2022 CCTB

中国肿瘤标志物学术大会

暨CACA整合肿瘤学峰会

暨第十六届肿瘤标志物青年科学家论坛

暨中国肿瘤标志物产业创新大会

论文集

Proceedings

目　　录

（按投稿先后排序）

TBM 优秀论文

16. **长链非编码 RNA AC100821.2 通过调控 miR512-5p/DDX6 轴促进鼻咽癌的进展**……程天仪、杨致远、游波*
17. **胞外囊泡中的 SCARB1 通过联合调控 M1 及 M2 巨噬细胞功能促进鼻咽癌转移**……陈文卉*、游波、尤易文
18. **基于生物信息学分析 DNAH14 基因在子宫内膜癌中的临床意义**……李楠*、陈蕾、段雨含、张琨
19. **合成 MRI 联合三维动脉自旋标记成像预测弥漫性胶质瘤分级及肿瘤细胞增殖活性的研究**……葛鑫*[1,2]、张静[2]
20. **Synthetic MRI 联合 DSC 在胶质瘤分级及肿瘤细胞增殖活性预测中的临床价值**……葛鑫*[1,2]、张静[2]
21. **集成磁共振成像预测胶质瘤 IDH1 表达的应用研究**……葛鑫*[1,2]、张静[2]
22. **血清 sTim-3 与 PG 联合检测对胃癌的诊断和预后评估中的价值**……秦源*[1]、陈玲丽[1]、陈鑫栋[1]、方红明[2]、黄飚[1]
23. **TRIB2 通过βTrCP 调节 TFRC 泛素化并抑制肝癌细胞铁死亡敏感性**……郭素素*、张骁、马丽芳、王佳谊
24. **miR-199-3p 过表达调控肺癌 A549 细胞生长、侵袭及上皮间质转化机制研究**……熊伟杰*、王云涛、何朗
25. **转录因子 FoxQ1 在肺癌患者血浆中的表达及预后诊断价值**……牟永平*、孙玉书、温珍平、贺晓花、李劭恒、陈永霞、高红叶
26. **影像组学在肝癌中的临床应用研究进展**……吴婧冉[1]、杜成[2]、刘渤娜*[2]
27. **曲妥珠单抗对 HER-2/neu 检测试剂的干扰研究**……肖雅*、渠文涛、史小芹
28. **儿童肾结石的血清代谢组学研究**……温钧翔*
29. **基于单细胞测序数据分析甲状腺乳头状癌的免疫特征**……韩君*
30. **血清 CA15-3 和 HER-2/neu 在诊断良恶性乳腺疾病的应用价值研**……田会会*、吴小田、高俊杰
31. **血清β-HCG 在早期异位妊娠诊断中的意义**……冉盼盼*
32. **基于 Bulk 和单基因转录组测序揭示铜死亡相关基因对肝细胞癌预后和免疫浸润的综合**……杨成雷*、郭颜林、吴宗泽、黄军涛、向邦德
33. **缺氧肿瘤细胞源性外泌体通过 ATP 酶途径促进脂肪细胞脂滴释放参与鼻咽癌恶性进展**……尹海朦*、游波、袁岭、尤易文

34. **乙酰化转移酶 NAT10 通过 DDX5/HMGB1 轴抑制 CD4+ T 细胞功能促进鼻咽癌的进展**……谢海静*、游波、尤易文

35. **IFN-γ 通过上调肿瘤细胞表面 HLA-E 表达抑制 NK 细胞杀伤**……郑慧*[1]、管晓琳[2]、孟欣[2]、郭林[1,2]、卢仁泉[1,2]

36. **一种用于发现肺癌血浆生物标志物的深度代谢组学分析方法**……李佳*

37. **逆转录转座子通过代谢重编程促进肺癌发生发展**……张蕊*[1]、孙泽国[2]、刘芃芃[1]、于津浦[1]、张为家[2]

38. **VAHS2 通过 Snail 依赖性 VEGF-D 信号通路促进肺鳞癌淋巴管生成**……刘芃芃*、张蕊、于津浦

39. **RB1CC1 介导的转录重编程使肿瘤细胞对铁死亡敏感**……薛翔飞*、张骁、马丽芳、王佳谊

40. **乳腺化生性癌的诊断和治疗进展**……孙红娜*、徐君南、孙涛

41. **血清 fPSA 与 PSA 的比值在 PSA 低值区的意义研究**……田会会*、蔡高灿

42. **线粒体转录延伸因子（TEFM）在人脑胶质瘤组织中的表达及预后意义**……刘如爱*[1]、罗中贵[1]、自加吉[1]、王心萌[1]、赵妤[2]、余敏[3]、熊伟[1]

43. **乳腺癌易感基因在乳腺癌中的作用研究进展**……张润娇*、于津浦

44. **KAP1 基因在人恶性胸膜间皮瘤（MPM）中表达的临床意义及对 MPM 细胞增殖和侵袭的影响**……王心萌*[1,2]、周崇熙[1,2]、李彬[1,2]、自加吉[1,2]、普元倩[1,2]、邱璐[3]、梅雯[4]、张也频[4]、熊伟[1,2]

45. **云南省青石棉污染区恶性胸膜间皮瘤与致瘤性猿猴病毒 SV40 的关联研究**……王播勇*[1,2]、陈欣[1,2]、普元倩[1,2]、李锦松[1,2]、自加吉[1,2]、梅雯[3]、赵一[3]、邱璐[4]、熊伟[1,2]

46. **脑膜转移瘤患者脑脊液中存在基因组不稳定性**……王鹏*、章巧玲、于津浦

47. **鉴定用于预测神经母细胞瘤预后和免疫微环境的糖基转移酶特征**……韩雷*、沙永亮、赵强、于津浦

48. **中国胃癌患者基因谱以及分子分型研究**……程亚楠*[1]、卜德超[2]、董莉[1]、赵屹[2]、于津浦[1]

49. **中国家族遗传性乳腺癌家系易感基因突变谱**……董莉*

50. **EphB1 通过 PI3K/AKT 信号通路促进食管鳞状细胞癌 EC-9706 细胞增殖、迁移、侵袭，并抑制其凋亡**……张键*、罗咏萍、刘毅、陈宗华

51. **长链非编码 RNA AC012073.1 对乳腺癌细胞迁移侵袭的影响及临床价值研究**……孔雪*、王传新

52. **ISG20 表达调控：一种神秘的抗病毒因子对癌症患者和正常人群的影响**……刘志颖、柳曙光、傅俊江*

53. **TMPRSS4 在癌症中的表达以及小分子抑制剂的调控研究**……谭琦、柳曙光、傅俊江*

54. **PSAT1 整合代谢重编程及与 IQGAP1 互作信号通路促进肺腺癌 EGFR-TKIs 耐药和转移**……罗鸣宇*、周烨、沈瑛

55. **解旋酶 DHX36 作为原癌基因促进肺癌的生长和转移的研究**……李婷[1]、杨晶[2]、傅俊江*[1]

56. **综合机器学习和生物信息学分析揭示胃癌干性特征并区分具有不同预后和免疫治疗反应的干性亚型**……邹远江、鞠铭伊、李耀、赵琳*

57. **肿瘤教育血小板 SNORA58 作为食管癌新型标志物的研究**……张倩茹*、宋兴国、宋现让

58. **质粒编码的 lncRNA-SLERCC 纳米颗粒介导的转染抑制肾细胞癌的进展**……毛卫浦*[1]、陈明[1]、李伟[2]

59. **环状 RNA ciRS-7-- 肾细胞癌的预后生物标志物和潜在的基因治疗靶点**……毛卫浦*、陈明

60. **血浆外泌体作为卵巢癌的新型肿瘤标志物**……李晓*、王世文、宋兴国、宋现让

61. **DEK 通过 β-catenin 调控幽门螺杆菌相关性胃癌增殖的机制研究**……范博洋*[1]、焦媛媛[1]、阮耀奇[1]、陈高正[1]、高雪菲[2]、孙洁[1]

62. **GSTT1 在卵巢癌紫杉醇耐药中的生物学研究**……张菁*

63. **miR-143/145 基因簇对食管癌细胞信号通路靶基因调控作用的研究进展**……罗堉楼*

64. **科罗索酸通过降低肝癌细胞中 CDK19 介导的 O 糖基化水平抑制肝癌生长**……马丽芳*、王佳谊*

65. **电化学发光法检测甲胎蛋白的性能验证及评价**……李德宪*、施立超、柳强、杨丽红、韩文

66. **血浆外泌体来源的小 RNA tRF-Lys-CTT-049 作为非小细胞肺癌生物标志物的研究**……周娜*、郑白冰、谢丽

222. **The E3 Ligase NEDD4 is A Potential Target in IGF Signal Pathway-driven Gastric Cancer**.....ke wang*[1]、xunliang jiang[1]、jipeng li[1,2]

223. **Nomogram to predict long-term overall survival and cancer-specific survival of radiotherapy patients with nasopharynx**.....ke wang*[1]、xunliang jiang[1]、jipeng li[1,2]

224. **A novel biomarker based on five tsDElncRNAs SLC25A5-AS1, RP11-336A10.4, FLJ42969, RP11-21L19.1 and RP11-406H23.2 can predict the prognostic risk of papillary renal cell carcinoma**.....Ji Ma*

225. **A case report of a patient with first phenotype of papillary thyroid carcinoma and heterochronous multiprimary tumor harboring germline MUTYH Arg19*/Gly286Glu mutations**.....mingbo wang*

226. **MYCN and MYC as potential biomarkers for poor prognosis in small cell lung cancer patients**.....Xuefeng Liang*、Yuji An、Wenhui Wang、Kejian Wang、Zhenglin Li、Lijun Sheng

227. **Identification of KRAS G12V associated clonal neoantigens and immune microenvironment in long-term survival of pancreatic adenocarcinoma**.....Chao Wang*、Jun Zhang

228. **Clinical features of patients with HER2-positive breast cancer and development of a nomogram for predicting survive**.....Yu Fan*、Yu Wang、Lijia He、Saber Imani、Qinglian We

229. **CLIP4 Shows Putative Tumor Suppressor Characteristics in Breast Cancer: An Integrated Analysis**.....Yu Fan*、Lijia He、Yu Wang、Shaozhi Fu、Yunwei Han、Juan Fan、Qinglian Wen

230. **The clinicopathological and prognostic significances of CDC73 expression in breast cancer：A pathological and bioinformatics analysis**.....ying e*、huachuan zheng、hang xue、congyu zhang、mingzhen zhao

231. **The effects of REG4 expression on the chemoresistance of ovarian cancer**.....Liwei Xiang*、huachuan zheng、hang xue、minwen ha

232. **The roles of ING5 in cancer: a tumor suppressor**.....huachuan zheng*、Hang Xue、Hua Jiang

233. **Oncogenic roles of GPR176 in breast cancer: A marker of aggressiveness and a target of gene therapy**……...Wenjing Yun*、Huachuan Zheng

234. **The oncogenic roles of GPR176 in ovarian cancer: a molecular target for aggressiveness and gene therapy**……Ning Yang*、Hang Xue、Wenjing Yun、Huachuan Zheng

235. **The effects of TRG-AS1/miR-196a-5p/ING5 axis on the gastric cancer**……ying chen*、huachuan zheng

236. **Transcriptional regulation of ING5 and its suppressive effects on gastric cancer**……Hang Xue、Huachaun Zheng

237. **The roles of BTG4 mRNA expression in cancers: a bioinformatics analysis**……..Hailan Xu*、Huachuan Zheng

238. **Survival Prediction of Patients Treated with Immune Checkpoint Inhibitors via KRAS/TP53/EGFR-single Gene Mutation**……..……shuai geng*

239. **The clinicopathological and prognostic significances of GPR176 in colorectal cancer**……Cuiyu Hu*、Hua-chuan Zheng、Hang Xue、Wen-jing Yun

240. **The roles of BTG3 mRNA expression in cancers: a bioinformatics analysis**……huachuan zheng*、Congyu Zhang

241. **Identification of a Prognostic Colorectal Cancer Model Including LncRNA FOXP4-AS1 and LncRNA BBOX1-AS1 Based on Bioinformatics Analysis**……zhiliang shi*[1,2]、guoqiang zhou[1]、jian guo[1]、xiaoling yang[1]、cheng yu[1]、chenglong shen[1]、xinguo zhu[2]

242. **The roles of parafibromin in cancer: a tumor suppressor**……huachuan zheng*、ying e、hang xue

243. **Identification of a novel mRNA-miRNA-lncRNA competing endogenous RNA network associated with prognosis of pancreatic cancer**……..……Yanrong Wang*

244. **Identification of Prognostic Biomarkers and Therapeutic Targets Among CCN Family Genes in Human Gastric Cancer**……Mengqi Yang *[1]、Huanting Chen[2]、Yajie Liu[1]

245. **Immune checkpoints TIM-3 expression in circulating and tumor-infilitrating $CD4^+$ and $CD8^+$ T cells in ovarian cancer patients**……..Jie Li*

246. **Reliability analysis of exonic-breakpoint fusions identified by DNA sequencing for predicting the efficacy of targeted therapy in non-small cell lung cancer**…… Weihua Li*[1]、Rui Wan[1]、Lei Guo[1]、Dong Jiang[2]、Lin Meng[2]、Jianming Ying[1]

247. **NEK9, a novel effector of IL-6/STAT3, regulates metastasis of gastric cancer by targeting ARHGEF2 phosphorylation**……Guofang Lu*、Siyuan Tian、Yi Sun、Jiaqiang Dong、Na Wang、Jiaoxia Zeng、Yongzhan Nie、Kaichun Wu、Bin Feng、Ying Han、Yulong Shang

248. **KRT80 expression works as a biomarker and a target for differentiation in gastric cancer**……Kaihang Shi [1]、Hang Xue[1]、Enhong Zhao[1]、Lijun Xiao[2]、Hongzhi Sun[3]、Huachuan Zheng*[1]

249. **A pair of neglected potential tumor diagnostic bio-markers: xanthine and xanthine oxidase**……Kaihang Shi [1]、Hang Xue[1]、Enhong Zhao[1]、Lijun Xiao[2]、Hongzhi Sun[3]、Huachuan Zheng*

250. **A lncRNA signature associated with tumor immune heterogeneity predicts distant metastasis in locoregionally advanced nasopharyngeal carcinoma**……Yelin Liang*[1]、Yuan Zhang[1]、Xirong Tan[1]、Han Qiao[1]、Songran Liu[1]、Linglong Tang[1]、Yanping Mao[1]、Lei Chen[1]、Wenfei Li[1]、Guanqun Zhou[1]、Yin Zhao[1]、Junyan Li[1]、Qian Li[1]、Shengyan Huang[1]、Sha Gong[1]、Ziqi Zheng[1]、Zhixuan Li[1]、Ying Sun[1]、Wei Jiang[2]、Jun Ma[1]、Yingqin Li[1]、Na Liu[1]

251. **The roles of REG4 expression in colorectal cancer: a potential marker for carcinogenesis and subsequent progression**……Congyu Zhang*[1]、Hua-chuan Zheng[2]、Hang Xue[2]

252. **Clinical value of PRC1 and DLGAP5 and immunosuppressive T cells overexpressing them in HCC based on bulk and single-cell RNA data**……Chenglei Yang*、Jiatai He、Rui Song、Bangde Xiang

253. **How Nanotechniques Could Vitalize the O-GlcNAcylation-Targeting Approach for Cancer Therapy**……Rui Yang、Daozhen Chen*

254. **Circulating lymphocyte subsets are prognostic factors in patients with nasopharyngeal carcinoma**……Jing Zhu*、Ruhua Fang、Zhiwen Pan、Xu Qian

255. **Circulating lymphocyte subsets are dynamic biomarkers for HPV negative head and neck squamous cell carcinoma during treatme**……Jie Zhou*、Jing Zhu、Xu Qian

256. **Identification of potential biomarkers for progression and prognosis of bladder cancer by comprehensive bioinformatics analysis**……Zhiyong Tan*、Jiansong Wang

257. **SMAD4 通过 HBx 转录激活和蛋白稳定的协同作用而促乙肝相关肝癌细胞增殖**……王朝敏

258. **Overexpression of Protein Phosphatase 2 Regulatory Subunit B"Alpha Promotes Glycolysis by Regulating Hexokinase 1 in Hepatocellular Carcinoma** ……Ning Jiao*、Qing Zhang

259. **Decreased expression of the lncRNA CASC2 predicts advanced clinicopathological features and serves as an unfavorable risk factor for cancer patient survival**……..Tianrui Xu*、Guoqiang Xu、Lixiu Zhu

260. **An Algorithm for the Early Diagnosis of Gastric Cancer based on Combined Serum Tumor Biomarkers** ……..Rui Ding*[1]、Honglei Li[1]、Qiang Xu[2]、Tingting You[1]、Linglin Zhang[3]、Zijian Guo[1]、Xiaowei Wang[4]、Man-Fung Tsoi[5]、Lin Zhang[6]、Zhongjuan Liu[1]、Xuzhen Qin[1,7]、Zhihong Qi[1]

261. **Association of BRCA1/2 mutations with prognosis and surgical cytoreduction outcomes in ovarian cancer patients: An updated meta-analys**……yazhuo wang*

262. **Development and Validation of Reassigned CEA, CYFRA21-1 and NSE-Based Models for Lung Cancer Diagnosis and Prognosis Prediction**……Jingmin Yuan*、Yan Sun、Hui Ren、Mingwei Chen

263. **RNA modifications meet tumors**……..Zhiyuan Yang、Bo You*

264. **PTEN promoter methylation predicts 10-year prognosis in hormone receptor positive early breast cancer patients that received adjuvant tamoxifen endocrine therapy**……Yu Fan*、Zhu Wang、Wang Yu、Yanping Wang、Hong Zheng、Xiaorong Zhong

265. **Investigated Diagnostic Value of Synthetic Relaxometry, Three-dimensional Pseudo-Continuous Arterial Spin Labelling and Diffusion-Weighted Imaging in the Grading of Glioma**……Xin Ge*[1,2]、Jing Zhang[2]

266. **Differentiation and prognostic stratification of acute myeloid leukemia by serum-based spectroscopy coupling with metabolic fingerprints**……Yang Chen*[1,2]、Zhengwei Duan[1]、Lijing Xiao[1]、Yingping Cao[3]、Yi Peng[4]、Wuping Liu[5]、Jianda Hu[1,2]

267. **TRIB2 modulates proteasome function to reduce ubiquitin stability and protect liver cancer cells against oxidative stress**……Susu Guo*、Xiao Zhang、Lifang Ma、Jiayi Wang

268. **Ubiquitin-specific protease 24 promotes hepatocellular carcinoma progression via YAP stabilization and deubiquitination**……Huizhuang Dan*[1]、Xinhua Xiao[2]、Yingli Wu[3]

269. **Identification of a 5-Gene-Based Signature to Predict Prognosis and Correlate Immunomodulators for Rectal Cancer**……Yi Lin*[1]、Qiang Ji[1]、Yichen Peng[1]、Chunna Yu[1]、Yi Zheng[1]、Xun Kang[1]、Jianwei Zheng[1]、Rixing Bai[1]、Wenmao Yan[1]、Xiaomin Wang[1,2]、Wenbin Li[1]

270. **Identification of a novel PAX5-GSE1 fusion gene acting as minimal residual disease biomarker in acute B-lymphocytic leukemia**……Haina Wang*、Jingjing Xue、Xuehong Zhang、Yuan Gao、Xin Zong、Zhijie Kang、Jinsong Yan

271. **CD155/SRC complex promotes hepatocellular carcinoma progression via inhibiting the p38 MAPK signaling pathway and correlates with poor prognosis**…….Anli Jin*[1]、CHUN-YAN ZHANG[1]、Wen-Jing ZHENG[1]、JING-RONG XIAN[1]、WEN-JING YANG[1]、TE LIU[2]、WEI CHEN[1]、TONG LI[1]、BEI-LI WANG[1]、BAI-SHEN PAN[1]、QIAN LI[1]、JIAN-WEN CHENG[1]、PENG-XIANG WANG[1]、BO HU[1]、JIAN ZHOU[1]、JIA FAN[1]、XIN-RONG YANG[1]、WEI GUO[1]

272. **Comprehensive analysis of HHLA2 as a prognostic biomarker and its association with immune infiltrates in hepatocellular carcinoma**……Lin Ding*[1]、QIAN YU[1]、SHUO YANG[1]、WEN-JING YANG[1]、TE LIU[2]、JING-RONG XIAN[1]、TONG-TONG TIAN[1]、TONG LI[1]、WEI CHEN[1]、CHUN-YAN ZHANG[1]、BEI-LI WANG[1]、BAI-SHEN PAN[1]、JIAN ZHOU[1]、JIA FAN[1]、XIN-RONG YANG[1]、WEI GUO[1]

273. **Bioinformatics analysis of key genes and their associations with immune infiltration and prognosis in hepatocellular carcinoma**……Danna Xie[1]、Baolin Qian[2]、Xun Li*[1,3]

274. **Nucleic acids and proteins carried by exosomes from various sources: biomarkers for liver disease**…… Danna Xie[1,3]、Baolin Qian[2]、Xun Li*[1,3]

275. **A Novel Cellular Senescence-related lncRNA Signature for Predicting the Prognosis of Breast Cancer Patients**……Fangxu Yin*[1]、Chong Hou[2]、Song Wang[3]、Zhenlin Yang[1]

276. **Investigation of BIRC5 and CDK12 molecular mechanism underlying acquired drug resistance of afatinib in lung adenocarcinoma**……xiaoxi zhu*、yuanzhi lu

277. **Genetically predicted circulating concentrations of micronutrients and the risk of hepatocellular carcinoma: a Mendelian randomization study**……Chenglei Yang[1]、Qiang Cai[2]、Siyu Chen[3]、Yuankuan Li[1]、Xi Wu[3]、Bangde Xiang*[1]

278. **Clinical prognostic value and potential molecular pathway of Cell division cycle associated 5(CDCA5) in hepatocellular carcinoma (HCC)** …….Cheng-Lei Yang*[1]、Guo-Qun Liu[3]、Kun-Ying Huang[2]、Ao Jia[3]、Bang-De Xiang[1]

279. **Identification of the target protein of the metastatic colorectal cancer-specific aptamer W3 as a biomarker by aptamer-based target cells sorting and functional characterization**……Wanming Li*[1]、Chia-Chun Wu[2]、Shuo Wang[1,4]、Linlin Zhou[1]、Lei Qiao[3]、Wei Ba[1]、Furong Liu[1]、Linan Zhan[1]、Hang Chen[1]、Jau-Song Yu[2]、Jin Fang[1]

280. **Association between telomere length and hepatocellular carcinoma risk: a Mendelian randomization study**……Chenglei Yang*[1]、Xi Wu[2]、Siyu Chen[2]、Bangde Xiang[1]

281. **Two molecularly distinct subtypes and immunosuppressive microenvironment of CK19-positive cancer stem cells in HBV-associated hepatocellular carcinoma based on scRNA-seq**……Chenglei Yang*[1]、Qiuyan Wang[2]、Bangde Xiang

282. **PD-L1 expression on circulating tumor cells can be a predictive biomarker to PD-1 inhibitors combined with radiotherapy and antiangiogenic therapy in advanced hepatocellular carcinoma**……Ke Su*、Yunwei Han

283. **Clinical significance of serum and tumor tissue transthyretin expression in surgically resected non-small cell lung cancer**……..……chunhua xu*

284. **Radiotherapy in Gastric Cancer Patients with Liver Metastases: A Propensity Score-Matched SEER Database Analysis**……..……Liyou Lian[1]、Shuwen Cheng[2]、Rujie Zheng[3]、Hongxia Yao[1]、Tianhui Chen[4]、Jinfei Chen*[5]

285. **Survival benefit after radiotherapy for pancreatic ductal adenocarcinoma patients with liver metastases: A propensity score-matched study**……Liyou Lian[1]、Shuwen Cheng[2]、Rujie Zheng[3]、Hongxia Yao[1]、Tianhui Chen[4]、Jinfin Chen*[5]

286. **Down-regulation of BMAL1 1 by miR-494-3p promotes hepatocellular carcinoma growth and metastasis by increasing GPAM-mediated lipid biosynthesis**……Tao Yang*[1]、Yi Yang[1]、Peng Yuan[1]、Zifeng Zhao[1]、Jinliang Xing[3]、Hongxin Zhang[1]、Jibin Li[2]

287. **Expression Profile and Prognostic Value of MELK in Human Breast Cancer**……Mengqi Yang *、Yajie Liu

288. **N7-Methylguanosine-Related lncRNA: Potential Biomarker for Predicting the Prognosis of Hepatocellular Carcinoma Patients**……Zhihao Xu*、Ning Zhang、Huake Cao、Songlin Xing、Feixu Chen

289. **YAP ISGylation increases its stability and promotes its positive regulation on PPP by stimulating 6PGL transcription**……Xiangfei Xue *、Xiao Zhang

290. **Kinectin 1 promotes the growth of triple-negative breast cancer via directly co-activating NF-kappaB/p65 and enhancing its transcriptional activity**……Lin Gao*[1]、Shanze Chen[2]、Malin Hong[1,3]、Wenbin Zhou[1]、Bilan Wang[4]、Junying Qiu[1]、 Jinquan Xia[1]、Pan Zhao[1,3]、Li Fu[5]、Jigang Wang[1,3]、Yong Dai[1]、Ni Xie[5]、He Yang[6]、 Hsien-Da Huang[8]、Xiang Gao[9]、Chang Zou[1,3,7]

291. **The essential roles of m6A RNA modification to stimulate ENO1-dependent glycolysis and tumorigenesis in lung adenocarcinoma**……Lifang Ma*、Jiayi Wang

292. **Yin Yang 1 promotes aggressive cell growth in high-grade breast cancer by directly transactivating kinectin 1**……Lin Gao*[1]、Wenbin Zhou[2]、Ni Xie[3]、Junying Qiu[4]、Jingyi Huang[1]、Zhe Zhang[1]、Malin Hong[1,5]、Jinquan Xia[1]、Jing Xu[1]、Pan Zhao[1,5]、Jing Jiang[6]、Hui Gong[6]、Jigang Wang[1,5]、Yong Dai[1]、Dixian Luo[6]、Chang Zou[1,5,7]

293. **MORTALIN-Ca2+ axis drives innate rituximab resistance in diffuse large B-cell lymphoma**……Qi Sun*[1]、Ling Yang[2]

294. **Survival and prognosis of metastatic breast cancer in young women: SEER 2010-2015**……Hongna Sun*、Junnan Xu、Tao Sun

295. **A Nomogram for Predicting Survival in Breast Infiltrating Duct Carcinoma Patients With Brain Metastasis: A Population-Based Study**……Hongna Sun*、Junnan Xu、Tao Sun

296. **Breast cancer brain metastasis: Current evidence and future directions**……Hongna Sun*、Junnan Xu、Tao Sun

297. **Primary Neuroendocrine Tumor of the Breast: Current Understanding and Future Perspectives**……Hongna Sun*、Junnan Xu、Tao Sun

298. **Identification of Immune-Related Target and Prognostic Biomarkers in PBMC of hepatocellular carcinoma**……Rui Hu*、Xiaozhou Zhou

299. **Diagnosis and Monitoring Value of Circulating Tumour Cells in Breast Cancer with an Optimised Microfluidic Device: A Retrospective Study**……Zhiyun Gong*、Renquan Lu

300. **Fecal microbiota characteristics of anxiety and depression patients in esophageal cancer screening: a case-control study**……Juan Zhu*[1]、Wenqiang Wei[2]

301. **Role of JAK-STAT1 signaling pathway in Helicobacter pylori infection induced gastric carcinogenesis**……..Xue Li*[1]、Kai-Feng Pan[2]、Markus Gerhard[3]、Raquel Mejiías-Luque[3]、Wen-Qing Li[2]

302. **Combinational use of Trabectedin and Pegylated Liposomal Doxorubicin for Recurrent Ovarian Cancer: A Meta-analysis of Phase III Randomized Controlled Trials**……..…Chao Li*、Zhiru Li

303. **MTERF1 promotes colorectal cancer progression by increasing mitochondrial OXPHOS and regulating the p-AMPK/mTOR signaling pathway**..……Qian-qian Liu*[1,2]、Bin Li[1]、Ru-ai Liu[1]、Bo-yong Wang [1]、Lei Ding[2]、Qinghua Cui[2]、Jie Lin[2]、Min Yu[2]、Wei Xiong

304. **NNMT-DNMT1 axis is essential for maintaining cancer cell sensitivity to oxidative phosphorylation inhibition**……..Yue Liu*

305. **A super-enhancer gene-based risk score model for predicting overall survival in patients with hepatocellular carcinoma**……..……..Xueyan Wei*

306. **Estrogen receptor response gene EGR3 mediates breast cancer cell resistance to tamoxifen through promoting MCL1 transcription**……Yu Xie*、Yue Wang、Junfang Qin、Mengci Yuan、Jing Yu

307. **Downregulation of lactate receptor GPR81 contributes to tamoxifen resistance via regulating FAO in Breast Cancer Cells**……..……Jing Yu*、Yu Xie、Meng-ci Yuan、Jun-fang Qin、Yue Wang

308. **Peripheral blood mononuclear cell DNA methylation markers enables early non-invasive detection for breast cancer**……tiantian wang*、chuanxin wang

309. **A novel long non-coding RNA AC073352.1 promotes metastasis and angiogenesis via interacting with YBX1 in breast cancer**……...……..Xue Kong*、Chuanxin Wang

310. **Long non-coding RNA STEAP2-AS1 promotes lung adenocarcinoma cells proliferation, migration, and invasion by interacting with ARNTL2 to upregulate DARS2**……Ming Li*、Cheng Zhan、Mingxiang Feng、Qun Wang

311. **Distinct prognostic values of adenosine deaminase isoenzymes-ADA1 and ADA2 in cancer**……Zhao-wei Gao*、Ke Dong

312. **Annotation and evaluation of base editing outcomes in multiple cell types using CRISPRbase**……..……..Fengbiao Mao*

313. **Heat-shock protein 90α is a potential prognostic and predictive biomarker in hepatocellular carcinoma: a large-scale and multicenter study**……Ke Su*、Yunwei Han、jianwen Zhang

314. **Intratumor Microbiome Influence Lung Cancer Recurrence**……Mantang Qiu*[1]、Yi Ma[1,2]、Haiming Chen[1]、Jun Wang[1]

315. **Identification of lung cancer breath biomarkers based on perioperative breathomics testing: A prospective observational study**……..……Mantang Qiu*[1]、Peiyu Wang[1]、Qi Huang[2]、Shushi Meng[1]

316. **Identifying Distinctive Tissue and Stool Microbial Signatures and the Tumor-promoting Effects of Deoxycholic Acid in Breast Cancer**……Na Wang[1,2]、Mengzhen Han[1,2]、Wenjie Han[1,2]、Tao Sun[1,2,3]、Junnan Xu*[1,2,3]

317. **Identification of Lung Adenocarcinoma and Benign Pulmonary Lesions Based on Immunologic Gene Set Variation Analysis in Peripheral Whole Blood**……Wenmin Zhu*[1]、Tingting Chen[1]、Yangkai Li[2]、Lin Lei[3]、Shanshan Cheng[1]、Sheng Wei[1]

318. **Transmembrane Protein 170B is a Prognostic Biomarker and Associated with Immune Infiltrates in Pancreatic Adenocarcinoma**……Zilong Zhang*、jin shang、yuxin liang、xiaolun huang

319. **Human Adipose Mesenchymal Stem Cells-derived Exosomes Ameliorate Hepatic Fibrosis by Regulating Choline Metabolism and PI3K/Akt/mTOR Pathway: Based on Transcriptomics and Metabolomics**……..Zilong Zhang*、jin shang、ying shi、xiaolun huang

320. **Prognostic value of inflammation-immunity-nutrition score in patients with hepatocellular carcinoma treated with anti-PD-1 therapy**……Zilong Zhang*、yuxin liang、jin shang、ying shi、xiaolun huang

321. **Decreased expression of Rab32 promotes hepatocellular carcinoma progression by preventing MAM formation**……Xiaoli Liu*[1]、Zeyu Yan[1]、Dalin Wang[1]、Jiming Tian[2]、Dan Wu[1]、Yinping Wang[1]、Jing Zhao[1]、Qichao Huang[1]、Yulu Du[1]、Jiniang Xing*[1]、Xiacheng Sun*[1]

322. **Survival benefit after radiotherapy for patients with malignant pleural mesothelioma: A propensity score-matched study**……Liyou Lian[1]、Shuwen Cheng[3]、Rujie Zheng[1]、Hongxia Yao[1]、Jinfei Chen[1]、Tianhui Chen*[2]

323. **Oestrogen-regulated super-enhancer-associated lncRNA NCALD plays a key role in luminal breast cancer progression by forming a complex with ERa to activate GRHL2**……yue Meng*、dianrong zhou、bing gu

324. **Expression of LncRNA LINC00205 and miR-628-5p in serum of breast cancer patients and their clinical diagnostic value**……guoping wang*[1]、yan zhang[2]

325. **Induction therapy with TPF and Sindelizumab for locally advanced Nasopharyngeal Carcinoma and its effect on lymphocyte subcohorte**……guoping wang*[1]、yan zhang[2]

326. **Overexpression of SCEL inhibits oral squamous cell carcinoma proliferation and metastasis by modulating the TGF-β1/Smad signaling pathway**……Danping Li*[1]、Limei Li[1]、Shu Wu[1]、Jun Zhao[1]、Haishan Zhang[1]、Qiaoli Chen[1]、Yingxi Mo[2]、Xiaoying Zhou[3]

327. **SRTdb: an omnibus for human tissue and cancer-specific RNA transcripts**……Qili Shi*[1]、Teng Liu[2]、Zhiao Chen[1]、Xianghuo He[1]、Shengli Li[2]

328. **Cervicovaginal microbiota disorder combining microenvironment profiles promotes the poor development of cervical cancerization**……Mingxuan Zhang*、Jintao Wang、Jiahao Wang、Le Zhang

329. **DiseaseMeth version 3.0: A major expansion and update of the human disease methylation database**……jie xing*、rui yang zhai、cong wang

330. **Identification and characterization of partially hypermethylation in under-methylated regions**……Xinyu Wang*、Lijun Dai、Qingran Qong、Jianzhong Su

331. **Di-methylation of CD147-K234 promotes the progression of NSCLC by enhancing lactate export**……Ke Wang*

332. **Anti-HIV Drug Elvitegravir Suppresses Cancer Metastasis via Increased Proteasomal Degradation of m6A Methyltransferase METTL3**……Long Liao*、Bin Li

333. **Abnormal regulation of miR-29b-ID1 signaling is involved in the process of decitabine resistance in leukemia cells**……..Jichun Ma*、Xiangmei Wen、Zijun Xu、Peihui Xia、ye jin、Jiang Lin、Jun Qian

334. **Predicting the Influence of Circ_0059706 Expression on Prognosis in Patients with Acute Myeloid Leukemia using Classical Statistics and Machine Learning**……..Jichun Ma*、Xiangmei Wen、Zijun Xu、Peihui Xia、Ye Jin、Jiang Lin、Jun Qian

335. **The downregulation of circ_0059707 in acute myeloid leukemia promotes cell growth and inhibits apoptosis by regulating miR-1287-5p**……Jichun Ma*、Xiangmei Wen、Zijun Xu、Peihui Xia、Ye Jin、Jiang Lin、Jun Qian

336. **CC-115 mediates GSDME-dependent pyroptosis in lung adenocarcinoma through Akt/Bax pathway**……Ting Zhang*

337. **Powerful correlation of GBP1 expression with prognosis and tumor immunity in pan-cancer**……王森钰*、张雅静、冯阳春

338. **GCA induces pyroptosis of lung cancer stem cells by regulating the formation of dTGN via GOLPH3 / MYO18A complex**……Feng Zhang*

339. **NMT1-mediated N-myristoylation of VILIP3 protein and cancer progression are suppressed by desloratadine in hepatocellular carcinoma**……Yan He*、Bin Li

340. **PAMR1 is a Favorable Prognostic Biomarker in Hepatocellular Carcinoma**……Xiaoping Zhou*

341. **Investigation of transcript variant 6 of TPD52L2 as a prognostic and predictive biomarker in basal-like MDA-MB-231 and MDA-MB-453 cell lines for breast cancer**……Xin Zhang*[1,2]、Daniel O'Brien[3]、Xiaohui Zhang[4]

342. **ncRNA-mediated high expression of SOX4 correlates with unfavorable outcomes and immune infiltration in hepatocellular carcinoma**……..……Li Jing、zhiyi han、xiaozhou zhou*

343. **FAT4 Overexpression in Peripheral Blood Mononuclear Cells is Associated With a Favorable Prognosis and Promotes Immune Cell Infiltration in Hepatocellular Carcinoma**……..Li Jing、zhiyi han、xiaozhou zhou*

344. **Nanoparticle delivery of miR-21-3p sensitizes melanoma to anti-PD-1 immunotherapy by promoting ferroptosis**……..Weinan Guo*、Zhenjie Wu、Jianru Chen、Sen Guo、Xiuli Yi、Chunying Li

345. **Clinical significance and immune cell infiltration of lnc-MAPKAPK5-AS1 in HCC: based on public databases and immunohistochemistry**……Xiangzhi Hu*[1]、Dedong Wang[1,2]、Jinbin Chen[3]、Pengzhe Qin[2,4]、Boheng Liang[2,4]、Di Wu[2,4]

346. **Identification and Validation of a Novel Multi-omics Signature for Prognosis and Immunotherapy Response of Endometrial Carcinoma**……Qiu Wang*、Zhicheng Wu、Xiaofeng Li、Ling Ji

347. **DNA Methylation-Specific Analysis of G Protein-Coupled Receptor-Related Genes in Pan-Cancer**……..……Meng yan Zhang*、Ji yun Zhao、Yan Zhang

348. **Development and Validation of a Novel Prognosis Prediction Model for Patients with Myelodysplastic Syndrome**……..……Haiping Liang*[1]、Liu Bei[2]

349. **Alternatively activated (M2) macrophage express SP to promote tumour growth and invasiveness and can be inhibited by aprepitant in Esophageal cancer**……yang zheng*、meixiang sang、baoen shan

350. **Value of multi-gene testing in the diagnosis of Bethesda I to III thyroid nodules: A prospective double-blind study**……Guozhi Zhang*、Xiaowei Qi、Lin Ren、Chunlin Tang、Ping Chen、Qiyun Shi、Hao Tian、Peng Tang、Linjun Fan、Li Chen、Shushu Wang、Ye Zhang、Wenting Yan、Ling Zhong、Yanli Guo、Yi Zhang

351. **Impact of salvage radiotherapy combined with chemotherapy on long-term outcomes of patients with recurrent nasopharyngeal carcinoma: a retrospective study**……..……Ying Li*[1,2]、Wei Liu[1,2]、Lihua Wang[1,2]、Wenquan Hong[1,2]、Youliang Weng[2]、Sufang Qiu[2]

352. **Development of small extracellular vesicle miRNA-based liquid biopsy for prostate cancer early diagnosis and risk classification**……Meng Han*[1,2]、Yuan Yin[4]、Cheng Zhou[2,3,6]、Bairen Pang[1,2,5]、Qi Wang[1,2,5]、Jie Gong[1,2]、Rui Su[2,3]、Jiukai Jin[2,3]、Yingzhi Chen[2,3]、Zhong Zheng[2,3]、Zhaohui Jiang[2,3]、Qi Ma[1,2,3]、Yue Cheng[1,2,3]、Zejun Yan[1,2,3]、Yong Li[5]、Junhui Jiang[1,2,3]

353. **Prognostic model on overall survival in elderly nasopharyngeal carcinoma patients: A recursive partitioning analysis identifying pre-treatment risk stratification**……Ying Li*[1,2]、Zongwei Huang[1,2]、Sunqin Cai[1,2]、Qin Ding[1,2]、Youliang Weng[2]、Sufang Qiu[2]

354. **Liquid biopsy of novel extracellular vesicle and particle cargos to improve prostate cancer diagnosis and progression monitoring**……...……Qi Wang*[1,2,3] 、Bairen Pang[1,2,3]、Meng Han[1,2]、Cheng Zhou[2,4,5]、Jie Gong[1,2]、Rui Su[2,4]、Jiukai Jin[2,4]、Yingzhi Chen[2,4]、Zejun Yan[1,2,4]、Zhong Zheng[2,4]、Zhaohui Jiang[2,4]、Junhui Jiang[1,2,4]、Yong Li[3]

355. **CXCL12 derived from CD248-expressing cancer-associated fibroblasts mediates M2-polarized macrophages to promote nonsmall cell lung cancer progression**……Jieheng Wu *[1,3]、Jiangwei Wu[1]、Qiaoling Zhang[1]、Zeyang Yang[1]、Rui Zhang[3]、Jian Zhang[2]、Zhu Zeng[1]

356. **Regulation Mechanism of Ell-associated Factor 2 in Cervical Carcinoma Microenvironment**……Fan Guo 、Weina Kong*、Miyessar Anwar、Xiumin Ma

357. **The oncogenic roles of JC polyomavirus T antigen in cervical cancer**……..……Hang Xue*、Huachuan Zheng

358. **A comprehensive platelet expression atlas resource PEA and platelet transcriptome landscape**……Gui-Yan Xie*

359. **ImmuCell AI-mouse: a tool for comprehensive prediction of mouse immune cell abundance and immune microenvironment depiction**……...……Ya-Ru Miao*

360. **GSCA: an Integrated Platform for Gene Set Cancer Analysis at Genomic, Pharmacogenomic, and Immunogenomic Levels**……....Gui-Yan Xie*

361. **The inactivation of ketone body metabolism induces an inflammatory microenvironment and facilitates the progression of renal clear cell carcinoma**……..……Ran Zhao*、Qian Zheng、Xiao ying Zhou

362. **The Predictive Model of key Biomarker in Liquid Biopsy for Prognosis of Bladder Cancer**……Xin Dong*、Baojun Wei、Wei Cui

363. **Ubiquitin Specific Protease 44: What we currently know**……Yujia Liu*、zhongjun wu、tingxiu xiang

364. **Detecting NAB2-STAT6 Fusion Variants and other Molecular Alterations in Intracranial Solitary Fibrous Tumors by Targeted RNA sequencing**……...…….Juan Ji*[1,2]、Yang Liu[1,2]

365. **Lactate metabolism as a dictator of patient outcomes and immune microenvironment in head and neck squamous carcinoma**……...…Xiaochuan Chen*、Junping Pan、Qin Ding、Hanxuan Yang、Sufang Qiu

366. **The value of MECOM/PRDM3 expression in predicting development and poor prognosis in lung adenocarcinoma**……Anqi Li*[1]、Meng Li[1]、Jing Wang[2]、Jiejun Zhou[1]、Meng Fan[1]、Mingwei Chen[1,2]

367. **dbCAC: a comprehensive database of genes and drugs in cancer-associated cachexia**……Longxiang Xie、Qiang Wang、Guo Zhao、Fangmei Nan、Qiongshan Li、Shengnan Wu、Xinyuan Liu、Yongsen Wang、Zhihan Zhou、Xiangqian Guo*

368. **Integrated analysis of lncRNA-miRNA-mRNA ceRNA network identified lncRNA EPB41L4A-AS1 as a potential biomarker in non-small cell lung cancer**……...……Meiqi Wang*

369. **Metabolic biomarkers for diagnosis of germinoma revealed by multi-omics and machine learning approaches**……HuaChun Yin*[1]、Yong Chen[4]、LuSheng Li[4]、Ying Xiong[3]、JingXin Tao[2]、ShengQing Lv[1]、Hui Yang[1]、Bo Li[2]、Song Li[1]

370. **Romidepsin enhances the killing ability of NKG2D-CAR-T cells through enhanced expression of NKG2DL against ovarian cancer cells**……Liang Wang*、lirui yu

371. **Reclassifying Early-Stage Colorectal Cancer into Two Subgroups with Different Overall Survival, Tumor Microenvironment, and Response to Immune Checkpoint Blockade Treatment**……..……..……Xiangxiang Liu*、Shukui Wang

372. **The oncomicroprotein MUCP1 promotes colorectal cancer progression by regulating lipid metabolism**……..……..……..Junjie Nie*、Shukui Wang

373. **Study on exosome mediated miR-1229 as metastasis markers of colorectal cancer and its mechanism**……Huiling Sun*、Shukui Wang

374. **H3K4me3-activated miR-1290 promotes the progression of CRC through KLF9/p53/MMP9 pathways**……Jian Qin*、Shukui Wang

375. **TBC1D3 induces TC-1 expression to promote human breast cancer cell metastasis**……Yong Shen*[1,2]、Qingxia Xu[1,2]

376. **Single-cell RNA sequencing of cancer patients reveals age-dependent tumour microenvironment alterations that facilitate response to immunotherapy**……Xiaoqiang Zhu *[1,2]、Jie Hong[1]、Jason W.H. Wong[2]、Youwei Zhang[3]、Haoyan Chen[1]

377. **Detection of telomerase activity based on an enzyme-free dual DNA electrochemical sensor**……Qingxia Xu*

378. **Hsa_circ_0007990 promotes breast cancer progression via inhibiting YBX1 protein ubiquitination and degradation**……Tao Xu*、Shukui Wang

379. **LncRNA MAFG-AS1 promotes proliferation and immune escape of breast cancer by interaction with EZH2**……Bei Pan*、Shukui Wang

380. **P3H1 as a novel prognostic biomarker correlates with immune infiltrate: a pan-cancer analysis**……Changmeng Wu*

381. **Comprehensive analysis of serum and gastric juice bile acid profiles and gastric microorganisms in patients with different stages of gastritis-cancer transformation process**……Luyao Zhang*[1,2]、Na Wang[1]、Xiaodong Qu[1]、Xingyu Zhao[1]、Qiang Dong[1]、Jiangyi Zhu[1]、yan Nie[1]、Yongquan Shi[1]

382. **A Gene Expression Signature in Predicting Prognosis of Colorectal Cancer with Peritoneal Metastasis**……Wenqing Xie*、Wanjun Liu、Qianxin Luo、Daici Chen

383. **Identification of the lipid metabolism related molecular subtypes and construction of a prognostic model in the Triple negative breast cancer**……Jun Yang*

384. **CXCR6 expression associated with checkpoint immunotherapy response in cutaneous melanoma**……Zhengyun Zou、Xinyu Su*

385. **Inactivation of epithelial sodium ion channel molecules serves as effectively diagnostic biomarkers in clear cell renal cell carcinoma**……Yao Wei*、Qian Zheng、Yifang Wang、Ran Zhao、Xiaoying Zhou

386. **Different onset patterns of acral melanoma: clinicopathological features and potential molecular mechanisms**……..…Zhengyun Zou*[1]、Rong Huang[1]、Mengke Zhao[2]、Jiayu Wang[3]、Kelin Zheng[3]、Xinyu Su[1]、Lanqun Qin[4]、Yirong Wu[1]

387. **NBS1 Interacts with CyclinB to Modulate Drug Sensitivity of Olaparib in Ovarian Cancer**……..……Ailing Zhong*、Renquan Lu、Lin Guo

388. **SLC22A3 methylation-mediated gene silencing predicts adverse prognosis in acute myeloid leukemia**……Yu Gu*、Zijun Xu、Jingdong Zhou、Jun Qian

389. **MUC20 as a novel prognostic biomarker in ccRCC correlating with tumor immune microenvironment modulation**……..…….Bo Xue*[1,2]、Dognwen Wang[1,2]

390. **Developing an m5C regulator–mediated RNA methylation modification signature to predict prognosis and immunotherapy efficacy in rectal cancer**……..……Rixin Zhang*、Min Yang

391. **Proteomic identification of novel small extracellular vesicle protein biomarkers for prostate cancer diagnosis and risk stratification**……Bairen Pang*[1,2,3,4]、Cheng Zhou[2,3,5]、Meng Han[1,2,3]、Qi Wang[1,2,4]、Jie Gong[1,2,3]、Rui Su[2,3]、Jiukai Jin[2,3]、Yingzhi Chen[2,3]、Zejun Yan[1,2,3]、Zhaohui Jiang[2,3]、Zhong Zheng[2,3]、Tianli Fan[6]、Yong Li[4]、Junhui Jiang[1,2,3]

392. **mitoSomatic: A tool for accurate identification of mitochondrial DNA somatic mutations without paired controls**……..……Wenjie Guo、Yang Liu、Liping Su、Shanshan Guo、Xiaoying Ji、kaixiang Zhou、Xu Guo、Xiwen Gu、Jinliang Xing*

393. **Mutational signature of mtDNA confers mechanistic insight into oxidative metabolism remodeling in colorectal cancer**……Yang Liu*、Wenjie Guo、Fan Peng

394. **Proteomic characteristics of gastric cancer related to Helicobacter pylori**……...……Jiameng Sun*

395. **Correlation between Immunohistochemical Markers Expression and Lymph Node Metastasis in Gastroenteropancreatic Neuroendocrine Neoplasms: A Nation-wide**

10-year Retrospective Clinical Epidemiological Study in China……..…Huan Yang*、Jin-hu Fan

396. **GRAP2 as a Promising Predictor of Prognosis and Immunotherapy Response for Patients with Breast Cancer**……..……Xin Meng*、Lin Guo、Renquan Lu
397. **Exploration of Reference Intervals for SCCA and CYFRA 211 levels in Southeast Chinese Population**…….……Minglei Jiang*
398. **COPS5 conferred the platinum-resistance in epithelial ovarian cancer**……Tianqing Yan *、Lin Guo、Renquan Lu
399. **Effect of EGFR amplification on survival of patients with EGFR mutation-positive non-small cell lung cancer receiving first-line EGFR-TKIs treatment**..…….....……..Yiquan Xu*、Gen Lin
400. **Systematic Analysis based on Publicly Available Databases Reveals IGF2BP3 as a Potential Pan-Cancer Biomarker for Prognosis and Response to Immunotherapy**……Yating Wu*[1,2]、Zhongqiu Wu[3]、Zhuolin Li[1,2]、Huimin Niu[1,2]、Xiaofeng Lai[1,2]、Hu Zhao[4]、Meng Zhao[1,2]、Shenghang Zhang[1,2]、Shuiliang Wang[1,2]
401. **A novel feedback regulated loop of circRRM2-IGF2BP1-MYC promotes breast cancer metastasis**……Ran Hao*[1]、Lei Zhang[1]、Yipeng Wang[1]、Jie Hu[1]、Yixin Qi[2]
402. **Single-cell characterization of macrophages in uveal melanoma uncovers a unique proliferative subset that confers a de novo subtype with a poor prognosis and aggressive behavior**……Ke Li*、lanfang sun、wencan wu、jie sun、meng zhou
403. **ATOH1 modulates cancer stem cell properties and tumorigenesis through activation of GAS1 in gastric adenocarcinoma Running Head: ATOH1 Regulates Gastric Cancer Stemness**……Xiaohui Zhong*[1,2]、Qing Zhong[3,4,5,6]、Hai-chun Chen[1,2]
404. **Characterization of Sialylation-Related Long Noncoding RNAs to Develop a Novel Signature for Predicting Prognosis, Immune Landscape, and Chemotherapy Response in Colorectal Cancer**…….……Mingxuan Zhou*、Min Yang、YuFang Hou、Rixin Zhang、Weiqi Wang、Zheng Yan、Tiegang Li、Wenqiang Gan、Silin Lv、Zifan Zeng、fang Zhang

405. **Individualized concurrent chemoradiotherapy or targeted radiotherapy by pre-treatment plasma EBV DNA in locoregionally advanced nasopharyngeal carcinoma**……Sunqin Cai*、Zongwei Huang、Sufang Qiu、Jun Lu、Yuhui Pan

406. **Machine Learning-Based Integration Develops a Robust Mitophagy-Related Multigene Model to Predict Patient Prognosis and Immune Microenvironment in Head and Neck Squamous Cell Carcinoma**……...……Qin Ding*、Yuhui Pan、Wei Liu、Sufang Qiu

407. **Prognostic relevance of PD-L1 expression on circulating tumor cells in metastatic breast cancer patients treated with anti-PD-1 immunotherapy**……Ying Zhou *[1,2]、Jinmei Zhou[3]、Xiaopeng Hao[4]、Haoyuan Shi[1,2]、Xuejie Li[1,2]、Anqi Wang[1,2]、Zhiyuan Hu[1,2,5,6]、Yanlian Yang[2,5]、Zefei Jiang[3]、Tao Wang[3]

408. **A Circular RNA Activated by TGFβ Promotes Tumor Metastasis through Enhancing IGF2BP3-mediated PDPN mRNA Stability**……Ke Li*、Jiawei Guo、Yue Ming、Shuang Chen、Tingting Zhang、Hulin Ma、Xin Fu、Jin Wang、Wenrong Liu Liu、Yong Peng

409. **Mitochondrial fragmentation is crucial for c-Myc-driven hepatoblastoma-like liver tumors**……...……Dalin Wang*[1,2]、Jiming Tian[3]、Zeyu Yan[4]、Qing Yuan[5]、Dan Wu[1]、Xiaoli Liu[1]、Shirong Yang[4]、Shanshan Guo[1]、Jianxun Wang[6]、Yongxiu Yang[3]、Jinliang Xing[1]、Jiaze An[2]、Qichao Huang[1]

410. **Methionine Deficiency Facilitates Antitumor Immunity by Altering m6A Methylation of Immune Checkpoint Transcripts**……Ting Li*[1,2]、Tan Yue-Tao[1]、Yan-Xing Chen[1]、Xiao-Jun Zheng[3]、Wen Wang[4]、Kun Liao[1]、Hai-Yu Mo[1]、Junzhong Lin[1,5]、Wei Yang[6]、Hai-Long Piao[4]、Rui-Hua Xu[1,7]、Huai-Qiang Ju[1,7]

411. **Whole-exome sequencing reveals the evolutionary trajectory of microvascular invasion in hepatocellular carcinoma from the perspective of tumor and circulating tumor DNA**……Chenhao Zhou*[1]、Jialei Weng[1]、Shaoqing Liu[1]、Qiang Zhou[1]、Xiaoqiang Zhu[2]、Ning Ren[1]

412. **Construction of a novel prognostic model of lung adenocarcinoma based on genes related to immunity and mitophagy**…...……..Di Zhu*[1]、Ting Huang[1]、Renyu Zhou[2]、Bo Yang[1]、Lilin Peng[1]、Lijuan Zhong[1]、Qianyuan Tian[1]、Yuanzhi Lu[1]

413. **Differences in serum cytokine levels between non-invasive and invasive lung adenocarcinoma**……..Bingjie Zeng 、Yueyang Qin、Xianzhao Wang、Lifang Ma*

414. **Lamprey Immunity Protein enables early detection and recurrence monitoring for bladder cancer through recognizing Neu5Gc-modified UMOD glycoprotein in urine**……..Hongming Teng*[2]、Qingwei Li[1]、Meng Gou[1]、Gang Liu[2]、Xu Cao[1]、Jiali Lu[1]、Yinglun Han[1]、Yang Yu[3]、Zhanfeng Gao[4]、Xiaoping Song[5]、Weijie Dong[2]、Yue Pang[1]

415. **Discovery and Validation of PARP4 DNA Methylation to Distinguish Malignant from Benign Thyroid Nodules**…….....……Mengxia Li[1]、Yifei Yin[2]、Hong Li[2]、Chenxia Jiang[3]、Rongxi Yang*[1]

416. **Prognostic Predictor and Immune Microenvironment Signatures of Aberrant Exon Skipping Events in Triple-Negative Breast Cancer**……..……Qingwang Chen*、Zehui Cao、Ruolan Zhang、Erfei Shang、Qiaochu Chen、Leming Shi、Yuanting Zheng

417. **Mitochondrial DNA Haplogroup M7: A Predictor of Poor Prognosis for Colorectal Cancer Patients in Chinese Population.** ……Zeyu Yan[1]、Qing Yuan[2]、Yiwei He[3]、Xianli He[1]、Qi Zhao[4]、Jinliang Xing[1]、Xu Guo*[1]

418. **Inactivation of adipose triglyceride lipase facilitates the proinflammatory response of nasopharyngeal carcinoma by modulating lipid droplets/PPAR-α signaling axis**……..…….Limei Li、Xiaoying Zhou*、Xue Xiao、Jun Zhao、Haishan Zhang

419. **Real-world clinical treatment outcomes in Chinese non-small cell lung cancer (NSCLC) with EGFR exon 20 insertion mutations(ex20ins)** ……..…CHAO SHI[1]、RU YUE XING[3]、MENG MENG LI[3]、JUN NAN FENG[1,2]、RUI SUN[1,2]、BING WEI[1,2]、YONG JUN GUO[1,2]、JIE MA[1,2]、HUI JUAN WANG*[3]

420. **CD105: Tumor diagnosis, prognostic marker and future tumor therapeutic target**……Lan Li*

421. **circRNF10 regulates tumorigenic properties and nature killer cell mediated cytotoxicity toward breast cancer via miR-934/PTEN/ PI3k-Akt axis**……..…Fei Liu、Baoen Shan、meixiang Sang*

422. **A comprehensive assessment of a newly designed non-exonic SNP-based NGS panel for HRD detection**……..……..Bing Wei[1]、JINXIANG ZHENG[1,2]、JUN LI[1,2]、ZHIZHONG WANG[1,2]、JIE MA*[1,2]

423. **PRPS1-mediated purine biosynthesis is critical for pluripotent stem cell survival and stemness**……xia huang*

424. **DAISM-DNNXMBD: Highly accurate cell type proportion estimation with in silico data augmentation and deep neural networks**……Yating Lin[1]、Haojun Li[1]、Xu Xiao[1,2]、Lei Zhang[3]、Kejia Wang[4]、Jingbo Zhao[5]、Minshu Wang[2,4]、Frank Zheng[5]、Minwei Zhang[6]、Wenxian Yang[7]、Jiahuai Han[2,3,8]、Rongshan Yu*[1,2,7]

425. **Multiplexed imaging mass cytometry reveals distinct tumor-immune microenvironments linked to immunotherapy responses in melanoma**……Xu Xiao[1]、Qian Guo[2]、Chuanliang Cui[2]、Yating Lin[1]、Lei Zhang[1]、Xin Ding[3]、Qiyuan Li[1]、Minshu Wang[1]、Wenxian Yang[4]、Yan Kong[2]、Rongshan Yu*[1,4]

426. **Molecular epidemiology and clinical characterization of human rhinoviruses circulating in Shanghai, 2012-2020**……Haixia Jiang*

427. **Cell surface vimentin as a novel biomarker and therapeutic target for advanced gastric cancer**……Heming Li 、Lu Xu、Mingfang Zhao*、Tao Han

428. **Specific vaginal and gut microbiomes of cervical cancer and a diagnostic value**……Mengzhen Han*

429. **Patients with Advanced Pancreatic & Biliary Cancer Appear More Vulnerable to SARS-CoV-2 Omicron Variant: An Observational Study during the COVID-19 Outbreak in Shanghai**……Heming Li [1]、Tao Han*[1]、Tingsong Chen[2]

430. **Lung abscess by Fusobacterium nucleatum and Streptococcus co-infection by metagenomic next-generation sequencing: a case series and review of the literature**……Na Wang[1,2]、Wenjie Han[1,2]、Mengzhen Han[1,2]、Tao Sun[1,2,3]、Junnan Xu*[1,2,3]

431. **DNA Methylation-Specific Analysis of G Protein Coupled Receptor-Related Genes in Pan-Cancer**……Mengyan Zhang、Jiyun Zhao、Yan Zhang*

432. **RAD21 Amplification Epigenetically Suppresses Interferon Signaling to Promote Immune Evasion in Ovarian Cancer**……peng deng、Jing Tan*

433. **Next-generation sequencing-based identification of EGFR and NOTCH2 complementary mutations in non-small cell lung cancer**……Lei Liu *

434. **A "one-stop shop" decision tree for diagnosing and phenotyping polycystic ovarian syndrome on serum metabolic fingerprints**……Ruimin Wang[1]、Lin Huang[1]、Kun Qian*[2]

435. **Diagnosis and prognosis of breast cancer by high-performance serum metabolic fingerprints**……Yida Huang、Kun Qian*

436. **The m6A demethylase ALKBH5 promotes tumor progression by inhibiting RIG-I expression and interferon alpha production through the IKKε/TBK1/IRF3 pathway in head and neck squamous cell carcinoma**……Hailong Ma*、Zhiyuan Zhang、Shufang Jin、Yue He、Jianjun Zhang

437. **Monitoring retinoblastoma by machine learning of aqueous humor metabolic fingerprinting**……Wanshan Liu、Kun Qian*

438. **Integrated Machine Learning and Bioinformatic Analyses Constructed a Tumor immune microenvironment -Related Classifier to Predict Prognosis and Immunotherapy Responses for Hepatocellular Carcinoma Patients**……Wangrui Liu*[1]、Tao Wang[1]、Jianfeng Xiang[1]、Jun Li[2]、Bo Zhai[1]

439. **Comprehensive characterization of alternative splicing in in hepatocellular carcinoma**……Shuai Zhao*[1]、Wangrui Liu[3]、Jun Li[2]、Jian Wang[1]

440. **A novel long noncoding RNA SP100-AS1 induces radioresistance of colorectal cancer via sponging miR-622 and stabilizing ATG3**……You Zhou、Jingting Jiang*

441. **N6-methyladenosine demethylase FTO promotes growth and metastasis of gastric cancer via m6A modification of caveolin-1 and metabolic regulation of mitochondrial dynamics**……You Zhou、Jingting Jiang*

442. **TRIM27 Is an Adverse Prognostic Biomarker and its Association with Immune and Molecular Profile in Right-sided Colon Cance**……Minghui Zhang[1,2,3,4]、Bowen Yang[1,2,3,4]、Lingyun Zhang[1,2,3,4]、Xiaoyu Guo[1,2,3,4]、Guangwei Zhang[5]、Xiaofang Che[1,2,3,4]、Ce Li[1,2,3,4]、Kezuo Hou[1,2,3,4]、Xiaojie Zhang[1,2,3,4]、Jinglei Qu[1,2,3,4]、Ti Wen[1,2,3,4]、Xiujuan Qu*[1,2,3,4]

443. **A copper-based biosensor for dual-mode glucose detection**……Xiaoyu Xu*

444. **Glaucoma characterization by machine learning of tear metabolic fingerprinting**……Jiao Wu、Kun Qian*

445. **Inhibiting ADRB2 signaling suppresses HCC chemoresistance by regulating HIF-1α expression**……Fuquan Wu、Zhiyu Cao*

446. **Plasmonic Alloys Reveal a Distinct Metabolic Phenotype of Early Gastric Cancer**……Haiyang Su*

447. **ADRB2 signaling promotes HCC progression and sorafenib resistance by inhibiting autophagic degradation of HIF1a**……Fuquan Wu、Zhiyu Cao*

448. **PRR15 deficiency facilitates malignant progression by mediating PI3K/AKT signalling and portends clinical efficacy and prognosis in triple-negative rather than non-triple-negative breast cancer**……Fengzhu Guo[1]、Jialu Ma[2]、Shuning Liu[1]、Chunxiao Li[1]、Jiani Wang[1]、Jinsong Wang[1]、Zhijun Li[1]、Cong Li[1]、Jingtong Zhai[1]、Fangzhou Sun[1]、Yantong Zhou[1]、Changyuan Guo[1]、Haili Qian[1]、Binghe Xu*[1]

449. **Study on novel fluorescent biosensors**……Yubin Zhou*、Junting Liang、Xiaoxian Zhu、Qing Zhou、Huizhi Chen

450. **Hierarchical magnetic nanoparticles for highly effective capture of small extracellular vesicles**……liang shi*

451. **mRNA sequencing and CyTOF analysis revealed ASPP2 altered the response patterns of hepatocellular carcinoma HepG2 cells to Usnic acid**……Yang Wang 、Liujia Chan、Yuheng Pang、Dexi Chen、Wenjing Wang*

452. **CD147 controls pancreatic cancer stem cell mitochondrial respiration and maintains stemness potentials via activating complex I core-subunit NDUFS1 mediated PAX2 demethylation**……樊新宇、李玲*

453. **Estrogen receptor response gene EGR3 mediates breast cancer cell resistance to tamoxifen through promoting MCL1 transcription_2**……Yu Xie*、Yue Wang、Junfang Qing、Mengci Yuan、Jing Yu

454. **A Four Oxidative Stress Gene Prognostic Model and Integrated Immunity-Analysis in Pancreatic Adenocarcinoma**……Hao Wang[1,2]、Tian Ruo-Fei[1]、Liang Xue[1]、Fan Jing[1]、Duan Zi-Chuan[1]、Fan Xin-Yu[1]、Zhang Jia-Jia[1]、Chen Zhi-Nan[1,2]、Yao Dong-Sheng[2]、Li Ling*[1]

455. **Circular RNA TAF4B Promotes Bladder Cancer Progression by Sponging miR-1298-5p and Regulating TGFA Expression**……Xiaofeng Li 、Qiu Wang、Ling Ji*

456. **Identification of the lipid metabolism related prognostic model in the Triple negative breast cancer**……yang jun、jun yang*

457. **NKD1 targets PCM1 to promote HHT therapeutic sensitivity of colorectal cancer via regulating cell cycle and apoptosis**……Jia Cao、Rong Ma、Jia Wang、libin Wang*

458. **Pan-cancer Analysis of magnesium-ITGAL and Its Positive Immune Effects in Head and Neck squamous cell carcinoma**……..……hanxuan yang、zongwei huang、ying li、sufang qiu*

459. **Reciprocal Regulation of ASPM and Foxm1 Amplifies the Oncogenic Progression in Human Hepatocellular Carcinoma**……..……Xunliang Jiang、Ke Wang、Jipeng Li*

460. **TransLnc: a comprehensive resource for translatable lncRNAs extends immunopeptidome**……Yongsheng Li*[1]、Dezhong Lv[2]、Zhenghong Chang[2]、Tao Pan[1]

461. **CCDC65, A Gene Knockout That Leads to Early Death of Mice, Acts as A Potentially Novel Tumor Suppressor in Lung Adenocarcinoma**……Ziyan Zhang、weiyi Fang*

462. **Chemically synthesized cinobufagin suppresses nasopharyngeal carcinoma metastasis by inducing ENKUR to stabilize p53 expression**……....Rentao Hou、Weiyi Fang*

463. **ENKUR expression induced by chemically synthesized cinobufotalin suppresses malignant activities of hepatocellular carcinoma by modulating β-catenin/c-Jun/MYH9/USP7/c-Myc axis**……Rentao Hou、Weiyi Fang*

464. **Targeting acetylcholine signaling modulates persistent drug tolerance in EGFR-mutant lung cancer and impedes tumor relapse**……Meng Nie、Na Chen、Zeping Hu*

465. **Evolutionary metabolic landscape from preneoplasia to invasive lung adenocarcinoma**……..Meng Nie、Ke Yao、Zeping Hu*

466. **N7-methylguanosine tRNA modification promotes esophageal squamous cell carcinoma tumorigenesis via the RPTOR/ULK1/autophagy axis**……..Hui Han、Shuibin Lin*

467. **Development and clinical validation of a novel microfluidic-based platform for CTC detection and downstream molecular analysis**……..Heng Zou、Yuan Wang、Wenchong Zhang、Tao Xu*

468. **Genome-wide CRISPR/Cas9 library screening identified critical drivers for cisplatin resistance in ESCC**……..Peipei Zhang、Weiguang Zhang、Junfei Jiang、Mingqiang Kang*

469. **Clinical and prognostic significance of perioperative change in red cell distribution width in patients with esophageal squamous cell carcinoma**……..……宋倩*

470. **Overexpression of PLCG1 is associated with Esophageal Squamous Cell Carcinoma (ESCC) Proliferation and Migration**……Weiguang Zhang*、Peipei Zhang、Junfei Jiang

471. **Super enhancer-driven genes-based identification of serum EFNA1 and MMP13 as potential biomarkers for early detection of esophageal squamous cell carcinoma**……..……Lingyu Chu[1,2]、hao chen[3]、wangkai Fang[2]、chaoqun Hong[1]、haiying Zou[2]、 yuhui Peng[1]、fangcai Wu[1]、yiwei Xu*[1]、jianjun Xie[2]

472. **LSD1-Demethylated LINC01134 Promotes Oxaliplatin Resistance by Facilitating SP1-mediated P62 Transcription in Hepatocellular Carcinoma**……Chunyuan Xue、Luyuan Ma、Nan Huo、Xiaofeng Kang、Zhong Chu、Xiaojie Xu*

473. **Cerebrospinal fluid circulating tumor DNA contributes to the detection and characterization of leptomeningeal metastasis in non-small cell lung cancer**……..……..Qian Miao*、gen lin、xinlong zheng、xiaobin zheng、longfeng zhang、kan jiang、biao wu、yiquan xu

474. **Liquid Biopsy for Predicting Postoperative Recurrence in Patients with Non-Small Cell Lung Cancer**……..Heng Zou、Chongwen Zhang、Yuan Wang、Tao Xu*

475. **PCMT1 has potential prognostic value and promotes cell growth and motility in breast cancer**……..……Yiwei Lin 、 Fangcai Wu 、 Yixuan Zhuang、Lingyu Chu、Tianyan Ding、Qiqi Qu、Xinhao Li、Yukun Cui、Chaoqun Hong*

476. **Prognostic value of lipid metabolism-related genes and serum ApoA1 in patients with NSCLC**……..……..……Ping Lu [1]、Lingyi Xiong[1]、Xinjun Liang*[2]

477. **Ferroptosis-related lncRNAs as prognostic signatures in cervical cancer**……Songtao Han[1]、Senyu Wang[2]、Yangchun Feng*[3]

478. **The diagnostic value of serum IGFBP1 in patients with colorectal cancer**……..Laifeng Wei*

479. **DNMT3B-mediated FAM111B methylation promotes papillary thyroid tumor glycolysis, growth and metastasis**……xiaofeng kang、Xiang Zhu、Chunyuan Xue、Nan Huo、Yuchen Han、Yimeng Du、Xiaojie Xu*

480. **microRNA-569 inhibits tumor metastasis in pancreatic cancer by directly targeting NUSAP1**……ce li、Xiujuan Qu*、Xiaohui Guo

481. **Systematic analysis of cuproptosis-related long non-coding RNA predicting prognosis in patients with lung squamous cell carcinoma**……Shanxiu Jin[1,2]、Cheng Du*[1]

482. **FERMT1 expression and correlated gene regulation in bladder urothelial carcinoma by bioinformatics analysis**……ce li、Xiujuan Qu*、Xiaohui Guo

483. **Identification of a Novel Tumor Mutation Burden and Major Histocompatibility Complex-Related Score to Predict Prognosis and Immunotherapy Response in Gastric Cancer**……Kanghui Xiang[1,2,3,4]、ti wen*[1,2,3,4]

484. **Construction and validation of an immune gene signature in esophageal cancer**……Jinhong Zhu*

485. **Bioinformatic analysis of lncRNA HAR1A and experimental validation**……Jinhong Zhu*

486. **ARA55 participates in TGFβ1-induced epithelial-mesenchymal transition in CNE2 nasopharyngeal carcinoma cells**……Zhaolei Cui、Yan Chen*

487. **Estrogen receptor response gene EGR3 mediates breast cancer cell resistance to tamoxifen through promoting MCL1 transcription_3**……Yu Xie*、Yue Wang、Junfang Qin、Mengci Yuan、Jing Yu

488. **A Pan-Cancer Landscape of IGF2BPs and Their Association with Prognosis, Stemness and Tumor Immune Microenviron-ment**……..Wei Shao、shoudu zhang、qian ding、qian xu*

489. **Dynamic risk profiling using blood indicators for severe myelosuppression after chemotherapy prediction in gastric cancer: An analysis from multi-center cohorts**……Bowen Yang[1]、Bo Jin[1]、Lingyu Fu[1]、Ying Liu[2]、Jie Zhang[3]、Jinghua Sun[4]、Ping Yu[1]、Jin Wang[1]、Xiaofang Che[1]、Yunpeng Liu[1]、Xiujuan Qu*[1]

490. **OSdream: an online prognostic and differential analysis tool for recurrence and metastasis of pan-cancer**……Huimin Li、Qiang Wang、Longxiang Xie、Lu Zhang、Xiangqian Guo*

491. **Hypoxia-related Markers Distinguish Oxygen Environment and Survival in Gliomas**……Weicheng Zheng*、Huangfeng Lin、Zhangying Zeng、Lei Qiao、Hailong Hao

492. **Discovery and clinical transformation of new subsets of liver cancer in China based on whole transcriptome sequencing**……Junjie Xu*[1]、Shi Jiang[2]、Xueyi Teng[3]、Chengchen Zhang[1]、Xiao Liang[1]、Xiujun Cai[1]

493. **A Comprehensive Evaluation and Identification of Novel Molecular Signature in Bladder Cancer**……王占旺[1]、金一[2]、何东[3]、朱煜星[1]、程雅新[1]、曹科*[1]

494. **Downregulation of POTEE inhibits cell growth, metastasis and cisplatin sensitivity of ovarian cancer cells, possibly via mediating actin polymerization**……Dan Yao、Xiaoqing Zhu*

495. **Identification and validation of a genomic mutation signature as a predictor for immunotherapy in NSCLC**……Zemin Wang、You Ge、Han Li、Pingmin Wei*

496. **Core transcription regulatory circuitry orchestrates the aberration of epigenetic and transcriptional patterns in triple-negative breast cancer**……Zhiying Xiong、Hui Zhi*

497. **BP180 is a Prognostic Factor in Head and Neck Squamous Cell Carcinoma**……Xue Meng[1,2,3,4]、MATSUMOTO FUMIHIKO[3]、TAISUKE MORI[2]、NAMI MIURA[2,4]、YOSHINORI INO[2]、KAORU ONIDANI[2]、KENYA KOBAYASHI[2]、YUSUKE MATSUZAKI[2,4]、SEIICHI YOSHIMOTO[2]、KATSUHISA IKEDA[3]、KAZUFUMI HONDA*[2,4]

498. **Proteomic analysis of small extracellular vesicles from the plasma of patients with hepatocellular carcinoma**……Wei Dong [1,2,3,4]、

Junfei Jin*[2,3,4]、Zeyu Xia[2,3,4]、Zehua Chai[2,3,4]、Zhidong Qiu[2,3,4]、Xuehong Wang[2,3,4]、Zebin Yang[2,3,4]、Junnan Wang[2,3,4]、Tingrui Zhang[2,3,4]、Qinqin Zhang[5]

499. **NAT10-mediated ac4C-mRNA modification promotes malignant progression and immunosuppression by reprogramming glycolytic metabolism in cervical cancer**……Xiaona Chen[1]、Yi Hao[2]、Quanwei Guo[1]、Sheng Zhong[1]、Tuotuo Chong[1]、Xiaomin Luo[1]、Keyi Ao[1]、Chichao Xia[1]、Minuo Yin[1]、Ming Ye[3]、Hui He[4]、Anwei Lu[1]、Yufei Long[1]、Jianjun Chen[5]、Xin Li[1]、Jian Zhang[6]、Xia Guo*[1]

500. **Trajectories of serum tumour marker impact on advanced-stage hepatocellular carcinoma outcomes after hepatic arterial infusion chemotherapy: A longitudinal, retrospective, multicentre, cohort study**……..Chao An *

501. **Hepatocyte-derived FGG-rich extracellular vesicles promote nasopharyngeal carcinoma lung metastasis through an IL6-related pre-metastatic microenvironment**……Kaiwen Zhang、Bo You、Yiwen You*

502. **PRDM16 serve as potential dignostic biomarkers in lung adenocarcinoma and down-regulated in tumor tissues and serum**…….……Meng Li、Anqi Li、Jiejun Zhou、Meng Fan、Mingwei Chen、Hui Ren*

503. **Comprehensive Analysis of 5-Methylcytosine Regulators in Adenocarcinoma of the pancreas**……Songlin Xing*

504. **Stiff cancer matrix reduces lenvatinib sensitivity of hepatocellular carcinoma through promoting mitophagy**……..Yunong Fu、Kunjin Wu、Kaibo Yang、Kai Qu*

505. **Development and Validation of a Prognostic Model Related to Pyroptosis-related Genes for Esophageal Squamous Cell Carcinoma Using Bioinformatics Analysis**……..……..……..……Weiguang Zhang、Peipei Zhang、Junfei Jiang、Kaiming Peng、Zhimin Shen、Mingqiang Kang*

506. **Diagnostic and Prognostic Potential of Circulating and Tissue BATF2 in Nasopharyngeal Carcinoma**……..……Zhaolei Cui、Yan Chen*

507. **Development of a diagnostic nomogram for intrahepatic cholangiocarcinoma**…..……..……..……..……..……Jiahua Liang[1]、Borui Xu[1]、Mingjian Ma[1]、Guangyan Zeng[2]、Zicheng Wang[1]、Li Huang*[1]

508. **The role of EphA7 methylation in the development of cervical cancer**……Wenfan Zhang、Shuang Chen、Jinhao Yang、Hongrun Zhao、Yuwei Liu、Zhuqing Sun、Rong Wang*

509. **Diagnostic and prognostic value of the cancer-testis antigen LDH-C4 in breast cancer**……Zhaolei Cui、Yan Chen*

510. **Diagnostic potential for circular RNAs in gastric carcinoma: A meta-analysis**……Zhaolei Cui、Yan Chen*

511. **Endogenous SARI induced cell apoptosis in nasopharyngeal carcinoma by targeting the intrinsic apoptotic pathway**……Zhaolei Cui、Yan Chen*

512. **Expression and Clinical Implications of Basic Leucine Zipper ATF-Like Transcription Factor 2 in Breast Cancer**……Zhaolei Cui、Yan Chen*

513. **Identification of Adriamycin Resistance Genes in Breast Cancer based on Microarray Data Analysis**……Zhaolei Cui、Yan Chen*

514. **Lactate Dehydrogenase C4 is associated with breast cancer prognosis and affects cancer cell proliferation and invasion**……Zhaolei Cui、Yan Chen*

515. **An ultrasensitive method for detecting short and rare cell-free DNA**……yu zhuang、feng shao*

516. **Performance of A PLK1-Based Immune Risk Model for Prognosis and Response Prediction of Breast Cancer**……Zhaolei Cui、Yan Chen*

517. **Plasma D-dimer and IL-6 associated with treatment response and progress free survival in advanced non-small cell lung cancer patients treated with anti-PD-1**……Chong Chen*

518. **Poor prognosis of stage I lung adenocarcinoma patients determined by elevated expression over pre/minimally invasive status of COL11A1 and THBS2 in the focal adhesion pathway**……Jun Shang、He Jiang、Leming Shi、Yuanting Zheng*

519. **Hypoxia related prognostic model based on four genes in gastric cancer**……Lina Wen*[1,2]、Zongqiang Han[3]

520. **The altered plasma metabolic profiles and its diagnostic potential for primary liver cancer**……Zhiying Liu*、Zhihang Zhou

521. **Differences of molecular events driving pathological and radiological progression of lung adenocarcinoma**……He Jiang、Jun Shang、Leming Shi、Yuanting Zheng*

522. **Co-expression and cooperation of RMP and IGF1r confers hypoxia induced metastasis of gastric cancer**……Wei Zhou、jingting jiang*

523. **PSMB7 induces M2-like TAM polarization and promotes immune infiltration and progression of lung adenocarcinoma**……Bingjie Zeng [1]、Dong Chenglai[2]、Zhou Hao [1]、Ma Lifang[1]、Wang Jiayi*[1]

524. **Comparison of Plasma and Serum miRNA Profiles by Small RNA Sequencing**……Haiyan Wang、Qingwang Chen、Naixin Zhang、Yaqing Liu、Wanwan Hou、Leming Shi、Yuanting Zheng*

525. **The role of circRUNX1 MDS-AML in the transformation process**……..邓发滑 [1]、韦四喜*[2]、胡华丽 [1]、王斯奇 [1]

526. **追踪线粒体 DNA 突变演变描绘卵巢癌转移**……徐智阳 [1]、周凯翔 [2]、王珍妮 [2]、刘洋 [2]、王兴国 [1]、高天 [1]、谢凡凡 [2]、袁晴 [2]、谷习文 [2]、刘淑娟 [1]、邢金良*[2]

527. **Cisplatin resistance-related multi-omics differences and the establishment of machine learning models**……Qihai Sui*

528. **Prognostic value of systemic immune-inflammation index in elderly patients with newly diagnosed colorectal cancers**……Chan Li[1]、Wei Tian[2]、Meng Li[1]、Ke Xie*[2]

529. **The Speckle-type POZ protein (SPOP) inhibits breast cancer malignancy by destabilizing TWIST1**……Chunli Wei、Junjiang Fu*、Xiaoyan Liu、Jingliang Cheng、Jiewen Fu

530. **The m6A demethylase ALKBH5-mediated upregulation of DDIT4-AS1 maintains pancreatic cancer stemness and suppresses chemosensitivity by activating the mTOR pathway**……Xiaomeng Liu、Bo Tang*

531. **HDAC11 Regulates Glycolysis through the LKB1/AMPK Signaling Pathway to Maintain Hepatocellular Carcinoma Stemness**……shiqian liu、bo tang*

532. **Long Non-Coding RNA LINC01572 Promotes Hepatocellular Carcinoma Progression via Sponging miR-195-5p to Enhance PFKFB4-Mediated Glycolysis and PI3K/AKT Activation**……Yudie Yang、Bo Tang*

533. **LINC00680 enhances hepatocellular carcinoma stemness behavior and chemoresistance by sponging miR-568 to upregulate AKT3**….haiqiang chen、bo tang*

534. **Study on the Correlation between Interleukin-27 and CXCL10 in Pulmonary Tuberculosis**……..……Jiahui Fan[1]、Yefeng Yang[2]、Liang Wang[3,4]、Xiaoqian Shang[1]、Li Zhang[4]、Hu Sun[4]、Yujie Ma[4]、Ying Li[3]、Jing Wang[2,3]、Xiumin Ma*[1,3]

535. **Cancer cell remodels myeloid-derived suppressor cell through TTLL12 activity to promote tumor progression**……Dongwen Chen、Peishan Hu、Chong Chen、Xinxin Huang、Shubiao Ye、Xiaojian Wu、Ping Lan*

536. **Exosomes from B7H3-CAR-T loaded with miR-145 and fluorouracil for targeted treatment of colorectal cancer**……Ruyue Yang、Dong Hu、Guidan Wang、Tingting Yang、Zhaoyi Wei、Gaofeng Liang*

537. **New star of therapeutic potential for liver cancer: exosomes derived from engineered liver cancer cells**……Dong Hu、Guidan Wang、Ruyue Yang、Tingting Yang、Zhaoyi Wei、Gaofeng Liang*

538. **Mesoporous magnetic nanoparticles linked aptamers were used to capture and detect exosomes**……..……..Guidan Wang、Ruyue Yang、Dong Hu、Tingting Yang、Zhaoyi Wei、Gaofeng Liang*

539. **VDR–SOX2 signaling promotes colorectal cancer s temness and malignancy in an acidic microenvironment**……Peishan Hu*、Dongwen Chen

540. **FDX1 as a cuproptosis-associated genes in diffuse large B-cell lymphoma-related biomarkers to guide clinical diagnosis, prognosis and therapy.** ……Ziyu Liu[1]、Nan Song[1]、Zhimin Wang[2]、Xiao Yang*[3]、Tianshu Gao[2]

541. **ANXA10 sensitizes MSI-H colorectal cancer to anti-PD-1 therapy via assembly of HLA-DR dimers** ……yiting sun、bowen yang、ce li、xiujuan qu*

542. **Tumor acidic microenvironment regulates malignant progression of colorectal cancer through SLC26A3-HuR/CUGBP1 axis**……Chong Chen*

543. **Tumor-associated macrophages promote gastric cancer progression via secreting IL-13 to activate the JAK-STAT3 axis**.....Xinxin Huang、Yufeng Chen、Peishan Hu*

544. **A Novel Proteogenomic Integration Strategy Expands the Breadth of Neo-Epitope Sources**……Xuan Dong*、Haitao Xiang、Fanyu Bu、Xiangyu Guan、Yuntong Zhao、Weicong Zhang、Yijian Li、Ying Gu

壁报交流

545. **曲美他嗪联合琥珀酸美托洛尔缓释片快速控制长期频发室性早搏一例**……徐汉友*

546. **高尿酸血症可能诱发运动性哮喘，救治成功中学生运动性哮喘一例**……徐汉友*

547. **急性酒精中毒及其他类中毒的 120 急诊医疗服务病例分析**……徐汉友*

548. **清开灵注射液联合生脉注射液或参麦注射液救治新型冠状病毒感染性肺炎**……徐汉友*

549. **其他铂类对比顺铂治疗局部晚期鼻咽癌的疗效和安全性的 Meta 分析**……李芷茹*、李超

550. **趋化因子 CXCL9、10、11 及 CXCR3 在晚期 NSCLC 患者免疫治疗监测中的临床意义**……朱晓斌*、朱敏、苏璇、张俊萍

551. **双硫仑联合铜通过靶向 NPL4 通路发挥抗胃癌作用的机制研究**……刘瑶*、郑振东、杜成、王美玲、王乃雪、陈禹潼、李宝磊、傅方伟、徐竹轩

552. **血清 HE4 在卵巢癌预后监测中的应用价值研究**……冉盼盼*

553. **血清 PGI、PGII及 PGR 结果反映胃黏膜状态的研究**……冉盼盼*

554. **构建“图灵图案”和纳米颗粒组成的智能水凝胶用于循环肿瘤细胞的捕获、培养和分析鉴定**……陈东亮*、杨大伟、任天莹

555. **LIPI 评分对 PD-1 抑制剂治疗的晚期胰腺癌患者预后的预测价值**……陈诗韵*、谭招丽、戴广海

556. **基于糖基转移酶基因的神经母细胞瘤预后模型的构建及功能分析**…沙永亮*、赵强

557. **EBV 通过增强干性和 EMT 促进休眠癌细胞的 VM 形成**……程天仪*、纪妍、游波

558. **MIR-1246 通过抑制巨自噬且促进分子伴侣介导的自噬共同促进鼻咽癌的恶性表型**……张盼盼*、雷伟、顾苗

559. **非小细胞肺癌免疫治疗生物标志物的研究进展**……刘兆喆*、陈潞君、谢晓冬

560. 阿司匹林协同吉西他滨抑制胆囊癌 GBC-SD 细胞生长的机制研究……罗凯*、张旭东、刘中原、王向坤、李仁锋

561. LCBP 风险评估模型在肺结节危险分层的临床应用……武曼*[1]、冯飞雪[1]、马艳侠[2]

562. TFF3 靶向抑制剂 AMPC 联合多西他赛在治疗他莫昔芬耐药乳腺癌中应用……郭慧*

563. CA19-9 和 CEA 联合检测在胆囊癌辅助诊断中的应用价值……宋少敏*、渠文涛

564. 晚期上皮性卵巢癌患者术前炎症指标联合 CA125、HE4 对肿瘤细胞减灭术满意度的预测价值……祖逸峥*[1]、哈春芳[2]

565. 血清 CA125 在心衰检测的临床意义研究……吴小田*

566. 标本前处理对 CEA 测定结果的影响……吴小田*

567. PGE2 与 COX-2 通过正反馈环促进结肠癌发生的研究进展……魏思桐*

568. 多指标联合血浆 ctDNA 中 HOXA7、SOX17 甲基化在肺结节早诊中的临床应用研究……冯飞雪*

569. 径向超声联合快速现场评估在肺外周病变的诊断价值……徐春华*

570. 生物钟基因 BMAL1 通过抑制 TGF-β1/Smads 通路在鼻咽癌增殖、转移中的作用和机制研究……赵朝芬*[1,2]、金风[1,2]、龙金华[1,2]、刘丽娜[1,2]、贺前勇[1,2]、李卓玲[1,2]、陈越[1,2]、黎钰欣[1,2]、徐歆宇[1,2]、周定安[1]

571. 晚期 HER-2 阳性乳腺癌原发灶与转移灶异质性研究……王慧*、张咪、杨姣、王凡、董丹凤、杨谨

572. 肿瘤来源的血清外泌体 miR-4321 作为非小细胞肺癌的诊断生物标志物……张哲*、谢丽

573. 内源性谷氨酸在 ADCY10 依赖条件下抑制 YAP 决定肺腺癌的铁死亡敏感性……张骁*

574. 外泌体传递的 miR-7 通过靶向 YAP 在非小细胞肺癌中逆转吉非替尼耐药……张骁*

575. 外泌体和 circRNA_101093 在肺腺癌铁死亡脱敏中的重要作用……张骁*

576. 肝癌血清标志物 NRP1 诊断价值研究……张骁*

577. TFCP2/YAP 转录复合体调控蛋白 CPE 对肝癌诊断价值研究……张聪聪*

578. Bcl-2-938 C>A 多态性与癌症发病及预后的关系……张聪聪*

579. Hippo/YAP 信号通路调控蛋白 ACAN 诊断价值研究……张聪聪*

580. **血浆外泌体 miR-320d 作为卵巢癌的新型肿瘤标志物**……王世文*、宋兴国、谢丽、宋现让

581. **基于 PBMC 高通量测序数据探讨原发性肝癌免疫相关生物标志物**……胡锐*、周小舟

582. **靶向 system XC-的 SLC3A2 亚基对于 m6A 阅读器 YTHDC2 成为肺腺癌的内源性铁死亡诱导剂至关重要**……马丽芳*、王佳谊

583. **基于活检组织在临床根治性放化疗队列中构建食管鳞癌放化疗敏感性多分子预测模型**……李植茂*[1,2]、黄河澄[2]、陈旭丽[2]、吴文智[1]、许秀娥[1]、郑雅琪[1]、王少洪[2]、许丽艳[1]、李恩民[1]

584. **食管鳞癌及癌前病变分子标志物的发现及联合诊断模型效能验证的研究**……郑雅琪*[1]、黄海花[2]、许秀娥[1]、李植茂[1]、楚曼宇[1]、于帅霞[1]、刘伟[3]、李恩民[1]、许丽艳[1]

585. **基于自噬相关基因构建 TP53 突变多发性骨髓瘤预后模型及免疫浸润细胞景观图谱**……郑焱华*[1,2,3]、高广勋[4]

586. **应用同步放化疗对隐匿性宫颈癌进行补救治疗的临床研究**……李芷茹*、李超

587. **红细胞分布宽度、中性粒细胞与淋巴细胞比值、癌胚抗原、糖类抗原 19-9 联合检测对胃癌诊断和分期的价值**……张华洋*

588. **APRI 评分与 HBV 相关肝细胞癌切除术患者预后的关联研究**……周运香*

589. **超级增强子区域遗传变异与 HBV 相关肝细胞癌术后生存期的关联分析**……韦雪艳*

590. **早期髓系来源抑制细胞通过下调 ARID1A 表达促进 luminal A 型乳腺癌上皮间充质转化过程**……陈桂冬*、李星晨、纪辰燕、刘芃芃、于津浦

591. **中国卵巢癌 DNA 损伤修复基因突变图谱分析**……叶英楠*、王珂、董莉、程亚楠、韩雷、张蕊、于津浦

592. **沙棘对人乳腺癌 MCF-7 细胞增殖、迁移、凋亡、周期的影响**……黄聪玲*

593. **肿瘤内微生物异质性影响肝癌肿瘤免疫微环境及其临床预后**……李胜男*[1,2]、宋天强[1]、徐亮[1]、于津浦[1]、陆伟[1]

594. **辛伐他汀联合贝伐珠单抗通过 HIF-1α-Wnt/β-catenin 通路抑制肺腺癌 A549 细胞增殖、迁移及侵袭并促进其凋亡**……涂昕*、青措、徐智

595. **ATP8B1 低表达通过胆碱代谢引发氧化还原高水平促进肺鳞癌发生发展**……张蕊*、张晓、刘芃芃、于津浦

596. **血管生成基因预测食管鳞癌患者预后和免疫特性:证据来自多组学分析和实验验证**……王帅元*[1]、梁英豪[2]、张嘉欣[1]、王文佳[1]、洪铱辰[2]、孙淼淼[1]、舒姣[1]、陈奎生[1]

597. **线粒体 DNA 基因组不稳定性在肝细胞癌中的研究进展**……刘秋龙[2]、邢金良[1]、高一钊[2]、王珍妮[1]、周凯翔[1]、张召辉[3]、周峰[3]、郭旭[1]

598. **白蛋白-球蛋白评分和肌少症联合指标预测接受腹腔镜肾切除术肾细胞癌患者的预后情况**……毛卫浦*、陈明

599. **七种肺癌相关抗体联合检测模型在肺结节诊断中的价值研究**……赖良、冯阳春*

600. **血浆外泌体 miR-44588 可以作为非小细胞肺癌的新型标志物**……吴亚雯*[1]、谢丽[2]、宋兴国[2]

601. **血浆外泌体 tRF-Asn-GTT-010 可以作为一种新型的 NSCLC 诊断生物标志物**……郑白冰*、宋兴国、谢丽

602. **血浆外泌体 tRF-Leu-TAA-005 作为非小细胞肺癌的新型诊断标志物**……李蕾*、郑白冰、宋兴国、谢丽

603. **肿瘤教育血小板 snoRA68 作为食管癌新型标志物的研究**……赵漩*、张倩茹

604. **乳腺癌前哨淋巴结超声造影识别影响因素的 logistic 回归分析**……骆云皓*[1,2]、罗俊[2]、曹文斌[2]、陈琴[2]、赵玮[1]、吴昊[2]、李超男[4]、刘瑜妍[3]

605. **eIF2α的磷酸化减轻急性肝损伤中的内质网应激和肝细胞坏死**……徐畅*

606. **环状 RNA circRNA_0072387 通过调节 miR-490/HDAC2 轴促进肝母细胞瘤进展**……徐畅*、孙奋勇

607. **智能响应型 DNA 纳米器件用于体内肿瘤相关 miRNA 的抗干扰成像**……陈天舒*

608. **《醛酮还原酶 1B10 测定试剂盒》经大规模多中心临床研究验证并获国家药监局三类诊断试剂注册批文**……窦亚玲*[1]、曹德良[2]、曹友德[3]、刘康龙[2]、曹哲[4]

609. **血清 PGI、PGII、G-17 联合检测在慢性萎缩性胃炎诊断中的研究价值**……李彦红*、许粉娟、蔡小冉

610. **肝癌干细胞标志物的研究进展和临床治疗意义**……徐韵*、贾永峰、刘霞

631. **PRMT1-MLXIP 蛋白复合体通过β-Catenin 信号通路促进胃癌细胞增殖和迁移的机制研究**……王锋*、周旭军、陈施彤

632. **一种新型宫颈癌前病变分子标志物及其应用**……崔倩文*、杨武林

633. **Let-7c-5p 靶向调控 CTHRC1 抑制食管鳞状细胞癌进展的研究**……郑雅心*[1]、张键[3]、黄春梅[1]、方霖[1]、康敏[2]

634. **乳腺癌合并直肠癌 1 例并文献复习**……于少雨、简亿*、朱梅、包宇航、杨美、郭敏、谢仟、胡晓倩

635. **人工智能在乳腺癌 HER2 IHC 0 和 1+准确判读中的作用**……吴偲*、岳萌、刘月平

636. **使用全幻灯片图像自动评估提高 Ki67 评分的一致性及预后分析**……蔡丽静*、刘月平

637. **基于 WSI 图像的人工智能模型提高三阴性乳腺癌 PD-L1 CPS 的精准判读**……李金泽*、王心然、刘月平

638. **TAE 序贯奥沙利铂+雷替曲塞联合安罗替尼二线治疗中晚期原发性肝癌的临床研究**……韩朝稳*、梁秀群、沈永奇、李凯旋、康中强、何沙

639. **微小膜壳缘虫感染对 ICR 小鼠小肠干细胞相关基因 mRNA 表达的影响**……杨汉蕾*

640. **DUOX1 基因在鼻咽癌中转录失活的研究**……张海山*

641. **新型快速高通量融合检测技术的开发与验证**……孙瑞[1,2]、王志中[1,2]、刘红霞[1,2]、马杰*[1,2]

642. **hnRNPM 细胞核亚定位调控可变剪接及肿瘤转移**……郭佳维、李科、明月、潘怡潼、刘文荣、沈舒、徐富滟、刘宇、程健、王瑾、王成弟、戴伦治、李为民、彭勇*

643. **灌洗液样本可作为基因检测的有效来源**……张成娟[1]、吴新新[2,3]、吴敏清[1]、常玉喜[2,3]、魏冰[2,3]、马杰*[2,3]

644. **miR-19a-3p/CDS1/ 脂滴 /NF-κB 信号通路轴对鼻咽癌炎症反应的影响**……周晓莹*、王怡方

645. **自主神经在口腔黏膜癌变及防治中的作用**……陈倩[1,2]、江涵[1,3]、神应强*[1]

646. **羰基化合物：一类新型肺癌诊断标志物**……张沫[1]、赖治臻[1]、张仁俊[1]、刘帅[1]、田洪涛[1]、李丹[1]、周江[2]、李智立*[1]

647. **HIGD1A 的表观遗传失活促进肾透明细胞癌转移的研究**……赵军*

648. **泛癌的蛋白糖基化修饰标志物研究**……赖治臻[1]、王志刚[1]、张继匀[1]、袁钟浩[1]、李丹[1]、徐雅莉[3]、张丹[1]、李娜[1]、周江[2]、李智立*[1]

649. **PSMB1 在 II/III 期结直肠癌复发转移中的作用及其机制研究**……蒋雪飞、刘依婷、冯杏芝、高倩玲、杨兰兰、龙家慧、杨孜欢*

650. **跨人群研究肺癌筛查中特征的肠道微生物标志物及评估其诊断效能**……韩文婕[1]、王娜[1]、韩梦真[1]、孙涛[2]、徐君南*[2]

651. **基于蛋白质糖基化修饰的肝癌诊断研究**……张继匀[1]、赖治臻[1]、丁锐[3]、袁钟浩[1]、周巾煜[2]、李丹[2]、秦绪珍[3]、周江[4]、李智立*[2]

652. **循环肿瘤细胞异倍体检测在鼻咽癌患者治疗和 预后中的临床意义**……汪玉兰[1,2]、程进[2]、黄倩*[2]

653. **原发性肺弥漫大 B 细胞淋巴瘤 1 例并文献复习**……简亿、于少雨*、朱梅、包宇航、杨美、余枝娟、胡晓倩、路庚辛

654. **急性淋巴细胞白血病化疗中诱发肺结核活动 1 例**……朱梅、包宇航、袁亚婷、黄敏、李小鹏、于少雨、杨美、简亿*

655. **原位突变检测新策略及其在肿瘤精准治疗中的应用研究**……汪慧聪、牛霞、郑直*

656. **氨基酸类代谢物：一类新型肺癌诊断标志物**……田洪涛[1]、仇宇明[1]、赖治臻[1]、张沫[1]、刘帅[1]、张仁俊[1]、李丹[1]、周江[2]、李智立*[1]

657. **肿瘤干细胞来源外泌体分离鉴定及表达特征分析**……产柳佳、王文敬*、王阳

658. **合并骨髓转移及弥散性血管内凝血的胃癌病人的临床病理特征及治疗**……杜格、曹泰源、翟晓慧、练磊、杨祖立、肖健*

659. **一种基于尿液 DNA 低深度全基因组甲基化测序的尿路上皮癌早期诊断和复发监测的新方法研究**……史悦、王平、慈维敏*

660. **基于全转录组测序的中国肝癌新亚群发现与临床转化研究**……徐俊杰*[1]、姜是[2]、滕学奕[3]、张程晨[1]、梁霄[1]、蔡秀军[1]

661. **基于相对表达秩序关系的差异基因识别算法 RankCompV3**……严婧、曾秋红、王先龙*

662. **基于肠道大肠杆菌及其代谢物靶基因构建胰腺癌特异性预后相关 mRNA-miRNA-lncRNA 三元调控网络**……曹舒清*[1]、郭晨洁[2]、陈梦[2]、张钰婧[3]、贾天琪[4]、张潇月[2]

663. **基于空间转录组学研究造釉型颅咽管瘤的异质性**……涂志伟[1]、王先龙*[1]、赵传[2]、林志雄[2]、林金城[1]、张恩[1]

699. 基于高效液相色谱-质谱联用(HPLC-MS)技术的血浆代谢组学在早期胃癌诊断中的应用研究……王峰[1]、庞瑞芳[2]、尹玉新[2]、戎龙*[1]

700. alstonine 通过 AMPK 活化和 PGC-1α/TFAM 上调抑制小鼠体外骨肉瘤细胞增殖和体内肿瘤生长……严沁*

701. 56℃灭活 30min 对糖类抗原 CA242、CA19-9 和 CA50 检测结果的影响……史琦、韩冉冉、渠文涛、史小芹

702. S100 β蛋白在脑梗死和脑出血患者中的诊断价值研究……张绿萍、渠文涛

703. 联合放射组学评分和液体活检的恶性肺结节诊断预测多维度模型……许露、朱晓莉

704. TPP1 介导的 DDR 及其下游信号通路在食管癌中的分子机制研究……文继林[1,2]、徐磊[2]、钟晓武[1,2]、郭晓兰[1,2]、方莉[1,2]

705. 基于生物信息学分析 Shelterin 在食管癌中表达及免疫浸润的临床意义……杨密渊[1,2]、钟晓武[1,2]、高川力[1,2]、袁梓纯[1,2]、王琴[1,2]、徐磊[1]、马强[1,2]、郭晓兰[1,2]

706. KDM4B 对胶质母细胞瘤细胞增殖影响的初步研究……王忠泽、李泽昆、孙伟、赵二虎、崔红娟

707. 基于转运 RNA 及其来源片段表达谱分析探讨乳腺癌细胞耐药机制……莫冬萍、严枫

708. 皮下瘤切除与否尿液蛋白质组的变化……高友鹤、衡姊琦

709. 新型血栓标志物对恶性肿瘤患者围手术期并发 VTE 的预警效能……张金彪[1]、曹蕾[1]、马飞[1]、代荣琴[2]

710. 血浆热休克蛋白 90α对胰腺癌诊断的临床意义……陈佳祺

711. 肿瘤相关巨噬细胞代谢基因预测卵巢癌预后价值的研究……李泽、田菁、任丽

712. FoxQ1 在结直肠癌同期放化疗抵抗中的作用机制研究……刘艳艳、蒋永新、刘珊、安倩、范雪梅

713. 肺癌组织来源外泌体的蛋白质组学研究……纪东瑞、张庆华

714. 阴沟肠杆菌促进肺上皮间充质转化促进肺癌增殖转移……林鑫、孙轶华

715. 长链非编码 RNA LINC AC008063.3 在头颈鳞癌中的生物学功能及临床意义……买尔哈巴·米吉提[1,2]、郑希望[1,2]、田然[1,2]、郭庆博[1,2]、董阳洋[1,2]、吴勇延[3]、高伟[3]

784. **Exploration of tumor-infiltrating immune cells on the prognosis of endometrial cancer**……Jiayi Zhou[2]、Jing He[1]、Yueming Zhang[1]、Qiao Gu[3]、Wenjie Hou[1]

785. **The circular RNA, circRARS, promotes aerobic glycolysis of non-small cell lung cancer by binding with LDHA**……Haoran Li[1]、Qi Huang[2]、Haifa Guo[3]、Xiao Li[1]、Mantang Qiu[1]

786. **Identification of a 5-microRNA prognostic signature of patients with chromophobe renal cell carcinoma**……Ziwei Liu[1,2]、Huiying Liang[1,2]

787. **Age-associated HAT1 expression instigates tumor heterogeneity and morphology in esophageal squamous cell carcinoma through the E2F transcription factor**…… Yuefeng Wu[1,2,3]、Bin Jiang[1]、Qi Wang[1]、Chuanqiang Wu[1]、Ming Wu[1]、Hai Song[1,2]

788. **Heterogeneous distribution pattern of CD3+ tumor-infiltrated lymphocytes (TILs) and high combined positive score (CPS) favored the prognosis of resected early stage small-cell lung cancer**……Ying Jin [1,2,3]、Liang Zhu[1,2]、Guoping Cheng[1,2]、Meijuan Wu[1,2]、Ming Chen[4]

789. **A Nomogram for Predicting Survival in Breast Infiltrating Duct Carcinoma Patients With Brain Metastasis: A Population-Based Study**…….. Hongna Sun、Jun nan Xu、Tao Sun

790. **Pan-cancer Analysis of LINC02535 and Its Oncogenic Role in Lung Adenocarcinoma**……Shuang Dai、Feng Luo

791. **Novel blood-based FUT7 DNA methylation is associated with lung cancer：especially for lung squamous cell carcinoma**……Yifei Fang[1]、Yunhui Qu[2]、Longtao Ji[3,4,5]、Hao S[6]、Jiaqi Li[4,5]、Yutong Zhao[3,5]、Feifei Liang[3,4,5]、Zhi Wang[3,4,5]、Jiao Su[1]、Liping Dai[3,4,5]、Songyun Ouyang[1]

792. **Perspectives for immunotherapy of EBV-associated GLELC: A relatively "hot" tumor microenvironment**……雷艳娜、刘明

793. **Survival Benefit of Radiation Therapy for Pancreatic Ductal Adenocarcinoma with Liver Metastases: A Propensity Score-Matched Study**……Liyou Lian[1]、Shuwen Cheng[5]、Rujie Zheng[3]、Hongxia Yao[1]、Tianhui Chen[2]、Jinfei Chen[4]

794. **NTF4 exerts dual roles via ANXA1 pathway in breast cancer progression**……Ran Sun[1,2]、Jin He[1]、Yijia Gong[1]、Yijiao Ning[1]、Chaoqun Deng[1]、Kexin Sun[1]、Mingjun Zhang[2]、Zhaobo Cheng[3]、Qin Xiang[1]、Xin Le[1]、Yongzhong Wu[3]、Tingxiu Xiang[1,3]

795. **Plasma autoantibodies IgG and IgM to PD1/PDL1 as potential biomarkers and risk factors of lung cancer**……Jiaqi Li、Man Liu、Xue Zhang、Longtao Ji、Ting Yang、Yutong Zhao、Zhi Wang、Feifei Liang、Liping Dai

796. **KLF15 suppresses tumor growth and metastasis in Triple-Negative Breast Cancer by downregulating CCL2 and CCL7**……Xin Le[1]、Quist Kanyomse[1]、Jun Tang[1]、Fengsheng Dai[1]、Youchaou Mobet[2]、Chang Chen[2]、Zhaobo Cheng[1]、Chaoqun Deng[1]、Yijiao Ning[1]、Renjie Yu[1]、Xiaohua Zeng [3]、Tingxiu Xiang[3]

797. **Establishment of Differential Model for NSCLC and Benign Pulmonary Nodules Based on Serum miRNAs**……Man Liu[1,3]、Jiaqi Li[1]、Longtao Ji[1]、Fenghui Liu[2]、Songyun Ouyang[2]、Yutong Zhao[1]、Zhi Wang[1]、Feifei Liang[1]、Liping Dai[1]

798. **Construction of lncRNA TYMSOS/hsa-miR-101-3p/CEP55 and TYMSOS/hsa-miR-195-5p/CHEK1 axis in non-small cell lung cancer**……Longtao Ji[1,2,3]、Jiaqi Li[2,3]、Feifei Liang[1,2,3]、Zhi Wang[1,2,3]、Yutong Zhao[2,3]、Fengqi Chen[2,3]、Yutong Li[1,2,3]、Liping Dai[1,2,3]

799. **BAP29 suppresses metastasis in triple negative breast cancer by inhibiting NOTCH pathway**……hefen sun、wei jin

800. **Differential Model Based on Novel Plasma Protein Markers for Lung Adenocarcinoma and Benign Pulmonary Nodules**……Yutong Zhao、Xue Zhang、Jiaqi Li、Longtao Ji、Zhi Wang、Feifei Liang、Liping Dai

801. **Potentially functional variants of MAP3K14 in the NF-κB signaling pathway genes predict survival of HBV-related hepatocellular carcinoma patients**……黄琼广

802. **Bioinformatics analysis and validation of the development and prognosis role of lnc-RAB11B-AS1 in hepatocellular carcinoma**……Xiangzhi Hu[1]、Dedong Wang[1,2]、Jinbin Chen[3]、Boheng Liang[2,4]、Pengzhe Qin[2,4]、Di Wu[2,4]

803. **Plasma D-dimer and IL-6 associated with treatment response and progress free survival in advanced non-small cell lung cancer patients treated with anti-PD-1 therapy**……..……Chong Chen

804. **MiRNA-625-3p promotes cell proliferation and metastasis of lung adenocarcinoma by targeting KLF9**……Zhi Wang[1,2,3]、Longtao Ji[1,2,3]、Feifei Liang[1,2,3]、Jiaqi Li[2,3]、Yutong Zhao[2,3]、Yutong Li[1,2,3]、Fengqi Chen[2,3]、Liping Dai[1,2,3]

805. **Potential Unreliability of ALK variant allele frequency in the efficacy prediction of targeted therapy in NSCLC**……Weihua Li、Wei Rao、Jianming Ying

806. **Reviewing the pathophysiological relationship between gut microbiota and depression to explore the optimal therapeutic pathway**……徐君南、韩文婕、孙涛

807. **Integrated proteomic analysis of human plasma and tumor tissue for liver cancer biomarker discovery**……..……Zuoliang Dong[1]、Li Ren[2]

808. **A positive feedback loop between ID3 and PPARγ via DNA damage repair regulates the efficacy of radiotherapy for rectal cancer**……..……Chuanzhong Huang、Ling Wang、Wankai Fu、Junxin Wu、Yunbin Ye

809. **Piezo1 protein affects the proliferation, cycle and apoptosis of esophageal squamous cell carcinoma through the p53 signaling pathway**……..……Lulu Wang[1]、Guanglei Chang[1]、Zhaobin Xu[1]、Miaomiao Yang[2]、Liguo Zhang[1]

810. **Mir-421 and Mir-550a-1 are Potential Prognostic Markers in Esophageal Adenocarcinoma**…….....……Guanglei Chang[1,2,3]、Lulu Wang[1,2,3]、Miaomiao Yang[4]、Zhaobin Xu[1,2,3]、Liguo Zhang[1,2,3]

811. **Peripheral Blood Markers Predictive of Outcome in Upper Gastrointestinal Cancers Patients Treated with Immune Checkpoint Inhibitors**……..……Peiwei Wang、Jia Feng、Xue Cui、Yao Jin、Zexi Xu、Xinyi Chen、Jiayan Wei、Jinsong Wang、Yiming Weng、Min Peng

812. **ENKUR expression induced by chemically synthesized cinobufotalin suppresses malignant activities of hepatocellular carcinoma by modulating β-catenin/c-Jun/MYH9/USP7/c-Myc axis**……Rentao Hou、Weiyi Fang

813. **Experimental study of interference with calcitonin assay**……..…..…Yixian Liu、Xiaofang Zhang、Zouliang Dong

814. **Systematic analysis of cuproptosis-related long non-coding RNA predicting prognosis in patients with lung squamous cell carcinoma**……Shanxiu Jin[1,2]、Cheng Du[2]

815. **ZNF503 combined with GATA3 is a prognostic factor in triple-negative breast cancer**……Siyu Liu、Jingjing Liu

816. **Antitumor effects of dictyophora polysaccharide against lung cancer by inhibiting recruitment of MDSCs**……xiaohong wang

817. **SLC7A5 promotes chemotherapy resistance of cervical cancer by mediating glutamine metabolism through ASNS**……Lei Tang、Jian-Zhong He、ye Liu、Fa-Min Zeng

818. **A Nomogram for Predicting Survival in patients with Unresectable Hepatocellular Carcinoma treated with intensity modulated radiotherapy**……Meiying Long[1]、Jianxu Li[2]、Moqin Qiu[3]、Meiying He[2]、Jialin Qiu[4]、Yingchun Li[4]、Hongping Yu[4]

819. **Cancer SLC6A6-Mediated Taurine Uptake Impairs CD8+ T Cell Antitumor Immunity via Regulating Immune Checkpoints**……Tianyu Cao、Qi Wang、Wenyao Zhang、Yuanyuan Lu、Daiming Fan、Yongzhan Nie、xiaodi Zhao

820. **Identification of gut microbial markers for diagnosis across populations in early lung cancer**……Junnan Xu、mengzhen Han、Tao Sun

821. **Dynamic changes of vaginal flora during cervical carcinogenesis and clinical potential of vaginal and gut microbes as diagnostic tools for cervical cancer**……Junnan Xu、mengzhen Han、Tao Sun

822. **The peripheral blood CD4+ T cells/platelets can be used as indicator for prognosis of patients with metastatic/recurrent breast cancer**……Xiaorui Li[1]、Yiwen Ma[1]、Shisheng Wang[2]、Tao Sun[1]

823. **The Oleanolic Acid Derivative ZQL-3d Exerts Anticancer Effects via miR-221-3p/ASPP2 and Modulates Trastuzumab Resistance in Breast Cancer**……Xiaorui Li[1]、Yiwen Ma[1]、Tao Sun[1]、Shisheng Wang[2]

824. **Necroptosis-related lncRNAs and Hepatocellular Carcinoma Undoubtedly Secret**……Keran Sun[1]、Xiaobing Chen[1]、Jingyuan Ning[2]、Lin Wei[2]

825. **Prognostic models for stomach adenocarcinoma patients based on hypoxia related long non code RNAs**……..……Lina Wen[1]、Zongqiang Han[2]

826. **Association of Genetic Variants of the Glycogen Metabolism Pathway with Risk of HBV-Related Hepatocellular Carcinoma**……Yang Zuo[1]、Yingchun Liu[1]、Guanqiao Jin[1]、Xueyan Wei[2]、Shicheng Zhan[2]、Junjie Wei[2]、Hongping Yu[1]

827. **Performance of A PLK1-Based Immune Risk Model for Prognosis and Response Prediction of Breast Cancer**……..……Zhaolei Cui

828. **Diagnostic performance and efficacy evaluation of NSE and CA125 in sarcomas**……Limei Min、Yuchen Ge、Hanxi Zhang、Wu Sun、Siyi Tan、Luxin Xue、Qin Wang、Zhijun Jia、Jie Shen、Baorui Liu、Xiaolu Wang、Rutian Li

829. **人类组蛋白修饰数据库 2.0**……..……..王洪利

830. **Prognostic of gastric cancer based on DNA methylation- driven EMT genes**……Te Ma

831. **Multi-Omics Integration Collective Variational Autoencoder for cancer-drug Sensitivity Prediction**……..…Cong Wang、yan zhang

832. **Acquired EGFR exon 19 deletion as a resistance mechanism to BRAF/MRK inhibition in BRAF V600E-mutant NSCLC** ……..…fang wu、yuxuan liu、yue zeng、yurong peng、yue pan、yizheng li

833. **Overexpression of ErbB3 promotes metastasis of ErbB2-positive breast cancer and its underlying molecular mechanisms**……Ruxue Jia、Zhuolin Li、Yating Wu、Huimin Niu、Xiaofeng Lai、Meng Zhao、Shenghang Zhang、Shuiliang Wang

834. **Mesenchymal stem cell promotes metastasis of bladder cancer with co-expression of ErbB2 and ErbB3 mainly via paracrine of NRG-1**……Zhuolin Li、Ruxue Jia、Yating Wu、Huimin Niu、Xiaofeng Lai、Jin Chen、Meng Zhao、Shenghang Zhang、Shuiliang Wang

835. **Long noncoding RNA lnc-POP1-1 upregulated by VN1R5 promotes cisplatin resistance in head and neck squamous cell carcinoma through interaction with MCM5**……Yingying Jiang 1、Wantao Chen2、Jianjun Zhang2

TBM 优秀论文

1. 创新改造快速血糖监测仪为无痛、体外监测势在必行

徐汉友*

湖州市安吉国际 LIASOM 医院

目的：为了减轻日益增多的糖尿病病人监测血糖的痛苦，非常迫切需要创新快速血糖监测方法。

方法：总结作者本人几十年的工作经历，创新一种无创体外快速血糖监测仪的方案。

结果：2013 最新研究成果，以 2010 年的一个具有全国代表性的成年人样本为基础，报道了中国成年人糖尿病发病率情况，指出成年人有近 12%患有糖尿病，而前期转化患病率可以达到大约 50%。据世界卫生组织报道，从 1980 年，到 2014 年，全世界糖尿病的患病人数由 1.08 亿，猛增到 4.22 亿，据估计，在 2019 年，就有 1500000 人直接死于糖尿病；而在 2012 年，据估计，有 2200000 人死因与血糖增高有关，因此，每天有成千上万的糖尿病人在服用或注射降血糖药物，快速血糖监测成糖尿病人的必备器械，特别是在初诊糖尿病病人初始强化控制血糖时，血糖波动大、不易控制的糖尿病病人，或危重症病人，每日快速血糖监测至少 7 次，或更多，或每小时测一次，这样一来，长时间或长期监测，病人的十指指尖肯定被扎遍了，清醒病人，每扎一次，痛苦一次，经常扎很是痛苦，还存在着容易被传染病传染、感染发炎等危险，更是给医护人员加大工作量和造成被传染病传染的风险，作者作为在普通内科工作几十年的医生，深感病人的上述痛苦，因此，为了减轻病人痛苦，特创新产生改造快速血糖监测仪为无痛、体外监测仪的创意，在此特提出以下创新方案：1、 像当今广泛使用的快速非接触式体温测定仪一样，创造发明简易快速体外末梢血糖监测仪，其基本构思为，5 号、或 7 号电池为电源的或可充电的轻型仪器，有开关、探头，有显示屏显示血糖数值。2、有质控系统，有高灵敏度和精确度。3、可把探头对准指尖、指头，或暴露的皮肤作为探查点，探查点范围应该固定和统一，利于质控。4、研究思路应为，先创新确定用什么方法，能在体外快速精确测定血糖，检测到血糖后，通过芯片或微电脑系统，在荧光屏上显示准确血糖数值，可先通过动物实验，通过常规方法测定血糖，与其反复验证其准确度和敏感性，再在人体试验比对，最后大工快成，再进入临床试验验证。5、很显然本项创意前途是光明的，但需要科学创新，就现有的物理、化学、生物化学、医学，等科学的发展，体外测定血糖的方法可能很快会成为现实。6、希望所有人不再被扎。

结论：本创新创意值得深入研究，为解除病人痛苦，为更好地控制糖尿病病人血糖、提高治疗糖尿病和其并发症的效果，为提高病人的生活质量和大众健康作贡献。分别用本研究的题目和关键词，在中国知网上检索，结果无此项研究报道；同样的，分别用英文关键词和英文题目，在 PubMed.gov（https://pubmed.ncbi.nlm.nih.gov/）检索，结果也无此项研究报道，说明本创新方案有创新开发利用价值。

关键字：创新创意；体外快速血糖仪；研究方案；糖尿病

2. 刺激和促进昏迷病人大脑苏醒的一种很有潜能的方法--刺激膀胱充盈、苏醒、排尿神经反射通路，促进昏迷病人大脑苏醒

徐汉友*

湖州市安吉国际 LIASOM 医院

目的：为了促进昏迷病人苏醒，提高病人生存生活质量，研究一套新的苏醒方法。

方法：本研究通过总结作者长期、反复的临床实践和观察，结合相关生理和病理生理知识和原理，诱发了新的创新和设想，就是刺激膀胱充盈、苏醒、排尿神经反射通路，促进昏迷病人大脑苏醒的一整套方法。

结果：在作者长期、反复的临床实践中，一种特别的病理生理现象被发现，就是，很多昏迷病人，在无尿时，总是一直处于昏迷状态，肢体常静止不动，当随着病人膀胱充盈、尿潴留，并且尿潴留逐渐加重时，病人会出现躁动，或由昏迷好转转变成昏睡或嗜睡，甚至能短暂苏醒，呼喊排尿，排尿后会再次进入排尿前的状态。正常人体生理反应事实告诉我们，正常成人和大部分小儿，夜间睡觉，自发性苏醒的主要原因是，因为膀胱充盈、有排小便刺激，或者说有短暂的轻度尿潴留，这些刺激反射，通过上行神经传导通路，传至大脑，刺激大脑及时苏醒，使正常人完成排尿的生理功能和行为，当小儿大脑神经组织发育不完全时，夜间睡觉，膀胱充盈、有排小便刺激，或者说有短暂的轻度尿潴留，这些刺激反射，通过上行神经传导通路，传至大脑，不能及时刺激大脑苏醒，不能完成正常排尿的生理功能和行为，小儿就会遗尿。这种创新和设想，以刺激排尿反射整个通路神经为切入点，通过物理手段、药物手段、中医中药手段、外科手段，等手段，刺激膀胱周围副交感传入神经或其感受器、骶部

脊髓的初级排尿中枢、脊髓的传入神经、脑干中枢调节系统及大脑皮层高级中枢，从而产生苏醒或（和）小便意感，从而达到临床治疗昏迷病人的目的。

结论：本研究创新设想，有坚实的生理和病理生理基础，也具有坚实科学的解剖学、组织学、生物化学与分子生物学基础，由此产生的科学创新设想，虽仅为设想，但是很有进一步研究价值，经国内外检索证实截至目前，在国内外还没有类似的研究报道，因此本研究论文值得参考应用。

关键字：膀胱充盈；尿潴留、排尿反射；昏迷；苏醒；治疗方法。

3. 论各行各业专业技术人员高级等职称评审晋升管理是行政行为，纠纷可行政诉讼

徐汉友*

湖州市安吉国际 LIASOM 医院

目的：为了提高卫生专业技术人员、教师，等各行各业专业技术人员职称晋升异议处理的公平和合理合法，提高其工作积极性和科技发展。

方法：总结本人司法经历，正当中国在大力开展依法治国时，我却经历了卫生系列高级职称评审晋升的不公平待遇，我多次提起行政复议，均被裁定不受理，2020 年至 2021 年，就此事不公平待遇和异议，再次提起行政复议和行政诉讼，再次被裁定不予受理，在上诉期间，我认真思考，并查阅了大量资料，发现，与卫生系列有直接关系的工伤管理和医疗事故管理，特别是工伤管理，一直以来是按行政管理行为管理的，其异议处理，是通过行政复议和行政诉讼受理处理和解决的，而作为专业技术人员职称晋升先驱，教师系列的晋升异议处理，到目前为止，均被行政复议和行政诉讼拒之门外，但由此引起教师系统的不满，并因此产生了此异议处理的众多法律科技的研究和成果及进展，此项中心成果就是，教师系列职称晋升异议的处理，应该和需要通过行政复议和行政诉讼这样一个司法程序才能公平处理和解决。结果：全国各行各业专业技术人员职称晋升的异议处理管理，也类似教师系列职称晋升异议的处理现状，据我所知，卫生系列专业技术人员高级等职称评审晋升及其他系列专业技术人员职称评审晋升异议的处理，也未得到通过行政复议和行政诉讼这样一个司法程序公平处理和解决，本人的案例就是证明，以此，借此机会，特研究总结、论证，卫生系列专业技术人员高级等职称评审晋升及其他系列专业技术人员职称评审晋升，包括教师系列，异议的处理，

应该和需要通过行政复议和行政诉讼这样一个司法程序才能公平处理和解决，现报告和说明论证如下：通过多项健康管理有关可行政诉讼的行政管理行为案例总结和分析，及类似卫生专业技术人员高级等职称评审晋升管理的同类情形，教育界教师职称评审晋升管理的现状总结和分析，发现现实社会有关人员，对教师职称评审晋升异议处理，不被行政复议和行政诉讼受理，怨言很大很多，而法学界和教育界专业人员，一直研究认为，教师职称评审晋升异议处理，应该是行政复议和行政诉讼受案范围，及其如此依法治国的很多益处，从而，通过类比、逻辑推理，得出结论，卫生专业技术人员高级等职称评审晋升管理的异议处理，也应该是行政复议和行政诉讼受案范围，其他各行各业专业技术人员职称评审晋升管理，也是行政行为，异议处理也属于行政复议和行政诉讼受案范围。

结论：各行各业专业技术人员高级等职称评审晋升管理是行政行为，纠纷可行政诉讼的研究结论，已被学术界所公认，迫切需要付诸现实，但现实司法系统的司法行为，与广大学术界和专业技术人员的期望背道而驰，不利于调动广大科技人员的积极性，改革势在必行，本研究为依法治国和国家复兴，做出贡献。

关键字：各行各业；职称晋升；卫生专业技术人员；教师；行政诉讼；行政复议；依法治国。

4. 如何从中国古典哲学角度看待原癌基因和抑癌基因

应力*

上海交通大学医学院附属第九人民医院

在我硕士一年级时，有一门开卷的课程叫做口腔基础医学，负责课程的人是我的导师，陈万涛教授。一共有 5 道题目，每题 20 分。当年因为一道题目打印时漏了资料，我总分是 C+，即 70-75。当年那道试卷最后一道题目是：你如何看待原癌基因和抑癌基因。我洋洋洒洒写了至少 300 多字，都写到背面去了。后来我一直把这道题目铭记在心。今天就是想拿出来和大家讨论一下。

关键字：中国古典哲学；基因

5. 血清 25 羟基维生素 D 与结直肠癌相关临床意义研究

常鑫*

宁夏医科大学

目的: 通过探讨血清 25 羟基维生素 D[25(OH)D]与结直肠癌临床病理特征、肿瘤标志物 CEA、CA199 以及 VEGF、EGFR 之间的相关性，为临床结直肠癌的诊疗提供理论依据。

方法: 选取结直肠癌患者 234 例，采用酶联免疫吸附法检测血清 25(OH)D 含量，采用电化学发光法测定血清 CEA、CA199 含量，同时应用免疫组织化学法检测结直肠癌病理组织中 VEGF、EGFR 的表达情况。

结果: 结直肠癌患者血清 25(OH)D 水平低于正常健康人群，其中女性患者血清 25(OH)D 水平显著低于男性患者，右半结肠癌患者血清 25(OH)D 水平低于左半结肠和直肠癌患者，肿瘤浸润深度突破肌层的患者血清 25(OH)D 水平显著低于未突破肌层患者，TNM 分期中 T4 期患者血清 25(OH)D 水平显著低于 T1、T2 和 T3 期，N1、N2 患者血清 25(OH)D 水平低于 N0，II、III、IV期患者血清 25(OH)D 水平低于I期，肿瘤分化程度为低分化与中分化者血清 25(OH)D 水平低于高分化者；结直肠癌患者 CEA 异常组血清 25(OH)D 水平低于正常组；VEGF、EGFR 阳性表达组血清 25(OH)D 水平低于阴性组(*以上 P 均*<0.05)。

结论： 血清 25(OH)D 水平与结直肠癌临床病理特征、肿瘤标志物、VEGF 和 EGFR 之间存在一定的相关性，通过对 25(OH)D 的研究，为结直肠癌的诊疗提供相关理论依据。

关键字: 25(OH)D；结直肠癌；肿瘤标志物；EGFR；VEGF；

6. CD55 蛋白在肺癌中的表达及临床意义

张月洋*[1]、黄安康[2]、王卫东[1]、龚永生[2]、金艳霞[1]

1. 湖北师范大学

2. 南京医科大学附属苏州医院

目的： 补体加速衰减因子（Complement decay-accelerating factor, CD55）为含 381 个氨基酸的糖基磷脂酰肌醇锚定的糖蛋白，是膜结合性补体调节蛋白的重要成员，在血液和多种组织中表达。前期通过转录组测序数据分析发现 CD55 在早期非小细胞肺癌（non-small cell lung

cancer, NSCLC）患者的外周血白细胞中表达下调，但其在肺癌中的表达以及功能还不明确。本研究检测肺癌血清中 CD55 的表达水平，探索其与患者临床病理特征和预后的关系。

方法：采集 15 例良性患者和 36 例肺癌患者的血清和临床病例检测指标，利用蛋白印迹法分析 CD55 在肺癌血清中的表达水平，利用 GEPIA 数据库分析 CD55 在肺癌组织中的 mRNA 表达变化；运用 SWISS-MODEL WORKSPACE 和 SPDBV 软件同源模建和分析 CD55 蛋白的 3D 结构；运用 STRING 数据库分析 CD55 蛋白与其他蛋白的相互作用；运用 Kaplan-Meier Plotter 数据库分析 CD55 表达与肺癌患者的生存关系；并利用 SPSS 软件回顾性分析 CD55 蛋白表达与患者血常规、肿瘤标志物、凝血指标和生化指标之间的关系。

结果：CD55 mRNA 在肺鳞癌组织中表达下降，在腺癌中无显著差异，CD55 蛋白在 31 例肺癌血清中的表达水平相比 15 例良性样本无明显变化。同源模建发现 CD55 蛋白的 3D 结构与 pdb 为 3iyp.1.E 的模板序列同源性为 99.74%，含有 8 个二硫键。进一步分析发现 CD55 低表达的肺癌患者生存时间更短，在早期肺癌中更明显。运用 SPSS 统计软件双变量相关分析发现，CD55 表达与早期肺癌患者血清中低密度脂蛋白和高尔基蛋白 73 有显著相关性。蛋白互作分析发现 CD55 蛋白与 CD59、C97、C2、C3、C4A、C4B、ICAM1、PIGA、EGF、EMR2 和 CEACAM8 有相互作用。

结论：CD55 表达与肺癌生存相关，且与肺癌患者生化指标有显著相关性，表明 CD55 有可能作为肺癌预后生存标志物，为探索 CD55 参与肺癌发生机制和预后判断提供参考依据。

关键字：肺癌；CD55 蛋白；表达；生存；生物信息学；数据库

7. Beclin 1 表达与肺鳞癌临床病理特征的关系及其抑癌机理

曾雨佳*、胡翠玉、薛航、梁宗英、郑华川

承德医学院附属医院

目的：探究肺鳞癌中 Beclin 1 表达的临床病理意义及抑癌作用。

方法：肺鳞癌 SQ-5 细胞过表达 Beclin 1，分别通过 CCK-8、海马能量监测、油红 O 染色、流式细胞术、β-半乳糖苷酶染色、transwell、免疫荧光和 Western 蛋白印迹检测细胞增殖、糖代谢、脂肪堆积、细胞周期与凋亡、衰老、迁移与侵袭、肿瘤生长及表型相关蛋白表达。Becn1 mRNA 表达水平与肺鳞癌临床病理特征相比较。

结果：与对照组比较，Beclin 1 抑制肺癌 SQ-5 细胞增殖、迁移与侵袭以及肿瘤生长，诱导凋亡、S/G2 期阻滞、促进脂肪积累、自噬与衰老，体内外实验 Becn1 转染体对顺铂耐药。转染体中 Bcl-2、β-连环蛋白和 HSP90 表达下调，LC-3B、ADFP、细胞色素 C、p-p38 和 p-NF-κB 表达升高。生物信息学分析表明，肺鳞癌中 Becn1 mRNA 表达上调 (p<0.05)，Becn1 基因表达与 N 分期、TNM 分期、TP53 野生型和不良预后呈现负相关(p<0.05)

结论：异常 Beclin 1 表达抑制肺鳞癌发生与演进，其过表达可逆转增殖和侵袭等恶性表型，可作为肺鳞癌预后潜在靶点。

关键字: 肺鳞癌；Beclin 1；临床病理意义；预后；基因治疗

8. HACE1 在恶性肿瘤中的研究进展

朱甜甜*、刘培民、李东东、郭军辉

河南省中医院（河南中医药大学第二附属医院）

HACE1 是一种 E3 泛素连接酶，作为一种重要的肿瘤抑制基因，其可通过激活细胞自噬、介导 Rac1 的泛素化、抑制活性氧依赖的谷氨酰胺成瘾等多种途径发挥抑制肿瘤进展的作用。HACE1 的下调及突变与多种肿瘤的发生、进展、侵袭及预后密切相关。此外，HACE1 还具有保护心脏，抗氧化应激，调节细胞动力学等多种生物学功能。本文通过查阅近年来有关 HACE1 的相关文献，旨在阐述其在恶性肿瘤中的作用机制，及其与恶性肿瘤发生、转移和预后的关系，为临床癌症药物研制提供新方向。

关键字: HACE1;肿瘤抑制基因;研究进展

9. 上调的自噬相关基因 ITGA6 作为肥胖直肠癌患者复发和远处转移相关的良好预后的生物标志物

刘超月、付佳、付晨*

中国医科大学

肠道癌症是世界上最致命的疾病之一。大量的研究已经证明自噬与肠道肿瘤发生的关系。越来越多的证据表明，自噬系统在直肠癌的生物学过程中起着关键作用,如肿瘤发生发展，复发和转移。一些人已经讨论将自噬作为对抗各种癌症的武器。肥胖影响消化系统的功能和内

分泌系统的功能，并且增加癌症发生的危险性。然而，自噬相关基因是否可以在肥胖人直肠癌的预测预后尚未确定。

背景：直肠癌（ROAD）是一种发病率高,预后差的疾病。现有的评估直肠癌患者预后的临床方法有个体化治疗存在侵入性、非系统性、主观性、数据少等缺陷，并且直肠癌肥胖患者可以引发体内诸多代谢紊乱，比如导致高血压、心脑血管疾病以及糖尿病等。肥胖可能增强了直肠癌的危险因素。 迫切需要识别潜在的预后标志物和新的直肠癌肥胖患者治疗靶点。

方法：基于美国国立癌症基因图谱（TCGA）和自噬基因数据库（HADb）数据集,我们整合了 173 名直肠癌患者的核糖核酸（mRNA）测序资料和临床资料，计算自噬相关的差异基因（ARGs）。功能分析表明，ARGs 在细胞生长，代谢途径中富集最为显著,表明肥胖的直肠癌患者的癌变机制较为复杂。基于基因组学和临床病理数据,我们将直肠癌肥胖患者的自噬相关基因分成高风险和低风险组。构建了一个生存分析模型来预测携带肥胖直肠癌患者的预后。接下来,我们评估了风险评分和自噬之间的相关性。最后,我们在 GEO 数据库 GSE56699 数据集中验证了该模型的预后性能。

结果：232 个 ARGs 在 173 例直肠上皮细胞和 3 例正常直肠表面上皮细胞中表达水平与 7 个独立因素分析，鉴定出 10 个差异 ARGs mRNA（MYC, ATG9B, LAMP1, BECN1, ATG4C, VMP1, ITGA6, CASP1, MAPK3, PEA15）。我们研究了功能性和通路性对所有差异 ARGs 进行富集分析，构建蛋白质相互作用网络。筛选候选的差异 ARGs 与直肠癌肥胖患者的生存相关，并构建自噬相关的单变量和多变量预后风险特征分别建立 Cox 比例风险模型。筛选出了 10 个自噬预后相关基因根据风险评分的中值，整个 TCGA 队列被分为高风险组和低风险组。而低风险组有更好的总生存率（OS）。最后，选取最佳独立预后的差异 ARGs 评估其与直肠癌复发和远端转移相关性。生存预测的预后风险模型的准确性和稳定性通过分析直肠癌肥胖患者生存状态、临床病理特征及风险评分的相关性来验证。并且根据临床数据对直肠癌肥胖患者进行了远端转移和复发分析。并据此构建预后模型，根据与 TNM 等临床分期相比，其预后性能更好。为了预测直肠癌肥胖患者的总生存率，我们建立了一个与基因和临床因素相关的列线图。接受者操作特征（ROC）曲线，一致性指数（Cindex）和校准曲线显示，该模型具有较好的准确性。并且该预后模型可以为后期患者治疗提供更多信息。筛选出来的自噬基因和预后之间的相关性风险评分分析表明，ITGA6 可作为直肠癌肥胖患者自噬治疗的新靶点，为直肠癌肥胖患者的自噬治疗提供新方向。

结论：自噬相关预后风险模型可以独立用于预测肥胖直肠癌患者的总生存期，并且自噬相关基因 ITGA6 还与直肠癌肥胖患者的复发与远端转移密切相关。对于患者来讲，它也可以潜

在地帮助个体化治疗和生物标志物的发展，最后，我们在肥胖直肠癌患者中发现了一个新的自噬治疗相关靶点 ITGA6（Integrin Subunit Alpha 6）。并系统地阐述了携带直肠癌肥胖患者发病的分子机制。我们的 ARG 预后模型被证明在监测，治疗和预后评估方面具有价值。

关键字: Autophagy; mRNA; ROAD; Fat; Prognosis; TCGA

10.血清来源的外泌体 mir-129-5p 标记作为结直肠癌的诊断生物标志物

董楠[1]、赵梁[1]、付晨*[2]

1. 沈阳市疾病预防控制中心

2. 中国医科大学

背景：结直肠癌（CRC）是一种常见的恶性肿瘤，总体预后不理想。血浆中来自外泌体的 miRNA 可能有希望成为肿瘤预后生物标志物，之前有证据表明，外泌体中的 miRNA 在肿瘤发生和发展过程中发挥重要作用，并且，外泌体 lncRNA 和 circRNA 介导的 ceRNA 网络的调节机制和预后作用尚未阐明。本文发现了 mir-129-5p 在细胞外泌体中的作用及其在 CRC 中的预后价值和免疫治疗。并可能成为大肠癌的潜在生物标记物。

方法：从 exoRBase 数据库中获得 CRC 和正常样本 EVs 中的 circRNA、lncRNA 和 mRNA 表达水平矩阵。差异表达的 circRNA，lncRNA 和 mRNA 使用 R 软件的 limma 软件包限制条件 $LogFC > 1$ 和 $p < 0.05$ 进行鉴定。基于工具预测 circRNA，lncRNA，mRNA 相关的 miRNA，根据竞争性内源 RNA 机制和差异表达基因，构建了 CRC 的 circRNA-miRNA-mRNA 和 lncRNA-miRNA-mRNA 调控网络。其中 miRNA 和从 BBCancer 数据库下载了 EVs 中相应的 miRNA 表达水平矩阵进行交集，筛选出血浆中生物标记物 mir-129-5p。使用 GEO 数据库中 GSE26334 数据集来证实 miR-129-5p 在 CRC 细胞系 HCT116 和 SW480 中有差异表达，用 Pearson 的临界值 $|r| > 0.3$ 且 $p < 0.05$ 筛选与 mir-129-5p 共表达的 mRNA。通过使用透射电子显微镜（TEM）和 Western-blot 鉴定从血清和培养介质中分离的外泌体。通过 RT-qPCR 和 ROC 曲线分析并且进一步验证 mir-129-5p 的表达水平和预后诊断价值。基于共表达的 mRNA 的基因集富集分析（GSEA）用于探索 mir-129-5p 的潜在分子功能。

结果：在 exoRBase 数据库中鉴定出 CRC 差异表达的 circRNA，lncRNA 和 mRNA，构建了 CRC 外泌体的 circRNA-miRNA-mRNA 和 lncRNA-miRNA-mRNA 调控网络。其中 mir-129-5p

的 FC 值为 3.92。 RT-qPCR 分析显示 CRC 血液样本中与正常人相比，CRC 细胞系和正常结肠上皮细胞相比，mir-129-5p 水平均上调。总体生存分析发现，mir-129-5p 的高表达与预后较差有关。最后，基于 mir-129-5p 和 12 个上调的 mRNA，GSEA 表明与 mir-129-5p 共表达的 mRNA 参与 EPHB-mediated forward signaling。

结论：该研究证实了大肠癌血浆中外泌体 mir-129-5p 可作为检测大肠癌转移的生物标志物。将循环外泌体 mir-129-5p 检测与肠镜相结合可以提高大肠癌转移的早期诊断率。EEF1A1P11-mir-129-5p-HNRNPA3 的 lncRNA-miRNA-mRNA 调控网络可用于揭示 CRC 的发生和发展过程。

关键字: 大肠癌，miRNA，细胞外囊泡，竞争性内源 RNA

11. 血清 S100β蛋白水平与黑色素瘤临床分期的关系

韩冉冉*、渠文涛

郑州安图生物工程有限公司

目的：探讨血清 S100β蛋白水平与黑色素瘤临床分期的关系。

方法：收集 40 例皮肤黑色素瘤患者的血清样本，作为实验组，其中I期患者 15 例，II期患者 10 例，III期患者 8 例，IV期患者 7 例，20 例健康体检者血清作为对照组。使用 S100 蛋白检测试剂盒（磁微粒化学发光法）在 AutoLumo A2000 plus 上进行检测，比较两组血清 S100β蛋白水平。采用四格表法计算各期黑色素瘤患者 S100β的敏感性。

结果：各期皮肤黑色素瘤患者血清 S100β蛋白水平均高于对照组，但I、II期与对照组差异无统计学意义（$P>0.05$）。I、II期皮肤黑色素瘤的诊断敏感性为 12.0%，远低于IV期的诊断敏感性 71.4%，III期患者的敏感性为 37.5%。

结论：血清 S100β蛋白在黑色素瘤患者的肿瘤临床各期含量不同,应该在恶性黑色素瘤患者临床各分期进行血清 S100β检测，提示血清 S100β可作为恶性黑色素瘤预后的标志物。

关键字: S100β；黑色素瘤；敏感性

12.血清样本灭活处理对 Cyfra21-1 检测结果的影响研究

周珊珊*、渠文涛、万鹏

郑州安图生物工程股份有限公司

目的：血清 Cyfra21-1 的检测对肺癌、尤其是非小细胞肺癌的治疗效果评价和预后监测具有重要的诊断价值。为保护检验人员，防止某些潜在传染源随血液样本的临床使用而传播，可对样本进行适当的灭活处理。临床血液样本经 56 ℃加热 30 min 是常用的一种灭活手段，但灭活后样本的检测结果是否受影响，一直是检验工作者关注的重点。本文评估了 56 ℃加热 30 min 灭活血清样本对 Cyfra21-1 指标的影响，为临床实验室检测 Cyfra21-1 的样本采取合适的处理方法提供参考依据。

方法：取 Cyfra21-1 检测样本 10 例，均分为 2 组，一组作为灭活前的对照组置于 2-8℃保存，另一组样本于 56℃条件下加热 30min 作为灭活后实验组。将处理完成的两组样本恢复至室温，采用 AutoLumo A2000 Plus 检测系统搭配相应的 Cyfra21-1 检测试剂盒平行考核两组样本 Cyfra21-1 的含量，并对灭活前后的结果进行比对分析，观察灭活对检测结果的影响。

结果：Cyfra21-1 参考值为 3.3 ng/mL，本研究评估了 1-200 ng/mL 浓度值范围内的 10 例梯度样本灭活前后 Cyfra21-1 检测结果的变化。与对照组相比，样本热灭活后，Cyfra21-1 的检测结果均有不同程度的降低，其中低值区样本在灭活处理之后基本降为零值，其灭活前检测结果为 2.31±1.33 ng/mL，灭活后检测结果为 0.01±0.01ng/mL；中间区段样本灭活前检测结果为 34.38±19.56 ng/mL，灭活后检测结果为 2.03±1.07ng/mL；高值区样本灭活前检测结果为 140.19±54.83 ng/mL，灭活后检测结果为 53.01±8.88ng/mL；结果差异有统计学意义（$P<0.05$）。

结论：血清样本在 56℃灭活 30min 处理后，Cyfra21-1 的检测结果显著降低，说明 Cyfra21-1 对热敏感，其在 56℃条件下不稳定，推测可能是由于高温导致蛋白变性或蛋白结合位点变性，使结果有显著差异。因此，临床实验室在进行 Cyfra21-1 检测时，血清样本不能进行灭活处理，否则会导致检测结果的不准确。

关键字：样本灭活；Cyfra21-1；降低；

13.CA242、CA19-9 和 CA72-4 在初诊胃癌患者血清中的表达及应用价值

韩冉冉*、韩冉冉

郑州安图生物工程有限公司

目的：探讨糖类抗原 242(CA242)、糖类抗原 19-9(CA19-9)和糖类抗原 724（CA72-4）在胃癌患者血清中的表达及临床应用价值。

方法：收集 2018 年 1 月至 2019 年 12 月 82 例初诊胃癌患者和 45 例健康体检者血清样本，采用磁微粒化学发光法检测研究对象血清 CA242、CA19-9 和 CA72-4 水平，并分析与胃癌临床分期的关系。通过受试者工作特征(ROC)曲线分析 CA242、CA19-9 和 CA72-4 检测对胃癌的诊断价值。

结果：胃癌组患者血清 CA242、CA19-9 和 CA72-4 水平分别为(152.8±31.5)U/mL、(631.7±196.2)U/mL、(189.3±12.9)U/mL，显著高于正常对照组的(9.8±2.4)U/mL、(23.1±6.4)U/mL、(6.4±1.2)U/mL，差异均有统计学意义（$P<0.05$）。III～IV期患者血清 CA242、CA19-9 和 CA72-4 水平(182.8±51.3)U/mL、(831.7±206.2)U/mL、(199.1±10.9)U/mL 显著高于 I～II期患者(102.8±21.3)U/mL、(331.7±76.2)U/mL、(108.5±30.8)U/mL，差异有统计学意义（$P<0.05$）。CA242、CA19-9 和 CA72-4 单项及联合检测灵敏度分别为 65.80%、74.36%、75.35%、92.30%，特异性分别为 72.53%、76.75%、68.31%、95.63%。

结论：血清 CA242、CA19-9 和 CA72-4 水平与肿瘤临床分期有关，可作为胃癌早期诊断的辅助诊断指标，联合检测有助于提高胃癌临床检测的灵敏度和特异性，值得临床推广应用。

关键词：CA242, CA19-9, CA72-4, 胃癌

14.HE4 在鉴别孕早期 CA125 假阳性上的应用价值

李晓燕*、渠文涛、史小芹

郑州安图生物工程股份有限公司

目的：CA125 是临床上常用的一种卵巢癌相关的肿瘤标志物，但是，由于 CA125 的灵敏度和特异性有限，临床上经常会出现一些由于生理或病理因素导致 CA125 假性升高的情况。

HE4 作为一种新型的卵巢癌标志物，特异性和灵敏度均有显著的提升，本文探讨了 HE4 在鉴别孕早期 CA125 假阳性上的应用。

方法：采用回顾分析的方法，分析 122 例孕妇人群的 CA125 和 HE4 检测结果，分析孕早期（怀孕前三个月）CA125 和 HE4 的阳性率。CA125 和 HE4 的检测使用的是安图生物的 AutoLumo A2000 及配套试剂。正常人群的参考区间：CA125 为 0-35U/ml；HE4 为 0-140 pmol/L。

结果：比较孕早期 CA125 和 HE4 检测结果的阳性率，CA125 的阳性率为 58.19%（71/122），结果分布 10.26-837U/ml，中位数 60.31U/ml； HE4 的阳性率为（3.28%）4/122，结果分布 25.16-150.29 pmol/L，中位数 40.36pmol/L。孕早期 CA125 的阳性率显著高于 HE4，也显著高于非妊娠健康人群，结果与文献报道一致。

结论：对于孕早期的人群，CA125 的检测结果会异常升高，这主要是妊娠期特殊的生理原因造成的，胎儿绒毛膜、羊水和母体蜕膜中均有大量的 CA125，当母体蜕膜细胞破坏和滋养层细胞与蜕膜细胞分离后，使胎儿绒毛膜、羊水和母体蜕膜中的 CA125 进入血液而致血清 CA125 异常增多。到孕中期，大部分人 CA125 会降到正常水平。孕早期 HE4 的阳性率较低，因此，HE4 可用于鉴别孕早期 CA125 的假阳性

关键词：CA125 偏高；孕妇；HE4；孕早期

15.鼻咽癌中低表达 m6A 去甲基化酶 FTO 和 ALKBH5 通过联合负调控 ARHGAP35 抑制其进展的研究

杨致远、尤易文*

南通大学附属医院

目的：本研究旨在探讨 m^6A 去甲基化酶 FTO 和 ALKBH5 对鼻咽癌细胞增殖、迁移等恶性生物学行为的影响及其对下游靶点 ARHGAP35 的稳定性的影响和调控作用。

方法：本实验随机选取初诊鼻咽癌患者 3 例，以健康人为对照，提取对应组织 RNA 后采用斑点印迹杂交和比色法验证鼻咽癌组织中 m^6A 的表达水平。鼻咽癌患者组织芯片针对 FTO 和 ALKBH5 染色、评分、生存分析两者在鼻咽癌患者不同临床分期的表达和预后影响。利用不同时间段的体外实验检测 FTO 和 ALKBH5 对鼻咽癌细胞恶性生物学行为的影响。通过 RNA 测序和 RNA N^6-methyladenine 测序技术预测可能的下游靶基因 ARHGAP35，同时

qRT-PCR, Western blot 以验证 FTO 和 ALKBH5 对 ARHGAP35 的作用，并使用与前同批组织芯片对 ARHGAP35 染色、评分、生存分析其在鼻咽癌患者不同临床分期的表达和预后影响。再次应用体外体内试验单独检测 ARHGAP35 对鼻咽癌细胞恶性生物学行为的影响。通过 Western blot 及 qRT-PCR 分析 m^{6}A 对下游靶 mRNA 稳定性的影响。应用体内外实验验证 FTO 和 ALKBH5 联合负调控 ARHGAP35 改善鼻咽癌的恶性进展。该研究所涉及关于体外实验中增殖：EDU,集落形成；迁移：Transwell,伤口愈合实验；体内实验中增殖：裸鼠皮下成瘤，转移：尾静脉肺转移造模。

结果: m^{6}A 在鼻咽癌患者组织标本中低表达，FTO 和 ALKBH5 在鼻咽癌中的表达与患者病情进展、总体生存率密切相关。在鼻咽癌细胞 CNE2 和 C666-1 中同时设置实验组为 shCtrl,shFTO,shALKBH5,shFTO+shALKBH5。单敲组和共敲组均不同程度抑制细胞的增殖、迁移和侵袭等相关恶性行为能力，但随着时间进展，单敲组对上述恶性行为能力的抑制作用会减弱，而共敲组还能维持较好的抑制作用。ARHGAP35 被验证为 FTO 和 ALKBH5 的联合下游靶基因，FTO 和 ALKBH5 也保持了其 mRNA 稳定。相比于单敲组，共敲组可明显上调 ARHGAP35 的表达。CNE2 和 C666-1 中过表达 ARHGAP35 可抑制细胞的增殖、迁移和侵袭。敲低共敲组的 ARHGAP35 的表达，共敲组细胞的恶性行为能力会被逆转。

结论： 本研究通过联合敲低鼻咽癌中 m^{6}A 去甲基化酶 FTO 和 ALKBH5 的表达，导致 ARHGAP35 表达显著上调，从而最终抑制鼻咽癌的进展。

关键字: 鼻咽癌，m6A，RNA 稳定性，ARHGAP35

16. 长链非编码 RNA AC100821.2 通过调控 miR512-5p/DDX6 轴促进鼻咽癌的进展

程天仪、杨致远、游波*

南通大学附属医院

目的: 本研究旨在探讨 lncRNA AC100821.2 对鼻咽癌细胞增殖、迁移和侵袭等恶性生物学行为的影响及其对 miR-512-5p/DDX6 分子轴的调控作用。

方法: GEO 数据库筛选出在鼻咽癌中上调的基因，并在鼻咽癌细胞中采用逆转录聚合酶反应(qRT-PCR)验证 AC100821.2 的表达。通过 EDU、Transwell、侵袭和集落形成等一系列细胞表型实验检测 AC100821.2 对鼻咽癌细胞恶性生物学行为的影响。应用核质分离实验检测

AC1000821.2 在细胞中的分布表达。通过 miRDB 在线预测靶基因网站通过 AC100821.2 的序列找出可能的下游靶 miRNA，并通过双萤光素酶报告基因检测实验验证 miR-512-5p 与 AC100821.2 的结合关系。在体内外均验证了 miR-512-5p 的恶性生物学作用。再次通过在线生信预测软件找出 miR-512-5p 的下游靶基因 DDX6，同样使用荧光素酶报告以及 qRT-PCR，Western blot，验证 miR-512-5p 与 DDX6 的结合关系以及相关表达量。4D label free 找到了 DDX6 下游靶 mRNA，并通过 western blot 以及 qRT-PCR 验证 DDX6 对下游靶 mRNA 稳定性的影响。通过体内外实验验证 AC100821.2 通过调控 miR-512-5p/DDX6 轴促进鼻咽癌的恶性进展。

结果：长链非编码 RNA AC100821.2 在鼻咽癌细胞 CNE2 中表达上调，AC100821.2 在鼻咽癌中的表达与患者总体生存率、病情进展快慢密切相关。在 CNE2 中过表达 AC100821.2 上调了细胞的增殖、迁移和侵袭等相关恶性行为能力，而 AC100821.2 siRNA 抑制了这些恶性生物学行为。AC100821.2 可与 miR-512-5p 结合，DDX6 被证实为 miR-512-5p 的靶基因，AC100821.2 可通过抑制 miR-512-5p 的表达上调 DDX6 在鼻咽癌细胞中的表达。

结论：本研究表明长链非编码 RNA AC100821.2 通过调控 miR-512-5p/DDX6 分子轴促进鼻咽癌进展。

关键字: lncRNA; miR-512-5p; DDX6; 鼻咽癌

17.胞外囊泡中的 SCARB1 通过联合调控 M1 及 M2 巨噬细胞功能促进鼻咽癌转移

陈文卉*、游波、尤易文（通讯作者）

江苏省南通大学附属医院

目的：远处转移是鼻咽癌治疗失败的主要因素，探索鼻咽癌转移的机制，寻找可靠的治疗靶点对改善预后、实现临床转化至关重要。巨噬细胞作为肿瘤微环境中的重要免疫细胞，已证实可调控转移。胞外囊泡是连接肿瘤微环境中各种细胞的重要桥梁，现有报道及我们前期研究表明胞外囊泡参与重塑鼻咽癌微环境。然而，鼻咽癌来源的胞外囊泡对巨噬细胞的作用及其调控巨噬细胞影响转移的功能尚不明确。本研究旨在探索鼻咽癌细胞来源的胞外囊泡通过调控巨噬细胞功能，影响鼻咽癌转移的作用及机制。

方法: 利用蛋白质谱、数据库分析、qRT-PCR、WB 等检测手段发现，与鼻咽癌来源的胞外囊泡共培后，巨噬细胞中 SCARB1、HAAO 和 CYP1B1 三者的表达水平显著升高。通过 ROS 流式、线粒体电镜实验及瑞氏-吉姆萨、乳胶珠实验进一步分析胞外囊泡中 SCARB1 如何通过 HAAO 促进 M1 型巨噬细胞铁死亡；以及通过 CYP1B1 抑制 M2 型巨噬细胞吞噬。并且通过裸鼠活体成像，免疫组化等方法从体内验证了胞外囊泡中的 SCARB1 通过巨噬细胞促进对鼻咽癌转移。并采用 IP 质谱、ChIP、萤光素酶报告等实验验证了胞外囊泡中的 SCARB1 是通过转录因子 KLF9 实现对 HAAO 及 CYP1B1 的调控。

结果: 鼻咽癌细胞来源的胞外囊泡中的高表达的 SCARB1 增加 M1 型巨噬细胞中 HAAO 表达量，使得 M1 型细胞铁死亡增多，浸润减少；与此同时，胞外囊泡中的 SCARB1 增加 M2 型细胞 CYP1B1 表达，以降低 M2 型巨噬细胞对鼻咽癌细胞的吞噬作用。最终二者共同联合影响了巨噬细胞功能，促进鼻咽癌转移。相关机制将为改善鼻咽癌患者的预后提供了新的治疗策略。

结论: 我们的研究表明鼻咽癌胞外囊泡中的 SCARB1 通过联合调控 M1 及 M2 型巨噬细胞功能促进了鼻咽癌的转移。

关键字: 鼻咽癌，胞外囊泡，巨噬细胞，铁死亡，吞噬

18.基于生物信息学分析 DNAH14 基因在子宫内膜癌中的临床意义

李楠*、陈蕾、段雨含、张琨

吉林大学第二医院

目的: 利用肿瘤综合数据库分析 DNAH14 基因对子宫内膜癌发展的影响及其临床意义。

方法: 全面检索 UALCAN、GEPIA、Kaplan-Meier plotter、TIMER、Mu Target、DAVID、STRING 等数据库，分析其表达、突变状态、频率、生存曲线、功能富集情况、基因相关性及信号通路，并进行生物信息学预测。

结果: DNAH14 高表达患者总体生存率和无疾病生存率均低于低表达患者，差异有统计学意义（$P<0.05$）；不同临床分期、年龄、更年期状态以及组织学类型中的分布存在显著差异（$P<0.05$)。子宫内膜癌患者存在 DNAH14 基因突变，提示良好预后。相关性分析显示，DNAH14 基因突变可能通过癌症中的蛋白多糖及 Wnt、T 细胞受体、Toll 样受体信号通路发

挥作用；另外，DNAH14 突变与免疫浸润水平相关；蛋白互作分析显示，DCTN3、HAP1、ACTR1、DNAH12、ACTR1B 等蛋白与 DNAH14 具有相互作用。

结论: DNAH14 在子宫内膜癌中呈高表达，其高表达与患者的不良预后相关。在子宫内膜癌患者中 DNAH14 基因突变，可能通过癌症中的蛋白多糖及 Wnt、T 细胞受体、Toll 样受体信号通路影响免疫浸润水平并改善预后，DNAH14 可能成为判断子宫内膜癌患者预后的指标。

关键字: 子宫内膜癌；DNAH14；基因突变；预后

19.合成 MRI 联合三维动脉自旋标记成像预测弥漫性胶质瘤分级及肿瘤细胞增殖活性的研究

葛鑫*[1,2]、张静 [2]

1. 兰州大学第二临床医学院

2. 兰州大学第二医院

目的：探讨合成磁共振成像联合三维动脉自旋标记(3D-ASL)成像对弥漫性胶质瘤分级诊断的应用价值及与肿瘤细胞增殖活性(Ki-67)的相关性。

方法：前瞻性分析 2020 年 8 月至 2021 年 6 月 66 例弥漫性胶质瘤患者的临床及影像表现。将 66 例患者分为低级别胶质瘤(LGG)组 25 例(WHO II 级)和高级别胶质瘤(HGG)组 41 例(WHO III、IV 级)。所有患者术前均接受常规 MRI、合成 MRI 及、3D-ASL 及常规 MR 增强检查，利用 GE ADW4.7 后处理软件测量肿瘤实质部分 T1、T2、质子密度(PD)、脑血流量(CBF)。术后病理切片通过免疫组化检测 Ki-67 阳性表达率。采用独立样本 t 检验或 Mann-Whitney U 检验比较 HGG 组与 LGG 组各定量参数的差异，采用受试者操作特征(ROC)曲线分析 T1、PD、CBF 和三者联合的诊断效能，利用 Spearman 检验分析各参数与 Ki-67 阳性表达率的相关性。

结果：HGG 组 T1[(1 573 ± 173)ms]、PD[(86.2 ± 2.4)pu]、CBF[(129 ± 48) ml·100g-1·min-1]均高于 LGG 组[分别为[(1 376 ± 134)ms、(83.0 ± 2.5)pu、(77 ± 49)ml·100g-1·min-1]，差异具有统计学意义(t 分别为-4.860、-5.077、-4.242,均 P<0.01)。ROC 证实 T1、PD、CBF 鉴别 HGG 组与 LGG 组的曲线下面积(AUC)分别为 0.847、0.843、0.777。多参数分析中，三者联合的诊断效能最高(AUC=0.973)，灵敏度和特异度分别为 87.8%和 100%。在 LGG 和 HGG 组中，

T1、T2、PD、CBF 与 Ki-67 阳性表达率无相关性；整体胶质瘤患者中，T1、PD、CBF 均与 Ki-67 阳性表达率呈程度正相关性(r 分别为 0.394、0.411、0.406, 均 $P<0.01$)；T2 与 Ki-67 阳性表达率无相关性(r=-0.100, $P=0.423$)。

结论：合成 MRI 和 3D-ASL 可无创地评估胶质瘤的病理分级并预测 Ki-67 的表达情况，其中 T1 和 PD 是较好的影像学新指标。

关键字：弥漫性胶质瘤；分级诊断；细胞增殖抗原；合成磁共振成像；动脉自旋标记

20.Synthetic MRI 联合 DSC 在胶质瘤分级及肿瘤细胞增殖活性预测中的临床价值

葛鑫*[1,2]、张静 [2]

1. 兰州大学第二临床医学院

2. 兰州大学第二医院

目的：探讨合成磁共振成像(synthetic MRI, sy-MRI)联合动态磁敏感对比成像(dynamic susceptibility contrast, DSC)在胶质瘤分级及细胞增殖活性预测中的临床价值。

方法：回顾性分析 60 例胶质瘤患者，其中低级别(low-grade glioma, LGG)22 例，高级别(high-grade glioma, HGG)38 例。所有患者术前行 sy-MRI 和 DSC 序列扫描，术后标本行 Ki-67 免疫组化染色。由两名放射科医师在 T1 mapping、T2 mapping、相对脑血流量(relative cerebral flow, rCBF)和相对脑血容量(relative cerebral volume, rCBV)伪彩图上，选取肿瘤实质最大层面画取 ROI，并测量增强前 T1 值(native-T1)、T2 值(native-T2)、增强后 T1(enhanced-T1)、增强前后 T1 值变化的百分比(ΔT1)、rCBF 和 rCBV。利用独立样本 t 检验或 Mann-Whitney U 检验比较两组间各参数的差异，利用 Spearman's 法分析各参数与 Ki-67 LI 之间的相关性，采用 ROC 曲线评估其在分级中的诊断效能。

结果：HGG 组ΔT1、rCBF 和 rCBV 均高于 LGG 组($P<0.01$)，HGG 组 enhanced-T1 低于 LGG 组($P<0.01$)，ΔT1、rCBF、rCBV 与 Ki-67 LI 均成正相关(r 值分别为 0.643、0.324、0.411，$p<0.05$)，enhanced-T1 与 Ki-67 LI 成负相关(r=－0.619, $P<0.01$)。Enhanced-T1、ΔT1、rCBF 和 rCBV 鉴别高、低级别胶质瘤的 AUC 分别为 0.972、0.990、0.775 和 0.849。

结论： Sy-MRI 能够反映组织微观结构信息，是胶质瘤分级诊断和预测肿瘤增殖活性的成像新技术，其中ΔT1 的诊断效能最高。此外，DSC 可用于胶质瘤微血管灌注的评估，是评估分级的重要补充。

关键词：胶质瘤；分级；细胞增殖；合成磁共振成像；动态磁敏感对比

21.集成磁共振成像预测胶质瘤 IDH1 表达的应用研究

葛鑫*[1,2]、张静 [2]

1. 兰州大学第二临床医学院

2. 兰州大学第二医院

目的：探讨集成磁共振成像定量弛豫图在预测胶质瘤异柠檬酸脱氢酶 1（IDH1）表达中的应用价值。

方法：本研究于 2020 年 8 月至 2021 年 9 月期间，前瞻性连续纳入 81 例经术后病理证实为胶质瘤的患者。所有患者均行轴位扩散加权成像（DWI）和增强前后集成磁共振成像。利用后处理工作站获得 DWI 表观扩散系数图（ADCmap）和集成磁共振成像定量弛豫图（T1map、T2map、PDmap 和 T1map+C），由两名放射医师分别独立在各参数图中勾画 ROI，计算得出胶质瘤 pre-T1、pre-T2、pre-PD、post-T1 和 ADC 值。免疫组织化学检测胶质瘤 IDH1 基因型（部分采用 DNA 测序验证），将入组病例分为 IDH1 突变型（IDH1m）和 IDH1 野生型（IDH1w）胶质瘤组。采用卡方检验或费舍尔精确检验比较组间分类资料差异，计量资料使用曼-惠特尼 U 检验，受试者工作特征曲线（ROC）用于评估诊断效能。

结果: IDH1m 胶质瘤 pre-T1 和 pre-PD 值显著低于 IDH1w 胶质瘤（*P* 分别为 0.022 和 0.015），IDH1m 胶质瘤 post-T1 和 ADC 值显著高于 IDH1w 胶质瘤（*P* 分别为 0.013 和<0.001），IDH1m 胶质瘤 pre-T2 值与 IDH1w 胶质瘤无显著性差异（*P*=0.928）。单参数分析中，ADC 值的 ROC 曲线下面积（AUC）高于 post-T1、pre-T1 和 pre-PD 值，但诊断效能相近（所有 *P*>0.05），多参数分析中，联合模型（pre-T1^{+}pre-PD^{+}post-T1^{+}ADC）的 AUC 达到了 0.805，特异性为 94.87%，显著提升了 post-T1、pre-T1 和 pre-PD 值的诊断效能（所有 *p*<0.05），但没有改善 ADC 值的诊断效能（*P*=0.190）

结论：集成磁共振成像定量弛豫图有助于鉴别胶质瘤不同 IDH1 基因型。Pre-T1、pre-PD、post-T1 和 ADC 值组建的多参数联合模型诊断效能优于集成磁共振成像单参数模型，可作为提高胶质瘤分子标记物鉴别诊断能力的有效策略。

关键字：集成磁共振成像；T1 弛豫时间；T2 弛豫时间；质子密度；胶质瘤；IDH1

22.血清 sTim-3 与 PG 联合检测对胃癌的诊断和预后评估中的价值

秦源*[1]、陈玲丽[1]、陈鑫栋[1]、方红明[2]、黄飚[1]

1. 浙江理工大学

2. 浙江萧山医院

目的：评估血清中可溶性 T 细胞免疫球蛋白及黏蛋白结构域分子 3(sTim-3)和胃蛋白酶原（PG）联合检测在胃癌(GC)中的临床应用价值。

方法：用时间分辨荧光免疫技术（TRFIA）对 69 例胃癌（GC）患者（其中 58 例首诊胃癌患者和 11 例 GC 术后患者），22 例胃部良性疾病（BGD）患者及 32 例健康人的血清 sTim-3、PGI、PGII 含量进行定量检测，通过接受者操作特征曲线（ROC）来分析 sTim-3 与 PG 联合检测对 GC 的临床诊断价值。

结果： GC 患者血清 sTim-3 水平（21.39±1.43 ng/mL）高于健康对照组（11.44 ± 0.52ng/mL），差异显著（P<0.0001）。GC 患者血清中 PGI 含量及 PGI/II 比值低于正常对照组，差异显著（P<0.001）。血清中 sTim-3 单独检测（AUC 0.8575, Sensitivity 77.59%, Specificity 90.63%）及 sTim-3+PGI/PGII 联合检测(AUC 0.9661, Sensitivity 86.21%, Specificity 96.88%)在 GC 中均具有较高的诊断价值。sTim-3+PG 联合检测还可以对胃癌复发进行有效的评估。

结论：sTim-3 +PGI/PGII 联合检测可以对 GC 进行辅助诊断和预后评估。

关键字：胃癌；时间分辨荧光免疫分析；Tim-3；血清标志物

23.TRIB2 通过βTrCP 调节 TFRC 泛素化并抑制肝癌细胞铁死亡敏感性

郭素素*、张骁、马丽芳、王佳谊

上海市胸科医院

目的：本部分旨在探究 TRIB2 调节铁稳态的机制，明确 TRIB2 调控肝癌细胞铁死亡敏感性的作用，为基于 TRIB2 的肝癌防治提供理论基础。

方法：采用流式细胞术检测细胞死亡与 ROS 水平。采用基于 ATP 的方法检测细胞增殖能力。采用基于 ELISA 的方法检测花生四烯酸与肾上腺酸水平。采用免疫共沉淀实验检测底物的泛素化。

结果：TRIB2 的敲除增加了肝癌细胞中不稳定铁并提高细胞对铁死亡的敏感性，TRIB2 的过表达则与之相反。进一步研究发现敲除 TFRC 可抑制 TRIB2 对不稳定铁的作用，证明 TFRC 是 TRIB2 调节细胞内铁稳态的靶点。免疫共沉淀实验证明βTrCP 可作为 TFRC 的 E3s 调控其泛素化水平。敲除βTrCP 可逆转 TRIB2 对不稳定铁和铁死亡相关 ROS 的抑制作用。

结论：本研究阐明了 TRIB2 通过 E3s βTrCP 促进 TFRC 泛素化并降低不稳定铁，最终降低肝癌细胞铁死亡敏感性的作用。

关键字: TRIB2, 铁稳态，铁死亡

24.miR-199-3p 过表达调控肺癌 A549 细胞生长、侵袭及上皮间质转化机制研究

熊伟杰*、王云涛、何朗

成都市第五人民医院

目的：探究 miR-199-3p 过表达靶向抑制 SOX5 对肺癌 A549 细胞生长、侵袭及上皮间质转化（EMT）的影响。

方法：荧光素酶实验检测 miR-199-3p 与 SOX5 靶向关系。构建 SOX5pcDNA 载体过表达 SOX5，将 miR-199-3p 与 pcDNA-SOX5 单独或联合转染 A549，将细胞随机分为对照组（Control 组）、

miR-199-3p 过表达组（mimic 组）、SOX5 组和 mimic+SOX5 组进行后续实验。克隆形成法检测肺癌 A549 细胞增殖情况，流式细胞术检测肺 A549 细胞凋亡情况，Transwell 检测肺癌 A549 细胞侵袭能力；荧光显微镜观察肺癌 A549 细胞 EMT 形态学变化；蛋白免疫印迹试验检测 Ki-67、PCNA、Bax、Bcl-2、Caspase-3、E-cadherin、N-cadherin、Vimentin 蛋白表达水平。

结果：与 SOX5 组比较，mimic+SOX5 细胞克隆形成率低，Ki-67、PCNA 蛋白水平降低，细胞凋亡率升高，Bax/BCl-2 和 cleaved Caspase-3/Caspase-3 比值升高，细胞侵袭数降低，E-cadherin 蛋白水平升高，N-cadherin、Vimentin 蛋白水平降低（$P<0.05$）。

结论：miR-199-3p 靶向 SOX5 抑制肺癌 A549 细胞增殖、侵袭和 EMT，并诱导细胞凋亡。

关键字：肺肿瘤；A549 细胞；细胞增殖；细胞凋亡；钙黏着糖蛋白类；SOXD 转录因子类；上皮间质转化

25.转录因子 FoxQ1 在肺癌患者血浆中的表达及预后诊断价值

牟永平*、孙玉书、温珍平、贺晓花、李劭恒、陈永霞、高红叶

内蒙古自治区肿瘤医院

目的：探讨血浆中转录因子叉头框 Q1 基因(Fork head box Q1,FoxQ1)表达水平与肺癌发病风险的关系，及其在肺癌预后中的诊断价值。

方法：收集内蒙古自治区肿瘤医院 2016 年 5 月至 2017 年 5 月接受治疗的肺癌患者 90 例，同期收治的年龄、性别与肺癌患者相匹配的 90 例健康体检人群。采集外周血液样本，通过酶联免疫(ELISA）方法检测 FoxQ1 在研究样本血浆中的表达情况，分析血浆 FoxQ1 蛋白表达水平与肺癌发病风险的关系，通过 Kaplan-Meier 来分析 FoxQ1 在血浆中的表达水平在肺癌预后诊断中的价值。

结果：肺癌患者血浆 FoxQ1 表达水平显著高于健康体检人群（中位数：195.44±44.39 *vs.* 177.57±38.56 (ng/ml)，t=-2.884, $P = 0.004$），晚期患者（TNM 分期为 III 期和 IV 期）血浆 FoxQ1 的表达水平显著高于早期患者（TNM 分期为 I 期和 II 期）（中位数：208.79 ±35.55 vs177.18 ±35.25（ng/mL）t=-5.76, $P<0.01$。以健康人群为参照，与 FoxQ1 表达低的个体相比，血浆 FoxQ1 表达高的个体肺癌发病风险上升（校正比值比为 2.36，95%可信区

间为 1.30 - 4.29）（$P < 0.05$）。分析 FoxQ1 表达量与预后关系，总体中位生存时间为 22.4±2.4 个月，其中低表达者中位生存时间 28.3±5.5 个月，高表达组为 16.2±2.1 个月，差异有统计学意义，x2=21.09 $P<0.01$，提示 FoxQ1 高表达患者预后不良。

结论： 血浆 FoxQ1 表达水平升高与肺癌发病风险升高显著正相关， FoxQ1 高表达患者预后不良，可用于临床病情评估。

关键字： 肺癌，血浆 FoxQ1，发病风险，预后诊断

26.影像组学在肝癌中的临床应用研究进展

吴婧冉[1]、杜成[2]、刘渤娜*[2]

1. 大连医科大学北部战区总医院培养基地

2. 中国人民解放军北部战区总医院

肝癌是常见恶性肿瘤之一。在全球范围，原发性肝癌发病率在所有癌症中居第六位，死亡率在所有癌症中居第三位。肝癌发病率高、早期症状隐匿、诊断滞后、多数患者确诊时已为中晚期，且预后差、死亡率高。因此早期发现、早期诊断、早期治疗直接影响肝癌的预后。现阶段针对肝癌的诊断及治疗方案正在不断完善，但肝细胞癌的预后情况仍然不容乐观。病理学方法是诊断肝癌的“金标准”，并且可以在一定程度上指导后续治疗。但由于完整的病理诊断需要取得手术标本，导致了病理诊断的滞后，同时术前的病理穿刺获得标本有限，无法整体评估肿瘤情况。传统影像学方法在诊治过程中有着无法替代的作用但是对于肝癌的诊断具有某些局限性，如影像学特征研究深度不足及影像医生主观性的特点等。影像组学作为一种新兴的、功能强大的非侵入性成像生物标志物，使用一系列数据挖掘算法和统计分析工具对图像特征进行高通量分析以获取与疾病相关的信息。目前已经在肝癌的诊断和鉴别、术前预测、肿瘤疗效评估等方面得到广泛地运用，表现出巨大的应用前景。本文围绕影像组学工作流程以及其目前在肝癌疾病中的诊断及鉴别诊断、影像基因组学及分子生物标志物、免疫治疗疗效预测等方面的临床应用进展进行综述 。

关键字： 肝癌；影像组学；影像生物标志物；人工智能

27.曲妥珠单抗对 HER-2/neu 检测试剂的干扰研究

肖雅*、渠文涛、史小芹

郑州安图生物工程股份有限公司

目的：曲妥珠单抗是一种抗 HER-2/neu 的单克隆抗体，它通过将自己附着在 HER-2/neu 上来阻止人体表皮生长因子在 HER-2/neu 上的附着，从而阻断癌细胞的生长，临床上主要用于治疗 HER-2/neu 过度表达的转移性乳腺癌。本文探讨了曲妥珠单抗对 HER-2/neu 检测试剂盒的检测结果是否有干扰。

方法：取 HER-2/neu 高、低值样本各一例，分别等分为三份，一份作为对照组 A，另外两份作为实验组 B 和 C；B 组加入 100 μg/mL 的曲妥珠单抗，C 组加入 400 μg/mL 的曲妥珠单抗。使用 AutoLumo A2000 plus 及配套试剂盒对三组样本进行检测，分析添加曲妥珠单抗后对检测结果是否有影响。

结果：和对照组 A 相比，B 组和 C 组的 HER-2/neu 检测结果偏差在-4.36%～6.92%之间，均小于±10%，结果差异有统计学意义（$P<0.05$），满足要求。

结论：考核 400 μg/mL 的曲妥珠单抗，对 HER-2/neu 检测试剂盒的检测结果无影响。人体表皮生长因子 2 检测试剂盒（磁微粒化学发光法）可以用于血清 HER-2/neu 的检测。

关键字：曲妥珠单抗；HER-2/neu；干扰；

28.儿童肾结石的血清代谢组学研究

温钧翔*

上海市第一人民医院

目的：本部分研究旨在采用超高效液相色谱串联质谱技术，分析儿童肾结石的特异性血清代谢谱，寻找与结石显著相关的小分子及代谢通路。

方法：1. 从 2018 年 1 月到 2019 年 7 月，以 30 例在复旦大学附属儿科医院肾脏科确诊为肾结石的儿童作为肾结石组，以 20 例在复旦大学附属儿科医院体检中心体检的健康儿童作为正常对照组，并采集血清样本。2.采用超高效液相色谱-四级杆/静电场轨道阱高分辨质谱技术分析 50 例血清样本，并采用主成分分析和正交偏最小二乘判别分析，结合代谢物

数据库，筛选和鉴定结石相关代谢小分子。3. 采用在线网站 MetaboAnalyst，并结合京都基因与基因组百科全书与人类代谢组数据库，寻找与儿童肾结石相关的代谢通路。

结果：1. 我们一共发现 40 种与儿童肾结石显著相关的代谢物，主要涉及视黄醇代谢、类固醇激素生物合成、卟啉和叶绿素代谢通路。2. 我们发现肾结石患儿血清中胆红素相对水平明显降低，而视黄醛、全反式维甲酸、孕酮和前列腺素 E2 相对水平明显增高。

结论：肾结石患儿具有独特的血清代谢谱，这可能与结石形成或机体代偿有关，有助于理解儿童肾结石发病机制以及开发新型防治策略。

关键字：肾结石，代谢组学，血清标志物

29.基于单细胞测序数据分析甲状腺乳头状癌的免疫特征

韩君*

北京康仁堂药业有限公司

目的：甲状腺乳头状癌(papillary thyroid carcinoma，PTC)的肿瘤免疫特征和异质性目前尚未完全阐明，本研究利用 GEO 数据库中的 GSE184362 数据集中的 3 个 PTC 样本和 3 个癌旁样本进行单细胞测序分析来揭示 PTC 的细胞异质性和免疫学特征。

方法：利用 Seurat 包对数据进行过滤质控，标准化，降维，聚类，对 PTC 的甲状腺细胞进行差异基因分析，利用 clusterProfiler 进行富集分析，利用 CellChat 进行细胞通讯分析，利用 Monocle 对 PTC 肿瘤组织和癌旁组织的 B 细胞进行拟时间分析，然后进行免疫组化验证。

结果：6 个样本经过质控筛选，得到 38934 个高质量细胞，经过降维，聚类等过程后，共得到 9 个主要的细胞亚群，不同样本之间具有明显的细胞数量异质性，证实了 PTC 的甲状腺细胞具有明显的免疫激活特性，PTC 细胞间具有更多的细胞通讯数目和更强的通讯强度，并且具有 CD23，CD70，CD6，CD86 等免疫信号的激活。细胞轨迹分析表明，PTC 肿瘤组织的部分 B 细胞特异性处于轨迹左上支，该分支的高表达基因于肿瘤坏死因子活性等信号通路密切相关。免疫组织化学验证显示与甲状腺正常组相比，HLA-DPA1 和 S100A4 在甲状腺癌中翻译水平升高，这与本文生信分析的结果相一致，进一步验证了本研究的可靠性。

结论：本研究采用多种生物信息学方法对其下游进行分析，阐明了 PTC 的免疫学特征，为 PTC 的药物开发及精准治疗提供了新的思路。

关键字：甲状腺乳头状癌；单细胞测序；免疫；细胞通讯；细胞轨迹

30.血清 CA15-3 和 HER-2/neu 在诊断良恶性乳腺疾病的 应用价值研究

田会会*、吴小田、高俊杰

郑州安图生物工程股份有限公司

研究目的：乳腺癌是女性中最常见的恶性肿瘤之一，特别在我国其发病率的增长速度超过了世界平均水平，死亡率仅次于肺癌而位居第二。据报道，2011 年我国城市女性乳腺癌发病率和死亡率分别排位在女性癌症的第 1 位和第 5 位，提示乳腺癌正严重威胁着女性的生命健康。由于该病早期没有明显症状，病人就医时通常已发展为晚期，如果能做到早诊断、早治疗，就可以提高患者的生存期及生存率。本文通过研究良恶性患者血清中 CA15-3 和 HER-2/neu 的值，以期为乳腺良恶性疾病的辅助诊断，疗效观察和预后判断提供一定的依据。

材料与方法：收集医院正常女性血清 84 例，乳腺良性病变患者血清 54 例，乳腺癌患者血清 36 例，采用试剂：郑州安图生物工程股份有限公司的糖类抗原 CA15-3 检测试剂盒（磁微粒化学发光法）、人表皮生长因子受体 2 检测试剂盒（磁微粒化学发光法）中试；仪器：全自动磁微粒化学发光仪 AutoLumo A2000 Plus。

结果：早期乳腺癌患者血清 CA15-3，HER-2/neu 与良性乳腺疾病患者及正常对照组之间有显著性差异，CA15-3 和 HER-2/neu 单个指标检测敏感度和准确度较低，2 个指标联合检测敏感度和准确度达到 81.45%和 83.04%；晚期乳腺癌患者 CA15-3 和 HER-2/neu 阳性率明显高于早期患者；复发转移乳腺癌病人两项指标均明显高于其他两组，但相互间无明显相关性，二者联合检测可提高对乳腺癌复发转移诊断的灵敏度和特异度；两项指标术后均明显低于术前，个别术后指标升高者提示预后不佳。

结论：CA15-3 和 HER-2/neu 联合检测对乳腺癌早期的诊断具有重要临床价值，且能提高诊断效能。对血清 CA15-3，HER-2/neu 连续动态监测将有助于判断疗效、疾病进展和预后，可对不同期乳腺癌的治疗，疗效观察和预后判断提供独立而客观的参考价值。

关键字：乳腺癌、良恶性乳腺疾病、CA15-3、HER-2/neu

31.血清β-HCG 在早期异位妊娠诊断中的意义

冉盼盼*

郑州安图生物工程股份有限公司

目的：探讨血清β-HCG 检测值对孕妇怀孕初期是否是异位妊娠、绒毛膜癌的早期诊断或正常怀孕鉴别的意义。

方法：收集河南省妇幼保健院门诊 2022 年 1 月-2022 年 7 月早孕期(4~7 周) 检查的 533 例孕妇检测β-HCG 的数据。分成正常怀孕组（323 例）、异位妊娠组（150 例）和绒毛膜癌（60 例）3 组，统计和分析 3 组人员的β-HCG 检测值。

结果：正常怀孕组β-HCG 结果是 58100±3695.3mIU/ml；异位妊娠组β-HCG 结果是 5900.1±1822.3mIU/ml；绒毛膜癌组β-HCG 结果是 101010.2±10693.6mIU/ml。异位妊娠与正常怀孕组比对 $P<0.05$；绒毛膜癌组与正常怀孕组比对 $P<0.05$；异位妊娠组与绒毛膜癌组比对 $P<0.05$，差异均有统计学意义。

结论：血清β-HCG 的检测值在早期异位妊娠诊断中具有很重要的意义。

关键字：β-HCG；异位妊娠；绒毛膜癌；早期诊断

32.基于 Bulk 和单基因转录组测序揭示铜死亡相关基因对肝细胞癌预后和免疫浸润的综合分析

杨成雷*、郭颜林、吴宗泽、黄军涛、向邦德

广西医科大学附属肿瘤医院

背景：肝细胞癌是一种高恶性的癌症，是最常见的恶性肿瘤之一，其预后预测具有挑战性。铜死亡是一种新发现的铜依赖性的调节性细胞死亡，其依赖于线粒体呼吸，直接与三羧酸循环脂酰化组分结合发挥作用。截至目前，作用于肝细胞癌中铜死亡相关基因的预后价值和其免疫微环境特征未见报道。

方法：在本研究中，先使用单变量 cox 回归分析筛选出铜死亡基因中与预后相关的基因，再对 TCGA 队列样本（361 例）进行差异分析，将得到的差异基因与铜死亡预后相关基因取交得到 TCGA 队列中与预后相关的铜死亡相关基因。然后使用最小绝对收缩和选择算子（LASSO）Cox 回归模型构建了 TCGA 队列中的多基因 signature。同时使用 ICGC 队列（231

例）和我们自己内部测序队列中的肝细胞癌（116 例）转录组和临床资料数据用于验证。随后，我们评估了三个队列中铜死亡相关的免疫微环境特征和功能富集结果。最后我们进一步在单细胞水平，探索了铜死亡相关基因在 T 细胞中的富集基于单细胞 RNA 测序。

结果：在 TCGA 队列中，大多数与铜死亡相关的基因（84.2%）在肝细胞癌组织和邻近正常组织之间差异表达。在单变量 Cox 回归分析中，16 个铜死亡相关的差异表达基因（DEG）与总生存率（OS）相关（均经校正 $p<0.05$），其中 9 个基因与预后相关。在多变量 Cox 回归分析中，风险评分是 OS 的独立预测因子（HR>1，$P<0.01$）。构建了 4 个基因 signature，按评分将患者分为高低两个风险组。与低风险组患者相比，高风险组患者的 OS 和预后皆显著降低。接受者操作特征（ROC）曲线分析证实了此模型的良好的预测能力。功能富集分析显示，高风险组中细胞分裂通路显著激活。同时在 ICGC 队列和内部测序队列中本风险评分模型的性能皆得到了验证。基于 bulk RNA-seq，铜死亡相关的肝细胞癌免疫微环境为显著富集 Treg 细胞和巨噬细胞。在单细胞水平进一步揭示了其与耗竭性增殖 T 细胞密切相关。

结论：一种新的铜死亡相关基因 signature 可用于预测肝癌的预后。铜死亡相关的 HCC 显著富集 Treg 细胞和巨噬细胞，并且与耗竭性增殖 T 细胞密切相关。本研究的结果为 HCC 患者有效的联合免疫治疗提供了理论依据。

关键字：肝细胞癌，铜死亡，预后，免疫浸润，单细胞转录组测序

33.缺氧肿瘤细胞源性外泌体通过 ATP 酶途径促进脂肪细胞脂滴释放参与鼻咽癌恶性进展

尹海朦*、游波、袁岭、尤易文

南通大学附属医院

目的: 研究缺氧肿瘤微环境中鼻咽癌细胞与常驻肿瘤基质细胞——脂肪细胞之间沟通串扰的机制。探究鼻咽癌(nasopharyngeal carcinoma， NPC)恶性进展中，缺氧肿瘤细胞通过外泌体动员脂肪细胞释放脂滴(lipid droplets, LDs)为其供能的可能性。论述阻断脂肪细胞 LDs 释放对裸鼠体内异体瘤生长的影响。

材料与方法: 统计鼻咽癌患者组织芯片中脂滴表面标记蛋白（Perilipin 2, PLIN2）和缺氧诱导因子（Hypoxia-inducible factor 1α，HIF-1α）的共定位情况以及与患者预后的相关性。选取鼻咽癌 CNE2 细胞和脂肪细胞作为研究对象，根据 Transwell 共培养模型，将脂肪细胞分

别与常氧和缺氧 CNE2 细胞共培养，用甘油三酯检测试剂盒分析培养基中的脂质含量。采用梯度离心法纯化缺氧 CNE2 源性外泌体，将脂肪细胞分别与去除和添加外泌体的条件培养基共培养，利用 C12 和 BODIPY 染料对培养基中的 LDs 进行定量。接着提取脂肪细胞培养基中的 LDs 与 CNE2 细胞共培养，用集落形成、EdU 和 CCK8 试剂盒检测细胞增殖能力的改变；用 Transwell 迁移实验和划痕实验检测细胞迁移能力的改变。然后通过转录组测序和 GSEA 分析，明确添加缺氧 CNE2 源性外泌体后，脂肪细胞中触发 LDs 释放的关键分子。利用 ChIP 实验和 Co-IP 实验探究具体的分子机制。最后在裸鼠模型中研究抑制脂肪细胞 LDs 释放对 NPC 恶性进展的作用。所有分析中 $P<0.05$ 被认为具有统计学意义，统计分析软件为 SPSS。

结果: 同时存在 PLIN2 和 HIF-1α高表达的鼻咽癌患者预后不良。在与缺氧 CNE2 细胞共培养的脂肪细胞培养基中，甘油三酯含量明显高于常氧组。在脂肪细胞培养基中添加缺氧 CNE2 源性外泌体后培养基中甘油三酯的释放增多。将纯化的 LDs 与 CNE2 细胞共培养后，CNE2 细胞的增殖和迁移能力增强。转录组测序和 GSEA 分析表明，AAA 型 ATP 酶（Vacuolar Protein Sorting 4 Homolog B,VPS4B）在常氧和缺氧外泌体组的脂肪细胞中差异表达。并且，添加 VPS4B 的特异性抑制剂 MSC1094308 后，脂肪细胞 LDs 释放减少，CNE2 细胞在裸鼠体内的成瘤能力被抑制，ChIP 实验结果表明，转录因子（Activating Transcription Factor 2，ATF2）在缺氧外泌体组的脂肪细胞中激活 VPS4B 的表达；Co-IP 实验证明脂肪细胞中 VPS4B 与膜联蛋白（Annexin A5，ANXA5）互作。体内抑制 ATF2-VPS4B-ANXA5 轴的表达可以抑制高脂饮食小鼠的成瘤能力。

结论: 肿瘤缺氧微环境中，鼻咽癌 CNE2 细胞通过释放外泌体激活脂肪细胞 ATP 酶途径依赖的 LDs 释放，促进 NPC 恶性进展。这种供能方式的发现为肥胖患者进展期的 NPC 治疗提供了新思路。

关键字: 外泌体，脂滴，鼻咽癌

34.乙酰化转移酶 NAT10 通过 DDX5/HMGB1 轴抑制 CD4+ T 细胞功能促进鼻咽癌的进展

谢海静*、游波、尤易文

南通大学附属医院

目的：鼻咽癌（NPC）是一种起源于鼻咽黏膜上皮细胞的恶性肿瘤，大部分患者主要分布在东亚和东南亚，中国是世界上发病率和死亡率最高的国家之一。鼻咽癌作为典型的“热肿瘤”，其肿瘤微环境中存在广泛的免疫抑制，尤其是 NPC 晚期患者，肿瘤免疫抑制显著增强，极大影响 NPC 治疗疗效。mRNA ac4C 乙酰化修饰作为 mRNA 修饰中唯一的乙酰化事件，与肿瘤免疫抑制、预后不佳密切相关。因此，加强对 NPC 肿瘤微环境中免疫抑制的机制研究具有十分重要的意义。

方法：我们通过 NPC 病人组织芯片分析发现 NPC 患者中 ac4C 乙酰化转移酶 NAT10 与临床分期、转移、复发及预后的相关性；ac4C 乙酰化免疫共沉淀测序（acRIP-seq）和 mRNA 转录组测序联合分析筛选出了下游差异基因，基于蛋白水平的差异，我们重点关注了这三个基因：DDX5、HLTF、CEBPG，并且通过测序结果中 IGV 可视化图和 acRIP-qPCR 探究 NAT10 对 DDX5、HLTF、CEBPG 的乙酰化修饰水平的作用；通过 Actd 稳定性试验和 CHX、MG132 翻译实验验证 NAT10 对 DDX5、HLTF、CEBPG 的具体作用机制；通过在线数据库预测以及蛋白互作、CHIP 寻找 DDX5、HLTF、CEBPG 共同调控的下游基因 HMGB1，并通过趋化因子阵列试剂盒分析其他可能受调控的分泌性蛋白。在 NAT10 转基因敲除鼠体内验证 NAT10 对免疫细胞的影响，并通过活体实验进一步验证 NAT10 抑制和 PD-1 治疗联用的效果。

结果：NPC 患者中 ac4C 乙酰化转移酶 NAT10 与临床分期、转移、复发及预后具有密切相关性；高通量测序发现 NAT10 促进 CEBPG、DDX5、HLTF mRNA ac4C 乙酰化；mRNA 稳定性试验和翻译实验证实 NAT10 促进 CEBPG、DDX5、HLTF mRNA 稳定性和翻译；蛋白互作实验显示 CEBPG、DDX5、HLTF 共同调控 HMGB1 的表达，CHIP 进一步显示 DDX5 调控 HMGB1 转录；NAT10 转基因敲除鼠外周血流式表明 NAT10 抑制 T 细胞的数量和功能，尤其是 CD4+T 细胞；此外在 B6 小鼠皮下成瘤模型中，在联用 NAT10 抑制剂 Remodelin 和 PD-1 抑制剂 Pembrolizumab 的情况下，可以进一步抑制肿瘤生长，增强 PD-1 治疗的敏感性。

结论：NPC 中高表达的 NAT10 通过促进 CEBPG、DDX5、HLTF ac4C 乙酰化提高其稳定性及翻译效率，进而促进 HMGB1 转录，分泌到肿瘤微环境中抑制 CD4+T 细胞的数量和功能，促进肿瘤细胞的免疫逃逸，抑制 NAT10 能够增加 PD-1 治疗敏感性。

关键字：鼻咽癌，ac4c 乙酰化修饰，NAT10，肿瘤微环境，免疫逃逸

35.IFN-γ通过上调肿瘤细胞表面 HLA-E 表达抑制 NK 细胞杀伤

郑慧*[1]、管晓琳 [2]、孟欣 [2]、郭林 [1,2]、卢仁泉 [1,2]

1. 复旦大学附属肿瘤医院检验科

2. 复旦大学上海医学院肿瘤学系

目的：HLA-E 是非经典 MHC-I 类分子，主要递呈某些肽段和 NK 细胞表面的抑制性受体结合，从而使肿瘤细胞逃避宿主的免疫监视。我们之前的研究已表明卵巢癌组织高表达 HLA-E 蛋白，然而，HLA-E 过表达与肿瘤微环境之间的关系尚不清楚。本研究旨在探讨肿瘤微环境如何上调 HLA-E 表达。

方法：我们通过人卵巢癌细胞系，用实时定量 PCR 分析 HLA-E 在转录水平的表达，以及利用 western blot 分析 HLA-E 在蛋白水平的表达。而细胞表面表达水平通过流式技术检测。NK 细胞杀伤能力通过肿瘤细胞 LDH 释放量检测。最后，卵巢癌患者 HLA-E 蛋白表达水平和无进展生存期之间的关系进行评估。

结果：我们发现细胞因子 IFN-γ可以通过激活 STAT1 信号通路上调 HLA-E 表达，并通过增加蛋白酶体活性而使细胞表面 HLA-E 表达升高。而且，我们观察到只有高水平的细胞膜表面 HLA-E 表达能抑制 NK 介导的细胞杀伤。在肿瘤微环境中，我们证实了 HLA-E 和 IFN-γ之间存在正相关关系。卵巢癌患者 HLA-E 表达水平和无进展生存期呈负相关。

结论：本研究表明 IFN-γ上调 HLA-E 表达并使肿瘤不易被免疫系统攻击。我们从一个全新的视角去探索肿瘤微环境和免疫逃逸之间的关系，并揭示了 IFN-γ治疗的促肿瘤作用。

关键字: HLA-E；NK 细胞；卵巢癌；免疫逃逸；肿瘤微环境

36.一种用于发现肺癌血浆生物标志物的深度代谢组学分析方法

李佳*

厦门市迈理奥科技有限公司

代谢组学从机体的动态代谢途径寻找生物标志物，有助于肿瘤的早期发现，实现肿瘤的早期诊断，但常规代谢组学方法易出现大量代谢物检测困难与定量不准确等问题，限制了代谢组学在临床的应用。本研究选择性别、年龄匹配的肺良性结节(n=50)和肺癌患者(n=50)，采用DeepMarker MT 代谢组学平台对血浆样本进行深度代谢组学分析，即通过高效化学同位素标记（High Performance Chemical Isotope Labeling，HP-CIL）技术对血浆中的代谢物进行化学衍生化处理，在 Agilent 6546 UHPLC-Q-TOF/MS 正离子模式下进行检测，并通过 IsoMS Pro 软件的三层级代谢物数据库对代谢物鉴定，最终在血浆中检测到 7330 个色谱峰对，其中有 6695 个代谢物（89.4%）可以被准确鉴定或者是推定得到。与肺良性结节相比，肺癌患者血浆的氨基酸代谢、胆汁酸合成代谢通路受到扰动较大，通过火山图与 PLS-DA 等分析筛选并鉴定出肺良性结节与恶性肿瘤患者血浆中显著差异的 45 种代谢物。因此，DeepMarker MT 代谢组学平台突破了常规代谢组学方法的瓶颈，体现了更高灵敏度、高覆盖率、高精准定量、高稳定性的全方位、多层面的领先优势，发现多个肺癌相关的潜在生物标志物，助力肺癌早诊领域的研究。

关键字: 肺癌；代谢组学； DeepMarker MT 代谢组学平台；高效化学同位素标记

37.逆转录转座子通过代谢重编程促进肺癌发生发展

张蕊*[1]、孙泽国[2]、刘芃芃[1]、于津浦[1]、张为家[2]

1. 天津医科大学肿瘤医院

2. 美国西奈山医学院

研究目的: 长散布元素-1（LINE-1，L1）是肿瘤遗传风险。L1 通过形成 L1 嵌合转录本（LCTs），在肿瘤发生发展中发挥重要作用。我们前期发现，LCT 能够改变肿瘤细胞花生四烯酸代谢。在本研究中，我们拟进一步探索全基因组 LCT 在肺癌发生发展中的功能。

材料与方法：我们开发了逆转录转座子基因融合估算程序，识别和量化来自 TCGA 肺癌队列（n=1146）和单细胞 RNA 测序数据集中的 LCT，并在天津肿瘤医院独立队列（n=134）中进一步验证这些 LCT。然后我们研究了肿瘤特异性 LCT（L1-FGGY）在肺鳞癌细胞增殖和小鼠肿瘤进展中的功能作用。

结果：LCT 与特定的代谢过程和线粒体功能相关，并与基因组不稳定性、低甲基化、肿瘤分期和肿瘤免疫微环境相关。基于 L1-FGGY 的功能分析表明，L1-FGGY 引起花生四烯酸代谢重编程，促进肿瘤生长，联合使用抗 HIV 药物 NVR 和代谢抑制剂 ML355 可有效抑制肿瘤生长。最后，我们确定了一组转录组特征，以将预后不良风险较高的肺鳞癌患者分层，这些患者可能受益于单独使用 NVR 或与抗代谢药物联合使用的治疗。

结论：本研究首次阐明了 LCT 在肺癌代谢重编程中的作用，为 LCT 预测预后提供了理论依据，并为提出肺癌治疗新策略提供了潜在的可能。

关键字：逆转录转座子，代谢重编程，肺癌

38.VAHS2 通过 Snail 依赖性 VEGF-D 信号通路促进肺鳞癌淋巴管生成

刘芃芃*、张蕊、于津浦

天津医科大学肿瘤医院

研究目的：肿瘤转移是肿瘤细胞进入淋巴管和血管，然后扩散到继发部位形成继发性肿瘤的过程。在血管生物学中，血管生成和抗血管生成治疗已被广泛研究，但导致淋巴管生成和淋巴转移的分子机制尚不清楚。

材料与方法：我们分析了来自癌症基因组图谱（TCGA）和基因表达综合数据库（GEO）的 937 例原发性肺鳞癌（LUSC）样本的 mRNA 表达谱，筛选与 LUSC 患者不良预后相关的差异表达最显著的基因，并在一个独立的中国 LUSC 队列中进行验证。我们重点研究了血管抑制素 2（VASH2），并通过在体外的 LUSC 细胞系 H520 中过表达 VASH2 来研究其在 LUSC 中增殖、凋亡、迁移、侵袭以及淋巴管生成中的生物学功能。我们还研究了 VASH2 靶向治疗 LUSC 异种移植小鼠模型的抗肿瘤疗效。

结果：我们发现了 12 个与 LUSC 患者预后不良密切相关的基因，其中 VASH2 在独立的中国 LUSC 队列中得到验证，并显示出很高的淋巴转移潜力。VASH2 在体内外均能促进 LUSC

细胞的增殖和侵袭。在 LUSC 细胞中过表达 VASH2 可通过上调血管内皮生长因子-D（VEGF-D）的产生促进人脐静脉内皮细胞（HUVECs）和人淋巴内皮细胞（HLECs）的扩增和管形成，而 VEGF-D 可通过敲减 Snail 而逆转。此外，通过干扰肿瘤组织中癌细胞的增殖和淋巴管生成，使用特异性抗体阻断 VASH2/VEGF-D 信号显著抑制小鼠肿瘤生长。

结论：总之，VASH2 以 Snail 依赖的方式促进淋巴管生成和肿瘤生长，这可能是早期诊断和预后预测的新生物标记物，也是 LUSC 的潜在治疗靶点。

关键字: VASH2；Snail；淋巴管生成；肺鳞状细胞癌；内皮生长因子-D（VEGF-D）

39.RB1CC1 介导的转录重编程使肿瘤细胞对铁死亡敏感

薛翔飞*、张骁、马丽芳、王佳谊

上海市胸科医院

目的：铁死亡是一种受调节的细胞死亡形式，也是癌症研究领域的一个重要课题。然而，使肿瘤细胞对铁死亡敏感的信号通路和因素仍然难以捉摸。本研究旨在探究 RB1 诱导卷曲蛋白 1（RB1-inducible coiled-coil 1，RB1CC1 或称为 FIP200）相关信号通路调节肿瘤细胞铁死亡敏感性的机制，为靶向 RB1CC1 进行肿瘤治疗提供理论基础。

方法：我们通过测量细胞死亡和脂质活性氧（Reactive oxygen species，ROS）的产生来确定细胞中铁死亡的水平。检测 4-羟基壬烯醛的表达和丙二醛的水平来判断组织中发生脂质过氧化的程度。通过免疫印迹和免疫组织化学实验分析 RB1CC1 和相关蛋白的表达情况。免疫荧光用于确定 RB1CC1 的亚细胞定位。我们构建了一系列 RB1CC1 突变体来研究 RB1CC1 核转位的机制。在电泳凝胶中补充 PhostagTM 试剂来观察代表了 RB1CC1 发生磷酸化的超移带。为了检查肿瘤细胞中铁死亡和 RB1CC1 依赖性转录程序，我们进行了染色质免疫沉淀测序分析。染色质构象捕获实验用于验证 RB1CC1 相关增强子和潜在的铁死亡相关基因启动子之间的相互作用。为了评估 Rb1cc1 基因在脂质过氧化中的必要性以及 c-Jun N-末端激酶（c-Jun N-terminal kinase，JNK）激动剂对于咪唑酮 Erastin（Imidazole ketone erastin，IKE）疗效的影响，我们构建了细胞源性异种移植小鼠模型。此外，我们使用肝细胞癌小鼠模型阐明了 Rb1cc1 在基于 IKE 的肝癌治疗中的重要性。

结果：RB1CC1 能被脂质 ROS 上调，并且第 537 位丝氨酸的磷酸化造成的 RB1CC1 的核转位对于肿瘤细胞中的铁死亡敏感是必不可少的。在诱导铁死亡后，核 RB1CC1 共享叉头盒

（Forkhead box，FOX）家族转录因子的结合基序，募集延伸复合体蛋白 3（Elongator complex subunit 3，ELP3）以加强与铁死亡相关的增强子内的组蛋白 H4K12Ac 修饰。这也刺激了铁死亡相关基因的转录。例如含卷曲螺旋域蛋白 3（Coiled-coilhelix- coiled-coil-helix domain containing 3，CHCHD3），其增强了线粒体功能，从而在诱导铁死亡后早期阶段就能起到促进线粒体 ROS 产生的效果。FDA 批准的能发挥 JNK 激活作用的一些药物能增强 RB1CC1 核转位并使肿瘤细胞对铁死亡更敏感，这强烈表明 JNK 位于 RB1CC1 的上游。RB1CC1 的核定位还与临床肺癌标本中的脂质过氧化水平相关。此外在使用铁死亡激动剂抑制小鼠肝脏肿瘤发生发展的治疗过程中，Rb1cc1 基因也是必需的。

结论：我们的研究结果表明，RB1CC1 相关信号使肿瘤细胞对铁死亡敏感，靶向 RB1CC1 可能对肿瘤治疗有益。

关键字：药物筛选，ELP3 介导的组蛋白修饰，增强子，核转位，Rb1cc1 敲除小鼠，ROS

40.乳腺化生性癌的诊断和治疗进展

孙红娜*、徐君南、孙涛

辽宁省肿瘤医院

乳腺化生性癌（MpBC）是一组罕见、形态学异质且极具侵袭性的疾病，病理可以分为多种组织学亚型。MpBC 定义为组织学上至少存在典型的上皮和间充质细胞 2 种成分。因其罕见，目前尚无针对 MpBC 的标准化治疗，治疗推荐多由浸润性导管癌外推而来。近年来，随着研究技术的提高，MpBC 越来越被重视。研究者对其进行了大量研究，并取得实质性进展。MpBC 多为三阴性乳腺癌（TNBC），与传统 TNBC 相比，MpBC 生存更差。手术、化疗和放疗仍然是 MpBC 的主要治疗方法。MpBC 具有遗传异质性，存在体细胞突变，最常见的是 TP53、PIK3CA、端粒酶逆转录酶（TERT）、表皮因子生长受体（EGFR）和磷酸酶及张力蛋白同源物（PTEN），这些基因均为潜在的治疗靶点。此外，在这些肿瘤中也观察到 PD-L1 的过表达，提示免疫治疗在MpBC 的治疗中可发挥作用。本研究对MpBC 各种类型的临床病理特征、发病机制、分子学改变、治疗及预后进行阐述，为 MpBC 的诊治提供参考依据。

关键字：乳腺化生性癌；临床病理特征；发病机理；分子学改变；靶向治疗；免疫治疗；预后

41.血清 fPSA 与 PSA 的比值在 PSA 低值区的意义研究

田会会*、蔡高灿

郑州安图生物工程股份有限公司

研究目的：在泌尿外科临床实践中，血清前列腺特异性抗原（PSA）及 PSA 为 4-10ng/mL 时，fPSA 与 PSA 的比值应用被认为是前列腺癌（PCa）筛查的最佳标志物。尽管 PSA 检测可用于前列腺癌诊断和治疗，但其对前列腺癌的敏感性和特异性不足，无法被视为早期检测恶性肿瘤的理想标志物。血清 PSA 水平升高不是前列腺癌的确诊指标；相反，低于参考范围的水平也不一定表明其不存在。早期研究显示，38%至 50%具有临床意义的前列腺癌患者的血清 PSA 水平在 0- 4ng/mL 之间。本文通过研究血清 fPSA 与 PSA 的比值在 PSA 低值区（0-4ng/mL）的意义，以期为前列腺癌的早期诊断和发现提供指导。

材料与方法：收集正常对照组男性血清 56 例，前列腺疾病患者血清 1086 例，使用 AutoLumo A2000 检测系统和配套试剂盒进行 PSA 和 fPSA 检测，并将 PSA 在 0-4ng/mL 之间且 f/t≤20%的数据根据临床诊断信息进行归纳分析。

结果：正常对照组 PSA 浓度在 0.26～3.55ng/mL 之间，f/t 在 25%～60%之间。PSA 浓度 1.0～2.99 ng/mL 且 f/t≤20%的患者中，有 68 例进行了活检，检出 6 例癌症，检出率为 8.8%；PSA 浓度 3.0～3.99 ng/mL 且 f/t≤20%的患者中，有 82 例建议活检，其中 54 例实施(65.8%)，8 例检出癌症，检出率为 14.8%。PSA 浓度 1.0～3.99 ng/mL 且 f/t＞20%的患者中，有 52 例进行了活检，检出 1 例癌症，检出率为 1.9%。

结论：虽然前列腺特异性抗原(PSA)在 1.0～3.99 ng/mL 范围内前列腺癌检出率较低，但在此范围内 fPSA 与 PSA 的比值仍具有相关性，f/t 越低，前列腺癌检出率相对会高。所以低 PSA 范围中 f/t 比值可能有助于鉴别前列腺癌。如果早期获得诊断，再结合前列腺指诊、影像学检查及前列腺组织活检等，可尽早地对 PSA<4ng/mL 的患者做出有价值的诊断提示，使之得到良好的治疗效果，为临床治愈赢得时间。

关键字: PSA，低值区，f/t，前列腺癌

42.线粒体转录延伸因子（TEFM）在人脑胶质瘤组织中的表达及预后意义

刘如爱*[1]、罗中贵[1]、自加吉[1]、王心萌[1]、赵妤[2]、余敏[3]、熊伟[1]

1. 大理大学基础医学院

2. 大理白族自治州第一人民医院病理科

3. 云南大学生命科学学院

目的：探讨线粒体转录延伸因子（TEFM）在脑胶质瘤组织中的表达及其与临床病理特征和预后的关系。

方法：收集大理州第一人民医院 2012 年 1 月~2017 年 6 月手术切除并经病理证实的 68 例脑胶质瘤组织及 35 例非肿瘤脑组织。采用免疫组化 SP 法检测以上组织中 TEFM 蛋白的表达水平，采用实时荧光定量 RT-PCR 检测以上组织中 TEFM mRNA 水平，分析脑胶质瘤组织和非肿瘤脑组织中 TEFM 蛋白和 mRNA 表达差异。分析 TEFM 基因 mRNA 表达量与临床病理参数的相关性。根据随访资料采用 Kaplan-Meier 分析 TEFM 基因 mRNA 表达量和患者预后的相关性。采用 COX 比例风险回归模型分析影响脑胶质瘤患者预后的因素。

结果：免疫组织化学结果显示，TEFM 蛋白主要表达于细胞质，且在不同级别脑胶质瘤组织中的阳性表达率（91.18%）明显高于非肿瘤脑组织中的阳性表达率（37.14%），组间差异极显著（$P<0.01$）。脑胶质瘤患者 TEFM 基因 mRNA 表达量与患者年龄、病理分级、病理类型、偏侧性与慕上位置均具有显著相关性（$P<0.05$）；Kaplan-Meier 生存分析显示，TEFM mRNA 表达水平显著影响脑胶质瘤患者的总体生存率（OS）和无疾病进展生存率（DFS），TEFM 高表达的患者 OS 和 DFS 显著缩短（Log-rank $p<0.05$）；COX 多因素回归分析显示，患者年龄、病理分级和病理类型是影响脑胶质瘤患者预后的独立因素（$P<0.05$）。

结论：TEFM 蛋白和 mRNA 在脑胶质瘤组织中比非肿瘤脑组织中表达显著升高，TEFM 可能参与脑胶质瘤的病理进展过程，且 TEFM 高表达的患者 OS 和 DFS 显著缩短。

关键字：线粒体转录延伸因子；脑胶质瘤；免疫组化；预后

43.乳腺癌易感基因在乳腺癌中的作用研究进展

张润娇*、于津浦

天津医科大学肿瘤医院

目的：乳腺癌易感基因 1/2 通过同源重组修复受损的 DNA。此外，乳腺癌的局部免疫微环境与患者的预后密切相关。但是在乳腺癌中，乳腺癌易感基因 1/2 表达与局部免疫抑制微环境的关系尚不清楚。本研究旨在探讨两者之间的相关性。

材料与方法：我们收集了 2014 年 1 月至 2018 年 10 月来自天津医科大学肿瘤医院 156 例乳腺癌患者新鲜的乳腺原发肿瘤、配对的正常组织以及外周血。分析了乳腺癌易感基因 1/2 胚系突变与原位微环境免疫状态的关系。

结果：结果表明乳腺癌易感基因 1/2 的胚系突变与乳腺癌易感基因 1/2 蛋白的表达并不一致，且乳腺癌易感基因 1/2 蛋白表达阴性的患者免疫细胞的比例高于乳腺癌易感基因 1/2 蛋白表达阳性的患者(p<0.05)。乳腺癌易感基因 1/2 蛋白表达阴性的患者 CD3+ T 细胞的程序性死亡配体 1、程序性死亡蛋白 1、细胞毒性 T 淋巴细胞抗原 4 的表达高于乳腺癌易感基因 1/2 蛋白表达阳性的患者(p<0.05)。乳腺癌易感基因 1 的蛋白表达与乳腺癌患者家族史(p= *0.006*)、局部淋巴结转移(p= 0.001)和 TNM 分期(p≤0.001)显著相关。乳腺癌易感基因 2 蛋白表达与局部淋巴结转移(p≤0.001)、III 期发生率(p= 0.003)和分子分型(p≤0.001)显著相关。此外，G1 组及病理 III 期患者的 5 年无病生存期较其他组及其他 TNM 分期患者更差。

结论：总之，对于乳腺癌易感基因 1/2 蛋白表达阴性的乳腺癌患者，免疫治疗可能是一种潜在的治疗方法。

关键字：乳腺癌；乳腺癌易感基因 1/2；临床病理特征；免疫细胞浸润；免疫检查点；预后

44.KAP1 基因在人恶性胸膜间皮瘤（MPM）中表达的临床意义及对 MPM 细胞增殖和侵袭的影响

王心萌*[1,2]、周崇熙[1,2]、李彬[1,2]、自加吉[1,2]、普元倩[1,2]、邱璐[3]、梅雯[4]、张也频[4]、熊伟[1,2]

1. 大理大学基础医学院

2. 云南省高校临床生物化学检验重点实验室

3. 楚雄师范学院化学与生命科学系

4. 楚雄彝族自治州第一人民医院病理科

目的：KRAB 相关蛋白 1（KRAB-associated protein 1, KAP1）又称转录中介因子 1β（transcriptional intermediary factor 1β, TIF1β），也称三结构域蛋白 28（tripartite motif-containing protein 28, TRIM28），是一种多功能的染色质解读器和转录中介因子，在诸多转录调控复合体中起桥梁作用。本研究旨在分析 KAP1 基因在人恶性胸膜间皮瘤（malignant pleural mesothelioma, MPM）细胞和组织中的表达，评价其与 MPM 患者预后的关系，并初步探讨 KAP1 基因在 MPM 中的作用机制。

方法：采用 RT-qPCR 分析人正常胸膜间皮细胞系（LP9）和上皮样型 MPM 细胞系（NCI-H28）、肉瘤样型 MPM 细胞系（NCI-H2052）、双相混合型 MPM 细胞系（NCI-H2452）中 KAP1 基因 mRNA 表达量；采用 RT-qPCR、Western blotting 和免疫组化检测 38 例 MPM 组织及 19 例非 MPM 胸膜组织中 KAP1 基因表达水平。构建 Kaplan-Meier 模型探讨 KAP1 基因表达量对 MPM 患者预后的影响。通过 siRNA 技术沉默 H2052 细胞中 KAP1 基因表达，观察其对 H2052 细胞周期、细胞增殖、侵袭和细胞凋亡等恶性生物学行为的影响。

结果：与非 MPM 胸膜细胞和组织相比，MPM 细胞和组织中 KAP1 基因的表达量均呈现显著的增高（P<0.01）。KAP1 基因表达量与 MPM 患者总生存率（OS）和无疾病进展生存率（DFS）均呈显著负相关（Logrank P＜0.05）。KAP1 作为转录激活因子，是 G2/M 转化和有丝分裂执行所必需的。siRNA 敲低 KAP1 基因表达导致 H2052 细胞周期出现 G2/M 期阻滞，G2/M 转换相关基因（AURKA、AURKB、BIRC5、INCENP、CDCA8、BMYB 和 FOXM1）表达水平显著下调（P<0.01），通过抑制 H2052 细胞有丝分裂进程，进而显著抑制细胞增殖和侵袭，导致细胞出现大量死亡。

结论: KAP1 基因在 MPM 细胞和组织中均呈现显著增高，且 KAP1 基因量与 MPM 患者的 OS 和 DFS 呈显著负相关。敲低 KAP1 基因导致 MPM 细胞出现 G2/M 期阻滞和 G2/M 基因表达下调，显著抑制 MPM 细胞增殖和侵袭，导致细胞死亡。

关键字: KRAB 相关蛋白 1；胸膜间皮瘤；免疫组化；有丝分裂；预后意义

45.云南省青石棉污染区恶性胸膜间皮瘤与致瘤性猿猴病毒 SV40 的关联研究

王播勇*[1,2]、陈欣[1,2]、普元倩[1,2]、李锦松[1,2]、自加吉[1,2]、梅雯[3]、赵一[3]、邱璐[4]、熊伟[1,2]

1. 大理大学基础医学院

2. 云南省高校临床生物化学检验重点实验室

3. 楚雄彝族自治州第一人民医院病理科

4. 楚雄师范学院化学与生命科学系

目的: 我国云南省楚雄彝族自治州大姚县 5% 的地表散布着蓝色的青石棉，是恶性胸膜间皮瘤（malignant pleural mesothelioma, MPM）的高发区。早年的流行病学调查资料显示，大姚县青石棉污染区恶性间皮瘤发病率达到 8.5/10 万人（1977-1983 年）、17.75/10 万人（1987-1995 年），高出一般人群几十倍。本研究旨在探讨致瘤性猿猴病毒 SV40 (Simian virus 40, SV40) 是否与云南省大姚县青石棉污染区 MPM 的发生相关。

方法: 收集大理大学第四附属医院（楚雄彝族自治州第一人民医院）和大姚县人民医院胸外科 2014 年 1 月～2019 年 12 月诊治的 51 例有石棉接触史的 MPM 患者肿瘤组织和 12 例非 MPM 患者的胸膜组织（包括肺大疱、肺结核等疾病）。同时，体外培养人正常胸膜间皮细胞系 Met5A（SV40 转化的间皮细胞）和 MPM 细胞系 NCI-H28（上皮样型）、NCI-H2052（肉瘤样型）、NCI-H2452（双相混合型）。提取各组细胞和组织基因组 DNA 后，用文献报道（Lopez-Rios F, Lancet, 2004）的 3 组低污染风险引物（SVINT、SVfor2 和 SVTA1）对 SV40 大 T 抗原（TAg） 的基因片段分别进行聚合酶链式反应（PCR）扩增检测。另外，用 2 种 SV40 相关抗体（Pab l01 和 Ab-2）分别进行 Western blotting 和免疫组织化学染色，检测 MPM 肿瘤组织和 MPM 细胞系中是否存在 SV40 TAg。

结果:（1）PCR、Western blotting 和免疫组化染色结果均显示 Met5A 细胞系中 SV40 为阳性，含有 SV40 TAg 基因和蛋白质。而各种 MPM 细胞系 NCI-H28、NCI-H2052 和 NCI-H2452 中

SV40 均为阴性。（2）在 12 例非 MPM 组织和 51 例 MPM 组织中，3 组低污染风险引物的 PCR 反应均为阴性。（3）在 12 例非 MPM 组织和 51 例 MPM 组织中，2 种抗体的免疫组化染色均未检测出 SV40 TAg。

结论：云南省青石棉污染区 MPM 的发生与 SV40 病毒感染的关系可能不密切，青石棉接触可能才是导致 MPM 发生的主要原因。

关键字：恶性胸膜间皮瘤(MPM)；青石棉；猿猴病毒 SV40；聚合酶链式反应；免疫组织化学

46.脑膜转移瘤患者脑脊液中存在基因组不稳定性

王鹏*、章巧玲、于津浦

天津医科大学肿瘤医院

目的：本研究旨在探讨脑膜转移瘤(MM)患者脑脊液基因组不稳定性。

方法：我们收集了 15 例 MM 患者和 1 例脑实质转移(BPM)患者的血液和脑脊液标本。基于 543 个肿瘤相关基因组成的 panel 测序数据，分析了所有患者脑脊液和血浆 cfDNA 的基因组不稳定性状况。同时有 9 名患者接受了低深度全基因组测序(WGS)分析，以验证基因组不稳定性的存在，然后应用非整倍体评分进行基因组评分。并使用诊断特异性分级预后评估(DS-GPA)评分来评估脑膜转移瘤患者的临床状况。

结果：MM 脑脊液 cfDNA 与血浆 cfDNA 基因组状态有显著性差异。其中 12 例患者脑脊液 cfDNA 检出基因组不稳定，其余 3 例基因组稳定。脑脊液和石蜡包埋组织切片显示 BPM 患者基因组稳定。所有患者血浆 cfDNA 均未发现基因组不稳定性。在 10 例基因组不稳定的 MM 患者中检测到 EGFR、ERBB2、ALK 和 KRAS 基因的敏感突变，MET 和 ERBB2 基因拷贝数增加，在 1 例基因组稳定的 MM 患者中检测到 EGFR 基因突变。值得注意的是，与基因组稳定的患者相比，基因组不稳定的 MM 患者总生存率较低，非整倍体评分和肿瘤突变负荷较高。此外，DS-GPA 分数较高的 MM 患者生存率较高。

结论：MM 患者脑脊液 cfDNA 而非血浆 cfDNA 存在基因组不稳定性，提示克隆进化。

关键字：基因组不稳定，脑脊液，脑膜转移，全基因组测序，无细胞 DNA

47.鉴定用于预测神经母细胞瘤预后和免疫微环境的糖基转移酶特征

韩雷*、沙永亮、赵强、于津浦

天津医科大学肿瘤医院

目的：神经母细胞瘤（Neuroblastoma , NB）是儿童最常见的实体瘤之一。糖基转移酶(Glycosyltransferases, GTs) 在肿瘤发展和免疫逃逸中起着至关重要的作用，并已被用作各种肿瘤的预后生物标志物。然而，对于 NB 中 GTs 的生物学功能和预后意义仍然知之甚少。

方法：收集来自 NCBI 基因表达数据库 (GEO) 和 TARGET(Therapeutically Applicable Research to Generate Effective Treatments)数据库的表达数据作为训练和测试数据。根据肿瘤进展状态，鉴定出差异表达的 GTs。我们通过支持向量机、最小绝对收缩和选择算子以及 Cox 回归构建了基于 GTs 的 NB 预后相关模型(GTscore)。

结果：通过应用机器学习算法，我们建立了基于 GTs 表达的，与 NB 预后相关模型(GTscore)。在这个模型中包括 4 个预后相关的 GTs。通过多个数据集验证，我们建立的 GTscore 是 NB 的独立预后风险因素。同时我们发现，在 NB 队列中，高 GTscore 组的患者年龄较大，MYCN 扩增，分期较高，临床风险评估为高风险人群。具有高 GTscores 的样本显示高二唾液酸神经节苷脂 (GD2) 和神经元特异性烯醇化酶表达水平。此外，在高 GTscore 组中观察到免疫细胞浸润较少。该 GTscore 还与趋化因子（CCL2、CXCL9 和 CXCL10）和免疫检查点基因（细胞毒性 T 淋巴细胞相关蛋白 4、颗粒酶 H,和颗粒酶 K)相关。在另外一种如 NB 一样来源于神经外胚层细胞的肿瘤--黑色素瘤中发现，低 GTscore 也与黑色素瘤患者抗 PD-1 免疫治疗的反应增强有关。

结论：我们构建的 GTscore 揭示了 GTs 表达与 NB 预后、GD2 表型和免疫浸润之间的关系，为预测 NB 的预后和免疫治疗反应提供了新的线索。

关键字: 糖基转移酶；神经母细胞瘤；预后模型；GD2；免疫微环境

48.中国胃癌患者基因谱以及分子分型研究

程亚楠*[1]、卜德超[2]、董莉[1]、赵屹[2]、于津浦[1]

1. 天津医科大学肿瘤医院

2. 中国科学院计算技术研究所

研究目的: 胃癌存在很大的异质性。基于基因组图谱精确、全面的分子分型为识别胃癌潜在的治疗靶点提供了充分证据，在指导胃癌患者的个体化精准治疗方面具有很大的潜力。

材料与方法: 我们对 206 份中国胃癌样本进行了 435 肿瘤相关基因的高通量测序进行全面的基因谱分析，其中包括 69 与临床治疗相关的靶基因。

结果: 206 例患者中至少 182 例患者(88.3%)存在 435 个基因中的一个突变，206 例患者中的至少 134 例(65.0%)存在患者一个拷贝数突变(SCNA)。在本研究中，我们发现了 5 个与临床病理特征密切相关的基因改变，包括 TP53、CDH1 和 KMT2D 基因突变，以及 ERBB2 和 CDKN1B 的 SCNA。根据 TCGA 胃癌分子分型将我国胃癌患者分为 EBV (N=4)、MSI-H (N=13)、染色体不稳定性(CIN) (N=54)和基因组稳定性(GS) (N=135) 4 种亚型。此外，206 例患者中 61 例(29.6%)为突变负荷高胃癌患者(TMB-H)。根据突变负荷和与临床治疗相关的基因进行聚类分析，将 206 例患者进一步分为 7 个亚组，分别为 TMB-H (G1, N=61)、ERBB2 扩增(G2, N=10)、ATM 丢失(G3, N=10)、BRCA2 突变(G4, N= 7)、CDKN2A/B 缺失(G5, N=10)、PI3KCA 突变(G6, N=9)和少突变(G7, N=99)。

结论: 我国胃癌患者具有独特的基因谱，基于突变负荷和与临床治疗相关的基因，我国患者可分为 7 个分子亚型，为选择最佳的个体化靶向治疗和免疫治疗提供了参考。

关键字: 胃癌；高通量测序；突变负荷；分子分型

49.中国家族遗传性乳腺癌家系易感基因突变谱

董莉*

天津医科大学肿瘤医院

目的: 乳腺癌已成为中国女性最常见的恶性肿瘤，约 5%~10%的乳腺癌患者具有遗传易感性，表现为家族聚集性。本研究的目的是探究在中国家族性乳腺癌家系中 43 个具有不同外显率的基因的胚系突变特征，分析其与中国家族性乳腺癌家系表型特征的相关性。

方法：本研究收集了 27 例家族性乳腺癌家系，包括 45 例患者和 71 例健康家系成员，共 116 例样本。利用二代测序技术（NGS）平台（Ion Torrent S5™测序系统），检测了 43 个肿瘤相关易感基因，筛选中国家族遗传性乳腺癌家系易感基因的突变，探究在中国家族性乳腺癌家系中 43 个具有不同外显率的基因的胚系突变特征，分析其与中国家族性乳腺癌家系表型特征的相关性。

结果：本研究共筛选出 81 个高质量胚系突变，分别位于 27 个基因上，其中 80.8%（21/26）为 DNA 损伤修复基因。在 81 个胚系突变中，21.0%（17/81）突变位于 BRCA1/2 基因上，BRCA1/2 基因仍然是最常见的突变基因。在 27 个家族性乳腺癌家系中，48.1%（13/27）由已知遗传易感基因突变导致，51.9%（14/27）原因未知。25.9%（7/27）的家系与 BRCA1/2 基因突变相关，22.2%（6/27）的家系与非 BRCA 基因突变相关，包括 BLM、BRIP1、MSH2、MSH6、RAD51C 和 RET 基因，说明在家族性乳腺癌患者家系中检测非 BRCA 基因突变，使得遗传性乳腺癌家系的检出率提高了 22.2%。在 96 例突变携带者中，41.7% (40/96) 携带 BRCA 突变，88.5% (85/96) 携带非 BRCA 突变，其中 30.2% (29/96) 同时携带 BRCA 突变和非 BRCA 突变。在收集的家族遗传性乳腺癌患者中，携带 BRCA 突变组和突变阴性组相比，BRCA 突变患者具有更高的区域淋巴结的转移率（*P*=0.049），而非 BRCA 突变患者和突变阴性患者相比，非 BRCA 突变的患者可能更容易伴发乳腺良性疾病（*P*=0.024）。

结论：本研究证明在适宜人群中开展 BRCA 基因及其他乳腺癌易感基因的检测十分必要，多个乳腺癌易感基因的检测对于筛选中国家族性/遗传性 BC 的潜在致病性种系突变更有价值。

关键字：家族性/遗传性乳腺癌；二代测序；易感基因；DNA 损伤修复；临床特征

50.EphB1 通过 PI3K/AKT 信号通路促进食管鳞状细胞癌 EC-9706 细胞增殖、迁移、侵袭，并抑制其凋亡

张键*、罗咏萍、刘毅、陈宗华

宜宾市第二人民医院

目的：研究促红细胞生成素产肝细胞受体 B1(Erythropoietin-producing human hepatocellular receptor B1，EphB1)对食管鳞状细胞癌 EC-9706 细胞增殖、迁移、侵袭及凋亡的影响，并探索其可能的作用机制。

方法：qRT-PCR 分析 40 对食管鳞癌患者的癌组织及邻近正常组织中 EphB1 表达情况，并分析其临床特征。在 EC-9706 细胞中分别转染 siEphB1 RNA 和 oeEphB1 RNA 及其阴性对照，qRT-PCR 和蛋白印迹试验检测转染效率；CCK8 实验分析 EphB1 对细胞活力的影响；Hoechst 33258 染色和流式细胞学实验检测细胞凋亡；划痕愈合实验及 Transwell 实验明确细胞迁移及侵袭能力；蛋白免疫印迹试验检测 EphB1 蛋白，增殖相关蛋白增殖细胞核抗原（PCNA），凋亡相关蛋白 Bad、Bcl-2、Caspase 3 及剪切型-caspase 3 蛋白，侵袭转移相关蛋白基质金属蛋白酶 9(MMP-9)、MMP-2、Snail、波形蛋白(Vimentin)、N-cadherin、E-cadherin 蛋白，以及 PI3K/AKT 通路相关蛋白 PI3K、AKT、P-AKT 的表达。

结果：研究结果发现 EphB1 在食管鳞癌组织和细胞系中高表达，EphB1 的表达水平与食管鳞癌患者的 TNM 分期、淋巴结转移和远处转移具有相关性。与对照组相比，通过细胞转染技术沉默 EphB1 和过表达 EphB1 使 EC-9706 细胞的增殖、迁移、侵袭能力明显降低或增强，并诱导或抑制细胞凋亡。在蛋白水平，siEphB1 和 oeEphB1 处理 EC-9706 细胞 48h 后，增殖相关蛋白 PCNA 蛋白表达水平分别显著降低或增加，并分别增加或降低促凋亡相关蛋白 Bad、cleaved-caspase 3 的表达水平，下调或上调抗凋亡蛋白 Bcl-2、Caspase 3 的蛋白表达，抑制或促进侵袭转移相关蛋白标记 MMP-9、MMP-2、Snail、Vimentin、N-cadherin 的蛋白活性，但上调或下调 E-cadherin 的表达水平。同时，Western blotting 实验结果还证实 EphB1 可诱导食管鳞癌 EC-9706 细胞中通路蛋白 PI3K、p-AKT 的活性增强。

结论：EphB1 可能通过调控 PI3K/AKT 信号通路促进食管鳞状细胞癌 EC-9706 细胞的增殖、迁移及侵袭，并抑制其凋亡。

关键字：食管鳞状细胞癌，EphB1，PI3K/AKT

51.长链非编码 RNA AC012073.1 对乳腺癌细胞迁移侵袭的影响及临床价值研究

孔雪*、王传新

山东大学第二医院

目的：探讨长链非编码 RNA（lncRNA）AC012073.1 在乳腺癌（BC）中的表达及对细胞迁移侵袭的影响，并对其临床价值进行研究。

方法： 运用高通量芯片和 TCGA 数据挖掘分析在 BC 组织中高表达并与患者预后不良相关的 lncRNAs。利用实时荧光定量 PCR（qRT-PCR）检测 AC012073.1 在乳腺癌细胞和血清中的表达水平。通过小干扰或质粒转染技术敲减或过表达 AC012073.1 并利用 Transwell 和划痕实验检测其对细胞迁移和侵袭能力的影响。利用 TargetScan 等数据库对下游作用靶点和功能富集分析进行预测，并运用 Cytoscape 软件绘制 ceRNA 调控网络。采用受试者工作曲线（ROC）分析血清 AC012073.1 对乳腺癌的诊断效能。

结果： 筛选发现一种新型 lncRNA AC012073.1，在乳腺癌组织中高表达（$P<0.001$）且与患者预后不良具有统计学关联性（$P=0.031$），乳腺癌细胞系中 AC012073.1 表达水平均高于正常乳腺上皮细胞，差异具有统计学意义。选择 MDA-MB-231 和 MCF-7 两株细胞进行功能实验，结果显示，敲减 AC012073.1 明显抑制细胞迁移和侵袭能力，反之过表达 AC012073.1 后，细胞的迁移和侵袭能力明显增强。下游靶点和基因通路分析显示 AC012073.1 可能通过调控肿瘤经典信号通路促进乳腺癌的进展。此外，qRT-PCR 结果显示，与健康对照相比，乳腺癌患者血清中 AC012073.1 显著升高（$P<0.001$），ROC 曲线结果显示曲线下面积（AUC）为 0.833，表明其对乳腺癌具有良好的诊断价值。

结论： 研究表明 AC012073.1 在乳腺癌中高表达,促进乳腺癌细胞的迁移和侵袭，并可能成为乳腺癌诊断和预后的生物标志物。

关键字: 长链非编码 RNA；乳腺癌；迁移；侵袭；生物标志物

52.ISG20 表达调控：一种神秘的抗病毒因子对癌症患者和正常人群的影响

刘志颖、柳曙光、傅俊江*

西南医科大学医学基础研究中心表观遗传学与肿瘤四川省高校重点实验室

背景:干扰素激活外切核酸酶基因 20kDa（Interferon Stimulated Exonuclease Gene 20kDa0, ISG20）抑制 SARS-CoV-2 等病毒入侵；然而，其在健康和癌症个体中的表达、调节与病毒易感性的细节仍有待阐明。

方法:本研究分析了健康和癌症个体中 ISG20 的表达、亚型信息、存活率、甲基化模式、免疫细胞浸润和新冠肺炎结局。使用虫草素（Cordycepin,CD）和 N6，N6-二甲基腺苷（N6, N6-dimethyladenosine ,m62A）处理癌细胞以表达 ISG20。

结果:我们发现 ISG20 mRNA 表达主要位于骨髓和淋巴组织。有趣的是，它在 11 种不同类型的癌症中的表达显著增加，这表明癌症患者可能不易感染 SARS-CoV-2。其中，ISG20 的高表达与宫颈鳞癌和腺癌以及皮肤黑色素瘤中的长生存期相关，表明 ISG20 可能是病毒预防和癌症进展的有利标志物。与配对正常组织相比，膀胱尿路上皮癌、直肠腺癌和甲状腺癌肿瘤组织中 ISG20 启动子甲基化显著降低，而乳腺浸润癌、肺鳞癌、肾透明细胞癌和胰腺癌中 ISG20 启动子甲基化则升高。肾透明细胞癌和胰腺癌组织中 ISG20 的高甲基化与 ISG20 的高表达相关，这表明 ISG20 的甲基化可能不是其高表达的基础。此外，ISG20 表达与免疫浸润水平显著相关，包括免疫淋巴细胞、趋化因子、受体、免疫抑制剂、免疫刺激剂和(Major Histocompatibility Complex, MHC)分子泛癌。胃癌的 ISG20 突变程度最高；未改变组的中位无进展生存时间（月）为 61.84，而突变组为 81.01。亚型 ISG20-001 和 ISG20−009 显示了相同的核糖核酸酶 T(Ribonuclease T, RNase-T）结构域，证明了在癌症患者的肿瘤发生和 SARS-CoV-2 感染抑制中的功能作用。此外，虫草素（CD）和 N6,N6-二甲基腺苷(m62A)都增加了 ISG20 在各种癌细胞系中的表达，这意味着二者在抗病毒/抗 SARS-CoV-2 的治疗潜力。

结论：本研究强调了在新冠肺炎大流行期间以 ISG20 为靶点对抗癌症的价值，并且从中药中提取的小分子，如 CD，可能通过促进 ISG20 表达而具有作为抗 SARS-CoV-2 和抗癌剂的潜力。

关键字：ISG20 表达；癌症；SARS-CoV-2；虫草素；N6，N6-二甲基腺苷

53.TMPRSS4 在癌症中的表达以及小分子抑制剂的调控研究

谭琦、柳曙光、傅俊江*

西南医科大学医学基础研究中心表观遗传学与肿瘤四川省高校重点实验室

背景：跨膜丝氨酸蛋白酶 4（transmembrane protease serines4, TMPRSS4）是 II 型编码丝氨酸蛋白家族的成员，位于染色体 11q23.3，分子量为 48kDa。主要存在于组织或器官的细胞表面，通过介导细胞信号的通路传导，调节各细胞间的相互作用功能。此外还具有潜在的降解细胞膜外基质的功能，可增加细胞在组织内的迁移和扩散，从而促进肿瘤细胞的生长、侵袭和转移。已有研究证明，TMPRSS4 与各种癌症的风险增加密切相关，在肿瘤组织和细胞中

高表达，包括胃癌、乳腺癌、肺癌等。因此通过调控 TMPRSS4 在肿瘤基因中的表达，可抑制肿瘤基因的 mRNA 转录水平来影响肿瘤细胞的发生发展。

方法：在公共数据库中分析了 TMPRSS4 的表达、亚型信息、突变率、生存率、甲基化。虫草素(CD)、百里醌(TQ)和 N6、N6-二甲基腺苷（m62A）用于治疗癌细胞。Westernblot 和 RT-PCR 检测 TMPRSS4 在 H1975, MCF7, 22RV1, H460 细胞系的表达。

结果:通过生物信息学我们分析了 TMPRSS4 在不同物种中高度保守，同时发现了 TMPRSS4 mRNA 的表达主要在近端消化道、肾脏和膀胱中高度表达，而 TMPRSS4 除在小脑、唾液腺、肝脏、肾脏、卵巢、平滑肌和淋巴结中表达较低外，在 36 个器官中表达较中。同时 TMPRSS4 在 CESC、COAD、LUSC、LUAD、OV、PAAD、READ、STAD、THCA、UCS、UCES 来源的癌症中表达显著升高，提示 TMPRSS4 与癌症风险的增加密切相关。与 TMPRSS2 相比，TMPRSS4 在正常、肺癌和 PAAD 组织中的表达均较高，因此 TMPRSS4 可能在肿瘤攻击正常组织中发挥重要作用。TMPRSS4 的高表达与 BLCA 中较长的 OS 相关，而在 KIRP 和 PAAD 中的 OS 较短。此外，亚型 TMPRSS4−004 包含 SRCR-2 和胰蛋白酶结构域，显示了其在包括 PAAD 在内的癌症患者的肿瘤发生的功能作用。CESC 和 LUSC 肿瘤组织中 TMPRSS4 启动子的低甲基化与 TMPRSS4 的高表达呈正相关，提示低甲基化是一种假定的机制。此外，CD、TQ 和 m62A 均以剂量依赖性的方式抑制 TMPRSS4 的表达，表明它们具有控制肿瘤细胞恶意增殖的治疗潜力。

结论:这项研究发现了在肿瘤细胞中通过靶向 TMPRSS4 抗击癌症的价值。并且强调了中药或中草药中的小分子抑制剂对癌症治疗的重要作用，如 CD 和 TQ 等，为 TMPRSS4 作为肿瘤治疗的潜在靶点提供了新的认识，通过干预 TMPRSS4 高表达也可能成为新的抗肿瘤策略。

关键字: TMPRSS4 的表达；癌症；虫草素(CD)；百里醌(TQ)；N6、N6-二甲基腺苷（m62A）

54.PSAT1 整合代谢重编程及与 IQGAP1 互作信号通路促进肺腺癌 EGFR-TKIs 耐药和转移

罗鸣宇*、周烨、沈瑛

上海交通大学医学院

目的：磷酸丝氨酸氨基转移酶 1（PSAT1）是丝氨酸合成通路关键酶之一，参与多种实体瘤发生发展。Erlotinib 等表皮生长因子受体酪氨酸激酶抑制剂（EGFR-TKIs）治疗肺腺癌疗效

显著，但极易耐药、转移并复发。本研究深入探讨了 PSAT1 在肺腺癌 EGFR-TKIs 耐药和转移中的作用及其新机制。

材料与方法：1. 构建肺腺癌耐 Erlotinib 细胞系，联合转录组学及代谢组学筛选具有表达差异的关键代谢酶。2. siRNA 敲低 PSAT1，观察对肺腺癌亲本和耐药细胞克隆形成及凋亡影响。3. 构建过表达野生型及失活突变 PSAT1 细胞系，验证其对肺腺癌细胞粘附、运动及对 Erlotinib 敏感性影响。4. 采用免疫共沉淀-蛋白质谱法寻找 PSAT1 相互作用蛋白，并结合转录组学寻找下游关键信号通路。5. 构建裸小鼠皮下移植瘤模型观察体内干预 PSAT1 是否影响肺腺癌对 Erlotinib 敏感性；构建裸小鼠尾静脉转移模型和胸内注射转移模型验证过表达 PSAT1 对肺腺癌体内转移及小鼠生存期的影响。6. 结合临床组织芯片以及公共数据库分析 PSAT1 与肺腺癌患者疾病进展和预后的关系。

结果：1. 耐药细胞中丝氨酸合成通路激活，从头合成丝氨酸含量显著增多，PSAT1 蛋白水平在 Erlotinib 适应性耐药及获得性耐药模型中均上调。2. 下调 PSAT1 显著抑制肺腺癌细胞及耐药细胞克隆形成，并恢复耐药细胞对 Erlotinib 的敏感性。机制研究发现敲低 PSAT1 显著升高肺腺癌细胞内活性氧水平，激活 JNK/c-Jun 信号通路，诱导耐药细胞凋亡，使用活性氧清除剂或 JNK 抑制剂能部分逆转细胞凋亡。3. 过表达野生型及酶活缺失突变 PSAT1 均能显著促进肺腺癌细胞粘附、运动及对 Erlotinib 耐药。4.蛋白质谱鉴定获得 2560 个可能与 PSAT1 结合的蛋白，验证发现 PSAT1 可不依赖其代谢酶活性与 IQ 结构域 GTP 酶活化蛋白（IQGAP1）发生蛋白互作，随后募集并激活下游信号转导与转录活化因子 3（STAT3）信号通路促进细胞运动。敲低 PSAT1 或 IQGAP1 可抑制 STAT3 信号通路，逆转过表达 PSAT1 细胞粘附及运动。同样，使用 STAT3 活性抑制剂及敲低 STAT3 可逆转过表达 PSAT1 细胞运动。5.体内实验表明持续敲低 PSAT1 增强皮下移植瘤对 Erlotinib 的敏感性，延缓适应性耐药及获得性耐药的发生；而过表达 PSAT1 可诱导亲本细胞对 Erlotinib 耐药及体内转移，显著缩短荷瘤小鼠生存期。6.临床数据显示 PSAT1 在肿瘤组织水平高于癌旁。患者肿瘤组织 PSAT1 水平与疾病进展和不良预后呈正相关。

结论：本研究阐明了 PSAT1 不仅通过丝氨酸合成通路调控肿瘤代谢网络，维持细胞内氧化还原稳态，还能不依赖于其酶活和 IQGAP1 互作，募集并激活下游 STAT3 信号通路，从而促进肺腺癌 EGFR-TKIs 耐药和转移。揭示 PSAT1 有望成为新的抗肿瘤代谢靶标，为深入研究 PSAT1 与肺腺癌恶性进展之间的关系提供实验理论基础，为靶向 PSAT1 抗肿瘤新药定向设计提供新的思路。

关键字：磷酸丝氨酸氨基转移酶 1；非酶活依赖蛋白互作；肺腺癌；EGFR-TKIs 耐药；肿瘤转移

55.解旋酶 DHX36 作为原癌基因促进肺癌的生长和转移的研究

李婷[1]、杨晶[2]、傅俊江*[1]

1. 西南医科大学医学基础研究中心表观遗传与肿瘤四川省高校重点实验室

2. 湖南理工学院化学化工学院

目的：解旋酶是一种广泛存在于原核、真核生物中的核苷酸二级结构，参与 DNA 的复制、转录等多种生命活动。而 DHX36 是解旋酶的一种，由我们实验室先前应用果蝇无雄基因序列同源分子克隆方法克隆出的 DNA/RNA 解旋酶盒的人的新的同源基因。有研究表明，DHX36 上调原癌基因的表达，促进癌症的发生，目前关于 DHX36 在肺癌中的研究较少，本研究旨在阐明 DHX36 与肺癌的作用关系，为肺癌的诊断、治疗、预后提供新的分子靶标。

方法： 在人肺腺癌细胞 A549、H460 细胞中过表达 DHX36 以及使用 DHX36 敲减慢病毒对 A549、H1975 细胞系 DHX36 进行敲减。使用实时细胞分析仪 (xCELLigence RTCA DP, Roche, Germany) 来分析细胞迁移、侵袭和生长指数。通过在 A549 细胞中建立 DHX36 稳定敲减细胞系后，与对照组细胞同时经原位皮下移植和尾静脉注射入裸鼠体内，分别记录原位瘤的生长曲线和裸鼠肺组织转移情况。通过收集 28 对肺腺癌与癌旁组织临床肿瘤样本，使用 Western Blot 分别检测 DHX36 在不同组织中蛋白水平表达差异。

结果：RTCA 结果显示，过表达 DHX36 组细胞的生长、侵袭、迁移曲线均高于对照组；而敲减 DHX36 以后，肺癌细胞的生长、侵袭和侵袭均受到抑制。在 28 对临床肺癌肿瘤样本中，我们发现有 26 对样本出现了 DHX36 在癌组织中高于癌旁组织的情况，这说明 DHX36 可能是作为促进肺癌发生发展的原癌基因。

结论：DHX36 可望成为肺癌的新的分子靶标。我们下一步将 DHX36 敲减在小鼠体内观察原位瘤生长和肺部转移。

关键字: DHX36；肺癌；生长转移

56.综合机器学习和生物信息学分析揭示胃癌干性特征并区分具有不同预后和免疫治疗反应的干性亚型

邹远江、鞠铭伊、李耀、赵琳*

中国医科大学

目的：胃癌是具有高度异质性且预后较差的恶性肿瘤，手术、放化疗等传统手段对胃癌的疗效均有限。随着对胃癌免疫基因组学的进一步了解，免疫疗法目前被认为是治疗胃癌最具前景的创新方法。由于肿瘤的发生、转移和耐药与肿瘤的干性特征息息相关，本文综合机器学习与生物信息学的方法探究胃癌干性特征及其与免疫微环境的关系，并基于干性特征提出新型的分子亚型，以预测患者的预后并筛选出对免疫治疗更敏感的人群。

方法：基于癌症基因组图谱（TCGA）、基因表达综合数据库(GEO)和祖细胞生物学联盟（PCBC）的 RNA 测序数据集，应用一类逻辑回归（OCLR）算法计算胃癌患者的干性指数（mRNAsi）。评价 mRNAsi 与胃癌预后、临床特征和肿瘤微环境的相关性。并基于加权共表达网络分析(WGCNA)和生存分析鉴定的生存相关干性核心基因，通过无监督共识聚类将患者分为两个亚型。全面探究不同干性亚型间预后特征、临床特性、体细胞突变、功能注释和免疫微环境模式的差异，深入分析不同干性亚型与免疫治疗和化疗效果之间的关系。最后通过多种机器学习方法构建了干性亚型预测模型并进行了验证。

结果：高 mRNAsi 的胃癌患者具有更高的微卫星不稳定性（MSI）和肿瘤突变负荷（TMB），总体生存期（OS）和无病生存期（DFS）明显长于低 mRNAsi 的患者；胃癌患者的 mRNAsi 与年龄、肿瘤组织学分级 Grade、T 分期、ACRG 分子分型以及 Lauren 分型之间均存在显著相关性，且与大部分的 T 淋巴细胞、B 淋巴细胞、树突状细胞和巨噬细胞等免疫细胞浸润程度都呈现负相关。根据干性特征区分的分子亚型中，干性亚型 I 的患者表现出更好的 OS，更高比例的 MSI 患者、较高的 TMB 和拷贝数变异负荷。此外，两种干性亚型具有明显不同的肿瘤免疫微环境状态，浆细胞、活化的 CD4+ T 淋巴细胞、M1 巨噬细胞和活化的树突状细胞等肿瘤杀伤性免疫细胞在干性亚型 I 中含量更高。肿瘤免疫功能障碍和排除（TIDE）预测、常见免疫检查点基因表达情况和免疫原性评分（IPS）的比较都表明干性亚型 I 对免疫治疗更敏感，是免疫疗法的优势人群。

结论：干性指数与胃癌患者的预后和免疫微环境具有显著的相关性，以干性特征聚类的新型分子亚型可以很好地预测胃癌患者的预后，有效区分免疫治疗的优势人群，为指导胃癌免疫治疗提供了新的方法和方向。

关键字：机器学习；胃癌；干性指数（mRNAsi)；分子亚型；免疫治疗

57.肿瘤教育血小板 SNORA58 作为食管癌新型标志物的研究

张倩茹*、宋兴国、宋现让

山东省肿瘤医院

食管癌是世界上第八大最常见的恶性肿瘤，也是导致癌症相关死亡的第六大原因。由于缺乏早期特异性症状和有效的筛查策略，相当数量的食管癌患者在诊断时已处于晚期。 因此，迫切需要敏感性和特异性理想的生物标志物用于食管癌早期诊断及协助临床决策。 最近，血小板已成为肿瘤发生的各个阶段的积极参与者，包括肿瘤生长、肿瘤外渗和转移。“肿瘤教育血小板”（TEPs)已成为一种很有前途的生物标志物来源，可通过血液液体活检对癌症进行非侵入性检测。多项研究表明 snoRNAs 的异常表达直接影响着肿瘤的发生、发展及预后。但是很少有研究讨论过 snoRNAs 在 TEPs 中的作用。在此,我们系统评估了食管癌中 snoRNAs 的失调，并阐明了 SNORA58 在血小板中的生物标志物潜力。

研究方法:1.采用低速离心法获得血小板沉淀。 通过高通量测序在 4 例食管癌患者和 4 例健康人中筛选出差异表达的 snoRNAs 分子; 2.设计相关差异表达 snoRNAs 分子的引物，RT-PCR 验证食管癌患者血小板和健康志愿者之间 snoRNAs 分子表达差异情况，计算诊断效能。

研究结果：与健康对照组相比，SNORA58 在食管癌患者血小板中表达上调。SNORA58 的诊断效能为 0.785，早期诊断效能为 0.797。

结论：总之，TEP SNORA58 可以作为食管癌非侵入性诊断和早期诊断的生物标志物，具有良好的诊断效能，为下一步 snoRNA 在血小板中的功能研究奠定了基础。

关键字: Esophagus cancer, SNORA58, SNORA68, SNORD93, Tumor-educated platelets (TEPs)

58.质粒编码的 lncRNA-SLERCC 纳米颗粒介导的转染抑制肾细胞癌的进展

毛卫浦*[1]、陈明 [1]、李伟 [2]

1. 东南大学附属中大医院

2. 上海市第十人民医院

背景：越来越多的证据证实，长非编码 RNAs（lncRNAs）在肾细胞癌（RCC）的进展中起着关键的调节作用。但是，lncRNAs 在基因治疗中的应用仍然很少。在此，我们通过在 RCC 细胞中引入质粒编码的肿瘤抑制因子 lncRNA-SLERCC（SLERCC），研究了一种传递系统的功效。

方法：我们通过芯片对成对的癌症和正常组织进行了 lncRNAs 表达分析，并在我们的临床数据和 TCGA 数据集中进行了验证。对质粒-SLERCC@PDA@MUC12 纳米颗粒（PSPM-NPs）进行体内和体外测试，包括细胞摄取、进入、CCK-8 检测、肿瘤生长抑制、组织学评估和安全性评价。此外，还进行了裸鼠异种移植模型的实验，以评估 PSPM-NPs 纳米治疗系统对 SLERCC 的治疗效果。

结果：我们发现 SLERCC 在 RCC 组织中表达下调，而外源性上调 SLERCC 可以抑制 RCC 细胞的转移。此外，高表达的 DNMT3A 被招募到 SLERCC 启动子上，诱发了异常的高甲基化，最终导致了 RCC 中 SLERCC 的表达下调。从机制上讲，SLERCC 可以直接与 UPF1 结合，通过 Wnt/β-catenin 信号通路发挥抑制肿瘤的作用，从而抑制 RCC 的进展和转移。随后，PSPM-NPs 纳米治疗系统可以有效地抑制 RCC 体内转移的生长。

结论：我们的研究结果表明，SLERCC 是一个有前途的治疗目标，针对跨膜转移标志物的质粒包封的纳米材料可能为 RCC 的治疗开辟了一条新的途径。

关键字: lncRNA-SLERCC；纳米颗粒；肾细胞癌；基因治疗；肿瘤抑制因子

59.环状 RNA ciRS-7---肾细胞癌的预后生物标志物和潜在的基因治疗靶点

毛卫浦*、陈明

东南大学附属中大医院

目的: 环状 RNA 是一类新的非编码 RNA，已被证明在肾细胞癌（RCC）的发展和进展中发挥关键作用。然而，人们对 ciRS-7 在 RCC 中的功能机制和治疗作用知之甚少。

方法: 为了研究 ciRS-7 的功能机制和治疗作用，我们进行了一系列的体外和体内实验，如实时定量 PCR、CCK-8、伤口愈合、trans-well、菌落形成、Edu、肿瘤异种移植和 NSG 小鼠的肺转移。采用 RNA pull-down、双萤光素酶报告法、荧光原位杂交法（FISH）和挽救实验来确定 ciRS-7、miR-139-3p 和 TAGLN 之间的关系。此外，我们用 PBAE 材料构建了 PBAE/si-ciRS-7 纳米复合物，并且评估了纳米复合物对体内肿瘤的治疗效果。

结果: ciRS-7 在 RCC 肿瘤组织和细胞系中高表达，ciRS-7 高表达与肿瘤大小、高 Fuhrman 分级和不良生存率相关。敲低 ciRS-7 能明显抑制 RCC 细胞在体内的增殖、侵袭、肿瘤生长和转移，而过度表达 ciRS-7 则有相反的效果。从机制上讲，ciRS-7 作为 miR-139-3p 的 "ceRNA"，通过 PI3K/AKT 信号通路阻止 TAGLN 的降解，促进 RCC 的进展和转移。此外，miR-139-3p 模拟物或抑制剂可以逆转 ciRS-7 过表达或沉默引起的恶性肿瘤行为的改变。此外，PBAE/si-ciRS-7 纳米复合物可以显著抑制 RCC 体内肿瘤的进展和转移。

结论: ciRS-7 通过调节 miR-139-3p/TAGLN 轴和激活 PI3K/AKT 信号通路来促进 RCC 的进展和转移，从而充当肿瘤的促癌因子。以 ciRS-7 为靶点的 PBAE/si-ciRS-7 纳米复合物的药物开发可能代表了一种有前途的 RCC 基因治疗策略。

关键字: ciRS-7；肾细胞癌；纳米复合物；预后

60.血浆外泌体作为卵巢癌的新型肿瘤标志物

李晓*、王世文、宋兴国、宋现让

山东省肿瘤医院

研究目的：卵巢癌（ovarian cancer, OC）在女性生殖道恶性肿瘤发病率中占第三位，死亡率高居第一，其发病隐匿，早期无典型症状，临床发现多为中晚期，死亡率高，预后极差，严

重威胁妇女生命。但是目前缺乏有效的早期诊断标志物，因此，迫切需要研究卵巢癌的早期诊断标志物。卵巢癌的发生、发展与自身产生外泌体密切相关。外泌体是来源于细胞的纳米级囊泡，含有大量的生物活性物质,包括蛋白质、核酸和脂质，在肿瘤的发生、发展中发挥着重要的作用。外泌体中具有多种 miRNAs，近年来的研究显示,外泌体 miRNAs 在肿瘤的早期诊断、临床分型及预后评估中具有重要意义，是一类极具潜力的肿瘤分子标志物。本研究旨在探索外泌体 miRNAs 在卵巢癌中的诊断价值，为卵巢癌的诊断和预后监测筛选新型肿瘤标志物。

研究方法：1.5 例健康人和 5 例卵巢癌患者血浆样本分离外泌体后进行 miRNAs 测序，筛选差异表达的 miRNAs。2.通过透射电镜（TEM），qNano，Western blot 验证分离出的血浆外泌体。3.收集 168 例健康人血浆样本，161 例卵巢癌患者和 36 例良性疾病患者的血浆样本，提取外泌体 RNA 后，通过 RT-qPCR 验证 miRNAs 的表达差异。4.分析外泌体 miRNAs 的表达特点。5.统计分析。

结果：1.在测序结果中，与健康样本相比，外泌体 miR-320d 在卵巢癌患者样本中表达显著下调（P<0.01）。2.透射电镜，qNano 和 Western blot 结果证明血浆中分离出的囊泡为外泌体。3.大样本结果验证与健康和良性疾病样本相比，外泌体 miR-320d 在卵巢癌样本中显著下调（P<0.0001）。4.MiR-320d 主要存在于外泌体中且含量稳定不受 RNA 酶的影响。5.外泌体 miR-320d 在淋巴结转移的患者中的含量显著低于非淋巴结转移的患者（P<0.001），此外，外泌体 miR-320d 的表达与卵巢癌分期呈负相关。

结论：血浆外泌体 miR-320d 可作为卵巢癌的新型循环肿瘤标志物。

关键字: 卵巢癌；外泌体；miRNAs；肿瘤标志物

61.DEK 通过β-catenin 调控幽门螺杆菌相关性胃癌增殖的机制研究

范博洋*[1]、焦媛媛 [1]、阮耀奇 [1]、陈高正 [1]、高雪菲 [2]、孙洁 [1]

1. 吉林医药学院

2. 延边大学

目的: 探究 DEK 调控幽门螺杆菌（Helicobacter pylori，H.pylori）相关性胃癌增殖的作用及分子机制。

材料与方法：应用生信数据库分析 DEK 与 H.pylori 相关性胃癌的相关性；构建 H.pylori 感染模型；应用 CCK-8、流式细胞术、免疫荧光染色等实验检测差异表达 DEK 对 H.pylori 感染细胞增殖活性、凋亡和自噬的影响；应用差异富集分析、PPI 等预测 DEK 调控 H.pylori 相关性胃癌增殖所涉及的关键因子；应用 Western blot 实验明确 DEK 与关键因子之间的调控关系。

结果：DEK 在胃癌组织中高表达($p<0.05$)，且其高表达与 H.pylori 感染、患者的不良预后密切相关；DEK 与 CagA 的表达呈正相关，且 DEK 可调控 H.pylori 感染模型的增殖活性；长期给予 H.pylori 裂解液刺激可上调正常胃上皮细胞 GES-1 和胃癌细胞 SGC-7901 的 Bcl2 蛋白表达水平、下调 cleaved-Caspase 3、Bax 和 LC3BII/LC3BI表达水平($p<0.01$)，而在此基础上进行 DEK 沉默可逆转 Bcl2、Bax 和 LC3BII/LC3BI表达变化；过表达β-catenin 可逆转 DEK 沉默所导致的 Bcl2、Bax、LC3B 表达变化($p<0.01$)。结论：DEK 可通过β-catenin 调控 H.pylori 相关性胃癌的非 Caspase 依赖性凋亡和自噬，从而影响 H.pylori 相关性胃癌的增殖。

关键字: DEK；β-catenin；幽门螺杆菌；胃癌；增殖

62.GSTT1 在卵巢癌紫杉醇耐药中的生物学研究

张菁*

复旦大学附属肿瘤医院

背景和目的：谷胱甘肽-S-转移酶 T1（glutathione-S-transferase theta 1, GSTT1）属于谷胱甘肽-S-转移酶二聚体的超基因家族，催化还原性谷胱甘肽（GSH）结合各种化合物，使外源性药物排出体外。卵巢癌是女性生殖系统最常见的恶性肿瘤之一，临床治疗主要采用肿瘤细胞减灭术以及紫杉醇和铂类为主的化疗，然而随着紫杉醇的广泛使用，卵巢癌耐药增加，影响了卵巢癌患者的治疗和预后。因此，研究卵巢癌紫杉醇耐药相关分子和机制对于卵巢癌的治疗至关重要。

方法：通过 GEO 数据库分析卵巢癌紫杉醇耐药相关通路。利用 GeneMANIA 数据库构建 GSTT1 相互作用分子模型，分析 GSTT1 相关信号通路，探索其生物学功能。联合 TISIDB 和 Kaplan-Meier Plotter 数据库对 GSTT1 在卵巢癌中的治疗进行分析。同时，构建紫杉醇耐药的 HO8910 和 SKOV3 细胞株，研究 GSTT1 的表达变化对耐药细胞株生物学的影响；通过蛋白芯片检测、Western blot 和细胞免疫荧光技术研究相关信号通路。

结果：在卵巢癌紫杉醇耐药中，上调基因主要富集于肿瘤蛋白聚糖通路和 WNT 信号通路。GSTT1 相关基因主要富集于生物代谢、氧化应激以及细胞解毒等生物功能。GSTT1 在卵巢癌紫杉醇耐药组织和细胞中高表达，下调 GSTT1 的表达影响卵巢癌紫杉醇耐药相关信号通路 JAK/STAT、PI3K/AKT、P53 以及 ROS 的调控，通过细胞免疫荧光发现 GSTT1 与磷酸化 STAT3 共定位于细胞核。

结论：GSTT1 可以通过多种信号通路参与卵巢癌紫杉醇耐药以及卵巢癌的发生和转移。GSTT1 可能成为卵巢癌治疗和预后的新靶点。

关键字: 谷胱甘肽-S-转移酶 T1；卵巢癌；紫杉醇耐药

63.miR-143/145基因簇对食管癌细胞信号通路靶基因调控作用的研究进展

罗堉楼*

新疆医科大学

食管癌是我国重点防治的恶性肿瘤之一，目前死亡负担仍不容乐观。新疆是中国食管癌高发地区之一，其中哈萨克族发病率远超全国平均水平，因此阐明调控食管癌发生发展的分子机制愈显必要。越来越多的报道提示 miR-143、miR-145 在食管癌中异常表达，深入参与其发生演进、放化疗抵抗等过程，并与预后相关。研究 miR-143、miR-145 在食管癌中的表达及靶基因调控作用有助于进一步阐明其分子机制，明确二者作为生物标志物和分子靶标的价值，从而为食管癌临床治疗提供新思路。

关键字: miRNA; miR-143; miR-145; 食管癌; 信号通路; 靶基因

64.科罗索酸通过降低肝癌细胞中CDK19介导的O糖基化水平抑制肝癌生长

马丽芳*、王佳谊*

上海市胸科医院检验科

目的：糖尿病是肝癌的重要危险因素，但其机制尚不清楚。科罗索酸（Corosolic acid，CA）已被证实具有降血糖和抗肿瘤的双重作用。本研究通过 CA 抑制高糖作用下肝癌细胞内的 O 糖基化水平探讨其抗肿瘤作用及其机制，为临床治疗糖尿病相关肝癌提供更加可靠的理论和实验依据。

方法：通过 CCK-8、软琼脂成瘤、IHC、Western-blot、RT-qPCR、裸鼠皮下移植瘤，免疫荧光、过表达与敲除质粒构建等实验方法探究 CA 通过 CDK19 介导 O 糖基化水平抑制肝癌生长的作用机制。

结果：（1）CA 抑制肝癌细胞的增殖，肝癌细胞的增殖活性随葡萄糖浓度的增加而增强。（2）YAP、OGT、SLC5A3、Nudt9 在肝癌组织中的表达相对正常肝组织的上调。YAP、OGT、O 糖基化表达随葡萄糖浓度的增加而升高，高糖培养下的肝癌细胞 HBP 通路被激活。（3）CA 抑制 HBP 通路的活性和高糖诱导的肝癌细胞 O 糖基化、YAP 的表达增强，CA 或胰岛素治疗可以显著减小裸鼠皮下移植瘤的大小和重量。CA 能够抑制 STZ 诱导小鼠的 OGT、YAP、O 糖基化、SLC5A3 和 Nudt9 表达的增加。（4）CA 能显著抑制高糖下 CDK19 的升高。CDK19 过表达导致细胞 YAP、OGT、O 糖基化表达增加，而 CDK19 敲除则相反。（5）OGT、YAP 过表达或敲除对 CDK19 的表达没有影响。YAP 基因敲除可阻止 CDK19 过表达引起的细胞 YAP、OGT、O 糖基化增加。（6）CA 处理或 CDK19 敲除处理的肝癌细胞的 YAP、OGT 和 O 糖基化水平显著降低，同时过表达 CDK19 可部分逆转 CA 处理后受损的 YAP、O 糖基化水平和转化表型。

结论：高糖能促进肝癌细胞增殖，而 CA 能抑制高糖诱导的肝癌细胞生长和裸鼠移植瘤生长。CA 可通过失活 CDK19/YAP/O 糖基化途径降低高糖培养下肝癌细胞的增殖能力，进而抑制肿瘤生长，提示 CA 可能是抗糖尿病相关肝癌的候选药物。

关键字：科罗索酸，肝癌，CDK19，O 糖基化

65.电化学发光法检测甲胎蛋白的性能验证及评价

李德宪*、施立超、柳强、杨丽红、韩文

杭州迪安医学检验中心有限公司

目的：参照美国临床和实验室标准协会（CLSI）的 EP 文件要求，对罗氏 E602 电化学发光免疫分析仪检测甲胎蛋白（AFP）的方法进行性能验证。

方法：选择新鲜混合血清标本（高值、低值）各 20 份，测量前先定标，做质控，质控在控制范围内，连续测定 20 次，计算 SD,CV,进行精密度验证；取一个月的质控（高、低）计算 CV,SD 进行中间精密度验证；收集 5 个样本与三甲医院相同检测系统进行正确度验证；留取试剂说明书所示分析测量范围上限和下限附近的高值和低值标本各一份，以 50ul 为一个体检单位，将高低值标本以 3:1、2:2、1:3 体积比例混合，加上高低值得到 5 个浓度水平的系列样本，浓度范围遍布整个预期可报告范围，至少重复检测 2 次进行分析测量范围验证；收集健康人群的 20 例样本进行参考区间的验证。其结果与厂家声称的性能指标或公认的质量目标进行比较。

结果：验证的混合血清批内精密度允许偏倚小于（1/4CLIA'88），中间精密度的允许偏倚小于（1/3CLIA'88）；正确度允许偏倚小于（1/2CLIA'88）；分析测量范围的计算以直接测定结果计算的相应浓度为 X，以通过稀释测定结果为 Y,计算回归方程 Y=bX+a，线性相关系数 r2=0.998，实际偏倚均在允许偏倚范围内；健康人群的 20 例样本结果，95% 的检测范围 0-7（ng/ml）以内。结论：对罗氏 E602 全自动电化学发光免疫分析仪检测甲胎蛋白（AFP）的分析性能进行方法学验证后，其分析性能符合厂家声称的性能指标或公认的质量目标和要求，能够保证临床检验结果的真实性、准确性和可靠性，能够更好地满足和服务于临床。

关键字：电化学发光分析；甲胎蛋白（AFP）；性能验证

66.血浆外泌体来源的小 RNA tRF-Lys-CTT-049 作为非小细胞肺癌生物标志物的研究

周娜*、郑白冰、谢丽

山东省肿瘤医院

目的：2022 年 2 月国家癌症中心发布的全国癌症统计数据显示肺癌位居我国癌症死亡人数榜首，其中非小细胞肺癌是肺癌中最常见的类型。在过去的几十年中，虽然非小细胞肺癌在诊断和治疗上均取得了重大进步，但是对早期非小细胞肺癌的诊断率仍低于 30%，因此深入挖掘新的非小细胞肺癌早期分子标志物仍是防治中的重点。tRNA 来源片段（tRFs）是一类新的小非编码 RNA，越来越多的研究表明其参与多种癌症的发生及发展过程。然而 tRFs 是否在非小细胞肺癌的早期诊断中有较大的意义仍然未知。本研究旨在筛选并验证可作为非小细胞肺癌生物标志物的 tRFs 分子，为非小细胞肺癌的早期诊断开辟新思路。

方法：采集 5 名确诊为非小细胞肺癌的病人血浆及 5 名健康人血浆，超速离心方法分离血浆外泌体并提取总 RNA，采用非编码 RNA 测序技术筛选并鉴定非小细胞肺癌相关的 tRFs；根据测序结果，将 Fold change≥2 作为判断标准且依据 $p<0.05$ 的原则，筛选出差异明显的 tRFs 分子进行验证，采用实时荧光定量 PCR 的方法对 tRF 的表达量进行检测。

结果：对 244 名非小细胞肺癌患者及 250 名健康查体者血浆外泌体 tRF-Lys-CTT-049 表达量检测后发现，非小细胞肺癌患者血浆外泌体中的 tRF-Lys-CTT-049 表达量明显降低（$p<0.05$）；通过 ROC 曲线评估该分子的诊断效能发现：AUC 曲线下面积为 0.7066，敏感度为 71.3%，特异度为 63.6%(95% CI: 0.661-0.753)。统计结果显示 tRF-Lys-CTT-049 表达水平与非小细胞肺癌密切相关。

结论：血浆外泌体 tRF-Lys-CTT-049 可作为非小细胞肺癌早期诊断的生物标志物，为非小细胞肺癌的诊断提供了新的思路，具有较好的应用前景。

关键字：非小细胞肺癌；外泌体；tRF-Lys-CTT-049；早期诊断

67.BCL-2 家族在恶性肿瘤治疗的研究进展(2)

徐瑞宇*

河北医科大学第四医院

细胞凋亡受阻是恶性肿瘤发生机制之一，凋亡信号与抗凋亡信号的平衡决定了细胞的生存与凋亡，促进细胞凋亡、增强细胞凋亡易感性成为抗癌治疗的重要方法之一。但传统肿瘤药物毒副作用与耐药性仍是癌症治疗的最大障碍之一，寻找新的抗肿瘤药物成为癌症治疗的重点。Bcl-2 是一类具有明显抗凋亡作用的蛋白质，与其基因同源性的共同构成一个大家族，包括抗凋亡蛋白（如 Bcl-2，Bcl-XL）、促凋亡蛋白也称凋亡前体蛋白（如 Bax、Bim），促凋亡蛋白中尤以 BH3-only 蛋白为核心成员，它仅含有凋亡调节蛋白的核心结构域，当接收到射线、或者药物毒性刺激，启动蛋白质加工修饰，促进细胞色素 c 凋亡诱导因子其他等凋亡因子的释放，从而促进细胞凋亡。抗凋亡蛋白通过与促凋亡蛋白中 BH 结构域结合，抑制促凋亡因子的释放，抑制凋亡的发生。研发设计抗凋亡蛋白抑制剂或促凋亡蛋白模拟物成为靶向治疗的一个思路。一些 BH3 类似物药物、Bcl-2 抑制剂已经进入临床阶段，前者模拟 BH3-only 蛋白中 BH3 结构域，竞争性结合 Bcl-2 家族蛋白，置换释放促凋亡因子，诱导细胞凋亡，从而达到抗肿瘤的作用。近年来研究显示 BH3 模拟物在多种系统肿瘤中已显示出良好的应用前景,如 ABT-199 治疗血液系统恶性肿瘤，单药或与其他药物联用治疗均能提高治疗效果,延长患者的生存时间。但很大一部分药物仍在进行特征鉴定.本文在概述 Bcl-2 蛋白家族作用机制的基础上,综述了多种已经广泛认可的 BH3 类似物、Bcl-2 抑制剂以及正在研究进展中的。

关键字: 凋亡，BCL-2 家族，抗肿瘤

68.食管鳞状细胞癌中 circATP5C1 基因的表达及其临床意义

赵晓茹*

河北医科大学第四医院

目的：探讨 circATP5C1 在食管鳞状细胞癌细胞中的表达，并分析其与食管癌细胞侵袭、迁移、增殖的关系。旨在为食管鳞癌的进展及防治寻找新的生物标志物。

方法：1. 应用 QFRT-PCR 法筛选出高表达 circATP5C1 的细胞株 KYSE150。2. 应用小干扰 RNA(small interfering RNA, siRNA)敲低 KYSE150 中 circATP5C1 的表达，并用 QFRT-PCR 法验证 KYSE150 细胞中 circATP5C1 的敲低效率。3. 应用 Transwell 迁移和侵袭实验检测敲低 circATP5C1 对食管鳞癌细胞 KYSE150 迁移和侵袭的作用影响;应用 CCK8 实验、克隆实验检测敲低 circATP5C1 对食管鳞癌细胞 KYSE150 增殖影响；应用划痕实验检测敲低 circATP5C1 对食管鳞癌细胞 KYSE150 迁移作用影响。

结果：1. QFRT-PCR 实验结果显示，与其他食管鳞状细胞癌比较，KYSE150 细胞株中 circATP5C1 显著高表达。2. QFRT-PCR 实验结果显示，与对照组相比，敲低组中 circATP5C1 表达水平显著降低。3. Transwell 实验结果显示，敲低 circATP5C1 表达能抑制食管鳞癌细胞 KYSE150 的迁移和侵袭能力；CCK8、克隆实验结果显示，敲低 circATP5C1 表达能抑制食管鳞癌细胞 KYSE150 的增殖能力；划痕实验结果显示，敲低 circATP5C1 表达能抑制食管鳞癌细胞 KYSE150 的迁移能力。

结论：环状 RNA circATP5C1 的表达水平下调在体外可以抑制食管鳞癌细胞 KYSE150 的迁移、侵袭、增殖能力，其机制有待进一步研究。

关键字: 食管鳞状细胞癌；circATP5C1；侵袭；迁移；增殖

69.多基因检测在 Bethesda I - III 型甲状腺结节诊断中的价值:一项前瞻性双盲研究

章国智*、齐晓伟、任林、唐春霖、陈萍、史绮韵、田浩、唐鹏、范林军、陈莉、王姝姝、张晔、阎文婷、钟玲、郭燕丽、张毅

陆军军医大学第一附属医院

背景：甲状腺超声检查可在 68%的健康人群中发现甲状腺结节，恶性风险为 7%-15%。恶性结节需及时手术治疗才能获得良好预后，然而绝大多数甲状腺结节无法根据症状和体征区分其良恶性。目前超声联合细针穿刺活检是诊断甲状腺结节的首选方法，但有一定的局限性，约 30%的甲状腺结节难以明确诊断。国际上广泛使用 Bethesda 甲状腺细胞学病理报告系统将甲状腺结节分为六类，恶性风险从 0%到 99%不等，其中 Bethesda I、Bethesda II 和 Bethesda III 类结节的恶性风险分别为 1%-4%、0%-3%和 5%-15%。Bethesda I-III 类结节占比约为 81.8%，此类结节指南建议再次细针穿刺活检或超声随访。然而，这并不是一个令人满意的处理方法，

10%的 Bethesda I 类结节再次细针穿刺活检仍不能明确诊断，最终术后病理明确为恶性，即使是细胞学诊断为良性的 Bethesda II 类结节，两年内超声随访的假阴性率也达到了 7.5%，Bethesda III 类结节中 15.9%被诊断为恶性。是否能利用甲状腺癌分子标记物提高上述结节诊断的准确性，从而避免患者假阴性风险和重复细针穿刺活检，目前尚无相关研究证据。本研究旨在探讨多基因检测在提高 Bethesda I-III 型甲状腺结节诊断准确性方面的潜在益处。

方法：研究纳入 2019 年 12 月至 2020 年 12 月在陆军军医大学第一附属医院接受细针穿刺活检的甲状腺结节患者 542 例，筛选出 Bethesda I-III 类甲状腺结节 181 例。基于下一代测序(NGS)对细针穿刺活检样本进行甲状腺癌相关的 16 个点突变基因和 26 个融合突变基因进行检测。对基因检测阳性结节进行手术治疗，以组织学病理为金标准，确定多基因检测的诊断性能，并与 BRAF V600E 基因突变结果进行$\chi 2$ 检验比较。

结果：181 例 Bethesda I-III 类甲状腺结节进行多基因，其中 71 例发现基因突变，45 例结节进行了手术治疗并获得了组织学病理结果。多基因检测正确分类恶性结节 21/24 个，良性结节 19/21 个。敏感性、特异度、阳性预测值、阴性预测值及准确率分别为 91%[73-98 (95%置信区间)]、86%[67-95 (95%置信区间)]、86%[71-97 (95%置信区间)]、90%[69-96 (95%置信区间)]、89%[77-95 (95%置信区间)]。多基因检测的诊断准确率显著高于 BRAF V600E 突变检测(89% vs 76%，$\chi 2$= 15.652, P <0.01)。

结论：多基因检测能提高 Bethesda I-III 类结节良恶性诊断的准确率，显著高于当前广泛采用的 BRAF V600E 单基因检测。

关键字：甲状腺癌；甲状腺结节；分子标记物；多基因检测；Bethesda 分类

70.基于血浆外泌体多组学分析的肺癌早期筛查诊断技术开发及产业化

廖才智*[1]、王霞[2]、Alain Wuthrich[3]

1. 广州康立明生物; 澳洲国立纳米生物工程研究所

2. 浙江大学医学院附属邵逸夫医院

3. 澳洲国立纳米生物工程研究所

研究目的：肺癌是全球范围内最常见的恶性肿瘤之一，其死亡率居所有癌症之首。目前，我国 70% - 80% 的肺癌患者确诊时已为中晚期，5 年生存率仅为 16.1%，而临床 I 期肺癌患

者十年生存率高达 88%。肺癌的早期筛查诊断或将成为提高患者生存率的关键 。目前临床常规的肺癌筛查诊断主要通过影像学结合组织病理活检分析。但目前诊断方法无法满足早期筛查的需求，无法动态和客观的反映肿瘤发展进程以及患者体内各肿瘤病灶的生物学信息。因此，寻找肺癌特异性表达的肿瘤标志物，发展无损、高灵敏、高特异的检测技术，可有效地补充和完善现有的肺癌早期筛查诊断模式，及时提供综合、动态的肿瘤生物学信息，为客观诊断和后续的精准治疗提供重要依据保障。

材料与方法：外泌体在细胞间信号转导、肿瘤微环境形成等生理及病理过程中具有重要作用。研究表明，外泌体及其携带的生化成分有望作为潜在标志物，用于无损、准确的肺癌早期筛查诊断。基于前期工作，这里我们进一步设计研发可用于一体化多组分分析外泌体携带的肿瘤特异蛋白及遗传物质的新型微流控-多组学分析技术平台，即在我们设计的微流控型芯片上实现病人血浆样品中多种外泌体膜蛋白、内部蛋白、内部 miRNA 的一步法分离检测。

结果：我们成功设计制备了一种包含血浆外泌体分离及后续原位检测外泌体膜蛋白表型、内部蛋白、内部 miRNA 的微流控集成芯片，实现了利用多组学技术对训练组和验证组（早期肺癌患者、肺部良性病变患者及健康人）血浆外泌体的膜蛋白、内部蛋白和 miRNA 表型的刻画表征和表型研究。我们进一步结合临床 CT 及组织病理活检数据，筛选优化统计分析方法，构建了肺癌早期筛查诊断模型并对其诊断的准确性进行了评估。

结论：针对目前早期肺癌诊断敏感性、特异性低的问题，本工作成功建立了一种基于血浆外泌体多组分信息的、快速灵敏的筛查诊断的新方法。基于我们开发的一体化血浆外泌体分离、分析方法，实现了同时对外泌体膜蛋白、内部蛋白及内部 miRNA 的多组学分析。通过与临床 CT 及组织病理活检分析结果的比较，我们构建的肺癌早期筛查诊断模型成功地对早期肺癌患者、肺部良性病变患者及健康人实验群体实现了精准的早期诊断。 因此，我们提出的基于血浆外泌体肿瘤相关生化信息谱图的肺癌早期筛查诊断技术平台，不仅有望为肺癌早期筛查诊断提供重要理论依据，甚至可为其他疾病的筛查诊断、 疗效监测及预后评估提供研究新思路。

关键字：肺癌，早期诊断，外泌体，微流控，多组学分析

71.肿瘤早期尿液标志物

高友鹤*

北京师范大学

肿瘤的早期诊断是医学最重要的问题之一。早期诊断可以给医生有效治疗的机会。尿液不像血液那样受身体稳态效应的控制，能够汇集大量的疾病相关变化，因此尿液能够更好地反映早期微小的变化，是生物标志物的更好体液来源。我们通过一系列的动物实验，发现在皮下瘤被摸到之前尿蛋白质组发生显著的变化，颅内接种的胶质瘤在核磁共振影像发现前发生尿蛋白质组的显著变化。还将探讨尿液为什么可以这么早期发现肿瘤的机制。通过一系列的实验研究，还将探讨尿蛋白质组对同样的肿瘤细胞株在不同器官接种，不同的肿瘤细胞株在同一器官接种所产生的各种不同变化。探索尿蛋白质组反映肿瘤发生发展的灵敏度和监测。除了易于控制混杂因素的接种瘤模型，还将通过动物模型探讨和人类肿瘤更接近的诱导肿瘤模型的尿蛋白质组在不同时间的表现。利用同一个人的前后对照，可以解决临床研究中大量混杂影响因素的对照问题，让尿液标志物更早地用于临床。利用临床样本，报告还将探讨通过个性化的比较方式，通过比较肿瘤被切除前后，化疗前后的尿蛋白质组的差别，以期为判断肿瘤切除的完全性或者化疗的早期疗效提供线索，为个体化的精准治疗提供研究范式。报告还将介绍尿液中大分子物质简便经济的膜保存方法。

关键字：早期诊断；尿液蛋白质组；个体化；精准医学

72.FASTKD1 与免疫细胞浸润相关并可预测乳腺癌不良预后

郭凡*、孔维娜、米叶沙尔·安尼娃尔、马秀敏

新疆医科大学附属肿瘤医院

背景：乳腺癌(BRCA)是世界上最常见的第二大癌症。目前，与非小细胞肺癌和膀胱癌等其他类型癌症相比，乳腺癌的免疫治疗进展较为缓慢。FAST 激酶结构域 1(FASTKD1)基因在乳腺癌中的作用尚未见报道。我们的研究确定了 FASTKD1 基因在乳腺癌中的表达及其潜在的生物学功能。

方法：利用癌症基因组图谱(TCGA)数据库和我们的免疫组化(IHC)队列，我们分析了 FASTKD1 在乳腺癌中表达与其临床特征之间的相关性，并评估了 FASTKD1 在乳腺癌中的预后价值。通过 LinkedOmics 数据库分析了 FASTKD1 在 BRCA 中的潜在生物学功能。通过 TIMER 数据库和我们的 IHC 队列对 FASTKD1 与乳腺癌免疫细胞浸润之间的关系进行了评估。

结果：研究发现，FASTKD1 在乳腺癌组织中表达量显著升高，而 FASTKD1 的高表达与其临床特征和不良预后有关。FASTKD1 可作为 BRCA 的独立预后因子。在肿瘤微环境(TME)中发现 FASTKD1 的表达与肿瘤浸润性免疫细胞呈正相关。此外，功能富集分析表明，FASTKD1 可能参与了 RNA 的运输和降解、剪接体、细胞周期和线粒体基因表达，以及线粒体 RNA 代谢，影响 BRCA 的发生发展。

结论：我们的研究结果提示，FASTKD1 可能是一种致癌基因，可作为乳腺癌的预后生物标志物，并与免疫浸润水平相关。但其潜在机制仍需进一步阐明。

关键字：乳腺癌，FASTKD1，免疫细胞浸润

73.电化学发光优化项目分配提升检测效率

姚晓宾*

河南省肿瘤医院

目的：优化电化学发光检测系统项目分配，提升检测效率，降低质控成本。

方法：收集了电化学发光 24 天的检测数据，导入模拟软件，对比试剂舱位调整后检测效率的变化。

结果：平均 TAT 变化不明显，无统计学差异，$P=0.68$；平均卸载 TAT 下降了 5.76±6.12 分钟，$P<0.01$；总检测时间下降了 21.30±19.46 分钟，$P<0.01$。试剂舱位下降了 30%，平行舱位下降了 68.42%。室内质控、性能验证和日常比对总检测数下降了 39.76%。

结论：多模块电化学发光检测系统优化试剂分配方案，能够提升检测效率，同时降低质控消耗。

关键字：电化学发光检测；试剂舱位；平均 TAT；平均卸载 TAT；总检测时间

74.泛素偶联酶 UBE2C 通过调控 MMP9 蛋白去泛素化影响非小细胞肺癌的进展

赵杰*[1,2]、代娟娟[2]、王丹丹[1,2]、梁超[1,2]、武艳[2]

1. 滨州医学院附属医院肿瘤科

2. 滨州医学院附属医院医学研究中心

目的：UBE2C 作为泛素-蛋白酶体系统的重要组成部分参与许多肿瘤的进展过程，本研究旨在探讨 UBE2C 调控 MMP9 在非小细胞肺癌（NSCLC）增殖、迁移中的影响，并阐明其作用机制。

方法：通过 GEPIA 数据库分析 UBE2C 在肿瘤组织中的表达水平，Kaplan-Meier 分析 UBE2C 表达水平与生存期之间的关系。H1299 和 H520 细胞中单独转染 pcDNA3.1，pcDNA3.1-Flag-UBE2C，shMMP9 或共转染 pcDNA3.1-Flag-UBE2C 和 shMMP9 质粒，实时荧光定量 PCR 和 Western blotting 法检测其转染效率。CCK8 法和克隆形成实验检测各组细胞增殖和克隆形成能力，Transwell 法检测各组细胞迁移和侵袭能力。Starbase 数据库分析 UBE2C 和 MMP9 的相关性。Western blotting 和免疫荧光实验检测 UBE2C 和 MMP9 的蛋白表达水平。CHX（cycloheximide，放线菌酮）追踪实验检测 UBE2C 对 MMP9 蛋白稳定性的影响。采用免疫共沉淀（co-immunoprecipitation，Co-IP）阐明 UBE2C 和 MMP9 相互作用及 UBE2C 调控 MMP9 的作用机制。

结果：GEPIA 数据库分析显示 UBE2C 在肺癌等多种肿瘤中表达上调。Kaplan-Meier 分析显示 UBE2C 的表达水平升高与总生存率（OS）和无进展生存期（PFS）呈负相关。与 pcDNA3.1 组相比，pcDNA3.1-Flag-UBE2C 组 H1299 和 H520 细胞的增殖、克隆形成、迁移和侵袭能力显著上调。Starbase 数据库分析显示 UBE2C 与 MMP9 的表达水平呈正相关。Western blotting 和免疫荧光实验证实上调 UBE2C 后可以促进 MMP9 蛋白的表达，并且 MMP9 蛋白表达与 UBE2C 表达水平呈剂量依赖性。CHX（cycloheximide,放线菌酮）追踪实验证明 UBE2C 可以增加 MMP9 的蛋白稳定性。免疫共沉淀（co-immunoprecipitation，Co-IP）实验证实 UBE2C 可以与 MMP9 发生相互作用，并通过抑制 MMP9 的泛素化修饰增强其蛋白的稳定性，进而促进 MMP9 的蛋白表达。与 pcDNA3.1-Flag-UBE2C 组相比，在 pcDNA3.1-Flag-UBE2C 组中转染 shMMP9 质粒后可以部分逆转 UBE2C 对 H1299 和 H520 细胞的增殖、克隆形成、迁移和侵袭能力的促进作用。

结论：UBE2C 在非小细胞肺癌组织中表达上调并与病人生存期呈负相关，并且 UBE2C 的表达水平与 NSCLC 细胞的增殖、迁移和侵袭能力密切相关。此外，UBE2C 通过抑制 MMP9 的泛素化修饰，增强 MMP9 的蛋白稳定性，从而上调其蛋白表达水平。同时，MMP9 在 UBE2C 调控的 NSCLC 恶性生物学特征中发挥重要作用。本研究通过探讨 UBE2C 在 NSCLC 发生发展中的作用机制，将为以 UBE2C 为靶点的肺癌治疗提供实验依据。

关键字: UBE2C ; MMP9;　非小细胞肺癌;　迁移

75.Hsa circ 0000594 作为肝母细胞瘤新的生物标志物和治疗靶点的研究

卞知玄*、潘秋辉

上海交通大学医学院附属上海儿童医学中心

各种研究表明，环状 RNA（circRNAs）的异常表达在多种癌症中起着关键作用。 然而，circRNA 在肝母细胞瘤中的作用尚不清楚。在本研究中，我们试图探讨 has_cric_0000594 在肝母细胞瘤中的潜在机制及其临床意义。在我们的研究中，通过原位杂交和 RT-qPCR 确定 hsa_circ_0000594 在肝母细胞瘤组织和匹配的正常肝组织中的表达模式。 通过 CCK-8、克隆形成实验，transwell 和流式细胞术检测肝母细胞瘤细胞的增殖、细胞活力、迁移和凋亡。通过双萤光素酶报告分子测定研究了 hsa_circ_0000594 与 miR-217 的相互作用。 生物信息学分析表明，SIRT1 可作为 miR-217 的靶基因。与成对的正常肝组织相比，hsa_circ_0000594 的表达水平在肝母细胞瘤组织中显著上调，并且与肝母细胞瘤的亚型显示出显著的相关性。敲除 hsa_circ_0000594 可抑制肝母细胞瘤的恶性表型。通过 hsa_circ_0000594 / mir-217 / SIRT1 调节轴，hsa_circ_0000594 在肝母细胞瘤发育中起关键作用，这可能成为肝母细胞瘤的新型诊断标志物和潜在的治疗靶标。

关键字: 环状 RNA，肝母细胞瘤

76.Hbprem：整合肝母细胞瘤中转录组、翻译组、转录后修饰组和翻译后修饰组学的网络数据库

卞知玄*、潘秋辉

上海交通大学医学院附属上海儿童医学中心

肝母细胞瘤（Hepatoblastoma, HB）是一种罕见且高度恶性的小儿肝肿瘤。其发病机制仍不清楚，由于 HB 患者的预后较差，因此有必要弄清 HB 发生发展的潜在分子机制。在本文中，我们探讨了 HB 组织和邻近正常肝组织的 RNA 和蛋白质中的转录，翻译，转录后和翻译后修饰。此外，我们还在前期大量高通量测序和质谱数据的基础上，进一步开发在线共享数据库。HBprem（http://www.hbpremdb.com/index.html），它是集 HB 中 mRNA，蛋白质，m6A RNA 甲基化，蛋白质 O 糖基化和磷酸化修饰测序和质谱结果为一体的数据库。HBprem 的首个版本包括 9999 个 mRNA，431 个 m6A 甲基化的 mRNA，8564 个蛋白，4546 个磷酸化的蛋白和 138 个 O 糖基化的蛋白。该数据库中提供了注释，定量和来源等详细信息。数据库界面简单友好，用户能通过输入基因名、基因 ID 等信息直接检索相关基因在肝母细胞瘤中的表达水平及修饰情况。该数据库可为广大肝母细胞瘤研究人员提供丰富资源，以了解和鉴定 HB 中的 mRNA，蛋白质，mRNA 修饰和蛋白质修饰。同时，HBprem 也接受其他研究学者上传相关测序和质谱数据，以不断完善肝母细胞瘤这一罕见儿童肿瘤的转录组、蛋白组学和转录后/翻译后修饰组学信息。

关键字：肝母细胞瘤，数据库

77.PAICS 参与胃癌发生发展且参与 DNA 损伤应答过程

黄楠*、孙奋勇

上海市第十人民医院

目的：PAICS 作为嘌呤从头合成中的关键酶，已报道和多种肿瘤的发生发展相关，但在胃癌中未有相关报道。嘌呤核苷酸为 DNA 合成的重要原材料，嘌呤合成途径相关酶是否参与 DNA 损伤应答过程未有相关报道，本研究旨在探索 PAICS 在胃癌中的生物学功能及是否参与 DNA 损伤应答过程。

方法：首先通过生信分析的方法检测了 TCGA 数据库中，PAICS 在胃癌中的表达及预后情况；其次体外实验通过 CCK8，克隆形成，流式细胞术检测了干扰 PAICS 后胃癌细胞的增殖凋亡情况，体内实验通过皮下成瘤实验检测干扰 PAICS 表达对胃癌细胞成瘤能力的影响；最后通过干扰 PAICS 后，检测 DNA 损伤修复标志物γH2AX 表达和免疫荧光、彗星实验验证 PAICS 是否参与 DNA 损伤修复过程。

结果：生信分析发现 PAICS 在胃癌中显著高表达，且和患者预后相关。CCK8、克隆形成实验、流式凋亡检测结果表明干扰 PAICS 后抑制胃癌细胞增殖，诱导凋亡。裸鼠成瘤实验证实干扰 PAICS 后降低胃癌细胞成瘤能力。彗星实验、γH2AX 表达和免疫荧光实验表明干扰 PAICS 后 DNA 出现损伤，免疫共沉淀实验表明 PAICS 能够和组蛋白去乙酰化酶 HDAC1/2 相互结合，影响组蛋白乙酰化来参与 DNA 损伤修复。药物敏感性的体内外实验表明，干扰 PAICS 能够增强胃癌细胞对化疗药物顺铂的敏感性。

结论：PAICS 在胃癌中发挥着癌基因的作用，能够促进胃癌的发生发展且和胃癌患者预后相关。同时 PAICS 能够和组蛋白去乙酰化酶 HDAC1/2 相互作用来维持基因组稳定性，干扰 PAICS 能够增强胃癌细胞对化疗药物顺铂的敏感性。

关键字: PAICS，DNA 损伤应答，胃癌，顺铂

78.低氧微环境中肿瘤与肿瘤相关巨噬细胞串扰的分子机制研究进展

白瑞雪*[1,2]、赵琳 [1]

1. 中国医科大学

2. 中国医科大学附属盛京医院

低氧微环境是许多实体肿瘤持续存在的一个病理特征，被认为是患者临床预后不良的重要影响因素之一，近年来已成为肿瘤研究的热点。最新研究结果表明，低氧肿瘤微环境极大程度地影响药物临床转化的成功率。将肿瘤细胞暴露在常氧环境中仅仅几分钟便足以改变肿瘤细胞生物学的信号通路，而大多数临床前研究是在常氧条件下而不是低氧状态下收集和处理肿瘤组织，这最终造成药物临床前和临床数据的不一致。因此，低氧微环境在肿瘤药物开发中具有关键作用，不容忽视。肿瘤相关巨噬细胞（TAMs）是肿瘤微环境（TME）中最丰富的免疫细胞，对肿瘤的发展和免疫治疗具有重要影响。TAMs 受到肿瘤细胞释放的各类因子的

吸引，大量聚集在肿瘤组织的低氧区域。TAMs 和低氧是一种致命的组合，因为低氧可诱导巨噬细胞转变为促瘤表型。尽管关于肿瘤低氧的研究越来越多，但低氧微环境中肿瘤和 TAMs 之间串扰的分子机制仍缺少全面的了解。因此，本文从低氧微环境中肿瘤细胞与 TAMs 相互作用的关键媒介和信号通路两个方面进行总结与讨论，以期能够更加深入地了解低氧驱动的肿瘤与 TAMs 细胞间通讯的分子机制，为低氧肿瘤发生发展的机制研究提供参考，为开发靶向肿瘤或 TAMs 的治疗策略研究提供思路。本文结果表明，在低氧微环境下，TAMs 和肿瘤细胞通过外泌体、细胞因子、生长因子、细胞坏死碎片、肿瘤代谢物以及细胞表面的配体和受体作用进行串扰。其中，外泌体是目前研究较多的细胞间通讯媒介，其内容物主要包括微小 RNA（miRNA）、长链非编码 RNA（LncRNA）、环状 RNA（CircRNA）和白介素（ILs）。低氧微环境下两种细胞的串扰能够促进肿瘤增殖、迁移、侵袭、血管生成、耐药、上皮间质转化（EMT）和肿瘤干细胞自我更新。同时，低氧微环境能够促进巨噬细胞的吞噬功能，从而发挥抑制肿瘤生长的作用。因此，低氧微环境是肿瘤进展中的一把双刃剑。此外，在低氧微环境下，肿瘤细胞分泌的因子可以促进巨噬细胞浸润、M2 型极化、PD-L1 表达、代谢重编程、炎性因子和血管内皮细胞生长因子释放并增强其 T 细胞的抑制功能。综上，低氧微环境中肿瘤细胞与 TAMs 之间的串扰是十分复杂的，更加深入地研究将有助于梳理其相互作用的特点，进而挑选出潜在的治疗靶点。

关键字：细胞间通讯；免疫治疗；低氧肿瘤；肿瘤靶向治疗

79.基于体细胞突变构建通路标志预测癌症免疫治疗反应

韩俊伟*、李香妹

哈尔滨医科大学

背景：肿瘤遗传变异与免疫治疗获益之间的关联已得到广泛认可。由于肿瘤基因组变异水平的异质性，基于基因的突变生物标志物的预测能力不稳定。最近的研究表明，由累积的基因突变激活的关键生物学通路可能作为预测免疫检测点抑制剂（immune checkpoint inhibitors, ICI）治疗疗效的有效生物标志物。此外，通路中不同位置的基因突变对通路功能有着不同的影响。因此，捕获由累积的基因突变激活的通路，且同时考虑体细胞突变基因在通路中的位置，可能为免疫治疗的预测和新药的开发提供新的见解。

方法：在本研究中，我们创新性地开发了一种推断个体通路突变扰动的分析方法（命名为individual Pathway Mutation Perturbation, iPMP），该方法不仅考虑了突变基因在通路中的位置信息，还考虑了他们对通路的累积影响。在 iPMP 中，我们首先将单个样本的体细胞突变映射到单个通路的基因上，并迭代计算通路图中从初始节点到结束节点的每个通路中基因的突变扰动评分（gene mutation perturbation score, GMPscores）。然后我们将通路扰动得分（pathway mutation perturbation score，PMPscore）模型定义为通路中所有基因的 GMPscores 加和。因此，iPMP 会生成一个完整的 PMPscores 矩阵，其中行代表通路，列代表患者。PMPscore 矩阵可以用于替代原始突变数据来识别通路与免疫治疗患者临床结果的关联。随后，我们使用 Wilcoxon 秩和检验识别 PMPscores 差异的通路，并保留 $p<0.05$ 的通路。为了进一步缩小候选通路的范围并防止过度拟合，我们进行了单变量 Cox 比例风险回归和 LASSO 回归分析，从而识别重要的候选通路。最后，通过将候选通路的 PMPscore 和多变量 Cox 比例风险回归系数加权，构建一个基于通路的风险模型，以对癌症免疫治疗患者进行分层，识别适合免疫治疗的患者。

结果：为了说明 iPMP 方法的效果，我们将其应用于接受 ICI 治疗的黑色素瘤队列，并识别了 7 个显著的扰动通路，之后构建了一个基于通路的风险评分模型。使用基于通路的风险评分模型，患者被分为两个具有显著差异的总生存期（overall survival, log-ranktest $p<0.0001$）和客观反应率（objective response rate, Chi-Square test $p= 7.10e-3$）的亚组。该通路风险评分模型的预后和预测能力在两个独立的黑色素瘤免疫治疗队列中得到一致验证。此外，通过多变量 Cox 分析，我们发现该通路风险模型在黑色素瘤训练集和验证集中都是独立的预后因子。最后，我们将 iPMP 方法应用于 ICI 治疗的非小细胞肺癌队列，所识别的基于通路的风险评分模型在肺癌训练和验证队列中也表现出良好的性能。

结论：总之，iPMP 方法可用于识别显著的突变扰动通路，构建基于通路的生物标志物，预测癌症患者的预后以及对免疫治疗的反应。为了方便 iPMP 方法的应用，我们已将其开发成一个开源的 R 包上传至 CRAN(https://CRAN.R-project.org/package=PMAPscore)。

关键字：体细胞突变， 免疫治疗标志，通路分析，患者预后

80.基于 TCGA 数据库的 COL22A1 基因突变与肺腺癌患者预后及浸润性免疫细胞的关系

余军林*、贾晓艳、李向荣

武汉科技大学附属孝感医院

目的:少数研究表明，COL22A1 基因在肿瘤中异常表达且与预后相关，然而其突变状态与肺腺癌的预后及浸润性免疫细胞的关系未知，因此，本研究着重探索 COL22A1 突变状态在肺腺癌中的预后预测价值及与浸润性免疫细胞的关系。

方法:从 TCGA 下载肺腺癌转录表达、突变数据及对应临床基线特征。通过 R 语言的“wilcox test”分析肺腺癌组织 COL22A1 突变组和野生组间的差异表达基因、肿瘤突变负荷及浸润性免疫细胞的差异浸润丰度。使用单因素及多因素 Cox 回归评估 COL22A1 突变状态与肺腺癌患者总生存期（OS）的关系。与 COL22A1 突变相关的基因进行 GO 富集及 KEGG 通路富集分析。CIBERSORT 工具估计浸润性免疫细胞的浸润丰度。

结果: 本研究中的 COL22A1 在肺腺癌的突变率为 10.59%。单因素及多因素 COX 分析表明，COL22A1 突变状态是肺腺癌患者独立预后因素（p=0.003, HR(95%CI):2.374(1.353-4.163)）。K-M 生存曲线显示，COL22A1 突变的患者的 OS 明显短于野生型患者（p<0.001）。GO 及 KEGG 富集分通路分析显示，与 COL22A1 突变相关的上调基因主要富集在细胞周期正调控、细胞周期过程正调控及细胞周期检查点等通路上，COL22A1 突变相关的下调基因主要富集在细胞紧密连接、囊泡内吞等通路上。相关性分析显示，在 COL22A1 突变的肺腺癌微环境中，M1 巨噬细胞（p=0.003）、活化 CD4 记忆 T 细胞（p=0.002）及 M0 巨噬细胞浸润丰度（p=0.066）增加，而未活化树突状细胞（p=0.027）及单核细胞（p=0.063）的浸润丰度降低。

结论: COL22A1 突变与肺腺癌预后不良及免疫细胞浸润相关，可作为肺腺癌预后不良的预测因子及潜在免疫治疗靶点。

关键字: COL22A1，肺腺癌，预后，浸润性免疫细胞

81.胸部 SMARCA4 缺陷型未分化肿瘤

卢红阳*、姜佳鹏、龚佳黎

中国科学院大学附属肿瘤医院（浙江省肿瘤医院）

胸部 SMARCA4 缺陷未分化肿瘤（SMARCA-UT）是最近描述的一种与吸烟相关的恶性肿瘤。SMARCA-UT 的发病机制是编码哺乳动物 switch/蔗糖非发酵（mSWI/SNF）ATP 酶依赖性染色质重塑复合物的亚单位的突变失活和表达缺失(该复合物可通过三磷酸腺苷水解核小体动员，并调节其他细胞过程，包括发育、分化、增殖和凋亡），特别是 SMARCA4 和 SMARCA2。该复合物的动态活性在调节基因表达程序的激活和抑制中起重要作用。研究表明，SMARCA4-UT 与恶性横纹样肿瘤（MRT）和卵巢小细胞癌（SCCOHT）具有相似的形态学特征和转录组学，但 SMARCA-UT 从基因组角度与 SCCOHT 和 MRT 不同。在临床表现方面，SMARCA4-UT 没有特定的临床表现。病变主要累及肺和胸膜，表现为易压迫周围组织的大浸润性肿块。SMARCA4-UT 预后差，无特异性治疗。目前可用的治疗包括 EZH2 抑制剂、化疗和抗 PD-1 阻滞剂。本文就 SMARCA4-UT 的病理特征、免疫组织化学、诊断、治疗和预后进行综述。

关键字: 胸部 SMARCA4 缺陷型未分化肿瘤；治疗；诊断；预后

82.肺部睾丸核蛋白癌

卢红阳*、陈静、李美慧

中国科学院大学附属肿瘤医院（浙江省肿瘤医院）

NUT(睾丸核蛋白)癌（NC）是一种具有高度侵袭性和致命性的恶性肿瘤。其特征是染色体 15 q l4 上睾丸基因核蛋白（NUTM1)重排，最常见的融合形式是 BRD4-NUT。NUT 癌可发生于不同器官，主要出现在中线器官，且肺是常见的发生部位。NC 几乎在所有年龄段的患者中都有发现，在男女性中的发生率基本一致。该肿瘤确诊时大多已属晚期，且缺乏有效治疗手段，预后极差。经过多年的研究，NC 的发生机制仍未完全明确，其治疗方法有待进一步探索。为了更全面地认识 NC，并探索其有效的治疗方法，本综述对 NC 的临床表现、病理学特征、诊断方法、治疗策略等进行了总结。

关键字: 睾丸核蛋白癌；BRD4-NUT；治疗；预后

83.肺唾液腺肿瘤-透明样透明细胞癌的文献综述

卢红阳*、王欣园、胡舒敏

中国科学院大学附属肿瘤医院（浙江省肿瘤医院）

肺透明细胞肺癌是一种罕见的肺唾液腺恶性肿瘤，占原发性肺肿瘤的不到 0.09%，没有特定的流行病学或临床特征。正确的诊断需要影像学、实验室、病理学、免疫组织化学和分子检查。肺透明细胞癌的特征是透明细胞和透明基质。肿瘤细胞由透明细胞和嗜酸性粒细胞组成。分子改变对于 t（12;22）（q13;q12）产生融合基因 EWSR1-ATF1 引起的肺透明细胞癌的病理学诊断具有重要意义。其他类型的基因融合也有报道。没有标准的治疗：主要治疗方法是手术切除，而化疗或放疗疗效尚不清楚。本文综述了肺透明细胞癌的临床特征、影像学及病理特征、免疫组化检查、突变分析、鉴别诊断、预后及治疗。

关键字： 肺透明细胞癌，病理学，分子特征，外科治疗

84.迈克 i3000 全自动化学发光免疫分析仪性能验证及评价

施立超*、柳强、杨丽红、韩文

杭州市迪安医学检验中心有限公司

目的：在仪器投入使用前，为了能够保证临床检验结果的准确性，提高临床检验的检测质量，有效地提高服务质量，现对迈克 i3000 全自动化学发光免疫分析仪进行验证及评价。

方法：根据 ISO15189 的要求，现对在该全自动免疫分析仪上检测的甲胎蛋白（AFP）、癌胚抗原（CEA）、糖类抗原 125（CA12-5）、糖类抗原 153(CA15-3)、糖类抗原 199(CA19-9)、糖类抗原 724(CA72-4)、铁蛋白(Ferr)、非小细胞肺癌相关抗原 21-1(CYFRA21-1)、总前列腺特异性抗原（PSA）、游离前列腺特异性抗原（fPSA）、神经元特异性烯醇化酶（NSE）共 11 个项目的精密度、正确度、分析测量范围、参考区间、临床可报告范围进行性能的验证与评价。

结果：批内精密度均小于 1/4CLIA’88（6.25%），批间精密度均小于 1/3CLIA’88（8.33%）；正确度允许误差均小于 1/2CLIA’88（12.5%）；分析测量范围的实际偏倚均小于允许偏倚（12.5%）；健康人群的 20 例样本进行验证，应不超过 2 例（10%）在验证区间外，若超过 2 例在参考区间外，则需要重复检测另外一组 20 例标本，参考区间的 20 例样本均不超过 2

例（10%）在验证区间外，验证通过；可报告范围的高限，至少选用 3 个高浓度样本，稀释倍数应为方法性能标明的最大稀释倍数并适当增加或减小稀释比例，每个高值样本重复测定 3 次，其相对偏倚均在允许范围（8.33%）之内。

结论：通过对迈克 i3000 全自动化学发光免疫分析仪进行验证及评价后，其分析性能符合质量目标和要求，能够保证临床检验结果的真实性、准确性和可靠性，能够更好地满足和服务于临床。

关键字：全自动发光免疫分析仪；精密度；正确度；分析测量范围；参考区间；临床可报告范围

85. 乙酰化相关 lncRNA 的筛选及候选基因 AC099850.3 对非小细胞肺癌增殖迁移的影响

徐晖*、周俊良

哈尔滨医科大学附属肿瘤医院

目的：分析乙酰化相关 lncRNAs 在非小细胞肺癌中的作用，为非小细胞肺癌患者的临床诊断和预后提供新的潜在的生物标志物。

方法：我们应用 TCGA 数据库，从 497 个非小细胞肺癌组织和 54 个正常组织中筛选出 399 个差异 lncRNAs (DElncRNAs)。结合临床预后信息，选取 12 个与预后相关的 lncRNA 进行分析。我们使用聚类软件将非小细胞肺癌患者分为两个亚组，并进行免疫细胞浸润分析、微环境分析和临床相关性分析。我们通过建立一个风险模型，进一步评估与预后相关的 lncRNA 在非小细胞肺癌患者中的预后价值。然后，基于 ceRNA 竞争机制，我们利用 GO 和 KEGG 分析了 105 个乙酰化相关 lncRNA 的富集途径。采用实时荧光定量 PCR 检测候选基因 lncRNA AC099850.3 在非小细胞肺癌组织及细胞中的表达水平。在 A549 细胞中敲减 AC099850.3，CCK-8 实验检测 A549 细胞增殖能力的变化，划痕实验检测 A549 细胞迁移能力的改变。

结果：105 个 DElncRNAs 与乙酰化调节因子相关。在 12 个与预后相关的 lncRNA 中，lncRNA AC099850.3 的危险比更高。我们发现，在 cluster1 和高危亚组中 AC099850.3 均显著增高，这可能是 NSCLC 患者预后的潜在生物标志物。在单因素或多因素 Cox 回归分析中，风险评分对肺癌的预后评估较好。乙酰化相关 lncRNAs 主要富集在与非小细胞肺癌发生发展密切相关的 MAPK 和 EGFR 信号通路中。RT-qPCR 结果证实 lncRNA AC099850.3 在 10 对肺癌

组织及细胞中表达较高。敲减 AC099850.3 后 A549 细胞增殖能力及迁移能力明显降低（P<0.01）。

结论：通过 TCGA 数据库筛选了非小细胞肺癌中乙酰化及预后相关的 lncRNAs，发现 lncRNA AC099850.3 在非小细胞肺癌的发生发展中起调节作用。AC099850.3 在非小细胞肺癌组织和细胞中高表达，并与非小细胞肺癌患者总体生存率相关。AC099850.3 促进非小细胞肺癌细胞增殖和迁移。

关键字：非小细胞肺癌，乙酰化，长链非编码 RNA，增殖，迁移

86.Gemin6 通过促进 AURKB 的 mRNA 成熟稳定 c-Myc 蛋白促进 NSCLC 的进展

刘柏杨*、陈勇彬

中国科学院昆明动物研究所

目的：肺癌是全球癌症死亡的主要原因，根据组织学特征，约 85%的患者被归为非小细胞肺癌(NSCLC)。我们前期通过对 NSCLC 患者的转录组数据分析发现 Gemin6（负责组装核糖核蛋白复合体(RNPs)的运动神经元(SMN)复合体的关键组成部分）相较于其他的 SMN 复合物成员在 NSCLC 癌组织中高表达，并且其高表达与较差的总体生存率相关。Gemin6 在肿瘤中的研究尚未见报道，解析其在 NSCLC 中的潜在功能与机制对未来 NSCLC 新肿瘤标志物的挖掘和治疗策略的创新具有一定意义。

方法：我们通过结合 TCGA 等多种数据库分析并结合 NSCLC 临床组织芯片验证 Gemin6 在 NSCLC 中的表达水平和患者预后的相关性。随后，通过体外生化实验、体内成瘤实验和药物筛选实验解析 Gemin6 在 NSCLC 中的潜在功能与机制并寻找可靶向其信号轴的 FDA 已批准药物。

结果：我们证实了 Gemin6 在 NSCLC 患者癌组织和 NSCLC 肿瘤细胞系中高表达且与患者的预后呈负相关。通过 GSCA 数据库和体外生化细胞实验发现 Gemin6 在肿瘤中高表达是由其启动子区域附近的低甲基化水平所引起的。除此之外，我们还发现敲降 Gemin6 在体外抑制了肿瘤细胞的增殖、迁移和细胞周期的转变，在体内抑制了异种移植瘤的形成。随后通过 GSEA 富集分析手段预测，Gemin6 可能参与了 c-Myc 信号通路。通过进一步的实验验证发现 Gemin6 促进了 AURKB mRNA 的成熟和蛋白的表达，导致 c-Myc Ser67 的磷酸化水平增

加，从而稳定 c-Myc 蛋白，参与 NSCLC 的肿瘤进展。通过针对 FDA 获批药物库筛选发现抗精神分裂症药物 Sertindole 可特异性抑制 Gemin6 的表达，进一步通过体内外实验验证发现 Sertindole 可抑制 Gemin6/AURKB/c-Myc 信号轴的功能进而抑制 NSCLC 的进展。

结论：我们的研究结果揭示了 Gemin6 在 NSCLC 进展中的致癌作用和具体的分子机制，此外利用 Sertindole 阻断 Gemin6 可能在未来被用作一种新的治疗策略。

关键字: Gemin6、c-Myc、NSCLC、Sertindole、AURKB

87.固有淋巴样 2 型细胞具有吞噬消化外来微生物和产生胞外诱捕网的新功能

杨义然*[1]、李艳 [2]、徐英杰 [3]、张寒晓 [3]、陈诗皓 [3]、王炜 [3]、孙英 [3]

1. 上海市胸科医院

2. 首都医科大学附属北京同仁医院，耳鼻喉研究所

3. 首都医科大学

研究背景：固有淋巴样 2 型细胞（Group 2 innate lymphoid cells，ILC2）是一群新型的缺乏特异性抗原识别受体和造血系主要细胞表面标志的固有免疫细胞，主要参与宿主寄生虫防御、过敏性疾病和组织修复等。最近研究发现 ILC2 可通过表达 MHC II 类分子活化 T 细胞，刺激 T 细胞向 Th2 细胞分化，但其具体机制尚未阐明。特别是 ILC2 是否具有摄取、加工抗原的能力，目前在世界范围内尚未有研究报道。

目的：探究 ILC2 在体内外是否具有吞噬外源性抗原并进行加工处理的生物学功能。

方法：采用重组小鼠 IL-33 滴鼻，从 8 周龄雌性 BALB/c 小鼠肺中分离 Lineage$^-$CD45$^+$ICOS$^+$ST2$^+$GATA3$^+$ ILC2。采用不同直径（50 nm、100 nm 和 1 μm）荧光微球分别加入阳性对照 RAW264.7 、阴性对照 Jurkat 和 ILC2 的培养皿中，使用激光共聚焦显微镜观察三种细胞与不同直径荧光微球共孵育后对荧光微球的吞噬情况以及吞噬后荧光微球和溶酶体的共定位情况；采用流式细胞术比较 ILC2 和 RAW264.7 吞噬 50 nm、100 nm 和 1 μm 荧光微球的能力；将 ILC2 和 RAW264.7 暴露于粪肠球菌不同时间后，采用透射电镜观察对细菌的吞噬和细菌在细胞内迁移情况，裂解细胞以观察胞内细菌的存活情况；采用免疫荧光技术观察在不同条件刺激下，ILC2 和 RAW264.7 细胞的胞外诱捕网的产生情

况；使用荧光素标记活的粪肠球菌滴鼻，观察比较肺脏 ILC2 与巨噬细胞在体内吞噬细菌的情况。

结果：①与阴性和阳性对照相比，小鼠肺 ILC2 在体外能够有效吞噬外来颗粒，包括不同直径的荧光微球和细菌，其吞噬能力低于巨噬细胞；②小鼠肺 ILC2 吞噬的荧光微球或细菌可以与溶酶体融合，进而细菌被杀灭，但杀灭细菌的时效较吞噬细胞长；③ILC2 能够在细菌、PMA 或 LTA 刺激后释放胞外诱捕网；④在体内与巨噬细胞相比，ILC2 有效吞噬滴鼻给入的细菌，且吞噬效率低于巨噬细胞。

结论：上述新发现表明 ILC2 对包括细菌在内的颗粒具有吞噬作用，此特性奠定了 ILC2 作为抗原提呈细胞的物质基础。ILC2 具有吞噬和降解细菌并产生胞外诱捕网的能力提示，该类细胞不仅可以参与 2 型免疫应答，还可能参与人体抵御外来微生物的第一道防线，在多种临床疾病中发挥抗感染免疫等更广泛的作用。

关键字：固有淋巴样 2 型细胞，吞噬作用，胞外诱捕网

88.负载 NO 的肿瘤靶向纳米脂质体对黑色素瘤的抑瘤作用研究

杨曰玲[1,2]、邹征云*[1,2]

1. 南京大学医学院附属鼓楼医院

2. 南京中医药大学鼓楼临床医学院

研究目的：近年来细胞免疫治疗在实体瘤中取得了突破性的进展，然而实体瘤肿瘤血管系统异常及负性免疫微环境，不利于抗肿瘤免疫细胞进入肿瘤内发挥抗肿瘤作用。因此，有效地提高免疫细胞在实体瘤中的穿透性是目前亟待解决的问题。本文构建了负载一氧化氮（Nitric oxide, NO）的肿瘤靶向纳米脂质体，并在黑色素瘤模型中评价其肿瘤靶向穿透性。

材料与方法：构建末端修饰肿瘤靶向肽 iRGD 的膜融合纳米微球，将 NO 供体包封至其内部，对微球进行表征；通过共聚焦显微镜观察纳米脂质体对肿瘤细胞膜的修饰作用及细胞定位；构建恶性黑色素瘤 3D 肿瘤细胞球模型，通过共聚焦显微镜观察纳米脂质体的分布；构建黑色素瘤皮下瘤模型，通过近红外活体成像观察纳米脂质体的肿瘤靶向性，并通过多重免疫荧光检测小鼠肿瘤血流灌注情况，通过流式细胞术检测小鼠肿瘤免疫微环境变化。

结果：MALDI-TOF-MS 分析证实成功构建纳米脂质体，且粒径与电荷可在 3 周内基本保持稳定；酶标仪检测 NO 释放浓度证实成功包封 NO 供体且在 3 天内稳定释放；共聚焦显微镜观察显示纳米脂质体通过与肿瘤细胞膜融合的方式将 NO 释放至细胞内，且具有肿瘤穿透性；近红外活体成像显示静脉回输的纳米脂质体可有效浸润至黑色素瘤皮下瘤组织深部，具有肿瘤靶向性；多重免疫荧光显示负载 NO 的纳米脂质体可以改善肿瘤的血管灌注，流式细胞术检测显示小鼠肿瘤免疫微环境中 M1 型巨噬细胞比例提高。

讨论：本文通过将负载 NO 的纳米载体递送至肿瘤微环境，实现主动肿瘤靶向，改善血管灌注，增加肿瘤微环境中免疫刺激的 M1 型巨噬细胞比例，使肿瘤转化为利于免疫治疗的“热”肿瘤。该脂质体的肿瘤靶向富集优势及免疫微环境调节优势，为肿瘤免疫治疗提供了新思路。

关键字：黑色素瘤；肿瘤微环境；纳米脂质体；巨噬细胞；一氧化氮

89.PPP2R3A 预测肝癌肝移植患者术后不良预后的临床意义

何佳佳*[1]、矫宁[2]、张庆[1]

1. 中国人民解放军总医院第三医学中心

2. 济南市济阳区人民医院

背景：蛋白磷酸酶 2 调节亚单位 B′α（PPP2R3A）基因表达对肝细胞癌（HCC）发生、发展和预后的影响尚不清楚。本研究旨在探讨 PPP2R3A 基因是否可用于预测肝癌肝移植术后肿瘤复发和生存率。

目的：明确 PPP2R3A 基因与肝癌的相关性，以及探索 PPP2R3A 基因对肝癌患者肝移植术后预后的预测价值。

方法：利用免疫组织化学染色法检测大样本量人肝癌组织和良性肝病组织中 PPP2R3A 基因的表达情况；运用 Wilcoxon 秩检验或 Mann-Whitney U 秩和检验分析 PPP2R3A 在不同组织及血清中的表达差异；采用卡方检验分析 PPP2R3A 的表达与肝癌临床病理指标之间的关系；COX 比例风险模型分析 PPP2R3A 的表达对肝癌肝移植患者预后的影响，以及联合 AFP 水平后对肝癌肝移植患者预后的意义。

结果：免疫组化显示肝癌组织中 PPP2R3A 蛋白主要定位于细胞质上，少部分表达在细胞膜上，PPP2R3A 蛋白在肝癌中高表达，其在肝癌组织中的表达强度明显高于癌旁组织（$p \leq 0.001$）；且显著高于良性肝病组织（$p \leq 0.001$）。相关分析表明，PPP2R3A 高表达与术前甲胎蛋白（AFP）

水平（*P*=0.003）和 TNM-t 分期（*P*≤0.001)相关. 单变量分析显示 PPP2R3A 高表达患者的 1、3、5 年生存率和无瘤生存率分别为 73.0%、39.1%、21.2%；40.0%、22.4%、0。低表达患者的 1、3、5 年生存率和无瘤生存率分别为 94.8%、71.2%、57.0%；71.4%、41.0%、38.8%。PPP2R3A 高表达患者生存率（*p* ≤0.001）和无瘤生存率（p=0.025）明显差于低表达患者。多变量分析表明， PPP2R3A 高表达（*p*=0.004）是影响 HCC 肝移植术后生存的独立风险因子；PPP2R3A 高表达（*p*=0.024）也是影响 HCC 患者肝移植术后肿瘤复发的独立风险因子。此外，肿瘤直径≥6cm（*p*=0.008）和肿瘤数量＞1 个（*p*=0.000）是影响 HCC 肝移植术后生存的独立风险因子。这项研究也显示 AFP≥400 ng/ml 时，PPP2R3A 高表达患者的术后总生存率（*p*≤0.001）和无瘤生存率（*p*＝0.023）均比低表达患者差。

结论：PPP2R3A 表达强度联合 AFP 可提高预测肝癌肝移植预后的准确性。

关键字: PPP2R3A；肝细胞癌；肝移植；预后

90.过表达 PPP2R3A 通过调节己糖激酶 1 促进肝癌细胞的糖酵解

矫宁*[1,2]、张庆 [1]

1. 中国人民解放军总医院第三医学中心

2. 济南市济阳区人民医院

目的：探索蛋白磷酸酶 2 调节亚单位 B′α（PPP2R3A）和己糖激酶 1（HK1）在肝细胞癌糖酵解过程中的调控关系。

方法：在 HepG2 和 Huh7 细胞中，通过慢病毒转染的方式过表达 PPP2R3A，采取小干扰 RNA 技术敲低 PPP2R3A 和 HK1 的表达。通过 RNA 测序，筛选与 PPP2R3A 基因显著相关的差异表达基因。通过检测培养基中的葡萄糖消耗量和乳酸生成量测定肝癌细胞的糖酵解水平。采用 QRT-PCR、Elisa、Westernblot 和免疫荧光法检测肝癌细胞中 PPP2R3A 和 HK1 的变化。采用细胞增殖、迁移和侵袭实验观察 PPP2R3A 对 HK1 的调控作用。

结果：RNA 测序数据分析显示，在肝癌细胞中，PPP2R3A 小干扰 RNA 显著下调了 HK1 的表达。过表达 PPP2R3A 促进了 HK1 的表达及糖酵解的水平，而敲低 PPP2R3A 抑制了 HK1 的表达和糖酵解的水平。在肝癌组织样本中，PPP2R3A 和 HK1 蛋白共定位于细胞质中，且

两者表达呈正相关。在过表达 PPP2R3A 的基础上抑制 HK1 可消除过表达 PPP2R3A 对肝癌细胞糖酵解、增殖、迁移和侵袭的促进作用。

结论：我们的研究结果显示了 PPP2R3A 和 HK1 在肝癌糖酵解过程中的调控关系，揭示了 PPP2R3A 在癌症中致癌作用的新机制。

关键字：肝细胞癌；PPP2R3A；己糖激酶 1；糖酵解

91. 甲基转移酶样 3 介导的 N6-甲基腺苷会提高碳离子放疗对非小细胞肺癌的耐药性

张沛茹*

复旦大学附属肿瘤医院

目的:了解 m6A 在非小细胞肺癌 (NSCLC) 碳离子放射治疗中的作用。

方法：使用能量为 333.82 MeV/u 的 IONTRIS 强度调制光栅扫描系统对人 NSCLC 细胞系（A549 和 H1975）进行碳离子照射。通过 CCK-8、伤口愈合和 transwell 侵袭试验分析 NSCLC 细胞的增殖、迁移和侵袭能力。通过实时 PCR 和 Western Blot 分析甲基转移酶样 3（METTL3）和 H2AX 的水平。皮下异种移植物用于评估体内 NSCLC 细胞的肿瘤发生能力。

结果：这项研究中，我们发现 METTL3 的水平及其介导的 m6A 修饰在碳离子放射治疗的 NSCLC 细胞中升高。敲除 NSCLC 细胞中的 METTL3 会损害体外和体内的增殖、迁移和侵袭。此外，我们发现 METTL3 介导的 m6A 修饰 mRNA 抑制 mRNA 的衰变并增强其表达，从而增强 DNA 损伤修复和细胞存活。

结论:我们证明了 METTL3 介导的 m6A 修饰对 NSCLC 中碳离子放射治疗的效率至关重要，这表明靶向 METTL3 介导的 m6A 修饰可能是 NSCLC 的潜在治疗策略。

关键字:碳离子放射治疗；非小细胞肺癌；甲基转移酶样 3；N6-甲基腺苷；H2AX

92.LIF 介导胰腺癌星形细胞-肿瘤细胞互作促进胰腺癌增殖的机制研究及诊断价值

蒋文娜*、任丽

天津医科大学肿瘤医院

目的：胰腺癌是高度恶性肿瘤，五年生存率低于 7%，被称为“癌中之王”。病理上胰腺癌细胞（PCC）和间质星状细胞（PSC）之间通过外分泌系统相互影响、共同促进肿瘤恶性进展，在临床上导致胰腺癌进展快、难以从常规化疗和靶向治疗中获益。近年来研究发现支链氨基酸（BCAA）代谢重构是影响胰腺癌预后和化疗敏感性的重要影响因素，代谢重编程成为胰腺癌重要遗传学标志事件（Kras 突变）的热点问题。鉴于此，本课题围绕着胰腺癌 BCAA 代谢紊乱及其所特有的肿瘤微环境，探讨白血病抑制因子介导胰腺癌星形细胞-胰腺癌细胞互作导致支链氨基酸代谢紊乱从而促进胰腺癌增殖的分子机制。

方法：收集 PDAC 患者癌与癌旁组织，利用微量液相色谱-串联质谱法（Nano-Liquid chromatography-tandem mass spectrometry, NanoLC-MS/MS）的方法，检测癌与癌旁组织间的差异蛋白，并对差异蛋白进行 KEGG 通路富集分析。收集 67 例 PDAC 患者与 54 例健康对照组血浆以及 PDAC 患者癌与癌旁组织，利用核磁共振波谱（Nuclear Magnetic Resonance, NMR）技术检测 BCAA 含量的变化。胰腺癌细胞与 αPSC 共同培养，应用 CCK-8 实验及平板克隆实验检测胰腺癌细胞的增殖能力。利用 Nano-LC-MS/MS 技术对与 αPSC 共培养后的胰腺癌细胞内 BCAA 及代谢酶表达水平进行检测。为了进一步探讨 BCKDK 的作用，应用 CCK-8 实验及平板克隆实验检测 BCKDK 对胰腺癌细胞增殖能力的影响。同时应用动物皮下瘤模型探究 BCKDK 在体内发挥的作用。胰腺癌细胞中加入人源重组的 LIF，分别处理不同的时间点，应用 NMR 技术对细胞内的 BCAA 含量进行检测。通过加入 BT2 及 BCAA 探讨 LIF 促进胰腺癌增殖的机制。应用 Western Blot 实验对 LIF 处理后胰腺癌细胞 BCKDK 及 Src 的表达水平进行检测，检测 LIF 促进 BCKDK 表达的分子机制。

结果：1.对 PDAC 患者癌与癌旁组织中的差异蛋白进行 KEGG 通路富集分析，结果显示与 BCAA 相关的通路有显著性差异，与健康对照组相比，BCAA 在 PDAC 患者血浆及组织中均显著升高。2.与αPSC 共培养后的胰腺癌细胞的增殖能力显著提升。Nano-LC-MS/MS 结果显 示与αPSC 共培养后的胰腺癌细胞内的 BCAA 分解代谢中的限速酶- BCKDK 表达水平显著提高。CCK-8 及平板克隆实验显示 BCKDK 可显著提高胰腺癌细胞的增殖能力且在动

物水平，BCKDK 抑制剂能够显著抑制肿瘤增殖，说明 BCKDK 在 PDAC 的进展中起到促进作用，而抑制 BCKDK 的表达水平，可阻碍 PDAC 的进展。3.白血病抑制因子处理肿瘤细胞后，支链氨基酸含量增加;且 BCKDK 及 p-BCKDHA 的表达升高，Src 的表达也随之升高。由于 BCKDK 的表达也受到与 Src 相互作用的影响，故而我们推测存在 LIF/Src/BCKDK 通路来调控 BCAA 的含量进而调控

结论: 胰腺癌中存在 BCAA 代谢紊乱，胰腺癌星形细胞通过分泌 LIF 导致胰腺癌 BCAA 代谢紊乱从而促进胰腺癌增殖。

关键字: 白血病抑制因子，细胞互作，肿瘤标志物，诊断

93.肺癌组织和外周血中 p53、PGP9.5、SOX2、GAGE 7、GBU4-5 和 MAGE A1 水平检测及其在临床诊疗中的价值探讨

邹淳缘*、许晓峰、卢仁泉、郭林

复旦大学附属肿瘤医院

探讨肺癌肿瘤组织和外周血中抑癌基因（p53）、蛋白基因产物（PGP9.5）、转录因子（SOX2）、肿瘤相关基因蛋白（GAGE 7）、解旋酶（GBU4-5）和黑色素瘤抗原（MAGE A1）蛋白水平的相关性，同时分析其在肺癌诊疗中的应用价值。

方法: 随机入组 2018 年 05 月至 2020 年 05 月入复旦大学附属肿瘤医院确诊肺癌患者共 100 例，临床 TNM 分期 I 期 25 例，II 期 45 例，IIIa 期 30 例；其中病理类型非小细胞 80 例，小细胞 20 例；取手术切除的肿瘤组织和癌旁组织，采用免疫组化染色法检测上述六种蛋白的阳性表达率，实时荧光定量 PCR（RT-PCR）法检测蛋白的相对表达水平，酶联免疫吸附（ELISA）法检测外周血六种蛋白的抗体阳性率。

结果: 肿瘤组织 p53、PGP9.5、SOX2、GAGE 7、GBU4-5 和 MAGE A1 蛋白的阳性表达率和相对表达水平均明显高于癌旁正常肺组织（$P<0.05$）；其与肿瘤的临床特征进行相关分析发现，肿瘤组织和外周血中的 p53、PGP9.5、SOX2、GAGE 7、GBU4-5 和 MAGE A1 蛋白的阳性表达率和相对表达水平与肿瘤 TNM 分期和分化级别有关（$P<0.05$），而与患者性别、年龄、肿瘤直径、病理类型均无关（$P>0.05$）。肿瘤组织六种蛋白的表达水平与外周血清表达具有较好的一致性（$P>0.05$）。

结论：肺癌肿瘤组织和外周血中 p53、PGP9.5、SOX2、GAGE 7、GBU4-5 和 MAGE A1 蛋白表达阳性对早期诊断肺癌有较好的应用价值，与肿瘤 TNM 分期和分化级别密切相关。

关键字：肺癌；抑癌基因 p53；蛋白基因产物 PGP9.5；转录因子 SOX2；肿瘤相关基因蛋白 GAGE 7；解旋酶 GBU4-5；黑色素瘤抗原 MAGE A1

94.HBx 基因整合通过 Bcl-2 途径抑制弥漫性大 B 细胞淋巴瘤的凋亡

王砚春*、卢仁泉、郭林

复旦大学附属肿瘤医院

目的：弥漫性大 B 细胞淋巴瘤（DLBCL）是非霍奇金淋巴瘤（NHL）最常见的病理类型，与乙型肝炎病毒（HBV）感染和 HBx 基因整合密切相关。本课题旨在研究 DLBCL 中 HBx 基因整合的细胞生物学效应与分子机制。

方法：采用测序技术检测 HBx 基因整合情况，通过体外细胞实验评估细胞生物学效应变化以及相关分子机制，并在实验动物和临床病例中验证。

结果：我们研究发现，对构建成功的 HBx 稳转 DLBCL 细胞进行测序分析，存在 HBx 的整合位点；染色体步移技术进一步验证转染细胞和临床组织中的 HBx 整合。细胞实验发现，与对照细胞相比，HBx 转染细胞的线粒体膜电位降低比例显著减少，染色体 DNA 断裂信号明显减少，凋亡细胞比例显著减少；因此，HBx 整合能够引起细胞凋亡水平降低的生物学效应。进一步研究发现，这一凋亡水平降低与 Bcl-2 及其下游剪切的 Caspase-3 和 PARP 蛋白的显著降低有关，揭示 DLBCL 中的 HBx-Bcl-2 凋亡分子机制。最后在临床上得以验证，血清 HBsAg 阳性的 DLBCL 患者，Bcl-2 的阳性细胞百分比显著低于抗原阴性患者（$P<0.001$）；动物实验结果也显示，裸鼠皮下成瘤的 HBx 转染细胞，Bcl-2 的蛋白表达显著降低。

结论：在弥漫性大 B 细胞淋巴瘤中，HBx 基因整合可以通过 Bcl-2 分子抑制细胞凋亡。

关键字：弥漫大 B 细胞淋巴瘤；乙型肝炎病毒；HBx 分子；Bcl-2 分子；凋亡

95.热疗对放射抵抗性结肠癌细胞的放射增敏作用与机制研究

周怡婷[1]、于剑[2]、梁珊珊*[1,2]、王若雨[1,2]

1. 辽宁省乳腺及消化肿瘤分子标志物高通量筛选及靶向药物转化重点实验室，大连大学附属中山医院

2. 大连大学附属中山医院肿瘤综合诊疗中心

目的：放射治疗是结肠癌综合治疗的重要手段，而多线治疗和复发肿瘤常呈现放射抵抗。因此，增加肿瘤细胞放射敏感性是提高疗效和减少副反应的关键。热疗是继手术、放疗、化疗及生物治疗以外的一种新的绿色的肿瘤治疗手段。本研究旨在探讨热疗对放射抵抗结肠癌细胞的放射增敏作用及其分子机制，为热疗联合放疗治疗结肠癌提供理论依据。

方法：以分割剂量（2Gy 四次，4G 四次，8G 两次），累计照射剂量 40Gy，构建放射抵抗结肠癌细胞株 HCT116R；显微镜下观察 HCT116 与 HCT116R 的形态，利用 CCK8 实验检测二者增殖情况，通过 western blot 实验检测两者的 EMT 相关标志物表达情况；照射处理两组细胞，利用平板克隆实验绘制辐射剂量-细胞存活率（SF）曲线，检测二者的放射敏感性；将 HCT116R 细胞设置对照组、热疗组（43℃）、照射组（4Gy）和联合处理组，通过平板克隆形成实验检测热疗对耐照射细胞的放射增敏情况；通过 Edu 荧光染色检测各组细胞处理后的凋亡情况；通过 western blot 检测各组细胞 DNA 损伤修复蛋白的表达情况。

结果：结肠癌 HCT116 细胞在体外经 X 线累计剂量照射至 40Gy 后，平板克隆实验证实成功构建放射抵抗性结肠癌 HCT116R 细胞，显微镜下观察，与原 HCT116 细胞相比，HCT116R 细胞形态呈间质样改变，但二者增殖情况未见显著差异；western blot 实验结果显示，HCT116R 细胞上皮标志物 E-Cad、ZO-1 表达下调，间质标志物 Vimentin、N-Cad 及β-Catenin 表达上调，HCT116R 细胞具有 EMT 表型；照射处理两组细胞后，平板克隆实验显示放射抵抗性 HCT116R 细胞的放射敏感性更低；引入热疗处理后，与对照组相比，联合处理组克隆形成率显著降低；Edu 荧光染色实验显示联合处理组产生的凋亡小体明显增多；Western Blot 结果显示，与对照组相比，γ-H2AX 蛋白表达显著上调；DNA 损伤修复相关蛋白 p-ATM、P53、P21、HSP90β和 HSPA8 蛋白表达均下调。

结论：累积剂量 40Gy 照射成功构建放射抵抗性结肠癌细胞并呈现 EMT 表型；热疗联合照射处理后能显著增强放射抵抗性结肠癌细胞的放射敏感性，这一作用可能通过抑制放疗引起的 DNA 双链断裂后损伤修复，继而诱导放射抵抗性结肠癌细胞凋亡而实现。

关键字：结肠癌 热疗 放射抵抗 放射增敏 DNA 损伤与修复

96.DRdriver：基于个体特异性网络识别耐药驱动基因

黄玉娥、周顺衡、姜伟*

南京航空航天大学

研究目的：耐药的发生是当前癌症治疗的主要限制因素之一。已有研究表明，基因突变在癌症耐药的发生过程中至关重要。此外，耐药具有异质性，使得耐药患者的治疗更加困难，迫切需要从个体的水平探索驱动耐药发生的基因。

材料与方法：本研究提出一个基于耐药患者个体特异性网络识别耐药驱动基因的方法：DRdriver。首先，通过与所有敏感患者比较，识别出每个耐药患者的差异突变，并将其所在的基因视为候选驱动基因。然后，从已知的基因调控网络中提取包含候选驱动基因及其调控靶点的子网作为每个耐药患者的个体特异性网络。接下来，利用遗传算法从候选驱动基因中识别耐药驱动基因，使其调控最多差异表达基因且最少不差异表达基因。

结果：与乘客基因相比，耐药驱动基因具有更高的突变频率，并且倾向于参与癌症和耐药的发生发展。此外，利用所有驱动基因的突变特征（mutational signature）和 LGG_替莫唑胺的驱动基因富集的通路，将耐药患者划分为不同的亚型，并从上皮间质转换（epithelial-mesenchymal transition；EMT）、DNA 损伤反应（DNA damage response；DDR）、肿瘤突变负荷（Tumor mutational burden；TMB）等方面验证了亚型的准确性。

结论：总之，本研究提出一个识别个性化耐药驱动基因的方法，为解锁耐药的分子机制和异质性提供了思路。

关键字：耐药性；异质性；驱动基因；个体特异性网络；遗传算法

97.ncFO：实验证实和预测的铁死亡相关 ncRNA 分析平台

周顺衡、黄玉娥、姜伟*

南京航空航天大学

研究目的：铁死亡（ferroptosis）是近年来发现的一类受调控的细胞死亡方式，该过程通常伴随着脂质过氧化和铁离子的积累。在癌症中诱导细胞铁死亡可有效地清除肿瘤细胞，为癌

症治疗提供新的药物作用靶点。而 ncRNA（non-coding RNA，非编码 RNA）虽然不具备蛋白质编码的能力，但被证实在铁死亡过程中扮演着重要的调控功能。目前，关于实验证实的铁死亡相关 ncRNA 的信息零散地分布在众多文献当中，需要进行系统地收集和整理。

材料与方法：首先，通过 PubMed 文献检索关键词，手动筛选经过实验证实的 ncRNA 与铁死亡的关联关系，并提取其中的 ncRNA 名字、ncRNA 类型、ncRNA 靶点等信息。此外，通过两种不同的策略进行铁死亡相关 ncRNA 的预测：（一）基于已知的铁死亡相关基因和实验证实的 ncRNA-基因调控关系，从而预测铁死亡相关的 ncRNA；（二）基于 TCGA 泛癌样本表达谱，通过与已知铁死亡相关基因计算表达相关性，得到与铁死亡基因共表达的 ncRNA，从而预测铁死亡相关的 ncRNA。最后，利用 R 语言和 PHP+Apache+MySQL 网站架构进行在线展示和分析。

结果：经过手动筛选文献证实的铁死亡相关 ncRNA，获取了 90 个实验证实的铁死亡相关 ncRNA 条目，其中包含 46 个 miRNA（microRNA，微小 RNA），21 个 lncRNA（long non-coding RNA，长非编码 RNA）和 17 个 circRNA（circular RNA，环形 RNA）。此外，通过调控预测了 598 个铁死亡相关 miRNA 和 178 个铁死亡相关 lncRNA。最后，通过共表达预测了 967 个铁死亡相关 miRNA 和 9632 个铁死亡相关 lncRNA。

结论：本工作系统地收集了实验证实和两种不同方法预测的铁死亡相关 ncRNA，方便用户对铁死亡相关 ncRNA 的研究和分析以及药物靶点的识别。铁死亡相关 ncRNA 分析平台的访问网址是 http://www.jianglab.cn/ncFO/。

关键字：铁死亡，ncRNA，miRNA，lncRNA，circRNA，癌症

98.CTpathway：一种基于通路交互的通路富集分析方法

刘海洲*、袁梦琴、姜伟

南京航空航天大学

目的：通路富集分析是一种常用的探索基因集功能的方法，它能够将成百上千个基因分配到不同的通路中，进而识别疾病风险通路。通路-通路之间通常会通过交互作用发挥功能。然而目前的通路富集分析方法忽略了通路之间的交互作用，并且对已有通路资源和先验生物知识的利用不充分。这些缺陷阻碍了从生物数据到生物知识的提取过程，亟待解决。

材料与方法：本研究提出了一种新的基于通路交互的通路富集分析方法 CTpathway。首先，整合了 8 个通路数据库的超过 2500 条通路信息、4600 对转录因子-基因调控关系以及 79000 对蛋白质-蛋白质互作关系构建了一个全局通路交互网络 GPCM，它包含超过 15000 个节点（基因）和 440000 条边。然后，通过多重-重启随机游走（multi-RWR）算法评估了 GPCM 中基因-基因的交互作用强度。接下来，通过整合基因差异表达和基因-基因交互作用强度计算了基因风险得分。最后，通过与随机比较识别了显著富集风险基因的通路。

结果：通过对包含 10 种癌症组织和血液样本的超过 8300 个表达谱进行分析，结果表明：与现有的方法相比，CTpathway 在准确性、可重复性和运行速度方面优势明显。对于多种癌型，CTpathway 不仅识别到了已知的风险通路，而且能够特异地识别其他方法忽视的重要通路。进一步地，对于不同时期（I、II、III、IV 期）的癌症样本，CTpathway 能准确地识别癌型对应的靶通路，而其他方法准确性较低。尤其是对于差异程度较小的早期（I 期）癌症，CTpathway 优势更为明显。此外，CTpathway 既能够应用于混合测序样本又适用于单细胞测序样本，帮助识别癌症组织和细胞类型特异的相关通路。

结论：综上，CTpathway 是一个快速、准确和稳定的通路富集分析方法。为了便于使用，本研究开发了 CTpathway 在线工具，网址为：http://www.jianglab.cn/CTpathway/。

关键字：通路富集分析方法；通路交互作用；风险通路；分子互作；网络分析

99.METTL3 通过 m6A 修饰 pri-miR-196b 促进结直肠癌细胞侵袭转移

李小蝶*[1]、梁丹露 [1]、张瑜 [1]、曾丽婷 [1]、曾佳煜 [1]、黄兰兰 [1,2]

1. 广东药科大学

2. 广东药科大学附属第一医院

目的：氮 6-甲基腺嘌呤（N6-methyladenine，m6A）修饰是 RNA 中广泛存在的甲基化修饰，其可以影响 RNA 的出核、剪切、稳定性和转录等过程。近年研究发现，参与 m6A 动态修饰相关酶及结合蛋白的异常表达与肿瘤的发生发展密切相关。甲基转移酶样 3（methyltransferase like 3，METTL3）是 m6A 甲基化酶复合体的重要成分，已有研究报道 METTL3 在多种恶性肿瘤中高表达并调控肿瘤的侵袭转移。然而 METTL3 调控结直肠癌细胞侵袭转移的分子机制有待进一步研究。

方法：我们利用免疫组化法分析结直肠癌组织及癌旁组织 METTL3 的表达水平；利用 Transwell、划痕试验等方法分析细胞的侵袭和迁移能力；利用 miRNA 测序、RNA 免疫共沉淀及 RNA 甲基化免疫共沉淀技术分析 METTL3 的下游靶基因。

结果：免疫组化结果显示，与癌旁组织相比 METTL3 在结直肠癌组织中高表达（p<0.05）。Transwell、划痕试验结果显示，过表达 METTL3 促进结直肠癌细胞侵袭和转移，然而敲降 METLL3 显著抑制结直肠癌细胞侵袭和迁移。miRNA 测序结果显示，敲降 METTL3 后导致 miR-196b 等 18 个 miRNA 表达水平下调。荧光定量 PCR 结果显示，过表达 METTL3 上调 miR-196b 表达水平同时下调 pri-miR-196b 的表达水平，然而抑制 METTL3 则相反。RNA 免疫共沉淀结果显示，METTL3 结合 pri-miR-196b。RNA 甲基化免疫共沉淀结果显示，敲降 METTL3 导致 pri-miR-196b m6A 水平降低。此外，过表达 miR-196b 可显著逆转因 METTL3 敲降导致的细胞迁移能力下降，而抑制 miR-196b 能显著下调因过表达 METTL3 导致的细胞迁移能力上升。

结论：METTL3 通过 m6A 修饰促进 pri-miR-196b 的成熟来调控结直肠癌细胞的侵袭转移。

关键字：结直肠癌；侵袭转移；METTL3；m6A；pri-miR-196b

100. 过表达 miR-150 在三阴性乳腺癌中作为免疫与预后标志物

赵梁*、董楠

沈阳市疾病预防控制中心

背景：微小核糖核酸（miRNA）从表观上可以调控大量癌症相关基因，并被认为是癌症生物学中的一个关键角色。MiR-150 能促进癌细胞的增殖、迁移和侵袭。然而。目前还没有研究 miR-150 过表达在乳腺癌肿瘤微环境中的作用。

方法：分析了来自多个独立大样本的 1961 名乳腺癌患者。这些结果通过体外实验进行了验证。使用 Transwell 实验评估了乳腺癌细胞对淋巴免疫细胞的吸引作用。

结果：miR- 150 的表达在三阴性乳腺癌（TNBC）亚型中是最高的。并与组织学等级相关（均为 $P < 0.001$）。在 METABRIC 数据库中，miR-150 高表达与更好的总生存率（OS）显著相关。在 METABRIC 和 TCGA 队列中，无论亚型如何，高的 miR-150 都与较好的总生存率（OS）显著相关。(除 TCGA 中的 TNBC 外，所有 p<0.05）。MiR-150 的表达与 Hallmark 免疫相

关基因组（异体移植排斥反应、IL6 信号传导、IFN-γ反应、炎症反应、IL2 信号传导和细胞凋亡）相关，与细胞溶解活性、CD8+T 细胞、CD4+记忆 T 细胞和树突状细胞的浸润有联系，以及与主要的免疫检查点分子（PD-1, CTLA4, IDO1, TIGIT, BTLA, 和 LAG3）相关，在 METABRIC 和 TCGA 数据库中结果一致（所有 $r > 0.65$，$P < 0.01$）。出乎意料的是，通过过表达 miR-150 并没有增加乳腺癌细胞系 MDA-MB231 或 BT-549 的生长、迁移和侵袭。另一方面，MiR-150 在 MDA-MB231 或 BT-549 乳腺癌细胞中的过表达，并且明显增加了对淋巴细胞系（Jurkart 细胞）的吸引，这可以通过添加 MiR-150 抑制剂这一现象被取消。通过比较 miR-150 过表达的细胞和对照组细胞的基因表达谱，我们发现许多与炎症相关的基因包括增强细胞迁移的 NF-κB 信号的基因被富集到 miR-150 过表达的乳腺癌细胞上，这意味着这可能是 miR-150 表达高的乳腺癌细胞如何吸引淋巴细胞到肿瘤微环境的机制。

结论：MiR-150 的过表达可以引起免疫细胞浸润和免疫反应，以及更好的乳腺癌患者的生存率。于此同时 miR-150 在乳腺癌细胞中的过表达并不促进癌细胞的增殖、迁移和侵袭。然而，却可以增加三阴性乳腺癌细胞对淋巴细胞的吸引。多种与炎症有关的基因的表达量在 miR150 过表达的 MDA-MB231 中更高。

关键字： MiR-150，乳腺癌，免疫细胞，浸润，预后

101. CDKN3 在 HPV16 阳性不同程度宫颈病变中的表达情况及临床意义

徐殿琴*[1]、朱小雨[1]、任吉[1]、谢璐鸿[2]、陈晓伟[2]、谯坤[2]、闵少菊[2]、谭玉洁*[1,2]

1. 贵州医科大学附属医院

2. 贵州医科大学

目的：探讨细胞周期依赖激酶抑制剂 3（Cyclin-dependent kinase inhibitor 3 ，CDKN3）在 HPV16 阳性不同程度宫颈病变中的表达及临床意义。

方法：访问并下载 GEO 数据集中 HPV16 阳性宫颈癌 GSE39001 数据，分析 CDKN3 mRNA 在 43 例 HPV16 阳性宫颈癌及 12 例宫颈正常组织表达差异性；并采用免疫组化的方法检测 12 例 HPV16 阳性宫颈癌、12 例 HPV16 阳性宫颈癌前病变、10 例 HPV16 阳性慢性宫颈炎及 7 例 HPV 阴性宫颈正常组织 CDKN3 蛋白的表达情况。

结果: HPV16 阳性宫颈癌中的 CDKN3 mRNA 表达水平明显高于宫颈正常组织；HPV16 阳性宫颈癌、HPV16 阳性宫颈癌前病变、HPV16 阳性慢性宫颈炎及 HPV 阴性宫颈正常四个组组织中 CDKN3 蛋白的阳性表达率分别为 91.7（11/12）%、58.3（7/12）%、0（0/10）%、0（0/7）%。

结论: CDKN3 可能是一种 HPV16 阳性癌前病变及宫颈癌诊断、治疗及预后的分子标志物，是宫颈癌中新的癌基因，为后续的机制研究及靶向治疗提供理论基础。

关键字： HPV16，宫颈癌，细胞周期依赖激酶抑制剂 3，CDKN3

102. 一种基于基因表达标签的乳腺癌新辅助化疗疗效预测方法

傅昌芳*、杨武林

中国科学院合肥物质科学研究院

研究目的：紫杉醇和蒽环类新辅助化疗广泛用于乳腺癌的治疗，但临床上仍然难以对治疗的敏感性进行预测。

材料与方法：在本研究中，我们应用 LASSO 逻辑回归方法开发了一个基因标签分类器，用于预测乳腺癌新辅助化疗的病理完全缓解(pCR)。进一步使用另外四个独立的测试集进一步评估分类器的预测准确率。同时对基因标签中的基因进行功能富集分析，并探讨分类器预测得分与免疫特征之间的相关性。

结果：我们通过建模找到了一个由 25 个基因组成的签名分类器，可以有效预测乳腺癌新辅助化疗的 pCR。对于基于 T/FAC 的训练集和测试集，分类期预测评分的 AUC 可以达到 0.9 以上，对于 T/AC 的测试集，AUC 也可以达到 0.7 以上，因此该签名分类器对 T/FAC 和 T/AC 方案都具有良好的预测能力。多变量模型显示分类器预测分值作为独立预测因子远优于其他临床参数。生物学功能富集分析表明，分类器所包含的基因标签主要富集于免疫相关的生物学过程。分类器预测评分与免疫评分呈显著正相关。pCR 和 RD 样本的免疫细胞类型也有显著差异。

结论：总之，我们构建了一个基于 25 个基因表达值的分类器，可以有效预测乳腺癌紫杉醇和蒽环类新辅助化疗的 pCR。同时，我们也发现免疫生态系统积极参与调节新辅助化疗的临床反应，有利于患者的预后。

关键字：乳腺癌；新辅助化疗；病理完全缓解；基因标签；免疫微环境

103. 卡介苗 Ag85A 高亲和抗原肽联合 PD-1 单抗的抗黑色素瘤研究

邹征云*[1,2]、张桂颖[1,2]、秦岚群[1,2]

1. 南京大学医学院附属鼓楼医院

2. 南京中医药大学

目的：利用免疫系统攻击肿瘤已成为抗肿瘤治疗领域强有力的手段，然而肿瘤内存在大量没有发挥抗肿瘤作用的病毒及细菌反应性 T 细胞，本研究拟通过外源性递送病毒或细菌高亲和力抗原肽，使其加载至肿瘤细胞表面空 MHC 分子上，诱导特异性 T 细胞靶向识别并杀伤肿瘤细胞，联合使用 PD-1 单抗，探索对恶性黑色素瘤的抑瘤效果及对免疫微环境的影响。

方法：采用不同的抗原亲和力预测网站预测常见病原体的 HLA-A*0201 高亲和力抗原肽；构建抗原肽与 PBMCs（HLA-A*0201 人群来源）、抗原肽与肿瘤细胞（人源黑色素瘤细胞系 A375）、抗原肽与肿瘤细胞及 T 细胞的共孵育系统，分别检测上清中γ-IFN 的表达、抗原肽的递呈及持续时间、T 细胞对肿瘤的杀伤能力；采用网站预测针对 57BL/6J 小鼠 MHC-I/II 类分子高亲和力抗原肽，将 20 只 C57BL/6J 小鼠平均分为抗原肽组、PD-1 单抗组、抗原肽联合 PD-1 单抗组、PBS 组，构建卡介苗免疫后 B16F10 黑色素瘤小鼠皮下瘤模型，瘤内注射抗原肽、腹腔注射 PD-1 单抗，治疗 28 天，观察各组小鼠体重、活跃度及重要脏器 HE 染色结果，进行生物安全性验证。分析各组小鼠肿瘤生长曲线与 T 细胞表型变化情况，比较不同治疗组的抗肿瘤效果及免疫效应。

结果：使用网站预测得到卡介苗 Ag85A 高亲和力抗原肽，将其与 PBMCs 共孵育后检测到上清中γ-IFN 表达升高；激光共聚焦显微镜结果显示，与肿瘤细胞共孵育后抗原肽可加载至肿瘤细胞表面，流式结果显示加载效应呈浓度依赖型，且 48h 后仍未衰减，持续时间稳定；CFSE/PI 染色结果提示抗原肽与肿瘤细胞、T 细胞共孵育可加强特异性 T 细胞对肿瘤细胞的杀伤能力；在体内实验中，小鼠在抗原肽组、PD-1 单抗组、联合治疗组、PBS 组均没有明显的体重及活跃程度变化，重要脏器 HE 染色没有发现明显的病理变化，提示单独瘤内注射抗原肽及其与 PD-1 单抗联合治疗均安全可行；肿瘤生长曲线显示，与 PBS 组相比，抗原肽组和联合治疗组有明显的抑瘤效果，结果具有统计学差异（$p=0.009$,$p=0.007$），且联合治

疗组抑瘤效果更显著；流式细胞术分析发现瘤内注射抗原肽可增加 T 细胞的记忆表型，无论是在肿瘤还是淋巴结中，相较于 PBS 组，抗原肽组和联合治疗组具有更多的效应记忆性 T 细胞（$p<0.05$）。

结论：瘤内注射病原体高亲和力抗原肽，可诱导特异性 T 细胞靶向识别并杀伤肿瘤细胞，与 PD-1 单抗联合治疗可有效抑制恶性黑色素瘤体积生长，增加 T 细胞的记忆表型，改善免疫微环境。

关键字：抗原递送；PD-1 单抗；卡介苗；记忆性免疫应答；免疫治疗；瘤内注射

104. 融合乏氧和免疫微环境的结直肠癌多组学驱动诊断模型

翟睿阳*、张岩

哈尔滨工业大学生命科学与技术学院

目的：由于肿瘤微环境中的乏氧和免疫活性是复杂的，随着肿瘤形成乏氧区域，导致免疫微环境发生改变。越来越多的研究证明结直肠癌（CRC）微环境中乏氧与免疫相互作用的临床意义以及对患者的生存状态的影响。因此，本研究通过探索结直肠癌免疫和乏氧相互作用，将其分类为不同的分子亚型，有利于开发新的生物标志物和靶向治疗。

研究方法：本研究综合使用 10 种聚类方法，根据 TCGA 的表达谱数据构建与乏氧-免疫相关的结直肠癌亚型。通过分析 TCGA 数据库的多组学数据，探索乏氧-免疫在结直肠癌中的相互作用机制，并鉴定出乏氧-免疫相关的遗传和表观遗传特征。之后，综合使用 LASSO、SVM-RFE、RF、XGBoost 四种机器学习算法筛选出的最显著的差异特征建立预后模型。之后本研究使用免疫治疗效应预测、潜在药物预测、肠道菌群分析等方法评估了基于风险评分的 CRC 治疗策略。

结果：使用乏氧标志基因和 ESTIMATE 打分将 TCGA 结直肠癌分为“高乏氧低免疫”、“低乏氧高免疫”和“混乱”三组。生存分析结果表明这三组之间存在极显著的差异：“高乏氧低免疫力”组的患者生存率最低，而“低乏氧高免疫力”组的患者预后最好。这说明免疫和乏氧状态对结直肠癌患者预后的影响是一种负相关关系。随后对结直肠癌多组学数据进行分析，确定了多组学特征中一些显著的乏氧免疫相关改变，包括 525 个差异 mRNA、136 个差异 lncRNA、24 个差异 miRNA、2420 个差异甲基化探针、490 个差异突变基因。综合使用四种

机器学习算法筛选出的最显著的差异特征建立预后模型，平均 1 年、3 年和 5 年 AUC 分别为 0.88、0.876 和 0.919，结果表明基于多组学的特征可有效评估结直肠癌患者的生存状态。同时，本研究评估了基于风险评分的 CRC 治疗策略：在 IPS 分析和 TIDE 分析中，发现低风险患者对免疫治疗有更好的反应；通过 GDSC 和 CTRP 数据库预测出 Docetaxel、Navitoclax、Pelitinib 等六种在高低风险患者中有显著差异效果的药物；通过 TCMA 数据库分析出 Blautia 和 Enterobacter 两种在高低风险患者中有最显著差异的肠道菌群。

结论：我们的研究基于乏氧-免疫状态探索了结直肠癌预后特征并凸显了该模型的性能，该研究结果有望阐述乏氧-免疫与结直肠癌之间的关系，并可能为开发新型结直肠癌乏氧免疫生物标志物和针对性靶向治疗提供帮助。

关键字： 结直肠癌；乏氧；免疫；机器学习；分子特征

105. HIF-1α/EZH2 双靶点药物抗肿瘤活性研究

王建民、杨程、陈国良、王立辉*

沈阳药科大学

实体肿瘤的发生和发展依赖于丰富的血管，肿瘤细胞距离血管越远，其周围氧浓度愈低。由于肿瘤内部缺氧以及一些癌基因的突变（例如 ERBB2、VHL 和 PTEN）会引起缺氧诱导因子 1α（HIF-1α,hypoxia-inducible factor-1α）的高表达。研究表明 HIF-1α在多种癌症中高表达，且在肿瘤的增殖、转移、血管形成和免疫逃逸中发挥重要作用。因此，HIF-1α被认为是抗肿瘤药物的理想靶标。然而，一些 HIF-1α抑制剂在最初会抑制肿瘤生长，但随后肿瘤表现为加速生长，提示抑制 HIF-1α会产生耐药性和免疫逃逸。表观遗传调控是一种基因型未改变而表型发生变化的可逆调控，其失调被认为是肿瘤发生发展以及耐药的关键因素。尽管 FDA 批准了一些用于血液恶性肿瘤治疗的表观药物，如组蛋白甲基转移酶 EZH2（Enhancer of zeste homolog 2）抑制剂 Tazemetostat 用于治疗上皮样肉瘤，但 Tazemetostat 对实体瘤疗效较差。研究表明，表观遗传药物除了有单一治疗的潜力外，还可能在与其他抗癌疗法的协同使用或在逆转获得性耐药方面发挥重要作用。因此，表观遗传药物与其他药物结合使用，可能是最有效且最具吸引力的策略。本研究使用计算机辅助药物设计的方法设计并合成一系列 HIF-1α/EZH2 双靶向药物，通过双萤光素酶报告基因及 Western blot 实验筛选可以同时抑制

HIF-1 转录及 EZH2 酶活性的药物，发现 W-03 具有良好的双靶向抑制效果。本研究旨在探讨双靶向药物的抗肿瘤活性，为实体瘤的治疗提供新策略。

研究目的：考察 W-03 对肿瘤细胞恶性表型的影响；考察 W-03 对体内外血管生成能力的影响；考察 W-03 对皮下异位移植瘤模型的作用效果。

材料与方法：利用平皿克隆、划痕实验及 Transwell 小室实验考察 W-03 对 A549 克隆、迁移、侵袭等生物学功能的作用；利用人脐静脉内皮细胞 HUVEC 小管形成实验、鸡胚绒毛尿囊膜实验以及 C57BL/6 皮下基质胶栓实验检测 W-03 对血管生成的作用；建立 A549 裸鼠皮下异位移植瘤模型，考察腹腔注射 W-03（25 mg/kg）对肿瘤生长速度的影响；通过免疫组化考察瘤组织中细胞增殖核抗原 Ki67 及血管生成相关标志物 CD31 的表达。

结果：1.W-03 对体外 A549 恶性表型的影响 W-03 可以显著抑制 A549 克隆形成数，且可以抑制缺氧条件下 A549 的迁移及侵袭能力。2.W-03 抑制血管形成 W-03 可以减少 VEGF 促血管生成作用下 HUVEC 管状结构的生成，且可以减少基质胶栓内暗红色血管的生成，同样可以显著减少鸡胚绒毛尿囊膜血管分支。3. W-03 减缓肿瘤生长速度相较于单药组（HIF-1α抑制剂 2-Methoxyestradiol 或 EZH2 抑制剂 Tazemetostat），W-03 显著减缓肿瘤生长速度，抑瘤率达 57%。且瘤组织中 Ki67 表达减少，微血管密度（MVD, microvessel density）显著降低。

结论:W-03 可以显著抑制体外肿瘤细胞的克隆、迁移、侵袭等生物学功能，且可以在体内外抑制血管形成。在体模型也显示 W-03 可以显著减缓肿瘤生长速度，具有较好地抗肿瘤活性。

关键字: 实体瘤；表观遗传调控；组蛋白甲基转移酶 EZH2；缺氧诱导因子 1α；W-03

106. 中国人神经纤维瘤病 1 型患者 NF1 基因新发杂合新突变（c.4963delA:p.K1655fs*41）的鉴定

杨丽莎 [1,2]、傅俊江*[1]

1. 西南医科大学医学基础研究中心表观遗传学与肿瘤四川省高校重点实验室，泸州 646000，四川

2. 西南医科大学附属医院产科，泸州 646000，四川

背景: 神经纤维瘤病 1 型（NF1）是一种常染色体显性、单倍体不足的多系统性疾病，发病率约为 1/3000。部分 NF1 患者可发展为良性或恶性肿瘤，占先证者的 45%。临床表现主要为皮肤牛奶咖啡斑、虹膜 lisch 结节、周围神经系统肿瘤或皮肤、皮下神经纤维瘤。NF1 基

因定位于染色体 17q11.2, 跨长 287kb，包含 60 个外显子（其中 3 个为选择性剪接外显子），编码由 2818 个氨基酸组成的神经纤维蛋白 1。神经纤维瘤病 1 型源于 NF1 基因的突变，表现出几乎完全的外显率。

方法：在本研究中，我们招募了一名患有 NF1 疾病并且伴有既往妊娠早期自然流产的中国年轻女性及家庭成员，提取其外周血 DNA，进行了全外显子组测序（WES）、Sanger 测序、短串联重复序列（STR）和共分离分析。

结果：结果显示，在该神经纤维蛋白 1 型（NF1）先证者中发现了的一种新的新发杂合病理性突变（c.4963delA:p.K1655fs*41）。NF1 蛋白的这种突变产生了一种截短蛋白，该截短蛋白在 C 端丢失了 NF1 蛋白的三分之一以上，包括一半 CRAL-TRIO 脂质结合结构域和核定位信号（NLS），从而导致患病（ACMG 标准：PVS1+PM2+PM6）。共分离和 STR 分析父母的基因型均为野生，表明先证者 NF1: c.4963delA: p.K1655fs*41 可能来自父亲或母亲生殖系的新发突变。不同物种 NF1 蛋白保守分析表明，不同物种间 NF1 蛋白高度保守。对不同人体组织中 NF1 mRNA 表达的分析显示，组织特异性低，这可能造成其临床表现或症状在各器官中不同。特别重要的是，我们又对先证者进行产前诊断，其结果显示，该位点在胎儿 NF1 基因的两个等位基因中均为野生型。目前，小孩已出生一个月，没有发现皮肤色素沉着和皮下结节等神经纤维瘤病相关临床表现。

结论：本研究成功地在 NF1 基因中鉴定出了一个新的、新发杂合移码突变 NF1: c.4963delA: p.K1655fs*41，该突变可能导致该中国家庭的神经纤维瘤蛋白异常。该新发突变是神经纤维瘤病的一个诊断标志物。所以，二代测序(NGS)包括 WES 和 STR 分析不仅阐明了 NF1 在该家系中的分子发病机制，还有助于该病的诊断、遗传咨询和临床治疗。

关键字：神经纤维瘤病 1 型（NF1）；全外显子测序（WES）；短串联重复序列；新发突变；移码突变

107. SMARCE1 通过协助 MYCN 介导的转录激活来促进神经母细胞瘤的发生

崔红娟*[1,2]、胡晓松 [1,2]

1. 西南大学，家蚕基因组生物学国家重点实验室

2. 西南大学，医学研究院

目的：SMARCE1（也称为 BAF57），是一种存在于所有高等真核生物的染色质重塑复合物基因。根据目前的研究进展发现 SMARCE1 在乳腺癌、胰腺导管癌等多种癌症中起着重要的作用。但是，SMARCE1 基因在神经母细胞瘤相关研究中未有报道。本论文着重于探索 SMARCE1 在神经母细胞瘤发生发展中扮演的重要角色。

材料与方法：本研究利用 R2 数据库对 SMARCE1 进行生物信息学分析；利用 RNA 干扰、蛋白质免疫印迹实验，荧光定量 PCR，生长曲线测定，BrdU 掺入实验和流式细胞术检测了 SMARCE1 的表达对神经母细胞瘤细胞增殖和自我更新的影响；利用双荧光素酶实验和 ChIP 实验探索了 SMARCE1 在神经母细胞瘤细胞中转录调控功能。

结果：利用 R2 数据库中分析发现，SMARCE1 基因的表达与神经母细胞瘤病人预后密切相关， SMARCE1 的高表达则预示着病人预后差，且神经母细胞瘤恶性程度越高的组织中 SMARCE1 的表达量也越高；在细胞水平上，利用 RNA 干扰技术和过表达 SMARCE1 质粒构建技术，在 BE2C 和 IMR32 细胞中稳定敲低和回复 SMARCE1 的表达。结果显示 SMARCE1 表达的降低可以显著性地抑制神经母细胞瘤细胞的增殖和克隆形成能力，并且将细胞周期阻滞在 G2/M 期。回复 SMARCE1 的表达则可以恢复这些现象。在动物水平上，小鼠体外成瘤实验结果证实 SMARCE1 能够促进肿瘤形成。在机制上，SMARCE1 直接与 MYCN 相互作用，协助 MYCN 转录调控下游靶基因 PLK1、ODC1 和 E2F2。同时，PLK1 过表达可以显著逆转 SMARCE1 敲低对 MYCN 扩增的神经母细胞瘤细胞增殖、集落形成和致瘤性的抑制作用。此外，我们发现 MYCN 通过与 SMARCE1 启动子的非规范 E-box 结合而直接调控 SMARCE1 的转录。

结论：在神经母细胞瘤进展过程中 SMARCE1 基因能够促进神经母细胞瘤细胞的增殖、自我更新。同时，SMARCE1 在 MYCN 扩增的神经母细胞瘤的发生中起关键作用。因此 SMARCE1 基因可能作为神经母细胞瘤靶向治疗的新型靶点，同时检测 SMARCE1 基因在神经母细胞瘤的表达情况对判断肿瘤病情的严重程度及预后具有重要的临床指导意义。

关键字: SMARCE1，MYCN，胶质母细胞瘤，增殖，自我更新

108. CBX3 通过稳定 EGFR 表达加速多形性胶质母细胞瘤的恶性进展

崔红娟*[1,2]、彭文 [1,2]

1. 西南大学，家蚕基因组生物学国家重点实验室

2. 西南大学，医学研究院

研究目的：CBX3 作为表观遗传的调节剂与 H3K9me2/3 特异性结合，在细胞命运转变过程中特定基因的转录调控上发挥着巨大的作用，在人类肿瘤的发生发展中发挥重要作用。本研究旨在阐释 CBX3 在胶质母细胞瘤增殖和迁移侵袭过程中的调控机制，为胶质母细胞瘤的临床治疗提供新的科学依据和新的靶点。

方法：利用 TCGA,CGGA 和 Rembrandt 数据库分析 CBX3 在癌旁组织和胶质母细胞瘤中的表达差异，并分析其对患者预后的影响，同时通过多个临床样本来进一步验证数据库预测结果。利用慢病毒 shRNA 感染技术，构建 CBX3 沉默的胶质母细胞瘤细胞系（LN229 和 U-87 MG），并通过 MTT、BrdU、流式检测、Soft Agar、小鼠颅内移植瘤实验，检测 CBX3 缺失对胶质母细胞瘤细胞增殖和迁移侵袭能力的影响。通过染色质免疫共沉淀实验、双萤光素酶报告基因系统检测和蛋白质免疫共沉淀等试验阐释 CBX3 在胶质母细胞瘤中的作用机制。

结果：在此项研究中，我们的研究报告了将 CBX3 鉴定为 GBM 的潜在治疗靶点。简而言之，我们通过生物信息学的技术发现了 CBX3 在 GBM 中显着上调并降低患者存活率。此外，功能实验测定表明，CBX3 在体外和体内显着促进 GBM 细胞的增殖、侵袭和肿瘤发生。机制上，我们使用靶向表皮生长因子受体 (EGFR) 酪氨酸激酶小分子抑制剂（厄洛替尼）证明了 CBX3 促进 GBM 的恶性进展是 EGFR 依赖性的。以前的研究表明，PARK2 和 STUB1 是 EGFR 特异性 E3 连接酶，我们通过 ChIP 检测证实了 CBX3 通过其 CD 结构域在转录水平直接抑制 PARK2 和 STUB1 的表达，以减少了 EGFR 的泛素化水平来保护其稳定性。此外，CBX3 的 CSD 结构域与 PARK2 相互作用并调节其泛素化以进一步降低其蛋白质水平。

结论：在胶质母细胞瘤细胞中，CBX3 抑制 E3 连接酶 STUB1 和 PARK2 的表达来保护 EGFR 的稳定性，从而进一步地加速了胶质母细胞瘤患者的恶性进程。这些结果揭示了一个 GBM 患者发病的未知机制，并证实 CBX3 是一个有前途的治疗靶点。

关键字: CBX3，EGFR, GBM, 泛素化

109. 单加氧酶 MOXD1 在胶质母细胞瘤中的作用研究

崔红娟*[1,2]、史鹏飞 [1,2]

1. 西南大学，家蚕基因组生物学国家重点实验室

2. 西南大学，肿瘤生物学与转化工程研究中心

目的：胶质母细胞瘤（Glioblastoma, GBM）是鉴定过的中枢神经系统中非常常见的原发性恶性肿瘤。GBM 患者预后差的主要原因是肿瘤内细胞的高度异质性以及可塑性，GBM 的浸润和迁移性质，以及较高的复发率。GBM 的发生发展也涉及许多基因和蛋白水平的变化，以及功能的改变。其中 GBM 患者治疗的制约因素或许是我们对胶质母细胞瘤在体内的发生发展的作用机制缺乏更加深层的理解。Monooxygenase DBH like 1 (MOXD1) 是一个多巴胺β羟化酶的类似物，属于铜II型抗坏血酸单加氧酶家族。最近的研究发现 MOXD1 在早期高风险群体胃癌中过度表达，其表达能够作为早期胃癌发育的标志基因。MOXD1 的下调能够抑制骨肉瘤细胞的生长。然而，有关 MOXD1 调控 GBM 生长的分子机制尚未有报道。本研究从分子细胞生物学等多个角度探究 MOXD1 在 GBM 生长发育中的作用，揭示 MOXD1 在胶质母细胞瘤生长发育中的分子机制。

方法：利用 TCGA、R2- GBM 临床数据库分析 MOXD1 与 GBM 患者的预后关系，随后采用 QRT-PCR 和 Western blot 探究 MOXD1 在星形胶质细胞系 SVGP12 及胶质母细胞瘤细胞系（A172、LN-229、U87 MG、U118 MG）中的表达情况。IHC 鉴别 MOXD1 在 GBM 不同级别中的表达。构建的 MOXD1 过表达载体导入 GBM 中，MTT 法测定细胞生长和增殖，采用划痕实验和 Transwell 侵袭实验测定 GBM 细胞的迁移能力和侵袭能力。采用 GSEA 和 R studio 分析 MOXD1 影响的信号途径，流式细胞术和 Western blot 鉴定 MOXD1 调控 GBM 生长的机制。

结果：MOXD1 普遍表达在人类正常组织和肿瘤组织中，且表达与 GBM 患者的生存预后密切相关，并与 GBM 患者的临床病理分级呈正相关趋势，而且，IDH 突变和 1p/19q 缺失的病

人中 MOXD1 的表达低。MOXD1 的敲低能够显著的抑制 GBM 细胞的增殖和 DNA 复制合成，同时诱导细胞阻滞在 G2/M 期；显著抑制了 GBM 细胞的迁移和侵袭能力；抑制了 GBM 细胞的克隆能力；抑制了小鼠颅内肿瘤的形成，并延长了小鼠的生存时间。GSEA 分析和 IP 实验也表明 MOXD1 能够参与β3GnT2 对 EGFR 的糖基化修饰。当 MOXD1 下调后，能够导致 GBM 细胞发生内质网应激，并引发线粒体途径的凋亡。

结论：本项研究中，发现了 MOXD1 的表达量与胶质母细胞瘤患者的生存预后不良呈现正相关趋势，MOXD1 通过协助β3GnT2 对 EGFR 的糖基化修饰来调控胶质母细胞瘤细胞内质网的稳定性，并促进细胞的增殖、迁移和成瘤。

关键字: MOXD1；β3GnT2；EGFR；胶质母细胞瘤；糖基化

110. E3 泛素连接酶 ARIH2 促进胃癌细胞增殖的机制研究

崔红娟*[1,2]、耿圣钧 [1,2]、彭文 [1,2]

1. 西南大学家蚕基因组国家重点实验室

2. 西南大学医学研究院

目的：Ariadne homolog 2 (ARIH2) 是 RING-between-RING (RBR) E3 连接酶家族的关键成员，其特征在于参与多泛素化过程的 RBR 结构域。然而，ARIH2 在胃癌发病机制中的分子机制和生物学功能仍不清楚。

材料与方法：本研究利用 R2 数据库分析了 ARIH2 与胃癌病人预后情况之间的关系；利用慢病毒感染技术在胃癌细胞系中敲低 ARIH2 的表达，通过蛋白质免疫印记，定量 PCR，生长增殖测定，BrdU 掺入实验、平板克隆实验和流式细胞术检测了 ARIH2 敲低对胃癌细胞增殖能力和细胞周期的影响；利用蛋白质免疫共沉淀实验探究了 ARIH2 促进胃癌细胞增殖的机制；在小鼠体内通过皮下注射胃癌细胞联合五氟尿嘧啶用药处理后检测敲低 ARIH2 对胃癌细胞化疗敏感性的调节。

结果与方法：通过 R2 数据库分析，我们发现 ARIH2 基因的高表达与胃癌患者预后差正相关；通过 RNA 干扰技术以及过表达质粒构建技术，我们在 MKN45 和 SGC7901 胃癌细胞株中下调和上调了 ARIH2 的表达；通过生长增殖测定、BrdU 掺入实验、平板克隆实验和流式细胞术，发现敲低 ARIH2 的表达显著降低了胃癌细胞的增殖能力，并且显著将细胞周期进程阻滞在 G2/M 期；通过软琼脂克隆形成实验和小鼠皮下成瘤实验，我们在体外和体内验证

了敲低 ARIH2 对胃癌细胞克隆形成能力和成瘤能力的抑制；进一步的机制研究表明，ARIH2 与 p21 相互作用并诱导 p21 泛素化，泛素的 K48 残基和 p21 的 K161 残基在 ARIH2 介导的 p21 泛素化中起关键作用。我们通过体外泛素化测定将 ARIH2 鉴定为 p21 的 E3 连接酶。此外，ARIH2 敲低诱导 DNA 损伤，进而诱导细胞凋亡，并在与五氟尿嘧啶联合治疗后调节胃癌细胞的化学敏感性。

结论：ARIH2 促进了 GC 细胞的增殖。 首次证实了 p21 和 ARIH2 之间的直接蛋白质相互作用，并确定了在 ARIH2 介导的 p21 泛素化中 p21 和泛素的关键氨基酸残基。 我们的研究为 GC 发病机制的鉴定和 GC 治疗靶点的确定提供了相关的见解。

关键字: ARIH2，p21，胃癌，泛素化

111. HECTD3 通过介导 c-MYC 的多聚泛素化调控胃癌的发展进程

崔红娟*[1,2]、张光辉 [1,2]

1. 西南大学家蚕基因组生物学国家重点实验室

2. 西南大学医学研究院

E3 泛素连接酶 HECTD3 与 E6 相关蛋白羧基末端同源，在生物修饰中发挥重要作用，包括免疫反应性、耐药性和凋亡。目前的研究表明，HECTD3 促进多发性肿瘤的恶性增殖并增加药物耐受性。我们的研究主要探讨了 HECTD3 在胃癌中的重要作用。在这里，我们发现 HECTD3 在胃癌中异常激活，临床预后数据库表明 HECTD3 在胃癌中高表达。HECTD3 的缺失抑制了细胞的增殖和克隆能力，并诱导胃癌细胞凋亡。在机制上，我们的发现揭示了 HECTD3 和 c-MYC 之间的相互作用，并且 HECTD3 的 DOC 结构域与 c-MYC 的 CP 和 bHLHZ 结构域相互作用。此外，我们发现 HECTD3 介导 c-MYC 的 K29 连接的多泛素化。然后，我们的研究也表明，HECTD3 的氨基酸 823（泛素酶活性位点）的半胱氨酸突变降低了 c-MYC 的多泛素化。我们的实验结果表明，HECTD3 通过介导 c-MYC 的 K29 位点连接的多泛素化促进胃癌的恶性增殖。HECTD3 可能成为治疗标志物。

关键字: HECTD3，c-MYC，胃癌，多聚泛素化

112. GRP78 调控内质网应激反应对结直肠癌细胞增殖和凋亡的作用研究

王子源*、李瑞雪、吴敏、吕凤红、郭甲森、黄尤光

云南省肿瘤医院

目的：GRP78 又称为免疫球蛋白重链结合蛋白（immunoglobulin heavy chain binding protein，Bip），主要定位在内质网上，GRP78 在各种类型的肿瘤细胞和组织中高表达，且部分文献报道其表达水平跟不良预后相关。在结直肠癌细胞中，内质网应激情况下，GRP78 在结直肠癌细胞中作用机制尚未明确，本研究旨在探讨内质网应激情况下 GRP78 表达是否影响结直肠癌细胞生物学行为，并探讨可能机制。

方法：利用毒胡萝卜素诱导结直肠癌细胞 RKO 细胞、HCT116 细胞内质网应激，在内质网应激情况下采用 MTT 和平板克隆形成实验检测敲低 GRP78 对结直肠癌细胞增殖能力的影响；应用 Western blot 检测内质网应激情况下，GRP78 敲低对 PI3K/AKT 通路蛋白、内质网应激相关蛋白、凋亡分子 cleaved-caspase12、cleaved-caspase3 蛋白表达的影响。

结果：内质网应激情况下，敲低 GRP78 可以有效抑制结直肠癌细胞 RKO、HCT116 的增殖，并下调 PI3K-AKT 通路蛋白的表达，上调内质网应激相关分子 PERK、IRE1α、ATF6 及凋亡分子 cleaved-caspase12、cleaved-caspase3 的表达。

结论：内质网应激情况下，GRP78 可能通过上调 PI3K/AKT 通路蛋白相对表达量、抑制内质网应激相关凋亡途径来促进结直肠癌细胞生存并抑制其凋亡。

关键字: GRP78；内质网应激；凋亡

113. 薯蓣皂苷对结肠癌细胞化学增敏作用研究

李瑞雪*、王子源、吕凤红、郭甲森、黄尤光

云南省肿瘤医院

背景：结肠癌化疗抵抗是晚期病人多功能器官衰竭致死的主要原因。薯蓣皂苷经过对多种实体肿瘤如肝癌、甲状腺癌、宫颈癌实验中证实具有较强的肿瘤恶性抵抗能力。小分子化合物联合传统药物提高其化疗增敏作用具有一定的潜力，但目前仍然缺乏相关实验室证据及进一步的机制研究。

方法：本课题以结肠癌作为研究对象， MTT 检测奥沙利铂、氟尿嘧啶、薯蓣皂苷的细胞毒性作用并计算 IC50，选择合适的联合用药浓度进行后续肿瘤恶性抵抗及化疗增敏实验。HCT116 与单药奥沙利铂或联合薯蓣皂苷，SW620 与单药 5 氟尿嘧啶或联合薯蓣皂苷，通过 EdU、细胞克隆形成实验验证药物的增殖抑制效应，流式细胞检测用药后细胞凋亡、周期，细胞划痕、Transwell 实验验证细胞侵袭、迁移能力。从机制层面，蛋白质免疫印迹检测相关凋亡蛋白、周期蛋白的特异靶点表达以及对 Notch 信号通路的调控作用。

结果：研究中我们证实奥沙利铂、5 氟尿嘧啶、薯蓣皂苷在结肠癌细胞系 HCT116、SW620 中均有抑制作用，薯蓣皂苷的细胞毒性作用最强，HCT116 与奥沙利铂、SW620 与 5 氟尿嘧啶均表现出更强的耐药潜力。以奥沙利铂 6.4μM 及薯蓣皂苷 0.8μM 共同刺激 HCT116 具有更强的增殖抑制，EdU 增殖比例、细胞集落形成明显减少，凋亡诱导增加，周期 G0/G1、G2/M 期阻滞，对细胞的侵袭、迁移能力明显抑制，证实双药联合具有协同作用。以 5 氟尿嘧啶 6.4μM 及薯蓣皂苷 0.8μM 共同刺激 SW620 具有相同趋势，但疗效弱于 HCT116。蛋白印迹法检测，双药刺激后 Bax、Caspase3、Caspase12、CDK2、CDK6、CyclinB1 表达降低、Bcl2 表达量上升，双药协同还可抵抗奥沙利铂引发的 Notch 通路激活。

结论：薯蓣皂苷可通过抑制 Notch 信号通路协同传统化疗药物，增强奥沙利铂、5 氟尿嘧啶在结肠癌中的化学抗性，更好抵抗肿瘤恶性。

关键字：薯蓣皂苷、结肠癌、化疗抵抗、肿瘤恶性、Notch 通路

114. 基于乳腺癌类器官放射损伤模型的 DNA 损伤修复分子标志物研究

姚良雪*[1]、于艳丽 [1]、梁珊珊 [1]、王若雨 [1,2]

1. 辽宁省乳腺及消化肿瘤分子标志物高通量筛选及靶向药物转化重点实验室

2. 大连大学附属中山医院肿瘤综合诊疗中心

研究目的：放射治疗在乳腺癌局部治疗和全身综合治疗中发挥重要作用，在早期术后和晚期复发与转移情况下广泛应用。乳腺癌的高度异质性使个体间和个体不同阶段的放射敏感性存在差异，因此，能够检测放射损伤反应并预测乳腺癌放射敏感性的体外乳腺癌类器官模型具有重要意义。本研究旨在构建乳腺癌类器官，建立放射损伤评估模型，检测照射损伤后相关 DNA 损伤修复分子标志物的表达情况，为探讨通过该模型预测放疗效果提供依据。

方法：构建乳腺癌类器官培养体系，对乳腺癌细胞系 MCF-7 、MDA-MB-231 和患者来源的乳腺癌组织进行培养；通过组织学与乳腺癌相关标志物的免疫组化检测乳腺癌类器官与原始组织的匹配情况；对构建的乳腺癌类器官进行 2、4、8、16Gy 的照射剂量处理，在光镜下记录各组的平均直径变化，通过 ATP 酶活性检测评估细胞活力绘制辐射生存 SF 曲线；通过流式细胞术评估照射损伤修复后的细胞凋亡和增殖情况；通过 Western Blot 和 RT-qPCR 检测照射后不同时间内乳腺癌类器官 DNA 双链断裂损伤修复蛋白的表达变化。

结果： HE 染色显示乳腺癌类器官形成微组织结构，具有明显的细胞异型性和病理性核分裂象。免疫组化结果显示 MCF-7 类器官呈现 ER、PR 阳性表达，HER2 阴性表达，符合 luminalA 型分子分型；MDA-MB-231 类器官呈现 ER、PR、HER2 阴性表达，符合三阴性分子分型；且患者来源的类器官与其原始肿瘤组织的分子分型保持一致。流式细胞术和 ATP 酶活性检测显示从 8Gy 开始，类器官存活率呈剂量依赖性下降，12Gy 时，类器官活力完全丧失。Western Blot 和 RT-qPCR 结果显示类器官模型在照射后γ-H2AX、P53 明显上调，DNA 损伤相关激活蛋白 p-ATM 在照射早期 48h 内表达上调，96h 修复完成后下调。

结论：乳腺癌类器官与原始肿瘤的形态学，组织病理学，激素受体状态相匹配且维持了肿瘤的遗传异质性。乳腺癌类器官模型下的肿瘤细胞较普通二维培养下的肿瘤细胞更耐照射，结合 DNA 修复标志物分析提示该模型下利于肿瘤细胞完成损伤修复过程。乳腺癌类器官模型是更接近体内的放射生物学体外研究模型。

关键字：乳腺癌类器官 ；放射生物学；个体化医学；DNA 损伤修复

115. 血清外泌体和血清 Glypican-1 在早期胰腺癌表达及临床诊断和预后意义

赵娟*

哈尔滨医科大学附属肿瘤医院

背景:本研究目的是通过酶联免疫吸附试验(ELISA)法检测血清外泌体及血清 GPC-1，探讨其是否可作为 PDAC 早期诊断和复发的预测因子。

方法:收集 PDAC、良性胰腺肿瘤(BPT)、慢性胰腺炎（CP)患者和健康对照者(HCs)血清样本。ELISA 法检测血清外泌体和血清 GPC-1 浓度，分析血清反复冻融过程中 GPC-1 的稳定性。

ROC 曲线评估 GPC-1 在早期胰腺癌诊断价值，Kaplan-Meier 曲线和多因素 Cox 回归分析评估 GPC-1 对胰腺癌预后价值。

结果:血清外泌体和血清 GPC-1 平均浓度为 1.45 和 0.80 ng/ml。在反复冻融条件下，GPC-1 表达稳定(d1-5 冻融 vs. d0 $P > 0.05$)。PDAC 组血清外泌体和血清 GPC-1 高于 HCs 组($P<0.0001$)，略高于 CP 和 BPT 组，无统计学差异($P > 0.05$)。PDAC、CP 和 BPT 患者术后 5 天外泌体和血清 GPC-1 表达较术前升高($P<0.05$)。高水平外泌体和血清 GPC-1 的患者无复发生存期(RFS)更短($P= 0.005$, $P= 0.007$)。多因素分析显示，外泌体和血清 GPC-1 是预测早期 RFS 的独立指标($P= 0.008$, $P= 0.029$)。

结论: ELISA 是一种有效的检测外泌体和血清 GPC-1 方法。GPC-1 在反复冻融循环过程稳定。GPC-1 可区分早期 PDAC 和 HC，但不能区分 PDAC 和 CP 和 BPT。外泌体和血清 GPC-1 是 PDAC 早期复发的独立预测因子。

关键字: 胰腺导管腺癌，外泌体，glypican 1，诊断，RFS

116. 人 SLC25A37 基因促进肺癌细胞的生长与迁移

孙志佳*[1]、亢小峰 [2]、薛春源 [2]、霍楠 [2]、李江波 [3]、韩雨辰 [2]、杜楠 [4]、徐小洁 [2]、王颖杰 [1]

1. 中国人民解放军空军特色医学中心

2. 军事医学研究院生物工程研究所

3. 军事医学研究院微生物流行病研究所

4. 解放军总医院第五医学中心

目的: 构建带 Flag 标签的人线粒体溶质载体蛋白 25A37（SLC25A37）的真核表达载体，验证其表达，检测其对人肺癌细胞生长的影响。

方法: 以人乳腺文库为模板采用 PCR 技术扩增出 SLC25A37 的编码区序列，双酶切后将其插入到 pCMV-Tag2B-Flag 载体中，构建 Flag 重组质粒；将重组质粒与空载体分别转染人肺癌 H460 细胞，Western blot 鉴定目的基因蛋白表达，CCK-8、克隆形成实验测定其对 H460 细胞生长的影响，划痕试验检测其对 H460 细胞运动迁移能力的影响。

结果: 双酶切鉴定表明，Flag-SLC25A37 真核表达质粒构建成功；转染 H460 细胞后融合蛋白表达。生长曲线、克隆形成及划痕实验结果表明，SLC25A37 可促进肺癌细胞的增殖和迁移。

结论: 携带 Flag 标签的人 SLC25A37 基因的真核表达载体能在人肺癌 H460 细胞中表达，且能促进该细胞的生长。该实验为进一步研究 SLC25A37 在肿瘤，尤其是肺恶性肿瘤中的功能奠定了基础。

关键字: SLC25A37；肺癌；H460 细胞；克隆

117. 结直肠癌患者癌组织端粒酶表达与临床病理特征关系的 Meta 分析

李江波*[1]、孙志佳 [2]、秦玲玫 [3]、王瑞官 [4]

1. 军事科学院军事医学研究院微生物流行病研究所

2. 中国人民解放军空军特色医学中心

3. 军事科学院军事医学研究院生物工程研究所

4. 解放军总医院第八医学中心

目的:采用 Meta 分析方法系统评价结直肠癌患者癌组织中端粒酶表达与临床病理特征间的关系，以求达到指导基础机制研究，临床治疗方案制定和癌症预后评估的目的。

方法: 在 PubMed、Cochrane、EMbase、web of Science、CNKI、重庆维普和万方数据库搜索国内外有关比较结直肠癌患者临床病理特征与患者癌组织中端粒酶表达研究的文章，检索的时间段为各个数据库建库到 2022 年 7 月 1 日。首先根据纳入与排除制定的相关标准对检索的文章进行初步的筛选，提取资料，并对筛选纳入的研究用 Cochrane 工具进行偏移的评估。采用 NOS 量表工具进行文献质量评价之后，用 RevMan5.3 软件实施 Meta 分析。

结果: 最终纳入 23 个研究，共计 1281 例病人。 根据 Meta 分析结果显示：结直肠癌患者癌组织中端粒酶的表达在肿瘤大小、肿瘤位置的差异不具有统计学意义（$P>0.05$），在肿瘤远处转移、Dukes 分期、分化程度、淋巴转移、临床分期、浸润深度的差异具有统计学意义（$P<0.05$）。

结论: 结直肠癌患者癌组织中端粒酶表达越强其恶性程度越高，端粒酶表达可能参与结直肠癌的分化、促进其浸润和转移。

关键字: 结直肠癌；端粒酶；系统评价

118. CD274（PD-L1）和 PDCD1LG2（PD-L2）结构变化的泛癌景观研究

付佳*、刘超月

中国医科大学

背景：PD-1 受体和 PD-L1 配体的相互作用是多种肿瘤类型的免疫疗法的目标。预测对免疫疗法反应的既定生物标志物包括微卫星不稳定性、肿瘤突变负担和 PD-L1 免疫组化。CD274（PD-L1）和 PDCD1LG2（PD-L2）的结构变异已在癌症中被观察到，但其综合情况尚不清楚。这里我们描述了 CD274 和 PDCD1LG2 结构变异的基因组情况和它们对肿瘤微环境的潜在影响，以及有这些改变的患者可以更好适应免疫疗法的证据。

方法:我们分析了含有 CD274 和 PDCD1LG2 结构变异的 514 个癌症病例的测序数据。数据来源包括大型泛癌症来源。Foundation Medicine, Inc(FMI)、The Cancer Genome Atlas (TCGA) 和 Oncology Research Information Exchange Network。为了评估免疫特征的富集程度，我们运行软件 ImSig 得到基因表达数据。我们整理了携带 CD274 和 PDCD1LG2 结构变异的患者的临床结果。

结果：从 25 项研究和数据集中，我们整理出 514 例具有 PD-L1 和 PD-L2 结构变异的癌症病例，包括 158 次重复，126 次缺失，97 次倒置，178 次易位，以及 96 次未分类的结构变异，总共有 655 个事件。我们在 PD-L1 和 PD-L2 的 3'-UTR 非翻译区观察到断裂位点“热点（hotspots）”。利用 TCGA 数据，我们观察到在 CD274 重组的肿瘤中，PD-L1 和 PD-L2 的表达显著上调，干扰素信号、巨噬细胞、单核细胞、T 细胞和免疫细胞增殖的特征也显著上调。与 CD274 非重排的、拷贝中性的肿瘤相比，$P<0.001$。此外，回顾了 12 项研究，其中包括 CD274 或 PDCD1LG2 结构变异的患者，包括重复、颠倒和拷贝数扩增，发现 73%(52/71) 的患者对 PD-1 免疫疗法有反应，且反应持久。

结论：我们评估了 CD274 和 PDCD1LG2 的结构变异显示，3'-UTR 经常受到影响，并且与配体和免疫特征的表达增加有关。在 CD274 重新排列的肿瘤中，富集的干扰素信号是特别值得关注的。因为已知干扰素暴露会驱动 PD-L1 和 PD-L2 的表达。来自研究的回顾性证据表明，这些基因组改变可以确定 PD-1 或 PD-L1 免疫疗法的候选人。我们期望这些发现将更好地定义 CD274 和 PDCD1LG2 在癌症中的结构变异在癌症中的变异，并支持我们的泛癌症前瞻性临床试验，以锁定这些改变在临床中的。

关键字: CD274，PDCD1LG2，结构改变，免疫治疗

119. NAMPT 和 PD-L1 双靶点抑制剂的抗肿瘤作用研究

杨媛、王义栋、秦铭泽、王立辉*

沈阳药科大学

研究目的: 近年来，靶向阻断 PD-1/PD-L1 相互作用的肿瘤免疫治疗已在临床上取得了良好的治疗效果，但大量患者出现原发性或继发性耐药。PD-1/PD-L1 单抗耐药机制复杂，目前已确证肿瘤高代谢导致 T 细胞增殖受到抑制，促进肿瘤免疫抑制微环境的形成，降低了单抗药物的疗效。NAMPT 是肿瘤细胞代谢中的关键酶，通过调控 NAD+的合成来影响肿瘤细胞的代谢，且肿瘤细胞中过表达的 NAMPT 会促进免疫抑制性细胞 MDSCs 的扩增，从而造成免疫抑制，但由于存在剂量限制性毒性的问题，NAMPT 抑制剂临床疗效并不理想。综上，同时抑制 PD-1/PD-L1 相互作用和 NAMPT 从理论上具有协同的免疫活化功能，并在一定程度上克服抗 PD-1/PD-L1 治疗耐药。因此，开发 PD-1/PD-L1 相互作用和 NAMPT 双重抑制剂将有望获得抗肿瘤活性突出、作用机制独特的化合物，具有重要的研究意义。

材料与方法: 在总结 NAMPT 和 PD-L1 两类抑制剂结构特征的基础上，通过建立两类抑制剂的药效团模型，以实验室前期报道的 PD-1/PD-L1 抑制剂和 NAMPT 抑制剂为先导化合物，运用药效团拼合原理和局部修饰策略，设计和合成抑制 NAMPT 和 PD-L1 的双靶化合物。在生化水平，采用 HTRF 检测法，以实验室前期合成的 PD-1/PD-L1 抑制剂 32 为阳性对照，测试双靶化合物对 PD-1/PD-L1 相互作用的抑制活性；采用 TR-FRET 检测法，以 FK-866 为阳性对照，测试双靶化合物对 NAMPT 的抑制率。在细胞水平，采用 MTT 法，以 FK-866 为阳性对照，选取 NAMPT 高表达的人卵巢癌细胞 A2780 为测试细胞株，考察化合物对肿瘤细胞生长抑制活性。NAD+水平下降是 NAMPT 活性抑制后的典型特征，采用 NAD+检测试剂盒检测化合物对 NAD+水平的影响，以验证化合物对 NAMPT 的抑制作用。采用 CCK-8 法考察化合物对人外周血单核细胞 PBMC 的毒性，通过在 CT26/PD-L1 和 $CD3^{+}$T 细胞共培育模型中，测试化合物对 T 细胞增殖和分化、释放 IFN-γ和 IL-2 能力以及杀伤肿瘤细胞功能的影响，进一步研究目标化合物的免疫调节活性。在体水平，通过内源性高表达 NAMPT 和 PD-L1 和外源性过表达 NAMPT 和 PD-L1 的两种动物模型进行双靶化合

物的药效学评价，并通过免疫正常和缺陷小鼠的对比，验证目标化合物的作用是否依赖免疫环境。

结果: 设计并合成了未见文献报道的能同时抑制 NAMPT 和 PD-L1 的化合物，并通过 MS、1H NMR 确证目标化合物的结构。在生化水平，发现双靶化合物能有效抑制 PD-1/PD-L 相互作用和 NAMPT 的活性。在细胞水平，化合物能有效抑制 A2780 细胞的生长活力，而且化合物对 PBMC 基本无毒性；共培养条件下，化合物能特异性阻断 PD-1/PD-L1 相互作用，恢复被 PD-1 激活抑制的 T 细胞增殖，提高 IFN-γ和 IL-2 释放水平，恢复肿瘤免疫微环境，提高 T 细胞杀伤肿瘤细胞的能力。在体实验的结果也表明双靶化合物能有效抑制小鼠肿瘤的生长。

结论: NAMPT 和 PD-L1 的双靶向治疗能有效抑制肿瘤的生长，有望为免疫治疗耐受的肿瘤提供一种有前景的治疗策略。

关键字: NAMPT，PD-L1，双靶点抑制剂，抗肿瘤

120. 血清外泌体 lncRNA 用于早期肺癌诊断的临床性能评价

于文俊*、郑沁杨、孟红委

上海市胸科医院

研究目的：探索用于早期肺腺癌诊断的血清外泌体 lncRNA，评价血清外泌体 lncRNA 的临床诊断性能。

材料与方法：我们前期利用基因芯片技术筛选 5 例正常人、5 例早期肺腺癌患者血清外泌体中差异表达的 lncRNAs。进一步利用 RT-qPCR 技术在 40 例肺部良性疾病、40 例早期肺腺癌患者中验证差异表达的前 20 条血清外泌体 lncRNAs，绘制 ROC 曲线评价血清外泌体 lncRNAs、传统肿瘤标志物（CEA、CYFRA21-1）的临床诊断性能，包括灵敏度和特异性。

结果：利用基因芯片技术筛选出差异表达的血清外泌体 lncRNAs 共 994 条，其中 815 条表达上调，179 条表达下调。利用 RT-qPCR 技术验证差异表达的前 20 条血清外泌体 lncRNAs，其中 lncRNA SLC6A12-9 在早期肺腺癌患者血清中表达量升高，与肺部良性疾病患者的血清表达量有显著差异。利用 ROC 曲线评价 lncRNA SLC6A12-9、CEA、CYFRA21-1 在早期肺腺癌的诊断灵敏度和特异性，发现三个标志物联合检测的灵敏度、特异性最高，分别是 95%、77.5%。

结论：血清外泌体 lncRNA SLC6A12-9 可用于肺癌的早期诊断，与 CEA 和 CYFRA21-1 联合检测可提高临床诊断性能。

关键字:外泌体，lncRNA，早期诊断，肺腺癌

121. miR-203a-3p 通过调控 Drp1 的表达促进食管鳞癌转移的作用研究

郭江豪[1,2]、杨雅亭[1,2]、魏夏杰[1,2]、朱庆国[1,2]、王晓燕[3]、鲍登克*[1,2]

1. 河南大学药学院肿瘤标志物与液体活检实验室

2. 开封市生物标志物与肿瘤液体活检重点实验室

3. 郑州大学第一附属医院

目的：探究 miR-203a-3p 通过调控 Drp1 的表达进而对食管癌转移的影响及其相关机制

方法：使用公共数据库分析 Drp1 与食管癌患者预后相关性。使用免疫组织化学（IHC)、免疫印迹法（Western Blot）、荧光定量 PCR（qPCR）等方法检测 Drp1 在食管癌组织样本中的表达。使用 Western Blot、Transwell 和裸鼠体内实验等研究 Drp1 异常表达及 Drp1 抑制剂 Mdivi-1 对食管癌细胞体内外转移的影响。使用 TargetScan、miRBase、miRBD 及 miRWalk 等在线分析与 Drp1 相互作用的 miRNA，并通过细胞划痕，Transwell，Western Blot、qPCR 及流式细胞术等方法研究 miR-203a-3p 对 Drp1 介导的食管癌转移的影响及其分子机制。

结果:1）利用公共数据库以及 Western blot、qPCR、IHC 等实验结果表明食管癌病人组织样本中 Drp1 的表达显著上调；使用统计学方法进行分析显示肿瘤病人中 Drp1 的高表达与食管癌的发展及食管癌病人的不良预后存在着重要的相关性。2）Western blot、细胞克隆、EdU、细胞划痕和 Transwell 实验等实验结果提示：Drp1 过表达显著促进食管癌细胞的增殖、迁移和侵袭能力。3） 转染 miR-203a-3p 后食管癌细胞中 Drp1 表达减少，细胞的增殖、迁移和侵袭能力降低。4） 流式细胞术、Western blot、划痕实验和 Transwell 等实验结果显示 miR-203a-3p 通过调控 Drp1 介导的 ROS-PGC1-α-Nrf1/2 途径抑制食管癌的转移。

结论：本研究表明 miR-203a-3p 能够抑制 Drp1 的表达进而抑制食管癌的转移，研究结果将为食管癌的治疗提供新的思路。

关键字: 食管癌、Drp1、miR-203a-3p、转移

122. 缺氧通过 TLR9 通路促进 TAMs 浸润和 HCC 进展的作用研究

司娇阳[1,2]、王佳鑫[1,2]、姚晓娟[1,2]、梁怡宣[1,2]、廖子谦[1,2]、鲍登克*[1,2]

1. 河南大学药学院肿瘤标志物与液体活检实验室

2. 开封市生物标志物与肿瘤液体活检重点实验室

目的：初步探索 TLR9 通路在缺氧诱导 TAMs 浸润和肝癌进展中的作用，研究结果将为深入探究肝癌微环境中缺氧与 TAMs 相互作用的分子机制提供新的见解。

方法：通过 Western blot、qRT-PCR、IHC 和公共数据库等分析缺氧标志分子 HIF-1α和 M2 型 TAMs 标志物 CD163 在肝癌组织样本中的表达及其相关性，并分析其与肝癌患者预后的关系。构建原位肝癌小鼠模型，采用 HE、qRT-PCR、IHC 等实验分析小鼠组织中缺氧对 TAMs 浸润和肝癌进展的影响。采用 Western blot、IF、FCM 等实验方法分析肝癌细胞缺氧对 TAMs M2 型极化和募集的影响。通过 Western blot、FCM 等实验探讨缺氧通过 TLR9 通路诱导 TAMs M2 型极化的作用机制。

结果：1、Western blot、qRT-PCR、IHC 等实验结果发现肝癌患者肿瘤组织中 HIF-1α和 M2 型 TAMs 在 HCC 组织中浸润显著增加。公共数据库分析发现，在肝癌组织中 HIF-1α与 CD163 的表达呈显著正相关，并与肝癌患者预后较差相关；2、构建原位肝癌小鼠模型结果表明，缺氧促进 TAMs 浸润和肝癌进展。3、qRT-PCR、Western blot、IF 和 FCM 实验结果发现肝癌细胞缺氧促使 TAMs 向 M2 型极化，同时采用迁移实验证实了肝癌细胞缺氧促进 TAMs 募集；4、Western blot 实验结果发现肝癌细胞缺氧条件培养基孵育巨噬细胞后，明显增加了 TLR9 及其下游相关分子的磷酸化水平；使用 TLR9 干涉片段或拮抗剂(ODN INH-18)能够显著抑制缺氧条件培养基介导的 TAMs M2 型极化。

结论：缺氧通过激活 TLR9 通路促进 TAMs 的浸润和肝癌进展。

关键字：肝癌，缺氧，肿瘤相关巨噬细胞，TLR9，肿瘤微环境

123. 线粒体转录因子 TFAM 在食管癌发生发展中的作用研究

杨笑天[1,2]、韩静如[1,2]、李雨佳[1,2,3]、杨琪[1,2,3]、陈慧[1,2]、吴远远[1,2]、鲍登克*[1,2]

1. 河南大学药学院肿瘤标志物与液体活检实验室

2. 开封市生物标志物与肿瘤液体活检重点实验室

3. 河南大学生命与科学学院

目的：以食管癌临床组织样本、TFAM 干涉/过表达食管癌细胞株及皮下荷瘤小鼠动物模型为基础，在多水平上系统地研究 TFAM 在食管癌发生发展中的作用。研究结果将为深入研究食管癌发生发展的分子机制和建立新的防治策略奠定理论基础。

方法：本研究使用公共数据库及免疫组化实验方法分析 TFAM 在食管癌组织样本中的表达以及分析其与食管癌病人预后相关性。采用慢病毒转染的方式构建干涉和过表达 TFAM 的食管癌细胞系，通过 MTS、克隆形成和 EdU 实验检测细胞增殖，并利用荷瘤小鼠皮下成瘤实验进行体内验证。 RNA-seq 和 Western blot 分析 TFAM 干涉对 cGAS-STING 通路的影响，以及靶向抑制 cGAS-STING 后对食管癌细胞增殖的影响。

结果：1）利用 Western blot、qPCR、IHC 以及公共数据库等实验方法检测食管癌病人组织样本中 TFAM 的表达，结果显示 TFAM 在 ESCC 组织中蛋白、mRNA 水平显著下调；随后使用统计学方法进行分析：结果显示肿瘤病人中 TFAM 的低表达与食管癌的发展及食管癌病人的不良预后存在着重要的相关性。2） MTS 、 EdU 、克隆形成实验及裸鼠皮下成瘤实验结果证明 TFAM 下调能显著促进食管癌细胞的体内外增殖能力。3）靶向抑制 cGAS-STING 后抑制食管癌细胞的体内外增殖。

结论：本研究表明 TFAM 在食管癌的发生发展中起着重要作用，对设计有效治疗药物有着重要的理论指导意义。

关键字: 食管癌、TFAM、cGAS-STING、增殖

124. 术前炎症指标联合 PET-CT 代谢参数在非小细胞肺癌预后中的应用

陈奕心、孙轶华*

哈尔滨医科大学附属第三医院

背景及目: 2020 年中国肺癌的发生率和死亡率居恶性肿瘤首位。虽然对于肺癌的检查手段和诊断方法有了很大进步，但患者的 5 年生存率仍不理想。手术治疗是目前非小细胞肺癌（Non-small lung cancer，NSCLC)最主要的治疗手段，为了更好预测患者的预后，术前的全面评估和开发准确特异的生物标志物是极其重要的。炎症不仅影响局部肿瘤微环境，还具有改变全身炎症反应的作用，在 NSCLC 的发生发展过程中扮演了重要的角色。基于这些全身炎症反应的相关指标，近年来受到了学界的广泛的关注。本研究综合分析全身炎症反应指标系统性免疫炎症指数 SII与肿瘤局部代谢参数 SUV-max 对可切除 NSCLC 患者预后的预测意义，探讨二者的相关性，并借助诺莫图（Nomogram），构建个体化预测模型。

方法: 收集 2013 年 10 月至 2016 年 2 月期间哈尔滨医科大学附属肿瘤医院收治的 140 例手术治疗的非小细胞肺癌患者的临床病例资料及预后信息。对所收集数据进行回顾性分析，组间比较采用$\chi 2$ 检验。采用受试者操作特征(Receiver operating characteristic，ROC)曲线方法确定 SII、NLR、PLR、SUV-max 的最佳截断值，并根据最佳截断值将患者分为高值组和低值组。采用 spearman 进行相关性分析。采用单因素和多因素 Cox 回归分析筛选影响预后的独立危险因素。采用 Kaplan-Meier 法绘制生存曲线，Log-rank 检验用于分析生存曲线之间的差异，$P<0.05$ 为差异有统计学意义。用 R 语言构建手术切除的 NSCLC 预后预测模型。应用一致性指数（C-index）和校准曲线评估模型的准确性和可靠性。以上数据分析均通过 spss26.0、Graphpad Prism8、RStudio(version 1.4.171)软件进行。

结果: SII 和 SUV-max 的最佳截断值分别为 413.40 和 5.40，在此临界值下 AUCSII为 0.765、AUCSUV-max 为 0.733 对 NSCLC 预后有预测作用。非小细胞肺癌患者 SII水平与 PET-CT 的代谢参数 SUV-max 具有轻等程度且显著的相关性（r=0.3179）95%CI：0.1599～0.4601（$P<0.001$）。多因素 Cox 分析结果显示淋巴结转移（HR=8.83，$P=0.001$）、累及胸膜（HR=6.90，$P<0.001$）、临床分期（III+IV期）（HR=8.53，$P=0.002$）、SII（≥413.40）（HR=3.42，$P<0.001$）、SUV-max（≥5.40）（HR=1.97，$P=0.007$）为影响预后的独立危险因素。基于上述 Cox 分析结果构建可切除 NSCLC 的预后预测模型，在内部验证中 5 年生存率的 C-index

为 0.732（95%CI：0.688～0.779）绘制术后 NSCLC 患者预后的 3 年及 5 年生存率的 ROC 曲线，其曲线下面积（AUC）的结果为训练集 3 年：0.827；5 年：0.709；验证集 3 年：0.719；5 年 0.731。根据上述独立预后因素构建的 3 年及 5 年生存概率模型，绘制 Kaplan-Meier 生存曲线，用 Log-rank 检验分析生存曲线之间的差异，差异有统计学意义（P<0.001）

结论: SII和 SUV-max 是影响可切除 NSCLC 预后的独立危险因素；SII和 SUV-max 具有轻等程度相关性；基于 SII和 SUV-max 构建的预后模型具有良好的准确性和可靠性。

关键字: 非小细胞肺癌；系统性免疫炎症指数；最大标准化摄取值；诺莫图

125. M2 型巨噬细胞通过 MIF/ERK/FBXW7 通路 影响乳腺癌的增殖和迁移

陈敏捷 、孙轶华*

哈尔滨医科大学附属肿瘤医院

背景及目的：近年来，我国乳腺癌发病率呈逐年上升趋势，据相关数据统计,我国乳腺癌的发病率已位居女性癌症的首位。乳腺癌的发生发展是一个多种因素相互调控的过程。乳腺癌组织中浸润的多种免疫细胞和基质细胞及各种细胞分泌的细胞因子都参与其中。肿瘤相关巨噬细胞（Tumor-associated macrophages, TAMs)作为乳腺癌微环境中的重要组分，通过分泌细胞因子来介导其与肿瘤细胞之间的相互作用，在乳腺癌细胞增殖迁移、逃避免疫反应及产生耐药性等方面起到促进作用。巨噬细胞迁移抑制因子（Macrophage migration-inhibitory factors, MIF)是一种促瘤细胞因子，在肿瘤组织中高表达。研究发现 TAMs 可以分泌 MIF，二者均与肿瘤的不良进展相关。然而，TAMs 分泌的 MIF 在乳腺癌中的作用尚未见相关报道。因此 TAMs 是否通过分泌 MIF 促进乳腺癌的进展值得深入研究。本课题旨在研究 M2 巨噬细胞来源的 MIF 对乳腺癌细胞的影响，并探究 MIF 影响乳腺癌的具体机制，从而为乳腺癌的临床治疗提供一个新的靶点。

方法：利用 PMA 诱导 THP-1 细胞分化为 M0 巨噬细胞、IL-4 和 IL-13 将 M0 巨噬细胞极化为 M2 型巨噬细胞；Western-blot 检测 M1 巨噬细胞和 M2 巨噬细胞表型标志物的表达和 M2 型巨噬细胞中 MIF 的蛋白表达情况；ELISA 法检测 M2 型巨噬细胞上清液中 MIF 的分泌量；沉默或过表达 M2 型巨噬细胞中的 MIF，使用 Western-blot 和 ELISA 验证转染效果；收集经过不同处理后的 M2 型巨噬细胞的上清液制备条件培养基，用于培养乳腺癌细胞 BT-549 和

MCF-7，CCK-8 实验检测乳腺癌细胞的增殖，划痕实验和 transwell 实验用于检测细胞迁移；利用共培养小室将转染 MIF 的 M2 型巨噬细胞与 BT-549 或 MCF-7 细胞共培养，Western-blot 检测 BT-549 和 MCF-7 细胞中 E-cadherin、Vimentin、P-ERK1/2、FBXW7（F 框/WD-40 域蛋白 7）的表达；向乳腺癌细胞中加入 ERK 通道阻断剂 U0126，然后将其与过表达 MIF 的 M2 型巨噬细胞共培养，Western-blot 检测 BT-549 和 MCF-7 细胞中 FBXW7、P-ERK1/2、E-cadherin、Vimentin 的表达，CCK-8 检测细胞增殖，划痕实验和 transwell 实验检测细胞迁移。

结果：M2 型巨噬细胞比 M0 型巨噬细胞分泌 MIF 增多。当与 M2 型巨噬细胞共培养后，BT-549 和 MCF-7 细胞的增殖和迁移增加，细胞中 EMT 相关蛋白 E-cadherin 表达减少，Vimentin 表达增加。当沉默 M2 型巨噬细胞中的 MIF 后，其促进 BT-549 和 MCF-7 细胞增殖迁移和 EMT 的能力被抑制；而过表达 MIF 的 M2 型巨噬细胞进一步促进 BT-549 和 MCF-7 细胞的增殖迁移和 EMT。沉默 MIF 后乳腺癌细胞中 FBXW7 的表达升高，过表达 MIF 后 FBXW7 的表达下降，而 P-ERK1/2 的变化与 FBXW7 相反。ERK 阻断剂可逆转 MIF 对 FBXW7 的抑制作用，恢复乳腺癌细胞中 FBXW7 的表达，并抑制乳腺癌细胞增殖迁移及 EMT。

结论：M2 型极化的巨噬细胞分泌 MIF 增多；MIF 通过激活乳腺癌细胞中 ERK 信号通路抑制 FBXW7 的表达，促进乳腺癌的增殖和迁移。

关键字：乳腺癌；肿瘤相关巨噬细胞；巨噬细胞迁移抑制因子；FBXW7；ERK 信号通路

126. 肺癌肺部菌群特征及其与宿主共代谢产物研究

孟红委*

上海市胸科医院

肺癌是世界范围内癌症死亡的首要原因。前人研究发现肺部菌群可能参与肺癌的发生发展，但是具体机制尚不清楚，而且由于多数研究的样本量较小和肺癌的异质性，目前关于肺癌肺部菌群的研究得出的一致结论有限，且缺乏肺癌代谢组学的相关研究。申请人通过采集肺癌、肺部良性疾病和健康对照组较多而全面的血浆样本进行前期研究，基于已有研究中肺癌患者的血浆代谢谱与健康人之间存在明显的差异，猜测肺部菌群可能通过影响宿主共代谢来参与肺癌的发生发展。因而本研究拟通过 16S rRNA 测序和代谢组学分析，对已采集的肺癌、肺部良性疾病和健康对照组配对的肺泡灌洗液和血浆样本进行肺部菌群和局部及全身代谢组

的变化研究，以筛选和挖掘出与肺癌相关的潜在生物标志物，并通过生信分析探索肺部菌群变化对肺癌患者的代谢表型的可能影响，初步探讨肺部菌群与肺癌患者代谢之间的机制，为肺癌的临床诊断提供新的依据并为肺癌发生发展的研究提供新的思路。

关键字: 肺癌；肺部菌群；16S rRNA；共代谢产物；生物标志物

127. 外泌体递送 lncRNA DARS-AS1 siRNA 对慢性应激诱导的 TNBC 侵袭转移的影响及机制研究

刘新利、张葛、禹瞳垚、尹大川、张辰艳*

西北工业大学

目的: 侵袭转移是导致临床三阴性乳腺癌（TNBC）患者高死亡率的主要原因。机体长期慢性应激（CUMS）可通过调控神经内分泌系统改变机体内稳态诱导恶性肿瘤的发生发展和侵袭转移。然而，有关 CUMS 对 TNBC 发生发展和侵袭转移的影响及其作用机制尚未阐明

方法: 利用体内外慢性应激模型（CUMS），观察 CUMS 状态下 lncRNA DARS-AS1 的表达变化及其对 TNBC 细胞增殖、迁移和侵袭的影响；并进一步通过 GO 分析、KEGG 分析、体外共培养、外泌体递药、RNAi 技术和裸鼠原位异种移植瘤模型，初步揭示 CUMS 状态对 TNBC 细胞侵袭转移的作用机制。

结果: 细胞水平实验结果表明，体外 CUMS 状态可诱导 lncRNA DARS-AS1 的高表达，进而促进 TNBC 细胞的增殖、迁移和侵袭。此外，裸鼠原位异种移植瘤模型结果表明，对荷瘤小鼠进行连续 5 周的 CUMS 模型干预，随后采用瘤内注射 DARS-AS1 siRNA 负载的 EXOs 递药系统治疗，能够显著抑制 CUMS 模型诱导的裸鼠体内 TNBC 原位成瘤和肝转移。进一步研究结果表明，CUMS 模型介导的 DARS-AS1 可作为 miR-129-2-3p 的分子海绵，通过竞争结合并上调 CDK1 的表达并激活下游 NF-κB/STAT3 信号通路，进而促进 TNBC 细胞的增殖和转移；采用 EXOs 递送 DARS-AS1 siRNA 或使用该信号通路特异性抑制剂 EVP4593 可通过阻断 NF-κB/STAT3 信号通路，从而抑制 TNBC 的体内成瘤和肝转移。

结论: DARS-AS1 是一种应激响应的促癌 lncRNA，其异常高表达能够促进 TNBC 的增殖、迁移和侵袭，提示 DARS-AS1 可作为临床转移性 TNBC 的潜在治疗靶点，同时 EXOs 可作为 DARS-AS1 siRNA 的新型高效递药载体在临床 TNBC 治疗中发挥作用。综上所述，本项目的研究成果将为临床转移性 TNBC 患者的治疗提供新靶点和一种高效、安全的递药载体。

（国家自然科学基金项目，52177226，82172063；陕西省重点研发计划项目，2021KW-62；陕西省创新能力支撑计划项目，2020TD-042；西北工业大学博士学位论文创新基金项目，CX2021096）

关键字：慢性应激（CUMS）,长链非编码 RNA（lncRNA）,CDK1，siRNA 载药外泌体（siRNA-loaded exosomes），乳腺癌肝转移（BCLM）

128. et-7c-5p 靶向调控 DUSP7/ERK 表达抑制大肠癌细胞 HCT8 的增殖

付娟娟[1]、侯志平*[1]、李思锦[2]、周龙妹[2]

1. 承德医学院

2. 承德医学院附属医院

目的：探讨 let-7c-5p 靶向 DUSP7 通过 MAPK-ERK 信号通路调控大肠癌增殖的作用及其潜在机制。

方法: TCGA 数据库中检测 let-7c-5p 在大肠癌组织与癌旁组织的表达情况及其与大肠癌患者临床病理分期的关系；RT-qPCR 法验证 let-7c-5p 在大肠癌及癌旁组织中的表达情况；利用转染的方法构建 let-7c-5p 高表达 HCT8 细胞系，通过 CCK8、EDU、细胞克隆形成实验及流式细胞术观察 let-7c-5p 对大肠癌增殖和凋亡的影响；通过 miRTarBase、TargetScan 和 GEPIA 等数据库预测和分析 let-7c-5p 靶基因；通过 GO 分析筛选信号通路并进行 WB 实验验证。

结果: TCGA 数据分析显示 let-7c-5p 在大肠癌组织的表达明显低于癌旁组织，且与临床分期有关。同时，在临床水平采用 RT-qPCR 技术验证 let-7c-5p 在大肠癌组织中的表达明显低于癌旁对照组。CCK-8 及 EdU 实验结果表明 let-7c-5p mimics 组细胞增殖能力显著低于对照组($P<0.05$)；let-7c-5p 显著抑制集落生成能力($P<0.05$)；流式结果表明 let-7c-5p mimics 组细胞凋亡率上升($P<0.05$)；利用生信软件预测 let-7c-5p 的靶点为 DUSP7 且其在大肠癌组织中呈高表达；通过 KEGG 富集分析锁定 MAPK 信号通路，WB 验证显示 let-7c-5p mimics 组细胞 ERK1/2 蛋白表达降低，Bax/Bcl-2 蛋白表达上升。

结论: let-7c-5p 通过抑制 DUSP7 调控 MAPK-ERK 信号通路抑制大肠癌的增殖，发挥抗肿瘤作用。

关键字:大肠癌; let-7c-5p；DUSP7；MAPK-ERK;

129. 肺癌样本 RNA 质量的影响因素研究

赵雅波、赵晋波、姜涛、吉晓鸿、熊延路、王雪娇*

空军军医大学唐都医院

目的:高质量的生物样本是医学研究的基石，RNA 完整性是衡量生物样本质量的关键指标，本研究拟探索影响肺癌组织样本 RNA 质量的因素，为优化肺癌生物样本取材及储存方法提供研究基础。

方法:从唐都医院胸腔外科生物标本库随机抽取-80℃储存的肺癌组织样本 282 例，评估样本储存年限和肿瘤大小、病理类型、年龄、性别等经典临床因素对 RNA 完整性的影响；选取新鲜肺癌手术样本 100 例，平均分成 5 组，评估不同离体时间（0h、0.5h、1h、2h、4h、8h、24h）对样本 RNA 完整性的影响；选取 4 只 C57/BL6N 小鼠的脑、肺、肝、肾组织，评估不同离体时间（0h、0.5h、1h、2h、4h、8h、24h）对不同组织 RNA 完整性的研究；通过 RT-qPCR 及 ELISA 探究不同条件下肺癌组织样本及小鼠组织样本中 3 种经典 RNA 酶（RNaseA/RNaseT1/RNaseH）含量及活性。

结果: 储存年限显著影响冰冻肺癌组织样本 RNA 质量，随着储存年限增加，RNA 逐步降解；年龄、性别、肿瘤大小、病理类型、病灶位置均不影响 RNA 完整性；离体时间 0.5h 内肺癌组织样本 RNA 无明显降解，0.5h 后随时间增加，RNA 完整性逐步减低；相比于其他脏器，肺组织 RNA 降解速率最快；RNaseA 含量及活性和样本 RNA 完整性呈负相关。

结论:储存年限是肺癌组织样本的-80℃保存的重要质量考量因素。0.5h 内离体操作对肺癌组织样本完整性无明显影响,抑制 RNaseA 的活性是保持 RNA 质量的有效途径。

关键字: 肺癌、组织样本、保存时间、RNA 完整性、RNaseA、质量控制

130. 整合酶介导基因盒位点特异性重组染色体反应模型的构建

张龙*

上海市胸科医院

背景:整合子在细菌耐药性的获得及传播中占据重要地位，对于整合子整合反应检测方法及反应机制的研究，可以加深整合子对细菌耐药性贡献的理解，为遏制耐药菌株的产生提供途径。

目的:在细菌染色体上构建第 1 类整合子反应模型，用于评价整合酶介导的基因盒位点特异性重组。

方法：PCR 分别扩增含氯霉素耐药基因 cat 的 CM 片段、含基因盒 aadA5 的 LacA5 片段、含 attI1 位点及强可变区启动子的 PcS 片段和敲入位点两侧的同源臂，重叠延伸 PCR 连接上述 5 个片段制备整合子模型敲入片段，通过同源重组将构建好的整合子模型片段敲入大肠埃希菌 JM109 染色体中。转入高表达整合酶的质粒 pHSint，在链霉素平板上筛选发生整合的菌株，并经 PCR 和测序验证。

结果:构建的整合子模型片段经测序与预期一致，整合子模型片段成功敲入大肠埃希菌 JM109 染色中。转入高表达整合酶的质粒 pHSint 后，在链霉素平板上成功筛选出基因盒 aadA5 发生整合的菌株，经 PCR 扩增并测序与预期一致。

结论:在大肠埃希菌中成功构建第 1 类整合酶介导基因盒位点特异性重组染色体反应模型，为进一步揭示整合子捕获与表达耐药性基因盒的调控机制奠定基础。

关键字: 整合子，同源重组，质粒，染色体

131. TFAM 通过 mtDNA-cGAS-STING 介导的自噬促进食管癌增殖的机制研究

韩静如[1,2]、杨笑天[1,2]、李雨佳[1,2,3]、杨琪[1,2,3]、陈慧[1,2]、吴远远[1,2]、鲍登克*[1,2]

1. 河南大学药学院肿瘤标志物与液体活检实验室

2. 开封市生物标志物与肿瘤液体活检重点实验室

3. 河南大学生命与科学学院

目的: 食管鳞状细胞癌是最常见的食管癌组织学亚型，也是中国食管癌发病的主要类型，因此研究食管癌发病机制以及寻找调控食管癌进展的信号通路至关重要。大量研究表明，线粒体功能障碍在癌症的发生和发展中有着多重作用，而线粒体转录因子 A (TFAM) 是调节线粒体 DNA(mtDNA)复制、转录和生物发生的关键因子，TFAM 下调会导致 mtDNA 由线粒体释放到胞浆诱发 mtDNA 应激。本研究的目的在于揭示 TFAM 在食管癌发生发展中的作用及其潜在的分子机制。

方法:本研究首先通过检测线粒体膜电位、ATP 生成以及 ROS 生成来分析 TFAM 下调与线粒体功能障碍之间的关系；采用共聚焦显微镜、ddPCR 等检测 mtDNA 应激形态以及胞浆 mtDNA 拷贝数，并通过靶向抑制 mPTP 和 VDAC1 来进一步研讨 mtDNA 释放机制；通过 RNA-seq 测序、Western blot、透射电镜以及共聚焦显微镜等方法进一步研究 mtDNA 应激在 TFAM 介导的自噬和食管癌细胞生长中的作用及机制。

结果:1）JC-1 染色、ATP 以及 ROS 生成实验结果显示，TFAM 下调导致线粒体功能障碍。2）共聚焦和 ddPCR 结果显示 TFAM 下调导致线粒体拟核呈异常分布，且增加了胞浆 mtDNA 拷贝数，阻断 mPTP 孔后显著抑制了胞浆 mtDNA 积聚。3）Western blot 和透射电镜结果显示 mtDNA 参与了自噬的发生，RNA-seq、共聚焦结果进一步证明 mtDNA 通过影响 cGAS-TING 通路促进食管癌细胞自噬。4）靶向抑制 cGAS-STING 通路或清除胞浆 mtDNA 后，显著抑制了自噬的发生和食管癌进展。

结论:本研究系统阐述了 TFAM 缺失介导的 mtDNA 应激促进食管癌发生的作用及潜在机制研究，为临床上治疗食管癌提供了新思路。

关键字: TFAM、mtDNA、cGAS-STING、自噬、食管癌

132. 色甘酸钠灌胃减轻葡聚糖硫酸钠诱导的 BALB/c 小鼠溃疡性结肠炎炎症

戈伊芹*

上海市胸科医院

目的：通过使用肥大细胞膜稳定剂色甘酸钠（Sodium Cromoglycate，Crom）稳定肥大细胞来探究其在小鼠溃疡性结肠炎造模过程中的作用。

方法：空白组小鼠自由饮用双蒸水；模型小鼠自由饮用 3%葡聚糖硫酸钠（dextran sulfate sodium，DSS）溶液构建溃疡性结肠炎模型；色甘酸钠组小鼠则在饮用 3% DSS 溶液同时灌胃服用色甘酸钠溶液，进而比较空白组、模型组和色甘酸钠组之间小鼠体质量改变、疾病活动指数（disease activity index，DAI）和病理评分以及脾脏免疫细胞浸润的变化。

结果：与空白组相比，模型组小鼠重度便血，DAI 评分升高，甲苯胺蓝染色显示肠道中肥大细胞数量增多。而定期给予色甘酸钠灌胃处理的小鼠便血减少，DAI 评分和病理评分较模型组降低。

结论：色甘酸钠灌胃可减轻小鼠溃疡性结肠炎炎症反应，间接表明肥大细胞参与了溃疡性结肠炎的发病。

关键字: BALB/c 小鼠，溃疡性结肠炎，色甘酸钠，肥大细胞

133. Romidepsin 促进靶向 NKG2DL-CAR-T 细胞对卵巢癌细胞的杀伤作用实验研究

王亮*、余丽蕊

福建省妇产医院

背景：为了提高嵌合抗原受体 T 细胞（chimeric antigen receptor T cell, CAR-T）在治疗以卵巢癌为代表的实体瘤中的效果，希望促进肿瘤细胞靶抗原上调，提高 CAR-T 的 cytotoxicity.

材料与方法：以卵巢癌细胞表面 NKG2D 配体为靶抗原，构建 NKG2D-CAR-T 细胞，创新性联合 Romidepsin 处理卵巢癌细胞 SKOV3，探究 SKOV3 表面 NKG2DL 的表达改变，并采用 LDH 释放试验验证 CAR-T 细胞的细胞杀伤作用，利用 ELISA 方法确定细胞因子的分泌。

结果：流式细胞术结果显示靶向 NKG2DL-CAR-T 细胞得到有效活化，Romidepsin 处理导致 SKOV3 表面 NKG2DL 表达增强；细胞毒性实验显示 Romidepsin 通过调控卵巢癌细胞 NKG2DL 表达增强从而提高 NKG2D-CAR-T 细胞对卵巢癌的杀伤能力（$P<0.05$）；IFN-γ 的分泌与杀伤作用同步升高（$P<0.05$），IL-2、PFP 在较低效靶比时存在统计学意义，而 PD-1 并未受到影响（$P\geq0.05$）。

结论：通过增强肿瘤细胞靶抗原的表达是解决 CAR-T 细胞在实体瘤上应用不佳的方法。

关键字: CAR-T 细胞，卵巢癌，NKG2DL，Romidepsin，细胞杀伤

134. 尿液 DNA 甲基化和突变在尿路上皮癌无创和精准诊断中的前瞻性、多中心临床研究

陈旭[1]、刘征[2]、吕强[3]、陈海戈[4]、范晋海[5]、魏强[6]、谭万龙[7]、廖洪[8]、徐涛[9]、杨进[10]、王少刚[11]、范建兵[12]、黄建[1]、林天歆*[1]

1. *中山大学孙逸仙纪念医院*
2. *华中科技大学同济医学院附属同济医院*
3. *江苏省人民医院*
4. *上海交通大学附属仁济医院*
5. *西安交通大学第一附属医院*
6. *四川大学华西医院*
7. *南方医科大学南方医院*
8. *四川省肿瘤医院*
9. *北京大学人民医院*
10. *成都大学附属医院*
11. *南方医科大学珠江医院*
12. *广州市基准医疗有限责任公司*

目的：目前尿路上皮癌的诊断和复发监测方法主要通过侵入性的膀胱或输尿管镜检查，现有无创尿液诊断技术在敏感性和/或特异性上难以满足临床需求。我们前期建立了尿液 DNA 甲基化诊断膀胱癌的技术。我们拟在全国的前瞻性大队列中进行 DNA 甲基化联合突变的技术优化和验证，最终开发出高敏感性和特异性的尿液无创诊断技术。

方法：我们在全国 11 个大型三甲医院前瞻性收集了 1187 例泌尿系统患者和健康人尿液，最终入组分析了 1092 例。其中包含膀胱和上尿路上皮癌共 623 例，其他泌尿系肿瘤共 97 例，良性疾病对照 338 例，健康人 31 例。基于 TCGA 和我国测序数据筛选建立检测 DNA 突变的 qPCR 检测方法，结合前期已建立的 2 个基因的甲基化方法，对上述样本进行检测，并将本技术与尿脱落细胞学和 FISH 进行诊断效能的比较分析。

结果：DNA 甲基化总体敏感性、特异性、准确性分别为 84.4%，86.8%和 85.4%。其中 NMIUC 和 MIUC 患者中敏感性分别为 82.2%和 94.5%，低级别和高级别患者中敏感性分别为 61%和 94.5%。联合甲基化和突变，性能较前提高到准确性 88.6%，敏感性为 86.8%、，特异性为 94.5%。联合 DNA 甲基化和突变总体敏感性、特异性、准确性分别为 89.1%，86%和 87.9%，较前有较大提升。其中健康人中特异性为 100%。无论是单用 DNA 甲基化或突变，或者联合两者，他们的敏感性显著高于尿脱落细胞学（40%）和 FISH（68.2%），而特异性相近（93.9%和 87.3%）。而且尿液 DNA 甲基化联合突变，在低分期、低分级肿瘤，以及 UTUC 展示出高的敏感性和准确性，显著优于脱落细胞学和 FISH。

结论：本研究是国内首个大样本的尿液 DNA 甲基化联合突变诊断尿路上皮癌的前瞻性、多中心临床研究，中期结果显示尿液 DNA 甲基化和突变检测是一种快速、高通量、无创、高诊断效能的方法，可用于早筛，可减少不必要的有创检查和盲目的二次手术，为尿路上皮癌精准诊断提供高效新方法。

关键字：尿路上皮癌，尿液无创诊断，DNA 甲基化，DNA 突变

135. 蛋白质组学和代谢组学在血液恶性肿瘤生物标志物筛选中的应用

郭璐璐*

上海市胸科医院

组学研究在质谱与测序技术的发展推动下已进入新时代，组学分析已成为筛选疾病诊断和预后监测标志物的新方法。组学技术如基因组、转录组、蛋白质组或代谢组，是对生物样本进行系统研究，多组学联合分析（Multi-omics）是将各组学的数据加以整合分析，解决单一组学无法全面解释生物系统宏微观变化的集成研究。血液系统恶性肿瘤发病率逐年提高，缺乏

早期特异性诊断标志物，故本文对转录组、蛋白质组、代谢组以及组学联合在血液肿瘤标志物中的研究进展进行阐述。

关键字：蛋白组学；血液恶性肿瘤

136. 基于 CTSL/ZBTB7B 表达的新型胃癌高危免疫分子亚型

崔凯飒、费伯健、黄朝晖*

江南大学附属医院

目的：胃癌的肿瘤微环境复杂且具有较强异质性，而肿瘤微环境与包括免疫治疗手段在内的治疗响应密切相关。因此，实施精准的癌症免疫治疗迫切需要开发鉴定出新的分子亚型。然而，现有大部分胃癌分子亚型的标志物基因和检测手段都较为复杂，限制了其临床应用。因此，有必要建立新的基于胃癌肿瘤微环境的双基因免疫分子亚型。

材料与方法：我们使用了 9 个独立的组织和单细胞水平的胃癌患者队列，来源于公共数据库和自行收集建立的验证队列，涵盖 2000 余名亚洲和欧美患者。运用单细胞测序、定量 RT-PCR、免疫组化染色以及多重免疫荧光检测进行相关基因/蛋白的检测。并且我们使用 9 种独立算法、5 种现有的胃癌分子亚型和一系列分子标签来评估胃癌肿瘤微环境和分子特征。

结果：我们在胃癌队列中筛选鉴定出分别与免疫检查点正相关和负相关的标志基因 CTSL（cathepsin L）和 ZBTB7B（zinc finger and BTB domain containing 7B）。CTSL 是人类半胱氨酸蛋白酶基因，其在胃癌组织表达上调并预测患者不良预后；ZBTB7B 是一个 CD4 系转录因子基因，其在胃癌组织表达下调并预测患者良好预后。基于此，我们建立了 CTSL/ZBTB7B 亚型系统，开发出具有独立预后价值的 CTSL 高 ZBTB7B 低的免疫分子亚型。该亚群患者的总生存与无复发生存率较差，但具有较高免疫细胞浸润和较低肿瘤纯度。对胃癌肿瘤微环境进一步刻画和验证发现，CTSL 在非恶性细胞类群，尤其是巨噬细胞中拥有较高丰度；而 ZBTB7B 则在恶性细胞类群中丰度较高。此外，CTSL 高 ZBTB7B 低的胃癌患者拥有相对较高的免疫检查点水平。CTSL/ZBTB7B 亚型系统既能兼容又能独立于现有一些胃癌分子分型系统，并且该亚型富集有多种癌症相关信号通路。泛癌分析表明这一高危亚群还同时在膀胱癌、头颈癌和卵巢癌中存在，表明该免疫分子亚型具有一定的普适性。

结论：我们基于 CTSL 和 ZBTB7B 的表达，确定了一个具有独特肿瘤微环境特征的胃癌高危亚群，表明了免疫激活和免疫抑制机制之间存在的平衡表型。本研究揭示依赖单一的免疫评估可能会导致胃癌风险的错误划分。此外，这一亚型显示出较高的免疫检查点和癌症相关信号通路水平，提示联合靶向其中的癌症信号通路可能会增强免疫检查点抑制剂在这些患者中的治疗响应。本研究提供了一种可用于癌症精准治疗的个性化预后方法，并提示在未来肿瘤基因的研究中应进一步考虑肿瘤微环境因素。

关键字：胃癌，分子分型，肿瘤微环境，预后

137. 术前炎症相关指标与可切除胃癌患者预后的相关性

陈奕心*

哈尔滨医科大学附属第三医院

目的：探讨术前外周血系统性免疫炎症指数(Systemic immune-inflammation index，SII)、中性粒细胞与淋巴细胞比值(Neutrophil to lymphocyte ratio，NLR)、血小板与淋巴细胞比值(Platelet to lymphocyte radio，PLR)与可切除胃癌患者预后的相关性及其临床意义。

方法：回顾性分析 2013 年 10 月-2015 年 2 月在我院收治的 226 例经手术治疗胃癌患者的临床病理资料。评估并比较 SII、NLR、PLR 在可切除胃癌患者中的预后价值。

结果：胃癌组 SII、NLR、PLR 明显高于健康对照组，差异均有统计学意义(P＜0.05)。多因素 Cox 回归分析结果显示 SII 高(HR=2.947，95% CI：1.345～6.454，P=0.007)、NLR 高(HR=2.876，95% CI：1.445～5.724，P=0.003)、T 分期越高(HR=5.885，95% CI：1.641～21.099，P=0.007)、有远处转移(HR=3.010，95% CI：1.472～6.154，P=0.003)是影响可切除胃癌患者预后的独立危险因素。SII 预测可切除胃癌患者结局的 ROC 曲线下面积为 0.840，灵敏度为 0.866，特异度为 0.680，高于 NLR 、PLR 及 CEA199，且差异有统计学意义(P＜0.05)。

结论：SII 对可切除胃癌患者生存结局的评估价值优于 NLR 和 PLR。

关键字：胃癌；系统性免疫炎症指数；中性粒细胞与淋巴细胞比值；血小板与淋巴细胞比值；预后

138. Nrf2、HIF-1a 在食管鳞癌的表达、临床意义及相关作用机制探讨

皮国良、金军*

湖北省肿瘤医院

目的：检测 Nrf2、HIF-1a 在食管鳞癌组织及癌旁组织中的表达并分析临床病理意义，初步探索 Nrf2 及 HIF-1a 在食管鳞癌发生发展过程中的作用机制。

方法：收集 2010-2021 年我院病理科 34 例食管癌根治术且未接受术前放化疗的原发性食管鳞癌组织切片，采用免疫组化分析食管鳞癌组织及癌旁组织的 Nrf2、HIF-1a、E-cadherin 及 mdm2 的阳性率。采用 Graphpad Prism5.0 软件分析 Nrf2、Hif-1a 不同的表达状态对术后 PFS 的影响。

结果：Nrf2 及 HIF-1a 在食管鳞癌组织中高表达并均与肿瘤浸润深度、T 分期及有无淋巴结转移密切相关，另外，Nrf2 还与病变的长度相关。Nrf2 在食管鳞癌组织的表达阳性率为 64.71%（22/34）高于癌旁组织 17.65%（6/34）（$P<0.05$）；HIF-1a 在食管鳞癌组织的表达阳性率为 73.53%（25/34）高于癌旁组织 44.12%（15/34）（$P<0.05$）；Ecadherin 及 mdm2 在食管鳞癌组织及癌旁组织之间阳性率差异明显（$P<0.05$）；食管鳞癌组织中 Nrf2 的表达与 HIF-1a、mdm2 表达呈正相关；与 E-cadherin 表达呈负相关。Nrf2 和 HIF-1a 的不同状态下患者术后 PFS 之间均无明显统计学差异。

结论：Nrf2、HIF-1a 在食管鳞癌中高表达,可能通过 Nrf2/HIF-1a 信号通路下调 E-cadherin 及上调 mdm2 促进了食管鳞癌发生和发展。

关键字：Nrf2；HIF-1a；食管鳞癌(ESCC)；作用机制

139. TET1 的表达与宫颈癌临床病理参数的相关性研究

谢璐鸿、任吉、谭玉洁*

贵州医科大学附属医院

目的：探讨宫颈癌组织中甲基胞嘧啶双加氧酶 1(TET1)、5-甲基胞嘧啶(5-mC)和 5-羟甲基胞嘧啶(5-hmC) 的表达及其与宫颈癌患者临床病理参数的关系。

方法：应用免疫组化法检测 TET1、5-mC、5-hmC 在 45 例宫颈癌患者及 20 例正常宫颈组织中的表达情况；分析 TET1、5-mC、5-hmC 在宫颈癌组织中的差异表达情况，及其与临床病理参数的相关性。

结果：与正常宫颈组织相比，宫颈癌组织中 TET1(27/45)和 5-hmC(30/45)以低表达为主，5-mC 以高表达为主(24/45)。宫颈癌中 TET1 的表达与 5-mC 呈负相关(r=-0.327, *P*=0.028)，与 5-hmC 呈正相关(r=0.481, *P*=0.001)。并且 5-mC 与 5-hmC 表达也呈负相关(r=-0.378, *P*=0.010)。在宫颈癌相关病理参数分析中得出 TET1、5-mC 和 5-hmC 的表达与淋巴结转移相关(*P*=0.040/0.029/0.020)，而 5-mC 和 5-hmC 的表达也与血管侵袭相关(*P*=0.007/0.048)。

结论：TET1、5mC、5hmC 可能参与宫颈癌的发展与转移过程。

关键字：TET1；5mC；5hmC；宫颈癌；病理参数

140. 甲状腺间变性癌中代谢相关竞争性内源 RNA 网络的构建

杜秋静[1]、周汝豪[2]、党文娇[1]、李倩[1]、郭剑津*[1]

1. 山西医科大学第三医院

2. 山西医科大学第二医院

研究目的：甲状腺间变性癌(anaplastic thyroid cancinoma, ATC)又称未分化甲状腺癌，是所有甲状腺癌中最不常见但最具侵袭性和致命性的甲状腺恶性肿瘤，中位生存期较短，主流治疗手段效果不佳。最近几年对 ATC 代谢谱的研究揭示了肿瘤的特异性依赖于从头脂肪生成的增加，本研究旨在识别 ATC 中与代谢相关的差异表达基因，探索其竞争性内源 RNA（ceRNA）网络调控机制，识别潜在的治疗靶标。

材料与方法：通过 Gene Expression Omnibus（GEO）数据库下载微阵列芯片数据集 GSE29265，借助 Strawberry Perl 软件分别获取信使 RNA（mRNA）和长链非编码 RNA（lncRNA）的表达谱，访问 Molecular Signatures Database 下载 gmt 文件用于代谢相关基因（MRGs）的提取。使用 R 软件对 mRNA 表达数据进行 ATC 患者和健康对照的差异分析并提取 MRGs 表达谱，分析与被提取的 mRNA 表达相关的 lncRNA，得到与代谢相关的 lncRNA。通过 mircode、miRDB、miRTarBase、TargetScan 数据库预测与代谢相关 lncRNA 互作的微小 RNA（miRNA）及其调控的 mRNA，再与差异 MRGs 取交集，得到 lncRNA-miRNA-mRNA 关系，构建 ceRNA 网络，并筛选关键靶标作 GSEA 富集分析。

结果：通过基因表达谱差异分析和数据提取获得 13 个与代谢相关的差异基因（CA4、DGKI、SORD、ADH1B、FMO2、HGD、EPHX2、ALDH1A1、RRM2、SPHK1、ACADL、GPX3、TPO），获得与 83 个代谢相关的 lncRNA。通过构建代谢相关 ceRNA 网络，筛选出 14 个 lncRNA，3 个 miRNA（hsa-miR-20b-5p、hsa-miR-33a-3p、hsa-miR-17-5p）和 1 个关键基因 RRM2 可能在 ATC 的发生发展过程中发挥重要作用。GSEA 富集分析结果表明，RRM2 在 ATC 中的高表达涉及 regulation of IFNA signaling、dopaminergic neurogenesis、metabolism of steroid hormones、biosynthesis of unsaturated fatty acids、nucleotide catabolism、pyroptosis 等信号通路。

结论：通过构建 ATC 中代谢相关 lncRNA 介导的 ceRNA 网络，分析鉴别出潜在的治疗靶点，可能在 ATC 发生发展中发挥重要作用，为后续实验研究提供研究基础。

关键字： 甲状腺间变性癌；代谢基因；ceRNA；lncRNA；miRNA

141. 肺腺癌类器官组织学表征与化疗药物反应研究

于艳丽[1]、房艳华[1]、梁珊珊*[1,2]、王若雨[1,2]

1. 辽宁省乳腺及消化肿瘤分子标志物高通量筛选及靶向药物转化重点实验室

2. 大连大学附属中山医院肿瘤综合诊疗中心

目的：肺腺癌是肺癌最常见的病理类型，患者来源的肿瘤类器官技术为个体化诊疗提供了新希望。本研究旨在构建肺癌类器官培养体系，并对比肺癌类器官与其来源的肿瘤组织对药物治疗反应的情况，探讨肺癌类器官技术在肺癌的个体化用药和预后中的作用，为肿瘤类器官成为临床前模型提供依据。

方法：构建肺癌类器官培养体系，对肺腺癌患者来源的肿瘤组织进行肺癌类器官体外培养，记录并量化类器官生长情况；探讨肺癌类器官的培养、传代、冻存和复苏的最佳条件；利用组织学 HE 染色观察肺癌类器官微组织与来源肺腺癌组织的形态特点；利用免疫组织化学染色检测肺腺癌标志物 TTF-1、Napsin-A、CK7、P63-α及 Ki67 在组织间的表达情况；利用 ATP 酶活性检测，评估类器官对常规化疗药物奥希替尼及顺铂反应，并对比平行临床疗效。

结果：成功构建了患者来源肺腺癌类器官模型，可长期稳定传代，并实现冻存后的复苏再培养；HE 染色显示肺腺癌类器官呈现微组织结构，具有明显的细胞异型性和病理性核分裂像；免疫组织化学染色显示肺腺癌标志物 TTF-1、Napsin-A、CK7、P63-α及 Ki67 在类器官与来

源肺腺癌组织间高度一致；常规化疗药物奥希替尼及顺铂杀伤实验对比平行临床疗效显示类器官与来源肺腺癌组织具有高度一致的药物敏感度。

结论：以肺腺癌患者组织样本构建的类器官模型能够重现体内肿瘤的组织形态学和生物标志物表征，维持了肿瘤的异质性，并具有与其来源肺腺癌组织相近的药物敏感度，在肺癌的个体化用药和预后中起到关键作用，具有作为肺腺癌研究可靠的临床前模型的潜力。

关键字：肺癌类器官；3D 培养，个体化医学；临床前模型

142. 乳腺癌采用 CA153、CA125 与 CEA 联合检验的诊断效果观察

陆晓洁*

杭州迪安医学检验中心有限公司

目的：探讨 CA153、CA125 与 CEA 的检验方法，观察其在乳腺癌诊断中的效果和作用价值，为临床工作的实践提供参考。

方法：将 120 例健康体检者作为健康组，120 例良性乳腺疾病患者作为良性组，120 例乳腺癌患者作为恶性组，分别对三组患者进行 CA153、CA125、CEA 检验，观察、对比各组患者的检验结果，以及恶性组单项 CA153、CA125、CEA 检验与三联检验对乳腺癌的检出率。

结果：与健康组和良性组相比较，恶性组患者不论是 CA153、CA125 还是 CEA 的检验结果，均显著更高，差异具有统计学意义。在乳腺癌检出中，恶性组 CA153、CA125、CEA 三联检验诊断的检出率，显著高于其中任何一单项检验诊断的检出率，差异同样具有统计学意义（$p<0.05$）。

结论：做好对乳腺癌的检验和诊断工作，是健康中国背景下，检验医学服务人民健康的一项重要任务。与健康人群以及良性乳腺疾病患者相比，乳腺癌患者的 CA153、CA125、CEA 水平均明显更高。不过在乳腺癌的诊断中，CA153、CA125、CEA 单项检验的检出率并不高，三联检验才具有更高的准确性和诊断价值。

关键字: CA153；CA125；CEA；乳腺癌

143. 表观沉默 IGFBP5 影响食管癌细胞增殖的分子机制

刘悦[1]、樊红*[1,2]

1. 东南大学医学院，南京，210009

2. 发育与疾病相关基因教育部重点实验室，南京，210018

食管癌是一种十分常见的消化系统肿瘤，其发病率和死亡率均居全球癌症前列，诱因比较复杂，具有高度侵袭性，预后效果差，五年生存率总体较低。组蛋白修饰常包括组蛋白甲基化和组蛋白乙酰化两种，在肿瘤中发挥着转录调控的作用。H3K27me3 是一种常见的抑制性组蛋白修饰，常富集于抑癌基因启动子区域，通过表观调控使抑癌基因表达失活，参与癌症的发生发展。IGFBP5 是 IGFBPs 家族中重要成员，是该家族中最保守的蛋白，在调控肿瘤细胞增殖、迁移和周期等过程中发挥着重要作用。目前，H3K27me3 的异常表达水平对食管鳞状细胞癌（Esophageal squamous cell carcinoma, ESCC）发生发展的影响尚不明确。结合本课题组前期研究发现，本文主要探究高水平 H3K27me3 表观沉默 IGFBP5 的表达，回复 IGFBP5 后对 ESCC 细胞生物学行为的影响和相关机制。本研究首先利用 ChIP-seq 技术，通过生物信息学分析 EC9706 细胞中 H3K27me3 富集的 DNA 片段的生物学特征及相关信号通路，联合 TCGA 数据库、GO 分析和 KEGG 信号通路分析，筛选目标靶基因 IGFBP5。通过相关功能试验 CCK-8，平板克隆实验和细胞划痕实验等，分析 IGFBP5 过表达对 ESCC 生物学行为的影响，最后通过 Western blot 实验检测 IGFBP5 对 IGF 信号通路的影响，探究 IGFBP5 基因受 H3K27me3 表观调控参与 ESCC 发生发展的分子机制。研究结果表明，IGFBP5 基因在食管鳞癌临床病例中表达水平显著下调；过表达 IGFBP5 基因可以抑制食管鳞癌细胞的增殖和迁移；过表达 IGFBP5 基因表达影响了 IGF 信号通路及相关靶分子的表达，抑制了 ESCC 的生长。总之，本文发现 IGFBP5 与 H3K27me3 之间存在显著的相关性，IGFBP5 的过表达可以抑制 ESCC 的增殖能力，揭示了 IGFBP5 可能是与食管鳞癌发生发展密切相关的潜在抑癌基因，对于食管鳞癌在临床上的诊断和治疗具有较大的参考价值。

关键字：食管鳞癌；H3K27me3；IGFBP5；细胞增殖；IGF 信号通路

144. 用我位点基因组编辑研究逆转座子重复序列的功能

郭雅彬*、马若骜

中山大学孙逸仙纪念医院

人类基因组含有大量逆转座子重复序列。其中 LINE-1（L1）是比例最高的逆转座子，占到基因组的 17%，也是人类基因组中唯一活跃的自主型转座子。Alu 是一类非自主型逆转座子，占基因组的 11%。尽管比例低于 L1，但 Alu 比 L1 短得多，故拷贝数反而比 L1 多得多。这两类逆转座子合起来已经占到人类基因组的近 30%。长久以来，人们对这些重复序列的功能所知甚少，一度将它们称为垃圾 DNA，但随着研究的深入，尤其是高通量测序的应用，人们逐渐开始认识它们的作用，比如有些研究显示这些逆转座元件和它们的结合蛋白能介导染色体不同部分之间的相互作用，对维持基因组的三维结构很重要。不过，由于它们的拷贝数太高，直接在基因组层面对它们进行操作还存在一定的困难。我们在前期研究中开发了一种称为 CReaC（Chromosome Rearrangement by CRISPR-Cas9）的方法，通过 sgRNA 的介导，让 Cas9 内切酶靶向数千到数十万的位点。令人惊奇的是，基因组经过 Cas9 大量切割的细胞仍然有少数能活下来，并且发生了全局性染色体重排（GCR）。基于这种操作，我们又开展了进一步的实验，研究基因组三维结构与表观遗传学的变化。Hi-C 实验显示通过编辑这些重复序列，染色体间的相互作用发生了明显的变化；ATAC-seq 也显示染色质的开放性发生了显著的变化，提示核小体的排布乃至核小体的密度都发生了改变。通过对高度重复的逆转座元件的编辑，我们有望更深刻地理解它们的功能。

关键字：逆转座子，基因组编辑，CRISPR，CReaC，染色体重排，Hi-C

145. SCTAE 在食管鳞癌中的临床诊断价值及生物学功能研究

邢磊[1]、张学顺[2]、任圣男[1]、杨丁全[1]、胡越[1]、任平[2]、陈芳芳*[1]

1. *吉林大学中日联谊医院*
2. *吉林大学第一医院*

目的：超灵敏食管癌诊断癌睾丸抗原标志物（super-sensitive cancer testis antigen in esophageal carcinoma，SCTAE)是一种新发现的在食管癌癌中高表达的癌睾丸抗原。我们通过回顾性临

床研究，探索 SCTAE 在食管鳞癌中的表达水平、诊断价值以及其在食管鳞癌生长、转移中的影响及生物学作用机制。

方法：我们利用 qRT-PCR、Western Blot 及免疫组织化学染色技术分析 SCTAE 在食管鳞癌组织中的表达水平，并通过 ELISA 法检测来自不同中心的食管鳞癌患者与健康受试者外周血中 SCTAE 蛋白浓度。使用 SCTAE 蛋白、抗 SCTAE 抗体刺激 2 种食管鳞癌细胞系（Eca-109、TE-1），同时进行 SCTAE 过表达/敲减实验。采用 CCK8 与 EdU 法检测其增殖能力变化；流式细胞术检测细胞周期及细胞凋亡；划痕实验和 Transwell 实验检测细胞转移能力变化。最后，我们使用通过免疫荧光、Western Blot 以及 ELISA 法验证 SCTAE 的生成场所及分泌方式；临近标记系统确定其作用位点，Western Blot 法检测其激活相关信号通路情况。

结果：SCTAE 在食管鳞癌组织中高表达，且与患者的细胞分化程度呈负相关，与淋巴结转移、临床分期、脉管受侵和神经受侵呈正相关；食管鳞癌患者的血清 SCTAE 蛋白浓度要显著高于健康对照组，在食管鳞癌的诊断中有着较强的灵敏度与特异性（AUC=0.994）。细胞实验结果表明：SCTAE 能够促进食管癌细胞的增殖、侵袭与迁移。SCTAE 的主要分布场所是在细胞胞浆内，通过经典的内质网-高尔基体途径分泌到细胞外，其表达和分泌均受血清浓度的调控。SCTAE 通过作用于细胞膜表面受体，激活 PI3K/Akt/mTOR/4E-BP1 信号通路促进食管鳞癌细胞的增殖，并能够显著推进 G1/S 期进展。

结论：本研究表明癌睾丸抗原 SCTAE 能够在食管鳞癌组织中特异性高表达，并证明 SCTAE 在食管鳞癌早期筛查中具有较高的诊断能力，有望作为一个食管鳞癌的血清学诊断标志物。同时，SCTAE 通过自分泌的方式分泌到细胞外，作用于细胞膜表面受体，通过激活 PI3K/Akt/mTOR/4E-BP1 通路，推动 G1/S 期进展，从而促进食管鳞癌细胞的增殖。

关键字: SCTAE，食管鳞癌，肿瘤标志物

146. 一种新型潜在的生物学标志物在肝细胞肝癌被发现——C18ORF54

马玉玉、田凤鸣、马秀敏*

新疆医科大学附属肿瘤医院

背景：近年来，肝细胞肝癌的发病率呈现上升趋势，本研究旨在通过生物信息学方法探究肝细胞肝癌中上调基因的分子机制来确定新的潜在的生物学标志物。

方法：GEO 数据库检索出肝细胞肝癌（GSE84402,GSE101685,GSE62232,GSE112790）的数据集，使用 R studio 软件筛选出差异表达上调基因，通过韦恩图确定 192 个共同上调基因进行 PPI 网络图绘制，而后分别进行 GO 和 KEGG 富集分析。通过 Cytoscape 确定 5 个 hub gene 进行 ROC 曲线，甲基化以及在正常组织和肝细胞癌症中 mRNA 差异表达来确定 C18orf54 为新的潜在的生物学标志物。接着，我们确定了 C18orf54 在染色体中的位置，并绘制出其 3D 结构，我们发现 C18orf54 在正常睾丸组织中高度表达，在正常肝脏中几乎不表达，但其却在肝癌组织中高度表达，我们紧接着进行 HE 染色，IHC 组化分析，IF 免疫荧光共定位，WB，和 Q-RTPCR 实验共同验证了 C18orf54 在肝细胞癌症患者的组织标本中的差异。通过在线数据库 Timer2.0 分析了 C18orf54 与肝细胞肝癌免疫浸润之间的相关性，使用 R studio 软件对基因 C18orf54 与肝细胞肝癌患者的预后和生存进行分析统计。最后，我们进行基因联合药物分析，有 4 种药物可能在降低 C18orf54 mRNA 的表达中有一定的效果。

结果：我们对四个肝细胞肝癌的数据库进行差异分析筛选出上调表达基因，其富集结果显示其主要富集于细胞周期和 DNA 复制通路。此外，通过 PPI 网络鉴定了 5 个 hub gene(BARD1, MSH2, H2AFX, H2AFZ, C18orf54)。ROC 曲线表明 5 个 hub gene 对肝细胞肝癌诊断有着高的灵敏度和特异度，5 个 hub gene 在肝细胞肝癌和正常组织间 mRNA 差异明显,甲基化分析发现 C18orf54 存在 5 个甲基化突变位点，综合分析后决定将其作为新的生物学靶点进行探索，随后进行基础实验验证发现 C18orf54 在肝细胞肝癌和正常组织间有着明显差异，通过在线数据库 Timer2.0 对 C18orf54 基因在肝细胞肝癌中的免疫浸润情况进行分析，发现在肝细胞肝癌中高表达 C18orf54 与 CD8+T cell,CD4+T cell, Tregs cell, B cell,中性粒细胞，巨噬细胞，NK cell 以及肿瘤相关纤维化细胞呈现负相关。接着对高表达 C18orf54 的肝细胞肝癌患者的预后和生存进行分析发现，高表达 C18orf54 肝细胞肝癌患者邻近肝组织炎症发病率更高，child-Pugh 等级分数更高，残留肿瘤复发率更高等。同样的在其亚组分型中也同样有着更差的预后。最后我们进行药物联合基因分析， 提出 Cyclosporine，Calcitriol，Quercetin，Testosterone 等可能对降低 C18orf54 的 mRNA 表达有一定的效果。

总结：C18orf54 可能在肝细胞肝癌的发展中起到关键作用，并可能成为肝细胞肝癌的潜在生物标志物。

关键词：肝细胞肝癌；C18orf54；生物标志物；生信分析

147. 生物钟基因 BMAL1 通过调控 PI3K/Akt/MMP-2/9 信号通路抑制耐辐射鼻咽癌细胞株 5-8FR 增殖、迁移和侵袭能力的研究

黎钰欣[2,3]、金风*[1,3]

1. 贵州省肿瘤医院

2. 贵州医科大学

3. 贵州医科大学附属医院

目的: 探究 BMAL1 基因对耐辐射鼻咽癌细胞株（5-8FR）的增殖、迁移和侵袭能力的影响及分子机制。

方法:小剂量分次照射构建鼻咽癌耐辐射细胞 5-8FR，运用克隆形成实验结果拟合多靶单击模型并计算放疗增敏比；通过蛋白质印迹实验检测 5-8FR 和对照组 5-8F 细胞株中 PI3K/Akt/MMP-2/9 信号通路相关蛋白的表达；构建 BMAL1 基因的高表达及敲除载体，分别转染鼻咽癌细胞株 5-8F 和耐辐射细胞株 5-8FR，获得 BMAL1 过表达（pcDNA-BMAL1）及其对照组（pcDNA）和干扰（BMAL1-shRNA）及对照组（con-shRNA）的稳转细胞株，蛋白质印迹实验验证感染效率，检测两组细胞过表达或干扰 BMAL1 基因后 PI3K/Akt/MMP-2/9 信号通路相关蛋白的改变情况；采用 CCK-8 法、划痕实验、Transwell 法检测 5-8F 与 5-8FR 以及过表达及干扰 BMAL1 后耐放疗细胞株 5-8FR 增殖、迁移和侵袭能力的变化。

结果: 鼻咽癌耐辐射细胞株中 BMAL1 基因表达下调，PI3K/Akt 通路蛋白及下游相关分子 MMP-2、MMP-9 表达增加，TIMP-2、TIMP-1 表达降低，同时增殖、迁移和侵袭能力增强。过表达 BMAL1 基因可抑制 PI3K/Akt 通路蛋白及下游相关分子 MMP-2、MMP-9 表达，促进 TIMP-2、TIMP-1 表达，抑制耐辐射鼻咽癌细胞的增殖、迁移和侵袭能力，干扰 BMAL1 基因则结果相反。

结论: BMAL1 基因可以逆转耐辐射鼻咽癌细胞株 PI3K/Akt/MMP-2/9 信号通路相关蛋白的表达，并抑制耐辐射鼻咽癌细胞株的增殖、迁移和侵袭能力。

关键字: 生物钟基因；鼻咽癌；耐辐射细胞株；增殖；迁移；侵袭

148. 生物钟基因 BMAL1 及缺氧诱导因子 HIF-1α对鼻咽癌细胞 HONE1 增殖、迁移和放疗敏感性影响的研究

唐雅雪、金风*

贵州医科大学附属肿瘤医院

目的：了解生物钟基因 BMAL1 及缺氧诱导因子-1α(hypoxia inducible factor-1α，HIF-1α) 对鼻咽癌细胞 HONE1 增殖、迁移及放疗敏感性的影响，同时初步探讨生物钟基因 BMAL1 能否影响 HIF-1α蛋白的表达，为进一步研究生物钟基因 BMAL1 与缺氧诱导因子 HIF-1α的相关性奠定基础。

方法:1、分别构建 BMAL1 基因过表达及干扰慢病毒、HIF-1α基因干扰慢病毒，转染鼻咽癌细胞株 HONE1，Western blot 验证 BMAL1 基因稳定过表达及敲低细胞株、HIF-1α基因敲低细胞株的建立，同时了解 BMAL1 基因过表达及敲低细胞株中 HIF-1α蛋白的表达情况；2、利用 CCK-8 细胞增殖实验、划痕实验分析细胞的增殖、迁移能力；3、用流式细胞凋亡术分析放疗后的细胞凋亡情况，克隆形成实验检测不同剂量（0Gy、2Gy、4Gy、6Gy）X 线照射后，BMAL1 及 HIF-1α对鼻咽癌细胞 HONE1 放疗敏感性的影响。

结果：1、构建 BMAL1 基因的过表达及干扰慢病毒，有效地上调和下调了鼻咽癌细胞株 HONE1 中 BMAL1 蛋白的表达，构建 HIF-1α基因的干扰慢病毒，有效地下调了鼻咽癌细胞株 HONE1 中 HIF-1α蛋白的表达，并分别成功筛选出稳转鼻咽癌细胞株；Western blot 结果显示，过表达 BMAL1 基因可以抑制鼻咽癌细胞 HONE1 中 HIF -1α蛋白表达，敲低 BMAL1 基因可以促进鼻咽癌细胞 HONE1 中 HIF -1α蛋白表达($P<0.05$)；2、CCK-8 细胞增殖实验及划痕实验表明，过表达 BMAL1 基因或敲低 HIF-1α基因能抑制鼻咽癌细胞 HONE1 的增殖能力及迁移能力($P<0.05$) ；3、流式细胞凋亡术结果显示，8Gy 照射 72 小时后，BMAL1 基因过表达组的细胞凋亡率高于过表达对照组，同样，HIF-1α基因敲低组的细胞凋亡率高于敲低对照组($P<0.05$)。不同剂量（0Gy、2Gy、4Gy、6Gy）X 射线照射后，克隆形成实验显示，BMAL1 基因过表达组或 HIF-1α基因敲低组的克隆形成率、细胞存活分数均低于其阴性对照组($P<0.05$) ，Sigmaplot 软件分析结果显示 BMAL1 基因过表达组或 HIF-1α基因敲低组 D0、Dq、SF2 值均低于阴性对照组，放射增敏比分别为 1.381、1.063。

结论：1、过表达 BMAL1 基因可以抑制鼻咽癌细胞 HONE1 增殖、迁移，增加放疗后的细胞凋亡率，提高放射敏感性；2、敲低 HIF-1α基因可以抑制鼻咽癌细胞 HONE1 增殖、迁移，

增加放疗后的细胞凋亡率，提高放射敏感性；3、在鼻咽癌细胞 HONE1 中，过表达 BMAL1 基因可以抑制 HIF-1α蛋白的表达，敲低 BMAL1 基因可以促进 HIF-1α蛋白的表达。

关键字：生物钟基因 BMAL1；缺氧诱导因子 HIF-1α；鼻咽癌；细胞增殖；细胞迁移；放疗敏感性

149. 血清多肽在肿瘤诊断中的研究进展

郭玲、汪静、李娜娜、苏亚娟*

哈尔滨医科大学附属第三医院

癌症是导致人类死亡的主要原因之一。尽管早期诊断可以有效提高生存率，但目前现有肿瘤标志物的灵敏度和特异性都低于预期目标，令人不满意。在寻找新的诊断指标过程中，血清中具有差异性的多肽受到了极大的关注。多肽标记物可以相对抵抗蛋白酶降解，即使蛋白被肿瘤细胞外间隙或循环中的蛋白酶降解，多肽也可能存活。因此，它可能提供比前体蛋白更多的信息。此外，以质谱为基础的高通量检测方法支持检测血液中更多的低分子量、肿瘤特异性肽。据报道，血清多肽模型提高了肿瘤的检测灵敏度和特异性。因此，血清中差异性多肽可以作为新型诊断标志物，提高肿瘤的早期诊断和鉴别诊断。

关键字：多肽；肿瘤；诊断

150. CNIH1 在宫颈癌中的预后和免疫分析

韩松涛[1]、王森钰[2]、冯阳春*[3]

1. 新疆医科大学附属中医医院

2. 新疆医科大学第二附属医院

3. 新疆医科大学附属肿瘤医院

目的：宫颈癌作为女性常见恶性肿瘤，改善其转移或复发患者预后至关重要。CNIH1 是 AMPA 受体辅助蛋白之一，主要参与免疫反应和信号转导。目前 CNIH1 在癌症预后和免疫调节中的作用鲜有报道。

方法：本研究从 UCSC XENA 和 GTEx 获取泛癌和宫颈癌数据。Cox 回归和 Kaplan-Meier 分析用于评估 CNIH1 在泛癌和宫颈癌中的预后价值。TIMER 和 CIBERSORT 用于评估 CNIH1 和免疫细胞的关系。

结果：CNIH1 在多种癌症中均有很高的表达量。Kaplan-Meier 显示 CNIH1 的表达与宫颈癌等癌症的 OS 密切相关。其次 ROC 曲线表明 CNIH1 在诊断宫颈癌等癌症中具有很高的诊断价值。最后，通过与免疫细胞的相关性研究表明 CNIH1 和免疫细胞存在一定的相关性。

结论：首次发现 CNIH1 在泛癌和宫颈癌中的作用，其可用以诊断宫颈癌以及评估宫颈癌的预后。

关键字：宫颈癌；CNIH1；诊断价值；预后；免疫细胞

151. SEC61G 在宫颈癌中的预后和免疫分析

韩松涛[1]、王森钰[2]、冯阳春*[3]

1. 新疆医科大学附属中医医院

2. 新疆医科大学第二附属医院

3. 新疆医科大学附属肿瘤医院

目的：研究表明，Sec61 γ亚基(SEC61G)在多种肿瘤中过度表达，可作为潜在的预后标志物。但 SEC61G 与宫颈癌之间的相关性仍不清楚。本次研究中，我们旨在证明 SEC61G 基因在宫颈癌中的预后价值和潜在生物学功能。

方法：本研究从 UCSC XENA 和 GTEx 获取泛癌和宫颈癌数据。Cox 回归和 Kaplan-Meier 分析用于评估 CNIH1 在泛癌和宫颈癌中的预后价值。TIMER 和 CIBERSORT 用于评估 SEC61G 和免疫细胞的关系。

结果：SEC61G 在多种癌症中均有很高的表达量。Kaplan-Meier 显示 SEC61G 的表达与宫颈癌等癌症的 OS 密切相关。其次，ROC 曲线表明 SEC61G 在诊断宫颈癌等癌症具有很高的诊断价值。最后，通过与免疫细胞的相关性研究表明 SEC61G 和免疫细胞存在一定的相关性。

结论：首次明确 SEC61G 在泛癌和宫颈癌中的作用，其可用以诊断宫颈癌及评估宫颈癌的预后。

关键字：宫颈癌；SEC61G；诊断价值；预后；免疫细胞；泛癌

152. MEIS1 作为人类肿瘤预后生物标志物和免疫治疗靶点的系统泛癌分析

李晗、王泽敏、卫平民*

东南大学

目的：研究表明，MEIS1 参与肿瘤细胞的增殖分化。虽然 MEIS1 已被证明在前列腺癌、非小细胞肺癌和食管鳞状细胞癌中作为肿瘤抑制因子调节肿瘤进展。目前还没有关于 MEIS1 的泛癌研究。本研究旨在探索 MEIS1 在泛癌中的作用。

方法：本研究利用 TCGA (The cancer genome atlas)和 GEO (Gene expression omnibus)数据集探讨 MEIS1 基因与癌症的关系。一些生物信息学方法探讨 MEIS1 的潜在作用，包括分析不同肿瘤中 MEIS1 表达与预后、肿瘤微环境(tumor microenvironment, TME)生物标志物、检查点基因(checkpoint genes, icpg)和免疫细胞浸润水平的关系。对 147 个 MEIS1 相关基因进行 GO 和 KEGG 分析。

结果：MEIS1 在大多数肿瘤中表达下调，其表达与癌症患者的预后及免疫浸润水平有关。因此，从基因富集分析的强度来看，细胞分化、细胞命运决定、转录失调等可能的功能参与了 MEIS1 对癌症的影响。

结论：本文证明，MEIS1 可能是未来癌症治疗的新靶点。

关键字: MEIS1，肿瘤，免疫，细胞增殖分化

153. 基于生物信息学方法分析铁死亡相关基因构建甲状腺癌预后模型预测价值及对肿瘤免疫微环境的影响

余幼林*、余军林、沈雄山、胡超华、卢婷、杨青青、刘程浩

武汉科技大学附属孝感医院

目的：基于生物信息学方法构建铁死亡相关基因甲状腺癌预后模型，评估预测价值，并进一步分析其与肿瘤免疫微环境的关系。

方法：基于 TCGA 数据库中甲状腺癌铁死亡相关基因的表达谱，建立 LASSO cox 回归模型。ROC 曲线评估模型生存期预测效能。Kaplan-Meier 生存曲线分析模型高低风险组生存差异。

PCA 分析模型分类的准确性。ssGSEA 分析模型风险评分与免疫细胞浸润及免疫功能之间的关联，单因素及多变量 COX 回归分析预后模型的独立性。

结果：确定 DPP4、 GSS、HMGCR、TFRC、PGD 5 个铁死亡相关基因的构建模型。ROC 曲线评估模型预测 1 年，5 年，10 年生存期 AUC 分别为 0.839、0.825、0.851。模型风险评分高风险组比低风险组预后更差（$p < 0.05$）。PCA 分析结果显示模型分类有较高准确性。ssGSEA 分析结果显示：模型风险评分高风险组对比低风险组：肿瘤微环境中的免疫细胞浸润丰度降低，免疫细胞功能减弱。COX 回归分析结果显示：模型可作为甲状腺癌独立预后预测因素（$p< 0.05$，HR：3.816，95% CI：1.141–12.764）。

结论：基于 DPP4、GSS、HMGCR、TFRC、PGD 5 个铁死亡相关基因构建预后评估模型及危险度评分系统，为预测甲状腺癌患者预后提供参考。铁死亡相关基因可能通过影响免疫细胞浸润和免疫细胞功能调控肿瘤免疫微环境。为甲状腺癌的免疫调控机制研究提供理论基础。

关键字：铁死亡；甲状腺癌；预后；肿瘤微环境

154. 基于牛血清白蛋白载体平台和超支化滚环扩增的高重现性高灵敏度电化学生物传感器用于 HPV 检测

何颖豪、洪国斧*

厦门大学附属第一医院

构建传统的 DNA 电化学生物传感器时，作为捕获探针的硫醇化单链 DNA (ssDNA)通过自组装的方式修饰于金电极表面。然而这种组装过程存在较大随机性，因此不同电极上分布的 ssDNA 存在显著差异，这极大的影响了传感器的检测重现性。本研究首先在电极表面修饰牛血清白蛋白（BSA）形成多孔的 BSA 层，其可改善随后修饰的 ssDNA 探针的位置分布和空间取向。将 BSA 载体平台与超支化滚环扩增相结合，开发出用于人乳头状瘤病毒（HPV）E6、E7 癌基因检测的高重现性和高灵敏度的电化学生物传感器。在目标序列存在时，电极表面通过超支化滚环反应积累了大量的扩增产物，其中包含不同长度的双链 DNA（dsDNA）与 ssDNA 片段，可结合大量亚甲基蓝（电化学指示剂），从而检测到明显的电化学信号。信号强度与目标物浓度在 50 fM 到 10 pM 间呈线性关系，检测限为 44.6 fM (S/N= 3)。通过 BSA 载体平台，检测的相对标准偏差从 9.09%降低到 4.37%，从而提高了重现性。本研究提出的检测策略为构建高重现性和高灵敏度的电化学生物传感器提供了一种新方法。

关键字：电化学生物传感器，牛血清白蛋白载体平台，超支化滚环扩增，人乳头状瘤病毒，高重现性

155. 2016-2020 年肿瘤患者铜绿假单胞菌感染及耐药趋势的回顾性研究

崔兆磊、陈燕*

福建省肿瘤医院

目的：回顾分析肿瘤患者临床标本分离的铜绿假单胞菌（PA）菌株相关信息，研究肿瘤患者感染 PA 的临床分布、耐药趋势，为临床上治疗肿瘤患者 PA 感染提供相关依据。

方法：回顾性分析 2016-2020 年福建省肿瘤医院临床标本分离的 PA 及相关数据，采用 WHONET5.6 和 SPSS22.0 统计软件对数据进行分析。

结果：从 2016 年 1 月到 2020 年 12 月，5 年共检出 PA 926 株，每年 PA 占临床分离菌株的比率分别为 8.61% （163/1893）、7.68%（170/2213）、7.62%（201/3637）、6.33%（182/2876）、7.36%（210/2852）;2018-2020 年 PA 分离率与 2015-2017 年的 PA 分离率相比有所降低，但无显著差异（p=0.084）。临床患者标本来源主要为呼吸道标本（65.12%），各类来源之间具有显著差异。ICU 患者、腹部肿瘤患者、胸部肿瘤患者和头颈部肿瘤患者的 PA 分离率有显著差异（p <0.05）。抗生素药敏试验表明，在 2016-2020 年，我院分离 PA 菌株对亚胺培南的耐药率大于 30%，；对庆大霉素、环丙沙星、头孢他啶的耐药率在 25%-3%之间，具有较大波动；对美罗培南的耐药率大于 20%；对头孢吡肟、左氧氟沙星、哌拉西林、哌拉西林/他唑巴坦的耐药率均小于 20%。我院肿瘤患者临床标本 PA 分离率与全国平均水平无显著差异，但分离的 PA 菌株对亚胺培南（31.43% *vs.* 23.2%, χ^2=10.416, p<0.05）的耐药率高于全国平均水平，对左氧氟沙星（13.82% *vs.* 17.47%, χ^2=10.262, p<0.05）、头孢吡肟（10.48% *vs.* 14.78%, χ^2=13.532, p<0.001）、哌拉西林（12.20% *vs.* 16.4%, χ^2=29.917，p<0.001）、哌拉西林/他唑巴坦（13.07% *vs.* 15.55%, χ^2=13.867, p<0.001）的耐药率低于全国平均水平，具有显著差异。

结论：肿瘤病人对某些药物的耐药率高于全国平均水平，但对某些药物的耐药率低于全国平均水平，这可能与肿瘤病人病种特殊性有关。研究结果提示我们，我们应该密切监测肿瘤患

者 PA 感染及耐药情况，同时在临床 PA 感染治疗中应合理使用抗菌药物，预防耐药菌株的产生。

关键字：铜绿假单胞菌；肿瘤患者；耐药性；抗生素

156. 血清肌酐与胱抑素 C 比值作为实体瘤免疫治疗的预测标志物

纪宏娟[1,2]、杜成*[1]

1. 中国人民解放军北部战区总医院

2. 锦州医科大学

背景与目的：PD-L1 是推荐用于免疫治疗的生物标志物，但一些 PD-L1 高表达的患者临床反应较差。考虑到 PD-L1 表达与免疫检查点抑制剂（ICIs）疗效之间的相关性不一致，需要更敏感的生物标志物来预测免疫治疗疗效。我们旨在评估血清肌酐/胱抑素 C 比值（CCR）与接受 ICIs 治疗的恶性实体瘤患者的总生存期（OS）之间的关联。

方法：2019 年 3 月-2021 年 10 月期间在北部战区总医院肿瘤科接受 ICIs 治疗的转移性实体瘤患者纳入本研究，收集这些患者的临床资料及相关血液学指标，包括性别、年龄、肿瘤部位、骨骼肌指数（SMI）、身体质量指数（BMI）、白蛋白、CCR 等。根据中位 CCR 值将患者分为高 CCR 组（CCR>0.78，n=90）和低 CCR 组（CCR<0.78，n=90），比较两组间临床特征、营养指标及总生存期差异。使用 Kaplan-Meier 方法评估 CCR 的预后价值。COX 回归用于评估与长期生存相关的危险因素。

结果：共纳入 180 例接受 ICIs 治疗的转移性实体瘤患者，中位年龄为 63 岁（范围 39-83 岁），男性患者占所有患者的 79%。生存分析显示，基线 CCR 水平较高组的 OS 优于较低组（25.15 个月 *vs.* 19.76 个月，*P*=0.039）。在单因素分析中，CCR（HR：0.63，95%CI：0.41-0.92，*P*=0.041）是 OS 的独立影响因素。

结论：本研究表明，CCR 可以准确、廉价地用于评估免疫治疗疗效，在 ICIs 治疗的转移性实体瘤患者中，CCR 低于 0.78 的患者预后较差。因此，CCR 可作为一种临床标志物用来预测免疫治疗的疗效。

关键字：血清肌酐/胱抑素 C；免疫治疗；实体瘤；预后

157. 鼻咽癌患者放疗前后外周血中免疫原性细胞死亡相关蛋白的水平变化及与炎症相关指标的相关性研究

徐露、龙金华*、金风

贵州省肿瘤医院

目的：射线诱导的肿瘤免疫原性细胞死亡与放疗的疗效相关。本文旨在探索临床常规分割剂量射线照射对鼻咽癌（nasopharyngeal carcinoma, NPC）患者免疫原性细胞死亡相关蛋白及炎症相关指标的表达水平的影响，深入理解放疗诱导的特异性抗肿瘤免疫应答的启动过程，指导临床实践。

材料与方法:1）纳入 38 例初治III-IV期局部晚期 NPC 患者，均接受诱导化疗+同步放化疗；2）另选 20 例健康志愿者与患者进行对照；3)采集患者治疗前、诱导化疗后、同步放化疗后共 3 组清晨空腹静脉血 3 mL，制备成血清；检测其中免疫原性细胞死亡相关蛋白-热休克蛋白 70（heat shock protein 70, HSP70）、钙网蛋白（calreticulin，CRT）和高迁移率族蛋白 1（high-mobility group box-1，HMGB-1）的含量；4)分析三种蛋白的表达与患者一般临床资料等相关性；5)收集患者治疗前外周血中中性粒细胞与淋巴细胞比值(neutrophils to lymphocytes ratio,NLR)、淋巴细胞与单核细胞比值(lymphocytes to monocytes ratio，LMR），球蛋白计数及治疗前后树突状细胞（dendritic cells, DCs）的占比。6)分析患者 NLR，LMR，球蛋白计数与三种蛋白的表达及一般临床资料是否有相关性；7）分析 NPC 患者治疗前后外周血中 DC 的变化。

结果：1）NPC 患者治疗前外周血中 HSP70 及 HMGB-1 含量较健康人群高（$p<0.05$）；2）放疗后 CRT 的含量显著高于治疗前 ($p<0.05$)，然而其差异表达与患者的近期疗效无显著相关性；3）HSP70 同步放化疗后较治疗前显著降低（$p<0.05$）；4）HMGB-1 诱导化疗后及同步放化疗后较治疗前含量均无显著差异（$p>0.05$）；5）治疗前 NLR 与 HSP70 呈负性相关（r=-0.335，$p<0.05$ ）；6）PDCs、MDCs 同步放化疗后较治疗前含量均无明显差异（$p>0.05$）。

结论：1、放疗能够诱导 NPC 患者 CRT 表达增加，这可能与后续的抗肿瘤免疫应答有关，CRT 可能是潜在的 NPC 肿瘤相关抗原（tumor-associated antigen，TAA）；2、治疗后的 HSP70 血清水平降低可能反映良好的预后，需后续随访进行证实。

关键字：鼻咽癌；免疫原性细胞死亡；钙网蛋白；热休克蛋白 70；高迁移率族蛋白 1；树突状细胞。

158. c-Jun/ABRACL 轴通过调节线粒体功能增强放疗抵抗

霍楠、亢小峰、薛春源、朱俊闻、杜祎萌、徐小洁*

生物工程研究所

研究目的：线粒体在辐射中起着决定细胞命运的关键作用，但在放射生物学领域，线粒体融合与分裂动态平衡和功能的精细调节与放疗敏感性之间的关系却并不十分清楚。

材料与方法：我们通过剂量递增法构建了辐射抵抗（IR-R）MCF-7 细胞系。随后，我们对 IR-S 及 IR-R 细胞进行转录组测序（RNA-Seq），结合 GEO 数据库（GSE#:197236）筛选出在辐射耐受细胞株中上调的基因。并进一步通过 RT-PCR 验证差异基因。随后通过 Kmplot 筛选出高表达生存率降低的基因。为了确定 ABRACL 在辐射中的功能，我们通过克隆形成、生存曲线测定、细胞凋亡和 ROS 流式检测 ABRACL 与辐射敏感性之间的关系。接下来，我们通过海马高通量分析、流式细胞技术、丙二醛（MDA）含量检测、Mito-tracker 线粒体探针与透射电镜检测了线粒体功能及形态变化。为了进一步研究 ABRACL 在辐射条件下表达升高的机制，我们利用 RT-PCR 以及 Western-blot 对照射后细胞 ABRACL 的转录及蛋白水平进行了分析。通过荧光素酶活性实验确定了调节 ABRACL 的上游转录因子。接下来，我们利用小鼠荷瘤实验验证了 c-Jun/ABRACL 轴在体内对放疗敏感性的调节作用。利用临床标本进行免疫组化染色，确定了 ABRACL 在放疗敏感与抵抗患者中的表达量高低，以及与 c-Jun 表达水平的相关性。通过分析 GEPIA 网站中 TCGA 收集的乳腺癌患者与肺癌患者数据，研究 ABRACL 与放疗治疗预后的相关性。

结果：我们成功构建了辐射抵抗的 IR-R MCF-7 细胞系。利用 RNA-Seq 与 GEO 数据库（GSE#:197236）筛选以及 RT-PCR 确定了 7 个基因在辐射抵抗中表达升高的基因。随后通过 Kmplot 筛选出高表达预后差的 ABRACL 因子。辐射条件下 ABRACL 敲低可减少克隆形成率、细胞生存率，增加细胞凋亡与 ROS 水平，而敲低 ABRACL 再回复后，克隆形成率与细胞生存率增加，细胞凋亡率与 ROS 水平降低，说明 ABRACL 能够介导放疗抵抗。辐射条件下 ABRACL 敲低导致线粒体耗氧率及线粒体膜电位水平下调、脂质过氧化物水平增加、同时促进线粒体裂变。当敲低 ABRACL 再回复后线粒体耗氧率及线粒体膜电位水平增加，脂质过氧化物水平下调。说明 ABRACL 通过调节线粒体分裂与融合稳态及线粒体功能来促进辐射抵抗。在辐射条件下，MCF-7 和 A549 细胞中 ABRACL 的转录与蛋白水平均升高。萤光素酶活性实验显示 ABRACL 的上游转录因子为 c-Jun。抑制 c-Jun/ABRACL 轴导致局部

放疗后小鼠肿瘤体积显著降低，凋亡率上升。当 ABRACL 回复后，肿瘤体积增加，凋亡率降低，说明 c-Jun/ABRACL 轴能够在体内介导放疗抵抗性。临床标本免疫组化染色结果显示 ABRACL 的表达水平与放疗敏感性呈负相关，c-Jun 与 ABRACL 的表达呈正相关。通过 GEPIA 数据库中的结果分析显示，ABRACL 是肿瘤放疗治疗的特异性标志物，ABRACL 高表达预示患者预后较差。

结论：c-Jun/ABRACL 轴在调节线粒体融合与分裂稳态和介导放疗抵抗中起重要作用，加入 c-Jun 抑制剂或抑制 ABRACL 能够改善和增加放疗敏感性。

关键字: 线粒体，辐射，ABRACL

159. 生物信息学分析 BATF2 在头颈部肿瘤的表达及其预后价值

崔兆磊、陈燕*

福建省肿瘤医院

目的：通过 TCGA 和 GEPIA 数据库分析 BATF2(basic leucine zipper transcription factor, ATF-like 2)在头颈部鳞状细胞癌(head and neck squamous cell carcinoma，HNSCC)中的表达和预后价值。

方法：利用 TCGA 数据库、GEPIA 数据库分析 BATF2 在不同癌症组织中的表达进行对比；在 TCGA 数据的基础上，通过 R 语言进行 BATF2 与基因的共表达及相关性分析，分析这些基因与 BATF2 可能存在的相互作用通路。通过 UALCAN 数据库分析 BATF2 的表达情况与 HNSCC 生存期的关系，评估预后价值，得到预后风险比（HR）森林图。

结果：BATF2 在 HNSCC 中的表达处于中等水平，WARS、GBP5、GBP1 与 BATF2 相关性最强，呈正相关；BATF2 表达与丝氨酸蛋白酶抑制剂因子 Serpin B3 呈正相关（r=0.13,*P*=0.0025）。BATF2 的表达在 HNSCC 患者预后评估中不具有统计学意义。

结论：BATF2 在 HNSCC 中呈中低水平表达，对 HNSCC 中所有癌种的生存期评估尚无统计学差异。

关键字: BATF2；生物信息学；HNSCC；预后

160. IMP-4 型金属β内酰胺酶合并膜孔蛋白 OmpK36 缺失引起 ST85 型产酸克雷伯菌对碳青霉烯类耐药

孙明月、许青霞*

河南省肿瘤医院

目的：本研究旨在对一株碳青霉烯类耐药产酸克雷伯菌(Carbapenem-resistant Klebsiella oxytoca，CRKOX)耐药机制及耐药基因分子特征进行分析。

方法：自一个 2 岁急性髓系白血病-M7 患儿血培养中分离出产酸克雷伯菌株。采用全自动细菌鉴定药敏系统对细菌做鉴定和药敏，MALDI-TOF MS 鉴定复核细菌。PCR 扩增和 DNA 序列分析耐药基因，多位点序列测定分型(multilocus sequence typing,MLST)对菌株进行分型，全基因组测序(Whole genome sequencing ,WGS)分析菌株耐药基因，比较基因组学对耐药基因进行研究。分析质粒接合转移模块，采用接合实验检测耐药基因可转移性。

结果：全自动细菌鉴定药敏系统和质谱鉴定为产酸克雷伯菌株，亚胺培南、美罗培南对菌株的 MIC 分别为 8μg/ml 和>8μg/ml，MLST 分型为 ST85 型。PCR 扩增和序列分析发现该菌株为产 IMP-4 型金属β内酰胺酶，该酶位于 62892bp 质粒的 IS26 相关的I类整合子上，接合实验显示 blaIMP-4 基因可转移至大肠埃希菌 EC600。全基因组测序显示此菌株染色体含有 blaOXY-1-1 型β-内酰胺酶基因，同时伴有 OmpK36 膜孔蛋白的缺失。

结论：本研究首次报道了 ST85 型碳青霉烯类耐药产酸克雷伯菌，其对碳青霉烯类抗生素耐药的机制为 IncN1 型质粒介导的 IMP-4 型金属β内酰胺酶的产生合并 OmpK36 膜孔蛋白缺失。

关键字：产酸克雷伯菌、blaIMP-4、ST85、IncN1、OmpK36

161. 关于吸烟及癌发生的因果通路研究

李慧芹、杜牧龙*

南京医科大学

研究目的：肺癌是全球范围内最常见的恶性肿瘤之一，肺癌的发病率位居全球第二，死亡率排名第一。吸烟是增加肺癌发生风险的主要环境因素。香烟烟雾中含有多种致癌物质，然而，烟草致癌物代谢相关的遗传变异是否直接参与肺癌发生尚不明确。本研究旨在探讨吸烟及其代谢参与肺癌发生之间的遗传学机制和因果关系，为肺癌的防治提供依据。

材料与方法：首先，我们利用大样本 GWAS 数据分析了 43 种烟草致癌物代谢酶与肺癌易感性的遗传学关联。然后，基于孟德尔随机化、中介分析和结构方程模型的多种因果推断策略，重点研究遗传变异、吸烟强度和体内代谢能力参与吸烟所致肺癌发生的遗传学机制。

结果：我们发现，*CYP2A6* 中的 rs56113850 C>T 与吸烟者的肺癌风险降低显著相关（OR= 0.88, 95% CI= 0.85-0.91, P= 2.18×10^{-16}），*CYP2A6* rs56113850 与吸烟状态之间存在交互作用（$P_{interaction}$= 0.028）。综合因果推断模型结果，我们发现在吸烟人群中，吸烟强度可介导 CYP2A6 活性对肺癌风险影响的 15.3%-82.3%，并且该通路也间接影响了 *CYP2A6* rs56113850 与肺癌易感性的遗传效应。

结论：这项大规模的人群研究发现了 CYP2A6 活性、吸烟和吸烟所致肺癌的因果级联关系，即 rs56113850 的 T 等位基因可降低 CYP2A6 的活性及其表达，继而通过减少香烟消费行为，降低肺癌发生风险，为深入理解肺癌的病因提供了新的见解。

关键字: CYP2A6 活性；吸烟；肺癌；因果推断

162. 早期胃癌淋巴结转移 3-基因甲基化预测模型前瞻性队列研究

陈尚、刘权、廖柯、殷磊、李一凡、罗迪贤*

华中科技大学协和深圳医院

背景：淋巴结转移(LNM)不仅是早期胃癌(EGC)治疗方案的决策因子，也是发生复发和进展最重要的危险因素。目前临床术前诊断早期胃癌的淋巴结转移方法（CT 影像）不佳，导致约 80%患者被过度治疗。DNA 甲基化作为最常见的表观遗传调控事件之一，与体细胞突变相比，个体同一类型肿瘤细胞之间甲基化谱具有相对一致性和组织特异性，DNA 甲基化特征已被应用于癌变检测的生物标志物。

方法：我们之前曾报道过一组 3-基因（FCGBP，GNAS，CCDC166）EGC 组织 LNM 特异 DNA 甲基化标志，并构建了 3-基因甲基化模型。采用 methylight qPCR 的方法检测 3-基因模型甲基化水平，用于 LNM 预测。在本研究中，我们运用一组之前确定的 EGC LNM 特异的 3-基因甲基化标记，进一步开展临床样本前瞻性研究，并验证和评估这组 DNA 甲基化标志物的临床应用。

结果：1. 为了评估 3-基因甲基化模型的临床运用场景和真实性能，2021.11-2022.8 在华中科技大学协和深圳医院从临床获得 EGC 新鲜组织镜检样本共 117 例，其中术后病理诊断为 LNM 阳性（LNM+） 19 例，LNM 阴性（LNM-）为 98 例,LNM+病例占比 16.23%，符合流行病学统计。卡方或费希尔精确检验统计 117 例临床资料信息，提示侵润程度和淋巴管浸润与 EGC LNM 显著相关。2. 根据 3-基因甲基化预测模型危险分数 cutoff 值设定为 0.233，将样本分为 LNM 高和低分险，LNM+/-的危险分数有统计学意义（T 检验，p=0.027）19 例转移阳性中有 9 例（47.4%）被预测出阳性，98 例转移阴性中有 83 例（84.7%）预测出阴性，准确率为 78.6%。3. 我们分析了传统临床术前方法（CT 影像）以及 3-基因联合浸润深度(ID)和淋巴管浸润(LVI)的联合模型，它们鉴别淋巴结转移状态的结果，明显的是 3-基因甲基化预测模型的结果比传统方法的预测结果更好，与病理诊断的结果具有更高的一致性。19 例病理诊断为 LNM 阳性中传统方法预测有 3 例（15.8%），3-基因模型和联合模型预测出 9 例（47.4%），98 例转移阴性中两模型分别预测出 74 例（75.5%），81 例（82.7%），其准确率为 65.8%和 76.9%。

结论：我们构建的 3-基因甲基化预测模型性能优于传统模型，预测结果与临床病理结果一致性高。当联合浸润深度和淋巴管浸润后，对预测 EGC LNM 状态的性能并没有显著的提高。3-基因甲基化预测模型在前瞻性入组队列中表现出良好的鉴别性能，具有很好的临床潜力，有望成为评估 EGC LNM 状态并辅助临床方案决策的有力工具。

关键字：早期胃癌，淋巴结转移，DNA 甲基化，预测模型，前瞻性研究

163. NGS 技术检测I期 NSCLC 常见靶向基因突变分布及共突变情况

吴婧冉[1]、杜成*[2]

1. 大连医科大学北部战区总医院培养基地

2. 中国人民解放军北部战区总医院

背景及目的：肺癌是最常见恶性肿瘤和癌症死亡的主要原因之一，非小细胞肺癌（NSCLC）是我国肺癌的主要病理类型，其 5 年生存率较低。NSCLC 的发生、发展与一系列驱动基因突变有关。二代测序(NGS)技术，能够同时对上百万甚至数十亿个 DNA 进行分析，可较全面地指导肺癌患者个体化治疗或进一步发现新的基因突变，已成为临床肿瘤学实践的基石。

NGS 技术在晚期非小细胞肺癌中已有了标准化的应用，但其在 NSCLC 早期阶段的使用仍然不常见。本研究探讨驱动基因在I期 NSCLC 中的突变特征。为早期 NSCLC 基于生物标志物的靶向治疗提供帮助。

方法：纳入 2019 年 6 月-2021 年 11 月就诊于我院共 443 例I期 NSCLC 患者，收集患者临床病理特征等基本信息。采用 NGS 技术，分析患者病理组织中 EGFR、ALK、ROS1、BRAF、KRAS、MET、RET、ERBB2、PIK3CA、PTEN、TP53、BRCA、NRAS、FGFR1/2/3、MEK1、HRAS、NF1、CDK4、CDKN2A、PALB2、TSC2、CHEK2、FANCA、IDH1 共 26 种基因的突变情况。

结果：I期 NSCLC 中，女性（50.79% vs 37.25%，P=0.026）和腺癌的患者（74.27% vs 5.19%，$p<0.05$）相较于男性及其他病理类型患者发生基因突变的频率更高。不同病变部位（左肺、右肺）及不同年龄组间(≥60 岁、＜60 岁)驱动基因突变率差异无统计学意义（$P>0.05$）。至少发生 1 种基因突变的患者例数为 390 例（88.04%）。突变频率最高的驱动基因为 EGFR（61.63%），其次是 TP53（18.96%）、KRAS（8.12%）、ALK 和 PIK3CA（2.93%）、ERBB2（2.71%）。EGFR 突变的患者中，EGFR 单突变 184 例（41.53%），EGFR-EGFR 共突变患者例数为 22 例（4.97%）。67 例（15.12%）合并其他基因共突变，其中最常见的共突变形式为 EGFR-TP53 共突变（39 例，8.80%），EGFR 合并其他 1 种基因突变的患者数量为 58 例（13.09%），EGFR 突变合并其他 2 种基因的共突变患者数量为 9 例（2.03%）。12 例（2.71%）患者发生了 ALK 的重排，其中 1 例 24 岁的男性患者同时出现 3 种 ALK 的重排（ALK-CD207; ALK-STEAP4; ZNF804B-ALK）。1 例 50 岁的女性腺癌患者发生了 ALK 基因的点突变，且同时伴有 EGFR 及 TP53 的共同突变。

结论：NSCLC 驱动基因突变的频率与临床病理特征有关，EGFR、TP53、KRAS 等基因在I期 NSCLC 中的突变频率较高，EGFR 突变患者中与其他基因的共突变发生较频繁。这些结果对 NSCLC 药物开发和靶向治疗提供参考，但仍需积累更多病例进一步分析。

关键字：非小细胞肺癌 驱动基因 二代测序技术 靶向治疗

164. PI3K 调节亚基 p85β Tyr464 位点磷酸化后核转位调控 EZH2/H3K27me3/RB1 信号轴促进肾癌发生

张燕华[1]、何宝玉[1]、熊祖泉[2]、张东[1]、张一帆[1]、陈承坤[1]、杨仕仪[1]、崔高平[1]、顾峻[1]、王婷[1]、林璋[1]、樊友本[3]、郝宇钧*[1]

1. 上海交通大学医学院附属仁济医院上海市肿瘤研究所

2. 复旦大学附属华山医院

3. 上海交通大学附属第六人民医院

目的：PI3K 作为多种肿瘤发生的关键信号分子，其亚基在肾透明细胞癌（ccRCC）中突变率低，仅调节亚基 p85β的表达与肿瘤大小和临床预后密切相关，那么 p85β在 ccRCC 中的作用、机制及临床应用值得深入研究。中晚期肾癌及术后复发病人的一线用药是多靶点酪氨酸激酶抑制剂（比如：舒尼替尼），近期研究表明，与单药相比，酪氨酸激酶抑制剂（Vorolanib）和 mTOR 抑制剂（依维莫司）联合用药可明显改善 ccRCC 患者的中位生存时间，所以探究肾癌的药物联合治疗具有极大的临床应用前景。

材料与方法：通过 TCGA 数据库生物信息学分析获得 PI3K 调控 ccRCC 进程的关键蛋白亚基 p85β；利用免疫荧光和免疫组化等确定 p85β在 ccRCC 细胞中的定位；通过磷酸化蛋白分析和体外激酶实验等鉴定出 p85β核转位依赖的磷酸化位点和该位点磷酸化的蛋白激酶；通过 Crispr/CAS9 基因编辑，细胞功能分析，体内皮下瘤和原位瘤实验等明确 p85β在 ccRCC 中的作用；利用 ChIP-PCR，免疫印迹和 RNA-seq 等方式阐明 p85β核转位影响的下游信号通路；利用 FAK 小分子抑制剂阻断 p85β核转位探索治疗 ccRCC 的新方案。

结果：在 ccRCC 患者中，仅 PI3K 调节亚基 p85β的表达与肿瘤大小，疾病分期及预后呈显著相关性；数据库及临床样本证实 p85β在肾癌中高表达，同时在细胞系及癌组织中均可观察到 p85β大量位于细胞核内；通过磷酸化蛋白分析和体外激酶实验等发现 p85β核转位依赖 Y464 位点酪氨酸磷酸化，并证实该磷酸化位点的激酶是 FAK；体内外功能实验验证核定位而非胞质定位的 p85β可促进 ccRCC 细胞及肿瘤的生长和转移；免疫印迹等阐明核定位 p85β会结合组蛋白甲基转移酶 EZH1/2，降低它们的泛素化水平而上调组蛋白 H3K27 三甲基化，引起抑癌基因 RB1 的表达抑制，促进细胞周期从 G1 期向 S 期转换，从而促进 ccRCC 的发生；ccRCC 肿瘤有高水平的 p85β或 p-p85β时，其对 FAK 抑制剂单独治疗及联合舒尼替尼治疗都具有更好的响应性。

结论：PI3K 的调节亚基 p85β被激酶 FAK 在 Y464 位点磷酸化后发生核转位，调控 EZH2/H3K27me3/RB1 信号轴而促进 ccRCC 的发生发展。FAK 抑制剂单药治疗和联合舒尼替尼的联合用药有望成为治疗 ccRCC 的新策略，其效果有赖于可作为标志物的 p85β或 p-p85β的表达水平。

关键字: PI3K；p85β核转位；p85β磷酸化；FAK；EZH1/2；RB1

165. 95 例消化道肿瘤免疫相关不良事件的临床分析

孙婧、史幼梧、杜丰、杨颖、孙志伟、余靖、肖艳杰、张晓东、贾军*

北京大学肿瘤医院

目的: 探讨消化系统恶性肿瘤中免疫检查点抑制剂（Immune checkpoint inhibitors, ICIs）导致免疫相关不良事件(Immune-related adverse events, irAEs)的特征及危险因素。

方法: 回顾性分析 2019 年 4 月至 2021 年 10 月北京大学肿瘤医院诊治的 95 例接受 ICIs 治疗的消化系统恶性肿瘤患者的临床资料、实验室检查结果及 irAEs 发生情况。irAEs 危险因素分析采用二元 Logistic 回归分析。

结果：95 例患者共应用 ICIs 治疗 458 例次，中位应用 3 例次（范围：1~33 例次）。irAEs 的发生率为 55.8%，3~4 级 irAEs 发生率为 9.5%。最常见的 irAEs 为皮肤毒性（27.4%）和内分泌 irAEs（22.1%）。内分泌 irAEs 中甲状腺功能减退最常见（16.8%），而肾上腺皮质功能减退（2%）和垂体炎（1%）少见。多数 irAEs 发生于免疫治疗初期，78.2%发生于 12 周内。过敏反应、皮疹最早发生，中位发生时间分别为 2 周（范围：0.9-3.1 周）和 3.8 周（范围：0.9-17.9 周），内分泌 irAEs 中位发生时间为 6.9 周（范围：3.0-52.1 周）。多因素分析显示，女性(OR=5.197, 95%CI 1.166-23.154, p=0.031)和微卫星高度不稳定（Microsatellite Instability-High，MSI-H） (OR=35.048, 95%CI 2.756-445.787, p=0.006)是内分泌 irAEs 发生风险增加的独立危险因素，免疫治疗联合化疗(OR=0.001, 95%CI 0.021-0.412, p=0.001）是内分泌 irAEs 的独立保护性因素。

结论:在消化道肿瘤中应用 ICIs 具有较好的安全性。女性和 MSI-H 患者出现内分泌 irAEs 风险增加，联合化疗可能降低内分泌 irAEs 发生风险。

关键字: 消化系统恶性肿瘤；免疫检查点抑制剂；免疫相关不良事件

166. 免疫原性细胞死亡相关基因模型在宫颈癌预后及抗肿瘤免疫中的意义

姜山 [1,2]、孙阳*[2]、崔兆磊 [2]、吴巧铃 [2]

1. 福建中医药大学

2. 福建省肿瘤医院

目的:基于免疫原性细胞死亡相关基因为宫颈癌患者构建预后模型。

方法：以肿瘤基因组图谱(Tumor Genome Atlas, TCGA)宫颈癌患者样本数据为基础，采用 LASSO 和 COX 回归方法获得免疫原性细胞死亡预后基因(IPGs)，构建 IPGs 评分体系，将患者分为高、低风险两组，以 GEO 数据集为验证组。通过 Kaplan-Meier 分析、ROC 分析、单因素和多因素变量 Cox 回归分析探讨风险评分对预后的作用。此外，我们将风险评分与肿瘤微环境中的免疫特征相关联，包括肿瘤微环境、肿瘤浸润免疫细胞、免疫治疗。并对高低风险组进行肿瘤突变负荷及化疗药物敏感性的差异分析。通过 Cox 回归筛选出 IPGs 中风险比（Hazard Ratio，HR）最高的关键基因 PDIA3，随后通过蛋白质印迹法、免疫荧光法、组织微阵列验证其在宫颈癌中的表达及其对患者预后的影响。

结果：免疫原性死亡预后模型显示出良好的预测能力。Cox 回归筛选出 4 种与预后相关 IPGs (PDIA3、CASP8、IL1 和 LY96)构建预后模型，在 TCGA 队列中高表达与 CESC 患者不良预后呈正相关，能作为宫颈癌的独立预测指标(HR= 1.058, P<0.01)，并在 GEO 得到进一步的验证。我们通过结合临床特征和 IPGs 特征构建了一个临床列线图，预测宫颈癌患者的生存可能性。校准曲线证实了列线图预测与实际之间的良好一致性。高风险组肿瘤微环境评分和免疫细胞浸润程度均低于低风险组，富集发现多为免疫信号通路。在 TIDE, MDSC 和 CAF 评分中高风险组低于低风险组，说明高风险组可能抑制了机体的免疫效应，IPGs 高表达患者的免疫效果更差，并且常用化疗药物在高风险组患者中敏感性均较低。根据蛋白质印迹与免疫荧光发现关键基因 PDIA3 在宫颈癌组织中高表达，组织微阵列差异分析表明 PDIA3 与患者预后不良相关。

结论：本研究基于 4 个 IPGs 探讨宫颈癌预后与免疫原性死亡的关系。通过探讨其生物行为特征和临床因素，结果表明 IPGs 风险评分可作为宫颈癌患者预后和免疫疗效的生物标志物，并为早期肿瘤筛查提供策略基础。其中关键基因 PDIA3 也具有重要的预后价值。因此我们

可以通过靶向治疗，影响免疫原性死亡在肿瘤免疫调节方面的强大作用，这将为宫颈癌患者的治疗提供新思路。

关键字：宫颈癌；免疫原性死亡；肿瘤免疫浸润；免疫治疗；预后

167. 早期肺腺癌患者血清中蛋白核心岩藻糖基化改变模式的研究

周洁君、李安琪、陈明伟*

西安交通大学第一附属医院

研究目的：肺癌（lung cancer）是肿瘤相关性死亡最重要的病因，其中腺癌（lung adenocarcinoma，LUAD）是最常见的亚型，预后不良，故进一步探寻其生物标志物和潜在的药物靶点尤为重要。本课题组前期研究发现肺腺癌中蛋白核心岩藻糖基化水平显著升高。本研究在前期研究基础上，利用基质辅助激光解吸电离飞行时间质谱技术进一步确认早期（I-II 期）肺腺癌中的特征性蛋白核心岩藻糖基化改变模式，以期为找寻新型肺癌生物标志物及治疗新靶点提供一定依据。

材料与方法：收集自 2020 年 10 月-2021 年 7 月期间于西安交通大学第一附属医院确诊的早期肺腺癌患者进行初次治疗前的血清标本，并收集肺部良性结节患者及健康体检人群血清标本作为对照组。使用凝集素技术提取出血清样本中有核心岩藻糖基化改变的蛋白，并通过凝集素印迹技术对提取样本进行验证。使用基质辅助激光解吸电离飞行时间质谱技术进一步解析早期肺腺癌中蛋白核心岩藻糖基化改变的具体模式。

结果：本研究共收集血清标本 179 例，其中早期肺腺癌血清标本 79 例，肺部良性结节患者血清标本 41 例，健康人血清标本 59 例。平均年龄 51.9±10.1 岁，男女比例 1.35:1。质谱分析结果显示：早期肺腺癌组与健康人组相比，血清中有 4 种蛋白（GKAP1、IGHG2、IGHG3、GPX3）核心岩藻糖基化水平显著降低（表达差异倍数>1.5 倍且 *P value*<0.05，后同）,有 46 种蛋白（IGHM、IGJ、CFAH、AACT 等）的核心岩藻糖基化水平显著升高。早期肺腺癌组与肺部良性结节患者组相比，血清中有 92 种蛋白（IGHG3、GKAP1、AACT、IGHG2、HPT、FINC 等）核心岩藻糖基化水平显著降低,有 10 种蛋白（CLUS、BTD、CALL5、IGJ、PIGR、AFAM、SAMP、CTSD、APOH、CPN2）的核心岩藻糖基化水平显著升高。早期肺腺癌组相对健康人组与肺部良性结节组核心岩藻糖基化水平均显著升高的有 6 种蛋白（CLUS、

CALL5、IGJ、CTSD、APOH、CPN2）,早期肺腺癌组相对健康人组与肺部良性结节组核心岩藻糖基化水平均降低的蛋白有 4 种（GKAP1、IGHG2、IGHG3、GPX3）。

结论：早期肺腺癌患者血清中的蛋白核心岩藻糖基化模式相对正常人和肺部良性结节患者均发生了显著改变。异常改变的糖基化模式有望作为潜在的肺癌生物标志物，异常的核心岩藻糖基化位点有望成为肺癌治疗新靶点。

关键字：肺腺癌；血清蛋白；核心岩藻糖基化；生物标志物

168. PIKE-A 调控 STAT3-FTO-SDHA-线粒体轴在 GBM 发展中的作用研究

孙明明[1]、山长亮[1]、张帅*[2]

1. 南开大学

2. 天津中医药大学

研究目的：神经胶质瘤是一种常见的恶性程度较高的脑实质肿瘤，生长于脑实质内部，常与正常脑组织混合。神经胶质瘤病因尚不清楚，也无明确的预防措施。随着细胞与分子生物学、遗传学研究的不断深入，研究神经胶质瘤关键调控分子，寻找有效治疗靶点已经成为神经胶质瘤的治疗亟待解决的问题。磷酸肌醇 3 激酶增强子（phosphoinositide (PI) 3-kinase enhancer,PIKE）是 centaurin 家族的一员，由 CENTG1 基因编码，包括 S，L 和 A 三种亚型。前期我们的研究发现，当 PIKE-A 被稳定敲低时，肿瘤细胞的增殖和生长明显受到抑制。近年来越来越多的研究结果已经证明了线粒体功能异常在肿瘤发生中起关键的作用。我们推测 PIKE-A 通过调节线粒体功能从而影响神经胶质瘤恶性发展，然而其具体分子机制还不清楚。因此，本文主要从 PIKE-A 调控琥珀酸脱氢酶（Succinate dehydrogenase, SDH）影响线粒体功能的角度，探讨 PIKE-A 在神经胶质瘤恶性发展中的作用机制。

材料与方法：为了探究 PIKE-A 在神经胶质瘤恶性发展中的作用机制，本课题首先构建了多种稳定敲低 PIKE-A 的神经胶质瘤细胞系，利用 OCR 分析试剂盒、ATP 检测试剂盒和线粒体膜电位检测试剂盒检测了细胞耗氧率（Oxygen Consumption Rate,OCR）、细胞内的 ATP 水平和线粒体膜电位。然后我们通过代谢组学来评估敲低 PIKE-A 前后的代谢产物的变化，RNA-seq 方法筛选有变化的代谢酶，qRT-PCR 实验确定 SDHA 为影响线粒体呼吸的关键代谢酶。在进一步探索 PIKE-A 调控线粒体呼吸的分子机制中，我们利用 qRT-PCR 实验和免

疫印迹实验检测 PIKE-A 是否可以影响 STAT3 的活性，另外，PIKE-A 可以通过 STAT3 调控 FTO 表达影响 SDHA 表达。我们利用线粒体膜电位检测试剂盒检测了 PIKE-A 可以通过 STAT3/FTO 影响线粒体膜电位。并且，我们利用细胞计数实验检测 PIKE-A 通过 STAT3/FTO 影响脑胶质瘤细胞增殖。

结果：在本研究中我们首先发现稳定敲低 PIKE-A 的神经胶质瘤细胞相对于对照组细胞，线粒体的功能如细胞耗氧率、细胞内 ATP 水平和线粒体膜电位降低。另外，代谢组学、RNA-seq 实验结果显示 PIKE-A 可以通过 SDHA 调控线粒体呼吸。在前期研究中，我们发现敲低 PIKE-A 导致 STAT3 活性降低。在本研究中，分子生物学实验结果显示，PIKE-A 通过 STAT3 促进 FTO 表达来增加 SDHA 的表达。并且，PIKE-A 通过 STAT3/FTO 依赖的方式调控线粒体呼吸和细胞增殖。

结论：在本研究中，我们发现了 PIKE-A 通过调控 SDHA 的表达来调控线粒体功能，从而促进癌症进展的分子机制。进一步的机制研究表明，PIKE-A 是 STAT3/FTO 的一个新的调节因子，调节 SDHA 的表达。在本研究中，我们揭示了 PIKE-A/STAT3/FTO/SDHA 促进线粒体代谢，从而在促进肿瘤生长中发挥关键作用。

关键字：PIKE-A；线粒体；SDHA；细胞增殖；神经胶质瘤

169. 体内版类器官药敏检测：OncoVee-MiniPDX 在胃癌患者术后辅助治疗的应用

毕臻乐、胡凯猛、闻丹忆*

上海立迪生物技术股份有限公司

研究目的：胃癌患者术后生存率仍较低，如何选择更为有效的方案以达到最佳的术后辅助治疗效果是临床亟待解决的问题。目前以条件重编程细胞、类器官和人源肿瘤异种移植模型(Patient-Derived Xenograft, PDX)等模型为代表的功能性检测平台在肿瘤患者药物选择上显示出较大的潜力。本研究旨在回顾性分析 PDX 及体内版类器官模型（OncoVee®-MiniPDX）在胃癌患者术后辅助治疗中的应用前景。

材料与方法：我们入组接受手术治疗后需要进行辅助治疗的胃癌患者 37 例，取其肿瘤手术样本进行 MiniPDX 检测，同时进行 PDX 建模。临床上患者按照指南进行术后用药，并随访其无进展生存期（Progression-free Survival, PFS）情况。MiniPDX 和 PDX 模型均检测临床

实际应用药物的敏感性结果。匹配 MiniPDX、PDX 和临床结局，通过回顾性分析评估体内版类器官和 PDX 在患者临床结局预测的相关性。

结果：37 例患者最终 PDX 建模成功 19 例，该 19 例患者的基线情况、MiniPDX 结果、PDX 结果及 PFS 均见表 1。相关性分析显示 MiniPDX 和 PDX 之间的系数为 0.594 (p<0.01)，MiniPDX 以及 PDX 肿瘤抑制率(Tumor growth inhibition rate, TGI)与患者 PFS 相关系数分别为 0.908 (p<0.01)和 0.779 (p<0.01) 。以 PDX TGI 40%和 MiniPDX TGI 45%分别为 cut-off 值对患者进行分层，Log-rank 检验结果显示：PDX TGI ≥40%以及 MiniPDX TGI ≥45%均能较好地区分患者 PFS (p=0.017 和 P=0.001)。

结论：无论是 PDX 还是 MiniPDX 均与临床生存结局存在较高的相关性，尤其是 MiniPDX。但是 MiniPDX 与 PDX 本身的相关性欠缺稳定，可能与体系误差有关。利用 PDX 和 MiniPDX 其 Cut-off 值进行临床分层具备较好的潜力，但仍需要更大样本量长期随访的前瞻性对照试验来验证。

关键字：类器官；体内；MiniPDX；PDX；胃癌；辅助治疗；药物敏感性

170. 蛋白质 O-糖基化分析新技术研究

秦洪强*

中国科学院大连化学物理研究所

糖基化是最重要的蛋白质翻译后修饰之一，它对于蛋白质的折叠、定位、构象稳定和活性等各方面具有重要影响。其中，O-糖基化参与了几乎所有重要的生命过程，如蛋白质相互作用、免疫应答、细胞通讯、细胞凋亡等，其异常与肿瘤等众多恶性疾病的发生、发展密切相关。然而，O-糖基化修饰是受到一系列糖基转移酶和糖苷酶共同调控，存在着高度的复杂性，如何实现蛋白质糖基化的高灵敏度、高通量分析是其在临床应用的关键。针对以上科学问题，我们的研究工作主要包括： 1）Mucin 型 O-GalNAc 糖基化分析新技术研究；2）O-GlcNAc 糖基化分析新技术研究。针对 O-GalNAc 型糖基化丰度低、N-连接糖基化干扰严重、缺乏糖苷酶的分析挑战，基于 O-连接糖肽在质谱碎裂时易产生糖链完全中性丢失的肽段特征，发展了基于理论去糖基化的策略，降低了谱图的复杂性和数据检索空间，将完整 O-GalNAc 糖肽的鉴定数目提高了 4 倍以上（Anal. Chem. 2017, 89, 1469）；针对 O-GalNAc 糖基化亲水性弱、富集效率低的挑战，提出了基于 Ti-IMAC 材料的 O-GalNAc 糖肽富集策

略，通过亲水-亲和协同效应增强糖肽的保留和提高富集效率，从 0.10 微升血清样品中鉴定到超过 300 条完整糖肽（常规亲水富集血清用量约需要 5.0 微升），并最终从 7.2 微升血清样品中鉴定到 2093 条完整糖肽，建立了迄今为止人源血清完整 O-GalNAc 糖基化的最大数据库，为候选标志物的筛选提供了数据库(Anal. Chem. 2021, 93, 7579)。将该方法应用于正常人与肝癌患者血清中 O-GalNAc 糖基化分析，为 O-GalNAc 型糖基化在临床肿瘤早期诊断的应用提供了关键技术支撑。O-GlcNAc 是与细胞内丝氨酸、苏氨酸残基连接，虽然其糖型结构简单，但是丰度远低于磷酸化等修饰，富集和检测更具挑战性。研究团队在糖肽富集与鉴定过程中引入‘可逆’的概念，实现糖肽的高效捕获、释放与鉴定，主要包括以下两方面：1）氧化标记-可逆富集策略，发展了基于化学氧化-可逆酰肼化学的富集策略，通过化学氧化法引入醛基，并利用醛基与酰肼、羟胺分别形成腙-肟之间的化学反应平衡，实现糖肽的捕获与可逆释放，其具有释放效率高、引入质量标签小的优势（Anal. Chem. 2021, 93, 16618）；2）可逆酶促标记策略，建立了基于糖苷内切酶 Endo-M 及其突变体的可逆化学酶促标记：一方面，利用 Endo-M N75Q 的突变体进行 O-GlcNAc 糖型的延长，显著增强糖肽的亲水性，提高糖肽的富集效率；另一方面，富集后的糖肽利用 Endo-M 等糖苷酶将延长糖链切除，降低质量标签对糖肽鉴定的干扰，真正意义上实现了 O-GlcNAc 糖肽的“无痕”富集(Angew. Chem. Int. Ed., 2022, DOI:10.1002/anie.202117849)。以上研究发现，鉴定到 RNA 甲基化结合蛋白发生 O-GlcNAc 修饰，为二者的交互作用以及肿瘤中调控机制的研究提供了新思路。

关键字：O-GalNAc 糖基化；O-GlcNAc 糖基化；交互作用；

171. TET1 参与宫颈癌疾病进展的作用机制研究

谢璐鸿、任吉、谭玉洁*

贵州医科大学附属医院

背景：甲基化修饰已被发现在调节基因表达与多种生物学过程中起着至关重要的作用。其中去甲基化修饰酶甲基胞嘧啶双加氧酶 1(TET1)通过调节关键致癌基因或抑癌基因启动子区 CpG 岛胞嘧啶修饰来影响肿瘤进展，但其在宫颈癌中的作用尚不清楚。

目的：探讨宫颈癌组织中 TET1、5-甲基胞嘧啶(5-mC)和 5-羟甲基胞嘧啶(5-hmC) 的表达及其与宫颈癌患者临床病理参数的关系。探讨 TET1 在宫颈癌发生发展中的作用及分子机制。

方法：利用 Western-blot 和免疫组织化学方法分析 TET1 在宫颈癌和癌旁组织中的表达水平。应用免组织化学方法检测 TET1、5-mC、5-hmC 在 45 例宫颈癌患者及 20 例正常宫颈组织中的表达情况；分析 TET1、5-mC、5-hmC 在宫颈癌组织中的差异表达情况，及其与临床病理参数的相关性。通过 RTCA、划痕试验和 Transwell 侵袭试验等体外试验和小鼠异种移植模型建立探究 TET1 对宫颈癌细胞生物学行为影响，进一步通过转录组测序和甲基化测序，分析 TET1 可能参与的细胞功能以及对宫颈癌发生发展的分子作用机制。

结果：发现宫颈癌中 TET1 的表达明显低于癌旁组织。与正常宫颈组织相比，宫颈癌组织中 TET1 和 5-hmC 以低表达为主，5-mC 以高表达为主。宫颈癌中 TET1 的表达与 5-mC 呈负相关，与 5-hmC 呈正相关。并且 5-mC 与 5-hmC 表达也呈负相关。在宫颈癌相关病理参数分析中得出 TET1、5-mC 和 5-hmC 的表达与淋巴结转移相关，而 5-mC 和 5-hmC 的表达也与血管侵袭相关。在宫颈癌细胞中敲低 TET1 后，宫颈癌细胞的增殖、侵袭与迁移能力以及体内肿瘤生长、转移均增强，相反，在 TET1 过表达后获得了相反的结果。转录组测序显示 TET1 基因敲除影响宫颈癌 Siha 细胞的主要信号通路包括 AMPK、自噬、mTOR、Rap1、PI3K/Akt 及 apoptosis 等，其中我们发现 TET1 的敲低能增强宫颈癌细胞自噬水平。另外。甲基化的 DNA 免疫沉淀测序(MeDIP-seq)，MeDIP 定量实时 PCR，发现 TET1 介导了自噬基因启动子区甲基化修饰。

结论：TET1 可能参与宫颈癌的发展与转移过程。TET1 对宫颈癌及宫颈癌细胞生物学的影响以及在此过程中通过修饰自噬基因的甲基化水平影响宫颈癌的进展，但具体机制仍需进一步研究。对宫颈癌的诊断、预后和分子靶向治疗具有重要的应用价值。

关键字：TET1；宫颈癌；病理参数；自噬

172. 血浆 Septin9 基因甲基化检测对中国人群结直肠癌的诊断价值：一项 Meta 分析

刘丹丹[1]、聂优[2]、王宏伟*[1]

1. 中国人民解放军总医院第四医学中心

2. 首都医科大学

结直肠癌（colorectal cancer，CRC）是人类癌症相关死亡第二大原因，已成为严重威胁全球健康的公共卫生问题。中国人口基数大，CRC 发病率、死亡率仍位居世界前列，正在面临

沉重的 CRC 负担，亟需一项简便、灵敏、易接受的高效筛查技术解决这一重大临床问题。血浆 Septin9 基因甲基化检测是一项被 FDA 批准的无创性、灵敏度和特异度高的 CRC 筛查技术。尽管，当前几项研究已经证实血浆 Septin9 基因甲基化检测对 CRC 诊断具有潜在价值，但基于中国人群的研究较少并缺乏大样本数据和一致性评价。

目的：荟萃基于中国人群的血浆 Septin9 基因甲基化 CRC 的相关研究，通过 Meta 分析方法学更精确评估血浆 Septin9 基因甲基化对 CRC 的诊断价值，旨在为血浆 Septin9 基因甲基化作为 CRC 规模性筛查策略提供依据，为降低中国人群 CRC 发病率、死亡率识别精准的预警标志。

方法：本研究对维普、万方、CNKI、Ovid、PubMed、Sinomed、Web of Science、EBSCO、Wiley online library、Science Direct、Springer 数据库进行检索并按照纳入标准筛查文献和进行质量评价。利用 Meta-Disc1.4 和 Stata 17.0 等软件对提取信息进行 Meta 分析。

结果：这项研究共检索文献 1397 篇，排除后纳入 15 篇。涉及研究对象：CRC 患者 2023 例，健康对照者 1289 例。Meta 分析显示：选用随机效应模型进行合并效应量，合并敏感度为：0.70（95% C I ：0.65 ～0.74)，合并特异度为 0.97（95% C I ：0.95～0.98)，合并阳性似然比：23.8（95% C I ：14.4 ～39.4)，合并阴性似然比：0.31（95% C I ：0.27 ～0.36)，诊断比值比为 77（95% C I ：47～128)，SROC 曲线下面积（AUC)为 0.90（95% C I ：0.87～0.93）。同时，回归分析提示：试剂盒品牌是敏感性和特异性的显著影响因素。

结论：血浆 Septin9 基因甲基化对中国人群 CRC 诊断具有潜在价值，有望成为中国人群规模性 CRC 筛查计划的检测技术，但需要进一步对试剂检测盒检测标准同质化做出努力。

关键字：结直肠癌；Septin9；基因甲基化；诊断；Meta 分析

173. 基于血小板相关基因构建结直肠癌预后风险预测模型的研究

刘琪[1]、冯焱[3]、程义凡[1]、张博文[1]、张澍[2]、尹晓然*[1]

1. 西安交通大学第二附属医院肿瘤科

2. 西安交通大学第二附属医院老年消化外科

3. 西安交通大学第一附属医院消化科

目的：构建基于血小板相关基因预测结直肠癌（Colorectal Cancer, CRC）患者的预后风险模型。

方法：从 TCGA 数据库获取 CRC 患者的全基因组表达数据，从 KEGG 和 GSEA 数据库获取血小板相关基因，通过差异分析获取差异表达的血小板相关基因。单因素 Cox、LASSO 回归筛选出与 CRC 预后相关的候选基因，多因素 Cox 用于构建预后模型的风险评分方程。Kaplan-Meier 生存分析、ROC 曲线分析对模型验证并评估其预测水平。多因素 Cox 判断该模型作为 CRC 患者预后的独立预测能力。基于预后模型风险评分与多个独立预测预后的临床因素绘制 Nomogram 图。

结果： 基于单因素、LASSO、多因素 Cox 筛选出 6 个与 CRC 患者预后关联的基因，并构建预后模型的风险评分方程。Kaplan-Meier 生存曲线显示，高风险组生存期明显低于低风险组（$p<0.05$）。ROC 曲线分析及多因素 Cox 分析显示，血小板相关基因预测模型具有良好的预测效能，1、3、5 年生存率的 AUC 分别为 0.727、0.687、0.591，并且可以独立预测患者的生存时间（HR=1.58, $P<0.001$）。进一步结合有预测效能的临床指标构建出 Nomogram 图，ROC 曲线分析结果显示，训练集中 AUC 值为 0.829，验证集中 AUC 值为 0.799。

结论：本研究基于血小板相关基因所构建的预测模型具有独立预测能力，而联合具有预测效能的临床指标的 Nomogram 模型能够更加有效预测 CRC 患者的预后，其中的相关基因可能是结直肠癌患者靶向治疗的潜在标志物。

关键字：结直肠癌；血小板相关基因；生物信息学；预测模型；生物标志物

174. 胰腺腺鳞癌的研究进展和治疗展望

张文、梁喜俊、丁劲*

海军军医大学

胰腺癌是一种预后极差的消化道恶性肿瘤，其总体五年生存率极低。胰腺腺鳞癌是一种预后更差的罕见胰腺恶性肿瘤，一般胰腺腺鳞癌被定位于肿瘤组织中同时存在腺状细胞成分和鳞状细胞成分。但目前胰腺腺鳞癌的发生机制尚不清楚，且缺乏针对性治疗方案。本文结合胰腺腺鳞癌与胰腺导管腺癌的相关研究，回顾了腺鳞癌的生物学特征、鳞癌起源假说及潜在腺鳞癌调控机制的进展，系统总结了胰腺腺鳞癌潜在的生物标志物及鳞癌可能的调控机制，并进一步提出了胰腺腺鳞癌可能的治疗新方向。因此，本文通过系统综述胰腺腺鳞癌的研究进展，为胰腺腺鳞癌的发生发展机制及治疗提供了新思路。

关键字: 腺鳞癌; 病理特征; 发病机制; 治疗

175. EB 病毒感染与 XRCC1- Arg399Gln 基因多态性在鼻咽癌发生中的交互作用研究

崔兆磊、陈燕*

福建省肿瘤医院

目的： 探讨 VCA-IgA、EA-IgA、Rta-IgG 三种抗体在鼻咽癌中的临床应用价值，评估 XRCCl-Arg399 Gln 单核苷酸多态性在鼻咽癌发病中的风险；研究 XRCCl-Arg399 Gln 单核苷酸多态性与 EB 病毒感染的交互作用。

方法：采用 ELISA 检测 2155 例未经治疗的鼻咽癌患者及 6957 例健康体检者血清中 VCA-IgA、EA-IgA、Rta-IgG 水平；采用病例对照研究，并按照性别和年龄 1∶1 配对，抽取全血基因组 DNA 进行 PCR 扩增，对扩增产物再进行酶连接检测反应扩增，最后测序分析得出 XRCC1 Arg399Gln 的基因型。

结果： VCA-IgA、EA-IgA、Rta-IgG 在鼻咽癌组中阳性率分别达 89.88%、46.59%和 63.25%；ROC 曲线分析显示，曲线下的面积 VCA-IgA>Rta-IgG >EA-IgA；危险度分析显示，VCA-IgA、EA-IgA 和 Rta-IgG 三项检测均阳性者危险度最高，其次为 VCA-IgA 和 Rta-IgG 两项阳性，三项抗体均阴性者危险度最低；VCA-IgA 抗体检测在鼻咽癌中以 41~60 岁阳性率最高

（*P*<0.01），而 Rta-IgG 阳性率随着年龄增加而增高，另外 VCA-IgA 以非角化未分化性鳞癌阳性率最高（*P*<0.01）；EA-IgA 阳性率与 T 分期具呈线性相关（*P*<0.01），三种抗体检测阳性率分别与 N 分期、临床分期均呈线性关系（*P*<0.01）；EB 病毒感染能增加鼻咽癌发病风险：VCA-IgA、EA-IgA 和 Rta-IgG 抗体三项阳性时可以增加鼻咽癌风险因素，但单项 VCA-IgA 阳性是鼻咽癌发病的最强危险因素，单因素分析显示与携带 XRCC-1 Arg399Gln 的 AA 基因型相比，携带 XRCC-1 Arg399Gln 的 GG 基因型可以增鼻咽癌发病风险；XRCC-1 Arg399Gln 的 GA 基因型与 VCA-IgA 存在交互作用（OR=20.755）。

结论：三种抗体诊断价值以 VCA-IgA 最优，其次是 Rta-IgG，EA-IgA 相对较弱。鼻咽癌筛查中，以 VCA-IgA、EA-IgA 和 Rta-IgG 三项阳性危险度最高，VCA-IgA 和 Rta-IgG 两项阳性危险度次之，而三项抗体均阴性者危险度最低；XRCC-1 基因的 Arg399Gln 基因多态性能够增加患鼻咽癌的风险，且 Arg399Gln 的 GA 基因型与 EB 病毒感染具有一定的交互作用。

关键字: XRCC1；鼻咽癌；基因多态性；VCA-IgA；EA-IgA；Rta-IgG

176. 肝细胞癌免疫治疗耐药的研究进展

王志杰、高鹏、丁劲*

海军军医大学

免疫检查点抑制剂（Immune checkpoint inhibitors，ICIs）的应用极大地丰富了我们对抗肝细胞癌（Hepatocellular carcinoma，HCC）的治疗方案，使受益患者取得了良好的长期生存率，然而由于 HCC 复杂的发病机制和免疫抑制的肿瘤微环境（Tumor microenvironment，TME），能够从中获益的患者很少且存在获益后耐药的情况。ICIs 的耐药与多种可能的因素有关，包括免疫抑制性的 TME、抗原的表达缺失及提呈受损、肿瘤的异质性及肠道微生物群的影响等，因此，积极探索可能的耐药机制以进一步提高 ICIs 的临床获益率至关重要。目前针对 HCC 免疫治疗的多种联合方案在一定程度上预防并逆转了耐药现象，同时，还有许多新的可以克服耐药的药物正在探索中。在本篇综述中，我们讨论了 HCC 中复杂的 TME，探讨了不同耐药分类中可能的免疫耐药机制，并回顾总结了目前应用中和探索中的免疫治疗联合方案。

关键字: 肝细胞癌；免疫检查点抑制剂；肿瘤微环境；免疫耐药

177. GALAD 和 BALAD-2 模型在原发性肝细胞癌诊断及短期疗效评价中的临床意义研究

崔兆磊、陈燕*

福建省肿瘤医院

目的：探讨 GALAD 模型在原发性肝细胞癌患者诊断价值以及 BALAD-2 模型在肝细胞癌短期疗效评估中的价值。

方法：收集某院 2017 年 8 月—2018 年 2 月 87 例首诊肝癌（HCC）患者、53 例肝脏良性疾病（BLD）患者、49 例表观健康体检者(HC)血清，采用微流控免疫荧光电泳技术检测血清中 AFP、AFP-L3 和 DCP 水平，建立基于性别、年龄和血清中 AFP、AFP-L3 和 DCP 水平的 GALAD 模型，分析 GALAD 模型对于肝癌患者的诊断价值；采用溴甲酚紫法检测血清中白蛋白及重氮法检测血清中胆红素水平，建立基于 ALB、BIL、AFP、AFP-L3 和 DCP 的 BALAD-2 模型，对随访资料完整的 41 例原发性肝癌患者动态观察治疗前后 BALAD-2 模型变化，分析 BALAD-2 模型与肝癌患者短期疗效的关系。

结果：GALAD 模型评分与患者的性别和年龄显著相关，差异有统计学意义,多数肝癌患者伴有乙肝病毒感染，肝硬化是肝癌的高危因素；肝癌患者血清 AFP、AFP-L3、DCP 水平以及 GALAD 模型评分均显著高于肝脏良性疾病组(p<0.05)和表观健康对照组(p<0.05)，差异均有统计学意义；GALAD 的特异性（94.3%）和准确性（60.8%）均高于 AFP（分别为 85.1%和 55.7%）、AFP-L3(分别为 71.3%和 55.0%）、DCP（分别为 85.1%和 59.1%）,特异性(95.1%)低于 AFP-L3(97.1%)和 DCP(97.1%)，高于 AFP(90.2%),研究表明，GALAD 模型诊断肝癌优于单一指标；肿瘤控制组治疗后 AFP、AFP-L3、DCP 水平以及 BALAD-2 较治疗前均显著下降（p<0.05）差异有统计学意义；肿瘤进展组 AFP、AFP-L3、DCP 和 BALAD-2 均未显著下降（P>0.05）。

结论：GALAD 模型可提高原发性肝癌的早期诊断率，BALAD-2 模型有助于肝细胞癌患者短期疗效评估。

关键字：原发性肝细胞癌；GALAD 模型；BALAD-2 模型；肿瘤标志物

178. GPC3 联合 PIVKA-II在 AFP 阴性肝癌的诊断预后价值

崔兆磊、陈燕*

福建省肿瘤医院

目的：探讨磷脂酰肌醇蛋白聚糖-3（GPC-3）和异常凝血酶原（PIVKA-II）联合检测对 AFP 阴性肝癌的诊断和预后价值，为患者的临床治疗提供参考。

方法：从福建省肿瘤医院 408 例肝癌首诊患者中筛选出 101 例 AFP 阴性肝癌患者作为实验组，并对其中 13 例接受肝癌手术治疗的患者进行疗效监测，同时选择同期入院的 114 例良性肝病患者以及 60 例体检的正常人群作为对照组进行前瞻性队列研究。收集肝癌实验组临床诊疗数据进行生存随访。检测研究对象血清中 GPC3 及 PIVKA-II的表达水平，建立 ROC 曲线并计算两者诊断指标以及在不同肿瘤分期的诊断敏感性；单因素分析 GPC3 和 PIVKA-II 与 AFP 阴性肝癌患者临床特征的相关性；分析手术患者治疗前后 GPC3 及 PIVKA-II的表达水平变化；比较治疗前 GPC3 和 PIVKA-II与肝癌患者预后相关性。

结果: AFP 阴性肝癌患者血清中 GPC3 及 PIVKA-II的表达水平显著高于良性肝病患者和正常对照者，差异有统计学意义。在 AFP 阴性肝癌患者中，GPC3 和 PIVKA-II单项及组合的 ROC 曲线下面积分别为 0.792，0.928 和 0.862；GPC3 和 PIVKA-II单项及联合检测的敏感性分别为 77.2%、86.1%和 83.2%，特异性分别为 82.2%、93.1%和 83.3%。GPC3 及 PIVKA-II随着肿瘤分期的增高而增高，在I期肝癌中的敏感性高达 86.5%和 83.8%。GPC3 水平与 AFP 阴性肝癌患者年龄相关，PIVKA-II水平与 AFP 阴性肝癌患者门脉癌栓情况相关；肝癌患者术后 GPC3 及 PIVKA-II血清水平较术前明显减少。肝癌患者的生存时间与治疗前 GPC3 及 PIVKA-II的表达水平无关，与临床分期显著相关。

结论: GPC3 及 PIVKA-II检测对于 AFP 阴性肝癌尤其是I期肝癌有较高的诊断价值，可用于 AFP 阴性肝癌术后疗效监测。

关键字: GPC3；PIVKA-II；AFP；肝癌；诊断

179. G 试验在肿瘤患者侵袭性念珠菌感染中的临床价值

崔兆磊、陈燕*

福建省肿瘤医院

目的: 讨论 G 试验在恶性肿瘤患者侵袭性念珠菌(invasive candidiasis, IC) 感染中的临床早期诊断价值及其临床特征之间的关系。

方法: 选取福建省肿瘤医院 2019 年 1 月至 2020 年 12 月期间 64 例侵袭性念珠菌感染(invasive candidiasis, IC)患者、58 例念珠菌黏膜定植者，采用免疫比浊法分别检测两组 G 试验与 pct 浓度，分析 G 试验早期诊断恶性肿瘤患者 IC 的灵敏度、特异度、阳性预测值、阳性预测值等指标，以受试者工作特征（ROC）曲线评估 G 试验在恶性肿瘤患者 IC 早期诊断中的价值，并比较 G 试验阳性率与患者临床特征之间的关系，以及与 PCT 联合检测对肿瘤患者 IC 的诊断价值。结果用 SPSS 26.0 分析。

结果: IC 组 G 试验浓度与黏膜定植组相比显著增高；64 例 IC 组患者中，白念珠菌比例高于非白念珠菌；G 试验诊断总体灵敏度为 56.25%，特异度为 87.9%，阳性预测值为 85.71%，阴性预测值为 67.1%，阳性似然比为 4.648，阴性似然比为 0.498，约登指数为 0.44；G 试验 ROC 曲线下面积 AUC 为 0.628；IC 患者 G 试验阳性率与病原菌、粒细胞、体温、合并感染的情况、治疗方法等临床特征无关；G 试验与 PCT 联合检测的灵敏度及特异度（分别为 75%、65.31%）高于二者单独检测（$P<0.05$），但阴阳预测值并未明显改变。

结论: G 试验对于恶性肿瘤患者 IC 的早期诊断具有一定临床可用性，能区分定植和感染，但其在恶性肿瘤的患者临床应用价值准确性一般，实验室应优化检测方法，临床连续检测 G 试验以减少假阳性和假阴性的发生，提高 IC 诊断的准备性。

关键字: (1,3)-β-D-葡聚糖；PCT；侵袭性念珠菌病；肿瘤患者

180. 非编码 RNA 在食管癌转移机制中的研究进展

庄宇、邵丰*

南京市胸科医院

近年来，随着分子生物学研究技术的革新和转录组学的深入研究，非编码 RNA 的作用和生物学功能得到了进一步的探索，其在基因的转录、翻译、细胞分化、遗传及表观遗传等生命活动中具有重要的调控作用。目前，大量研究证实非编码 RNA 可在表观遗传学、转录水平、转录后水平等多个重要节点调控肿瘤的进展。越来越多的研究表明，非编码 RNA 与食管癌发生发展有关，如果能够通过研究发现与食管癌发生转移相关的非编码 RNA，从而指导食管癌的诊断与治疗，大大改善中晚期食管癌的预后，这将对我国的食管癌防治工作产生重大的影响。本文着重强调 miRNA、lncRNA 及 circRNA 在食管癌进展中主要生物学功能，并总结其在食管癌发生转移中的异常表达及其调控机制，以期为食管癌的诊断和治疗提供新思路和新方法。

关键字: 非编码 RNA ；食管癌； 转移机制；预后

181. Logistic 回归结合 ROC 曲线分析标志物模型在肝硬化合并肝癌患者中的诊断价值

崔兆磊、陈燕*

福建省肿瘤医院

目的：评价血清异常凝血酶原（PIVKA-II）、高尔基体蛋白 73（GP73）、甲胎蛋白（AFP）和甲胎蛋白异质体（AFP-L3）四种肝癌标志物不同检测模型在肝硬化合并肝癌患者中的诊断价值，建立最佳诊断模型。

方法：以治疗前 170 例肝硬化合并肝癌、60 例肝硬化、60 例慢性乙型肝炎患者和 60 例健康体检者为研究对象，检测 PIVKA-II（化学发光酶免疫检测法）、GP73（酶联免疫法）、AFP（电化学发光法）和 AFP-L3（微量离心柱法）的血清水平，建立单项检测的 ROC 曲线，确立各指标的最佳诊断临界值（cutoff 值）。使用 SPSS 做多变量观察值的 ROC 曲线，建立 Logistic 回归方程，评价多变量检测模型的诊断指标，确定最佳诊断模型。

结果：单项检测时，PIVKA-II的曲线下面积（AUCROC）最大（0.920），敏感性和特异性分别为 91.2%和 85.6%。多项联合检测时，PIVKA-II和 AFP 联合检测的多变量检测模型曲线下面积（AUCROC）最大（0.951），敏感性和特异性分别为 87.6%和 91.1%，为乙肝肝硬化合并肝癌的最佳诊断模型。最佳诊断模型的肝癌风险概率值在早期肝癌患者中的敏感性为 66.7%，在小肝癌的敏感性为 67.7%。

结论： PIVKA-II和 AFP 联合检测为乙肝肝硬化合并肝癌的最佳诊断模型，利用肝癌风险概率值可从乙肝肝硬化患者中及时诊断出早期肝癌和小肝癌，提高患者生存率。

关键字: 肝细胞癌；甲胎蛋白；异质体；异常凝血酶原；高尔基体蛋白

182. PIVKA-II 对肝癌患者疗效评价和预后评估的价值

崔兆磊、陈燕*

福建省肿瘤医院

目的：探讨异常凝血酶原（PIVKA-II）在肝癌患者疗效评价和预后评估中的应用价值。

方法：采集治疗前 163 例肝癌患者的血清，检测患者异常凝血酶原（PIVKA-II）和甲胎蛋白（AFP）浓度，探讨其对肝癌患者疗效评估的价值，采用卡方检验分析患者临床病理特征与 PIVKA-II 浓度的关系，采用 Kaplan-Meier 法计算总生存率及无进展生存率，单因素分析采用 Log-rank 法，多因素分析采用 Cox 回归模型。

结果：肝癌进展组 PIVKA-II、AFP 浓度显著高于缓解组，差异具有统计学意义（$p<0.05$）。PIVKA-II 高表达与 AFP、AST、ALT 有统计学意义（$\chi^2=13.664$，$P<0.001$；$\chi^2=4.013$，$P=0.045$；$\chi^2=5.504$，$P=0.019$）。随访 1-55 个月，163 例肝癌患者的 1 年总生存率为 57.67%，平均 OS 为 33.66 个月（95% CI：28.55~38.77）。3 年总生存率为 34.36%，平均 OS 为 23.76 个月（95% CI：19.24~28.28），中位 OS 为 16 个月（95% CI：9.39~22.61）。1 年无进展生存率为 38.04%，平均 PFS 为 26.61 个月（95%CI：21.93~31.3），中位 PFS 为 25 个月（95%CI：16.01~33.99）。单因素生存分析显示：肿瘤转移、血管侵犯、门脉癌栓、PIVKA-II、AFP、AST、ALT、ALB、TBIL、PT 对患者预后具有统计学意义（P 均<0.01）。Cox 回归模型多因素分析结果显示：PIVKA-II（$P=0.003$；HR=1.975，95%CI:1.269~3.073）、AFP（$P=0.028$；HR=1.663，95%CI:1.057~2.616）、TBIL（$P=0.042$；HR=1.530，95%CI:1.016~2.304）、血管侵犯（$P=0.002$；HR=2.523，95%CI:1.387~4.588）、肿瘤转移（$P=0.022$；HR=2.008，95%CI:1.107~3.642）、

门脉癌栓（*P=0.003*；HR=1.970，95%CI: 1.256~3.092）、PT（*P*=0.030；HR=1.636，95%CI: 1.050~2.551）对患者预后具有统计学意义。

结论：PIVKA-II、AFP 在肝癌中的表达水平，可成为预测肝癌患者发生发展及预后的分子标记物，对肝癌患者疗效评价和预后评估具有一定价值。

关键字：原发性肝癌；PIVKA-II；AFP；疗效评估；预后

183. SARI 蛋白在乳腺癌中的表达及其临床意义

崔兆磊、陈燕*

福建省肿瘤医院

目的：探讨 SARI 蛋白在乳腺癌中的表达及其临床意义。

方法：采用免疫组化技术检测 SARI 蛋白在乳腺癌及其癌旁组织中的表达，探讨 SARI 蛋白表达水平与乳腺癌的临床病理特征及预后的关系。

结果：基于高通量的乳腺癌组织芯片免疫组化分析显示，在 87 例乳腺癌石蜡标本中，93.1%（81/87）的组织中 SARI 蛋白低呈现低表达或不表达，其中 80 例（98.8%）SARI 无表达，1 例（1.2%）SARI 蛋白低表达，6 例(6.9%)BATF2 高表达。SARI 蛋白在乳腺癌组织及旁组织表达差异无相关性（*P*=0.950）。SARI 的表达水平与乳腺癌的临床病理分级密切相关（*P*=0.000），患者年龄是影响乳腺癌预后的独立因素（*P*=0.027）。

结论：SARI 蛋白在乳腺癌中存在低表达，可能发挥肿瘤抑癌因子的作用，其临床意义有待于进一步被证实。

关键字：乳腺癌；SARI；临床病理特征

184. SARI 过表达对 CNE2 鼻咽癌细胞生物学活性的影响及其机制研究

崔兆磊、陈燕*

福建省肿瘤医院

目的：构建 SARI 基因过表达真核表达载体并完成鉴定。研究 SARI 基因过表达对 CNE2 鼻咽癌细胞的生物学特性的影响并初步探讨相关分子机制。

方法：钓取并克隆 SARI 基因的全长 cDNA 序列，纯化后用 Bgl II 和 Xba I 进行双酶切消化，经 T_4 DNA 连接酶作用，连接至 pDsRed2-C-RFP 真核表达载体，连接产物经转化、挑取克隆、扩增培养后，提取小量质粒，进行 DNA 测序鉴定，并用 Bgl II 和 Xba I 内切酶消化酶消化连接产物，琼脂糖凝胶电泳鉴定。重组质粒转染 SARI 阴性表达的 CNE2 细胞，荧光显微镜观察 SARI-RFP 融合蛋白的表达。Western blot 检测转染后 SARI-RFP 融合蛋白的表达。pDsRed2-SARI-RFP 真核表达载体转染至 CNE2 细胞，通过 CCK-8 比色绘制生长曲线、Transwell 小室侵袭实验、划痕修复实验、Caspase-3 活性检测、DNA 片段电泳检测等实验，探讨 SARI 过表达对 CNE2 鼻咽癌细胞生长增殖、凋亡等生物学特性的影响。Western blot 检测内源性线粒体凋亡途径相关蛋白的表达变化，探讨 SARI 过表达对 CNE2 细胞增殖、凋亡影响的分子机制。

结果：DNA 测序结果表明，SARI 全长 cDNA 序列已正确连接至 pDsRed2-C-RFP 载体。双酶切鉴定结果显示，pDsRed2-SARI-RFP 真核表达载体的构建成功。重组质粒转染至 CNE2 细胞后可表达 SARI-RFP 融合蛋白。CCK-8 比色、Transwell 小室侵袭、划痕修复实验结果显示 SARI 过表达组细胞生长增殖、侵袭迁移能力显著低于空载体对照组和空白对照组（P ＜0.05）；Caspase-3 活性及 DNA 梯状电泳结果显示，SARI 过表达诱导 CNE2 细胞产生凋亡，明显高于空载体对照组和空白对照组（P ＜0.05）。Western blot 检测显示 SARI 过表达组 CNE2 细胞较空载体对照组和空白对照组 Bcl-2 表达下调，Bax、Cytochrome C 表达上调，同时伴有凋亡途径相关蛋白 Caspase-3 和 Caspase-9 剪接激活以及 PARP 的表达上调。

结论：成功构建 pDsRed2-SARI-RFP 真核表达载体； SARI 过表达可明显抑制鼻咽癌 CNE2 细胞增殖和侵袭迁移能力，诱导细胞凋亡； SARI 可能通过激活线粒体内源性凋亡途径诱导 CNE2 鼻咽癌细胞凋亡，发挥抑癌作用。

关键字：鼻咽癌；CNE2；SARI；过表达；凋亡；分子机制

185. 鼻咽癌不同患者血浆 EB 病毒 DNA 与肿瘤疗效关系探讨

崔兆磊、陈燕*

福建省肿瘤医院

目的：评价血浆 EBVDNA 在鼻咽癌筛查和早期诊断价值，探讨不同患者血浆 EBVDNA 含量与肿瘤疗效的关系。

方法：以 2017 年 1 月至 2017 年 12 月来福建省肿瘤医院就诊的鼻咽癌首诊患者为研究对象，按入组标准分为鼻咽癌首诊组 485 例和治疗组 238 例。用磁珠提取法结合实时荧光定量 PCR 测定研究对象的 EBVDNA 含量。建立 EBVDNA 检测数据库并分析首诊组患者治疗前血浆 EBVDNA 的诊断效能以及与 TNM 分期、临床分期的关系，治疗组患者在治疗过程中不同首诊血浆 EBVDNA 的下降速率和治疗后不同血浆 EBVDNA 与疗效的关系以及复发时的患者血浆 EBVDNA 变化趋势。

结果：485 例首诊患者的 ENDNA 扩增检出率为 93.6%，与健康体检者相比（5.2%），差异有统计学意义。EBDNA 诊断鼻咽癌的 ROC 曲线下面积为 0.964（0.951-0.977），敏感性为 93.6% ，特异性为 94.8% ，准确性为 88.4% ，阳性预测值 94.8%，阴性预测值为 93.6% 。患者治疗前血浆 EBVDNA 含量与 TNM 分期和临床分期正相关，TNM 及临床分期早期的患者 EBDNA 含量显著低于中晚期，首诊血浆 EBVDNA 含量>10000copies/ml 的患者通过三次放化疗的下降为 0 的病例百分比显著低于血浆 EBVDNA≤10000copies/ml 患者，差异有统计学意义。复发患者血浆 EBVDNA 呈上涨趋势。EBDNA 的复发检出率为 90%。首诊 EBVDNA 含量为 0~200copies/ml 的复发患者甚至在治疗过程中可持续检测到低含量的 EBDNA。

结论：血浆 EBVDNA 含量检测有助于鼻咽癌的筛查和早期诊断，首诊患者血浆 EBVDNA 含量越高，分期越晚。治疗过程中 EBVDNA 含量变化可反映治疗效果，治疗后 EBVDNA 含量持续复制或上升患者有较高的复发风险。

关键字：鼻咽癌；EB 病毒；疗效

186. 鼻咽癌患者鼻咽溃疡医院感染及临床分析

崔兆磊、陈燕*

福建省肿瘤医院

目的：调查分析鼻咽癌患者放疗过程中鼻咽溃疡发生医院感染的菌种分布、耐药性及其临床特征，总结临床经验，为医院感染的预防工作提供理论依据。

方法：随机选取医院 184 例鼻咽癌发生鼻咽溃疡的住院患者作为研究对象，通过对临床资料的回顾性分析，研究患者医院感染的临床特征与病原菌类型。

结果：184 例鼻咽癌鼻咽溃疡的住院患者中有 64 例发生医院感染，感染率高达 37%，共检出病原体 90 株 ，以肺炎克雷伯菌（26.9），铜绿假单胞菌（19.2%），金黄色葡萄球菌（15.4）为主，真菌比例较低。鼻咽癌患者行放化疗过程中鼻咽腔黏膜发生发射性反应 ，形成鼻咽溃疡，易造成医院感染 。肿瘤分期晚，肿瘤体积大，激素类药物的应用并发感染的概率高。发生医院感染的危险因素包括住院时间、鼻咽黏膜完整性、体内白细胞水平、抗菌药物。

结论：为预防医院感染，鼻咽癌患者在行放化疗时，应积极关注其鼻咽黏膜完整性，预防性保护，及时送检分泌物标本，合理用药。

关键字：鼻咽癌；鼻咽溃疡；感染

187. 红细胞冷凝集对血常规多项参数结果的影响分析

崔兆磊、陈燕*

福建省肿瘤医院

目的：研究红细胞冷凝集对血细胞分析各项检测参数检测结果的影响及处理办法。

方法：选取本院 2017 年 12 月—2018 年 3 月冷凝集标本 83 例，用 SysmexXN-9000 全自动血细胞分析仪检测 37℃水浴前、后的红细胞计数（RBC）、血细胞比容（Hct）、红细胞平均容积（MCV）、红细胞平均血红蛋白含量（MCH）、血红蛋白浓度（Hb）、红细胞平均血红蛋白浓度（MCHC）、白细胞计数（WBC）、血小板计数（PLT）等参数，再进行结果比较

结果：RBC、HCT、MCV、MCH、MCHC 的结果水浴前后对比差异有统计学意义（$P<0.05$），而 Hb、WBC 和 PLT 水浴前后结果无统计学意义($P<0.05$)。

结论：冷凝集标本会引起血细胞分析过程中多项参数检测结果严重失真并出现直方图、散点图异常及仪器报警提示。因此，在血细胞分析检测时应保证实验室温度，检验人员应加强质量控制，仔细审核分析检验结果，及时发现冷凝集标本，立即进行 37℃水浴 30min 后，即刻上机检测。同时应注意运送过程中的保温，对标本及检验试剂和用具作适当的加温处理，有助于解除标本凝集，从而使血常规各参数的检测结果得到校正。

关键字：冷凝集；血常规；水浴

188. 肌钙蛋白 T 和 N 端 B 型脑利钠肽前体对乳腺癌患者蒽环类药物序贯曲妥珠单抗治疗致心脏毒性的预测价值

崔兆磊、陈燕*

福建省肿瘤医院

目的：探讨 cTnT 与 NT-ProBNPHER2 阳性乳腺癌患者接受蒽环类药物序贯曲妥珠单抗治疗所致的心脏毒性的预测价值。

方法：选取 2018 年 1 月-2021 年 3 月福建省肿瘤医院治疗的 70 例乳腺癌患者，按照发生心脏毒性和未发生心脏毒性分为两组，比较两组在基线期临床病理参数的差异；比较两组 cTnT 与 NT-proBNP 水平在基线和终点的动态变化，ROC 曲线分析 cTnT 与 NT-proBNP 对心脏毒性的诊断价值；将 cTnT 与 NT-proBNP 纳入 COX 回归分析，评估两生物标志物对心脏毒性的预测价值。

结果：两组在基线时期高血压、高血脂发生率、ER、PR 阳性率无明显统计学差异（$P>0.05$），心脏毒性组基线高尿酸血症发生率高于非心脏毒性组，差异有统计学意义（$p<0.05$）；在基线时两组 cTnT 与 NT-proBNP 差异均无统计学意义（$P>0.05$）。然而在终点时间时，发生心脏毒性组 cTnT 与 NT-proBNP 水平明显高于未发生心脏毒性组，差异具有显著统计学差异（$P<0.01$）；ROX 曲线分析 cTnT 与 NT-ProBNP 诊断心脏毒性的曲线下面积分别为 0.883 和 0.892，最佳诊断阈值分别为 8.66 和 194.30；COX 回归分析提示患者 cTnT 与 NT-proBNP 对心脏毒性具有一定的预测价值，cTnT 与 NT-proBNP 任一指标高于阈值者发生心脏毒性的风险是两指标均正常者的其发生心脏毒性的可能性是 cTnT 和（或）NT-ProBNP 没有超过阈值者的 17.94 倍（HR=17.94）。

结论：cTnT 与 NT-proBNP 可以作为 HER2 阳性乳腺癌患者接受蒽环类药物序贯曲妥珠单抗治疗导致心脏毒性的预测指标。

关键字：乳腺癌；心脏毒性；肌钙蛋白 T；N 端脑钠肽前体

189. 基于 CRISPR/Cas9 系统靶向敲减 miR-21 对鼻咽癌放疗抵抗的影响

崔兆磊、陈燕*

福建省肿瘤医院

目的：本研究拟通过 CRISPR/Cas9 系统靶向敲减 CNE2 细胞中的 miR-21，评估对 CNE2 细胞生物学特性的影响并探讨分子机制。

方法：通过 CRISPR/Cas9 系统对放疗抗拒的 CNE2-R 和正常 CNE2 鼻咽癌细胞株进行内源性 miR-21 基因敲除，通过 T7EN1 酶切和 Real-time PCR 验证敲除效果。通过设置体外相关实验，探讨 miR-21 基因敲除对 CNE2-R 和正常 CNE2 细胞增殖状态、克隆形成、凋亡状态等生物学特性的影响，进行放疗敏感性及侵袭能力的比较。通过生物信息学分析预测 miR-21 在鼻咽癌中参与调控的信号通路，免疫印迹进一步验证。

结果：CRISPR/Cas9 载体系统可有效敲减对 CNE2-R 和 CNE2 细胞系中内源性 miR-21 基因，编辑效率接近 50%。miR-21 靶向敲减可明显抑制 CNE2-R 和 CNE2 细胞的生长增殖，克隆形成及侵袭转移等能力，并诱导细胞凋亡。生物信息学分析共找到 28 个 KEGG，并筛选出共同交集的通路。免疫印迹显示，miR-21 敲减组 PI3K/AKT/mTOR 通路相关蛋白及其磷酸化水平发生明显改变。Meta 分析结果显示，miR-21 联合其他 miRNA 分子表达谱在诊断鼻咽癌中的灵敏度、特异度及曲线下面积（AUC）分别为 0.78、0.79 和 0.85。本项目研究结果证实，内源性 miR-21 与 CNE2-R 细胞的放疗抗拒有关，靶向敲减 miR-21 可通过阻断 PI3K/AKT/mTOR 信号通路来抑制 CNE2-R 和 CNE2 细胞的生长增殖，诱导细胞凋亡，从而增加放疗的敏感性。

结论：靶向敲减 miR-21 可通过抑制 PI3K/AKT/mTOR 信号通路抑制 CNE2-R 和 CNE2 细胞的生长增殖，诱导细胞凋亡，增加放疗的敏感性。

关键字：CRISPR/Cas9；miR-21；鼻咽癌；放疗抵抗；机制

190. 降钙素原在非霍奇金淋巴瘤患者伴感染中的诊断价值

崔兆磊、陈燕*

福建省肿瘤医院

目的：分析降钙素原(Procalcitonin，PCT)在非霍奇金淋巴瘤（NHL）患者中的影响因素、评估感染诊断价值，探讨其在临床中的合理应用。

方法： 收集 2017 年 1 月 1 日至 2020 年 12 月 31 日入住福建省肿瘤医院 736 例 NHL 患者病例，根据临床特点划分感染组与非感染组，并对两组患者的血清 PCT 水平进行比较；分析 NHL 非感染组基础血清 PCT 水平与肿瘤病理分型、肿瘤分期、肿瘤进程以及中性粒细胞数等影响因素，并进行多因素及独立影响因素分析；分析 80 例 NHL 患者在基础状态、感染状态、有效抗感染治疗后的三个阶段血清 PCT 检测值；分析感染组血清 PCT 水平与感染部位和致病菌类型之间关系。

结果：血清 PCT 水平在组织病理学类型、IPI 评分（0-2 与 3-4 分）、肿瘤分期、肿瘤进展和性别等方面有明显差异（$p<0.05$），与患者年龄无显著性差异（$P>0.05$），肿瘤转移和肿瘤进展是非感染 NHL 患者血清 PCT 水平升高的独立影响因素。I-III 与 IV 期比较，血清 PCT 诊断肿瘤 IV 期转移的 ROC 曲线下面积为 0.6532，最佳临界值为 0.065ng/mL，敏感度、特异性分别为 61.1%、59.9%，阳性预测值、阴性预测值分别为 56.3%、64.6%。血清 PCT 诊断感染 ROC 曲线下面积为 0.7885，最佳临界值为 0.120ng/mL，敏感度、特异性分别为 54.9%、89%，阳性预测值、阴性预测值分别为 65.6%、83.8%；在 80 例 NHL 患者中，其基础值、抗感染有效治疗后与感染阶段比较，血清 PCT 水平统计学均具有显著差异（$P<0.001$）。血清 PCT 水平在血流感染和局部感染之间统计学有显著差异（$P<0.001$）；在血流感染中血清 PCT 水平在 G+和 G-之间统计学存在差异（$P=0.012$，<0.05），凝固酶阴性葡萄球菌（coagulase-negative staphylococcus，CNS）血流感染组与污染组的血清 PCT 水平差异具有统计学意义（$P=0.007$，<0.05），诊断 CNS 感染的 ROC 曲线下面积为 0.7143，最佳临界值为 0.165ng/mL，患者 PCT 诊断指标敏感度、特异性、阳性预测值、阴性预测值分别为 60%、85.71%、75%、60%。

结论：血清 PCT 水平有望作为诊断 NHL 患者是否转移的参考指标；可作为 NHL 伴感染诊断和抗感染治疗监测指标，诊断感染 cut-off 值为 0.12ng/mL；同时对区分 NHL 患者血流感

染与局部感染、区分血流感染 G+与 G-菌、血浆 CNS 血流感染与污染具有一定价值；建议 NHL 患者入院进行常规 PCT 检查，建立患者的 PCT 基础值，作为后续感染诊断对照。

关键字：降钙素原；非霍奇金淋巴瘤；影响因素；感染

191. 卵巢癌患者血小板参数的变化情况分析

崔兆磊、陈燕*

福建省肿瘤医院

目的：探讨血小板七项参数 PLT、PDW、MPV、PCT、P-LCR、PNR 、PLR 在卵巢癌患者化疗前后的变化。

方法：收集在福建省肿瘤医院诊断为卵巢癌的患者、卵巢癌后进行化疗的患者以及体检人员的临床资料。通过各类检验方法回顾性分析各组间血小板七项参数的差异性。

结果：PLT、MPV、P-LCR 的临界值分别为 225.000、9.750、22.550 时，对卵巢癌的临床分期具有一定的预测价值。PLT、PCT、PLR 的临界值分别 312.500、0.265、179.935 时，对卵巢癌的诊断具有一定的预测价值。卵巢癌患者 PLT、PCT、PLR 较体检组的高，接受化疗后 PLT、PCT、PLR 显著低于化疗前。血小板参数受不同病理类型，肿瘤直径、不同年龄段等的影响并不大。

结论：血小板的各项参数(PLT、PCT、PLR)在卵巢癌的诊断以及分期，化疗效果等方面可以起到判断预测效果，各项差异有统计学意义。

关键字：血小板参数；卵巢癌患者；化疗前后

192. 乳酸脱氢酶 C4 在骨肉瘤中的表达与生物学功能研究

崔兆磊、陈燕*

福建省肿瘤医院

目的：通过分析乳酸脱氢酶 C4（LDH-C4）在骨肉瘤（OS）组织中的表达情况，探讨其表达水平与骨肉瘤患者临床病理资料之间的相关性，明确 LDH-C4 表达上调后对骨肉瘤细胞 MG63 生物学行为能力的影响及相关分子机制。

方法：采用免疫组织化学染色方法对高通量骨肉瘤组织芯片进行检测，分析骨肉瘤组织中 LDH-C4 蛋白的表达水平与骨肉瘤患者临床病理特征的相关性。构建 LDHC 慢病毒过表达载体并感染骨肉瘤细胞 MG63，采用不同感染复数（MOI）和嘌呤霉素浓度筛选稳定感染的 MG63 细胞系。采用 RT-PCR 方法检测各组骨肉瘤细胞蛋白和 LDHC mRNA 表达情况。通过 CCK-8 实验、平板克隆形成实验、划痕修复实验以及 Transwell 细胞迁移、侵袭实验，检测上调 LDH-C4 后对骨肉瘤细胞 MG63 增殖和迁移侵袭等能力的影响。通过比色法检测乳酸和丙酮酸表达水平,葡萄糖氧化酶法检测葡萄糖消耗量。通过 Western blot，分析 LDH-C4 过表达对 AKT/mTOR 信号转导通路相关蛋白表达的影响。

结果：LDH-C4 蛋白主要表达于骨肉瘤细胞的细胞质中，软骨肉瘤表达在细胞核中，低表达/阴性表达占 54.29%（38/70），相关性分析结果显示，在骨肉瘤患者中临床分期和肿块直径与 LDH-C4 的表达水平呈负相关关系（$p<0.05$）。过表达 LDH-C4 在 CCK-8 实验、平板克隆实验、细胞划痕实验和 Transwell 小室迁移侵袭实验显示感染组 MG63 细胞的增殖能力、克隆能力、迁移能力和侵袭能力可被明显抑制。3.能量代谢实验结果显示感染组骨肉瘤细胞 MG63 葡萄糖摄取率降低，乳酸生成减少，丙酮酸生成增多。Western blot 实验发现过表达 LDH-C4 后，下调了感染组 PI3K、AKT、mTOR 蛋白表达，HIF-1α蛋白无明显变化。

结论：在骨肉瘤组织中 LDH-C4 为中低表达状态，并与骨肉瘤患者临床分期及瘤体直径相关。上调 LDH-C4 可明显降低 MG63 骨肉瘤细胞体外的生长增殖、克隆形成以及侵袭和迁移能力。LDHC 过表达抑制细胞正常氧化耗能，通过抑制糖酵解和负向调控 PI3K/AKT/mTOR 信号通路发挥其生物学功能。

关键字：骨肉瘤；乳酸脱氢酶 C4；过表达；分子机制

193. 乳酸脱氢酶 C4 在乳腺癌中的表达及临床意义

崔兆磊、陈燕*

福建省肿瘤医院

目的：检测 LDH-C4 在乳腺癌中的表达，明确其表达阳性率，分析 LDH-C4 表达与乳腺癌临床病理特征和预后的关系。

方法：基于高通量乳腺癌组织芯片 HBre-Duc140Su02，通过免疫组化技术检测 LDH-C4 蛋白在乳腺癌细胞中的表达水平。基于 HBreD145Su02 高通量组织芯片已建立的临床资料和随访

数据库，分析 LDH-C4 表达与肿瘤组织分化程度、淋巴结转移、肿瘤大小、临床分期等临床病理特征的关系，应用 Kaplan–Meier 法绘制生存曲线，估计生存率，分析 LDH-C4 表达与乳腺癌预后的关系。采用 COX 比例风险模型进行多因素风险分析。

结果：LDH-C4 在乳腺癌细胞中的表达率为 91.5%，其阳性表达与患者年龄、肿瘤大小、临床分期、病理分级、淋巴结是否转移均无关（*P* 均>0.05），LDH-C4 阳性患者的十年生存率显著低于 LDH-C4 阴性表达患者（$p<0.05$）。

结论：LDH-C4 表达与乳腺癌预后相关，可作为乳腺癌预后判断的一项重要指标。

关键字：乳酸脱氢酶 C4；乳腺癌；预后

194. 乳酸脱氢酶 C4 在乳腺癌中的表达及其对乳腺癌细胞生物学功能的影响

崔兆磊、陈燕*

福建省肿瘤医院

目的：研究乳酸脱氢酶 C4（LDH-C4）在乳腺癌组织中的表达，探讨 LDH-C4 对乳腺癌预后判断的价值；探讨 LDH-C4 表达上调对 MCF-7 乳腺癌细胞中的生物学影响及分子机制。

方法：通过免疫组织化学分析 158 例乳腺癌石蜡组织中 LDH-C4 蛋白在的表达情况。分析乳腺癌不同临床病理参数与 LDH-C4 蛋白表达的相关性。对随访资料进行 Cox 回归模型，研究 LDH-C4 蛋白在乳腺癌预后判断的临床价值。通过慢病毒载体将外源 LDHC 基因导入 MCF-7 乳腺癌细胞中，通过稀释法结合绿荧光蛋白表达筛选 LDH-C4 阳性表达的单克隆细胞系。通过平板克隆、CCK-8 细胞增殖、细胞划痕、Transwell 小室等细胞生物学实验，研究 LDH-C4 表达上调对 MCF-7 细胞生物学行为的影响；Western blot 法检测 PI3K/AKT/mTOR 信号通路相关分子，探讨 LDHC 基因上调对乳腺癌 MCF-7 细胞生物学影响的可能机制。

结果：158 例乳腺癌石蜡组织切片免疫组化染色，LDH-C4 蛋白染色集中在细胞质中，呈淡棕色到深棕色，阳性率为 91.8%（145/158），其中低表达（-/+）和高表达（++/+++）分别为 41.8%（66/158）、58.2%（92/158）。经卡方检验，乳腺癌临床分期晚、腋窝淋巴结转移率高，患病年龄低者 LDH-C4 呈高表达（$p<0.05$）；Kaplan-Meier 法进行生存分析并经 Log-rank 检验结果显示，乳腺癌 LDH-C4 高表达者预后差（*P*=0.035）；Cox 回归分析显示临床分期（*P*=0.000）和 LDH-C4 表达水平（*P*=0.002）是乳腺癌预后的独立因素。2. 通过慢病毒感

染成功筛选 LDH-C4 过表达的单克隆化的乳腺癌 MCF-7 细胞系；细胞学实验结果显示，LDH-C4 蛋白过表达可增强乳腺癌 MCF-7 侵袭和迁移能力，而对细胞生长增殖无显著影响；免疫印迹法初步显示，过表达 LDH-C4 蛋白可上调乳腺癌 MCF-7 细胞中 AKT 和 mTOR 蛋白的表达。

结论：LDH-C4 在乳腺癌组织中具有很高的表达阳性率，其表达与临床分期、腋窝淋巴结转移相关；高 LDH-C4 蛋白水平预示乳腺癌不良预后。过表达 LDH-C4 可增强 MCF-7 细胞增殖、侵袭和迁移能力，其机制可能与 AKT/mTOR 细胞信号通路的激活有关。

关键字：乳腺癌，LDH-C4，预后，MCF-7

195. 乳腺癌合并甲状腺癌患者的临床病理特征分析

崔兆磊、陈燕*

福建省肿瘤医院

目的：通过分析乳腺癌合并甲状腺癌的临床病理特征，探讨甲状腺癌、甲状腺激素功能及甲状腺相关抗原抗体在乳腺癌发生发展的作用。

方法：回顾性分析福建省肿瘤医院 2001 年 1 月-2017 年 12 月期间收治的乳腺癌合并甲状腺癌患者 76 例（合并癌组），并随机收集同期收治的单纯乳腺癌患者（对照组）116 例，同时收集患者治疗前甲状腺激素（T3、T4、FT3、FT4、TSH）、甲状腺自身抗原和抗体（TG 、TPOAb、TGAb)、临床病理（TNM 分期、临床分期、淋巴转移、原发结节大小）和乳腺癌免疫组化指标（ER、PR、HER-2、Ki-67）等；通过 SPSS 25.0 软件统计分析合并癌组和对照组各临床病理和免疫组化指标，进一步探讨甲状腺癌在乳腺癌发生发展中的作用。

结果：合并癌组的淋巴受累率高于对照组（60.9% *VS.* 37.7%），具有统计学差异（$p<0.05$）；甲状腺的功能状态：合并癌组与对照组 T3（1.74 *VS.* 1.68）和 TSH（2.19 *VS.* 10.27）具有统计学差异（$p<0.05$）；甲状腺相关抗原抗体：合并癌组与对照组 TPOAb（3.693 *VS.* 12.3) 和 TG（10.71 *VS.* 2.77）的表达水平具有统计学差异（$p<0.05$）；其他病理特征：合并癌组与对照组在 ER、PR、HER-2、Ki-67 和 TNM 分期等免疫组化和病理特征上不具有统计学意义（$p>0.05$）。

结论：乳腺癌合并甲状腺癌组的淋巴受累率明显高于对照组（60.9% *VS.* 37.7%）；同时发现乳腺癌合并甲状腺癌组 T3 和 TG 表达水平高于对照组，TSH 和 TPOAb 表达水平低于对照

组，提示甲状腺癌在乳腺癌的发生发展中起作用，其机制可能与 T3 和 TG 的升高和 TSH 和 TPOAb 降低有关。

关键字：乳腺癌；甲状腺癌；甲状腺激素

196. 探讨妇科恶性肿瘤患者局部感染及围手术期预防用药选择

崔兆磊、陈燕*

福建省肿瘤医院

目的：分析我院妇科恶性肿瘤患者宫颈非厌氧菌感染菌种分布及耐药性，为多重耐药菌管理提供依据，探讨妇科恶性肿瘤患者围手术期预防用药的选择。

方法：回顾性分析 2016-2017 年 482 例妇科恶性肿瘤患者感染情况，并收集临床分离株，采用 K-B 纸片扩散法结合 VITEK II MIC 法进行病原菌药敏试验，按照美国临床实验室标准化委员会（CLSI）标准判断结果，采用 WHONET5.5 进行统计。

结果：宫颈部位发生感染率为 59.43%，其中大肠埃希菌检出率占据首位，构成比为 64.9%，其次是粪肠球菌、肺炎克雷伯菌、铜绿假单胞菌，前四位构成比合计高达 91.50%。大肠埃希菌和肺炎克雷伯菌对头孢唑啉、头孢呋辛、头孢曲松耐药率均高于 50%，两者产超广谱 β-内酰胺酶（ESBL）菌检出率分别为 62.47%和 41.94%。肠球菌对红霉素耐药率为 88.37%，对环丙沙星和左旋氧氟沙星耐药率高于 30%，屎肠球菌对多数抗菌药物耐药率均保持较高水平，金黄色葡萄球菌耐药率相对较低，本实验室未检出耐碳青霉烯类的肠杆菌科细菌和耐万古霉素及利奈唑烷的阳性球菌。

结论：妇科恶性肿瘤患者宫颈感染率较高，且耐药现象严重，需加强多重耐药菌管理及防治。妇科恶性肿瘤患者宫颈感染主要病原菌为大肠埃希菌、粪肠球菌、肺炎克雷伯菌、铜绿假单胞菌，其对第一、二代头孢菌素、头孢曲松及头孢噻肟耐药率高，是否可应用其他抗菌药物作为妇科恶性肿瘤围手术期预防用药值得探讨。

关键字：妇科恶性肿瘤；用药；感染

197. 丝切蛋白-1、磷酸化丝切蛋白-1、CD11c 与鼻咽癌的临床相关性研究

曾林梅[1]、龙金华*[2]、金风[2]、吴伟莉[2]、李媛媛[2]、罗秀玲[2]、贺晓燕[2]、杨勇[2]、李娟[2]、龙萃[2]

1. 贵州医科大学附属肿瘤医院

2. 贵州医科大学附属肿瘤医院

目的：研究丝切蛋白 1（cofilin-1）、磷酸化丝切蛋白 1（P-cofilin-1）及树突状细胞（dendritic cells, DCs）亚群在鼻咽癌（nasopharyngeal carcinoma，NPC）病理组织中的表达情况，并深入探讨其表达状况与鼻咽癌临床预后之间的相关性。

方法：采用回顾性分析方法，纳入了 97 例 NPC 患者，免疫组化检测治疗前鼻咽部病理组织中的 cofilin-1、P-cofilin-1 及 CD11c+DCs 的表达情况。观察生存情况，采用 SPSS 24.0 统计学分析软件包进行统计学处理与分析。

结果：cofilin-1 的表达与 NPC 治疗前的 M 分期、UICC 总分期、治疗后转移、骨转移及无远处转移生存期（Distant Metastasis-Free Survival，DMFS）之间差异有统计学意义（$p<0.05$），而与其他临床特征差异无统计学意义（$P>0.05$）。P-cofilin-1 的表达与 NPC 治疗后转移、骨转移及 DMFS 之间差异有统计学意义（$p<0.05$），而与其他临床特征差异无统计学意义（$P>0.05$）。CD11c 的表达与 NPC 患者的总生存期（Overall survival time，OS）之间差异有统计学意义（$p<0.05$），而与 DMFS 及其他临床特征差异无统计学意义（$P>0.05$）。

结论：NPC 患者的病理切片中 cofilin-1、P-cofilin-1、CD11c 均有表达；cofilin-1 的表达越高肿瘤细胞发生转移的的风险越高，相反 P-cofilin-1 的表达越高肿瘤细胞发生转移的风险越低；CD11c 表达越高总生存时间越长。cofilin-1、P-cofilin-1、CD11c 可能是 NPC 患者生存及预后的生物标志物。

关键字：鼻咽癌；丝切蛋白-1；磷酸化丝切蛋白-1；树突状细胞亚群

198. 血浆热休克蛋白 90α和 EBV DNA 定量检测对鼻咽癌的诊断和预后评价

崔兆磊、陈燕*

福建省肿瘤医院

目的: 检测鼻咽癌患者血浆中 HSP90α和 EBV DNA 治疗前、后及健康人中的表达情况，探讨其在鼻咽癌诊断与临床病理特征关系以及疗效评价和预后评估中的作用。

方法: 应用定量酶联免疫吸附法和实时定量 PCR 方法检测 92 例初治鼻咽癌患者治疗前后、放化疗后转移或复发以及持续缓解鼻咽癌患者血浆中 HSP90α和 EBV DNA 的表达情况，并以 30 名健康体检者为对照。

结果: 血浆中 HSP90α水平为 87.28ng/ml 诊断鼻咽癌的敏感度为 92.1%，特异度为 86.0%。血浆 EB DNA 中位拷贝数为 4900/ml 对初诊鼻咽癌患者的诊断敏感性为 89.0%，特异性为 92.0%。92 例鼻咽癌患者经过治疗后均达到完全缓解或者部分缓解。鼻咽癌患者治疗前血浆中 HSP90α和 EBV DNA 水平显著高于治疗后和健康对照者。血浆中 HSP90α与鼻咽癌临床分期相关，与性别、年龄、病理分型（T、N）无关(P>0.05)，治疗后完全缓解患者降至健康对照者水平。部分缓解患者仍高于健康对照者水平，而完全缓解与部分缓解患者的治疗后血浆 HSP90α降至健康对照者水平。在半年内远处转移的患者治疗后血浆中 HSP90α和 EBV DNA 水平均明显高于未发生远处转移患者和健康对照者。血浆中 HSP90α和 EBV-DNA 表达之间存在相关性。

结论： 血浆 HSP90α水平作为辅助诊断鼻咽癌的指标有一定的临床意义。血浆中 HSP90α与 EBV-DNA 检测有助于判断鼻咽癌的诊断、病情监测和预后评估具有重要价值。

关键字: 鼻咽癌；HSP90；EBV DNA；实时定量 PCR；预后；诊断

199. 血清 miRNA-223 在非小细胞肺癌化疗疗效监测中应用

崔兆磊、陈燕*

福建省肿瘤医院

目的: 探讨 microRNA-223（miRNA-223, miR-223）作为非小细胞肺癌（NSCLC）晚期（III-IV 期）患者化疗疗效评价指标的可行性。

方法：收集 14 例非小细胞肺癌晚期患者化疗前及化疗第一周期后血清，提取总 RNA 后采用实时荧光定量 PCR 方法检测血清 miRNA-223 水平变化，计算各个患者化疗第一周期后相对化疗前的变化量，并依据临床对患者疗效进行的化疗疗效评估（RECIST），将 14 例样本分为疾病进展（PD, progressive disease）组、疾病稳定(SD, stable disease) 组、部分缓解(PR, partial response)组，比较三组患者化疗第一周期后血清 miR-223 变化量，探讨不同组别血清 miR-223 作为 NSCLC 患者化疗疗效评估指标的可行性。

结果：数据统计显示，miRNA-223 在 PR 组中化疗后表达水平低于化疗前的水平，其相对表达含量为 0.70±0.32，在 SD 组中化疗后相对表达含量为 1.18±0.34，在 PD 组中化疗前后相对表达含量最高，为 2.84±0.87。化疗后 miR-223 相对化疗前的表达水平与患者年龄(u=23.00, *P*=0.848)、性别(u=10.00, *P*=0.157)、TNM 分期（u=20.00, *P*=1.000）差异无统计学意义。PR、SD、PD 组间 miR-223 化疗后水平呈趋势性变化，差异具有统计学意义（χ^2=8.9, *P*=0.012）。

结论：血清 miR-223 在化疗一个周期后的变化水平能较好预示 NSCLC 患者的化疗疗效，提示血清 miR-223 可作为 NSCLC 患者化疗疗效评价指标之一，对于实现肺癌个性化治疗有着重要的临床意义。

关键字：微小核糖核酸 223；非小细胞肺癌；早期疗效监测；实时定量聚合酶链反应

200. 血清多指标联合检测对肺癌的诊断价值

崔兆磊、陈燕*

福建省肿瘤医院

目的：探讨血清中癌胚抗原（CEA）、特异性烯醇化酶(NSE)、胃泌素释放肽前体(Pro-GRP)、细胞角蛋白 19 片段(CYFRA21-1)、鳞状细胞癌抗原（SCC）和胱抑素 C(Cys C)联合检测对肺癌诊断的价值。

方法：将研究对象分为健康对照组（医院体检者）和肺癌患者组（初次确诊肺癌患者），分别收集他们的 CEA、NSE、CYFRA21-1、Pro-GRP、SCC 及 Cys C 数据，进行比较；进而分析 CEA、NSE、CYFRA21-1、Pro-GRP、SCC 及 Cys C 单独检测和联合检测的检验效能，从不同类型的患者和疾病的不同阶段分析它们在肺癌中的诊断价值，结合 ROC 曲线，从而选出最优的肿瘤标志物组合，提高临床对肺癌的检出率。

结果：CEA、NSE、CYFRA21-1、Pro-GRP、SCC 及 Cys C 在年龄、性别表达上无显著差异。通过单因素方差分析，得出 CEA、CYFRA21-1、NSE、Pro-GRP 在 T1 期到 T4 期间，表达水平依次递增；CYFRA21-1 与 NSE 在 TNM 期中I期到IV期，表达水平递增；CYFRA21-1 在鳞癌中，表达水平高于另外两种癌症；Pro-GRP 在小细胞癌的表达水平最高；SCC 随着肿瘤增大和淋巴转移其表达水平上升；Cys C 随着肿瘤增大表达水平上升，随着肿瘤多处转移减小。通过对数据进行相应 t 检验和卡方检验，得出正常组和健康对照组的差异是有统计学意义的。通过绘制 ROC 曲线，得出联合检测是可以提高诊断率的。其中两两联合检测中 Pro-GRP+SCC 高达 0.905，CEA+NSE 高达 0.976，明显比单独检测敏感度高。通过相关性分析，得出 CEA 与 CYFRA21-1、NSE 之间有相关性，Pro-GRP 与 NSE 之间有相关性，其余各项之间是可以起互补的作用。

结论：CEA、NSE、CYFRA21-1、Pro-GRP、SCC 及 Cys C 在肿瘤不同分期、癌症种类、肿瘤大小和肿瘤转移中表达水平存在差异；并且这些指标的联合检测是可以提高肺癌早期的辅助诊断率；肺癌表达 Cys C 水平和正常人表达的水平具有一定差异。

关键字：肺癌；血清标志物；联合检测

201. 应用四项新型凝血指标评估妇科肿瘤手术患者的凝血功能

崔兆磊、陈燕*

福建省肿瘤医院

目的：检测妇科肿瘤患者手术前、后凝血及纤溶分子标志物的变化及探讨其临床意义。

方法：以 55 例健康体检者为对照组，92 例妇科肿瘤患者为研究组（良性肿瘤组 38 例、恶性肿瘤 54 例）。研究组于术前、术后 1d、3 d、5 d、7 d 分别采血，采用高敏化学发光免疫分析方法检测上述标本中凝血酶-抗凝血酶复合物（TAT）、纤溶酶-α2-抗纤溶酶复合物（PIC）、组织型纤溶酶原激活剂及其抑制剂-1 复合物（tPAI·C）、血栓调节蛋白（TM）的表达水平。

结果：恶性肿瘤组术前的四项指标水平均较健康对照组及良性肿瘤组升高（p<0.05），良性肿瘤组术前仅 TAT 及 TM 水平高于健康对照组（p<0.05）；恶性肿瘤组术后 1d、3d、5d 的 PIC 及 TAT 水平均高于术前（p<0.05），tPAI·C 仅在术后第 1d 较术前高（p<0.05），但 TM 水平术前术后无差异（P>0.05），但均高于正常组；良性肿瘤组术后四项指标仅在术后第一

天短暂性的升高，术后 3d 即恢复至术前水平或者正常水平。除了术后第一天的 TM，恶性肿瘤组 tPAI·C、TM、TAT、PIC 表达均明显高于同一时期的良性肿瘤组。

结论：妇科恶性肿瘤患者机体内存在着明显的凝血与纤溶系统功能的异常，TAT、PIC、t-PAI-C、TM 等指标的动态检测和分析有利于血栓前状态的判断，对预警血栓形成具有重要意义。

关键字：妇科肿瘤；凝血及纤溶系统标志物 凝血酶-抗凝血酶复合物/TAT、纤溶酶-抗纤溶酶复合物/PIC；组织型纤溶酶原激活抑制复合物/tPAI·C；血栓调节蛋白/TM

202. 双氢青蒿素对 HepG-2 细胞的影响

杨韬、王涛、苏海翔*

甘肃省医学科学研究院/甘肃省肿瘤医院

目的：研究双氢青蒿素(dihydroartemisinin，DHA)对人肝癌 HepG-2 细胞凋亡及自噬的影响。

方法：采用不同浓度(0、2.5、5、10、20、40、80、160、320 μmol·L－1) DHA 作用于 HepG-2 细胞 24h、48h、72h 后，CCK-8 法检测 DHA 对细胞增殖的影响，计算 DHA 对 HepG-2 细胞的半抑制浓度 (Half maximal inhibitory concentration，IC50)，并于显微镜下观察细胞变化。Chou-Talalay 法分析 DHA 与索拉非尼(Sorafenib，Sora)联用的联用指数(combination index，CI)。克隆形成实验检测 DHA 对 HepG-2 细胞增殖的影响。划痕实验测定 DHA 对 HepG2 细胞迁移能力的影响。Hoechst 33342 染色检测 DHA 处理 HepG-2 细胞 48h 后凋亡水平的变化。自噬抑制剂二磷酸氯喹(chloroquine diphosphate，CQ)预处理 HepG-2 细胞，后用(0、20、40、60、80 μmol·L－1) DHA 作用于处理后的 HepG-2 细胞 24h、48h，CCK-8 法检测细胞活性。MDC 染色观察 DHA 处理 HepG-2 细胞 48h 后自噬的变化。

结果：不同浓度 DHA 干预 HepG-2 细胞 24h、48h、72h 后，细胞增殖抑制率显著升高，并呈剂量依赖性。DHA 与 Sora 联用对 HepG-2 细胞具有较好的协同抑制细胞增殖作用。DHA 显著抑制 HepG-2 细胞增殖和迁移。DHA 诱导 HepG-2 细胞自噬，与 CQ 联用后明显降低 DHA 对 HepG-2 的细胞毒性。

结论：DHA 对 HepG2 细胞的增殖、迁移具有抑制作用。DHA 与 Sora 联用具有协同抑制 HepG2 细胞增殖的作用。DHA 诱导 HepG-2 细胞凋亡，其机制与 DHA 诱导 HepG-2 细胞自噬有关。

203. 肿瘤患者念珠菌感染的危险因素及药敏分析

崔兆磊、陈燕*

福建省肿瘤医院

目的：分析福建省肿瘤医院肿瘤患者念珠菌感染的临床特点、流行病学特征及导致感染发生的可能危险因素，为临床念珠菌感染的预防和诊疗提供参考依据。

方法：回顾性分析我院 2015-2017 年恶性肿瘤患者念珠菌感染的 60 例临床资料，对可能的危险因素进行单因素及多因素 logistic 回归分析，估计各危险因素的 OR 值并统计病原菌药敏试验结果作进一步分析。

结果：在念珠菌感染中，根据单因素卡方检验分析结果显示，应用广谱抗生素、住院天数（≥14 天）、术后引流管留置数量（≥4 个）及天数（≥7 天）、放化疗和是侵入性操作是发生念珠菌感染的危险因素（$P<0.05$）。Logistic 分析中，应用广谱抗生素、术后引流管留置天数（≥7 天）、住院天数（≥14 天）和侵入性操作的 OR 值分别为 11.177、1.925、15.154、4.613 均是发生感染的独立危险因素（$P<0.05$）。白念珠菌仍是最主要的病原菌（73%），常见真菌对常见抗真菌药物的敏感性由高到低依次为：两性霉素 B,5-氟胞嘧啶，伊曲康唑，伏立康唑，氟康唑。

结论：肿瘤患者住院治疗的周期长，放化疗，术后引流管插管数量多时间长，侵入性操作，术后广谱抗生素应用不规范等是引起念珠菌感染危险因素，临床应对存在危险因素的患者重点预防感染并掌握引起真菌感染病原菌的分布及耐药性，同时合理应用抗真菌药物以及同时注意及时送检合格标本。

关键字：肿瘤患者；念珠菌感染；药敏分析；危险因素

204. 多倍体巨大肿瘤细胞子代细胞通过过表达整合素αvβ6抵抗失巢凋亡促进下咽癌转移

刘慧婷、张振新、游波、尤易文*

南通大学附属医院

目的：下咽癌（Hypopharyngeal carcinoma，HPC）是指发生于梨状窝（占 70%以上）、环状软骨后区、喉咽后壁区的喉咽部恶性肿瘤，约占头颈部恶性肿瘤的 5%左右。资料显示：初

诊患者约 70%–90%已处于临床晚期（III~IV期），约 65%–80%伴颈部淋巴结转移。下咽癌是头颈部鳞状细胞癌中预后最差的癌症，5 年生存率仅约 25%–40%。下咽癌预后不良与复发密切相关，复发者大多同时伴有远处转移，且再次放化疗效果不佳，生存期短，预后极差。有研究表明，休眠的多倍体巨大肿瘤细胞（Polyploid giant cancer cells，PGCCs）及其子细胞（Daughter cells，DCs）是肿瘤发生、发展、侵袭、转移和化疗耐药的关键因素。本研究旨在探索 HPC-PGCCs 的特征和其在临床预后中的作用；化疗药物诱导的 HPC- DCs 是否通过过表达整合素 αvβ6（ITGB6），参与失巢凋亡抵抗的调控，促进下咽癌复发与转移。

方法：通过统计下咽癌患者病理组织切片中 PGCCs 的数量并探究其与 HPC 临床特征和预后间的关系。用紫杉醇酯质体（Paclitaxel，PTX）构建 HPC-PGCCs，HPC-DCs 诱导体系；利用免疫印迹实验（Western Blot）检测上皮间充质转化（Epithelial-mesenchymal Transition，EMT）、干细胞特性、细胞周期相关蛋白等表达水平；使用光学显微镜、细胞免疫荧光、流式细胞倍体实验、活死细胞分析实验、细胞黏附实验等探索 HPC-PGCCs 和 HPC-DCs 的细胞形态和生物功能学特征。通过高通量转录组测序筛选出 HPC 普通细胞和 HPC-DCs 之间的差异表达基因 ITGB6 并验证；在体外 HPC-PGCCs，HPC-DCs 诱导体系和体内裸鼠尾静脉转移模型中探究 ITGB6 对 HPC 失巢凋亡抵抗及转移的作用。

结果：PGCCs 的数量与 HPC 患者临床高分期、病理低分化、淋巴结转移和预后不良显著相关。PTX 诱导的 HPC-PGCCs 具有巨大核或多核的核特征，具有 G2/M 期停滞，细胞干性，混合 EMT、MET 和休眠癌细胞样特征，并且能够通过“爆裂样”和“出芽样”分裂生成 HPC-DCs。HPC-DCs 具有低粘附性、凋亡抵抗和高转移性的特征。高表达的 ITGB6 可以抑制 HPC 细胞失巢凋亡，并在体外 HPC-PGCCs，HPC-DCs 诱导体系和体内裸鼠尾静脉转移模型中促进其转移。高表达的 ITGB6 与 HPC 患者不良的临床特征和预后密切相关。

结论：研究结果显示：PTX 可成功诱导 HPC-PGCCs，HPC-DCs 的形成，并且 HPC-DCs 凋亡抵抗和远处转移能力增强。我们的研究首次阐释了在 HPC 治疗后，高表达 ITGB6 抑制失巢凋亡，促进远处转移。靶向 ITGB6 或联合使用常规化疗药物与 ITGB6 抑制剂有助于抑制 HPC 复发与转移。

关键字：下咽癌，转移，多倍体巨大肿瘤细胞，整合素αvβ6，失巢凋亡抵抗

205. 鼻咽癌多倍体巨大肿瘤细胞形成、分裂过程中的时空特异性超级增强子及核心转录因子分析

夏天、尤易文、游波*

南通大学附属医院

目的：复发转移是鼻咽癌(Nasopharyngeal carcinoma,, NPC)致死的主要因素。研究报道，多倍体巨大肿瘤细胞(PGCCs)，一种特殊的肿瘤休眠细胞，与肿瘤复发转移、预后不佳等密切相关。课题组在前期研究中成功构建 NPC-PGCCs 诱导体系，明确 NPC-PGCCs 的形成与鼻咽癌复发转移密切相关。本研究旨在解析普通 NPC 向 PGCCs 转化、PGCCs 休眠期维持、子细胞分裂的特定时空变化过程中超级增强子图谱的变化及其转录复合体组成。

方法：利用 RNA-seq 技术对普通 NPC 细胞、NPC-PGCCs、出芽分裂状态 PGCCs with budding、爆炸性分裂出的子代细胞 Daughter cells 进行全方位的 RNA 表达检测分析；利用 H3K27ac-ChIP-seq、ATAC-Seq 技术对普通 NPC 细胞、NPC-PGCCs、出芽分裂状态 PGCCs with budding、爆炸性分裂出的子代细胞 Daughter cells 进行全方位的染色质开放状态及增强子修饰状态分析。结合 RNA-seq、H3K27ac-ChIP-seq、ATAC-Seq 系统分析普通 NPC 向 PGCCs 转化、PGCCs 休眠期维持、子细胞分裂的特定时空变化过程中超级增强子图谱的变化及解析其过程中的关键转录复合体。利用裸鼠 NPC 原位转移模型、裸鼠 NPC 复发模型进一步明确 NPC 向 PGCCs 转化、PGCCs 休眠期维持、子细胞分裂的特定时空变化过程中关键超级增强子及其转录复合体的调控作用。

结果：为深入探究 PGCCs 形成、休眠、分裂及爆炸性复发提供了原创性数据。首次绘制普通 NPC 向 PGCCs 转化、PGCCs 休眠期维持、子细胞分裂的这一特定时空变化过程的增强子图谱及关键调控转录因子图谱。明确转录因子 ETV2、STAT4 在调控 PGCCs 形成及休眠状态维持中的作用。明确转录因子 E2F1、FOSL1、JUN 在 PGCCs 爆炸性分裂即 NPC 休眠后的爆炸性复发与转移中的作用。放化疗同时抑制 E2F1、FOSL1、JUN，可抑制 NOC 治疗后的复发与转移，提高患者生存率。

结论：研究结果提示，核心转录因子 E2F1、FOSL1、JUN 可调控 NPC-PGCCs 的爆炸性分裂。常规放化疗过程中，同时抑制 E2F1、FOSL1、JUN，可抑制 NPC 治疗后的爆炸性复发与转移，改善患者预后。

关键字：鼻咽癌，多倍体巨大肿瘤细胞，超级增强子，核心转录因子，时空特异性

206. KIF18B 通过调节线粒体更新及运动促进鼻咽癌恶性进展

夏天、姚慧、游波*

南通大学附属医院

目的：鼻咽癌（Nasopharyngeal carcinoma，NPC）是起源于鼻咽部黏膜上皮细胞的恶性肿瘤，具有高侵袭性、高转移性的特征。一旦转移，治疗效果极差，中位生存期仅 10-15 个月，5 年生存率仅约 20%-30%，转移成为 NPC 患者死亡的主要原因。肿瘤细胞通过驱动蛋白在微管上的动态变化，调控细胞器沿微管运输与胞内定位，促进转移。本研究中，我们探究了驱动蛋白 KIF18B 促进鼻咽癌转移的机制及其在 NPC 个体化治疗中的运用。

方法：通过 GEO 数据库，蛋白印迹实验和 qRT-PCR 评估 KIF18B 在 NPC 中的表达；使用共聚焦显微镜观察 KIF18B 的表达对微管及细胞器功能的影响；利用 RNA-seq 对不同表达 KIF18B 细胞中的差异表达基因进行全面分析，通过透射电镜分析、蛋白质印迹法、免疫荧光分析 KIF18B 敲低诱导产生的线粒体自噬作用；使用抑制剂或促进剂验证线粒体自噬与微管乙酰化对 NPC 恶性生物学行为表型的影响，并通过体内裸鼠实验加以验证；通过检测细胞能量代谢观察不同处理下细胞代谢能力；利用类器官模型分析针对 KIF18B 与破坏微管结构的临床用药。

结果：KIF18B 在 NPC 中异常高表达，与患者的临床预后相关。高表达 KIF18B 的细胞更易转移且具有更强的恶性生物学表型。特别是，NPC 中敲低 KIF18B 的表达与α微管结构改变和线粒体核周重新分布相关，同时促进线粒体自噬，并且抑制细胞恶性生物学行为。KIF18B 敲低显著抑制 HDAC6 的活性以提高微管乙酰化水平，利诺司他/ACY 是 HDAC6 的选择性抑制剂，在类器官模型中检测 KIF18B 水平，通过针对性用药验证了个体化治疗的可行性。

结论：研究结果提示，KIF18B 通过调控微管网络，调控线粒体沿微管运输与胞内定位，从而促进肿瘤转移等恶性生物学行为。

关键字：鼻咽癌，转移，微管，乙酰化，类器官

207. miR-598-3p 靶向调控 RMP 抑制胃癌细胞增殖和侵袭迁移的实验研究

王琦、蒋敬庭*

常州市第一人民医院

目的：探讨 miR-598-3p 靶向调控 RPB5 调节蛋白(RMP)基因对人胃癌细胞 SGC-7901 恶性增殖和侵袭迁移的影响及其作用机制。

方法：筛选 SGC-7901 细胞株行后续实验，分别建立稳定过表达或敲减 RMP 和 miR-598-3p 的 SGC-7901 细胞株。采用溴脱氧尿苷(BrdU)、细胞计数试剂盒(CCK-8)检测细胞增殖活力，平板克隆形成实验检测细胞集落形成能力，划痕实验检测细胞迁移能力，Transwell 实验检测细胞侵袭能力，双萤光素酶报告基因法分析 miR-598-3p 的结合靶点，蛋白质印迹(Western blot)检测相关通路相关蛋白表达水平，两样本间比较使用 t 检验。

结果：稳定过表达和敲减 RMP 或 miR-598-3p 的 SGC-7901 细胞株建立成功。敲减 RMP 能显著降低 SGC-7901 的增殖能力，BrdU(8.867±1.159 比 26.03±3.630, t=7.704, P<0.01)，CCK-8(0.560±0.052 比 1.020±0.107, t=6.708, P<0.01)，迁移能力(336.0±21.07 比 252.7±36.12, t=3.452, p<0.05)，侵袭能力(36.33±7.371 比 127.3±10.69, t=12.14, P<0.01)。过表达 RMP 能显著提高 SGC-7901 细胞的增殖能力，BrdU(56.40±6.560 比 24.80±4.423, t=6.918, P<0.01)，CCK-8(2.105±0.142 比 1.028±0.110, t=10.35, P<0.01)，迁移能力(131.3±20.11 比 257.0±29.14, t=6.148, P<0.01)，侵袭能力(347.7±41.14 比 135.0±17.69, t=8.226, P<0.01)。生物信息学预测 miR-598-3p 与 RMP 的 3'UTR 位点结合，并通过双荧光素报告系统验证。过表达或敲减 miR-598-3p 能分别降低和提高 SGC-7901 细胞株的增殖、迁移及侵袭能力，而 RMP 的回复表达能挽救 miR-598-3p 引起的细胞增殖、侵袭及迁移的抑制。miR-598-3p 通过靶向 RMP 抑制 p70 核糖体蛋白 S6 激酶(p70s6k1)/凋亡蛋白(Bad)和核因子-κB(NF-κB)通路发挥功能。

结论：miR-598-3p 靶向 RMP 基因抑制 p70s6k1/Bad 和 NF-κB 通路降低 SGC-7901 细胞的增殖、集落形成、迁移及侵袭能力。

关键字：miR-598-3p；胃癌；RMP；转移；增殖

208. FGF7（成纤维细胞生长因子-7）在肺癌类器官组织形成中的作用研究

李彦佼[1,2]、房艳华[1,2]、梁珊珊*[1,2]、王若雨[1,2]

1. 辽宁省乳腺及消化肿瘤分子标志物高通量筛选及靶向药物转化重点实验室

2. 大连大学附属中山医院肿瘤综合诊疗中心

目的：FGF7 是典型的肿瘤有丝分裂原，在肿瘤维持和增殖分化中发挥重要作用，也是体外肿瘤类器官培养体系中的关键细胞因子，但其具体作用和对肿瘤类器官形成的影响尚不明确。本研究旨在探讨 FGF7 在肺癌类器官形成中的作用，初步探索其在肺癌形成与维持中的机制。

方法：利用肺癌类器官培养体系（全因子）和 FGF7 缺失培养体系（-FGF7）在体外培养患者来源的肺癌组织，观测肺癌类器官形态差异，记录各组类器官的平均直径变化及成球情况，统计形成率，利用 ATP 酶活性检测三维肺癌类器官的生长速率；收取培养形成的肺癌类器官，进行组织学表征，利用免疫组化染色检测肿瘤标志物 Ki-67、CDK1、PCNA，以及干细胞标志物 CD44、CD133、EpCAM、SOX2、OCT4 的表达情况，对比两组类器官间以及来源组织的差异情况，分析 FGF7 可能参与肺癌类器官形成与维持生长的机制。

结果：FGF7 缺失培养体系下培养出的肺癌类器官平均直径和成球率均低于全因子培养体系，传代之后此现象更为明显；ATP 酶活性检测结果显示 FGF7 缺失培养体系中的肺癌类器官生长速率明显低于全因子培养体系；免疫组化染色结果显示，全因子培养体系中的肺癌类器官与来源组织的标志物表达情况基本一致，FGF7 缺失培养体系培养出的肺癌类器官 Ki-67、CDK1、PCNA 的表达明显降低，干细胞标志物 CD44、EpCAM 表达升高，CD133、SOX2 和 OCT4 表达维持或未检测到。这些结果表明，FGF7 为肺癌类器官的生长增殖提供了良好的条件（不含 FGF7 组因自第二代开始增殖减慢，成球较少，仅收集第一代进行了免疫组化染色。）

结论：FGF7 对肺癌类器官的形成和维持生长中起重要作用；FGF7 缺失培养条件下肺癌类器官仍可形成，但增殖指标下降，同时影响干细胞亚群分布，CD44+EpCAM+亚群比例升高。以上结论提示 FGF7 在肺癌的发生和发展过程中具有关键作用。

关键词：FGF7；肺癌类器官；3D 培养；肿瘤干细胞

209. 基于生物信息学分析 CLDN7 及其免疫相关细胞在乳腺癌中的表达及临床预后模型建立

范晓杰、刘月平*

河北医科大学第四医院

目的：应用生信分析 CLDN7 及其相关免疫基因在乳腺癌（BRCA）中的表达，并构建 CLDN7 相关免疫基因来预测 BRCA 预后状态的列线图。

方法：从 TCGA 数据库中获得 BRCA 数据集,运用 CIBERSORT 算法对转录组样本测序数据进行分析。运用 Timer2.0 在线分析 BRCA 转录组中 CLDN7 与免疫基因相关性。CCLE 下载 51 种 BRCA 细胞株的 RNA-seq 数据，进行 CLDN7 相关免疫基因 KEGG 和 GO 富集分析。将 CLDN7 相关免疫基因进行风险评估，差异表达基因纳入风险预后模型，构建列线图。最后，IF 和 IHC 验证 CLDN7 在 BRCA 细胞株和组织中的真实表达。

结果：CIBERSORT 分析显示，与癌旁样本相比，BRCA 中 B 细胞、T 细胞、M0 巨噬细胞、M1 巨噬细胞、树突状静息细胞的比例显著增加。Time2.0 分析结果显示，CLDN7 mRNA 表达于 B 细胞，$CD4^+$T 细胞，$CD8^+$T 细胞呈负相关，与 M0 巨噬细胞呈正相关。GSEA 分析 CLDN7 主要参与了 B 细胞信号通路和细胞缝隙连接通路。CLDN7 信号通路分析鉴定出 15 相关的免疫刺激基因，37 个相关的免疫抑制基因，主要参与 NF-kappa B 信号通路和 T 细胞受体信号通路。将 52 个相关基因采用单因素 Cox 回归分析与 OS 之间的相关性，得到 19 个与预后相关基因。将预后相关基因纳入模型构建 C-index=0.76 BRCA 的预后列线图，来预测个体的 3 年和 5 年生存概率。最后，IF 验证 CLDN7 在 BRCA 细胞存在较高表达，IHC 验证 CLDN7 在 BRCA 组织中蛋白水平较高。

结论：研究结果为 CLDN7 在 BRCA 肿瘤免疫中的作用提供了证据，提示 CLDN7 可能是 BRCA 的潜在免疫治疗靶点，其相关免疫标记是 BRCA 中一个很有前途的预后生物标志物。

关键字：CLDN7；免疫细胞；乳腺癌；预后；列线图

210. 低氧微环境通过促进 Caveolin1 介导的肿瘤源性细胞外囊泡 LAMB2 分选促进胃癌腹膜转移

李冬阳、车晓芳*、刘云鹏

中国医科大学附属第一医院

目的：胃癌易发生腹膜转移，且缺乏有效治疗手段，预后极差。低氧是实体肿瘤的重要且普遍存在的微环境特征，细胞外囊泡（EV）是细胞间进行信息传递的重要工具。然而，低氧微环境如何通过影响 EV 来促进胃癌腹膜转移尚不清楚。本研究旨在探讨低氧微环境下，胃癌细胞来源 EV 对周边常氧胃癌细胞的影响及可能机制。

方法：构建人低氧耐性胃癌细胞系，蛋白组学分析低氧耐性胃癌细胞系与常氧胃癌细胞系表达差异蛋白。超速离心法提取细胞外囊泡后，利用电镜、粒径分析及 Western blot 法对细胞外囊泡进行表征。PKH26 染色法确认靶细胞对细胞外囊泡的摄取。免疫沉淀、质谱分析以及 Duolink 实验探讨蛋白相互作用。Transwell 小室探讨细胞迁移及侵袭能力。基质胶、人腹膜间皮细胞粘附试验探讨胃癌细胞粘附能力。小鼠腹膜转移模型进行体内实验验证。利用胃癌腹膜转移患者腹水中的细胞外囊泡进行临床验证。

结果：1. 经长期低氧培养建立的低氧耐性胃癌细胞系转移能力增强、细胞外囊泡（EV）分泌增多，且其 EV 可促进常氧胃癌细胞发生腹膜转移。2. 通过蛋白组学分析低氧耐性胃癌细胞系与常氧胃癌细胞系蛋白差异，结合胃癌在线数据及细胞外囊泡数据库数据分析，并经验证发现低氧耐性胃癌细胞-EV 中 Caveolin1（CAV1），Lamininb2（LAMB2）高表达。 3. 低氧耐性胃癌细胞源性 EV-CAV1 可促进常氧胃癌细胞腹膜转移；敲减 CAV1 后 EV 中，而非细胞中 LAMB2 明显减少；LAMB2 被常氧胃癌细胞摄取后通过激活 AKT 通路促进了常氧胃癌细胞的腹膜转移；小鼠腹膜转移模型证实 EV-CAV1 确实可促进常氧胃癌细胞腹膜转移；胃癌腹膜转移患者腹水标本证实，腹水-EV 中 CAV1 和 LAMB2 高表达。这些结果提示，低氧胃癌细胞通过 CAV1 介导 LAMB2 向 EV 分选而促进常氧胃癌细胞的腹膜转移。4. 通过免疫沉淀质谱分析及 Duolink 实验鉴定出 CAV1 的结合蛋白 ROCK1，并发现敲减 ROCK1 及应用 Y27632 抑制 ROCK1 活性后，CAV1 磷酸化水平而非 CAV1 蛋白水平降低、且 EV-LAMB2 减少；进一步经位点突变实验证实 CAV1 Y14 位点磷酸化是其促进 LAMB2 向 EV 分选的关键。这些结果提示，ROCK1 通过促进 CAV1 Y14 磷酸化促进了 LAMB2 向 EV 的分选。

结论：低氧微环境下，胃癌细胞中的 ROCK1 通过介导 CAV1 Y14 的磷酸化促进 LAMB2 分选进入 EV；而 EV-LAMB2 被周边常氧状态的胃癌细胞摄取后，通过激活 AKT 通路促进其发生腹膜转移发生。EV-CAV1 及 EV-LAMB2 有望成为预测胃癌腹膜转移的生物标志物，及治疗胃癌腹膜转移的潜在靶点。

关键字：低氧微环境、细胞外囊泡、胃癌腹膜转移、Caveolin1

211. lncRNA RUN12 在胃癌中的表达及相关的机制研究

黄志艺[1,2]、邹长棪[2]、林贤东*[2]

1. 福州大学化学学院

2. 福建省肿瘤医院

目的：探讨 lncRNA RUN12 基因表达与胃癌的进展的关系及相关的机制研究。

方法：收集胃腺癌患者 81 例，分析 RNU12 表达与胃癌病理特征的关系。利用慢病毒载体构建过表达和敲低 RNU12 的胃癌 AGS 细胞系，并通过 RT-qPCR、MTT 法、划痕实验和 transwell 侵袭实验，检测 RNU12 在胃癌细胞中的生物学功能。通过 lncRNASNP2 等数据库预测 RNU12 可能结合的 miRNA 及下游作用的靶基因，并利用 RIP、双萤光素酶实验进行验证。通过回复实验评估下游靶基因 BLID 与 RNU12 的关系。建立斑马鱼胃癌异种移植模型，探索 RNU12 与胃癌进展的关系。

结果：RUN12 在胃癌组织中低表达，而且其表达与病理特征密切相关。体外实验表明，RNU12 过表达抑制胃癌细胞的侵袭性。RNU12 和 BLID 的 3'UTR 都有 hsa-miR-575 结合位点，并且 Hsa-miR-575 是 RNU12 抑制剂和 BLID 阻滞剂。BLID 在 RNU12 介导的胃癌细胞体外恶性行为起重要作用。斑马鱼胃癌移植模型研究表明，RNU12 过表达抑制胃癌细胞的增值和转移。RIP、双萤光素酶实验及回复实验显示，RUN12 通过 miR-575/BLID 信号轴调控胃癌的进展。同时，RNU12 可以抑制多种促瘤因子的作用，如 CCND1、PCNA、Cyclib D1、N-钙粘蛋白波形蛋白和 BCL-2。

结论：RNU12 在胃癌中异常表达，且与临床病理特征密切相关。RUN12 通过 miR-575/BLID 信号轴调控胃癌的进展。RUN12 可能是胃癌潜在肿瘤分子标志物。作者：黄志艺福州大学化学院 邹长棪福建省肿瘤医院 林贤东福建省肿瘤医院

关键字: RNU12；胃癌；肿瘤标志物

212. 淋巴细胞在肝癌免疫系统中的空间转录分布的定量分析：一个与生存和基因表达相关的生物标志物

苗雨曦*

中国医科大学

背景：众所周知，肿瘤微环境（TME）会影响肝细胞癌（HCC）的预后。尽管数字病理学和人工智能已被应用于现代医学和肿瘤学。但很少有定量的生物标志物被确定用于预测通过在细胞水平上对 TME 的自动分析来预测 HCC 的预后和指导治疗。

方法：365 例 HCC 患者的组织病理学图像和临床数据来自 TCGA（The Cancer Genome Atlas），并从 PAIP2019（Pathology Artificial Intelligence Platform）中收集了 60 个 HCC 病理图像和癌症病灶注释。基于 DenseNet 的 HCC 分割模型（F1-score, 0.904）和基于 Hover-Net 的细胞检测模型（F1-score, 0.914）。PAIP2019 和 MoNuSac 数据集。每个 TME 的组织病理学图像通过分割模型被分割成两个区域。包括：1）包括基质的非肿瘤区域；2）HCC 细胞集中的肿瘤区域。细胞检测模型识别图像上的单细胞，本研究指定淋巴细胞，并计算淋巴细胞与总细胞数的比率（RLTCC）。然后 RLTCC 与临床生存结果、HCC 主要风险因素和 RNA 表达谱相关联。

结果：肿瘤区域的 RLTCC 与预后没有明显关系。非肿瘤区域 RLTCC（RLTCC in NT）较高的患者组比 NT 中 RLTCC 较低的患者组显示出更好的总生存率（OS），无论 HCC 风险因素如何，非肿瘤区 RLTCC 较高的患者群体比 NT 区 RLTCC 较低的患者群体的总生存期（OS）要好（中位 OS= 45.7 *vs.* 18.6 month；log risk ratio= -1.6±1.1，P=0.006）。这些患者的基因表达高与癌症抗原表达有关的基因（p<0.05）（较高的基因表达+33.7%），T 细胞识别癌细胞（+32.0%），T 细胞启动和激活（+32.2%），免疫细胞定位到肿瘤（+31.9%），和杀死癌细胞（+24.7%）。那些有 HCC 病因的乙型和丙型肝炎患者在 NT 中的 RLTCC 较高（分别为 17/21 名患者，占 81.0%；23/29 名，占 79.3%）。相比之下，有饮酒习惯的患者显示出相同的分布（26/53 名，占 49.1%）。B/C 型肝炎组的 RLTCC 在统计学上高于饮酒组（p<0.05）。

结论：一个数字化的预后性生物标志物，TME 的非肿瘤患者中的 RLTCC 被确定为一个重要的预后指标，并且它被证明与 T 细胞介导的癌症免疫相关的 RNA 基因表达相关。这是一项关于系统性治疗的临床反应与数字生物标志物的关系的回顾性分析。

关键字:肿瘤微环境；肝癌；预后标志物；淋巴细胞

213. Activation of PI3K/AKT pathway is a potential mechanism of treatment resistance in small cell lung cancer

Ying Jin *[1]、Yamei Chen[1]、Huarong Tang[1]、Xiao Hu[1]、Shawna M. Hubert[2]、Qian Li[3]、Dan Su[1]、Haimiao Xu[1]、Yun Fan[1]、Xinmin Yu[1]、Qixun Chen[1]、Jinshi Liu[1]、Wei Hong[1]、Yujin Xu[1]、Huan Deng[1]、Dapeng Zhu[1]、Pansong Li[3]、Yuhua Gong[3]、Xuefeng Xia[3]、Carl M. Gay[2]、Jianjun Zhang[2]、Ming Chen[4]

1. Zhejiang Cancer Hospital

2. Department of Thoracic/Head and Neck Medical Oncology, the University of Texas MD Anderson Cancer Center, Houston, Texas 77030, USA

3. 北京吉因加研究院

4. 中山大学肿瘤防治中心

Purpose: Here we have investigated treatment resistance mechanisms in small-cell lung cancer (SCLC) by focusing on comparing the genotype and phenotype in tumor samples of treatment-resistant and treatment-sensitive SCLC.

Methods: We conducted whole-exome sequencing (WES) on paired tumor samples at diagnosis and relapse from 11 limited-stage (LS)-SCLC patients and targeted sequencing of 1,021 cancer-related genes on cell free DNA (cfDNA) at baseline and paired relapsed samples from 9 additional LS-SCLC patients. Furthermore, we performed label-free mass spectrometry- (MS-) based proteomics on tumor samples from 28 chemo-resistant and 23 chemo-sensitive patients with extensive-stage (ES)-SCLC. The main findings were validated in vitro in chemo-sensitive versus chemo-resistant SCLC cell lines and analyses of transcriptomic data of SCLC cell lines from a public database.

Results: Genomic analyses demonstrated that at relapse of LS-SCLC, genes in the PI3K/AKT signaling pathway were enriched for acquired somatic mutations or high frequency acquired CNVs. Pathway analysis on differentially upregulated proteins from ES-SCLC cohort revealed enrichment in the HIF-1 signaling pathway. Importantly, 7 of 62 PI3K/AKT pathway genes containing acquired somatic copy number amplifications were enriched in HIF-1 pathway.

Analyses of transcriptomic data of SCLC cell lines from public databases confirmed upregulation of PI3K/AKT and HIF-1 pathways in chemo-resistant SCLC cell lines. Furthermore, chemotherapy-resistant cell lines could be sensitive to PI3K inhibitors in vitro.

Conclusions: PI3K/AKT pathway activation may be one potential mechanism underlying therapeutic resistance of SCLC. This finding warrants further investigation and provides a possible approach to reverse resistance to chemo/radiotherapy.

Key words: small cell lung cancer, whole-exome sequencing, mechanism of treatment resistance, PI3K/AKT pathway

214. Hypermethylated PCDHGB7 as a universal cancer only marker and its application in early cervical cancer screening

Shihua Dong*

Shanghai Epiprobe Bio Technology Co., Ltd

Background: Epigenetic aberrations have been intensively studied in diverse cancers. However, universal features shared among all cancer types have received minimal attention in the era of precision medicine. For primary cervical cancer screening, the high false-positive rate of the human papillomavirus (HPV) test and cervical cytology and the urgent need in distinguishing between high-grade squamous intraepithelial lesion (HSIL) and low-grade squamous intraepithelial lesion (LSIL) call for potent biomarkers.

Methods: We analyzed PCDHGB7 methylation in 17 types of cancer in TCGA datasets (n= 7,069) and verified it in 13 types of clinical cancer samples (n= 727) by bisulfite-PCR pyrosequencing. Next, we concentrated on cervical cancer and detected PCDHGB7 methylation in 86 primary tissues, 404 cervical smears, and 273 vaginal secretions by bisulfite-PCR pyrosequencing and methylation-sensitive restriction enzymes-based quantitative PCR (MSRE-qPCR), and evaluated it as a biomarker for early cervical cancer screening.

Results: Here, we found PCDHGB7 was universally hypermethylated in 17 cancer types from TCGA datasets, which was proven in 13 types of clinical cancer samples with a high area under

the curve (AUC) value (≥ 0.85). The methylation detection of PCDHGB7 can be applied to early cervical cancer screening in cervical smears and even in self-sampled vaginal secretions with a sensitivity of 90.9% and specificity of 90.4%. Furthermore, the methylation status of PCDHGB7 can clearly distinguish HSIL and LSIL, which will contribute to early theranostic management of cervical cancer.

Conclusions: Hypermethylated PCDHGB7 could serve as a pan-cancer (or "universal-cancer-only methylation", UCOM) marker and its implementation would greatly improve the currently used cervical cancer screening strategy and benefit womens health.

Key words： PCDHGB7, DNA methylation, UCOM marker, cervical cancer, early screening

215. Folate-Receptor Positive Circulating Tumor Cell Is a Potential Diagnostic Marker of Prostate Cancer

Shenyi Lian*、Lujing Yang、Qin Feng、Ping Wang、Yue Wang、Zhongwu Li

Peking University Cancer Hospital & Institute

Folate-receptor positive circulating tumor cells (FR+CTCs) shows an important role in the diagnosis and dynamic monitoring for many solid tumors; however, the application of FR+CTCs in prostate cancer remains unclear. We explored the potential application of FR+CTCs in this retrospective study. The levels of FR+CTCs were detected in 30 prostate cancer patients and 7 bladder cancer patients in Peking University Cancer Hospital from August 2017 to August 2021. Clinical and pathology data were collected. One-way ANOVA was used to compare the difference in FR+CTCs levels in patients with prostate cancer, bladder cancer, and benign disease. The area under the receiver operating curve (AUROC) was used to compare the accuracy of FR+CTCs and tPSA in the diagnosis of prostate cancer. We found that levels of FR+CTCs were significantly higher in cancer patients (both prostate and bladder cancer) than in patients with benign urinary disease (p<0.001). Besides, FR+CTCs level was consistently high in the prostate cancer patients with different tPSA levels (p<0.001), and it was significantly higher in the patients with f/tPSA levels <0.16 than in those patients with f/tPSA levels >0.16 (12.20 ± 1.31 *vs.* 8.73 ± 0.92 FU/3 ml, p= 0.043). The diagnosis efficiency of FR+CTCs is better than the tPSA in prostate cancer patients

with tPSA <10 ng/ml (0.871 *vs.* 0.857). In the prostate cancer patients with tPSA <10 ng/ml and f/tPSA <0.16, a combination of FR+CTCs and tPSA (AUROC, 0.934) further increased the diagnosis efficiency of each of these biomarkers alone (FR+CTCs, 0.912; tPSA, 0.857). Therefore, FR+CTCs could serve as an early diagnosis marker in the prostate cancer patients with uncertain tPSA levels.

Key word: circulating tumor cells, prostate cancer, folate-receptor positive, diagnosis, biomarkers

216. Emergency medical service at a first aid station by emergency call120 for acute alcohol poisoning and other kinds of poisoning

Hanyou Xu*

Department of Internal Medicine, INTERNATIONAL LIASOM Hospital in Anji , Huzhou city, Zhejiang Province, China.

Objective: In order to promote and enhance the clinical outcome for acute alcohol poisoning and other kinds of poisoning by emergency medical service, so as to promote the public health, Chinese quality of life, the well-being， and better social behavior and image, the emergency medical service at our first aid station by emergency call120 for patients of acute alcohol poisoning and other kinds of poisoning were summarized and analysed.

Method: By retrospective analysis, from 2014-11-1 to 2016-10-31, all the patients of acute alcohol poisoning and other kinds of poisoning called for 120 emergency medical service at our first aid station were enrolled for this research. The new data, new special clinical syndromes, medical treatment and the prognosis or clinical results were summarized and calculated.

Results: The per cent of patients of acute alcohol poisoning and other kinds of poisoning is 15.6% among the patients of all 120 emergency calls to our first aid station in the research period. And the per cent of patients of acute alcohol poisoning is 87.1% among all the patients of poisoning. There have been 6 dead patients of acute alcohol poisoning when the 120 emergency calls were done. The most new special clinical syndrome of acute alcohol poisoning is that about 72.7% suffered patients are lying on the public places with astonished bad behaviors and images, mostly

on the road, inns, or streets. Which the normal public order were disturbed. Another special clinical syndrome of acute alcohol poisoning is that about one quarter patients are suffering from traumas and injuries in different degrees by their poisonings induced.Our research has indicated that our treatments and emergency medical service for the acute alcohol poisoning and other kinds of poisoning are satisfied by all the patients and their accompanying relatives. And the patients with only acute alcohol poisoning are not needed inward treatment as inpatients. And the strategy methods for treatment acute alcohol poisoning are outlined. Which is different from some habit treatment of acute alcohol poisoning.

Conclusions: Our research firstly reported the data of 120 emergency medical service for poisoning including acute alcohol poisoning and other kinds of poisoning, firstly reported that about 72.7% acute alcohol poisoning suffered patients are lying on the public places with astonished bad behaviors and images, mostly on the road, inns, or streets. Which the public normal order were disturbed. The new finding further displays that the acute alcohol poisoning is not simply as eating food. Which has not been paid attention to by related workers. But it is a severe disease which destroys the public health, the well-being， quality of life and strong, and the social behavior, image and spirit. The research calls for treating it as carefully as possible to enhance and recover the harming of acute alcohol poisoning, national policy must be created as soon as possible to prevent and mend the sufferings, and international cooperation is needed as well as possible to cure the world wide enlarged alcohol poisoning.

Key words: Alcohol poisoning; emergency medical service; poisoning; emergency medicine; poisoning behavior.

217. An important proposal: The new laws and regulations about protection of life's physiology and their health must be established.

Hanyou Xu*

Department of Internal Medicine, INTERNATIONAL LIASOM Hospital in Anji , Huzhou city, Zhejiang Province, China.

Objective: As the modern science and technology developed, the radio controlling the space craft and physiology of human being and man-made patho-physiology changes have been being in a easy way like the hand movements of normal adult man.As I am doctor with more than 30 years experience. Some radio controlling technologies have been applied for civil use to diagnose and treat patients. Also, I have been experiencing that the normal physiology of human-being have been being interfered by the powerful people who control the radio micro-controlling system and harm their rivals or enemies. In this way, the diseases and suffering from the man-made radio controlling induced pathology have been being faced by me and all others.In order to protect life's physiology and their health of mankind and others, I researched as this paper.

Methods: Summarized facts of the mankind and experiences of mine. Created the results and suggestions.

Results: In modern technology developed time, nearly all the world people known, the life and the health of people can be controlled or interfered by the outsiders. These weapons have been grabbed by the leaders, powers or politicians. The leaders or the politicians must not controlled or interfered the health of other countrymen to get own the health of countrymen well-up than other countries for political great job gaining.All the people around the world must have the same rights to live freely and heath. The politicians and the leaders controlling the power must not interfere the people's physiology and their health.Therefore, it is very imperative to set up the new order of freedom about people's physiology and their health interfered by the radio and micro outsiders. These new orders must be created at present new technology era at once. And the related laws and regulations to protect people's physiology and their health from interfering by the radio and micro outsiders must be established.So as the new laws and regulations about protection of animal's or

other life's physiology and their health must be established.As the aims of the United Nations are "The Peace, dignity and equalityon a healthy planet". The UN,One place where the worlds nations can gather together, discuss common problems and find shared solutions.The UN has evolved over the years to keep pace with a rapidly changing world. But one thing has stayed the same: it remains the one place on Earth where all the world's nations can gather together, discuss common problems, and find shared solutions that benefit all of humanity. As the United Nations Secretary-General António Guterres has said,"In the end, it comes down to values [...] We want the world our children inherit to be defined by the values enshrined in the UN Charter: peace, justice, respect, human rights, tolerance and solidarity".So , in order to let all the people around the world living in the" Peace, dignity and equality on a healthy planet", and in" justice, respect, human rights, tolerance and solidarity", the new laws and regulations about protection of life's physiology and their health from interfering by the radio and micro outsiders must be established by the UN,WHO and every countries and regions.

Conclusion: In this regards, I am making these proposals to the UN ,WHO, nations and may lead to all the countries and regions with the goodwill aims to .set up the related laws and regulations and to let the all people around the world to know the factual situation and acting to support my proposals and gain the normal and healthy world far from outsiders interfering ours heart beat,respiration,temperature,blood pressure,sleep,thinking,memory,eating,urination,defecating.....In this way, we can cure lots of man made diseases,like the fever,cough,ache,vomiting,cancer,shock,coma,even death or sudden death, et al. all the natural developed diseases which the devil outsiders all can interfere and induce looked like the natural developed diseases.

Key words : Proposals; freedom of physiology; health protection; radio controlled health destroy.

218. Selective multiplexed enrichment for the detection and quantitation of low-fraction DNA variants via low-depth sequencing

宋萍*

上海交通大学生物医学工程学院

DNA sequence variants with allele fractions below 1% are difficult to detect and quantify by sequencing owing to intrinsic errors in sequencing-by-synthesis methods. Although molecular-identifier barcodes can detect mutations with a variant-allele frequency (VAF) as low as 0.1% using next-generation sequencing (NGS), sequencing depths of over 25,000×are required,thus hampering the detection of mutations at high sensitivity in patient samples and in most samples used in research. Here we show that low-frequency DNA variants can be detected via low-depth multiplexed NGS after their amplification, by a median of 300-fold, using polymerase chain reaction and rationally designed ‘blocker’ oligonucleotides that bind to the variants. Using an 80-plex NGS panel and a sequencing depth of 250×, we detected single nucleotide polymorphisms with a VAF of 0.019% and contamination in human cell lines at a VAF as low as 0.07%. With a 16-plex NGS panel covering 145 mutations across 9 genes involved in melanoma, we detected low-VAF mutations (0.2–5%) in 7 out of the 19 samples of freshly frozen tumour biopsies, suggesting that tumour heterogeneity could be notably higher than previously recognized.

Key words : 癌症诊断，低突变频率，放大检测，二代测序

219. miR-195-5p 调控 MIB1 对前列腺癌细胞增殖、迁移和侵袭的影响

陈彬*、白国辉、马小彦、谭璐琳、许厚强

贵州大学

Mind bomb 1 (MIB1) is a well-known E3 ubiquitin ligase. MicroRNAs (miRNAs or miRs) have been found to serve important functions in cancer cell physiology. However, the clinical significance and biological function of MIB1 and miRNAs in prostate cancer (PCa) are yet to be fully elucidated. The current study predicted the interaction between MIB1 and miR-195-5p using TargetScan, and the results were confirmed by performing a dual-luciferase reporter assay. The results revealed that the expression of MIB1 was increased, while the expression of miR-195-5p was decreased in PCa tissues (MIBI, $P<0.001$; miR-195-5p, $P<0.01$) and various cell lines, including PC-3 (MIBI, $P<0.001$; miR-195-5p, $p<0.05$), VCaP (MIBI, $P<0.001$; miR-195-5p, $P<0.01$), 22Rv1 (MIBI, $P<0.001$; miR-195-5p, $p<0.05$), DU145 (MIBI, $P<0.001$; miR-195-5p, $P<0.01$) and LNCaP (MIBI, $P<0.001$; miR-195-5p, $p<0.05$). Knockdown of MIB1 in VCaP and DU145 cells significantly inhibited cell proliferation, migration and invasion, while miR-195-5p exerted the opposite effects. Additionally, MIB1 overexpression restored the miR-195-5p overexpression-induced repression of cell proliferation and invasion. The current study identified that the MIB1 gene was an effector of cell proliferation, migration and invasion in PCa. Furthermore, the novel miR-195-5p may regulate PCa cell proliferation and invasion by regulating MIB1, indicating its potential therapeutic application for PCa in the future.

关键字: prostate cancer, miR-195-5p, mind bomb 1, proliferation, migration, invasion

220. Development and Validation of a Metabolic Gene-Based Prognostic Signature for Hepatocellular Carcinoma

Jialei Weng*[1]、Chenhao Zhou[1,2]、Qiang Zhou[1]、Wanyong Chen[1,3]、Yirui Yin[1]、Manar Atyah[1]、Qiongzhu Dong[2,3,4]、Yi Shi[5]、Ning Ren[1,3]

1. Zhongshan Hospital, Fudan University

2. Department of Molecular and Cellular Oncology, The University of Texas MD Anderson Cancer Center, Houston, Texas

3. Institute of Fudan Minhang Academic Health System, Minhang Hospital, and Key Laboratory of Shanghai Municipal Health Commission, Fudan University, Shanghai, China

4. Institutes of Biomedical Sciences, Fudan University, Shanghai, China

5. Biomedical Research Centre, Zhongshan Hospital, Fudan University, Shanghai, China

Background: Hepatocellular carcinoma (HCC) is a malignant tumor with great variation in prognosis among individuals. Changes in metabolism influence disease progression and clinical outcomes. The objective of this study was to determine the overall survival (OS) risk of HCC patients from a metabolic perspective.

Patients and Methods: The model was constructed using the least absolute shrinkage and selection operator (LASSO) COX regression based on The Cancer Genome Atlas (TCGA, n=342) dataset. The International Cancer Genome Consortium (ICGC, n=232), GSE14520 (n=242) datasets, and a clinical cohort (n=64) were then used to assess the prognostic value of the signature.

Results: A 10 metabolic gene-based signature was constructed and verified as a robust and independent prognostic classifier in public and real-world validation cohorts. Meanwhile, the signature enabled the identification of HCC molecular subtypes, yielding an AUC value of 0.678 [95%CI: 0.592-0.763]. Besides, the signature was associated with metabolic processes like glycolysis, supported by a clear correlation between the risk score and expression of rate-limiting enzymes. Furthermore, high-risk tumor was likely to have a high tumor infiltration status of immunosuppressive cells, as well as elevated expression of some immune checkpoint molecules. For final clinical translation, a nomogram integrating the signature and tumor stage was

established, and showed improved predictive accuracy of 3- and 5-year OS and brought more net benefit to patients.

Conclusion: We developed a prognostic signature based on 10 metabolic genes, which has proven to be an independent and reliable prognostic predictor for HCC and reflects the metabolic and immune characteristics of tumors.

Key words : hepatocellular carcinoma, metabolism-related gene, signature, prognosis

221. miR-1301-3p is a potential prognostic biomarker for esophageal carcinoma and acts by downregulating NBL1 expression

Jianting Du*、Yang Zhang、Bin Zheng、Chun Chen

Fujian Medical University Union Hospital

Background: Esophageal cancer (ESCA) is one of the most aggressive and lethal human malignant cancers. It is associated with poor overall survival (OS) and ranks sixth among the causes of cancer-related mortalities. MiR-1301-3p plays vital roles in a majority of malignancies. The aim of this study was to investigate the correlation between miR-1301-3p/NBL1 axis and prognosis of ESCA patients.

Methods: We compared the miR-1301-3p expression levels between ESCA and normal esophageal tissues using MiRNAseq data retrieved from The Cancer Genome Atlas (TCGA) database. We employed UALCAN web platform, starBase v3.0 database, R software and GEPIA web platform to perform statistical analysis and data visualization. We then used TargetScan Human, miRDB and DIANA Tools databases to predict the miR-1301-3p target genes. Finally, we analyzed the expression patterns of the target genes as well as their prognostic value in ESCA.

Results: There was an overexpression of miR-1301-3p in most malignancies, including ESCA (P<0.001). The miR-1301-3p expression levels were significantly related to age and histologic grade in primary ESCA (p<0.05), with high expression of miR-1301-3p being significantly associated with poor prognosis (Hazard ratio [HR]=1.88, P=0.012). NBL1 was identified as a potential target gene for miR-1301-3p and a negatively correlation in expression

levels between the two genes was observed (r=-0.282, *P*<0.001). Notably, NBL1 was significantly downregulated in ESCA *(P*<0.001) and its low expression was significantly associated with poor prognosis of ESCA patients (HR=0.53, *P*=0.0063).

Conclusion: miR-1301-3p is a potential biomarker for predicting prognosis of ESCA patients. It may regulate ESCA progression by regulating NBL1 expression.

Key words : esophageal cancer; miR-1301-3p; NBL1; prognostic biomarker; survival

222. The E3 Ligase NEDD4 is A Potential Target in IGF Signal Pathway-driven Gastric Cancer

ke wang*[1]、xunliang jiang[1]、jipeng li[1,2]

1. 空军军医大学西京医院

2. 空军军医大学西京医院实验外科

Heterogeneity has always been a challenge in targeted therapy of gastric cancer (GC). Searching for therapeutic targets based on the molecular subtypes of GC will provide more precise treatment for stratified patients. IGF1/IGF1R pathway is highly activated in some subtypes of GC that exhibits poor survival and chemotherapy resistance, indicating the therapeutic significance of targeting IGF1/IGF1R pathway in GC. As an E3 ligase of key tumor suppressor PTEN, NEDD4 functions as an oncogene in various types of tumors. However, the role and underlying mechanisms of NEDD4 in gastric cancer (GC) remain elusive. Here, we investigated the therapeutic benefit of targeting NEDD4 in GC with high activation of IGF1 signaling. We found that IGF1/IGF1R is highly activated in part of GC cell lines and GC tissues, which is significantly correlated with the prognosis of GC patients. Using a Dox-induced NEDD4 gene silence system, we found that knockdown of NEDD4 inhibits the IGF1/IRS1/AKT signaling and proliferation of IGF1R-dependent GC cells both in vitro and in vivo. However, knockdown of NEDD4 has no effect on the phosphorylation level of AKT and proliferation of IGF1R-independent GC cells. Moreover, rescue experiment showed that a PTEN-IRS1 axis is required for NEDD4-mediated regulation of AKT activation. Taken together, we demonstrated that NEDD4 promotes

proliferation of GC cells with high activation of IGF1 signaling in a PTEN-dependent manner, suggesting the distinctive clinical significance of NEDD4-targeted strategy in GC treatment.

Key words : Gastric cancer; E3 ligase; NEDD4; PTEN; IGF1 signaling

223. The E3 Ligase NEDD4 is A Potential Target in IGF Signal Pathway-driven Gastric Cancer

ke wang*[1]、xunliang jiang[1]、jipeng li[1,2]

1. 空军军医大学西京医院

2. 空军军医大学西京医院实验外科

Heterogeneity has always been a challenge in targeted therapy of gastric cancer (GC). Searching for therapeutic targets based on the molecular subtypes of GC will provide more precise treatment for stratified patients. IGF1/IGF1R pathway is highly activated in some subtypes of GC that exhibits poor survival and chemotherapy resistance, indicating the therapeutic significance of targeting IGF1/IGF1R pathway in GC. As an E3 ligase of key tumor suppressor PTEN, NEDD4 functions as an oncogene in various types of tumors. However, the role and underlying mechanisms of NEDD4 in gastric cancer (GC) remain elusive. Here, we investigated the therapeutic benefit of targeting NEDD4 in GC with high activation of IGF1 signaling. We found that IGF1/IGF1R is highly activated in part of GC cell lines and GC tissues, which is significantly correlated with the prognosis of GC patients. Using a Dox-induced NEDD4 gene silence system, we found that knockdown of NEDD4 inhibits the IGF1/IRS1/AKT signaling and proliferation of IGF1R-dependent GC cells both in vitro and in vivo. However, knockdown of NEDD4 has no effect on the phosphorylation level of AKT and proliferation of IGF1R-independent GC cells. Moreover, rescue experiment showed that a PTEN-IRS1 axis is required for NEDD4-mediated regulation of AKT activation. Taken together, we demonstrated that NEDD4 promotes proliferation of GC cells with high activation of IGF1 signaling in a PTEN-dependent manner, suggesting the distinctive clinical significance of NEDD4-targeted strategy in GC treatment.

Key words : Gastric cancer; E3 ligase; NEDD4; PTEN; IGF1 signaling

224. A novel biomarker based on five tsDElncRNAs SLC25A5-AS1, RP11-336A10.4, FLJ42969, RP11-21L19.1 and RP11-406H23.2 can predict the prognostic risk of papillary renal cell carcinoma

Ji Ma*

Zhejiang Sci-Tech University

Background: Long non-coding RNA (lncRNA) has attracted attention of researchers in recent years because of its potential role in cancer. Tissue-specific differentially expressed lncRNAs (tsDElncRNAs) play an important role in the occurrence and development of papillary renal cell carcinoma (pRCC). The prognosis of pRCC remains poor and the research of developing prognostic lncRNA biomarkers of pRCC has been launched. However, tsDElncRNAs of pRCC have not been screened and whether they can be used as prognostic biomarkers has not been evaluated.

Methods: RNA-seq data obtained from the pRCC project of TCGA database (TCGA-KIRP) were analyzed by using bioinformatics tools, including the screening of prognostic tsDElncRNAs, the establishment of a prognostic risk prediction model, and the correlation analysis between risk score and clinical characteristics (e.g. age, gender, pathological stage, tumor stage, etc.).

Results: 441 pRCC tsDElncRNAs were obtained. Univariate Cox regression analysis showed that 53 tsDElncRNAs were significantly associated with the prognosis of pRCC (p<0.05). In multivariate Cox regression analysis, a prognostic risk model containing five tsDElncRNAs SLC25A5-AS1, RP11-336A10.4, FLJ42969, RP11-21L19.1 and RP11-406H23.2 were established and separated pRCC patients into high and low risk groups according to the risk score. The overall survival (OS) between the two groups was significantly different in the training, test and the whole data set (p<0.0001). The area under curves (AUCs) in 1, 3, and 5 years showed that the model was of high efficiency in prognosis prediction. In the correlation analysis between risk score and clinical characteristics, it was found that the prognosis risk was not related to gender, age, weight, laterality, serum calcium level, hemoglobin, platelets, white cells, erythrocyte sedimentation rate

and tumor type (p > 0.05), but related to vital status, race, height, tumor recurrence, primary lymph node (PLN) presentation and TNM stage (p<0.05).

Conclusions: The biomarker based on the five tsDElncRNAs can predict the prognostic risk effectively, and can be used as a target of precise treatment and screening of pRCC patients before operation.

Key words: papillary renal cell carcinoma, long non-coding RNA, survival analysis, prognosis, biomarker

225. A case report of a patient with first phenotype of papillary thyroid carcinoma and heterochronous multiprimary tumor harboring germline MUTYH Arg19*/Gly286Glu mutations

mingbo wang*

Dong'e County People's Hospital

MUTYH-associated polyposis (MAP) is an autosomal recessively inherited disease with multiple system tumors mainly in alimentary system. Tumor occurrence of MAP patients is highly heterogeneous in space and time. MAP is associated with germline biallelic mutations in MUTYH. The targeted next-generation sequencing technology and Sanger sequencing are the important methods to screen MUTYH mutations now. Herein, we identified a patient with heterochronous multiprimary tumor carring MUYTH Arg19*/Gly286Glu compound heterozygous mutations. The patient in this case had a first phenotype of thyroid cancer at age 44, which earlier 2 years than the alimentary system cancers. In conclusion, our case report creases the in-depth understanding of the MAP heterogeneous phenotype and further reminds recommendations for improvement of health management and genetic counseling, special treatment plans.

Key words : case report, MUTYH Arg19*/Gly286Glu mutations

226. MYCN and MYC as potential biomarkers for poor prognosis in small cell lung cancer patients

Xuefeng Liang*、Yuji An、Wenhui Wang、Kejian Wang、Zhenglin Li、Lijun Sheng

山东第一医科大学第三附属医院肿瘤内科

Background: Extensive-stage small cell lung cancer (ES-SCLC) has an extremely poor prognosis, with a median survival of about 8 to 10 months. Platinum-containing two-drug regimens have always been the best choice for first-line therapy. With the deepening of understanding of the molecular biology of SCLC, its genetic background and mechanisms of oncogenesis remain largely unknown. Significant variability in first-line treatment efficacy among different ES-SCLC patients, which makes an urgent need to identify novel prognostic biomarkers to accurately predict patient response to maximize benefit.

Methods: Here we investigated the mutation profiles of 21 ES-SCLC patients using comprehensive next-generation sequencing (NGS) targeting 416 cancer-relevant genes. Upon receiving etoposide combined with cisplatin or carboplatin therapy, the progression-free survival (PFS) and overall survival (OS) was monitored. The association of specific genetic alterations and first-line chemotherapy efficacy was analyzed.

Results： The probability of gene mutation (including point mutation, insertion/deletion mutation, single copy number deletion) in TP53 and RB1 genes was 100% and 90.5%, respectively. The patients carrying MYCN-amplified had significantly shorter OS(P=0.014) and decreased PFS(P=0.082) comparing to those carrying wildtype MYCN. Combined analysis of MYC gene family members, MYC, MYCN, MYCL amplification did not show significant correlation with PFS(P=0.820) and OS(P=0.382). PFS(P=0.049) and OS(P=0.014) were significantly reduced in the state of hyperamplification of MYC, MYCN, and MYCL.

Conclusions: Our results demonstrated that MYCN-amplified and hyperamplification of MYC, MYCN and MYCL can serve as simple but effective biomarker for poor prognosis of first-line treatment in ES-SCLC patients.

Key words: extensive-stage small cell lung cancer, prognosis biomarkers, next-generation sequencing, MYCN, MYC, MYCL

227. Identification of KRAS G12V associated clonal neoantigens and immune microenvironment in long-term survival of pancreatic adenocarcinoma

Chao Wang*、Jun Zhang

Department of Oncology, Shanghai Jiaotong University school of medicine affiliated Ruijin hospital

Objective： To investigate the molecular characteristics in tumor immune microenvironment that affect long-term survival of patients with pancreatic adenocarcinoma (PAAD).

Methods: The tumor related genetic features of a female PAAD patient (over 13-year survival) who suffered from multiple recurrences and metastases, and six operations over one decade were investigated deeply. Genomic features and immune microenvironment signatures of her primary lesion as well as six metastatic tumors at different time-points were characterized.

Results: High-frequency clonal neoantigenic mutations identified in these specimens revealed the significant associations between clonal neoantigens with her prognosis after each surgery. Meanwhile, the TCGA and ICGC databases were employed to analyse the function of KRAS G12V in pancreatic cancer. Conclusions: The genomic analysis of clonal neoantigens combined with tumor immune microenvironment could promote the understandings of personalized prognostic evaluation and the stratification of resected PAAD individuals with better outcome.

Key words: KRAS G12V, Neoantigen, Pancreatic adenocarcinoma, Immune

228. Clinical features of patients with HER2-positive breast cancer and development of a nomogram for predicting survival

Yu Fan*、Yu Wang、Lijia He、Saber Imani、Qinglian Wen

The affiliated hospital of southwest medical university

Background: Different estrogen receptor (ER) and progesterone receptor (PR) expression patterns have important biological and therapeutic implications in patients with human epidermal

growth factor receptor 2 (HER2)-positive breast cancer. However, little is known about hormone receptor (HR)-positive and triple-positive subtypes, making therapy selection and survival prognosis difficult. This study investigated the clinical characteristics and nomogram-predicted survival of patients with HER2-positive breast cancer. Materials and methods: Data on patients with HER2-positive breast cancer were retrieved from the Surveillance, Epidemiology, and End Results database. Comparisons were carried out between single HR-positive and double HR-positive/double HR-negative subtypes. A nomogram-based model of predicted outcomes was developed. Results: This cohort study included 34 819 patients with breast cancer (34 606 women and 213 men). Single HR-positive and double HR-positive/double HR-negative subtypes showed distinct clinicopathological characteristics. Multivariable Cox regression analysis showed that patients with ER-positive/PR-negative/HER2-positive [hazard ratio (HR)= 1.24; 95% confifidence interval (CI): 1.14-1.39], ER-negative/PR-positive/HER2-positive (HR= 1.56; 95% CI: 1.23-1.97), and ER-negative/PR-negative/HER2-positive (HR= 1.56; 95% CI: 1.43-1.70) subtypes had worse breast cancer-specifific survival than patients with the triple-positive subtype. Thirteen clinical parameters were included as prognostic factors in the nomogram: age, sex, race, grade, histology type, bone, brain, liver, and lung metastasis, TNM (tumor-node-metastasis) staging, and molecular subtype. The C-index was 0.853 (95% CI: 0.845-0.861). Calibration plots indicated that the nomogram-predicted survival was consistent with the recorded 3-year and 5-year prognoses. Conclusions: Signifificant differences in survival rates were observed between single HR-positive and double HR-positive/ double HR-negative subtypes. A nomogram accurately predicted survival. Different treatment strategies may be required for HER2-positive patients with single HR-positive and double HR-positive tumors to ensure optimal treatment and benefifits.

Key words: HER2-positive breast cancer, clinical features, triple-positive breast cancer, nomogram, breast cancer-specific survival

229. CLIP4 Shows Putative Tumor Suppressor Characteristics in Breast Cancer: An Integrated Analysis

Yu Fan*、Lijia He、Yu Wang、Shaozhi Fu、Yunwei Han、Juan Fan、Qinglian Wen

The affiliated hospital of southwest medical university

Background: CAP-Gly domain containing linker protein family member 4 (CLIP4) plays an important role in cancers. However, its expression, prognostic value, and biological effect in breast cancer remain unclear. Methods: Data on patients diagnosed with breast cancer were retrieved from the TCGA_x0002_BRCA and other public omics databases. The expression profile of CLIP4 was analyzed using Oncomine, bc-GenExMiner, and TCGA. The prognostic value of CLIP4 was determined by Kaplan-Meier Plotter and Human Protein Atlas. Identifification of genes co-expressed with CLIP4 and potential mechanism analyses were performed using UALCAN, STRING, Metascape, and GSEA. The epigenetic characteristics of CLIP4 were determined by DiseaseMeth and MEXPRESS. Results: CLIP4 was downregulated and its expression was negatively correlated with estrogen receptor (ER), progesterone receptor (PR), human epidermal growth factor receptor type 2 (HER2) status, Nottingham prognostic index (NPI), and Scarff-Bloom-Richardson (SBR) grade in breast cancer, whereas it was positively linked to basal-like and triple negative breast cancer status. Ectopic expression of CLIP4 was related with poor prognosis. In the analysis of genes co-expressed with CLIP4, GSEA showed that the Hedgehog (Hh), JAK-STAT, ERBB, Wnt signaling pathway, cell adhesion molecules, and pathways in cancer were dissimilarly enriched in the CLIP4 expression high phenotype. Analysis of the genetics and epigenetics of CLIP4 indicated that its expression was negatively correlated with DNA methylation. Conclusion: Methylated CLIP4 may be a novel prognostic and therapeutic biomarker for breast cancer.

Key words: DNA methylation, CAP-Gly domain containing linker protein family member 4, breast cancer, prognosis, biomarker, integrated analysis

230. The clinicopathological and prognostic significances of CDC73 expression in breast cancer：A pathological and bioinformatics analysis

ying e*、huachuan zheng、hang xue、congyu zhang、mingzhen zhao

Department of Oncology and Experimental Center, The Affiliated Hospital of Chengde Medical University

Parafibromin is a protein encoded by oncosuppressor CDC73 gene, whose mutation results in the hyperparathyroidism-jaw tumor syndrome (HPT-JT) and parathyroid carcinoma, Down-regulated parafibromin is positively linked to the tumorigenesis of lung, gastric, colorectal and ovarian cancers. Parafibromin expression was detected by RT-PCR, bioinformatics analysis, Western blot and immunohistochemistry, and compared with clinicopathological characteristics of breast cancer. CDC73-related genes and pathways were analyzed using bioinformatics analysis. Parafibromin expression was found to be higher in breast cancer than normal tissues at both mRNA and protein levels (p<0.05). Among triple-negative breast cancers, it was higher in basal-like 1 than basal-like 2 patients (p<0.05), and mesenchymal than immunomodulatory patients (p<0.05). CDC73 mRNA expression was positively correlated with white race, non-filtration of immune cells, favorable luminal subtypes of PAM50 and prognosis of the breast cancer patients (p<0.05). The differential genes of CDC73 was classified into enzyme inhibitor, peptide, and keratinization by KEGG (p<0.05), and into ribosome, TGF-β, oxidation phosphorylation, inositol phosphate metabolism, arachidonic acid metabolism, linoleic acid metabolism, ERBB and VEGF signal pathway by GSEA (p<0.05). The positively-correlated genes of CDC73 were involved in cell mobility, response to interferon α, nuclear pore and basket, histone methytransferase. The negatively-correlated genes of CDC73 were involved in mitochondrial respiratory chain, thermogenesis, and ribosome. Parafibromin expression was higher in invasive ductal than lobular carcinoma (p<0.05), and mucinous adenocarcinoma than others (p<0.05). Parafibromin immunoreactivity was positively associated with high overall survival rate of the breast cancer patients as an independent factor (p<0.05). These findings suggested that up-regulated expression of parafibromin was seen in breast cancer and was closely linked to favorable prognosis of the

breast cancer patients. It was involved in the tumorigenesis and subsequent progression via the regulation of metabolism, ribosome and cytokines.

Key words: breast cancer; parafibromin; pathobiological behaviors; prognosis

231. The effects of REG4 expression on the chemoresistance of ovarian cancer

Liwei Xiang*、huachuan zheng、hang xue、minwen ha

Department of Oncology and Experimental Center, The Affiliated Hospital of Chengde Medical University

Although ovarian cancer usually responds well to platinum-based and taxane-based first-line chemotherapy, most patients develop recurrence and chemoresistance. REG4 is a secretory protein involved in cell differentiation and proliferation, and up-regulated in gastrointestinal and ovarian cancers. We found a higher REG4 expression in ovarian cancer than normal tissues ($p<0.05$) according to Oncomine, and REG4 expression was negatively associated with overall, progression-free or post-progression survival rate of ovarian cancer patients receiving platinum or paclitaxel treatment ($p<0.05$) according to KM plotter. REG4 overexpression resulted in either cisplatin or paclitaxel resistance, and apoptosis resistance in ovarian cancer cells ($p<0.05$). REG4 transfectants showed a stronger migration and invasion of ovarian cancer cells treated with cisplatin or paclitaxel ($p<0.05$). Additionally, cisplatin or paclitaxel exposure led to the overexpression of p-PI3K, p-Akt, p-mTOR, GST-π, surviving, and Bcl-2 in REG4 transfectants, compared with control ($p<0.05$). These suggested that REG4 expression was up-regulated in ovarian cancer, and associated with poor survival and chemotherapy resistance. REG4 promoted the occurrence, development, and chemotherapy resistance of ovarian cancer by regulating cell proliferation, apoptosis, migration, invasion and PI3K/Akt/m-TOR signaling pathway.

Key words: REG4, ovarian cancer, chemoresistance

232. The roles of ING5 in cancer: a tumor suppressor

huachuan zheng*、Hang　Xue、Hua Jiang

The Affiliated Hospital of Chengde Medical University

As Class II tumor supressor, ING5 contains plant homeodomain, nuclear localization signal, novel conserved region, and leucine zipper-like domains. ING5 proteins form homodimer via their N-terminal domain into a coiled-coil structure, and heterodimers with ING4, histone H3K4me3, HAT complex, Tip60, Cyclin A1/CDK2, INCA1 and EBNA3C for the transcription of targe genes. The acetylated proteins upregulated by ING5 are preferentially located in nucleus and act as transcription cofactors, chromatin binding and DNA binding functions, while those downregulated by ING5 mostly in cytoplasm and contribute to metabolism. ING5 promotes the autoacetylation of HAT p300, p53, histone H3 and H4 for the transcription of downstream genes (Bax, GADD45, p21, p27 and so forth). Transcriptionally, YY1 and SRF can up-regulate ING5 mRNA expression by the interaction of YY1-SRF-p53-ING5 complex with ING5 promoter. Translationally, ING5 is targed by miR-196, miR-196a, miR-196b-5p, miR-193a-3p, miR-27-3p, miR-200b/200a/429, miR-1307, miR-193, miR-222, miR-331-3p, miR-181b, miR-543 and miR-196-b. ING5 suppressed proliferation, migration, invasion and tumor growth of various cancer cells via the suppression of EGFR/PI3K/Akt, IL-6/STAT3, Akt/NF-κB/ NF-κB/MMP-9, or IL-6/CXCL12 pathways. ING5-chemoresistance was closely linked to anti- apoptosis, overexpression of chemoresistant genes, the activation of PI3K/Akt, NF-κB and Wnt/ β-catenin signal pathways. Histologically, ING5 abrogation in gastric stem-like and Pdx1- positive cells caused gastric dyplaisa and carcinoma, and conditional ING5 knockout in gastric chief and pdx1-positive cells increased MNU-induced gastric carcinogenesis. Intestinal ING5 deletion increased AOM/DSS-induced colorectal carcinogenesis and decreased high-fat-diet weight. The overexpression and nucleocytoplasmic translocation of ING5 were seen during carcinogenesis, and ING5 expression was inversely linked to aggressive behaviors and poor prognosis in a variety of cancers. These findings indicated that ING5 might be used for a molecular marker for carcinogenesis and subsequent progression, and as a target for gene therapy if its chemoresistant function was ameliorated.

Key words: ING5; cancer; tumor suppressor

233. Oncogenic roles of GPR176 in breast cancer: A marker of aggressiveness and a target of gene therapy

Wenjing Yun*、Huachuan Zheng

The Affiliated Hospital of Chengde Medical University

G-protein-coupled receptor 176 (GPR176) is a member of the G-protein-coupled receptor 1 family, and couples to the unique G-protein subclass Gz/Gx to reduce cAMP production. In this study, GPR176 expression was analyzed by RT-PCR, bioinformatic analysis, western blot, and immunohistochemistry, and its association with clinicopathological characteristics of breast cancer was determined. GPR176-related genes and pathways were subjected to bioinformatic analysis. We also explored the effects of GPR176 on the phenotypes of breast cancer cells. Lower expression of GPR176 mRNA was seen in breast cancer than in normal mucosa, but the opposite pattern was found for its protein (p<0.05). GPR176 mRNA was associated with female sex, low T staging, non-Her-2+ subtypes, non-mutant p53 status, and no purity of immune cells in breast cancer (p<0.05). GPR176 methylation was negatively correlated with its mRNA level and T staging in breast cancer, and was higher in breast cancer than in normal tissues (p<0.05). GPR176 protein expression was associated with older age, smaller tumor size, and the non-luminal-B subtype of breast cancer (p<0.05). The genes differentially expressed between cases with high and low GPR176 expression were involved in receptor-ligand interaction, RNA maturation, hormone, sm-like protein family, cell cycle, proteasome, DNA replication, ECM-receptor interaction, focal adhesion, and p53 signal pathway, among others (p<0.05). GPR176-related genes were categorized into those involved in cell mobility, membrane structure, nerve development, Hippo signal pathway, mitochondrial respiratory chain, and non-alcoholic fatty diver disease, among others (p<0.05). GPR176 knockdown weakened the proliferation, glucose catabolism, anti-apoptosis, anti-pyroptosis, migration, invasion, and epithelial-mesenchymal transition of breast cancer cells. These results indicate that GPR176 might be involved in the tumorigenesis and subsequent progression of breast cancer by deteriorating aggressive phenotypes. It might be

employed as a biomarker to indicate the aggressive behaviors and poor prognosis of breast cancer and as a target of gene therapy.

Key words: breast cancer, GPR176, aggressiveness, prognosis, target therapy

234. The oncogenic roles of GPR176 in ovarian cancer: a molecular target for aggressiveness and gene therapy

Ning Yang*、Hang Xue、Wenjing Yun、Huachuan Zheng

The Affiliated Hospital of Chengde Medical University

Introduction: G-protein-coupled receptor 176 (GPR176) is a member of the G-protein coupled receptor (GPCR) 1 family and produces a 515 amino acid glycosylated protein.

Materials and Methods: In the present study, GPR176 expression was detected using immunohistochemistry (IHC) and compared with clinicopathological characteristics of ovarian cancer using bioinformatics analysis. GPR176-related genes and pathways were analyzed using bioinformatics analysis. In addition, the effects of GPR176 on the phenotypes of ovarian cancer cells were investigated.

Results: GPR176 mRNA expression positively correlated with older age,clinicopathological staging, tumor residual status, and unfavorable survival of ovarian cancer (p<0.05) but negatively with purity loss, infiltration of B cells, and CD8+ T cells (p<0.05). Gene Set Enrichment Analysis (GSEA) showed that differential expression of the GPR176 gene was involved in focal adhesion, ECM-receptor interaction, ribosome, oxidative phosphorylation, actin skeleton, cytokine-cytokine receptor interaction, gap junction, and cell adhesion molecules (p<0.05). STRING and Cytoscape were used to determine the top 10 nodes (FN1, COL1A1, MMP2, COL1A2, COL3A1, THBS1, ACAN, DCN, COL5A1, LUM) which were downregulated in ovarian cancer (p<0.05). Kyoto Encyclopedia of Genes and Genomes (KEGG) analysis indicated that GPR176-related genes were categorized into the AGE-RAGE signaling pathway in diabetic complication, ECM receptor interaction, protein digestion and absorption, ECM structural constituent and organization, and collagen trimer (p<0.05). GPR176 overexpression promoted the proliferation,anti-apoptosis, anti-pyroptosis, migration and invasion of ovarian cancer cells with

overexpression of N-cadherin, Zeb1, Snail, Twist1, and underexpression of gasdermin D, caspase 1, and E-cadherin. These results indicated that GPR176 might be involved in the progression of ovarian cancer by deteriorating aggressive phenotypes.

Conclusion: GPR176 could potentially be used as a biomarker to indicate the aggressive behavior and poor prognosis of ovarian cancer and a target of genetic therapy.

Key words: ovarian cancer, GPR176, aggressiveness, prognosis, target therapy

235. The effects of TRG-AS1/miR-196a-5p/ING5 axis on the gastric cancer

ying chen*、huachuan zheng

The Affiliated Hospital of Chengde Medical University

Summary: ING5 acts as epigenetic readers of the H3K4Me3 histone and targets histone acetyltransferase or histone deacetylase (HDAC) protein complexes for local chromatin remodeling. Here, we found that TRG-AS1 might competitively bind to ING5 mRNA with miR-196a-5p, finally to promote ING5 expression. TRG-AS1, miR-196a-5p inhibitor and ING5 suppressed the proliferation (p<0.05), induced apoptosis (p<0.05), and inhibited migration, and invasion (p<0.05) in gastric cancer cells, while TRG-AS1 knockdown and miR196a-5p had the opposite results. TRG-AS1 blocked the effects of miR196a-5p on the proliferation, apoptosis and invasion of gastric cancer cells， but deteriorated the miR196a-5p inhibitor (p<0.05). TRG-AS1 expression was lower in gastric cancer than normal tissues (p<0.05), and positively correlated with T stage, clinicopathological staging, histological grading and dedifferentiation, histological grading and favorable prognosis of gastric cancer (p<0.05). The differential genes of TRG-AS1 included cytokine-cytokine receptor interaction, CXCR chemokine binding, immunoglobulin and T cell receptor complexes, complement activation, immune and immunodeficiency, GRCR ligand binding, signaling by interleukin, immunoregulattion, phospholipids in phagocytosis, and so forth (p<0.05). miR196a-5p expression was high in gastric cancer than normal tissues (p<0.05), and negatively associated with N stage, diffuse-type carcinoma, dedifferentiation, Helicobacter pylori infection and poor prognosis (p<0.05). The differential genes of miR-196a-5p included protein

digestion and absorption, pancreatic secrtion, aspartic-type peptidase, intermediate filament, and keratinization,cytokine-cytokine receptor interaction, GPCRS class A rhodopsinlike, platelet activation signaling and AGGR, oxidative phosphorylation, and so forth (p<0.05).

Key words : Gastric cancer; ING5; TRG-AS1; miR-196-5p.

236. Transcriptional regulation of ING5 and its suppressive effects on gastric cancer

Hang Xue、Huachaun Zheng

The Affiated Hospital of Chengde Medical University

Background: ING5 acts as an epigenetic reader of H3K4Me3 and targets histone acetyltransferase or histone deacetylase complexes for local chromatin remodeling. However, its transcriptional regulation and suppressive effects on gastric cancer remain elusive.

Method : Luciferase assay, EMSA, and ChIP were used to identify the cis-acting elements and trans-acting factors of the ING5 gene. We also analyzed the effects of SAHA on the aggressive phenotypes of SGC-7901 ING5 transfectants, and the effects of different ING5 mutants on the aggressive phenotypes of SGC-7901 cells. Finally, we observed the effects of ING5 abrogation on gastric carcinogenesis.

Results： A promoter of ING5 was located from -50 bp upstream to the transcription start site, a suppressor between -2000 and -1000 bp, and an enhancer between -800 and -100 bp. EMSA and ChIP showed that both SRF (-717 to -678 bp) and YY-1 (-48 to 25 bp) interacted with the promoter of ING5 and up-regulated ING5 expression in gastric cancer via SRF-YY1-ING5-p53 complex formation. ING5, SRF, and YY1 were overexpressed in gastric cancer, compared with the levels in normal mucosa (p<0.05), and associated with worse prognosis of gastric cancer patients (p<0.05). ING5 had positive relationships with SRF and YY1 mRNA expression in gastric cancer (p<0.05). SAHA treatment caused early arrest at S phase in ING5 transfectants of SGC-7901 (p<0.05), and either 0.5 or 1.0 μM SAHA enhanced their migration and invasion (p<0.05). The wild-type (WT) and mutant ING5 transfectants showed lower viability and invasion than the control (p<0.05) with low CDC25, VEGF, and MMP-9 expression. Gastric

adenocarcinoma was observed in Atp4b-cre; ING5f/f, Pdx1-cre;ING5f/f, and K19-cre;ING5f/f mice. The latter 2 mice had a high susceptibility to chemically-induced gastric carcinogenesis.

Conclusion： ING5 mRNA might be a good marker of gastric carcinogenesis, aggressiveness, and poor prognosis. ING5 expression was shown to be positively regulated by the interaction of SRF-YY1-ING5-p53 complex with the ING5 promoter from -50 bp upstream to the transcription start site. ING5 deletion in parietal, stem-like, and Pdx1-positive cells of gastric epithelium might contribute to the histogenesis of gastric cancer.

Key words： Gastric cancer · ING5 · transcriptional regulation ·tumor suppressor

237. The roles of BTG4 mRNA expression in cancers: a bioinformatics analysis

Hailan Xu*、Huachuan Zheng

The Affiated Hospital of Chengde Medical University

Objective: BTG4 has anti-proliferative property by arresting cell cycle, and suppresses the oocytes and embryos development and carcinogenesis. This study aimed to clarify the clinicopathological and prognostic significances of BTG4 mRNA expression in cancers.

Materials and methods: We performed a bioinformatics analysis of BTG4 mRNA expression through Oncomine, TCGA and Kaplan-Meier databases up to July 1, 2017.

Results: Down-regulated BTG4 expression was observed in gastric and lung cancers, compared with normal tissues ($p<0.05$), but versa for breast and ovarian cancers ($p<0.05$). TCGA database showed that BTG4 expression was negatively related to the overall survival rate of gastric cancer patients ($p<0.05$). It was higher in male than female patients with lung cancer ($p<0.05$), and in squamous cell carcinoma than adenocarcinoma patients ($p<0.05$). Cox's analysis showed that younger age, T staging, lymph node metastasis and low BTG4 expression were independent factors for worse prognosis of the lung cancer patients ($p<0.05$). BTG4 expression was negatively correlated with T staging and distant metastasis of breast cancer patients ($p<0.05$). According to Kaplan-Meier plotter, we found that BTG4 expression was negatively correlated with overall, progression-free, post-progression or relapse-free survival rates of the patients with gastric, lung

or ovarian cancer, even stratified by aggressive parameters (p<0.05). It was the same for the distant-metastasis-free survival rate of the patients with the breast cancer carrying wild-type p53 (p<0.05). However, the converse was true for the overall and relapse-free survival rates of breast cancer patients (p<0.05) or for the overall survival of T2 or M0 gastric cancer patients.

Conclusion: BTG4 expression might be considered as a potential marker to indicate carcinogenesis, histogenesis, aggressive behaviors, and prognosis.

Key words: BTG4, bioinformatics analysis, carcinogenesis, aggressive behaviors, prognosis

238. Survival Prediction of Patients Treated with Immune Checkpoint Inhibitors via KRAS/TP53/EGFR-single Gene Mutation

shuai geng*

Strategic Support Force Medical Center

Background: Immune checkpoint inhibitors (ICIs) have become an effective treatment option for cancer. KRAS, EGFR and TP53 are common mutated oncogenes in cancer whose single gene status may predict the therapeutic effect of clinical ICIs. In this efficacy evaluation, we aimed to clarify whether the single gene mutation status of KRAS, EGFR or TP53 affects the survival benefits of ICIs in cancer patients.

Methods: We used PubMed, Cochrane Library, web of science, and clinical trials Gov database to retrieve qualified documents, the time was up to January 2022. Hazard ratios (HRS) and 95% confidence intervals (CIs) were used to determine the single gene mutation status and no progression of KRAS, EGFR or TP53.

Results: A total of 19 studies included 7029 cancer patients treated with ICIs. The results showed that KRAS, EGFR or TP53 single gene mutation could significantly improve PFS and OS in patients receiving ICIs, but the degree of improvement was different. The risk of prolongation of PFS (HR= 1.48, 95% CI= 1.19-1.85, P= 0.0004) and OS (HR= 1.68, 95% CI= 1.36-2.07, P<0.00001) caused by TP53 single gene mutation was relatively high, the risk ratio of prolongation of PFS (HR= 1.38, 95% CI= 1.21-1.57, P<0.00001) and OS (HR= 1.56, 95% CI=

1.20-2.04, *P*= 0.001) caused by EGFR single gene mutation was the second, the risk ratio of prolongation of PFS (HR= 1.33, 95% CI= 1.12-1.57, *P*= 0.001) and OS (HR= 1.39, 95% CI= 1.18-1.63, *P*<0.00001) caused by KRAS single gene mutation was relatively low, and the results were significantly different.

Conclusion: In cancer patients, KRAS, EGFR or TP53 single gene status is correlated with the benefits of immunotherapy PFS and OS, which suggests that gene sequencing should be carried out in time in the process of clinical treatment to determine the gene mutation of patients and better predict the clinical treatment effect of ICIs.

Key words: Immune checkpoint inhibitors; Cancer; Gene mutation; Progression free survival; Overall survival; Survival benefit

239. The clinicopathological and prognostic significances of GPR176 in colorectal cancer

Cuiyu Hu*、Hua-chuan Zheng、Hang Xue、Wen-jing Yun

The Affiliated Hospital of Chengde Medical University

G protein-coupled receptor 176 (GPR176) is a member of the G-protein coupled receptor 1 family, and produces 515-aa glycosylated protein. Here, we found that GPR176 expression was higher in colorectal cancer than normal tissue at both mRNA and protein levels (p<0.05), opposite to its methylation (p<0.05). GPR176 mRNA expression was positively correlated with white race, depth of invasion, lymph node metastasis, TNM staging and short survival times of colorectal cancer (p<0.05). Immunohistochemically, GPR176 expression was positively correlated with lymphatic invasion, liver metastasis, distant metastasis, and differentiation of colorectal cancer (p<0.05). GPR176 methylation was negatively correlated with its mRNA expression, male gender, younger age, Afican-American race, N stage, clinicopathological stage, and p53 mutation (p<0.05). The differential genes of GPR176 were involved in ECM constituent, interaction and organization, synaptic membrane, angiogenesis, ECM-receptor interaction, DNA replication, cell adhesion molecules, neuroactive ligand receptor interaction, and so forth (p<0.05). GPR176-related genes were categorized into protein digestion and absorption, extracellular matrix,

collagen signal pathways, proteasome, transmembrane transporter, mitochondrial membrane, transport signal pathways, and so on (p<0.05). The results indicated that GPR176 might be employed to reflect the aggressiveness of colorectal cancer in clinical practice.

Key words: colorectal cancer, GPR176, aggressiveness, prognosis

240. The roles of BTG3 mRNA expression in cancers: a bioinformatics analysis

huachuan zheng*、Congyu Zhang

The Affiliated Hospital of Chengde Medical University

Abstract: BTG3 is reported to be a tumor suppressor and suppresses proliferation and cell cycle progression. Here, we performed a bioinformatics analysis of BTG3 mRNA expression through Oncomine, TCGA and KM plotter databases. Up-regulated BTG3 expression was found in gastric, lung, breast and ovarian cancers, compared with normal tissues (p<0.05). BTG3 expression was found to negatively associate with histological grading and dedifferentiation of gastric cancer (p<0.05), and tumor size of lung cancer (p<0.05). Pulmonary adenocarcinoma patients had a higher BTG3 expression than squamous cell carcinoma ones (p<0.05). A higher BTG3 expression was seen in invasive ductal than lobular carcinomas (p<0.05). According to KM plotter, BTG3 expression was positively correlated with overall, progression-free or post-progression survival rate of gastric and ovarian cancer patients, even stratified by aggressive parameters (p<0.05). However, the converse was true for overall, progression-free relapse-free, post-progression or distant-metastasis-free survival rates in lung and breast cancers, even stratified by different subgrouping (p<0.05). According to TCGA database, BTG3 expression was positively linked to overall survival rate of lung cancer patients as an independent factor (p<0.05). These findings suggested that BTG3 overexpression was positively linked to carcinogenesis, histogenesis and aggressive behaviors, and employed to evaluate the prognosis of cancers.

Key words: BTG3; bioinformatics analysis; carcinogenesis; aggressive behavior; prognosis

241. Identification of a Prognostic Colorectal Cancer Model Including LncRNA FOXP4-AS1 and LncRNA BBOX1-AS1 Based on Bioinformatics Analysis

zhiliang shi*[1,2]、guoqiang zhou[1]、jian guo[1]、xiaoling yang[1]、cheng yu[1]、chenglong shen[1]、xinguo zhu[2]

1. Changshu NO.2 People's Hospital

2. 苏州大学附属第一医院

Background: Knowledge about the prognostic role of long noncoding RNA (lncRNA) in colorectal cancer(CRC) is limited. Therefore, we constructed a lncRNA-related prognostic model based on data from the Gene Expression Omnibus (GEO) and The Cancer Genome Atlas (TCGA).

Materials and Methods: CRC transcriptome and clinical data were downloaded from the GSE20916 dataset and the TCGA database, respectively. R software was used for data processing and analysis. The ifferentiallncRNA expression within the two datasets was first screened, and then intersections were measured. Coxregression and the Kaplan–Meier method were used to evaluate the effects of various factors on prognosis. The area under the curve (AUC) of the receiver operating characteristic curve and a nomogram based on multivariate Cox analysis were used to estimate the prognostic value of the lncRNA-related model. Gene Ontology (GO) and Kyoto Encyclopedia of Genes and Genomes (KEGG) enrichment analyses were applied to elucidate the significantly involved biological functions and pathways.

Results: A total of 11 lncRNAs were crossed. The univariate Cox analysis screened out two lncRNAs, which were analyzed in the multivariate Cox analysis. A nomogram based on the two lncRNAs and other clinicopathological risk factors was constructed. The AUC of the nomogram was 0.56 at 3 years and 0.71 at 5 years. The 3-year nomogram model was compared with the ideal model, which showed that some indices of the 3-year model were consistent with the ideal model, suggesting that our model was highly accurate. The GO and KEGG enrichment analyses showed that positive regulation of secretion by cells, positive regulation of secretion,positive regulation of exocytosis, endocytosis, and the calcium signaling pathway were differentially enriched in the two-lncRNA-associated phenotype.

Conclusions: A two-lncRNA prognostic model of CRC was constructed by bioinformatics analysis. The model had moderate prediction accuracy, LncRNA BBOX1-AS1 and lncRNA FOXP4-AS1 were identified as prognostic biomarkers.

Key words: bioinformatics analysis, colorectal cancer, lncRNA, prognostic model

242. The roles of parafibromin in cancer: a tumor suppressor

huachuan zheng*、ying e、hang xue

The Affiliated Hospital of Chengde Medical University

The hyperparathyroidism-jaw tumor (HPT-JT) syndrome is an autosomal dominant disease, and resulted from CDC73 mutation, which encodes parafibromin protein. WT1 transcriptionally down-regulated CDC73, and CDC73 is translationally targeted by miR-182-3p and miR-155. In the nucleus, parafibromin binds to RNA polymerase II and PAF1 complex for transcription. Parafibromin transcriptionally increases the expression of c-myc, decreases CPEB1 expression by interacting with H3M4, and reduces Cyclin D1 expression by binding to H3K9. RNF20/RNF40/parafibromin complex induces monoubiquitination of H2B-K120. SHP2-mediated dephosphorylation of parafibromin promotes the parafibromin/ β-catenin interaction, and induces the expression of Wnt target genes, which is blocked by PTK6-mediated phosphorylation. Parafibrominom physically associates with the CPSF and CstF complexes that are essential for INTS6 mRNA maturation. In the cytosol, parafibromin binds to hSki8 and eEF1Bγ for the destabilization of p53 mRNA, to JAK1/2-STAT1 for STAT1 phosphorylation, and to actinin-2/3 for bundle/cross-linking actin filaments. CDC73 knockout mice in parathyroid developed parathyroid and uterine tumors as a model for HPT-JT syndrome. Conditional deletion of CDC73 in mesenchymal progenitors results in the embryos with no development of the heart and liver, while its abrogation in mature osteoblasts and osteocytes increases cortical and trabecular bone. Heterozygous germline mutations cause HPT-JT, and are associated with parathyroid carcinogenesis. CDC73 mutation and parafibromin loss were decreased from parathyroid adenoma, atypical adenoma to carcinoma. Additionally, down-regulated parafibromin was closely linked to

the tumorigenesis, subsequent progression or poor prognosis of head and neck cancers, gastric, lung, colorectal, and ovarian cancers, and its overerexpression might reverse the aggressiveness of these cancer cells. Therefore, parafibromin might be employed as a biological marker of malignancies and a target for their genetic therapy.

Key words: parafibromin; cancer; tumor suppressor

243. Identification of a novel mRNA-miRNA-lncRNA competing endogenous RNA network associated with prognosis of pancreatic cancer

Yanrong Wang*

Southwest Medical University

Aim: To identify a novel competitive endogenous RNA (ceRNA) network related to the prognosis of pancreatic cancer (PCa).

Methods: Based on the intersection of four human gene expression datasets obtained from Gene Expression Omnibus (GEO) database, a ceRNA network was constructed using a variety of bioinformatics tools.

Results: A total of 132 up-regulated mRNAs and 58 down-regulated mRNAs were identified. Through the stepwise reverse prediction from mRNA to lncRNA and the verification through expression and survival analysis, 16 hub genes, 1 key miRNA and 3 key lncRNAs were identified. Finally, a ceRNA network composed of LINC01578, PVT1, TNRC6C-AS1, miR-16-5p, ITGA2, ITGA3, COL8A1, COL12A1, FN1 and RUNX2 was constructed.

Conclusion: The current study successfully constructed a novel human PCa-related ceRNA network, and provided potential targets for the clinical treatment of PCa.

Key words: pancreatic cancer, competing endogenous RNA, long noncoding RNA, miRNA, bioinformatic analysis

244. Identification of Prognostic Biomarkers and Therapeutic Targets Among CCN Family Genes in Human Gastric Cancer

Mengqi Yang *[1]、Huanting Chen[2]、Yajie Liu[1]

1. Peking University Shenzhen Hospital

2. 深圳市宝安区人民医院

Background: Gastric cancer (GC) is a deadly malignancy with an ever-increasing incidence worldwide. Research studies should be conducted to discover reliable prognostic biomarkers and novel therapeutic targets to prolong patients' survival. Our bioinformatics analysis first identified highly expressed WISP1 in GC tissues compared with healthy controls. WISP1 is a member of cellular communication network (CCN) family which exerts regulatory functions on cell proliferation, differentiation, and migration. To date, the expression and prognostic values of CCN family members in GC remain unclear.

Methods: We first selected three gene chips from Gene Expression Omnibus and obtained the commonly up-expressed genes in these datasets. We next assessed the genetic alteration and functions enrichment using cBioPortal and Metascape databases, as well as DAVID tool. The mRNA and protein expressions of CCN family in patients with GC were analyzed with GEPIA, ONCOMINE, and HPA databases. We analyzed the prognostic value of distinct CCN family members in patients using the Kaplan–Meier plotter database. We explored which transcription factors involved in the regulation of CCN family genes via the TRRUST database and the effect CCN family gene on the immune cells in gastric tumor microenvironment via the TIMER database.

Results: mRNA deregulation of CCN family genes was the most common alteration in patients with GC. The functions of CCN family were mainly involved in intercellular interactions. WISP1 was significantly elevated while WISP2 were reduced from GEPIA database. However, most CCN family genes were highly expressed in GC tissues with different pathological types in ONCOMINE. And a significant correlation was found between the expression of NOV and WISP1 and the pathological stage of patients with GC. Importantly, Patients with low

transcription levels of WISP1/2/3 and NOV were associated with a significantly better prognosis in patients with GC. Our data revealed that WT1 and STAT3 are key transcription factors for CCN family. In addition, we found significant associations between the expression of CCN family genes and the infiltration of immune cells.

Conclusions: These findings may provide useful and novel information for the identification of potential prognostic biomarkers and therapeutic targets for GC.

Key words: gastric cancer, prognostic biomarkers, therapeutic targets, CCN family, tumor microenvironment

245. Immune checkpoints TIM-3 expression in circulating and tumor-infilitrating $CD4^+$ and $CD8^+$ T cells in ovarian cancer patients

Jie Li*

tongji hospital, huazhong university of science and technology

Immune checkpoints inhibitors (ICC) are promising therapeutic approach, however limited efficacy has shown in clinical trials, like KEYNOTE-100. Success of PD-1/PD-L1 blockade brings promise to ovarian cancer (OC) treatment, but also with the declining efficacy, for its primary and acquired resistance. T cell immunoglobulin and mucin domain-3 (TIM-3), as an immunosuppressive biomarker in T cells, reported to be elevated in PD-1/PD-L1 inhibitors therapy. In this study, we analyzed Tim-3 and other key immunosuppressive biomarkers expression in $CD4^+$ and $CD8^+$ T cells from tumor sites, compared with ascites and peripheral blood from the same OC patients and peripheral blood from healthy volunteers. We also investigated the correlation between the levels of Tim-3 expression in $CD4^+$ and $CD8^+$ T cells and clinicopathological features including serum levels of CA125 and disease stage.

Key words: ovarian cancer, immune checkpoints, tumor microenvironment

246. Reliability analysis of exonic-breakpoint fusions identified by DNA sequencing for predicting the efficacy of targeted therapy in non-small cell lung cancer

Weihua Li*[1]、Rui Wan[1]、Lei Guo[1]、Dong Jiang[2]、Lin Meng[2]、Jianming Ying[1]

1. Departments of Pathology, National Cancer Center/National Clinical Research Center for Cancer/Cancer Hospital, Chinese Academy of Medical Sciences and Peking Union Medical College

2. 北京诺禾致源

Background: Diverse genomic breakpoints of fusions that localize to intronic, exonic or intergenic regions have been identified by DNA next-generation sequencing (NGS), but the role of exonic breakpoints remains elusive. We investigated whether exonic-breakpoint fusions could predict matched targeted therapy efficacy in non-small cell lung cancer (NSCLC).

Methods: NSCLC samples were analyzed by DNA NGS, RNA NGS, immunohistochemistry (IHC) and fluorescence in situ hybridization.

Results: Using DNA NGS, kinase fusions were identified in 685 of 7148 (9.6%) NSCLCs, with 74 harboring exonic-breakpoint fusions, mostly anaplastic lymphoma kinase (ALK) fusions. RNA NGS and IHC revealed that 11 of 55 (20%) exonic-breakpoint fusions generated no aberrant transcript/protein, possibly due to open reading frame disruption or different gene transcriptional orientations. Four cases of genomic-positive but RNA/protein-negative fusions were treated with matched targeted therapy, but progressive disease developed within 2 months. Nevertheless, 44 of 55 (80%) exonic-breakpoint fusions produced chimeric transcripts/proteins, possibly owing to various alternative splicing patterns, including exon skipping, alternative splice site selection and intron retention. Most of these genomic- and RNA/protein-positive fusion cases showed a clinical response to matched targeted therapy. Particularly, there were no differences in objective response rate (P=0.714) or median progression-free survival (P=0.500) between intronic-breakpoint (n=56) and exonic-breakpoint ALK fusion subtypes (n=11) among ALK RNA/protein-validated patients who received first-line crizotinib.

Conclusions: Exonic-breakpoint fusions may generate in-frame fusion transcripts/proteins or not, and thus are unreliable for predicting the efficacy of targeted therapy, which highlights the

necessity of implementing RNA or protein assays for functional validation in exonic-breakpoint fusion cases.

Key words: non-small cell lung cancer, DNA sequencing, exonic-breakpoint fusion, alternative splicing, targeted therapy

247. NEK9, a novel effector of IL-6/STAT3, regulates metastasis of gastric cancer by targeting ARHGEF2 phosphorylation

Guofang Lu*、Siyuan Tian、Yi Sun、Jiaqiang Dong、Na Wang、Jiaoxia Zeng、Yongzhan Nie、Kaichun Wu、Bin Feng、Ying Han、Yulong Shang

Xijing Hospital of Digestive Diseases,Fourth Military Medical University

Rationale: Inflammatory stimuli from the tumor microenvironment play important roles in cancer progression. However, the mechanism of promotion of cancer metastasis by inflammation in gastric cancer (GC) is poorly understood.

Methods: The roles of NEK9 were validated via loss-of-function and gain-of-function experiments in vitro and in an animal model of metastasis. Cytoskeletal reorganization-associated molecules were detected by GST pull-down. The regulation of ARHGEF2 by NEK9 was investigated by phosphoproteomics analysis, immunoprecipitation (IP) and in vitro kinase assay. The transcriptional regulation of miR-520f-3p was studied using luciferase reporter and chromatin immunoprecipitation (ChIP). The expression of these proteins in GC tissues was examined by immunohistochemistry.

Results: NEK9 directly regulates cell motility and RhoA activation in GC. The phosphorylation of ARHGEF2 by NEK9 is the key step of this process. NEK9 is a direct target of miR-520f-3p, which is transcriptionally suppressed by IL-6-mediated activation of STAT3. A decrease in miR-520f-3p leads to the amplification of IL-6/STAT3 by targeting GP130. A simultaneous elevation of the levels of NEK9, GP130 and p-STAT3 was confirmed in the lymph nodes and distant metastases. An increase in NEK9, GP130 and STAT3 is associated with reduced overall survival of GC patients.

Conclusion: This study demonstrates that activation of STAT3 by IL-6 transcriptionally suppresses miR-520f-3p and diminishes the inhibitory effects of miR-520f-3p on NEK9 and GP130. An increase in GP130 enhances this signaling, and NEK9 directly influences cell motility and RhoA activation by targeting the phosphorylation of ARHGEF2. Targeting the IL-6-STAT3-NEK9 pathway may be a new strategy for GC treatment.

Key words: Gastric cancer, Metastasis, NEK9, Inflammation, Phosphorylation

248. KRT80 expression works as a biomarker and a target for differentiation in gastric cancer.

Kaihang Shi [1]、Hang Xue[1]、Enhong Zhao[1]、Lijun Xiao[2]、Hongzhi Sun[3]、Huachuan Zheng*[1]

1. The Affiliated Hospital of Chengde Medical University

2. 承德医学院

3. 锦州医科大学附属第一医院

Keratin 80 (KRT80) is a filament protein that participates in cell differentiation and the integrity of the epithelial barrier. Here, KRT80 expression was higher in gastric cancer compared with normal mucosa at both mRNA and protein levels by qRT-PCR and Western blot (p<0.05), opposite to KTR80 methylation (p<0.05). There was a negative relationship between promoter methylation and expression level of KRT80 gene at in gastric cancer (p<0.05). KRT80 mRNA and protein expression was positively correlated with the differentiation of gastric cancer (p<0.05), while KRT80 methylation was negatively associated with gastric cancer differentiation and p53 mutation (p<0.05). The expression of KRT80 mRNA was positively linked to no infiltration of immune cells, the short survival time of gastric cancers (p<0.05). The differential genes of KTR80 mRNA were involved in ligand-receptor interaction, estrogen signal pathway, peptidase, filament and cytoskeleton, keratinocyte differentiation, vitamin D receptor, muscle contraction, and B cell-mediated immune (p<0.05). KRT80-related genes were classified into cell adhesion and junction, cadherin binding, skin and epidermis development, and so forth (p<0.05). KRT80 knockdown suppressed proliferation, anti-apoptosis, anti-pyroptosis, migration, invasion and epithelial-mesenchymal transition in gastric cancer cells (p<0.05). These findings indicated that

up-regulated expression of KRT80 played a crucial part in gastric carcinogenesis, and might be considered as a biological marker for aggressive behaviors and poor prognosis. Its silencing might be used as an approach of target therapy for gastric cancer patients.

Key words: gastric cancer, KRT80, biological behaviors, prognosis, gene therapy

249. KRT80 expression works as a biomarker and a target for differentiation in gastric cancer.

Kaihang Shi [1]、Hang Xue[1]、Enhong Zhao[1]、Lijun Xiao[2]、Hongzhi Sun[3]、Huachuan Zheng*[1]

1. The Affiliated Hospital of Chengde Medical University

2. 承德医学院

3. 锦州医科大学附属第一医院

Keratin 80 (KRT80) is a filament protein that participates in cell differentiation and the integrity of the epithelial barrier. Here, KRT80 expression was higher in gastric cancer compared with normal mucosa at both mRNA and protein levels by qRT-PCR and Western blot (p<0.05), opposite to KTR80 methylation (p<0.05). There was a negative relationship between promoter methylation and expression level of KRT80 gene at in gastric cancer (p<0.05). KRT80 mRNA and protein expression was positively correlated with the differentiation of gastric cancer (p<0.05), while KRT80 methylation was negatively associated with gastric cancer differentiation and p53 mutation (p<0.05). The expression of KRT80 mRNA was positively linked to no infiltration of immune cells, the short survival time of gastric cancers (p<0.05). The differential genes of KTR80 mRNA were involved in ligand-receptor interaction, estrogen signal pathway, peptidase, filament and cytoskeleton, keratinocyte differentiation, vitamin D receptor, muscle contraction, and B cell-mediated immune (p<0.05). KRT80-related genes were classified into cell adhesion and junction, cadherin binding, skin and epidermis development, and so forth (p<0.05). KRT80 knockdown suppressed proliferation, anti-apoptosis, anti-pyroptosis, migration, invasion and epithelial-mesenchymal transition in gastric cancer cells (p<0.05). These findings indicated that up-regulated expression of KRT80 played a crucial part in gastric carcinogenesis, and might be

considered as a biological marker for aggressive behaviors and poor prognosis. Its silencing might be used as an approach of target therapy for gastric cancer patients.

Key words: gastric cancer, KRT80, biological behaviors, prognosis, gene therapy

250. A lncRNA signature associated with tumor immune heterogeneity predicts distant metastasis in locoregionally advanced nasopharyngeal carcinoma

Yelin Liang*[1]、Yuan Zhang[1]、Xirong Tan[1]、Han Qiao[1]、Songran Liu[1]、Linglong Tang[1]、Yanping Mao[1]、Lei Chen[1]、Wenfei Li[1]、Guanqun Zhou[1]、Yin Zhao[1]、Junyan Li[1]、Qian Li[1]、Shengyan Huang[1]、Sha Gong[1]、Ziqi Zheng[1]、Zhixuan Li[1]、Ying Sun[1]、Wei Jiang[2]、Jun Ma[1]、Yingqin Li[1]、Na Liu[1]

1. Sun Yat-sen University cancer center

2. Affiliated Hospital of Guilin Medical University

Purpose: Distant metastasis is the primary reason for locoregionally advanced nasopharyngeal carcinoma (LA-NPC) associated deaths. Here, we assessed the utility of long noncoding RNAs (lncRNAs), which were newly characterized as metastasis regulators, for metastasis prediction in LA-NPC.

Experimental Design: Microarrays were employed to profile lncRNAs in the discovery cohort (n= 56). The differential analysis identified metastasis-related lncRNAs, which were further measured using RT-qPCR assay in the Guangzhou training cohort (n= 177). A penalized Cox regression method was adopted to develop a lncRNA signature, followed by validations in Guangzhou internal (n= 177) and Guilin external cohorts (n= 150). Furthermore, the lncRNA signature was assessed for associations with tumor heterogeneity using bioinformatic analysis, the finding of which was confirmed with immunohistochemistry.

Results: A nine-lncRNA signature was constructed to classify patients into high-risk and low-risk groups in the training cohort. Patients in the high-risk group had a significantly higher risk of distant metastasis (HR 6.04, 95% CI 2.82–12.94, P<0.001). Validation in the Guangzhou internal and Guilin external cohorts yielded similar results and verified that the nine-lncRNA signature

was an independent and consistent factor of LA-NPC metastasis. Integrative analyses showed that the nine-lncRNA signature correlated with immune activity and tumor lymphocyte infiltration, which was validated using a digital pathology method. Patients in the low-risk group had significant activation of the immune microenvironment and had more B cell and CD8+ T cell infiltration.

Conclusions: In this multicenter retrospective cohort study, we identified an immune-associated signature, which can serve as a promising biomarker for metastasis prediction in LA-NPC.

Key words: nasopharyngeal carcinoma, distant metastasis, immune-related lncRNA signature

251. The roles of REG4 expression in colorectal cancer: a potential marker for carcinogenesis and subsequent progression

Congyu Zhang*[1]、Hua-chuan Zheng[2]、Hang Xue[2]

1. The First Affiliated Hospital of Jinzhou Medical University

2. 承德医学院附属医院

Abstract: REG4 is a potent activator of EGFR/Akt/AP-1 pathway, and protects cancer cell against apoptotic induction. Here, we performed a meta-, bioinformatics and pathological analysis of REG4 expression in colorectal cancer. The effects of REG4 on the phenotypes and related proteins were also investigated in colorectal cancer cells. We- found a higher REG4 mRNA expression in colorectal cancer than normal mucosa (p<0.05), but opposite for its protein. REG4 mRNA expression was negatively correlated with lymph node metastasis, distant metastasis, TNM staging and adenocarcinoma subtype, but positively with MSI status, BRAF mutation and favorable overall survival of cancer (p<0.05). According to bioinformatics databases, REG4 mRNA expression was higher in colorectal adenoma and cancer than normal tissues (p<0.05), and negatively correlated with lymph node metastasis, distant metastasis, TNM staging and overall survival rate, but positively with MSI status and BRAF mutation in colorectal cancer (p<0.05). These findings indicated that REG4 expression might be employed as a potential marker to indicate colorectal carcinogenesis and subsequent progression, even prognosis. REG4-related

genes included chemokine activity, taste receptor, protein-DNA and DNA packing complex, nucleosome and chromatin, generation of second messenger molecules, PD1 signaling, epigenetic regulation and DNA methylation, transcription repression and activation by DNA binding, insulin signal pathway, sugar metabolism and transfer, neurotransmitter receptor, and so forth (p<0.05). REG4 expression was positively with lymph node metastasis, TNM staging, dedifferentiation and unfavorable overall survival of colorectal cancer (p<0.05). REG4 exposure or transfectants showed G2/S progression, apoptotic induction, a high proliferation, migration and invasion in comparison with the control or mock (p<0.05). These findings indicated that REG4 expression might be employed as a potential marker to indicate gastric carcinogenesis and subsequent progression, even prognosis.

Key words: REG4; colorectal cancer; meta analysis; bioinformatics analysis; ; biomarker, prognosis, phenotypes

252. Clinical value of PRC1 and DLGAP5 and immunosuppressive T cells overexpressing them in HCC based on bulk and single-cell RNA data

Chenglei Yang*、Jiatai He、Rui Song、Bangde Xiang

Guangxi Medical University Cancer Hospital

Purpose: Despite immune checkpoint inhibitor (ICI) has recently taken on an extremely important role in tumors, only a minority of hepatocellular carcinoma (HCC) patients are effective. The clinical value of PRC1 and DLGAP5 in HCC and its relationship with immune microenvironment have been rarely reported.

Methods: Key genes related to doubling time of HCC tumors were identified using WGCNA, and their expression was analyzed against our in-house RNA sequencing database, the Gene Expression Omnibus and the Cancer Genome Atlas database. We explored correlations between key genes and the immune microenvironment based on the TISCH and TIMER database, as well as clinicopathological characteristics and prognosis of HCC in patients at our center.

Results: WGCNA identified PRC1 and DLGAP5 as key genes in HCC. PRC1 and DLGAP5 were over-expressed in HCC tissues relative to normal tissues based on analysis of 2,154 patients and 1,344 controls. The genes gave respective areas under the summary receiver operator characteristic curve of 0.95 (95%CI 0.93-0.97) and 0.94 (95%CI 0.92-0.96). High expression of PRC1 and DLGAP5 positively correlated with tumor recurrence and microvascular invasion, was an independent risk factor for poor overall survival. PRC1 and DLGAP5 were co-expressed in proliferative T cells over-expressing immunosuppressive markers PDCD1, CTLA4, HAVCR2, LAG3 and TIGIT based on single-cell RNA-sequencing datasets. Conclusions: PRC1 and DLGAP5 significantly upregulated in HCC are associated with poor prognosis and show strong diagnostic potential. PRC1 or DLGAP5 combined with CD8 T cell markers may serve as predictive biomarkers for the efficacy of ICI combination therapy.

Key words: hepatocellular carcinoma; PRC1; DLGAP5; clinical value; immune microenvironment

253. How Nanotechniques Could Vitalize the O-GlcNAcylation-Targeting Approach for Cancer Therapy

Rui Yang、Daozhen Chen*

Affiliated Wuxi Maternity and Child Health Care Hospital of Nanjing Medical University

Accumulated data indicated that many types of cancers have increased protein O-GlcNAcylation at cell surface and inside cells. The aberrant O-GlcNAcylation is considered a potential therapeutic target. Although several types of compounds capable of inhibiting O-GlcNAcylation have been developed, their low solubility, poor permeability and delivery efficiency have impeded the application for in vivo and pre-clinical studies. Nanocarriers have the advantages of controllable drug release and active cancer-targeting capability. Moreover, nanoparticles can improve drug delivery efficiency and reduce the non-specific distribution in normal tissues by the enhanced permeability and retention (EPR) effect in cancer. Taking the advantage of O-GlcNAc-specific antibodies or lectins, nanoparticles could further improve their

cancer-targeting capability. Although nanocarriers targeting the canonical N- and O-linked glycosylation has been extensively investigated for cancer detection and therapy, application of nanotechniques for the specific targeting of O-GlcNAcylation has not been actively pursued. This review summarizes the general features GlcNAcylation and its alterations in cancers. Analyses are focused on the following areas: How the nanocarriers may improve the solubility and/or cell permeability of O-GlcNAc transferase (OGT) inhibitors; The modification of nanocarriers with lectins or antibodies for active targeting of O-GlcNAc; The nanocarriers-mediated co-delivery of OGT inhibitors and conventional drugs, which may lead to synergistic effects. Unsolved issues impeding the research progression on O-GlcNAcylation-targeting scheme are also discussed.

Key words: O-GlcNAcylation; Nanocarriers; OGT inhibitor; Targeted therapy; Lectin; Combined therapy

254. Circulating lymphocyte subsets are prognostic factors in patients with nasopharyngeal carcinoma

Jing Zhu*、Ruhua Fang、Zhiwen Pan、Xu Qian

Zhejiang Cancer Hospital

Background: Nasopharyngeal carcinoma (NPC) is a geographically and racially variable disease which has a high incidence in Southeast China. According to previous studies on tumor immunity, we compared multiple clinical parameters and blood indexes with outcome regarding to Epstein-Barr virus (EBV) status in NPC patients.

Methods: According to the EBV load at diagnosis, 220 NPC patients who receiving concurrent chemoradiotherapy (CRT) were divided into two groups, EBV DNA≥1500 copies/mL and EBV DNA<1500 copies/mL, respectively. We compared clinical parameters with peripheral blood mononuclear cells, lymphocyte subsets and biochemical indexes. We also analyzed distant metastases and overall survival rate regarding to these characteristics.

Results: In most cases, the two groups showed the same trend. Most blood indexes were decreased during CRT and the decrease of the absolute count was more significant than percentage. Patients with younger age showed the higher $CD3^+$ and $CD3^+CD8^+$ percentage. Patients whose

EBV DNA≥1500 copies/mL showed higher N classification than those with EBV DNA<1500 copies/mL at first diagnosis. Within patients with EBV DNA≥1500 copies/mL, higher $CD3^+CD8^+$ percentage or lower $CD3^-CD56^+$ percentage had better OS rates, and $CD3^+CD8^+$ percentage was an independent prognostic factor by multivariate survival analyses.

Conclusions: CRT caused an overall decrease of blood cells in NPC patients. Among all the blood indexes, $CD3^+CD8^+$ percentage showed its correlation with age and was an independent prognostic factor in patients with EBV DNA≥1500 copies/mL at first diagnosis, which is worthy for further large cohort study.

Key words: Nasopharyngeal carcinoma, Cancer immunity, EBV, Circulating lymphocyte subsets, Chemoradiotherapy, Follow-up

255. Circulating lymphocyte subsets are dynamic biomarkers for HPV negative head and neck squamous cell carcinoma during treatment

Jie Zhou*、Jing Zhu、Xu Qian

Zhejiang Cancer Hospital

Background: Locally advanced head and neck squamous cell carcinoma (LAHNSCC) frequently develops recurrences and/or metastases. This study researched the systemic changes in circulating immune cell subsets in response to treatment and their contribution to HPV negative LAHNSCC outcomes.

Methods: We measured peripheral blood mononuclear cells by flow cytometry in 38 healthy individuals and 70 LAHNSCC patients after surgical resection followed by concurrent chemoradiotherapy (CRT).

Results: Patients who developed distant metastases showed a higher $CD3^+CD8^+$ cell percentage (P=0.004) and a lower $CD3^+CD4^+$ cell percentage (P=0.024), CD4/CD8 cell ratio (P=0.005), $CD4^+CD45RA^+$ cell percentage (P=0.014) and count (P=0.033) after tumor removal than those without distant metastases. Systemic T-cell loss, especially $CD3^+CD4^+$ cell count and percentage reduction, and a higher CD4/CD8 cell ratio can predict better survival after CRT.

Conclusions: The $CD3^+CD4^+$ cell count and percentage as well as the CD4/CD8 cell ratio have prognostic value and the potential to stratify LAHNSCC patients with distant metastases. Monitoring the circulating lymphocyte subsets can better evaluate the treatment effect and formulate personalized treatment.

Key words: Head and neck cancer, cancer immunity, circulating lymphocyte subsets, immune response, liquid biopsy, follow-up

256. Identification of potential biomarkers for progression and prognosis of bladder cancer by comprehensive bioinformatics analysis

Zhiyong Tan*、Jiansong Wang

The Second Affiliated Hospital of Kunming Medical University

Background: Bladder cancer (BLCA) is a highly malignant tumor that develops in the urinary system. Identification of biomarkers in progression and prognosis is crucial for the treatment of BLCA.

Methods: BLCA-related differently expressed genes (DEGs) were authenticated by screening the DEGs and weighted gene co-expression network analysis (WGCNA). LASSO and SVM-RFE algorithms were utilized to screen the feature genes in BLCA. Survival analysis was performed using the Kaplan-Meier curve provided by the 'survival' R package. The BLCA samples were clustered by hclust based on the immune-score matrix calculated by the single sample GSEA (ssGSEA) algorithm. The immune-, stromal- and estimate- scores of each BLCA patient were calculated by applying the ESTIMATE algorithm. The ssGSEA was conducted to explore the function of characteristic genes in BLCA. The expression of characteristic genes in clinical cancer tissue and peri-cancerous tissue of BLCA patients was verified using qRT-PCR assays.

Results: A total of 189 BLCA-related DEGs were identified. Fourteen feature genes were defined by LASSO and SVM-RFE algorithms. Five characteristic genes, including SMYD2, GAPDHP1, ATP1A2, CILP, and THSD4, were related to the OS of BLCA. The correlation analysis of five characteristic genes and clinicopathological factors showed that five genes played a role in the

progression of BLCA. Additionally, the expression of five characteristic genes in clinical cancer tissues and pericarcinomatous tissues from BLCA patients was verified by qRT-PCR, which was consistent with the result from the public database.

Conclusions: Finally, we discovered five prognostic genes linked to BLCA progression, which might serve as a theoretical basis for prognosis and treatment targets for BLCA patients.

Key words: bladder cancer, prognosis, progression, biomarker, WGCNA

257. SMAD4 通过 HBx 转录激活和蛋白稳定的协同作用而促乙肝相关肝癌细胞增殖

王朝敏*

天津医科大学附属肿瘤医院

Purpose: Hepatitis B virus (HBV) plays a crucial role in the progression of hepatocellular carcinoma (HCC). It is known that HBV-encoded X protein (HBx) can induce genetic alterations in some oncogenes and that SMAD4 is relevant for the development of some cancers, especially HBV-related HCC. Previously, it has been reported that HBx can promote SMAD4 protein expression in liver fibrosis and HCC but, as yet, its regulatory mechanism has not been fully elucidated. Here, we aimed to investigate the correlation between and regulatory mechanism behind HBx and SMAD4 in HCC.

Methods: mRNA and protein expression of SMAD4 in HCC tissues was detected by qRT-PCR, Western blotting and IHC. CCK-8 and colony forming assays, as well as xenograft murine models were used to evaluate the effects of HBx and SMAD4 on the proliferation and tumorigenicity of HCC cells. Luciferase reporter, immunofluorescence, Co-IP and truncation assays were performed to assess the regulatory relationship between HBx and SMAD4.

Results: We found that SMAD4 was highly expressed in HBV-positive HCC patient samples and correlated with a poor prognosis. The proliferation of HCC cells with a high SMAD4 expression was found to be enhanced in vitro and in vivo, and knocking down HBx while replenishing SMAD4 rescued HCC cell proliferation. Mechanically, we found that HBx regulates SMAD4 expression at the transcriptional level via TFII-I and can bind to SMAD4 to repress its

ubiquitination. The binding region comprised the MH2 domain of SMAD4. Furthermore, we found that SMAD4 can promote HBx expression through a positive feedback mechanism.

Conclusions: From our data we conclude that SMAD4 is modulated spatiotemporally via both transcriptional activation and protein stabilization by HBx in HCC cells. Our data shed light on the molecular mechanism underlying HBx-induced hepatocarcinogenesis.

Key words: Hepatocellular carcinoma; SMAD4; HBx; proliferation

258. Overexpression of Protein Phosphatase 2 Regulatory Subunit B"Alpha Promotes Glycolysis by Regulating Hexokinase 1 in Hepatocellular Carcinoma

Ning Jiao*、Qing Zhang

Department of Organ Transplantation, The Third Medical Center of PLA General Hospital, Beijing 100039, China

Objective: To investigate the regulatory relationship of Protein Phosphatase 2 Regulatory Subunit B"Alpha (PPP2R3A) and hexokinase 1 (HK1) in glycolysis of hepatocellular carcinoma (HCC).

Methods: In HepG2 and Huh7 cells, PPP2R3A expression was silenced by small interfering RNA (siRNA) and overexpression by plasmid transfection. The PPP2R3A-related genes were searched by RNA sequencing. Glycolysis levels were measured by glucose uptake and lactate production. QRT-PCR, elisa, western blot and immunofluorescence assay were performed to detect the changes of PPP2R3A and HK1. Cell proliferation, migration and invasion assay were used to study the roles of HK1 regulation by PPP2R3A.

Results: RNA sequencing data revealed that PPP2R3A siRNA significantly downregulated the expression of HK1. PPP2R3A gene overexpression promotes, while gene silencing suppresses, the level of HK1 and glycolysis in HCC cells. In HCC tissue samples, PPP2R3A and HK1 were colocalized in the cytoplasm, and their expression showed a positive correlation. HK1 inhibition abrogated the promotion of glycolysis, proliferation, migration and invasion by PPP2R3A overexpression in liver cancer cells.

Conclusion: Our findings showed the correlation of PPP2R3A and HK1 in the glycolysis of HCC, which reveals a new mechanism for the oncogenic roles of PPP2R3A in cancer.

Key words: Hepatocellular carcinoma; PPP2R3A; Hexokinase 1; Glycolysis

259. Decreased expression of the lncRNA CASC2 predicts advanced clinicopathological features and serves as an unfavorable risk factor for cancer patient survival

Tianrui Xu*、Guoqiang Xu、Lixiu Zhu

Department of Radiotherapy, Yunnan Cancer Hospital, the Third Affiliated Hospital of Kunming Medical University, Kunming, China

Background: Cancer susceptibility candidate gene 2 (CASC2) exhibits low expression in different carcinomas and is involved in cancer progression. The aimed of this study was to assess the value of CASC2 as a prognostic marker for cancers.

Methods: Two authors independently searched five databases for eligible studies from inception to June 2, 2022. Combined hazard ratios (HRs), odds ratios (ORs), and 95% confidence intervals (CIs) were calculated using Review Manager 5.4. Stata MP 16.0 was utilized to perform the publication bias and sensitivity analyses. We validated the results by Gene Expression Profiling Interaction Analysis 2 (GEPIA2).

Results: Twenty studies involving 1414 people encompassing 11 malignancies across five systems, were considered. CASC2 downregulation was markedly correlated with shorter overall survival (OS) in cancer patients (HR= 0.49; 95% CI, 0.41–0.60; P<0.00001). Furthermore, CASC2 downregulation was associated with advanced TNM stage (OR= 0.32; 95% CI, 0.25–0.42; P<0.00001), larger tumor size (OR= 0.48; 95% CI, 0.31–0.75; P= 0.001), and poor tumor differentiation (OR= 0.39; 95% CI, 0.27–0.56; P<0.00001) but not with age, sex, or distant metastasis. CASC2 downregulation was directly related to poor differentiation in digestive system cancers (OR= 0.53; 95% CI, 0.31–0.91; P= 0.02). Low CASC2 expression was related to negative lymph node metastasis in digestive system (OR= 1.96; 95% CI, 1.08–3.55; P= 0.03) and female reproductive system cancers (OR= 2.11; 95% CI, 1.16–3.85; P= 0.01).

Conclusions: CASC2 expression is directly correlated with prognostic and clinicopathological characteristics in tumor patients, indicating that CASC2 might be a viable therapeutic target and a predictor of poor prognosis.

Keywords: Cancer, lncRNA CASC2, Meta-analysis, Prognosis

260. An Algorithm for the Early Diagnosis of Gastric Cancer based on Combined Serum Tumor Biomarkers

Rui Ding*[1]、Honglei Li[1]、Qiang Xu[2]、Tingting You[1]、Linglin Zhang[3]、Zijian Guo[1]、Xiaowei Wang[4]、Man-Fung Tsoi[5]、 Lin Zhang[6]、 Zhongjuan Liu[1]、 Xuzhen Qin[1,7]、 Zhihong Qi[1]

1. Department of Laboratory Medicine, Chinese Academy of Medical Sciences and Peking Union Medical College Hospital, Beijing 100730, China

2. Department of General Surgery, Chinese Academy of Medical Sciences and Peking Union Medical College Hospital, Beijing 100730, China

3. Department of Anatomic Pathology, Chinese Academy of Medical Sciences and Peking Union Medical College Hospital, Beijing 100730, China

4. Abbott Shanghai Co., Ltd, Shanghai

5. Centre of Epidemiology Versus Arthritis, University of Manchester

6. Centre of Cancer Research, Victorian Comprehensive Cancer Centre, Melbourne, Victoria, Australia

7. NMPA Key Laboratory for Quality Evaluation of In Vitro Diagnostics

Background: Ideal biomarkers for early diagnosis of gastric cancer are limited, we aim to set up an algorithm to diagnose gastric cancer in Chinese population using clinical routine biomarkers.

Methods: 173 patients with gastric cancer and 210 healthy volunteers were included in this study. Serum carcinoembryonic antigen (CEA), cancer antigen 19-9 (CA19-9), cancer antigen 72-4 (CA72-4), cancer antigen 125 (CA125), pepsinogen 1 (PG1), pepsinogen 2 (PG2), progastrin-releasing peptide (ProGRP), sialic acid (SA), myogenin (MYOG), C-reactive protein (CRP), ferritin (FER) and α-1-acid glycoprotein (AGP) levels were measured in a central laboratory using commercial chemiluminescence method. Age, gender, and biomarkers were selected to set up an algorithm for diagnosis of gastric cancer using R package.

Results: CRP, FER, PG1, PG2, CA125, ProGRP, CEA, CA19-9, CA72-4, age, and gender were selected for a binary logistic regression model with the AUC of 0.93 and sensitivity of 88.4%, specificity of 79.5%. A simpler algorithm including age, gender, CEA, CA19-9, CA72-4, PG1, PG2, and PG1/PG2 ratio were set up with a bit lower diagnostic efficacy as the sensitivity, specificity, and AUC of 90%, 72%, and 0.90, separately. These algorithms have better performance for diagnosis of gastric cancer compared with single tumor biomarker.

Conclusions: Our findings indicated that new algorithms with combined serum tumor biomarkers, age and gender might be a useful and practical way for early-stage gastric cancer screening.

Key words: Gastric cancer, Early diagnosis, Serum biomarker, Algorithm

261. Association of BRCA1/2 mutations with prognosis and surgical cytoreduction outcomes in ovarian cancer patients: An updated meta-analysis

yazhuo wang*

Hebei General Hospital

Aim: This meta-analysis was conducted to evaluate the impact of BRCA mutations on survival outcomes and assess whether the BRCA status was an independent predictor of complete cytoreduction.

Methods: We searched the PubMed, Cochrane, EMBASE, Scopus, Web of Science, and Google Scholar databases for studies that evaluated the associations among BRCA mutations, ovarian cancer survival and surgical cytoreduction before August 2021 based on specific inclusion and exclusion criteria.

Results: We identified 62 articles that compared the clinical features, survival outcomes and optimal surgical cytoreduction rates between BRCA-positive patients and BRCA-negative patients. The results showed that BRCA mutation carriers were diagnosed with ovarian cancer at a younger age than the age at which nonmutation carriers were diagnosed. In addition, BRCA mutation carriers were more likely to be in International Federation of Gynecology and Obstetrics (FIGO) stage III-IV, and the pathological grade was commonly grade 3. The pathological type of

BRCA mutation carriers was more likely to be high-grade serous carcinoma. Patients with BRCA mutations had higher response rates to platinum-based chemotherapy than the controls. However, patients in both groups had equivalent rates of surgical cytoreduction, and BRCA-positive patients had longer overall survival times (HR=0.65; 95% confidence interval (CI): 0.59, 0.73; P <0.001) and longer PFS (HR=0.72; 95% CI: 0.63, 0.82; P <0.001).

Conclusion: BRCA mutations appear to be associated with improved OS and PFS in patients with ovarian cancer. However, we did not find any difference in the surgical resection rate between participants in the two groups.

Key words: BRCA; mutation; ovarian cancer; survival; surgical cytoreduction

262. Development and Validation of Reassigned CEA, CYFRA21-1 and NSE-Based Models for Lung Cancer Diagnosis and Prognosis Prediction

Jingmin Yuan*、Yan Sun、Hui Ren、Mingwei Chen

The First Affliated Hospital of Xi'an Jiaotong University

Background: The majority of lung cancer(LC) patients are diagnosed at advanced stage with a poor prognosis. However, there is still no ideal diagnostic and prognostic prediction model for lung cancer.

Methods: Data of CEA, CYFRA21-1 and NSE test of patients with LC and benign lung diseases (BLDs) or healthy people from Physical Examination Center was collected. Samples were divided into three data sets as needed. Reassign three kinds of tumor markers (TMs) according to their distribution characteristics in different populations. Diagnostic and prognostic models were thus established, and independent validation was conducted with other data sets.

Results: The diagnostic prediction model showed good discrimination ability: the area under the receiver operating characteristic curve (AUC) differentiated LC from healthy people and BLDs (diagnosed within 2 months), being 0.88 and 0.84 respectively. Meanwhile, the prognostic prediction model did great in prediction: AUC in training data set and test data set were 0.85 and 0.8 respectively.

Conclusion: Reassigned CEA, CYFRA21-1 and NSE can effectively predict the diagnosis and prognosis of LC. Compared with the same TMs that were considered individually, this diagnostic prediction model can identify high-risk population for LC screening more accurately. The prognostic prediction model could be helpful in making more scientific treatment and follow-up plans for patients.

Key words: Lung cancer; CEA; CYFRA21-1; NSE; Screening; Prognosis

263. RNA modifications meet tumors

Zhiyuan Yang、Bo You*

Affiliated Hospital of Nantong University

RNA modifications occur through the whole process of gene expression regulation, including transcription, translation, and post-translational processes. They are closely associated with gene expression, RNA stability, and cell cycle. RNA modifications in tumor cells play a vital role in tumor development and metastasis, changes in the tumor microenvironment, drug resistance in tumors, construction of tumor cell-cell “internet”, etc. Several types of RNA modifications have been identified to date and have various effects on the biological characteristics of different tumors. In this review, we discussed the function of RNA modifications, including N^6-methyladenine(m^6A), 5-methylcytosine (m^5C), N^7-methyladenosine(m^7G), N^1-methyladenosine (m^1A), pseudouridine(Ψ), and adenosine-to-inosine (A-to-I), in the microenvironment and therapy of solid and liquid tumors.

Key words: Tumor, RNA modification, non-coding RNA, tumor microenvironment, tumor therapy

264. PTEN promoter methylation predicts 10-year prognosis in hormone receptor positive early breast cancer patients that received adjuvant tamoxifen endocrine therapy

Yu Fan*、Zhu Wang、Wang Yu、Yanping Wang、Hong Zheng、Xiaorong Zhong

四川大学华西医院

Purpose: There remains a lack of biomarkers for endocrine therapy resistance in patients with breast cancer (BC), which is proving to be a great challenge. In vitro experiments have shown that downregulation of PTEN expression leads to resistance to tamoxifen (TAM) in BC cells. We aimed to investigate the predictive role of tumor PTEN promoter methylation and PTEN expression in long-term survival after TAM adjuvant therapy in patients with early-stage BC.

Methods: From 2001 to 2013, 105 patients with stage I–III BC who were treated with standardized adjuvant TAM for 5 years or until relapse in West China Hospital (WCH) were enrolled in this study. PTEN expression and DNA methylation of three specified sequences from the PTEN promoter in primary tumors were measured using immunohistochemistry and pyrosequencing. A cohort of 159 hormone receptor-positive patients receiving TAM treatment from The Cancer Genome Atlas (TCGA) database was used for verification.

Results: Median follow-up time for the WCH cohort was 141.7 months. The low, moderate, and high PTEN expression groups had differing 10-year disease-free survival (DFS) (42.3%, 55%, 81%, respectively, $P = 0.027$) and overall survival (OS) rates (65%, 84.2%, 90.5%, respectively, $P = 0.027$). Higher methylation levels of the second sequence (-819 to -787 bp), rather than the first (-1143 to -1107 bp) or third sequence (-663 to -593 bp), independently increased the risk of disease recurrence (hazard ratio= 2.60) and death (hazard ratio= 3.79) in the WCH cohort, according to multivariate Cox regression analysis. Importantly, out of the five CpG islands located within this sequence, only high methylation of the -796 CpG island predicted shorter DFS and OS. In TCGA validation cohort, there was also a trend of higher methylation of the -796 CpG island correlating with shorter disease-free intervals, with borderline significance ($P = 0.057$).

Conclusions: Low PTEN expression and high methylation of its promoter (sequence -819 to -787 bp) in tissue predicts poor DFS and OS in hormone-receptor positive early BC patients who received adjuvant TAM.

Key words: Breast cancer; PTEN; tamoxifen; promoter methylation; 10-years survival

265. Investigated Diagnostic Value of Synthetic Relaxometry, Three-dimensional Pseudo-Continuous Arterial Spin Labelling and Diffusion-Weighted Imaging in the Grading of Glioma

Xin Ge*[1,2]、Jing Zhang[2]

1. Second Clinical School, Lanzhou University

2. 兰州大学第二医院

Background: To investigate the performance of synthetic relaxometry, three-dimensional pseudo-continuous arterial spin labelling (pCASL) and diffusion-weighted imaging (DWI) in differentiating high-grade gliomas (HGGs) from low-grade gliomas (LGGs) and to compare with the conventional MRI.

Methods: Seventy-two patients with gliomas (including 27 LGGs and 45 HGGs) were studied using synthetic magnetic resonance imaging (sy-MRI), pCASL, and DWI with a 3.0T MR scanner. T1 relaxometry (T1), T2 relaxometry (T2), as well as proton density (PD) from sy-MRI, cerebral blood flow (CBF) from pCASL, apparent diffusion coefficient (ADC) from DWI and enhancement quality (EQ), proportion enhancing (PE) from conventional contrast enhanced image based Visually-Accessible-Rembrandt-Images (VASARI) scoring system, were all analyzed by two radiologists. The Student's t-test, Mann-Whitney U-test or Fisher's exact test was used to compare the parameters between LGGs and HGGs. The diagnostic performance of each parameter and their combination for glioma grading were analyzed.

Results: Significant statistical differences in T1, PD, CBF, ADC, EQ and PE are observed between LGGs and HGGs (all P<0.001). The ADC values have higher discrimination abilities

compared with other univariable parameters, with the AUC of 0.905. AUC values for conventional contrast-enhanced method, EQ and PE from VASARI, and conventional contrast-free method, CBF+ADC, are 0.873 and 0.912 respectively. The combined T1, PD, CBF and ADC model had the best performance for differentiating LGGs and HGGs with AUC, sensitivity and specificity of 0.993, 95.5%, 100%, respectively.

Conclusions: Relaxometry parameters derived from synthetic MRI contributed to the discrimination of low-grade gliomas from high-grade gliomas. Proposed contrast-free approach combining T1, PD, CBF and ADC showed a strong discriminative power, and outperformed conventional approaches.

Key words: Glioma, Grading, Magnetic resonance imaging, Synthetic relaxometry, Three-dimensional pseudo-continuous arterial spin labelling, Diffusion-weighted imaging

266. Differentiation and prognostic stratification of acute myeloid leukemia by serum-based spectroscopy coupling with metabolic fingerprints

Yang Chen*[1,2]、Zhengwei Duan[1]、Lijing Xiao[1]、Yingping Cao[3]、Yi Peng[4]、Wuping Liu[5]、Jianda Hu[1,2]

1. Fujian Medical University

2. 福建医科大学附属协和医院，福建省血液病研究所

3. 福建医科大学附属协和医院，检验科

4. 福建医科大学医学技术与工程学院，眼视光学系

5. 厦门大学电子科学系，福建省等离子体与磁共振研究重点实验室

Acute myeloid leukemia (AML) is a heterogeneous disease characterized by complex molecular and cytogenetic abnormalities. New approaches to predict the prognosis of AML have increasingly attracted attention. There were 98 non-M3 AML cases and 48 healthy controls were enrolled in the current work. Clinically routine assays for cytogenetic and molecular genetic analyses were performed on the bone marrow samples of AML patients. Meanwhile, metabolic profiling of these AML subjects were also performed on the serum samples by combining Ag nanoparticles-based

surface-enhanced Raman spectroscopy (SERS) with proton nuclear magnetic resonance (NMR) spectroscopy. Although most of the routine biochemical test showed no significant differences between the M0~M2 and M5 groups, the metabolic profiles were significantly different either between AML subtypes or between prognostic risk subgroups. Specific SERS bands were screened to serve as potential markers for AML subtypes. The results demonstrated that the classification models for M0~M2 and M5 shared two bands (i.e., 1328 and 741 cm^{-1}), all came from nucleic acid signals. Furthermore, Metabolic profiles provided various differential metabolites responsible for different AML subtypes, and we found altered pathways mainly included energy metabolism like glycolysis, pyruvate metabolism, and metabolisms of nucleic acid bases as well as specific amino acid metabolisms. It is concluded that integration of SERS and NMR provides the rational and could be reliable to reveal AML differentiation, and meanwhile lay the basis for experimental and clinical practice to monitor disease progression and prognostic evaluation.

Key words: acute myeloid leukemia, metabolic profiling, nuclear magnetic resonance, prognosis, surface-enhanced Raman scattering

267. TRIB2 modulates proteasome function to reduce ubiquitin stability and protect liver cancer cells against oxidative stress

Susu Guo *、Xiao Zhang、Lifang Ma、Jiayi Wang

Shanghai Tenth People&amps Hospital

Objectives: This part of the study aims to explore a new way that TRIB2 does not rely on E3s to regulate the UPS and substrate ubiquitination, and to clarify the new mechanism that TRIB2 affects the occurrence and development of liver cancer, providing new ideas for the treatment of liver cancer.

Methods: IB was used to investigate the relationship between TRIB2 and Ub. PCBP2, the intermediate protein between TRIB2 and PSMB5, was identified by MS. Immunoprecipitation and PLA were used to explore the interaction between the proteins. Immunohistochemistry was used

to explore the correlation between TRIB2 and PCBP2 in different liver cancer tissues. Mutants were constructed by PCR to explore the specific sites where TRIB2 interacts with PCBP2. The effects of TRIB2 on the proliferation and tumorigenesis ability of HCC cells were investigated by 3D culture and nude mouse tumorigenesis experiments.

Results: We reveal that TRIB2 decreased Ub levels largely by stimulating proteasome degradation. In the proteasome, PSMB5 was critical for the function of TRIB2, although it did not directly interact with TRIB2. TRIB2 acts as an upstream protein to inhibit the K48 ubiquitination of PCBP2 and improve the stability of PCBP2 protein. Therefore, a model showing that TRIB2 cooperates and stimulates PCBP2 to reduce Ub levels was established. Additionally, the reduction in Ub levels induced by TRIB2 and PCBP2 was dependent on K48-ubiquitination. The interaction between PCBP2 and TRIB2 relied on the DQLVPD element of TRIB2 and the KH3 domain of PCBP2, which was necessary to maintain the viability of the liver cancer cells and promote tumor growth. Mechanistically, GPX4 functioned as one of the terminal effectors of TRIB2 and PCBP2 to protect liver cancer cells from oxidative damage.

Conclusion: The data indicates that TRIB2 plays a critical role in regulating UPS by modulating PSMB5 activity in proteasome to reduce Ub flux and that targeting TRIB2 might be helpful in liver cancer treatments by enhancing the oxidative damage induced by therapeutic agents.

Key words: TRIB2, proteasome, ubiquitin, oxidative stress

268. Ubiquitin-specific protease 24 promotes hepatocellular carcinoma progression via YAP stabilization and deubiquitination

Huizhuang Dan*[1]、Xinhua Xiao[2]、Yingli Wu[3]

1. Guangdong Provincial People' hospital

2. 广州市妇女儿童医疗中心

3. 上海交通大学医学院

Ubiquitin-specific protease 24 (USP24) is a member of the deubiquitinating enzyme family, which plays an important role in human tumor diseases. However, the mechanisms by which USP24

facilitates tumor development, especially in hepatocellular carcinoma (HCC), remain unclear. Clinically, we found that USP24 is overexpressed in human HCC tissues compared with adjacent non-tumoral tissues. Moreover, Kaplan–Meier survival analysis showed a poor overall survival rate in patients with USP24-overexpressing tumors. Analyses of univariate and multivariate Cox proportional hazard models indicated that USP24 is a prognostic biomarker for poor outcome. Using in vitro and in vivo assays, we demonstrated that knockdown of USP24 inhibited HCC cell growth, migration, and invasion. Mechanistically, the oncoprotein Yes-associated protein (YAP) in Hippo pathway was identified as an important molecule for USP24-mediated oncogenic activity in HCC. We observed that USP24 interacted with YAP and inhibited YAP degradation via deubiquitination in HCC cells. Interestingly, our data showed that the expression levels of USP24 were positively associated with those of YAP in HCC cell lines and clinical samples. Functionally, overexpression of YAP abolished the proliferation inhibition of HCC cells mediated by silencing USP24 in vitro. These data suggest that USP24 acts as a novel prognostic marker, offering potential therapeutic opportunities for HCC.

Key words: Ubiquitin-specific protease 24, YAP, Hepatocellular carcinoma,deubiquitination

269. Identification of a 5-Gene-Based Signature to Predict Prognosis and Correlate Immunomodulators for Rectal Cancer

Yi Lin*[1]、Qiang Ji[1]、Yichen Peng[1]、Chunna Yu[1]、Yi Zheng[1]、Xun Kang[1]、Jianwei Zheng[1]、Rixing Bai[1]、Wenmao Yan[1]、Xiaomin Wang[1,2]、Wenbin Li[1]

1. Beijing Tiantan Hospital, Capital Medical University

2. 北京大学肿瘤医院

Background and Objectives: Specific tumor markers that could aid in survival prognosis and guide treatment decisions, similar to the 21-gene assay in breast cancer, have yet to be identified in rectal cancer. The objective of this study was to identify a gene signature for rectal cancer and to evaluate its prognostic value for survival prediction.

Methods: Two datasets containing data regarding rectal cancer were downloaded from the GEO. Differentially expressed genes (DEGs) were obtained, and univariable Cox analyses were carried out to identify genes correlated with overall survival (OS) using data from TCGA. Multivariable Cox and LASSO regression were applied to establish the prognostic signature. Then, a time-dependent ROC curve was generated to evaluate the model, and validated the prognostic value in the GSE133057 dataset. Patients were assigned into high-risk group and low-risk group according to the risk-score calculated by the model. A nomogram was constructed to estimate survival predictability for the 3-, 4- and 5-year OS in TCGA and GSE133057. Subsequently, our research investigated the relationship between the 5-gene-based risk-score and clinicopathological features. Thenceforth, functional annotation and enrichment were carried out between the low- and high-risk groups via GO, KEGG and GSEA. Moreover, we searched for possible gene-targeted miRNAs by using TargetScan, and analyzed the functional state at the single-cell level by the CancerSEA tool. Finally, the low and high-risk groups were assessed for TMB, MSI, mutation, ssGSEA, immune cell infiltration, and the presence of immune checkpoint molecules.

Results: A total of 468 DEGs between rectal cancer and normal tissues were found in the analysis of both datasets. A signature for rectal cancer prognosis consisting of 5 genes (CLIC5, ENTPD8, PACSIN3, HGD and GNG7) was identified by univariable and multivariable Cox regression and LASSO regression. By using the TCGA dataset in training, survival analyses according to the risk score showed significantly worse overall survival (OS) in the high-risk group (*P*= 0.004*4*, log-rank= 6.328). Similar survival trends were validated in the GSE133057 dataset. The model exhibited high performance in time-dependent ROC curve as well as nomogram among both training and validating dataset. Notably, the risk-score was associated with vascular invasion (*P*= *0.038*), and besides a superior independent prognostic factor. Afterwards, the GO and KEGG annotations indicated that low- and high-risk groups were differentially enriched in autophagy-, immune-, cell cycle-, infection-, and apoptosis-associated terms and pathways. Markedly, the mutation landscape was also different between the low- and high-risk groups. Then, hsa-miR-6887 was predicted to be a common microRNA of 5 genes by TargetScan. Unexpectedly, the functional states of differentiation, apoptosis and quiescence were significantly related to the 5-gene signature in the single-cell GSE81861 dataset. Furthermore, the low- and high-risk groups showed significant differences with respect to nonregulatory CD4+ T cells and CD8+ T cells. Strikingly,

Heat map plot showed that genes in our model were correlated with immunoinhibitors, particularly CLIC5 and GNG7.

Conclusion: Our results suggest that a 5-gene-based signature can serve as a novel prognostic biomarker for the evaluation of rectal cancer patients, and indicate pertinent tumor immunomodulators to benefit clinical decision-making.

Key words: CLIC5, ENTPD8, PACSIN3, HGD, GNG7, Rectal Cancer, Prognosis

270. Identification of a novel PAX5-GSE1 fusion gene acting as minimal residual disease biomarker in acute B-lymphocytic leukemia

Haina Wang*、Jingjing Xue、Xuehong Zhang、Yuan Gao、Xin Zong、Zhijie Kang、Jinsong Yan

Department of Hematology, Liaoning Key Laboratory of Hematopoietic Stem Cell Transplantation and Translational Medicine, Second Hospital of Dalian Medical University, Dalian, China

Aim: To validate the RNA-sequencing (RNA-seq) result that GSE1 is a novel fusion partner of PAX5, and to figure out whether the new fusion gene can act as a biomarker of minimal residual disease (MRD) during acute B-lymphocytic leukemia (B-ALL) treatment process. To verify whether PAX5-GSE1 fusion gene acts as a dominant negative on wild-type PAX5 and to elucidate its function in B-ALL development.

Methods: RNA-seq was employed to find new molecular occurrence in a 22-year-old male diagnosed with B-ALL patient. STAR-Fusion software was used to detect the fusion transcripts. Reverse transcription polymerase chain reaction (RT-PCR) and sanger sequencing were performed to validate the novel fusion gene. Chromosome karyotype analysis with standard G-banding and fluorescence in situ hybridization (FISH) were carried out to further verify the existence of the fusion gene in patient bone marrow sample. Standard curve was established and the gene expression of PAX5-GSE1 in bone marrow samples before and post induction chemotherapy were quantified by quantitative real-time RT-PCR (qRT-PCR). Expression plasmid containing the fusion gene was constructed, and western blotting and immunofluorescence were used to examine the subcellular localization of this fusion gene. The luciferase reporter vector pGL3-CD19 was

constructed and dual-luciferase reporter assay was performed to detect the dominant negative effect of the PAX5-GSE1 fusion gene on wild type PAX5. Gene set enrichment analysis (GSEA) by the JAVA program was selected to compare the RNA expression profiling between PAX5-GSE1 fusion positive patient and negative B-ALL patients.

Results: A new fusion gene PAX5-GSE1 formed by exon 5 of PAX5 and exon 2 of GSE1was found by RNA-seq. Its existence was confirmed by RT-PCR and sanger sequencing. G-band karyotyping and FISH analyses performed on bone marrow sample revealed the following complex karyotype: 47,XY,del(1)(q22),+6,t(9;16)(p13;q24),-10,+22[3]/46,XY[10]. qRT-PCR results showed that the expression level of PAX5-GSE1 fusion gene in bone marrow was very high at the initial stage, yet significantly decreased after induction chemotherapy, indicating a coincidence of the fusion gene expression level with the clinical progression of disease. Western blotting and immunofluorescent results showed a nuclear localization of the fusion gene. Luciferase reporter assay revealed that PAX5-GSE1 can dramatically inhibit wild-type PAX5 transcriptional activity in a dominant-negative and dose-dependent manner. Transcriptome data analysis showed that 172 genes were up-regulated and 22 genes were down-regulated in PAX5-GSE1 positive patient compared with other negative B-ALL patients (FC > 2 and Q<0.05). Functional annotation was performed using the differentially expression genes, and the results showed that HALLMARK ALLOGRAFT REJECTION, HALLMARK COMPLEMENT, KEGG NATURAL KILLER CELL MEDIATED CYTOTOXICITY and KEGG ALLOGRAFT REJECTION pathways are enriched. In GSEA analysis, genes related to allograft rejection pathway both in Hallmark and KEGG database were significantly upregulated with normalized enrichment score (NES) 1.61 and 1.47, and P value 0.001 and 0.027.

Conclusions: We found a novel fusion gene PAX5-GSE1 in one B-ALL patient, which can be used as a molecular biomarker to monitor the MRD. In vitro experiments showed that PAX5-GSE1 localizes in the nucleus and has a dominant negative inhibitory effect on wild-type PAX5. Bioinformatics analysis showed that PAX5-GSE1 positive patient may have the risk of immune rejection after transplantation.

Key words: Fusion gene; PAX5-GSE1; B-ALL; MRD biomarker; Dominant negative inhibition

271. CD155/SRC complex promotes hepatocellular carcinoma progression via inhibiting the p38 MAPK signaling pathway and correlates with poor prognosis

Anli Jin*[1]、Chun-Yan Zhang[1]、Wen-Jing Zheng[1]、Jing-Rong Xian[1]、Wen-Jing Yang[1]、Te Liu[2]、Wei Chen[1]、Tong Li[1]、Bei-Li Wang[1]、Bai-Shen Pan[1]、Qian Li[1]、Jian-Wen Cheng[1]、Peng-Xiang Wang[1]、Bo Hu[1]、Jian Zhou[1]、Jia Fan[1]、Xin-Rong Yang[1]、Wei Guo[1]

1. Department of Laboratory Medicine, Zhongshan Hospital, Fudan University, Shanghai

2. 上海中医药大学上海老年医学研究所

Background: Hepatocellular carcinoma (HCC) is a prevalent malignancy with poor prognosis. As a cell adhesion molecule, poliovirus receptor (PVR/CD155) is abnormally overexpressed in tumor cells and related to tumor proliferation and invasion. However, the potential role and mechanism of CD155 have not yet been elucidated in HCC.

Methods: Immunohistochemistry, RT-PCR and western blot assays were used to determine CD155 expression in HCC cell lines and tissues. Cell Counting Kit-8 and colony formation assays were used to examine cell proliferation. Transwell and wound healing assays were used to evaluate cell migration and invasion. Cell apoptosis and cycle distribution were assessed by flow cytometry. Cox regression and Kaplan-Meier analyses were performed to explore the clinical significance of CD155. The role of CD155 in vivo was evaluated by establishing liver orthotropic xenograft mice model. RNA-sequencing, bioinformatics analysis and co-immunoprecipitation assay were used to explore the downstream signaling pathway of CD155.

Results: CD155 was up-regulated in HCC tissues and represented a promising prognostic indicator for HCC patients (n=189) undergoing curative resection. High CD155 expression enhanced cell proliferation, migration and invasion, and contributed to cell survival in HCC. CD155 overexpression also induced epithelial-mesenchymal transition in HCC cells. CD155 function in HCC involved SRC/p38 MAPK signaling pathway. CD155 interacted with SRC homology-2 domain of SRC and promoted SRC activation, further inhibiting the downstream p38 MAPK signaling pathway in HCC.

Conclusions: CD155 promotes HCC progression via the SRC/p38 MAPK signaling pathway. CD155 may represent a predictor for poor post-surgery prognosis in HCC patients.

Key words: Hepatocellular carcinoma; Poliovirus receptor; Epithelial-mesenchymal transition; Prognosis; SRC.

272. Comprehensive analysis of HHLA2 as a prognostic biomarker and its association with immune infiltrates in hepatocellular carcinoma

Lin Ding*[1]、Qian Yu[1]、Shuo Yang[1]、Wen-Jing Yang[1]、Te Liu[2]、Jing-Rong Xian[1]、Tong-Tong Tian[1]、Tong Li[1]、Wei Chen[1]、Chun-Yan Zhang[1]、Bei-Li Wang[1]、Bai-Shen Pan[1]、Jian Zhou[1]、Jia Fan[1]、Xin-Rong Yang[1]、Wei Guo[1]

1. Department of Laboratory Medicine, Zhongshan Hospital, Fudan University, Shanghai, China

2. 上海中医药大学上海老年医学研究所

Background: Inhibitory immune checkpoint proteins promote tumor immune escape and are associated with inferior patient outcome. However, the biological functions and regulatory roles of one of its members, HHLA2, in the tumor immune microenvironment have not been explored.

Methods: Random Forest analyses (371 cases), qRT-PCR (15 cases), and immunohistochemical staining (189 cases) were used to validate the prognostic value of HHLA2 in hepatocellular carcinoma(HCC) patients. Bioinformatic analyses were further performed to explore the biological functions and potential signaling pathways affected by HHLA2. Moreover, ESTIMATE, single sample gene set enrichment analysis, CIBERSORT, TIMER, and other deconvolution methods were used to analyze the composition and infiltration level of immune cells. Multiplex immunofluorescence assays were employed to validate the fractions of suppressive immune cells, and HHLA2-related molecular alterations were investigated. Finally, the clinical response to chemotherapy and immune checkpoint blockade was predicted by TIDE, Submap, and several other in silico analyses.

Results: RandomForest analysis revealed that HHLA2 was the most important inhibitory immune checkpoint associated with HCC patient prognosis (relative importance=1). Our HCC cohorts

further revealed that high HHLA2 expression was an independent prognostic biomarker of shorter overall survival (P<0.01) and time to recurrence (P<0.001) for HCC patients. Bioinformatics experiments revealed that HHLA2 may accelerate the cell cycle of cancer cells. Additionally, we found that high expression of HHLA2 was associated with immune infiltrates, including some immunosuppressive cells, cytokines, chemokines, and corresponding receptors, resulting in an immunosuppressive environment. Notably, HHLA2 expression was positively correlated with the infiltration of exhausted $CD8^+$ T cells, which was validated by immunofluorescence. Genomic alteration analyses revealed that promoter hypermethylation of HHLA2 may be associated with its low expression. More importantly, patients with high HHLA2 expression may be more sensitive to chemotherapy and have better responses to immunotherapy.

Conclusions: High expression of HHLA2 is an independent prognostic biomarker for HCC patients. It can activate the cell cycle and foster an immunosuppressive tumor microenvironment by enriching exhausted $CD8^+$ T cells. Promoter hypermethylation might lead to low expression of HHLA2 in HCC. Thus, targeting HHLA2 may be a practical therapeutic strategy for HCC patients in the future.

Key words: HHLA2, tumor microenvironment, immune infiltration, prognosis, hepatocellular carcinoma

273. Bioinformatics analysis of key genes and their associations with immune infiltration and prognosis in hepatocellular carcinoma

Danna Xie[1]、Baolin Qian[2]、Xun Li*[1,3]

1. The Affiliated Hospital of Southwest Medical University

2. The First Affiliated Hospital of Harbin Medical University

3. The First Hospital of Lanzhou University

Background: Hepatocellular carcinoma (HCC) is a malignant tumor characterized with high morbidity. The development of HCC is regulated by genes. This study intends to identify key genes and construct a new model for predicting prognosis of HCC.

Methods: Three gene datasets GSE45267, GSE87630, and GSE102079 were downloaded from the GEO database to draw Venn diagrams, and then differentially expressed genes (DEGs) were selected. The enrichment analysis of DEGs was performed, STRING was used to construct a protein interaction (PPI) network, cytoscape was used for visualization analysis, and cytoHubba was used to screen candidate genes. Next, key DEGs were screened by survival analysis. Finally, a new prognostic model was constructed. The calibration curve and time-dependent ROC curve were drawn to verify and compare the prediction accuracy.

Results: 72 DEGs were selected and 10 Hub genes were confirmed by GO/KEGG enrichment analysis and PPI network. Subsequently, 4 key genes (CYP3A4, SLC10A1, CDC20, AURKA) related to prognosis were screened out and were proved to effectively distinguish HCC tissues from normal liver tissue by principal component analysis. Moreover, the results suggested that the key genes were linked with the immune infiltration. Finally, new prognostic model incorporating key genes and TNM staging were successfully constructed. Calibration analysis indicated that there was good agreement between predicted value and actual observed value. The time-dependent ROC curves revealed the area under the curve (AUC) for 1, 3, and 5, year OS/DSS were 0.774, 0.884, 0.815 and 0.871, 0.811, 0.847, respectively.

Conclusions: The 4 genes obtained in this study were potential biomarkers affecting the prognosis and related to immune infiltration of HCC. Based on key genes and TNM staging, new prognostic model of HCC was successfully constructed, and its prediction accuracy and distinguishing ability were better than TNM staging.

Key words: Hepatocellular carcinoma; Bioinformatics; Immune infiltration; Prognostic model

274. Nucleic acids and proteins carried by exosomes from various sources: biomarkers for liver disease

Danna Xie[1,3]、Baolin Qian[2]、Xun Li*[1,3]

1. The Affiliated Hospital of Southwest Medical University

2. The First Affiliated Hospital of Harbin Medical University

3. The First Hospital of Lanzhou University

Exosomes have been a research topic of great interest to scholars. Exosomes are extracellular membrane-encapsulated vesicles, which are released into the extra-cellular space or biological fluids by different cells through exocytosis. As a new way of inter-cellular signal communication, exosomes participate in mediating various pathological and physiological processes by transmitting a variety of biologically active substances. Liver disease has characteristics of high incidence and high risk. Increasing evidence shows that exosomes have attractive application prospects in liver disease-related research. Therefore, this article mainly reviewed the potential roles of exosomes from different sources, aiming to bring enlightenments to diagnosis and treatment of liver disease.

Key words: liver disease, exosomes, nucleic acid, protein, biomarker

275. A Novel Cellular Senescence-related lncRNA Signature for Predicting the Prognosis of Breast Cancer Patients

Fangxu Yin*[1]、Chong Hou[2]、Song Wang[3]、Zhenlin Yang[1]

1. Binzhou Medical University Hospital

2. 滨州医学院烟台附属医院

3. 天津医科大学总医院

Background: Long non-coding RNA (lncRNA), a key regulator of breast cancer (BC) development, is associated with cellular senescence. Cellular senescence has been induced in several studies as a therapeutic strategy for cancer. However, the predictive value of cellular

senescence-related lncRNA (CSRL) in BC has not been fully established. Based on CSRL, we constructed a predictive model for the prognosis of BC patients.

Materials and methods: CSRL expressions, clinic-pathological and overall survival information were obtained from The Cancer Genome Atlas (TCGA) and cellular senescence databases. Univariate Cox regression、least absolute shrinkage and selection operator (Lasso) regression and multivariate Cox regression analyses were performed to obtain lncRNAs associated with cellular senescence. The accuracy of the model was assessed by survival analysis, receiver operating characteristic (ROC) curves, and principal component analysis (PCA). Next, prognostic nomograms combining cellular senescence and clinical characteristics were created and showed good predictive efficacies for survival risk stratification. Gene set enrichment analysis (GSEA) was performed to explore functional differences between high-risk and low-risk groups, while single-sample gene set enrichment analysis (ssGSEA) was used to explore the relationship between predictive signatures and immune status. Finally, correlations between predictive signatures and treatment responses in BC patients were analyzed.

Results: We constructed a signature consisting of nine cellular senescence-associated lncRNAs (LINC01871, LINC01235, LINC00987, EGOT, SEMA3B-AS1, AL358472.3, AC098484.1, AP000851.2, MAPT-AS1). The CSRL markers were established to be independent predictors for the prognosis of BC patients. Compared to clinic-pathological variables, the cellular senescence-associated lncRNA signature (CSRLSig) had high diagnostic efficiency, with an area under the subject working characteristic curve of 0.772. ssGSEA revealed that tumor and immune-related pathways were mainly enriched in the high-risk group while predictive signatures were significantly associated with immune status of BC patients. High-risk group patients were more sensitive to the targeted therapeutic agent (gefitinib) and the conventional chemotherapeutic agents (cisplatin, paclitaxel, etoposide, doxorubicin and gemcitabine). The expression of nine prognostic genes was verified in MCF-7 and MCF-10A in in vitro experiments.

Conclusion: we developed a prognostic model associated with cellular senescence in BC consisting of nine lncRNAs (LINC01235, AC098484.1, LINC00987, LINC01871, AP000851.2, MAPT-AS1, SEMA3B-AS1, AL358472.3, and EGOT). The model newly identified BC immune-related lncRNAs. The nine CSRL are potential molecular biomarkers and therapeutic targets for BC patients.

Key words： cellular senescence, lncRNA, breast cancer, immune microenvironment, drug therapy

276. Investigation of BIRC5 and CDK12 molecular mechanism underlying acquired drug resistance of afatinib in lung adenocarcinoma

xiaoxi zhu*、yuanzhi lu

暨南大学

Introduction: Resistance to the second epidermal growth factor receptor tyrosine kinase inhibitor (EGFR-TKI) afatinib is the most significant challenge in the clinical treatment of non-small cell lung cancer (NSCLC), and the underlying mechanisms remain unclear.

Methods: Genomic signatures likely to confer afatinib resistance in NSCLC were identified through data mining of public databases and comprehensive bioinformatics analysis. An acquired afatinib-resistant lung adenocarcinoma cell line (HCC827 AR) was established by chronic exposure to afatinib in vitro. The expression of baculovirus IAP repeat protein 5 (BIRC5) was detected by western blot, and the cell viability of HCC827 AR was determined by CCK8.In addition, we collected clinicopathological data and public database cancer genes to analyze the correlation between CDK12 and lung cancer; we constructed low-expressing CDK12 lung cancer cell line stably using lentivirus. based on these cell models. The correlation between CDK12 and lung cancer cell phenotype was verified by CCK8 cell proliferation assay, clone formation assay, migration assay, and flow cytometry. And the use of CDK12 inhibitor Dinaciclib on the growth of lung cancer cells. Finally, Western blot was used to detect the downstream targets of CDK12 to explore the molecular mechanism of CDK12 acting on BIRC5.

Results: Overexpression of BIRC5 in NSCLC tissues. Overexpression of BIRC5 correlated with tumor stage and age, gender, smoking, and lymph node metastasis. BIRC5 expression is associated with progression and poorer survival in LUAD, and BIRC5 and its related genes are involved in apoptosis, cell cycle, and DNA damage-related processes and pathways. BIRC5 is overexpressed in lung adenocarcinoma cell line afatinib-resistant cells. The BIRC5 inhibitor YM155 has inhibitory effects on afatinib-resistant cells. CDK12 knockdown expression NSCLC

cell line was successfully constructed. CDK12 knockdown inhibited the proliferation and migration of NSCLC cells, induced G1 phase arrest (p<0.05), and the survival of lung cancer cells resistant to CDK12 inhibitor Dinaciclib, and promoted lung cancer cell apoptosis. Genes significantly down-regulated by CDK12 include c-Myc, BIRC5. CDK12 can significantly increase the apoptosis of drug-resistant cells by inhibiting the expression of the anti-apoptotic protein BIRC5 in afatinib-resistant cells.

Conclusions: We investigated the expression profile and potential functional analysis of BIRC5 in NSCLC. It was demonstrated that overexpression of BIRC5 resulted in NSCLC resistance to afatinib, and BIRC5-specific inhibitors might reverse the drug-resistant phenotype and promote cell death in lung cancer cells. At the same time, Dinaciclib can reverse the drug resistance of lung cancer cells by inhibiting the expression of BIRC5. Therefore, CDK12 and BIRC5 may be effective targets for the treatment of drug resistance of lung cancer cells, and inhibition of CDK12 and BIRC5 may become a new strategy for lung cancer treatment.

Key words： Non-small cell lung cancer; Afatinib resistance; BIRC5; CDK12; Dinaciclib

277. Genetically predicted circulating concentrations of micronutrients and the risk of hepatocellular carcinoma: a Mendelian randomization study

Chenglei Yang[1]、Qiang Cai[2]、Siyu Chen[3]、Yuankuan Li[1]、Xi Wu[3]、Bangde Xiang*[1]

1. Guangxi Medical University Cancer Hospital

2. Xiangyang Central Hospital, Affiliated Hospital of Hubei University of Arts and Science

3. The First Clinical Medical School, Guangxi Medical University

Objective： Exploring the causal relationship between micronutrients and the risk of hepatocellular carcinoma by Mendelian randomization.

Methods： Two-sample MR analysis was used to explore the causality of micronutrients on HCC. SNPs related to micronutrients were obtained from genome-wide association studies (GWAS). Also, the SNPs were screened in GWAS of HCC and PhenoScanner V2 to exclude those associated with HCC (P＜0.05) and confounders (p<5×10^{-8} and r2>0.8). Then, F statistics were

performed on the remaining SNPs to exclude weak instrumental variables ($F < 10$). The TwoSampleMR package performed Mendelian randomization (MR) analysis in R (Version 4.0.1) to establish the causal relationship between micronutrients and HCC risk. When only 1 SNP was considered as a genetic instrument, the Wald ratio was used to generate effect estimates. IVW fix effects models were used when the number of SNPs was 2, and IVW multiplicative random effects models were used if the number of SNPs was more than 2. Other methods such as MR-Egger, simple mode, weighted mode, and weighted median were employed for MR estimates. Sensitivity analyses, which included assessments of directional heterogeneity and pleiotropy, were performed to test the robustness of MR estimates,. Directional heterogeneity was assessed using the Cochran Q statistic calculated by the inverse variance weighted (IVW) and MR egger methods, and pleiotropy was measured by MR-Egger regression. Impacts of causal estimation were evaluated using the "leave-one-out analysis". Sensitivity analyses were not conducted if the number of SNPs was small (less than three). A value of $P<0.05$ was considered significant in sensitivity analysis

Results: The causal relationships between 48 SNPs (7 SNPs belong to calcium, 6 SNPs belong to magnesium, 2 SNPs belong to copper, 3 SNPs belong to zinc, 3 SNPs belong to phosphorus, 1 SNPs belong to selenium, 4 SNPs belong to β-carotene, 2 SNPs belong to vitamin A, 1 SNPs belong to vitamin B6, 5 SNPs belong to vitamin B12, 1 SNPs belong to vitamin E, 10 SNPs belong to vitamin C, 3 SNPs belong to folate), selected as instrumental variables, and HCC risk were evaluated using data from GWAS of 168 HCC patients and 372,016 controls. The MR analysis showed that calcium, magnesium, copper, zinc, phosphorus, selenium, β-carotene, vitamins A, B6, B12, E, C, and folate had no causal relationship with HCC risk. In IVW and MR-Egger analysis, no directional heterogeneity was detected for the associations between micronutrients and HCC. Also, no pleiotropy with a small intercept was identified by MR-Egger regression. The "leave-one-out analysis" showed that no given SNP had any significant impact on causal estimation.

Conclusion: Our study, as the study to analyze the causal relationship between multiple circulating micronutrients and the risk of HCC using the MR method, did not provide evidence to support that the 13 micronutrients analyzed in the study were risk factors for HCC. This provides a reference for subsequent research, and also suggests that intake of micronutrients may not prevent HCC and its associated risks.

Key words: hepatocellular carcinoma; Mendelian randomization; micronutrients; causal inference

278. Clinical prognostic value and potential molecular pathway of Cell division cycle associated 5(CDCA5) in hepatocellular carcinoma (HCC)

Cheng-Lei Yang*[1]、Guo-Qun Liu[3]、Kun-Ying Huang[2]、Ao Jia[3]、Bang-De Xiang[1]

1. Department of Hepatobiliary Surgery, Guangxi Medical University Cancer Hospital, Nanning 530021, Guangxi Province, PR China

2. 广西医科大学基础医学院

3. 广西医科大学第一临床医学院

Objective: The purpose of this study is to investigate the prognostic value and possible molecular pathway of CDCA5 in hepatocellular carcinoma (HCC) and its relationship with the immune microenvironment of HCC.

Methods: Based on bioinformatics, public databases and our in-house RNA sequencing (RNA-seq) data, we explored the CDCA5 mRNA expression level. Meanwhile, the protein expression level of CDCA5 in HCC was also investigated using immunohistochemical analysis based on our RNA-seq database. In combination with TIMER immune database and TISCH single cell database, immune infiltration level and single cell localization of CDCA5 in HCC were investigated. Additionally, the potential molecular pathways that CDCA5 involved in HCC were explored according to TCGA database.

Results: Firstly, 1649 HCC samples and 1044 non-cancerous tissues were included from GEO, TCGA and our in-house RNA-seq database. The results of comprehensive meta-analysis suggested that CDCA5 mRNA expression level in HCC was significantly higher than non-HCC tissues (SMD=1.61). Besides, CDCA5 was proved that it had strong diagnostic ability for distinguishing HCC from non-tumor tissues (AUC=0.94). Furthermore, immunohistochemical analysis indicated that CDCA5 protein expression was up-regulated in HCC as well. However, no significant statistical difference was found the enrichment of $CDCA5^{+}$T cells between primary and early recurrent HCC. Clinical pathological parameters analysis showed that up-regulated CDCA5

was associated with adverse clinical characteristics and worse survival and prognosis of HCC patients. Secondly, 16457 single cells from 18 HCC tumor tissues were used for cell classification and marker gene identification by Seurat. 28 subpopulations and 10 cell types were identified, in which cells expressing CDCA5 were defined as $CDCA5^{+}T$ cells that highly expressed proliferation genes MKI67, CD4, CD8A, GZMH and immune exhaustion cell marker genes (TIGIT, CTLA4, PDCD1 and HAVCR2). $CDCA5^{+}T$ cells were related to cell division, mitotic nuclear division, cell proliferation, DNA replication, cell cycle and p53 signaling pathway by GO and KEGG analysis, which might play an important role in the HCC immune microenvironment. Finally, We found that microRNA-1286 (miRNA-1286) may directly target CDCA5 expression. GO and KEGG analysis indicated that highly expressed CDCA5 may be involved in cell division related pathways to regulate HCC progression. CDK1, CCNA2, CCNB1, TOP2A and BUB1B were identified as hub genes by protein-protein interaction (PPI) network.

Conclusion: CDCA5 was up-regulated in HCC, and its high CDCA5 expression has strong diagnostic ability in differentiating HCC from non-HCC tissues. Up-regulated CDCA5 expression was associated with poor survival outcomes in HCC patients. Immune infiltration and single cell localization of CDCA5 and HCC patients were discovered a population of proliferative $CDCA5^{+}T$ cells related to the HCC immune microenvironment.

Key words: CDCA5, HCC, immune infiltration, single cell localization, molecular pathway

279. Identification of the target protein of the metastatic colorectal cancer-specific aptamer W3 as a biomarker by aptamer-based target cells sorting and functional characterization

Wanming Li*[1]、Chia-Chun Wu[2]、Shuo Wang[1,4]、Linlin Zhou[1]、Lei Qiao[3]、Wei Ba[1]、Furong Liu[1]、Linan Zhan[1]、Hang Chen[1]、Jau-Song Yu[2]、Jin Fang[1]

1. China Medical University

2. Chang Gung University

3. Shengjing Hospital of China Medical University

4. Shenyang Agricultural University

Metastasis is a leading cause of cancer-related deaths. Hence, the discovery of more reliable metastasis-related biomarkers is crucial to improve the survival rate of cancer patients. W3 is an aptamer previously produced by the subtractive cell-SELEX using metastatic colorectal cancer cells as target cells and non-metastatic cells as negative cells. In this study, we aimed to evaluate whether the target molecule of W3 can potentially act as a metastatic biomarker. First, we obtained two cell subpopulations with different expression levels of the target molecule by W3-based cell sorting. Subsequently, we demonstrated that $W3^{high}$ cells have a higher metastatic potential than W3low cells both in vitro and in vivo. Further, immuno-histochemical analysis revealed that W3 target expression is positively associated with metastasis and poor prognosis of CRC patients. Usi ng mass spectrometry (MS) combined with pull-down, we identified that Ephrin type-A receptor 2 (EphA2) is the target of W3. EphA2's potential as a metastatic predictor was demonstrated by capturing W3-positive circulating tumor cells from CRC patients using a W3 probe. Based on these results, we put forward a stratagem for cell-SELEX-based biomarker discovery: selecting an aptamer through subtractive cell-SELEX towards the phenotype of interest; evaluating the functional phenotype of the target molecule by aptamer-based target cell sorting and analysis of clinical samples; and identifying the aptamers target molecule using MS and aptamer-based target

enrichment. This stratagem not only shortens the time for the clinical application of aptamers but also enables a more targeted and efficient discovery of biomarkers.

Key words: Aptamer W3; Cell-SELEX; Metastatic colorectal cancer; Tumor biomarker; EphA2; Circulating tumor cell

280. Association between telomere length and hepatocellular carcinoma risk: a Mendelian randomization study

Chenglei Yang*[1]、Xi Wu[2]、Siyu Chen[2]、Bangde Xiang[1]

1. Guangxi Medical University Affiliated Tumor Hospital

2. The First Clinical Medical School, Guangxi Medical University

Background: Hepatocellular carcinoma (HCC), one of the common cancers that threaten the health of people worldwide, has been suggested to be associated with telomere length (TL). However, the causal relationship between TL and HCC is unknown. This study aimed to explore the causal relationship between TL and HCC using a Mendelian randomization analysis that can circumvent the effects of confounding and reverse causality in the Asian population and European population, respectively.

Methods: The summary statistics of TL-associated SNPs were obtained from a genome-wide association study (GWAS) in the Asian population (N= 23096). Data of TL-associated SNPs in the European population (N= 472174) and the GWAS summary statistics of HCC in the Asian population (1,866 cases, 195,745 controls) and the European population (168 cases, 372,016 controls) were downloaded from the publicly GWAS database. Next, instrumental variables (IVs) are screened under strict criteria. The information on these SNPs of HCC from the GWAS dataset was extracted. Two-sample Mendelian randomization (MR) was performed in Asians and Europeans using five methods: inverse variance weighting (IVW), weighted median estimate, MR-Egger regression, weighted-mode estimate, and simple-mode estimate. To robust the result, sensitivity analysis was performed to detect the heterogeneity and horizontal pleiotropy. leave-one-out analysis was performed to examine SNPs with driving effects.

Results: Nine single nucleotide polymorphisms (SNPs) associated with TL in Asian and 98 SNPs in European populations were selected as IVs from GWAS, respectively. No sufficient evidence for a causal relationship between heritable TL and the HCC risk was found in Asian (IVW analysis OR= 1.023, 95% CI -0.294, 0.340, *P*= 0.887) and European populations (IVW analysis OR= 0.9997, 95% CI 0.9992, 1.0001, *P*= 0.1574). Other methods also achieved similar results. IVW analysis and MR-Egger regression showed that there is no heterogeneity among IVs in Asians (IVW, Q (df) 12.14 (8), *P*= 0.145; MR-Egger, Q (df) 10.81 (7), *P* = 0.147) and Europeans (IVW, Q (df) 104.42 (97), *P*= 0.285; MR-Egger, Q (df) 103.72 (96), *P* = 0.277). While, MR-Egger regression found no horizontal pleiotropy in Asians (intercept β= -0.034, *P*= 0.384) and Europeans (intercept β= -8.76E-06, *P*= 0.424). The leave-one-out analysis found no SNP with driving effect.

Conclusions: This study demonstrated that heritable TL was not significantly associated with the HCC risk in Asian and European populations.

Key words: Mendelian randomization; Telomere length; Hepatocellular carcinoma; Single nucleotide polymorphism; Genome-wide association study

281. Two molecularly distinct subtypes and immunosuppressive microenvironment of CK19-positive cancer stem cells in HBV-associated hepatocellular carcinoma based on scRNA-seq

Chenglei Yang*[1]、Qiuyan Wang[2]、Bangde Xiang[1]

1. Guangxi Medical University Cancer Hospital

2. 广西医科大学，广西基因组与个体化医学重点实验室

Background and Aims: The high heterogeneity in hepatocellular carcinoma (HCC) is one of the important reasons for its poor therapeutic effect. Cancer stem cells (CSCs) have unique stem cell-like self-renewal and differentiation potentials, which are the most fundamental factor leading to tumor heterogeneity. Keratin 19 (CK19), a marker of CSC, is found to be expressed in approximately 4-28% of HCCs. The over-expression of CK19 was an important poor prognostic

marker for HCC and was incorporated into various HCC molecular typing systems. However, the understanding of CK19^{+}CSC classification and immune microenvironment in HBV-associated HCC is limited.

Methods: Tissue samples were collected from 11 patients with HBV-related HCC (discovery cohort), including 7 CK19-positive, 3 CK19-negative samples tumor tissues and 5 adjacent tissues. Then scRNA-seq experiments were performed using the Singleron platform. Surgically resected tumor tissue and paired para-cancerous tissue samples from 96 patients with HBV-related HCC were collected for bulk RNA sequencing and their clinicopathological data were recorded(validation cohort 1). HCC cell lines (HCC_97L, HCC_LM3) were selected to construct a stem cell-enriched nude mouse model. We selected the normal liver cell line LO2 with low CK19 expression, the cholangiocarcinoma cell line HCCC9810 with significantly high CK19 expression, and hepatocellular carcinoma with relatively high CK19 expression (HUH7, SNU182, HCC_97 and HCC_LM3), as well as HCC_97L and HCC_LM3 primary nude mouse tumorigenic tissues (Tissue_97 and Tissue_LM3) to conduct scRNA-seq as validation cohort 2. In addition, the published spatial transcriptome data of CK19^{+}HCC patient tissues (including tumor and non-tumor) was used to uncover the spatial distribution of TAM_SPP1. The results of the analyses for scRNA-seq data were validated using validation cohort 1 or 2, Spatial transcriptome, immunohistochemistry or multiplex immunofluorescence and in vitro and in vivo experiments.

Results: In this study, we sequenced a total of 64,581 single cells derived from human HCC and adjacent tissues. We delineated the transcriptome profile of human CK19^{+} HCC, which is classified into 11 major cell types, including cancer cells, immune cells, and stromal cells. First, we found CK19^{+}CSCs co-express multiple consensus markers of CSCs in malignant cells, such as EPCAM, PROM1, SOX9, CD24, ALDH1A1, DLK1 and LGR5. Then, the heterogeneity of malignant cells in CK19^{+} HCC patients was revealed at the single-cell level and two molecularly distinct cellular subtypes were found in CK19-positive CSCs, verified by validation cohort 2. The foetal hepatocyte subtype regulated by the MYC transcription factor has strong stemness characteristics. The adult HHyP subtype, which is regulated by SOX9, possesses stronger metastatic ability and worse prognosis. CLDN4 was identified as a marker that differentiates the two cellular subtypes of CK19^{+}CSC. Moreover, myeloid-derived cells were classified into 7 categories in the discovery cohort. The immune microenvironment of suppressive SPP1-positive

tumor-associated macrophages (TAM_SPP1) in CK19^{+} HCC is further elucidated. We found that CK19^{+} HCCs were significantly enriched in SPP1-TAM subset cells compared with CK19-negative HCCs. TAM_ SPP1 promoted tumor invasion and metastasis at the tumor invasive front of CK19^{+} HCC by activating angiogenesis, EMT, hypoxia and Kras signaling pathways. And patients with high TAM_SPP1 enrichment had shorter overall survival and disease -free survival. In addition, we further disclosed the microenvironment of T/NK cell immune exhaustion. Relative to non-tumor CD8_GZMH, CD8_NR4A1, NK_CD160 and NK_CD16 cell subsets were significantly reduced and T_MKI67 was significantly enriched in CK19^{+}HCC, whereas only NK_CD160 was reduced in CK19-negative HCC. The cytotoxic CD8_GZMH was significantly reduced in CK19^{+}HCC compared to CK19-HCC. We further found that T_MKI67 expresses multiple immune checkpoint markers, such as HAVCR2, TIGIT, CTLA4, LAG3 and PDCD1, verified by validation cohort 1.

Conclusions: Our findings provide a comprehensive transcriptomic landscape of human CK19^{+}HCC at single-cell resolution. Stem-strong foetal hepatocyte and high-metastatic adult HHyP subtypes were identified in CK19^{+}CSC, with distinct regulatory mechanisms in these subtypes. Enrichment of SPP1-TAM and T_MKI67 were found in CK19^{+}HCC. These findings provide the basis for effective immuno-oncology therapy in HCC.

Key words: Hepatocellular carcinoma, cancer stem cell, keratin 19, single-cell transcriptome sequencing, immunosuppressive microenvironment

\

282. PD-L1 expression on circulating tumor cells can be a predictive biomarker to PD-1 inhibitors combined with radiotherapy and antiangiogenic therapy in advanced hepatocellular carcinoma

Ke Su*、Yunwei Han

The Affiliated Hospital of Southwest Medical University

Aim: A programmed death 1 (PD-1) inhibitor coupled with radiotherapy and antiangiogenic therapy is a potential therapeutic strategy for advanced hepatocellular carcinoma (HCC). We aimed to determine if circulating tumor cells (CTCs) positive for programmed death-ligand 1 (PD-L1) could be employed as a predictive biomarker in HCC patients receiving triple therapy.

Methods: In this study, HCC patients received a PD-1 inhibitor in combination with intensity-modulated radiotherapy (IMRT) and antiangiogenic therapy. Following IMRT, the PD-1 inhibitor was administrated once every 3 weeks, while the antiangiogenic drug was given once a day. Treatment was continued until the disease progressed. Two mL of peripheral blood was collected at baseline, 1 month, and 3 months after treatment for CTC enrichment using the CytoSorter® system with a CytoSorter™ CTC PD-L1 Kit (Watson Biotech., China).

Result: A total of 47 HCC patients receiving the triple therapy were enrolled in this study. Patients with<2 PD-L1+ CTCs at baseline had a higher objective response rate (ORR) and longer overall survival (OS) than those with ≥ 2 PD-L1+ CTCs (56.5% *vs.* 16.7%, p= 0.007; not reach *vs.* 10.8 months, p= 0.001, respectively). The count of PD-L1+ CTCs was found to be an independent predictive biomarker of OS. Furthermore, the objective response was more likely to be achieved in patients with a dynamic decrease in PD-L1+ CTC counts at 1 month after treatment.

Conclusions: Our study demonstrated that PD-L1+ CTCs could be a predictive biomarker for HCC patients receiving PD-1 inhibitors in combination with IMRT and antiangiogenic therapy.

Key words: programmed death-ligand 1, circulating tumor cells, hepatocellular carcinoma, programmed death 1 inhibitor, radiotherapy, antiangiogenic therapy

283. Clinical significance of serum and tumor tissue transthyretin expression in surgically resected non-small cell lung cancer

chunhua xu*

Nanjing Chest Hospital

Objective: Transthyretin (TTR) is a traditional biomarker for nutritional and inflammatory. The present study was conducted to explore the clinical value of TTR in serum and tumor tissue in patients with surgically resected non-small cell lung cancer (NSCLC).

Methods: TTR expression levels were determined in paraffin-embedded NSCLC tissue specimens using immunohistochemistry. Serum TTR expression levels were measured from patients with lung cancer and healthy controls using enzyme-linked immunosorbent assay (ELISA).

Results: The expression levels of TTR were significantly higher in lung cancer tissues than in paracancerous tissues, and TTR expression was significantly associated with TNM stage (P=0.002) and lymph node metastasis (P=0.032). Multivariate analysis revealed that increased expression of TTR was an independent risk factor for overall survival (P=0.012) and progression-free survival (P=0.011) in NSCLC patients. The expression levels of TTR in serum from lung cancer patients were lower than those of healthy controls (P=0.002). A high expression of TTR in tumor tissue was associated with a higher serum level (r=0.799, P=0.001).

Conclusions: TTR expression is upregulated in lung cancer patients, and its expression was correlated with poor prognosis in NSCLC patients.

Key words: Non-small cell lung cancer; Transthyretin; Expression; Prognosis

284. Radiotherapy in Gastric Cancer Patients with Liver Metastases: A Propensity Score-Matched SEER Database Analysis

Liyou Lian[1]、Shuwen Cheng[2]、Rujie Zheng[3]、Hongxia Yao[1]、Tianhui Chen[4]、Jinfei Chen*[5]

1. First Affiliated Hospital of Wenzhou Medical University

2. Nanjing University Medical School

3. Department of Radiology, the First Affiliated Hospital of Wenzhou Medical University

4. Department of Cancer Prevention/Zhejiang Cancer Institute, Cancer Hospital of the University of Chinese Academy of Sciences (Zhejiang Cancer Hospital)

5. Department of Oncology, First Affiliated Hospital of Wenzhou Medical University

Background and purpose: Gastric cancer with liver metastases (GCLM) remains a challenge in clinical practice. The purpose of the study was to access the therapeutic role of radiotherapy in GCLM patients in the Surveillance, Epidemiology, and End Results (SEER) database.

Materials and methods: Data on GCLM patients were extracted from the SEER database. Propensity score matching (PSM) was used to minimize bias between radiotherapy and no-radiotherapy groups. The therapeutic role of radiotherapy was evaluated by comparing Kaplan-Meier (KM) curves and Cox proportional hazard models presented with hazard ratio (HR) and 95% confidence intervals (CI).

Results: A total of 2300 patients with microscopically confirmed GCLM were extracted from the database, including 356 patients who received radiotherapy that was 1:1 PSM with patients who did not receive radiotherapy. GCLM patients could not benefit from radiotherapy (HR: 1.08, 95% CI: 0.93-1.26, P= 0.33). Multivariate analyses revealed receiving surgery, chemotherapy and low grade were protective prognostic factors. The median overall survival (OS) time of radiotherapy and no-radiotherapy groups were both 7 months (P > 0.05). The median OS time of chemotherapy with radiotherapy was shorter than those chemotherapy alone (8 months, 95% CI 8-10 months versus 10 months, 95% CI 9-12 months, P > 0.05). The median OS time of surgery with radiotherapy was similar to those with surgery alone (11 months, 95% CI 8-17 months versus 11 months, 95% CI 6-22 months, P > 0.05).

Conclusion: Radiotherapy is not associated with better prognosis in GCLM patients. Radiotherapy combined with chemotherapy or surgery does not prolong the OS.

Key words: Gastric cancer; Liver metastases; Radiotherapy; Overall survival; Propensity score.

285. Survival benefit after radiotherapy for pancreatic ductal adenocarcinoma patients with liver metastases: A propensity score-matched study

Liyou Lian[1]、Shuwen Cheng[2]、Rujie Zheng[3]、Hongxia Yao[1]、Tianhui Chen[4]、Jinfin Chen*[5]

1. First Affiliated Hospital of Wenzhou Medical University

2. Nanjing University Medical School

3. Department of Radiology, the First Affiliated Hospital of Wenzhou Medical University

4. Department of Cancer Prevention/Zhejiang Cancer Institute, Cancer Hospital of the University of Chinese Academy of Sciences (Zhejiang Cancer Hospital)

5. Department of Oncology, First Affiliated Hospital of Wenzhou Medical University

Background: Pancreatic ductal adenocarcinoma (PDAC) patients are commonly metastasized to the liver, which are extremely chemo-resistant. While radiotherapy is commonly used to treat metastatic tumors, survival benefits after radiotherapy for PDAC patients with liver metastases remains uncertain. Thus, we aimed to evaluate survival benefits after radiotherapy for PDAC patients with liver metastases.

Methods: Data on PDAC patients with liver metastasis were extracted from the Surveillance, Epidemiology, and End Results (SEER) database. The bias between radiotherapy and no-radiotherapy groups was minimized using propensity score matching (PSM). Kaplan-Meier and Cox proportional hazard models were used to explore the therapeutic role of radiotherapy presented with hazard ratio (HR) and 95% confidence intervals (CI).

Results: Overall, 12,945 PDAC patients with liver metastasis were extracted from the SEER database, including 473 patients who underwent radiotherapy (1:1 matched with patients without radiotherapy). We found that PDAC patients with liver metastasis receiving radiotherapy alone could significantly prolong the OS (HR: 0.78, 95% CI: 0.682-0.882, P<0.001) or receiving

radiotherapy in combination with either surgery or chemotherapy could also prolong the OS (HR: 0.752, 95% CI: 0.661-0.855, *P*<0.001; HR: 0.784, 95% CI 0.689-0.892, *P= 0.008*, respectively). Radiotherapy appeared to prolong the OS (with median OS increasing from 1 month to 4 months). Additionally, we found that several protective prognostic factors including younger age, low stage, and receiving chemotherapy and surgery (all *P*<0.001).

Conclusions: PDAC patients with liver metastases could benefit from radiotherapy alone or in combination with either surgery or chemotherapy, suggesting radiotherapy was most effective for PDAC patients with liver metastases, especially for younger age (< 65 year), low stage, and receiving chemotherapy and surgery.

Key words: pancreatic ductal adenocarcinoma; radiotherapy; liver metastasis; propensity score; prognosis.

286. Down-regulation of BMAL1 1 by miR-494-3p promotes hepatocellular carcinoma growth and metastasis by increasing GPAM-mediated lipid biosynthesis

Tao Yang*[1]、Yi Yang[1]、Peng Yuan[1]、Zifeng Zhao[1]、Jinliang Xing[3]、Hongxin Zhang[1]、Jibin Li[2]

1. Department of Pain Treatment, Tangdu Hospital, the Fourth Military Medical University, Xi'an, Shaanxi, 710038, China

2. 空军军医大学教学实验中心

3. 空军军医大学生理与病理生理学教研室

Background & Aims: The circadian clock presents daily rhythmicity to numerous crucial biological processes and its disruption is related to carcinogenesis in several kinds of cancer. As a core circadian rhythm component, brain and muscle arnt-like protein 1 (BMAL1) dysregulation has been shown to contribute to aberrant metabolism in human diseases. However, the biological functions of BMAL1, especially its involvement in aberrant lipid metabolism in hepatocellular carcinoma (HCC), remain elusive. Methods: The expression of BMAL1 and its clinical significance was determined in tissues and cell lines of HCC. In addition, biological functions of BMAL1 in HCC cells and the underlying molecular mechanisms were explored both in vitro and

in vivo. Moreover, therapeutic application of BMAL1 in the treatment of HCC was also explored. Results: We established that BMAL1 was often down-regulated in HCC cells primarily due to the up-regulation of miR-494-3p. Down-regulation of BMAL1 was remarkably linked to dismal survival in individuals with HCC. BMAL1 down-regulation enhanced HCC cell growth, as well as metastasis. Mechanistically, through cooperating with EZH2, BMAL1 transcriptionally suppressed glycerol-3-phosphate acyltransferase mitochondrial (GPAM) expression, a pivotal enzyme involved in the regulation of lipid biosynthesis, leading to reduced levels lysophosphatidic acid (LPA), which has long been known as mediator of oncogenesis. Particularly, treatment with SR8278, an activator of BMAL1, exhibited a therapeutic influence on HCC. Conclusions: BMAL1 has as critical anti-oncogenic role in HCC, providing a strong research evidence for BMAL1 as a prospective HCC therapeutic target.

Key words: BMAL1, GPAM, EZH2, lipid biosynthesis, growth, metastasis, hepatocellular carcinoma

287. Expression Profile and Prognostic Value of MELK in Human Breast Cancer

Mengqi Yang *、Yajie Liu

Peking University Shenzhen Hospital

Background: The Ser/Thr protein kinase MELK (maternal embryonic leucine zipper kinase) involved in various processes such as cell cycle regulation, self-renewal of stem cells, apoptosis and splicing regulation. MELK has already been considered as an attractive therapeutic target for managing cancer. However, a comprehensive analysis of the expression and prognostic value of MELK on breast cancer (BC) patients is still lacking.

Methods: The expression profile of MELK in BC and its subgroups were evaluated via UALCAN, ONCOMINE and GEPIA databases. Genetic alterations and co-expression profiles of MELK were performed using the cBioportal database. The prognostic value of MELK in BC and its subgroups was analyzed using Kaplan Meier plotter database. The correlation analysis of MELK and immune cell infiltration in BC was analyzed by the TIMER database.

Results: MELK was significantly highly expressed in BC than adjacent normal tissues, but it was not remarkably correlated with the tumor stage. There was a positive correlation between high MELK mRNA expression and Chromosome-associated kinesin KIF4A. More importantly, high mRNA expression of MELK was significantly associated with shorter overall survival (OS) in BC patients. Interestingly, increased MELK was associated with worse OS in HER-2 positive BC patients, while no prognostic value of MELK was observed in triple negative BC patients.

Conclusion: Our studies suggest that MELK may be regarded as novel biomarkers for predicting potential prognosis values and potential therapeutic targets of HER-2 positive BC patients. These data warrant further functional validation for MELK as a potential therapeutic target in HER-2 positive BC.

Key words: MELK, Breast cancer, prognosis, biomarker, therapeutic target

288. N7-Methylguanosine-Related lncRNA: Potential Biomarker for Predicting the Prognosis of Hepatocellular Carcinoma Patients

Zhihao Xu*、Ning Zhang、Huake Cao、Songlin Xing、Feixu Chen

Anhui Medical University

Research Intent: The most common type of liver cancer, carcinoma, is one of the most fatal malignancies with its high heterogeneity and recurrence rate. Traditional TNM staging often fails to accurately predict patient prognosis and survival. Suitable biomarkers and subtle molecular subtypes of hepatocellular carcinoma urgently need to be identified to provide accurate and effective treatment for patients with different prognoses. The N7-Methylguanosine (m7G) modification is an emerging RNA modification that is thought to be associated with RNA shearing, splicing, and robustness, and is further involved in cancer development. Long non-coding RNAs (lncRNA) have received much attention for their important regulatory roles. In this study we researched into the prognostic significance of m7G-related lncRNA using public database. Our study aims to explore the prognostic value of m7G-related lncRNA, to generalize the molecular

subtypes of hepatocellular carcinoma and to provide a prognostic model with robust predictive power for the clinic.

Materials and Methods: Data collection and normalization RNA-sequencing files (FPKM, normalized with Fragments Per Kilobase of transcript per Million mapped reads) for the liver samples, together with corresponding clinical information on tumour samples and normal samples were downloaded from The Cancer Genome Atlas (TCGA, https://portal.gdc.cancer.gov/) and Genotype-Tissue Expression (GTEx, https://www.gtexportal.org/) databases. Based on previous publications, m7G-regulator genes were collected from Gene Set Enrichment Analysis (GSEA, https://www.broadlnstitute.org/gsea/). A total of 29 regulators' expression matrixes were extracted from our dataset.Annotation and Identification of m7G-related lncRNA Alignment and annotation of sequences were performed using Genome Reference Consortium Human Build 38 (GRCH38). Derived from recognizing the Ensemble ID, 15,203 lncRNA were identified. Pearson correlation analysis was then carried out to explore the correlation between m7G-regulators and lncRNA to obtain m7G-related lncRNA. In our study, a lncRNA whose expression was correlated with one or more m7G-regulator was considered as m7G-related lncRNA (| Pearson | > 0.5, P<0.01).m7G-related lncRNA Signature Model Establishment and Verification Combining with clinical data, univariate analysis was first implemented to screen prognostic m7G-related lncRNA. Thereafter, we used the R package "glmnet" for regression analysis using the lasso-cox method combining clinical information such as follow-up time and status, where we set up 10-fold cross-validation to obtain the optimal model. We constructed an m7G-related lncRNA Signature model including 9 m7G-related lncRNA and corresponding coefficient. The risk score can be calculated with this formula:Annotation of DEG function between risk groups Here we used the R package "limma" (version 3.40.6) for the analysis of variance to obtain differential genes between the risk groups. Furthermore, we performed an enrichment analysis of the differentially expressed mRNA in order to determine the potential mechanisms of conversion of low-risk groups to high-risk groups. In this study, the "ClusterProfiler" package, a highly integrated module, was used to investigate the potential biological functions of differentially expressed genes in GO and KEGG.Predicting possible treatment strategies and potential drugs Potential ICB response was predicted with TIDE algorithm. TIDE is an algorithm for predicting potential immunotherapy responses. By using gene expression markers, TIDE examines two different mechanisms of

tumour immune escape, including dysfunction of tumour-infiltrating cytotoxic T lymphocytes (CTLs) and rejection of CTLs by immunosuppressive factors. There is a link between high TIDE scores and poor efficacy and a short survival rate after immune checkpoint blockade therapy. Using the largest publicly available pharmacogenomics database, we predicted chemotherapeutic response for each sample. The prediction process was implemented by R package “pRRophetic”. By using ridge regression, the half-maximal inhibitory concentration (IC50) of samples was estimated.

Result: Firstly, compared with expression in normal tissue, the expression of most m7G regulators notably increased, including: AGO2, CYFIP1, DCP2, EIF3D, GEMIN, IFIT5, LARP1, METTLE1, NCBP1, NCBP2, NCBP3, NUDT16, NUDT4, WDR4, EIF4E, EIF4G3, NUDT4B, SUSPN. DCPS, EIF4A1, NSUN2 and NUDT3 were found downregulated, while no significance was found in LSM1, NCBP2, NUDT11, EIF4E3 and EIF4E1B. Next, with the expression profiles of the m7G regulators and lncRNA, we used the PEARSON formula to calculate the correlation coefficients and p values of the m7G regulators and lncRNA. In our study, a lncRNA whose expression was correlated with one or more m7G regulator was considered as m7G-related lncRNA (| Pearson | > 0.5, P<0.01). 718 m7G-related lncRNA were identified. In a two-to-one ratio, we randomly divided the cohort into a training group and a test group. We calculated a Signature model that included nine lncRNAs and corresponding coefficients by the LASSO-cox regression algorithm. A risk score is assigned to each sample, which can be calculated with the formula shown below: Risk Score= 0.0387730768087211 * PRRT3-AS1 + 0.465820036186531 * TMCC1-AS1+0.353800453818159*AL031985.3+0.0134643432540013*NRAV+0.0843470300047088*PLEKHA8P1+0.0941066638321154*RPL13P5+0.0511736005029239*POLH-AS1+0.0154659366031976*AL158166.1+0.400107643735815*MKLN1-AS The AUC for the training group were 0.81, 0.79 and 0.79 for one, three and five years respectively, while the AUC for the test group were all 0.71.We then divided the TCGA cohort into two groups based on risk scores, a low risk group and a high risk group, with significant differences between the two groups in scores for survival, Tumour Mutation Burden, Stem Score, and immune infiltration. Also, higher levels of immune checkpoint and glycolysis-related gene expression in the high-risk group predicted higher levels of immune escape. We also carried out enrichment analyses of differential genes and

showed that the high-risk group was significantly enriched in cycles such as immune cell formation and cell cycle.

Conclusion: In our present study, m7G-related lncRNA was proved to be closely related to patient survival, immune and metabolic levels, thus influencing the development of hepatocellular carcinoma tumours. And we constructed and evaluated a m7G-related lncRNA Signature model with fine predictive capability help predict the prognosis of HCC patients. m7G modifications and lncRNA will be a promising way for the diagnosis and treatment of HCC.

Key words: hepatocellular carcinoma, N7-methylandenosine, long non-coding RNA, computational biology and bioinformatics, immunology

289. YAP ISGylation increases its stability and promotes its positive regulation on PPP by stimulating 6PGL transcription

Xiangfei Xue *、Xiao Zhang

Shanghai Chest Hospital, Shanghai Jiao Tong University

Yes-associated protein (YAP) activation is crucial for tumor formation and development, and its stability is regulated by ubiquitination. ISGylation is a type of ubiquitination like post-translational modification, whereas whether YAP is ISGylated and how ISGylation influences YAP ubiquitination-related function remains uncovered. In addition, YAP can activate glucose metabolism by activating hexosamine biosynthesis pathway (HBP) and glycolysis, and generate a large number of intermediates to promote tumor proliferation. However, whether YAP stimulates pentose phosphate pathway (PPP), another tumor-promoting glucose metabolism pathway, and the relationship between this stimulation and ISGylation needs further investigation. Here, we found that YAP was ISGylated and this ISGylation inhibited YAP ubiquitination, proteasome degradation, interaction with-beta-transducin repeat containing E3 ubiquitin protein ligase (βTrCP) to promote YAP stability. However, ISGylation-induced pro-YAP effects were abolished by YAP K497R (K, lysine; R, arginine) mutation, suggesting K497 could be the major YAP ISGylation site. In addition, YAP ISGylation promoted cell viability, cell derived xenograft (CDX) and patient

derived xenograft (PDX) tumor formation. YAP ISGylation also increased downstream genes transcription, including one of key enzymes of PPP, 6-phosphogluconolactonase (6PGL). Mechanistically, YAP promoted 6PGL transcription by simultaneously recruiting SMAD family member 2 (SMAD2) and TEA domain transcription factor 4 (TEAD4) binding to the 6PGL promoter to activate PPP. In clinical lung adenocarcinoma (LUAD) specimens, we found that YAP ISGylation degree was positively associated with 6PGL mRNA level, especially in high glucose LUAD tissues compared to low glucose LUAD tissues. Collectively, this study suggested that YAP ISGylation is critical for maintaining its stability and further activation of PPP. Targeting ISGylated YAP might be a new choice for hyperglycemia cancer treatment.

Key words: ubiquitination, proteasome, promoter, ISG15, LUAD

290. Kinectin 1 promotes the growth of triple-negative breast cancer via directly co-activating NF-kappaB/p65 and enhancing its transcriptional activity

Lin Gao*[1]、Shanze Chen[2]、Malin Hong[1,3]、Wenbin Zhou[1]、Bilan Wang[4]、Junying Qiu[1]、Jinquan Xia[1]、Pan Zhao[1,3]、Li Fu[5]、Jigang Wang[1,3]、Yong Dai[1]、Ni Xie[5]、He Yang[6]、Hsien-Da Huang[8]、Xiang Gao[9]、Chang Zou[1,3,7]

1. The Second Clinical Medical College, Jinan University (Shenzhen People's Hospital)

2. Department of Respiratory and Critical Care Medicine, First Affiliated Hospital of Southern University of Science and Technology; The Second Clinical Medical College, Jinan University (Shenzhen People's Hospital), Shenzhen Institute of Respiratory Diseases

3. Shenzhen Public Service Platform on Tumor Precision Medicine and Molecular Diagnosis, the Second Clinical Medical College, Jinan University (Shenzhen People's Hospital)

4. Department of Pharmacy, West China Second University Hospital of Sichuan University

5. Guangdong Provincial Key Laboratory of Regional Immunity and Diseases, Department of Pharmacology and International Cancer Center, Shenzhen University Health Science Center

6. Department of Integrated Chinese and Western Medicine, Jinan University

7. School of Life and Health Sciences, The Chinese University of Kong Hong

8. Warshel Institute for Computational Biology, The Chinese University of HongKong

9. Department of Neurosurgery, State Key Laboratory of Biotherapy, West China Hospital, Sichuan University

Triple-negative breast cancer (TNBC) is the most challenging subtype of breast cancer. Various endeavor has been made to explore the molecular biology basis of TNBC. Herein, we reported a novel function of factor Kinectin 1 (KTN1) as a carcinogenic promoter in TNBC. KTN1 expression in TNBC was increased compared with adjacent tissues or luminal or Her2 subtypes of breast cancer, and TNBC patients with high KTN1 expression have poor prognosis. In functional studies, knockdown of KTN1 inhibited the proliferation and invasiveness of TNBC both in vitro and in vivo, while overexpression of KTN1 promoted cancer cell proliferation and invasiveness. RNA- seq analysis revealed that the interaction of cytokine-cytokine receptor, particularly CXCL8 gene, was upregulated by KTN1, which was supported by the further experiments. CXCL8

depletion inhibited the tumorigenesis and progression of TNBC. Additionally, rescue experiments validated that KTN1-mediated cell growth acceleration in TNBC was dependent on CXCL8 both in vitro and in vivo. Furthermore, it was found that KTN1 enhanced the phosphorylation of NF-κB/p65 protein at Ser536 site, and specifically bound to NF-κB/p65 protein in the nucleus and cytoplasm of cells. Moreover, the transcription of CXCL8 gene was directly upregulated by the complex of KTN1 and NF-κB/p65 protein. Taken together, our results elucidated a novel mechanism of KTN1 gene in TNBC tumorigenesis and progression. KTN1 may be a potential molecular target for the development of TNBC treatment.

Key words : triple-negative breast cancer; KTN1; CXCL8; NF-κB/p65; cell invasion

291. The essential roles of m6A RNA modification to stimulate ENO1-dependent glycolysis and tumorigenesis in lung adenocarcinoma

Lifang Ma*、Jiayi Wang

上海市胸科医院检验科

Background: Lung adenocarcinoma (LUAD) is the most common subtype of lung cancer. Patient prognosis is poor, and the existing therapeutic strategies for LUAD are far from satisfactory. Recently, targeting N6-methyladenosine (m^6A) modification of RNA has been suggested as a potential strategy to impede tumor progression. However, the roles of m6A modification in LUAD tumorigenesis is unknown.

Methods: Global m6A levels and expressions of m6A writers, erasers and readers were evaluated by RNA methylation assay, dot blot, immunoblotting, immunohistochemistry and ELISA in human LUAD, mouse models and cell lines. Cell viability, 3D-spheroid generation, in vivo LUAD formation, experiments in cell- and patient-derived xenograft mice and survival analysis were conducted to explore the impact of m6A on LUAD. The RNA-protein interactions, translation, putative m6A sites and glycolysis were explored in the investigation of the mechanism underlying how m6A stimulates tumorigenesis.

Results: The elevation of global m6A level in most human LUAD specimens resulted from the combined upregulation of m6A writer methyltransferase 3 (METTL3) and downregulation of eraser alkB homolog 5 (ALKBH5). Elevated global m6A level was associated with a poor overall survival in LUAD patients. Reducing m6A levels by knocking out METTL3 and overexpressing ALKBH5 suppressed 3D-spheroid generation in LUAD cells and intra-pulmonary tumor formation in mice. Mechanistically, m6A-dependent stimulation of glycolysis and tumorigenesis occurred via enolase 1 (ENO1). ENO1 mRNA was m6A methylated at 359 A, which facilitated it's binding with the m6A reader YTH N6-methyladenosine RNA binding protein 1 (YTHDF1) and resulted in enhanced translation of ENO1. ENO1 positively correlated with METTL3 and global m6A levels, and negatively correlated with ALKBH5 in human LUAD. In addition, m6A-dependent elevation of ENO1 was associated with LUAD progression. In preclinical models, tumors with a higher global m6A level showed a more sensitive response to the inhibition of pan-methylation, glycolysis and ENO activity in LUAD.

Conclusions: The m6A-dependent stimulation of glycolysis and tumorigenesis in LUAD is at least partially orchestrated by the upregulation of METTL3, downregulation of ALKBH5, and stimulation of YTHDF1-mediated ENO1 translation. Blocking this mechanism may represent a potential treatment strategy for m6A-dependent LUAD.

Key words: METTL3, ALKBH5, YTHDF1, translation, lung cancer, RNA-protein interaction

292. Yin Yang 1 promotes aggressive cell growth in high-grade breast cancer by directly transactivating kinectin 1

Lin Gao*[1]、Wenbin Zhou[2]、Ni Xie[3]、Junying Qiu[4]、Jingyi Huang[1]、Zhe Zhang[1]、Malin Hong[1,5]、Jinquan Xia[1]、Jing Xu[1]、Pan Zhao[1,5]、Jing Jiang[6]、Hui Gong[6]、Jigang Wang[1,5]、Yong Dai[1]、Dixian Luo[6]、Chang Zou[1,5,7]

1. The Second Clinical Medical College, Jinan University (Shenzhen People' s Hospital)

2. Department of Thyroid and Breast Surgery, Department of General Surgery, The Second Clinical Medical College, Jinan University (Shenzhen People's Hospital), The First Affiliated Hospital of Southern University of Science and Technology

3. Biobank, Shenzhen Second People's Hospital, Shenzhen, Health Science Center, First Affiliated Hospital of Shenzhen University

4. Medical Laboratory of Shenzhen Luohu People's Hospital

5. Shenzhen Public Service Platform on Tumor Precision Medicine and Molecular Diagnosis, the Second Clinical Medical College, Jinan University

6. Department of Laboratory Medicine, Huazhong University of Science and Technology Union Shenzhen Hospital (Nanshan Hospital)

7. School of Life and Health Sciences, The Chinese University of Kong Hong

Invasive cancer growth and metastasis account for the poor prognosis of highgrade breast cancer. Recently, we reported that kinectin 1 (KTN1), a member of the kinesin-binding protein family, promotes cell invasion of triplenegative breast cancer and high-grade breast cancer cells by augmenting the NF-κB signaling pathway. However, the upstream mechanism regulating KTN1 is unknown. Therefore, this functional study was performed to decipher the regulatory cohort of KTN1 in high-grade breast cancer. Bioinformatic analysis indicated that transcription factor Yin Yang 1 (YY1) was a potential transactivator of KTN1. High YY1 expression correlated positively with pathological progression and poor prognosis of high-grade breast cancer. Additionally, YY1 promoted cell invasive growth both in vitro and in vivo, in a KTN1-dependent manner. Mechanistically, YY1 could transactivate the KTN1 gene promoter. Alternatively, YY1 could

directly interact with a co-factor, DEAD-box helicase 3 X-linked (DDX3X), which significantly co-activated YY1-mediated transcriptional expression of KTN1. Moreover, DDX3X augmented YY1-KTN1 signalingpromoted invasive cell growth of breast cancer. Importantly, overexpression of YY1 enhanced tumor aggressive growth in a mouse breast cancer model. Our findings established a novel DDX3X-assisted YY1-KTN1 regulatory axis in breast cancer progression, which could lead to the development novel therapeutic targets for breast cancer.

Key words: breast cancer; DDX3X; growth; invasion; KTN1; YY1

293. MORTALIN-$Ca2^+$ axis drives innate rituximab resistance in diffuse large B-cell lymphoma

Qi Sun*[1]、Ling Yang[2]

1. Shanghai Chest Hospital

2. Department of Cellular and Genetic Medicine, School of Basic Medical Sciences; Fudan University, Shanghai 200032, China

Diffuse large B-cell lymphoma (DLBCL) is the most common subtype of B Non-Hodgkin lymphoma (NHL), and rituximab plus chemotherapy remains standard treatment of DLBCL. Although rituximab monotherapy has a remarkable response rate, drug resistance with unclear mechanisms and lack of effective second-line therapy limit the survival benefits of lymphoma patients. Here we report that, in DLBCL patients, MORTALIN is highly expressed, and correlates with rituximab-based therapy resistance and poor survival. Mechanistically, gain- and loss-of-function experiments reveal the Voltage-dependent anion channel 1 (VDAC1)-binding protein, MORTALIN, regulates mitochondria-associated membrane to release $Ca2^+$ from endoplasmic reticulum stores and confers AP1-mediated proliferation and YY-1-mediated FAS downregulation. These dual mechanisms contribute to rituximab resistance. In mouse models, genetic depletion of MORTALIN markedly increases the antitumor activity of rituximab. We shed mechanistic light on a MORTALIN-$Ca2^+$-CaMKII-AP1-mediated proliferation and MORTALIN-$Ca2^+$-CaMKII-inhibited death receptor in DLBCL rituximab resistance, and propose MORTALIN as the novel potential target in DLBCL.

Key words: Glucose regulated protein 75, Lymphoma, Drug resistance, Calcium signaling, Cell proliferation, Apoptosis

294. Survival and prognosis of metastatic breast cancer in young women: SEER 2010-2015

Hongna Sun*、Junnan Xu、Tao Sun

Department of Medical Oncology, Cancer Hospital of China Medical University, Liaoning Cancer Hospital & Institution, Shenyang, China

Objective: Female breast cancer is the most frequent malignant tumor with an estimated 2.3 million new cases, followed by lung cancer, and the fifth-biggest cause of cancer-related fatalities globally. While breast cancer is the leading cause of cancer death in women. Although breast cancer in young women (BCYW) is not as common as in older individuals, the incidence of BCYW is increasing. Due to the particular considerations regarding pregnancy, fertility preservation, early menopause, body image, lactation, and quality of life, BCYW deserves unique management. We sought to estimate the survival and prognosis of such patients.

Methods: We extracted primary breast cancer patients data between 2010 and 2015 from the Surveillance Epidemiology and End Results (SEER) database. We included patients under 70 years and divided them into two groups by age (＜40 *vs.* 40-69 years). Through Kaplan-Meier curves and Log-rank test, we analyzed and compared the overall survival (OS) and breast cancer-specific survival (BCSS) of metastatic breast cancer in young women and older patients among tumor subtypes. Furthermore, we divided metastatic BCYW into training and validation sets to create a nomogram for predicting patients risk and prognostic variables. The univariate and multivariate Cox proportional hazards model was used to determine essential independent prognostic factors for metastatic BCYW. A nomogram was developed to predict 1-, 3-, and 5-year OS based on the independent factors. The receiver operating characteristic (ROC) curve, concordance index (C-index), and calibration curves were employed to test the nomogram models prediction capacity as well as clinical applicability value.

Results: Kaplan-Meier curves suggest that patients under 40 years have longer OS and BCSS than older patients. Whereas these survival benefits are limited in HR+ or/and HER2+ patients, triple-negative breast cancer (TNBC) in young women has similar unfavorable outcomes to older patients. Cox regression analysis demonstrated that race, marital status, tumor subtypes, surgery, liver metastasis, brain metastasis, and lung metastases were independent risk and prognostic factors for OS of BCYW patients. We used these independent variables to construct the nomogram. The training groups C-index for OS prediction was 0.721 (95% CI: 0.697–0.745), while the validation groups was 0.703 (95% CI: 0.664–0.742). The 1-, 3-, and 5-year AUCs in the training group were 0.802, 0.846, and 0.861, respectively, whereas the validation groups were 0.639, 0.703, and 0.692. The calibration curves for the probability of survival at 1-, 3-, and 5-year OS showed high agreement in the training group and satisfactory concordance in the validation group between the prediction by actual observation and nomogram.

Conclusion: We defined the clinicopathologic characteristics, comprehensively analyzed and compared the OS and BCSS of breast cancer between two age groups among tumor subtypes. Patients under 40 years have longer OS and BCSS than older patients, while these survival benefits are limited in HR+ or/and HER2+ patients, except for TNBC, which needs further investigation. In addition, we developed an efficient predictive nomogram to predict 1-, 3- and 5-year OS of metastatic BCYW. These nomograms can aid oncologists in distinguishing, assessing and evaluating the risk and prognosis of metastatic BCYW, which can help oncologists select next treatment strategies for BCYW.

Key words: Breast cancer in young women, Overall survival, Breast cancer-specific survival, Nomogram, Prognostic factors, SEER.

295. A Nomogram for Predicting Survival in Breast Infiltrating Duct Carcinoma Patients With Brain Metastasis: A Population-Based Study

Hongna Sun*、Junnan Xu、Tao Sun

Department of Medical Oncology, Cancer Hospital of China Medical University, Liaoning Cancer Hospital & Institution, Shenyang, China

Objective: Female breast cancer is the most frequent malignant tumor and the fifth-biggest cause of cancer-related fatalities globally. Breast cancer can spread to bone, liver, lung, and brain, and metastasizing to the brain has the worst outcomes. Brain metastases attack nearly 25% of advanced breast cancer patients, significantly lowering their quality of life and overall survival (OS). The most frequent histological subtype of breast cancer is infiltrating duct carcinoma (IDC). However, several researches have focused on brain metastasis diagnostic and prognostic nomograms in newly diagnosed breast infiltrating duct carcinoma (BIDC) patients. The goal of the research was to create a nomogram utilizing the SEER (Surveillance Epidemiology and End Results) database, determining the independent factors that affect the prognosis of patients with brain metastases to make an optimal therapy plan for them.

Methods: We used the SEER database to determine 936 patients with brain metastases of breast infiltrating duct carcinoma (BIDC) and separated these patients into training (n=655) and validation (n=281) cohorts at random. The Cox proportional hazards model, both univariate and multivariate, was used to identify essential independent prognostic variables for brain metastasis of BIDC, and a nomogram was developed to forecast 1-, 2-, and 3-year overall survival (OS). In addition, we applied Kaplan-Meier curves to analyze survival and used the Log-rank test to compare the differences among the survivals. The receiver operating characteristic curve (ROC) and concordance index (C-index), and calibration curves were employed to test the nomogram models prediction capacity and clinical applicability value. All tests were two-tailed, and *P* values <0.05 were statistically significant. All statistical analyses were using R software (version 4.1.3; http://www.R-project.org).

Results: The major primary site was the upper outer (22.3%). The opportunity of tumors occurring in the left and right mammary was similar. Most tumors were grade II (32.4%) or grade III (48.9%), although tumor grade was unknown in 15.3% of patients. Hormone receptor-positive (HR^+)/human epidermal growth factor receptor 2-negative ($HER2^-$) breast cancer was the commonest subtype (40.5%), followed by HR-/HER2-(19.3%) and $HR^+/HER2^+$ (18.5%). In addition to brain metastasis, 618 patients (66.0%) had bone metastasis, 298 (31.8%) had liver metastasis and 428 (45.7%) had lung metastasis. Seven significant independent predictive indicators of OS (age, race, grade, tumor subtypes, surgery, chemotherapy, and liver metastasis) were discovered through univariate and multivariate Cox proportional hazard models, and we used these six independent variables to construct the nomogram. Then, we used the ROC and C-index, and calibration curves to test the nomogram models prediction capacity and clinical applicability value. The training groups C-index for OS prediction was 0.704 (95% CI: 0.677–0.731), whereas the validation cohorts C-index was 0.678 (95% CI:0.639–0.717), indicating that the model exhibited acceptable accuracy of prediction. The ROC curve demonstrated high predictive ability as well as clinical utility. The 1-, 2-, and 3-year AUC in the training group were 0.789, 0.786, and 0.778, respectively, and 0.745, 0.760, 0.740 in the validation group. Between the prediction by actual observation and nomogram, the calibration plot for the probability of survival at 1-, 2-, and 3-year OS demonstrated well accordance in the training group and satisfying concordance in the validation group.

Conclusions: We firstly developed an efficient predictive nomogram to predict 1-, 2- and 3-year OS in BIDC patients with brain metastases. These nomograms can aid oncologists in distinguishing, assessing and evaluating the risk and prognosis of BIDC with brain metastasis, which can help oncologists select next treatment strategies for BIDC brain metastasis patients.

Key words: infiltrating duct carcinoma, breast cancer, brain metastases, nomogram, prognostic factors, SEER.

296. Breast cancer brain metastasis: Current evidence and future directions

Hongna Sun*、Junnan Xu、Tao Sun

Department of Medical Oncology, Cancer Hospital of China Medical University, Liaoning Cancer Hospital & Institution, Shenyang, China

Breast cancer is the most common cancer in women and the second leading cause of cancer-related deaths after lung cancer. Metastasis of the central nervous system is a terrible event for breast cancer patients, affecting their survival and quality of life. Compared with hormone receptor-positive/human epidermal growth factor receptor 2-negative breast cancer patients, brain metastases are more likely to affect patients with triple-negative breast cancer and human epidermal growth factor receptor 2-positive breast cancer. The treatment of breast cancer has improved greatly in the last two decades. However, brain metastases from breast cancer remain the leading cause of morbidity and mortality. Patients with breast cancer brain metastasis have been in an inferior position due to the lack of clinical research in this field, and they are often explicitly excluded from almost all clinical trials. The occurrence and progression of brain metastases will result in severe cognitive impairment and adverse physical consequences, so we must have a good understanding of the molecular mechanisms of breast cancer brain metastasis. In this article, we have retrieved the latest literature of molecules and pathways associated with breast cancer brain metastasis, summarized common therapy strategies, and discussed the prospects and clinical implications of targeting the molecules involved.

Key words: blood–brain barrier, breast cancer brain metastasis, drug resistance, immunotherapy, molecular mechanisms, targeted therapy

297. Primary Neuroendocrine Tumor of the Breast: Current Understanding and Future Perspectives

Hongna Sun*、Junnan Xu、Tao Sun

Department of Medical Oncology, Cancer Hospital of China Medical University, Liaoning Cancer Hospital & Institute, Shenyang, China

Primary neuroendocrine carcinoma of the breast (NECB) is characterized with heterogeneity, rarity, and poor differentiation, which is probably an underestimated subtype of breast cancer, including small cell NECs and large cell NECs. The diagnostic criteria for NECB have been constantly updated as the disease changes and the understanding increases. According to the latest WHO Classification, primary neuroendocrine neoplasm (NEN) of the breast consists of well-differentiated neuroendocrine tumors (NET), extremely aggressive neuroendocrine carcinomas (NEC) as well as invasive breast cancers of no special type (IBCs-NST) with neuroendocrine differentiation. The accurate diagnosis of NECB remains a challenge for its low incidence, which needs multi-disciplinary methods. For the rarity of the disease, there is a lack of large samples and prospective clinical research. For these invasive tumors, there are no standardized therapeutic guidelines or norms, and the treatment often refers to nonspecific breast cancer. In addition, the prognosis of such patients remains unknown. In 2003, the World Health Organization (WHO) listed NECB as an independent entity for the first time, while few features of NECB were clarified. In this review, it presents the WHO Classification, clinicopathologic characteristics, diagnosis, treatment, and prognosis of these patients. In addition, it summarizes the latest studies on molecular features of NECB, aiming to provide new therapeutic perspectives for the disease.

Key words: primary neuroendocrine carcinoma of the breast, neuroendocrine neoplasia, clinicopathologic characteristics, diagnosis, treatment, prognosis, literature review

298. Identification of Immune-Related Target and Prognostic Biomarkers in PBMC of hepatocellular carcinoma

Rui Hu*、Xiaozhou Zhou

Department of Liver Disease, Shenzhen Traditional Chinese Medicine Hospital, Shenzhen 518033, China

Hepatocellular carcinoma (HCC) is the third leading cause of cancer-related deaths worldwide, and is characterized by insidious onset, rapid progression and poor prognosis. In recent years, several biomarkers have been identified for early screening of HCC, although novel prognostic biomarkers still need to be explored. In this study, we compared the transcriptomes of 6 deceased and 6 living HCC patients using DESeq2, edgeR and Limma programs, and identified 43 differentially expressed genes (DEGs). The top 10 DEGs were validated by RNA-Seq analysis of peripheral blood mononuclear cells (PBMCs) isolated from HCC patients of different BCLC stages. The expression levels of METTL7B, CLDN18, SOCS3, ITGA9 and S100P correlated positively with the BCLC stage. Moreover, CLDN18 and S100P proteins were also significantly upregulated in the tumor tissues, but only CLDN18 was associated with HCC stage, tumor grade and poor prognosis. Functional annotation of CLDN18 in HCC revealed enrichment of the cellular senescence, mRNA surveillance, metabolism of xenobiotics by cytochrome P450 and Human T-cell leukemia virus 1 infection pathways, along with biological processes such as cell cycle, inflammatory response and cellular ketone metabolism. In addition, CLDN18 was also associated with tumor infiltrating immune cells, suppressive immune cell markers, T lymphocyte depletion and activation of HCC, and low expression of CLDN18 was associated with higher CD8+T cell infiltration and better survival rates. These results suggest that CLDN18 is a potential prognostic marker and immunotherapeutic target for HCC.

Key words: Biological techniques; Hepatocellular carcinoma; CLDN18; prognosis; immune infiltration; T cells

299. Diagnosis and Monitoring Value of Circulating Tumour Cells in Breast Cancer with an Optimised Microfluidic Device: A Retrospective Study

Zhiyun Gong*、Renquan Lu

Department of Clinical Laboratory, Fudan University Shanghai Cancer Center

Background and aims: More excellent detection system of circulating tumor cells (CTCs) is demand. Here we performed CTCs detection with a novel automatic device.

Materials and methods: 137 breast cancer patients, 49 patients with benign breast diseases and 42 healthy volunteers were enrolled. Peripheral blood was obtained and followed CTCs detection. The performance was verified by spiking assay and clinical samples. The number of CTCs and $CD45^+$ CTCs were analyzed along with clinicopathologic features. A short-term follow-up review was presented for treatment monitoring by CTC and $CD45^+$ CTCs.

Results: In general, CTCs were found in 86.86% of patients with malignant breast cancer and 63.27% of patients with benign breast diseases but only 1 in healthy group. The sensitivity and specificity of 74.5% and 90.1% respectively when the cut-off was 2. The significant differences of CTC level were found between malignant and non-malignant group (P<0.01), tumor progression (P=0.0216) and tumour size (P=0.0326). In follow-up, the 65.22% of patients exhibited reduction in CTCs count because treatment. Additionally, dual-positive CTC ($CD45^+/CK^+$) exerted descending pattern during treatment period in patients undergone chemotherapy, target-therapy, hormonotherapy and radiotherapy.

Conclusion: A qualified performance of this novel platform was validated in our study. CTCs and $CD45^+$ CTCs both have clinical significance in breast cancer diagnosis and monitoring.

Key words: Breast cancer, Circulating tumour cells, Tumour progression, Dual-positive CTC

300. Fecal microbiota characteristics of anxiety and depression patients in esophageal cancer screening: a case-control study

Juan Zhu*[1]、Wenqiang Wei[2]

1. national cancer center/cancer hospital, chinese academy of medical sciences and peking union medical

2. 中国医学科学院肿瘤医院

Objective: To identify psychological distress-associated gut microbiota among screening population for esophageal cancer.

Methods: Based on the Natioanl Cohort of Esophageal cancer, we characterized the microbial characteristics of fecal samples collected through FOBT card from screeners diagnosed anxiety and depression (N=23) and paired non-anxiety and non-depression screeners (N=46). We described and compared the microbial characteristics including α diversity, β diversity, and relative abundance at phylum, family, genus and species levels between the two groups.DNA was extracted using the MOBIO PowerSoil kit. The V4 region of the 16S rRNA gene was sequenced using the MiniSeq and processed using QIIME1. LEfSe was used to identify differentially abundant microbes.

Results: The intestinal microbial environments of screeners by phylum were all composed primarily of Firmicutes, Bacteroidetes, and Proteobacteria, and the corresponding top genera were Faecalibacterium, Roseburia, and Prevotella. Compared with controls, the ranking of the top five genera in the anxiety and depression group changed. Screeners with positive anxiety and depression symptoms had greater abundances of Pediococcus, Erysipelatoclostridium, Granulicatella, Kluyvera, Shuttleworthia, Vagococcus, Faecalicatena, and lower greater abundances of Gemmiger, Veillonella, Ruminococcus, Anaerovorax, and Barnesiella at the genus level. Compared with controls, screeners with anxiety and depression symptoms had a less relative abundance of Gemmiger (1.4 *vs.* 2.3%, *P*= 0.025), Ruminococcus (0.6 *vs.* 0.8%, *P*= 0.037), and Veillonella (0.6 *vs.* 1.3%, *P*= 0.020) at genus level.

Conclusion: Altered microbial characterization among participants with anxiety and depression was found in esophageal cancer screening in China, which was informative for the optimization of

endoscopic screening programs for upper gastrointestinal cancer in China, and had potential clinical implications for the treatment of psychological diseases. Large-scale prospective cohort studies are needed to confirm our findings.

Key words: Esophageal Cancer; Screening; Anxiety; Depression; Microbiome

301. Role of JAK-STAT1 signaling pathway in Helicobacter pylori infection induced gastric carcinogenesis

Xue Li*[1]、Kai-Feng Pan[2]、Markus Gerhard[3]、Raquel Mejiías-Luque[3]、Wen-Qing Li[2]

1. The Cancer Hospital of the University of Chinese Academy of Sciences（Zhejiang Cancer Hospital）

2. 北京大学肿瘤医院

3. Technical University of Munich

Purpose: Helicobacter pylori (H. pylori) infection induces a number of pro-inflammatory signaling pathways contributing to gastric inflammation and gastric cancer (GC). Many immune responses initiated by cytokines secreted upon H. pylori infection signal through JAK-STAT signaling. The links between H. pylori infection, JAK-STAT signaling and tumorigenesis are poorly understood.

Materials and Methods: Proteomic and phosphoproteomic profiling were performed through liquid chromatography tandem mass spectrometry on a human cohort of 111 gastric lesions and 58 GC and 185 advanced GC together with paired adjacent normal tissues, respectively. 67 subjects with gastric lesions were prospectively followed for 280 to 702 days (median 370 days). Immunohistochemistry was used to confirm STAT1 activation and PD-L1 expression in gastric biopsies. Gastric epithelial cells were infected with H. pylori and phosphorylated STAT1 (p-STAT1) and its target gene PD-L1 were detected by Western Blot. Multivariable logistic regression and cox regression models were used for association analysis and prognosis analysis.

Results: In depth tissue proteomics revealed that STAT1 was up regulated along the cascade of progression of gastric lesions from gastritis to intestinal metaplasia and then to gastric cancer. Based on follow-up study, STAT1 was positively associated with progression of gastric lesions with an odds ratio of 2.65 (P=0.28). The expression of STAT1 in gastric cancer is independently

associated with prognosis with hazard ratio (95%CI) of 2.34(1.04-5.30). STAT1 is highly phosphorylated in advanced gastric cancer tissues compared with adjacent normal tissues (Wilcoxon test, *P*=0.02) and patients with higher STAT1 phosphorylation presented worse prognosis. STAT1 was activated in human H. pylori-positive gastritis, while in GC, STAT1, and its target gene, PD-L1, were significantly elevated. H. pylori infection activated JAK-STAT1 signaling pathway and downstream program in gastric cancer cell lines presenting higher phosphorylation of STAT1 and up-regulated expression of PD-L1, which depended on cytokines produced by immune cells. STAT1 and PD-L1 were upregulated in gastric tumor tissues compared with adjacent normal tissues and were highly correlated with CD8+ immune cells infiltration and were associated with poor prognosis based on the TCGA-STAD database.

Conclusions: STAT1 is a risk factor for progression of gastric lesions and gastric cancer prognosis. H. pylori infection induces PD-L1 expression in the gastric epithelium and during GC development in a STAT1 and immune cell-dependent manner. PD-L1 may allow transformed epithelial cells to progress to GC and later determine GC prognosis.

Key words: Gastric cancer; Helicobacter pylori; STAT1; PD-L1

302. Combinational use of Trabectedin and Pegylated Liposomal Doxorubicin for Recurrent Ovarian Cancer: A Meta-analysis of Phase III Randomized Controlled Trials

Chao Li*、Zhiru Li

Sichuan Qionglai Medical Center Hospital

Background: In recent years, pegylated liposomal doxorubicin (PLD) has been used to improve the survival of patients with ovarian cancer; however, it is unclear whether the combinational use of PLD with other drugs is more effective. Therefore, this study aimed to evaluate the efficacy and safety of trabectedin combined with PLD in treating recurrent ovarian cancer by meta-analysis.

Methods: PubMed, Medical Literature Analysis and Retrieval System Online (MEDLINE), Excerpta Medica Database (EMBASE), Cochrane Library clinical controlled trials (CENTRAL) and ClinicalTrials.gov databases were searched to retrieve all potentially eligible clinical trials as of May 15, 2022. Pooled hazard ratios (HRs), risk ratios, and 95% confidence intervals (CIs) were calculated using Review Manager software 5.4 (RevMan 5.4).

Results: A total of 1248 patients with recurrent ovarian cancer from two phase III randomized control trials were included in the meta-analysis. Meta results revealed that trabectedin combined with PLD chemotherapy significantly improved overall survival (OS) in patients with BRCA-mutated recurrence (HR, 0.49; 95% CI, [0.33-0.73]; p= 0.0004) and in patients with platinum-sensitive recurrence whose platinum-free interval (PFI) was 6 -12 months (HR, 0.66; 95% CI, [0.52 -0.84]; p= 0.0005). In addition, progression-free survival (PFS) was significantly improved in patients with recurrent ovarian cancer compared with PLD alone (HR, 0.86; 95% CI, [0.74-0.99]; p= 0.03); PFS was significantly improved in patients with BRCA gene-mutated recurrence (HR, 0.58; 95% CI, [0.40-0.58]; p = 0.004), and in patients with platinum-sensitive recurrence (HR, 0.73; 95% CI, [0.56-0.95]; p = 0.02). Trabectedin combined with PLD was more prone to grade 3-4 toxic side effects than PLD alone (p<0.05); however, fatal adverse events related to non-toxic side effects occurred.

Conclusion: Trabectedin combined with PLD significantly improves OS and PFS in patients with BRCA-mutated and/or platinum-sensitive recurrent ovarian cancers. The potential use of trabectedin combined with PLD for treating recurrent ovarian cancer should be selected according to the PFI and BRCA gene mutation status of patients.

Key words: trabectedin, pegylated liposomal doxorubicin, meta-analysis, chemotherapy, relapsed ovarian cancer

303. MTERF1 promotes colorectal cancer progression by increasing mitochondrial OXPHOS and regulating the p-AMPK/mTOR signaling pathway

Qian-qian Liu*[1,2]、Bin Li[1]、Ru-ai Liu[1]、Bo-yong Wang [1]、Lei Ding[2]、Qinghua Cui[2]、Jie Lin[2]、Min Yu[2]、Wei Xiong[1]

1. Dali University

2. School of Life Sciences, Yunnan University, Kunming, Yunnan, 650091, China

Objective: Human mitochondrial transcription termination factor 1 (MTERF1) has been demonstrated to play an important role in mitochondrial energy metabolism; however, the molecular mechanism in CRC remains largely unknown. Methods and Results: we found that MTERF1 expression was significantly increased in colon cancer tissues compared with normal colorectal tissue by western blotting, immunohistochemistry and tissue microarrays (TMA). Overexpression of MTERF1 in the HT29 cell line promoted cell proliferation, migration and invasion, xenograft tumor formation and cell cycle transition at G1/S phase and inhibited cell apoptosis, whereas knockdown of MTERF1 in HCT116 cells appeared the opposite phenotype to HT29 cells. Furthermore, MTERF1 can increase mitochondrial DNA (mtDNA) replication, transcription and protein synthesis in colorectal cancer cells, increase the mitochondrial crista density, mitochondrial membrane potential, and oxygen consumption rate (OCR) and reduce the ROS production in colorectal cancer cells, thereby enhancing mitochondrial oxidative phosphorylation (OXPHOS) activity. Mechanistically, we revealed that MTERF1 regulates the AMPK/mTOR signaling pathway in cancerous cell lines, and we also confirmed the involvement of the AMPK/mTOR signaling pathway in both xenograft tumor tissues and colon cancer tissues. Conclusion: our data reveal an oncogenic role of MTERF1 in CRC progression, indicating that MTERF1 may represent a new therapeutic target in the future.

Key words: colorectal cancer; MTERF1; cell proliferation; mtDNA; oxidative phosphorylation; AMPK/mTOR

304. NNMT-DNMT1 axis is essential for maintaining cancer cell sensitivity to oxidative phosphorylation inhibition

Yue Liu*

TONGJI UNIVERSITY

Lacking a clear understanding for molecular mechanism determining cancer cell sensitivity to oxidative phosphorylation (OXPHOS) inhibition limits the development of OXPHOS-targeting cancer treatment. Here, our screen identified cancer cell lines sensitive or resistant to OXPHOS inhibition. OXPHOS inhibition sensitive cancer cells possess increased OXPHOS activity and silenced nicotinamide N-methyltransferase (NNMT) expression. NNMT expression negatively correlates with OXPHOS inhibition sensitivity and functionally downregulates intracellular level of S-Adenosyl methionine (SAM). Expression of DNA methyltransferase 1 (DNMT1), a SAM consumer, positively correlates with OXPHOS inhibition sensitivity. NNMT overexpression and DNMT1 inhibition render OXPHOS inhibition sensitive cancer cells resistant. Importantly, treatments of OXPHOS inhibitors (Gboxin and Berberine) hamper the growth of mouse tumor xenografts by OXPHOS inhibition sensitive but not resistant cancer cells. What's more, our retrospective study of 62 tumor samples from a clinical trial demonstrates that administration of Berberine reduces tumor recurrence rate of NNMTlow/DNMT1high but not NNMThigh/DNMT1low colorectal adenomas (CRAs). These results thus reveal a critical role of NNMT-DNMT1 axis in determining cancer cell reliance on mitochondrial OXPHOS and suggest that NNMT and DNMT1 are faithful biomarkers for OXPHOS-targeting cancer therapies.

Key words: OXPHOS, cancer, biomarker, NNMT, SAM, DNA methylation

305. A super-enhancer gene-based risk score model for predicting overall survival in patients with hepatocellular carcinoma

Xueyan Wei*

Guangxi Medical University

Background: Super-enhancer (SE) refers to a regulatory element with super transcriptional activity, which can enrich transcription factors and drive gene expression. SE-related genes play an important role in the pathogenesis of malignant tumors, including hepatocellular carcinoma (HCC). This study aimed to establish a SE-related gene expression signature for predicting prognosis in patients with HCC.

Methods: The SE-related genes were obtained from the human super-enhancer database (SEdb). Data from the transcriptome analysis and related clinical information from the HCC were obtained from The Cancer Genome Atlas (TCGA) and the International Cancer Genome Consortium (ICGC) database. The upregulated SE-related genes from TCGA-LIHC were identified by the DESeq2R package. Univariate Cox analysis was used to screen out SE-related genes associated with the overall survival (OS) of HCC patients. Multivariate Cox regression analyses were carried out to construct the prognostic signature.

Results: We identified 82 target genes of SE from the intersection of 724 SE-related genes and 6,029 upregulated genes (Log2FC>1 and $p<0.05$) in HCC. Multivariate Cox regression analyses identified 5 target genes significantly associated with the OS of HCC and subsequently applied to construct the prognostic signature. According to the median risk score, HCC patients were divided into high-risk and low-risk groups. The Kaplan-Meier (KM) curve showed that the prognosis of the high-risk group was significantly worse ($P<0.001$). The model trained by the TCGA-LIHC dataset had a good prediction capacity, evidenced by the area under the curve (AUC) values of 0.727, 0.767, and 0.690 for predicting the 1, 3, and 5 years OS, respectively. This models prognostic value was further validated in the LIRI-JP dataset and HCC samples (n=65). Furthermore, we found that infiltration of M0 macrophages was higher in the high-risk group

patients. In addition, higher levels of immune checkpoint molecules were found in the high-risk group, emphasizing that immunotherapy may be more effective in this patient population.

Conclusion: Our novel SE-related gene model has a high potential to predict the prognosis of HCC patients. This five-gene signature has huge prospects for clinical application as a therapeutic target for HCC.

Key words: hepatocellular carcinoma,super enhancer, prognostic model, immune, overall survival

306. Estrogen receptor response gene EGR3 mediates breast cancer cell resistance to tamoxifen through promoting MCL1 transcription

Yu Xie*、Yue Wang、Junfang Qin、Mengci Yuan、Jing Yu

Nankai University

Background: Estrogen receptor (ER) positive breast cancer is a common disease in globally women, and endocrine therapy is a well-establish strategy. Currently, with widely application of endocrine medicine, drug resistance become an intractable problem increasingly. Early growth response protein (EGR) 3 is a well-established ER response factor. Whereas the role of EGR3 in ER-relevant endocrine therapy resistance is still confusing.

Purpose: We supposed EGR3 is a properly biomarker in endocrine therapy resistance which play a crucial role in resistant breast cancer cells. The study aims to investigate the necessity of EGR3 expression in resistant cells and clarify the mechanism of EGR3 mediating in tamoxifen treatment.

Methods: With the representativeness of tamoxifen in endocrine medicine, MCF7 and T-47D tamoxifen resistance cell lines was established. Firstly, EGR3 expression in tamoxifen treatment and resistant samples from the Gene Expression Omnibus database was re-analysis. The key role of EGR3 in resistance to tamoxifen treatment was investigated by manipulating expression. The responsibility of EGR3 to estrogen(E2) oestrone (E1) prolactin(PRL) action was detected by ligand stimulation. To clarify the EGR3 regulatory mechanism, the downstream factor was investigated and cell survival-related gene MCL1 was found. The function of EGR3 and MCL1 in resistance cells was investigated through tamoxifen-inducing apoptosis and proliferation assay. At

the last, the action mechanism of EGR3 was investigated through CHIP and dual-luciferase report system.

Results: 1. EGR3 expression was higher in the tamoxifen treated and resistant samples. 2. With EGR3 knockdown, tamoxifen-resistant MCF7 cell line (MCF7-TamR) growth was impaired upon tamoxifen treatment; consistently, EGR3 forcing expressing given resistance to tamoxifen in MCF7. 3. Treating with estrone and estradiol, EGR3 expression was influenced by ER signaling both in MCF7 and MCF7-TamR and was aberrant in resistant cells. 4. MCL1 is the downstream effector in EGR3-regulated apoptosis and proliferation in tamoxifen resistance. 5. EGR3 functions as a transcriptional factor binding to the MCL1 promoter and facilitating MCL1 transcription.

Conclusion: EGR3 is a key factor participating in abnormal ER signal that attenuating tamoxifen-induced apoptosis and inhibition of proliferation through facilitating MCL1 transcription. The current study reveals the negative role of EGR3 in tamoxifen-induced cancer cell suppression, which makes clear that EGR3 is a good indicator and a potential target to improve endocrine therapy resistance.

Key words: Breast cancer; endocrine therapy resistance; estrogen receptor; tamoxifen; MCF7; EGR3; MCL1

307. Downregulation of lactate receptor GPR81 contributes to tamoxifen resistance via regulating FAO in Breast Cancer Cells

Jing Yu*、Yu Xie、Meng-ci Yuan、Jun-fang Qin、Yue Wang

Nankai University

Objective: Tamoxifen is a commonly used endocrine therapy drug in estrogen receptor (ER)-positive breast cancer patients. However, drug resistance remains a major limiting factor in tamoxifen therapy for breast cancer. G protein-coupled receptor 81 (GPR81) as a lactate receptor, has been found to play an important role in lipid metabolism. Our study explores the role and underlying mechanism of GPR81 in inducing tamoxifen resistance by regulating fatty acid

oxidation (FAO), aiming to provide new insights into the relationship between breast cancer metabolism and resistance.

Methods: Tamoxifen-resistant T47D cell lines were established and compared the concentration of lactate in the tumor microenvironment. The expression of GPR81 was examined by qPCR and western blot, respectively. After lactate treatment, CCK-8 and clone formation assays were used to detect the proliferative capacity in tamoxifen-resistant T47D cells. The differential gene-enriched signaling pathways were obtained from the RNA-seq dataset of the GEO database. Furthermore, the level of FAO was identified by qPCR, western blotting, and immunofluorescence staining.

Results: Here, we detected lower concentration of lactate in the cell culture supernatant of tamoxifen-resistant T47D cell lines. Accordingly, lactate receptor GPR81 expression was significantly decreased in both mRNA and protein levels in resistance cell lines. Meanwhile, there may be a strong negative correlation between GPR81 and disease staging according to the Human Protein Atlas database and UALCAN database. CCK-8 and clone formation assays further determined that lactate-regulated GPR81 affects tamoxifen resistance. For the RNA-seq results, the differential expressed genes were mainly enriched in the metabolic pathway, PI3K pathway and cancer-related pathways. Interestingly, FAO was upregulated in Tamoxifen-resistant T47D cell lines, and lactate can reverse this upregulation by stimulating GPR81.

Conclusions: In summary, our data suggest that GPR81 may be a key molecule, which can regulate FAO through lactate stimulation to contribute tamoxifen resistance in breast cancer cells.

Key words: GPR81; Lactate; Tamoxifen resistance; Fatty acid oxidation

308. Peripheral blood mononuclear cell DNA methylation markers enables early non-invasive detection for breast cancer

tiantian wang*、chuanxin wang

The Second Hospital of Shandong University

Background: The immune system can monitor the development of tumors, while DNA methylation is involved in the bodys immune response to tumors. Peripheral blood mononuclear

cell (PBMC) DNA carrying cancer-specific epigenetic aberrations may become a non-invasive approach for early detection of breast cancer (BC). Thus, we aimed: 1) to analyze DNA methylation changes in PBMC of BC and identify candidate methylation markers, and 2) develop a new assay for the detection of BC by multiplex quantitative methylation-specific PCR assay (mBC-MSP) and evaluate its performance in the early diagnosis of BC.

Methods: In this study, we examined the genome-wide methylation profile of PBMC from 50 BC and 30 normal controls using Infinium 850K BeadChips and identified specific DNA methylation changes in BC. The BC prediction diagnostic markers were then validated in a cohort (n=200) using pyrosequencing and MethylTarget sequencing. A mBC-MSP assay was established and the performance of this diagnostic method was analyzed in an independent cohort (n=522) and also compared with the traditional tumor markers CA153、CA125 and CEA.

Results: We discovered a total of 282 differentially methylated CpG positions (DMPs) between BC and normal controls, including 171 hypo-methylated DMPs and 111 hyper-methylated DMPs, genes associated with DMPs were enriched in the pathways involved in immune monitoring system. Eight significant DMPs markers were selected and further validated using pyrosequencing and MethylTarget sequencing, and finally four hyper-methylated DMPs passed the validation, and their methylation levels were higher in the early stage BC than in the late stage BC. A mBC-MSP assay was established based on the above four hyper-methylated DMPs, which is able to accurately distinguish BC from normal controls, yielded an area under the curve (AUC) of (0.925, 0.918), sensitivity (83.1%, 80.3%), and specificity (90.4%, 89.1%) in both the training and validation set. More importantly, compared with CA153、CA125 and CEA, the mBC-MSP assay had a higher sensitivity for early-stage BC (stage 0， 92.0% vs. 0% , 0%, 5.9%) and a higher sensitivity for minimal tumor with diameter ≤ 1.5 cm (92.2% vs. 0%, 2.0%, 0%).

Conclusions: The mBC-MSP assay based on DNA methylation markers of PBMC can provide a noninvasive, accurate, rapid and high-throughput method for early diagnosis of BC, and are more sensitive than traditional tumor markers for early-stage and minimal tumor.

Key words: DNA methylation, Peripheral blood mononuclear cell, breast cancer, marker, early detection

309. A novel long non-coding RNA AC073352.1 promotes metastasis and angiogenesis via interacting with YBX1 in breast cancer

Xue Kong*、Chuanxin Wang

The second hospital of Shandong university

Background: Patients with breast cancer (BC) metastasis have poor prognosis and the mechanisms of BC metastasis are not completely understood. Long non-coding RNAs (lncRNAs) have been shown to have crucial roles in BC progression. However, the underlying mechanisms by which lncRNA-drive BC metastasis is unknown.

Methods: The lncRNA microarray and TCGA database analysis were used to screen the target lncRNA AC073352.1, and its expression levels in breast cancer tissues and clinical significance were confirmed by in situ hybridization. The roles of AC073352.1 in BC progression were further investigated by gain and loss of functions assays in vitro and in vivo. The regulatory mechanism of AC073352.1 was studied by RNA pull-down, Western blot and RNA immunoprecipitation analysis. Co-culture and exsome labeling experiments were performed to assess exosomal AC073352.1 transferred by BC cells into endothelial cells. The role of exosomal AC073352.1 in angiogenesis was further investigated by tube formation.

Results: In this study, we identified a novel lncRNA AC073352.1 that was significantly upregulated in BC tissue and was associated with advanced TNM stages and poor prognosis. In addition, AC073352.1 was found to promote BC metastasis in vitro and in vivo. Mechanistically, we elucidated that AC073352.1 interacts with YBX1 and stabilized its expression. Knock down of YBX1 reduced cell migration and invasion, and could partially reverse BC metastasis driven by AC073352.1. Moreover, AC073352.1 might be packaged into exosomes by binding to YBX1 in BC cells resulting in angiogenesis.

Conclusions: Collectively, AC073352.1 could serve as a biomarker for prognosis and a therapeutic target in BC.

Key words: Breast cancer, LncRNA, Metastasis, YBX1, Exosome, Angiogenesis

310. Long non-coding RNA STEAP2-AS1 promotes lung adenocarcinoma cells proliferation, migration, and invasion by interacting with ARNTL2 to upregulate DARS2

Ming Li*、Cheng Zhan、Mingxiang Feng、Qun Wang

Zhongshan Hospital, Fudan University

Objective: Circadian rhythm plays an important role in tumorigenesis and developing malignant tumors. However, the roles and mechanisms of circadian rhythm in the development and metastasis of cancer cells are still not clear. Though ARNTLS serves as one of the core genes of circadian rhythm, there are few studies on its regulation and mechanism of lung cancer. We sought in this study to firstly define the expression, prognostic effects, and potential regulatory roles of ARNTL2 in lung adenocarcinoma. We subsequently fully explored the non-coding RNA regulatory mechanism and regulated target genes of ARNTL2 in lung adenocarcinoma to determine ARNTL2's regulatory mechanism. Finally, we clarified the key regulatory role of the "non-coding RNA - ARNTL2 - target gene" regulatory axis in the tumorigenesis and development of lung adenocarcinoma through a series of cytological and animal assays.

Methods: First, the expression and prognostic significance of ARNTL2 in lung adenocarcinoma were identified by data from the The Cancer Genome Atlas (TCGA) and the single-cell transcriptome sequencing database of our department. Subsequently, long non-coding RNA (lncRNA) regulatory mechanisms and target genes of ARNTL2 were fully explored by Immunoprecipitation sequencing of RNA (RIP-Seq) method and high-throughput transcriptome sequencing of RNA (RNA-Seq) method in A549 and H1299 cells, respectively. Further, we take full advantage of molecular techniques such as bioinformatics analysis, Chromatin Immunoprecipitation (ChIP), Western blot, Immunofluorescence and Fluorescence in situ hybridization; cytological and animal experimental methods such as cell migration and invasion assay (Transwell assay), angiogenesis assay, and nude mice tumorigenesis assay, etc., to fully

explore the regulatory effects and mechanisms of “LncRNA - ARNTL2 - target gene” regulatory axis in the proliferation, migration, and invasion of lung adenocarcinoma.

Results: In the first part of the study, we found that ARNTL2, a circadian core element, was significantly differentially expressed in multiple malignancies compared with normal tissues. In particular, the expression of ARNTL2 was upregulated in lung adenocarcinoma (*P*<.001) and significantly associated with worse prognosis (overall survival, OS: *P*=6e-05; recurrence-free survival, RFS: *P*=.00455). Through bioinformatics analysis, cytology, and animal experiments, we discovered the effect of ARNTL2 in cell proliferation, migration, and invasion of lung adenocarcinoma. In the second part of the study, we found that LncRNA STEAP2-AS1 was an important non-encoding RNA interacting with ARNTL2 in A549 and H1299 cells by RIP-Seq. LncRNA STEAP2-AS1 was also upregulated in lung adenocarcinoma (*P*<.05), and the OS of the LncRNA STEAP2-AS1 high-expression group was significantly worse than the low-expression group (*P*=.0015). Finally, we found that LncRNA STEAP2-AS1 was mainly expressed in the cytoplasm and had the role of transferring the transcription factor ARNTL2 through the cytoplasm to the nucleus by LncRNA-FISH and immunofluorescence assays. In the third part of the study, we further found that DARS2 could be one of the target genes of ARNTL2 through RNA-Seq in A549 and H1299 cells. DARS2 was also up-regulated in lung adenocarcinoma (*P*<.05), and the prognosis of DARS2 high-expression group was significantly poorer (OS: *P*=.00372; RFS: *P*=.0113). We then predicted the possible binding sites in the promoter region of ARNTL2 and DARS2 by bioinformatics. ChIP-qPCR and Dual-luciferase reporter gene assays showed that the “1143-1150” region of the DARS2 transcription start site up 2KB promoter sequence was the binding site of ARNTL2, which had a sequence of “E-box” elements. In the fourth part of the study, we verified and explored the regulatory mechanisms and roles of the LncRNA STEAP2-AS1/ARNTL2/DARS2 axis in lung adenocarcinoma. Results showed that the downregulated expression of LncRNA STEAP2-AS1/ARNTL2/DARS2 axis could significantly inhibit the cell proliferation (CCK-8: A549 *P*<.01; H1299 *P*<.01; EdU: A549 *P*<.0001; H1299 *P*<.0001; Colony formation: A549 *P*<.001; H1299 *P*<.001), migration (Would healing: A549 *P*<.0001; H1299 *P*<.0001; Transwell migration: A549 *P*<.0001; H1299 *P*<.0001), invasion (Transwell invasion: A549 *P*<.0001；H1299 *P*<.0001), and angiogenesis of A549 and H1299 cells (A549 *P*<.0001; H1299 *P*<.0001). In the reverse assay, overexpression of DARS2 in the A549 and

H1299 cells with the downregulating of LncRNA STEAP2-AS1 expression could significantly reversed the proliferation, migration, invasion, and angiogenesis of cancer cells.

Conclusion: The present study elucidates for the first time in lung adenocarcinoma cells that ARNTL2 undergoes "Cytoplasmic-Nuclear translocation" through the LncRNA STEAP2-AS1-dependent guidance effect and binds to the promoter region of the target gene DARS2 to promote the expression. LncRNA STEAP2-AS1/ARNTL2/DARS2 axis plays an important role in promoting cell proliferation, migration, and invasion of lung adenocarcinoma. Our findings will shed light, to some extent, on the key roles and regulatory mechanisms of the circadian element ARNTL2 in the development and progression of lung adenocarcinoma.

Key words: lung adenocarcinoma, LncRNA STEAP2-AS1/ARNTL2/DARS2 axis, cell proliferation, migration, and invasion, regulatory mechanism

311. Distinct prognostic values of adenosine deaminase isoenzymes-ADA1 and ADA2 in cancer

Zhao-wei Gao*、Ke Dong

Tangdu hospital, Air Force Medical University

Objective: Adenosine deaminase (ADA) play an important role in immune response, which includes two isoenzymes: ADA1 and ADA2. This study aim to explore the roles of ADA1 and ADA2 in cancers.

Methods: Enzyme assay was used to detected the ADA1 and ADA2 activities in serum from cancer patients. Kaplan-Meier (KM) plotter was used to analyze the prognostic value of ADA1 and ADA2. TIMER2.0 was used to explore how ADA1 and ADA2 correlating with immune infiltration and immune checkpoints.

Results： There were no significant change for serum ADA1 activities in most cancer, while serum ADA2 activities were increased in most cancer. For prognosis, high ADA1 was associated with the poor survival for several cancers, including ESCC, HNSC , KIRC, KIRP, LIHC, LUAD and UCEC. However, high ADA2 expression showed a favorable prognosis in BRCA, CESC, HNSC, KIRC, KIRP, LUAD, OV, PAAD, Sarcoma and THYM. ADA1 showed a moderately positive

correlation with multiple infiltrating immune cells in most cancers. ADA2 was positive correlated with B cells, CD8 T cells, Monocyte/macrophage and DCs, and was strong negatively correlated with Myeloid-derived suppressor cells.

Conclusion： Although as the isoenzyme, ADA1 and ADA2 showed the opposite prognostic value and different correlative pattern with immune infiltrating. These data demonstrated the distinct roles of ADA1 and ADA2 in cancer development, and ADA2 might act as a protective factor.

Key words: ADA1, ADA2, Cancer, Prognosis, Immune infiltration

312. Annotation and evaluation of base editing outcomes in multiple cell types using CRISPRbase

Fengbiao Mao*

Peking University Third Hospital

Currently, base editing (BE) systems based on CRISPR/Cas9 technology have been developed rapidly, and can create designed single-nucleotide alterations in a precise and efficient manner. A growing number of studies have indicated that BE system is a powerful tool to manipulate genetic base editing in vitro and in vivo. Consequently, the CRISPR/Cas9 BE data is increasing rapidly, posing a challenge for researchers to access all related information of base editing outcomes. Moreover, the off-target effect remains uncertain, and the on-target efficiency differs among various BE systems. Hence, an integrated resource and analysis platform is urgently needed for comprehensive annotation and evaluation of the off-target effect and the on-target efficiency among various BE systems.Herein, we developed CRISPRbase (http://crisprbase.maolab.org/), by integrating 1,252,935 records of base editing outcomes in more than 50 cell types from 17 species. CRISPRbase helps to evaluate putative editing precision of different BE systems by integrating multiple annotations, functional predictions and a blasting system for single-guide RNA sequences. We systematically assessed the editing window, editing efficiency and product purity of six mainstream BE systems. As far as we know, CRISPRbase is the first database for CRISPR-mediated base editing and has several advantages. It (i) is fitted with the effect prediction

of BE off-target by using ANNOVAR and OncoBase; (ii) has a blast system based on curated sgRNA sequences for better decision-making and (iii) provides comprehensive annotations of BE outcomes. We systematically assessed the editing window, editing efficiency and product purity of various BE systems. The product purities of both adenine base editor (ABE) and cytosine base editor (CBE) were relatively low, indicating that more efforts are needed to minimize the off-target effect by engineering deaminases. Remarkably, more than half of cancer-related off-target mutations were non-synonymous and extremely damage to protein functions in most common tumor types. Luckily, most of these cancer-related mutations were passenger mutations rather than cancer driver mutations, indicating a weak effect of off-target mutation on carcinogenesis. In summary, CRISPRbase curates base editing events in various cell types from multiple species and provides a blast system to search similar sgRNA designs based on curated records. Therefore, CRISPRbase is a powerful and convenient tool to study the outcomes of different base editors and help researchers choose appropriate BE designs for functional studies. We believe that our CRISPRbase would be a novel and fundamental tool for researchers.

Key words: CRISPR-Cas9; base editor; off-target effect; editing efficiency; product purity

313. Heat-shock protein 90α is a potential prognostic and predictive biomarker in hepatocellular carcinoma: a large-scale and multicenter study

Ke Su*、Yunwei Han、jianwen Zhang

The Affiliated Hospital of Southwest Medical University

Background: Although the diagnostic value of plasma heat-shock protein 90α (HSP90α) in hepatocellular carcinoma (HCC) has been previously reported, the causal effect of the plasma HSP90α levels on HCC prognosis remains largely unclear. To this extent, we sought to assess whether the plasma HSP90α act as a prognostic factor for HCC patients.

Methods: A total of 2150 HCC patients were included in this retrospective study between August 2016 and July 2021. Plasma HSP90α levels were tested within a week before treatment and their association with prognosis was assessed.

Results: An optimal cut-off value of 143.5 for the HSP90α based on the overall survival (OS) was determined using the X-tile software. HCC patients with HSP90α <143.5 ng/mL (low HSP90α) before and after propensity score matching (PSM) indicated longer median OS (mOS) relative to those with HSP90α ≥143.5 ng/mL (high HSP90α) (37.0 *vs.* 9.0 months, $p < 0.001$; 19.2 *vs.* 9.6 months, $p < 0.001$; respectively). In addition, the high HSP90α plasma level is an independent poor prognostic factor for OS in HCC patients. In our subgroup analysis, including the supportive care group, surgery group, transarterial chemoembolization (TACE) group, adjuvant TACE group, an immune checkpoint inhibitor (ICI) plus targeted therapy group, and TACE plus ICI group, the high HSP90α group demonstrated better OS compared to the low HSP90α group. Moreover, in the supportive care, TACE, ICI plus targeted therapy, TACE plus ICI groups, and high HSP90α levels were also an independent poor prognostic factors for OS.

Conclusions : Our study confirmed that the plasma HSP90α level can be used as a prognostic biomarker for HCC.

Key words: Heat-shock protein 90α, Hepatocellular carcinoma, Biomarker, Overall survival, Primary liver cancer, Transarterial chemoembolization, Immune checkpoint inhibitor, Targeted therapy, Prognostic factor, Predictive biomarker

314. Intratumor Microbiome Influence Lung Cancer Recurrence

Mantang Qiu*[1]、Yi Ma[1,2]、Haiming Chen[1]、Jun Wang[1]

1. Peking University People's Hospital

2. 上海市肺科医院

Most recurrence of lung cancer occur within 3 years after surgery, but the key factors responsible for cancer recurrence and the underly mechanism have not been clearly discovered. Here, we collected lung cancer tissues with shorter (average 1.3 years, Recurrence group) and longer (average 5.01 years, Non-Recurrence group) recurrence-free survival. By 16S rRNA gene sequencing, we found intratumor microbiome diversity was significantly lower in Recurrence group than that in Non-Recurrence group, and several well-known butyrate-producing bacteria

was enriched in Recurrence group. Both the intratumor microbiome signature (AUC= 0.887) and circulating microbiome DNA (AUC=0.717 in validation set) can accurately predict lung cancer recurrence. Among butyrate-producing bacterial enriched in Recurrence group, we proved that intratumor injection of Roseburia can promote xenograft tumor growth of lung cancer. Mechanistically, bacteria-derived butyrate could promote lung cancer metastasis by increasing expression of long noncoding RNA H19 in tumor cells through inhibiting HDAC2 and increasing H3K27 acetylation at H19 promoter, and inducing M2 macrophage polarization. Our results provide evidence for the cross-talk between intratumor microbiome and lung cancer metastasis and define butyrate as the key molecular mediator, suggesting the potential prognostic and therapeutic value of microbiome for cancer research.

Key words: lung cancer, intratumor microbiome, recurrence, butyrate, lncRNA H19

315. Identification of lung cancer breath biomarkers based on perioperative breathomics testing: A prospective observational study

Mantang Qiu*[1]、Peiyu Wang[1]、Qi Huang[2]、Shushi Meng[1]

1. Departmeng of Thoracic Surgery, Peking University People's Hospital

2. 郑州大学附属第一医院胸外科

Background: Breathomics testing has been considered a promising method for detection and screening of lung cancer. This study aimed to identify breath biomarkers of lung cancer through perioperative dynamic breathomics testing.

Methods : The discovery study was prospectively conducted between Sept 01, 2020 and Dec 31, 2020 in Peking University People's Hospital in China. High-pressure photon ionization time-of-flight mass spectrometry was used for breathomics testing before surgery and 4 weeks after surgery. 28 volatile organic compounds (VOCs) were selected as candidates based on a literature review. VOCs that changed significantly postoperatively were selected as potential breath biomarkers for lung cancer. An external validation was conducted to evaluate the performance of these VOCs for lung cancer diagnosis. Multivariable logistic regressions were

used to establish diagnostic models based on selected VOCs. Findings In the discovery study of 84 patients with lung cancer, perioperative breathomics demonstrated 16 VOCs as lung cancer breath biomarkers. They were classified as aldehydes, hydrocarbons, ketones, carboxylic acids, and furan. In the external validation study including 157 patients with lung cancer and 368 healthy individuals, patients with lung cancer showed elevated spectrum peak intensity of the 16 VOCs after adjusting for age, sex, smoking, and comorbidities. The diagnostic model including 16 VOCs achieved an area under the curve (AUC) of 0.952, sensitivity of 89.2%, specificity of 89.1%, and accuracy of 89.1% in lung cancer diagnosis. The diagnostic model including the top eight VOCs achieved an AUC of 0.931, sensitivity of 86.0%, specificity of 87.2%, and accuracy of 86.9%.Interpretation Perioperative dynamic breathomics is an effective approach for identifying lung cancer breath biomarkers. 16 lung cancer-related breath VOCs (aldehydes, hydrocarbons, ketones, carboxylic acids, and furan) were identified and validated. Further studies are warranted to investigate the underlying mechanisms of identified VOCs.

Key words: Lung cancer; Breathomics; Volatile organic compounds; Diagnosis

316. Identifying Distinctive Tissue and Stool Microbial Signatures and the Tumor-promoting Effects of Deoxycholic Acid in Breast Cancer

Na Wang[1,2]、Mengzhen Han[1,2]、Wenjie Han[1,2]、Tao Sun[1,2,3]、Junnan Xu*[1,2,3]

1. Liaoning Cancer Hospital

2. 中国医科大学肿瘤医院

3. 大连理工大学肿瘤医院

Objective: An increasing body of literature supports that both mammary and intestinal microbiota dysbiosis are associated with the initiation and progression of breast tumors. However, the microbial features for breast tumors patients were wide variation in different research, and the replicable biomarkers for early-stage breast tumors diagnosis remain elusive. We aim to identify the different microbial signatures, seek specific tumor-related biomarkers, and establish the Random Forest Models for the early diagnosis of breast cancer (BC).

Materials and Methods: We demonstrate a machine learning-based method to investigate breast tissue and gut microbial differences among benign breast disease, BC, and healthy population using 16S rRNA sequence data retrieved from 8 studies. The raw sequencing data were downloaded based on the published accession number form National Center for Biotechnology Information Sequence Read Archive database. QIIME 2.0 and R software (version 3.6.1) was used to consistent processing for downloaded FASTQ data to avoid the biases from bioinformatics analyses. A naive Bayes classifier was trained on the RDP v16 reference database to assign taxonomy using the Vsearch software. An in vitro cell experiment was performed to assess the effects of deoxycholic acid (DCA), *Clostridium* metabolite produced, on cell proliferation cycle and apoptosis in BC.

Results: After re-analysing with a total of 768 breast tissue samples and 1,311 fecal samples, we identified that Halomonas and Shewanella were the most representative genera of BC tissue. In the intestines of BC patients, Bacteroides was frequently and significantly enriched. Halomonas, the most characteristic BC-associated biomarker, appear at tissue and gut sites. Random Forest Models were established to discriminate BC from non-cancer populations. The areas under the curve (AUC) were 74.27 % and 68.08 % using breast carcinoma tissues and stool samples, respectively. The model were validated for effectiveness via cohort-to-cohort transfer (average AUC=0.65) and leave-one-cohort-out (average AUC=0.66). The in-vitro results showed that deoxycholic acid (DCA), *Clostridium* metabolite produced, promotes HER2-positive BC cells proliferation, stimulates G0/G1 phase cells to enter S phase and did not affect cell apoptosis.

Conclusions: The results in this study extend our knowledge on the microbial profile of breast tumors. Microbial changes may be present in both tissues and gut of BC,and specific markers could contribute to the early diagnosis of BC. The in vitro experiments confirm that intestinal enrichment *Clostridium* metabolite DCA promotes proliferation of BC cells. We propose that as a non-invasion and convenient method, detection of stool-based biomarkers is easy to be clinically accepted.

Key words: breast cancer, 16S rRNA, microbiome, intestine, cancer diagnosis, random forest, Clostridium, deoxycholic acid

317. Identification of Lung Adenocarcinoma and Benign Pulmonary Lesions Based on Immunologic Gene Set Variation Analysis in Peripheral Whole Blood

Wenmin Zhu*[1]、Tingting Chen[1]、Yangkai Li[2]、Lin Lei[3]、Shanshan Cheng[1]、Sheng Wei[1]

1. Tongji Medical College, Huazhong University of Science and Technology

2. 华中科技大学同济医学院附属同济医院

3. 深圳市慢性病防治中心

Objective: To explore the value of immunologic gene set variation in peripheral whole blood for diagnosing lung adenocarcinoma(ADC) and benign pulmonary lesions.

Method: Using RNA-seq data from the Gene Expression Omnibus, gene set variation analysis was conducted to characterize the activity changes of immunologic gene sets in patients with ADC or benign pulmonary lesions. The diagnostic gene sets were screened by the least absolute shrinkage and selection operator. A random forest model was created for obtaining the genes included in the diagnostic model. An artificial neural network (ANN) was constructed using the genes screened from diagnostic gene sets to identify ADC and benign pulmonary lesions. The diagnostic model was further validated by the peripheral whole blood samples from Chinese patients.

Results: 244 ADC and 220 benign pulmonary lesions samples were clustered into distinct clusters based on immunologic gene set variation analysis in peripheral whole blood. 10 diagnostic gene sets screening from immunologic gene sets were in benign pulmonary lesions and 14 in ADC. Genes from gene sets in benign pulmonary lesion and ADC enriched in different biology functions. 30 genes were screened from 24 diagnostic gene sets by random forest model. These genes were used to identify ADC and benign pulmonary lesions in a ANN model with the AUC 0.885 (95% CI: 0.848-0.920). The model was validated in the Chinese patients with AUC 0.666(95% CI: 0.568-0.762). All genes in ANN were correlated to the abundance ratio of certain types of immune cells.

Conclusion: The activity changes of immunologic gene sets in peripheral whole blood could help to distinguish ADC and benign pulmonary lesions.

Key words: lung adenocarcinoma, benign pulmonary lesion, immunologic gene sets, peripheral whole blood, diagnosis

318. Transmembrane Protein 170B is a Prognostic Biomarker and Associated with Immune Infiltrates in Pancreatic Adenocarcinoma

Zilong Zhang*、jin shang、yuxin liang、xiaolun huang

Department of Hepatobiliary-Pancreatic Surgery, Cell Transplantation Center, Sichuan Provincial People's Hospital, University of Electronic Science and Technology of China

Background: Pancreatic adenocarcinoma (PAAD) is among the most common types of cancer with a poor prognosis. Transmembrane protein 170B (TMEM170B) has been reported to suppress breast cancer proliferation, metastasis, and tumorigenesis and is related to prognosis. However, its role in PAAD and the underlying molecular mechanisms are yet to be investigated.

Patients and methods: We performed a comprehensive analysis of RNA sequencing data obtained from the Gene Expression Omnibus (GEO) and The Cancer Genome Atlas (TCGA) databases to determine TMEM170B expression. Immunostaining and real-time polymerase chain reaction (RT-PCR) were done to determine TMEM170B expression in human pancreatic cancer cell lines and tissue specimens. Furthermore, the correlation of TMEM170B with clinicopathological features and PAAD prognosis was investigated, and the mechanisms were explored through enrichment analysis and immune cell infiltration analysis.

Results: TCGA and GEO dataset analysis revealed that TMEM170B expression in PAAD tissue samples was significantly lower than that in non-tumorous tissues, which was further confirmed by immunohistochemistry and RT-PCR. Low TMEM170B expression was associated with poor differentiation (p= 0.014). Multivariate analysis identified that TMEM170B is an independent indicator for overall survival [hazard ratio (HR)= 0.116, 95% confidence interval (CI)= 0.014–0.995; p= 0.049] and disease-free survival (HR= 0.19, 95% CI= 0.04–0.910; p= 0.038) in patients with PAAD. Additionally, TMEM170B was involved in immune-related gene sets, including those related to chemokine signaling pathways and innate and adaptive immunity. High

TMEM170B expression was linked to antitumor immune microenvironment with a high infiltration of B cells, T cells, dendritic cells, monocytes, M1 macrophages, neutrophil and natural killer cells and a low infiltration of Tregs and myeloid-derived suppressor cells (all $p<0.05$).

Conclusion: The findings suggest that low TMEM170B expression is remarkably correlated with poor PAAD prognosis, which might provide a therapeutic target for PAAD.

Key words : TMEM170B, prognosis, pancreatic cancer, biomarker, immune infiltration

319. Human Adipose Mesenchymal Stem Cells-derived Exosomes Ameliorate Hepatic Fibrosis by Regulating Choline Metabolism and PI3K/Akt/mTOR Pathway: Based on Transcriptomics and Metabolomics

Zilong Zhang*、jin shang、ying shi、xiaolun huang

Department of Hepatobiliary-Pancreatic Surgery, Cell Transplantation Center, Sichuan Provincial People's Hospital, University of Electronic Science and Technology of China, Chengdu, China

Abstract: Liver fibrosis is a chronic liver disease with presence of the progressive wound healing response caused by liver injury. Currently, there are no approved therapies for liver fibrosis. Exosomes derived from human adipose mesenchymal stem cells (hADMSCs-Exo) have displayed a prominent therapeutic effect on liver diseases. However, few studies have evaluated therapeutic effect of hADMSCs-Exo in liver fibrosis and cirrhosis, and its precise mechanisms of action remains unclear. Herein, we investigated in vitro and in vivo antifibrotic efficacy of hADMSCs-Exo, and identified important metabolic changes and the detailed mechanism through transcriptomic and metabolomic profiling. We found hADMSCs-Exo could inhibit the proliferation of activated hepatic stellate cells, promote their apoptosis, arrest G1 phase, effectively inhibit the expression of profibrogenic proteins and epithelial-to-mesenchymal transition (EMT) in vitro. Moreover, it could significantly decrease the expression of collagen deposition and EMT progression, improve liver function and reduce liver inflammation in liver cirrhosis mice model. In addition, Transcriptome analysis revealed that the key mechanism of

hADMSCs-Exo anti-hepatic fibrosis was the regulation of PI3K/AKT/mTOR signaling pathway. Metabolic analysis showed that hADMSCs-Exo affected the changes of metabolites in lipid metabolism and mainly regulated choline metabolism, which involved in PI3K/AKT/mTOR pathway to anti-liver fibrosis. Thus, our study indicates that hADMSCs-Exo can attenuated hepatic stellate cell activation and suppressed the progression of liver fibrosis, which holds the significant potential of hADMSCs-Exo for use as extracellular nanovesicles-based therapeutics in the treatment of liver fibrosis and possibly other intractable chronic liver diseases.

Key words: Liver fibrosis, human adipose mesenchymal stem cells, exosomes

320. Prognostic value of inflammation-immunity-nutrition score in patients with hepatocellular carcinoma treated with anti-PD-1 therapy

Zilong Zhang*、yuxin liang、jin shang、ying shi、xiaolun huang

Department of Hepatobiliary-Pancreatic Surgery, Cell Transplantation Center, Sichuan Provincial People's Hospital, University of Electronic Science and Technology of China, Chengdu, China

Background: There are no validated biomarkers that can predict the clinical benefit of immune checkpoint blockers against the programmed cell death protein 1 (PD-1) treatments in hepatocellular carcinoma (HCC). This study aimed to investigate the prognostic value of inflammation-immunity-nutrition score (IINS) in patients with HCC treated with anti-PD-1 therapy.

Methods: A consecutive series of 101 HCC patients treated with PD-1 inhibitors in Sichuan Provincial Peoples Hospital between January 2018 and August 2020 were enrolled in the retrospective study. IINS (0–6) was constructed based on pretreatment high-sensitivity C-reactive protein (hsCRP), lymphocyte (LYM), and albumin (ALB). The patients were divided into high and low IINS groups according to IINS values. Prognostic values of each variable were evaluated with univariate and multivariate time-dependent Cox regression analyses. Survival curves were calculated and compared using the Kaplan–Meier method and log-rank test. The prognostic

performance of IINS was further compared with that of other traditional prognostic indicators by receiver operating characteristic (ROC) curve and the areas under the ROC curve.

Results: Patients with low IINS had longer overall survival (OS) (HR: 4.711, 95% CI: 1.80–12.37, *p*= .001) and progression-free survival (HR: 3.411, 95% CI: 1.79–6.51, *p*<.0001) than those with high IINS. The multivariate analysis identified IINS (HR: 3.746, 95% CI: 1.05–13.38, *p*= .042) and tumor number (HR: 5.111, 95% CI: 1.075–24.299, *p*= .04) as independent prognostic factors. According to ROC analysis, IINS (AUC=0.729, 95% CI: 0.597–0.861, *p*= .002) presented better prognostic performance than other traditional prognostic indicators. The area of the IINS-CA19-9 under the ROC curve (AUC) was higher than that of the IINS or CA19-9 levels for the prediction of OS.

Conclusion: The results suggest that IINS may be an independent prognostic indicator for HCC patients treated with anti-PD-1 therapy. IINS-CA19-9 classification may be more effective in predicting clinical benefit of anti-PD-1 therapy in HCC patients.

Key words: biomarkers, hepatocellular carcinoma, inflammation-immunity-nutrition score, prognosis, programmed cell death protein 1

321. Decreased expression of Rab32 promotes hepatocellular carcinoma progression by preventing MAM formation

Xiaoli Liu*[1]、Zeyu Yan[1]、Dalin Wang[1]、Jiming Tian[2]、Dan Wu[1]、Yinping Wang[1]、Jing Zhao[1]、Qichao Huang[1]、Yulu Du[1]、Jiniang Xing*[1]、Xiacheng Sun*[1]

1. Fourth Military Medical University

2. Lanzhou University

Background: Our previous study found that the formation of MAM in HCC cells was reduced and related to the poor patient prognosis. Screening by mass spectrometry revealed that the expression of small GTPase Rab32 in MAM of HCC was significantly reduced. In addition, decreased Rab32 is associated with MAM deficiency and HCC cell viability increase. However, the mechanism of Rab32 regulates the MAM formation and tumor progression in HCC remains to be systematically elucidated.

Methods: We compared Rab32 expression and clinicopathological characteristics using paired HCC and adjacent noncancerous liver tissues from 100 patients by immunohistochemistry analyses. Furthermore, cell proliferation, viability and apoptosis were determined in HCC cell lines with Rab32 knockdown or over-expression and MAM formation decrease or increase through EdU, CCK-8 and apoptosis assays, and tumor growth was monitored in nude mice xenograft model. Finally, we systematically investigated the role of Rab32 in regulation of MAM formation by living cell imaging, transmission electron microscope (TEM) and immunoprecipitation.

Results: The expression of Rab32 was significantly lower in HCC tissues than in paired peritumor tissues (P<0.01). Specifically, lower expression of Rab32 was found in HCC with more tumor number (P<0.01), larger tumor size (P<0.01), vascular invasion (p<0.05), and advanced TNM stage (P<0.01). Rab32 expression was a prognostic factor for both survival and recurrence after curative resection. To be specific, functionally, the down-regulation of Rab32 in HCC cells promoted cell proliferation and apoptosis resistance. In contrast, up-regulation of Rab32 obviously inhibited these characteristics. Mechanistically, decreased Rab32 expression could decrease the phosphorylation of the mitochondrial membrane protein, protein tyrosine phosphatase interacting protein-51 (PTPIP51) which could interact with the endoplasmic reticulum protein vesicle-associated membrane protein-associated protein B (VAPB) in a PKA-dependent manner to inhibit MAM formation. Consistently to this, increased Rab32 expression enhanced MAM formation via this mechanism.

Conclusions: Down-regulating Rab32 expression promoted HCC cells proliferation in vivo and in vitro by inhibiting the interaction between PTPIP51 and VAPB to decrease MAM formation in a PKA-dependent manner. Taken together, our study implicated Rab32 as a potential therapeutic target for HCC. In addition, Rab32 contributed to further understand the essential function of MAM and regulation mechanism of MAM formation in HCC cells.

Key words: Rab32，mitochondria associated ER membrane(MAM)， HCC

322. Survival benefit after radiotherapy for patients with malignant pleural mesothelioma: A propensity score-matched study

Liyou Lian[1]、Shuwen Cheng[3]、Rujie Zheng[1]、Hongxia Yao[1]、Jinfei Chen[1]、Tianhui Chen*[2]

1. First Affiliated Hospital of Wenzhou Medical University

2. Cancer Hospital of the University of Chinese Academy of Sciences (Zhejiang Cancer Hospital)

3. Nanjing University Medical School

Background: Malignant pleural mesothelioma (MPM) is an aggressive cancer with dismal survival. While radiotherapy is commonly used to treat malignant tumors, survival benefits after radiotherapy for MPM patients remains uncertain. Thus, we aimed to evaluate survival benefits after radiotherapy for MPM patients.

Materials and Methods: Data on MPM patients were extracted from the Surveillance, Epidemiology, and End Results (SEER) database. The bias between the radiotherapy and no-radiotherapy groups was minimized using propensity score matching (PSM). Kaplan-Meier (KM) and Cox proportional hazard models were used to explore the therapeutic role of radiotherapy presented with hazard ratio (HR) and 95% confidence intervals (CI).

Results: Overall 7,299 patients with microscopically confirmed primary MPM were extracted for further analyses and among them, 803 (11%) underwent radiotherapy. We found the radiotherapy group had statistically significant higher median overall survival (OS), compared to the group without radiotherapy (12 months vs. 8 months, respectively; HR: 0.868, 95% CI 0.785-0.961) and after adjustment for PSM, the statistical significance remained (HR: 0.874, 95% CI: 0.789-0.968). We found reduced OS after radiotherapy for MPM patients with lung metastases (2 months vs. 8 months, respectively; HR: 2.446, 95% CI 1.303-4.592). Additionally, patients in a combination of radiotherapy with surgery had better OS compared with surgery alone (19 months vs. 13 months, respectively; HR: 0.758, 95 CI%:0.659-0.872). We also found that the OS in combination with surgery, chemotherapy and radiotherapy group significantly improved, compared to radiotherapy with chemotherapy or with surgery (20 months vs. 11 months; HR: 0.612, 95% CI: 0.518-0.722).

Conclusion: We found radiotherapy prolonged the OS for MPM patients, though radiotherapy should be administered with caution for MPM patients with metastases.

Key words: Keywords: malignant pleural mesothelioma; radiotherapy; propensity score matching; metastases; overall survival.

323. Oestrogen-regulated super-enhancer-associated lncRNA NCALD plays a key role in luminal breast cancer progression by forming a complex with ERa to activate GRHL2

yue Meng*、dianrong zhou、bing gu

guangdong provincial peoples hospital

Background: Luminal breast cancer is one of the most popular subtype, which has a sustained risk of late disease recurrence and death. Super-enhancer assoicated lncRNAs may play prominent roles in driving tissue-specific gene expression in the tumorigenesis. However， the biological function of specific transcription dysregulated SE-lncRNAs in luminal breast cancer and the underlying mechanisms are still largely unknown.

Method: The ChIP-seq data, RNA-seq and Hi-C data were used to analyze super-enhancer regulated SE-lncRNA NCALD. The ChIP-seq data, ChIP-qPCR, EMSA, supershift-EMSA and Dual-luciferase reporter assay were conducted to explore the transcription of SE-lncRNA NCALD activated by estrogen receptor (ERα). RT-qPCR was used to detect the expression of SE-lncRNA NCALD, RT-qPCR and Western blotting were used to determine the expression of ERα and GRHL2. RNA pull-down and RIP were employed to investigate the interaction between SE-lncRNA NCALD and ERα. FISH, ChIP-qPCR were used to elucidate the interaction between SE-lncRNA NCALD ERα and GRHL2. The effect of SE-lncRNA NCALD on malignant phenotypes was examined through in vitro and in vivo assays.

Results: To identify the significant overexpressed SE-lncRNAs in luminal breast cancer, three pairs of luminal breast cancers and para-carcinoma tissues were examined by a SE-lncRNA

microarray. SE-lncRNA NCALD was chosen owing its significant specifically overexpressed in luminal breast cancer. We found that The expression level of SE-lncRNA NCALD is regulated by super-enhancers (SEs) driven by ERα. High expression levels of SE-lncRNA NCALD was associated with poor prognosis. Knockout experiments showed SE-lncRNA NCALD was essential for the growth of tumors. Moreover, we demonstrated SE-lncRNA NCALD can regulate the expression of the master transcriptional factor GRHL2 by recruitment of ERα in the promoter of GRHL2.

Conclusion: Our study demonstrated that SE-lncRNA NCALD was transcriptionally activated by super-enhancers driven by ERα and exhibited lineage-specific expression pattern. SE-lncRNA NCALD can promote cancer progression by interacting with ERα and regulating expression of GRHL2

Key words: Luminal breast cancer, SE-lncRNA NCALD, LncRNA, GRHL2, ERα

324. Expression of LncRNA LINC00205 and miR-628-5p in serum of breast cancer patients and their clinical diagnostic value

guoping wang*[1]、yan zhang[2]

1. Chengdu No. 5 Peoples Hospital affiliated to Chengdu University of Traditional Chinese Medicine

2. 四川省泸州市人民医院

Objective ： to investigate the expression levels of long-chain non-coding RNA (LncRNA) LINC00205 and microrna-628-5p (Mir-628-5p) in serum of patients with breast cancer and their clinical diagnostic value.

Methods: from November 2019 to January 2022,92 patients with breast cancer, 92 patients with benign breast diseases and 92 healthy controls were selected. The serum levels of LncRNA LINC00205, miR-628-5p and carcinoembryonic antigen (CEA) were compared among the three groups, and the relationship between the serum levels of LncRNA LINC00205, Mir-628-5p and clinicopathological characteristics of breast cancer was analyzed The correlation between the

expression of LncRNA LINC00205 and miR-628-5p in serum was analyzed, and the diagnostic value of LncRNA LINC00205, Mir-628-5p and CEA in breast cancer was analyzed.

Results: the levels of serum LncRNA LINC00205 and CEA were gradually increased (P & Lt; 0.05) , and the expression level of miR-628-5p was gradually decreased (p & Lt; 0.05) in the groups of health examination, benign breast disease and breast cancer The expression levels of LncRNA LINC00205 and miR-628-5p were correlated with lymph node metastasis, differentiation and clinical stage (P & LT; 0.05) The expression level of LncRNA LINC00205 was negatively correlated with that of miR-628-5p (R= -0.540, P & Lt; 0.05) , and the area under the curve (AUC) of serum LncRNA LINC00205, Mir-628-5p, CEA in the diagnosis of NSCLC was 0.870.0862,0.713, respectively, the cut-off values were 1.41,0.79.4.52 μg/l, the sensitivity was 80.7% , 77.6% , 48.2% , the specificity was 88.5% , 85.7% , 89.4% , the AUC of serum LncRNA LINC00205 and mir-628.5 P was 0.954. The sensitivity of serum LncRNA LINC00205 and mir-628.5 P was significantly higher than that of serum LncRNA LINC00205, the sensitivity was 93.5% and the specificity was 84.9% .

Conclusion: the expression of LncRNA LINC00205 and miR-628-5p in serum of patients with breast cancer is higher than that of normal controls, and the combination of LncRNA LINC00205 and miR-628-5p can be used as a marker for diagnosis of breast cancer.

Key words: Microrna-628-5p; long-chain non-coding RNA LINC00205; breast cancer; diagnostic value

325. Induction therapy with TPF and Sindelizumab for locally advanced Nasopharyngeal Carcinoma and its effect on lymphocyte subcohorte

guoping wang*[1]、yan zhang[2]

1. Chengdu No. 5 Peoples Hospital affiliated to Chengdu University of Traditional Chinese Medicine

2. 四川省泸州市人民医院

Objective: To investigate the efficacy of TPF regimen combined with Sindelizumab in the treatment of locally advanced Nasopharyngeal Carcinoma (NPC)and its effect on

lymphocyte .Methods: Sixty patients with locally advanced nasopharyngeal Carcinoma (NPC) treated with induction therapy of TPF regimen (Control Group, N= 60) and TPF regimen combined with Sindelizumab (Trial Group, N= 60) from January 2020 to January 2022 were analyzed retrospectively， serum Tumor Markers [squamous Cell Carcinoma Antigen (SCCAG) , Serum Ferritin (SF) , Cytokeratin 19 fragment (CYFRA21-1)] were measured before and after squamous-cell Carcinoma treatment.Results： the Serum Levels of Sccag, SF and CYFRA21-1 in the experimental group were significantly lower than those in the Control Group on the 14th day after chemotherapy (P <0.05) , and the serum levels of CD3+、CD4+、CD4+/CD8 T lymphocyte in the experimental group were significantly lower than those in the Control Group on the 14th day after chemotherapy (P <0.05) , the serum levels of CD3+、CD4+、CD4+/CD8+ were higher than those in the control group, while the serum levels of CD8+ were lower than those in the control group (P <0.05) . The ORR, DCR, PFS and OS of the experimental group were higher than those of the control group (P <0.05).The incidences of nausea, vomiting, Granulocytopenia, thrombocytopenia, muscle and joint pain were not different between the two groups (P>0.05) , after the treatment of symptomatic improvement.In the test group, fever, hypothyroidism and skin reaction were all grade I and II, which were improved after symptomatic treatment.Conclusions: Induction therapy with TPF regimen combined with Sindelizumab for locally advanced nasopharyngeal carcinoma is effective, less toxic and has little effect on the immune system. It is helpful for the recovery of t lymphocyte subsets and reduces the toxic and side effects such as Myelosuppression.

Key words: Sindelizumab, locally advanced nasopharyngeal carcinoma, tumor markers, lymphocyte subpopulation

326. Overexpression of SCEL inhibits oral squamous cell carcinoma proliferation and metastasis by modulating the TGF-β1/Smad signaling pathway

Danping Li*[1]、Limei Li[1]、Shu Wu[1]、Jun Zhao[1]、Haishan Zhang[1]、Qiaoli Chen[1]、Yingxi Mo[2]、Xiaoying Zhou[3]

1. Affiliated Stomatological Hospital of Guangxi Medical University

2. Guangxi Medical University Cancer Hospital

3. Life Science Institute, Guangxi Medical University

OBJECTIVE: Sciellin (SCEL) is a precursor protein of the epithelial keratinized envelope.Previous studies have shown that sciellin (SCEL) is a potential biomarker for a variety of malignant tumors. However, the role and mechanism of SCEL in oral squamous cell carcinoma (OSCC) remain unclear.

METHODS: The mRNA expression of SCEL in OSCC tissues and compared with normal tissues was analyzed based on the TCGA database and was further validated by qRT-PCR. IHC staining was applied to analyze the protein expression of SCEL. CCK8 and colony formation assays were used to evaluate cell proliferation. A scratch healing assay and transwell assay were used to determine cell migration and invasion.

RESULTS: We found that the mRNA level of SCEL decreased significantly in OSCC compared with normal oral epithelium ($P<0.001$). The lower levels of SCEL in OSCC were correlated with the patients with lymph node metastasis ($p<0.05$). The AUC of SCEL mRNA and protein level in OSCC was 0.7455 ($p<0.05$) and 0.7956 ($p<0.05$), respectively. Besides, overexpression of SCEL remarkably impedes the proliferation, colony formation capacity, migration, and invasion of OSCC cell lines ($p<0.05$). In addition, the expression of transforming growth factor-β1 (TGF-β1), Smad2/3/4($p<0.05$), was decreased in OSCC cells with SCEL overexpression, indicating that SCEL might suppress the TGF-β1/Smad signaling pathway.

CONCLUSIONS: The expression of SCEL decreased with the increase of OSCC malignancy and may inhibit the growth and metastasis of OSCC by attenuating the TGF-β1/Smad signaling

pathway. Hence，SCEL could serve as a valuable diagnostic biomarker and therapeutic target for OSCC.

Key words: OSSS; SCEL; TGF-β1/Smad; differentiation; metastasis

327. SRTdb: an omnibus for human tissue and cancer-specific RNA transcripts

Qili Shi*[1]、Teng Liu[2]、Zhiao Chen[1]、Xianghuo He[1]、Shengli Li[2]

1. Fudan University Shanghai Cancer Cente

2. Shanghai Jiao Tong University

The production of functional mature RNA transcripts from genes undergoes various pre-transcriptional regulation and post-transcriptional modifications. Accumulating studies demonstrated that gene transcription carries out in tissue and cancer type-dependent ways. However, RNA transcript-level specificity analysis in large-scale transcriptomics data across different normal tissue and cancer types is lacking. We applied reference-based de novo transcript assembly and quantification of 27,741 samples across 33 cancer types, 29 tissue types, and 25 cancer cell line types. We totally identified 231,836 specific RNA transcripts (SRTs) across various tissue and cancer types, most of which are found independent of specific genes. Almost half of tumor SRTs are also tissue-specific but in different tissues. Furthermore, we found that 10 ~ 20% of tumor SRTs in most tumor types were testis-specific. The SRT database (SRTdb) was constructed based on these resources. Taking liver cancer as an example, we showed how SRTdb resource is utilized to optimize the identification of RNA transcripts for more precision diagnosis of particular cancers. Our results provide a useful resource for exploring transcript specificity across various cancer and tissue types, and boost the precision medicine for tumor patients.

Key words: RNA transcript, Pan-cancer analysis, Transcriptional diversity, Precision tumor diagnosis, Tissue specificity analysis

328. Cervicovaginal microbiota disorder combining microenvironment profiles promotes the poor development of cervical cancerization

Mingxuan Zhang*、Jintao Wang、Jiahao Wang、Le Zhang

Department of Epidemiology, School of Public Health, Shanxi Medical University

Cervical cancer poses a serious threat to women's health. Emerging evidence indicates that cervicovaginal microbiota (CVM) and vaginal microenvironment change may play an essential role in the cervical carcinogenic process. However, the influence and function of CVM under different microenvironment conditions and their interaction in cervical lesions remain unclear. A total of 510 participants with different stages of cervical lesions were detected for CVM and vaginal microenvironment profile by 16S rDNA sequencing and vaginal pH, H2O2, and cleanness. The co-occurrence network and generalized multifactor dimensionality reduction (GMDR) model were used to examine the correlation and interaction between microbial taxa and microenvironment profile. The Kyoto Encyclopedia of Genes and Genomes (KEGG) was employed to estimate microbial functions. Our results demonstrated the associations of cervical lesions with CVM disorder and abnormal vaginal microenvironment. In deteriorated vaginal microenvironment, diverse anaerobes (such as Gardnerella, Prevotella, and Peptoniphilus) increased with the severity of cervical cancerization, while Lactobacillus gradually depleted. An interaction of abnormal vaginal pH (>4.5), non-Lactobacillus-dominant (the relative abundance of Lactobacillus<80%), and high CVM diversity (Shannon index≥0.81) on the risk of squamous cell carcinoma of the cervix was revealed by GMDR model. In precancerous cervical lesions, abnormal vaginal pH and H2O2 were correlated to Lactobacillus depletion and created a positively co-occurring relationship with anaerobes. The CVM function significantly varied with the vaginal microenvironment changing in different stages of cervical lesions. Our findings suggested that CVM dysbiosis, especially combined with an abnormal vaginal microenvironment, could promote the progress of cervical lesions, highlighting the significance of assessing vaginal microecology for the prevention and control of cervical cancerization.

Key words: cervical cancerization, cervicovaginal microbiota, vaginal microenvironment, 16s rDNA sequencing

329. DiseaseMeth version 3.0: A major expansion and update of the human disease methylation database

jie xing*、rui yang zhai、cong wang

Harbin Institute of Technology

DNA methylation has a growing potential for use as a biomarker because of its involvement in disease. DNA methylation data have also substantially grown in volume during the past five years. To facilitate access to these fragmented data, we proposed DiseaseMeth version 3.0 based on DiseaseMeth version 2.0, in which the number of diseases including increased from 88 to 162 and High-throughput profiles samples increased from 32,701 to 49,949. Experimentally confirmed associations added 448 pairs obtained by manual literature mining from 1472 papers in PubMed. The search, analysis and tools sections were updated to increase performance. In particular, the search function now provides for the functional enrichment of genes from localized GO and KEGG annotation. We have also developed a unified analysis pipeline for identifying differentially DNA methylated genes (DMGs) from the original data stored in the database. 22,718 DMGs were found in 99 diseases. These DMGs offer application in disease evaluation using two self-developed online tools, Methylation Disease Correlation and Cancer Prognosis & Co-Methylation. All query results can be downloaded and can also be displayed through a box plot, heatmap or network module according to whichever search section is used. DiseaseMeth version 3.0 is freely available at http://diseasemeth.edbc.org/.

Key words: DNA methylation、database、diseases

330. Identification and characterization of partially hypermethylation in under-methylated regions

Xinyu Wang*、Lijun Dai、Qingran Qong、Jianzhong Su

Wenzhou Medical Universiy

DNA methylation plays key regulatory role in regulation of gene transcription by multiple features such as length, genome location, and CpG density, So the regulatory programs of DNA methylation is very complex and has not yet been fully understood. Through deep analysis of hypermethylated CpG sites in the under-methylated regions by a new computing framework hyperUMR we designed, we observed a bimodal methylation status, named partially and fully Hyper. Partially Hyper could not be quantified by traditional mean methylation level of CpG within a predefined regions. Compared with fully Hyper, partially Hyper exhibits a more complex transcriptional regulation pattern, and it associates with up-regulation of gene expression maybe mediated by inhibiting the methylation-sensitive repressors. Pan-cancer analysis verified the universality of partially Hyper. Our study provides a computational tool for the precise identification of DNA methylation patterns, suggesting the complexity of regulational role of DNA methylation.

Key words: DNA methylation; Pan-Cancer; Partially methylated; Transcritpional regulation; UMR

331. Di-methylation of CD147-K234 promotes the progression of NSCLC by enhancing lactate export

Ke Wang*

Fourth Military Medical University

CD147 is a tumor-associated glycoprotein that regulates cell metabolism. However, CD147 methylation and its subsequent role in cancer cell metabolism remain unclear. Here, we detect CD147 di-methylation in 16 non-small-cell lung cancer (NSCLC) tissues using liquid

chromatography-tandem mass spectrometry. CD147 is di-methylated to CD147-K234me2 by lysine methyltransferase 5A (KMT5A). The increase in KMT5A expression boosts the levels of CD147-K234me2, further promoting the interaction between CD147 and monocarboxylate transporter 4 (MCT4), which enhances the translocation ofMCT4 from the cytoplasm to the membrane. Overexpression of CD147-K234me2 and KMT5A enhances glycolysis and lactate export in NSCLC cells. Clinical analysis shows that high CD147-K234me2 expression is significantly related to cancer progression and overall survival, and has prognostic significance in individuals with NSCLC, especially for those in the early stages. Our findings indicate that CD147-K234me2 plays a critical role in cancer metabolism, and it can be a highly promising therapeutic target for NSCLC.

Key words: CD147; di-methylation; NSCLC; lactate export

332. Anti-HIV Drug Elvitegravir Suppresses Cancer Metastasis via Increased Proteasomal Degradation of m6A Methyltransferase METTL3

Long Liao*、Bin Li

The Fifth Affiliated Hospital of Guangzhou Medical University

N6-methyladenosine (m6A) methylation is an abundant modification in eukaryotic mRNAs. Accumulating evidence suggests a role for RNA m6A methylation in various aspects of cancer biology. In this study, we aimed to explore the biological role of RNA m6A modification in tumor metastasis and to identify novel therapeutic strategies for esophageal squamous cell carcinoma (ESCC). Integration of genome-wide CRISPR/Cas9 functional screening with highly invasive and metastatic ESCC subline models led to the identification of METTL3, the catalytic subunit of the N6-adenosine-methyltransferase complex, as a promoter of cancer metastasis. METTL3 expression was upregulated in ESCC tumors and metastatic tissues. In vitro and in vivo experiments indicated that METTL3 increased m6A in EGR1 mRNA and enhanced its stability in a YTHDF3-dependent manner, activating EGR1/Snail signaling. Investigation into the regulation of METTL3 expression found that KAT2A increased H3K27 acetylation levels in the METTL3

promoter region and activated transcription of METTL3, whereas SIRT2 exerted the opposite effects. Molecular docking and computational screening in a Food and Drug Administration-approved compound library consisting of 1,443 small molecules identified compounds targeting METTL3 to suppress cancer metastasis. Elvitegravir, originally developed to treat human immunodeficiency virus (HIV) infection, suppressed metastasis by directly targeting METTL3 and enhancing its STUB1-mediated proteasomal degradation. Overall, RNA m6A modifications are important in cancer metastasis, and targeting METTL3 with elvitegravir has therapeutic potential for treating ESCC.

Key words: m6A modification, METTL3, tumor metastasis, histone H3K27 acetylation, drug repositioning

333. Abnormal regulation of miR-29b-ID1 signaling is involved in the process of decitabine resistance in leukemia cells

Jichun Ma*、Xiangmei Wen、Zijun Xu、Peihui Xia、ye jin、Jiang Lin、Jun Qian

Affiliated People's Hospital of Jiangsu University

Decitabine (DAC) is an inhibitor of DNA methyltransferase used to treat leukemia, but primary or secondary resistance to DAC may develop during therapy. The mechanisms related to DAC resistance remain poorly understood. miR-29b expression in various leukemia cell lines and AML patients by RQ-PCR, and the associated with prognosis was analyzed. To observed the effect of miR-29b on DAC resistance by increasing or inhibiting its expression. Methylation level of cells deal with DAC and DAC-resistant cells was analyzed by BSP. To observed the effect of ID1 on DAC resistance in vivo and vitro. In this study, we find that miR-29b expression was decreased in various leukemia cell lines and AML patients and was associated with poor prognosis. In DAC-sensitive cells, miR-29b inhibited cell growth, promoted apoptosis, and increased the sensitivity to DAC. Similarly, it exerted anti-leukemic effects in DAC-resistant cells. When the miR-29b promoter in DAC-resistant cells was demethylated, its expression was not up-regulated. Furthermore, the expression of ID1, one of the target genes of miR-29b, was down-regulated in

miR-29b transfected leukemic cells. ID1 promoted cell growth, inhibited cell apoptosis, and decreased DAC sensitivity in leukemic cells in vitro and in vivo. ID1 was down-regulated in DAC-sensitive cells treated with DAC, while it was up-regulated in DAC-resistant cells. Interestingly, the ID1 promoter region was completely unmethylated in both DAC-resistant cells and sensitive cells before DAC treatment. The growth inhibition, increased DAC sensitivity, and apoptosis induced by miR-29b can be eliminated by increasing ID1 expression. These results suggested that DAC regulates ID1 expression by acting on miR-29b. Abnormal ID1 expression of ID1 that is methylation independent and induced by miR-29b may be involved in the process of leukemia cells acquiring DAC resistance.

Key words: Decitabine, Drug resistance, miR-29b, ID1, Acute myeloid leukemia

334. Predicting the Influence of Circ_0059706 Expression on Prognosis in Patients with Acute Myeloid Leukemia using Classical Statistics and Machine Learning

Jichun Ma*、Xiangmei Wen、Zijun Xu、Peihui Xia、Ye Jin、Jiang Lin、Jun Qian

Affiliated People's Hospital of Jiangsu University

Various circular RNA (circRNA) molecules are abnormally expressed in acute myeloid leukemia (AML), and associated with disease occurrence and development, as well as patient prognosis. The roles of circ_0059706, a circRNA derived from ID1, in AML remain largely unclear. circ_0059706 expression in de novo AML patients was detected by RQ-PCR, and its association with prognosis was analyzed. To evaluate the prospects for application of circ_0059706 levels in AML in machine learning algorithms, we developed seven types of machine learning algorithm. Further, circ_0059706 efffect on cell growth and apoptosis was detected by CCK8 and FCM. Here, we reported circ_0059706 expression in Chinese patients with de novo AML and its association with prognosis. We found that circ_0059706 expression was significantly lower in bone marrow mononuclear cells from patients with AML than in those from controls (P<0.001). Survival analysis of patients with AML divided into two groups according to high and low circ_0059706 expression showed that overall survival (OS) of patients with high circ_0059706 expression was

significantly longer than that of those with low expression (P<0.05). Further, female patients with AML and those aged > 60 years in the high circ_0059706 expression group had longer OS than male patients and those younger than 60 years. Multiple regression analysis showed that circ_0059706 was an independent factor affecting prognosis of all patients with AML. To evaluate the prospects for application of circ_0059706 in machine learning predictions, we developed seven types of algorithm: logistic regression (LR), random forest (RF), gradient boosting (GB), neural network (NNK), support vector machine (SVM), k-NearestNeighor (KNN), and Gaussian naïve Bayes (GNB). The GB model exhibited higher performance in prediction of one-year prognosis, while the GB and LR models showed better performance in three-year prognosis prediction. We analyzed the importance of variables included in the GB, LR, and RF algorithms, which had good modeling performance. Circ_0059706 expression level was the most important variables among all 26 factors included in the GB and RF algorithms and also among the most important in the LR algorithm. Further, circ_0059706 overexpression inhibited cell growth and increased apoptosis of leukemia cells in vitro. These results provide evidence that high expression of circ_0059706 is propitious for patient prognosis and suggest circ_0059706 as a potential new biomarker for diagnosis and prognosis evaluation in AML, with high predictive value and good prospects for application in machine learning algorithms.

Key words: circ_0059706, acute myeloid leukemia, machine learning, prognosis, biomarker

335. The downregulation of circ_0059707 in acute myeloid leukemia promotes cell growth and inhibits apoptosis by regulating miR-1287-5p

Jichun Ma*、Xiangmei Wen、Zijun Xu、Peihui Xia、Ye Jin、Jiang Lin、Jun Qian

Affiliated People's Hospital of Jiangsu University

Acute myeloid leukemia (AML) is the most common type of hematological malignancy. Recently, increasing reports have shown that many circular RNAs can act as effective targets for AML. However, the roles of circ_0059707 in AML remain largely unclear. In this study, we found that the expression levels of circ_0059707 were significantly decreased in AML patients than in

normal healthy controls (P<0.001). Low expression levels of circ_0059707 were also associated with a poor prognosis. Furthermore, circ_0059707 overexpression inhibited cell growth, promoted apoptosis in leukemia cells, compared with control group. Circ_0059707 and empty plasmid transfected cells were injected subcutaneously into BALB/c nude mice. We found tumor volume of mice in the circ_0059707 group was significantly lower than in the control (P<0.01). Nuclear pyknosis, nuclear fragmentation, nuclear dissolution, and cell necrosis were observed in circ_0059707 group by HE staining. Circinteratome analysis showed that 25 microRNAs (miRNAs), including miR-1287-5p, hsa-miR-1825, and hsa-miR-326, may be potential targets for circ_0059707; of these miRNAs were analyzed and intersected by the GEO database GSE51908 and GSE142700. miR-1287-5p were lower in AML patients compared with controls in both the GSE51908 and GSE142700 datasets. Moreover, we demonstrated that miR-1287-5p expression was down-regulated in AML patients and up-regulated in overexpressed circ_0059707 cells. Collectively, our research demonstrated that the downregulation of circ_0059707 was highly evident in de novo AML patients. Analysis also demonstrated that circ_0059707 inhibited cell growth and promoted apoptosis by up-regulating miR-1287-5p.

Key words: circular RNA, acute myeloid leukemia, circ_0059707, prognosis

336. CC-115 mediates GSDME-dependent pyroptosis in lung adenocarcinoma through Akt/Bax pathway

Ting Zhang*

The First Affiliated Hospital of Chengdu Medical College

Background: Chemotherapeutic agents remain the treatment foundation for various solid tumors, including lung cancer. CC-115 is a novel compound with antitumor activity that has been used in phase I clinical trials in some tumors. However, whether CC-115 has significant anticancer effects on lung adenocarcinoma remains unclear.

Methods: We used human lung adenocarcinoma cell lines (A549 and H1650) for the in vitro determination of the anticancer effects of CC-115 and a xenograft mouse model to determine the potential therapeutic efficacy of CC-115 in vivo. We generated GSDME-knockdown cell lines and

their corresponding control cell lines by transfection with lentiviral constructs. The Akt activator SC79 was used to detect the role of Akt on pyroptosis. Bax knockout was generated to elucidate the role of Bax in CC-115-mediated pyroptosis. Functional experiments were performed using LDH, IL-1β, and IL-18 release assays, flow cytometry, western blotting, and qRT-PCR.

Results: In this study, we found that CC-115 induced lytic cell death in A549 and H1650 cells by way of cell swelling and large bubbles on the cytoplasmic membrane, typical of pyroptosis, a novel form of programmed cell death and plays an important role in chemotherapy. We further demonstrated that CC-115 exerted antitumor effects in lung adenocarcinoma through GSDME-mediated pyroptosis, and GSDME cleavage is based on caspase-3 activation. Moreover, CC-115, as a dual inhibitor of DNA-PK and mTOR, can significantly inhibit the phosphorylation of Akt and relieve the inhibitory effect of Akt on Bax, inducing pyroptosis via the Bax-mitochondrial intrinsic pathway. In contrast, the effects of CC-115 on inducing pyroptosis can be abrogated by treatment with the Akt activator SC79 or Bax knockout. Moreover, CC-115 significantly reduced tumor volume and weight by promoting the expression of Bax and GSDME-N in a xenograft mouse model.

Conclusions: Collectively, our results revealed that CC-115 exerts its anticancer effect by regulating GSDME-mediated pyroptosis through the Akt/Bax-mitochondrial intrinsic pathway. CC-115 is promising as a therapeutic drug candidate for lung adenocarcinoma.

Key words: CC-115, GSDME, pyroptosis, Bax, lung adenocarcinoma

337. Powerful correlation of GBP1 expression with prognosis and tumor immunity in pan-cancer

王森钰*、张雅静、冯阳春

新疆医科大学附属肿瘤医院

Background: Guanylate binding protein 1 (GBP1) is the most studied member of the GBP family, which has anti-microbial and anti-angiogenesis effects, but the researchs in the field of cancer are still not comprehensive. This study intended to perform a pan-cancer analysis of GBP1 by bioinformatics methods.

Methods: Several databases such as TCGA were used to explore GBP1 mRNA and protein expression, and the correlation of GBP1 expression with prognosis, immune checkpoint genes, immune infiltration and tumor microenvironment (TME) was analyzed. In addition, we compared the expression differences of GBP1 in different clinical stages and analyzed GBP1 related proteins and genes. Finally, the enrichment analysis was conducted.

Results: The expression of GBP1 mRNA was up-regulated in ESCA, GBM, HNSC, KIRC and STAD, down-regulated in KICH, KIRP, LIHC, LUAD, LUSC, PRAD, THCA, PAAD and UCEC. The expression of GBP1 protein was up-regulated in colon cancer, ovarian cancer, KIRC, PAAD, HNSC and GBM, and down-regulated in breast cancer and LIHC. The expression of GBP1 was the highest in GBM cell lines and the lowest in LAML cell lines. Prognostic analysis showed that high GBP1 expression was associated with longer overall survival (OS) and progression - free interval (PFI) for BLCA, CESC, COAD, OV, READ and SKCM, and shorter OS and PFI for KIRP, LGG and THYM. GBP1 expression was significantly different at different clinical stages in cancers such as KIRP. The correlation of GBP1 with GBP4, GBP5, IRF1, STAT1 and TAP1 genes was the strongest. More importantly, GBP1 was significantly correlated with immune checkpoint genes, immune infiltration, TME and participated in multiple immune-related pathways.

Conclusion: Powerful role in tumor immunity, which we think can be combined with prognostic studies, is a good way to address the problem of low survival in cancer patients. GBP1 is expected to become an important tumor marker.

Key words: guanylate binding protein 1, expression, prognosis, tumor immunity, pan-cancer

338. GCA induces pyroptosis of lung cancer stem cells by regulating the formation of dTGN via GOLPH3/ MYO18A complex

Feng Zhang*

The First Affiliated Hospital of Chengdu Medical College

Background: Lung cancer remains one of the leading causes of death worldwide. Cancer stem cells (CSCs) are the underlying reason for tumor recurrence, progression, and therapeutic

resistance. Targeting CSCs may contribute to the treatment of lung cancer and improve clinical outcomes. Through rigorous and systemic analysis, we were able to screen out Golgicide A (GCA) from 441 potential candidates in the FDA-approved pyroptosis compound library, and the anticancer mechanism was further studied.

Methods: Induction of stem cell formation by serum-free suspension culture, cck-8 was used to detect the cell viability, detection of cell membrane integrity by LDH release assay, caspase-1 activity assay, western blot, ELISA, flow cytometry were used to analyze pyroptosis in cells. Confocal microscopy was used to detect protein co-localization, the quantification of fluorescence intensity and the co-localization was analyzed by Image J software. Co-IP was performed to assess the interaction between GOLPH3 and MYO18A. Animal study was conducted to evaluate the effect of GCA on tumor growth in vivo.

Results: GCA induces cell death through pyroptosis both in H1650- and A549-drived CSCs (Fig 1); GCA can lead to disassembly of the trans-Golgi network (TGN) and recruit NLRP3 (Fig 2); GCA enhanced the binding of GOLPH3 / MYO18A, resulting in TGN dispersion (Fig 3); In xenograft animal models, GCA can inhibit tumor growth (Fig 4).

Conclusion: GCA induced pyroptosis via formation of dTGN by promoting the combination of GOLPH3 and MYO18A in LCSCs to exert anti-tumor effects.Our studies provide a novel molecular insight of anti-cancer activities of GCA in LCSCs.

Key words: Golgicide A, pyroptosis, lung cancer stem cells, trans-Golgi network

339. NMT1-mediated N-myristoylation of VILIP3 protein and cancer progression are suppressed by desloratadine in hepatocellular carcinoma

Yan He*、Bin Li

The Fifth Affiliated Hospital of Guangzhou Medical University

Hepatocellular carcinoma (HCC) is one of the most common malignant tumors. Identification of the underlying mechanism of hepatocellular carcinoma progression and development of new therapeutic drugs are urgently needed. Here, a compound library consisting of 419 FDA-approved

drugs was taken to screen potential anticancer drugs. A series of functional assays showed that desloratadine, an antiallergic drug, can repress proliferation in HCC cell lines, cell-derived xenograft (CDX), patient-derived organoid (PDO) and patient-derived xenograft (PDX) models. N-myristoyl transferase 1 (NMT1) was identified as a target protein of desloratadine by drug affinity responsive target stability (DARTS) and surface plasmon resonance (SPR) assays. Upregulation of NMT1 expression enhanced but NMT1 knockdown suppressed tumor growth in vitro and in vivo. Metabolic labeling and mass spectrometry analyses revealed that Visinin-like protein 3 (VILIP3) was a new substrate of NMT1 in protein N-myristoylation modification, and high NMT1 or VILIP3 expression was associated with advanced stages and poor survival in HCC. Mechanistically, desloratadine binds to Asn-246 in NMT1 and inhibits its enzymatic activity, disrupting the NMT1-mediated myristoylation of the VILIP3 protein and subsequent NFκB/Bcl-2 signaling. Conclusively, this study demonstrates that desloratadine may be a novel anticancer drug and that NMT1-mediated myristoylation contributes to HCC progression and is a potential biomarker and therapeutic target in HCC.

Key words: N-myristoylation, cancer biomarker, drug repurposing, small molecule drug, target identification

340. PAMR1 is a Favorable Prognostic Biomarker in Hepatocellular Carcinoma

Xiaoping Zhou*

The First Affiliated Hospital of Chengdu Medical College

Background: Peptidase domain containing associated with muscle regeneration 1 (PAMR1) is downregulated in breast cancer and cervical cancer while appearing to inhibit cervical cancer cell invasion and metastasis. This study aimed to evaluate the role of PAMR1 in hepatocellular carcinoma (HCC) and explore the associated molecular mechanisms.

Methods: GSE45267, GSE101685, GSE121248 and GSE14520 mRNA microarray datasets from Gene Expression Omnibus (GEO) were analysised to obtain diferentially expressed genes (DEGs) between HCC and liver normal tissues.We evaluated expression of PAMR1 in HCC databases,

including TCGA, GEPIA, and Kaplan-Meier Plotter and verified by real time PCR and immunohistochemistry (IHC) .Then,we screened and GO enrichment analyzed for genes closely related to changes in PAMR1 expression by cBioPortal and DAVID plateform. Meanwhile, we use TIMER and GEPIA databases to investigate the relationships between PAMR1 expression and infiltrated immune cells. In addition, GSEA was used to predict potential hallmarks associated with different expression of PAMR1 on transcriptional sequences from TCGA database.

Results: In total, The four datasets revealed 15 DEGs, 3 upregulated and 12 downregulated, including the candidate gene PAMR1. PAMR1 was proved significantly downregulated in HCC at the mRNA and protein expression levels. The Kaplan-Meier analysis revealed that low PAMR1 expression was associated with poor overall, relapse-free, progression-free, and disease-specific survival. Gene Ontology analysis suggested that genes related to PAMR1 in HCC was mainly enriched in the regulation of extracellular matrix organization, collagen fibril organization, cell adhesion, and blood vessel development. PAMR1 expression was positively correlated with immune infiltrates, including six immune cells (B cells, $CD8^+$ T cells, $CD4^+$ T cells, neutrophils, macrophages, and dendritic cells). In addition, Gene Set Enrichment Analysis showed that genes downregulated in the low-PAMR1 HCC subgroup were significantly enriched in an inflammatory response, hypoxia, epithelial-mesenchymal transition, KRAS signaling, and TNF-α signaling via NF-kB.

Conclusion: PAMR1 is typically downregulated in HCC, so PAMR1 overexpression may be a favorable prognostic factor in these patients.

Key words: PAMR1; hepatocellular carcinoma;GO analysis; immune infiltrates; GSEA

341. Investigation of transcript variant 6 of TPD52L2 as a prognostic and predictive biomarker in basal-like MDA-MB-231 and MDA-MB-453 cell lines for breast cancer

Xin Zhang*[1,2]、Daniel O'Brien[3]、Xiaohui Zhang[4]

1. Weifang People's Hospital

2. Key Laboratory of Human Spine Biomechanics of Weifang City

3. Bioinformatics Core, Mayo Clinic

4. Department of Breast Surgery, Peking Union Medical College Hospital, Chinese Academy of Medical Science

Background: Basal-like breast cancer (BLBC) exhibits worse pathological features than other breast cancer subtypes, and patients diagnosed with BLBC have short disease-free and overall survival times. Thus, the identification of novel biomarkers and therapeutic targets for BLBC is of upmost importance. Although TPD52L2 is upregulated in multiple cancers, little is known about its roles in BLBC. Methods: RNA levels were analyzed between breast cancer tissues and paired adjacent normal tissues using RNA-seq data from The Cancer Genome Atlas (TCGA). TPD52L2 stable knockdown and inducible knockout cell lines were established using basal-like MDA-MB-231 and MDA-MB-453 cell lines. Cell proliferation assays in vitro and tumor growth analysis in vivo were performed to determine the function of TPD52L2 during BLBC progression. Transwell assays wereused to estimate the regulatory effect of TPD52L2 on BLBC cell migration. The expression profile of all tpd52l2 transcripts was analyzed to assess the functional protein isoform. Association of transcript variant 6 (V6) expression with pathological parameters was carried out using the clinical data of the BRCA cohort. Results: We identified V6 of TPD52L2 as a novel biomarker and regulator of BLBC progression. TPD52L2 is upregulated in BLBCs and associated with patient outcomes. TPD52L2 knockdown suppresses tumor growth, and V6 correlates with cancer-related phenotypes in BLBC. Clinical data further proved that V6 is associated with different pathological features, such as pathological stage and pathological tumor status, and independently predicts patient outcomes and responses to therapies. Conclusions: Our

findings demonstrate that V6 of TPD52L2 is a novel biomarker for BLBC patients. V6 promotes cell proliferation and migration and has marked oncogenic roles in determining the malignant phenotypes of BLBC.

Key words: TPD52L2, BLBC progression, proliferation, metastasis, prognosis, pathological features

342. ncRNA-mediated high expression of SOX4 correlates with unfavorable outcomes and immune infiltration in hepatocellular carcinoma

Li Jing、zhiyi han、xiaozhou zhou*

Department of Liver Disease, Shenzhen Traditional Chinese Medicine Hospital, Shenzhen, China

The activity and number of immune cells in the tumor microenvironment are closely related to the overall survival of patients with hepatocellular carcinoma (HCC). The sex-determining region Y-box 4 (SOX4) gene is abnormally expressed in various tumor tissues and is critical for tumor development. However, the correlation between SOX4 expression in HCC and tumor immunity is unclear. SOX4 expression was explored using data from The Cancer Genome Atlas, Gene Expression Omnibus, and UALCAN databases. Real-time reverse transcription quantitative polymerase chain reaction and western blotting were used to analyze SOX4 expression in several liver cancer cell lines. Additionally, correlations among SOX4 expression, cancer immune characteristics, and infiltrated immune cell gene marker sets in patients with HCC were analyzed using data from the Tumor Immune Estimation Resource, Gene Expression Profiling Interactive Analysis, and Tumor-Immune System Interactions databases. Moreover, we evaluated SOX4 expression in HCC tissues and the correlation of SOX4 expression with survival rate. Subsequently, noncoding RNAs (ncRNAs) responsible for SOX4 overexpression were identified using expression, correlation, and survival analyses. SOX4 expression was significantly upregulated in HCC and was correlated with a poor prognosis. Additionally, SOX4 upregulation in HCC was positively correlated with immune cell infiltration, several biomarkers of immune cells, and immune checkpoint expression. Finally, the MCM3AP-AS1/hsa-miR-204-5p axis was

identified as the most likely upstream ncRNA-related pathway for SOX4 in HCC. These results indicated that ncRNA-mediated upregulation of SOX4 was correlated with immune infiltration level and poor prognosis in HCC.

Key words: SOX4; Hepatocellular carcinoma; Immune cells; noncoding RNA; Prognosis.

343. FAT4 Overexpression in Peripheral Blood Mononuclear Cells is Associated With a Favorable Prognosis and Promotes Immune Cell Infiltration in Hepatocellular Carcinoma

Li Jing、zhiyi han、xiaozhou zhou*

Department of Liver Disease, Shenzhen Traditional Chinese Medicine Hospital, Shenzhen, China

Purpose: To identify prognostically relevant genes in hepatocellular carcinoma, and to investigate whether gene expression in peripheral blood mononuclear cells (PBMCs) and hepatocellular carcinoma tissues can be used as a diagnostic and prognostic marker.

Methods: Using RNA-sequencing, gene expression was examined in PBMCs from patients with advanced hepatocellular carcinoma who survived or died. The expression of the top 10 genes in the survival group was validated. The Gene Expression Omnibus and The Cancer Genome Atlas databases were used to analyze FAT atypical cadherin 4 (FAT4) transcript levels in PBMCs and in hepatocellular carcinoma and normal tissues. The correlation between FAT4 expression and immune cell infiltration was also explored using Tumor Immune Estimation Resource, Gene Expression Profiling Interactive Analysis 2, and the Tumor and Immune System Interaction Database.

Results: FAT4 expression was lower in hepatocellular carcinoma than in normal PBMCs and tissues. Kaplan–Meier analysis suggested that downregulated FAT4 was associated with a relatively poor prognosis. FAT4 overexpression was positively correlated with immune cell infiltration, several immune cell markers, and immune checkpoint expression. MicroRNAs

regulating FAT4 expression were identified using correlation, expression, and survival analyses. Hsa-miR-93-5p was the most likely upstream microRNA of FAT4 in hepatocellular carcinoma.

Conclusion: FAT4 is highly expressed in PBMCs and hepatocellular carcinoma tissues, indicating a favorable prognosis and immune cell infiltration in hepatocellular carcinoma, and revealing the potential role of miRNA-93-5p-mediated downregulation of FAT4 in hepatocellular carcinoma immunology. Our findings provide a new direction for the development of novel immunotherapy targets for hepatocellular carcinoma.

Key words: Biomarker; FAT Atypical Cadherin 4; Hepatocellular Carcinoma; Immune Cell Infiltration; MicroRNA; Peripheral Blood Mononuclear Cell

344. Nanoparticle delivery of miR-21-3p sensitizes melanoma to anti-PD-1 immunotherapy by promoting ferroptosis

Weinan Guo*、Zhenjie Wu、Jianru Chen、Sen Guo、Xiuli Yi、Chunying Li

Xijing Hospital, the Airforce Military Medical University

Background: Although anti-PD-1 immunotherapy is greatly effective in melanoma treatment, low response rate and treatment resistance significantly hinder its efficacy. Tumor cell ferroptosis triggered by IFN-γ that is derived from tumor-infiltrating CD8+T cells greatly contributes to the effect of immunotherapy. However, the molecular mechanism underlying IFN-γ-mediated ferroptosis and related potentially promising therapeutic strategy warrant further clarification. MiRNAs participate in ferroptosis execution and can be delivered systemically by multiple carriers, which have manifested obvious therapeutic effects on cancer.

Methods: MiRNAs expression profile in IFN-γ-driven ferroptosis was obtained by RNA sequencing. Biochemical assays were used to clarify the role of miR-21-3p in IFN-γ-driven ferroptosis and the underlying mechanism. MiR-21-loaded gold nanoparticles was constructed and systemically delivered to testify its role in anti-PD-1 immunotherapy in pre-clinical transplanted tumor model.

Results: miRNAs expression profile of melanoma cells in IFN-γ-driven ferroptosis was firstly obtained. Then, up-regulated miR-21-3p was proved to facilitate IFN-γ-mediated ferroptosis by potentiating lipid peroxidation. MiR-21-3p increased the ferroptosis sensitivity by directly targeting TXNRD1 to enhance lipid ROS generation. Further, miR-21-3p overexpression in tumor synergized with anti-PD-1 antibody by promoting tumor cell ferroptosis. More importantly, miR-21-loaded gold nanoparticles were constructed, and the systemic delivery of them increased the efficacy of anti-PD-1 antibody without prominent side effects in pre-clinical mice model. Ultimately, ATF3 was found to promote miR-21-3p transcription in IFN-γ-driven ferroptosis.

Conclusions: MiR-21-3p up-regulation contributes to IFN-γ-driven ferroptosis and synergizes with anti-PD-1 antibody. Nanoparticle delivery of miR-21-3p is a promising therapeutic approach to increase immunotherapy efficacy without obvious systemic side effects.

Key words: Melanoma, immunotherapy, nanoparticle, miRNA, ferroptosis

345. Clinical significance and immune cell infiltration of lnc-MAPKAPK5-AS1 in HCC: based on public databases and immunohistochemistry

Xiangzhi Hu*[1]、Dedong Wang[1,2]、Jinbin Chen[3]、Pengzhe Qin[2,4]、Boheng Liang[2,4]、Di Wu[2,4]

1. Department of Public Health and Preventive Medicine, School of Medicine, Jinan University

2. Guangzhou Center for Disease Control and Prevention, Guangzhou, 510440, PR China.

3. Guangzhou key laboratory for clinical rapid diagnosis and early warning of infectious diseases, KingMed School of Laboratory Medicine, Guangzhou Medical University, Guangzhou, Guangdong 510180, China.

4. Institute of Public Health, Guangzhou Medical University & Guangzhou Center for Disease Control and Prevention, Guangzhou, 510440, PR China.

The oncogenic or tumor suppressor roles of MAPKAPK5-AS1 in multiple cancers suggest its complexity in modulating the progression of various cancers. We investigated the expression status and methylation level of MAPKAPK5-AS1 in hepatocellular carcinoma (HCC) through data mining from The Cancer Genome Atlas (TCGA) and Gene Expression Omnibus (GEO) and discussed its significance in prognosis and immunity. MAPKAPK5-AS1 was co-expressed with its

protein-coding gene MAPKAPK5 in HCC and exhibited upregulation in HCC tissues due to the hypomethylation of its promoter region. High expression of MAPKAPK5-AS1 was associated with a poor prognosis. Further enrichment analysis showed that it was involved in multiple tumorigenic pathways, such as collagen degradation, FOXM1 pathway, and chemical carcinogenesis DNA adducts. In addition, changes in the expression of MAPKAPK5-AS1 affected plasma cells, T cells CD4 memory resting, NK cells, macrophages M0/M1, and mast cells resting in the tumor microenvironment (TME), and MAPKAPK5-AS1 was found to have obvious correlations with 15 immune cell marker genes. Based on the Sangerbox database, positive relationships were observed between MAPKAPK5-AS1 expression, immune checkpoints (ICP), tumor mutational burden (TMB), and microsatellite instability (MSI), which implied that the MAPKAPK5-AS1 high expression group might exhibit a better effect on immunotherapy. In addition, MAPKAPK5-AS1 expression was verified sensitive to multiple targeted drugs by using CellMiner. Finally, immunohistochemistry served as an external verification to report the expression pattern of MAPKAPK5 protein in HCC as well as its prognostic significance. The above results revealed that MAPKAPK5-AS1 might be involved in the occurrence and development of HCC as an oncogene and a potential therapeutic target through modulating the substance metabolism and immune response.

Key words: hepatocellular carcinoma (HCC), MAPKAPK5-AS1, MAPKAPK5, prognosis, immune infiltration.

346. Identification and Validation of a Novel Multi-omics Signature for Prognosis and Immunotherapy Response of Endometrial Carcinoma

Qiu Wang*、Zhicheng Wu、Xiaofeng Li、Ling Ji

Peking University Shenzhen Hospital

Purpose: Cancer development and immune escape involve DNA methylation, copy number variation and other molecular events. However, there are remarkably few studies integrating

multi-omics genetic profile in endometrial cancer (EC). This study aimed to develop a multi-omics signature for prognosis and immunotherapy response of endometrial carcinoma.

Methods: The gene expression, somatic mutation, copy number alteration and DNA methylation data of EC were analyzed from UCSC Xena database. Then, a multi-omics signature was constructed by machine learning model, ROC curve comparing its prognostic power with traditional clinical features. Two computational strategies were utilized to estimate the signature's performance in predicting immunotherapy response in EC. Further validation focused on the most frequently mutant molecule, ARID1A, in the signature. Association of ARID1A with survival, MSI (Microsatellite-instability), immune checkpoints, TIL (tumor infiltrating lymphocyte) and downstream immune pathways were explored.

Results: The signature consisted of 22 multi-omics molecules, showing excellent prognostic performance in predicting the overall survival of patients with EC (AUC= 0.788). After stratifying patients into high and low risk group according to the signature's median value, low risk patients displayed a greater possibility to response to immunotherapy. Further validation on ARID1A suggested it could induce immune checkpoints up-regulation, promote interferon response pathway and interact with Treg (regulatory T cell) to facilitate immune activation in EC.

Conclusion: A novel multi-omics prognostic signature of EC was identified and validated in this study, which could guide clinical management of EC and benefit personalized immunotherapy.

Key words: Prognosis; Immunotherapy; Endometrial Carcinoma; ARID1A; Regulatory T cell

347. DNA Methylation-Specific Analysis of G Protein-Coupled Receptor-Related Genes in Pan-Cancer

Meng yan Zhang*、Ji yun Zhao、Yan Zhang

Harbin Intitute of Technology

Tumor heterogeneity presents challenges for personalized diagnosis and treatment of cancer. The identification method of cancer-specific biomarkers has important applications for the diagnosis and treatment of cancer types. In this study, we analyzed the pan-cancer DNA methylation data

from TCGA and GEO, and proposed a computational method to quantify the degree of specificity based on the level of DNA methylation of G protein-coupled receptor-related genes (GPCRs-related genes) and to identify specific GPCRs DNA methylation biomarkers (GRSDMs) in pan-cancer. Then, a ridge regression-based method was used to discover potential drugs through predicting the drug sensitivities of cancer samples. Finally, we predicted and verified 8 GRSDMs in adrenocortical carcinoma (ACC), rectum adenocarcinoma (READ), uveal Melanoma (UVM), thyroid carcinoma (THCA), and predicted 4 GRSDMs (F2RL3, DGKB, GRK5, PIK3R6) which were sensitive to 12 potential drugs. Our research provided a novel approach for the personalized diagnosis of cancer and informed individualized treatment decisions.

Key words: G protein-coupled receptor; DNA methylation; biomarker; drug sensitivity

348. Development and Validation of a Novel Prognosis Prediction Model for Patients with Myelodysplastic Syndrome

Haiping Liang*[1]、Liu Bei[2]

1. LANZHOU UNIVERSITY

2. The First Hospital of Lanzhou University

Background: Somatic mutations are widespread in patients with Myelodysplastic Syndrome (MDS) and are associated with prognosis. However, a practical prognostic model for MDS that incorporates somatic mutations urgently needs to be developed.

Methods: A cohort of 201 MDS patients from the Gene Expression Omnibus (GEO) database was used to develop the model, and a single-center cohort of 115 MDS cohorts from Northwest China was used for external validation. Kaplan-Meier analysis was performed to compare the effects of karyotype classifications and gene mutations on the prognosis of MDS patients. Univariate and multivariate Cox regression analyses and Lasso regression were used to screen for key prognostic factors. The shinyapps website was used to create dynamic nomograms with multiple variables. The time-dependent receiver operating characteristic (ROC) curves, calibration plots, and decision

curve analysis (DCA) were used to evaluate the models discrimination, accuracy and clinical utility.

Results: Six risk factors (age, BM blast percentage, ETV6, TP53, EZH2, and ASXL1) were considered as predictor variables in the nomogram. The nomogram showed excellent discrimination, with respective the area under the ROC curve (AUC) values of 0.850, 0.839, 0.933 for the training cohort at 1 year, 3 years and 5 years; 0.715, 0.802 and 0.750 for the testing cohort at 1 year, 3 years and 5 years; and 0.668, 0.646 and 0.731 for the external validation cohort at 1 year, 3 years and 5 years. The calibration curves and decision curve showed that the nomogram had good consistency and clinical practical benefit. Finally, a stratified analysis showed that MDS patients with high risk had worse survival outcomes than patients with low risk.

Conclusion: We developed a nomogram containing six risk factors, which provides reliable and objective predictions of prognosis for MDS patients.

Key words: Myelodysplastic Syndrome, somatic mutation, prognosis, nomogram

349. Alternatively activated (M2) macrophage express SP to promote tumour growth and invasiveness and can be inhibited by aprepitant in Esophageal cancer

yang zheng*、meixiang sang、baoen shan

The fourth hospital of HeBei Medical University

Background & Aims: The role of alternatively activated (M2) macrophages on pro-tumor phenotypes have been well documented in many cancer except esophageal cancer (ECA).Considering their close relationship with chronic tissue injuries as well as enhanced timour invasiveness and growth, we aimed to investigate the direct effect of M2 macrophages on ECA. Besides,multidrug resistance presents a major problem in ECA, and new anti-tumor strategies are desperately needed. The substance P (SP)/neurokinin-1 receptor (NK1R) complex has been discovered to be pivotal in the development of a variety of human cancers, and NK1R antagonists, such as the clinical drug aprepitant, are promising future anticancer agents. Yet, the role of the SP/NK1R complex as a potential anticancer target in ECA is still unknown.The peptide substance

P (SP) is a widely distributed neuronal transmitter that, after binding specifically to the neurokinin-1 receptor (NK1R), triggers a broad variety of functions. Recently, it has become apparent that SP can induce tumor cell proliferation, angiogenesis, and migration via the NK1R, and that the SP/NK1R complex is an integral part of the cancer cell itself and its tumor microenvironment. Therefore, the use of NK1R receptor antagonists as a novel and promising approach for treating patients with cancer is currently under intense investigation. Aprepitant, a non-peptide NK1R antagonist, is a clinical drug approved by the Food and Drug Association (FDA) for the use in chemotherapy-induced nausea and vomiting. Importantly, no significant toxic side effects have been described for aprepitant so far, even when given in high doses.

Methods: M2 macrophages in 25 ECA clinical specimens were quantified using immunohistochemistry and quantitative PCR. The pro-tumour functions and the underlying molecular mechanisms of M2 macrophages in ECA were investigated in vitro co-culture system. We used the three Human ECA cell lines TE1, KYSE150, and KYSE170, as previously described. Cell proliferation was evaluated using CCK-8, We also used transwell, DAPI staining, flow cytometric to detect the growth, invasiveness and apoptosis. Human tumor samples from 25 adult with esophagus cancer were analyzed by quantitative PCR to detect the SP/NK1R.

Results: M2 macrophage express SP to promote tumor growth and invasion, therapeutic targeting with the NK1R antagonists aprepitant, led to growth inhibition , invasion weakened and apoptosis in TE1, KYSE150, and KYSE170 cells in a dose-dependent manner. Intriguingly, ECA cells predominantly expressed the truncated splice variant of NK1R. Human fibroblasts showed only dismal NK1R expression and were significantly more resistant. Stimulation of Esophagus cells with SP, NK1R's natural ligand, caused increased growth rates and abrogated the anti-proliferative effect of NK1R antagonists. Expression analysis of 25 human esophagus cancer samples confirmed the clinical relevance of NK1R, we found the expression were significantly higher for the tr-NK-1R. Most importantly the NK1R antagonists induce apoptosis in Esophagus cancer cells

Conclusions: M2 macrophages contribute to poor prognosis in ECA and promote tumour invasiveness through SP. Besides,for the first time, we describe the NK1R in its truncated splice variant as a potent target in human esophagus cancer cells and an inhibitory effect in vitro by NK1R antagonists.

Key words: M2 macrophages, Esophagus cancer, Truncated neurokinin-1 receptor, Aprepitant

350. Value of multi-gene testing in the diagnosis of Bethesda I to III thyroid nodules: A prospective double-blind study

Guozhi Zhang*、Xiaowei Qi、Lin Ren、Chunlin Tang、Ping Chen、Qiyun Shi、Hao Tian、Peng Tang、Linjun Fan、Li Chen、Shushu Wang、Ye Zhang、Wenting Yan、Ling Zhong、Yanli Guo、Yi Zhang

Department of Breast and Thyroid Surgery, Southwest Hospital, Army Medical University, Chongqing 400038, China.

Background: Bethesda I to III thyroid nodules need to be managed with ultrasound follow-up or repeated fine-needle aspiration (FNA) biopsy based on the Guidelines of American Thyroid Association. In clinical practice, patients with Bethesda I to III thyroid nodules can be unclear in many cases, despite repeated FNA. If the nodules in such cases can be reliably diagnosed as benign or malignant, invasive diagnostic procedures can be avoided in cases in which they are not required. The purpose of this study was to examine the potential benefits of multi-gene testing in terms of improving the accuracy of diagnosis of Bethesda I to III thyroid nodules.

Methods: Between December 2019 and December 2020, patients with thyroid nodules who underwent FNA at The First Affiliated Hospital of Army Military Medical University were enrolled. The study cohort included 542 patients (129 men and 413 women; mean age, 48.7 years; age range, 22–73 years). Among 658 nodules included, 181 were Bethesda I to III thyroid nodules and 45 were resected. Prospective analysis of the FNA samples was conducted with next-generation sequencing (NGS) assay of 16 genes for point mutations and 26 types of gene fusions. The results were compared with surgical outcomes to determine the diagnostic performance of NGS. Further, the results were compared with the results of BRAF V600E mutation analysis by the $\chi 2$ test.

Results: A total of 181 Bethesda I to III thyroid nodules were tested for multiple genes, and mutations were found in 71 nodules. With multi-gene testing, it was possible to correctly classify 21 out of 24 cancers and 19 out of 21 benign nodules. The overall sensitivity, specificity, positive predictive value, negative predictive value, and accuracy were 91% [confidence interval (CI)

73-98], 86% [confidence interval (CI) 67-95], 86% [confidence interval (CI) 71-97], 90% [confidence interval (CI) 69-96], and 89% [confidence interval (CI) 77-95], respectively. The diagnostic accuracy of multi-gene testing was significantly higher than that of the BRAF V600E mutation test (89% vs. 76%, $\chi 2 = 15.652$, $P<0.01$).

Conclusions: Mutations with malignant characteristics were detected in both Bethesda I and Bethesda III thyroid nodules. Some Bethesda II thyroid nodules had mutations with malignant characteristics and were eventually diagnosed as cancer. Multi-gene testing for Bethesda I to III thyroid nodules can be used to accurately distinguish between malignant and benign nodules and has a higher accuracy than the BRAF V600E mutation test.

Key words: Multi-gene testing; Thyroid nodules; Bethesda classification; Papillary thyroid carcinoma; Differentially expressed genes.

351. Impact of salvage radiotherapy combined with chemotherapy on long-term outcomes of patients with recurrent nasopharyngeal carcinoma: a retrospective study

Ying Li*[1,2]、Wei Liu[1,2]、Lihua Wang[1,2]、Wenquan Hong[1,2]、Youliang Weng[2]、Sufang Qiu[2]

1. Clinical Oncology School of Fujian Medical University, Fujian Cancer Hospital

2. 福建省肿瘤医院

Background: It remains controversial that the application of chemotherapy has an impact on recurrent nasopharyngeal carcinoma (rNPC) patients with salvage radiotherapy. Here, we aimed to evaluate treatment outcomes of rNPC patients and derive a prognostic model to assess the benefit of chemotherapy in patients with re-radiotherapy.

Methods: Totally 340 rNPC patients treated with salvage intensity-modulated radiotherapy (IMRT) or chemoradiotherapy (CRT) from October 2006 to September 2019 were included in this study. Overall survival (OS) was the primary outcome. Kaplan-Meier method was employed to detect the prognostic difference with Log-rank tests. The Cox regression analysis was performed

to explore the potential prognostic factors while the multivariate Cox analysis was used to identify candidate variables for the prognostic model of OS.

Results: The 5-year actuarial rates of OS, progression-free survival, loco-regional progression-free survival, and distant metastases-free survival didn't show significant difference between the IMRT and CRT groups (*ps* > 0.05). Age at recurrence was found to be the only independent prognostic factor for OS (HR = 2.076, 95% CI 1.490-2.894, $p < 0.001$). Three factors (age at recurrence, rStage, and initial treatment) were identified for the prognostic model. We found that rNPC patients suffered poor OS in the high-risk group ($p < 0.001$). In the low-risk group, CRT failed to induce survival benefits when compared to RT alone ($p = 0.036$).

Conclusions: Salvage RT combined with chemotherapy cannot improve survival outcomes for rNPC. More novel clinical trials should be explored to develop individualized strategies to improve survival and minimize toxicities.

Key words: nasopharyngeal carcinoma, recurrence, salvage radiotherapy, chemoradiotherapy, prognostic model

352. Development of small extracellular vesicle miRNA-based liquid biopsy for prostate cancer early diagnosis and risk classification

Meng Han*[1,2]、Yuan Yin[4]、Cheng Zhou[2,3,6]、Bairen Pang[1,2,5]、Qi Wang[1,2,5]、Jie Gong[1,2]、Rui Su[2,3]、Jiukai Jin[2,3]、Yingzhi Chen[2,3]、Zhong Zheng[2,3]、Zhaohui Jiang[2,3]、Qi Ma[1,2,3]、Yue Cheng[1,2,3]、Zejun Yan[1,2,3]、Yong Li[5]、Junhui Jiang[1,2,3]

1. Translational Research Laboratory for Urology, the Key Laboratory of Ningbo City, Ningbo First Hospital, The Affiliated Hospital of Ningbo University, Ningbo 315600, Zhejiang, China.

2. Ningbo Clinical Research Center for Urological Disease, Ningbo 315600, Zhejiang, China.

3. Department of Urology, Ningbo First Hospital, The Affiliated Hospital of Ningbo University, Ningbo 315600, Zhejiang, China.

4. School of Basic Medical Sciences, Zhengzhou University, Henan 450001, China.

5. St George and Sutherland Clinical Campuses, School of Clinical Medicine, UNSW Sydney, Kensington, NSW 2052, Australia.

6. Zhejiang University School of Medicine, Zhejiang University, Hangzhou 310030, Zhejiang, China.

Background: Based on GLOBOCAN 2020 estimates, over 1.4 million new cases of prostate cancer (PCa) and 375,304 deaths were reported worldwide and PCa was the most frequently diagnosed cancer in 112 countries in 2020. The incidence of PCa in China is increasing due to the improved detection approaches. Problematically, the current standard marker, prostate specific antigen (PSA), cannot differentiate among benign prostate changes, early stage and advanced stage of PCa. Surgical biopsies are often not a true representation of the molecular profile given complex tumor heterogeneity. Magnetic resonance imaging has a somewhat improved selection for biopsy, but the utility is still limited by occasional false negatives and false positives. Therefore, non-invasive methods detecting novel biomarkers with higher sensitivity and specificity are in a great demand for earlier detection, better diagnosis and prognosis, and more accurate therapeutic determination in PCa patients Liquid biopsy of human body fluids has recently emerged as an appealing non-invasive strategy to support early cancer diagnosis, selection for biopsy, active surveillance for low-risk cancer, and surveillance post-treatment for

recurrence. It has demonstrated unparalleled advantages over conventional tissue biopsy and may complement or even replace medical imaging as a first- or second-line screening tool for earlier cancer detection and better surveillance of cancer metastasis and prognosis. Small extracellular vesicles (sEVs) are nano-sized extracellular vesicles (40-150 nm in diameter) released by cells into biological fluids that contain a plethora of biomolecules such as proteins, nucleic acids, and lipids, and are potent and clinically valuable tools for PCa early diagnosis and prognosis as they are highly representative of their cell of origin. EVs are expected to be considerably advantageous over existing methods of using PSA due to EVs having a higher cell specificity.

Aim: The aim of the study was to identify sEV miRNA profiles from PCa cell lines, human urine, and tissue samples and validate the potential miRNAs in a set of independent human urine and tissue samples for early diagnosis and risk grading of PCa and improving patient-individualized treatment options.

Methods: In this study, sEVs were isolated by ultracentrifugation and confirmed by Transmission Electron Microscopy (TEM) for morphology, and Nanoparticle Tracking Analysis Technology (NTA) for size and concentration, and Western Blotting (WB) for common sEV markers, respectively. The expression differences of sEV miRNAs between PCa cell lines (22RV1, LNCaP, and PC3) and a normal prostate epithelial cell line (RWPE-1) or between low-medium-risk group, and high-risk group PCa urine and tissue samples (N=3/per group) and control samples (N=3/per group) were compared using next generation sequencing. The candidate sEV miRNA markers selected are being validated in PCa cell lines and a large set of PCa urine samples by quantitative real-time PCR (qRT-PCR).

Results: Total 30 candidate sEV miRNAs were identified from PCa cell lines and urine and tissue samples. We demonstrated 1) miR-222-3p was significantly differently expressed in sEVs urine and tissues in PCa patients compared with control subjects. 2) miR-424-5p, miR-664a-5p, and miR-766-3p were significantly differentially expressed in the urine and tissue sEVs of controls and low- and intermediate-risk patients. Among them, sEV miR-424-5p was decreased in PCa cells compared with normal prostate cells, while miR-664a-5p was increased in primary PCa cells compared with metastatic cells. 3) miR-34c-5p and miR-181b-2-3p were significantly different in urine and tissue sEVs between control subjects and high-risk PCa patients, and their expression

levels were significantly decreased in metastatic PCa cells compared with normal prostate epithelial cells.

Conclusion: We have discovered a panel of potential sEV miRNAs from PCa cell lines, human PCa urine, and tissues, which hold promise for developing a non-invasive, liquid biopsy for early diagnosis and progression risk classification to reduce unnecessary biopsy and aid in patients' treatment option. The validation of these candidate biomarkers is in progress in our laboratory.

Key words: Prostate cancer; extracellular vesicle; miRNA; liquid biopsy; diagnosis; risk classification

353. Prognostic model on overall survival in elderly nasopharyngeal carcinoma patients: A recursive partitioning analysis identifying pre-treatment risk stratification

Ying Li*[1,2]、Zongwei Huang[1,2]、Sunqin Cai[1,2]、Qin Ding[1,2]、Youliang Weng[2]、Sufang Qiu[2]

1. Clinical Oncology School of Fujian Medical University, Fujian Cancer Hospital

2. 福建省肿瘤医院

Background: We aimed to evaluate the optimal management for elderly patients with nasopharyngeal carcinoma (NPC) with intensity-modulated radiotherapy (IMRT).

Methods: 301 elderly patients with NPC diagnosed from 2015 to 2019 were enrolled. Overall survival (OS) was the primary endpoint. The univariate and multivariate Cox regression analysis were preformed to identify potential prognostic factors. The recursive partitioning analysis (RPA) was used for risk stratification. Kaplane-Meier survival curves were applied to evaluate the survival endpoints, and log-rank test was used to assess the difference between groups. The prognostic index (PI) was constructed to further predict patients' prognoses displayed by nomogram model. The area under the receiver operating characteristic (ROC) curves (AUC) and the calibration curves were applied to assess this model.

Results: Based on RPA-based risk stratification, we demonstrated that elderly NPC patients who were treated with IC followed by RT had similar OS compared with those with IC combined with CCRT in the intermediate- (stage I-III and pre-treatment EBV > 1840 copies/ml) and high-risk groups (stage IV). IMRT alone maybe an optimal treatment option in the low-risk group (stage I-III with pre-treatment EBV < 1840 copies/ml). We established an integrated PI which was indicted with stronger prognostic power than it based on each separately for elderly NPC (The AUC of PI was 0.87, 0.81, and 0.79 for 1-, 3-, 5-year prediction of OS, respectively).

Conclusion: We present a robust model for clinical stratification which could guide individual therapy for elderly NPC patients.

Key words: Nasopharyngeal carcinoma, Elderly patients, Recursive partitioning analysis, Prognostic model, Geriatric assessment

354. Liquid biopsy of novel extracellular vesicle and particle cargos to improve prostate cancer diagnosis and progression monitoring

Qi Wang*[1,2,3]、Bairen Pang[1,2,3]、Meng Han[1,2]、Cheng Zhou[2,4,5]、Jie Gong[1,2]、Rui Su[2,4]、Jiukai Jin[2,4]、Yingzhi Chen[2,4]、Zejun Yan[1,2,4]、Zhong Zheng[2,4]、Zhaohui Jiang[2,4]、Junhui Jiang[1,2,4]、Yong Li[3]

1. 宁波第一医院外泌体团队

2. Ningbo Clinical Research Center for Urological Disease, Ningbo 315600, Zhejiang, China.

3. St George and Sutherland Clinical Campuses, School of Clinical Medicine, UNSW Sydney, Kensington, NSW 2052, Australia.

4. Department of Urology, Ningbo First Hospital, The Affiliated Hospital of Ningbo University, Ningbo 315600, Zhejiang, China.

5. School of Medicine, Zhejiang University, Hangzhou 310030, Zhejiang, China.

Background: Prostate cancer (PCa) is the most frequently diagnosed cancer in 112 countries and the second leading cause of cancer-related death in men in developed countries. With the improved popularization screening of PCa, the incidence of disease in China is increasing year by year. The current common PCa diagnostic methods in clinic include serum prostate-specific

antigen (PSA), digital rectal examination (DRE), magnetic resonance imaging (MRI) and transrectal ultrasound (TRUS) analysis. Serum PSA test has low specificity with high rates of false-positive or negative results. TRUS is unreliable for detecting PCa because it is insensitive to high-risk PCa groups and leads to overdiagnosis in low-risk groups. The sensitivity and specificity of MRI are also lower. The current gold standard for PCa diagnosis, tissue biopsy, is costly, discomfort/invasive, time-consuming, inaccurate due to tumor heterogeneity and not suitable for early diagnosis and accurate risk stratification, with some risks for patients. Late diagnosis and inaccurate risk identification can significantly affect patients' correct treatment choice, leading to a poor prognosis due to an inappropriate treatment decision.Liquid biopsy is a new developing research area, and a sensitive, non-invasive test to detect cancer development without painful tissue biopsies. It detects extracellular vesicles (EVs) shed by tumor cells into the bloodstream. Detection of tumor specific markers allows for more accurate therapy decision making in cancer patients. In addition to EVs as a good source for cancer biomarker research, two small extracellular particles (EPs), exomere and supermere, have been recently reported in Nature Cell Biology (2018, 2021) and are attracting a great interest in EV area. These two interesting small particles have distinct cargo profiles and functions from EVs and need to be deeply investigated.As one type of liquid biopsies, EVs and EPs, released by all kinds of cell types, are present in all biological fluids and transmits all kinds of nucleic acids, lipids, proteins, and other biological information to other cells. EVs and EPs can be divided into four main subtypes: large extracellular vesicles (lEVs), small extracellular vesicles (sEVs), exomeres and supermeres. Their contents highly reflect the information of their cell origin and have significant clinical values for the early diagnosis and prognosis of PCa patients.

Aims: The study aims are 1) to isolate different subpopulations of EVs (lEVs and sEVs) and EPs (exomeres and supermeres) using different PCa cell lines and human PCa plasma samples; 2) to perform proteomic profiling subpopulations of EVs and EPs to find biomarker difference for PCa diagnosis and progression monitoring.

Methods: Five PCa cell lines (PC3, DU145, LNCaP, C42B, 22RV1) and one normal prostate epithelial cell line (RWPE-1) were cultured, and PCa patient (n=5) and non-cancer control subjects (n=5) were recruited in the Ningbo First Hospital. sEVs, lEVs, exomeres and supermeres were isolated from supernatants of culture and plasma of PCa patients and controls by

ultracentrifugation. The EVs, exomeres and supermeres were characterized by transmission electron microscopy (TEM), nanoparticle tracking analysis (NTA) and Western blotting (WB), atomic force microscopy (AFM), Zeta potential analyzer and nano flowcytometry. In addition, LC-MS/MS proteomics will be used to determine the expression differences of proteins between PCa cell lines and a normal control prostate cell line or between PCa patients and non-cancer control subjects.

Results: We have successful established a stable and repeatable method based on a series of gradient ultracentrifugation conditions to isolate four different EV and EP subpopulations (lEVs, sEVs, exomeres and supermeres) from PCa cell lines and human PCa plasma samples. We are detecting the differences of protein expression using these isolated EV and EP subpopulations for biomarker discovery and validation in our ongoing investigation.

Conclusion: We have successfully established an EVs and EPs isolation method using PCa cell lines and human PCa plasma samples. These different EV subpopulation hold promise for PCa novel biomarker discovery and validation for early diagnosis and progression monitoring. Proteomic profiling of these EV and EP subpopulations is under way in our laboratory.

Key words: Prostate cancer, liquid biopsy, extracellular vesicles, exomeres, supermeres, diagnosis, progression.

355. CXCL12 derived from CD248-expressing cancer-associated fibroblasts mediates M2-polarized macrophages to promote nonsmall cell lung cancer progression

Jieheng Wu *[1,3]、Jiangwei Wu[1]、Qiaoling Zhang[1]、Zeyang Yang[1]、Rui Zhang[3]、Jian Zhang[2]、Zhu Zeng[1]

1. Department of Immunology, Guizhou Medical University

2. Department of Thoracic Surgery, The Affiliated Hospital of Guizhou Medical University, 550001, Guiyang, China

3. Department of Immunology, The Fourth Military Medical University, Xi'an 710032, China

Nonsmall cell lung cancer (NSCLC) is among the most prevalent malignant tumours threatening human health. In the tumour microenvironment (TME), cancer-associated fibroblasts (CAFs) induce M2-polarized macrophages, which strongly regulate tumour progression. However, little is known about the association between CAFs and M2 macrophages. CD248 is a transmembrane glycoprotein found in several cancer cells, tumour stromal cells, and pericytes. Here, we isolated CAFs from tumour tissues of NSCLC patients to detect the relationship between CD248 expression and patient prognosis. We knocked down the expression of CD248 on CAFs to detect CXCL12 secretion and macrophage polarization. We then examined the effects of CD248-expressing CAF-induced M2 macrophage polarization to promote NSCLC progression in vitro and in vivo. We found that CD248 is expressed mainly in NSCLC-derived CAFs and that the expression of CD248 correlates with poor patient prognosis. Blocking CXCL12 receptor (CXCR4) drastically decreased M2 macrophage chemotaxis. CD248 promotes CAFs secreting CXCL12 to mediate M2-polarized macrophages to promote NSCLC progression both in vitro and in vivo. Collectively, our data suggest that CD248-positive CAFs induce NSCLC progression by mediating M2-polarized macrophages.

Key words: CD248；cancer-associated fibroblasts；CXCL12；M2 macrophages；Nonsmall cell lung cancer

356. Regulation Mechanism of Ell-associated Factor 2 in Cervical Carcinoma Microenvironment

Fan Guo、Weina Kong*、Miyessar Anwar、Xiumin Ma

Tumor Hospital Affiliated to Xinjiang Medical University

Purposes: ELL-associated factor 2 (EAF2) plays an important role in transcription elongation and the regulation of gene expression in mammalian cells. EAF2's depletion has been demonstrated to enhance cell proliferation and greatly increase the risk of cancer. Even so, its expression and prognostic role in cervical carcinoma (CC) remains controversial.

Methods: To solve this issue, we comprehensively investigated the role of EAF2 in CC through various databases including ONCOMINE, UALCAN, Kaplan-Meier Plotter and TIMER.

Results: In all, we found that the EAF2 was highly expressed in CC tissue and was significantly correlated with better patient survival. Among the CNAs, amplification was the dominant alteration. Then the co-expression profile and enrichment analysis of EAF2 were related to the potential signaling pathways. The function of genes such as Kinase LYN, mi-RNA133A-133B and transcription factor OCT1 were also enriched in CC. The positively relation EAF2 expression to 6 immune cells revealed that EAF2 expression may affect development of patients with CC partially due to immune infiltration.

Conclusions: Taken together, our data suggest that EAF2 might be a potential prognostic marker and therapeutic target for CC patients.

Funding: This study was supported by grants from Natural Science Foundation of Xinjiang Uygur Autonomous region (2021D01C402), State Key Laboratory of Pathogenesis, Prevention and Treatment of High Incidence Diseases in Central Asia (SKL-HIDCA-2021-14).

Key words: ELL-associated factor 2 (EAF2), Cervical carcinoma, Prognosis, Immune cells

357. The oncogenic roles of JC polyomavirus T antigen in cervical cancer

Hang Xue*、Huachuan Zheng

Chengde Medical University Affiliated Hospital

Abstract

Background: According to pathological and transgenic data, there is a close link between JC polyomavirus (JCPyV) T antigen and various epithelial cancers. The aim of this study was to explore the role of T antigen in cervical tumorigenesis.

Methods: The phenotypes were observed in T antigen-overexpressing HeLa cells by Cell Counting Kit-8 assay, Annexin V staining, Transwell assay, and a xenograft model. Phenotype-related and T antigen partner proteins were screened by western blot. Nested, real-time, and in situ PCR were used to detect T antigen in cervical cancer.

Results: Overexpression of T antigen promoted the proliferation, anti-apoptosis, anti-pyroptosis, chemoresistance, migration, invasion, and epithelial-mesenchymal transition of HeLa cells. All mutants impaired the positively regulated effects of T antigen on proliferation. According to a general PCR, the positive rate of T antigen was higher in cervical cancer than in adjacent cervical intraepithelial neoplasia (CIN) and normal tissues ($p<0.05$), in line with the JCPyV copy number ($p<0.05$). T antigen-positive cells were detectable in the nuclei of cervical cancer, CIN, and squamous cells by in situ PCR. Strong nuclear immunoreactivity against T antigen was observed in cervical cancers, but not in CIN or normal squamous epithelium.

Conclusions: JCPyV T antigen may insert into the genome of cervical squamous epithelial cells and encode T antigen for its oncogenesis. T antigen participates in the aggressive progression of these cells by promoting proliferation, anti-apoptosis, anti-pyroptosis, migration, invasion, epithelial-mesenchymal transition, and chemoresistance.

Key words: JC polyomavirus; T antigen; oncogenesis; cervical cancer

358. A comprehensive platelet expression atlas resource PEA and platelet transcriptome landscape

Gui-Yan Xie*

huazhong university of science and technology

Platelet is important component in blood and RNAs in platelets can be potential biomarkers for noninvasive disease monitoring. However, a comprehensive investigation for expression profile in platelets is lacking. Here, we curated 2069 high quality datasets of mRNA and miRNA expression profiles from human platelets of healthy and disease samples to investigate the transcriptome characteristics of platelets. We detected about 5000 protein-coding and 2000 non-coding genes on average in platelets of RNA-seq healthy samples. Although total numbers of genes in platelets of disease samples varied dramatically from 3069 to 13678, the top 500 expressed genes were identical more than 88.4% averagely. Six of the top ten highly expressed genes in platelets were from mitochondria. Moreover, genes in platelets, whole blood and PBMC are 7162, 10,512 and 9336 averagely, respectively. The top 500 genes in platelets shared<200 genes with PBMC or blood. Compared with healthy samples, the platelet expression profiles are altered in cancer patients, which genes enriched in ribosome biogenesis and immune-related processes are down-regulated. Finally, we documented all platelets expression data into a database named platelet expression atlas (PEA, http://bioinfo.life.hust.edu.cn/PEA). PEA as the state-of-art platelet expression repository across different diseases will benefit the blood research community.

Key words: platelet; transcriptome; differentially expressed genes; specifically expressed genes; database.

359. ImmuCellAI-mouse: a tool for comprehensive prediction of mouse immune cell abundance and immune microenvironment depiction

Ya-Ru Miao*

Huazhong University of Science and Technology

Motivation: Immune cells are important components of the immune system and are crucial for disease initiation, progression, prognosis, and survival. Although several computational methods have been designed for predicting the abundance of immune cells, very few tools are applicable to mouse. Given that mouse is the most widely used animal model in biomedical research, there is an urgent need to develop a precise algorithm for predicting mouse immune cells.

Results: We developed a tool named ImmuCellAI-mouse (Immune Cell Abundance Identifier for mouse) to estimate the abundance of 36 immune cell (sub)types from gene expression data by hierarchical strategy. Benchmark results showed high accuracy of ImmuCellAI-mouse in predicting most immune cell types, with correlation coefficients between predicted value and real cell proportion of most cell types being larger than 0.8. We applied ImmuCellAI-mouse to a mouse breast tumor dataset and revealed the dynamic change of immune cell infiltration during treatment, which is consistent with the findings of the original study but with more details. We also constructed an online server for ImmuCellAI-mouse, on which users can upload expression matrices for analysis. ImmuCellAI-mouse will be a useful tool for studying the immune microenvironment, cancer immunology, and immunotherapy in mouse models, providing an indispensable supplement for human disease studies.Availability and implementation Software is available at http://bioinfo.life.hust.edu.cn/ImmuCellAI-mouse/

Key words： immune cell, cancer, immunotherapy

360. GSCA: an Integrated Platform for Gene Set Cancer Analysis at Genomic, Pharmacogenomic, and Immunogenomic Levels

Gui-Yan Xie*

College of Life Science and Technology, Huazhong University of Science and Technology

Background: Cancer initiation and progression are caused by several gene dysregulations. Gene set analysis (GSA) could improve the signal-to-noise ratio and identify biological insights on the gene set level. However, there is no platform for exploring cancer genomic data using GSA methods.

Results: In this study, we upgraded our GSCALite to GSCA (http://bioinfo.life.hust.edu.cn/GSCA) for cancer GSA at genomic, pharmacogenomic, and immunogenomic levels. In this improved GSCA, we integrated expression, mutation, drug sensitivity, and clinical data from four public data sources for 33 cancer types. We added several new features to GSCA, including associations between immune infiltration with gene expression and genomic variations, and associations between gene set expression scores and clinical outcomes. GSCA has four main functional modules for cancer gene sets to explore, analyze, and visualize expression, genomic variations, tumor immune infiltration, drug sensitivity, and their associations with clinical outcomes. To prove the usefulness of GSCA, we used two case studies of seven cell cycle genes and three mTOR genes to identify their associations between expression, mutation and clinical associations in different cancer types, which was unable to identify on single-gene level.

Conclusions: In conclusion, GSCA is a user-friendly web server and a useful resource for conducting hypothesis tests using GSA methods at genomic, pharmacogenomic, and immunogenomic levels.

Key words： Keywords: gene set, cancer analysis, pharmacogenomics, immunogenomics, clinical outcomes

361. The inactivation of ketone body metabolism induces an inflammatory microenvironment and facilitates the progression of renal clear cell carcinoma

Ran Zhao*、Qian Zheng、Xiao ying Zhou

Guangxi Medical University

Abnormal metabolism of the ketone body is closely related to the occurrence and development of the tumor. Previously, we found that key enzymes for ketogenesis, including ACAT1, BDH2, HMGCL, and HMGCS2 are significantly inactivated and positively correlated with a worse outcome in patients with clear cell renal cell carcinoma (ccRCC). To further address the tumor-suppressive role of ketogenesis enzymes in ccRCC, we comprehensively analyzed the transcriptome of ccRCC cell lines which is ectopically overexpressed by these four genes, respectively. RNA-seq analysis showed that differentially expressed genes affected by elevating ACAT1, BDH2, HMGCL, and HMGCS2 respectively in ccRCC cells were remarkably focused on the TNF-α/NF-κB inflammatory signaling pathway, in which downregulation of C-X-C pro-inflammatory chemokines, such as CXCL1, CXCL2, CXCL5, and CXCL8 was observed. Based on the TCGA database, we found a higher transcriptional level of these pro-inflammatory chemokines above in ccRCC, which were closely associated with the worse prognosis of patients. By TISIDB network analysis, we found that the transcription levels of four key enzymes in ketone metabolism were not significantly correlated with neutrophil infiltration but negatively correlated with macrophage infiltration. Then using HE staining and IHC staining, we found that there were a large number of macrophages in ccRCC tissues and a large number of neutrophils in para-cancerous tissues. In addition, TCGA database analysis showed that VEGFA was negatively correlated with the transcription levels of four key ketogenic enzymes in ccRCC. In summary, ketone body metabolism affects the tumor immune microenvironment and then might affect the occurrence and evolution of ccRCC.

Key words： ccRCC; metabolite; inflammatory cytokines; immune microenvironment

362. The Predictive Model of key Biomarker in Liquid Biopsy for Prognosis of Bladder Cancer

Xin Dong*、Baojun Wei、Wei Cui

Department of Laboratory, National Cancer Center/Cancer Hospital, Chinese Academy of Medical Sciences and Peking Union Medical College

Purpose: The aim of present study was to explore the expressive status of overexpressed in lung cancer-1 (OLC1) gene in bladder urothelial carcinoma, and analyzed the correlation between the aberrant expression of OLC1 and the clinicopathological features. On the basis of clarifying the expression of OLC1 gene in the tumor tissue of bladder cancer patients, explore the relationship between OLC1 expression and the prognosis of bladder cancer patients. Determine the expression of OLC1 in blood and urine before operation, and evaluate the possibility of OLC1 as a biopsy marker for predicting the prognosis of bladder cancer.

Methods: The mRNA expression of OLC1 was examined in 70 bladder cancer tissues and 38 corresponding normal urothelial samples by reverse real-time quantitative polymerase chain reaction (qRT-PCR); and OLC1 protein expression was examined in 114 bladder cancer specimens by immunohistochemical staining，OLC1 protein expression was examined in 52 bladder cancer patient serum by ELISA. Kaplan-Meier analyses were performed to determine the association between OLC1 expression and progression-free survival (PFS) and overall survival (OS) of the patients.

Results: The mRNA and protein expression of OLC1 was markedly up-regulated in the tumor tissues($p<0.05$) and serum($p<0.05$) of the bladder cancer patients, especially in those with the muscle invasive bladder cancer (stage T2-T4, $p<0.001$), and of the smoker patients ($p<0.05$). The 5-year OS rate for the patients with high level OLC1 in the tumor was considerably lower than those with low level OLC1 ($p=0.04$). Additionally the 5-year OS rate for the smoking patients with high level OLC1 protein was significantly lower than those of non-smoking patients with low level OLC1 ($p=0.01$).

Conclusions: OLC1 was overexpressed in bladder urothelial carcinoma which correlated with the tumor invasion, overall survival, and smoking history of the patients, suggesting that OLC1 is a potential biopsy prognosis biomarker for bladder cancer.

Key words: OLC1, Prognosis Biomarker, Bladder cancer.

363. Ubiquitin Specific Protease 44: What we currently know

Yujia Liu*、zhongjun wu、tingxiu xiang

first affiliated hospital of chongqing medical university

USP44 (ubiquitin specific peptidase 44) is an important molecule that counters the signal induced by ubiquitin conjugases and ligases by removing ubiquitin from substrates. Current research has implicated USP44 activity in various cancers. Absence of USP44 results in functional changes of crucial carcinogenic and tumor suppressor proteins, directly or indirectly leading to chromosome mis-segregation, aneuploidy and tumorigenesis in vivo. In this review, we discuss recent advances regarding of the functions of USP44, focusing our attention on the molecules interacting with USP44 and the biological processes in which these interactions are involved, revealing the possibility of USP44 as a therapeutic target in cancers.

Key words： USP44; ubiquitin; ubiquitin–proteasome system; mechanism

364. Detecting NAB2-STAT6 Fusion Variants and other Molecular Alterations in Intracranial Solitary Fibrous Tumors by Targeted RNA sequencing

Juan Ji*[1,2]、Yang Liu[1,2]

1. Department of Pathology, Sichuan Cancer Hospital & Institute, Chengdu, China

2. 电子科技大学附属肿瘤医院

Background: Intracranial solitary fibrous tumor (SFT) is a rare tumor with a propensity for recurrence and metastasis. NAB2-STAT6 is the driver gene of SFT. Both NAB2 and STAT6 are located on chromosome 12q13. Thus, there is a tendency to miss some new fracture sites with the fluorescence in situ hybridization (FISH) test. Here, we sought to establish the repertoire of genetic alterations by RNA sequencing and clinicopathological features of intracranial SFT.

Methods: Clinicopathologic data were collected on a cohort of seven intracranial solitary fibrous tumor. RNA sequencing was used to detect the repertoire of genetic alterations. Immunohistochemical assays were also performed to assess STAT6, CD34 and BCL2 expression in the intracranial SFTs.

Results: NAB2-STAT6 fusion was detected in about 72% of cases, and the main fusion site was NAB2exon6-STAT6exon16/17. The fusion variant was not related to clinical prognosis, which is consistent with previous reports. Of note, we detected a new KCNQ1-IGF2 gene fusion with RNA sequencing, which is a pathognomonic hallmark of SFT. Analysis of immunostaining expression for SFTs revealed that BCL2 has the highest susceptibility (100%), followed by STAT6(86%) and CD34(86%).

Conclusions: STAT6 stain is highly specific and sensitive for SFT. In addition to NAB2-STAT6 fusion, KCNQ1-IGF2 gene fusion, which is involved in the overexpression of vascular endothelial growth factor (VEGF), was detected by RNA sequence. These results provide additional evidence for the use of antiangiogenics in the treatment or recurrence of refractory SFT.

Key words: solitary fibrous tumor, intracranial, NAB2-STAT6, IGF2, RNA sequencing

365. Lactate metabolism as a dictator of patient outcomes and immune microenvironment in head and neck squamous carcinoma

Xiaochuan Chen*、Junping Pan、Qin Ding、Hanxuan Yang、Sufang Qiu

Clinical Oncology School of Fujian Medical University, Fujian Cancer Hospital, Fuzhou, China

Objective: Head and neck squamous cell carcinoma (HNSCC)treatment is facing clinical challenges. Head and neck squamous cell carcinoma (HNSCC)is a major public health concern because of delayed diagnosis and poor prognosis. Recent studies and research reports have highlighted the important integral function o performed by the tumor microenvironment (TME) in the prediction of clinical outcomes as well as the efficacy. Lactate metabolism mediates many cancers initiation and progression development, including metastasis, angiogenesis, and immunosuppression. However, the prognostic values significance of lactate metabolism-related genes (LMRGs) and the role of TME in HNSCC remain to require further elucidation.

Methods: We built a prognostic multigene signature with LMRGs and systematically correlated the risk signature with immunological characteristics in TME. The most important prognostic gene among risk signatures was screened by machine learning analysis.

Results: LMRGs-related prognostic model showed good prediction performance. The immunological signaling pathways are linked to connected with low-risk scores. Low-risk scores are associated with immune signaling pathways. A high proportion of immunomodulators were shown to be inversely associated with linked to the risk signature. Samples with low-risk scores were found to exhibit greater higher levels of $CD8^+$ T cells infiltration, suggesting that the low-risk subgroup may have shaped an inflammatory TME. Furthermore, immune therapy might be more effective for the low-risk subtype of HNSCC patients ($P < 0.001$). Machine learning analysis revealed highlighted that PYGL was the most important prognostic gene among risk signatures. The inflammatory phenotype was characterized by the least expression of PYGL, which was observed to be inversely linked to CD8+ T-cell infiltration, as determined by immunofluorescence analyses.PYGL exhibited the lowest expression in the inflamed phenotype,

which was negatively correlated with CD8+ T-cell infiltration, according to immunofluorescence analyses.

Conclusion: Our study identified and validated a promising LMRGs signature associated with inflamed TME, which can effectively predict may accurately efficaciously anticipate forecasting the survival of HNSCC patients. PYGL might be a novel biomarker to predict immune efficacy.

Key words: head and neck squamous cell carcinoma, lactate metabolism, tumor microenvironment, prognostic model, TCGA

366. The value of MECOM/PRDM3 expression in predicting development and poor prognosis in lung adenocarcinoma

Anqi Li*[1]、Meng Li[1]、Jing Wang[2]、Jiejun Zhou[1]、Meng Fan[1]、Mingwei Chen[1,2]

1. *The First Affiliated Hospital of Medical College of Xi'an Jiaotong University*

2. *陕西省第二人民医院*

Background: lung cancer is one of the most common cancers in the world, and lung adenocarcinoma (LUAD) is the main pathological type. The MDS1 and EVI1 complex locus (MECOM, also known as PRDM3) is a zinc finger transcription factor highly associated with many malignancies. However, the correlation between MECOM and the clinicopathological features and prognosis of LUAD is still unclear.

Materials and methods: The relationship between the expression of MECOM and the clinicopathological features and prognosis of LUAD was determined by searching The Cancer Genome Atlas (TCGA), GEPIA, KM plotter and UALCAN databases. The expression level of MECOM in lung adenocarcinoma cell lines, tissues and serum was determined by Real-time quantitative polymerase chain reaction (qRT-PCR), western blotting, immunohistochemical staining and ELISA to establish the receiver operating characteristic curve (ROC) to assess the diagnostic efficacy of MECOM.

Results: TCGA database showed that the mRNA level of MECOM was significantly degraded in non-small cell lung cancer tissues ($p<0.05$), while GEPIA and KM plotter database indicated that

the low expression of MECOM was only associated with poor prognosis in LUAD (p<0.05). In addition, UALCAN database displayed that the expression of MECOM was correlated with the gender, age, smoking habit, clinical stage, lymph node metastasis status and TP53 mutation status of LUAD patients (p<0.05). Compared with lung (bronchial) epithelial cell line, the mRNA and protein levels of MECOM in lung adenocarcinoma cell lines were significantly down regulated (P <0.05), and the expression of MECOM in tumor tissues was significantly lower than that in paracancerous tissues (p<0.05). Compared with healthy people, the expression of MECOM in serum of LUAD was significantly decreased (p<0.05). Further analysis showed that the expression of MECOM was correlated with gender, stage, tumor size, lymph node metastasis and distant metastasis (p<0.05), but not with age and smoking habit. The area under the curve (AUC) of MECOM for predicting LUAD was 0.804, and for predicting stage was 0.762. The AUC of CEA and CA125 for predicting stage was 0.814 and 0.820, respectively. Although the AUC of MECOM for predicting stage was lower than that of tumor markers, we found that the combined diagnosis of tumor markers and MECOM for stage was as high as 0.889, which can significantly improve the diagnostic value.

Conclusions: MECOM may be a potential diagnostic marker for LUAD, and its low expression may be related to the poor prognosis of LUAD.

Key words: MECOM; PRDM3; Clinicopathological features; Prognostic; Lung adenocarcinoma

367. dbCAC: a comprehensive database of genes and drugs in cancer-associated cachexia

Longxiang Xie、Qiang Wang、Guo Zhao、Fangmei Nan、Qiongshan Li、Shengnan Wu、Xinyuan Liu、Yongsen Wang、Zhihan Zhou、Xiangqian Guo*

Henan university

Aim: Cancer-associated cachexia (CAC) is a devastating and multifactorial syndrome, characterized by anorexia and loss of body weight with specific losses of adipose tissue and skeletal muscle. About half of patients with advanced cancer show a syndrome of cachexia, which has profoundly impacted on quality of life, symptom burden and usage of healthcare resources.

Hence, it is urgent to ascertain the molecular mechanisms behind cancer cachexia, and develop effective medical intervention strategies for reversing cachexia, that is why hundreds of cachexia relevant papers are published per year in recent decades. However, the information of CAC related genes and drugs are scattered and dispersed across a large amount of literatures without systematic recording and integrating.

Material and Methods: Here, we presented a database calling dbCAC (database of genes and drugs in Cancer-Associated Cachexia), which collected experimental validated functional proteins, non-coding RNAs and drugs in CAC. In total, dbCAC contains 293 CAC genes (252 protein-encoding genes and 41 non-coding genes) and 254 CAC drugs which are retrieved from 602 studies.

Results: By user-friendly interface of dbCAC, user can search, browse, analyze, download these CAC genes and their related information. Furthermore, we have collected a total of 22985 tumor cases with both gene expressional profiles and clinical survival information from 160 gene expression profiling datasets, which includes 132 GEO (Gene Expression Omnibus) datasets, 26 TCGA (The Cancer Genome Atlas) datasets, 1 ICGC (International Cancer Genome Consortium) dataset and 1 published literature. By these tumor expression profiles, we built a prognosis analysis module for the CAC genes.

Conclusion: dbCAC provides a relatively comprehensive repository of the CAC related genes and drugs, and is expected to help researchers acquire insights into CAC. dbCAC is freely available at http://bioinfo.henu.edu.cn/Cachexia/Cac.html

Key words: cancer-associated cachexia; gene; drug; prognosis; TCGA; GEO

368. Integrated analysis of lncRNA-miRNA-mRNA ceRNA network identified lncRNA EPB41L4A-AS1 as a potential biomarker in non-small cell lung cancer

Meiqi Wang*

Harbin Medical University Cancer Hospital

Background: Recent evidence has indicated that long noncoding RNAs (lncRNAs) can function as competing endogenous RNAs (ceRNAs) to modulate mRNAs expression by sponging microRNAs (miRNAs). However, the specific mechanism and function of lncRNA-miRNA-mRNA regulatory network in non-small cell lung cancer (NSCLC) remains unclear.

Materials and Methods: We constructed a lung cancer related lncRNA-mRNA network (LCLMN) by integrating differentially expressed genes (DEGs) with miRNA-target interactions. We further performed topological feature analysis and random walk with restart (RWR) analysis of LCLMN. Gene Ontology (GO) and Kyoto Encyclopedia of Genes and Genomes (KEGG) pathway analysis were performed to investigate the target DEGs in LCLMN. The expression levels of significant lncRNAs in NSCLC were validated by quantitative real-time PCR (RT-qPCR). The prognostic value of the potential lncRNA was evaluated by Kaplan-Meier analysis.

Results: A total of 33 lncRNA nodes, 580 mRNA nodes and 2105 edges were identified from LCLMN. Based on functional enrichment analysis and co-expression analysis, lncRNA EPB41L4A-AS1 was demonstrated to be correlated with the tumorigenesis of NSCLC. RT-qPCR results confirmed that the expression levels of lncRNA EPB41L4A-AS1 in NSCLC tissues were downregulated compared with adjacent non-cancerous tissues. Kaplan-Meier analysis showed that high expression of lncRNA EPB41L4A-AS1 was associated with better overall survival (OS) in NSCLC patients. Further investigation identified that high expression levels of COL4A3BP, CDS2, PURA, PDCD6IP and TMEM245 were also correlated with better OS in NSCLC patients.

Conclusions: In this study, we constructed a lncRNA-miRNA-mRNA ceRNA network to investigate potential prognostic biomarkers for NSCLC. We found that lncRNA EPB41L4A-AS1 could function as a regulator in the pathogenesis of NSCLC.

Key words: Non-small cell lung cancer, Long non-coding RNAs, Competing endogenous RNAs, LncRNA-miRNA-mRNA regulatory network, Overall survival

369. Metabolic biomarkers for diagnosis of germinoma revealed by multi-omics and machine learning approaches

HuaChun Yin*[1]、Yong Chen[4]、LuSheng Li[4]、Ying Xiong[3]、JingXin Tao[2]、ShengQing Lv[1]、Hui Yang[1]、Bo Li[2]、Song Li[1]

1. Department of Neurosurgery, Xinqiao Hospital, The Army Medical University

2. 重庆师范大学生命科学学院

3. 陆军军医大学

4. 重庆医科大学附属儿童医院神经外科

Background: Germinoma accounts for two-thirds of intracranial germ cell tumours (iGCTs). Patients with germinomas have 5-year survival rates of ≥90% after radiotherapy. Accurate and early diagnosis is crucial for therapeutic planning and strategies for germinomas. Negative tumour markers may distinguish germinoma from a non-germinoma germ cell tumour (NGGCT), but not similar neoplasia. Liquid biopsies rely upon detection of circulating tumour cells, cell free DNA, RNA, proteins and metabolites present in biofluids of patients. The cerebrospinal fluid (CSF)-derived liquid biopsies are widely accepted as a non-invasive method for diagnosing tumour. Metabolic from CSF alterations, used as diagnostic biomarkers of germinoma, remain poorly understood.

Methods: The global metabolic profiles of CSF in 57 patients (26 germinoma, 23 non-iGCT, and 8 NGGCT) and tumour in 7 patients (3 germinoma and 4 NGGCT) were evaluated by metabolomics, and the tumour also were evaluated by RNA-seq profiles. The common clinic molecular Alpha-fetoprotein and beta subunit of human chorionic gonadotrophin (β-HCG) in CSF were detected by enzyme-linked immunosorbent assay. OSPF, a multi-step machine learning method consists of four popular algorithms: orthogonal partial least-squares discriminant analysis, support vector machine recursive feature elimination, permutation test, and fold change, was

applied to identify diagnostic signatures for germinoma via nested cross validation. Multi-omics integration analysed dysregulated pathways in germinoma pathogenesis from transcriptome, metabolomic and genome-wide methylation profile. Meanwhile, the altered immune microenvironment analysed by CIBERSORT between germinoma and NGGCT.

Results: Using OSPF framework, 52 differential metabolites (DMs) were screened, and a combined 3-marker signature [N-Acetylaspartylglutamate (NAAG), dodecanoic acid (DAA)and β-HCG] were identified based on SVM classifier model. The 3-marker signature with the highest area under the receiver operating characteristic curve (AUC; 84%), sensitivity (95%) and specificity (68.8%) distinguished germinoma from non-iGCT, and high AUC (85.8%) distinguished germinoma from NGGCT. The concentration of top20 DMs in the different regions were exhibited. Of these, NAAG, n1-methyl-2-pyridone-5-carboxamide, adenine and l-glutamate showed significant changes in different regions. Survival analysis indicated that germinoma patients with high amounts of DAA presented with poor prognosis. Further multi-omics integration research regarding the different pathogenesis between germinoma and NGGCT found that germinoma had active nicotinate and nicotinamide metabolism, fewer immune-suppressing phenotype cells, and more anti-tumour immune cells.

Conclusions: A combination of two metabolites (NAAG, DAA) and β-HCG is proposed as a potential diagnostic signature for germinoma. Abnormal activation of nicotinamide metabolism and diverse immune microenvironments suggest a differential pathophysiologic mechanism for germinoma and NGGCT, providing new insights on potential therapeutic strategies for iGCTs.

Key words: germinoma; diagnostic signatures; differential metabolites; multi-omics integration; machine learning method

370. Romidepsin enhances the killing ability of NKG2D-CAR-T cells through enhanced expression of NKG2DL against ovarian cancer cells

Liang Wang*、lirui yu

Fujian Maternity and Child Health Hospital

Background： Upregulation of tumor cell targeting antigens and improvement in the cytotoxicity ofchimeric antigen receptor T cell (CAR-T) is expected to facilitate better treatment efficacy for solid tumors represented by ovarian cancer. Materials and Methods Killer cell lectin-like receptor subfamily K member 1 (NKG2D) ligands are the target antigen for ovarian cancer. NKG2D-CAR-T cells were constructed for NKG2D ligand on the ovarian cancer cell surface. We used flow cytometry to evaluate the expression of NKG2DL on SKOV3. Innovatively combined with Romidepsin to treat ovarian cancercell SKOV3, for evaluating the cell killing of this combined strategy, we verified the cytotoxicity of CART cells by LDH release test and determined the secretion of cytokines by ELISA. Results The results offlow cytometry showed effective activation of the NKG2D-CAR-T cells, and Romi depsin treatmentresulted in increased expression of NKG2DL on the surface of SKOV3. C ytotoxicity test showed that Romidepsin could enhance the killing ability of NKG2D-CAR-T cells against ovarian cancer cells by regulating their NKG2DL expression (P<0.05). The killing effects and secretion of IFN-γ increased synchronously (P<0.05). Levels of IL-2 and PFP were statistically significant at a low target ratio butPD-1 remained unaffected (P≥0.05). Conclusions Enhancing the expression of tumor target antigen could address the issue of poor application of CAR-T cells in solid tumors.

Key words: CAR-T cells, ovarian cancer, NKG2DL, Romidepsin, cytotoxicity

371. Reclassifying Early-Stage Colorectal Cancer into Two Subgroups with Different Overall Survival, Tumor Microenvironment, and Response to Immune Checkpoint Blockade Treatment

Xiangxiang Liu*、Shukui Wang

Nanjing First Hospital, Nanjing Medical University

Purpose: The traditional TNM staging system is often insufficient to differentiate the survival discrepancies of colorectal cancer (CRC) patients at early stages (TNM-I/II). Our study aimed to reclassify early-stage CRC patients into several subgroups with different prognoses and explore their suitable therapeutic methods.

Materials and methods: Single-cell RNA (scRNA) sequencing data, bulk RNA sequencing data, and clinicopathological information of CRC patients were enrolled from the TCGA and GEO databases. The tumor microenvironment of CRC tissues was accessed by the ESTIMATE algorithm. The prognostic genes were identified by Cox regression analysis. GO and KEGG analyses were conducted in the DAVID database. GSEA analysis was performed for annotation of the correlated gene sets.

Results: We successfully reclassified early-stage CRC patients into two subgroups and discovered that patients in cluster-2 underwent worse overall survival than those in cluster-1. GSEA analysis showed that immune-associated gene sets were positively enriched in cluster-2. Besides, the differentially expressed genes (DEGs) between cluster-1 and cluster-2 patients also participated in immune-related biological processes and signaling pathways. Moreover, we found that more immune cells infiltrated the microenvironment of cluster-2 patients compared to that of cluster-1 patients, such as Tregs and tumor-associated macrophages. ScRNA sequencing analysis uncovered that most of the enriched immune-associated signaling in cluster-2 patients was mainly attributed to these upregulated immune cells whose infiltration levels were also high in CRC tissues rather than in normal tissues. In addition, we demonstrated that the expression of immune checkpoint genes was significantly higher in cluster-2 patients compared to cluster-1 patients. ScRNA

sequencing analysis revealed that the infiltrated $CD8^+$T cells in CRC were naïve T cells and can be activated into effector T cells after immune checkpoint blockade (ICB) treatment.

Conclusion: Early-stage CRC patients can be divided into two subgroups, which have different overall survival rates, tumor microenvironment, and response to ICB therapy.

Key words: colorectal cancer, prognosis, bioinformatics analysis, tumor microenvironment

372. The oncomicroprotein MUCP1 promotes colorectal cancer progression by regulating lipid metabolism

Junjie Nie*、Shukui Wang

Nanjing First Hospital

Background: Long non-coding RNAs (lncRNAs) exercise critical roles in cancer development and progression. The purpose of this study is to identify aberrantly expressed lncRNAs in colorectal cancer (CRC) and provide new targets for CRC diagnosis and therapy.

Methods: Ribosome profiling sequencing (Ribo-seq) were performed to identify lncRNAs capable of binding to ribosomes, and from which LINC00969 was selected for elevated expression in CRC. Plasmids construct, Mass spectrometry, Immunofluorescence, Co-immunoprecipitation, and Western blot were used to verify lncRNA-encoded microprotein, and we named it MUCP1. Gain- and loss-of-function studies were performed to examine the biological roles of MUCP1 in CRC progression. RNA sequencing, qRT-PCR, Western blot and Cellular cholesterol levels assay were performed to analyze MUCP1-regulated downstream target genes and signaling pathways. Cell derived xenograft were used to analyze the effects of MUCP1 on CRC metastasis.

Results: LINC00969 was up-regulated in CRC tissues and its elevated levels were associated with distal metastasis and poor prognosis. Mechanistically, LINC00969 encoded a novel microprotein MUCP1 that directly interacted with SCD1 to facilitated cholesterol synthesis, and which led to the activation of MAPK signaling pathway. MUCP1 knockdown inhibited while overexpression promoted CRC cell migration and invasion. MUCP1 overexpression promoted CRC growth and metastasis in mouse tumor models.

Conclusions: MUCP1 is a new oncomicroprotein that has tumor promoting effect in CRC and it may serve as a potential prognostic biomarker and therapeutic target for CRC.

Key words: NcRNA; MUCP1; Invasion and metastasis; MAPK pathways; Lipid metabolism; CRC

373. Study on exosome mediated miR-1229 as metastasis markers of colorectal cancer and its mechanism

Huiling Sun*、Shukui Wang

Nanjing First Hospital, Nanjing Medical University

Background: Existing evidence has shown that miRNAs are involved in carcinogenesis and cancer progression through regulating the expression of their target genes, and that exosome-mediated miRNAs play an important role in cancer progression and metastasis, suggesting that miRNAs in exosomes may be potential biomarker in cancer.

Methods: To elucidate the role of miR-1229 in exosomes in CRC, we performed quantitative real-time PCR(qRT-PCR), western blot and immunohistochemical(IHC) assays, FISH, Transwell migration/invasion (with Matrigel) assays, in vitro scratch assay, luciferase reporter assay, Western blot and RT-qPCR analysis in vitro. In vivo, LoVo tumor-bearing mice and liver metastasis mice model were applied.

Results: Preliminary studies of our group observed that miR-1229 in exosomes was significantly downregulated in serum and tissue samples of colorectal cancer (CRC) with metastasis. As target genes of miR-1229, IGF2 and IGF2BP3 were markedly overexpressed in tissue samples of CRC metastasis, and promoted the proliferation, invasion and metastasis of cancer cells, indicating that exosome-mediated miR-1229 has a potential clinical value as a biomarker to predict CRC metastasis.In this research project, serum and tissue samples of CRC with or without metastasis is collected to investigate the value of exosome-mediated miR-1229, in the early diagnosis and prognosis of CRC metastasis; the regulation of IGF2/IGF2BP3 and downstream signaling pathway is investigated to determine the role of signaling pathway in vascular permeability,

proliferation, invasion and metastasis of cancer cells in vivo and in vitro; and the mechanisms underlying CRC metastasis is explored as well.

Conclusions: This study will provide clinicians with new insights on clinical diagnosis and the molecular pathogenesis of CRC metastasis.

Key words: colorectal cancer; exosome; miR-1229; metastasis; biomarker

374. H3K4me3-activated miR-1290 promotes the progression of CRC through KLF9/p53/MMP9 pathways

Jian Qin*、Shukui Wang

Nanjing First Hospital, Nanjing Medical University

Background: Colorectal cancer (CRC) ranks third in incidence and second in mortality among cancers worldwide. Emerging researches showed that microRNAs (miRNAs) play an important role in CRC progression. Here, we aimed to investigate the expression and regulatory mechanism of miR-1290 in CRC.

Materials and methods: All clinical samples were collected from Nanjing First Hosptial. RNA-sequencing, quantitative real-time PCR (qRT-PCR) and western blot were used to test gene expression. The effects of miR-1290 on CRC cell proliferation, migration, invasion, and apoptosis were measured by colony formation, EdU, wound healing assay, Transwell assays, flow cytometry, and animal experiments. The target of miR-1290 was identified through algorithm prediction and dual-luciferase reporter assay. Chromatin immunoprecipitation (ChIP) assay was implemented to validate the H3K4me3 level of miR-1290 promoter in CRC.

Results: miR-1290 is significantly overexpressed in CRC primary tissues and metastatic tissues compared to that in normal tissues, and up-regulated miR-1290 is correlated with poor overall survival (OS) of CRC patients. Functional experiments showed that miR-1290 can promote the proliferation, migration, invasion and inhibit apoptosis of CRC cells. Mechanistically, miR-1290 directly targets KLF9 and promotes the malignancy progression of CRC cells through regulating

MMP9 and p53 expression, subsequently. In addition, high H3K4me3 levels in miR-1290 promoter region activate its transcription in CRC.

Conclusions: In summary, our study demonstrated the expression and regulatory mechanism of miR-1290 in CRC which supports the notion that therapeutic targeting of miR-1290 may be a promising treatment approach for CRC patients.

Key words: miR-1290, colorectal cancer, KLF9, p53, MMP9

375. TBC1D3 induces TC-1 expression to promote human breast cancer cell metastasis

Yong Shen*[1,2]、Qingxia Xu[1,2]

1. Henan Cancer Hospital

2. 郑州大学附属肿瘤医院

Rationale: TBC1D3 can promote the migration of human breast cancer cells, but the molecular mechanism of breast cancer metastasis is not clear. The mechanism of TC-1 in the regulation of human breast cancer metastasis by oncogene TBC1D3 remains unknown.

Methods: We performed qRT-PCR and westen assays to investigate the role of TBC1D3 in promoting TC-1 expression and activating wnt/β-catenin signaling pathway. Transwell cell migration assay and wound healing assay were used to investigate the effect of TBC1D3 and TC-1 on the migration of human breast cancer cells. Immunohistochemical study was used to evaluate the role of TBC1D3 and TC-1 in metastasis and recurrence of breast cancer.

Results: TBC1D3 promoted the transcription and protein expression of TC-1 and promoted the migration of human breast cancer cells. TC-1 could also promote the metastasis of breast cancer. After knockdown TC-1, TBC1D3 could no longer promote the migration of human breast cancer cells. Both TBC1D3 and TC-1 could activate wnt/β-catenin signaling pathway. After using wnt/β-catenin signal inhibitor XAV-939, TBC1D3 could not activate wnt/β-catenin signaling pathway and could not promote the migration of human breast cancer cells. After knockdown TC-1, TBC1D3 could no longer activate wnt/β-catenin signaling pathway. Clinically, the higher the immunohistochemical scores of TBC1D3, TC-1 and β-catenin, the more likely breast cancer

patients were to metastasize. The 5-year recurrence rate of TBC1D3, TC-1 and β-catenin positive patients was also significantly higher than that of negative patients.

Conclusions: TBC1D3 promotes the migration of breast cancer cells by promoting the expression of TC-1 and activating wnt/β-catenin signaling pathway.

Key words: Breast cancer; TBC1D3; TC-1; β-catenin, Migration

376. Single-cell RNA sequencing of cancer patients reveals age-dependent tumour microenvironment alterations that facilitate response to immunotherapy

Xiaoqiang Zhu *[1,2]、Jie Hong[1]、Jason W.H. Wong[2]、Youwei Zhang[3]、Haoyan Chen[1]

1. Renji Hospital, School of Medicine, Shanghai JiaoTong University

2. 香港大学李嘉诚医学院

3. 徐州市中心医院

Background: Immunotherapy has revolutionized the cancer treatment. While cancer incidence increases with age and age-associated changes in immune function have been well characterized, the effect of age-related differences in immune populations on the efficacy of immunotherapy remains unknown.

Methods: We collected clinical data from 3544 patients treated with immune checkpoint blockade (ICB) at the pan-cancer level. Single-cell sequencing data from 191 samples with multiple cancer types were analyzed to illustrate the age-associated alterations of tumor microenvironment (TME) and linked them with ICB response. Animal models were utilized to compare the anti-PD1 treatment efficiency between young and aged mice.

Results: Older patients responded more efficiently to ICB treatment. Further Cox regression screening on age revealed that patients aged above 47 responded better and had longer progression-free survival (PFS) than younger counterparts. Older patients displayed lower burden of loss of heterozygosity (LOH) and copy number variation (CNV) but higher tumor mutation burden (TMB) and TCR clones. scRNA-seq analysis revealed the activated adaptive immune response in older patients, mainly reflected by increased proportions of dysfunctional T cells

marked by CXCL13 , LAYN and immune checkpoint molecules, and tumor-associated macrophages marked by SPP1, CX3CR1 and CCL13. This phenotype was confirmed in multiple cancer types and observed in ICB-responsive patients at single-cell resolution and supported by animal models. Spatial transcriptomic data revealed actual interactions between these T cells and TAMs with increased strength in older patients.

Conclusions: By performing systemic evaluation using large clinical cohorts and single-cell sequencing data, we revealed that older patients tended to be more responsive to ICB treatment and had longer PFS, addressing the importance of age when considering ICB treatment.

Key words: Single-cell sequencing, Cancers, Ageing, Immunotherapy, Tumor microenvironment

377. Detection of telomerase activity based on an enzyme-free dual DNA electrochemical sensor

Qingxia Xu*

Henan cancer hospital

Purpose: To explore that telomerase is a potential tumor biomarker.

Methods: An enzyme-free and isothermal fluorescence strategy, dual-3D DNA walker based on catalytic hairpin assembled DNAzyme (CHA-DNAzyme), for ultrasensitive detection of telomerase activity is described.

Results: Upon incubation with telomerase, the telomerase primer is elongated to form telomeric repeat sequences (TR). The elongated TR stochastically moves along the predesign track by continuous strand displacement reaction to assemble the intact DNAzyme (CHA walker). Then, the activated DNAzyme autonomously moves along the other track by hydrolyzing DNA hairpins to release fluorescent-labeled DNA fragments from AuNPs (DNAzyme walker). As a result, a large amount of fluorescence is recovered to analyze telomerase activity. The use of CHA walker and DNAzyme walker endows the sensing strategy with high sensitivity and signal transfer efficiency. The strategy exhibits a wide analytical range from 10 to 1000 HeLa cells mL^{-1} with a low detection limit of 7 cells mL^{-1}. The strategy not only can detect telomerase activity in different tumor cells, but also quantifies telomerase activity of cancer cells from accumulated

normal cells. In addition, the practicability of the strategy is validated by detecting telomerase activity in human serum.

Conclusion: The sensing method holds great potential for the clinical diagnosis of cancers.

Key words: Telomerase; Fluorescent; Three-dimensional DNA walker; Catalytic hairpin

378. Hsa_circ_0007990 promotes breast cancer progression via inhibiting YBX1 protein ubiquitination and degradation

Tao Xu*、Shukui Wang

General Clinical Research Center, Nanjing First Hospital, Nanjing Medical University

Objective: Breast cancer (BC) is the most common diagnosed malignant tumor and the leading cause of cancer in females worldwide. Although great advances in early detection and treatment strategy lead to the steadily declined mortality, recurrence and metastasis still occurred frequently and remained the major reasons for cancer deaths in BC patients. Circular RNA (circRNA) is generated by special alternative splicing, with the properties of stability, high conserved and tissue, temporal and disease specificity. Increasing evidence has demonstrated that circRNA exerts critical functions in cancer progression. However, the detailed biological functions and molecular mechanisms of circRNAs in BC remain far from understood. This study aimed to investigate the possible role of circRNA in the progression of BC.

Methods: Differentially expressed circRNAs in BC were filtered by integrating breast tumor-associated somatic CNV data and circRNA high-throughput sequencing. Aberrant hsa_circ_0007990 expression and its host gene copy number were detected in BC cell lines via qRT-PCR. The expression level of hsa_circ_0007990 in BC tissues was validated via situ hybridization (ISH). Sanger sequencing was used to identify the head-to-tail splicing site of hsa_circ_0007990. Loss- and gain-of-function experiments in vitro and in vivo were performed to explore the potential biological function of hsa_circ_0007990 in BC. The underlying mechanisms of hsa_circ_0007990 were investigated through MS2 RNA pull-down, mass spectrometry, RNA

immunoprecipitation, RNA fluorescence in situ hybridization and immunofluorescence experiments, chromatin immunoprecipitation and luciferase reporter assay.

Results: The levels of hsa_circ_0007990 were elevated in BC tissues and BC cell lines, which was partly due to host gene copy number gains. Functional assays showed that hsa_circ_0007990 promoted BC cells growth. Mechanistically, hsa_circ_0007990 could interact with YBX1 and stabilize its protein levels by preventing ubiquitin/proteasome-dependent protein degradation, thus enhancing the expression of cell cycle-associated gene E2F1. Rescue experiments suggested that hsa_circ_0007990 invoked BC progression through YBX1.

Conclusion: In general, our study demonstrated that hsa_circ_0007990 modulated the ubiquitination and degradation of YBX1 protein, and further regulated E2F1 expression to promote BC progression. We explored the possible function and molecular mechanism of hsa_circ_0007990 in BC and provided a novel candidate target for the treatment of BC.

Key words: circRNA, breast cancer, YBX1, ubiquitination

379. LncRNA MAFG-AS1 promotes proliferation and immune escape of breast cancer by interaction with EZH2

Bei Pan*、Shukui Wang

Nanjing First Hospital, Nanjing Medical University

Aim: Understanding the complicated mechanisms of lncRNAs in breast cancer (BC), one of the deadliest cancers worldwide, contributes to provide potential targets for BC to assist in diagnosis and treatment.

Methods: The expression of lncMAFG-AS1 in BC cell lines were detected by qRT-PCR and immunofluorescence. Fluorescence in situ hybridization (FISH) and Nucleocytoplasmic separation assay were utilized to probe the location of lncRNA in BC cells. Bioinformatics analysis for lncRNA expression in TCGA and GEO databases, correlation of the expression with cancer-related pathways and tumor immunity. Cell cycle and apoptosis-related genes as well as target genes of lncMAFG-AS1 expression were measured by western-blot. Clone formation, EdU,

flow cytometry, and nude mouse tumorigenesis assays were used to probe the function of lncMAFG-AS1 in breast cancer cells in vivo and in vitro. RNA pulldown and Chromatin immunoprecipitation (ChIP) were conducted to identify the specific binding of lncMAFG-AS1-EZH2 complex and the H3k27me3 modification of CDKN2A. $CD8^+$ T cells sorting and co-culture with tumor cells were used to detect the resistance of tumor cells to the damage ability of $CD8^+$ T cells.

Results: Analyzing the openly available microarray data from TCGA-BRCA, GSE54002 and GSE42568, MAFG-AS1 was found overexpressed in breast cancer tissues compared with normal mammary tissues. Additional, MAFG-AS1 was up-regulated in a panel of breast cancer cells compared with a normal mammary cell. Consistently, immunofluorescence staining results by constructing MAFG-AS1 probes on tissue microarrays containing 42 pairs of breast cancer tissues showed that MAFG-AS1 expression was significantly elevated in breast cancer tissues compared to the paracancerous ones.We found that proliferation ability of BC cells were suppressed when MAFG-AS1 was knocked down. EdU and clone formation assay demonstrated that loss of MAFG-AS1 could reduce the growth of breast cancer cells, whereas overexpressed MAFG-AS1 showed higher cell proliferation ability in breast cancer. Next, we observed Xenografts on the side of up-regulated MAFG-AS1 showed increased volume compared with that in the control side. These results suggested that MAFG-AS1 could promote breast cell growth both in vivo and vitro. Subsequently, GSEA analysis of the sequencing data showed that cycle-related gene sets were significantly enriched in response to MAFG-upregulated. Then, results of flow cytometry approved MAFG-AS1 knockdown suppressed the transition from G1 to S phase, whereas up-regulated MAFG-AS1 promoted cell cycle activity. Consistent with the data above, western bolt showed cell cycle related protein expression were reduced by si-MAFG-AS1.We next investigated the mechanisms underlying the effect of a MAFG-AS1 on breast cancer development. FISH and nuclear fractionation assay showed MAFG-AS1 located in both cell nucleus and cytoplasm. The significant association of MAFG-AS1 with the cell cycle inspired us to explore the mechanism of its regulation of the cell cycle. After analysis of differentially expressed genes of transcriptome sequencing, we focused on CDKN2A, a key cell cycle regulator, whose expression was significantly decreased after MAFG-AS1 knockdown. Moreover, we observed the expression of CDKN2A was negatively correlated with MAFG-AS1 both at mRNA and protein

level. CCk8 assay shown that si-CDKN2A abolished the inhibitory proliferation effects of MAFG-AS1 knockdown, which further verified by the EDU assay. Recently studies revealed that nuclear located lncRNAs can play a role in recruiting PRC2 to prevent transcription of target genes by catalyzing the trimethylation of H3K27. GSEA analysis were performed to verify the correlation between MAFG-AS1 and PRC2. Further, RNA pull down assay was conducted and the results of western blot showed MAFG-AS1-1 probe combined with EZH2 protein directly, indicating MAFG-AS1 was required for EZH2 effects. It is known that EZH2 plays pivotal functions in cell cycle via targeting tumor suppressor, and CDKN2A is thought to be one of the key targets. Accordingly, the results of ChIP-PCR shown that EZH2 and H3K27me3 were occupied at the CDKN2A promoter locus and the enrichment of EZH2 and H3K27me3 was reduced after MAFG-AS1 depletion. Then, we found loss-of-EZH2 inhibited the proliferation-promoting effects of MAFG-AS1 overexpression.We analyzed the BRCA-TCGA data and divided the patients into low and high immunity groups, and observed high MAFG-AS1 expression was associated with low immune infiltration in breast cancer patients (p<0.01). EZH2 has been reported to play an important regulatory role in the immune microenvironment of cancer, which mediates CXCL9/10 to suppress its expression, thereby turning the cancer from “hot” to “cold”. Since we have found that MAFG-AS1 can be involved in its regulation by binding to EZH2, qRT-PCR was utilized to assess CXCL9/10 expression and showed that overexpression of MAFG-AS1 resulted in an expressively decrease in CXCL9 but no significant change in CXCL10 expression, indicating that MAFG-AS1 was involved in the EZH2-CXCL9 regulatory pathway. Subsequently, we co-cultured T47D cells with normal human CD8+T cells. The CXCL9/10 of the culture medium were detected by ELISA, and the results showed that overexpression of MAFG-AS1 lead to increased CXCL9 secretion with or without co-culture with CD8+T. Meanwhile, we performed crystalline violet staining and PI staining on the co-cultured cells, and it was seen that upregulated MAFG-AS1 resulted in increased resistance of damaged effect of CD8+T cells and a decreased proportion of apoptotic breast cancer cells. Similarly, IF with constructing MAFG-AS1 and CD8 probes on breast cancer tissue microarrays showed that MAFG-AS1 was significantly correlated with expression of CD8. Collectively lncMAFG-AS1 participated the EZH2-mediated CXCL9 level repression to inhibit immune infiltration.

Conclusions: Our data highlighted that aberrant lncMAFG-AS1 level affected tumorigenesis and correlates with immune infiltration of BC, suggesting that it might be a potential target for BC.

Key words: Breast cancer, lncRNA, Immune, EZH2

380. P3H1 as a novel prognostic biomarker correlates with immune infiltrate: a pan-cancer analysis

Changmeng Wu*

Laboratory Medicine Center, Peking University Shenzhen Hospital, Guangdong 518000, China.

Prolyl 3-hydroxylase 1(P3H1) is a member of the collagen prolyl hydroxylase family that plays an important part in the development and progression of tumors. However, its prognostic value and the correlation of P3H1 expression and tumor immunity in some cancer remain unclear. In general, we found that P3H1 was abnormally overexpressed in multiply tumors and distinct associations exist between P3H1 expression and prognosis of tumor patients by analysis online data. Moreover, we identified a strong correlation between P3H1 expression and immune checkpoint gene expression in diverse cancers. We observed that P3H1 expression was highly associated with immune-infiltrated tumor microenvironment in top 5 cancer types. Remarkably, a positive correlation between P3H1 expression and tumor mutation burden and neoantigen in colon adenocarcinoma (COAD) was observed. Furthermore, P3H1 was involved in the extracellular matrix organization and immune-related pathways in COAD. Finally, drug sensitivity analysis revealed that high P3H1 group has higher sensitivity in diverse drugs for the therapy of COAD compared to low P3H1 group. Our study provides a comprehensive insight for revealing the significant role of P3H1 in the survival, RNA modification, tumor immune, microenvironment of human cancers, and anticancer drug sensitivity analysis of COAD.

Key words: P3H1; COAD; immune infiltrate

381. Comprehensive analysis of serum and gastric juice bile acid profiles and gastric microorganisms in patients with different stages of gastritis-cancer transformation process

Luyao Zhang*[1,2]、Na Wang[1]、Xiaodong Qu[1]、Xingyu Zhao[1]、Qiang Dong[1]、Jiangyi Zhu[1]、yan Nie[1]、Yongquan Shi[1]

1. Xijing Hospital, Air Force Medical University,

2. 安徽医科大学第一附属医院

Objective: Serum and gastric juice bile acid concentrations and gastric microorganisms have been demonstrated to be closely related to the development of gastric cancer, but the specific bile acids and bacteria (other than H. pylori) that play a key role remain elusive.Here, we attempted to systematically characterize the serum and gastric juice bile acid profiles and the linkage between bile acids and gastric microorganisms in patients with different stages of gastritis cancer transformation.

Methods: A total of 73 patients (including 19 with chronic gastritis, 22 with intestinal metaplasia, 11 with dysplasia, and 22 with gastric cancer) were enrolled in the study. Patients with chronic gastritis were used as controls to compare bile acid profiles and gastric microorganisms between groups, to screen for between-group differences, and to look for associations between bile acids and microorganisms.

Results: The serum LCA-3S, isoalloLCA, TLCA-3S and NorDCA levels were significantly higher in the gastric cancer and precancerous lesions (intestinal metaplasia and dysplasia) compared to the chronic gastritis, while β-UDCA was significantly lower. A significant positive correlation was found between serum LCA-3S, isoalloLCA, GLCA-3S, GLCA, DCA-3S and NorDCA levels and the degree of disease. The process of gastritis-cancer transformation is accompanied by changes in the structure of the microbial community in the stomach. Campylobacter, Helicobacter pylori, s_Streptococcus and Olsenella were significantly enriched in gastric cancer, and Veillonellaceae, c_Negativicutes, f_Comamonadaceae and g_Prevotella were

enriched in precancerous lesions. And gastric microbial alterations correlated with changes in serum and gastric juice bile acid profiles.

Conclusion: High concentrations of DCA and LCA may be involved in the transformation of normal gastric cells to cancer cells, and gastric microbial dysbiosis may, together with bile acids, contribute to the inflammatory-cancerous progression of chronic gastritis.

Key words: bile acid profile; gastric microbiota; gastric precancerous lesion; chronic gastritis; intestinal metaplasia; dysplasia; gastric cancer

382. A Gene Expression Signature in Predicting Prognosis of Colorectal Cancer with Peritoneal Metastasis

Wenqing Xie*、Wanjun Liu、Qianxin Luo、Daici Chen

The Sixth Affiliated Hospital, Sun Yat-sen University

Background: Peritoneal metastasis (PM) is an advanced stage of colorectal cancer (CRC) and confers a poor prognosis. Preoperative diagnosis of PM is difficult, and the molecular mechanism is unclear, which has long been considered as an untreatable condition. Our analysis aimed to develop and validate that a new gene signature in predicting prognosis for improvement of personalized patient management.

Materials and methods: Our research performed whole transcriptome sequencing (RNA-seq) on 18 CRC specimens (9 patients with PM) and expanded the sample for label-free proteomic analysis on 33 CRC specimens (18 patients with PM). Quantitative real-time polymerase chain reaction (qRT-PCR) analysis and immunohistochemical (IHC) with an independent cohort of samples were performed to validate the microarray data. The overall survival (OS) of CRC patients was analyzed by Kaplan-Meier analysis.

Results: The entire microarray dataset was processed to identify differentially expressed genes (DEGs) in PM compared to none. 496 upregulated and 397 downregulated DEGs were common for proteomics and RNA-seq. Gene ontology (GO) analyses and Kyoto Encyclopedia of Genes and Genomes (KEGG) analyses were applied to analyze the function of genes after categorizing the DEGs. GO analysis contained mitochondrial translation and cell adhesion. The results of

KEGG analysis indicated that the pathway of complement and coagulation cascades and protein digestion and absorption were closely associated with the genes regardless of whether they were identified by the proteomic or RNA-seq analysis. The qRT-PCR analysis showed that the gene expression for MCCC2, MIF, ABCC1 and ORMDL1 was elevated. Importantly, MCCC2, ABCC1, and ORMDL1 were consistent with the results in the microarray dataset. In contrast, USP47、MMP2、UCHL1、CD248 were downregulated as microarray dataset. The result of the IHC analysis indicated that MCCC2 and ORMDL1 were elevated in PM samples. Kaplan-Meier analysis showed that a high level of MCCC2 and ORMDL1 was correlated with favorable OS (*P*= *0.016*).

Conclusion: A gene signature including MCCC2 and ORMDL1 performed well for the detection of patients with PM, and may serve as biomarkers to predict favorable outcomes in CRC with PM.

Key words: Colorectal cancer; Peritoneal metastasis; Prognosis; MCCC2; ORMDL1

383. Identification of the lipid metabolism related molecular subtypes and construction of a prognostic model in the Triple negative breast cancer

Jun Yang*

Medical Oncology Department of Breast Tumors

Background: Triple negative breast cancer (TNBC) is a highly heterogeneous disease with a high tumor mutation burden, which represents the worst outcome among all the breast cancer subtypes. The disturbed lipid metabolism is an early event in the development of tumor, which is related with the tumor metastasis and treatment drug-resistance. Our study aims to identify a lipid metabolism signature to predict prognosis and immunotherapy responses of TNBC patients.

Methods: We systematically analyzed 743 lipid metabolism related genes (LMRGs) of 223 samples in TNBC from TCGA datasets and screened out prognostic genes by univariate Cox regression. Unsupervised clustering was performed to stratify TNBC patients into different lipid metabolism patterns with distinct clinical characteristics. Lasso regression analyses and

multivariate Cox regression were used to identify prognostic LMRGs. A lipid metabolism related risk model was constructed with 6 prognositc LMRGs and was validated in GSE135565.

Results: In our results, TNBC patients were stratified into 3 distinct clusters with LMRGs. Cluster 2 patients had the worst survival outcomes and Cluster 3 patients had the highest TMB and the lowest infiltrating immune cells. We also identified and validated a prognostic risk model based on six genes including ELOVL1, HSD11B2, ELOVL3, SLC27A2, SUMO2 and ARV1. The Risk-Score was demonstrated as a significant factor for prognosis, which was independent of clinical tumor-node-metastasis (TNM) stage. The Risk-Score was negatively correlated with infiltration levels of most immune cells, especially type 2 T helper cell and activated CD4 T cell. In addition, patients with lower Risk-Score had higher immune checkpoint genes (PD-1, PD-L1, PD-L2 and LAG3) expression and showed better efficacy from immunotherapy.

Conclusion: Our work elucidated the relevance of lipid metabolism genes and TNBC patient's prognosis. The risk model might be a promising tool for predicting prognosis and guiding personalized treatment for TNBC patients.

Key words: Triple negative breast cancer, lipid metabolism, molecular subtype, prognostic model, tumor microenvironment

384. CXCR6 expression associated with checkpoint immunotherapy response in cutaneous melanoma

Zhengyun Zou、Xinyu Su*

Affiliated Drum Tower Hospital, Medical School of Nanjing University

Objective: To investigate the role of C-X-C motif chemokine receptor (CXCR6) in predicting immune checkpoint therapy response in cutaneous melanoma.

Methods: The expression of CXCR6 and its relationship with prognosis were analyzed in Skin Cutaneous Melanoma (SKCM). Then, correlations between CXCR6 expression and PDCD1/CD274 expression, immunocyte infiltration level and glycolytic activity level in SKCM were presented based on TCGA database. Finally, the role of CXCR6 in tumor microenvironment (TME) was clarified by utilizing the single cell transcriptome data of SKCM.

Results: The expression of CXCR6 gene in primary and metastatic tumor tissues was significantly higher than that in normal skin tissue (both p<2.22*10-22), and higher CXCR6 expression in SKCM samples got a better survival than lower expression samples (p= 3.59*10-5, HR= 0.748). CXCR6 expression was significantly positively correlated with both PDCD1 and CD274 expression in SKCM by utilizing TIMER2.0 tumor dataset, respectively. Higher CXCR6 expression was associated with higher immune score and stromal score in SKCM samples by utilizing ESTIMATE algorithm. CXCR6 expression was positively correlated with the infiltration level of immunocytes in $CD8^+$ T cells, memory activated $CD4^+$ T cells and M1 macrophages while it was reversed in memory resting $CD4^+$ T cells and M2 macrophages by utilizing CIBERSORT algorithm. Glycolysis-associated gene sets, HALLMARKER_GLYCOLYSIS, REACTOME_GLYCOLYSIS and WP_GLYCOLYSIS_AND_GLUCONEOGENESIS, were enriched in patients with lower CXCR6 expression by utilizing GSEA analysis. Based on the single cell transcriptome data of SKCM (GSE72056), we found that CXCR6 was obviously expressed in $CD8^+$ T cells while its ligand, CXCL16, was in macrophages. Utilizing CellphoneDB function, we found intense cell-to-cell interaction among $CD8^+$ T cells and macrophages via CXCR6-CXCL16 chemokine axis. Utilizing irGSEA and scMetabolism functions, we found that the given high inflammation level indicators and the low glycolysis level indicators both congregated in areas marked as $CD8^+$ $CXCR6^+$ T cells on UMAP plot.

Conclusion: CXCR6 could serve as a predictor to immunotherapy response and a target to improve the efficacy of ACT in SKCM, and its preliminary mechanisms by exploring the effects of CXCR6/CXCL16 chemokine axis on the landscape of TME in SKCM enhanced the feasibility of the above conclusion.

Key words: CXCR6； cutaneous melanoma； immunotherapy

385. Inactivation of epithelial sodium ion channel molecules serves as effectively diagnostic biomarkers in clear cell renal cell carcinoma

Yao Wei*、Qian Zheng、Yifang Wang、Ran Zhao、Xiaoying Zhou

Guangxi Medical University

Background: Non-voltage-gated sodium channel, also known as the epithelial sodium channel (ENaC), formed by heteromeric complexes consisting of SCNN1A, SCNN1B, and SCNN1G, is responsible for maintaining sodium ion and body fluid homeostasis in epithelial cells. However, no systematic study of SCNN1 family members were conducted in renal clear cell carcinoma (ccRCC) to date.

Methods: The transcription and protein expression levels of SCNN1 family members in ccRCC were analyzed based on the TCGA database, and were confirmed by quantitative RT-PCR and immunohistochemical staining assays, respectively. The area under curve (AUC) assay was used to evaluate the prognostic value of SCNN1 family members as a classification of ccRCC patients. CCK8, scratch, and transwell assays were applied to access the proliferation, migratory and invasive capacity of ccRCC cells.

Results: The expression of SCNN1 family members was significantly downregulated in ccRCC compared with normal kidney tissues, which might be due to the DNA hypermethylation. It is worth noting that the areas under curve of SCNN1A, SCNN1B, and SCNN1G were 0.965, 0.979, and 0.988 based on the TCGA database ($p<0.0001$), respectively. The diagnostic value was even higher when combing these three members together (AUC=0.997, $p<0.0001$). have high diagnostic values for ccRCC independently. Intriguingly, the mRNA level of SCNN1A was lower in the patients with advanced pathological stages, while SCNN1B and SCNN1G were increased with the progression of ccRCC, and remarkably associated with a worse outcome for patients. To our surprise, ectopic overexpression of the SCNN1 family members independently promoted the proliferation of ccRCC cell line 786-O. The migratory capacity was suppressed by SCNN1A but increased by SCNN1G.

Conclusion: The aberrantly decreased expression of SCNN1 family members could serve as valuable biomarkers for the diagnosis of ccRCC. But their biological role in ccRCC is inconsistent.

Key words: clear cell renal cell carcinoma; epithelial sodium channel; hypermethylation; diagnostic biomarker.

386. Different onset patterns of acral melanoma: clinicopathological features and potential molecular mechanisms

Zhengyun Zou*[1]、Rong Huang[1]、Mengke Zhao[2]、Jiayu Wang[3]、Kelin Zheng[3]、Xinyu Su[1]、Lanqun Qin[4]、 Yirong Wu[1]

1. Nanjing Drum Tower Hospital, the Affiliated Hospital of Nanjing University Medical School

2. Nanjing Drum Tower Hospital Clinical College of Nanjing Medical University

3. Nanjing Drum Tower Hospital Clinical College of Nanjing University of Chinese Medicine

4. The Affiliated Changzhou No. 2 People's Hospital of Nanjing Medical University

Objectives : To analyse different onset patterns of acral melanoma in Chinese population, focusing on the role of trauma in the formation and development of acral melanoma.

Methods: 303 consecutive patients with acral melanoma were retrospectively collected at Nanjing Drum Tower Hospital, the Affiliated Hospital of Nanjing University Medical School and the corresponding clinical classification was proposed. According to the different onset characteristics, we divided these 303 patients into four types: type 1: trauma type or nevus-free type, whose lesions became malignant because of the formation of pigmented nevi or repeated ulceration after trauma; type 2: pigmented nevus type, whose lesions may progress from congenital or acquired pigmented nevi without any trauma, and were never broken; type 3: pigmented nevi with trauma, in which patients suffered from ulceration or bleeding resulted from trauma in the presence of pigmented nevi; type 4: pigmented nevi with natural ulceration, in which patients suffered from ulceration naturally without trauma in the presence of pigmented nevi. There were 47, 56, 84, and 116 patients in the four types, respectively. In addition, we analyzed the clinicopathological

features, genetic aberrations and tumor immune microenvironment of patients with different onset patterns.

Results: Our study found that traumatic events accounted for a large proportion of acral melanoma in China, with type1 and type 3 accounting for 15.5% and 28.3%, respectively. In general, type 2 showed the best pathologically biological behavior, with the lowest rate of nodular melanoma subtype, significantly lowest Ki67 positive rate, highest ulcer-free rate, earliest T stages and lowest rate of lymph node metastasis. The histological subtype of type1 was mainly nodular melanoma with advanced T stages. In these 105 patients, the top ten altered genes (including somatic mutations and copy number variations) were CCND1, KIT, NRAS, RB1, CDK4, FGF19, BRAF, NF1, MDM2 and CRKL. The copy number variations of CCND1, RB1, FGF19, and IL7R and mutations of ARID2 were more common, while the copy number variations of CDK4 and TERT were less frequent in acral melanoma with trauma history. Meanwhile, type 2 patients had the lowest incidence of the copy number variations of CCDN1 and RB1, while posssessed the highest copy number variations of CDK4. In type 1 patients, the mutation rate of BRAF was markedly lower than the overall level (0%, 0 of 15), while the mutation rate of NRAS was far higher (26.7%, 4 of 15). In type 2 patients, BRAF mutation rate was the highest (28.6%, 4 of 14), while NRAS was the lowest (7.1%, 1 of 14). Tumor mutation burden was generally low in acral melanoma. Especially, patients with trauma history (type 1 and type 3) had significantly high tumor mutation burden than those without any traumatic factors (type 2) (p= 0.021). The overall level of immune infiltration was low in acral melanoma microenvironment. Specifically, patients in type 1 had the highest proportion of M2 macrophages in the invasive margin and showed an immunosuppressive microenvironment. Type 2 patients had the lowest proportion of NK cells in the tumor center.

Conclusions: This study summaries a new clinical classification of Chinese acral melanoma and provides a possible microscopic rationale for the potential association between trauma and acral melanoma.

Key words: Acral melanoma; clinical classification; trauma; potential molecular mechanisms

387. NBS1 Interacts with CyclinB to Modulate Drug Sensitivity of Olaparib in Ovarian Cancer

Ailing Zhong*、Renquan Lu、Lin Guo

Fudan University Shanghai Cancer Center

Dysfunction of the DNA repair pathway contributes to tumorigenesis and drug resistance. NBS1 is a key molecular involved in homologous recombination (HR) repair after DNA double-strand damage. MRN plays a crucial role in DNA replication, repair and transcription, which is also important for maintaining the secondary structure of DNA; therefore, their activity must be precisely controlled to ensure genome stability. We previously described that NBS1 expression was significantly correlated with CyclinB expression based on protein microarray analysis. CyclinB is a cell-cycle regulatory protein that has been shown to be involved in the activation of DNA damage repair checkpoints by inducing G2/M phase arrest, promoting apoptosis, and participating in the regulation of chemotherapeutic drug sensitivity by inducing nuclear degradation, as shown by immunofluorescence assays. In this study, NBS1-downregulated cells were generated using lentivirus-mediated RNAi. Using a qPCR-based HR assay kit to detected HR efficiency. The sensitivity of NBS1 to olaparib was investigated by cell proliferation, colony formation assays and flow cytometry. Our results demonstrated that the inhibition of NBS1 expression activated the CyclinB signaling pathways and sensitized ovarian cancer to X-ray and Olaparib treatment both in vitro and in vivo. NBS1 may be a potential therapeutic target for epithelial ovarian cancer (EOC).

Key words: NBS1, CyclinB, Olaparib, DNA damage repair, EOC

388. SLC22A3 methylation-mediated gene silencing predicts adverse prognosis in acute myeloid leukemia

Yu Gu*、Zijun Xu、Jingdong Zhou、Jun Qian

Affiliated People's Hospital of Jiangsu University

Background: We screened out several hypermethylated solute carrier (SLC) family genes in acute myeloid leukemia (AML) by reduced representation bisulfite sequencing (RRBS). SLC22A3 encodes an organic cation transport protein, which is critical for drug transportation and cellular detoxification. SLC22A3 is significantly downregulated and associated with tumor progression and worse prognosis in a variety of solid tumors. However, there are no data available regarding the role of SLC22A in AML. This study aimed to explore the regulatory mechanism of DNA methylation on SLC22A3 expression, as well as its clinical significance in AML prognosis.

Methods and Results: SLC22A3 was identified as the sole prognosis-associated gene among SLCs based on TCGA and Beat AML databases. Bone marrow mononuclear cells (BMMNCs) from AML, MDS patients and healthy donors were enrolled in this study. SLC22A3 methylation was significantly increased in AML compared with controls and MDS patients, and meanwhile the expression level of SLC22A3 was decreased. SLC22A3 hypermethylation presented obvious association with some specific clinical characteristics and affected survival time of AML patients as an independent risk indicator. SLC22A3 expression changed regularly as the disease complete remissions and relapses. Demethylation drug 5-aza-2'-deoxycytidine (DAC) activated transcription and increased mRNA expression of SLC22A3 in leukemia cell lines and AML fresh BMMNCs. Knockdown of SLC22A3 in leukemia cells enhanced cell proliferation and suppressed cell apoptosis. Data from public programs were used for auxiliary screening of probable molecular mechanisms of SLC22A3 in antileukemia effect.

Conclusions: Our results showed that increased methylation and decreased expression of SLC22A3 may be indicators of poor prognosis in AML. Methylation-silenced SLC22A3 expression may have potential guiding significance on anti-leukemia effect of DAC.

Key words: acute myeloid leukemia, methylation, SLC22A3, 5-aza-2'-deoxycytidine

389. MUC20 as a novel prognostic biomarker in ccRCC correlating with tumor immune microenvironment modulation

Bo Xue*[1,2]、Dognwen Wang[1,2]

1. Shanxi Medical University； National Cancer Center/National Clinical Research Center for Cancer/Cancer Hospital & Shenzhen Hospital，Chinese Academy of Medical Sciences and Peking Union Medical College

2. 中国医学科学院肿瘤医院深圳医院

Tumor microenvironment (TME) broadly participates in genesis development of clear cell renal cell carcinoma (ccRCC). To recognize the immune and stromal modulation in TME, we screened the differentially expressed TME-related genes generated by the ESTIMATE algorithm in ccRCC specimens. Following the construction of protein interaction (PPI) network and univariate COX regression, mucin 20 (MUC20) was judged to be a predictive factor. Further analysis, including immunohistochemistry (IHC) showed that MUC20 was positively correlated with survival and negatively correlated with the clinicopathologic characteristics (grade, clinical and TNM stages) in ccRCC patients. Gene Set Enrichment Analysis suggested that the low-expression MUC20 group was primarily enriched in immune-related activities, inflammation and epithelial-mesenchymal transition. Based on the CIBERSORT analysis for tumor-infiltrating immune cells (TICs), MUC20 was positively correlated with CD8+ T cells and resting mast cells and negatively correlated with activated CD4+ memory T cells, Treg cells, and plasma cells, implying that MUC20 may contribute to immune component in TME. Additionally, the patients with low MUC20 expression had better response to immune checkpoint blockades (ICBs) and 17 potential anticancer drugs were screened regarding calculating IC50 value. Thus, MUC20 may contain a value of prognosis assessment for ccRCC patients and indicate the immune modulation status of TME, which provided a novel insight for comprehensive immunotherapy.

Key words: Mucin 20, ccRCC, prognostic biomarker, TME, tumor-infiltrating immune cell

390. Developing an m5C regulator–mediated RNA methylation modification signature to predict prognosis and immunotherapy efficacy in rectal cancer

Rixin Zhang*、Min Yang

Institute of Materia Medica, CAMS & PUMC

Rationale: Cancer immunotherapy based on immune checkpoint inhibitors (ICI) has emerged as an evolutionary approach for various tumor types. Despite a great success in advanced colorectal cancer (CRC), only a small fraction of cases could respond to ICI treatment. Therefore, there is an urgent need to identify effective biomarkers to determine the responsiveness to ICI treatment. Recently, aberrant 5-methylcytosine (m5C) RNA modification has emerged as a key player in the pathogenesis of cancer involving tumorigenesis, metastasis, as well as drug resistance and relapse. Nonetheless, potential clinical significance of m5C RNA methylation regulators in CRC remains elusive. Here, we aim to explore the predictive signature based on m5C regulators-related genes for characterizing the immune landscapes, predicting the prognosis and response to therapies.

Methods: RNA-sequence data of CRC samples from The Cancer Genome Atlas (TCGA) were used as the training set, while the RNA data from Gene Expression Omnibus (GEO) data sets and immunohistochemistry (IHC) data from tissue microarray (TMA) were used for validation. We evaluated the prognostic values of these m5C regulators-related genes in patients with CRC by univariate Cox analysis, and eventually obtained a novel signature based on three m5C regulators-related genes in patients with rectal adenocarcinoma (READ) using a least absolute shrinkage and selection operator (LASSO)-Cox regression analysis. Furthermore, we systematically identified the correlation between the three-gene signature risk model and clinical data, altered pathways, mutational features, tumor immune microenvironment, immunotherapy efficiency, and potential applicable drugs. Moreover, the m5C RNA methylation-associated molecular pattern was constructed by unsupervised clustering analysis, which was defined as cluster-1, and -2.

Result: A novel m5C regulators–based signature (DNMT1, NSUN4, and NSUN7) in READ was initially constructed that classified cases into the high- and low-risk subgroups. Our results

demonstrated that READ patients in the low-risk subgroup were associated with prolonged survival in the training set and different validation cohorts. Notably, the signature was an independent prognostic factor, which exhibited more powerful survival prediction compared to conventional clinicopathological features. To facilitate the clinical viability of the m5C regulators–based signature, a highly reliable scoring nomogram was created. The comprehensive results revealed that the low-risk patients showed a greater degree of immune cell infiltration, stronger immunoreactivity phenotype, higher expression of immune stimulators, increased tumor burden mutation, and superior response to ICI therapy. However, the high-risk patients showed enriched pathways of cancer hallmarks and oncogenic signaling, presented lower immune cell infiltration, immune-suppressive state as well as decreased neoantigen load, which demonstrated a more insensitive to immunotherapy. In line with the clinical characteristics of the low-risk group, cluster-2 exhibited a relatively hot immune microenvironment and better immunotherapeutic response. Additionally, the m5C regulators–based signature markedly correlated with drug susceptibility.

Conclusions: We conducted the first and most comprehensive m5C RNA methylation regulators landscape analysis of patients with READ and developed a reliable m5C regulators–based risk model to predict the prognosis, clarify the molecular and tumor microenvironment (TME) status, and identify patients who will benefit from immunotherapy or chemotherapy. Our study could provide vital guidance to improve prognostic stratification and optimize personalized therapeutic strategies for patients with READ.

Key words: Rectal cancer, m5C RNA methylation regulators, prognosis, tumor immune microenvironment, immunotherapy

391. Proteomic identification of novel small extracellular vesicle protein biomarkers for prostate cancer diagnosis and risk stratification

Bairen Pang*[1,2,3,4]、Cheng Zhou[2,3,5]、Meng Han[1,2,3]、Qi Wang[1,2,4]、Jie Gong[1,2,3]、Rui Su[2,3]、Jiukai Jin[2,3]、Yingzhi Chen[2,3]、Zejun Yan[1,2,3]、Zhaohui Jiang[2,3]、Zhong Zheng[2,3]、Tianli Fan[6]、Yong Li[4]、Junhui Jiang[1,2,3]

1. Ningbo First Hospital

2. Ningbo Clinical Research Centre for Urological Disease, Ningbo 315600, Zhejiang, China.

3. Department of Urology, Ningbo First Hospital, The Affiliated Hospital of Ningbo University, Ningbo 315600, Zhejiang, China

4. St George and Sutherland Clinical Campuses, School of Clinical Medicine, University of New South Wales, Sydney 2052, NSW, Australia

5. School of Medicine, Zhejiang University, Hangzhou 310030, Zhejiang, China

6. Department of Pharmacology, School of Basic Medicine, Zhengzhou University, Zhengzhou 450001, Henan, China

Background: Accurate diagnosis and stratification of prostate cancer (PCa) prognostic risk group in clinic with the current standard of diagnostic biomarker, prostate specific antigen (PSA) is challenging. The current gold standard for PCa diagnosis, tissue biopsy has many side effects and requests high costs. Extracellular vesicles (EVs), as a new star of liquid biopsy for PCa diagnosis and monitoring progression, has attracted huge interest due to its potential to complement the inaccurate PSA screening and invasiveness of tissue biopsy. Liquid biopsy of EV biomarkers has many advantages over other approaches such as circulating tumour cells (CTC) or circulating tumour DNA (cfDNA), and holds promise for PCa precision medicine.

Objectives: Our objective in this study was to discover novel small EV (sEV) protein biomarkers in a panel of PCa cell lines using proteomics, and then validate these identified potential markers in sEVs of plasma and urine samples from PCa patients for predicting the presence of “clinically significant cancer” and the prognostic risk group.

Methods: In this study, primary PCa cell line (22Rv1), metastatic PCa cell lines (PC-3, DU145 and LNCaP), and a normal prostate epithelial cell line (RWPE-1) were used to isolate sEVs and the isolated sEVs were further confirmed by nanoparticle tracking analysis (NTA), transmission electron microscopy (TEM) and western blot. sEVs (n=3) from different PCa cell lines were analysed with label-free LC-MS/MS proteomics and the identified potential biomarkers are being validated in EVs of plasma and urine from different stages of PCa patients using parallel reaction monitoring (PRM) targeted proteomics and Western botting.

Results: The isolated sEVs from different PCa cell lines and a normal prostate epithelial cell line were confirmed by NTA, TEM and Western blot. We identified total 20 new protein sEV biomarkers from PCa cell lines such as DNAJA1, Histone H4, et al, which have never been reported in PCa EVs. These sEV markers are associated with cancer invasion, migration, regulation, microenvironment and metastasis. Our preliminary validation in both cell lines and clinical samples shows the unique expression patterns of 5 sEV markers within our identified protein panels are promising and demonstrate the potential for the value of diagnosis and prognosis. Targeted proteomics further confirmed sEV markers LAMB1 and Histone H4 diagnostic and prognostic value in human plasma and urine, respectively. The validation in a large set of plasma and urine samples from different stages of PCa patients is in progress in our laboratory.

Conclusion: We have identified a panel of promising novel sEV protein biomarkers from PCa cell lines and these potential candidates hold promise for PCa diagnosis and stratification of stages for PCa.

Key words: Extracellular vesicle, prostate cancer, proteomics, biomarker, liquid biopsy, diagnosis, prognosis

392. mitoSomatic: A tool for accurate identification of mitochondrial DNA somatic mutations without paired controls

Wenjie Guo、Yang Liu、Liping Su、Shanshan Guo、Xiaoying Ji、kaixiang Zhou、Xu Guo、Xiwen Gu、Jinliang Xing*

State Key Laboratory of Cancer Biology and Department of Physiology and Pathophysiology, Fourth Military Medical University, Xi'an, China.

Objective: Mitochondrial DNA (mtDNA) somatic mutations in cancer have drawn increasing attention. Currently, somatic mtDNA mutations in tumor were identified by next-generation sequencing (NGS) of paired tumor and control samples. However, recent profiling of mtDNA variations across different tissues has revealed the presence of mtDNA variants with uncertain germline or somatic origin. Furthermore, there are commonly encountered situations where matched control tissues are not available, thus complicating the identification of mtDNA somatic mutations in tumor. Recently, a few of bioinformatic tools, focusing specifically on nuclear DNA, have been developed to identify somatic mutations in tumor without matched normal controls. Nevertheless, these approaches are unsuitable for identifying mtDNA somatic mutations due to the specific characteristics of mtDNA. Therefore, a novel method for accurate identification of mtDNA somatic mutations in tumor in mtDNA NGS data is urgently needed, particularly in scenarios where matched control is not available.

Methods: In this study, the ground truth mtDNA variants orthogonally validated by triple-paired tumor, para-tumor, and blood samples were used to develop mitoSomatic. mitoSomatic is a machine learning tool for accurate identification of mtDNA somatic mutations in a specific tissue sample without control. First, ground truth somatic and germline mtDNA variants, generated by orthogonal validation of triple-paired samples, were split into three exclusive data sets: training, validation, and testing sets. As the optimal classification algorithm, the random forest model was then developed with the training set, with parameters fine-tuned by evaluating the performance with the validation set. Finally, mitoSomatic performance was evaluated by 6 testing sets. A

tab-formatted mtDNA variant table was used as the input file for the mitoSomatic package to report the variant type.

Results: In this study, ground truth somatic and germline mtDNA variants generated by orthogonal validation of paired tumor, para-tumor and peripheral blood mononuclear cell (PBMC) samples from 157 hepatocellular carcinoma (HCC), 24 colorectal carcinoma (CRC) and 18 renal cell cancer (RCC) patients in our laboratory were used to generate training, validation, and testing datasets to develop mitoSomatic. We demonstrated that mitoSomatic achieved area under the curve (AUC) values over 0.99 for identifying somatic mtDNA variants without paired control in three tumor types. In addition, mitoSomatic was also applicable in non-tumor tissues such as para-tumor and blood samples, suggesting the flexibility of mitoSomatic's classification capability. Furthermore, analysis of triple-paired samples identified a small group of variants with uncertain somatic/germline origin, whereas application of mitoSomatic significantly facilitated the prediction of their possible source. Finally, control-free evaluation of public pan-cancer NGS dataset with mitoSomatic revealed a substantial number of variants that were probably misclassified by conventional tumor-control comparison, further emphasizing the usefulness of mitoSomatic.

Conclusion: In the present study, a novel machine learning tool, mitoSomatic, was for the first time developed to accurately identify somatic and germline variants in mtDNA from various tumor tissues, with a unique advantage of being applicable even without paired controls. The remarkable performance of mitoSomatic was also extended to para-tumor tissues and PBMCs, indicating its generalized application. More importantly, this tool will greatly improve the accuracy of identifying somatic/germline origin of mtDNA variants, which can provide a better understanding of mtDNA mutational profiles.

Key words: mitochondrial DNA, somatic mutations, machine learning, next-generation sequencing

393. Mutational signature of mtDNA confers mechanistic insight into oxidative metabolism remodeling in colorectal cancer

Yang Liu*、Wenjie Guo、Fan Peng

Fourth Military Medical University

Background: Mitochondrial dysfunction caused by mitochondrial DNA (mtDNA) mutations and subsequent metabolic defects are closely involved in tumorigenesis and progression in a cancer-type specific manner. To date, mutational pattern of mtDNA somatic mutations in colorectal cancer (CRC) tissues and its clinical implication are still not completely clear.

Methods: In the present study, we generated a large mtDNA somatic mutation dataset from three CRC cohorts (432, 1,015 and 845 patients, respectively) and then most comprehensively characterized the CRC-specific evolutionary pattern and its clinical implication.

Findings: Our results showed that the mtDNA control region (mtCTR) with a high mutation density exhibited a distinct mutation spectrum characterizing a high enrichment of L-strand C > T mutations, which was contrary to the H-strand C > T mutational bias observed in the mtDNA coding region (mtCDR) (P<0.001). Further analysis clearly confirmed the relaxed evolutionary selection of mtCTR mutations, which was mainly characterized by similar distribution of HVS and non-HVS mutation density. Moreover, significant negative selection was identified in mutations of mtDNA complex V (ATP6/ATP8) and tRNA loop regions. Although our data showed that oxidative metabolism was commonly increased in CRC cells, mtDNA somatic mutations in CRC tissues were not closely associated with mitochondrial biogenesis, oxidative metabolism and clinical progression, suggesting a cancer-type specific relationship between mtDNA mutations and mitochondrial metabolic functions in CRC cells.

Interpretation: In conclusion, our study identified the CRC-specific evolutionary mode of mtDNA mutations, which is possibly matched to specific mitochondrial metabolic remodeling and confers new mechanic insight into CRC tumorigenesis.

Key words: mitochondrial DNA, somatic mutations, evolutionary selection, metabolic remodeling, colorectal cancer

394. Proteomic characteristics of gastric cancer related to Helicobacter pylori

Jiameng Sun*

Chinese Academy of Medical Sciences & Peking Union Medical College

Objective: This study will investigate the proteomic differences between *Helicobacter pylori* positive (Hp^+) and *Helicobacter pylori* negative (Hp^-) gastric cancer(GC).

Methods: Samples of tumor tissue and tissue adjacent to carcinoma from 1 Hp+ and 1 Hp- patient were collected. Three different sites were collected from each tissue sample. High-performance liquid chromatography-mass spectrometry (HPLC-MS) was used for proteomic analysis, and the differentially expressed proteins (DEPs) were screened by statistical analysis. Further bioinformatics functional analysis software was applied to identify key signaling pathways and related molecules.

Results: A total of 5536 proteins were identified in Hp+ and Hp- tumors and paracancerous tissues by LC-MS. Statistical analysis showed that proteins expression in different parts of Hp+ and Hp- tumors was significantly different, showing tumor heterogeneity, which was related to energy metabolism, cell proliferation and invasion, cell survival and death, immune response, virus infection and other functions.In gastric cancer, 1630 and 1843 proteins were significantly altered in tumor and paracancerous tissues, respectively (| fold change | ≥2) , and 764 differentially expressed proteins (| fold change | ≥2) were found in Hp+ and Hp- gastric cancer tumor tissues, which are associated with immune response, cell migration, cell proliferation and invasion, cell survival and death. In particular, DEPs associated with bacterial growth were found in both Hp+ and Hp- tumors.

Conclusion: Hp^+ and Hp^- gastric tumors exhibit tumor heterogeneity by proteome. There are significant differences in proteomic characteristics between gastric cancer tumors and adjacent, Hp-positive and Hp-negative tumors, which affect the body energy metabolism, immune response, cell proliferation and invasion, survival and death. Our study was to utilize proteomic analysis to provide new clues and ideas for the further study of gastric cancer.

Key words: Helicobacter pylori; Gastric cancer; proteome

395. Correlation between Immunohistochemical Markers Expression and Lymph Node Metastasis in Gastroenteropancreatic Neuroendocrine Neoplasms: A Nation-wide 10-year Retrospective Clinical Epidemiological Study in China

Huan Yang*、Jin-hu Fan

Cancer Hospital, Chinese Academy of Medical Sciences

Background: Previous research on the correlation between different pathological features and the development of gastroenteropancreatic neuroendocrine neoplasms (GEP-NENs) is rare in China.

Objective: To explore the correlation between immunohistochemical markers expression and lymph node metastasis in GEP-NENs.

Methods: In the seven regions of China, we conveniently selected at least one general hospital and one cancer hospital. All inpatient cases with confirmed pathology in the selected 23 hospitals were reviewed and patients' general information, clinical features and treatment information were collected based on the designed case report form (CRF).

Results: A total of 2010 GEP-NENs cases were included in this study. The most common primary sites for GEP-NENs were the pancreas (31.5%) and rectum (29.6%), followed by the cardia (11.6%) and body (15.4%) of stomach. The mean age of the patients at diagnosis was 51.7±14.0 years.The majority of pancreatic NENs (p-NENs) patients were female, while the number of male patients of gastric NENs (g-NENs) was significantly higher. Among patients with immunohistochemical biomarker test information, there was a significant difference in the positive rate of S-100 in patients without lymph node metastasis and with lymph node metastasis ($\chi2$=5.330, P=0.021). According to the stratification analysis of primary sites, lymph node metastasis in intestinal NENs was associated with the Choromogranin A and S-100 protein ($\chi2$=5.530, P=0.019; $\chi2$=6.518, P=0.011).

Conclusion: SD-100 protein expression may play a role in the diagnosis of GEP-NENs' lymph node metastasis, especially in intestinal neuroendocrine neoplasms. More studies on the

immunohistochemical commonality and heterogeneity of GEP-NENs are needed to improve diagnosis efficiencies.

Key words: Gastroenteropancreatic Neuroendocrine Neoplasms, Immunohistochemical Biomarker, Lymph Node Metastasis

396. GRAP2 as a Promising Predictor of Prognosis and Immunotherapy Response for Patients with Breast Cancer

Xin Meng*、Lin Guo、Renquan Lu

Fudan University Shanghai Cancer Center

Purpose： Growing evidence has supported the clinical implications of tumor microenvironment (TME) for predicting outcomes and immunotherapeutic efficacy. However, few molecular markers can characterize the immune profile reliably or predict the clinical prognosis due to the heterogeneity of breast cancer. Here, we explore new biomarkers essential for CD8+T cells recruitment and subsequent immunotherapeutic efficacy.

Methods： The ESTIMATE algorithm was applied to quantify the immune components and matrix components in 1109 breast cancer cases from TCGA database. The differentially expressed genes were sorted by the immune score and the stromal score. Univariate cox regression analysis and PPI network were used to identify key genes. After assessing their prognostic values, GRAP2 was found to be a predictive factor with results confirmed by immunohistochemistry analysis, tumor mutation analysis, correlation analysis with levels of CTLA-4 and PD-L1 and the extent of infiltrated CD8+T cell. Chemokine profiles showed a positive correlation of GRAP2 expression with antitumor-effect chemokines, (e.g. CXCL9, CXCL10 and CX3CL1). Results were confirmed by qPCR and ELISA analysis.

Results： We carried out a comprehensive analysis to uncover the role of GRAP2 in breast cancer using bioinformatics methods and experimental data. We found that GRAP2 was a favorable biomarker for improving cancer immunotherapy efficiency by chemokine secretion and CD8+T cells infiltration in the tumor environment.

Conclusions： Our findings emphasize the essential significance of GRAP2 for the prognostic value of breast cancer patients and highlight its potential to enhance therapeutic efficacy of ICB.

Key words： GRAP2, prognosis, immunotherapy, chemokine, CD8+T cell infiltration

397. Exploration of Reference Intervals for SCCA and CYFRA 211 levels in Southeast Chinese Population

Minglei Jiang*

Fudan University Shanghai Cancer Center

Background: Tumor makers are a promising method of cancer diagnostics. Appropriate reference interval is key in the clinical usage of tumor markers. We aimed to establish a reference interval of serum SCCA and CYFRA 21-1 for Chinese population.

Methods: One thousand subjects apparently health Chinese adults were recruited from 3 research sites. Electrochemiluminescence immunoassays (ECLIA) were used to measure the serum SCCA and CYFRA 21-1 levels.

Results: Reference intervals of serum SCCA and CYFRA 21-1 were not in agreement with those recommended by the manufacturers. The 95% reference interval is 0.553 to 3 ng/ml for SCCA and 1.06 to 4.93 ng/ml for CYFRA 211. The mean reference values of SCCA and CYFRA21-1 were statistically different according to gender (female, 1.38 ng/ml vs male, 1.15 ng/ml for SCCA, and female, 2.19 ng/ml vs male, 2.41 ng/ml for CYFRA21-1, respectively), and age (≥50 years, 1.09 ng/ml *vs.* <50 years, 1.31 ng/ml for SCCA, and ≥50 years, 2.47 ng/ml *vs.* <50 years, 2.15 ng/ml for CYFRA21-1,), respectively.

Conclusion: 3 ng/ml and 4.93 ng/ml are recommended as the upper limit for SCCA and CYFRA 21-1 in Southeast Chinese population, respectively.

Key words： Tumor makers

398. COPS5 conferred the platinum-resistance in epithelial ovarian cancer

Tianqing Yan *、Lin Guo、Renquan Lu

Fudan University Shanghai Cancer Center

Development of platinum resistance is one of the major causes of epithelial ovarian cancer (EOC) treatment failure. COP9 signalosome subunit 5 (COPS5) was found to take part in the progression of EOC in our previous study. Herein, we aim to uncover the potential utility of COPS5 in EOC chemoresistance. COPS5 levels were analyzed to define clinic pathologic correlates using a matched tissue microarray and online datasets. The effect of COPS5 inhibition by the lentivirus mediated short hairpin RNA on cell viability, proliferation and migration were accessed in vitro and in vivo. Results showed that COPS5 was upregulated in patients after platinum-resistance. Kaplan-Meier survival curves revealed that COPS5 overexpression was correlated with shorter PFS and OS. COPS5 downregulation inhibited the cell proliferation, migration, and reduced the sensitivity of EOC to platinum. Overall, our data indicated that COPS5 inhibition might represent a new therapeutic strategy for overcoming platinum-resistance in patients with EOC.

Key words： COP9 signalosome subunit 5, ovarian cancer, platinum-resistance

399. Effect of EGFR amplification on survival of patients with EGFR mutation-positive non-small cell lung cancer receiving first-line EGFR-TKIs treatment

Yiquan Xu*、Gen Lin

College of Clinical Medicine for Oncology, Fujian Medical University

Background: Non-small cell lung cancer (NSCLC) patients with Epidermal growth factor receptor (EGFR) mutation generally respond well to EGFR-tyrosine kinase inhibitors (EGFR-TKIs). However, the effect of EGFR amplification on the survival of patients with EGFR mutations receiving first-line EGFR-TKIs treatment remained unclear.

Methods: This multicenter, retrospective and real-world study included two cohorts that enrolled patients were histologically or cytologically confirmed with metastatic NSCLC, had EGFR mutation confirmed by NGS of tissue specimens and had first-line treatment with EGFR-TKI. The cohort 1 was used to detect the efficacy of EGFR amplification on patients carrying EGFR mutations, and the cohort 2 was used to compare the genomic features of those groups. Next-generation sequencing was performed to detect EGFR amplification of the enrolled patients. The molecular profile and outcomes between EGFR mutant NSCLC patients with or without EGFR amplification were evaluated.

Results: The cohort 1 enrolled 355 patients from 4 cancer centers between January 2013 to March 2022. No significant differences between the three groups, including Non-EGFR amplification and EGFR amplification, and the EGFR uncertain amplification in progression-free survival (10.0 months *vs.* 10.8 months *vs.* 9.9 months, p= 0.384). Furthermore, PFS was not significantly different in patients treated with first or third-generation EGFR TKIs between these three groups (p= 0.183 and p= 0.273, respectively). In addition, there were no differences in overall response rate between these three groups (63.16% *vs.* 74.07% *vs.* 54.55%, respectively, p= 0.056) as well as disease control rate (95.79% *vs.* 100% *vs.* 92.73%, p= 0.073). The cohort 2 included 10,087 patients of NSCLC, and the incidence of EGFR amplification in advanced EGFR mutant NSCLC patients is as low as 10%. There are gene mutations such as MYC, TP53 and alteration of cell cycle signaling pathway (p<0.05) were significantly associated with EGFR mutant patients with EGFR amplification than without.

Conclusions: EGFR amplification have no effect on efficacy of EGFR mutant patients treated with EGFR-TKI treatment, and may due to the concomitant genetic mutations of MYC and alteration of cell cycle signaling pathway.

Key words: Non-small cell lung cancer (NSCLC); Epidermal growth factor receptor; Gene amplification; Mutation; Efficacy

400. Systematic Analysis based on Publicly Available Databases Reveals IGF2BP3 as a Potential Pan-Cancer Biomarker for Prognosis and Response to Immunotherapy

Yating Wu*[1,2]、Zhongqiu Wu[3]、Zhuolin Li[1,2]、Huimin Niu[1,2]、Xiaofeng Lai[1,2]、Hu Zhao[4]、Meng Zhao[1,2]、Shenghang Zhang[1,2]、Shuiliang Wang[1,2]

1. Affiliated Dongfang Hospital （the 900th Hospital）of School of Medicine, Xiamen University

2. 福建医科大学附属福总临床医学院（第九〇〇医院）检验科

3. 福建医科大学附属福总临床医学院（第九〇〇医院）超声诊断科

4. 福建医科大学附属福总临床医学院（第九〇〇医院）普通外科

Background: Cumulative studies have increasingly demonstrated that IGF2BP3, an m6A "reader", plays important role in development and immunology of multiple types of cancer. To gain a landscape knowledge of IGF2BP3 in tumor biology, a systematic analysis based on publicly available databases was carried out in current study.

Methods: The expression of IGF2BP3 was explored with the TIMER, GEPIA, and BioGPS databases. The effect of IGF2BP3 on prognosis was analyzed via GEPIA and Kaplan-Meier plotter. The TISIDB database was used to determine IGF2BP3 expression in different immune and molecular subtypes of human cancers. The relationships between IGF2BP3 expression and tumor-infiltrated immune cells were analyzed via the TIMER databases. The correlations between IGF2BP3 expression and immune checkpoints (ICP), neoantigens (NEO), tumor mutational burden (TMB), microsatellite instability (MSI) and DNA mismatch repair genes (MMRs) in human cancers were analyzed via the SangerBox database. The genomic alterations of IGF2BP3 were investigated with the c-BioPortal database. IGF2BP3 co-expression networks were studied by the LinkedOmics database.

Results: Our results indicated that the expression of IGF2BP3 was higher in multiple human cancers than in paired normal tissue. IGF2BP3 expression was showed to strongly correlate with prognosis, ICP, NEO, TMB, and MSI in cancer. It was revealed that IGF2BP3 may play an

essential role in the tumor microenvironment (TME) and participate in immune regulation. Furthermore, IGF2BP3 co-expression networks were demonstrated to mainly participate in the regulation of adaptive immune response, T cell activation, and B cell activation.

Conclusion: Our systematic bioinformatic analysis reveals that IGF2BP3 may serve as a potential novel pan-cancer biomarker for prognosis and response to immunotherapy. It is strongly recommended to figure out the specific role of IGF2BP3 in certain cancer and its underlying molecular mechanism in the future.

Key words: IGF2BP3, pan-cancer biomarker, systematic bioinformatic analysis, cancer progression, prognosis, immunotherapy

401. A novel feedback regulated loop of circRRM2-IGF2BP1-MYC promotes breast cancer metastasis

Ran Hao*[1]、Lei Zhang[1]、Yipeng Wang[1]、Jie Hu[1]、Yixin Qi[2]

1. Hebei Medical University

2. The Fourth Hospital of Hebei Medical University

Background: Metastasis is the leading cause of mortality in patients with breast cancer (BC). Studies demonstrate that circular RNAs (circRNAs) were involved in BC progression, while the molecular mechanisms remain largely unclear.

Methods: The microArray circRNA profiles were used to explore the differential expression circRNAs in BC and paracancerous normal tissues, and the quantitative reverse transcription-polymerase chain reaction was used to validate their expression level in clinical samples and cell lines. Nuclear/cytosolic fractionation and fluorescence in situ hybridization (FISH) assays were performed to examine circRRM2 subcellular location. The scratch wound healing and transwell assays were conducted to evaluate the impact of circRRM2 on BC cell migration and invasion. We predicted miRNAs that might bind with cricRRM2 and the downstream target genes using bioinformatics analysis and explored their expression levels and prognostic value in BC. FISH, RNA immunoprecipitation, Co-immunoprecipitation, Western blot,

and rescue experiments were implemented to figure out circRRM2 function and underlying mechanisms in BC.

Results: The present study revealed several aberrant circRNAs in BC tissues and observed that circRRM2 was upregulated in tumor tissues of 40 patients with BC. High circRRM2 was significantly associated with advanced N stage in patients with BC. Gain- and loss- of function experiments revealed that circRRM2 promoted the migration and invasion of cells and functioned as an oncogene in BC. Mechanism studies showed that circRRM2 competed with miR-31-5p/miR-27-3p to upregulate the IGF2BP1 expression. Furthermore, IGF2BP1 upregulated the circRRM2 level via interacting with MYC, which functioned as the transcriptional factor of circRRM2. Thus, the positive feedback loop that is composed of circRRM2/IGF2BP1/MYC was identified.

Conclusions: This study confirms that upregulated circRRM2 functions an oncogenic role in BC metastasis. The positive feedback loop of circRRM2/IGF2BP1/MYC enforces the circRRM2 expression, which might offer a potential target for BC treatment.

Key words: circular RNA; breast cancer; metastasis; feedback loop; MYC

402. Single-cell characterization of macrophages in uveal melanoma uncovers a unique proliferative subset that confers a de novo subtype with a poor prognosis and aggressive behavior

Ke Li*、lanfang sun、wencan wu、jie sun、meng zhou

wenzhou medical university

Background: Uveal melanoma (UM) is the most common primary intraocular malignancy with high metastatic potential and a poor prognosis. Macrophages represent one of the most abundant infiltrating immune cells and exhibit diverse functions in cancers. However, the cell heterogeneity and functional diversity of macrophages in UM are yet to be fully elucidated.

Methods: The present study retrospectively analyzed single-cell RNA sequencing (scRNA-seq) data of 63,264 cells isolated from 11 UM samples, and deconstructed the different subsets of macrophages in UM. We then leveraged cell type-specific transcriptional signatures and single-sample gene set enrichment analysis to decompose cell type proportions in bulk RNA-seq data from the TCGA cohort and bulk microarray data from three GEO cohorts for clinical assessment on tumor behavior and prognosis. Bulk RNA-seq and immunohistochemistry (IHC) assays were carried out using the in-house cohort to validate the proposed subtyping scheme.

Results: Using the scRNA-seq analysis of macrophages, we identified a previously unrecognized, transcriptionally distinct subset of macrophages independent of the conventional M1/M2 dichotomy, termed Prol-MΦ, enriched for proliferation signaling. We demonstrated that the increased Prol-MΦ infiltration was associated with aggressive behaviors and worse survival outcomes in single-cell and bulk RNA-seq cohorts, which were further validated in multicenter microarray cohorts. A macrophage-based de novo subtyping scheme was proposed by integrating the transcriptional signatures of Prol-MΦ and machine learning to stratify patients into Prol-MΦ-enriched or Prol-MΦ-depleted subtypes with significantly different clinical outcomes, which was validated using public multicenter cohorts and a cohort from our institution via bulk RNA-seq and IHC assays.

Conclusions: This study uncovered a novel macrophage subset associated with aggressive behaviors and worse survival outcomes in UM tumors. Following further translational investigation, our findings may highlight a potential therapeutic strategy via targeting macrophage subsets to control the metastatic disease and consistently improve the outcome of patients with UM.

Key words: uveal melanoma, macrophages, single-cell RNA sequencing

403. ATOH1 modulates cancer stem cell properties and tumorigenesis through activation of GAS1 in gastric adenocarcinoma Running Head: ATOH1 Regulates Gastric Cancer Stemness

Xiaohui Zhong*[1,2]、Qing Zhong[3,4,5,6]、Hai-chun Chen[1,2]

1. School of PE and Sport Science, Fujian Normal University

2. Key Laboratory of sports function evaluation of General Administration of sports of the people's Republic of China

3. Department of Gastric Surgery, Fujian Medical University Union Hospital, Fuzhou, China

4. Department of General Surgery, Fujian Medical University Union Hospital, Fuzhou, China

5. Key Laboratory of Gastrointestinal Cancer (Fujian Medical University), Ministry of Education, Fuzhou, China

6. Fujian Key Laboratory of Tumor Microbiology, Department of Medical Microbiology, Fujian Medical University, Fuzhou, China

Objective: Gastric cancer stem cells (GCSCs) are considered tumor-initiating cells with self-renewal ability, which have high tumorigenicity and chemoresistance. Therefore, the vital to developing therapies is to determine the key factors of GCSCs. This study aimed to explore the role of atonal bHLH transcription factor 1 (ATOH1) in GCSC maintenance and its relevance to gastric cancer (GC) progression.

Methods: Bioinformatics analyses of local and public databases were applied to analyze ATOH1 expression, signaling pathways, and clinical significance. In vitro cell culture, spheroids, patient-derived organoids, and in vivo nude or Cre recombinase–mediated conditional preclinical mouse models were utilized. Molecular assays included ChIP-Seq, Co-IP, western blotting, qPCR, and immunocyto/histochemistry.

Results: ATOH1 was significantly downregulated in human GC and was closely related to chemotherapy resistance. DNMT1-mediated ATOH1 promotor hypermethylation leads to downregulation of ATOH1 in GC. By gene silencing and ectopic overexpression, we found that ATOH1 upregulated GAS1 transcriptional activity, with subsequent inhibition of the

RET/AKT/mTOR signaling axis.Functionally, ATOH1 overexpression impaired tumor spheroids and organoid formation. Furthermore, the overexpression of ATOH1 impaired tumor growth in gastric tumor xenograft mouse models. Conversely, conditional ATOH1 knockout conferred a significant reduction in the tumor burden of Tg(Tff1-CreERT2); APCfl/fl; p53fl/fl mice. Clinicopathological analysis indicated that abnormal overexpression of ATOH1 correlated with better prognosis and chemosensitivity in human GC.

Conclusion: We demonstrate that ATOH1 impacts GC progression by regulating GCSC properties, which could serve as a useful prognosis stratification marker for GC and provide personalized therapeutic approaches.

Key words: Gastric cancer, ATOH1, GAS1, cancer stem cell, mouse model

404. Characterization of Sialylation-Related Long Noncoding RNAs to Develop a Novel Signature for Predicting Prognosis, Immune Landscape, and Chemotherapy Response in Colorectal Cancer

Mingxuan Zhou*、Min Yang、YuFang Hou、Rixin Zhang、Weiqi Wang、Zheng Yan、Tiegang Li、Wenqiang Gan、Silin Lv、Zifan Zeng、fang Zhang

Institute of Materia Medica Chinese Academy of Medical Science

Background: Aberrant sialylation plays a key biological role in tumorigenesis and metastasis, including tumor cell survival and invasion, immune evasion, angiogenesis, and resistance to therapy. It has been proposed as a possible cancer biomarker and a potential therapeutic target against tumors. Nevertheless, the prognostic significance and biological features of sialylation-related long noncoding RNAs (lncRNAs) in colorectal cancer (CRC) remain unclear. This study aimed to develop a novel sialylation-related lncRNA signature to accurately evaluate the prognosis of patients with CRC and explore its potential molecular mechanism.

Methods: We identified sialylation-related lncRNAs using the Pearson correlation analysis in The Cancer Genome Atlas (TCGA) dataset. Univariate and stepwise multivariable Cox analyses were

used to establish a signature based on seven sialylation-related lncRNAs in TCGA dataset, and the risk model was validated in the Gene Expression Omnibus (GEO) dataset. Comprehensive research was done on the correlation between the sialylation lncRNA signature and clinical characteristics, enriched pathways, mutation, and tumor immune microenvironment. In addition, we verified the expression levels of seven lncRNAs in the CRC cell lines and normal cell lines using real-time quantitative polymerase chain reaction (qRT-PCR). Finally, combined drug sensitivity analysis (Genomics of Drug Sensitivity in Cancer [GDSC]/The Cancer Therapeutics Response Portal [CTRP]/Profiling Relative Inhibition Simultaneously in Mixtures [PRISM]) was conducted.

Result: Kaplan–Meier curve analysis revealed that CRC patients in the low-risk subgroup had a better survival outcome than those in the high-risk subgroup in the training set, testing set, and overall set. Multivariate analysis demonstrated that the sialylation-related lncRNA signature was an independent prognostic factor for overall survival (OS), progression-free survival (PFS), and disease-specific survival (DSS) prediction. The sialylation lncRNA signature–based nomogram exhibited a robust prognostic performance. Furthermore, enrichment analysis illustrated that cancer hallmarks and oncogenic signaling were more enriched in the high-risk group, while inflammatory responses and immune-related pathways were more associated with the low-risk group. The comprehensive analysis suggested that low-risk patients had a stronger activity of immune response pathways, greater immune cell infiltration, and higher expression of immune stimulators. Finally, the combined drug sensitivity analysis indicated that the sialylation-related lncRNA signature could serve as a potential predictor for chemosensitivity.

Conclusions: This is the first and most systemic exploration of the clinical significance of sialylation-related lncRNAs in patients with CRC. We successfully developed and validated the novel seven sialylation-related lncRNA signature, which displayed accurate performance in predicting the prognosis, immune status, and chemotherapy sensitivity in CRC patients. The present study may provide innovative perspectives in clinical outcome prediction for CRC patients and contribute to deepening the theoretical foundation for immunotherapy improvement and individualized antitumor treatment.

Key words: Sialylation, long noncoding RNA, colorectal cancer, prognostic signature, immune microenvironment

405. Individualized concurrent chemoradiotherapy or targeted radiotherapy by pre-treatment plasma EBV DNA in locoregionally advanced nasopharyngeal carcinoma

Sunqin Cai*、Zongwei Huang、Sufang Qiu、Jun Lu、Yuhui Pan

福建省肿瘤医院，福建医科大学肿瘤临床医学院

Background: To investigate the value of pre-treatment Epstein-Barr virus DNA (pre-DNA) for individualized concurrent therapy during intensity-modulated radiotherapy (IMRT).

Methods: In total, 491 patients with newly diagnosed locoregionally advanced nasopharyngeal carcinoma (LA-NPC), undergoing radical induction chemotherapy (IC) + concurrent targeted radiotherapy (CTRT) or chemoradiotherapy (CCRT) were retrospectively reviewed. The cut-off value of pre-DNA was calculated by receiver operating characteristics curve based on the primary endpoint, disease-free survival (DFS). The log-rank and chi-squared tests were respectively used to evaluate the difference of survival and toxicities between CCRT and CTRT groups. Potential independent prognostic factors were identified by multivariate cox proportional hazard analysis.

Results: CCRT and CTRT groups did not differ in survival among the original cohort. The cut-off value of pre-DNA was 4315 copies/ml (area under curve, 0.627; sensitivity, 0.661; specificity, 0.609). Besides, the CCRT and CTRT groups showed equivalent survival outcomes for low-risk patients with pre-DNA < 4315 copies/ml. However, CCRT group showed preferable survival in 3-year DFS (78.0% *vs.* 64.3%, *P*=0.045), and distant metastasis-free survival (DMFS; 79.3% *vs.* 66.1%, *P*= 0.048) than CTRT for high-risk patients with pre-DNA ≥ 4315 copies/ml. According to multivariate analysis, CCRT was considered as a protective factor for DMFS in high-risk group. However, CCRT embraced a higher incidence of hematologic toxicities than CTRT during entire radiotherapy.

Conclusions: For low-risk patients, CTRT may be superior to CCRT due to similar survival outcomes and lower incidence of toxicities. Pre-DNA may be a useful predictor to guide individualized concurrent therapy during IMRT in LA-NPC.

Key words: Nasopharyngeal carcinoma, targeted therapy, Epstein-Barr virus DNA, nimotuzumab.

406. Machine Learning-Based Integration Develops a Robust Mitophagy-Related Multigene Model to Predict Patient Prognosis and Immune Microenvironment in Head and Neck Squamous Cell Carcinoma

Qin Ding*、Yuhui Pan、Wei Liu、Sufang Qiu

Clinical Oncology School of Fujian Medical University, Fujian Cancer Hospital, Fuzhou, China

Purpose: Head and neck squamous cell carcinoma (HNSCC) treatment is facing clinical challenges. Mitophagy in cancer cells is related to the tumor high energetic metabolism. The tumor immune microenvironment (TME) strongly influences clinical outcomes and treatment efficiency. However, the correlation of mitophagy and TME remains unknown in HNSCC.

Methods: Based on machine learning, a prognostic multigene signature was built with mitophagy-related differentially expressed genes (MPGs), which was associated with TME by gene set enrichment analysis (GSEA), in the TCGA cohort. Moreover, we systematically correlated risk signature with immunological characteristics in TME, which included immune checkpoints, tumor-infiltrating immune cells (TIICs), immunomodulators. To further invalidate CSNK2A2, we employed immunohistochemistry to examine its expression.

Results: MPGs-related prognostic model showed good prediction performance. Patients who had high-risk scores had significantly shorter progression-free survival (PFS) and overall survival (OS) than those with low-risk scores, according to the results of the survival analysis (p<0.0001). The CD8+ T cells infiltrated less in samples with higher risk scores. The immunological characteristic markers were expressed at higher levels in the low-risk group. Furthermore, immune therapy might be effective for the low-risk subtype of HNSCC patients (p<0.001). Samples with higher risk scores were more sensitive to chemotherapy. CSNK2A2 was validated to be higher expressed in HNSCC tissues, according to immunohistochemistry.

Conclusion: We have constructed a prognostic signature and provided innovative insights that may improve HNSCC management, which might give a more precise prognostic prediction. CSNK2A2 might be a novel biomarker to predict immune efficacy.

Key words: mitophagy; head and neck squamous cell carcinoma; tumor microenvironment; prognostic model; CSNK2A2

407. Prognostic relevance of PD-L1 expression on circulating tumor cells in metastatic breast cancer patients treated with anti-PD-1 immunotherapy

Ying Zhou *[1,2]、Jinmei Zhou[3]、Xiaopeng Hao[4]、Haoyuan Shi[1,2]、Xuejie Li[1,2]、Anqi Wang[1,2]、Zhiyuan Hu[1,2,5,6]、Yanlian Yang[2,5]、Zefei Jiang[3]、Tao Wang[3]

1. Fujian Medical University

2. CAS Key Laboratory of Standardization and Measurement for Nanotechnology, CAS Key Laboratory for Biomedical Effects of Nanomaterials and Nanosafety, CAS Center for Excellence in Nanoscience, National Center for Nanoscience and Technology of China, Beijing, China

3. Breast Cancer Department, The Fifth Medical Center of PLA General Hospital, Beijing, China

4. Department of General Surgery, The First Medical Center of PLA General Hospital, Beijing, China

5. School of Nanoscience and Technology, Sino-Danish College, University of Chinese Academy of Sciences, Beijing, China

6. School of Chemical Engineering and Pharmacy, Wuhan Institute of Technology, Wuhan, China

Rationale: Breast cancer has become the leading cause of cancer mortality in women. Although immune checkpoint inhibitors targeting programmed death-1 (PD-1) are promising, it remains unclear whether PD-L1 expression on circulating tumor cells (CTCs) has predictive and prognostic values in predict and stratify metastatic breast cancer (MBC) patients who can benefit from anti-PD-1 immunotherapy.

Methods: Twenty six MBC patients that received anti-PD-1 immunotherapy were enrolled in this study. The peptide-based Pep@MNPs method was used to isolate and enumerate CTCs from 2.0

ml of peripheral venous blood. The expression of PD-L1 on CTCs was evaluated by an established immunoscoring system categorizing into four classes (negative, low, medium, and high).

Results: Our data showed that 92.3% (24/26) of patients had CTCs, 83.3% (20/26) of patients had PD-L1-positive CTCs, and 65.4% (17/26) of patients had PD-L1-high CTCs. We revealed that the clinical benefit rate (CBR) of patients with a cut-off value of ≥ 35% PD-L1-high CTCs (66.6%) was higher than the others (29.4%). We indicated that PD-L1 expression on CTCs from MBC patients treated with anti-PD-1 monotherapy was dynamic. We demonstrated that MBC patients with a cut-off value of ≥ 35% PD-L1-high CTCs had longer PFS (P<0.05) and OS (P<0.01) compared with patients with a cut-off value of<35% PD-L1-high CTCs.

Conclusion: Our findings suggested that PD-L1 expression on CTCs could predict the therapeutic response and clinical outcomes, providing a valuable predictive and prognostic biomarker for patients treated with anti-PD-1 immunotherapy.

Key words: circulating tumor cells, breast cancer, programmed death-ligand 1, programmed death-1, prognostic

408. A Circular RNA Activated by TGFβ Promotes Tumor Metastasis through Enhancing IGF2BP3-mediated PDPN mRNA Stability

Ke Li*、Jiawei Guo、Yue Ming、Shuang Chen、Tingting Zhang、Hulin Ma、Xin Fu、Jin Wang、Wenrong Liu Liu、Yong Peng

West China Hospital, Sichuan University

Aim: Metastasis is the leading cause of cancer-related death, where TGFβ-induced epithelial–mesenchymal transition (EMT) process confers on cancer cells increased metastatic potential. However, the involvement of circRNAs in this process still remains obscure. Therefore, it is urgent to identify circRNAs involved in tumor metastatic process and determine their feasibility as therapeutic targets against metastasis.

Methods: Bioinformatics analysis of RNA-Seq data from TGFβ-treated MCF10A cells was performed to screen the metastasis-related circRNAs. *in vitro* experiments and *in vivo* mouse

metastasis models were performed to investigate the biological functions of IREC. Molecular Strategies were performed to reveal the mechanisms of metastasis-promoting effect of IREC. Analysis of IREC levels in two independent cohorts of colorectal cancer patients was performed to determine associations of IREC expression and metastasis or overall survival.

Results: In this study, we identified that a highly conserved circRNA derived from ITGB6, IREC (ITGB6-related circRNA), was robustly induced by TGFβ and significantly upregulated in metastatic cancer samples. Moreover, IREC potently promoted EMT process and tumor metastasis *in vitro* and *in vivo*. The metastasis-promoting effect of IREC is largely attributed to its capacity of directly interacting with IGF2BP3 to stabilize *PDPN* mRNA, which encodes a critical effector protein to induce EMT and metastasis. Importantly, in vivo delivery of PEI-coated IREC siRNA complex dramatically suppressed tumor metastasis and extended survival of mice with pulmonary metastasis.

Conclusion: our study underscores the feasibility and therapeutic potential of manipulating IREC expression to treat metastatic cancers.

Key words: circRNA, TGFβ, tumor metastasis, IGF2BP3, PDPN

409. Mitochondrial fragmentation is crucial for c-Myc-driven hepatoblastoma-like liver tumors

Dalin Wang*[1,2]、Jiming Tian[3]、Zeyu Yan[4]、Qing Yuan[5]、Dan Wu[1]、Xiaoli Liu[1]、Shirong Yang[4]、Shanshan Guo[1]、Jianxun Wang[6]、Yongxiu Yang[3]、Jinliang Xing[1]、Jiaze An[2]、Qichao Huang[1]

1. Air Force Medical University

2. Department of Hepatobiliary Surgery, Xijing Hospital, Fourth Military Medical University, Xi'an, China.

3. The First Clinical Medical College of Lanzhou University, Lanzhou, China.

4. Department of General Surgery, Tangdu Hospital, Fourth Military Medical University, Xi'an, China.

5. Institute of Medical Research, Northwestern Polytechnical University, Xi'an, China.

6. Department of general surgery, 986th Hospital of air force, Xi'an, China.

Hepatoblastoma is the most common liver cancer in children, and the aggressive subtype often has a poor prognosis and lacks effective targeted therapy. Although aggressive HB is often

accompanied by abnormally high expression of the transcription factor c-Myc, the underlying mechanism remains unclear. In this study, we found that mitochondrial fragmentation was enhanced by c-Myc overexpression in human aggressive HB tissues and was associated with poor prognosis. Then, a mouse model resembling human HB was established via hydrodynamic injection of c-Myc plasmids. We observed that liver-specific knockout of mitochondrial fusion molecule MFN1 or overexpression of mitochondrial fission molecule DRP1 promoted the occurrence of c-Myc-driven liver cancer. In contrast, when MFN1 was overexpressed in the liver, tumor formation was delayed. In vitro experiments showed that c-Myc transcriptionally upregulated the expression of DRP1 and decreased MFN1 expression through upregulation of miR-373-3p. Moreover, enhanced mitochondrial fragmentation significantly promoted aerobic glycolysis and the proliferation of HB cells by significantly increasing ROS production and activating the AKT/mTOR and NF-κB pathways. Taken together, our results indicate that c-Myc-mediated mitochondrial fragmentation promotes malignant transformation and progression of HB by activating ROS-mediated multi-oncogenic signaling.

Key words: Hepatoblastoma; mitochondrial fragmentation; Drp1; Mfn1; c-Myc; ROS

410. Methionine Deficiency Facilitates Antitumor Immunity by Altering m6A Methylation of Immune Checkpoint Transcripts

Ting Li*[1,2]、Tan Yue-Tao[1]、Yan-Xing Chen[1]、Xiao-Jun Zheng[3]、Wen Wang[4]、Kun Liao[1]、Hai-Yu Mo[1]、Junzhong Lin[1,5]、Wei Yang[6]、Hai-Long Piao[4]、Rui-Hua Xu[1,7]、Huai-Qiang Ju[1,7]

1. Sun Yat-sen University Cancer Center

2. Department of Gastroenterology and Urology, Hunan Cancer Hospital/The Affiliated Cancer Hospital of Xiangya School of Medicine, Central South University

3. Research Department of Medical Sciences, Guangdong Provincial People's Hospital, Guangdong Academy of Medical Sciences

4. CAS Key Laboratory of Separation Science for Analytical Chemistry, Dalian Institute of Chemical Physics, Chinese Academy of Sciences

5. Department of Colorectal Surgery, Sun Yat-sen University Cancer Center

6. Guangdong Provincial Key Laboratory of Molecular Oncologic Pathology, Southern Medical University

7. Research Unit of Precision Diagnosis and Treatment for Gastrointestinal Cancer, Chinese Academy of Medical Sciences

Objective: Methionine metabolism is involved in a myriad of cellular functions, including methylation reactions and redox maintenance. Nevertheless, it remains unclear whether methionine metabolism, RNA methylation and antitumor immunity are molecularly intertwined.

Design: The antitumor immunity effect of methionine-restricted diet (MRD) feeding was assessed in murine models. The mechanisms of methionine and YTH domain-containing family protein 1 (YTHDF1) in tumor immune escape were determined *in vitro* and *in vivo*. Moreover, the MRD or YTHDF1 depletion synergizes with PD-1 blockade used to block tumor progress.

Results: We found that dietary methionine restriction reduced tumor growth and enhanced antitumor immunity by increasing the number and cytotoxicity of tumor-infiltrating $CD8^+$ T cells in different mouse models. Mechanistically, the S-adenosylmethionine derived from methionine metabolism promoted the N6-methyladenosine (m^6A) methylation and translation of immune checkpoints, including PD-L1 and VISTA, in tumor cells. Furthermore, a methionine-restricted

diet or m^{6}A-specific binding protein YTHDF1 depletion inhibited tumor growth by restoring the infiltration of CD8$^+$ T cells, and synergized with PD-1 blockade for better tumor control. Clinically, YTHDF1 expression correlated with poor prognosis and immunotherapy outcomes for cancer patients.

Conclusions: Methionine and YTHDF1 play a critical role in anticancer immunity through regulating the functions of T cells. Targeting methionine metabolism or YTHDF1 could be a potential new strategy for cancer immunotherapy.

Key words: Immunotherapy; Methionine metabolism; YTHDF1; m6A methylation

411. Whole-exome sequencing reveals the evolutionary trajectory of microvascular invasion in hepatocellular carcinoma from the perspective of tumor and circulating tumor DNA

Chenhao Zhou*[1]、Jialei Weng[1]、Shaoqing Liu[1]、Qiang Zhou[1]、Xiaoqiang Zhu[2]、Ning Ren[1]

1. *Zhongshan Hospital, Fudan University*

2. *香港大学生物医学院*

Background & Aims: Relapse of hepatocellular carcinoma (HCC) due to vascular invasion is common, but the genomic mechanisms underlying HCC vascular invasion remain unclear, and molecular determinants of high-risk relapse cases are lacking. We aimed to reveal the evolutionary trajectory of microvascular invasion (MVI) and develop a predictive signature for relapse in HCC.

Methods: Whole-exome sequencing was performed on tumor and peritumor tissues, portal vein tumor thrombus (PVTT), and circulating tumor DNA (ctDNA) to compare the genomic profiles between 5 HCC patients with MVI and 5 patients without MVI. We also conducted an integrated analysis of the exome and transcriptome to develop and validate a prognostic signature in two public cohorts and one cohort from Zhongshan Hospital, Fudan University.

Results: Shared genomic landscapes and identical clonal origins among tumor, PVTT, and ctDNA were observed in MVI (+) HCC, suggesting that genomic changes favoring metastasis occur at the

primary tumor stage and are inherited in metastatic lesions and ctDNA. There was no clonal relatedness between the primary tumor and ctDNA in MVI (-) HCC. HCC had dynamic mutation alterations during MVI and exhibited genetic heterogeneity between primary and metastatic tumors, which can be comprehensively reflected by ctDNA. A relapse-related gene signature named RGSHCC was developed based on the significantly mutated genes associated with MVI and shown to be a robust classifier of HCC relapse.

Conclusions: We characterized the genomic alterations during HCC vascular invasion and revealed a previously undescribed evolution pattern of ctDNA in HCC. A novel multiomics-based signature was developed to identify high-risk relapse populations.

Key words: Hepatocellular carcinoma; Microvascular invasion; Whole-exome sequencing; Circulating tumor DNA; Relapse

412. Construction of a novel prognostic model of lung adenocarcinoma based on genes related to immunity and mitophagy

Di Zhu*[1]、Ting Huang[1]、Renyu Zhou[2]、Bo Yang[1]、Lilin Peng[1]、Lijuan Zhong[1]、Qianyuan Tian[1]、Yuanzhi Lu[1]

1. The First Affiliated Hospital of Jinan University

2. Jinan University

Background: Lung cancer is the most common cancer worldwide, lung adenocarcinoma (LUAD) is the principal histological subtype of Lung cancer with heterogeneously morphological features and driver genetic alterations with high aggressiveness and poor prognosis. However, there were few unified prognostic model for clinical management of this disease. This study was dedicated to develop a novel prognostic model for LUAD based on immune-related genes (IRGs) and mitophagy-related genes (MRGs).

Methods: The differentially expressed IRGs (DE-IRGs) and MRGs (DE-MRGs) in LUAD were certificated by differential analysis and Venn diagrams. The univariate Cox and multivariate Cox analysis were executed to excavate the immune-mitophagy-relevant (IMR) prognostic genes. The

IMR signature was created and affirmed in distinct datasets. Independent prognostic predictors were authenticated by Cox analysis. CIBERSORT algorithm was applied to probe the linkage between the gene signature and immune infiltrating cells. Chemotherapy drug sensitivity and immunotherapy responsiveness were projected by 'pRRophetic' package and Tumor Immune Dysfunction and Exclusion (TIDE) website.

Results: A grand total of 41 DE-IRGs and 8 DE-MRGs in LUAD were mined. Based on univariate Cox and multivariate Cox analysis, four IMR prognostic genes, namely VDAC1, DTL, IGHM, and MBP, were selected to establish a IMR gene signature. Then, we confirmed the signature by internal and external validation sets. The risk score was demonstrated as a credible independent prognostic predictor by the Cox regression analysis. The result of CIBERSORT manifested that the proportion of T cells CD4+ memory activated and Macrophages M0 were elevated in the patients with higher risk scores, while the proportion of B cells memory, Plasma cells, T cells CD4 memory resting, and Mast cells resting were superior in the patients with lower risk scores. Drug sensitivity analysis suggested that the signature may be able to act as a chemosensitivity predictor.

Conclusion: Taken together, this study discovered the IMR prognostic genes and developed a risk signature for the overall survival projection of LUAD, which will be of great significance in developing prognostic molecular biomarkers, clinical prognosis prediction, and treatment strategy decision for LUAD patients.

Key words: lung adenocarcinoma, immune-related genes, mitophagy-related genes, prognosis, risk signature

413. Differences in serum cytokine levels between non-invasive and invasive lung adenocarcinoma

Bingjie Zeng 、Yueyang Qin、Xianzhao Wang、Lifang Ma*

Shanghai Tongji Hospital

Background: The incidence and mortality of lung cancer remain high and become the leading cause of cancer death. Lung adenocarcinoma is one of the main histological subtypes of lung

cancer. Previous studies have shown the role of inflammation in the development of lung cancer, but the relationship between cytokines and lung adenocarcinoma is still unclear. To further differentiate and explore the association of cytokines with the risk of non-invasive and invasive lung adenocarcinoma, we studied and assessed serum cytokine levels in patients with two types of lung adenocarcinoma.

Methods:A cohort study of 90 non-invasive lung adenocarcinomas and 90 invasive lung adenocarcinomas was retrospectively included, and the clinical characteristics were recorded in detail. The differences in the levels of 12 serum cytokines (IFN-α, IFN-γ, IL-10, IL-12P70, IL-17A, IL-1β, IL-2, IL-4, IL-5, IL-6, IL-8, and TNF-α) between the two groups of lung adenocarcinoma patients were analyzed and evaluated. Associations of cytokines with patient-related clinical outcomes were assessed by logistic regression analysis.

Results: The mean age of the patients was 56.6 years, and the proportions of males and females were 38.9% and 61.1%, respectively. IFN-α, IL-1β, IL2, IL6, TNF-α, IL4, and IL8 were significantly increased in patients with invasive lung adenocarcinoma compared with the non-invasive lung adenocarcinoma group. And further research found that smoking is one of the important influencing factors of invasive lung adenocarcinoma, and the changes of 4 cytokines IL-1β, IL-6, IL-8, and TNF-α in the smoking group of patients with invasive lung adenocarcinoma were significantly higher. For obvious, suggesting the role of inflammation in the development of invasive lung adenocarcinoma.

Conclusions: We found differences in preoperative serum cytokine levels between invasive and non-invasive lung adenocarcinoma patients, which may serve as potential serum biomarkers to aid clinical differential diagnosis and assess disease progression.

Key words: Invasive lung adenocarcinoma; Non-invasive lung adenocarcinoma; Cytokine; Inflammation.

414. Lamprey Immunity Protein enables early detection and recurrence monitoring for bladder cancer through recognizing Neu5Gc-modified UMOD glycoprotein in urine

Hongming Teng*[2]、Qingwei Li[1]、Meng Gou[1]、Gang Liu[2]、Xu Cao[1]、Jiali Lu[1]、Yinglun Han[1]、Yang Yu[3]、Zhanfeng Gao[4]、Xiaoping Song[5]、Weijie Dong[2]、Yue Pang[1]

1. 辽宁师范大学

2. Dalian Medical University

3. 大连医科大学附属第二医院

4. 大连医科大学附属中心医院

5. 大连大学附属中山医院

The clinical management of bladder cancer (BCa) is hindered by the lack of reliable biomarkers. We aimed to investigate the potential of lamprey immunity protein (LIP), a lectin that specifically binds to multi-antennary sialylated *N*-glycolylneuraminic acid (Neu5Gc) structures on UMOD glycoproteins in the urine of BCa patients. Primary BCa patients had higher levels of LIP-bound Neu5Gc in urine, compared to that of the healthy participants and patients receiving postoperative treatment. In addition, lectin chip assay and mass spectrometry were used to analyze the glycan chain structure, which can recognize the UMOD glycoprotein decorated with multi-antennary sialylated Neu5Gc structures. Furthermore, compared with urine samples from healthy patients (N= 2821, T/C= 0.12 ± 0.09) or benign patients (N= 360, T/C= 0.11 ± 0.08), the range of urine T/C ratio detected using LIP test paper was 1.97 ± 0.32 in patients with bladder cancer (N= 518) with significant difference ($P < 0.0001$). Our results indicate that LIP may be a tool for early BCa identification, diagnosis, and monitoring. Neu5Gc-modified UMOD glycoproteins in urine and Neu5Gc-modified N-glycochains and sialyltransferases may function as potential markers in clinical trials.

Key words: Biomarkers; Urinary Bladder Neoplasms; Lampreys; LIP; Polysaccharides

415. Discovery and Validation of PARP4 DNA Methylation to Distinguish Malignant from Benign Thyroid Nodules

Mengxia Li[1]、Yifei Yin[2]、Hong Li[2]、Chenxia Jiang[3]、Rongxi Yang*[1]

1. Nanjing Medical University

2. 徐州医科大学附属淮安医院/淮安第二人民医院

3. 南通大学附属医院

Background: Thyroid cancer (TC) is the most common endocrine malignancy and approximate 85% TCs are papillary thyroid cancer (PTC). However, the principal method in clinical practice, fine needle aspiration biopsy, always causes 20-30% indeterminate nodules, of which about 60% patients were over- or under-treated at initial surgery. Therefore, malignancy evaluation of thyroid nodules is an important but challenging issue. In this study, we screened out differentially methylated and expressed PARP4 gene by examining whole-genome DNA methylation profiles and expression profiles, and further validated the target sites with two independent case-control studies.

Methods: In the discovery round, we measured methylation and expression levels of 32 fresh-frozen (FF) tissue samples including 15 early-stage PTC and 17 benign thyroid nodule (BTN) cases from the Affiliated Huai'an Hospital of Xuzhou Medical University and the Second People's Hospital of Huai'an using Illumina Infinium Human Methylation EPIC 850K beadchip array and RNA-Sequencing.Subsequently, two independent studies with formalin-fixed and paraffin-embedded (FFPE) tissue samples were performed for validation. One hundred and ninety early-stage PTC and 190 age- and gender- matched BTN patients in validation I were collected from the same hospital mentioned above. Women accounted for 78.95% in both groups. The median ages in PTC and BTN patients were 51.00 and 53.00 years, respectively. Likewise, validation II consisted of 186 early-stage PTC and 191 age- and gender-matched BTN cases, who were collected from the Affiliated Hospital of Nantong University. PTC and BTN groups had the same median ages of 49.00 years, and the proportions of women patients were 78.49% and 77.49%. Methylation level of patients in validation studies was determined by matrix-assisted laser desorption ionization time-of-flight (MALDI-TOF) mass spectrometry.

Results: Differentially methylated and expressed genes were selected following the criteria, and cg20765408 and cg21812277 located at 5'-UTR of *PARP4* gene were obtained (Figure 1). Meanwhile, we designed a 212 bp amplicon covering the two target CpG sites for MALDI-TOF mass spectrometry in validation studies (Figure 2A). The average methylation levels of cg20765408 were 0.41 and 0.78 in PTCs and BTNs (FDR-corrected *P* value= 1.89E-04; Figure 2B). Cg21812277 also had an obvious hypomethylation in PTC than in BTN cases (0.21 *vs.* 0.56, FDR-corrected *P* value= 3.25E-05; Figure 2C). Further, we also observed consistent methylation change in FFPE tissue samples measured by MALDI-TOF mass spectrometry (Figure 3A-B) and found that DNA methylation levels in FFPE samples examined by MALDI-TOF mass spectrometry were positively correlated with those in FF samples by 850K beadchip array (for cg20765408: Spearman's rho= 0. 65, *P* value= 0.001; for cg21812277: Spearman's rho= 0. 64, *P* value= 0.002; Figure 3C). Next, we conducted the validation of hypomethylated *PARP4* in two independent studies with nearly 800 cases and found PTC cases presented a significant hypomethylation of *PARP4* in both validation study I [odd ratios (ORs) ≧ 1.72 per -10% methylation, *P* values ≦ 1.73E-13] and validation study II (ORs ≧ 1.64 per -10% methylation, *P* values ≦ 1.49E-13) (Figure 4A-B). Besides, we developed a predictive model by setting validation study I as training set and validation study II as test set (Figure 1). In training set, we defined a formula where risk score= 2.99 (constant) - 0.45 × CpG_1 - 3.98 × CpG_2.3 - 2.72 × CpG_4 + 0.18 × CpG_5, and supplemented the predictive model with five variables including age group (< 55 years= 0, ≧ 55 years= 1), gender (men= 1, women= 2), thyroid stimulating hormone (TSH), free triiodothyronine (FT3), and free tetraiodothyronine (FT4). Nomogram displayed the PTC risk of each patient (Figure 5A) and calibration curve showed a high agreement between predicted and actual probabilities of early-stage PTC (Figure 5B). Area under the receiver operating characteristic (ROC) curve (AUC) of the model was 0.825 (sensitivity: 81.3%, specificity: 77.2%) (Figure 5C). Also, the decision curve analysis (DCA) showed that the predictive model could increase the clinical benefits for early-stage PTC diagnosis (Figure 5D). In test set, the model still performed well with the AUC of 0.815 (sensitivity: 83.1%, specificity: 71.8%) (Figure 5E-F).

Conclusion: In summary, our study revealed and verified the potential of a novel biomarker, DNA methylation of *PARP4* gene, in discriminating between the early-stage PTC and benign thyroid nodules, offering an insight into the utility of DNA methylation in early diagnosis in PTC.

Key words: thyroid nodules; differential diagnosis; DNA methylation; PARP4 gene; biomarker

416. Prognostic Predictor and Immune Microenvironment Signatures of Aberrant Exon Skipping Events in Triple-Negative Breast Cancer

Qingwang Chen*、Zehui Cao、Ruolan Zhang、Erfei Shang、Qiaochu Chen、Leming Shi、Yuanting Zheng

Fudan University

Background: Exon skipping (ES) is defined as the procedure of mature RNA processing where a selected exon is excluded from the pre-mRNA. As one essential type of alternative splicing (AS) event, aberrant ES plays an important role in the pathogenesis of cancer and the formation of the tumor microenvironment. However, characterization of aberrant ES profiles in the malignancy and prognosis of triple-negative breast cancer (TNBC) is little known and urgently needed.

Methods: We quantified the percent spliced in (PSI) values for ES events in 360 tumor tissues and 88 adjacent-normal tissues from the Fudan University Shanghai Cancer Center (FUSCC) TNBC cohort. Then, we performed differential comparative analysis to obtain cancer-associated ES events (CAES). Unsupervised cluster analysis was performed to analyze the characteristics of immune infiltration in the microenvironment. Additionally, univariate Cox and stepwise multivariate Cox regression analyses were conducted to find the prognosis associated with CAES and the best prognostic CAES model. Finally, pathway enrichment and gene set enrichment analysis (GSEA) was further employed to reveal the significant pathways for prognosis-related CAES signatures.

Results: A total of 277 CAES were identified (|delta PSI tumor - normal| > 0.10, FDR<0.05), including 101 up-regulated and 176 down-regulated in tumor samples. Enrichment of 241 parent genes revealed 84 GO pathways with statistical significance (FDR<0.05), with the top pathways related to cell adhesion molecule binding, cell leading edge, etc. Unsupervised clustering analysis with CAES identified three clusters with different immune microenvironment components, immune score, and stromal score in TNBC (P<0.05). Univariate and multivariate Cox regression

analyses identified six CAES associated with better prognoses (P<0.05). Results of GSEA showed the CAES signature might confer a strong tumor metabolism phenotype in the high-risk group with elevated activities in folate biosynthesis and phospholipase D pathways of tumorigenesis (P<0.05).

Conclusions: Our study characterized the CAES in TNBC patients with the ability to function as the immune microenvironment signatures and prognostic predictors, which improved our understanding of the relationship between ES events and TNBC.

Key words: Alternative splicing, exon skipping, TNBC, prognostic predictor, immune microenvironment

417. Mitochondrial DNA Haplogroup M7: A Predictor of Poor Prognosis for Colorectal Cancer Patients in Chinese Population.

Zeyu Yan[1]、Qing Yuan[2]、Yiwei He[3]、Xianli He[1]、Qi Zhao[4]、Jinliang Xing[1]、Xu Guo*[1]

1. Fourth Military Medical University

2. 西北工业大学

3. 南京医科大学

4. 中山大学肿瘤防治中心（中山大学附属肿瘤医院、中山大学肿瘤研究所）

Haplogroups and single nucleotide polymorphisms (SNP) of mitochondrial DNA (mtDNA) were associated with the prognosis of many types of cancer patients. However, whether mtDNA haplogroups contribute to clinical outcomes of colorectal cancer (CRC) in Chinese population remains to be determined. In this study, mtDNA of tissue samples from 445 CRC patients from Northwestern China was sequenced to evaluate the association between haplogroup and prognosis. The mtDNA sequencing data of 1015 CRC patients from Southern China were also collected for result validation. We found that patients with mtDNA haplogroup M7 had a significantly higher death risk when compared to patients with other haplogroups in both Northwestern (HR= 3.093, 95% CI= 1.768-5.411, P<0.001) and Southern (HR= 1.607, 95% CI= 1.050-2.459, P= 0.029) China. Then, a haplogroup M7-based mtSNP classifier was selected by using LASSO Cox

regression analysis. A nomogram comprising the mtSNP classifier and clinicopathological variables was developed to predict prognosis of CRC patients (AUC 0.735, 95% CI= 0.679-0.791). Furthermore, patients with high- and low-risk scores calculated by the haplogroup M7-based mtSNP classifier exhibited significantly different overall survival (OS) and recurrence-free survival (RFS) (all P<0.001). Finally, RNA-seq and immunohistochemical analyses indicated that the poor prognosis of patients with haplogroup M7 may be related to mitochondrial dysfunction and immune abnormalities in CRC tissues. In conclusion, the haplogroup M7 and haplogroup M7-based mtSNP classifier seems to be a practical and reliable prognostic predictor for CRC patients, which provides a potential tool of clinical decision making for patients with haplogroup M7 in Chinese population.

Key words: mitochondrial DNA, haplogroup, single nucleotide polymorphisms, colorectal cancer, prognosis.

418. Inactivation of adipose triglyceride lipase facilitates the proinflammatory response of nasopharyngeal carcinoma by modulating lipid droplets/PPAR-α signaling axis

Limei Li、Xiaoying Zhou*、Xue Xiao、Jun Zhao、Haishan Zhang

广西医科大学

Objectives: Previously, we have shown that Epstein-Barr virus (EBV) encoded latent membrane protein LMP2A promotes the migration of nasopharyngeal carcinoma (NPC) cells by inhibiting the expression of adipose triglyceride lipase（ATGL）, which is the first and rate-limiting step of adipose triacylglycerol lipolysis. Here, we aim to further investigate the effect of ATGL in NPC biological malignant behavior via remodeling lipid droplets.

Methods: BODIPY staining and TG/T-CHO detection kits were used to examine the accumulation of lipid droplets (LDs), the relative concentration of triglyceride, and total cholesterol. The growth of NPC cells was assessed both in vivo and in vitro. Wound healing and

transwell were applied to detect cellular invasion and metastasis ability. Flow cytometry was performed to analyze the apoptosis of cells. RNA sequencing was utilized to investigate the expression of differential expression genes and signaling pathways in ATGL-overexpressing cells and their corresponding control cells. qPCR, ELISA, and western blot assay were further taken to explore the underlying molecular mechanisms of ATGL in regulating NPC cell growth, survival, and motility.

Results: We found that the mRNA expression of ATGL was significantly downregulated in NPC cell lines and NPC primary tissues in contrast with normal controls. When overexpressing ATGL in NPC cell lines, reduced intracellular LDs, TG concentration, and ROS were observed, but no difference in the T-CHO concentration. In addition, ATGL inhibited NPC cell proliferation, colony formation, migration, and invasion in vitro, and suppressed their tumorigenesis in vivo. Furthermore, we observed that the overexpression of ATGL led to apoptosis of NPC cells, with higher expression of caspase 3, BAX, PARP, and lower expression of Bcl-xl. Nevertheless, knocking down ATGL demonstrated the opposite effect in NPC cells. RNA-seq analysis indicated that the activation of TNF-α/NF-κB signaling pathway might be the main mechanism for the tumor suppressor effect of ATGL via retarded LDs accumulation in NPC cell lines. Western blot results confirmed a higher expression of nuclear NF-κB (p65) in ATGL overexpressing NPC cells, suggesting activation of the NF-κB signaling pathway. However, the downstream pro-inflammatory factors of NF-κB were significantly decreased in ATGL overexpression NPC cells, including IL6, IL8, IL1α, and CXLC2. Interestingly, we discovered that the PPAR-α signaling pathway was activated, with an upregulated of PPAR-α, PGC1-a, and GCLC when ATGL was expressed higher. As well, a chemical antagonism of PPAR-α significantly increased the transcriptional of pro-inflammatory factors mentioned above. Therefore, ectopic overexpression of ATGL impeds inflammatory responses of NPC cells by activating the PPAR-α signaling pathway.

Conclusion: The inactivation of ATGL induces alternations in lipid catabolism and promoted the malignant behavior of NPC by the PPAR-α/proinflammatory signaling pathway. ATGL might serve as a potential target for the treatment of NPC.

Key words: Nasopharyngeal carcinoma，ATGL，Lipid metabolism remodeling，NF-kB，PPAR-α

419. Real-world clinical treatment outcomes in Chinese non-small cell lung cancer (NSCLC) with EGFR exon 20 insertion mutations(ex20ins)

CHAO SHI[1]、RU YUE XING[3]、MENG MENG LI[3]、JUN NAN FENG[1,2]、RUI SUN[1,2]、BING WEI[1,2]、YONG JUN GUO[1,2]、JIE MA[1,2]、HUI JUAN WANG*[3]

1. Henan Cancer Hospital

2. 河南省分子病理学重点实验室

3. 郑州大学附属肿瘤医院 ,河南省肿瘤医院呼吸内科

Background: EGFR exon 20 insertions (EGFR ex20ins) constitute a heterogeneous subset of EGFR-activating alterations. However, the effectiveness of standard therapy in patients with EGFR ex20ins remains poor.

Methods: In our study, we retrospectively collected next-generation sequencing (NGS) data from 7831 Chinese NSCLC patients, and analyzed the relationship between EGFR ex20ins variations and medical records.

Results: Our data showed that EGFR ex20ins account for up to 3.5% of all EGFR mutation non-small-cell lung cancer (NSCLC) patients and 1.6% of all NSCLC patients in China. 38 different variants of EGFR ex20ins were identified in 129 NSCLC patients. We observed that the patients with EGFR ex20ins may benefit from the antiangiogenesis agents significantly (*P=0.027*). In EGFR ex20ins near loop group, patients received 2nd/3rd -generation EGFR-TKI therapy treatment as 1st-line treatment had longer median progression-free survival (PFS) than those initiated treatment with 1st-generation EGFR-TKI or chemotherapy. Patients with co-mutations of EGFR ex20ins near loop and TP53 tended to have shorter OS in 2nd/3rd-generation EGFR-TKI therapy (*P=0.039*). Additionally, median PFS was significantly longer in patients harboring EGFR ex20ins far loop variants received chemotherapy as a 1st-line setting (*P=0.037*).

Conclusions: Overall survival was significantly longer in EGFR ex20ins patients with antiangiogenesis agents. For the choice of first-line strategy, NSCLC with EGFR ex20ins near loop variants may benefit from 2nd/3rd -generation EGFR-TKI, while patients harboring EGFR

ex20ins far loop variants might have better outcomes from chemotherapy. TP53 could serve as a potential predictive marker in poor prognosis for EGFR ex20ins near loop patients.

Key words： EGFR exon20 insertion; near loop; far loop; clinical treatment outcomes; NSCLC

420. CD105: Tumor diagnosis, prognostic marker and future tumor therapeutic target

Lan Li*

Shanghai Chest Hospital

Cancer is one of the diseases with the highest morbidity and mortality rates worldwide, and its therapeutic options are inadequate. The endothelial glycoprotein, also known as CD105, is a type I transmembrane glycoprotein located on the surface of the cell membranes and it is one of the transforming growth factor-β (TGF-β) receptor complexes. It regulates the responses associated with binding to transforming growth factor β1 egg (Activin-A), bone morphogenetic protein 2 (BMP-2), and bone morphogenetic protein 7 (BMP-7). Additionally, it is involved in the regulation of angiogenesis This glycoprotein is indispensable in the treatment of tumor angiogenesis, and it also plays a leading role in tumor angiogenesis therapy. Therefore, CD105 is considered to be a novel therapeutic target. In this study, we explored the significance of CD105 in the diagnosis, treatment and prognosis of various tumors, and provided evidence for the effect and mechanism of CD105 on tumors.

Key words: CD105; Tumor therapy; Targeted therapy; Marker

421. circRNF10 regulates tumorigenic properties and nature killer cell mediated cytotoxicity toward breast cancer via miR-934/PTEN/ PI3k-Akt axis

Fei Liu、Baoen Shan、meixiang Sang*

the Fourth Hospital of Hebei Medical University

Circular RNAs (circRNAs) have drawn lots of attention in tumorigenesis and progression. However, circRNAs as crucial regulators in multitudinous biological processes have not been systematically identified in breast cancer (BC). In the present study, we found that has_circ_0028899 (also called circRNF10) was obviously downregulated in BC tissues, and higher levels of circRNF10 was markedly associated with a favorable prognosis of BC patients. The results from CCK8, Colony formation, Transwell invasion and migration, ELISA, and NK cell mediated cytotoxicity assays indicated that overexpression of circRNF10 could obviously inhibit the proliferation, migration, and invasion of BC cells, and enhances the killing efficiency of NK cells against BC cells. Based on these biological phenomenon, we further explored the possible role and mechanism of circRNF10 in BC cells. We predicted circRNF10-bound miRNAs using bioinformatics analyses, and verified by a series of biological experiments, including luciferase reporter assay, RIP, FISH, and Western blot. These results suggested that circRNF10 serve as a molecular sponge of miR-934 to further regulate the expression of PTEN as well as PI3k/Akt/MICA signaling in BC. In conclusion, our study revealed that circRNF10 functions as a tumor suppressor gene in BC by sponging miR-934 and suppressing the PI3K/Akt/MICA signaling pathway.

Key words: Breast cancer, circRNF10, miR-934, NK, PTEN

422. A comprehensive assessment of a newly designed non-exonic SNP-based NGS panel for HRD detection

Bing Wei[1]、JINXIANG ZHENG[1,2]、JUN LI[1,2]、ZHIZHONG WANG[1,2]、JIE MA*[1,2]

1. Henan Cancer Hospital

2. 河南省分子病理学重点实验室

Background: Ovarian cancer is a global problem and has no effective screening strategy. The recognition of homologous recombination deficiency (HRD) as a biomarker to predict the efficiency of Platinum-based or PARPis treatment. Whole Genome Sequencing (WGS) and Whole Exome Sequencing (1) can detect tumor HRD status but have several disadvantages restricting their clinical application.

Methods: This study developed a non-exonic SNP-based Tg-NGS panel that followed several principles. Then we comprehensively examined this panel both on 9 standards and 27 clinical ovarian cancer tissues, to describe its performance in HRD detection by comparing it with WGS and/or SNP microarray methods.

Results: First, based on 7 principles, high-frequency SNP loci were screened out, and a non-exonic SNP-based Tg-NGS panel was designed. The SNP sites of the panel had similar uniformity with Affymetrix OncoScan™ Assay but less number (52,592 vs. 217,611). Second, the HRD scores calculated by the panel and WGS were both consistent with the reference value of standards, and using sequenza to analyze the ASCN value was most reliable. At the same time, the tumor purity threshold of 30% and the raw sequencing depth ≥300x were highly recommended for the panel detection. In the end, the results on clinical samples revealed the panel performed better in HRD analysis than SNP microarray.

Conclusions: This newly developed kit is promising in clinical application to guide PARP inhibitors or platinum drugs using in ovarian cancer and other cancer therapy.

Key words: SNP-based NGS panel, Ovarian cancer, Chinese population, CNV, HRD

423. PRPS1-mediated purine biosynthesis is critical for pluripotent stem cell survival and stemness

xia huang*

Shanghai Chest Hospital

Introduction: Pluripotent stem cells (PSCs) have a unique energetic and biosynthetic metabolism compared with typically differentiated cells. However, the metabolism profiling of PSCs and its underlying mechanism are still unclear.

Methods: we analyzed the metabolism profiling by UHPLC-MS in PSCs and somatic cells. Then, we assessed the effects of ectopic expression or knockout (KO) of PRPS1 or PRPS2 on purine metabolite levels, drug sensitivity, and stemness in PSCs.

Results: Here, we report PSCs metabolism profiling and identify the purine synthesis enzymes, phosphoribosyl pyrophosphate synthetase 1/2 (PRPS1/2), are critical for PSCs stemness and survival. Ultra-high performance liquid chromatography/mass spectroscopy (UHPLC-MS) analysis revealed that purine synthesis intermediate metabolite levels in PSCs are higher than that in somatic cells. Ectopic expression of PRPS1/2 did not improve purine biosynthesis, drug resistance, or stemness in PSCs. However, knockout of PRPS1 caused PSCs DNA damage and apoptosis. Depletion of PRPS2 attenuated PSCs stemness and assisted PSCs differentiation.

Conclusions: Our finding demonstrates that PRPS1/2-mediated purine biosynthesis is critical for pluripotent stem cell stemness and survival.

Key words: PRPS1/2; Pluripotent stem cells; Purine biosynthesis; Stemness; Apoptosis

424. DAISM-DNNXMBD: Highly accurate cell type proportion estimation with in silico data augmentation and deep neural networks

Yating Lin[1]、Haojun Li[1]、Xu Xiao[1,2]、Lei Zhang[3]、Kejia Wang[4]、Jingbo Zhao[5]、Minshu Wang[2,4]、Frank Zheng[5]、Minwei Zhang[6]、Wenxian Yang[7]、Jiahuai Han[2,3,8]、Rongshan Yu*[1,2,7]

1. Xiamen University

2. National Institute for Data Science in Health and Medicine, Xiamen University

3. School of Life Science, Xiamen University

4. School of Medicine, Xiamen University

5. Amoy Diagnostics

6. Department of Critical Care Medicine, The First Affiliated Hospital of Xiamen University

7. Aginome Scientific, Xiamen

8. Research Unit of Cellular Stress of CAMS, Cancer Research Center of Xiamen University, School of Medicine, Xiamen University

Computational cell type deconvolution methods were developed to understand the cellular heterogeneity in disease-related tissues from bulk RNA-seq data. Due to the presence of strong batch effects, the performance of existing methods could fluctuate greatly when applied to different datasets even with the latest development in batch normalization or platform-agnostic signature designs. To tackle this issue, we proposed a DNN-based cell abundance estimation method with datasetspecific training data populated from a certain number of calibrated samples from a target dataset using DAISM, a data augmentation method using an in silico mixing strategy. DAISM-DNN enables accurate cell type proportions prediction and is robust to random errors in the ground truth cell type proportions of calibration samples. The evaluation results demonstrate that the DAISM-DNN pipelineoutperforms other existing methods consistently and substantially for all the cell types under evaluation inreal-world datasets. Importantly, we showed that with strict SOPs, it is possible to create a "train once, reuse many times" DAISM-DNN model for multiple biomedical experiments without the need for retraining.

Key words: cell type deconvolution, deep learning, data augmentation

425. Multiplexed imaging mass cytometry reveals distinct tumor-immune microenvironments linked to immunotherapy responses in melanoma

Xu Xiao[1]、Qian Guo[2]、Chuanliang Cui[2]、Yating Lin[1]、Lei Zhang[1]、Xin Ding[3]、Qiyuan Li[1]、Minshu Wang[1]、Wenxian Yang[4]、Yan Kong[2]、Rongshan Yu*[1,4]

1. Xiamen University

2. Peking University Cancer Hospital and Research Institute

3. Zhongshan Hospital Xiamen University

4. Aginome Scientific

Background: Single-cell technologies have enabled extensive analysis of complex immune composition, phenotype and interactions within tumor, which is crucial in understanding the mechanisms behind cancer progression and treatment resistance. Unfortunately, the knowledge on cell phenotypes and their spatial interactions at present has only limited utilization in guiding pathological stratification on patients based on their immune microenvironments for better clinical decisions.

Methods: Here we used imaging mass cytometry to simultaneously quantify 35 proteins in a spatially resolved manner on tumor tissues from 26 melanoma patients (14 responders and 12 nonresponders) receiving anti-programmed cell death-1 (anti-PD-1) therapy.

Results: Combined single-cell and spatial analysis reveals highly dynamic tumor microenvironments (TMEs) that are characterized with variable tumor and immune cell phenotypes and their spatial organizations in melanomas, and many of these multicellular features are associated with response to anti-PD-1 therapy. We further identify six distinct TME archetypes based on their multicellular compositions, and find that patients with different TME archetypes responded differently to anti-PD-1 therapy. Finally, we find that classifying patients based on the gene expression signature derived from TME archetypes predicts anti-PD-1 therapy response across multiple validation cohorts.

Conclusions: Our results demonstrate the utility of multiplex proteomic imaging technologies in studying complex molecular events in a spatially resolved manner for the development of new strategies for patient stratification and treatment outcome prediction.

Key words: Imaging mass cytometry, tumor microenvironment, melanoma, immunotherapy, single-cell imaging

426. Molecular epidemiology and clinical characterization of human rhinoviruses circulating in Shanghai, 2012-2020

Haixia Jiang*

shanghai chest hospital

Human rhinoviruses (HRVs) cause acute upper and lower respiratory tract infections and aggravation of asthma and chronicobstructive pulmonary disease. The 5' untranslated region (5' UTR) and the VP4/VP2 region are widely used for genotyping of HRVs. Members of the species Rhinovirus A and Rhinovirus C have been reported to be more frequently associated with severe disease than members of the species Rhinovirus B. We report the clinical and molecular epidemiological characteristics of HRVs circulating from 2012 to 2020 in Shanghai. A total of 5832 nasopharyngeal swabs from patients with acute respiratory infections were collected. A real-time reverse transcription polymerase chain reaction assay was used for virus detection. The 5' untranslated region and VP4/VP2 region were amplified and sequenced for genotyping and phylogenetic analysis. The overall rate of rhinovirus detection was 2.74% (160/5832), with members of species A, B, and C accounting for 68.13% (109/160), 20.00% (32/160), and 11.88% (19/160) of the total, respectively. A peak of HRV infection was observed in autumn (5.34%, 58/1087). Patients in the 3- to 14-year-old age group were the most susceptible to HRV infection ($\chi 2$= 23.88, *P*= 0.017). Influenza virus and Streptococcus pneumoniae were detected more frequently than other pathogens in cases of coinfection. Recombination events were identified in 10 strains, which were successfully genotyped by phylogenetic analysis based on the 5' UTR-VP4/VP2 region but not the 5' UTR region alone. We observed a high degree of variability in the relative distribution of HRV genotypes and the prevalence of HRV infection in Shanghai

and found evidence of recombination events in the portion of the genome containing the 5' UTR and the VP4/VP2 region between HRV-C strains and HRV-A-like strains. This study is important for surveillance of the spread of HRVs and the emergence of new variants.

Key words: Human rhinovirus, genotyping, epidemiology, recombination

427. Cell surface vimentin as a novel biomarker and therapeutic target for advanced gastric cancer

Heming Li、Lu Xu、Mingfang Zhao*、Tao Han

The First Hospital of China Medical University

Background: Circulating tumor cells (CTCs) have clinical relevance, but their role in advanced gastric cancer (GC) is limited because epithelial-mesenchymal transition (EMT) occurs more abundantly in the CTCs of advanced GC patients than early disease, and these CTCs are challenging to identify with standard detection methods.

Methods: To fill this gap, we established a new CTCs detection technique platform relying upon a novel biomarker, cell surface vimentin (CSV), and compared CTCs enumeration in GC patients using both EpCAM and CSV in a prospective head-to-head study to capture regular and EMT-CTCs, respectively. Blood samples were collected from 127 GC patients (61 with resectable disease and 66 with unresectable disease) and 10 healthy donors. The phenotype and enumeration were characterized under a confocal microscope. Spiking assays and whole-exome sequencing (WES) were performed to verify the reliability of this novel marker and technique. Additionally, bioinformatics analysis and tandem mass tag (TMT) quantitative proteomics were performed to screen potential potent inducers of CSV+CTC formation. Both in vitro and in vivo experiments were investigated to explore the molecular mechanism of CSV expression regulation and its role in GC metastasis.

Results: CSV-specific antibody 84-1 detected CTCs from GC patients' peripheral blood samples with high sensitivity verified by spiking assays and WES. Additionally, compared to the EpCAM detection method, the CSV-specific positive selection CTCs assay was significantly better for evaluating the therapeutic response and prognosis in advanced GC patients and successfully

predicted disease progression as early as 6.14 months ahead of radiology evaluation. In vitro and in vivo experiments further revealed that insulin-like growth factor-I (IGF-I) induced the translocation of vimentin from the cytoplasm to the cell surface and EMT progression. Blocking CSV with pritumumab in combination with the IGF-IR signaling pathway inhibitor GSK1838705A suppressed GC metastasis in a mouse model.

Conclusions: Utilizing the CSV method provides new insights into using CTCs capture to assess disease status and a new approach to personalized medicine in advanced GC patients.

Key words: cell surface vimentin (CSV), gastric cancer (GC), circulating tumor cells (CTCs), insulin-like growth factor-I (IGF-I), epithelial-mesenchymal transition (EMT)

428. Specific vaginal and gut microbiomes of cervical cancer and a diagnostic value

Mengzhen Han*

China Medical University

Objective: To investigate the vaginal and gut microbes changes during the carcinogenesis of cervical cancer and the auxiliary diagnostic value of cervical cancer-related vaginal and gut microbial markers.

Methods: We studied 416 female vaginal 16S rRNA sequencing data and 116 gut 16S rRNA sequencing data from 8 studies. The vaginal samples were divided into Normal group (n=180), cervical intraepithelial neoplasia (CINs) group (n=152) and cervical cancer (Cervical_cancer) group (n=84) according to the severity. The gut samples were divided into Normal group (n=51) and cervical cancer (Cervical_cancer) group (n=65). Reads were processed using VSEARCH. We used Shannon index, Chao1 index, Simpson diversity index, Beta diversity index, LEfSe analysis, co-abundance network analysis and KEGG enrichment analysis to explore microbiome differences between groups. We constructed random forest models based on genus and validated the models to test their diagnostic effectiveness. In addition, we investigated the differences in major metabolic pathways between the cervical cancer and non-cancer groups by the Kyoto Encyclopedia of Genes and Genomes (KEGG) and Cluster of Orthologous Groups (COG).

Results: Compared to the non-cancerous population, patients with cervical cancer had unique microbial community characteristics in both vaginal and gut ecological niches. The increase in vaginal microbial diversity and abundance was positively correlated with disease severity and was accompanied by a decrease in commensal bacteria such as Lactobacillus spp. and an increase in pathogenic bacteria such as Gardnerella spp. The diversity and abundance of gut flora were reduced in patients with cervical cancer, and there were significant changes in microbial composition, including enrichment of Bacteroides and Prevotella and reduced abundance of Faecalibacterium and Roseburia. Overall, cervical carcinogenesis resulted in two ecological sites of microbial change that differed significantly from the non-cancerous population. In addition, co-abundance analysis revealed differences in the complexity of the flora network in women with different pathological characteristics. To determine the optimal microbiota profile for noninvasive diagnosis, our predictive model based on biomarkers obtained at the genus level in two ecological regions achieved high accuracy in the diagnosis of cervical cancer (vaginal model AUC=91.58%; gut model AUC=99.95%). Potential functional pathways analysis based on the KEGG database indicated significant differences in the predicted profile functions between the normal women microbiomes and cervical cancer women microbiomes.

Conclusion: Significant differences were found in vaginal and gut microbes in patients with cervical cancer compared to the non-cancerous population. The phenomenon of dynamic changes of microbes occurring in the vagina in response to changes in disease severity is also present, and the microflora is involved in the development of cervical cancer. The prediction models constructed at the genus level in both ecological sites have good diagnostic value for cervical cancer.

Key words: cervical cancer; 16S rRNA; vaginal; gut; CIN; ROC; KEGG

429. Patients with Advanced Pancreatic & Biliary Cancer Appear More Vulnerable to SARS-CoV-2 Omicron Variant: An Observational Study during the COVID-19 Outbreak in Shanghai

Heming Li [1]、Tao Han*[1]、Tingsong Chen[2]

1. 中国医科大学附属第一医院

2. The first hospital of China Medical University

Background: There is a great controversy about lethal effect of Omicron Variant on vulnerable populations and the measure of full-open or zero community transmission policy. Thus, we designed an observational study to evaluate the outcomes of Omicron-infected patients with pancreatic & biliary cancer (the so-called “King of Cancer”) in order to provide potential evidence for the most appropriate strategy to counter Omicron transmission in Shanghai.

Methods: Omicron infected patients with advanced pancreatic & biliary cancer were enrolled from April 15 to May 31, 2022. Four groups were set in this study: Group 1, Omicron-infected cancer patients (N=4); Group 2, non-infected cancer patients (N=4); Group 3, infected non-cancer-afflicted subjects (N=4); Group 4, non-infected non-cancer-afflicted subjects (N=4). On Day 0, 7 and 14 after infection, the blood samples were dynamically collected from all subjects. The primary endpoints were disease severity and survival.

Results: By the endpoints in this observational study, Patients No. 2, 3 and 4 died separately at Day 11, 25 and 13 after viral infection, all of whom were patients with advanced cancer, with the death rate up to 75%. Group 1 presented an overall T cell exhaustion status compared with other groups with obviously lower T cell populations and higher B cell% and CD4+T/CD8+T ratio (p<0.05). Time-course cytokine monitoring results showed that IL-1β was significantly decreased in Group 1 (p<0.05) and generally kept at a low level without obvious fluctuation. IL-6 was markedly increased in infected cancer patients (P<0.01), but remained a low level and had no apparent change during the whole infection process in non-cancer-afflicted subjects. Furthermore,

several inflammatory parameter indexes indicated a tight association of Omicron infection with disease course and prognosis of Omicron-infected cancer patients.

Conclusions: For patients with advanced pancreatic & biliary cancer, the strict & comprehensive control strategy for COVID-19 epidemic in Shanghai provided a guarantee of low infection and death rate. Conclusively, this policy shall be persisted upon the consideration of the welfare of vulnerable populations.

Key words: Pancreatic & biliary cancer; COVID-19; SARS-CoV-2 Omicron; Immunosuppression; Vulnerable population.

430. Lung abscess by Fusobacterium nucleatum and Streptococcus co-infection by metagenomic next-generation sequencing: a case series and review of the literature

Na Wang[1,2]、Wenjie Han[1,2]、Mengzhen Han[1,2]、Tao Sun[1,2,3]、Junnan Xu*[1,2,3]

1. 辽宁省肿瘤医院

2. 中国医科大学肿瘤医院

3. 大连理工大学肿瘤医院

Objective: Lung abscess is a necrotizing infection leading to loss of healthy lung tissue. The most common microbiome of lung abscess was Klebsiella pneumonia, Staphylococcus aureus, Streptococcus, Mycobacterium, Actinomyces and Nocardia. The routine culture is time-wasting or false-negative results and clinicians could only choose empiric therapy or use broad-spectrum antibiotic, which could significantly contribute to the problem of resistance or aggravate the condition. The aim of this study was to carry out detecting pathogens in patients with lung abscesses using metagenomic next-generation sequencing.

Materials and methods: We report three patients of a routine-culture-negative lung abscess. Presenting symptoms included fever, cough, dyspnea, chest pain and a computed tomography scan revealed a lesion in the lungs. We extracted DNA from bronchoalveolar lavage fluid and pleural

fluid from 3 patients. The library prepared from samples DNA was sequenced on a MBGISEQ-2000RS sequencing platform. Raw reads were mapped to labortary-developed microbial databases and NCBI-nt database.

Results: Our study revealed Fusobacterium nucleatum and Streptococcus as the most represented microbial pathogen in 3 patients. And Streptococcus that co-infection with Fusobacterium nucleatum is not confined to the same species, S. constellatus in case 1 and case3, S. intermedius in case 2. Case 1 and 3 responded to standard treatment of piperacillin-tazobactam or meropenem and drainage intervention, case 2 responded to biapenem alone and all 3 patients gradually improved and discharged. The literature review also suggested that various Streptococcus species (S. anginosus, S. pneumoniae, S. viridans) could also cause lung abscess. Because of the sequence similarity, the sequences of Streptococcus were easily multiple mapped to more than one species rather than fully matched to a dominant species. Virulence genes RadD that associated with co-infections in Fusobacterium nucleatum were also detected and the coverage is 66.5% in case 1, 59.7% in case 2.

Conclusions: Our data demonstrated that mNGS could be a promising alternative diagnostic tool for pathogen detection and pathogen lists prompt us it will be important to focus on the Streptococcus genus rather than the dominant Streptococcus in terms of pathogen determined of co-infection by shotgun mNGS.

Key words:co-infection, Fusobacterium nucleatum, Streptococcus, lung abscess, shotgun metagenome next-generation sequencing

431. DNA Methylation-Specific Analysis of G Protein Coupled Receptor-Related Genes in Pan-Cancer

Mengyan Zhang、Jiyun Zhao、Yan Zhang*

Harbin Intitute of Technology

Tumor heterogeneity presents challenges for personalized diagnosis and treatment of cancer. The identification method of cancer-specific biomarkers has important applications for the diagnosis and treatment of cancer types. In this study, we analyzed the pan-cancer DNA methylation data

from TCGA and GEO, and proposed a computational method to quantify the degree of specificity based on the level of DNA methylation of G protein-coupled receptor-related genes (GPCRs-related genes) and to identify specific GPCRs DNA methylation biomarkers (GRSDMs) in pan-cancer. Then, a ridge regression-based method was used to discover potential drugs through predicting the drug sensitivities of cancer samples. Finally, we predicted and verified 8 GRSDMs in adrenocortical carcinoma (ACC), rectum adenocarcinoma (READ), uveal Melanoma (UVM), thyroid carcinoma (THCA), and predicted 4 GRSDMs (F2RL3, DGKB, GRK5, PIK3R6) which were sensitive to 12 potential drugs. Our research provided a novel approach for the personalized diagnosis of cancer and informed individualized treatment decisions.

Key words: G protein-coupled receptor; DNA methylation; biomarker; Drug sensitivity

432. RAD21 Amplification Epigenetically Suppresses Interferon Signaling to Promote Immune Evasion in Ovarian Cancer

peng deng、Jing Tan*

sun yat-sen university

Prevalent copy number alteration (CNA) is the most prominent genetic characteristic associated with ovarian cancer (OV) development, but its role in immune evasion has not been fully elucidated. In this study, we identified RAD21, a key component of the cohesin complex, as a frequently amplified oncogene that could modulate immnue response in OV. Through interrogating RAD21-regulated transcriptional program we found that RAD21 directly interacts with YAP/TEAD4 transcriptional co-repressors and recruits NuRD complex to suppress interferon (IFN) signaling. In multiple clinical cohorts, RAD21 overexpression is inversely correlated with IFN signature gene expression in OV. We further demonstrated in murine syngeneic tumor models that RAD21 ablation potentiated anti-PD-1 efficacy with increased intratumoral CD8+ T-cell effector activity. Our study identified a previously unrecognized RAD21-YAP/TEAD4-NuRD co-repressor complex in immune modulation, and thus provided a potential target and biomarker for precision immunotherapy in OV.

Key words: Copy number amplification, RAD21, immune invasion , Ovarian cancer

433. Next-generation sequencing-based identification of EGFR and NOTCH2 complementary mutations in non-small cell lung cancer

Lei Liu *

chengde medical college

Although targeted therapy has emerged as an effective treatment strategy for non-small cell lung cancer (NSCLC), some patients cannot benefit from such therapy due to the limited number of therapeutic targets. The present study aimed to identify mutated genes associated with clinicopathological characteristics and prognosis and to screen for mutations that are not concurrent with applicable drug target sites in patients with NSCLC. Tumor tissue and blood samples were obtained from 97 patients with NSCLC. A lung cancer-specific panel of 55 genes was established and analyzed using next-generation sequencing (NGS). The results obtained from the clinical cohort were compared with the NSCLC dataset from The Cancer Genome Atlas (TCGA). Subsequently, 25 driver genes were identified by taking the intersection of the 55 lung-cancer-specific genes with three databases, namely, the Catalog of Somatic Mutations in Cancer database, the Network of Cancer Genes database and Vogelsteins list. Functional annotation and protein-protein interaction analysis were conducted on these 25 driver genes. The $\chi 2$ test and logistic regression were used to evaluate the association between mutations in the 25 driver genes and the clinicopathological characteristics of 97 patients, and phosphatase and tensin homolog (PTEN) and kirsten rat sarcoma viral oncogene homolog (KRAS) were associated with stage at diagnosis and sex, respectively, while epidermal growth factor receptor (EGFR) was associated with sex, stage at diagnosis, metastasis, CEA and CYFRA21-1. Moreover, the association between the 25 driver gene mutations and overall survival were examined using Cox regression analysis. Age and Notch homolog 2 (NOTCH2) mutations were independent prognostic factors in TCGA dataset. The correlations between statistically significant mutations in EGFR, KRAS, PTEN and NOTCH2 were further examined, both in the clinical data and TCGA

dataset. There was a negative correlation between EGFR and NOTCH2 mutations (correlation coefficient, -0.078; *P*=0.027). Thus, the present study highlights the importance of NOTCH2 mutations and might provide novel therapeutic options for patients with NSCLC who do not harbor EGFR mutations.

Key words： next-generation sequencing, EGFR, mutation, non-small cell lung cancer

434. A "one-stop shop" decision tree for diagnosing and phenotyping polycystic ovarian syndrome on serum metabolic fingerprints

Ruimin Wang[1]、Lin Huang[1]、Kun Qian*[2]

1. Shanghai jiaotong University

2. State Key Laboratory for Oncogenes and Related Genes, School of Biomedical Engineering, Institute of Medical Robotics and Med-X Research Institute, Shanghai Jiao Tong University, Shanghai

Polycystic ovary syndrome (PCOS) is a common endocrine disease regulated by metabolic disorders, the effective intervention of which depends on diverse phenotypes (e.g., insulin resistance (IR)). Serum metabolic fingerprint (SMF) holds promise in characterizing the pathogenesis stress related to diseases; yet, PCOS diagnosis and phenotyping are time-consuming and challenging due to the lack of an integrated metabolic tool. Here, we introduce a nanoparticle-enhanced laser desorption/ionization mass spectrometry (NPELDI MS) platform for one-time serum metabolic fingerprinting, and identify the metabolic heterogeneity associated with obesity in PCOS patients. We construct a decision tree based on the acquired SMFs, and perform real-world simulation on independent internal and external cohorts. The decision tree yieldes the area under the receiver operating characteristic curves (AUC) of 0.967 for PCOS diagnosis and AUC of 0.898 for phenotyping, respectively. The technical robustness of the "one-stop shop" decision tree across laboratories is validated for clinical utility. The decision tree aims to improve PCOS management in comparison to clinical assessment, leading to a potential reduction in multiple blood tests and physician workload.

Key words: polycystic ovarian syndrome, serum metabolic fingerprints, mass spectrometry, diagnosis, phenotyping

435. Diagnosis and prognosis of breast cancer by high-performance serum metabolic fingerprints

Yida Huang、Kun Qian*

Shanghai Jiao Tong University

High-performance metabolic analysis is emerging in diagnosis and prognosis of breast cancer (BrCa). Still, advanced tools are in demand to deliver the application potentials of metabolic analysis. Here, we employed fast nanoparticle-enhanced laser desorption/ionization mass spectrometry (NPELDI-MS) to record serum metabolic fingerprints (SMFs) of BrCa in seconds, achieving high reproducibility and low consumption of direct serum detection without treatment. Subsequently, machine learning of SMFs generated by NPELDI-MS functioned as an efficient readout to diagnose BrCa from non-BrCa with an area-under-the-curve (AUC) of 0.948. Further, a metabolic prognosis scoring system was constructed using SMFs with effective prediction performance toward BrCa (p<0.005). Finally, we identified a biomarker panel of 7 metabolites that were differentially enriched in BrCa serum and their related pathways. Together, our work provided an efficient serum metabolic tool to characterize BrCa and highlighted certain metabolic signatures as potential diagnostic and prognostic factors of diseases including but not limited to BrCa.

Key words: Diagnosis, prognosis, breast cancer, serum metabolic fingerprints, mass spectrometry.

436. The m6A demethylase ALKBH5 promotes tumor progression by inhibiting RIG-I expression and interferon alpha production through the IKKε/TBK1/IRF3 pathway in head and neck squamous cell carcinoma

Hailong Ma*、Zhiyuan Zhang、Shufang Jin、Yue He、Jianjun Zhang

Department of Oral Maxillofacial-Head and Neck Oncology, Shanghai Ninth People's Hospital, College of Stomatology, Shanghai Jiao Tong University School of Medicine

Background: N6-methyladenosine (m6A) RNA modification plays a critical role in various physiological and pathological conditions. However, the role of m6A modification in head and neck squamous cell carcinoma (HNSCC) remains elusive.

Methods: In this study, the expression of m6A demethylases was detected by HNSCC tissue microarray. m6A-RNA immunoprecipitation (MeRIP) sequencing and RNA sequencing were used to identify downstream targets of ALKBH5.Comprehensive identification of RNA-binding proteins by mass spectrometry (ChIRP-MS) was used to explore them6A "readers". Tumor-infiltrating lymphocytes were analyzed in SCC7-bearing xenografts in C3H mice.

Results: Here, we demonstrate the downregulation of m6A status and upregulation of two demethylases in HNSCC. Silencing the m6A demethylase alkB homolog 5, RNA demethylase (ALKBH5) suppresses tumor progression in vitro and in vivo. m6A-RNA immunoprecipitation sequencing reveals that ALKBH5 downregulates the m6A modification of DDX58 mRNA. Moreover, RIG-I, encoded by the DDX58 mRNA, reverses the protumorigenic characteristics of ALKBH5. ChIRP-MS demonstrates that HNRNPC binds to the m6A sites of DDX58 mRNA to promote its maturation. ALKBH5 overexpression inhibits RIG-I-mediated IFNα secretion through the IKKε/TBK1/IRF3 pathway. The number of tumorinfiltrating lymphocytes in C3H immunocompetent mice is reduced by ALKBH5 overexpression and restored by IFNα administration. Upregulation of AKLBH5 negatively correlates with RIG-I and IFNα expression in HNSCC patients.

Conclusions: These findings unveil a novel mechanism of immune microenvironment regulation mediated by m6A modification through the ALKBH5/RIG-I/IFNα axis, providing a rationale for therapeutically targeting epitranscriptomic modulators in HNSCC.

Key words: ALKBH5, N6-methyladenosine, RIG-I, Interferon alpha, Head and neck squamous cell carcinoma

437. Monitoring retinoblastoma by machine learning of aqueous humor metabolic fingerprinting

Wanshan Liu、Kun Qian*

SJTU

The most common intraocular pediatric malignancy, retinoblastoma (RB), accounts for ~10% of cancer in children. Efficient monitoring is critical for management of RB but very challenging, which can enhance living quality of patients and 5-year survival ratio of RB up to 95%. However, due to the limitation of conventional detection methods, RB monitoring is still insufficient in regions with limited resources and the mortality may even reach over 70% in such areas. Here, we developed an RB monitoring platform by machine learning of aqueous humor metabolic fingerprinting (AH-MF), using nanoparticle enhanced laser desorption/ionization mass spectrometry (LDI MS). We recorded the direct AH-MF of RB free of sample pre-treatment, with both high reproducibility (coefficient of variation<10%) and sensitivity (low to 0.3 pmol) at sample volume down to 40 nL only. Meanwhile, the speed was within seconds per aqueous humor sample by on-chip microarrays toward large screening tests, while the throughput was sufficient with total ion count of ~108 and 228 m/z signals. Further, we differentiated early and advanced RB patients with area-under-the-curve over 0.9 and accuracy over 80%, through machine learning of AH-MF. Finally, we identified a metabolic biomarker panel of 7 metabolites through accurate MS and MS/MS with pathway analysis to monitor RB. Our work would contribute to advanced metabolic analysis of eye diseases including but not limited to RB and screening of new potential metabolic targets toward therapeutic intervention.

Key words: aqueous humor; metabolic fingerprinting; retinoblastoma; mass spectrometry; biomarkers

438. Integrated Machine Learning and Bioinformatic Analyses Constructed a Tumor immune microenvironment -Related Classifier to Predict Prognosis and Immunotherapy Responses for Hepatocellular Carcinoma Patients

Wangrui Liu*[1]、Tao Wang[1]、Jianfeng Xiang[1]、Jun Li[2]、Bo Zhai[1]

1. Affiliated Hospital of Youjiang Medical College for Nationalities

2. 上海第十人民医院

Background: The occurrence and development of hepatocellular carcinoma (HCC) is a complex biologic process, and the influence of tumor immune microenvironment (TIME) and malignant tumor phenotypes remains unclear.

Methods: Based on the immune-related indicators from ImmPort and InnateDB, we first clustered the samples and analyzed the differentially expressed genes among immune subtype using machine-learning methods. A total of 790 HCC samples from TCGA, LIRI-JP, GSE76427 were enrolled as discovering, testing and validation cohorts. ICI score was constructed based on Boruta algorithm and used to evaluate independent prognostic and predictive immunotherapy response implications.We also conducted clinical cohort verification at our center to prove the predictive effect of ICIscore on HCC.

Results: First, according to the immune gene expression level, immune cell abundance, immunescore and stromalscore, we obtained three independent immune subtypes with significance in survival and heterogeneity differences of HCC. Secondly, differentially expressed genes (DEGs) among 1022 immune subtypes divide HCC samples into three immune genotyping with significant difference in prognosis and TIME. Third, the ICI score, novel immunophenotyping of HCC, was established and significantly differs gender, stage, progression

and DNA variation profiles of HCC (p<0.05). Additionally, ICI score could markedly predict responses to immunotherapies via chemokine signaling, focal adhesion and JAK/STAT signaling pathways.

Conclusion: This study first describes that tumor microenvironment and immunophenotyping clusters improve the accuracy of the prognosis of HCC patients. The new independent prognostic indicators discovered in HCC highlight the relationship between tumor phenotype and the immune environment.

Key words: hepatocellular carcinoma, tumor microenvironment, immune checkpoint molecules, immunologic and hallmark gene sets,integrating machine learning

439. Comprehensive characterization of alternative splicing in in hepatocellular carcinoma

Shuai Zhao*[1]、Wangrui Liu[3]、Jun Li[2]、Jian Wang[1]

1. Xinhua Hospital Affiliated to Shanghai Jiaotong University School of Medicine

2. 上海第十人民医院

3. 上海交通大学医学院附属仁济医院(东院)

In hepatocellular carcinoma (HCC), alternative splicing (AS) is related to tumor invasion and progression. We used HCC data from a public database to identify AS subtypes by unsupervised clustering. Through feature analysis of different splicing subtypes and acquisition of the differential alternative splicing events (DASEs) combined with enrichment analysis, the differences in several subtypes were explored. Finally, in keeping with the differences between these subtypes, DASEs identified survival-related AS times, and were used to construct risk proportional regression models. In this study, AS was found to be useful for the classification of HCC subtypes, which changed the activity of tumor-related pathways through differential splicing effects, affected the tumor microenvironment, and participated in immune reprogramming. In summary, we described the clinical and molecular characteristics of HCC splicing subtypes, and constructed an extremely effective prognostic model, providing a new approach for the personalized treatment of HCC patients.

Key words: hepatocellular carcinoma; alternative splicing; subtype classification; pathway; immune system

440. A novel long noncoding RNA SP100-AS1 induces radioresistance of colorectal cancer via sponging miR-622 and stabilizing ATG3

You Zhou、Jingting Jiang*

Department of Tumor Biological Treatment, The Third Affiliated Hospital of Soochow University; Jiangsu Engineering Research Center for Tumor Immunotherapy; Institute of Cell Therapy, Soochow University, Changzhou, 213003, China

Although radiotherapy is an essential modality in the treatment of colorectal cancer (CRC), the incidence of radioresistance remains high clinically. Long noncoding RNAs (lncRNAs) reportedly play critical roles in CRC radioresistance by regulating genes or proteins at the transcriptional or post-translational levels. This study aimed to identify novel lncRNAs involved in radioresistance. We found that SP100-AS1 (lncRNA targeting antisense sequence of SP100 gene) was upregulated in radioresistant CRC patient tissues using RNA-seq analysis. Importantly, knockdown of SP100-AS1 significantly reduced radioresistance, cell proliferation, and tumor formation in vitro and in vivo. Mechanistically, mass spectrometry and bioinformatics analyses were used to identify the interacting proteins and microRNAs of SP100-AS1, respectively. Moreover, SP100-AS1 was found to interact with and stabilize ATG3 protein through the ubiquitination-dependent proteasome pathway. In addition, it could serve as a sponge for miR-622, which targeted ATG3 mRNA and affected autophagic activity. Thus, lncRNA SP100-AS1 could act as a radioresistance factor in CRC patients via RNA sponging and protein stabilizing mechanisms. In conclusion, the present study indicates that SP100-AS1/miR-622/ATG3 axis contributes to radioresistance and autophagic activity in CRC patients, suggesting it has huge prospects as a therapeutic target for improving CRC response to radiation therapy.

Key words: colorectal cancer, radioresistance, SP100-AS1, ATG3, autophagic activity

441. N6-methyladenosine demethylase FTO promotes growth and metastasis of gastric cancer via m6A modification of caveolin-1 and metabolic regulation of mitochondrial dynamics

You Zhou 、Jingting Jiang*

Department of Tumor Biological Treatment, The Third Affiliated Hospital of Soochow University; Jiangsu Engineering Research Center for Tumor Immunotherapy; Institute of Cell Therapy, Soochow University, Changzhou, 213003, China

Gastric cancer (GC) is the fifth most common tumor and the third most deadly cancer worldwide. N6-methyladenosine (m6A) modification has been reported to play a regulatory role in human cancers. However, the exact role of m6A in GC remains largely unknown, and the dysregulation of m6A on mitochondrial metabolism has never been studied. In the present study, we demonstrated that FTO, a key demethylase for RNA m6A modification, was up-regulated in GC tissues, especially in tissues with liver metastasis. Functionally, FTO acted as a promoter for the proliferation and metastasis in GC. Moreover, FTO enhanced the degradation of caveolin-1 mRNA via its demethylation, which regulated the mitochondrial fission/fusion and metabolism. Collectively, our current findings provided some valuable insights into FTO-mediated m6A demethylation modification and could be used as a new strategy for more careful surveillance and aggressive therapeutic intervention.

Key words: gastric cancer, N6-methyladenosine, FTO, caveolin-1, metastasis

442. TRIM27 Is an Adverse Prognostic Biomarker and its Association with Immune and Molecular Profile in Right-sided Colon Cancer

Minghui Zhang[1,2,3,4]、Bowen Yang[1,2,3,4]、Lingyun Zhang[1,2,3,4]、Xiaoyu Guo[1,2,3,4]、Guangwei Zhang[5]、Xiaofang Che[1,2,3,4]、Ce Li[1,2,3,4]、Kezuo Hou[1,2,3,4]、Xiaojie Zhang[1,2,3,4]、Jinglei Qu[1,2,3,4]、Ti Wen[1,2,3,4]、Xiujuan Qu*[1,2,3,4]

1. Department of Medical Oncology, The First Hospital of China Medical University

2. Key Laboratory of Anticancer Drugs and Biotherapy of Liaoning Province, The First Hospital of China Medical University, China Liaoning Province Clinical Research Center for Cancer, Shenyang, 110001, China

3. Liaoning Province Clinical Research Center for Cancer, Shenyang, 110001, China

4. Key Laboratory of Precision Diagnosis and Treatment of Gastrointestinal Tumors, Ministry of Education, Shenyang, 110001, China

5. Smart Hospital Management Department, The First Hospital of China Medical University, Shenyang,110001, China

Right-sided colon cancer (RCC), as an independent tumor entity, have a poor prognosis. It is imperative to find immune microenvironment-related genes for predicting RCC patients' prognosis and explore their function in RCC. Using weighted gene coexpression network analysis (WGCNA), differentially expressed analysis, and univariate Cox analysis, we identified tripartite motif-containing 27 (TRIM27) as a risk signature from The Cancer Genome Atlas (TCGA) and the Gene Expression Omnibus (GEO) datasets. It predicted a poorer overall survival and increased lymph node metastasis, which were then validated in our 48 clinical samples. Using immunohistochemistry (IHC), we found TRIM27 was highly expressed in both cancer cells and surrounding immunocytes, and its expression in tumor or immune cells both predicted a worse prognosis. Afterward, the functional mechanism, immune and molecular characteristics of TRIM27 were explored using GSEA, Estimate, Cibersort, and GSVA at the single-cell, somatic mutation, and RNA-seq level. Patients with TRIM27 high-expressed tumor cells presented lower CD4+ T cells infiltration and activation of the mTORC1/glycolysis pathway. In addition, TRIM27 high patients were characterized by hypermetabolism, higher tumor purity, more BRAF mutation,

and more chromosomal instability. Collectively, TRIM27 is an important immune-related prognostic biomarker in RCC patients. It may function via activating mTORC1/glycolysis pathway and suppressing $CD4^+$ T cells. These results suggest TRIM27 could be a promising therapeutic target in RCC.

Key words： right-sided colon cancer, tripartite motif-containing 27, immune related gene, prognostic biomarker, $CD4^+$ T infiltration

443. A copper-based biosensor for dual-mode glucose detection

Xiaoyu Xu*

Shanghai Jiao Tong University

Glucose is a source of energy for daily activities of the human body and is regarded as a clinical biomarker, due to the abnormal glucose level in the blood leading to many endocrine metabolic diseases. Thus, it is indispensable to develop simple, accurate, and sensitive methods for glucose detection. However, the current methods mainly depend on natural enzymes, which are unstable, hard to prepare, and expensive, limiting the extensive applications in clinics. Herein, we propose a dual-mode Cu_2O nanoparticles (NPs) based biosensor for glucose analysis based on colorimetric assay and laser desorption/ionization mass spectrometry (LDI MS). Cu_2O NPs exhibited excellent peroxidase-like activity and served as a matrix for LDI MS analysis, achieving visual and accurate quantitative analysis of glucose in serum. Our proposed method possesses promising application values in clinical disease diagnostics and monitoring.

Key words: Cu_2O Nanoparticle, colorimetric, mass spectrometry, glucose, biosensor.

444. Glaucoma characterization by machine learning of tear metabolic fingerprinting

Jiao Wu、Kun Qian*

Shanghai Jiao Tong University

Glaucoma is a common optic neuropathy disease affecting over 76 million people. Both timely diagnosis and progression monitoring are critical but challenging. Conventional characterization of glaucoma needs a combination of methods, calling for tedious procedures and experienced doctors. Herein, we built a platform through machine learning of tear metabolic fingerprinting (TMF) using nanoparticle enhanced laser desorption/ionization mass spectrometry. We obtained direct TMF noninvasively, with fast speed and high reproducibility, using trace tear samples (down to 10 nL). Consequently, we screened glaucoma patients against healthy controls with the area under the curve (AUC) of 0.866, through machine learning of TMF. Further, we differentiated primary open-angle glaucoma (POAG) from primary angle-closure glaucoma (PACG) and identified early-stage POAG. Finally, we constructed a biomarker panel of six metabolites for glaucoma characterization (including screening, subtyping, and early diagnosis) with AUC of 0.827-0.891, showing related metabolic pathways. Our work would provide insights into eye diseases not limited to glaucoma.

Key words: Glaucoma, Metabolic fingerprinting, Tear, Biomarkers, Mass spectrometry

445. Inhibiting ADRB2 signaling suppresses HCC chemoresistance by regulating HIF-1α expression

Fuquan Wu、Zhiyu Cao*

the Eighth Medical Center of PLA General Hospital

Background: Chemoresistance of hepatocellular carcinoma (HCC) is a major clinical problem. There has been evidence that adrenergic signaling is closely related to tumor progression as well as chemoresistance. The present study aims to determine the function of β2-adrenergic receptor (ADRB2) signaling in chemoresistance of HCC.

Methods: Change in proportion of ADRB2 positive cells in HCC cell lines undergoing chemotherapy was tested. The effects of inhibiting ADRB2 signaling on cisplatin and doxorubicin chemoresistance of HCC cells were then detected via in vitro proliferation and apoptosis assays. Subsequently, the expression of HIF-1α during this process was observed by western-blot assays. Moreover, the efficacy of inhibiting ADRB2 signaling on cisplatin chemoresistance of HCC cells was examined again after HIF-1α stabilization.

Results: The proportion of ADRB2 positive cells in HCC cell lines markedly increased in response to chemotherapy. ICI118,551-mediated inhibition of ADRB2 signaling further reduced the viability of HCC cells undergoing chemotherapy. Meanwhile, HIF-1α was confirmed to be further down-regulated. HIF-1α stabilization abolished the effect of blocking ADRB2 signaling on viability suppression of HCC cells undergoing chemotherapy.

Conclusion: Our data uncovers that inhibiting ADRB2 signaling plays a critical role in suppressing HCC chemoresistance via decreasing HIF-1α expression.

Key words: ADRB2, HCC, chemoresistance, HIF-1α

446. Plasmonic Alloys Reveal a Distinct Metabolic Phenotype of Early Gastric Cancer

Haiyang Su*

Shanghai Jiao Tong University

Gastric cancer (GC) is a multifactorial process, accompanied by alterations in metabolic pathways. Non-invasive metabolic profiling facilitates GC diagnosis at early stage leading to an improved prognostic outcome. Herein, mesoporous PdPtAu alloys are designed to characterize the metabolic profiles in human blood. The elemental composition is optimized with heterogeneous surface plasmonic resonance, offering preferred charge transfer for photoinduced desorption/ionization and enhanced photothermal conversion for thermally driven desorption. The surface structure of PdPtAu is further tuned with controlled mesopores, accommodating metabolites only, rather than large interfering compounds. Consequently, the optimized PdPtAu alloy yields direct metabolic fingerprints by laser desorption/ionization mass spectrometry in seconds, consuming 500 nL of native plasma. A distinct metabolic phenotype is revealed for early GC by sparse learning, resulting in precise GC diagnosis with an area under the curve of 0.942. It is envisioned that the plasmonic alloy will open up a new era of minimally invasive blood analysis to improve the surveillance of cancer patients in the clinical setting.

Key words: diagnosis, gastric cancer, metabolites, porous alloys, surface plasmon resonance

447. ADRB2 signaling promotes HCC progression and sorafenib resistance by inhibiting autophagic degradation of HIF1a

Fuquan Wu、Zhiyu Cao*

the Eighth Medical Center of PLA General Hospital

Background & Aims: Considerable evidence suggests that adrenergic signaling played an essential role in tumor progression. However, its role in hepatocellular carcinoma (HCC) and the underlying mechanisms remain unknown.

Methods: The effect of adrenaline in hepatocarcinogenesis was observed in a classical diethylnitrosamine-induced HCC mouse model. Effects of ADRB2 signaling inhibition in HCC cell lines were analyzed in proliferation, apoptosis, colony formation assays. Autophagy regulation by ADRB2 was assessed in immunoblotting, immunoflfluorescence and immunoprecipitation assays. In vivo tumorigenic properties and anticancer effects of sorafenib were examined in nude mice. Expression levels of ADRB2 and hypoxia-inducible factor-1a (HIF1a) in 150 human HCC samples were evaluated by immunohistochemistry.

Results: We uncovered that adrenaline promoted DEN-induced hepatocarcinogenesis, which was reversed by the ADRB2 antagonist ICI118,551. ADRB2 signaling also played an essential role in sustaining HCC cell proliferation and survival. Notably, ADRB2 signaling negatively regulated autophagy by disrupting Beclin1/VPS34/Atg14 complex in an Akt-dependent manner, leading to HIF1a stabilization, reprogramming of HCC cells glucose metabolism, and the acquisition of resistance to sorafenib. Conversely, inhibition of ADRB2 signaling by ICI118,551, or knockdown ADRB2 expression, led to enhanced autophagy, HIF1a destabilization, tumor growth suppression, and improved anti-tumor activity of sorafenib. Consistently, ADRB2 expression correlated positively with HIF1a in HCC specimens and was associated with HCC outcomes.

Conclusions: Our results uncover an important role of ADRB2 signaling in regulating HCC progression. Given the effificacy of ADRB2 modulation on HCC inhibition and sorafenib resistance,adrenoceptor antagonist appears to be a putative novel treatment for HCC and chemoresistance.

Lay summary: ADRB2 signaling played an essential role in sustaining hepatocellular carcinoma cell proliferation and survival. ADRB2 signaling negatively regulated autophagy, leading to hypoxia-inducible factor-1a stabilization, reprogramming of hepatocellular carcinoma cells glucose metabolism, and the acquisition of resistance to sorafenib. Adrenoceptor antagonist appears to be a putative novel treatment for hepatocellular carcinoma and chemoresistance.

Key words: ADRB2, HCC, autophagy, sorafenib, HIF1a

448. PRR15 deficiency facilitates malignant progression by mediating PI3K/AKT signalling and portends clinical efficacy and prognosis in triple-negative rather than non-triple-negative breast cancer

Fengzhu Guo[1]、Jialu Ma[2]、Shuning Liu[1]、Chunxiao Li[1]、Jiani Wang[1]、Jinsong Wang[1]、Zhijun Li[1]、Cong Li[1]、Jingtong Zhai[1]、Fangzhou Sun[1]、Yantong Zhou[1]、Changyuan Guo[1]、Haili Qian[1]、Binghe Xu*[1]

1. National Cancer Center/National Clinical Research Center for Cancer/Cancer Hospital, Chinese Academy of Medical Sciences and Peking Union Medical College

2. 河北医科大学

Background and aims： Triple-negative breast cancer (TNBC) is the most aggressive subtype of breast neoplasms with a higher risk of recurrence and metastasis compared with non-TNBC. Owing to the lack of effective receptor targets, conventional chemotherapy still represents the mainstay of therapeutic strategies combating TNBC, which is prone to being resistant to chemotherapeutic agents, thereby resulting in a dismal prognosis.

Methods： Bioinformatic analyses were performed for the identification of differentially expressed genes (DEGs), pan-cancer analysis, and partial mechanistic exploration. TNBC and non-TNBC cells with proline rich 15 (PRR15) knockdown/overexpression were constructed using lentivirus and applied to a vast array of *in vitro* and *in vivo* assays to determine the biological roles of PRR15, such as quantitative polymerase chain reaction, IncuCyte proliferation assay, wound

healing assay, transwell invasion assay, tumour xenografts, and pulmonary metastasis models. We also screened anti-neoplastics with higher inhibitory efficiency against PRR15-deficient TNBC through high-throughput drug sensitivity testing (397 compounds) and validated the underlying pathways via RNA sequencing, Western blot, immunohistochemistry, and pharmacological blockade in mice. Medical records and tumour tissues of patients with TNBC were collected and evaluated to investigate the clinical value of PRR15.

Results: To gain insight into the factors influencing the differences in malignant behaviours between TNBC and non-TNBC, we identified PRR15 as a DEG for the two, which was previously described as an oncogenic gene in breast cancer. However, we found that PRR15 showed decreased expression and anticipated a favourable prognosis in TNBC rather than non-TNBC. PRR15 loss significantly facilitated the proliferation, migration, and invasive ability of TNBC cells, which was abolished by PRR15 restoration, without marked effects on non-TNBC cells. PRR15 defect conferred on TNBC cells the potentiation of tumourigenesis and lung metastasis colonisation relative to the control group. Furthermore, PI3K/Akt signalling might be responsible for the aggressive properties regulated by PRR15 perturbation, which were verified via molecular biological and histopathological assessments. Meanwhile, the epithelial–mesenchymal transition effect was also implicated. Our TNBC cohort demonstrated PI3K/Akt activation in the tumour foci of patients with PRR15 downregulation, and PI3K inhibitor LY294002 reversed the lung metastatic capacity of TNBC in mice substantially. Moreover, in patients with TNBC, decreased PRR15 level was positively correlated with more aggressive clinicopathological characteristics, enhanced metastasis, and worse disease-free survival, with implications for chemotherapy efficacy.

Conclusions: Taken together, we examined the function of PRR15 in TNBC through laboratory experiments for the first time in this study. These findings reveal that PRR15 impairment promotes malignant progression by orchestrating PI3K/Akt signalling in TNBC rather than in non-TNBC, affects the response of TNBC cells to anti-tumour agents, and acts as a novel indicator of clinical therapeutic efficacy and disease outcomes in TNBC.

Key words: triple-negative breast cancer, PRR15, PI3K/Akt signalling, metastasis, drug sensitivity, prognosis

449. Study on novel fluorescent biosensors

Yubin Zhou*、Junting Liang、Xiaoxian Zhu、Qing Zhou、Huizhi Chen

Guangdong Medical University

Objective: Biosensors are a significant analytical approach, which have been widely applied in the field of food safety, environmental monitoring and disease diagnosis. Among the different types of biosensors, fluorescence-based biosensors have shown great potential in the application of analysis, owing to their advantages of simple design, rapid detection and high sensitivity. Currently, most of the fluorescent biosensors quantitate based on the absolute static fluorescence intensity. However, this mode may suffer the interference from some factors such as background fluorescence. Kinetic-based detection mode may be a solution to address the above-mentioned problem. This report will show some developed kinetic-based fluorescent biosensors and demonstrate their applications in the detection of different types of analytes (including tumor biomarkers).

Method: “Click-Chemistry” approach was employed for the efficient synthesis of several kinetic-based biosensors. The sensors were then characterized by a range of techniques to make sure they have the needed properties for biosensing. The developed sensors were tested in different analytes to demonstrate their sensing potential. Finally, qualitative and quantitative analysis were established.

Results: Several fluorescence kinetic-based biosensors have been successfully and characterized. The synthesized products were then characterized to present the required properties as biosensors. The biosensors are capable of qualitative and quantitative analysis for different analyses, which demonstrate the great potential of being a novel analytical approach. The sensitivity of the sensors needs to be further improved.

Conclusion: In the report, several fluorescent biosensors quantitated by kinetic mode have been successfully constructed. The sensing performance has been tested in different analytes. Theoretically, kinetic-based biosensing mode is not affected by the absolute statistic fluorescence intensity, which may address the issues such as background fluorescence interference. The kinetic-based biosensors are promising to be a novel biosensing platform.

Key words:biosensors; fluorescent sensors; kinetics; biomarkers

450. Hierarchical magnetic nanoparticles for highly effective capture of small extracellular vesicles

liang shi*

The Eighth Affiliated Hospital,Sun Yat-sen University

Small extracellular vesicles (EVs) have various functions through the transfer of specific biomolecules. However, it is still challenging to capture small EVs with high sensitivity and specificity. Herein, inspired by the unique burry structure and the strong adhesion ability of pollen grains, we presented a novel Fe3O4@MgSiO3 hierarchical magnetic nanoparticles (HNPs) as nanocarriers for the capture of small EVs. The NPs were generated through the solvothermal method and further modified with branching dendrimers to exhibit a hierarchical morphology. The enlarged surface area facilitated high-efficient capture of small EVs through specific recognition of aptamer probes and the small EVs surface markers. Besides, the magnetic core of the NPs allowed them to be isolated under the action of an external magnetic field, and thus the captured small EVs could be easily separated from plasma. These results indicated that the HNPs could serve as excellent nanocarriers for small EVs capture and related biomedical applications.

Key words: Small extracellular vesicles capture; Magnetic nanoparticles; Dendrimer; Aptamer; Hierarchical structure

451. mRNA sequencing and CyTOF analysis revealed ASPP2 altered the response patterns of hepatocellular carcinoma HepG2 cells to Usnic acid

Yang Wang、Liujia Chan、Yuheng Pang、Dexi Chen、Wenjing Wang*

Capital Medical University Beijing Youan Hpspital

Abstract

Objective: In this study, we had demonstrated that ASPP2 altered response of HepG2 cells to Usnic acid (UA) by using mRNA sequencing and CyTOF.

Materials and methods:CCK8 assay was used to detect cytotoxicity of UA on HepG2 cells. AnnexinV-RPE assay, and TUNEL assay, and cleaved caspase 3 assay were performed to examine the apoptotic cell death induced by UA. Transcriptomic sequencing and single cell of mass cytometry were used to analyze dynamic response of HepG2shcon and HepG2shASPP2 cells to UA treatment.

Results: We have demonstrated that UA could inhibit proliferation in HepG2 cells in a concentration-dependent manner. Apoptotic cell death was significantly induced by UA in HepG2 cells, while, knock down ASPP2 could increase resistance of HepG2 cells to UA. Data from mRNA-Seq indicated that knockout of ASPP2 in HepG2 cells affected cell proliferation, cycle and metabolism. ASPP2-knockdown resulted in increased stemness and decreased apoptosis of HepG2 cells under the action of UA. CyTOF analysis confirmed the above results, ASPP2-knockdown increased oncoproteins in HepG2 cells, and altered response patterns of HepG2 cells to UA .

Conclusion: Our data suggested that natural compound UA could inhibit liver cancer HepG2 cells, meanwhile, ASPP2-knockdown could affect response patterns of HepG2 cells to UA. The above results indicate that ASPP2 could be a research target in chemo-resistance of liver cancer.

Key words:RNA-Seq, CyTOF, Stemness, chemo-resistance

452. CD147 controls pancreatic cancer stem cell mitochondrial respiration and maintains stemness potentials via activating complex I core-subunit NDUFS1 mediated PAX2 demethylation

樊新宇、李玲*

空军军医大学

Background: Pancreatic cancer is a highly refractory malignant disease with metastasis and chemoresistance mainly derived from cancer stem cells (CSCs). Deregulating cellular energetics has recently emerged as a new hallmark of cancer. However, the attribution of pancreatic CSC metabolic characteristics to stemness potential maintaining and corresponding mechanisms are remained to be explored.

Methods: Pancreatic CSCs were obtained from patient-derived xenografts or cancer cells that enriched as tumorspheres or sorted as $ALDH^+$ subpopulation. Metabolic properties were assessed by OCR, ECAR and mitochondrial complex activities. Stemness potentials were analyzed by CSC ratios, tumorsphere formation, stemness gene expression and *in vivo* limiting dilution tumorigenesis assay. Bioinformatics data mining, transcriptome and methylation sequencing, PCR array, ChIP assay and multiplex fluorescence immunohistochemistry were performed to identify the mechanism of stemness enrichment by mitochondrial metabolism.

Results: Pancreatic CSCs preferred to undergo mitochondrial OXPHOS and maintained stemness by enhancing mitochondrial complex I activity. CD147 promoted stemness potentials and tumorgenicity of pancreatic CSCs by increasing OXPHOS and mitochondrial complex I activity. Complex I core-subunit NDUFS1 was significantly increased in pancreatic CSCs and mediated CD147 promoted stemness potential by enhancing SIRT1-DNMT1 induced-PAX2 demethylation. NDUFS1 was significantly correlated with CD147 in pancreatic cancer patient tissues and the co-expression was associated with poor patient survival. CD147 promoted NDUFS1 transcription via activating STAT3 phosphorylation.

Conclusion: This study demonstrated that CD147, highly expressed in pancreatic CSCs, enhanced SIRT1-DNMT1-PAX2 stemness signaling by promoting STAT3-NDUFS1 mediated complex I activity in mitochondrial OXPHOS. Our study suggests that targeting CD147 may become a novel therapeutic strategy for pancreatic cancer.

Key words: pancreatic cancer, cancer stem cell, mitochondrial OXPHOS, CD147

453. Estrogen receptor response gene EGR3 mediates breast cancer cell resistance to tamoxifen through promoting MCL1 transcription_2

Yu Xie*、Yue Wang、Junfang Qing、Mengci Yuan、Jing Yu

Nankai University

Background: Estrogen receptor (ER) positive breast cancer is a common disease in globally women, and endocrine therapy is a well-establish strategy. Currently, with widely application of endocrine medicine, drug resistance become an intractable problem increasingly. Early growth response protein (EGR) 3 is a well-established ER response factor. Whereas the role of EGR3 in ER-relevant endocrine therapy resistance is still confusing.

Purpose: We supposed EGR3 is a properly biomarker in endocrine therapy resistance which play a crucial role in resistant breast cancer cells. The study aims to investigate the necessity of EGR3 expression in resistant cells and clarify the mechanism of EGR3 mediating in tamoxifen treatment.

Methods: With the representativeness of tamoxifen in endocrine medicine, MCF7 and T-47D tamoxifen resistance cell lines was established. Firstly, EGR3 expression in tamoxifen treatment and resistant samples from the Gene Expression Omnibus database was re-analysis. The key role of EGR3 in resistance to tamoxifen treatment was investigated by manipulating expression. The responsibility of EGR3 to estrogen(E2)oestrone(E1)prolactin(PRL) action was detected by ligand stimulation. To clarify the EGR3 regulatory mechanism, the downstream factor was investigated and cell survival-related gene MCL1 was found. The function of EGR3 and MCL1 in resistance cells was investigated through tamoxifen-inducing apoptosis and proliferation assay. At the last, the action mechanism of EGR3 was investigated through CHIP and dual-luciferase report system.

Results: 1. EGR3 expression was higher in the tamoxifen treated and resistant samples. 2. With EGR3 knockdown, tamoxifen-resistant MCF7 cell line (MCF7-TamR) growth was impaired upon tamoxifen treatment; consistently, EGR3 forcing expressing given resistance to tamoxifen in MCF7. 3. Treating with estrone and estradiol, EGR3 expression was influenced by ER signaling both in MCF7 and MCF7-TamR and was aberrant in resistant cells. 4. MCL1 is the downstream effector in EGR3-regulated apoptosis and proliferation in tamoxifen resistance. 5. EGR3 functions as a transcriptional factor binding to the MCL1 promoter and facilitating MCL1 transcription.

Conclusion: EGR3 is a key factor participating in abnormal ER signal that attenuating tamoxifen-induced apoptosis and inhibition of proliferation through facilitating MCL1 transcription. The current study reveals the negative role of EGR3 in tamoxifen-induced cancer cell suppression, which makes clear that EGR3 is a good indicator and a potential target to improve endocrine therapy resistance.

Key words： Breast cancer; endocrine therapy resistance; estrogen receptor; tamoxifen; MCF7; EGR3; MCL1

454. A Four Oxidative Stress Gene Prognostic Model and Integrated Immunity-Analysis in Pancreatic Adenocarcinoma

Hao Wang[1,2]、Tian Ruo-Fei[1]、Liang Xue[1]、Fan Jing[1]、Duan Zi-Chuan[1]、Fan Xin-Yu[1]、Zhang Jia-Jia[1]、Chen Zhi-Nan[1,2]、 Yao Dong-Sheng[2]、 Li Ling*[1]

1. *National Translational Science Center for Molecular Medicine, Fourth Military Medical University*
2. *暨南大学细胞生物学系*

Objective: Pancreatic adenocarcinoma (PAAD) is a common gastrointestinal tumor with the poorest prognosis, is the seventh leading cause of cancer-related death in the world, with number of patients growing steadily. Oxidative stress has a great impact on various pathophysiological activities of cells, including the occurrence and development of tumors. However, the relationship between oxidative stress related genes and the with PAAD patients' prognosis remains to be explored thoroughly.

Materials and methods: The Cancer Genome Atlas (TCGA) included 170 pancreatic cancer tissue samples and 4 adjacent tissues samples, the 170 patients' RNA-Seq data were randomly divided into training set and validation set (106:64), the differential oxidative stress related genes (DEOSGs) were identified with a training set of TCGA database and three Gene Expression Omnibus (GEO) datasets (GSE28735, GSE62165 and GSE62452). Using univariate Cox regression analysis, Kaplan-Meier analysis and multivariate Cox regression analysis DEOSGs, to constructing a prognostic model for pancreatic adenocarcinoma and evaluated its predictive value. With the median value of risk score as the cut-off value, patients were classified into high and low risk groups, and then further gene set enrichment analysis (GSEA) was performed to clarify the differences of prognostic correlated signaling pathways in high risk and low risk groups. Furthermore, we analyzed the immune checkpoint related genes and synthetic driver genes of T cell proliferation in high and low risk groups. To validate the expression level of four prognostic genes in PADD, the protein expression of Model related genes in PADD were inquired in the CPTAC database (https://cptac-data-portal.georgetown.edu/). And, the mRNA levels of above four genes were determined with quantitative real-time PCR (qPCR) in 15 paired pancreatic cancer tissue/ adjacent tissues samples.

Results: In TCGA database, a total of 2994 genes were identified as DEGs at mRNA level. Three datasets in GEO were also screened and 4603, 7291 and 4428 genes were identified as DEGs in GSE28735, GSE62165 and GSE62452, respectively. 356 DEGs are shared by the four data sets, of which 55 genes were related to oxidative stress. a total of 52 genes were all used for further analysis, considering the gene expression level [mean value of fragments per kilobase of transcript per million mapped reads (FPKM)> 1]. 22 genes were identified as PAAD prognostic-associated genes with $P < 0.05$ by univariate cox regression analysis, 12 genes were retained through Kaplan-Meier analysis, then these genes were used for multivariate Cox regression analysis. Finally, four genes (MET, CDK1, CTTN, FYN) with $P < 0.1$ were selected to construct the prognostic model, the risk score of the model was calculated as follows: risk score= (0.8481 × MET expression) + (0.3674 × CDK1 expression) - (0.2532 × CTTN expression) - (0.7350 × FYN expression). In addition, time ROC analysis indicated that the prediction model was credible, as the areas under the curve (AUCs) of 1 and 2 years' survival for the training set were 0.87 and 0.91, and for the test set were 0.74 and 0.81. And further gene set enrichment analysis (GSEA) indicated

that lots of immune related pathways, metabolic pathways and DNA repair pathways were significantly enriched in the high risk group as compared with the low risk group. Immune infiltration analysis results shown that 23 out of 28 immune cells were significantly altered between high and low risk groups. 19 cells (Activated B cell, Activated CD8+T cell, Activated dendritic cell, Central memory CD4+T cell, Effector memory CD4+T cell, Effector memory CD8+T cell, Eosinophil, Immature B cell, Immature dendritic cell, Macrophage, Mast cell, MDSC, Monocyte, Natural killer T cell, Natural killer cell, Plasmacytoid dendritic cell, Regulatory T cell, T follicular helper cell, and Type 1 T helper cell) were negatively correlated with risk score. On the contrary, 4 cells that including CD56dim natural killer cell, Neutrophil, Type 17 T helper cell and Type 2 T helper cell were positively correlated with risk score (P <0.05). The results of differential expression analysis of 25 immune checkpoint genes showed that CD47, TNFSF9 and PVR were positively correlated with risk score; while HLA-DQB1, CD96, SIRPA, CD48, HLA-DRB1, BTN2A2, HLA-DOA, HLA-DPA1, HLA-DPB1, HLA-DMB, HLA-DMA, BTNL9, HLA-DRA, CD27 and HLA-DOB showed a opposite trend. For synthetic driver genes in T cell proliferation, LTBR, IL1RN, BATF, AHNAK, SLC10A7, CLIC1, RAN, CDK2, CDK1 and AHCY were positively correlated with risk score; while CXCL12, NFYB, FOSB, CYP27A1, GPD1 and ITM2A have a opposite trend. Final verification result that we found the protein levels of four prognostic genes in PADD were significantly enhanced in CPTAC database. Meanwhile, consistent with the protein levels results, the mRNA levels of MET, CDK1, CNND and FYN were all significantly upregulated in PADD as compare to adjacent tissues samples.

Conclusions: We have constructed an oxidative stress related prognostic model to predict the prognosis of PAAD patients. Further analysis indicated that the risk score was related to immune infiltration levels, especially the immune response and activation of T cells. Our work in this study might become a promising clinical guidance for individualized immunotherapy.

Key words: pancreatic adenocarcinoma, oxidative stress, survival, prognostic model, immune infiltration

455. Circular RNA TAF4B Promotes Bladder Cancer Progression by Sponging miR- 1298-5p and Regulating TGFA Expression

Xiaofeng Li 、Qiu Wang、Ling Ji*

Peking University Shenzhen Hospital

Background: Bladder cancer (Bca) is the most common malignant tumor of the urinary system. Circular RNAs (circRNAs) have been recognized as key regulators in tumorigenesis. However, the molecular mechanisms underlying circRNAs involved in the progression of BCa remain largely unknown.

Methods: We detected the expression level of circular RNA TAF4B (circTAF4B) by qRT- PCR assay. Cell proliferation was evaluated by CCK-8 and colony formation assays. Wound healing and Transwell assays were performed to measure cell migration and invasion capability. Moreover, we performed qRT-PCR and western blotting assays to determine the expression levels of epithelial-mesenchymal transition (EMT) markers. A nuclear/cytoplasmic fractionation assay was used to measure the subcellular location of circTAF4B. RNA pull-down and dual-luciferase reporter assays were used to detect the target microRNA of circTAF4B. A mouse xenograft model was produced to analyze the effect of circTAF4B on the tumorigenesis of BCa.

Results: In this study, we identified a novel circular RNA, circTAF4B, that is significantly upregulated in BCa and correlated with poor prognosis. Downregulated circTAF4B abolished the growth, metastasis and EMT process in BCa cells. Mechanistically, we found that circTAF4B facilitated the expression of transforming growth factor A (TGFA) by sponging miR-1298-5p. Finally, circTAF4B enhanced the proliferation and EMT process of BCa cells in vivo.

Conclusion: In summary, our study demonstrated that circTAF4B played a carcinogenic role in the growth, metastasis, and EMT process of BCa by regulating the miR-1298-5p/ TGFA axis. Thus, circTAF4B may become a diagnostic and therapeutic target for BCa.

Key words: Keywords: bladder cancer, circTAF4B, miR-1298-5p, TGFA, progression

456. Identification of the lipid metabolism related prognostic model in the Triple negative breast cancer

yang jun、jun yang*

Cancer Hospital of China Medical University

Background: Triple negative breast cancer (TNBC) is a highly heterogeneous disease with a high tumor mutation burden, which represents the worst outcome among all the breast cancer subtypes. The disturbed lipid metabolism is an early event in the development of tumor, which is related with the tumor metastasis and treatment drug-resistance. Our study aims to identify a lipid metabolism signature to predict prognosis and immunotherapy responses of TNBC patients.

Methods: We systematically analyzed 743 lipid metabolism related genes (LMRGs) of 223 samples in TNBC from TCGA datasets and screened out prognostic genes by univariate Cox regression. Unsupervised clustering was performed to stratify TNBC patients into different lipid metabolism patterns with distinct clinical characteristics. Lasso regression analyses and multivariate Cox regression were used to identify prognostic LMRGs. A lipid metabolism related risk model was constructed with 6 prognositc LMRGs and was validated in GSE135565.

Results: In our results, TNBC patients were stratified into 3 distinct clusters with LMRGs. Cluster 2 patients had the worst survival outcomes and Cluster 3 patients had the highest TMB and the lowest infiltrating immune cells. We also identified and validated a prognostic risk model based on six genes including ELOVL1, HSD11B2, ELOVL3, SLC27A2, SUMO2 and ARV1. The Risk-Score was demonstrated as a significant factor for prognosis, which was independent of clinical tumor-node-metastasis (TNM) stage. The Risk-Score was negatively correlated with infiltration levels of most immune cells, especially type 2 T helper cell and activated CD4 T cell. In addition, patients with lower Risk-Score had higher immune checkpoint genes (PD-1, PD-L1, PD-L2 and LAG3) expression and showed better efficacy from immunotherapy.

Conclusion: Our work elucidated the relevance of lipid metabolism genes and TNBC patient's prognosis. The risk model might be a promising tool for predicting prognosis and guiding personalized treatment for TNBC patients.

Key words: Triple negative breast cancer, lipid metabolism, molecular subtype, prognostic model, tumor microenvironment

457. NKD1 targets PCM1 to promote HHT therapeutic sensitivity of colorectal cancer via regulating cell cycle and apoptosis

Jia Cao、Rong Ma、Jia Wang、libin Wang*

General Hospital of Ningxia Medical University

Background: Colorectal cancer (CRC) is one of the most common malignant tumors with poor diagnosis and prognosis. Homoharringtonine (HHT) has a certain killing effect on a variety of solid tumors including CRC; Naked cuticle homolog 1 (NKD1) is abnormally expressed in many malignant tumors and closely related to tumor biological functions; However, whether NKD1 is involved in regulating the therapeutic sensitivity of HHT on CRC and underlying mechanism remain unclear.

Methods: CCK-8, clone formation and Edu experiments were used to detect the inhibitory effect of HHT on the proliferation of CRC cells; The effect of HHT on cell cycle and apoptosis were detected by immunoblotting, flow cytometry and immunofluorescence staining; Transcriptome sequencing and bioinformatics analysis screened drug delivery target NKD1 of HHT. The relationship between HHT and NKD1 was verified by RT-PCR, Western blot, loss of function in vitro and xenograft tumor formation in vivo. Quantitative proteomics were used to screen the biological function, signal pathway and downstream target protein PCM1. PRM, Western bolt and CO-IP, IF were verified the regulation and interaction relationship between NKD1 and PCM1. The degradation pathway of PCM1 was detected by MG132 and CHX. Loss of function or gain of function verified the effect of NKD1 combined with PCM1 on CRC cells proliferation, cell cycle and apoptosis.

Results: HHT significantly inhibited the cell proliferation and promoted cell cycle arrest and apoptosis; HHT suppressed the NKD1 expression in a concentration- and time-dependent manner. NKD1 was up-regulated in colorectal tumor tissues and cells, knockdown of NKD1 combined

with HHT promoted cell cycle arrest and apoptosis, indicating that NKD1 was involved in regulating the sensitivity of HHT to CRC treatment. HHT and NKD1 were both enriched in cell cycle and apoptosis biological processes, and leading to the decrease of PCM1 protein expression. Moreover, the NKD1 interacts with PCM1, and overexpression of PCM1 effectively reversed the promoting effects of HHT and NKD1 on CRC cell cycle and apoptosis.

Conclusion: HHT targeting NKD1 to inhibit the proliferation and promote apoptosis of CRC cells, and HHT-NKD1-PCM1 regulatory axis was involved in regulating the therapeutic sensitivity of HHT to CRC.

Key words: Colorectal cancer; NKD1; PCM1; cell cycle; apoptosis

458. Pan-cancer Analysis of magnesium-ITGAL and Its Positive Immune Effects in Head and Neck squamous cell carcinoma

hanxuan yang、zongwei huang、ying li、sufang qiu*

Clinical Oncology School of Fujian Medical University, Fujian Cancer Hospital

Background: Recent studies have proposed that Integrin subunit alpha L (ITGAL) is crucial to activate $CD8^+$ T cells by participating in magnesium-mediated immune synapse formation and specific cytotoxicity. However, the functional roles and regulated mechanisms of ITGAL in multiple cancers' immune microenvironment are largely unknown.

Aims: This study aims to analyse the relationship between ITGAL expression and Pan-cancer prognosis and immune microenvironment, and to provide a targeted antitumor strategy for ITGAL by influencing tumor immune microenvironment to treat head and neck cancer.

Methods: ITGAL expression in pan-cancer and the association with prognosis and immune microenvironment were identified by analyzing gene expression profiles from "TCGA" and "GEO" database with bioinformatics tools and methods.

Results: ITGAL was generally expressed in 27 pan-cancer tissues, and closely related to tumor prognosis. Analysis of "TCGA" and "GEO" databases by "Biomarker Exploration of Solid Tumors (BEST)" showed that high expression of ITGAL was associated with good prognosis in

CESC, LUAD, SARC, HNSC and SKCM. Among of these cancers, we used 2 algorithms for the functional enrichment and found ITGAL participated in immune regulation-related pathways, especially in leukocyte-mediated cytotoxicity, lymphocyte-mediated immunity, adaptive immune response, cytokine signaling in the immune system, antigen processing and presentation. Then, we used 4 algorithms for immune infiltration analysis, and found ITGAL was positively correlated with infiltration of B cells, $CD8^+$ T cells, $CD4^+$ T cells, M1 macrophages in tumor tissues. In order to further analyze the relationship between ITGAL and immune infiltration of HNSC, "IOBR" was used to showed that ITGAL was related to $CD8^+$T cell infiltration, T cell inflamed GEP and T cell inflamed. And it was validated with two immunotherapy cohorts. We divided the HNSC immune microenvironment into four types: immune-depleted(D), fibrotic(F), immune-enriched(IE), non-fibrotic and immune-enriched/fibrotic(IE/F), the results showed that ITGAL was closely related to IE， which is related to good prognosis. Single-cell analysis of HNSC showed ITGAL expression was the highest in $CD8^+$T cells. Finally, we found that, in HNSC, patients with high ITGAL expression were more likely to respond to Anti-PD-1/PD-L1 and Anti-PD-1 monotherapy.

Conclusion: ITGAL is significantly associated with $CD8^+$T cells and plays an important role in the tumor immune microenvironment of pan-cancer. Furthermore, our findings may provide a targeted antitumor strategy for ITGAL by influencing tumor immune microenvironment to treat head and neck cancer.Appendix:CESC: Cervical squamous cell carcinoma and endocervical adenocarcinoma LUAD: Lung adenocarcinoma SARC: Sarcoma HNSC: Head and Neck squamous cell carcinoma SKCM: Skin Cutaneous Melanoma

Keywords: ITGAL, Head and Neck squamous cell carcinoma, Pan-cancer, multi-omics, immunotherapy

459. Reciprocal Regulation of ASPM and Foxm1 Amplifies the Oncogenic Progression in Human Hepatocellular Carcinoma

Xunliang Jiang、Ke Wang、Jipeng Li*

Xijing Hospital of Fourth Military Medical University

Hepatocellular carcinoma (HCC) is a high-incidence tumor with an extremely poor prognosis. Fork-head box protein M1 (FoxM1) is an important transcriptional regulator, which promotes tumor progression in most cancers including HCC. However, the regulation mechanism of FoxM1 itself remains largely unclear. Here, we discovered a novel role of Abnormal spindle-like microcephaly（ASPM）in HCC, as a non-kinase protein that directly bind to FoxM1 and enhance its stability by preventing its proteasomal degradation. In addition, silencing ASPM in vivo and in vitro inhibited the proliferation and viability of HCC cells, while overexpression of ASPM had opposite effects. Furthermore, supplementation of FoxM1 could partially compensate for the weakened proliferative capacity of HCC caused by ASPM deletion. Meanwhile, FoxM1 also activated the expression of ASPM through transcription, thereby promoting the proliferation of HCC cells. Thus, the positive feedback loop between ASPM and FoxM1 continuously promote the progress of HCC. Besides, the ASPM-FoxM1 loop had been verified in clinical samples. Collectively, our study uncovers a previously unknown tightly coupled positive feedback signaling loop between ASPM and FoxM1,crucial for HCC progression. This positive feedback loop would be a very promising biomarker for HCC patients and an important potential therapeutic target.

Key words: human hepatocellular carcinoma; positive feedforward loop; transcription factor; FoxM1; protein degradation

460. TransLnc: a comprehensive resource for translatable lncRNAs extends immunopeptidome

Yongsheng Li*[1]、Dezhong Lv[2]、Zhenghong Chang[2]、Tao Pan[1]

1. Hainan Medical University

2. 哈尔滨医科大学

LncRNAs are not only well-known as non-coding elements, but also serve as templates for peptide translation, playing important roles in fundamental cellular processes and diseases. Here, we describe a database, TransLnc (http://bio-bigdata.hrbmu.edu.cn/TransLnc/), which aims to provide comprehensive experimentally supported and predicted lncRNA peptides in multiple species. TransLnc currently documents approximate 583,840 peptides encoded by 33,094 lncRNAs. Six types of direct and indirect evidences supporting the coding potential of lncRNAs were integrated, and 65.28% peptides entries were with at least one type of evidence. Considering the strong tissue-specific expression of lncRNAs, TransLnc allows users to access lncRNA peptides in any of the 34 tissues involved in. In addition, both the unique characteristic and homology relationship were also predicted and provided. Importantly, TransLnc provides computationally predicted tumour neoantigens from peptides encoded by lncRNAs, which would provide novel insights into cancer immunotherapy. There were 220 791 and 237 915 candidate neoantigens binding by major histocompatibility complex (MHC) class I or II molecules, respectively. Several flexible tools were developed to aid retrieve and analyse, particularly lncRNAs tissue expression patterns, clinical relevance across cancer types. TransLnc will serve as a valuable resource for investigating the translation capacity of lncRNAs and greatly extends the cancer immunopeptidome.

Key words: LncRNA; immune; MHC; immunopeptidome; cancer

461. CCDC65, A Gene Knockout That Leads to Early Death of Mice, Acts as A Potentially Novel Tumor Suppressor in Lung Adenocarcinoma

Ziyan Zhang、weiyi Fang*

Integrated Hospital of Traditional Chinese Medicine, Southern Medical University

CCDC65 is a member of coiled-coil domain-containing protein family and was only reported in gastric cancer by our group. We first observed that it is downregulated in lung adenocarcinoma based on TCGA database and immunohistochemistry. Reduced CCDC65 protein was shown as an unfavorable factor promoting the clinical progression in lung adenocarcinoma. Subsequently, $CCDC65^{-/-}$ mice were found possibly dead of hydrocephalus. Compared with the $CCDC65^{+/+}$ mice, the downregulation of CCDC65 in $CCDC65^{+/-}$ mice significantly increased the formation ability of lung cancer induced by urethane. In subsequent investigation, we observed that CCDC65 functions as a tumor suppressor repressing cell proliferation in vitro and in vivo. Molecular mechanism showed that CCDC65 recruits E3 ubiquitin ligase FBXW7 to induce the ubiquitination degradation of c-Myc, an oncogenic transcription factor in tumors, and reduces the binding with ENO1 promoter and thus suppresses the expression of ENO1 in mRNA level. In addition, CCDC65 also recruited FBXW7 to degrade ENO1 protein by ubiquitinated modulation. The downregulated ENO1 further reduced the phosphorylation activation of AKT1, which thus inactivated cell cycle signal. Our data demonstrated that CCDC65 is a potential tumor suppressor by recruiting FBWX7 to suppress c-Myc/ENO1-induced cell cycle signal in lung adenocarcinoma.

Key words: CCDC65; c-Myc; ENO1; Knockdown mice; Ubiquitin degradation; Cell cycle

462. Chemically synthesized cinobufagin suppresses nasopharyngeal carcinoma metastasis by inducing ENKUR to stabilize p53 expression

Rentao Hou、Weiyi Fang*

Cancer Center, Integrated Hospital of Traditional Chinese Medicine, Southern Medical University, Guangzhou, Guangdong, China.

Clinically, the metastasis of tumor cells is the key factor of death in patients with cancer. In this study, we used a model of metastatic nasopharyngeal carcinoma (NPC) to explore the effects of a new chemical, cinobufagin (CB), combined with cisplatin (DDP). We observed that chemically synthesized CB strongly decreased the metastasis of NPC. Furthermore, a better therapeutic effect was shown when CB was combined with DDP. Molecular analysis revealed that CB induced ENKUR expression by deregulating the PI3K/AKT pathway and suppressing c-Jun, an oncogenic transcriptional factor that binds to the ENKUR promoter and negatively modulated its expression in NPC. ENKUR as a tumor suppressor binds to MYH9 and decreases its expression by recruiting β-catenin via its enkurin domain to prevent its nuclear accumulation, which therefore suppresses c-Jun-induced MYH9 expression. Subsequently, downregulated MYH9 reduces the enlistment of E3 ligase UBE3A and thus decreases the UBE3A-mediated ubiquitination degradation of p53, a key tumor suppressor that decreases epithelial-mesenchymal transition (EMT). Clinical sample analysis demonstrated that the ENKUR expression level was significantly reduced in NPC tissues. Its decreased expression substantially promoted clinical progression and reflected poor prognosis for patients with NPC. This study demonstrated that CB induced ENKUR to repress the β-catenin/c-Jun/MYH9 signal and thus decreased UBE3A-mediated p53 ubiquitination degradation. As a result, the EMT signal was inactivated to suppress NPC metastasis.

Key words: Cancer cell metastasis; Cinobufagin; ENKUR; P53; Nasopharyngeal carcinoma

463. ENKUR expression induced by chemically synthesized cinobufotalin suppresses malignant activities of hepatocellular carcinoma by modulating β-catenin/c-Jun/MYH9/USP7/c-Myc axis

Rentao Hou、Weiyi Fang*

Cancer Center, Integrated Hospital of Traditional Chinese Medicine, Southern Medical University, Guangzhou, China

ENKUR plays a crucial role in lung and colorectal cancers. Chemically synthesized cinobufotalin(CB) showed its significant anti-cancer effect in nasopharyngeal carcinoma. However, the roles of ENKUR and CB along with their correlation are still unknown in hepatocellular carcinoma (HCC). In this study, ENKUR expression in HCC tissue and cells were detected. The relationship between ENKUR expression and clinical pathology was also assessed. In vivo and in vitro experiments were conducted to explore the effects and molecular basis of ENKUR and CB in HCC. ENKUR expression was correlated with HCC progression and patient prognosis. Furthermore, ENKUR could inhibit tumor proliferation, metastasis, and sorafenib resistance in HCC. Mechanistic studies showed that ENKUR or its Enkurin domain could bind to MYH9 and decrease its expression by binding to β-catenin and inhibiting its nuclear transfer, thus decreasing c-Jun level. Low expression of MYH9 suppressed recruitment of deubiquitination enzyme USP7, promoting degradation of the c-Myc. Therefore, cell cycle and EMT signals were suppressed. CB as a safe and effective anti-cancer compound up-regulates the expression of ENKUR via inhibiting PI3K/AKT/c-Jun-mediated transcription suppression. These findings show that ENKUR induced by CB antagonizes β-catenin/c-Jun/MYH9/USP7 pathway, thus increasing c-Myc ubiquitin degradation and finally suppressing cell cycle and EMT signals.

Key words: Chemically synthesized cinobufotalin, Hepatocellular carcinoma, Sorafenib, Malignant activities

464. Targeting acetylcholine signaling modulates persistent drug tolerance in EGFR-mutant lung cancer and impedes tumor relapse

Meng Nie、Na Chen、Zeping Hu*

Tsinghua University

Purpose: Although first-line epidermal growth factor receptor (EGFR) tyrosine kinase inhibitor (TKI) therapy is effective for treating EGFR-mutant non-small cell lung cancer (NSCLC), it is now understood that drug-tolerant persister (DTP) cells escaping from initial treatment eventually drives drug resistance.

Material and Methods: Integration analysis of metabolomics and transcriptomics on DTP cells and minimal residual diseases (MRD). Functional assays and mechanistic studies using genetic and pharmacological interventions with in vitro and in vivo models. Tumor tissue and plasma samples from clinical NSCLC patients were collected.

Results: We initially detected elevation of the neurotransmitter acetylcholine (ACh) levels in DTP cells. Extending these insights beyond in vitro work, we deployed EGFR-TKI-regressed mouse model and also found the accumulation of ACh. Plausibly explaining the elevated ACh levels that we detected in both cell lines and mice, we established that administration of EGFR-TKI caused upregulated expression of ACh biosynthesis enzyme choline acetyltransferase (ChAT) through YAP mediation. Genetic manipulation and pharmacological inhibition of ACh metabolism and signaling reduced DTP formation in vitro and in vivo. Furthermore, we demonstrated ACh mediated drug tolerance in part through WNT signaling in an ACh muscarinic receptor-3 (M3R)-dependent way, constituting the ACh-M3R-WNT axis. Importantly, plasma ACh levels and tumor ChAT expression of human NSCLC patients correlated with response to EGFR-TKI treatment and progression-free survival. Therapeutically, combination of EGFR-TKI with ACh/M3R signaling inhibition using the FDA-approved drug, Darifenacin, impeded tumor relapse in mice, demonstrating a prospective combination therapeutic strategy to manipulate the emergence of drug tolerance.

Conclusions: We identify the EGFR-TKI-induced ACh metabolism reprogramming pathway in DTP cells, which display a potential trigger of WNT signaling activation, an important contributor to drug tolerance. Moreover, this metabolic adaption during initial EGFR-TKI therapy implies that targeting ACh-M3R-WNT axis may represent a promising therapeutic modality to improve the efficacy of existing therapies. Taken together, our study provides a view for the design of more effective and personalized intervention strategies for patients receiving EGFR-TKI therapy.

Key words: Drug-tolerant persister, ACh metabolism reprogramming, EGFR-TKI therapy

465. Evolutionary metabolic landscape from preneoplasia to invasive lung adenocarcinoma

Meng Nie、Ke Yao、Zeping Hu*

Tsinghua University

Purpose: Metabolic reprogramming evolves during cancer initiation and progression. Before progression to invasive LUAD, there is step-wise evolution of pre-neoplasia and pre-invasive lesions, ranging from atypical adenomatous hyperplasia (AAH) to atypical pre-invasive adenocarcinoma in situ (AIS), minimally invasive adenocarcinoma (MIA), and eventually invasive adenocarcinoma (IAC). However, thorough understanding of metabolic evolution from preneoplasia to lung adenocarcinoma (LUAD) is still limited.

Materials and Methods: Large-scale targeted liquid chromatography-mass spectrometry (LC-MS)-based metabolomics analysis was performed on the tumor and paired normal adjacent tissue (NAT) obtained from a cohort (cohort 1) including 181 patients across different histological subtypes (n = 12 for AAH, n = 22 for AIS, n = 19 for MIA and n = 128 for IAC). In addition, we also characterized the dynamic alterations in circulating metabolites of plasma samples obtained from another independent cohort (cohort 2) including 92 patients across varying histological grades (n = 10 for benign diseases, n = 32 for AIS, n = 22 for MIA and n = 28 for IAC).

Results: We observe the progressive metabolic alterations from AAH to AIS, MIA, and IAC, suggesting that metabolic reprogramming emerges in premalignant lesions. Moreover, we reveal that different panels of circulating plasma metabolite biomarkers accurately distinguish early

LUAD and benign diseases, which holds promise for non-invasive and low-cost early diagnosis. Notably, metabolomics clustering of IAC patients identifies three metabolic subtypes (S-I, S-II, and S-III) with distinct clinical characteristics. Pathway enrichment analysis shows that bile acid metabolism is aberrantly activated in S-III compared to S-I and S-II, and associates with poor prognosis. Functionally, we demonstrate that modulating bile acid metabolism can affect the migration of LUAD.

Conclusions: The metabolomics analysis of patients with different stages deciphers evolutionary metabolic trajectory from preneoplasia to invasive LUAD, thus providing a comprehensive understanding of the neoplastic and invasive progression of LUAD and further offering an opportunity to expedite the translation of basic research to more precise diagnosis and therapy in the clinic.

Key words: Metabolic reprogramming, cancer initiation, cancer progression

466. N7-methylguanosine tRNA modification promotes esophageal squamous cell carcinoma tumorigenesis via the RPTOR/ULK1/autophagy axis

Hui Han、Shuibin Lin*

The first affiliated hospital, Sun Yat-sen University

Objective: Esophageal cancer is a deadly cancer that causes over 400,000 deaths worldwide annually and is therefore a great challenge for global health. It is of great significance to identify effective therapeutic targets for treatment of Esophageal cancer. Mis-regulated RNA modifications promote the processing and translation of oncogenic mRNAs to facilitate cancer progression, while the molecular mechanisms remain unclear. Here we sought to investigate the function and mechanisms of tRNA m^7G modification in regulation of cancerous mRNA translation and esophageal squamous cell carcinoma (ESCC) tumorigenesis.

Methods: ESCC clinical samples, ESCC cell lost-of-function and gain-of-function assays, xenograft models, conditional knockout and conditional knockin mice and in vivo ESCC initiation/progression models were used to study the physiological functions of tRNA m^7G

modification in ESCC tumorigenesis. tRNA modification and expression profiling, mRNA translation profiling and rescue assays were performed to uncover the underlying molecular mechanisms.

Results: We first analyzed the expression of tRNA m^7G methyltransferase complex proteins METTL1 and WDR4 using The Cancer Genome Atlas (TCGA) datasets and revealed that the mRNAs of both METTL1 and WDR4 are elevated in multiple cancers. Especially, METTL1 and WDR4 are significantly up-regulated in ESCCs and associated with poor ESCC prognosis. Using our cohort of ESCC samples, we further conformed that the m^7G tRNA modification and expression of METTL1/WDR4 in tumor tissues are up-regulated compared to their corresponding controls. Functionally, depletion of METTL1 or its partner WDR4 results to impaired proliferation and increased apoptosis of ESCC cells in vitro. Xenograft models revealed that targeting METTL1 inhibited the tumorigenesis of ESCC cells in vivo. Notably, forced expression of wild type METTL1 but not its catalytic inactive mutant could promote ESCC cell proliferation and colony-formation, suggesting that the tRNA m^7G methyltransferase activity of METTL1 is essential for its function in promoting ESCC progression. We further analyzed the m^7G tRNA modification and expression profiling using our previously established TRAC-seq (tRNA reduction and cleavage sequencing) method and identified 19 m^7G-modified tRNAs. Our TRAC-seq data demonstrated that METTL1 knockdown leads to reduced tRNA m^7G modification and m^7G-modified tRNA expression. Moreover, polyribosome-bound mRNAs sequencing (polyribosome-seq) revealed that METTL1 depletion selectively reduces the mRNA translation of a subset of oncogenic transcripts, including the genes related to mTOR signaling and autophagy in m^7G related codon dependent manner. Rescue assays revealed that overexpression of RPTOR or knockdown of ULK1 inhibited the hyperactivated autophagy and rescued the impaired proliferation of ESCC cells, suggesting that RPTOR/ULK1/autophagy axis is an essential downstream target that facilitates METTL1's function in regulation of ESCC progression. Furthermore, in vivo ESCC initiation and progression studies using *Mettl1* conditional knockout and knockin mice uncovered the critical oncogenic function of METTL1 in promoting ESCC tumorigenesis.

Conclusions: METTL1/WDR4 mediated tRNA m^7G modification promotes ESCC initiation and progression through RPTOR/ULK1/autophagy axis. Our data uncovered novel molecular insights

into the tRNA modification in regulation of selective oncogenic mRNA translation and ESCC tumorigenesis, suggesting that targeting METTL1 and its downstream signaling axis could be a promising strategy for ESCC treatment.

Key words: METTL1; N7-methylguanosine; autophagy; RPTOR; esophageal squamous cell carcinoma

467. Development and clinical validation of a novel microfluidic-based platform for CTC detection and downstream molecular analysis

Heng Zou、Yuan Wang、Wenchong Zhang、Tao Xu*

晶准生物医学（深圳）有限公司

Background: Circulating tumor cells (CTCs), which are the key to cancer metastasis, carry abundant cellular and genetic information of primary and metastasis tumor sites, and are promising biomarkers for cancer screening, diagnosis, monitoring, and prognosis in clinical utility. The sensitivity, specificity, and downstream analysis are critical for the clinical applications of CTCs. However, most current methods can only provide cell counting, lacking the capability for downstream genetic analysis, which is far from the clinical needs. Only by fully exploiting the multidimensional characteristics of CTCs, could it be more useful in clinical practice for improving the treatment design for personalized medicine.

Methods: In this work, an inertial focusing-based microfluidic platform was designed for CTCs isolation and characterization. Buffy coats layer was collected by density gradient centrifugation from the 4 mL blood samples. Our platform would enrich target CTCs, which are 13-15 μm in size, in 15 mins. Immunofluorescence staining was performed using anti-CD45, anti-Pan-CK, and anti-N-Cadherin to identify CTCs in epithelial and mesenchymal states. Anti-PD-L1, anti-HER2, and anti-VEGF were used for PD-L1, HER2, and VEGF proteins assessment in the clinical experiment, respectively. Then, AO/PI staining was performed to evaluate the integrity and viability of CTCs, which is essential for downstream analysis. To validate the clinical utility, CTCs were isolated from patients of various cancer types, stages, and treatments. After enrichment,

CTCs were collected by a single cell picking system and then performed qPCR on the genetic mutations, including EGFR (19del), KRAS (G12D), and BRAF (V600E).

Results: CTCs were enriched and identified in 567 patients with a CTCs positive rate (≥1/4mL) as high as 95.1%. An IF protocol was established to identify the collected tumor cells with the criteria defined as follows: PanCK+, DAPI+, CD45- cells with the nucleus to a cytoplasmic ratio greater than 0.8. After enrichment from our platform, CTCs demonstrate a normal morphology under the microscope, and 90.55 ± 4.79% of CTCs are alive. These results indicate that our platform was able to enrich CTCs from clinical samples and maintain their integrity and viability of CTCs. Furthermore, genetic mutations of EGFR (19del), KRAS (G12D) and BRAF (V600E) could be successfully detected in lung cancer and colorectal cancer samples, consistent with clinical tissue detection. Only one exception is different from the tissue sample, mainly due to tumor heterogeneity.

Conclusions: This novel microfluidic-based platform for enrichment and identification of CTCs demonstrated the diagnostic value for clinical utility. The high integrity and viability of enriched CTCs enable downstream molecular analysis, e.g., genetic mutations. Our results demonstrate the great prospect of genotyping, providing a reliable approach for guiding precise oncotherapy, especially for patients whose tissue biopsies are unavailable.

Key words: microfluidic platform, circulating tumor cells, CTC enrichment, molecular analysis

468. Genome-wide CRISPR/Cas9 library screening identified critical drivers for cisplatin resistance in ESCC

Peipei Zhang、Weiguang Zhang、Junfei Jiang、Mingqiang Kang*

Fujian Medical University Union Hospital

Background: Esophageal squamous cell carcinoma (ESCC) is a highly lethal and common tumor. Cisplatin is an essential drug in the treatment of advanced ESCC. However, ESCC is also resistant to cisplatin, so it is important to explore the molecular mechanism of its resistance.

Methods: MTT assays was used to detect the resistance concentration of Ec109 cell to cisplatin. Genome-wide CRISPR/Cas9 library (GeCKO) was used to construct stably transfected cells. Cells were cultured with cisplatin IC_{20}, and harvested for sgRNA sequencing after 10 passages. The differential genes were ranked using the robust rank aggregation (RRA) algorithm of the MAGeCK software, and the RRA score represented the importance of the gene. GO and KEGG were used in the follow-up bioinformatics analysis.

Results: The IC_{50} and IC_{20} concentrations of the Ec109 cells against cisplatin were 3.72 ug/mL and 1.32 ug/mL. According to the negative screening strategy, 839 differential genes were identified; according to the positive screening strategy, 801 differential genes were identified (p value<0.05). Activation of the mitophagy pathway was found in the resistance of Ec109 cells to cisplatin. Ulk1, BNIP3, RHOT2 and ATG9A exert critical roles in the resistance.

Conclusion: Some genes including Ulk1, BNIP3, RHOT2 and ATG9A, related to the mitophagy pathway, may be involved in the resistance of ESCC to cisplatin.

Key words: Esophageal squamous cell carcinoma (ESCC); cisplatin; CRISPR/Cas9; mitophagy

469. Clinical and prognostic significance of perioperative change in red cell distribution width in patients with esophageal squamous cell carcinoma

宋倩*

中国科学院大学附属肿瘤医院（浙江省肿瘤医院）

Background: Numerous studies reported the prognostic significance of the red cell distribution width (RDW) in patients with esophageal squamous cell carcinoma (ESCC), while the relationship between perioperative change in red cell distribution width and survival of patients with ESCC after surgery has not been assessed.

Methods： A total of 594 patients with newly diagnosed ESCC after surgery were enrolled in the study. Perioperative change in red cell distribution width (delta RDW) (delta RDW=Post-RDW–Pre-RDW) was counted according to data within one week before surgery and

two weeks after surgery. The median of delta RDW was selected to be the cut off value to investigate the relationship between delta RDW and Overall survival (OS).

Results： 99 (16.7%) patients had pathological stage 1a-1b, 202 (34.0%) patients had pathological stage 2a-2b, and 293 (49.3%) patients had pathological stage 3a-3c.There were 179 (30.1%) patients who had vessel invasive, and 415 (69.9%) patients without vessel invasive. There were 216 (36.4%) patients who had nerve infiltration, and 378 (63.6%) without nerve infiltration. In univariate analysis, five parameters including delta RDW(≥0.44 vs.<0.44) (*P*=0.039, HR= 1.337, 95% CI=1.014-1.762) significantly correlated with worse OS. Multivariate analysis revealed that delta RDW(≥0.44 vs.<0.44) was an independent prognostic marker for OS (*P=0.033*, HR= 1.356, 95% CI=1.025-1.793). Kaplan-Meier curves shown that delta RDW≥0.44 was significantly associated with worse OS (*P*= 0.039).

Conclusions: Perioperative change in red cell distribution width predicts worse survival in patients with ESCC after surgery.

Key words: red cell distribution width, esophageal squamous cell carcinoma, perioperative change, survival, prognosis

470. Overexpression of PLCG1 is associated with Esophageal Squamous Cell Carcinoma (ESCC) Proliferation and Migration

Weiguang Zhang*、Peipei Zhang、Junfei Jiang

Fujian Medical University Union Hospital

Background: The occurrence and development of esophageal squamous cell carcinoma (ESCC) involve multiple factors. Despite the progress made in diagnosis and treatment, the prognosis of esophageal cancer is still dismal. Potential avenues for the treatment of ESCC can be discovered by improving our understanding of key processes in ESCC progression. PLCG1 has been reported to influence the biological behaviors of tumors, such as tumor growth, invasion, and metastasis, which are key in promoting tumor development. However, the effect of PLCG1 on the malignant biological behavior of ESCC has not been clarified.

Methods: Datasets were downloaded from The Cancer Genome Atlas (TCGA) and GEPIA2 to analyze PLCG1 expression. ESCC Cancerous and Para cancerous tissues were analyzed by qRT-PCR, Western Blot, and IHC. Furthermore, we assessed the relationship between the PLCG1 expression and patient prognosis. The effect of silencing the PLCG1 gene on the proliferation, migration, and invasive ability of EC109 cells were investigated by Cell Counting Kit-8 (CCK8), Wound-healing, and Cell migration assays, respectively.

Results: Based on TCGA and GEPIA2 datasets, PLCG1 expression was upregulated in ESCC and correlated with poor prognosis. Moreover, PLCG1 expression was related to the TNM staging. We also found that PLCG1 mediated the proliferation and migration of ESCC in vitro.

Conclusions: Our data demonstrate that PLCG1 can be considered a potential biomarker and a potential therapeutic target for ESCC.

Key words: PLCG1; Esophageal Squamous Cell Carcinoma; Proliferation; Migration

471. Super enhancer-driven genes-based identification of serum EFNA1 and MMP13 as potential biomarkers for early detection of esophageal squamous cell carcinoma

Lingyu Chu[1,2]、hao chen[3]、wangkai Fang[2]、chaoqun Hong[1]、haiying Zou[2]、yuhui Peng[1]、fangcai Wu[1]、yiwei Xu*[1]、jianjun Xie[2]

1. Department of Clinical Laboratory Medicine, the Cancer Hospital of Shantou University Medical College

2. 汕头大学医学院

3. 中山大学肿瘤防治中心（中山大学附属肿瘤医院、中山大学肿瘤研究所）

Background: Super-enhancers (SEs) play a key role in promoting cancer progression. Here, we aimed to identify secreted proteins encoded by SE-driven genes as diagnostic biomarkers for esophageal squamous cell carcinoma (ESCC).

Methods: We integrated ChIP-Seq, secretome data, GEO data and Kaplan-Meier survival analysis to screen protential secreted proteins encoded by SE-driven genes. Using enzyme-linked immunosorbent assay (ELISA), targeted secreted proteins were selected in a small size of samples and varified in a multi-center validation stage (345 in test cohort and 231 in validation cohort).

Receiver operating characteristics (ROC) curve were used to calculate diagnostic accuracy. Change in serum levels of targeted secreted proteins were further analyzed in 85 ESCC patients before and after surgery.

Results: EFNA1, MMP13, PROC and SEMA3C were identified as secreted proteins encoded by SE-driven genes, but only serum EFNA1 and MMP13 had significantly higher levels in patients with ESCC compared to normal controls (p<0.05). ROC curve showed that EFNA1 combined with MMP13 provided an area under the curve (AUC) of 0.809, 54.0% sensitivity and 90.5% specificity in the test cohort, and could differentiate early-stage ESCC patients from normal controls (0.797, 51.1%, and 90.5%). Similar results were obtained in the validation cohort (0.806, 42.6%, 89.4%, and 0.831, 48.1%, 89.4%). In addition, the levels of serum EFNA1 and MMP13 were significantly reduced after surgical resection (p<0.05).

Conclusions: Our study suggested that EFNA1 and MMP13 as secreted proteins encoded by SE-driven genes might help to diagnose early-stage ESCC.

Key words: esophageal squamous cell carcinoma; early diagnosis; super-enhancers; EFNA1; MMP13

472. LSD1-Demethylated LINC01134 Promotes Oxaliplatin Resistance by Facilitating SP1-mediated P62 Transcription in Hepatocellular Carcinoma

Chunyuan Xue、Luyuan Ma、Nan Huo、Xiaofeng Kang、Zhong Chu、Xiaojie Xu*

Institute of Bioengineering, Academy of Military Medical Sciences, Academy of Military Sciences

Background and aims: Oxaliplatin (OXA) is one of the most commonly-used chemotherapeutics in advanced HCC, the resistance of which poses a big challenge. Long non-coding RNA (lncRNA) plays a vital role in chemoresistance. Therefore, elucidating the underlying mechanisms and identifying predictive lncRNAs for OXA resistance is needed urgently.

Methods: RNA-Seq and fluorescence in situ hybridization (FISH) were utilized to investigate the OXA-resistant lncRNA. Survival analysis was to determine the significance of LINC01134 and p62 expression. Luciferase, RIP and ChIP assay were to explore the mechanisms of LINC01134

regulating p62 expression. Effects of LINC01134/SP1/p62 axis on OXA resistance were evaluated by viability, apoptosis assay and mitochondrial function characterized by GSH/GSSG ratio, oxygen consumption rate (OCR), mitochondrial membrane potential (MMP) and mitochondrial morphology. Xenografts were used to estimate in vivo regulation of OXA resistance by the axis. ChIP, cell viability and xenograft assay were to identify the demethylase for upregulating LINC01134 in OXA resistance.

Results: LINC01134 was identified as one of the most upregulated lncRNAs. Higher expression of LINC01134 predicted poorer OXA-therapeutic outcome. LINC01134 upregulated p62 expression and positively correlated with anti-oxidative pathway by recruiting SP1 transcription factor to p62 promoter. LINC01134/SP1/p62 axis regulates OXA resistance by altering apoptosis, intracellular ROS production and mitochondrial homeostasis both in vitro and in vivo. Demethylase LSD1 was responsible for LINC01134 upregulation in OXA-R cells. Clinically, LINC01134 expression was positively correlated with p62 and LSD1 while SP1 positively correlated with p62 expression in HCC.

Conclusions: We established LSD1/LINC01134/SP1/p62 as a critical axis for HCC OXA resistance. Evaluating LINC01134 expression in HCC will be effective to predict OXA effect. For treatment-naive patients, targeting LINC01134/SP1/p62 axis may be a promising strategy to overcome HCC chemoresistance.

Key words: LINC01134, SP1, p62, hepatocellular carcinoma, Oxaliplatin

473. Cerebrospinal fluid circulating tumor DNA contributes to the detection and characterization of leptomeningeal metastasis in non-small cell lung cancer

Qian Miao*、gen lin、xinlong zheng、xiaobin zheng、longfeng zhang、kan jiang、biao wu、yiquan xu

Fujian Cancer Hospital

Background: Cerebrospinal fluid (CSF) reveals a unique genetic signature of Leptomeningeal metastases (LM) and has a potential role as a source of liquid biopsy in non-small cell lung cancer (NSCLC) patients. However, studies in patients with LMs are scarce.

Methods: Patients with LM from NSCLC were retrospectively analyzed. Circulating tumor DNA (ctDNA) of CSF and paired extracranial tumor or plasma were tested by next-generation sequencing (NGS). Clinical outcomes were compared with Kaplan-Meier log-rank test and Cox proportional hazards methodologies.

Results: We reviewed charts of 80 patients with LM treated at Fujian Cancer Hospital. A total of 57 CSF and of which 30 contemporaneously paired CSF and extracranial samples tested by NGS were analyzed. Mechanism of resistance to targeted therapy, such as concomitant T790M and T797S mutation, MET dysregulation, and the co-occurrence of tumor protein p53 gene (TP53) plus retinoblastoma 1 (RB1) loss, revealed in CSF. Most interestingly, ctDNA of CSF revealed EGFR mutations in 4 patients previously diagnosed with wild-type and prolonged survival with targeted therapy. In matched genetic profile of CSF and extracranial lesions, CSF showed superior sensitivity and abundant dysregulation of cell cycle regulator Copy Number Variations (CNVs), lower T790M mutation and higher EGFR amplification, while MYC amplification was significantly differentially expressed. After the diagnosis of LM, the median overall survival (OS) was 14.1 months [95% confidence interval (CI): 10.7–17.5 months]. Univariate analyses and multivariate Cox analyses demonstrated that patients with CDKN2A/CDKN2B co-mutation had inferior median OS compared without CDKN2A/2B mutations and with unknown (7.2 versus 17.1 versus 12.1 months, P=0.013).

Conclusions: CSF-based ctDNA testing contributes to the phenotypic detection and unique characterization of resistance mechanisms of LM in NSCLC. CDKN2A/2B mutation maybe a poor prognostic factor in LM patients.

Key words: Non-small cell lung cancer (NSCLC); leptomeningeal metastasis (LM); cerebrospinal fluid (CSF); circulating tumor DNA (ctDNA)

474. Liquid Biopsy for Predicting Postoperative Recurrence in Patients with Non-Small Cell Lung Cancer

Heng Zou、Chongwen Zhang、Yuan Wang、Tao Xu*

晶准生物医学（深圳）有限公司

Background： Lung cancer is one of the most common malignant cancers. Non-small cell lung cancer (NSCLC) accounts for about 80% of all lung cancers and there is no efficient clinical methods or indicators that could predict the recurrence risk of NSCLC patients after surgery. In this study, we combined microfluidic-based circulating tumor cells (CTCs) enumeration and microRNA-223 (miR-223) testing to evaluate the clinical values of liquid biopsy in predicting the recurrence in NSCLC patients.

Method: The whole blood samples were obtained from 60 early-stage NSCLC patients at ShenZhen Cancer Hospital Chinese Academy of Medical Sciences, People's Hospital of Maoming, and The First Affiliated Hospital of Guangdong Pharmaceutical University between December 2018 and October 2020. CTCs and serum mir-233 were tested one day before and 2 months after the surgery. CTCs were isolated by the inertial focusing-based microfluidic platform (CTC100, Cellomics). The platform would enrich target CTCs, which are 13-15 μm in size, in 15 mins. Immunofluorescence staining was performed using anti-CD45, anti-Pan-CK, and anti-N-Cadherin to identify CTCs in epithelial and mesenchymal states. Serum mir-233 was evaluated by real time quantitative polymerase chain reaction (qPCR). The Kaplan-Meier curves were used to evaluate relapse-free survival (RFS) and compared by the log-rank test.

Result： Compare to the pre-surgical level, CTCs and mir-233 decreased significantly in NSCLC patients that received surgical treatment. Kaplan-Meier curves showed that the RFS was

significantly longer in patients with decreased CTCs (p=0.041), and in patients with decreased miR-223 (p=0.014). Patients were further categorized by the change of CTCs and miR-223, Kaplan-Meier curves demonstrated that the patients with increased level of both CTCs and miR-223 had significant shorts RFS than the rest of patients (p=0.013).

Conclusion： Both CTCs and mir-233 significantly decrease in NSCLC patients who received surgical treatment. The change of CTCs enumeration and mir-233 level are both predictive of outcome in NSCLC patients receiving surgical therapies. By combining the CTCs enumeration and mir-233, we successfully developed a liquid-biopsy based predictor that may be used to assess the risk of post-operative recurrence in NSCLC patients.

Key words: Liquid biopsy; NSCLC; microfluidic; circulating tumor cell; microRNA-223; relapse -free survival

475. PCMT1 has potential prognostic value and promotes cell growth and motility in breast cancer

Yiwei Lin、Fangcai Wu、Yixuan Zhuang、Lingyu Chu、Tianyan Ding、Qiqi Qu、Xinhao Li、Yukun Cui、Chaoqun Hong*

the Cancer Hospital of Shantou University Medical College

Breast cancer (BC) is one of the frequently diagnosed cancer, and the leading cause of cancer-related death among women worldwide. The roles of protein L-isoaspartate (D-aspartate) O-methyltransferase (PCMT1) in human cancer have been exploring, however, the clinical significance and biological function of PCMT1 in BC are not yet clear. In this study, immunohistochemical assay was carried out to detected the expression of PCMT1 protein in 221 cases of BC tissues, and its correlation with clinicopathological parameters and prognosis of patients were further analyzed. Loss-of-function studies were conducted to explore the biological function of PCMT1 in regulating cell growth, migration, and invasion of MCF-7 cell. In our results, we found that PCMT1 protein was located in the cytoplasm of breast cancer cells, and PCMT1 expression was only obviously correlated with progesterone receptor expression of patients (p<0.05). Based on the TCGA-BRCA data set, the results showed that high expression of

PCMT1 gene was significantly correlated with shorter overall survival (OS), disease specific survival (DSS) and progress free survival (PFS) of breast cancer patients. Survival analysis showed that PCMT1 protein high-expression was an independent unfavorable prognostic factor for breast cancer patients. The in vitro experiments revealed that PCMT1 could regulate growth, migration and invasion capacity of MCF-7 cell, and modulate the expression of AKT/GSK3β/mTOR signaling pathway, EMT and cell cycle-associated protein. In conclusion, PCMT1 was an potential unfavorable prognostic biomarker for BC patient and might influence the AKT/GSK3β/mTOR signaling pathway to regulate the growth and motility of MCF-7 cell.

Key words: PCMT1, breast cancer, prognosis, cell growth, cell motility

476. Prognostic value of lipid metabolism-related genes and serum ApoA1 in patients with NSCLC

Ping Lu [1]、Lingyi Xiong[1]、Xinjun Liang*[2]

1. Hubei Cancer Hospital, the Seventh Clinical School Affiliated of Tongji Medical College, Huazhong University of Science and Technology, Wuhan, China

2. 湖北肿瘤医院

Objective: Altered lipid metabolism exhibited by cancer cells, this study was conducted to explore the prognostic values of lipid metabolism-related genes and serum lipids for non-small-cell lung cancer (NSCLC) patients.

Methods: Differential expression of the lipid metabolism-related genes were conducted by tumor immune estimation resource (TIMER) analysis. The gene expression profiling interactive analysis (GEPIA) tool was used to confirm the differential gene expression levels of lipid metabolism-related genes in lung adenocarcinoma (LUAD) and lung squamous cell carcinoma (LUSC). Using a Kaplan-Meier plotter (K-M plotter), the prognostic value of lipid metabolism-related genes was assessed. In addition, a retrospective study was conducted on patients with stage IV NSCLC diagnosed in Hubei Cancer Hospital. The chi-squared and Fisher's exact probability tests were used to analyze count data. Survival curves were analyzed using the Kaplan-Meier. The Cox regression model was used to analyze the prognosis value of serum lipids.

Results: TIMER dataset showed that expressions of CD36, LDLR, ACSS2, FASN and SCD were relatively low in both LUAD and LUSC, whereas ACLY exhibited significantly elevated expression. The GEPIA tool identified CD36 and ACSS2 as having downregulated expression in both LUAD and LUSC. Interestingly, we observed that high expression of CD36 had positive impacted on OS in LUAD (P= 0.01, HR= 0.66 (0.49 – 0.91)), while a negative impact in LUSC was exhibited (P= 0.01, HR= 1.43 (1.09 – 1.87)). According to the results of chi-square test and Fisher's exact test, ApoA1 was significantly related to gender (P<0.01), smoking status (P= 0.02), drinking status (P= 0.04), CHOL (P<0.001), TG (P<0.01), HDL-C (P<0.001) and LP(a) (P<0.001). High ApoA1 was associated with poor OS (ApoA1: 25.2 vs 31.2 months, P= 0.02) in univariate analysis. Multivariate Cox Regression model confirmed that ApoA1 was an independent prognostic factors for OS (P= 0.03, HR= 1.74, 95% CI: 1.07–2.83).

Conclusion: These findings suggest that lipid metabolism-related genes and serum lipids can be used as prognostic biomarkers for determining prognosis in NSCLC.

Key words: Lung cancer; Lipid Metabolism; Gens; Serum lipids; Survival Prognosis

477. Ferroptosis-related lncRNAs as prognostic signatures in cervical cancer

Songtao Han[1]、Senyu Wang[2]、Yangchun Feng*[3]

1. Traditional Chinese Medicine Hospital Affiliated to Xinjiang Medical University

2. 新疆医科大学第二附属医院

3. 新疆医科大学附属肿瘤医院

Background： Cervical cancer is one of the most common gynecological tumors. Second, ferroptosis is an iron-dependent new type of programmed cell death that is different from apoptosis, necrosis, and autophagy, and plays a role in ischemic organ damage and cancer.

Methods： In this study, multi-data mining was performed to identify ferroptosis-related lncRNAs in cervical cancer patients through expression and regulatory relationships.304 patients were divided into training set (n=210) and validation set (n=94). A prognostic model was constructed on

the training set, and prognostic efficacy, relationship between clinicopathological features, and immune infiltration analysis were evaluated.

Results： In this study, a Risk score prognostic model was constructed. The five-year survival prognostic AUC values of the model in the training set and validation set were 0.741 and 0.792, respectively. The Kruskal-Wallis test found that Risk score constructed by ferroptosis-related lncRNAs was significantly related to the clinicopathological characteristics of cervical cancer. Through the analysis of immune infiltration, it was found that the gene expression of TNFRSF18 immune checkpoint was different under the Risk score grouping. Finally, it was verified from TCGA and clinical samples that the MYOSLID gene was up-regulated in cervical cancer tissues.

Conclusion： The Risk score model constructed by ferroptosis-related lncRNAs can be used as an important indicator of the prognosis of cervical cancer, and the differential expression of MYOSLID gene in cervical cancer has been found.

Key words： Cervical cancer, Ferroptosis, lncRNA, Prognosis, MYOSLID, Cancer therapy

478. The diagnostic value of serum IGFBP1 in patients with colorectal cancer

Laifeng Wei*

Jiangmen Central Hospital Affiliated to Sun Yat-sen University

Objective: Colorectal cancer (CRC) is one of the most common malignant cancers in the world with high incidence and mortality. It is necessary to explore novel biomarkers for early detection of CRC. Some literatures have reported that the levels of circulating insulin-like growth factor binding protein-1 (IGFBP-1) were increased and showed a diagnostic value in some malignancies. However, the relationship between IGFBP-1 expression and CRC, especially about the diagnostic value, is rarely reported. Therefore, this study aimed to assess the diagnostic performance of IGFBP-1 in patients with CRC.

Methods: Firstly, the IGFBP-1 expression profile data of peripheral blood of CRC patients were downloaded from GEO database, and its expression and diagnostic efficacy in colorectal cancer were analyzed. Secondly, serum IGFBP-1 levels were detected by enzyme-linked immunosorbent

assay (ELISA) in 138 colorectal cancer patients and 190 normal controls. Receiver operating characteristic curves were applied to calculate the accuracy of diagnosis.

Results: In the GEO dataset GSE164191, statistical analysis found that blood IGFBP-1 mRNA expression level was higher in CRC patients compared to normal controls (P=0.027, The ROC curve analysis showed an area under the curve (AUC) of 0.600 (95%CI: 0.4980-0.7012), a sensitivity of 20.33% and a specificity of 90.16% for distinguishing CRC from normal controls. In addition, the levels of serum IGFBP-1 protein in the CRC group were significantly higher than that in normal controls group (P<0.0001). The diagnostic value of serum IGFBP1 was demonstrated by ROC. Versus normal group, the AUC of all CRC was 0.874 (95% CI: 0.835-0.932) and early-stage colorectal cancer was 0.812 (95% CI, 0.795-0.908). With an optimized cutoff of 1294.1060 ng/mL, IGFBP-1 showed certain diagnostic value with specificity of 90.53%, sensitivities of 63.04% and 55.88% in CRC and early-stage CRC, respectively. Clinical data analysis showed that the levels of IGFBP-1 were significantly associated to age (p<0.05) and gender (p<0.05).

Conclusions: Our study demonstrated that IGFBP-1 might be served as a potential biomarker for the diagnosis of early-stage CRC.

Key words: colorectal cancer, IGFBP-1, serum, biomarker, diagnosis

479. DNMT3B-mediated FAM111B methylation promotes papillary thyroid tumor glycolysis, growth and metastasis

xiaofeng kang、Xiang Zhu、Chunyuan Xue、Nan Huo、Yuchen Han、Yimeng Du、Xiaojie Xu*

军事医学研究院

Over the past decades, the incidence of thyroid cancer (TC) rapidly increased all over the world, with the papillary thyroid cancer (PTC) accounting for the vast majority of TC cases. It is crucial to investigate novel diagnostic and therapeutic targets for PTC and explore more detailed molecular mechanisms in the carcinogenesis and progression of PTC. Based on the TCGA and

GEO databases, FAM111B is downregulated in PTC tissues and predicts better prognosis in PTC patients. FAM111B suppresses the growth, migration, invasion and glycolysis of PTC both in vitro and in vivo. Furthermore, estrogen inhibits FAM111B expression by DNMT3B methylation via enhancing the recruitment of DNMT3B to FAM111B promoter. DNMT3B-mediated FAM111B methylation accelerates the growth, migration, invasion and glycolysis of PTC cells. In clinical TC patient specimens, the expression of FAM111B is inversely correlated with the expressions of DNMT3B and the glycolytic gene PGK1. Besides, the expression of FAM111B is inversely correlated while DNMT3B is positively correlated with glucose uptake in PTC patients. Our work established E2/DNMT3B/FAM111B as a crucial axis in regulating the growth and progression of PTC. Suppression of DNMT3B or promotion of FAM111B will be potential promising strategies in the estrogen induced PTC.

Key words: Papillary thyroid cancer; FAM111B; DNMT3B; Glycolysis; Estrogen

480. microRNA-569 inhibits tumor metastasis in pancreatic cancer by directly targeting NUSAP1

ce li、Xiujuan Qu*、Xiaohui Guo

the First Hospital of China Medical University

MicroRNAs (miRNAs) are known to be involved in the development and progression of pancreatic cancer (PC). In this study, the prognostic significance and mechanistic role of microRNA-569 in PC were explored. Quantitative real-time PCR was used to detect the expression of microRNA-569 in PC tissues and cell lines. Scratch test and Transwell assay were conducted to detect migration and invasion ability. The xenograft nude mice model was used to determine tumor metastasis in vivo. The direct targets of microRNA-569 were determined by using bioinformatics analysis and a dual-luciferase reporter assay. The expression level of microRNA-569 was down-regulated in PC patients with a poor prognosis. In vitro and in vivo experiments indicated that over-expression of microRNA-569 inhibited the migration and invasion of PC cells. MicroRNA-569 negatively regulated NUSAP1 by directly binding its untranslated region. Further mechanism research implied that the ZEB1 pathway was involved in

microRNA-569/NUSAP1 mediation of the biological behaviors in PC. These data demonstrated that microRNA-569 may exert a tumor-suppressing effect in PC and maybe a potential therapeutic target for PC patients.

Key words: miR-569, NUSAP1, pancreatic cancer, metastasis, ZEB1

481. Systematic analysis of cuproptosis-related long non-coding RNA predicting prognosis in patients with lung squamous cell carcinoma

Shanxiu Jin[1,2]、Cheng Du*[1]

1. 中国人民解放军北部战区总医院

2. 大连医科大学

Background： Cuproptosis is a newly proposed copper dependent cell death mode that induces protein toxic stress and eventually leads to cell death. The main mechanism is that CU^{2+} directly combines with the ester acylation components in the tricarboxylic acid cycle. Therefore, regulating cuproptosis in tumor cells is a new therapeutic approach. we will discuss whether cuproptosis related lncrna can be used to predict the prognosis of patients with lung squamous cell carcinoma（LSCA）.

Methods： A total of 19 genes related to cuproptosis（NFE2L2、NLRP3、SLC31A1、FDX1…) were identified through previous published articles. A total of 16 lncRNAs related to cuproptosis were identified by screening with the correlation coefficient of 0.4. The information of 504 lung squamous cell carcinoma patients were downloaded from TCGA public database and analyzed in R language (R version 4.2.1). We randomly divided them into train set and test set. The prognosis model was constructed by lasso-Cox regression in the train set and verified in the test set. In addition,the biological functions of the characterized lncRNAs were analyzed by Gene Ontology (GO) and Kyoto Encyclopedia of Genes and Genomes (KEGG).The gene mutation analysis obtained information on genetic alterations from the cBioPortal database. Finally,the relationship between characterized lncRNAs and immune checkpoint was also discussed.

Results： We finally identified four lncRNAs prognostic marker（AC079414.3、AC019080.1、AL449423.1、AC002467.1）for model construction, and divided them into high-risk and low-risk groups according to the median value. Kaplan-Meier analysis revealed hat the overall survival (P=0.002) and progression free survival (p<0.001) between the high- and low-risk groups was statistically significant. The areas under the ROC curve in one year, three years and five years are 0.603, 0.630 and 0.603. Univariate and multivariate Cox regression analysis also revealed that risk score was an independent prognostic factor. In the model we constructed, there was significant difference in tumor mutation burden between high-risk and low-risk groups (p<0.001). Patients with high and low tumor mutation burden who had low risk scores also had better prognosis (p<0.001). The main mutations were TTN and TP53 gene mutations in LUSC patients. In addition , the immune function was analyzed by heatmap, and it was found that the immune function of high-risk group was more active. Some immune checkpoint genes were significantly different between the two groups (p<0.05). Patients in the high-risk group responded better to immunotherapy than those in the low-risk group. Finally , we also found that risk scores were significantly associated with drug sensitivity in LUSC.

Conclusion: We investigated the potential mechanisms of LUSC development from the perspective of cuproptosis-related lncRNAs,and identified 4 lncRNAs as biomarkers to predict the prognosis of LUSC patients.

Key words: lung squamous cell carcinoma, cuproptosis, lncRNAS , TCGA , prognostic marker

482. FERMT1 expression and correlated gene regulation in bladder urothelial carcinoma by bioinformatics analysis

ce li、Xiujuan Qu*、Xiaohui Guo

the First Hospital of China Medical University

Fermitin family member 1(FERMT1) is a member of the fermitin family, includes a FERM domain and a pleckstrin homology domain.Abnormal FERMT1 expression is associated with carcinogenesis.We used sequencing data from the Cancer Genome Atlas database(TCGA) and Gene Expression Omnibus(GEO) to analyze FERMT1 expression and gene regulation networks in

bladder urothelial carcinoma (BLCA).Expression was analyzed by GEPIA and Oncomine database,and its relationship with clinical pathological parameters was identified by UALCAN database.Then,FERMT1 alteration landscape was described by cBioPortal database.Differential gene expression with FERMT1 was analyzed by LinkedOmics ,while protein-protein interaction and TF-miRNA network were identified by using NetworkAnalyst.Consistently,TIMER database was applied to assess correlations between FERMT1 expression and tumor immune infiltration level.FERMT1 was found up-regulated with amplification in tumor tissues in multiple BLCA cohorts. A significant association was found between the expression of FERMT1 and the pathological indicators of BLCA patients.Regulator networks revealed several key genes and transcript factor POU3F2 interacted with FERMT1 in BLCA.Notably, FERMT1 expression has significant correlation with B cells' and CD8+T cells' infiltrating levels .Our results demonstrate that data mining efficiently reveals information about FERMT1 expression and potential regulatory networks in BLCA,which laid a solid foundation for deep research of the role of FERMT1 in carcinogenesis.

Key words : FERMT1; PDAC

483. Identification of a Novel Tumor Mutation Burden and Major Histocompatibility Complex-Related Score to Predict Prognosis and Immunotherapy Response in Gastric Cancer

Kanghui Xiang[1,2,3,4]、ti wen*[1,2,3,4]

1. The First Hospital of China Medical University

2. Key Laboratory of Anticancer Drugs and Biotherapy of Liaoning Province, The First Hospital of China Medical University, Shenyang, China

3. Liaoning Province Clinical Research Center for Cancer, The First Hospital of China Medical University, Shenyang, China

4. Key Laboratory of Precision Diagnosis and Treatment of Gastrointestinal Tumors, Ministry of Education, The First Hospital of China Medical University, Shenyang, China

Tumor burden mutation (TMB) may predict clinical response to immune-checkpoint blockade (ICB) in STAD, whereas it only reflects tumor characteristics and could not alone optimally identify patients who benefit from ICB. Therefore, we take into account the molecular characteristics of the tumor (TMB) and the host (Major Histocompatibility Complex) to develop a novel TMB and MHC-related score (TMS) to predict overall survival (OS) and sensitivity to ICB of patients with gastric cancer. Differentially expressed gene and univariate cox analyses were used to derive TMB-, MHC-I, and MHC-II-related hub genes in The Cancer Genome Atlas (TCGA) database. The Least Absolute Shrinkage and Selection Operator (LASSO) analysis was applied for further selection and the selected genes were inputted into stepwise regression to develop TMS which was validated in Gene Expression Omnibus (1) datasets. The patient's response to immunotherapy was inferred by the tumor immune dysfunction and exclusion (TIDE) score and immunophenoscore (IPS) and validated in the Kim cohort. TMS was developed based on AKAP5, HBA2, HCAR1, INHA, HABP2, and PRICKLE1. Furthermore, higher TMS was identified as a poor factor for OS in TCGA and GEO datasets. According to the TIDE score and IPS, patients with lower TMS would react to immunotherapy better. Notably, in the Kim cohort,

the TMS beat the TMB, microsatellite instability (MSI) status, and Epstein-Barr virus (EBV) status on the receiver operating characteristic curve, indicating that a lower TMS was associated with better responses to ICB. Higher TMS is also associated negatively with the abundance of CD8+ T cells, M1 macrophages, and other immune cells. In the high-TMS group, several genes from the human leukocyte antigen family and immunological checkpoints were less expressed. According to our findings, a lower TMS may imply better OS outcome and immunotherapy response.

Key words: Gastric cancer; Tumor mutation burden; Major histocompatibility complex; Prognosis; Immunotherapy response

484. Construction and validation of an immune gene signature in esophageal cancer

Jinhong Zhu*

Harbin Medical University Cancer Hospital

Background: Esophageal cancer (EC) is one of the deadliest solid malignancies, mainly consisting of esophageal squamous cell carcinoma (ESCC) and adenocarcinoma (EAC). Robust biomarkers that can improve patient risk stratification are needed to optimize cancer management. We sought to establish potent prognostic signatures with immune-related gene (IRG) pairs for ESCC and EAC.

Methods: We obtained differentially expressed IRGs by intersecting the Immunology Database and Analysis Portal (ImmPort) with the transcriptome data set of The Cancer Genome Atlas (TCGA)-ESCC and EAC cohorts. A novel rank-based pairwise comparison algorithm was applied to select effective IRG pairs (IRGPs), followed by constructing a prognostic IRGP signature via the least absolute shrinkage and selection operator (LASSO) regression model. We assessed the predictive power of the IRGP signatures on prognosis, tumor-infiltrating immune cells, and immune checkpoint inhibitor (ICI) efficacy in EC. Kaplan-Meier survival analysis and receiver operating characteristic curves (ROC) were used to evaluate the clinical significance of IRGPs.

Univariate and multivariate Cox regression analyses were performed to investigate the association of overall survival (OS) with IRGPs and clinical characteristics.

Results: We built a 19-IRGP signature for ESCC (n=75) and a 17-IRGP signature for EAC (n=78), with an area under the ROC curve (AUC) of 0.931 and 0.803, respectively. IRGP signature-derived risk scores stratified patients into low- and high-risk groups with significantly different OS in ESCC and EAC (P<0.001). Nomogram and decision curve analysis were used to evaluate the clinical relevance of the prognostic signatures, achieving a C-index of 0.973 in ESCC and 0.880 in EAC. The risk scores were associated with immune and ESTIMATE (Estimation of STromal and Immune cells in MAlignant Tumor tissues using Expression data) scores and the composition of immune cells in the tumor microenvironment. The association between risk score and human leukocyte antigens (HLAs), mismatch repair (MMR) genes, and immune checkpoint molecules demonstrated its predictive value for ICI response. Differential immune characteristics and predictive value of the risk score were observed in EAC.

Conclusions: The established immune signatures showed great promise in predicting prognosis, tumor immunogenicity, and immunotherapy response in ESCC and EAC.

Key words: Esophageal cancer (EC); immune-related gene pair; prognosis; signature

485. Bioinformatic analysis of lncRNA HAR1A and experimental validation

Jinhong Zhu*

Harbin Medical University Cancer Hospital

Background: With an attempt to identify causal genes for NSCLC by mining public databases, we found that lncRNA Highly Accelerated Region 1A (HAR1A) is significantly downregulated in lung adenocarcinoma (LUAD) and negatively associated with prognosis. This study aimed to validate the implication of the LncRNA HAR1A in NSCLC tumorigenesis.

Methods: The impacts of lncRNA HAR1A on proliferation and apoptosis NSCLC cells as well as downstream signaling pathways were examined by CCK-8 assay, flow cytometry, and western blot. The tumor-suppressing potential of lncRNA HAR1A was further investigated in the

xenograft nude model. RNA-sequencing data from The Cancer Genome Atlas (TCGA) was used for Bioinformatics analysis. We built a predictive signature with lncRNA HAR1A-related gene using the LASSO COX regression model. Nomogram and decision curve analysis were used to assess the risk model's discrimination ability and clinical benefit. The R package pRRophetic was used to examine whether this signature can predict patient response to anti-tumor drugs.

Results: We found that knockdown of lncRNA HAR1A accelerated NSCLC cell proliferation but inhibited apoptosis, whereas the depletion of the lncRNA HAR1A led to the opposite results. LncRNA HAR1A regulated cellular activities through the STAT3 signaling pathway. Moreover, in vivo experiments demonstrated that infection with lentiviral lncRNA HAR1A significantly suppressed the tumorigenic capacity of NSCLC cells. Moreover, in silico analysis indicated that a 23-gene signature derived from lncRNA HAR1A-related cancer cell survival genes discerned LUAD patients with a significantly higher risk of inferior overall survival. The risk score was an independent predictor of prognosis in LUAD after adjusting for clinical characteristics. Nomogram and DCA confirmed that the signature performed robustly in predicting overall survival. Furthermore, the signature could also distinguish LUAD patients who were more likely to benefit from chemotherapy or targeted therapies.

Conclusions: our results suggest that lncRNA HAR1A functions as a tumor suppressor in NSCLC by regulating the STAT3 signaling pathway. LncRNA HAR1A may be a novel therapeutic target for NSCLC. The gene signature of lncRNA HAR1A-related cancer cell survival genes was robustly predictive of prognosis and sensitivity to anti_x0002_tumor drugs.

Key words: LncRNA HAR1A, STAT3, proliferation, prognostic signature, LUAD

486. ARA55 participates in TGFβ1-induced epithelial-mesenchymal transition in CNE2 nasopharyngeal carcinoma cells

Zhaolei Cui、Yan Chen*

Fujian Cancer Hospital

Objective: ARA55 (androgen receptor coactivator 55kDa protein) was first identified as a TGFβ1-inducible protein and function as a molecular scaffold in coordinating protein-protein interactions. Herein, we focused on validating the functional role of ARA55 in TGFβ1-induced epithelial-mesenchymal transition (EMT) in human CNE2 nasopharyngeal carcinoma cells.

Methods: Expression of ARA55 in the CNE2 cells was stimulated by TGFβ1 (5ng/ml), and a commercial RNA interference plasmid (siRNA-ARA55) was utilized to silence ARA55 expression in response to TGFβ1 induction.

Results: Our results manifested that forced expression of ARA55 enhances growth as well as migration and invasion of the CEN2 cells. In contrast, cells depleted of ARA55 resulted in suppressed cell proliferation and metastasis capability, along with a down-regulation of N-cadherin and up-regulation of Claudin-1. Further co-immunoprecipitation analysis exhibited that induced ARA55 yields a direct physical interaction with Smad7 in TGFβ1 signaling.

Conclusions: Our data demonstrate that ARA55 exerts a causative role and functions as a critical regulator in TGFβ1-mediated EMT in CNE2 nasopharyngeal carcinoma cells through binding with Smad7.

Key words: ARA55; nasopharyngeal carcinoma; CNE2; Smad7

487. Estrogen receptor response gene EGR3 mediates breast cancer cell resistance to tamoxifen through promoting MCL1 transcription_3

Yu Xie*、Yue Wang、Junfang Qin、Mengci Yuan、Jing Yu

Nankai University

Background: Estrogen receptor (ER) positive breast cancer is a common disease in globally women, and endocrine therapy is a well-establish strategy. Currently, with widely application of endocrine medicine, drug resistance become an intractable problem increasingly. Early growth response protein (EGR) 3 is a well-established ER response factor. Whereas the role of EGR3 in ER-relevant endocrine therapy resistance is still confusing.

Purpose: We supposed EGR3 is a properly biomarker in endocrine therapy resistance which play a crucial role in resistant breast cancer cells. The study aims to investigate the necessity of EGR3 expression in resistant cells and clarify the mechanism of EGR3 mediating in tamoxifen treatment.

Methods: With the representativeness of tamoxifen in endocrine medicine, MCF7 and T-47D tamoxifen resistance cell lines was established. Firstly, EGR3 expression in tamoxifen treatment and resistant samples from the Gene Expression Omnibus database was re-analysis. The key role of EGR3 in resistance to tamoxifen treatment was investigated by manipulating expression. The responsibility of EGR3 to estrogen(E2)\oestrone(E1)\prolactin(PRL) action was detected by ligand stimulation. To clarify the EGR3 regulatory mechanism, the downstream factor was investigated and cell survival-related gene MCL1 was found. The function of EGR3 and MCL1 in resistance cells was investigated through tamoxifen-inducing apoptosis and proliferation assay. At the last, the action mechanism of EGR3 was investigated through CHIP and dual-luciferase report system.

Results: 1. EGR3 expression was higher in the tamoxifen treated and resistant samples. 2. With EGR3 knockdown, tamoxifen-resistant MCF7 cell line (MCF7-TamR) growth was impaired upon tamoxifen treatment; consistently, EGR3 forcing expressing given resistance to tamoxifen in MCF7. 3. Treating with estrone and estradiol, EGR3 expression was influenced by ER signaling both in MCF7 and MCF7-TamR and was aberrant in resistant cells. 4. MCL1 is the downstream

effector in EGR3-regulated apoptosis and proliferation in tamoxifen resistance. 5. EGR3 functions as a transcriptional factor binding to the MCL1 promoter and facilitating MCL1 transcription.

Conclusion: EGR3 is a key factor participating in abnormal ER signal that attenuating tamoxifen-induced apoptosis and inhibition of proliferation through facilitating MCL1 transcription. The current study reveals the negative role of EGR3 in tamoxifen-induced cancer cell suppression, which makes clear that EGR3 is a good indicator and a potential target to improve endocrine therapy resistance.

Key words: Breast cancer; endocrine therapy resistance; estrogen receptor; tamoxifen; MCF7; EGR3; MCL1

488. A Pan-Cancer Landscape of IGF2BPs and Their Association with Prognosis, Stemness and Tumor Immune Microenviron-ment

Wei Shao、shoudu zhang、qian ding、qian xu*

nanyang normal university

The human insulin-like growth factor 2 mRNA binding protein (IMP1-3 or IGF2BP1-3) plays essential roles in RNA regulate splicing, translocation, stability, and translation into proteins. However, the immune and stemness mechanisms of IGF2BPs in cancers are remain poorly understood. This study aimed to present a pan-cancer analysis of IGF2BPs to investigate the relationship between IGF2BPs and tumor microenvironments. We comprehensively analysed the IGF2BPs expression patterns, clinical prognostic value and the association of tumor immune microenvironment (TIME). The results showed that IGF2BPs expression increases in most malignant tumors and diverse cancer cell lines, and lower survival rate across multiple tumors. Importantly, the IGF2BPs expression were significantly related to the degree of tumor immune infiltration and cancer stemness. Further, immunohistochemistry confirmed that the expression of IGF2BP2/3 were higher in multiple cancer tissues. Interestingly, high IGF2BPs expression was associated with poor prognosis in patients with glioma. Function experiments showed that knockdown of IGF2BP3 alleviated GSC and glioma cell proliferation, invasion and migration in

vitro. Overall, our results provide a valuable resource that will be useful in guiding oncologic and therapeutic analyses of the role of IGF2BPs family in cancers.

Key words: insulin-like growth factor 2(IGF2) messenger RNA; pan-cancer; prognosis signature; tumor mi-croenvironment; glioma stem cells; drug response.

489. Dynamic risk profiling using blood indicators for severe myelosuppression after chemotherapy prediction in gastric cancer: An analysis from multi-center cohorts

Bowen Yang[1]、Bo Jin[1]、Lingyu Fu[1]、Ying Liu[2]、Jie Zhang[3]、Jinghua Sun[4]、Ping Yu[1]、Jin Wang[1]、Xiaofang Che[1]、Yunpeng Liu[1]、Xiujuan Qu*[1]

1. Department of Medical Oncology, the First Hospital of China Medical University

2. 郑州医科大学附属肿瘤医院

3. 大连医科大学附属第一医院

4. 大连医科大学附属第二医院

Aim: This research aimed to develop and validate a prediction model for individual severe myelosuppression risk assessment in postoperative patients with gastric cancer.

Methods: Medical records of postoperative patients with gastric cancer from four medical centers were post-structured using medical record knowledge mapping technology between 2009 and 2021. The Gastric Cancer Myelosuppression Risk Index (GCMRI) based on a dynamic Bayesian model that utilized real-time examination results to obtain the risk probability of severe myelosuppression, was developed in the training cohort. Accuracy of GCMRI was validated in internal validation and external validation cohorts. Finally, patients were categorized into three severe myelosuppression probability groups (Low-risk, Medium-risk, and High-risk) based on GCMRI.

Results: Gender, stage N, platelet count, hemoglobin, white blood cell count, neutrophil count, and lymphocyte count were identified as being associated with severe myelosuppression. In internal validation cohort, the AUCs of GCMRI were 0.8859 (95% CI: 0.8582-0.9136) and 0.8882 (95% CI: 0.865–0.9144) at 4th and 8th cycles separately. The classification performance of

GCMRI was better than that of the logistic model with static features in most cycles of chemotherapy. These results were also validated in the external cohort.

Conclusions: The GCMRI is a reliable predictive tool for severe myelosuppression in post-operative patients with gastric cancer and might be able to predict which patients suffer severe myelosuppression in subsequent chemotherapy.

Key words: Gastric Cancer, Severe myelosuppression, Blood biopsy, Predictive modeling, Personalized medicine

490. OSdream: an online prognostic and differential analysis tool for recurrence and metastasis of pan-cancer

Huimin Li、Qiang Wang、Longxiang Xie、Lu Zhang、Xiangqian Guo*

Henan university

Objective: Recurrence and metastasis are the main causes for cancer deaths, and are major challenges for tumor treatment success. Thus, uncovering the mechanisms of tumor recurrence and metastasis, accurate prediction of metastasis and recurrence, would facilitate early diagnosis and stratification of tumor patients with distinct risks, and guide further proper treatment and management. However, to date, the prognosis biomarker and analysis tool to predict recurrence and metastasis are still lacking.

Materials and methods: We collected 149 gene expression profiling datasets with clinical follow-up data of almost 30 cancer types, which include a total of 23341 samples from The Cancer Genome Atlas (TCGA), Gene Expression Omnibus (GEO) databases and literatures. To do the prognosis and differential analysis, the univariate, multivariate Cox regression analysis, nomogram and Kaplan-Meier plot are used to evaluate recurrence and metastasis prognostic values with R package ggplot2, ggpubr, magrittr, survminer and survival, and box plot and heatmap are used to perform the differential analysis of recurrence and metastasis with R package pheatmap, ggplot2, ggpubr, ggsci.

Results: We constructed an easy-to-use tool named Online Survival and Differential analysis of Recurrence and Metastasis of pan-cancer (OSdream), aiming to facilitate identifying biomarkers

to predict recurrence and metastasis, to uncover the potential mechanism of recurrence and metastasis of cancers. OSdream was designated to have two functions (prognosis and differential analysis) and four modules (module RFS and MFS for prognosis analysis, module DEGs of Recurrence and DEGs of Metastasis for differential analysis). By module RFS (Recurrence-free survival) and module MFS (Metastasis-free survival), Kaplan-Meier plot, univariate and multivariate Cox regression analysis results could be outputted with the hazard ratio (HR) and p-value, in addition, nomogram will be constructed according to the multivariate Cox analysis results. To use modules of DEGs of recurrence or metastasis, user needs to enter one or multiple genes, and then box plot and heatmap will be showed to present differential analysis results.

Conclusions: OSdream is a valuable web tool to investigate the potency of genes in predicting RFS and MFS, potential mechanisms of genes in recurrence or metastasis in cancers. OSdream is freely accessible at https://bioinfo.henu.edu.cn/OSdream/OSdream.html.

Key words: OSdream, metastasis, recurrence, survival, pan-cancer

491. Hypoxia-related Markers Distinguish Oxygen Environment and Survival in Gliomas

Weicheng Zheng*、Huangfeng Lin、Zhangying Zeng、Lei Qiao、Hailong Hao

School of Medical Technology and Engineering, Key Laboratory of Medical Bioinformatics

Objective: Tumor microenvironment (TME) is crucial for tumor cells. It was reported that hypoxic TME was related to glioma progression and drug resistance. However, at present, the assessment of the oxygenic microenvironment of glioma only depends on subjective pathological diagnosis. There are no effective models to evaluate the oxygenic content of TME in patients. Therefore, this study intends to construct molecular markers related to the oxygenic microenvironment of glioma and apply them to the clinical diagnosis and treatment.

Methods: Glioma cell lines cultured in different oxygenic microenvironment were used to construct the TME model. Subsequently, high-throughput sequencing was performed on it. Later, identification methods of differential genes were used to identify molecular markers related to

hypoxic microenvironment. The molecular markers were subsequently applied to several independent gliomas tissue profiles. Survival analysis and KEGG functional enrichment analysis were used to verify their accuracy, and the difference of the immune microenvironment of glioma in different oxygenic microenvironment was detected by Cibersort.

Result: In this study, a molecular marker composed of eight genes which could robust estimate oxygen content in TME was identified from the TME model. Cluster analysis of the molecular marker in gliomas profiles showed that high-grade gliomas TME possesses significant hypoxic characteristics while individual in lower grade gliomas (LGG) differs. After the samples were divided into normoxic and hypoxic groups using this marker, several interesting findings have been made. It was confirmed in both TME models and independent datasets that HIF1A expression was always higher under normoxic conditions. In the meantime, a significant prognostic difference between the two groups was found and confirmed in independent datasets. Further more, Cibersort analysis further revealed the difference in the immune microenvironment between the two groups.

Conclusion: The molecular marker found in this study could effectively evaluate the oxygenic content of TME, which provides valuable basis for accurate diagnosis and treatment of glioma patients

Key words: glioma, Tumor microenvironment, hypoxia, normoxia, biomarker

492. Discovery and clinical transformation of new subsets of liver cancer in China based on whole transcriptome sequencing

Junjie Xu*[1]、Shi Jiang[2]、Xueyi Teng[3]、Chengchen Zhang[1]、Xiao Liang[1]、Xiujun Cai[1]

1. Run Run Shaw Hospital Affiliated to Zhejiang University

2. 宁波市第一医院

3. 中国科学院生物物理所

Objective: Based on the transcriptome sequencing data of Chinese patients with liver cancer, we found new subpopulations of liver cancer and identified specific markers, so as to provide new ideas for accurate diagnosis and individualized treatment of liver cancer.

Method: High throughput transcriptome sequencing was performed on 296 samples of cancer tissues and paracancerous tissues from patients with liver cancer from Run Run Shaw Hospital Affiliated to Zhejiang University, and the obtained data were subjected to gene differential expression analysis, functional enrichment analysis, immune infiltration, lineage analysis of metabolic pathways, co-expression network analysis and so on. We analyzed the specific differentially expressed genes of HCC_1, and verified in the tissue microarray of liver cancer patients treated with sorafenib to identify the HCC_1 subgroup marker genes and efficacy marker genes.

Results: We found a new subgroup of hepatocellular carcinoma—HCC_1, that is very similar to cholangiocarcinoma. Transcriptome sequencing data analysis showed that HCC_1 and ICC are highly similar in terms of prognosis, immune infiltration, metabolic pathway and hypoxia status. In the tissue microarray of liver cancer patients treated with sorafenib, the subgroup marker gene CEACEM5/6 of HCC_1 and the efficacy marker gene FGFR1 were identified.

Conclusion: HCC_1 is a new subgroup of hepatocellular carcinoma which is very similar to cholangiocarcinoma and has a similar expression profile. CEACEM5/6 can be used as a marker gene of HCC_1 to distinguish it from other HCC samples, and FGFR1 can predict the response to sorafenib in liver cancer patients.

Key words: Primary liver cancer; HCC_ 1; CEACEM5/6 ; FGFR1

493. A Comprehensive Evaluation and Identification of Novel Molecular Signature in Bladder Cancer

王占旺[1]、金一[2]、何东[3]、朱煜星[1]、程雅新[1]、曹科*[1]

1. *中南大学湘雅三医院*
2. *湖南省肿瘤医院*
3. *中南大学*

Background: Muscle-invasive bladder cancer (MIBC) develops lymph node (LN) metastasis or distant metastasis, leading to recurrence and poor prognosis. The five-year survival rate of MIBC with LN or distant metastasis is only 8.1%; therefore, there is an urgent need to identify reliable biomarkers for prognosis and treatment regimen for patients with bladder cancer (BLCA) .

Methods: SEER database was used to select important clinical characteristics for MIBC. Then, weighted gene co-expression network analysis (WGCNA) was employed to identify differentially expressed genes (DEGs) to recognize significant co-expression modules by calculating the correlation between the modules and clinical data. Furthermore, Cox regression and lasso analysis were applied to screen prognostic hub genes and establish the risk predictive model. Bladder cancer cell lines (UMUC3 and 5637) were used for experimental validation in vitro.

Results: Cox analysis of 122,600 MIBC patients showed that the N stage was the most important clinical factor. A total of 4,597 DEGs were calculated between N0 and N+ patients, and WGCNA with these DEGs in 368 samples revealed that expression of turquoise was positively and strongly correlated with the N stage. Eight genes were identified as important prognostic candidates using lasso regression based on Cox analysis and STRING database. Combining GEO datasets, literature, and clinical factors, we identified LAMA2 and RUNX2 as novel prognostic biomarkers. CCK8 assay showed that depletion of LAMA2 or RUNX2 significantly inhibited the proliferation of BLCA cells, and flow cytometry indicated that knockdown of LAMA2 or RUNX2 promoted the apoptosis of BLCA cells. Transwell assay also showed that silencing of LAMA2 or RUNX2 weakened the migration and invasiveness of BLCA cells.

Conclusions: We constructed a new eight-gene risk model to provide novel prognostic biomarkers and therapeutic targets for BLCA.

关键字: Muscle-invasive bladder cancer; WGCNA; metastasis; TCGA; prognosis

494. Downregulation of POTEE inhibits cell growth, metastasis and cisplatin sensitivity of ovarian cancer cells, possibly via mediating actin polymerization

Dan Yao、Xiaoqing Zhu*

Chongqing Medical and Pharmaceutical College

Background: A previous study has shown that expression of POTE ankyrin domain family member E (POTEE) exhibits correlation with progression of high-grade serous ovarian cancer. However, the function and mechanism underlying have not been elucidated so far.

Methods: The expression and prognosis of POTEE in ovarian cancer was investigated by analyzing data from The Cancer Genome Atlas (TCGA). A tissue microarray with 54 ovarian cancer tissue samples was adopted to confirm the expression of POTEE in ovarian cancer progression. The knockdown efficiency of POTEE was verified by Real-time reverse transcription PCR and western blotting. Cell growth, migration and invasion were evaluated by Cell Counting Kit-8 assay and transwell assay. Tumorigenesis and cisplatin sensitivity of ovarian cancer cells were investigated by xenograft nude mouse model. F-actin expression and distribution were detected by western blotting and phalloidin staining, respectively.

Results: It was firstly confirmed that POTEE demonstrated upregulation in tumor tissues compared to normal tissues and its expression showed correlation with poor survival in patients. Further exploration found that POTEE downregulation significantly reduced cell growth of ovarian cancer cells both in vitro and in vivo. Next, it was shown that knockdown of POTEE affects migration and invasion of ovarian cancer cells with cell cycle changes and induction of apoptosis. Moreover, POTEE expression was verified to mediate cisplatin sensitivity of ovarian cancer cells. Mechanistically, POTEE may play these roles in ovarian cancer via participating in actin polymerization.

Conclusions: In summary, the findings of this study revealed that POTEE may serve as a biomarker of ovarian cancer and could be an intervention target for treatment.

Key words: Ovarian cancer; POTE ankyrin domain family member E (POTEE); cisplatin sensitivity; actin polymerization

495. Identification and validation of a genomic mutation signature as a predictor for immunotherapy in NSCLC

Zemin Wang、You Ge、Han Li、Pingmin Wei*

Southeast University

Background: Non-small cell lung cancer (NSCLC) is mainly composed of lung adenocarcinoma and lung squamous cell carcinoma, which is the main cause of death in lung cancer worldwide. Currently, the benefits of immune checkpoint inhibitor (ICI) therapy prediction via emerging biomarkers have been identified, and the association between genomic mutation signatures and immunotherapy benefits has been widely recognized as well. However, the evidence about NSCLC remains limited.

Methods: In this study, we analyzed 310 immunotherapy patients with NSCLC from the Memorial Sloan Kettering Cancer Center (MSKCC) cohort. Lasso Cox regression was used to construct a genomic mutation signature (GMS), and the prognostic value of GMS could be able to verify in the Rizvi cohort (N= 240) and Hellmann cohort (N= 75). We further conducted immunotherapy-related characteristics analysis in TCGA cohort (N= 1052).

Results: A total of seven genes (ZFHX3, NTRK3, EPHA7, MGA, STK11, EPHA5, TP53) were identified for GMS model construction. Compared with GMS-high patients, patients with GMS-low had longer overall survival (P<0.001) in the MSKCC cohort and progression-free survival (P<0.001) in the validation cohort. Multivariate Cox analysis revealed that GMS was an independent predictive factor for NSCLC patients in both the MSKCC and validation cohorts. Meanwhile, we found that GMS-low patients reflected enhanced anti-tumor immunity in TCGA cohort.

Conclusions: Our study indicated that GMS had not only potential predictive value for the benefit of immunotherapy, but also may serve as a potential biomarker to guide clinical ICI treatment decisions for NSCLC.

Key words: Non-small cell lung cancer, Genomic mutation signature, Immunotherapy, Immune checkpoint inhibitor, Biomarker

496. Core transcription regulatory circuitry orchestrates the aberration of epigenetic and transcriptional patterns in triple-negative breast cancer

Zhiying Xiong、Hui Zhi*

Harbin Medical University

Triple negative breast cancer (TNBC) constitutes the most aggressive molecular subtype among breast tumors owing to high heterogeneity, aggressive nature, and lack of treatment options. The continuous and robust aberrant transcriptional program in tumorigenesis results from super enhancers (SEs) which is driven by core transcriptional regulatory circuitry (CRC).Here we apply integrated epigenomic and transcriptomic profiling from normal adult breast and TNBC cell lines to uncover super enhancer heterogeneity. With SE-based modeling of regulatory wiring, we reconstruct an interconnected core transcriptional regulatory circuitry. Analysis of prognostic survival and assessments of transcription factor (TF) dependencies demonstrate EOMES and other core regulatory (CR) TFs are critical to maintenance of TNBC cell growth and proliferation. Using in situ Hi-C technology, we characterize the comparative and dynamic 3D chromatin organization in TNBC cells, and identify TNBC specific CTCF-mediated chromatin loops. From this, we constructed networks revealing the regulation of genes by super enhancers orchestrated by CR TFs on specific chromatin loops in normal breast and TNBC, respectively. Presenting an updated exploratory analysis of networks, we identified EOMES as a valuable biomarker and therapeutic target for TNBC.Our study highlights the decisive role that CRC played during carcinogenesis in TNBC, and further advocates for elucidating the causation between 3D structural aberration and epitranscriptomic dysregulation to provide insights for novel therapeutic interventions.

Key words: Triple-negative breast cancer; Core transcription regulatory circuitry; Super enhancer; Epigenetic and transcriptional dysregulation

497. BP180 is a Prognostic Factor in Head and Neck Squamous Cell Carcinoma

Xue Meng[1,2,3,4] 、 MATSUMOTO FUMIHIKO[3] 、 TAISUKE MORI[2] 、 NAMI MIURA[2,4] 、 YOSHINORI INO[2]、KAORU ONIDANI[2]、KENYA KOBAYASHI[2]、YUSUKE MATSUZAKI[2,4]、 SEIICHI YOSHIMOTO[2]、KATSUHISA IKEDA[3]、KAZUFUMI HONDA*[2,4]

1. Shengjing Hospital of China Medical University

2. 日本国立癌症研究中心

3. 日本顺天堂大学

4. 日本医科大学

Background/Aim: Prognosis plays a vital role in head and neck squamous cell carcinoma (HNSCC) patient management and decision-making, the identification of prognostic factor BP180 was required in HNSCC. Patients and Methods: Protein expression of bullous pemphigoid antigen II (BP180) was verified by immunohistochemistry (IHC) in a tissue microarray study of 202 cases.

Results: IHC analysis revealed that protein expression of BP180 among HNSCC patients differed significantly in the presence and absence of neural invasion, and according to T status in laryngeal and pharyngeal cancer subgroups. Overall survival and multivariate analysis showed that positive BP180-IHC and advanced clinical stage were significant independent positive predictors of mortality in HNSCC patients. In addition, in the oral cancer subgroup, independent positive predictors were positive BP180-IHC, advanced N status and neural invasion. In laryngeal and pharyngeal cancer subgroups, predictors were positive BP180-IHC and advanced clinical stage.

Conclusion: BP180 is a prognostic factor in head and neck squamous cell carcinoma.

Key words: BP180, collagen XVII, head and neck squamous cell carcinoma (HNSCC), prognostic, tissue microarray (TMA)

498. Proteomic analysis of small extracellular vesicles from the plasma of patients with hepatocellular carcinoma

Wei Dong [1,2,3,4]、Junfei Jin*[2,3,4]、Zeyu Xia[2,3,4]、Zehua Chai[2,3,4]、Zhidong Qiu[2,3,4]、Xuehong Wang[2,3,4]、Zebin Yang[2,3,4]、Junnan Wang[2,3,4]、Tingrui Zhang[2,3,4]、Qinqin Zhang[5]

1. Xiangya Hospital, Central South University

2. Guangxi Key Laboratory of Molecular Medicine in Liver Injury and Repair, the Af filiated Hospital of Guilin Medical University, Guilin, 541001, Guangxi, China

3. Guangxi Health Commission Key Laboratory of Basic Research in Sphingolipid Metabolism Related Diseases, the Affiliated Hospital of Guilin Medical University, Guilin, 541001, Guangxi, China

4. China–USA Lipids in Health and Disease Research Center, Guilin Medical University, Guilin, 541001, Guangxi, China

5. Department of Thyroid and Breast Surgery, Nanxishan Hospital of Guangxi Zhuang Autonomous Region, Guilin, 541002, Guangxi, China

Purpose： Liver cancer is one of the most common tumors with the seventh highest incidence and the third highest mortality. Many studies have shown that small extracellular vesicles (sEVs) play an important role in liver cancer. Here, we report comprehensive signatures for sEV proteins from plasma obtained from patients with hepatocellular carcinoma (HCC), which might be valuable for the evaluation and diagnosis of HCC.

Methods： We extracted sEVs from the plasma of controls and patients with HCC. Differentially expressed proteins in the sEVs were analyzed using label-free quantification and bioinformatics analyses. Western blotting (WB) was used to validate the abovementioned sEV proteins.

Results： Proteomics analysis was performed for plasma sEVs from 21 patients with HCC and 15 controls. Among the 335 identified proteins in our study, 27 were significantly dysregulated, including 13 upregulated proteins that were involved predominantly in the complement cascade (complement C1Q subcomponent subunit B (C1QB), complement C1Q subcomponent subunit C (C1QC), C4B-binding protein alpha chain (C4BPA), and C4B-binding protein beta chain (C4BPB)) and the coagulation cascade (F13B, fibrinogen alpha chain (FGA), fibrinogen beta chain (FGB), and fibrinogen gamma chain (FGG)). We verified increased levels of the C1QB,

C1QC, C4BPA, and C4BPB proteins in the plasma sEVs from patients with HCC in both the discovery cohort and validation cohort.

Conclusions： The complement cascade in sEVs was significantly involved in HCC progression. C1QB, C1QC, C4BPA, and C4BPB were highly abundant in the plasma sEVs from patients with HCC and might represent molecular signatures.

Key words： Proteomics, extracellular vesicles, hepatocellular carcinoma, complement

499. NAT10-mediated ac4C-mRNA modification promotes malignant progression and immunosuppression by reprogramming glycolytic metabolism in cervical cancer

Xiaona Chen[1]、Yi Hao[2]、Quanwei Guo[1]、Sheng Zhong[1]、Tuotuo Chong[1]、Xiaomin Luo[1]、Keyi Ao[1]、Chichao Xia[1]、Minuo Yin[1]、Ming Ye[3]、Hui He[4]、Anwei Lu[1]、Yufei Long[1]、Jianjun Chen[5]、Xin Li[1]、Jian Zhang[6]、Xia Guo*[1]

1. Shenzhen Hospital, Southern Medical University

2. 深圳大学附属华南医院

3. 新疆医科大学附属肿瘤医院

4. 香港大学深圳医院

5. 南方医科大学

6. 南方科技大学

Accumulating evidence has shown that metabolic reprogramming, immune evasion, and hallmarks of cancer are essential for the progression of cervical squamous cell carcinoma (CSCC) progression. However, the exact mechanisms by which mRNA N4-acetylcytidine (ac4C) affects glycolytic metabolism and immunosuppression are unclear. Here, we found that N-Acetyltransferase 10 (NAT10) expression was significantly elevated in CSCC tissues and this was associated with poor prognosis of patients. Mechanistically, HOXC8 activation in the promoter of NAT10 facilitated NAT10 transcription, which stimulated ac4C modification of

FOXP1 mRNA and enhanced FOXP1 transcript translation efficiency to activate GLUT4 and KHK expression. More importantly, the results showed that NAT10-mediated FOXP1 upregulation induced higher level of glycolysis and led to continuous increase of lactic acid secreted by CSCC cells, a metabolic preference of regulatory T cells (Tregs). Thus, lactic acid-enriched tumor microenvironment (TME) contributed to increasing the abundance of tumour-infiltrating Treg cells, forming an immunocompetent TME. Moreover, NAT10 knockdown synergized with anti-PD-L1 blockade therapy, resulting in tumor regression. Taken together, our findings revealed the critical oncogene role of NAT10 in initiating the interaction between cancer cell glycolysis and the immune response by regulating the ac4C-FOXP1-GLUT4/KHK axis, which could serve as a potential target for synergistic metabolic therapy and immunotherapy in CSCC.

Key words： Cervical squamous cell carcinoma, N4-acetylcytidine, NAT10 acetyltransferases, FOXP1, glycolysis, immunosuppression, PD-L1 blockade therapy

500. Trajectories of serum tumour marker impact on advanced-stage hepatocellular carcinoma outcomes after hepatic arterial infusion chemotherapy: A longitudinal, retrospective, multicentre, cohort study

Chao An *

Chinese PLA General Hospital

Background: Hepatic arterial infusion chemotherapy (HAIC) using FOLFOX regimen (oxaliplatin plus fluorouracil and leucovorin) is a promising option for advanced hepatocellular carcinoma (Ad-HCC). However, most patients with Ad-HCC who received HAIC need to more accurate surveillance. Serum tumour marker-based MoRAL score (11×√protein induced by vitamin K absence-II [PIVKA] +2×√alpha-foetoprotein [AFP]) can reflect both tumour burden and aggressiveness, but its definition remains controversial.

Aim: This study aims to characterize MoRAL score trajectories after HAIC and compare its monitoring ability with serum AFP trajectorie and PIVKA trajectories, respectively. Moreover, we examine the MoRAL score trajectories impact on survival outcomes.

Methods: This retrospective, multi-center study protocol was approved by the Institutional Review Board of all participating institutions and conducted following the principles of the 1964 Declaration of Helsinki. The requirement for written informed consent was waived because of the retrospective nature of this study. From May 2014 to June 2020, 889 eligible patients with Ad-HCC underwent HAIC were retrospectively enrolled from seven hospitals. All patients were assigned to training cohort (n= 532), internal test cohort (n= 125), and external test cohort (n= 232). A latent class growth mixed model was applied to distinguish potential AFP level, PIVKA level and MoRAL score dynamic changing trajectories. Inverse-probability-of-treatment weighted analyses were performed to eliminate unmeasured confounders through marginal structural models. Multivariate Cox proportional hazard regression analyses were used to determine the prognostic factors for survival in patients with Ad-HCC. Performance of these serum tumour markers for survival prediction was compared by areas under receiver operating characteristic (AUC) analysis with Delong test.

Results: The median follow-up time was 31.2 months (6.4-77.2 months). A total of 889 patients with Ad-HCC, who underwent HAIC with AFP and PIVKA repeatedly measured 3 to 10 times, were enrolled in the study. Three distinct trajectories of these serum tumour markers were identified using the latent class growth mixture model: high-rising (35.1 %; n= 312), low-stable (48.9%; n= 435), and sharp-falling (AFP serological response, 16.0%; n= 142). Multivariate Cox proportional hazard regression analyses found that > 65 years old age, tumor size >7 cm, ALBI grade 2, higher AFP level, AFP trajectorie, PIVKA trajectories and MoRAL score trajectories were associated with survival outcomes. Among these risk factors, MoRAL score trajectories achieved the best performance (AUCs of 0.823 in internal test cohort and 0.817 in external test cohort), outperforming significantly those of AFP trajectorie (AUCs of 0.802 in internal test cohort and 0.798 in external test cohort) and PIVKA trajectories (AUCs of 0.762 in internal test cohort and 0.757 in external test cohort). Compared with the low-stable class, the aHRs for death were 7.29 (2.56, 11.20) and 0.49(0.40, 0.86) for the high-rising and sharp-falling class, adjusted by age, baseline major tumor size, intrahepatic lesions number, logAFP, and logPIVKA (smooth).

Furthermore, high-rising class had a significantly higher HR in the subgroup of age < 65 years old (hazard ratio[HR]:12.01, 95% confidence interval[CI]: 6.02, 19.62), ALBI grade 2 (HR: 5.78, 95% CI: 3.99, 10.21) and tumor size > 7cm (HR: 7.01, 95%CI: 4.28, 21.12) (*P= 0.008*, 0.022 and 0.015 for interaction, respectively).

Conclusions: The MoRAL score trajectories based on longitudinal, multiparametric tumor markers showed outstanding performance for predicting survival outcomes after HAIC treatment in Ad-HCC, which provide a monitoring potential tool for improving clinical decision-making.

Key words： Hepatic arterial infusion chemotherapy; MoRAL score trajectories; Advanced hepatocellular carcinoma; Survival outcomes

501. Hepatocyte-derived FGG-rich extracellular vesicles promote nasopharyngeal carcinoma lung metastasis through an IL6-related pre-metastatic microenvironment

Kaiwen Zhang、Bo You、Yiwen You*

AFFILIATED HOSPITAL OF NANTONG UNIVERSITY

Distant metastasis accounts for nasopharyngeal carcinoma (NPC)-related mortalities. Recently, extracellular vesicles(EVs) are increasingly being demonstrated as critical mediators of bi-directional tumor-host cell interactions, controlling organ-specific infiltration, adaptation and colonization at the secondary site. However, mechanisms underlying the pre-metastatic niche formation are poorly understood.Peripheral blood was collected from NPC patients with metastasis and non-metastasis, and EVs were extracted for mass spectrometry analyses. EVs intervention experiments verified the effect of FGG-rich EVs on the proliferation and metastasis of NPC in vitro and in vivo. Combined EVs tracking experiments and transcriptome sequencing to analyze the effect of FGG-rich EVs on the pre-metastatic microenvironment. The related pathways of FGG-rich EVs affecting IL6 expression were verified by western blotting experiments. Rescue experiments were performed by IL6 knockout mice.Mass spectrometry analysis confirmed that

peripheral blood EVs of NPC patients with distant metastasis were rich in FGG, and found that it was secreted by LO2 cells. FGG-rich EVs promote NPC lung metastasis in vivo. Further experiments confirmed that FGG-rich EVs were taken up by lung endothelial cells and promoted the release of IL6 through the Toll-like receptor pathway, thereby forming a pre-metastatic microenvironment with microthrombosis and increased vascular permeability, ultimately leading to lung metastasis. IL6-KO mice confirmed that the pre-metastatic microenvironment caused by FGG-rich EVs is IL6-dependent. Furthermore, we found that IL6 could further promote the secretion of FGG-rich EVs from LO2, thus forming a positive feedback loop. On top of this, we found that non-extracellular vesicle components released by NPC cells prompted LO2 to secrete FGG-rich EVs.NPC-associated hepatocyte-derived FGG-rich EVs promote lung endothelial cells to secrete IL6 through the TLR3/TLR8/p65 pathway to form a pre-metastatic microenvironment, thereby promoting NPC lung metastasis.

Key words： nasopharyngeal carcinoma ; extracellular vesicle; metastasis; FGG; IL6

502. PRDM16 serve as potential dignostic biomarkers in lung adenocarcinoma and down-regulated in tumor tissues and serum

Meng Li、Anqi Li、Jiejun Zhou、Meng Fan、Mingwei Chen、Hui Ren*

the First Affiliated Hospital of Xi'an Jiaotong University

Background: The transcription factor PR domain containing 16 (PRDM16) is known to play a significant role in the determination and function of brown and beige fat and some malignances. However, the role of PRDM16 in lung adenocarcinoma (LUAD) has not been well addressed.

Methods: GEPIA, UALCAN, and Kaplan–Meier (KM) plotter were conducted to determine the relationship between the expression of PRDM16, clinicopathological features, and prognosis in non-small cell lung cancer (NSCLC). Immunohistochemical staining (IHC), western blot and qRT-PCR were conducted to evaluate the mRNA and protein expression in lung adenocarcinoma (LUAD) tissue and cell lines. Meanwhile, clinical data and serum of 95 patients with LUAD and 30 healthy person admitted to the First Affiliated Hospital of Xi'an Jiaotong

University from January 2020 to June 2021 were collected. Elisa were performed to explored the PRDM16 expression in serum beteween LUAD patients and healthy controls and the relationship bewtween PRDM16 and clinicopathological features , then receiver operating characteristic (ROC) curve analysis was performed to assess the auccercy of PRDM16 and tumor biomarkers in the diagnosis and prediction tumor staging of LUAD.

Results: Online database showed that the mRNA levels of PRDM16 were down-regulated in NSCLC (p<0.05), and the low expression of the PRDM16 was associated with the age, gender, smoking duration, poor stage, nodal metastasis status, TP53 mutation and wores prognosis in LUAD (p<0.05). The mRNA and protein expression levels of PRDM16 were also found down-regulated in the LUAD tissues and cell lines by IHC, western blot and qRT-PCR. Decreased serum PRDM16 were illustrated that correlated with worse staging and lymph node metastasis. In addition, PRDM16 has a good diagnostic accuracy for LUAD(AUC=0.804, p<0.05), and its combination with CEA, CA125 and NSE showed a higher prediction accuracy in the prediction tumor staging of LUAD (AUC=0.979, p<0.05).

Conclusion: PRDM16 may serve as potential biomarkers in the diagnosis and prediction tumor staging of LUAD.

Key words： PRDM16, biomarker, lung adenocarcinoma diagnosis

503. Comprehensive Analysis of 5-Methylcytosine Regulators in Adenocarcinoma of the pancreas

Songlin Xing*

AnHui Medical University

Comprehensive Analysis of 5-Methylcytosine Regulators in Adenocarcinoma of the pancreas

Introduction： Adenocarcinoma of the pancreas (PAAD) is a highly lethal disease, with a low early diagnosis rate. According to the 2021 statistics of the National Cancer Center of China, pancreatic cancer ranks 7th in the incidence of malignant tumors in men, 11th in women, and 6th in the mortality rate related to malignant tumors. Cytosine methylation is a mature epigenetic mechanism that forms 5-methylcytosine (5mC) and affects global gene expression, where

methylation regulators are widely involved. DNA 5mC modification plays important roles in cancer progression including proliferation, metastasis, angiogenesis, and apoptosis. However, We conducted an extensive bioinformatics analysis of the mechanism of action of methylation modulators in individuals with pancreatic cancer in this study. In order to explore the mechanism and clinical application of 5mC methylation regulators in PAAD, we combined the transcriptional level and pathway interaction level, and conduct a step-by-step study. Finally, in order to fully explore the mechanism of action of methylation modification and metastasis in pancreatic cancer and study its clinical application, it is necessary to explore some specific tissues, such as establishing and validating a wide range of clinical samples. The 5mC process has special significance in PAAD. According to previous studies, the prediction model established by 5mC has excellent clinical performance and its specific expression of methylation regulators in pancreatic cancer. Therefore, we conclude that studies on methylation regulators are of interest. Finally, we constructed a clinical risk score model with good prognostic effect based on methylation modulators, which contributes to the clinical prognostic tools of pancreatic cancer.

Materials and Method： After screening, we downloaded 179 PAAD samples and 332 normal samples from the Cancer Genome Atlas (TCGA) and GTEx database. By reading published literatures, we first collected 22 5mC regulators and analyzed their expression differences through the "GGPLOT2" package in R software. In addition, Spearman correlation test was used to determine whether gene expression was normally distributed using "Corrplot" package in R software. Furthermore, Pathway-based sets and Gene ontology categories were analyzed through ConsensusPathDB website. Then the ssGSEA algorithm was applied to calculate the enrichment score of each sample in each pathway which is typical in cancer successively and the relationship between the sample and the pathway was obtained. In addition, univariate and multivariate Cox regression analyses were performed. Based on the results, a nomogram was developed using the "RMS" software package to predict overall recurrence rates at 1, 3, and 5 years. We developed a risk prediction model based on four regulatory factors to study the prognostic impact of a range of regulatory factors in patients with pancreatic cancer. Lasso method was used for dimensionality reduction calculation and a prognostic model was established. Finally, we evaluated the relationship between risk score and immune infiltration.All the analysis methods and R package were implemented by R version 4.0.3.

Results： We found that 22 5mC regulators differently expressed in PAAD compared with normal tissues. The results showed a broad positive relationship among the 22 regulators However, the correlations of NTHL1, SMUG1, MBD3, and NEIL1 seem to be more clustered. The correlation between the four regulatory factors was high, but the correlation was lower than that of other regulatory factors in the PPI network interaction diagram. we selected 10 pathways with enrichment or concentrated functions as follows: Epigenetic regulation of gene expression, Displacement of DNA glycosylase by APEX1; TET1,2,3 and TDG demethylate DNA; Base excision repair - Homo sapiens (human); Base Excision Repair; SUMO E3 ligases SUMOylate target proteins, SUMOylation; MTHFR deficiency; DNA methylation; DNA Repair. We found the relationship between 22 methylation regulators and pathways and identified three highly correlated pathways: DNA repair, P13K_AKT_mTOR_Pathway and TGFβ. Finally, using univariate Cox regression analysis, the results suggested that age is associated with the prognosis of PAAD. And we developed a risk prediction model based on four regulatory factors to investigate the prognostic impact of a range of regulatory factors in patients with pancreatic cancer. Lasso method was used for dimensionality reduction calculation and a prognostic model was established. The model includes risk score formulas for four regulators. Each gene has a weight.our risk prediction model performed well in. The five-year predicted AUC value reached 0.832, In the KM curve, high risk group and low risk group are distinguished. The results show that the prediction is very effective. And with a 95% confidence interval, HR value was 2.443. The following results were observed in an analysis of immune cell correlation between the risk prediction model and samples from pancreatic cancer patients. In the TIMER algorithm, we observed that the risk score was negatively correlated with T cell CD4+ and Macrophage. In EPIC algorithm, immune cells B cell and B cell showed a significant negative correlation, while NK cell showed a positive correlation with the score. In MCPCOUNTER algorithm, Expression of T cell is negatively correlated with risk score. Finally, in the QUANTISEQ, only the Macrophage M1, uncharacterized cells are positively related, while the Macrophage M2, Monocyte, NK cell, T cell $CD8^+$ T cell regulatory(Tregs) showed negative correlation. These results indicate that our risk prediction model based on 5mC methylation regulator is likely to be associated with immune microenvironment.

Discussion： In this study, we validated or modified previous conclusions about 5mC methylation in pancreatic cancer based on the differential expression of regulators in cancer samples. At the same time, we have further explored the association of methylation regulators at the pathway level. In addition, the prediction of risk models based on methylation regulators also demonstrated good clinical predictive efficacy.

Key words： 5mC regulators， methylation, function, clinical riskscore

504. Stiff cancer matrix reduces lenvatinib sensitivity of hepatocellular carcinoma through promoting mitophagy

Yunong Fu、Kunjin Wu、Kaibo Yang、Kai Qu*

The First Affiliated Hospital of Xi 'an Jiaotong University

Physical traits of cancer are closed related to biological characteristics of malignant cell. Whether stiffness of HCC affects their sensitivity to lenvatinib remains unclear. Here, we report stiff HCC is insensitive to lenvatinib treatment. HCC cells cultured on stiff hydrogel have lower cell apoptosis and mitochondrial damage after lenvatinib treatment. In addition, HCC cells on stiff hydrogel exhibit fragment mitochondrial morphology, enhanced mitochondrial motility and improved mitophagy under mitochondrial stress. Furthermore, we find stiff extracellular matrix downregulates global H3K27me3 and restores expression of FIS1, which facilitates mitochondrial fission and mitophagy. Finally, we find that mitophagy is improved in parallel with H3K27me3 downregulation in stiff HCC tissue. We propose that stiff extracellular matrix improves mitophagy and empowers mitochondrial homeostasis. Targeting mitophagy is a promising strategy to overcome insensitivity of stiff HCC to lenvatinib.

Key words： HCC, Lenvatinib sensitivity, Stiffness, Mitophagy,

505. Development and Validation of a Prognostic Model Related to Pyroptosis-related Genes for Esophageal Squamous Cell Carcinoma Using Bioinformatics Analysis

Weiguang Zhang、Peipei Zhang、Junfei Jiang、Kaiming Peng、Zhimin Shen、Mingqiang Kang*

Fujian Medical University Union Hospital

Background: Esophageal squamous cell carcinoma (ESCC) is one of the most lethal malignant tumors worldwide, and a larger number of ESCC patients have unsatisfactory overall survival (OS) rates. While pyroptosis participates in the development of a variety of malignancies, the function of pyroptosis-related genes (PRGs) in ESCC is still obscure. The aim of this study was to construct the pyroptosis-related prognostic model for ESCC, which will be developed to stratify the risk hazards of ESCC patients and to provide theoretical evidence for individualized treatment.

Methods: RNA-seq data of ESCC were download from the NCBI Gene Expression Omnibus (GEO) database. Gene ontology (GO) analysis and Kyoto Encyclopedia of Genes and Genomes (KEGG) analysis were used to explore the potential biological functions or pathways. OS was considered as the primary prognosis outcome in this study. The riskscore was constructed by Least Absolute Shrinkage and Selection Operator (LASSO) Cox regression analysis. The pyroptosis-related prognostic modelwas constructed based on all independent prognostic factors and verified by C-index, Receiver operating characteristic (ROC) curves, and Calibration curves, and the role of the riskscore in ESCC immunotherapy was evaluated by the Tumor Immune Dysfunction and Exclusion (TIDE) algorithm.

Results: The current study found 31 differentially expressed PRGs (P<0.001), and functional enrichment analysis showed these PRGs were enriched in positive regulation of cytokine production, interleukin-1 beta production. Univariate and multivariate Cox regression analysis were applied to validate that the riskscore based on four prognostic PRGs (HMGB1, IL-18, NLRP7, and PLCG1) was an independent prognostic factor for ESCC, and the C-index of

prognostic model related to the riskscore (C-index =0.705) was higher than that of Tumor Node Metastasis (TNM)stage (0.620). The low-risk group showed a better efficacy of immune checkpoint inhibitors.

Conclusions: The riskscore related to PRGs was one of the independent prognostic factors for ESCC. Moreover, the prognostic model related to the riskscore could be used to predict the OS of ESCC patients effectively. However, there still were several limitations in this study, such as no external validation sample. In summary, our data provides a novel perspective in exploring the potential prognostic biomarkers of ESCC.

Key words: Pyroptosis; prognostic model; esophageal squamous cell carcinoma (ESCC); bioinformatics

506. Diagnostic and Prognostic Potential of Circulating and Tissue BATF2 in Nasopharyngeal Carcinoma

Zhaolei Cui、Yan Chen*

Fujian Cancer Hospital

Objective: At present, there is still a lack of effective markers for early diagnosis and prognostic monitoring of nasopharyngeal carcinoma (NPC). A large number of studies have shown that the basic leucine zipper ATF-like transcription factor 2 (BATF2) gene is closely related to the occurrence and development of a variety of malignant tumors. However, the expression of BATF2 in NPC and its clinical significance is still unclear.

Methods: A high-throughput tissue microarray combined with immunohistochemistry (IHC) was used to detect the expression of BATF2 proteins in NPC tissues, and to explore its relationship with clinicopathological characteristics and the prognosis of NPC. Meanwhile, a quantitative reverse transcription-polymerase chain reaction (qRT-PCR) was used to detect the expression of BATF2 mRNA in serum and serum-derived exosomes of NPC patients.

Results: The IHC showed that BATF2 was mainly localized to the nucleus of NPC tissue cells. Survival analysis showed that the NPC patients with a positive BATF2 expression enjoyed a longer duration of overall survival than those with a negative BATF2 expression. The positive

expression rates of BATF2 mRNA in serum and serum exosomes of NPC patients were 51.47% and 48.52%, respectively. The AUCs of NPC patients diagnosed by serum and exosomal BATF2 and healthy control groups were 0.9409 and 0.8983, respectively. The BATF2 levels of serum and exosomes of NPC patients in the treatment group were higher than those in the initial group, but lower than those in the recurrence group.

Conclusion: BATF2 is expected to be a promising prognostic marker for NPC. BATF2 in serum and serum exosomes can be used as an important biomarker for diagnosis, efficacy evaluation, and recurrence monitoring of NPC.

Key words: BATF2; nasopharyngeal carcinoma; exosome; diagnosis; prognosis

507. Development of a diagnostic nomogram for intrahepatic cholangiocarcinoma

Jiahua Liang[1]、Borui Xu[1]、Mingjian Ma[1]、Guangyan Zeng[2]、Zicheng Wang[1]、Li Huang*[1]

1. The First Affiliated Hospital, Sun Yat-sen University, Guangzhou, China

2. 中山大学附属第八医院

Introduction： Intrahepatic cholangiocarcinoma (ICC) is an aggressive malignancy and surgical resection remains the curative therapy of ICC at early stage. ICC patients are typically asymptomatic and precise diagnosis of ICC remains clinically challenging. This study aims to develop an integrative diagnostic nomogram model for ICC.

Methods: A cohort of 27 ICC patients with pathologically confirmed and 11 patients with benign biliary disease were enrolled in our department between 2013 and 2015. Preoperative diagnostic examinations including radiologic imagings (contrast-enhanced ultrasound (CEUS), contrast-enhanced CT (CECT)) and serum tumor biomarkers (CYFRA 21-1, CEA and CA19-9). Diagnostic performance of above examinations were analyzed by the receiver operator characteristic (ROC) and a diagnostic nomogram model integrating above examinations was also developed.

Results: Analysis of the area under the ROC curves (AUC) of each preoperative diagnostic examinations revealed that the integrative nomogram model had better discriminatory ability

(0.979) than any other methods (AUC of CYFRA 21-1, CEA, CA19-9, CEUS and CECT, were 0.813, 0.729, 0.760, 0.850 and 0.878). The C-index values of the integrative nomogram model (0.97) was also significantly superior to CA19-9, CYFRA 21-1, CEA, CEUS or CECT (0.760, 0.813, 0.729, 0.850 and 0.878). Furthermore, the integrative nomogram model showed good predictability by calibration curves analysis.

Conclusion: The integrative nomogram model represent a promisingly quantitative, easily available and precise diagnostic tool for ICC.

Key words: Intrahepatic cholangiocarcinoma, serum tumor biomarkers, radiologic imagings, nomogram

508. The role of EphA7 methylation in the development of cervical cancer

Wenfan Zhang、Shuang Chen、Jinhao Yang、Hongrun Zhao、Yuwei Liu、Zhuqing Sun、Rong Wang*

Tianjin medical university

Objective: Aberrant methylation of EphA7 has been reported in the process of carcinogenesis but not in cervical cancer (CC). Therefore, an integration study was performed to explore the association between EphA7 hypermethylation and CC and validate the potential value of EphA7 hypermethylation in the diagnosis of cervical cancer. Furthermore, the regulation mechanisms of EphA7 expression in cervical carcinogenesis was investigated.

Methods: First, data on EphA7 methylation and expression in cervical cancer were extracted and analyzed via bioinformatics tools. Subsequently, CRISPR-based methylation perturbation tools (dCas9-Tet1/DNMT3a) were constructed to further demonstrate the association between DNA methylation and EphA7 expression. Then, the clinical value of EphA7 methylation in cervical cancer was validated in cervical tissues and Thinprep cytologic test (TCT) samples. Next, MTT, Transwell assays, apoptosis signals and PI3K/AKT pathway were evaluated to investigate the biological function of EphA7 in CC cells. The IC50 was generated by exposing CC cells to varying concentrations of cisplatin. The association between EphA7 methylation and

radiotherapy and tumour purity was analysed by Linkedomics. Ultimately, CRISPR-based pull down in situ revealed the transcription factors (TFs) bind to the EphA7 promoter. The interaction between TFs and EphA7 methylation was elucidated via knockout and 17-β oestradiol(E2) treatment.

Results: Pooled analysis showed that EphA7 promoter methylation levels were significantly increased in CC compared with normal tissues ($P<0.001$) and negatively correlated with EphA7 expression. Moreover, CRISPR-based methylation perturbation tools (dCas9-Tet1/DNMT3a) demonstrated that DNA methylation participates in the regulation of EphA7 expression directly. Consistent with these findings, the methylation level and the positive rate of EphA7 gradually increased with severity from normal to cancer stages in TCT samples ($P<0.01$). In additionally, EphA7-demethylation restrained progression and promoted apoptosis by impairing the PI3K/AKT pathway in CaSki and SiHa cells. EphA7 hypermethylation was positively correlated with tumour purity and a poor response to chemoradiotherapy ($p<0.05$). SP1 is located in the promoter regulating DNMT1 of EphA7. E2 upregulate EphA7 gene expression with demethylation through the ER/SP1 axis.

Conclusions: EphA7 hypermethylation is present in CC and EphA7-demethylation inhibits cervical carcinogenesis and enhances the sensitivity of cisplatin. E2 induces EphA7-demethylation, which suggest EphA7 is a highly promising diagnosis and therapeutic target for CC.

Key words: EphA7, DNA methylation, Cervical cancer, SP1, 17-β oestradiol

509. Diagnostic and prognostic value of the cancer-testis antigen LDH-C4 in breast cancer

Zhaolei Cui、Yan Chen*

Fujian Cancer Hospital

Objective: Lactate dehydrogenase C4 (LDH-C4) is a cancer/testis antigen (CTA) that is expressed abnormally in certain malignant tumors. However, the expression and clinical significance of LDH-C4 in breast cancer (BC) have not been determined.

Methods: Quantitative reverse transcription-polymerase chain reaction (RT-PCR) was adopted to investigate the expression of LDHC mRNA in the serum or serum-derived exosomes of patients with BC. The expression of LDH-C4 protein in BC tissues was also evaluated by using high-throughput tissue microarray analysis and immunohistochemistry.

Results: The results showed that LDHC mRNA was highly expressed in the serum and serum-derived exosomes of BC patients. The area under the curve (AUC) of serum and exosome LDHC in distinguishing BC from healthy individuals was estimated to be 0.9587 and 0.9464, respectively. The LDHC level in the serum-derived exosomes of patients with BC was significantly associated with tumor size and positively correlated with the expression of HER2 and Ki-67 (all with $p<0.05$). Serum and exosome LDHC levels in BC patients were negatively correlated with medical treatment and positively correlated with recurrence. Survival analysis showed that LDH-C4 expression was negatively associated with BC prognosis.

Conclusion: Serum and serum-derived exosome LDHC may be an effective indicator for diagnosis and therapeutic efficacy, as well as a predictor for the recurrence of BC. LDH-C4 may be a biomarker to determine the prognosis of BC.

Key words: lactate dehydrogenase C4, breast cancer, serum, exosome, diagnosis, prognosis

510. Diagnostic potential for circular RNAs in gastric carcinoma: A meta-analysis

Zhaolei Cui、Yan Chen*

Fujian Cancer Hospital

Background: Circular RNAs (circRNAs) are potential, novel biomarkers for the early diagnosis of gastric carcinoma. Herein, a meta-analysis was conducted to assess the diagnostic potential for circRNAs in gastric carcinoma.

Methods: Online databases were searched for eligible studies. Study quality was judged using the Quality Assessment for Studies of Diagnostic Accuracy (QUADAS) checklist-II tool. STATA 12.0 and Meta-Disc 1.4 software were used for statistical analysis.

Results: Twelve studies consisting of 1278 patients and 1250 paired controls were considered for meta-analysis. The pooled sensitivity and specificity of circRNAs for gastric carcinoma was compared to normal controls and found to be 0.68 (95%CI: 0.66 - 0.71) and 0.70 (95%CI: 0.68 -0.73), respectively. A corresponding area under the receiver operating characteristic curve of 0.78 was identified. Moreover, stratified analysis demonstrated an improved diagnostic value for circRNAs when tissue and plasma specimens were combined.

Conclusions: This meta-analysis demonstrates that circRNAs are promising biomarkers for gastric carcinoma.

Key words: circRNAs；gastric carcinoma；meta-analysis

511. Endogenous SARI induced cell apoptosis in nasopharyngeal carcinoma by targeting the intrinsic apoptotic pathway

Zhaolei Cui、Yan Chen*

Fujian Cancer Hospital

The SARI (suppressor of AP-1, regulated by IFN) gene, also named as BATF2, is associated with the risk of several kinds of cancers, and loss of SARI expression is frequently detected in aggressive and metastatic cancer. Nevertheless, the functional of SARI in nasopharyngeal carcinoma (NPC) remains exclusive. In this study, we discovered that knock-down of SARI expression suppressed cell growth and colony formation, inhibited invasion, promoted apoptosis, and induced G0/G1 and G2/M arrest in human CNE2 nasopharyngeal carcinoma cells. Of note, SARI restoration could trigger the mitochondrial pathway in CNE2 cells. Our data provide evidence that SARI exerts a role as a tumor suppressor gene in leukemia, possibly by inhibiting proliferation and promoting apoptosis via the mitochondrial pathway.

Key words: suppressor of AP-1, regulated by IFN; SARI; CNE2; nasopharyngeal carcinoma

512. Expression and Clinical Implications of Basic Leucine Zipper ATF-Like Transcription Factor 2 in Breast Cancer

Zhaolei Cui、Yan Chen*

Fujian Cancer Hospital

Objective: Basic leucine zipper ATF-like transcription factor 2 (BATF2) has been reported to participate in the occurrence and development of some malignancies. But little is known about its roles in breast cancer (BC). In this work, we aimed to explore the expression pattern and clinical implications of BATF2 in BC.

Methods: We assessed the differences in BATF2 mRNA expression between cancerous and noncancerous tissues in BC using online databases. In external validations, BATF2 protein expression in BC tissues was quantitated using a tissue microarray and immunohistochemical (IHC) analysis, and BATF2 mRNA expression in serum and serum-derived exosomes of BC patients using qRT-PCR.

Results: There were low-to-moderate levels of increases in BATF2 protein expressions in BC cases. BATF2 mRNA expression was negatively correlated with androgen receptor (AR) and positively correlated with BRCA2, Mki67, and TP53 expressions. Subgroup analyses showed that triple-negative breast cancer (TNBC) patients with high BATF2 mRNA expressions had a longer overall survival (OS). Our IHC analysis revealed a positive rate of BATF2 protein expression of 46.90%. The positive rates of BATF2 mRNA expressions in the serum and exosomes were 45.00% and 41.67%, respectively. Besides, the AUCs of serum and exosomal BATF2 mRNA for BC diagnosis were 0.8929 and 0.8869, respectively.

Conclusions: BC patients exhibit low-to-moderate increases in BATF2 mRNA expression levels in cancerous tissues, of which low BATF2 mRNA expression serves as an indicator of a poor TNBC prognosis. The high BATF2 protein expression can be a potential indicator of a better BC prognosis. Serum and exosomal BATF2 mRNA levels also serve as promising noninvasive biomarkers for BC diagnosis.

Key words: BATF2; breast cancer; bioinformatics; serum; exosomes; biomarker

513. Identification of Adriamycin Resistance Genes in Breast Cancer based on Microarray Data Analysis

Zhaolei Cui、Yan Chen*

Fujian Cancer Hospital

Objective: Breast cancer is a common malignant tumor with increasing incidence worldwide. This study aimed to investigate the molecular mechanisms of the adriamycin (ADR) resistance in breast cancer.

Methods: The GSE76540 dataset downloaded from the National Center for Biotechnology Information (NCBI) Gene Expression Omnibus (GEO) database was adopted for analysis. Differentially expressed genes (DEGs) in chemo-sensitive cases and chemo-resistant cases were identified using the GEO2R online tool respectively. Go analysis and KEGG enrichment analysis of DEGs were carried out by using the DAVID online tool. The protein-protein interaction (PPI) network was constructed using the Search Tool for the Retrieval of Interacting Genes (STRING) and visualized with Cytoscape software. The impact of key tumor genes on the survival and prognosis were described.

Results: A total of 1481 DEGs were excavated, including 549 up-regulated genes and 932 down-regulated genes. According to the GO analysis, the DEGs were significantly enriched in: extracellular matrix organization, positive regulation of transcription from RNA polymerase II promoter, lung development, positive regulation of gene expression, axon quidance and so on. The results of KEGG pathway enrichment analysis showed that the most enriched DEGs can be detected in: pathways in cancer, PI3K AKT signaling pathway, focal adhesion, ras signaling pathway and so on. In the PPI network analysis, hub genes of CDH1, ESR1, SOX2, AR, GATA3, FOXA1, KRT19, CLDN7, AGR2, ESRP1, RAB25, CLDN4, IGF1R, CLDN3 and IRS1 were detected. Finally, there is a correlation filter out these hub genes in resistance of ADR.

Conclusions: Hub genes associated with ADR resistance were identified using bioinformatic techniques. The results of this study may contribute to the development of targeted therapy for breast cancer.

Key words: breast cancer, microarray data analysis, adriamycin resistance

514. Lactate Dehydrogenase C4 is associated with breast cancer prognosis and affects cancer cell proliferation and invasion

Zhaolei Cui、Yan Chen*

Fujian Cancer Hospital

Objective: Human lactate dehydrogenase C4 (LDH-C4) is a known cancer/testis antigen (CTA). Nevertheless, its clinical effects and molecular role remains unclear in breast cancer (BC).

Methods: Expression of LDH-C4 in BC tissue, paired adjacent normal tissue, and cell lines were quantified by qRT-PCR, western blotting and immunohistochemistry. Additionally, we assessed the clinical and prognostic significance of LDH-C4 in BC by Kaplan-Meier method. Cell proliferation, migration and invasion, and cell apoptosis were measured by means of a cell counting kit-8, clone forming, Transwell assay, and TUMMEL, respectively. Invio an

Results: Expression levels of LDH-C4 were markedly upregualted in BC cells and tumor tissues but not expressed in normal BC tissue. Furthermore, survival showed that high LDH-C4 expression conferred reduced survival rates (P<0.05). Functional analyses revealed that LDH-C4 overexpression and down-regulation attenuated cell proliferation, invasion, and migration as well as energy metabolism in BC cells. LDH-C4 could affect mTOR activity.

Conclusions: Expression of LDH-C4 in BC may serve as a potential indicator for poor prognosis. LDH-C4 displays tumor suppressive behavior, warranting future investigations into its therapeutic potential in the treatment of BC.

Key words: lactate dehydrogenase C4; breast cancer; invasion; migration; mechanism

515. An ultrasensitive method for detecting short and rare cell-free DNA

yu zhuang、feng shao*

Department of Thoracic Surgery, Nanjing Chest Hospital

Cell-free DNA (cfDNA) promises to serve as surrogate biomarkers for noninvasive molecular diagnostics. Recent findings demonstrated that the cfDNA with a short size was highly associated with diseases. However, the short cfDNA cannot be effectively detected by current targeted sequencing methods. To address this gap, we developed One-PrimER Amplification (OPERA) system which could successfully detect DNA fragments as short as 50bp with almost 100% library conversion rate. With multiplex primers, OPERA could reach the limit of detection to 0.1 copies of Y chromosome and distinguish copy number variation of 1.03-fold increase. By suppressing single-strand errors, OPERA achieved 75% sensitivity at mutant allele fractions of 0.02% in reference samples and detected 57.1% (12/21) stage I lung cancer patients with 100% specificity.

Key words: cell-free DNA ;biomarkers;NSCLC

516. Performance of A PLK1-Based Immune Risk Model for Prognosis and Response Prediction of Breast Cancer

Zhaolei Cui、Yan Chen*

Fujian Cancer Hospital

Objective: Polo-like kinase 1 (PLK1) belongs to a family of serine/threonine-protein kinases and acts as a powerful oncogene in tumor occurrence and development. We aimed to assess potential correlations between PLK1 expression and immune infiltration in BRCA and construct a PLK1-based immune risk model applicable for prognosis and response prediction.

Methods: We collected gene expression data of PLK1 in BRCA patients from TCGA. Associations of PLK1 expression with immune cell infiltration and immunomodulators were

critically analyzed. A prognostic risk model based on seven genes for PLK1-related immunomodulators was established, and a nomogram was depicted for survival prediction.

Results: PLK1 expression was significantly associated with BRCA prognosis, clinical stage progression, and tumor classification. The PLK1 gene was significantly enriched in T cell and B cell receptors, and molecules of the chemokine signaling pathway. Specifically, PLK1 expression was positively correlated with the degree of activated CD8+T cell, regulatory T cell (Tregs), and negatively correlated with M2 macrophage infiltration. The seven-gene-based risk model could serve as an independent prognostic factor of BRCA. The risk model was markedly correlated with PD-1/PD-L1 (both $P<0.001$) immune checkpoints expression and tumor mutation burden (TMB). Patients at high and low risk of BRCA identified by the risk model revealed different responses to anti-PD-1 and/or anti-CTLA4 therapy, as well as common chemotherapy drugs like cisplatin, paclitaxel, and gemcitabine.

Conclusion: This PLK1-based immune risk model can effectively predict the prognosis and tumor progression of BRCA, identify gene mutations, and assess patient benefits from immunotherapy and chemotherapy regimens.

Key words: Polo-like kinase 1; breast cancer; immune infiltration; risk model; prognosis

517. Plasma D-dimer and IL-6 associated with treatment response and progress free survival in advanced non-small cell lung cancer patients treated with anti-PD-1

Chong Chen*

Tianjin Medical University Cancer Institute and Hospital

Background: The treatment response of immune checkpoint inhibitors (ICIs) remains unexpected and there is significant individual variability in the efficacy of different patients with advanced non-small cell lung cancer. This study aims to find peripheral blood biomarkers predicting the efficacy and PFS (progression-free survival) of anti-programmed death-1 (anti-PD-1) treatment in

patients with advanced non-small cell lung cancer (NSCLC), which can be used to guide the adjustment of anti-PD-1 treatment regimens to bring greater clinical benefit to NSCLC patients.

Methods: A systematic review of 103 patients with advanced or recurrent NSCLC who received anti-PD-1 therapy (pembrolizumab or carrelixumab) inpatiently at Tianjin Medical University Cancer Hospital between January 2018 and April 2021. The cut-off values for carcinoembryonic antigen (CEA), cytokeratin19 fragment 21-1 (CYFR21-1), squamous cell carcinoma (SCC), tissue polypeptide-specific antigens (TPSA), D-dimer and serum inflammatory markers were determined by receiver operating characteristic curve analysis. Tumor response was assessed by computed tomography according to the Response Evaluation Criteria in Solid Tumors, version 1.1.

Results: Peripheral blood biomarkers IL-6 and D-dimer can predict the clinical value of treatment effect at 6-8 weeks of anti-PD-1 treatment, with AUC areas corresponding to 0.765 and 0.804. Analyses of survival showed that IL-6 ≥ 8.03 pg/mL and DD≥ 917.2 ng/mL were independent predictors of progression-free survival (PFS). A PFS prediction model for anti-PD-1 treatment of NSCLC using the new cut-off values: using "IL-6 ≥ 8.03 pg/mL" or "DD ≥ 917.20 ng/mL" as a score of “1”. The results showed that the higher the score of combined IL-6 and D-dimer, the shorter the PFS time.

Conclusions: High expression of IL-6 in patients with advanced NSCLC predicts poor efficacy and short duration of PFS with anti-PD-1 therapy; Increasing the cut-off value of D-dimer to 917.20ng/mL predicts the occurrence of disease progression in anti-PD-1 treated NSCLC patients, while high expression of D-dimer predicts short duration of PFS. Combined application of inflammatory index (IL-6) and fibrinolytic index (D-dimer) scores to predict the efficacy of anti-PD-1-treated NSCLC patients and to establish a predictive model for PFS in anti-PD-1-treated NSCLC.

Key words： advanced non-small cell lung cancer； anti-PD-1； D-dimer； PFS

518. Poor prognosis of stage I lung adenocarcinoma patients determined by elevated expression over pre/minimally invasive status of COL11A1 and THBS2 in the focal adhesion pathway

Jun Shang、He Jiang、Leming Shi、Yuanting Zheng*

Fudan University

Patients with adenocarcinomas in situ (AIS) and minimally invasive (MIA) lung adenocarcinoma (LUAD) are curable by surgery, whereas 20% stage I patients die within five years post-operative. We hypothesize that poor-prognosis stage I patients may exhibit key molecular characteristics deviating from AIS/MIA. Focal adhesion (FA) was identified as the only pathway significantly perturbed at both genomic and transcriptomic levels by comparing 98 AIS/MIA and 99 LUAD. Then, two FA genes (COL11A1 and THBS2) were found strongly upregulated from AIS/MIA to stage I while steadily expressed from normal to AIS/MIA. Furthermore, unsupervised clustering separated stage I patients into two molecularly and prognostically distinct subtypes (S1 and S2) based on COL11A1 and THBS2 expressions (FA2). Subtype S1 resembled AIS/MIA, whereas S2 exhibited more somatic alterations and activated cancer-associated fibroblast. The simple knowledge-driven model was validated with 12 external datasets, showing potential in identifying high-risk stage I patients for more intensive post-surgery treatment.

Key words: lung adenocarcinoma, pre/minimally invasive, molecular subtypes, prognosis, COL11A1, THBS2, overfitting-resistant, unsupervised clustering

519. Hypoxia related prognostic model based on four genes in gastric cancer

Lina Wen*[1,2]、Zongqiang Han[3]

1. 首都医科大学附属北京世纪坛医院

2. 中国抗癌协会肿瘤标志专委会

3. 北京小汤山医院

Objective: Mining hypoxia related prognostic markers to provide reference for the prevention and treatment of gastric cancer.

Method: Transcriptome data of gastric cancer were downloaded and sorted from TCGA database, and the information of hypoxia related genes were extracted. The differentially expressed hypoxia genes were analyzed, and the functions were explored by go and KEGG enrichment. Then clinical data were also downloaded from TCGA. The differential prognostic genes were screened through unicox, and a prognosis model were further established through multicox. The prognostic model was evaluated by survival curve, risk curve, univariate and multivariate independent prognostic analysis and multivariate ROC curve. The correlation between prognostic model genes and clinical features was investigated by clinical correlation analysis.

Result: 41 differentially expressed hypoxia genes were discovered, and hypoxia related biological processes, cellular components, molecular functions and signaling pathways were enriched. STC1, DUSP1, ZFP36, DCN, BGN PIM1, SERPINE1, CAV1, EFNA3, LOX, AKAP12, PLAUR were identified as prognostic genes, but only SERPINE1, CAV1, EFNA3, PLAUR were optimized as a prognostic model. survival curve, risk curve, univariate and multivariate independent prognostic analysis and multivariate ROC curve analyses indicated this prognostic model could effectively distinguish the groups with good prognosis from those with poor prognosis of gastric cancer. The expression level of SERPINE1, CAV1, EFNA3 and risksore were associated with grade, while those of EFNA3 and PLAUR were related to age.

Conclusion: The prognostic model base on four genes of SERPINE1, CAV1, EFNA3, and PLAUR colud effectively indicate clinical outcomes of gastric cancer.

Key words： hypoxia, prognosis model, gastric cancer

520. The altered plasma metabolic profiles and its diagnostic potential for primary liver cancer

Zhiying Liu*、Zhihang Zhou

The second affiliated hospital of Chongqing medical university

Background: Liver cancer（LC）, as the third most morbid and deadly cancer worldwide, is facing great challenges in non-invasive diagnosis and early detection. The diagnosis of liver cancer does not rely on pathological biopsy, which is quite different from other cancer types.Liquid biopsy is an ideal alternative for cancer monitoring.Metabolic reprogramming is one of the hallmarks of cancer.It is promising to apply the characteristics of altered metabolic profiles to distinguish liver cancer from high-risk populations such as liver cirrhosis（Cir）.

Methods: We performed a comprehensive metabolomic analysis of the peripheral plasma of liver cancer(n=54),Cir(n=35), and healthy normal controls（NC, n=10）, and compared the metabolite changes measured.The samples were subjected to untargeted metabolomic analysis using high performance gas chromatography-mass spectrometry (GC-MS) to identify differential metabolites.Potential metabolic markers contributing to the diagnosis of liver cancer were screened by the receiver operating characteristic (ROC) curves and binary logistic regression analysis. The phenotypic functions of potential metabolites were validated in hepatocytema cell linesusing CCK-8 assay and would healing assay.

Results: Detailed metabolomic analysis revealed significant clustering separation of plasma metabolic profiles in the groups of liver cancer, cirrhosis and normal controls, identifying eight candidate metabolic biomarkers(Increased plasma levels of trans-trans-muconic acid and oxoglutaric acid, decreased levels of triethylene glycol、2-picolinic acid、heptaethylene glycol、N-formylglycine 、 citrulline and 4-(dimethylamino)azobenzene in liver cancer). Potential metabolites combination with better diagnostic performance for liver cancer was screened out compared with the Cir group, consisting of trans-trans-muconic acid, triethylene glycol and N-formylglycine.The area under the receiver-operating characteristic curve (AUC), sensitivity and specificity of this panel is 0.943, 92.6% and 97.1%, separately. This metabolite panel contributed to improved diagnostic performance of alpha-fetoprotein (AFP). The AUC, sensitivity and

specificity of combination of this metabolic panel and AFP were 0.985, 98.2%, and 94.3%, respectively, significantly better than 0.856, 66.7%, 91.4% for alpha-fetoprotein (AFP) alone (P<0.005). The diagnostic accuracy of this group was 87.6% for LC and 86.4% for AFP-negative (AFP<20 ng/ml) liver cancer. More importantly, changes in triethylene glycol and N-formylglycine were specific for the early-stage liver cancer, and their diagnostic performance was significantly more remarkable than that of AFP (AUC: 0.994 vs. 0.811, P<0.005). However, compared with NC, the change characteristics of heptaethylene glycol and 2-picolinic acid are more discriminative.

Conclusions: We have identified a metabolite combination of trans-trans-muconic acid, triethylene glycol and N-formylglycine as an ideal novel diagnostic regimen for primary liver cancer.Specifically,combination of triethylene glycol and N-formylglycinecan be used to effectively distinguish early-stage liver cancer from liver cirrhosis.These metabolites have the potential to become novel biomarkers for monitoring hepatocarcinogenesis in the cirrhotic population.

Key words： Primary liver cancer; novel metabolic biomarker; early-stage liver cancer; monitor

521. Differences of molecular events driving pathological and radiological progression of lung adenocarcinoma

He Jiang、Jun Shang、Leming Shi、Yuanting Zheng*

Fudan University

Introduction: Ground-glass opacity (GGO)-related lung adenocarcinoma (LUAD) has been detected increasingly in the clinic and its inert property and superior survival indicate unique biological characteristics. However, we do not know much about them in adenocarcinoma in situ (AIS), minimally invasive adenocarcinoma (MIA) and invasive lung adenocarcinoma (IAC), which hampers identification of key reasons of the inert property of GGO-related LUAD.

Methods: Using whole-exome sequencing and RNA sequencing, taking into account both radiological and pathological classifications of the same 197 patients concomitantly, we

systematically interrogate the genes driving the progression from GGO to solid nodule and potential reasons for the inertia of GGO.

Results: Identifying the differences between GGO and solid nodule, we found that molecular commonalities of GGO-related IAC and AIS/MIA included lower TP53 mutation frequency and less active cell proliferation-related pathways. Identifying the differences in mGGO between AIS/MIA and IAC, we noticed that EGFR mutation frequency and CNV load were significantly higher in IAC than in AIS/MIA. Regulatory T cell was also higher in IAC, while CD8+ T cell steadily decreased from AIS/MIA to IAC. Besides, we also discovered molecular events that may drive the progression from GGO to solid nodule and AIS/MIA to IAC concomitantly, including TMB, APOBEC-related mutation, cell proliferation and matrix remodeling associated genes. Finally, we constructed a transcriptomic signature to quantify the development from GGO to solid nodule (G2S), which was an independent predictor of patients' prognosis in 11 external LUAD datasets.

Conclusions: Our results provide deeper insights for the indolent nature of GGO.

Key words： lung adenocarcinoma, ground-glass opacity, pathological progression, radiological progression, molecular events

522. Co-expression and cooperation of RMP and IGF1r confers hypoxia induced metastasis of gastric cancer

Wei Zhou、jingting jiang*

The third affiliated hospital of soochow university

The hypoxic tumor microenvironment (TME) is a universal feature in solid tumors and it is associated with a poor clinical prognosis. However, the underlying mechanisms for this remain poorly explored. This research demonstrates that hypoxic conditions promote the expression and maintenance of a functional complex between RMP and IGF1r. Oxygen deprivation induces AMPK activation and the downstream AGC kinase PKN3; PKN3 phosphorylates RMP at Ser-371, inducing a metastasis in gastric cancer. In accordance with this, cells expressing non-phosphorylatable RMP (S371A), exhibit reduced metastatic potential. The integrity of the

RMP and IGF1r complex was found to be important, as PKN3 binds and phosphorylates RMP. In the hypoxic TME, the expression of miR-598-3p decreased, which lead to the deregulation of RMP and IGF1r expression. This work uncovered the AMPK/IGF1r/PKN3 axis. In addition, this research elucidated the mechanism in which, in an RMP-dependent manner, this astrix confers a metastatic phenotype to gastric cancer in response to oxygen deprivation.

Key words： Tumor microenvironment, Hypoxia, RMP, IGF1r, Gastric cancer

523. PSMB7 induces M2-like TAM polarization and promotes immune infiltration and progression of lung adenocarcinoma

Bingjie Zeng [1]、Dong Chenglai[2]、Zhou Hao [1]、Ma Lifang[1]、Wang Jiayi*[1]

1. Shanghai Tongji Hospital

2.新乡医学院第一附属医院

As an important pathological type of lung adenocarcinoma, invasive lung adenocarcinoma has a rapid increase in incidence. Its main characteristics are high degree of immune infiltration, short survival time and poor prognosis. Many evidences showed that tumor-associated macrophages (TAM) affect the occurrence and development of cancer. However, the specific mechanism by which PSMB7 affects the polarization of TAM and affects tumor development in lung adenocarcinoma is still unknown. In this study, we evaluated the expression of PSMB7 and its relationship with tumor immune infiltration through databases and human lung adenocarcinoma samples. The BMDM derived from mice was extracted and the THP-1 monocyte cell line were used to study PSMB7-mediated polarization of M2-like TAM in vitro. The expression of PSMB7 was silenced to detect the TAM functional phenotype and cytokine secretion. Atomization of NTHi lysate was used to stimulate the mouse lung cancer model to simulate the inflammatory tumor microenvironment, and to explore the relationship between PSMB7 and lung tumor immune infiltration. PSMB7 was highly expressed in lung adenocarcinoma, and strongly expressed in lung adenocarcinoma with immune infiltration phenomenon (p<0.05), and its protein expression is positively correlated with the expression of M2-like TAM identification markers

(p<0.05).In vitro studies have shown that there is a significantly high level of PSMB7 protein in M2-like macrophages (P<0.001). Knockdown of PSMB7 will affect the differentiation of M2-like macrophages into M1.In vivo studies confirmed that the expression of PSMB7 in lung tumor tissues of lung cancer mice stimulated by NTHi was significantly increased, and the surface marker of M2-like macrophages CD206 was significantly increased (P<0.001), suggesting that PSMB7 may be involved in the polarization of M2-like macrophages, And promote the development of lung adenocarcinoma's own tumor cells through paracrine. PSMB7 can induce TAM polarization and is highly expressed in M2 TAM, especially in lung adenocarcinoma with high degree of immune invasion. PSMB7 induces TAM polarization and secretes cytokines, activates JAK-STAT signal to promote the proliferation and invasiveness of lung adenocarcinoma.

Key words：PSMB7；Lung adenocarcinoma；TAM；proliferation

524. Comparison of Plasma and Serum miRNA Profiles by Small RNA Sequencing

Haiyan Wang、Qingwang Chen、Naixin Zhang、Yaqing Liu、Wanwan Hou、Leming Shi、Yuanting Zheng*

Fudan University

Background: Accumulated evidence has revealed that extracellular microRNAs (miRNAs) could be potential biomarkers for the diagnosis and therapy of various human diseases. Blood-derived plasma and serum are the most commonly used samples for miRNA analysis of liquid biopsy. However, the question about plasma or serum which is preferable remains unclear and needs to be elucidated.

Methods: We performed small RNA sequencing for paired plasma and serum samples which passed the quality control from 7 healthy individuals, 3 replicates per sample. Then we analyzed the number of detected miRNAs among all individuals and in each individual. Hierarchical clustering analysis and Pearson correlation analysis were applied to assess the heterogeneity and similarity in miRNA expression profiles of plasma and serum. Furthermore, the coefficient of variation was calculated to evaluate the technical variability of miRNA quantitation. Finally,

differentially expressed analysis was conducted to compare the difference in miRNA quantitation of plasma and serum, and KEGG and GO pathway enrichment analysis was carried out to reveal the significant pathway for differential miRNA signatures.

Results: All 42 samples passed the quality control of small RNA sequencing and entered the subsequent analysis. Among the major extracellular RNA biotypes, miRNA accounted for the highest proportion in both plasma and serum, where the proportion of miRNA in plasma was slightly higher compared with serum (47.3% *vs.* 42.9%). In plasma and serum, 573 miRNAs and 522 miRNAs were detected, respectively. Besides, we found that miRNA expression between plasma and serum was highly correlated, with a correlation coefficient of 0.99 (p<0.05). Lower biological and technical variability of miRNA expression was displayed in plasma than in serum. Furthermore, we identified three differentially expressed miRNAs (hsa-miR-1246, hsa-let-7i-3p, and hsa-miR-939-5p) with higher levels in serum than in plasma, which is mainly involved in organelle, ion binding, cell adhesion, and blood coagulation pathway.

Conclusions: This study displayed the high miRNA detection and low miRNA variability in plasma than in serum, which suggested the superiority of using plasma for miRNA analysis of blood-based liquid biopsy.

Key words： extracellular miRNA, plasma, serum, small RNA sequencing, liquid biopsy

525. The role of circRUNX1 MDS-AML in the transformation process

邓发滑[1]、韦四喜*[2]、胡华丽[1]、王斯奇[1]

1. 贵州医科大学医学检验学院

2. 贵州医科大学附属医院临床检验中心

Background: Myelodysplastic syndrome (MDS) is a disease with complex pathogenesis and characterized by ineffective hematopoiesis. Clonal proliferation of hematopoietic stem cells drives the transformation between MDS and acute myeloid leukemia (AML). CircRNA, a class of non-doding RNA, was recently discovered to play various roles in the development of multiple diseases which including hematologic malignancies. There was a result of RNA-seq hinted

circRUNX1 was differentially expressed between MDS and AML, therefore, we try to delve into the role of circRUNX1 to explore the association about AML transport of MDS, and bring new horizons to the study of hematological tumors.

Methods: Total RNA was extracted from the bone marrow of patients with AML, MDS and healthy donors, qRT-PCR was performed to identify the different transcripts expression of circRUNX1 of the cohort. CircRUNX1 knockdown/overexpression cell lines were constructed by lentivirus transfection, and CCK-8 assay was used to detect the cell viability; flow cytometry was used to detect cell apoptosis; bioinformatics analysis was used to predict combine and construct ceRNA networks, and KEGG and GO analysis was preformed to predict the potential biological fuctions of ceRNA networks. Then, double luciferase reporter assay was used to verify the interaction relationships between circRUNX1 and its target miRNA; expression of proteins were detected by western blot.

Results: Among peripheral blood of 100 AML patients, 70 MDS patients and 100 healthy control, we found that total circRUNX1 was significantly downregulated, and hsa_circ_0002360 as one of the transcripts of circRUNX1 has more significant difference than other transcripts. In addition, we successfully overexpressed hsa_circ_0002360 in SKM-1 cell, and knockdown hsa_circ_0002360 in THP-1 cells with lentiviral vector, and the result of CCK-8 shown that upregulated hsa_circ_0002360 could inhibit cell viability and promoted cells apoptosis.

Key words： ceRNA networks; MDS; AML transformation

526. 追踪线粒体 DNA 突变演变描绘卵巢癌转移模式

徐智阳[1]、周凯翔[2]、王珍妮[2]、刘洋[2]、王兴国[1]、高天[1]、谢凡凡[2]、袁晴[2]、谷习文[2]、刘淑娟[1]、邢金良*[2]

1. 空军军医大学西京医院

2. 空军军医大学基础医学院生理与病生教研室

Background: Ovarian cancer (OC) is the most lethal gynecologic tumor characterized by high-rate metastasis. Challenges in accurately delineating the metastatic pattern have greatly

restricted the improvement of treatment in OC patients. Increasing studies have leveraged mitochondrial DNA (mtDNA) mutations as efficient lineage-tracing markers of tumor clonality.

Methods: We applied multi-region sampling and high-depth mtDNA sequencing to portray the metastatic patterns in advanced-stage OC patients. Somatic mtDNA mutations were profiled from a total of 149 primary and 246 metastatic tumor tissue samples in 35 OC patients.

Findings: Our results revealed remarkable sample-level and patient-level heterogeneity. In addition, distinct mtDNA mutational patterns were observed between primary and metastatic OC tissues. Further analysis identified the different mutational spectra between shared and private mutations among primary and metastatic OC tissues. Analysis of clonality index calculated based on mtDNA mutations supported monoclonal tumor origin in 15 of 17 patients with bilateral ovarian cancers. Notably, mtDNA-based spatial phylogenetic analysis revealed distinct patterns of OC metastasis, in which linear metastatic pattern exhibited low degree of mtDNA mutation heterogeneity and short evolutionary distance, whereas parallel metastatic pattern showed the opposite trend. Moreover, a mtDNA-based tumor evolutionary score (MTES) related to different metastatic patterns was defined. Our data showed that patients with different MTES responded differently to the combined debulking surgery and chemotherapy. Finally, we observed that tumor-derived mtDNA mutations were more likely to be detected in ascitic fluid than plasma samples

Key words: Ovarian cancer; Mitochondrial DNA mutation; Metastatic pattern; Tumor evolution

527. Cisplatin resistance-related multi-omics differences and the establishment of machine learning models

Qihai Sui*

Zhongshan hospital Fudan university

Objectives: Platinum-based chemotherapies are currently the first-line regimen for the treatment of non-small cell lung cancer. This study will improve our understanding of the causes of resistance to cisplatin, especially in LUAD and provide a reference for therapeutic decisions in clinical treatments.

Methods: Cancer Cell Line Encyclopedia (CCLE), The Cancer Genome Atlas (TCGA) and Zhongshan hospital affiliated to Fudan University (zs-cohort) were used to identify the multi-omics differences related to platinum chemotherapy. Cisplatin-resistant mRNA and miRNA models were constructed by Logistic regression, classification and regression tree and C4.5 decision tree classification algorithm with previous feature selection performed via least absolute shrinkage and selection operator (LASSO). qRT-PCR and western-blotting of A549 and H358 cells, as well as immunohistochemistry and single-cell Seq data of tumor samples were applied to verify the tendency of certain genes.

Results: 661 cell lines were divided into three groups according to the IC50 value of cisplatin, and the top 1/3 (220) with a small IC50 value were defined as the sensitive group while the last 1/3 (220) were enrolled in the insensitive group. TP53 was the most common mutation in the insensitive group, in contrast to TTN in the sensitive group. 1348 mRNA, 80 miRNA, and 15 metabolites were differentially expressed between 2 groups (P<0.05). According to the LASSO penalized logistic modeling, 6 of the 1348 mRNAs, FOXA2, BATF3, SIX1, HOXA1, ZBTB38, IRF5, were selected as the associated features with cisplatin resistance and for the contribution of predictive mRNA model (all of adjusted P-values<0.001). 3 of 6 (BATF3, IRF5, ZBTB38) genes were finally verified in cell level and patients in zs-cohort.

Conclusions: somatic mutations, mRNA expressions, miRNA expressions, metabolites and methylation were related to the resistance of cisplatin. The models we created could help in the prediction of the reaction and prognosis of patients given platinum-based chemotherapies.

Key words： cisplatin, drug resistance, machine learning, IC50

528. Prognostic value of systemic immune-inflammation index in elderly patients with newly diagnosed colorectal cancers

Chan Li[1]、Wei Tian[2]、Meng Li[1]、Ke Xie*[2]

1. People's Hospital of Xinjin

2.四川省医学科学院·四川省人民医院

Background: Cancer is a significant public health problem. Colorectal cancer is one of the most frequently diagnosed cancers in the world and a leading cause of death. Elderly patients usually have increased comorbidities and limited tolerance to cancer therapy, but using an accurate prognostic tool allows selection of an appropriate treatment for the older patient to achieve the best outcome and avoid ineffective treatments. In this paper we evaluated the predictive value of the Systemic Immune-inflammation Index, SII, in determining the one-year survival, tumor differentiation status and cumulative probability of survival in elderly patients with newly diagnosed colorectal cancer.

Methods: A total of 103 patients with newly diagnosed colorectal cancer from Sichuan Provincial Peoples hospital, January to December 2014, were studied retrospectively. The SII was calculated based on counts of platelets, neutrophils and lymphocytes and the enrolled patients were divided into high and low SII groups. The relationship between SII and age, tumor differentiation and one-year survival were determined together with the association between Ki-67 expression and SII.

Results: A high SII was correlated with higher tumor differentiation stage, poor one-year survival and lower cumulative probability of survival. Patients with low SII had improved survival, better tumor differentiation (Stage I-II) and higher cumulative probability of survival. The SII was not associated with Ki-67 expression.

Conclusions: For elderly patients with newly diagnosed colorectal cancer, this pre-therapeutic, noninvasive, and easily available test has the potential to become a useful prognostic tool for survival prediction and to help clinicians develop an optimal treatment regimen.

Key words: systemic immune-inflammation index; predictive value; elderly patients; newly diagnosed; colorectal cancers

529. The Speckle-type POZ protein (SPOP) inhibits breast cancer malignancy by destabilizing TWIST1

Chunli Wei、Junjiang Fu*、Xiaoyan Liu、Jingliang Cheng、Jiewen Fu

Southwest Medical University

Epithelial-mesenchymal transition (EMT) inducing transcription factor TWIST1 plays a vital role in cancer metastasis. How the tumor-suppressive E3 ligase, Speckle-type POZ protein (SPOP), regulates TWIST1 in breast cancer remains unknown. In this study, we report that SPOP physically interacts with, ubiquitinates, and destabilizes TWIST1. SPOP promotes K63-and K48-linked ubiquitination of TWIST1, predominantly at K73, thereby suppressing cancer cell migration and invasion. Silencing SPOP significantly enhances EMT, which accelerates breast cancer cell migration and invasiveness in vitro and lung metastasis in vivo. Clinically, SPOP is negatively correlated with the levels of TWIST1 in highly invasive breast carcinomas. Reduced SPOP expression, along with elevated TWIST1 levels, is associated with poor prognosis in advanced breast cancer patients, particularly those with metastatic triple-negative breast cancer (TNBC). Taken together, we have disclosed a new mechanism linking SPOP to TWIST1 degradation. Thus SPOP may serve as a prognostic marker and a potential therapeutic target for advanced TNBC patients.

Key words : The Speckle-type POZ protein (SPOP); TWIST1; Stabilization; Triple-negative breast cancer (TNBC); Metastasis; Prognosis

530. The m6A demethylase ALKBH5-mediated upregulation of DDIT4-AS1 maintains pancreatic cancer stemness and suppresses chemosensitivity by activating the mTOR pathway

Xiaomeng Liu、Bo Tang*

Tianjin Medical University Cancer Institute and Hospital

Background: Chemoresistance is a major factor contributing to the poor prognosis of patients with pancreatic cancer, and cancer stemness is one of the most crucial factors associated with chemoresistance and a very promising direction for cancer treatment. However, the exact molecular mechanisms of cancer stemness have not been completely elucidated.

Methods: m^6A-RNA immunoprecipitation and sequencing were used to screen m^6A-related mRNAs and lncRNAs. qRT–PCR and FISH were utilized to analyse DDIT4-AS1 expression. Spheroid formation, colony formation, Western blot and flow cytometry assays were performed to analyse the cancer stemness and chemosensitivity of PDAC cells. Xenograft experiments were conducted to analyse the tumour formation ratio and growth in vivo. RNA sequencing, immunoblot and bioinformatics analyses were used to identify the downstream pathway of DDIT4-AS1. IP, RIP and RNA pulldown assays were performed to test the interaction between DDIT4-AS1, DDIT4 and UPF1. Patient-derived xenograft (PDX) mouse models were generated to evaluate chemosensitivities to GEM.

Results: DDIT4-AS1 was identified as one of the downstream targets of ALKBH5, and recruitment of HuR onto m^6A-modified sites is essential for DDIT4-AS1 stabilization. DDIT4-AS1 was upregulated in PDAC and positively correlated with a poor prognosis. DDIT4-AS1 silencing inhibited stemness and enhanced chemosensitivity to GEM (Gemcitabine). Mechanistically, DDIT4-AS1 promoted the phosphorylation of UPF1 by preventing the binding of SMG5 and PP2A to UPF1, which decreased the stability of the DDIT4 mRNA and activated the mTOR pathway. Furthermore, suppression of DDIT4-AS1 in a PDX-derived model enhanced the antitumour effects of GEM on PDAC.

Conclusions: The ALKBH5-mediated m^{6}A modification led to DDIT4-AS1 overexpression in PDAC, and DDIT-AS1 increased cancer stemness and suppressed chemosensitivity to GEM by destabilizing DDIT4 and activating the mTOR pathway. Approaches targeting DDIT4-AS1 and its pathway may be an effective strategy for the treatment of chemoresistance in PDAC.

Key words: ALKBH5, stemness, chemosensitivity, DDIT4-AS1, UPF1

531. HDAC11 Regulates Glycolysis through the LKB1/AMPK Signaling Pathway to Maintain Hepatocellular Carcinoma Stemness

shiqian liu、bo tang*

TIANJIN MEDICAL UNIVERSITY CANCER INSTITUTE&HOSPITAL

Background: Hepatocellular carcinoma (HCC) contains a subset of cancer stem cells (CSC) that cause tumor recurrence, metastasis, and chemical resistance. Histone deacetylase 11 (HDAC11) mediates diverse immune functions and metabolism, yet little is known about its role in HCC CSCs. In this study, we report that HDAC11 is highly expressed in HCC and is closely related to disease prognosis.

Methods: qRT-PCR and IHC were applied to examine HDAC11 levels in normal and chemoresistant HCC tissues. Cancer cell stemness and chemosensitivity were evaluated by spheroid formation, colony formation, Western blot and flow cytometry assays. RNA-seq combined with ChIP-seq was used to identify target genes, and ChIP, IP and dual luciferase reporter assays were applied to explore the underlying mechanisms.

Results: Depletion of HDAC11 in a conditional knockout mouse model reduced hepatocellular tumorigenesis and prolonged survival. Loss of HDAC11 increased transcription of LKB1 by promoting histone acetylation in its promoter region, thereby activating the AMPK signaling pathway and inhibiting the glycolysis pathway, which in turn leads to the suppression of cancer stemness and HCC progression. HDAC11 overexpression reduced HCC sensitivity to sorafenib.

Conclusion: This study finds that HDAC11 suppresses LKB1 expression in HCC to promote cancer stemness, progression, and sorafenib resistance, suggesting the potential of targeting HDAC11 to treat HCC and overcome kinase inhibitor resistance.

Key words: HDAC11, HCC, stemness, AMPK

532. Long Non-Coding RNA LINC01572 Promotes Hepatocellular Carcinoma Progression via Sponging miR-195-5p to Enhance PFKFB4-Mediated Glycolysis and PI3K/AKT Activation

Yudie Yang、Bo Tang*

TIANJIN MEDICAL UNIVERSITY CANCER INSTITUTE & HOSPITAL

Background: Accumulating evidence indicates that type 2 diabetes mellitus (T2DM) is a risk factor for hepatocellular carcinoma (HCC), and T2DM-associated HCC represents a common type of HCC cases. We herein identify an lncRNA LINC01572 that was aberrantly upregulated in T2DM-related HCC via high-throughput screening. Based on this, the study was undertaken to identify the functional role and mechanism of LINC01572 in HCC progression.

Methods: RT-qPCR was used to detect the expressions of LINC01572 in HCC tissues and cell lines. Gain- or loss-of-function assays were applied to evaluate the in vitro and in vivo functional significance of LINC01572 in the HCC cell proliferation, migration, and invasion using corresponding experiments. Bioinformatics, RIP, RNA pull-down, and luciferase reporter assays were performed to explore the regulatory relationship of the LINC01572/miR-195-5p/PFKFB4 signaling axis.

Result: In this study, we profiled lncRNAs in HCC tissues and corresponding adjacent tissues from HCC patients with T2DM by RNA sequencing. Our data showed that LINC01572 was aberrantly upregulated in HCC tissues as compared with control, especially in those with concurrent T2DM. The high level of LINC01572 was correlated with advanced tumor stage, increased blood HbA1c level, and shortened survival time. The overexpression of LINC01572

significantly promoted HCC cell proliferation, migration, invasion, and epithelial-to-mesenchymal transition (EMT), while the knockdown of LINC01572 had the opposite effects on HCC cells. A mechanistic study revealed that LINC01572-regulated HCC progression via sponging miR-195-5p to increase the level of PFKFB4 and subsequent enhancement of glycolysis and activation of PI3K-AKT signaling.

Conclusion: LINC01572 acts as ceRNA of miR-195-5p to restrict its inhibition of PFKFB4, thereby enhancing glycolysis and activates PI3K/AKT signaling to trigger HCC malignancy.

Key words: Keywords: T2DM-related HCC, LINC01572, MiR-195-5p, PFKFB4, glycolysis

533. LINC00680 enhances hepatocellular carcinoma stemness behavior and chemoresistance by sponging miR-568 to upregulate AKT3

haiqiang chen、bo tang*

Tianjin Medical University Cancer Institute & Hospital

Background: Hepatocellular carcinoma (HCC) has an extremely poor prognosis due to the development of chemoresistance, coupled with inherently increased stemness properties. Long non-coding RNAs (LncRNAs) are key regulators for tumor cell stemness and chemosensitivity. Currently the relevance between LINC00680 and tumor progression was still largely unknown, with only one study showing its significance in glioblastoma. The study herein was aimed at identifying the role of LINC00680 in the regulation HCC stemness and chemosensitivity.

Methods: QRT-PCR was used to detect the expression of LINC00680, miR-568 and AKT3 in tissue specimen and cell lines. Gain- or loss-of function assays were applied to access the function of LINC00680 in HCC cells, including cell proliferation and stemness properties. HCC stemness and chemosensitivity were determined by sphere formation, cell viability and colony formation. Luciferase reporter, RNA immunoprecipitation (RIP), and RNA pull-down assays were performed to examine the interaction between LINC00680 and miR-568 as well as that between miR-568 and AKT3. A nude mouse xenograft model was established for the in vivo study.

Results: We found that LINC00680 was remarkably upregulated in HCC tissues. Patients with high level of LINC00680 had poorer prognosis. LINC00680 overexpression significantly enhanced HCC cell stemness and decreased in vitro and in vivo chemosensitivity to 5-fluorouracil (5-Fu), whereas LINC00680 knockdown led to opposite results. Mechanism study revealed that LINC00680 regulated HCC stemness and chemosensitivity through sponging miR-568, thereby expediting the expression of AKT3, which further activated its downstream signaling molecules, including mTOR, elF4EBP1, and p70S6K.

Conclusion: LINC00680 promotes HCC stemness properties and decreases chemosensitivity through sponging miR568 to activate AKT3, suggesting that LINC00680 might be a potentially important HCC diagnosis marker and therapeutic target.

Keywords: Hepatocellular carcinoma, LINC00680, miR-568, AKT3, Stemness, Chemosensitivity

534. Study on the Correlation between Interleukin-27 and CXCL10 in Pulmonary Tuberculosis

Jiahui Fan[1]、Yefeng Yang[2]、Liang Wang[3,4]、Xiaoqian Shang[1]、Li Zhang[4]、Hu Sun[4]、Yujie Ma[4]、Ying Li[3]、Jing Wang[2,3]、Xiumin Ma*[1,3]

1. Tumor Hospital Affiliated to Xinjiang Medical University

2. 海南医科大学第二附属医院呼吸内科

3. 中亚高发疾病发病机制与防治国家重点实验室临床检验中心

4. 新疆医科大学第一附属医院

Objective: To investigate the correlation between interleukin-27 and CXCL10 and other cytokines in pulmonary tuberculosis and to further explore the related miRNAs through bioinformatics.

Methods: Collect the lesion tissue and peripheral blood of pulmonary tuberculosis patients and the peripheral blood of healthy controls. Immunohistochemical staining and qRT-PCR were used to observe the expression of interleukin-27, CXCL9, CXCL10, and CXCL11. Then, predict the key miRNA, qRTPCR was used to verify the expression of miRNA in the peripheral blood and evaluated the correlation between them.

Results: Both immunohistochemical staining and qRT-PCR indicated that the expressions of IL-27, CXCL9, CXCL10, and CXCL11 were significantly increased in tuberculosis patients, and IL-27 was significantly correlated with CXCL10 (r= 0:68). Key molecules such as has-let-7b-5p, has-miR-30a-3p, and has-miR-320b were screened out. Among them, has-let-7b-5p was significantly downregulated, and has-miR-30a-3p was significantly upregulated; they were related to interleukin-27 and CXCL10.

Conclusion: Our data shows that interleukin-27 and CXCL10 are significantly related in pulmonary tuberculosis, and has-let-7b-5p and has-miR-30a-3p are also related to interleukin-27 and CXCL10. It laid the foundation for subsequently exploiting the potential biomarkers in tuberculosis disease.

Key words: pulmonary tuberculosis, Interleukin-27, CXCL10, has-let-7b-5p, has-miR-30a-3p

535. Cancer cell remodels myeloid-derived suppressor cell through TTLL12 activity to promote tumor progression

Dongwen Chen、Peishan Hu、Chong Chen、Xinxin Huang、Shubiao Ye、Xiaojian Wu、Ping Lan*

The Sixth Affiliated Hospital of Sun Yat-sen University

Background: Immune checkpoint inhibitors (ICIs), exemplified by antibodies targeting programmed death 1 (PD-1) or programmed death ligand 1 (PD-L1), have achieved the long-term survival of 10–30% of treated individuals. The majority of patients treated with ICIs as single agents reap limited or no benefits at all.One of the major challenges limiting the efficacy of anti–PD-1/PD-L1 therapy in nonresponding patients is the underlying mechanisms that inhibit immune system to recognize and kill tumor cells. Further studies are urgently needed to explore regulatory targets to increase response rates and extend their use to a larger number of patients and tumor types. Therefore, our study aimed to find out new therapeutic targets to regulate the infiltration of immune cells in tumor microenvironment and improve the efficacy of ICIs. We analyzed the expression of TTLL12 in colorectal cancer (CRC) cohorts and revealed that TTLL12 was upregulated in CRC and negatively correlated with immune score (IS), immune cell subsets (ICS), effector and memory CD8+T cell (EM CD8+T cell), type 1 T helper cell (Th1) and natural

killer (NK) cells infiltration. In this study, we analyzed the role of TTLL12 in cancer cells and modulation of the tumor immune microenvironment.

Methods: Based on the proteomics characterizing tumor tissues and paired non-tumor tissues from CRC patients in our center, we used ssGSEA analysis to define IS, ICS, EM CD8+T cell, Th1 and NK cells of tumor samples according to previously reported immune-related gene signatures. Potential target was found out for further investigation. Quantitative real-time reverse transcription polymerase chain reaction (qRT-PCR) and immunohistochemistry were further used to analyze the transcriptional and protein levels of the potential target in CRC samples as well as its relationship with the outcomes of CRC patients. Subsequently, based on stable knockdown or overexpression cell lines, our study investigated whether the potential target could influence the proliferation of tumor cells in vitro as well as in subcutaneous tumor model of nude mice. Two subcutaneous tumor models of immunocompetent mice were further used to explore whether the potential target could regulate anti-tumor immunity. Mechanistically, by using flow cytometry and neutralizing antibody to deplete specific immune cells in vivo, our study confirmed the immune subset regulated by the potential target. Then, mass spectrometry of cell culture supernatant was used to further explore how the potential target influenced the immune subset. Finally, we assessed whether the potential target could enhance the anti-tumor efficacy of anti-PD-1 therapy in an immunocompetent mouse model.

Results: Our quantitative proteomic profiling and analysis revealed TTLL12 to be a highly expressed signature protein in tumor and negatively correlated with IS, ICS, EM CD8+T cell, Th1 and NK cells infiltration, which indicated that TTLL12 might negatively regulate anti-tumor immunity. Clinically validation of CRC samples also confirmed the higher transcriptional and protein levels of TTLL12 in CRC, and higher TTLL12 was found to be related to poor distant metastasis-free survival in CRC by using Kaplan-Meier analysis. In vitro cell proliferation experiment and in vivo nude mouse subcutaneous tumorigenesis experiment proved that TTLL12 could not influence the proliferation of CRC and melanoma cells, while TTLL12 could promote tumor progression in two subcutaneous tumor models of immunocompetent mice, which indicated that TTLL12 depended on the host immunity to promote tumor progression. Flow cytometry analysis revealed that TTLL12 could reshape the immune microenvironment by upregulating myeloid-derived suppressor cell (MDSC) and suppressing CD8+T cells as well as

NK cells. In vivo, MDSC depletion by using anti-Ly6G antibody abolished the immune protective effect of knockdown of TTLL12, which suggested that tumor TTLL12 depended on MDSC and in turn suppressed CD8+T cell and NK cell during tumor progression. Mass spectrometry of cell culture supernatant indicated that chemokine ligand 9 (CCL9) was less secreted from TTLL12-knockdown tumor cells and influenced the recruitment of MDSC. Finally, knockdown of TTLL12 enhanced the anti-tumor efficacy of anti-PD-1 therapy in an immunocompetentmouse model.

Conclusion: In conclusion, TTLL12 is upregulated in tumor and related to poor distant metastasis-free survival in CRC. In vitro and vivo experiments reveal that TTLL12 depends on MDSC to suppress CD8+T cell and NK cell during anti-tumor immunity. Furthermore, TTLL12 could promote the secretion of chemokine CCL9 from tumor cells and contribute to the recruitment of MDSC. Knockdown of TTLL12 enhances the anti-tumor efficacy of anti-PD-1 therapy in animmunocompetentmouse model and thus could be a potential therapeutic target.

Key words: Anti-tumor immunity, TTLL12, MDSC

536. Exosomes from B7H3-CAR-T loaded with miR-145 and fluorouracil for targeted treatment of colorectal cancer

Ruyue Yang、Dong Hu、Guidan Wang、Tingting Yang、Zhaoyi Wei、Gaofeng Liang*

Henan University of Science and Technology

We constructed a CAR-T-derived exosome delivery system, in which exosomes from B7H3-CAR-T cells were loaded with miR-145 and fluorouracil (5-FU) to achieve the purpose of targeted drug delivery and gene combination immunotherapy for colorectal cancer. In this study,the targeted drug delivery system was successfully constructed and characterized by TEM and DLS , CAR-T cell-derived exosomes can successfully recognize and target tumor sites, in addition to carrying granzyme and perforin for antitumor effects. Furthermore, exosomes have good tissue cell penetration ability compared with CAR-T cells. Exosomes carrying miR-145 can inhibit the proliferation, migration and invasion of HCT-116 cells, when combined with 5-FU, the antitumor effect will be significantly enhanced.

Key words: CAR-T-derived exosome , miR-145 ,5-FU,Colorectal cancer

537. New star of therapeutic potential for liver cancer: exosomes derived from engineered liver cancer cells

Dong Hu、Guidan Wang、Ruyue Yang、Tingting Yang、Zhaoyi Wei、Gaofeng Liang*

School of Basic Medical Science, Henan University of Science and Technology

Gene therapy has provided new ideas and strategies in cancer treatment. In addition, it has been reported that exosomes derived from tumor cells (TEX) can not only participate in the formation of immunosuppressive microenvironment, but also have obvious "homing effect". The exosomes(Exos) still show a good state after loading small molecules. This undoubtedly makes TEX a kind of excellent nano drug loading material, which can not only target tumors but also load therapeutic drugs. In this study, hepatocellular carcinoma cell-derived Exos were used as loading substrates, microRNA-26a(miR-26a) and Programmed death ligand-1 antibody(anti-PD-L1) were loaded into Exos to prepare engineered Exos with targeted gene therapy and immunotherapy ,and to evaluate the effect on liver cancer.

Key words : Exosome, MicroRNA, PD-L1, Liver cancer

538. Mesoporous magnetic nanoparticles linked aptamers were used to capture and detect exosomes

Guidan Wang、Ruyue Yang、Dong Hu、Tingting Yang、Zhaoyi Wei、Gaofeng Liang*

Henan University of Science and Technology

Exosomes is secreted to the outside of the cells of a utricle, size is around 30 ~ 150 nm, almost all of the cells can be released, It has shown great potential as a novel molecular marker in disease diagnosis, such as Alzheimers disease diagnosis and tumor diagnosis. However, exosomes isolation and detection remains a difficult problem, which limits its further application. This article propose a magnetic bead complex with gold nanoparticles for efficient exosome capture and

detection. The hydrothermal synthesis of Fe_3O_4 gives it a large specific surface area and mesoporous structure, making the composite structure an efficient platform for exosomes capture. In addition, eluting captured exosomes with 1M NaCl opens up the possibility of using downstream exosomes for Alzheimers disease diagnosis. This composite material has a wide range of application prospects in biomedical and clinical applications.

Key words: Magnetic nanoparticles,Isolation of exosomes ,Alzheimer&s disease,

539. VDR–SOX2 signaling promotes colorectal cancer stemness and malignancy in an acidic microenvironment

Peishan Hu*、Dongwen Chen

The Sixth Affiliated Hospital, Sun Yat-sen University

The acidic tumor microenvironment provides an energy source driving malignant tumor progression. Adaptation of cells to an acidic environment leads to the emergence of cancer stem cells. The expression of the vitamin D receptor (VDR) is closely related to the initiation and development of colorectal carcinoma (CRC), but its regulatory mechanism in CRC stem cells is still unclear. Our study revealed that acidosis reduced VDR expression by downregulating peroxisome proliferator-activated receptor delta (PPARD) expression. Overexpression of VDR effectively suppressed the stemness and oxaliplatin resistance of cells in acidosis. The nuclear export signal in VDR was sensitive to acidosis, and VDR was exported from the nucleus. Chromatin immunoprecipitation (ChIP) and assay for transposase-accessible chromatin with high-throughput sequencing (ATAC-seq) analyses showed that VDR transcriptionally repressed SRY-box 2 (SOX2) by binding to the vitamin D response elements in the promoter of SOX2, impairing tumor growth and drug resistance. We demonstrated that a change in the acidic microenvironment combined with overexpression of VDR substantially restricted the occurrence and development of CRC in vivo. These findings reveal a new mechanism by which acidosis could affect the stemness of CRC cells by regulating the expression of SOX2 and show that abnormal VDR expression leads to ineffective activation of vitamin D signaling, resulting in a lack of efficacy of vitamin D in antineoplastic process.

Key words: colorectal carcinoma, vitamin D receptor， SRY-box 2 (SOX2)， acidic tumor microenvironment，cancer stem cell phenotype

540. FDX1 as a cuproptosis-associated genes in diffuse large B-cell lymphoma-related biomarkers to guide clinical diagnosis, prognosis and therapy.

Ziyu Liu[1]、Nan Song[1]、Zhimin Wang[2]、Xiao Yang*[3]、Tianshu Gao[2]

1. Liaoning University of traditional Chinese Medicine

2. Affiliated Hospital of Liaoning University of traditional Chinese Medicine

3. Second Affiliated Hospital of Liaoning University of traditional Chinese Medicine

Background: Ferredoxin 1 (FDX1) plays an important role in various cancers; however, its effects on patient prognosis and immune infiltration in diffuse large B-cell lymphoma remain unclear.

Methods: In this study, the expression profiles and clinical information of patients with diffuse large B-cell lymphoma were obtained from the Cancer Genome Atlas (TCGA) database. Using the Wilcoxon rank-sum test, the FDX1 expression levels were compared between diffuse large B-cell lymphoma and normal breast tissues. Functional enrichment analyses were performed to explore the potential signaling pathways and biological functions that are involved. Immune cell infiltration was assessed using single-sample gene set enrichment analysis. The Kaplan-Meier method and Cox regression analysis were used to identify the prognostic value of FDX1. A nomogram was constructed to predict the overall survival (OS) rates at one-, three-, and five-years post-cancer diagnosis.

Results: FDX1 was overexpressed in diffuse large B-cell lymphoma and significantly associated with increased age. Multivariate Cox analysis identified FDX1 as an independent negative prognostic marker of OS. The receiver operating characteristic curves was generated with a AUC index of 0.944. Functional enrichment analysis showed that the enrichment pathways included the stress response of copper ions, the regulation of ion transmembrane transport, cell response to chemokines, immune response mediated by immunoglobulin and retinol metabolism. Moreover,

the overexpression of FDX1 was negatively correlated with the levels of immune cell infiltration of Macrophages and T helper cells.

Conclusions: Therefore, FDX1 maybe a novel prognostic biomarker.

Key words: FDX1, cuproptosis, diffuse large B-cell lymphoma, diagnosis, prognosis

541. ANXA10 sensitizes MSI-H colorectal cancer to anti-PD-1 therapy via assembly of HLA-DR dimers

yiting sun、bowen yang、ce li、xiujuan qu*

Department of Medical Oncology, the First Hospital of China Medical University

Objective: Microsatellite instability-high (MSI-H) is a hypermutation pattern that occurs in genomic microsatellites, which occurs due to functional defects in DNA mismatch repair in tumor tissues, namely mismatch repair deficient (dMMR). Colorectal cancer (CRC) originates from normal colon epithelium, and genomic instability is a key factor driving its occurrence. MSI-H/dMMR has occurred in different types of cancer, with a high incidence in CRC, accounting for about 15% of the overall and 5% of metastatic CRC. This subtype of patients is the dominant population in immune checkpoint blockade (ICB) treatment. Nonetheless, several studies have found that only about 40% of MSI-H/dMMR CRC patients benefit from ICB therapy, and a substantial majority of patients do not respond to treatment or do not benefit consistently. Therefore, it is crucial to further stratify MSI-H/dMMR CRC patients, to screen the characteristic genes of those who benefit from immunotherapy, and to explore their molecular mechanism.

Methods: The single-cell transcriptome data of CRC was analyzed in this study, and quality control and batch effect correction were performed. The Seurat R package was used for cell clustering analysis, and the t-distribution random neighbor embedding method was used to visualize the cell clustering. Cell type annotations were performed by SingleR R package and CellMarker database. Single cell pseudotime trajectories were constructed with Monocle 2 for intestinal cancer epithelial cells to infer the occurrence and development of cancer cells and analyze the gene expression changes in the pseudotime trajectories. Screening of differentially expressed genes in cell clusters by R package Seurat. Conduct pathway enrichment analysis for

each cell through single sample gene enrichment analysis (single sample GSEA) and annotate biological functions through the Hallmark database gene sets. Peripheral blood mononuclear cells (PBMC) were extracted from healthy human peripheral blood by density gradient centrifugation. The survival rates of tumor cells were detected after co-culture of tumor cells and PBMC. The functions of ANXA10 in MSI-H CRC cells were further confirmed by in vitro and in vivo experiments.

Results: Single-cell clustering analysis of colorectal epithelial cells suggested the diversity of colorectal tumor cells. This study identified several epithelial cell subsets, including left colon-specific cancer cell subsets, mixed cancer cell subsets, advanced cancer cell subsets and MSI-H cancer cell subsets. In the branch of MSI-H cancer cells, the enrichment of immune-related pathways gradually increased. ANXA10 was a characteristic gene of the MSI-H cancer cell subset. ANXA10 improved the survival rate of MSI-H CRC cells under the action of PBMC and the sensitivity of cancer cells to anti-PD-1 therapy. ANXA10 promoted assembly of HLA-DR dimers in MSI-H CRC cells by increasing the expression level of CD74.

Conclusions: ANXA10 was a characteristic gene of the MSI-H cancer cell subset with the highest enrichment of immune-related functions. In MSI-H CRC cell lines, ANXA10 could significantly increase the sensitivity of cancer cells to anti-PD-1therapy. ANXA10 promoted the expression levels of HLA-DR dimers by increasing the expression of CD74, and ultimately improved the sensitivity of MSI-H CRC cells to anti-PD-1 therapy.

Key words: microsatellite instability-high； colorectal cancer； data analysis in single-cell transcriptome sequencing；ANXA10；sensitivity to anti-PD-1 therapy

542. Tumor acidic microenvironment regulates malignant progression of colorectal cancer through SLC26A3-HuR/CUGBP1 axis

Chong Chen*

The Sixth Affiliated Hospital of Sun Yat-sen University

Tumor stem cells play an important role in tumorigenesis, recurrence, drug resistance and metastasis. Tumor microenvironment is an important factor to determine the phenotype of tumor stem cells.Clarifying the molecular mechanism of tumor microenvironment regulating the phenotype of tumor stem cells will provide clues for finding the key targets of recurrence, drug resistance and metastasis of colorectal cancer, and provide new ideas for clinical treatment strategies and prognosis of patients with colorectal cancer.In ARGO and TCGA databases, SLC26A3 was lowly expressed in colorectal tumors and negatively correlated with the expression of acidic environment marker CAIX. RT-qPCR,Westernblot and cell immunofluorescence experiment showed that the expression of SLC26A3 was low in colorectal cancer cells, and was further reduced after acid treatment.After knocking down SLC26A3, the expression of tumor dry markers increased, and the ball-forming ability and drug resistance of tumor cells were enhanced. This trend will be reinforced by further acid treatment.The expression of HuR in tumor cells decreased while the expression of CUGBP1 increased after knocking down SLC26A3. co-IP experiment showed that there was interaction between SLC26A3 protein and CUGBP1/ HuR protein. RIP experiment showed CUGBP1 and HuR proteins interacted with some EMT-related RNA, indicating that CUGBP1 and HuR are RNA binding proteins and regulate the malignant phenotype of tumor cells.

Key words: colorectal cancer, relapse, drug resistance, tumor microenvironment

543. Tumor-associated macrophages promote gastric cancer progression via secreting IL-13 to activate the JAK-STAT3 axis

Xinxin Huang、Yufeng Chen、Peishan Hu*

The Sixth Affiliated Hospital of Sun Yat-sen University

BACKGROUND: Gastric cancer is one of the most common malignant tumors, and tumor metastasis is the leading cause of death. Tumor-associated macrophages (TMA) are important components in the tumor immune microenvironment and are involved in the progression of several types of tumors. However, the mechanism of TMA in promoting the malignant progression of gastric cancer remains unclear.

AIM: To investigate whether TAM can activate the JAK-STAT3-APOBEC3G axis of gastric cancer cells through IL-13, thereby promoting the stemness phenotype of gastric cancer cells and leading to the malignant progression of gastric cancer.

METHODS: Firstly, a co-culture model of macrophages and gastric cancer stem cells was established, followed by an analysis of co-cultured macrophages and gastric cancer stem cells using real-time qPCR and Western blot, RNA-seq, and mass spectrometry to identify molecular immunoregulation-related APOBEC3G, inflammation-related IL-13, which play a crucial role in macrophages and gastric cancer tumor stem cells. The specific mechanism of the IL-13-STAT3-APOBEC3G axis regulating the phenotype of gastric cancer stem cells was clarified using the ChIP-seq technique, ATAC-seq, RIP-seq technique, RNA pulldown, CRISPR, and other techniques.

RESULTS: 1. the co-culture of macrophages and gastric cancer stem cells contributed to the phenotype of gastric cancer stem cells and polarized macrophages to a non-inflammatory type.2. transcriptome sequencing analysis screened that APOBEC3G was significantly increased in gastric cancer stem cells after co-culture, and the expression of APOBEC3G was positively correlated with macrophage enrichment.3. knockdown of APOBEC3G inhibited the self-renewal ability of gastric cancer stem cells and the development of gastric cancer.4. increased IL-13 secretion by macrophages after co-culture and IL-13 upregulated APOBEC3G expression in

gastric cancer stem cells; STAT3 was significantly and positively correlated with APOBEC3G expression.5. c-MYC is a transcription factor located upstream of the APOBEC3G gene and a target gene downstream of STAT3. In a co-culture model, cMYC expression was found to be elevated in gastric cancer stem cells under an acidic environment. Knockdown of IL13 in macrophages significantly suppressed c-MYC expression. A further prediction of c-MYC binding sites on the APOBEC3G gene revealed that c-MYC further inhibited APOBEC3G expression by acting on sites in the promoter region of APOBEC3G. IL13 regulates the expression of APOBEC3G through the STAT3-c-MYC signaling axis.

Key words: Gastric cancer，Tumor-associated macrophages，IL-13 ，STAT3

544. A Novel Proteogenomic Integration Strategy Expands the Breadth of Neo-Epitope Sources

Xuan Dong*、Haitao Xiang、Fanyu Bu、Xiangyu Guan、Yuntong Zhao、Weicong Zhang、Yijian Li、Ying Gu

BGI RESEARCH

Simple Summary: Tumor-specific antigens are ideal targets for cancer immunotherapy. Mass spectrometry, which is the main method that directly identifies neo-epitopes presented on tumor cells, focuses mainly on peptides derived from annotated protein-coding exomes. However, non-canonical peptides arising from alterations at genomic, transcriptional, and posttranslational levels have been identified in several pioneering studies, making it necessary to develop an integrated proteogenomic approach that can comprehensively identify neoantigens derived from all genomic regions. Our novel strategy combining database searches with a de novo peptide sequencing method accurately identified multiple types of non-canonical peptides in the colorectal cancer cell line, HCT116. This practical proteogenomic strategy can be applied to neoantigen discovery in clinical tumor samples, improving cancer immunotherapy.Abstract: Tumor-specific antigens can activate T cell-based antitumor immune responses and are ideal targets for cancer immunotherapy. However, their identification is still challenging. Although mass spectrometry can directly identify human leukocyte antigen (HLA) binding peptides in tumor cells, it focuses on

tumor-specific antigens derived from annotated protein-coding regions constituting only 1.5% of the genome. We developed a novel proteogenomic integration strategy to expand the breadth of tumor-specific epitopes derived from all genomic regions. Using the colorectal cancer cell line HCT116 as a model, we accurately identified 10,737 HLA-presented peptides, 1293 of which were non-canonical peptides that traditional database searches could not identify. Moreover, we found eight tumor neo-epitopes derived from somatic mutations, four of which were not previously reported. Our findings suggest that this new proteogenomic approach holds great promise for increasing the number of tumor-specific antigen candidates, potentially enlarging the tumor target pool and improving cancer immunotherapy.

Key words: mass spectrometry; immunopeptidome; neo-epitope; immunotherapy

壁报交流

545. 曲美他嗪联合琥珀酸美托洛尔缓释片快速控制长期频发室性早搏一例

徐汉友*

湖州市安吉国际 LIASOM 医院

目的：为了快速、方便、更好地救治长期频发室性早搏，解除病人痛苦，提高生活质量，为新药研究提供临床观点和证据，特做此项研究。

方法：总结快速救治长期频发室性早搏成功的一例病人，分析其病情和用药特点和原理，把经验分享给同行，期望参考应用，促进医药科技发展，从而救治更多的病人。

结果：病人 1 年余前，无明显诱因出现心慌胸闷，呈持续性，无其他明显不适，在三甲医院，等多家医院诊治，诊断为心律失常，用药不详，不见好转，心率 80 次/分，律不齐，可闻及频发早搏，各瓣膜听诊区未及病理性杂音。2020-05-02 日，一医院动态心电图报告：频发室性早搏，占心搏的 3%；2020-06-18 日，一三甲医院冠状动脉 CTA：右冠细小，余冠状动脉未见明显异常。2021-04-16 日本院心电图报告：频发室性早搏、三联律。入院当天,上午 11：00 首次口服药物，下午 15:30 开始输液，之后不久，就感觉到心慌胸闷明显好转，当时未查体，第二天上午 08:30 查房时，已发现频发室性早搏早已纠正，心率持续规整，应该在上午 08:30 之前早已恢复正常心率，病人感觉心慌停止，胸闷明显好转，稍觉胸闷。目前病人持续窦性心律，自觉无明显不适，已治愈出院。病人的入院诊断为：1.心律失常、频发室性期前收缩；2.冠状动脉粥样硬化性心脏病；、3.腔隙性脑梗死；4.高血压 3 级；5.高尿酸血症；6.高脂血症；7.颈动脉硬化；8、颈动脉斑块。本病人患病特点：长期饮酒；有高血压病史；高血脂；高尿酸；动脉粥样硬化，就是长期频发室性早搏的诱因和原因，病人长期频发室性早搏持续心慌胸闷，相当痛苦。本病人治疗特点：以曲美他嗪片 20mgTID 及琥珀酸美托洛尔缓释片口服 23.75mgQD 为主药；以其他药物治疗为辅助治疗，曲美他嗪通过保护病人缺氧或缺血状态下的能量代谢，阻止心肌细胞内 ATP 的下降，保证了心肌细胞离子泵的正常功能，维持心肌细胞内环境稳定和生物电活动的正常运行，加上琥珀酸美托洛尔缓释片口服 23.75mgQD 缓慢地降低了心肌细胞的自律性等对心脏的进一步保护，从而快速地纠正了长期的频发室性早搏，其他药物的辅助治疗也很重要，为心肌细胞、心脏功能的正常运行提供保障。

结论：通过本病例的治疗成功，我们可以这样总结，对于长期饮酒病人，同时伴有“三高”或“四高”的动脉粥样硬化、冠心病病人，若患有频发室性早搏，可参考应用，以曲美他嗪片 20mgTID 及琥珀酸美托洛尔缓释片口服 23.75mgQD 为主药，辅以银杏叶提取物注射液 52.5mg 静滴 QD、阿司匹林肠溶片(拜阿司匹林)口服 100mgQD、麝香保心丸 42 粒口服 2 丸 TID、阿托伐他汀钙片(立普妥)口服 20mgQD，很可能会很快纠正此类频发室性早搏，当然在临床实践中，可以根据病情，实施个体化辅助治疗，调整药物。曲美他嗪片 20mgTID 及琥珀酸美托洛尔缓释片口服 23.75mgQD 的主药组合，可制备复合新药，以方便病人服用，提高治疗效果。

关键字：频发室性早搏；复杂心律失常；曲美他嗪；美托洛尔缓释片；新药创新

546. 高尿酸血症可能诱发运动性哮喘，救治成功中学生运动性哮喘一例

徐汉友*

湖州市安吉国际 LIASOM 医院

目的：为了重视高尿酸血症及其并发症的防治，特做此研究。

方法：通过总结临床诊治的一例不常见病例，提出防治高尿酸血症及其并发症的重要性和方法。

结果：2020-10-22 日，在值急诊夜班时，接诊一急诊中学生，患者：杨某某，男，15 岁，学生，住张家港锦丰镇一居民小区，住院号：2020004669。患者因“运动后喘息 1 小时左右”入住我院，其病例特点如下：1.病史：约 1 小时前，在学校进行 1000 米赛跑时，跑过 600 米后，病人觉眼前全是空白色，觉呼吸困难、喘憋，乏力，呕吐一次胃内容物，量较多不详，急忙停止赛跑，休息，不见明显好转，遂急联系家长来本院急诊科急救，平素体质健康，1 年前及半月前，曾 2 次类似此病情发作一次，但比本次病情轻，经休息后逐渐恢复正常。主要辅助检查：尿酸 1146umol/L，第三天复查尿酸 640umol/L。经治疗后治愈出院。

讨论和启示：运动性哮喘是支气管哮喘的一种特殊类型，发病率不是很高，但各个年龄组均可发病，其原因就是运动，其诱发原因会很多，包括感染、环境污染等，但高尿酸血症诱发运动性哮喘，还未见报道，由于上述病例特点，可以说明，病人接连发生的运动性哮喘，与其高尿酸血症有关系，也就是说，病人的高尿酸血症，很可能是病人运动性哮喘的诱发因素。

通过中国知网查询，截至目前，还没有发现高尿酸血症与运动性哮喘，存在因果关系的研究报道。据一项近期报道的研究，广州市 7-10 岁儿童的高尿酸异常率较高，男生和女生分别为 15.9%,31.2%，而且，与体质量指数（BMI）、腰围（WC）、收缩压（SBP）呈正相关。这项研究说明，中国儿童的高尿酸血症已非常严重。

结论：通过救治成功该病例，我们可以得到很多启示，对我们今后防病治病，会有很大帮助，具体如下：1、重视高尿酸血症的防治，因为，高尿酸血症，不仅是痛风和痛风性关节炎的病因，而且也是心脑血管疾病、肾功能衰竭等疾病的独立危险因素。2、不仅重视中老年人的高尿酸血症、痛风和痛风性关节炎的防治，也应该重视青少年，甚至婴幼儿高尿酸血症的防治，因为，少年儿童年龄组以下的人群，相比于其他年龄组，更未受到重视，现状是，各个年龄组的高尿酸血症，甚至痛风和痛风性关节炎及其后遗症，均未得到有效防治，更不用说青少年，甚至婴幼儿高尿酸血症的防治了。3、高尿酸血症患者，不论是中老年人，不能剧烈活动，即使青少年高尿酸血症患者，也不能剧烈活动，这样可能防治运动性哮喘，等急危重疾病的发生，从而及时挽救生命，解除病痛，提高生活质量。4、对于青少年，或年龄更小的高尿酸血症的防治，应该注意尽早体检发现，尽早控制尿酸，才能不至于，造成急危重病了，才被发现，更不能带病成长，带病学习、生活和工作。

关键字：高尿酸血症；运动性哮喘；少年；防治方法。

547. 急性酒精中毒及其他类中毒的 120 急诊医疗服务病例分析

徐汉友*

湖州市安吉国际 LIASOM 医院

目的：为了提高 120 急诊医疗服务对急性酒精中毒及其他类中毒的救治效果，促进大众健康和提高生活质量、国人素质及提高优良的社会风貌，特总结我院急性酒精中毒及其他类中毒的 120 急诊医疗服务病例分析。

方法：回顾性分析总结我院从 2014 年 11 月 1 日至 2016 年 10 月 31 日，2 年内，受理因急性酒精中毒及其他类中毒而拨打 120 急救电话，所接诊的 120 急诊医疗服务病例，分析总结，急性酒精中毒及其他类中毒的患病临床特点，及主要原则性救治措施和效果。

结果：急性酒精中毒及其他类中毒占所有 120 呼救病人的 15.6%。急性酒精中毒占 120 急诊医疗服务中毒病人的绝大多数，为 87.1%，急性酒精中毒有发生院前死亡病例，而且 120 急诊医疗服务到达这些死亡病例现场时，病人早已死亡，无法挽回生命。急性酒精中毒病人患病的显著临床特点，就是中毒后，横卧、昏迷、昏睡在街道、马路、餐厅等公共场所，行为污浊，占中毒病人的 72.7%；急性酒精中毒病人患病的另一显著临床特点就是，中毒后合并自伤、他伤、车祸及内科疾病，占 24%。本院救治急性酒精中毒及其他类中毒的治愈和显著好转率达 92%，100%的病人都被正确妥善处理，单纯急性酒精中毒病人无住院者，均为留观。

结论：本研究首次总结报道中毒病人的 120 急诊医疗服务病例分析，首次统计发现急性酒精中毒病人患病的显著临床特点，就是中毒后，横卧、昏迷、昏睡在街道、马路、餐厅等公共场所，行为污浊；急性酒精中毒作为常见疾病，并未被有关人员重视，但其患病特点，大大降低了大众健康和生活质量，严重有损国人素质及社会风貌和形象，因此本研究严厉的要求和提示，立即重视防治急性酒精中毒疾患国家政策的出台；对于急性酒精中毒病人，应该认真全面地治疗；并加强国际合作，共同治愈逐渐严重的不良饮酒对人类所害。

关键字： 中毒；急诊医疗服务；酒精中毒；急诊急救；中毒后行为。

548. 清开灵注射液联合生脉注射液或参麦注射液救治新型冠状病毒感染性肺炎

徐汉友*

湖州市安吉国际 LIASOM 医院

目的：为了救治新型冠状病毒感染性肺炎，增强病人体质,治疗可能遗留肺纤维化等后遗症，因此，中药清开灵注射液联合生脉注射液或参麦注射液救治这些病人，显得非常必要。

方法：本人作为高年资执业医师，自本次传染病暴发以来，非常关心疫情的发展和动态，并不断了解和学习疫情的具体防治措施和效果，作为医生、药学和中药学执业药师，根据本人多年的临床经验，特总结出救治新型冠状病毒感染性肺炎，增强病人体质,治疗可能遗留肺纤维化等后遗症的药物治疗方案，供参考利用。

结果：按照中药清开灵注射液、生脉注射液和参麦注射液最新说明书分析，中药清开灵注射液联合生脉注射液或参麦注射液应用于疫情临床各类病情的病人，应用时，根据病情，用药

剂量做相应的加减，危重病人应用常用量的最大量，按照中药注射液现代药理作用应用于临床，是切合实际的，必要时参考中医药辨证施治。而且越早用越好，每组药疗程至少为 15 天，参麦和生麦注射液用药时间可再长一些。从本人多年临床应用效果证实，其效果与药物说明书和临床研究报道非常相符，在此特殊时期，本人创新地提出应用两种中成药注射液联合应用的临床治疗策略，两种药物联合应用，取长补短，增强其疗效，降低其副作用，清开灵注射液具有清热解毒、化痰通络、醒脑开窍的功能，用于热病、神昏、中风偏瘫、神志不清，对急性肝炎、肺炎、上呼吸道感染、脑血栓形成、脑出血见上述证候者，效果明显，专业人士应该知道，现代药理研究发现，她具有解热作用、保护脑组织作用及抗肝损伤作用，等。而生脉注射液功能主治益气养阴，复脉固脱。用于气阴两亏，脉虚欲脱的心悸、气短、四肢厥冷、汗出、脉欲绝及心肌梗塞、心源性休克、感染性休克等具有上述证候者。参麦注射液益气固脱，养阴生津，生脉；用于治疗气阴两虚型之休克、冠心病、病毒性心肌炎、慢性肺心病、粒细胞减少症，能提高肿瘤病人的免疫机能，与化疗药物合用时，有一定的增效作用，并能减少化疗药物所引起的毒副反应。已经众所周知，参麦注射液和生脉注射液，主要中药成分相同，现代药理学研究已发现，生脉注射液均具有对血压、微循环、血液系统、心血管系统、免疫系统、神经内分泌系统、炎症反应，等均有调节和保护作用，增强病人抵抗力，对缺氧、缺血的脑组织有较好的保护作用，增强机体对缺氧的耐受力，延长常压缺氧下机体生存时间，等良好作用；参麦注射液也有类似于生脉注射液的现代药理作用。清开灵注射液为“凉药”，而生脉注射液和参麦注射液属于“补药”，因此，清开灵注射液联合生脉注射液或参麦注射液能相互弥补抵消二者的副作用，达到益气、养阴、生脉，增强病人的抵抗力，对因治疗抗新型冠状病毒；对症治疗生脉、强心、增加白细胞、保肝、保护大脑神经组织、保护肺组织，等扶正祛邪保护、促进人体生理功能正常强健的作用，而此三种药物单独应用，则无上述好的效果，因此，在此非常时期，应用清开灵注射液联合生脉注射液或参麦注射液治疗，治疗新型冠状病毒感染性肺炎各种病情的病人均适合，只是在用药剂量上，结合病人病情给以加减，危、重症病人可用常用量的最大量，一般病人用常用量。

结论：根据清开灵注射液、生脉注射液、参麦注射液的药理作用，及现今新型冠状病毒感染性肺炎病人，常遗留不同程度的后遗症病情，应用清开灵注射液联合生脉注射液或参麦注射液给以治疗，既可以增强病人体质、抗病毒,改善症状，从而降低死亡率、提高治愈率、治疗遗留的肺纤维化等后遗症，提高大众生活质量，减轻病人及其家人痛苦。

关键字：新型冠状病毒感染性肺炎；治疗方案；治疗后遗症；增强体质；中成药；抗病毒

549. 其他铂类对比顺铂治疗局部晚期鼻咽癌的疗效和安全性的 Meta 分析

李芷茹*、李超

四川省人民医院邛崃医院

背景：以顺铂为基础的同步放化疗（CCRT）已被确定为局部晚期鼻咽癌的主要治疗方法和标准治疗方法。顺铂的副反应影响其治疗的依从性，寻找铂替代物一直是研究热点，不同铂治疗结果存在差异，因此我们进行一项 meta 分析比较了基于其他铂衍生物（卡铂、奈达铂、洛铂）和基于顺铂的方案用于治疗局部晚期鼻咽癌的疗效与安全性。

方法：系统检索 PubMed，Embase，Cochrane 图书馆，Web of Science 以及 ClinicalTrial.gov 等 5 个医学出版物数据库，以检索截至 2022 年 2 月 15 日的所有潜在合格临床试验，使用 Review Manager 软件 5.4(RevMan 5.4)计算合并风险比(HRs)、风险比(RRs)和 95%置信区间(CIs)。

结果：从 1265 份记录中，包括 6 项随机对照临床试验在内的 8 篇文章符合条件，共有 1907 例局部晚期鼻咽癌患者。基于其他铂的化疗方案 OS,PFS,DMFS,LRFS 与基于顺铂的化疗方案无统计学差异。 治疗期间的严重急性血液学（＞3 级）副反应 中性粒细胞减少，白细胞减少，血小板减少与顺铂治疗组相当，值得注意的是贫血在基于其他铂治疗的患者发生率较高。 非血液学毒副反应如恶心，呕吐，体重下降的风险在顺铂治疗组风险更高，其他非血液学毒副反应及晚期毒副反应 两组患者均无统计学差异。

结论：其他铂类为基础的化疗方案与顺铂为基础的方案疗效相当，可能成为一种有效的顺铂替代方案，未来还需要更多的高水平证据支持。

关键字：顺铂，其他铂，鼻咽癌，荟萃分析

550. 趋化因子 CXCL9、10、11 及 CXCR3 在晚期 NSCLC 患者免疫治疗监测中的临床意义

朱晓斌*、朱敏、苏璇、张俊萍

山西白求恩医院（山西医学科学院）

目的：目前，免疫治疗已经广泛应用于非小细胞肺癌的一线治疗，但个体间对免疫治疗的反应性有很大差异，因此筛选出具有预测性能的标志物是至关重要的。

方法：纳入就诊于山西白求恩医院 38 例接受抗 PD-1(programmed cell death 1)免疫治疗的晚期非小细胞肺癌（Non-small Cell Lung Cancer,NSCLC）患者，在治疗前和治疗后疗效评价日分别收集患者外周血，用 ELISA 方法检测 CXCL9、10、11 及 CXCR3 的浓度，根据疗效评价分为疾病控制组（Disease Control Rate,DCR）和疾病进展组（Disease progression,PD），分析 CXCL9、10、11 及 CXCR3 与免疫治疗的疗效及预后的相关性。

结果：治疗前 DCR 组的 CXCL9、10 水平均明显高于 PD 组，且有统计学意义（*P* 值＜0.05）。治疗后 DCR 组 CXCL9 水平高于 PD 组，且有统计学差异（*P* 值＜0.05）。比较趋化因子水平变化率发现 DCR 组 CXCL9 变化率明显高于 PD 组，呈增高趋势，差异有统计学意义（*P* 值＜0.05）；通过 ROC 曲线对 CXCL9、10、11 及 CXCR3 对免疫治疗疗效的预测能力进行评估，发现 CXCL9 对疗效的预测能力最强（AUC 值 88.9%），其次为联合组（AUC 值 85.4%），且均有统计学差异（*P*<0.01）。Logistic 回归分析显示治疗后 CXCL9 升高及无淋巴结转移为疗效受益的独立影响因素；通过 ROC 曲线将 CXCL9 变化率分为高低变化率组，KM 法生存分析示 CXCL9 高变化率组的患者 PFS 明显长于低变化率组（*P*=0.02）。

关键字：晚期 NSCLC；PD-1 抑制剂；CXCL9；生物标志物

551. 双硫仑联合铜通过靶向 NPL4 通路发挥抗胃癌作用的机制研究

刘瑶*、郑振东、杜成、王美玲、王乃雪、陈禹潼、李宝磊、傅方伟、徐竹轩

中国人民解放军北部战区总医院

目的：检测双硫仑(Disulfiram，DSF)联合铜离子对人胃癌细胞系 HGC-27 及 SGC-7901 的杀伤效应，通过全基因组学及生物信息学技术并体外验证 ROS/MAPK 通路和 NPL4 通路在抗癌过程的作用。

方法：1.体外培养两种胃癌细胞系：HGC-27、SGC-7901；采用 CCK8 探究合适的药物作用浓度对 HGC-27，SGC-7901 细胞系 24h 增殖能力的影响并设立 Control 组、Cu 组、DSF 组、DSF/Cu 组，进行加药处理，观察细胞形态学变化；选取 HGC-27 药物处理后，进行全基因组学检测，运用生物信息学技术分析其中发生变化的机制；用流式细胞术及荧光显微镜技术验证基因组学中差异显著的 ROS/MAPK 通路相关的氧化应激及凋亡现象；采用免疫蛋白印迹和激光共聚焦技术检测蛋白降解相关分子 NPL4 及 K48-ubiquitin 蛋白的变化。2.采用 IBM SPSS26 软件及 GraphPad prism 8.0 和 Flow Jo 10.0，Image J 分析实验数据，各组实验数据用(±S)表示；采用 t 检验方法进行两组之间数据的比较；应用单因素方差分析对多组数据进行比较，$P<0.05$ 为差异具有统计学意义。

结果：1. DSF/Cu 抑制 GC 细胞活力。根据实验经验和文献综述，我们选择 0.2μM 作为铜离子工作浓度，0.24μM 双硫仑用于 HGC-27，0.30μM 用于 SGC-7901。与单独使用 DSF、Cu 相比，DSF/Cu 共处理抑制了 HGC-27 和 SGC-7901 的细胞活力。DSF/Cu 处理后，细胞存活率下降到 50%左右，细胞收缩，细胞间隙变宽，最终细胞死亡。但用铜或 DSF 处理后，细胞死亡和形态变化不明显，然后将 DSF 与铜复合，细胞活力明显受到抑制，细胞失去形态。我们认为，这是由于铜的低浓度显著增强双硫仑的细胞毒性。2. DSF/Cu 通过调节 MAPK 通路中基因表达水平发挥细胞毒作用。运用 RNA-seq 测序分析，检测 HGC-27 细胞在 0.24μM DSF（含或不含 0.2μM Cu）中暴露 24 小时后的转录组变化，根据变化情况筛选出其中发生变化的 19000 多个基因。与空白处理的细胞相比，暴露于 DSF/Cu 的细胞中有 445 个基因上调，99 个基因下调，而单独使用 DSF 处理的细胞中分别有 82 个和 55 个基因上调。KEGG 分析表明 MAPK 信号通路可能参与 DSF/Cu 诱导的细胞毒性。接下来，我们通过 qRT-PCR 分析验证了 RNA-seq 的数据。八个 MAPK 通路相关基因（FOS、JUN、GADD45A、CACANA1、

DUSP2、HSPA1A、HSPA6、DDIT3）的 mRNA 在 DSF/Cu 作用下显著增加。此外，据报道，ROS 的表达与 MAPK 通路的激活有关。3. DSF/Cu 提升了细胞内 ROS 水平。药物处理 2h 后，使用 DCFH-DA 探针代表 ROS 并用流式细胞术记录并通过荧光显微镜观察胞内 ROS 水平表达，结果表明， DSF/Cu 组平均荧光强度更高，通过在 DSF/Cu 中添加 ROS 清除剂 N-乙酰-L-半胱氨酸（NAC），ROS 平均表达量及表达强度均降低。 由此推断 ROS 水平升高可能是 MAPK 通路被激活的原因之一。4. ROS 的产生与 MAPK 介导的细胞凋亡密切相关。为了验证 MAPK 介导的细胞凋亡，采用 TUNEL 凋亡检测试剂盒研究细胞凋亡。药物暴露 24h 后，DSF、DSF/Cu 可分别诱导细胞凋亡。当同时暴露于 DSF/Cu 时，凋亡细胞数目急剧增加。此外，活性氧抑制剂 NAC 减少了活性氧相关凋亡的增加。这些结果表明，ROS 超载会引起 MAPK 介导的细胞凋亡。5. DSF/Cu 增加 K48 泛素化蛋白的表达并诱导 NPL4 聚集。当 NPL4 聚集时，它不能将 K48 泛素化蛋白运输到蛋白酶体进行降解。K48 泛素化蛋白的表达在细胞质中上调并逐渐增加。同时，当 DSF 与铜络合时，NPL4 水平受到抑制。此外，DSF 和 DSF/Cu 均导致不溶性聚集内源性 NPL4 的形成，对预提取产生抗性，聚集状态在 DSF/Cu 中更为明显。6. 在生物信息学网站 KM-Plotter 的分析结果表明，NPL4 和 UFD1 作为 P97 辅因子在癌组织中高表达，且高表达患者预后较差，而 P97 表达相反。这证明 NPL4 不仅在细胞水平发挥关键作用，并且 NPL4 高表达患者临床上可选择双硫仑作为治疗药物。

结论：1. DSF 能够抑制胃癌细胞 HGC-27、SGC-7901 增殖，联合低浓度 Cu2+后 DSF 细胞毒活性增强。2. DSF/Cu 激活了 ROS/MAPK 通路，并且诱发了 ROS 相关的细胞凋亡；3. DSF/Cu 诱导 NPL4 呈聚集状态，阻碍 NPL4 发挥转运泛素化蛋白至蛋白酶体降解，不可降解蛋白累积增多致细胞内 ROS 水平升高，诱发了 ROS 相关凋亡；4. NPL4 高表达可预测胃癌患者不良生存预后，对于 NPL4 高表达的患者可选择双硫仑治疗。

关键字：胃癌；双硫仑；铜；NPL4 ROS/MAPK；凋亡

552. 血清 HE4 在卵巢癌预后监测中的应用价值研究

冉盼盼*

郑州安图生物工程股份有限公司

目的：卵巢癌是女性生殖器官常见的恶性肿瘤之一，具有发现晚、致死率高的特点，对女性生命造成了严重的威胁。CA125 是目前临床应用最为广泛的卵巢癌肿瘤标志物之一，但是

在早期卵巢癌筛查中特异性不高，HE4 作为一种新型的卵巢癌肿瘤标志物，具有相对较高的灵敏度和特异性，对卵巢癌的早期筛查、治疗效果评价及预后检测具有重要意义。本文重点研究了 HE4 在卵巢癌患者的预后监测中的应用价值。

方法： 跟踪 8 例卵巢癌术后患者，检测患者手术前及术后 0-20 个月的 HE4，CA125 浓度值；采用试剂：郑州安图生物工程股份有限公司的人附睾蛋白 4 检测试剂盒（磁微粒化学发光法）、糖类抗原 125 检测试剂盒（磁微粒化学发光法）；仪器：全自动磁微粒化学发光仪 AutoLumo A2000 Plus。

结果：8 例卵巢癌患者手术前 HE4、CA125 检测值远高于相应的参考值，术后 HE4、CA125 值均降到正常水平，其中有 3 例患者术后 20 个月无复发表现，有 5 例术后复发患者。5 例复发者有 3 例患者在术后 12 个月 HE4 结果升高为阳性，在术后 15 个月 CA125 才检测为阳性；1 例患者术后在术后 7 个月 HE4 结果为升高为阳性，在术后 12 个月 CA125 才检测为阳性；1 例患者术后在术后 11 个月 HE4 结果为阳性，在术后 16 个月 CA125 才检测为阳性。

结论：在卵巢癌的预后监测中，HE4 较 CA125 能够更早的反应出卵巢癌的复发情况，就有较高的临床应用价值。

关键字：HE4；CA125；卵巢癌；预后监测

553. 血清 PGI、PGII及 PGR 结果反映胃黏膜状态的研究

冉盼盼*

郑州安图生物工程股份有限公司

目的：胃蛋白酶原（PG）是胃蛋白酶的前体，由胃黏膜组织分泌进入血液中，根据生化特性、免疫原性、细胞来源及组织内分布可将 PG 分为 PGI、PGII两个亚群。组分 1-5 免疫原性近似，称为 PGI(PG A)，主要由胃体和胃底腺体的主细胞和黏液颈细胞分泌；组分 6-7 免疫原性近似，称为 PGII(PG C)，主要来源于全胃腺(胃底、胃体、幽门的腺体)；十二指肠上段的 Brunner 腺、前列腺和胰腺也产生少量 PGII。正常情况下合成的 PG 大部分进入胃腔，在酸性胃液作用下生成胃蛋白酶，仅少量 PG(约 1%) 透过胃黏膜毛细血管进入血循环，故可通过检测血清 PG 判断胃黏膜状态。

方法：收集医院胃粘膜正常人血清 101 例，浅表性胃炎患者血清 63 例，慢性轻-中度萎缩性胃炎患者血清 58 例，慢性重度萎缩性胃炎患者血清 59 例，胃癌患者血清 55 例，采用郑州

安图生物工程股份有限公司的胃蛋白酶原I检测试剂盒（磁微粒化学发光法）、胃蛋白酶原II检测试剂盒（磁微粒化学发光法）在全自动磁微粒化学发光仪 AutoLumo A2000 Plus 上进行定量检测 PGI和 PGII浓度值，同时计算 PGR(PGI/PGII)。

结果：胃粘膜正常的人血清 PGI浓度值约为 70.3±3.2ng/ml，PGII浓度值约为 10.2±0.5ng/ml，PGR 约为 6.9±0.2；浅表性胃炎患者血清 PGI浓度值约为 88.5±4.6ng/ml，PGII浓度值约为 20.2±1.2ng/ml，PGR 约为 4.4±0.2；慢性轻-中度萎缩性胃炎患者血清 PGI浓度值约为 53.5±8.6ng/ml，PGII浓度值约为 17.2±1.6ng/ml，PGR 约为 3.1±0.4；慢性重度萎缩性胃炎患者血清 PGI浓度值约为 9.3±2.2ng/ml，PGII浓度值约为 11.5±1.1ng/ml，PGR 约为 0.8±0.2；胃癌患者血清 PGI浓度值约为 4.5±0.6ng/ml，PGII浓度值约为 9.8±0.6ng/ml，PGR 约为 0.5±0.1。

结论：浅表性胃炎患者 PGI及 PGII浓度值升高，PGR 降低；慢性轻-中度萎缩性胃炎患者 PGI正常，PGII升高，PGR 降低；慢性重度萎缩性胃炎及胃癌患者 PGI降低，PGII正常，PGR 降低；同时 PGR 越低胃癌风险越高。

关键字：PGI、PGII、PGR、胃黏膜

554. 构建“图灵图案”和纳米颗粒组成的智能水凝胶用于循环肿瘤细胞的捕获、培养和分析鉴定

陈东亮*、杨大伟、任天莹

聊城市人民医院

目的：本文构建“图灵图案”和纳米颗粒协同作用的智能水凝胶微流体界面用于高效捕获、培养和临床药物分析循环肿瘤细胞。通过调控“图灵图案”中峰-谷相对高度、峰-峰宽度以及表面粗糙度探究其结构尺度与 CTCs 捕获效率和培养稳定传代的细胞株之间的关系，建立对乳腺癌、肝癌、食道癌动物和患者外周血中 CTCs 的捕获、培养进行细胞迁移、细胞侵袭、细胞状态、细胞蛋白分泌量和临床药敏性分析等研究，探讨疾病状态下 CTCs 与实体瘤各种临床指标及疾病转归的关系，为病人进行个体化的治疗提供理论和实验依据。

材料与方法：1、构建“图灵图案”与纳米颗粒协同作用智能水凝胶界面的微流体及其表征；2、未改性水凝胶表面、改性水凝胶表面、微流体界面对细胞的生物相容性、粘附和生长增殖研究；3、微流体界面对外周血中活体 CTCs 的高效捕获及培养。收集乳腺癌、宫颈癌、肺癌动物和患者的外周血，并对外周血梯度离心后取中间带有 CTCs 的液体，将悬液滴加在 4.5cm^2

的水微流体界面上。对比全自动 CTCs 扫描仪上检测 CTCs 的数量来确定微流体界面捕获效率；4、将培养成功的 CTCs 细胞株和实体瘤细胞株进行临床药敏性分析。捕获和培养乳腺癌、宫颈癌、肺癌动物和患者的外周血中 CTCs 进行生物学研究（细胞计数、细胞迁移、细胞侵染、细胞状态、细胞蛋白分泌含量等）和临床药敏性分析，发现疾病状态下 CTCs 与实体瘤发生变化的重要参数，如分子分型、免疫原性、耐药性等，探讨疾病状态下 CTCs 与实体瘤各种临床指标及疾病转归的关系。

结果：1、构建“图灵图案”与纳米颗粒协同作用智能水凝胶界面的微流体；2、通过聚合物的摩尔比和含水量调控水凝胶力学性能，包括应力-应变与韧性；3、对比未改性水凝胶表面、改性水凝胶表面、微流体界面上 MCF-7、HeLa、HCC827 细胞的贴附态；4、水凝胶微流体界面可高效捕获外周血中 CTCs。

结论：1、运用化学交联和梯度脱水的方法成功构建 “图灵图案”与纳米颗粒协同作用智能水凝胶界面的微流体；2、在应力-应变与韧性表征中当摩尔比(nAc/nAM)为 0.2 时，应力达到最大为 130KPa，韧性达到 510KJ/m^3。含水量(ms/m)为 0.5 时，应力达到最大 248KPa，韧性达到 698KJ/m^3；3、MCF-7、HeLa、HCC827 细胞成功在水凝胶微流体界面粘附；4、水凝胶微流体界面捕获外周血中 CTCs 的效率大于 90%。

关键字：图灵图案，纳米结构，协同作用，水凝胶微流体，高效捕获，培养，分析，CTCs

555. 观察血清异常糖链糖蛋白表达和细胞免疫功能对肺癌预后的影响

任占良*

陕西中医药大学附属医院

目的：观察血清异常糖链糖蛋白（TAP）表达和细胞免疫功能对肺癌患者预后的影响。

方法：选取 2016 年 1 月—2017 年 5 月陕西中医药大学附属医院收治的 49 例肺癌患者的临床资料，依据治疗方式不同分为观察组（肺癌根治术加术后辅助化疗，n=28）和对照组（化疗，n=21)。分别于治疗前及治疗后 1、3 个月检测两组患者血清 TAP 表达和细胞免疫功能指标，卡氏（Karnofsky，KPS）功能状态评分。

结果：两组患者治疗前 TAP 表达阳性率比较，差异无统计学意义（$\chi 2=1.647$，$P>0.05$）；观察组治疗后 TAP 表达阳性率较治疗前显著下降，差异有统计学意义（比较治疗后 1 个月

与治疗前，χ2=4.2486，*P*=0.0393；比较治疗后 3 个月与治疗前，χ2=31.2391，*P*=0.0000，*p*<0.05）；对照组治疗后 TAP 表达阳性率较治疗前无明显变化（比较治疗后 1 个月与治疗前，χ2=0.8281，*P=0.3628*；比较治疗后 3 个月与治疗前，χ2=2.4846，*P*=0.1150，*P*>0.05）；两组间治疗后 1、3 个月 TAP 表达对比存在差异（治疗后 1 个月，χ2=9.819，*P*=0.007；治疗后 3 个月，χ2=6.716，*P*=0.035，*p*<0.05）。观察组治疗后 CD4+/CD8+比值较治疗前升高（比较治疗后 1 个月与治疗前，t=-9.6353，*P*=0.0000；比较治疗后 3 个月与治疗前，t=-6.7035，*P*=0.0000，*p*<0.05），对照组治疗后 CD4+/CD8+比值较治疗前下降（比较治疗后 1 个月与治疗前，t=-1.6487，*P*=0.1050；比较治疗后 3 个月与治疗前，t=2.1757，*P*=0.0340，*P*>0.05）；治疗后 1、3 个月，观察组 CD4+/CD8+比值均显著高于对照组，差异有统计学意义（*P*<0.01）。治疗后 3 个月生活质量评分（KPS 评分），观察组有效率 57.14%，对照组有效率 38.09%，治疗后观察组生活质量评分较对照组明显升高，有统计学意义（χ2=7.2746，*P=0.0070*，*p*<0.05）。

结论：血清 TAP 和细胞免疫功能可作为评估肺癌预后疗效、复发的指标，有临床应用价值。

关键字： 肺癌；异常糖链糖蛋白；细胞免疫功能；预后

556. 基于糖基转移酶基因的神经母细胞瘤预后模型的构建及功能分析

沙永亮*、赵强

天津医科大学附属肿瘤医院

目的：基于糖基转移酶基因构建神经母细胞瘤（NB）预后模型，为预测 NB 的预后及肿瘤治疗提供新的思路和方向。

方法：将 GEO85047 作为训练集，TARGET 数据库作为验证集进行外部验证。利用 SVM-LASSO-Cox 构建糖基转移酶基因的预后模型，根据评分中位数将样本分为高风险组和低风险组。采用 Kaplan-Meier 法进行生存分析，ROC 曲线评估模型对预后的预测效能，单因素和多因素 Cox 回归分析评估模型和其他临床因素与肿瘤预后相关性。分析模型与免疫细胞浸润的关系。免疫组化检测神经节细胞瘤及 NB 组织中 B3GALT4 表达。将 Sh-B3GALT4、B3GALT4 质粒转染到 NB 细胞株 9464D、975A2，实时荧光定量 PCR 检测细胞 B3GALT4 mRNA 表达水平，CCK-8、克隆实验检测细胞增殖能力，Transwell 实验检测细胞侵袭、迁移能力。

结果：共筛选出 10 个差异基因（PIGZ、GALNT7、GALNT2、GALNT14、EXTL2、DPY19L3、CHPF2、B3GNT5、B3GALT4 及 ALG3），并构建风险模型。在训练集，根据中位风险值将患者分为高风险组和低风险组，生存分析显示两组生存时间存在显著差异（P<0.01），预后风险模型 1 年、3 年以及 5 年生存率的预测结果 AUC 分别为 0.807、0.825 及 0.837。多因素 Cox 回归分析显示患者年龄、分期和预后模型均是患者的独立预后因素。在验证集，根据中位风险值将患者分为高风险组和低风险组，生存分析显示两组生存时间存在显著差异（P<0.01），预后风险模型 1 年、3 年以及 5 年生存率的预测结果 AUC 分别为 0.654、0.675 及 0.662。多因素 Cox 回归分析显示患者年龄、分期和预后模型均是患者的独立预后因素。Cibersort 法分析结果显示高风险组 NB 患者肿瘤中有较多的 CD4+T 细胞、CD8+T 细胞浸润。临床样本免疫组化结果验证显示，B3GALT4 基因在 NB 组织中显著低表达。上调 B3GALT4 可显著抑制 9464D、975A2 细胞的增殖、侵袭及迁移能力。

结论：通过生物信息分析技术成功构建基于糖基转移酶表达水平的 NB 患者预后模型，所确定的 B3GALT4 有望成为判断 NB 患者预后的指标和潜在治疗靶点。

关键字：糖基转移酶；神经母细胞瘤；预后

557. EBV 通过增强干性和 EMT 促进休眠癌细胞的 VM 形成

程天仪*、纪妍、游波

南通大学附属医院

血管拟态 (VM) 被定义为由肿瘤细胞组成的血管通道样结构，已证明通过提供血液循环与癌细胞的生长相关。然而，VMs 是否可以在休眠的癌细胞中形成仍然难以捉摸。 我们之前的研究表明，多倍体巨癌细胞（PGCC）是一种特定的休眠细胞，与头颈癌的预后不良有关。在这里，我们证明了 EBV 可以促进 PGCC 在体内和体外形成 VM。 更重要的是，我们揭示了部分由 LMP2A 介导的激活 ERK 通路是造成干性的原因，干性表型的获得对 PGCCs 的恶性生物学行为至关重要。 此外，上皮-间质转化 (EMT) 过程在 PGCC 中扮演重要角色，而 EMT 的进展对于 EBV 阳性 PGCC 形成 VM 也至关重要。我们的发现首次表明 EBV 在 PGCC-VM 中产生了可塑性，并提供了一种新的靶向抗肿瘤策略。

关键字：ebv，血管拟态，多倍体巨细胞，休眠癌细胞，鼻咽癌

558. MIR-1246 通过抑制巨自噬且促进分子伴侣介导的自噬共同促进鼻咽癌的恶性表型

张盼盼*、雷伟、顾苗（通讯作者）

南通大学附属医院

目的：自噬目前主要分为巨自噬、微自噬和分子伴侣介导的自噬（Chaperone-mediated autophagy, CMA）。自噬参与鼻咽癌(nasopharyngeal carcinoma,NPC)的发生和发展，但 CMA 在 NPC 中的作用还未知。此外，microRNA (miRNAs)调节基因表达参与肿瘤的发生和发展并且已被证实能够影响肿瘤的自噬，然而 miRNAs 是否调控 CMA 尚未见报道。因此，识别与 miRNA 和自噬靶点相关的恶性表型将为 NPC 的治疗提供新的思路。

方法：首先利用 miRNA 微阵列结合 TCGA 及 GEO 数据库检测 miR-1246 在 NPC 和头颈癌中的表达；原位杂交检测 miR-1246 表达及与鼻 NPC 的预后相关性。体内外实验分析 miR-1246 在 NPC 恶性表型中的作用。接着，利用 miRNA 靶点网站分析 miR-1246 在自噬中发挥作用的靶点 ATG12(自噬相关因子 12)。利用共聚焦显微镜等观察自噬小体、自噬溶酶体。通过数据库分析 RUNX3(RUNX 家族转录因子 3)不仅是 miR-1246 的下游靶分子也可以作为转录因子调控 CMA 中的关键分子 LAMP2A，接着利用 WB 和 qRT-PCR 分析 RUNX3 和 LAMP2A 在 NPC 细胞系的表达。体内外实验分析 RUNX3 和 LAMP2A 在 NPC 恶性表型中的作用。通过 WB、qRT-PCR、免疫组化、萤光素酶检测分析 miR-1246 与 RUNX3、RUNX3 与 LAMP2A 之间的互作关系。最后通过蛋白质组学验证 miR-1246 调控 CMA 并进一步阐明 miR-1246 调节自噬的机制。

结果：首先利用 miRNA 微阵列结合 TCGA 及 GEO 数据库，发现 miR-1246 在 NPC 和头颈癌中的表达水平显著升高。原位杂交检测发现 miR-1246 与 NPC 不良临床结果相关。体内外实验证明了 miR-1246 促进 NPC 恶性表型。接着，利用 miRNA 靶点网站分析 miR-1246 在自噬相关的靶点 ATG12。利用共聚焦显微镜等观察到自噬小体、自噬溶酶体在 miR-1246 被抑制的情况下显著增多。通过数据库分析 RUNX3 不仅是 miR-1246 的下游靶分子也可以作为转录因子调控 CMA 中的关键分子 LAMP2A，接着利用 WB 和 qRT-PCR 发现 RUNX3 在 NPC 细胞系中低表达，LAMP2A 在 NPC 细胞系中高表达。体内外实验证实 RUNX3 可以抑制 NPC 细胞的生长和转移，而 LAMP2A 对 NPC 细胞的作用则相反。通过 WB、qRT-PCR、

免疫组化、萤光素酶实验发现 miR-1246 与 RUNX3、RUNX3 与 LAMP2A 之间存在结合位点并且 miR-1246 抑制 RUNX3 的表达，RUNX3 抑制 LAMP2A 的表达。最后通过蛋白质组学揭示 miR-1246 通过靶向抑制 RUNX3 而促进 LAMP2A 的表达，进而促进 CMA，引起恶性生物学行为。并通过生信分析及细胞外酸化率(Extracellular acidification rat,ECAR)检测发现 CMA 促进肿瘤糖酵解从而促进 NPC 的增殖和转移。

结论：我们的研究揭示了 miR-1246 不仅通过靶向 ATG12 抑制巨自噬还可以通过靶向抑制 RUNX3 而促进 LAMP2A 的表达，进而促进 CMA 并促进肿瘤糖酵解引起 NPC 恶性表型的机制，为 NPC 的治疗提供了新的思路。

关键字：鼻咽癌，自噬，恶性表型，MIR-1246

559. 非小细胞肺癌免疫治疗生物标志物的研究进展

刘兆喆*、陈潞君、谢晓冬

中国人民解放军北部战区总医院

免疫治疗的出现为非小细胞肺癌（non-small cell lung cancer, NSCLC）的治疗带来了重大的变革，然而，基于癌症类型的异质性，并非所有患者都能从免疫治疗中获益，因此寻找可靠的生物标志物用于指导临床免疫治疗成为关键。与目前临床上常用的组织学活检相比，基于生物标志物检测不仅具有早期、无创等优势，而且还可以反映肿瘤的生物学特征与机体的免疫状态。本文就生物标志物在非小细胞肺癌中的研究进展进行综述，旨在为非小细胞肺癌的免疫治疗疗效和预后评估提供参考。

关键字：非小细胞肺癌；外周血生物标志物；免疫治疗；综述

560. 阿司匹林协同吉西他滨抑制胆囊癌 GBC-SD 细胞生长的机制研究

罗凯*、张旭东、刘中原、王向坤、李仁锋

郑州大学第一附属医院

目的：探讨阿司匹林协同吉西他滨对胆囊癌 GBC-SD 细胞生长的抑制及其机制。

方法：本研究利用不同浓度吉西他滨（0.2、1、5、10μmol•L-1）及阿司匹林（0.5、1、4mmol•L-1）分别处理胆囊癌 GBC-SD 细胞。对数生长期的 GBC-SD 细胞随机被分为空白对照组、吉西他滨组、阿司匹林组、吉西他滨联合阿司匹林组。运用 CCK-8 技术检测各组胆囊癌细胞的增殖能力；采用流式细胞仪检测各组胆囊癌细胞的凋亡率；运用 Western blot 实验检测各组胆囊癌细胞中 p-PI3K 及 PI3K 蛋白的相对表达量。此外，通过裸鼠移植瘤动物实验探讨阿司匹林及吉西他滨对 GBD-SD 裸鼠移植瘤的影响。

结果：4 组吉西他滨处理的 GBC-SD 细胞随着药物浓度增加（0.2、1、5、10μmol•L-1）以及处理时间的延长（24h、48h、72h），细胞生长抑制率增加，呈时间和浓度依赖性（$P<0.05$）。不同浓度的阿司匹林（0.5、1、4mmol•L-1）单独处理 GBC-SD 细胞 24h 或 48h，细胞生长抑制率的增加也呈时间和浓度依赖（$P<0.05$）。0.2μmol•L-1 及 1μmol•L-1 吉西他滨处理胆囊癌细胞 GBC-SD 48h 后，其相应凋亡率分别为：（12.5±1.9）%,（16.4±2.3）%，高于对照组（5.4±2.5）%，差异显著（$p<0.05$）。与单独用药相比，吉西他滨联合阿司匹林组培养 48h 后细胞生长抑制率（59.3±5.4）%高于吉西他滨组（29.7±2.9）%和阿司匹林组（26.9±2.5）%（$p<0.05$）。吉西他滨联合阿司匹林组细胞凋亡水平（36.1±8.6）%高于阴性对照组（4.5±1.1）%、吉西他滨组（15.3±2.1）%和阿司匹林组（12.9±3.1）%（$p<0.05$）。Western blot 结果显示，吉西他滨增加 p-PI3K 的表达，而阿司匹林降低 p-PI3K 的表达。PI3K 特异性抑制剂 LY294002 或 Wortmannin 可增强吉西他滨诱导的 GBC-SD 细胞生长抑制率和凋亡率（$p<0.05$）。在裸鼠实验中，用药干预 18 天后吉西他滨联合阿司匹林组肿瘤体积（69±59）mm3 小于阴性对照组（1791±247）mm3 及阿司匹林组（1153±166）mm3 和吉西他滨组（378±87）mm3（$p<0.05$）。吉西他滨联合阿司匹林组肿瘤重量（0.23±0.15）g 也小于阴性对照组（2.02±0.35）g，阿司匹林组（1.35±0.24）g 和吉西他滨组（0.45±0.19）g（$p<0.05$）。

结论： 通过体内体外实验发现阿司匹林可通过抑制 PI3K 通路活性增加胆囊癌细胞对吉西他滨的敏感性。

关键字：胆囊癌；吉西他滨；阿司匹林；PI3K；凋亡；增殖

561. LCBP 风险评估模型在肺结节危险分层的临床应用

武曼*[1]、冯飞雪 [1]、马艳侠 [2]

1. 陕西中医药大学

2. 陕西中医药大学附属医院

目的：应用基于肿瘤标志物结合影像诊断的 LCBP 风险评估模型对肺部结节危险分层，预测患者疾病发生恶性的概率。

方法：收集 2020 年 1 月 6 日--2021 年 4 月 30 日在陕西中医药大学附属医院就诊的 57 例肺部 CT 检查有肺结节的患者为实验组，50 例肺部 CT 检查未发现肺结节的患者为对照组。采集患者血样，使用化学发光免疫分析法测定 ProGRP、CEA、SCC-Ag 和 CYFRA21-1 血清生物学标志物指标，结合临床资料、病理诊断以及影像学表现分析，应用 LCBP 风险评估模型对肺结节进行危险分层。

结果：两组血清学标志物 CEA, SCC-Ag，CYFRA21-1 差异具有统计学意义（P <0.05），ProGRP 差异无统计学意义(P> 0.05)；影像学指标结节大小以及有无毛刺征对肺结节恶性概率的评估具有统计学意义(P <0.05)。LCBP 模型计算出的恶性概率 ROC 曲线下面积（AUC）为 0.746，危险分层 ROC 曲线下面积（AUC）为 0.716， LCBP 模型对肺结节的不同危险分层具有较高的敏感性和特异性。

结论：基于血清学标志物和影像学表现以及临床资料的 LCBP 风险评估模型对肺结节的危险分层具有良好的鉴别能力。

关键字：肺结节；生物学标志；影像学；LCBP 风险评估模型

562. TFF3 靶向抑制剂 AMPC 联合多西他赛在治疗他莫昔芬耐药乳腺癌中应用

郭慧*

清华伯克利深圳学院

目的：探究 TFF3 靶向抑制剂联合多西他赛在他莫昔芬耐药乳腺癌治疗中的应用 1. 体外研究：前期成功构建 MCF7 和 T47D 他莫昔芬耐药细胞系。(a)westen blot 测量他莫昔芬耐药乳腺癌细胞中的 TFF3 表达。(b)利用流式细胞技术分析 AMPC 对于细胞周期，细胞凋亡影

响。(c)TFF3 靶向抑制剂 AMPC 在耐药细胞系中的半抑制浓度，以及在 2D 细胞集落形成，3D 细胞培养。(d)各类化疗药物在耐药乳腺癌中的效果。(e)AMPC 和多西他赛联合作用指数(CI)。(f) AMPC 联合多西他赛在 2D 细胞集落形成，3D 细胞培养中的效果。(g)AMPC 联合多西他赛在凋亡相关蛋白 BCL2, BCL-XL,BAK,BAX,BID, BIM,Caspase3/7 影响。2. 体内研究：将 5×10^6MCF7 耐药细胞注射到 BALB/c 裸鼠乳腺脂肪垫中，待肿瘤长到 100mm^3 时将老鼠随机分为正常对照组，AMPC 组，多西他赛组，AMPC+多西他赛组，每组 6 只。AMPC 组老鼠每日腹腔注射药物 AMPC 20mg/kg，多西他赛组每 4 日腹腔注射多西他赛 5mg/kg，AMPC+多西他赛组同时注射 AMPC 和多西他赛。药物治疗 14 天后牺牲老鼠，取小鼠肿瘤以及血清。肿瘤做免疫组化测量 TFF3, ki67 表达。ELISA 测量血清中 TFF3 的表达量。

结果：1.体内研究（a）TFF3 在他莫昔芬耐药的 MCF7 和 T47D 细胞中表达增强。(b)AMPC 可以明显降低 TFF3 的表达，阻止乳腺癌细胞在 G2 期，并且增加癌细胞早期和晚期凋亡。(c)AMPC 在乳腺癌中的半抑制浓度约 1μM，在 2D 细胞集落形成 和 3D 细胞培养中有明显地抑制癌细胞生长作用。（d）在蒽环类，铂类，氟嘧啶类，紫杉烷类化疗药物中耐药细胞对于多西他赛敏感。(e)AMPC 和多西他赛联合具有协同效用。(f)AMPC 联合多西他赛可以明显降低耐药乳腺癌细胞集落形成和抑制 3D 细胞生长。(g)AMPC 联合多西他赛抑制抗凋亡蛋白 BCL2,BCL-XL 表达，更好地促进凋亡相关蛋白 BAK，BAX，BID，BIM，Caspase3/7 的表达。2.体内研究：MPC 和多西他赛可以降低裸鼠乳腺癌肿瘤的生长，AMPC 联合多西他赛明显降低肿瘤体积并且部分出现肿瘤完全消退。肿瘤免疫组化提示 AMPC 联合多西他赛降低 Ki67 表达。免疫组化和血清 ELISA 结果提示小鼠 AMPC 组可以降低 TFF3 表达量，而多西他赛增加 TFF3 表达，AMPC 联合多西他赛仍可以降低 TFF3 的表达量。AMPC 可以增强多西他赛在他莫昔芬耐药乳腺癌治疗作用。

关键字：乳腺癌；他莫昔芬；耐药；多西他赛；TFF3；AMPC

563. CA19-9 和 CEA 联合检测在胆囊癌辅助诊断中的应用价值

宋少敏*、渠文涛

郑州安图生物工程股份有限公司

目的：探讨肿瘤标志物 CA19-9 和 CEA 联合检测在胆囊癌辅助诊断中的应用价值。

方法：共收集 110 例样本，其中 50 例原发性胆囊癌患者为对照组，30 例同期胆囊良性病变患者和 30 例健康者为对照组和健康组，在 Auto Lumo A2000 Plus 使用配套试剂进行 CA19-9 和 CEA 检测，分析统计各指标单独检测及两种联合检测的特异性与灵敏度，采用 ROC 分析血清 CA19-9，CEA 水平对胆囊癌的诊断价值。

结果：单独使用 CA19-9、CEA 诊断胆囊癌有较高特异性，但敏感性较低。将 CA19-9 和 CEA 联合检测时，敏感性为 82.8%，特异性 88.2% ，与良性病变组和健康组相比，胆囊癌患者血清 CA19-9，CEA 水平明显升高，差异具有统计学意义（p<0.05）；两项联合诊断的灵敏度，准确度，特异度，均高于各项单独检测，差异具有统计学意义（p<0.05）。ROC 曲线分析显示，血清 CEA，CA19- 9 水平联合诊断胆囊癌的 ROC 曲线下面积明显大于单独指标诊断（p<0.05）。

结论：肿瘤标志物 CA19-9 和 CEA 联合检测可以提高胆囊癌的诊断率，具有一定的临床应用价值，值得推广应用。

关键字: CA19-9；CEA；胆囊癌

564. 晚期上皮性卵巢癌患者术前炎症指标联合 CA125、HE4 对肿瘤细胞减灭术满意度的预测价值

祖逸峥*[1]、哈春芳 [2]

1. 福建医科大学妇儿临床医学院

2. 宁夏医科大学总医院妇科

目的：探讨晚期上皮性卵巢癌（AEOC）患者术前炎症指标联合糖类抗原 125（CA125）、人附睾蛋白 4（HE4）对初次肿瘤细胞减灭术满意程度的预测价值。

方法：回顾性分析自 2016 年 1 月至 2021 年 12 月于宁夏医科大学总医院经过初次肿瘤细胞减灭术的 AEOC 患者 144 例，其中满意组 101 例，不满意组 43 例。应用 MedCalc 20.0 软件绘制 ROC 曲线评估比较患者术前 NLR、MLR、PLR、CA125、HE4 单一预测及 PLR、CA125、HE4 两两联合预测不满意肿瘤细胞减灭术（SODS）的临床价值。

结果：1.不满意组术前 NLR、MLR、PLR、CA125、HE4 水平均高于满意组，差异有统计学意义（*P* 均＜0.05）；2.术前血清学指标单一预测 SODS 中，CA125 的 AUC 最大为 0.849（95%CI:0.780-0.903），其敏感性、特异性、准确性、阳性预测值、阴性预测值、阳性似然比、阴性似然比分别为 83.72%、73.27%、56.99%、57.14%、91.36%、3.13、0.22；3.术前血清学指标两两联合预测 SODS 中，术前 PLR＞262.11 联合 CA125＞748.4U/mol 的特异性最高为 94.06%。

结论：术前 PLR＞262.11 联合 CA125＞748.4U/mol 预测 AEOC 患者 SODS 的特异性高，在临床实践中可能成为预测 SODS 的有效手段。

关键字：晚期上皮性卵巢癌；肿瘤细胞减灭术；炎症指标；糖类抗原 125；人附睾蛋白 4

565. 血清 CA125 在心衰检测的临床意义研究

吴小田*

安图生物工程股份有限公司

目的：心力衰竭（heart failure）简称心衰，是指由于心脏的收缩功能和（或）舒张功能发生障碍，不能将静脉回心血量充分排出心脏，导致静脉系统血液淤积，动脉系统血液灌注不足，从而引起心脏循环障碍症候群，此种障碍症候群集中表现为肺淤血、腔静脉淤血。近年来心衰的发病率仍将继续增长，已经成为世界范围内的主要健康负担。 因此寻找新的心衰标志物，对该病进行早期预防至关重要，目前临床最常用的标志物有 BNP 和 NT -ProBNP，两者临床应用价值相似，但是 NT -ProBNP 更易于检测，更灵敏，是临床上更为理想的心衰标志物，在急性心衰（AHF）和慢性心衰（CHF）患者的临床诊断、危险分层、预后评估及疗效检测中均有重要意义。血清 CA125 是卵巢癌的辅助诊断指标，另子宫内膜癌、乳房癌、胃肠道癌一些恶性肿瘤及卵巢囊肿、子宫内膜病、宫颈炎及子宫肌瘤等良性妇科病中血清 CA125 也会有不同程度的升高，近年来很多研究证实 CA125 和心功能相关，因此对该情况进行研究。

方法：选取 93 例心衰患者血清，采用磁微粒化学发光法在安图 AutoLumo A2000 全自动化学发光测定仪上检测，首先使用血清 NT -ProBNP 确认其为阳性，然后使用糖类抗原 CA125 检测试剂盒（磁微粒化学发光法）进行检测，确认其血清 CA125 浓度。

结果：93 例患者中血清 CA125 结果在 39-553IU/ml 之间，均不同程度的高于 95%正常人参考值范围（界值 35IU/ml），且血清 CA125 与 NT -ProBNP 基本呈现正相关。

结论：心衰患者血清中 CA125 病理生理机制还不清楚，查阅文献资料发现可能跟心衰患者血清中的炎症因子水平上升、血液循环淤血可引起胸膜间皮细胞信号肽分泌、心衰患者血清中的原癌基因存在异常增多等有关。因本次研究样本数量有限，还需进一步验证与心衰的诊断及预后相关性，另外 CA125 在多种良性和恶性疾病患者体内都可以有不同程度的升高，临床上如何更加准确区分 CA125 高表达及降低和心功能的确切关系也需更进一步大规模的试验设计及临床分析支持。目前来看，联合 CA125 和 NT -ProBNP 的检测，在治疗心衰、预测 、预后方面可能有更积极的意义。

关键字：心衰；CA125；NT -ProBNP

566. 标本前处理对 CEA 测定结果的影响

吴小田*

安图生物工程股份有限公司

目的：CEA 是一种具有人类胚胎抗原特性的、细胞内富含多糖的酸性蛋白复合物，分子量约 200KD，其中含有 50~85%的碳水化合物。正常成人的血液中很难测出，主要存在于内胚层上皮细胞分化而来的癌肿细胞表面（尤其是腺癌），也是一种膜抗原和可溶性抗原，越过细胞膜进入体液中，故可在多种体液中检测出。CEA 属于非器官特异性肿瘤相关抗原，分泌 CEA 的肿瘤大多位于空腔脏器，如胃肠道、呼吸道、泌尿道等。正常情况下，CEA 经胃肠道代谢，而肿瘤状态时的 CEA 则进入血液和淋巴循环，引起血清 CEA 异常增高。在临床上，CEA 增高常见于结直肠癌、肺癌和胃癌，也可见于乳腺癌、卵巢癌、肝癌、胰腺癌、宫颈癌等。结肠炎、胰腺炎、肾功不全、肝硬化、肝炎等良性疾病及大量吸烟者体内 CEA 也会轻度升高。CEA 测定的主要用途是用于手术治疗、化疗、放疗等疗效监测。一般手术切除后 6 周，CEA 水平恢复正常，否则提示有残存肿瘤，若 CEA 浓度持续不断升高，或其数值超过正常 5-6 倍者均提示预后不良。肿瘤复发或转移常伴随着 CEA 水平的显著升高，

连续定量检测血清 CEA 含量，对肿瘤病情辅助判断更具有意义。本研究旨在研究标本前处理对 CEA 测定结果的影响。

方法：选取 20 例体检人群标本，均无相关疾病就及抽烟史，使用康健普通管采集 5ml 标本，两种方式处理：规范处理是 37℃孵育 30min，然后 4000r 离心 10min；不规范处理是 37℃孵育 15min，然后 4000r 离心 3min。使用癌胚抗原检测试剂盒（磁微粒化学发光法）在安图 AutoLumo A2000 全自动化学发光测定仪上每个标本重复 5 孔检测，分析其重复性及结果。

结果：20 例患者标本，规范处理结果均为阴性，每个标本 5 孔重复性在 3%以内，不规范处理的 CV 最大增大到 40%，结果可升高到 7.5ng/ml（界值为 5ng/ml）。

结论：血液标本的采取的是检验人员无法直接控制的，不规范的前处理可能会造成标本纤维蛋白析出，血红蛋白升高等进而影响到测量结果，其中有些异常可能无法通过肉眼判断，给后期的临床诊断和异常结果原因查找造成很大的困难，因此标本前处理过程在体外诊断过程中至关重要。

关键字: CEA；标本前处理

567. PGE2 与 COX-2 通过正反馈环促进结肠癌发生的研究进展

魏思桐*

内蒙古医科大学

结肠癌是常见的消化系统肿瘤，其具有高发病率和致死率。近年来，结肠癌的治疗具有多样性，包括联合化疗、抗 EGFR 和抗血管生成剂等治疗方式，但这些治疗方式的效果欠佳，均不能完全有效地缓解病情。目前已有研究表明，结肠癌的发生发展与前列腺素（PG）上调有关，并且研究中指出易感受试者的癌前细胞转为恶性细胞也与 PG 的上调相关。前列腺素 E2（PGE2）是在结肠癌中生成最多且最重要的前列腺素成员。通过环氧合酶-2（COX-2）诱导产生的 PGE2 可以促进肿瘤细胞的增殖、迁徙和转移、血管的生成和耐药性的抵抗。COX-2 和 PGE2 形成了一种正反馈的关系，COX-2 诱导 PGE2 的生成，反之 PGE2 的上调进一步增加了 COX-2 的表达。正反馈的机制是 PGE2 信号增加了相关蛋白 1（YAP1）的表达和转录活性，导致 COX-2 和前列腺素 E 受体 4 基因（EP4）的表达增加。正反馈环会促进结肠癌细胞系的增殖和结肠组织的再生。此途径的组成性激活可能会导致息肉和结肠肿瘤

的形成。在小鼠实验中已证实 PGE2 通过激活 NF-κB、EP4-PI3K 和 EP4-丝裂原活化蛋白激酶信号传导诱导小鼠结肠癌干细胞（CSC）扩张，并促进小鼠肝转移瘤的形成。此外，在家族性腺瘤性息肉病中，PGE2 的表达也增强。有研究证实，使用非甾体类抗炎药的受试者结肠癌发病率低，因此，PGE2 信号通路可能被用于靶向治疗以减缓 CSC 扩张和结直肠癌进展，其具体的作用机制还需进一步研究。

关键字： 结肠癌、前列腺素 E2、环氧合酶-2

568. 多指标联合血浆 ctDNA 中 HOXA7、SOX17 甲基化在肺结节早诊中的临床应用研究

冯飞雪*

陕西中医药大学附属医院

目的： 探讨结节直径、毛刺征、癌胚抗原（CEA）、细胞角蛋白 19（CYFRA21-1）、ctDNA 中 HOXA7、SOX17 甲基化对肺结节患者的早期诊断价值。

方法： 选取 2021 年 12 月至 2022 年 6 月我院收治的恶性肺结节性患者 25 例，良性结节患者 9 例，作为肺癌组和良性结节组，另选择同期于我院行体格检查的 17 例健康体检者作为对照组。比较三组间患者吸烟史、结节直径、毛刺征、血清 CEA 和 CYFRA21-1 水平及血浆 ctDNA SOX17 甲基化率，并通过二分类 Logistic 回归分析筛选癌变患者的独立为危险因素，然后得出预测模型方程，最后采用 ROC 曲线评价模型的诊断效能。

结果： 单因素分析表明，肺癌组患者结节直径、毛刺征、血清 CEA、CYFRA21-1 水平、HOXA7 及 SOX17 甲基化率明显高于良性结节组和健康对照组，差异具有统计学意义（p<0.05）。患者结节直径、毛刺征、血清 CEA 和 CYFRA21-1 水平升高及 HOXA7 和 SOX17 甲基化率是恶性肺结节的独立危险因素（p<0.05），最终预测模型为 P=1 / [1+e-(-9.026+0.031 结节直径+0.00616 毛刺征+1.956CEA+1.069CYFRA21-1+0.021HOXA7 甲基化率+0.038SOX17 甲基化率)]。其中，预测模型的 AUC 为 0.982，相较于单个指标显著提升，差异有统计学意义（p<0.05）。

结论： 结节直径、毛刺征、CEA、CYFRA21-1、ct DNA HOXA7、SOX17 甲基化率检测对肺癌患者具有较高的诊断价值，基于以上指标建立的联合预测模型可明显提升诊断效能。

关键字： 肺结节；肺癌；血清肿瘤标志物；循环肿瘤 DNA；甲基化；诊断价值

569. 径向超声联合快速现场评估在肺外周病变的诊断价值

徐春华*

南京市胸科医院

目的：评价径向超声经引导鞘管支气管镜肺活检术（EBUS-GS-TBLB）联合快速现场评估（ROSE）在肺外周病变（PPLs）诊断中的价值。

方法：对 2018 年 2 月至 2020 年 8 月于南京市胸科医院就诊发现的 158 例 PPLs 患者行 EBUS-GS-TBLB 检查，随机将患者分为 EBUS-GS-TBLB 联合 ROSE 组（ROSE 组）和不联合 ROSE 组（No-ROSE 组）中，观察两组的诊断率、操作时间、活检次数和并发症的差异。

结果: ROSE 组诊断率为 85.7%，No-ROSE 组诊断率为 70.3%，两组诊断敏感度差异有统计学意义（$P<0.05$）。ROSE 组平均操作时间和活检次数均少于 No-ROSE 组，两组差异有统计学意义（$P<0.01$）。两组患者均无严重气胸、咯血等并发症。

结论： ROSE 提高了诊断率，缩短了操作时间，将 ROSE 技术联 EBUS-GS-TBLB 应用于诊断 PPLs 高效安全。

关键字：径向超声；经支气管肺活检；快速现场评价；肺外周病变

570. 生物钟基因 BMAL1 通过抑制 TGF-β1/Smads 通路在鼻咽癌增殖、转移中的作用和机制研究

赵朝芬*[1,2]、金风[1,2]、龙金华[1,2]、刘丽娜[1,2]、贺前勇[1,2]、李卓玲[1,2]、陈越[1,2]、黎钰欣[1,2]、徐歆宇[1,2]、周定安[1]

1. 贵州医科大学附属医院

2. 贵州医科大学附属肿瘤医院

目的：拟探讨生物钟基因 BMAL1 抑制鼻咽癌增殖、转移的分子机制。

方法：1、BMAL1 在鼻咽癌组织及细胞系中的表达及意义研究：免疫组化检测 41 例鼻咽慢性炎症组织和 71 例鼻咽癌组织中 BMAL1 的表达。PCR 和 Western blot 分别检测鼻咽癌细胞株和人永生化鼻咽上皮细胞 NP69 中 BMAL1 的表达水平。2、BMAL1 对鼻咽癌细胞增殖、侵袭转移及上皮-间质转化的影响研究：平板克隆、CCK8 及裸鼠皮下成瘤实验检测 BMAL1 对鼻咽癌细胞体外、体内增殖能力的影响；划痕愈合、Transwell 侵袭迁移实验检测 BMAL1

对鼻咽癌细胞体外侵袭迁移能力的影响；荧光活体成像、HE 染色判断裸鼠尾静脉注射模型转移情况。PCR 和 Western blot 检测 BMAL1 对鼻咽癌细胞中 EMT 相关指标在转录和蛋白水平表达的影响。3、BMAL1 抑制鼻咽癌增殖、转移的分子机制研究：利用生物信息学技术，ChIP 实验，双萤光素酶报告基因实验，免疫荧光共定位实验及 Co-IP 等一系列分子生物学手段验证其机制。

结果：1、BMAL1 在鼻咽癌组织及细胞系中的表达研究结果显示：（1）BMAL1 在鼻咽癌组织和细胞中表达降低；（2）BMAL1 在鼻咽癌组织中的表达与鼻咽癌患者 M 分期有关(p=0.006)。2、BMAL1 对鼻咽癌细胞增殖、侵袭转移及上皮-间质转化的研究结果显示：（1）过表达 BMAL1 可抑制鼻咽癌细胞的增殖能力、侵袭及迁移能力，敲低 BMAL1 则相反；（2）过表达 BMAL1 可抑制鼻咽癌细胞的 EMT。3、BMAL1 抑制鼻咽癌增殖、转移的机制研究结果显示：（1）在 TGF-β1 启动子区存在 5 个 BMAL1 的结合位点，BMAL1 可以直接结合在 TGF-β1 启动子区域，能够抑制 TGF-β1 的转录活性；（2）过表达 BMAL1 可抑制 TGF-β1/Smads 通路活性；（3）在重组人 TGF-β1 的诱导下，鼻咽癌细胞增殖能力增强，TGF-β1/Smads 信号通路活性增强，鼻咽癌细胞发生 EMT，细胞侵袭和迁移能力增加；过表达 BMAL1 后，TGF-β1 不再促进 TGF-β1/Smads 信号通路活性，EMT 受到抑制，细胞侵袭和迁移能力减弱；（4）在鼻咽癌细胞及组织中 BMAL1 与 EZH2 存在共定位关系及相互作用，BMAL1 结合 EZH2 后可抑制 TGF-β1 转录及蛋白表达；（5）BMAL1 联合 TGF-β1 在预测鼻咽癌是否转移上具有一定的诊断价值。

结论：BMAL1 在鼻咽癌中表达下调，其表达水平与鼻咽癌的发展及转移有关。BMAL1 可抑制鼻咽癌细胞的增殖、上皮-间质转化及侵袭转移能力，其机制与抑制 TGF-β1/Smads 信号通路活性有关。推测可能成为鼻咽癌新的预后标志物和治疗靶点。

关键字：鼻咽癌；生物钟基因 BMAL1；TGF-β1/Smads 信号通路；增殖；转移

571. 晚期 HER-2 阳性乳腺癌原发灶与转移灶异质性研究

王慧*、张咪、杨姣、王凡、董丹凤、杨谨

西安交通大学第一附属医院

研究目的：比较晚期人表皮生长因子受体 2（human epidermal growth factor-2,HER-2）阳性乳腺癌患者原发灶与转移灶基因突变特征差异、肿瘤突变负荷（Tumor Mutation Burden，TMB）差异；探索原发灶与转移灶克隆演化规律。

材料与方法：本研究共纳入 24 名晚期 HER-2 阳性乳腺癌患者（21 例转移性患者及 3 例局部晚期患者），对收集到的 31 份组织样本（22 份原发灶样本+9 份转移灶样本，包括 7 对配对的原发灶与转移灶组织）进行了包含 618 种癌症相关基因的靶向测序。计量资料采用 Wilcoxon 秩和检验。以 $P< 0.05$ 为差异有统计学意义。

结果：1、HER-2 阳性乳腺癌患者原发灶组织与转移灶组织中最常见的突变基因均为 *TP53*（73%*vs.*78%）。*NOTCH3*、*ARID1A*、*SETD2* 等基因的突变频率在原发灶中高于转移灶（分别为 32%*vs.*22%，27%*vs.*11%，18%*vs.*11% ）。而 *PIK3CA*、*PRKCH*、*SLX4*、*AR*、*BARD1*、*NOTCH1*、*PPM1D* 等基因的突变频率在转移灶中高于原发灶（分别为 56%*vs.*36%、44%*vs.*14%、44%*vs.*27%、33%*vs.*14%、33%*vs.*14%、33%*vs.*23%、22%*vs.*5%）。*ESR1* 基因在转移灶中突变频率为 22%，而在原发灶中未检出。*ERBB2* 基因在原发灶及转移灶中的突变频率较接近，分别为 23%和 22%。原发灶组织的 TMB 显著高于转移灶组织 TMB，差异有统计学意义（P=0.0156）。2、P12 患者的乳腺原发灶与淋巴结转移灶（同时期）的基因检测结果表明，该患者原发灶与转移灶基因突变特征高度一致，原发灶中 93.3%的突变基因可在转移灶中检出。而 P2 患者的原发灶与肝转移灶（非同时期，经多线治疗后出现肝转移）的基因检测结果表明，原发灶与转移灶基因突变一致性较差，原发灶中仅有 15.7%的突变基因可在转移灶中检出，且转移灶较原发灶出现新的突变基因，包括 *NOTCH1*、*NCOR2*、*PRKCH*、*ESR1* 等。3、对患者 P12 进行原发灶与淋巴结转移灶克隆演化分析发现，由原发灶向转移灶形成的过程中，由主干突变簇形成了 2 支分支突变簇，且在转移灶中发生 *PRKCH*、*DUSP4*、*CALR*、*SLX4*、*JARID2* 等基因突变的突变簇的细胞比例较原发灶明显升高。对患者 P24 原发灶与淋巴结转移灶进行克隆演化分析发现，由原发灶向转移灶形成的过程中，发生 *POLE*、*CHEK2*、*JARID2*、*NBN*、*FANCG* 等基因突变的突变簇的细胞比例始终较高，而在转移灶中发生 *SLX4*、*TGFBR2*、*NOTCH1*、*MST1R*、*APC* 等基因突变的突变簇的细胞比例相比于原发灶明显下降。

结论：晚期 HER-2 阳性乳腺癌患者的转移灶较原发灶更常发生与耐药及疾病进展相关的基因突变；原发灶的 TMB 显著高于转移灶；原发灶与转移灶的克隆演化规律可为疾病进展、转移的发生机制提供分子水平依据。

关键字: HER-2 阳性乳腺癌；基因组学；肿瘤突变负荷；克隆演化

572. 肿瘤来源的血清外泌体 miR-4321 作为非小细胞肺癌的诊断生物标志物

张哲*、谢丽

山东省肿瘤研究防治院（山东省肿瘤医院）

研究目的：非小细胞肺癌(NSCLC)，是全球最常见的肺癌亚型，也是肺癌患者高发病率和高死亡率的主要原因，并且这些患者的存活率相对较低。因此，迫切需要研究一种针对 NSCLC 患者特异性诊断的生物学标志物。miRNA 是一种 20-24nt 的非编码 RNA，通过直接结合其 3‘非翻译区(3’UTR)，在多细胞生物中参与转录后调控基因表达。有研究表明，外源性 miRNA 是不同癌症中重要的预测或预后的生物标志物。本研究旨在确定血清外泌体生物标志物是否可以作为非小细胞肺癌（NSCLC）患者的生物学标志物。

材料和方法：1.通过高通量测序筛选出差异表达的 miRNA。2.收集山东省肿瘤医院 191 例非小细胞肺癌患者血清和 218 例健康供体血清。3.采用超速离心法从 NSCLC 患者(n=191)和健康供体(n=218)的血清中提取外泌体。4.使用透射电镜、qNano 和 Western Blot 实验验证了所提取物质为外泌体。5.用 qPCR 验证了血清外泌体 miRNA 的表达。

结果：1.血清外泌体来源的 miR-4321 在血清外泌体中稳定表达。2.与健康对照组相比，NSCLC 患者血清外泌体 miR-4321 的表达显著增高(P<0.0001)，曲线下面积(AUC)为 0.6798，其表达差异具有统计学意义。

结论：本研究结果表明，血清外泌体 miR-4321 在诊断肺癌方面具有潜在的临床价值，是 NSCLC 患者的一种很有前途的诊断生物标志物。

关键字: 非小细胞肺癌、miRNA、外泌体、肿瘤标志物

573. 内源性谷氨酸在 ADCY10 依赖条件下抑制 YAP 决定肺腺癌的铁死亡敏感性

张骁*

上海市胸科医院

目的：由于胱氨酸摄取受损，抑制胱氨酸-谷氨酸反转运体 system Xc-后，可诱导一种新发现的细胞死亡形式——铁死亡。Yes 相关蛋白(YAP)表达由己糖胺生物合成途径(HBP)依赖的 O-连接的β-N-乙酰氨基葡萄糖酰化(O-GlcNAc 糖基化)维持。谷氨酰胺-果糖-6-磷酸转氨酶(GFPT1)是 HBP 的限速酶，可以被腺苷酸环化酶(ADCY)介导的蛋白激酶 A (PKA)介导的磷酸化抑制。由于内源性谷氨酸在肺腺癌(LUAD)中积累后的结果尚未明确，以及积累的内源性谷氨酸是否通过影响肺腺癌细胞中的 ADCY/PKA/HBP/YAP 轴来决定铁死亡敏感性尚不清楚。因此，本研究主要探究内源性谷氨酸的积累是否会影响铁死亡敏感性。

方法：测定细胞活力、细胞死亡、脂质活性氧(ROS)与丙二醛(MDA)的产生，以评估抑制 system Xc-后对铁死亡的反应。TMTs 及定量蛋白组学被用来探索影响肺腺癌细胞铁死亡敏感性的关键蛋白。免疫印迹法和实时定量 PCR 分析蛋白质和基因表达。进行共免疫沉淀(co-IP)分析以鉴定蛋白质-蛋白质相互作用和翻译后修饰。使用合适的试剂盒测量代谢物水平。使用荧光素酶报告分析、染色质免疫沉淀(ChIP)和电泳迁移率偏移分析(EMSA)评估转录受调节情况。使用细胞来源的异种移植(CDX)和患者来源的异种移植(PDX)小鼠模型进行给药和限制性细胞稀释实验。临床结果、药物疗效和 ADCY10 表达之间的联系使用患者来源的原代肺腺癌细胞和患者组织进行评估。

结果：抑制 system Xc-后内源性谷氨酸的积累已被证明通过抑制肺腺癌细胞中的 YAP 来确定铁死亡的敏感性。当 GFPT1 受抑制，YAP O-GlcNAc 糖基化和表达不能在肺腺癌细胞中维持。YAP 的磷酸化和泛素化进而增强。在各种不同的肺腺癌细胞中，ADCY10 作为一个关键的下游靶点，使谷氨酸对 PKA 依赖的 GFPT1 的抑制作用多样化。我们还发现 ADCY10 的促肿瘤作用和促铁死亡作用是分别由两种信号通路介导的。ADCY10 高表达的晚期肺腺癌对铁死亡更加敏感。此外，具有获得性治疗抗性的肺腺癌细胞也倾向于更高表达 ADCY10，并且更可能对铁死亡敏感。最后，不同程度的二次不稳定铁增加是由于 system Xc-抑制后期未能维持 YAP 刺激的铁蛋白转录补偿引起的，这进一步解释了为什么各种肺腺癌细胞的铁死亡敏感性并不相同。

结论：内源性谷氨酸对肺腺癌细胞中 system Xc-抑制后的铁死亡敏感性起关键作用，对晚期和/或耐药肿瘤的肺腺癌患者，以铁死亡为基础的治疗是一个很好的选择。

关键字：铁死亡敏感性标志物；XBP1 剪接；铁蛋白；Hippo 通路；GFPT1；HBP 依赖的 O-GlcNAc 糖基化；

574. 外泌体传递的 miR-7 通过靶向 YAP 在非小细胞肺癌中逆转吉非替尼耐药

张骁*

上海市胸科医院

表皮生长因子受体(epidergrowth factor receptor, EGFR) T790M 突变是第一代和第二代酪氨酸激酶抑制剂(tyrosine kinase inhibitor, TKIs)发生耐药的主要机制，miR-7 在 T790M 突变发展中的作用尚不清楚。在这里，我们通过免疫印迹(IB)和酶联免疫吸附试验(ELISA)分析蛋白表达。RT-qPCR 分析 mRNA 表达；检测细胞存活率、细胞迁移、克隆形成及凋亡实验以评价细胞对吉非替尼的反应；免疫共沉淀分析用于鉴定蛋白质-蛋白质之间的相互作用。证实了在吉非替尼敏感性 PC9 细胞中 miR-7 的水平明显高于吉非替尼耐药 H1975 细胞，并且 miR-7 过表达促进了吉非替尼治疗后 H1975 细胞的凋亡。此外，我们发现外泌体可以将 miR-7 从 PC9 细胞转移到 H1975 细胞，通过与 YAP 结合逆转吉非替尼耐药，并改变 H1975 细胞的耐药表型。此外，我们发现通过 GW4869 抑制外泌体 miR-7 后，可增加 PC9 细胞对吉非替尼的体内化疗耐受性。值得注意的是，我们检测到健康对照组血清外泌体中的 miR-7 显著高于肺癌患者，高 miR-7 表达与接受吉非替尼治疗的肺癌患者的高敏感性以及更长的生存期相关。因此，外泌体 miR-7 可以作为 EGFR T790M 耐药突变的潜在生物标志物和治疗靶点。

关键字：NSCLC；T790M；miR-7；外泌体；吉非替尼；YAP

575. 外泌体和 circRNA_101093 在肺腺癌铁死亡脱敏中的重要作用

张骁*

上海市胸科医院

目的: 铁死亡是一种由铁依赖的脂质过氧化物过度积累引起的细胞程序性死亡，最近发现铁死亡与肺腺癌相关。细胞内的抗氧化系统可抑制铁死亡。本研究的目的是探究细胞外系统是否以及如何使肺腺癌细胞对铁死亡脱敏。

方法: 研究对象为人肺成纤维细胞 MRC-5、WI38 和人肺腺癌细胞 H1650、PC9、H1975、H358、A549 和 H1299 细胞系，肿瘤和匹配的肺腺癌邻近组织，健康个体和肺腺癌患者的血浆。研究方法为采用免疫组织化学和免疫印迹法分析蛋白表达；采用逆转录 PCR 法分析 mRNA 表达；采用细胞活力、细胞死亡和脂质活性氧生成评估铁死亡敏感性；采用透射电镜观察外泌体；采用点击化学标记法检测花生四烯酸定位；采用 RNA 下拉、RNA 免疫沉淀、光激活核糖体增强交联和免疫沉淀法检测 RNA 和蛋白质之间的相互作用；采用蛋白质组学分析 RNA 调控的蛋白；采用代谢组学分析代谢物；采用细胞来源的异种移植、患者来源的异种移植、细胞植入肺内肺腺癌小鼠模型和肺腺癌患者的血浆/组织标本来验证分子机制。

结果: 肺腺癌患者的血浆外泌体特异性降低了肺腺癌细胞的脂质过氧化，并使肺腺癌细胞对铁死亡脱敏。其机制为外泌体 circRNA_101093 (cir93)提高肺腺癌细胞内 cir93 水平，以此调控花生四烯酸代谢。花生四烯酸是一种多不饱和脂肪酸，对铁死亡至关重要，参与质膜过氧化。cir93 与脂肪酸结合蛋白 3 相互作用，促进花生四烯酸转运以及其与牛磺酸的反应。因此，花生四烯酸减少并且其产物 n -花生四烯酰牛磺酸增多。此外，研究发现 NAT 可抑制花生四烯酸进入质膜。在临床前的体内模型中，减少外泌体可以促进基于铁死亡的治疗效果。

结论: 外泌体和 cir93 是肺腺癌细胞对铁死亡脱敏的关键，阻断外泌体可能有助于肺腺癌的治疗。

关键字:外泌体, circRNA_101093, 铁死亡, 脱敏, 肺腺癌, 脂质过氧化, 多不饱和脂肪酸, 牛磺酸, N-花生四烯酸牛磺酸, RNA-蛋白质相互作用

576. 肝癌血清标志物 NRP1 诊断价值研究

张骁*

上海市胸科医院

研究背景与目的: NRP1 是一种 I 型跨膜糖蛋白，最初被发现在神经轴突导向和胚胎血管生成中发挥作用。NRP1 可以促进肿瘤发生的血管生成，细胞存活，迁移，侵袭和化学耐受。近年来，NRP1 被发现是抗肿瘤免疫的关键障碍。NRP1 与免疫细胞表达的配体 semaphorin-4a（Sema4a）相互作用，增强肿瘤内调节性 T 细胞（Tregs）的功能和存活，进而限制抗肿瘤免疫反应。在之前的研究中，ChIP-seq 分析数据显示 NRP1 可能是促肝癌 Hippo 信号通路主要转录因子 TEAD 的新型靶基因。然而，NRP1 是否刺激肿瘤发生并作为肝癌中的新型肿瘤标志物仍然未知。

材料与方法: 所有细胞均购买自中科院细胞库，患者标本及健康对照样本于 2015 年 5 月至 2016 年 11 月在上海市瑞金医院收集。qPCR 实验以及免疫印迹实验分别检测指定分子的 mRNA 及蛋白表达水平。酶联免疫吸附测定实验检测血清中肝癌相关蛋白表达水平。采用独立样本 t 检验，方差分析，Mann-Whitney 检验，Wilcoxon 标记秩和检验和 Kruskal-Wallis 检验比较组间连续变量差异。进行 Spearman 等级相关检验以计算等级变量之间的相关系数。用 ROC 曲线下面积（AUC-ROC）评估诊断价值。$p<0.05$ 认为具有统计学意义。

结果: TEAD 直接结合到 NRP1 的启动子上以刺激其在肝癌细胞中的转录。NRP 表达在肝癌组织中比正常组织显著上调，同时 NRP1 可促进肝癌细胞活力和集落形成，并抑制肝癌细胞凋亡。我们发现肝癌患者血清 NRP1 浓度显著高于健康个体），乙肝患者，丙肝患者，肝硬化患者，乳腺癌患者，结肠癌患者，胃癌患者肺癌患者。血清 NRP1 预测肝癌的最佳诊断阈值为 68pg / ml，灵敏度为 93.7%，特异性为 98.7%，说明血清 NRP1 是肝癌中较好的诊断标志物。

结论与讨论: Hippo/YAP 信号通路是通过控制细胞增殖和凋亡来控制器官大小的一条高度保守的信号通路。Hippo 信号通路上游激酶可对下游的 YAP 产生磷酸化修饰，对 YAP 产生抑制作用。一旦上游的核心激酶对 YAP 的抑制作用减弱，YAP 将与 TEAD 等转录因子相结合，促进下游基因的转录，起到促进癌症发生发展等多种作用。本研究发现 TEAD 靶基因 NRP1 有成为新型肝癌血清标志物潜力，为基础研究向临床转化提供了新依据。

关键字: NRP1；肿瘤标志物；Hippo 信号通路；TEAD；YAP；肝癌

577. TFCP2/YAP 转录复合体调控蛋白 CPE 对肝癌诊断价值研究

张聪聪*

上海市胸科医院

研究背景与目的: 肝癌是全世界发病率及死亡率最高的恶性肿瘤之一。因缺乏高特异性以及高灵敏度的早期诊断标志物，导致肝癌患者通常无法得到及时治疗。目前用于临床诊断的经典肝癌临床现有肝癌早期诊断肿瘤标志物存在一定比例假阳性及假阴性问题，开发新型肝癌诊断标志物对肝癌患者早期治疗，降低肝癌患者死亡率有着极其重要的意义。YAP 是一种共转录因子，可促进一系列下游原癌基因的转录，具有很强促肝癌功能。我们前期研究中发现另一种促肝癌分子 TFCP2 作为 YAP 相关转录因子的募集者，可招募一系列下游转录因子，从而促进肝癌形成，而且其自身也可发挥转录因子作用。本研究旨在探讨 TFCP2/YAP 转录复合体调控蛋白 CPE 在肝癌中的诊断价值。

材料与方法: 所有细胞均购买自中科院细胞库，患者标本及健康对照样本于 2015 年 3 月至 2017 年 3 月在上海市瑞金医院收集，qPCR 实验以及免疫印迹实验分别检测指定分子的 mRNA 及蛋白表达水平。双荧光报告实验检测 CPE 启动子荧光基因的活性。酶联免疫吸附测定实验检测血清中肝癌相关蛋白表达水平。运用的统计学方法包括 t 检验，Bonferroni 多重比较分析，进行 Spearman 等级相关检验以计算等级变量之间的相关系数。使用 ROC 曲线下面积（AUC-ROC）评估诊断价值。$p<0.05$ 认为具有统计学意义。

结果: 我们发现 CPE 的 mRNA 以及蛋白表达均受 TFCP2 和 YAP 调控，而且 CPE 启动子区域存在 TFCP2 结合基序，突变该基序后，TFCP2 和 YAP 丧失对 CPE 启动子调控作用。在肝癌患者的血清中，CPE 表达水平为 813.084 ± 199.118 pg/ml，明显高于正常人群(41.55± 9.074 pg/ml，n=100)，乙型肝炎(32.493 ± 7.019 pg/ml, n=42)和胃癌患者 (53.147±13.155 pg/ml, n=29)。此外，CPE 表达水平和 AFP（R=0.644，p=0.000），谷丙转氨酶 ALT（R=0.454，p=0.000）以及谷草转氨酶 AST（R=0.351，p=0.001）均存在正相关性。CPE 的 ROC 曲线下面积为 0.937，优于 AFP。CPE 的最佳诊断阈值为 75pg / ml，此时敏感度为 90.7%，特异性为 97.5%。

结论与讨论: CPE 是 M14 家族的金属羧肽酶的成员，可参与肽激素和神经递质（包括胰岛素）的生物合成，也具有一定程度促癌作用。此外，该基因突变与 2 型糖尿病有关。本研究中，我们发现 CPE 受促癌通路 YAP/TFCP2 调控，TFCP2 为直接调控 CPE 表达的转录因子，

而 YAP 起到关键促 CPE 转录作用。YAP 转录相关膜表面蛋白作为肝脏肿瘤标志物已有一系列报道，本研究中我们又发现了新型 YAP 调控膜表面蛋白 CPE 有成为新型肝癌诊断标志物潜力，证明了 YAP 相关转录通路的强促肝癌作用。

关键字：肝癌；TFCP2；YAP；CPE；肿瘤标志物

578. Bcl-2 -938 C>A 多态性与癌症发病及预后的关系

张聪聪*

上海市胸科医院

目的：细胞凋亡是一个高度程序化的细胞死亡，它可以通过两个主要途径实现：死亡受体途径和线粒体途径。Bcl-2 家族蛋白通过调控线粒体外膜完整性在调控线粒体凋亡途径中发挥重要作用。Bcl-2 是一种抗凋亡调控蛋白，通常在多种癌症中高表达。Bcl-2 有两段功能不同的启动子区域，分别被命名为 P1 和 P2。而-938 位点就是位于 Bcl-2 的 P2 启动子区域。Bcl-2 -938 位点 多态性与细胞周期的调控以及细胞的存活相关。有研究表明，Bcl-2 -938CC 基因型更容易发生无菌性松动，也可能引发重度抑郁症的临床症状。此外，Bcl-2 基因 -938 位点多态性可能与癌症的发病以及预后相关，有一些相关的研究曾报道它们潜在的关系，然而，并没有一个明确的结论被得出。这篇文章通过荟萃分析来探索-938 位点多态性（C>A)与癌症的发病以及预后的关系。

方法：文章通过搜索 PubMed, EMBASE, Cochrane Library, OVID 以及 Web of Science databases 等数据库获得文献。相对危险度（Odds ratio，OR）以及 95%置信区间（95%CI）用来衡量 Bcl-2 -938 C>A 位点的多态性与癌症发病率的关系，并采用显性模型（dominant model） (WM + MM vs WW； W：野生型基因，M：突变型基因),隐性模型（recessive model） (MM vs WM + WW),纯合子比较模型（homozygote comparison） (MM vs WW),杂合子比较模型（heterozygote comparison ）(WM vs WW)以及等位基因模型 allelic model (M vs W)。风险比（Hazard ratio，HR）以及 95%置信区间用来衡量 Bcl-2 -938 位点的各种不同基因型与癌症预后的关系。

结果：根据纳入的 26 篇文献来看，Bcl-2 -938 位点的多态性与癌症发病的风险有显著关系，这种显著性体现在包括隐性模型 (OR=1.35 95%CI: 1.07-1.69, *P*=0.01), 等位基因模型(OR=1.14, 95%CI: 1.01-1.28, *P*=0.03) 以及 纯合子比较模型 (OR=1.40, 95%CI: 1.05-1.85, *P*=0.02)

三种遗传模型中。此外，经过多种基因型比对的预后分析，发现 Bcl-2 -938 位点的多态性与癌症的预后关系不明显。(AA *vs.* CA: HR=0.99, 95%CI: 0.77-1.27, *P*=0.93; AA *vs.* CC: HR=0.92, 95%CI: 0.65-1.30, *P*=0.63; AC *vs.* CC: HR=0.94, 95%CI: 0.80-1.11, *P*=0.48 ; CC *vs.* AA+CA: HR=1.21, 95%CI: 0.69-2.13, P=0.50; AA *vs.* CC+CA: HR=0.99, 95%CI: 0.48-2.04, *P*=0.97)。

结论：Bcl-2 -938 位点多态性与癌症发病的风险有显著关系，尤其是 Bcl-2 -938 位点如果是 AA 基因型，则该种基因型的人群有很大可能发生癌症。这一结论为癌症的预防和筛查提供了新的研究方向。作为检验科的研究人员与工作人员，我们应继续探索 Bcl-2 -938 位点多态性在不同癌症类型中与癌症发病率的关系。如果能发现新的肿瘤易感基因筛查位点，就可以更好地预防该基因型人群发生癌症，从而降低癌症发病率，达到精准医疗的目的。

关键字: Bcl-2，癌症，预后，发病率，荟萃分析

579. Hippo/YAP 信号通路调控蛋白 ACAN 诊断价值研究

张聪聪*

上海市胸科医院

研究背景与目的: Hippo/YAP 信号通路是通过控制细胞增殖和凋亡来控制器官大小的一条高度保守的信号通路。YAP 可与多种转录因子如 TEAD，CREB 以及 TFCP2 等相结合，促进下游基因如 CTGF，BICC1 的转录，起到促肝癌作用。在肝癌中，肝特异性高表达 YAP 的转基因小鼠很快出现了肝损伤的症状，并最终形成了肝癌。YAP 调控膜蛋白在肝癌中高表达并可释放入血，本研究旨在探索探索 YAP 调控膜蛋白是否可作为肝癌肿瘤标志物对肝癌进行早期精准诊断。

材料与方法: 所有标本收集于上海市瑞金医院 2015 年 5 月至 2016 年 12 月期间。细胞系购买自中科院细胞库。RNA 抽提后经反转录获取 cDNA 并进行定量 PCR 分析。酶联免疫吸附测定试剂盒购自上海颖心实验设备有限公司。统计学方法包括 t 检验，Bonferroni 多重比较分析，Spearman 等级相关检验，ROC 曲线下面积等。$p<0.05$ 被认为具有统计学意义。

结果: 过表达 YAP 后，ACAN 的 mRNA 表达显著上升，而 YAP 敲减后 ACAN 的表达水平显著下降。在肝癌细胞 7402 以及 7721 细胞系中过表达几种常见和 YAP 结合的转录因子 CREB，TEAD，TFCP2 以及 RUNX2 等，我们发现仅有 CREB 过表达可促进 ACAN 的 mRNA

表达，而 TEAD，TFCP2 以及 RUNX2 对 ACAN 表达影响并不明显。ACAN 的启动子序列 -610～-599nt 存在 CREB 结合基序，直接受 YAP 以及 CREB 调控。与正常人群相比，我们发现肝癌患者血清中 ACAN 表达水平明显升高，而且在乙型肝炎，丙型肝炎等肝脏良性疾病以及胃癌，肠癌，乳腺癌以及肺癌患者血清中并未见到 ACAN 表达水平上升。ACAN 的表达和 AFP，谷丙转氨酶 ALT 以及谷草转氨酶 AST 均存在正相关关系。ACAN 的 ROC 曲线下面积为 0.978，最佳诊阈值为 66ng/ml，检测的敏感度为 96.4%，特异度为 98.2%，诊断效能一定程度上优于 AFP。

结论与讨论：软骨蛋白聚糖（Aggrecan, ACAN）主要由软骨细胞分泌产生，是由带负电荷的糖胺聚糖共价连接于核心蛋白所组成的糖复合物。ACAN 具有细胞间信息传递，维持细胞表型，介导与其他基质间相互作用，保持组织整体功能等重要作用。本研究中我们发现肝癌患者血清中 ACAN 表达水平明显升高，而且 ACAN 有成为新型肝癌血清标志物潜力，为肝癌患者的早期治疗以及精准医疗提供了可能性。

关键字： ACAN；Hippo/YAP 信号通路；肝癌；YAP；AFP

580. 血浆外泌体 miR-320d 作为卵巢癌的新型肿瘤标志物

王世文*、宋兴国、谢丽、宋现让

山东省肿瘤医院

研究目的：卵巢癌（ovarian cancer, OC）是妇科肿瘤中最常见的死亡原因之一。卵巢解剖位置隐匿，发病时无典型的症状和体征，往往出现恶性腹水或腹部肿块时已处于晚期，手术、放化疗等治疗效果较差，5 年生存率仅 25%，而早期患者的 5 年生存率可达 70%。因此，开发新的、灵敏的、微创的早期卵巢癌诊断标志物对降低其死亡率至关重要。在过去的几十年里，微小 RNA（miRNAs）在癌症的发生和进展中起着重要的作用，因此引起了极大的关注。此外，miRNAs 可以在循环血液中长期稳定存在（如包裹在外泌体中）,不仅可以通过外泌体的分泌和转移在肿瘤细胞之间和肿瘤细胞微环境的沟通中发挥重要的作用，同时表达失衡的外泌体 miRNAs 还可以作为新型的肿瘤标志物。本研究旨在探索外泌体 miRNAs 在卵巢癌中的诊断价值，为卵巢癌的诊断和预后监测筛选新型肿瘤标志物。

研究方法：1.5 例健康人和 5 例卵巢癌患者血浆样本分离外泌体后进行 miRNAs 测序，筛选差异表达的 miRNAs。2.通过透射电镜（TEM），qNano，Western blot 验证分离出的血浆外

泌体。3.收集 168 例健康人血浆样本，161 例卵巢癌患者和 36 例良性疾病患者的血浆样本，提取外泌体 RNA 后，通过 RT-qPCR 验证 miRNAs 的表达差异。4.分析外泌体 miRNAs 的表达特点。5.统计分析。

结果：1.在测序结果中，与健康样本相比，外泌体 miR-320d 在卵巢癌患者样本中表达显著下调（*P*<0.01）。2.透射电镜，qNano 和 Western blot 结果证明血浆中分离出的囊泡为外泌体。3.大样本结果验证与健康和良性疾病样本相比，外泌体 miR-320d 在卵巢癌样本中显著下调（*P*<0.0001）。4.MiR-320d 主要存在于外泌体中且含量稳定不受 RNA 酶的影响。5.外泌体 miR-320d 在淋巴结转移的患者中的含量显著低于非淋巴结转移的患者（*P*<0.001），此外，外泌体 miR-320d 的表达与卵巢癌分期呈负相关。

结论：血浆外泌体 miR-320d 可作为卵巢癌的新型循环肿瘤标志物。

关键字：卵巢癌；外泌体；miRNAs；肿瘤标志物

581. 基于 PBMC 高通量测序数据探讨原发性肝癌免疫相关生物标志物

胡锐*、周小舟

深圳市中医院

目的：利用高通量测序技术挖掘原发性肝癌患者外周血单个核细胞（PBMC）免疫相关 mRNA 差异表达，结合肿瘤所处整体免疫环境探讨差异基因在免疫评估和预后判断中的潜在应用价值，为原发性肝癌免疫相关标志物的鉴定奠定基础。

方法：根据纳入标准和排除标准纳入原发性肝细胞癌（HCC）患者 103 例及健康对照组 51 例，采集外周血 6ml 并提取 PBMC 用于高通量测序，利用生物信息学分析技术对获得的 mRNA 表达矩阵进行差异分析，结合 ImmPort 共享数据库筛选出免疫相关差异基因，完成目标基因显著性富集分析及 KEGG 通路分析，完善免疫相关基因与临床预后、巴塞罗那分期（BCLC）的相关性研究。

结果：1.与健康对照组相比，HCC 组 PBMC 中 PPARG、ADM、PTGFR、EDNRB、CXCL2、IL10、SOCS3、IL1B、SEMA6B、SDC1、MUC5AC、IL1A、AGTR1、ACKR1、TNFRSF11B、PGLYRP4、DKK1、S100A16 共 18 个免疫相关 mRNA 显著上调（$p<0.05$）；2.免疫相关 DEGs 主要参与刺激反应、信号转导、细胞群增殖、免疫反应等生物过程，执行调节 G 蛋白偶联

受体、血管紧张素受体、血管紧张素II型受体、前列腺素等受体活性的分子功能。KEGG 分析显示免疫相关 DEGs 主要富集在 IL-17、AGE-RAGE、NF-κB、TNF 和钙信号等通路；3. 免疫相关 DEGs 与 PBMC 中活化的 CD8+ T 细胞、效应 CD8+记忆 T 细胞、中性粒细胞、NK 细胞、DC 细胞等多种免疫细胞密切相关；4.生存分析发现腹水的出现意味着更差的预后（p=0.00026）,且肝功能越差患者的生存时间越短（p<0.0001），此外 ADM，SOCS3，AGTR1 低表达与 HCC 较长的 OS 相关（p<0.05）；5.BCLC 分期比较中，SDC1 在 C-D 期显著上调（p=0.04），而 MUC5AC 随着分期的升高，呈降低趋势（p=0.05）。ADM、SOCS3 和 ATGR1 在 BCLC A-B 期组和 C-D 期组无显著性差异，但总体呈上调趋势，随着分期发生动态变化；

结论：1. 18 个免疫相关 mRNA 在 HCC 组 PBMC 中显著上调，这些基因大多参与了刺激反应、信号转导、细胞增殖及免疫应答等生物过程，并在 IL-17、AGE-RAGE、NF-κB、TNF 等信号通路中富集，与循环免疫细胞群（包括活化的 CD8+T 细胞、中性粒细胞、NK 细胞、DC 细胞等）浸润丰度密切相关；肿瘤细胞可能通过释放信号因子，激活炎症相关通路，诱导外周免疫相关基因差异表达，进而调控循环免疫细胞群浸润丰度，诱导免疫抑制。2. PBMC 中 ADM，SOCS3，AGTR1 高表达与 HCC 不良预后相关，SDC1 在晚期 HCC 中呈高表达趋势（p=0.04），可能为原发性肝癌免疫相关预后标志鉴定提供新的研究方向。

关键字：原发性肝癌；免疫相关标志物；mRNA；免疫细胞

582. 靶向 system XC-的 SLC3A2 亚基对于 m6A 阅读器 YTHDC2 成为肺腺癌的内源性铁死亡诱导剂至关重要

马丽芳*、王佳谊

上海市胸科医院检验科

m6A 阅读器 YTHDC2 已被确定通过抑制溶质载体 7A11 (SLC7A11) 依赖性抗氧化功能来抑制肺腺癌 (LUAD) 肿瘤发生。 SLC7A11 是 system XC- 的主要功能亚基，抑制 system XC- 可诱导铁死亡。然而，抑制 SLC7A11 是否足以使 YTHDC2 成为 LUAD 中的内源性铁死亡诱导剂尚不清楚。在这里，我们发现将 YTHDC2 诱导至高水平可诱导 LUAD 细胞中的铁死亡，但不会在肺和支气管上皮细胞中诱导。除了 SLC7A11、溶质载体 3A2 (SLC3A2)，system XC-的另一个亚基对 YTHDC2 诱导的铁死亡同样重要。 YTHDC2 m6A

依赖性破坏 Homeo box A13 (HOXA13) mRNA 的稳定性，因为在其 3'非翻译区 (3'UTR) 内鉴定了一个潜在的 m6A 识别位点。有趣的是，HOXA13 作为转录因子来刺激 SLC3A2 的表达。因此，YTHDC2 通过以 m6A 间接方式抑制 HOXA13 来抑制 SLC3A2。小鼠实验进一步证实了 YTHDC2、SLC3A2 和 HOXA13 之间的关联，并证明 SLC3A2 和 SLC7A11 对于 YTHDC2 受损的肿瘤生长和体内诱导的脂质过氧化都很重要。此外，SLC7A11、SLC3A2 和 HOXA13 的较高表达表明 YTHDC2 抑制的 LUAD 患者的临床结果较差。总之，YTHDC2 被认为是一种强大的内源性铁死亡诱导剂，靶向 system XC- 的 SLC3A2 亚基对于这一过程至关重要。增加 YTHDC2 是治疗 LUAD 的另一种基于铁死亡的疗法。

关键字： HOXA13; METTL3; RNA stability; SLC3A2; Transcriptional regulation; m(6)A RNA methylation

583. 基于活检组织在临床根治性放化疗队列中构建食管鳞癌放化疗敏感性多分子预测模型

李植茂*[1,2]、黄河澄 [2]、陈旭丽 [2]、吴文智 [1]、许秀娥 [1]、郑雅琪 [1]、王少洪 [2]、许丽艳 [1]、李恩民 [1]

1. 汕头大学医学院

2. 汕头市中心医院

研究目的：构建并验证一种食管鳞癌根治性放化疗敏感性多分子预测模型，用于预测局部晚期食管鳞癌(ESCC)患者对根治性放化疗(CCRT)的治疗反应。

材料与方法：我们纳入了 136 例经组织病理学确诊为 ESCC 的患者进行一项 CCRT 治疗效果的巢式队列研究（ChiCTR1800016249）。91 例患者被分配到训练队列，45 例患者被分配到验证队列，所有患者都接受了 CCRT 治疗并根据 RECIST 1.1 评估 CCRT 治疗反应，分为完全缓解（CR）和非完全缓解（<CR）。对 18 例治疗前肿瘤活检组织（CR：*n*=8；＜CR：*n*=10）采用 LC-MS/MS 质谱分析技术获得蛋白质组表达谱，采用 Wilcox 秩和检验和非配对 t 检验对蛋白质组表达谱进行疗效差异蛋白筛选。通过查找相关文献资料获得候选蛋白分子，并进行免疫组化染色实验。采用 Logistic 回归分析构建食管鳞癌根治性放化疗敏感性多分子预测模型。采用 Cox 比例风险回归模型构建食管鳞癌根治性放化疗 5 年总生存（OS）及 5 年无进展生存（PFS）预测模型。最后通过 ROC 曲线对上述模型的准确性进行验证。

结果：136 例 ESCC 患者中，92 例被评估为<CR，44 例被评估为 CR。通过 LC-MS/MS 质谱分析技术获得 8678 个蛋白分子。根据 Wilcox 秩和检验和非配对 t 检验 p<0.05，Fold Change（CR *vs* <CR）>1.2 或<1/1.2 的条件筛选得到 257 个疗效差异蛋白。其中 107 个疗效差异蛋白是表达上调的，即为对放化疗敏感蛋白，150 个疗效差异蛋白是表达下调的，即为对放化疗抵抗蛋白。通过查找相关文献资料获得 10 个候选蛋白分子，分别为 RPIA、CAPN1、CAPN2、ACAT2、NOTCH3、PPIA、CXCL13、SOX9、THBD 和 HLA-DQA2。免疫组化染色结果发现 RPIA、CAPN1 和 CAPN2 在不同治疗反应组中的表达是有差异的。将 10 个候选蛋白分子纳入分析最终得到由 RPIA、CAPN2 和 ACAT2 组成的一个 3 分子分类预测模型。该模型在训练队列和测试队列中的 AUC 分别为 0.8333 (0.7369-0.9298)和 0.7866 (0.6409-0.9324)。利用上述 3 个蛋白分子构建食管鳞癌根治性放化疗生存预测模型发现，3 分子模型（RPIA、CAPN2 和 ACAT2）对于 5 年总生存（OS）和 5 年无进展生存（PFS）的预测效能在训练队列和测试队列中的 AUC 分别为 0.7913/0.5101 和 0.6508/0.6235。2 分子模型（RPIA 和 CAPN2）对于 5 年 OS 的预测效能在训练队列和测试队列中的 AUC 分别为 0.7873 和 0.5455。单分子 ACAT2 对于 5 年 OS 和 5 年 PFS 的预测效能在训练队列和测试队列中分别为 0.8833/0.7096 和 0.6267/0.7284。

结论：我们构建的由 RPIA、CAPN2 和 ACAT2 组成的 3 分子分类预测模型对于 ESCC 患者 CCRT 治疗反应具有良好的预测效能。ACAT2 对接受 CCRT 治疗的 ESCC 患者 5 年 OS 和 5 年 PFS 具有中等预测效能（本研究由 2021 年广东省科技专项资金项目（210713116901849）资助）。

关键字：食管鳞癌、根治性放化疗、治疗反应、放化疗敏感性分子标志物

584. 食管鳞癌及癌前病变分子标志物的发现及联合诊断模型效能验证的研究

郑雅琪*[1]、黄海花[2]、许秀娥[1]、李植茂[1]、楚曼宇[1]、于帅霞[1]、刘伟[3]、李恩民[1]、许丽艳[1]

1. 汕头大学医学院

2. 汕头大学医学院第二附属医院

3. 黑龙江工程学院

目的：食管癌起病隐匿、进展快、侵袭性强，患者在确诊时往往已经处于晚期，五年总生存率在 20%左右。而I期食管癌的五年生存率可达 70%，说明食管癌早期诊断和早期干预可以改善食管癌预后。本研究目的在于找到有效的早期诊断分子标志物或组合，辅助临床食管癌早期干预及治疗，提升食管癌及癌前病变早诊率，降低死亡率。

方法：我们通过分析 124 例食管癌患者手术样本以及 20 例正常食管活检样本的蛋白质组学数据，整合食管癌基因组信息来初步筛选出 CYHR1 等 9 个蛋白，然后通过小样本的正常食管（*n*= 20）与食管鳞癌（*n*= 18）活检样本进行免疫组化实验，进一步筛选出 CYHR1 等五个在食管癌中高表达的蛋白。在此基础上，通过免疫组织化学实验，评估随机划分为训练集（*n*= 157）和内部测试集（*n*= 79）共 236 名参与者（包括 60 例正常食管，93 例食管癌癌前病变和 83 例食管鳞癌）食管活检组织中，CYHR1 等 5 个蛋白分子的表达水平。使用 ROC 曲线（receiver operating characteristic curve）评估单分子和多分子联合模型诊断两类食管癌病变在训练集中的诊断效能，并在内部测试集中进行验证，对单个分子做 ROC 曲线分析，选择 “灵敏度+特异度-1”即约登指数最大处的免疫组化评分作为截断值。

结果：对食管癌蛋白组和正常食管蛋白质组数据做重叠分析得到 2427 个仅在食管癌中表达的蛋白分子，主要富集在细胞周期相关通路。这 2427 个蛋白中有 40 个蛋白在基因组层面发生了拷贝数扩增，进一步筛选出 21 个在食管癌中表达上调的蛋白（Fold-Change (Tumor/non-tumor) > 1.2, P<0.05）。综合考虑拷贝数变异频率、细胞定位、文献报道和是否有商品化可用于免疫组化实验的抗体，最终选择 CYHR1、ECT2、RAD9A、TONSL、KDM2A、YEATS4、IGHMBP2、RCE1 和 MDM1 等 9 个蛋白进行初步的小样本免疫组化检测。结果显示，CYHR1、ECT2、RAD9A、TONSL 和 KDM2A 等五个蛋白分子在食管鳞癌活检组织中的表达相对正常食管上调（P<0.01），IGHMBP2、RCE1 和 MDM1 在食管鳞癌和正常食管活检组织中的表达差异无统计学差异（P > 0.05），YEATS4 在食管鳞癌组织中的表达相

对正常食管下调（*P*<0.05），因此，选择 CYHR1 等五分子进行后续验证实验。在训练集和内部测试集中，CYHR1 等 5 个蛋白分子在癌前病变组织中的表达相对正常食管有上调的趋势，在食管癌鳞组织中的表达相对正常食管和癌前病变食管均显著升高（*P*<0.001）。在区分正常食管与食管鳞癌时，五分子联合诊断模型的诊断效能明显优于单分子，其 AUC 达 0.940（95% CI 0.897-0.983），此时敏感度特异度分别为 78.18% 和 100.00 %，且联合模型的诊断效能在内部测试集中也保持了较高的稳定性，AUC 为 0.943（95% CI 0.873-1.000），敏感度和特异度分别为 89.29 %和 100 %；在区分正常食管与癌前病变食管时，五分子联合模型的诊断效能较单分子也有所提升，在训练集中 AUC 为 0.694（95% CI 0.594-0.794），敏感度和特异度分别为 45.16 %和 95.00 %，而在内部测试集中 AUC 更高，为 0.751（95% CI 0.615-0.886），敏感度和特异度分别为 61.29 %和 76.27 %；在区分癌前病变食管与食管鳞癌时，五分子联合模型的诊断效能也明显优于单分子，在训练集中 AUC 为 0.896（95% CI 0.839-0.952），敏感度和特异度分别为 78.16 %和 91.94 %，而在内部测试集中 AUC 为 0.874（95% CI 0.776-0.973），敏感度和特异度分别为 82.14 %和 90.32 %。

结论：CYHR1 等 5 个蛋白的表达与食管癌进展密切相关，联合检测这些生物标志物可提高诊断效能，有助于早期诊断食管鳞癌，鉴别食管癌前病变的高危人群，具有潜在的临床应用前景，有待通过大样本和多中心进行验证（本研究由国家重点研发计划精准医学研究重点专项（2016YFC0901400）和李嘉诚基金会交叉学科研究基金（2020LKSFG07B）资助）。

关键字：食管鳞癌；癌前病变；早期诊断；生物标志物

585. 基于自噬相关基因构建 TP53 突变多发性骨髓瘤预后模型及免疫浸润细胞景观图谱

郑焱华*[1,2,3]、高广勋[4]

1. 空军军医大学第二附属医院（唐都医院）血液内科

2. 国家血液系统疾病临床医学研究中心陕西分中心

3. 陕西省血液疾病临床医学研究中心

4. 空军军医大学第一附属医院（西京医院）血液内科

目的：多发性骨髓瘤（MM）是第二常见的血液系统恶性肿瘤。其特征是骨髓内浆细胞增殖紊乱。与非 TP53 突变的 MM 患者相比，TP53 突变患者的总生存期较短，预后较差。自噬

是一种促生存机制，通过自噬机制，MM 细胞对蛋白酶体抑制剂产生耐药性，并避免有毒蛋白质的过度蓄积。本研究的目的是建立一种基于自噬相关基因（ARG）的预后模型，用于预测 TP53 突变 MM 患者的生存结果并绘制免疫浸润细胞的景观图谱。

方法：有关 TP53 突变的 MM 患者的信息从 GEO 数据库下载。通过检索人类自噬数据库获得 ARGs。通过微阵列数据的线性模型，对有或没有 TP53 突变的 MM 患者中的差异表达基因（DEG）进行鉴定和分析。Cox 比例风险回归用于确定独立预后 ARG 并构建风险特征。使用时间依赖性受试者操作特征（t-ROC）曲线来探讨预后模型的预测准确性。构建诺模图以更精确地预测 5 年、8 年和 10 年总生存率（OS）的概率。此外，我们利用 CIBERSORT 算法探讨了 TP53 突变 MM 患者中 22 种免疫浸润细胞在高危组和低危组之间的分布差异。

结果：三个差异表达的 ARG（CASP8、MAPK8、RB1CC1）最终纳入构建风险模型。5 年、8 年和 10 年 OS 对应 tROC 曲线的曲线下面积（AUC）分别为 0.735、0.686 和 0.662。根据中位阈值（-1.724549），MM 患者被分为高风险组和低风险组。基于 ARG 的风险评分模型是与 OS 相关的独立预后因素，风险比（HR）为 3.29（95%CI 2.35-4.60，P<0.001）。在 22 种免疫浸润细胞亚型中，13 个免疫细胞在高风险组和低风险组之间存在统计学差异。高风险组的 CD8+T 细胞、γδT 细胞、活化 NK 细胞、活化树突状细胞、单核细胞、静息肥大细胞和 M0、M1 型巨噬细胞的丰度低于低风险组（p *值*<0.05），而记忆 B 细胞、浆细胞、幼稚 CD4+T 细胞、静息 NK 细胞、活化的肥大细胞在高危组中较高（p<0.05）。

结论：我们建立了一个纳入三个 ARGs 的风险模型，表明该模型是一个独立的预后因素。列线图在预测 TP53 突变 MM 患者长期生存率方面效能较好。

关键字：多发性骨髓瘤，自噬，预后，风险，TP53 突变，免疫浸润细胞

586. 应用同步放化疗对隐匿性宫颈癌进行补救治疗的临床研究

李芷茹*、李超

四川省人民医院邛崃医院

目的：探讨隐匿性宫颈癌术后使用同步放化疗进行补救治疗与根治性再手术比较的疗效及不良反应。

方法：回顾自贡市第一人民医院和成都市第五人民医院 2009 年～2019 年仅行单纯筋膜外子宫切除术，术后病理为浸润性宫颈癌病例 37 例，放疗组 20 例均行根治性同步放化疗及三维腔内近距离治疗，手术组 17 例行经腹或腹腔镜下广泛性子宫切除术+盆腔淋巴结切除术±腹主动脉旁淋巴结切除术，术后 5 例依据高危因素行辅助盆腔外照射及同步化疗，观察两组患者的复发与生存情况，及手术并发症、放化疗毒副反应。

结果：手术组中位随访时间 48 个月（15-106 个月），有 3 例患者出现复发转移，放疗组中位随访时间 56 个月（21-112 个月），3 例患者转移性复发，手术组和放疗组的 5 年总生存率和无病生存率分别为 93.2%和 95.1%（p= 0.278），88.8%和 90.8%（p= 0.111），手术组术后并发症包括 5 例淋巴水肿（I级），2 例膀胱功能障碍（I级和 III 级各 1 例），2 例肾积水（I级），2 例不全肠梗阻（I级）和 2 例盆腔淋巴囊肿（I 级和 III 级各 1 例）。放疗组毒副反应包括I～II级急性直肠反应 7 例、I～II级急性膀胱反应 7 例，淋巴水肿 3 例；3 级泌尿道和消化道不良反应各 1 例，分别表现为尿痛伴肉眼血尿和肠梗阻，无远期并发症发生。

结论：对于单纯子宫切除术后隐匿性宫颈癌患者根治性再手术与补救性同步放化疗疗效相当，并发症均可耐受，但再次手术后仍需放化疗患者并发症增加，采用精确放疗技术可能降低远期并发症。

关键字：放化疗；手术；隐匿性；宫颈癌；疗效

587. 红细胞分布宽度、中性粒细胞与淋巴细胞比值、癌胚抗原、糖类抗原 19-9 联合检测对胃癌诊断和分期的价值

张华洋*

贵州医科大学研究生院

目的：探究红细胞分布宽度（RDW）、中性粒细胞与淋巴细胞比值（NLR）与传统肿瘤标志物癌胚抗原（CEA）、糖类抗原 19-9（CA19-9）联合检测对胃癌诊断和分期的价值。

方法：回顾性纳入 2014 年 11 月至 2021 年 11 月就诊于贵州医科大学附属医院的胃癌患者、癌前状态及癌前病变患者、慢性非萎缩性胃炎患者。胃癌患者根据国际抗癌联盟（UICC）2016 年第八版 TNM 分期系统进行分期，并根据 TNM 分期结果进一步分为I-II期组及III-IV期组。制定纳入标准和排除标准，详细记录所有研究对象的一般资料、RDW、NLR、CEA、CA19-9、胃镜检查结果、病理报告和影像学资料等。比较各组间 RDW、NLR、CEA 和 CA19-9

水平的差异，运用受试者工作特征曲线（ROC），比较 ROC 曲线下面积(AUC)，分析 RDW、NLR、CEA、CA19-9 单独及联合检测对胃癌的诊断和分期的价值，并探讨 RDW、NLR、CEA、CA19-9 与胃癌患者临床病理特征之间的关系。

结果: 本研究共纳入胃癌患者 313 例（其中 TNM 分期I-II期患者 127 例，III-IV期 186 例）、癌前状态及癌前病变患者 144 例（其中慢性萎缩性胃炎患者 64 例、慢性萎缩性胃炎伴肠上皮化生患者 61 例、胃上皮内瘤变患者 19 例）、慢性非萎缩性胃炎患者 137 例。通过统计学分析得出：1.胃癌组 RDW、CEA、CA19-9 水平高于癌前状态及癌前病变组、慢性非萎缩性胃炎组，差异有统计学意义（$p<0.05$）。2.胃癌III-IV期组 RDW 水平高于胃癌I-II期组、癌前状态及癌前病变组、慢性非萎缩性胃炎组，差异有统计学意义（$p<0.05$）；胃癌III-IV期组、胃癌I-II期组 CEA、CA19-9 水平高于癌前状态及癌前病变组、慢性非萎缩性胃炎组，差异有统计学意义（$p<0.05$）；胃癌III-IV期组 CEA、CA19-9 水平高于胃癌I-II期组，差异无统计学意义（$P>0.05$）。3.运用 ROC 曲线分析 RDW、NLR、CEA、CA19-9 对胃癌的诊断效能，单项检测中 RDW 对胃癌组患者的诊断效能（AUC=0.647）低于 CEA（AUC=0.801）、CA19-9（AUC=0.749）；两项指标联合检测时，CEA+CA19-9 的诊断效能（AUC=0.865）高于 CEA+RDW（AUC=0.815）、CA19-9+RDW（AUC=0.800）；RDW、CEA、CA19-9 三项指标联合检测的诊断效能最高（AUC=0.896）；NLR 的诊断效能较差（AUC=0.557），且敏感度低（35.5%）。4.运用 ROC 曲线分析 RDW、CEA、CA19-9 对胃癌I-II期患者的诊断效能，RDW 的诊断效能（AUC=0.576）低于 CEA（AUC=0.754）、CA19-9（AUC=0.758）；两项指标联合检测时，CEA+CA19-9 诊断效能（AUC=0.847）高于 CEA+RDW（AUC=0.785）、CA19-9+RDW（AUC=0.770）；RDW、CEA、CA19-9 三项指标联合检测对胃癌I-II期的诊断效能最高（AUC=0.869）。5.高 CEA 水平可能与胃癌的远处转移有关；高 RDW 水平可能与胃癌 TNM 分期、远处转移、浸润深度、淋巴结转移有关；高 NLR 水平可能与胃癌患者年龄、TNM 分期、远处转移、淋巴结转移有关；CA19-9 水平与胃癌患者临床病理特征无明显相关。

结论: 1.胃癌组 RDW、CEA、CA19-9 水平高于癌前状态及癌前病变组、慢性非萎缩性胃炎组。2.胃癌III-IV期组 RDW 水平高于胃癌I-II期组、癌前状态及癌前病变组、慢性非萎缩性胃炎组；胃癌III-IV期组、胃癌I-II期组 CEA、CA19-9 水平高于癌前状态及癌前病变组、慢性非萎缩性胃炎组。3.RDW、CEA、CA19-9 三者联合检测可提高对胃癌和胃癌I-II期的诊断效能。4.NLR 对胃癌的诊断效能较差。5.高 RDW 水平可能与胃癌 TNM 分期、远处转移、

浸润深度、淋巴结转移有关；高 NLR 水平可能与胃癌患者年龄、TNM 分期、远处转移、淋巴结转移有关；高 CEA 水平可能与胃癌的远处转移有关。

关键字：胃癌；红细胞分布宽度；中性粒细胞与淋巴细胞比值；癌胚抗原；糖类抗原 19-9

588. APRI 评分与 HBV 相关肝细胞癌切除术患者预后的关联研究

周运香*

广西医科大学

目的：评估天冬氨酸转氨酶与血小板计数比值指数（APRI）对 HBV 相关肝细胞癌（HCC）切除术患者术后总生存率（OS）的预测价值。

方法：采用回顾性队列研究方法，收集 2012 年 1 月至 2016 年 12 月期间在广西医科大学附属肿瘤医院行切除术治疗的 1031 例 HBV 相关 HCC 患者的术前临床资料。通过 Kaplan-Meier 生存曲线确定连续变量 APRI 的 cutoff 值。采用 Kaplan-Meier 法绘制患者不同 APRI 组的生存曲线，并通过 Log-rank 检验评估两组人群的生存差异。运用逐步多因素 Cox 回归筛选患者 OS 独立影响因素。采用限制性立方条图（RCS)评价患者 APRI 与死亡风险的相关性。建立列线图模型评估 APRI 对 OS 的预测能力并内部验证。

结果：RCS 显示 APRI 与死亡风险呈非线性关联（非线性 $P<0.001$）。多因素 Cox 回归结果显示：APRI、BCLC 分期、AFP、性别和肿瘤大小是 OS 独立影响因素，高 APRI 组死亡风险是低 APRI 组 2.1 倍。患者 OS 的列线图显示 APRI 对 OS 的预测能力仅次于 BCLC 分期。在建模组中预测 OS 列线图的 C-index 为 0.71（95% CI：0.68-0.74），在验证组中预测 OS 列线图的 C-index 为 0.69（95% CI:0.64-0.75）。1 和 5 年 OS 校正曲线显示列线图模型具有良好的校准度，临床决策曲线（DCA）显示模型具有良好的临床应用价值。

结论：APRI 是 HBV 相关 HCC 切除术患者 OS 独立影响因素，基于 APRI 对患者预后进行分层，有利于进行个体化治疗和随访

关键字: APRI 评分；肝细胞癌 ；乙型肝炎病毒；总生存率；列线图

589. 超级增强子区域遗传变异与 HBV 相关肝细胞癌术后生存期的关联分析

韦雪艳*

广西医科大学

目的：探讨超级增强子区域遗传变异与肝细胞癌（hepatocellular carcinoma, HCC）术后患者总生存期(Overall Survival，OS)的关联。

方法：本研究纳入 2007 年 7 月至 2017 年 12 月于广西医科大学附属肿瘤医院行肝癌切除术治疗的 866 例 HBV 相关 HCC 患者为研究对象。采用两阶段的多因素 Cox 比例风险回归分析超级增强子区域遗传变异与 HCC 患者术后 OS 之间的关联。

结果：年龄、AFP、有无癌栓和 BCLC 分期均与 HCC 患者术后 OS 相关。调整年龄，性别，吸烟史，饮酒史，乙型肝炎病毒（hepatitis B virus,HBV）感染，BCLC 分期，AFP，肝硬化，是否癌栓等因素后，Cox 比例风险回归分析发现 GLUL rs61805159 位点 AA 基因型和 AXIN2 rs4791170 位点 AA 基因型均可增加患者术后的死亡风险，BMF rs546220 位点 AA 基因型可降低患者术后的死亡风险，且均呈剂量-反应关系（p<0.05）。进一步分析 SNP-SNP 之间的联合作用，携带 2-3 个风险基因型（风险基因型: rs61805159 GA/AA 、rs546220 CC、rs4791170 GA/AA）的高风险组患者比携带 0-1 个风险基因型患者的中位生存时间（MST）缩短,MST 分别是 69.7 和 39 个月。多因素 Cox 比例风险回归模型分析，校正吸烟、饮酒、BCLC 分期、是否发生癌栓多个因素后发现携带 2~3 个风险基因型 HCC 术后患者发生死亡的风险是携带 0-1 个风险基因型患者的 1.65 倍，（HR=1.65，95%CI=1.36-2.01，P<0.001）。

结论: rs61805159 AA 和 rs4791170 AA 均可增加患者术后的死亡风险，rs546220 AA 可降低患者术后的死亡风险，且均存在剂量反应关系；rs61805159、rs546220 和 rs4791170 的联合作用可能影响肝细胞癌术后患者的生存结局，其风险基因型的联合作用使肝细胞癌术后患者 MST 缩短。

关键字: 肝细胞癌；总生存期；超级增强子；单核苷酸多态性

590. 早期髓系来源抑制细胞通过下调 ARID1A 表达促进 luminal A 型乳腺癌上皮间充质转化过程

陈桂冬*、李星晨、纪辰燕、刘芃芃、于津浦

天津医科大学肿瘤医院

目的：早期髓系来源抑制细胞（eMDSCs）是一种新的 MDSCs 亚群，与经典 MDSCs 相比具有更强的免疫抑制能力。在前期研究中，我们发现 eMDSCs 高浸润与乳腺癌的不良预后相关，但具体机制尚不清楚。

方法：我们构建了 21 个特征性基因来评估乳腺癌组织内 eMDSCs 的浸润状况，同时通过体外细胞实验探索 eMDSCs 对细胞行为的影响。此外，我们通过蛋白质组学的方法探索乳腺癌细胞中 eMDSCs 的目标蛋白，并在乳腺癌细胞中进行验证。

结果：21 个特征性基因能够很好地预测乳腺癌组织样本中 eMDSCs 的浸润情况，这一结果在我们收集到的乳腺癌样本中得到了验证，并且发现 eMDSCs 高浸润会影响乳腺癌患者的预后，特别是在 luminal A 型乳腺癌中。我们还在体外细胞实验中发现 eMDSCs 通过促进上皮-间质转化（EMT），加速细胞迁移和侵袭过程。eMDSCs 在 luminal A 型乳腺癌中明显下调了 ARID1A 的表达，这一蛋白与 EMT 密切相关，是乳腺癌患者的一个重要预后因素。此外，与 eMDSCs 共培养或敲除 ARID1A 后，luminal A 型乳腺癌细胞中 EMT 相关基因发生明显变化，而 ARID1A 的过表达明显逆转了这一过程。

结论：总之，eMDSCs 通过抑制 ARID1A 的表达促进 luminal A 型乳腺癌的 EMT 过程，为开发常规疗法后复发的 luminal A 型乳腺癌的新型治疗方案提供新的启示。

关键字：乳腺癌，早期髓系来源抑制细胞，ARID1A，上皮间充质转化

591. 中国卵巢癌 DNA 损伤修复基因突变图谱分析

叶英楠*、王珂、董莉、程亚楠、韩雷、张蕊、于津浦

天津医科大学肿瘤医院

目的：DNA 损伤修复基因（DDR）突变在卵巢癌的发生发展中起到了重要作用，近年来对于 DDR 基因中的 BRCA1/2 在卵巢癌中的研究比较深入，而对于其他基因的分布及其与卵巢癌患者临床特征之间的关系仍缺乏详细的探讨。

方法：本研究纳入 122 例卵巢癌患者的外周血样本和其中 67 例患者肿瘤组织标本，通过二代测序技术对 19 个 DDR 基因进行检测，分析其变异情况、分布特点和其与临床病理特征相关性。

结果：122 例卵巢癌患者共检出 38 例胚系突变阳性患者，突变率 31.15%，突变基因全部为同源重组修复（HRR）基因，其中 22 例为 BRCA1 突变，7 例为 BRCA2 突变，8 例为 RAD51D 突变，1 例 ATM 突变，主要的突变类型为移码突变。胚系突变阳性患者中有家族史和有乳卵家族史的比例均高于阴性患者，病理类型以浆液性腺癌为主，且对铂类化疗药物治疗敏感性更高。67 例肿瘤组织样本中检出阳性患者 46 例，突变率 68.66%，突变位点主要集中于 TP53 基因，其次为 HRR 基因，仅 1 例携带 PMS2 突变。4 例胚系 HRR 突变阴性患者肿瘤组织 HRR 突变阳性。HRR 基因突变阳性患者，发病年龄提前，有家族史和有乳卵家族史的比例更高，且对铂类化疗药物治疗敏感性更高。

结论：HRR 多基因检测对于提示卵巢癌患者发病风险，指导卵巢癌患者精准治疗有重要价值。因此，开展 HRR 多基因检测，特别是组织层面的检测将使更多的卵巢癌患者从中获益。

关键字：卵巢癌，DNA 损伤修复基因，多基因检测，二代测序

592. 沙棘对人乳腺癌 MCF-7 细胞增殖、迁移、凋亡、周期的影响

黄聪玲*

内蒙古医科大学研究生院

目的：探讨沙棘对人乳腺癌 MCF-7 细胞增殖、迁移、凋亡、周期的影响。

方法：以 20%的乙醇为提取媒介制备沙棘提取物。实验分为空白组、阴性对照组、盐酸阿霉素（0.01mg/ml）、沙棘浓度低（0.1mg/ml）、中（0.3mg/ml）、高（0.5mg/ml）剂量组，采用 MTT 法检测肿瘤细胞抑制率，细胞划痕法检测细胞迁移率。之后将实验分成阴性对照组、盐酸阿霉素（0.01mg/ml）、沙棘浓度低（0.3mg/ml）、中（0.5mg/ml）、高（0.7mg/ml）剂量组，流式细胞术检测肿瘤细胞凋亡率细胞周期的变化。

结果:与阴性对照组比较，沙棘浓度低、中、高剂量组 MCF-7 细胞抑制率显著升高（P<0.01）、细胞迁移率显著降低（P<0.01），且有明显量-效关系。与阴性对照组相比，沙棘浓度低、中、高剂量组 G0/G1 期细胞数量占比明显升高（P＜0.05）。

结论：沙棘提取物可以抑制人乳腺癌 MCF-7 细胞增殖，降低细胞的迁移率，并且可以通过细胞周期变化加快细胞凋亡。

关键字：沙棘；乳腺癌；增殖；迁移；凋亡；周期

593. 肿瘤内微生物异质性影响肝癌肿瘤免疫微环境及其临床预后

李胜男*[1,2]、宋天强[1]、徐亮[1]、于津浦[1]、陆伟[1]

1. 天津市肿瘤医院（天津医科大学肿瘤医院）

2. 天津市第二人民医院

目的：研究表明肿瘤内微生物能够调控多种类型肿瘤的发生发展。本研究旨在表征乙肝相关性肝细胞肝癌的肿瘤内微生物异质性并构建基于肿瘤内微生物特征的肝癌分子分型，从而揭示肿瘤内微生物异质性与肝癌发生发展之间的相关性。

方法：收集 30 例乙肝相关性肝细胞肝癌患者的手术切除癌组织及其配对癌旁组织，12 例慢性乙型肝炎患者的肝穿刺慢乙肝组织，采用微生物宏基因组测序技术（mNGS）检测肝组织内的微生物构成及其特征，并通过非度量多维尺度分析（NMDS）构建基于微生物特征的肝癌分子分型。基于转录组测序数据利用 EPIC 及 CIBERSORT 对不同分子分型肝癌的肿瘤免疫微环境进行分析，并通过免疫组织化学染色进行验证，进一步采用基因集变异分析（GSVA）探讨肝癌免疫微环境与代谢通路之间的相关性。最后，我们通过加权基因共表达网络分析（WGCNA）及 Cox 回归分析建立了不同分子分型间的三基因预后基因风险模型，并利用 TCGA-LIHC 的临床数据进行验证。

结果：相比于慢性乙肝组织，肝癌组织的肿瘤内微生物异质性下降。基于肝癌组织微生物异质性鉴定出两种肝癌分子分型（细菌优势亚型及病毒优势亚型），不同分子分型的临床预后及病理特征显著不同。与病毒优势亚型相比，细菌优势亚型具有更加抑制性的肿瘤免疫微环境，同时伴随多条代谢通路上调。基于不同分子分型的差异表达基因，我们筛选出包含 CSAG4、PIP4P2、TOMM5 的三基因预后模型，Kaplan-Meier 生存曲线表明高风险组生存率明显低于低风险组。

结论：基于肿瘤内微生物特征的肝癌分子分型能够表征肿瘤异质性，其与临床病理特征及肿瘤微环境差异密切相关，可作为肝癌预后的新生标志物。

关键字：肝癌，肿瘤内微生物，分子分型，免疫微环境

594. 辛伐他汀联合贝伐珠单抗通过 HIF- 1α-Wnt/β-catenin 通路抑制肺腺癌 A549 细胞增殖、迁移及侵袭并促进其凋亡

涂昕*、青措、徐智

成都市郫都区人民医院

目的：研究辛伐他汀（Sim）联合贝伐珠单抗（Beva）对人肺腺癌 A549 细胞增殖、迁移、侵袭及凋亡的影响，并探讨其可能的作用机制。

方法：采用 CCK-8 法和平板克隆形成实验检测 4、8、12、16 和 20 mol/L Sim 或 1、2、4、5 和 6 mg/mL Beva 及 2 药联合对 A549 细胞增殖的影响，并计算 Beva 的半数抑制浓度（IC50）以及联合用药指数（CI）；分别采用划痕愈合实验、Transwell 小室法和 FCM 法检测 Sim 单药、Beva 单药以及 2 药联合对细胞迁移、侵袭及凋亡的影响；运用 qRT-PCR 法检测缺氧诱导因子- 1α(HIF- 1α) 的表达水平；蛋白印迹法检测增殖相关蛋白增殖细胞核抗原（PCNA），侵袭迁移相关蛋白基质金属蛋白酶 9(MMP-9)、波形蛋白（Vimentin），凋亡相关蛋白 Bax、Bcl-2 以及 HIF- 1α、β-连环蛋白（β-catenin）的表达水平。

结果：不同浓度的 Sim、Beva 及 2 药联合处理组均可抑制 A549 细胞增殖（*P* 均＜0.05），Beva 24h 和 48h 的 IC50 值分别为（5.272±0.3448）mg/mL 和（3.434±0.3115）mg/mL，2 药联合的 CI 值均＜1，表现为协同效应。Sim 联合 Beva 处理组细胞的克隆形成数、迁移及侵袭能力均明显低于对照组和各单药组(*P* 均＜0.05)，且 2 药处理组 PCNA、MMP-9、Vimentin 蛋白的表达水平明显低于对照组和各单药组(*P* 均＜0.05)。Sim 单药（8umol/L）无明显促凋亡作用（*P*＞0.05），但联合 Beva 可增加 Beva 的促凋亡作用，且可上调促凋亡蛋白 Bax，下调抗凋亡蛋白 Bcl-2 的表达水平(*P* 均＜0.05)。与对照组相比，Beva 作用 A549 细胞后 HIF- 1α mRNA、HIF- 1α蛋白和β-catenin 蛋白表达明显增高，而 Sim 作用后其表达明显降低(*P* 均＜0.05)；与单用 Beva 相比，2 药联合处理组 HIF- 1α mRNA、HIF- 1α蛋白和β-catenin 蛋白表达明显下降(*P* 均＜0.05)。

结论：Sim 联合 Beva 可在体外协同抑制肺腺癌 A549 细胞增殖，并可抑制其迁移和侵袭并促进其凋亡，其机制可能与 Sim 可削弱 Beva 诱导的 HIF-1α 表达升高，进而负向调控 HIF-1α-Wnt/β-catenin 信号通路相关。

关键字：肺腺癌，辛伐他汀，贝伐珠单抗，缺氧诱导因子

595. ATP8B1 低表达通过胆碱代谢引发氧化还原高水平促进肺鳞癌发生发展

张蕊*、张晓、刘芃芃、于津浦

天津医科大学肿瘤医院

研究目的：翻转酶 ATPase I 类 8b 型成员 1(ATP8B1)对于维持细胞膜的稳定性和极性至关重要，并且可以将特定的磷脂从外膜转移到细胞内膜。尽管 ATP8B1 在细胞功能中起重要作用，但 ATP8B1 在肿瘤中的研究很少，其在肺鳞癌(LUSC)患者中的预后价值仍不清楚。本研究拟探索 ATP8B1 在 LUSC 发生发展中的作用机制。

材料与方法：通过分析 TCGA LUSC 数据库和天津医科大学肿瘤医院 109 例 LUSC 样本，分析 ATP8B1 的表达与不良预后的相关性。随后进一步构建了 H520SH-ATP8B1 和 SK-MES-1SH-ATP8B1 的 LUSC 细胞系，并建立异种移植小鼠模型，探究 ATP8B1 敲低如何在体外和体内促进细胞增殖、迁移和侵袭。

结果：通过研究 TCGA 数据库和天津医科大学肿瘤医院队列中 109 例 LUSC 样本的 RNA 测序数据，我们发现 ATP8B1 低表达与 LUSC 患者的不良预后相关。细胞实验和异种移植小鼠模型的结果表明，ATP8B1 敲低首先诱导线粒体功能障碍并促进 ROS 产生。同时，ATP8B1 敲低通过上调胆碱激酶（CHKA）依赖性胆碱代谢途径促进谷胱甘肽合成，从而维持细胞内高水平的氧化还原（REDOX）稳态，从而加剧 LUSC 的癌变和进展。

结论：我们提出 ATP8B1 作为 LUSC 中的一种新的预测性生物标志物，靶向 ATP8B1 导致的代谢紊乱可能是 LUSC 一种新的治疗策略。

关键字：ATP8B1，胆碱代谢，氧化还原，肺鳞癌

596. 血管生成基因预测食管鳞癌患者预后和免疫特性 :证据来自多组学分析和实验验证

王帅元*[1]、梁英豪[2]、张嘉欣[1]、王文佳[1]、洪铱辰[2]、孙淼淼[1]、舒姣[1]、陈奎生[1]

1. 郑州大学第一附属医院

2. 郑州大学医药科学院

研究目的：食管鳞状细胞癌(ESCC)是一种侵袭性疾病，五年生存率(OS)<15%。主要原因是转移而非局部肿瘤，血管生成在其中扮演着重要的角色。血管生成对肿瘤转移、治疗和预后有重要影响。然而，食管鳞癌（ESCC）中血管生成基因的表达模式、对治疗的影响及与预后关系尚未有系统报道。本研究旨在对食管鳞癌中血管生成基因进行首次全面多组学探索，并构建了基于血管生成的分型及预后特征。

材料与方法：我们收集了来自 TCGA 和 GEO 数据库中三个不同队列共 376 例食管鳞癌患者。我们从多组学层面详细研究了血管生成基因的表达改变及改变的可能驱动因素，鉴别了四种血管生成相关表型，探索不同的血管生成表型在微环境、免疫和肿瘤相关通路的异质性，并生成血管生成指数（AI）以预测生存、抗血管治疗及免疫治疗反应，另外在外部队列及体外实验中得到验证。

结果：血管生成在 ESCC 预后及抗肿瘤免疫反应方面起重要作用，体细胞突变、拷贝数变异、甲基化和转录因子调节血管生成相关基因从而促进 ESCC 进展。我们在 ESCC 中确定了四种表型，四种分型表现出明显不同的肿瘤微环境、免疫浸润细胞及癌症通路。重要的是，我们发现四种分型具有各自独特的免疫治疗生物标志物。此外，提出 AI 来量化肿瘤血管生成能力，并使用外部队列及相应细胞验证了它作为预后及免疫治疗预测指标的准确性。

结论：我们对 ESCC 患者进行了首次也是最全面的血管生成基因多组学分析，确定了四种结局、肿瘤特征及免疫景观各异的血管生成表型，这些分组不仅提供了患者预后，还有助于筛选抗血管生成治疗的优势人群。AI 预测预后及免疫治疗反应，为临床医生对 ESCC 的个体化免疫阻断治疗及抗血管生成治疗提供指导。

关键字：食管鳞癌，血管生成，多组学，TME，免疫治疗，预后

597. 线粒体 DNA 基因组不稳定性在肝细胞癌中的研究进展

刘秋龙[2]、邢金良[1]、高一钊[2]、王珍妮[1]、周凯翔[1]、张召辉[3]、周峰[3]、郭旭[1]

1. 空军军医大学基础医学院生理与病理生理教研室

2. 陕西中医药大学医学技术学院

3. 中国人民解放军陆军第七十一集团军医院

肝细胞癌（hepatocellular carcinoma，HCC）发病率呈逐年上升趋势，但筛查和诊断方法仍有限。线粒体 DNA（mitochondrial DNA，mtDNA）是真核细胞中重要的遗传物质，其基因组不稳定性（mitochondrial genome instability，mtGI）与癌症发生进展密切相关。mtGI 主要包含单碱基替换、片段插入缺失、拷贝数变异等多种 mtDNA 变异形式。既往研究在 HCC 患者中发现大量 mtDNA 变异，因此探索 mtDNA 变异与 HCC 的关系有利于进一步阐明 HCC 发病机制，为 HCC 临床早期诊断及治疗提供更多可能性。本文将围绕 mtDNA 变异与 HCC 研究进展进行综述。

关键字：肝细胞癌；线粒体 DNA；突变；液体活检

598. 白蛋白-球蛋白评分和肌少症联合指标预测接受腹腔镜肾切除术肾细胞癌患者的预后情况

毛卫浦*、陈明

东南大学附属中大医院

目的：我们进行了一项多中心临床研究，构建了一个基于白蛋白-球蛋白评分和肌少症（CAS）相结合的新型指数，可以全面反映患者的营养和炎症状态，并评估 CAS 在肾细胞癌（RCC）患者中的预后价值。

方法：2014 年至 2019 年期间收集了来自三个中心的 443 名接受肾切除手术的患者（训练集 343 人，测试集 100 人）。采用 Kaplan-Meier 曲线分析白蛋白-球蛋白比率（AGR）、白蛋白-球蛋白评分（AGS）、肌少症和 CAS 对 RCC 患者总生存期（OS）和癌症特异性生存期（CSS）的影响。接受者操作特征（ROC）曲线被用来评估 AGR、AGS、肌少症和 CAS 对预后的预测能力。

结果：高 AGR、低 AGS 和非肌少症与较高的 OS 和 CSS 有关。根据 CAS，训练集包括 60 名（17.5%）CAS-1 级患者，176 名（51.3%）CAS-2 级患者和 107 名（31.2%）CAS-3 级患者。较低的 CAS 与较长的 OS 和 CSS 有关。多变量 Cox 回归分析显示，CAS 是 OS 的独立危险因素（1 级对 3 级：aHR=0.08；95%CI：0.01-0.58，*p*=0.012；2 级对 3 级：aHR=0.47；95%CI：0.25-0.88，*p*=0.018）和 CSS（1 级对 3 级：aHR=0.12；95%CI：0.02-0.94，*p*=0.043；2 级对 3 级：aHR=0.31；95%CI：0.13-0.71，*p*=0.006）在接受肾切除的 RCC 患者中。此外，CAS 在预测 OS（AUC=0.687）和 CSS（AUC=0.710）方面的准确性高于 AGR、AGS 和肌肉疏松症。此外，在测试组中也得到了类似的结果。

结论：本研究开发的新型 CAS 指数反映了患者的营养和炎症状态，可以更好地预测 RCC 患者的预后。

关键字：CAS 组合；白蛋白-球蛋白评分；肌少症；预后指标；肾切除术

599. 七种肺癌相关抗体联合检测模型在肺结节诊断中的价值研究

赖良、冯阳春*

新疆医科大学附属肿瘤医院

目的：探讨血清中七种抗原（p53、GAGE 7、PGP9.5、CAGE、MAGE A1、SOX2、GBU4-5）对应抗体检测在肺癌诊断中的价值。

方法：收集 2021 年 8 月至 2022 年 2 月新疆医科大学附属肿瘤医院影像学初筛有肺部结节的患者，最终纳入确诊的肺癌患者 90 例，良性结节患者 18 例。在未进行任何治疗前采用 ELISA 法检测其血清中七种抗体的含量。构建七项指标联合诊断肺癌的 Logistics 回归模型，ROC 曲线计算各指标及七项指标联合检测模型的诊断价值。

结果：p53、GAGE 7、PGP9.5、CAGE、MAGE A1、SOX2、GBU4-5 抗体诊断肺癌的灵敏度分别为 88.9%、38.9%、66.7%、77.8%、61.1%、66.7%和 72.2%；特异度分别为 92.2 %、95.6%、67.8%、78.9%、58.9%、88.9%、57.8%和 62.2%。七项联合诊断模型的灵敏度为 90%，特异度为 94.4%，阳性预测值为 98.8%，阴性预测值为 65.4%，阳性似然比为 16.1，阴性似然比为 0.1，诊断符合率为 90.7%。

结论：利用七种肺癌相关抗体构建的诊断模型对于肺部结节的诊断有较好的诊断意义。

关键字：肺癌；肺癌相关抗体；肺结节；诊断

600. 血浆外泌体 miR-44588 可以作为非小细胞肺癌的新型标志物

吴亚雯*[1]、谢丽[2]、宋兴国[2]

1. 山东第一医科大学

2. 山东省肿瘤研究防治院（山东省肿瘤医院）

液体活检，也称为液态活检或者液相活检，是指通过采集人体体液作为检测样本从而反映肿瘤分子特征和动态变化的检测技术。相比于传统的肿瘤检测方法(如影像学检查、组织检查等) ，液体活检以其取样方式灵活安全、无创便捷、可以规律反复多次取样、依从性高等特点而迅速发展，有望在肿瘤早期预警及辅助诊断，即通过无创手段获取更多疾病信息从而实现肿瘤精准诊治。现如今，肺癌的肿瘤标志物为癌胚抗原（CEA）、神经元特异性烯醇化酶（NSE）、细胞角蛋白 19 片段（CYFRA21-1）、胃泌素释放肽前体和鳞状细胞癌抗原（SCCA）。但这些标志物单一诊断检测敏感性 特异性较低。所以，对于肺癌的早期诊断仍需进一步研究。外泌体是一种细胞外囊泡(30-100nm)，从活细胞中释放出来，可以运输到邻近的细胞或远处的细胞。新的研究表明，外泌体在肿瘤微环境中起着至关重要的作用，从而参与调节多种癌症相关的生物过程，如细胞增殖、血管生成和转移等。最近，外泌体介导的 MicroRNA 转移被发现是癌症进展中的一种新的机制。MicroRNA (miRNA) 是一类由内源基因编码的长度约为 22 个核苷酸的非编码单链 RNA 分子，它们在动植物中参与转录后基因表达调控。本研究旨在探讨 miRNA 在非小细胞肺癌中与健康志愿者中表达是否存在差异，而成为有力的新型肿瘤标志物。

方法：首先，本研究通过高通量测序选择了 10 个在未接受治疗的 NSCLC 患者和健康志愿者中差异表达的血浆外泌体 miRNA。

结果：然后在 183 例非小细胞肺癌与 213 例健康志愿者血浆中经超速离心得外泌体后提取 RNA，用 qRT-PCR 技术进一步验证。发现相比于健康志愿者，外泌体 miR-4458 在非小细胞肺癌中表达下调。其 AUC(曲线下面积）为 0.6683。

结论：我们的结果发现血浆外泌体 miR-4458 可以作为非小细胞肺癌有利的肿瘤标志物。

关键字：非小细胞肺癌 液体活检 外泌体 miRNA

601. 血浆外泌体 tRF-Asn-GTT-010 可以作为一种新型的 NSCLC 诊断生物标志物

郑白冰*、宋兴国、谢丽

山东省肿瘤医院

背景： 根据全球癌症统计数据，肺癌仍然在癌症死亡总数中占据首位。非小细胞肺癌（NSCLC）约占总肺癌的 85%，是肺癌高发病率和高死亡率的主要原因。非小细胞肺癌的高死亡率主要是因为患者错过了最佳治疗期和发生了肿瘤转移。因此，迫切需要研究非小细胞肺癌的早期诊断标志物。小非编码 RNAs 作为生物标志物的研究吸引了很多关注，最近的研究表明，tRNA 也可以作为小非编码 RNA（tsRNA）的主要来源之一。随着高通量技术的发展，越来越多的新的 tsRNA 逐渐被发现。根据其在成熟 tRNA 或前体 tRNA 上的切割位置，tsRNA 大致可分为两类：tiRNAs 和 tRFs。最近研究表明 tRFs 具有作为癌症诊断标志物的潜能。然而，外泌体 tRFs 作为生物标记物在非小细胞肺癌（NSCLC）中的作用尚未得到研究。本研究旨在探讨 tRFs 是否可以在外泌体中检测到，以及它们是否可以作为诊断性的生物标志物。

材料与方法：通过透射电子显微镜（TEM）、qNano 和 western 印迹法对从 NSCLC 患者血浆中分离的外泌体的表征进行鉴定。通过高通量测序在 NSCLC 患者和健康志愿者的血浆外泌体中筛选出差异表达的 tRFs，之后在 244 例 NSCLC 患者和 250 例健康志愿者血浆外泌体中经 qRT-PCR 进一步验证。ROC 曲线用于研究 tRFs 作为 NSCLC 诊断标志物的诊断效能。

结果：我们通过高通量测序选择了 10 个在未接受治疗的 NSCLC 患者和健康志愿者中差异表达的血浆外泌体 tRFs, 在 244 例 NSCLC 患者和 250 例健康志愿者中经 qRT-PCR 进一步验证，发现 tRFs 在血浆外泌体中高表达，同时发现 tRF-Asn-GTT-010 在 NSCLC 患者的血浆外泌体中显著下调，其曲线下面积（AUC）为 0.7574，经进一步分析发现与晚期 NSCLC 患者相比外泌体 tRF-Asn-GTT-010 在早期患者中也呈现显著下调，其 AUC 为 0.7345。这预示外泌体 tRF-Asn-GTT-010 可能具有作为 NSCLC 诊断标志物的潜能。

结论：我们的研究结果发现 tRFs 在外泌体中显著富集同时外泌体 tRF-Asn-GTT-010 能是 NSCLC 患者新的、有前景的非侵入性诊断生物标志物，与 NSCLC 发生密切相关。

关键字：外泌体、tRF-Asn-GTT-010、非小细胞肺癌、诊断标志物

602. 血浆外泌体 tRF-Leu-TAA-005 作为非小细胞肺癌的新型诊断标志物

李蕾*、郑白冰、宋兴国、谢丽

山东省肿瘤医院

非小细胞肺癌是癌症特异性死亡的主要原因。非小细胞肺癌发病率高，5 年生存率低，大多数非小细胞肺癌患者在被发现时都处于中晚期，但其发生发展的分子机制仍有待阐明。先前的研究表明，非编码 RNA 作为生物标记物与多种癌症的发生和发展有关，且生物标记物检测的实施大大延长了非小细胞肺癌患者的总存活率。tRF 作为 tRNA 衍生片段，是一种长度为 14-35nt 的非编码单链 RNA，已被发现在癌症的病理生理学中具有重要价值。然而，tRF 在非小细胞肺癌中的表达模式和临床意义研究不明。因此，本研究的目的是评估 tRF-Leu-TAA-005 在非小细胞肺癌患者血浆外泌体中的表达，并确定其诊断价值。我们依据非小细胞肺癌患者及健康人血浆外泌体 tRF 测序结果，按照 FC＞2 且 P＜0.05，筛选出差异明显的 tRF 进行验证。本实验纳入非小细胞肺癌患者 244 例和健康人 250 例，通过 QPCR 对血浆外泌体中 tRF-Leu-TAA-005 的表达量进行检测。然后利用 ROC 曲线对 tRF-Leu-TAA-005 作为非小细胞肺癌诊断标志物的诊断效能进行了分析。实验发现，与健康人群相比，非小细胞肺癌患者血浆外泌体 tRF-Leu-TAA-005 表达水平明显减少（p＜0.0001）。ROC 曲线下面积为 0.7420，敏感性为 68.4%，特异性为 72.4%。因此，我们的结果表明血浆外泌体 tRF-Leu-TAA-005 可能是一种新的、开创性的非小细胞肺癌诊断标志物。

关键字：外泌体，非小细胞肺癌，tRF-Leu-TAA-005，诊断标志物

603. 肿瘤教育血小板 snoRA68 作为食管癌新型标志物的研究

赵漩*、张倩茹

山东肿瘤医院

食管癌，是发生在食管上皮组织的恶性肿瘤，占所有恶性肿瘤的 2%。吸烟、喝酒是引起食管癌病见病因，中国是食道癌高发地区，北方地区发病率多于南方地区，男性多于女性，以

40 岁以上者居多。由于缺乏早期特异性症状和有效的筛查策略，相当数量的食管癌患者在诊断时已处于晚期。 因此，迫切需要敏感性和特异性理想的生物标志物用于食管癌早期诊断及协助临床决策。 最近，“肿瘤教育血小板”（TEPs)已成为一种很有前途的生物标志物来源，可通过血液液体活检对癌症进行非侵入性检测。snoRNA 被认为是一类具有相似结构和功能的非编码 RNA，根据其特有序列特征分为 C/D box 和 H/ACA box 两类。越来越多的研究发现 snoRNA 是癌症进程中的重要调控因。但是很少有研究讨论过 snoRNAs 在 TEPs 中的作用。 在此,我们系统评估了食管癌中 snoRNAs 的失调，并阐明了 snoRA68 在血小板中的生物标志物潜力。

关键字：食管癌；snoRNA；血小板

604. 乳腺癌前哨淋巴结超声造影识别影响因素的 logistic 回归分析

骆云皓*[1,2]、罗俊[2]、曹文斌[2]、陈琴[2]、赵玮[1]、吴昊[2]、李超男[4]、刘瑜妍[3]

1. 四川大学华西第二医院青白江妇女儿童医院/成都市青白江区妇幼保健院

2. 四川省医学科学院·四川省人民医院

3. 电子科技大学

4. 成都中医药大学

目的：分析不同影响因素对乳腺癌前哨淋巴结超声造影定位失败的影响。

方法：回顾性分析四川省人民医院 2017 年 01 月至 2022 年 02 月行超声造影定位乳腺癌前哨淋巴结的患者，分析不同影响因素对超声造影定位失败的影响。首先对纳入研究的影响因素进行单因素分析，连续变量采用独立样本 t 检验，分类变量采用卡方检验，再对具有统计学意义的影响因素进行二分类 logistic 回归分析，$p<0.05$ 具有统计学意义。

结果：总共纳入患者 1430 例，显影失败率为 7.48%(107/1323)。单因素分析结果显示，患者年龄、超声造影操作者、造影设备、造影剂注射点位数、肿瘤位于左乳或右乳、病理类型、病理组织学分级、分子分型、ER%、PR%、HER-2 等因素与超声造影识别乳腺癌前哨淋巴结显影失败无关($P>0.05$)，腋窝淋巴结有转移、既往手术史、既往新辅助治疗史、肿瘤位于外上象限、肿瘤最大径线、临床预后分期、Ki-67%与显影失败有关($p<0.05$)。logistic 回归分析结果显示，既往手术史、腋窝淋巴结有转移、既往新辅助治疗史与显影失败具有显著相关

性(p<0.05)，是超声造影识别乳腺癌前哨淋巴结失败的独立影响因素，其各自显影的成功率分别为 87.86%(123/140)，84.69%(260/307)，76.23%(93/122)，其 ROC 曲线下面积为 0.77(95% CI: 0.71~0.82)。

结论：腋窝淋巴结有转移、既往接受过乳腺手术、既往接受过乳腺癌新辅助治疗是超声造影识别乳腺癌前哨淋巴结显影失败的独立影响因素。

关键字: 乳腺癌；前哨淋巴结；超声造影；影响因素；logistic 回归分析

605. eIF2α的磷酸化减轻急性肝损伤中的内质网应激和肝细胞坏死

徐畅*

上海市第十人民医院

目的：已经明确坏死和内质网（ER）应激与急性和慢性肝损伤有关。激活的真核生物起始因子 2α（eIF2α）减少了蛋白质的合成，降低了 ER 中蛋白质折叠的负荷。本研究旨在分析 eIF2α磷酸化对急性肝损伤中肝细胞坏死的影响。

方法：给雄性 BALB/c 小鼠注射衣霉素或 d-半乳糖胺，并将 LO2 细胞与衣霉素共孵育以诱导急性肝损伤。利用 4-苯基丁酸（PBA）和 salubrinal 分别抑制内质网应激和 eIF2α的去磷酸化。分析小鼠和细胞模型中的 eIF2α磷酸化、内质网应激和肝细胞坏死情况。

结果：衣霉素或 d-半乳糖胺可在小鼠和 LO2 细胞中显著诱导 ER 应激和坏死，以及 eIF2α磷酸化。内质网应激加剧了衣霉素诱导的小鼠和 LO2 细胞肝细胞坏死。升高的 eIF2α磷酸化可显著减轻小鼠和 LO2 细胞的肝细胞 ER 应激和肝细胞坏死。有趣的是，肿瘤坏死因子受体 1（TNFR1）蛋白水平与坏死并不完全同步。在经 d-半乳糖胺处理的小鼠中，TNFR1 表达降低，而细胞与衣霉素孵育 12 和 24h，发现内质网应激可在衣霉素培养的细胞中部分恢复 TNFR1 的表达并增加坏死的发生。

结论：这些结果表明，ER 应激可介导独立于 TNFR1 信号的肝细胞坏死，而升高的 eIF2α磷酸化可减轻急性肝损伤期间的 ER 应激。附注：通讯作者：孙奋勇 联系方式：sunfenyong@263.net

关键字: eIF2α磷酸化，ER 应激，急性肝损伤，肝细胞坏死

606. 环状 RNA circRNA_0072387 通过调节 miR-490/HDAC2 轴促进肝母细胞瘤进展

徐畅*、孙奋勇

上海市第十人民医院

目的：越来越多的报道证实环状 RNA 与多种癌症的发生发展密切相关。然而，在肝母细胞瘤 (Hepatoblastoma, HB) 中环状 RNA 的生物学作用仍未明确。本研究旨在阐明 hsa_circ_0072387 (circ72387) 在肝母细胞瘤进展过程中的潜在机制。

方法：在 HB 组织和细胞系 HepG2 和 Huh6 中，通过定量聚合酶链反应（qPCR）检测 circ72387、hsa-miR-490（miR490）和组蛋白去乙酰化酶 2（HDAC2）的表达水平，通过蛋白质印迹法评估 HDAC2 的蛋白水平。细胞计数试剂盒 8（CCK-8）和克隆形成测定用于检测 HB 细胞系的增殖。miR490 与 circ72387 之间的相互作用由 CircInteractome 预测并通过 Dual-Luciferase 报告基因验证，而 miR490 与 HDAC2 之间的相互作用由 Targetscan 预测并通过蛋白质印迹分析验证其相关性。

结果：结果显示，circ72387 在 HB 组织和细胞中上调，miR490 在 HB 细胞中下调。值得注意的是，circ72387 的沉默显著抑制了肝母细胞瘤细胞的增殖，但对凋亡无显著影响。

结论：Circ72387 通过与 HDAC2 竞争性结合 miR490 促进 HB 细胞的增殖，miR490 在 HB 中充当 miR490 的分子海绵。Circ72387 通过 circ72387-miR490-HDAC2 调控轴在 HB 进展中发挥重要作用，有望成为 HB 的新型诊断标志物和潜在治疗靶点。

关键字：环状 RNA，肝母细胞瘤，Hsa_circ_0072387，Hsa-miR-490，HDAC2

607. 智能响应型 DNA 纳米器件用于体内肿瘤相关 miRNA 的抗干扰成像

陈天舒*

上海交通大学医学院附属上海儿童医学中心

微小 RNA（miRNA）作为肿瘤标志物已经广泛用于癌症的早期诊断、治疗以及预后判断等。由于凋亡或受损细胞的泄露或分泌，在细胞外体液包括血液、尿液和唾液中也发现了大量肿

瘤相关 miRNA，称之为循环 miRNA。因此，在以 miRNA 作为肿瘤标志物来对肿瘤组织和肿瘤细胞进行原位成像时，去除环境干扰，降低背景信号，成为了巨大的挑战。因此我们设想，是否可以基于肿瘤组织和细胞与血液和其他组织之间的差异，提出一种消除血液和其他组织的干扰的 miRNA 成像策略。已有研究表明，肿瘤血管和肿瘤细胞内还原型谷胱甘肽（Glutathione，GSH）浓度是正常血液和正常细胞内含量的数百倍，本文设计了一种谷胱甘肽（GSH）响应的 DNA 纳米器件用于 miRNA 的检测。该纳米器件以金纳米颗粒为载体，携带两种 DNA 组件，分别针对 GSH 和靶标 miRNA 引发响应，并且两者之间有依赖关系，即针对靶标 miR-21 的组件响应必须以针对 GSH 的组件响应为前提条件，否则，即使在靶标 miR-21 存在的条件下，也不能产生最终的阳性信号。在细胞层面及活体层面的原位成像结果表明，该智能 DNA 纳米器件在动物水平上实现了肿瘤的原位检测，消除了血液和其他组织的干扰，对基于体内分析的疾病临床诊断和预后具有重要价值。

关键字：微小 RNA；DNA 纳米器件；成像分析；谷胱甘肽；肿瘤

608. 《醛酮还原酶 1B10 测定试剂盒》经大规模多中心临床研究验证并获国家药监局三类诊断试剂注册批文

窦亚玲*[1]、曹德良[2]、曹友德[3]、刘康龙[2]、曹哲[4]

1. 中国医学科学院北京协和医院

2. 湖南省肿瘤医院

3. 湖南省人民医院（湖南师范大学附属第一医院）

4. 湖南莱拓福生物科技有限公司

目的：研究显示醛酮还原酶 1B10（Aldo-keto reductase1B10，AKR1B10）是诊断肝细胞肝癌（hepatocellular carcinoma，HCC）的一个新型特异性血清标志物，湖南莱拓福生物科技有限公司以此开发出《醛酮还原酶 1B10 测定试剂盒》，可以定量检测人血清 AKR1B10 蛋白含量。本研究主要为验证该产品对 HCC 的临床灵敏度和特异性，判断其临床应用的有效性；以及通过血清 AKR1B10 浓度变化与 HCC 患者病情变化的相关性，确定该产品用于对 HCC 手术患者进行动态监测以辅助判断疾病进程或手术治疗效果的临床应用价值。

方法：采取多中心、同步盲法、金标准对照等方法，选取中国医学科学院北京协和医院、湖南省肿瘤医院、湖南省人民医院等多中心非随访病例 1483 例，经病理确诊为 HCC 的随访

病例 101 例，样本类型为非抗凝血清样本。采用湖南莱拓福生物科技有限公司生产的《醛酮还原酶 1B10 测定试剂盒（时间分辨荧光免疫分析法）》测定血清 AKR1B10 的临床灵敏度和特异性，以及随访受试者手术前后血清 AKR1B10 平均浓度变化与患者病情变化的相关性。同期检测 HCC 患者血清 AFP 的临床灵敏度和特异性，探讨 AKR1B10 与 AFP 联合检测的临床意义。

结果：1483 例非随访病例使用该产品与病理诊断结果对比分析显示，《醛酮还原酶 1B10 测定试剂盒（时间分辨荧光免疫分析法）》对原发性肝细胞肝癌的总体临床灵敏度为 71.90%（95%CI：67.63%,76.16%）；特异度为 82.29%（95%CI：79.89%,84.50%）；总符合率为 79.30%（95%CI：77.17%,81.30%）。101 例随访病例中，受试者接受有效手术治疗后，其血清 AKR1B10 平均水平呈下降趋势，至术后 3~4 天平均水平降至参考区间以下，术后 1~3 月受试者血清 AKR1B10 平均水平亦在正常参考区间以下。424 例同期检测 AKR1B10 和 AFP 的 HCC 患者血清样本结果显示 AKR1B10 的灵敏度 71.93%高于 AFP 的灵敏度 63.44%。在 AFP 阴性的 HCC 样本中 AKR1B10 的阳性率为 73.5%，提示 AKR1B10 和 AFP 联合应用对 HCC 诊断具有互补性。继而分析 AKR1B10 和/或 AFP 对 HCC 诊断的总阳性率高达 90.33%，证明二者联合应用能显著提高 HCC 诊断性能。目前该试剂盒已通过国家药品监督管理局审评，获得三类诊断试剂注册批文。

结论：AKR1B10 是一种可用于检测 HCC 的有效血清标志物，其诊断性能优于 AFP；AKR1B10 水平随着原发性肝癌的切除而显著下降，可及时评估病情、指导治疗；AKR1B10 对 AFP 阴性 HCC 患者有诊断价值，二者联用显著提高 HCC 诊断性能。临床试验结果显示湖南莱拓福生物科技有限公司生产的《醛酮还原酶 1B10 测定试剂盒（时间分辨荧光免疫分析法）》临床性能可较好满足临床需求。

关键字：醛酮还原酶 1B10；AKR1B10；肝细胞肝癌；HCC；血清标志物；AFP；联合应用

609. 血清 PGI、PGII、G-17 联合检测在慢性萎缩性胃炎诊断中的研究价值

李彦红*、许粉娟、蔡小冉

郑州安图生物工程股份有限公司

慢性萎缩性胃炎(CAG)是胃癌演变过程中极为重要的癌前病变，在中国具有较高的发病率。目前，CAG 的诊断主要依赖胃镜和病理活检。胃镜检查会对患者带来一定痛苦和心理恐惧，且花费较大，在我国开展大规模的胃镜筛查难以实现。近年来血清学诊断法凭借简便、经济、非侵入性的优势逐步被广泛应用，即通过检测胃蛋白酶、胃泌素等血清学指标诊断 CAG。胃蛋白酶原(PG)由泌酸腺的主要细胞合成，其血清水平可反映不同部位胃黏膜的形态与功能。胃泌素-17（G-17）是胃窦部 G 细胞分泌的胃肠激素，受 G 细胞功能和数量影响，通过刺激壁细胞分泌胃酸，促进胃黏膜生产和分泌来增加胃肠道运动功能，在调节消化道功能和维持其结构完整有着重要作用。本文通过研究慢性萎缩性胃炎患者血清中 PGI、PGII、G17 的值以及 PGI 与 PGII 的比值（PGR）的值，以期为慢性萎缩性胃炎的诊断提供一定的依据。

关键字: PGI、PGII、PGR、G-17

610. 肝癌干细胞标志物的研究进展和临床治疗意义

徐韵*、贾永峰、刘霞

内蒙古医科大学基础医学院

肝癌是全球第五大最常见癌症和第三大癌症相关死亡原因。其中肝细胞癌 (HCC) 是最常见的肝癌。最近，已经提出导致 HCC 的肿瘤生长、转移和复发以及化疗和放疗失败的原因是肝癌干细胞（LCSC）。肝癌疗法会杀死大部分肿瘤细胞，但最终可能会导致失败的原因是它们不能消除 LCSCs，这些 LCSCs 会存活下来再生新的肿瘤。明确每个组织的 LCSC 标志物，LCSCs 的细胞和信号传导功能是基于 LCSC 生物标志物靶向 LCSCs 进行更好识别和诊断的关键。这些标记物对于分离 LCSCs 和分析其生物学特性以有效地靶向它们用于治疗目的是必要的。目前已经提出 LCSCs 恶性生物学特性的标志物有：$CD133^+$和 $EpCAM^+$（侵袭性）、$ALDH^+$（醛脱氢酶）和 $OV\text{-}6^+$（化学抗性）、$CD44^+$和 $ICAM\text{-}1^+$（转移性）、$CD90^+$（循环性）、$CD13^+$（化疗耐药）、$1B50\text{-}1^+$（自我更新）、$SALL4^+$（增殖），其中多数基

因表达具有致瘤特征。识别特定的 LCSCs 生物标志物与改善预后和最终患者生存有关。针对肿瘤细胞表面抗原的抗体疗法通过抑制特定信号通路或增强直接免疫效应子的激活来改善临床预后。在某些情况下，这些抗体药物与能够选择性靶向化疗药物的生物活性药物结合。通过开发靶向抗体，有望在许多癌症中消除潜在的耐药细胞亚群。此外，使用抗体阻断信号传导是根除肝 LCSC 并因此治愈这些患者的潜在策略。抗体药物还可以通过抗体依赖性细胞毒性/补体依赖性细胞毒性机制发挥作用，从而增强针对 LCSCs 的免疫反应。目前揭示了特异性靶向 LCSCs 在提高现有疗法效力方面的明显优势，未来需要更有效的肝脏 LCSC 标志物来识别和设计更特异性的抗 LCSC 标志物疗法，为开发新的治疗方案提供重要框架，从而带来长期的临床益处。

关键字: 肝癌干细胞；肝细胞癌；治疗意义

611. 肿瘤细胞通过旁分泌维持肿瘤相关成纤维细胞在微环境中的促癌作用

刘亚轩*、云芬、贾永峰

内蒙古医科大学

肿瘤相关成纤维细胞（CAF）是肿瘤基质组织的重要成分，在肿瘤发生发展的过程中发挥着重要的作用，通过重塑细胞外基质，形成血管、调节代谢功能，维持肿瘤细胞干性，抑制免疫反应和促进肿瘤细胞的增殖、迁移、侵袭和耐药性形成来维持肿瘤的恶性行为。肿瘤细胞通过多种方式诱导成纤维细胞，肿瘤细胞分泌的 TGF-β1 和 IL1 通过活化 NF-kβ信号通路诱导基质成纤维向 CAF 的转化，癌细胞分泌的外泌体 microRNA、长链非编码 RNA（LncRNA）通过下游丝裂原活化蛋白激酶（MAPK）、NF-Kβ信号转导和转录激活子 3（STAT3）将正常的成纤维细胞重新编程为 CAF。肿瘤细胞通过不同的衍生外泌体诱导 CAF 的形成，同时也可以将基质中的不同细胞诱导分化成为 CAF，通过 TGF-β1、肝细胞生长因子（HGF）和血小板衍生生长因子（PDGF）等细胞因子诱导血小板肝星状细胞、间充质干细胞、脂肪细胞、内皮细胞、上皮细胞分化。即使是坏死的癌细胞依然可以通过损伤相关模式（DAMP）促进 CAF 的恶性行为。研究发现肿瘤细胞受到免疫因子、化疗药物等外界刺激后会增加细胞因子的分泌，来增强周围细胞的促肿瘤作用。同时肿瘤的旁分泌功能对周围细胞异质性有显著作用，已有研究表明肿瘤周围的间质细胞会因为距离不同而呈现不同的表型和功能。通

过对肿瘤微环境认识的深入，我们发现仅仅针对癌细胞本身的治疗方式很难达到或是维持我们想要的效果。治疗癌症要切断肿瘤细胞对微环境的影响。

关键字：肿瘤细胞、肿瘤相关成纤维细胞、肿瘤微环境

612. 循环肿瘤 DNA 在非小细胞肺癌中的作用

张文仙*、云芬、贾永峰、康畅元

内蒙古医科大学

肺癌是临床上最常见的肿瘤之一，发病率及死亡率极高，其组织病理学可分为非小细胞肺癌和小细胞肺癌两大类，并以非小细胞肺癌最为常见，约占肺癌总发病率的 85%。由于其起病隐匿，大部分患者确诊时已晚，因此早期诊断极为重要。对于非小细胞肺癌，临床上主要采用低剂量螺旋电子计算机断层扫描、纤维支气管镜等进行诊断，但是由于其只能监测到宏观疾病，存在着明显的滞后性；组织活检虽是确诊肺癌的金标准，但无法避免肿瘤的异质性，且有创，故使用受到一定程度的限制，而 ctDNA 检测就弥补了以上的不足。循环肿瘤 DNA（circulating tumor DNA，ctDNA）是来自肿瘤基因组的 DNA 片段，由肿瘤细胞产生并释放于血液循环系统中，主要由单链或双链 DNA 以及单链与双链 DNA 的混合物组成，它从多个肿瘤多个部位释放，从而克服了肿瘤的异质性。ctDNA 是一种可重复性的无创“液体活检”诊断技术，具有易于动态血液样本采集，更为精确、灵敏，价格低廉，无不良反应等优点，更易被患者所接受，研究显示肿瘤 ctDNA 出现可能比临床影像学阳性要提前数月以上，因此 ctDNA 可作为肿瘤的早期筛查和术后微小残留病灶以及复发的检测；不仅如此，越来越多的证据表明,ctDNA 能够识别免疫治疗反应,评估疗效和生存时间，也因此用作癌症治疗效果的长期跟踪。ctDNA 还可用于肺癌敏感基因以及耐药基因检测以便靶向治疗和指导耐药治疗。目前敏感基因研究最多的是 EGFR 突变。大量研究显示 NSCLC 的 ctDNA 检测组织中的 EGFR 突变,灵敏度为 60％～75％、特异性为 90％～100％，ctDNA 与组织一致性为 79％～89%。对于耐药，其中约有 50%～60%患者发生 EGFR 第 20 号外显子 T790M 点突变而产生耐药，但研究发现，通过 ctDNA 检测 T 790M突变会出现假阴性，因此需要结合组织活检确认。尽管 ctDNA 检测非常重要，但也存在一定弊端，其在早期检测的敏感性不够高，因此还不能完全取代组织活检，提高 ctDNA 早期检测敏感性的方法需进一步研究探讨。

关键字：非小细胞肺癌；ctDNA；微小残留病灶

613. 靶向 FAPα阳性肝星状细胞克服结直肠癌肝转移模型中抗血管生成药物耐药

齐明*、范舒然、陈敏锋、叶文才、张冬梅

暨南大学

血管劫持（vessel co-option）已被证明可介导结直肠癌肝转移 (CRCLM) 对抗血管生成治疗的抵抗。目前针对血管劫持的机制研究主要集中在“劫持者”肿瘤细胞上，而对“被劫持者”窦状毛细血管的功能及作用尚未被探讨。我们研究发现在贝伐单抗 CRCLM 异种移植中，血管劫持的发生与肝星状细胞(HSCs)中成纤维细胞活化蛋白α (FAPα)的表达增加有关，而在携带 CRCLM 异种移植的 HSC 特异性条件 Fap 敲除小鼠中，该蛋白的表达显著减弱。在机制上，贝伐珠单抗治疗诱导缺氧可上调肿瘤细胞中成纤维细胞生长因子结合蛋白 1 (FGFBP1)的表达。功能获得或丧失实验显示，抗贝伐单抗的肿瘤细胞来源的 FGFBP1 通过增强 HSCs 旁分泌 FGF2-FGFR1-ERK1/2-EGR1 信号通路诱导 FAPα表达。FAPα促进 HSCs 细胞分泌 CXCL5，激活肿瘤细胞及骨髓源性抑制细胞（MDSC）的 CXCR2，促进肿瘤细胞的上皮-间充质转化（EMT）和 MDSC 的募集。这些发现在 CRCLM 患者来源的肿瘤组织中得到了进一步的验证。靶向 $FAP\alpha^+$ HSCs 有效地破坏了“被劫持”的窦状血管，克服了贝伐珠单抗的耐药性。本研究强调了 $FAP\alpha^+$ HSCs 在血管劫持中的作用，并为克服血管劫持介导的贝伐珠单抗耐药提供了一种有效的策略。

关键字: vessel co-option； 结直肠癌肝转移；FAPα；抗血管新生药物耐药

614. Sirtuin 6 在食管癌中发挥致癌作用并诱导自噬

袁千钦*、孙奋勇

上海市第十人民医院

目的：Sirtuin6（Sirt6）是 Sirtuin 家族成员，通过催化启动子区域组蛋白脱乙酰化来抑制 HIF1α 和 MYC 诱导的基因转录，进而抑制有氧糖酵解过程以及细胞生长。有文献报道 Sirt6 在前列腺癌、乳腺癌以及非小细胞肺癌中表达升高，表明其可能在不同癌种中发挥特定作用。目前，Sirt6 在食管癌中的作用尚不明确，本研究旨在探索 Sirt6 在食管癌细胞中发挥的作用，阐明其作用机制。

方法：采用 RT-qPCR、免疫组织化学检测 Sirt6 在食管鳞状细胞癌组织中的表达水平。分析 Sirt6 表达与临床特征相关性。通过生物学实验研究 Sirt6 影响细胞增殖的机制和下游分子。通过 LC3II/I和自噬通量研究 Sirt6 对自噬的影响。采用 WB 和 IP 鉴定与 Sirt6 互作的蛋白。

结果：Sirt6 在食管鳞状细胞癌组织中表达上调，其上调与临床特征密切相关，如肿瘤淋巴结转移、细胞分化等。Sirt6 促进细胞增殖，并诱导食管癌细胞中的关键抗凋亡因子 Bcl2 表达，且明显诱导细胞自噬。Sirt 6 与 ULK1 特异性相互作用，并通过调节 mTOR-ULK1 信号通路诱导自噬。

结论：Sirt6 的 mRNA 和蛋白水平在食管鳞状细胞癌组织中均显著升高，其过表达与临床病理、分期和细胞分化密切相关。Sirt6 能够促进细胞增殖，并通过调节 mTOR-ULK1 信号通路诱导自噬。

关键字：食管癌；自噬

615. 多不饱和脂肪酸在预防和促进癌症中的作用的 meta 分析

袁千钦*、孙奋勇

上海市第十人民医院

目的：每年世界上有近 800 万人死于癌症。致癌作用是一个涉及一系列 DNA 结构改变的过程，这些改变会影响其稳定性并阻止正常的细胞繁殖和发育。影响癌症的因素很多。其中包括营养因素。多不饱和脂肪酸的摄入越来越多地与具有炎症成分的慢性疾病（如癌症）的预防和发展相关联。本文综述了多不饱和脂肪酸及其与肿瘤（主要是前列腺癌、乳腺癌和结肠癌）的关系。

方法：初步搜索得到了 92 篇精选的参考文献。最后经过筛选，40 项动物和体外实验研究以及流行病学研究被包括在内。

结果：动物实验研究和体外实验显示ω3 多不饱和脂肪酸对癌症的保护作用。然而，人体研究是矛盾的。尽管有明显证据表明ω3 多不饱和脂肪酸在预防结肠癌中具有保护作用。

结论：饮食中ω3 多不饱和脂肪酸与癌症风险之间存在相关性，但需要进一步的研究来证实它们对这种疾病发展的影响。

关键字：多不饱和脂肪酸；癌症

616. 信号通路变异导致抗 PD1/PD-L1 抗体耐药的研究进展

魏子栓*

河北医科大学第四医院科研中心

人体内 T 细胞表面表达 PD1 蛋白与其配体 PD-L1 的结合，帮助肿瘤进行免疫逃逸，促进肿瘤进展。针对 PD1/PD-L1 通路的免疫治疗可有效阻断免疫抑制信号，起抗肿瘤作用。在过去的十年中，抗 PD1/PD-L1 治疗取得了巨大的成功。然而，只有一小部分患者表现出临床反应。大多数患者不能从抗 PD1/PD-L1 治疗中获益。此外，很多初期应答者会产生获得性抵抗。因此，了解免疫检查点抑制剂的耐药机制是有必要的。目前，研究人员已经确定了肿瘤免疫原性不足、巨噬细胞功能障碍、T 细胞不可逆耗竭等等主要耐药机制。本综述主要讲解一些致癌信号通路及基因突变导致的耐药。在这里，我们详细探讨潜在的机制，寻找有助于提高患者药效的生物标志物，并讨论可能缓解抗 PD1/PD-L1 耐药性的策略。

关键字：免疫检查点；PD1；PD-L1；耐药

617. 环状 RNA 在食管癌中的研究进展

刘烈*

河北医科大学第四医院

环状 RNA 是一种具有环状结构的内源性非编码 RNA，可竞争性与 microRNA 特异性结合，从而调节相关基因的表达。其除具有海绵作用外，还具有调节亲本基因的表达、转录翻译和蛋白质修饰的作用。它可以作为潜在的诊断和治疗的生物标志物，从而进一步评估预后。虽然，近年来对于食管癌的化疗、放疗和外科手术取得了重大的进展，但食管癌的发病率和死亡率仍然很高，并易早期转移，患者的 5 年生存率仍然很低。本文综述了 circRNA 的功能，并探讨了 circRNA 作为食管癌中生物标志物的研究进展。

关键字：环状 RNA，食道癌，生物标记物

618. PD-L1 在癌症中的表达

刘晶晶*

河北医科大学第四医院

逃避免疫系统是癌症的一个特征，它使癌细胞逃避免疫细胞的攻击。癌细胞可表达多种免疫抑制信号蛋白，引起免疫细胞功能障碍和凋亡。其中一种抑制分子是程序性死亡配体-1 (PD-L1)，它与 T 细胞、B 细胞、树突状细胞和自然杀伤 T 细胞上表达的程序性死亡-1 (PD-1)结合，从而抑制抗癌免疫。因此，抗 PD-L1 和抗 PD-1 抗体已经被用于癌症的治疗，显示出良好的效果。然而，只有一部分患者对治疗有反应。进一步了解其对 PD-L1 表达的调控，有助于提高抗 PD-L1 和抗 PD-1 治疗效果。研究表明 PD-L1 的表达受信号通路、转录因子和表观遗传因子的调控。PI3K 和 MAPK 通路均参与 PD-L1 调控，但控制 PD-L1 和细胞增殖的下游分子可能不同。转录因子缺氧诱导因子-1α和信号转导和转录-3 的激活作用于 PD-L1 的启动子以调控其表达。此外，miR-570、miR513、miR-197、miR-34a 和 miR-200 等 microRNA 对 PD-L1 具有负调控作用。在临床上，选择既能控制 PD-L1 表达又能控制细胞增殖的分子，可以提高靶向治疗的疗效。

关键字: 肿瘤，PD-1，机制

619. 人参皂苷 Rg1 靶向同源重组修复蛋白 CtIP 抑制肝母细胞瘤生长的机制研究

唐晓晨*

上海交通大学医学院附属上海儿童医学中心

人参皂苷 Rg1 是中草药人参的主要药理活性成分，被广泛用于中枢神经系统和免疫相关疾病的临床治疗。最近有研究表明它也具有抗肿瘤作用。肝母细胞瘤（hepatoblastoma，HB）在儿童肝恶性肿瘤中占比 80%，通常于 5 岁前诊断。完整手术切除是治疗 HB 的主要方法，而化疗可作为无法完全切除肿瘤患者的另一选择。然而，由于化疗药物的耐药和毒性过大等副作用，限制了 HB 患者的治疗效果。中药辅助治疗基于毒副作用少、器官刺激小等特点已在临床上得到广泛应用。研究报道 Rg1 可通过不同的发病机理影响多种肿瘤的进展，而 Rg1 对 HB 的发展及潜在的抗肿瘤机制尚未明确。

目的：探究人参皂苷 Rg1 靶向同源重组修复蛋白 CtIP 抑制 HB 生长的机制，并探讨抗肿瘤药物与 Rg1 联合应用靶向治疗 HB 的效果。

方法：1.确定 Rg1 的 IC50 值，通过 CCK-8 实验、克隆形成实验和流式细胞术检测 Rg1 对 HB 细胞生长的影响；2.收集 HB 肿瘤组织及其配对的正常组织，采用荧光实时定量 PCR 检测 CtIP 的表达水平；3.利用 Western blotting、免疫荧光分析、HR 及 NHEJ 报告实验研究 Rg1 靶向 CtIP 抑制 HB 生长的机制；4.通过 CCK-8 实验、克隆形成实验和免疫荧光分析评价 Rg1 与抗肿瘤药物联合应用靶向 HB 的治疗效果。

结果：1. Rg1 显著抑制 HB 细胞生长；2. CtIP 在 HB 组织中高表达；3. Rg1 特异靶向抑制 CtIP 并刺激 HB 细胞产生 DNA 双链断裂；4. Rg1 可提高 HB 细胞对抗肿瘤药物的敏感性。

结论：Rg1 通过直接靶向同源重组修复蛋白 CtIP，破坏 HB 细胞的同源重组修复并刺激产生 DNA 双链断裂，进而抑制 HB 生长，同时 Rg1 与抗肿瘤药物联合应用可提高 HB 治疗效果。

关键字：人参皂苷 Rg1，CtIP，肝母细胞瘤，同源重组修复

620. 用于超快递送反义 DNA 的类精子纳米载体

唐晓晨*

上海交通大学医学院附属上海儿童医学中心

尽管各种纳米材料已被设计为细胞内递送工具，但以下方面已成为限制其发展的障碍，例如复杂且耗时的合成过程，以及相对有限的应用领域（即生物传感或细胞成像）。在这里，我们开发了一种新型纳米递送系统，称为“纳米精子”，具有低细胞毒性和高生物相容性。在该系统中，我们仅以 DNA 为材料，合成头部为银纳米团簇，尾部为功能片段的纳米结构，其形状像精子，实现超快递送和成像/治疗的双重功能。作为模型，我们分析了“纳米精子”携带不同结构的 DNA 用于成像或 survivin-asDNA 用于肿瘤治疗的可能性。因此，这项工作构成了一种新型的双功能高速递送载体，成功填补了以 DNA 模板纳米团簇作为递送载体的肿瘤治疗领域的空白。

关键字：纳米载体，银纳米簇，药物递送，反义 DNA，生存素

621. cfDNA 作为结直肠癌诊断标记价值的一项荟萃分析

王欣悦*、孙奋勇

上海市第十人民医院

目的：通过荟萃分析系统地评价 cfDNA 作为结直肠癌非侵入性生物标志物的诊断价值。

方法：检索自 2017 年 8 月 7 日至 2020 年 11 月发表在 Pubmed，Embase 和 Cochrane Libray 数据库上的研究，筛选出报道了 cfDNA 作为结直肠癌非侵入性生物标志物诊断价值的有关文章，汇总之前荟萃分析的 14 项研究，通过统计软件量化分析 cfDNA 作为结直肠癌非侵入性生物标记物的诊断价值。

结果：2 项关于定量检测循环 cfDNA 用于结直肠癌诊断的研究符合纳入标准。汇总之前的 14 项研究共 16 项，最终包括 1683 名结直肠癌患者和 2539 名健康志愿者作为对照进行分析。最终结果显示：总的敏感度，0.742（95% CI，0.720-0.762）；特异性，0.887（95% CI，0.874-0.999）；阳性似然比，7.084（95% CI，4.885-10.271）；阴性似然比，0.289（95% CI，0.224-0.373）；诊断优势比，29.755（95% CI，17.383-50.932）；曲线下面积，0.8878（95% CI，0.84-0.94）。未检测到发表偏倚。

结论：本次更新的荟萃分析提示循环 cfDNA 诊断结直肠癌的敏感性不甚理想，但特异性尚可。

关键字：荟萃分析

622. RAP80 是食管鳞状细胞癌患者预后的独立生物标志物

王欣悦*、孙奋勇

上海市第十人民医院

目的：食管鳞状细胞癌是中国食管癌最常见的病理类型，尤其在我国中部的河南省。目前，靶向脱氧核糖核酸损伤修复因子是一种很有前途的癌症治疗方法。本小组致力于探索在食管鳞癌中过表达的 DNA 损伤修复因子，以提供潜在的治疗靶点。RAP80/UIMC1（含泛素相互作用基序 1）为 DNA 损伤修复因子之一，本文中对其在食管鳞状细胞癌中的作用和价值进行研究。

方法：通过比对 100 对食管鳞癌组织和邻近正常组织的免疫组化结果，筛选 DNA 损伤修复因子。采用 Pearson χ2 检验分析 RAP80 与患者临床特征的关系。细胞功能学实验和异种移植荷瘤实验研究了 RAP80 对细胞生长、凋亡及 G2/M 检查点调节的影响。通过流式分析和 WB 研究 RAP80 对 ATM 活性的影响。采用荧光共聚焦检测 RAP80 在 DNA 损伤修复过程中的作用。

结果：RAP80/UIMC1 在 ESCC 组织中高度过表达，此外，RAP80 基因水平被证实是 ESCC 患者总生存期的独立预后生物标志物。RAP80 在体外和体内促进细胞增殖，在早期和晚期抑制细胞凋亡，并参与 G2/M 检查点调节。机制研究表明，RAP80 通过蛋白酶体-泛素化途径积极调节 ATM 活性，促进细胞周期 G2/M 期的转变。RAP80 正向调节 USP13 的稳定性以促进内皮细胞的增殖。此外，抑制 RAP80 极大地提高了内皮细胞对 ATM 抑制剂 KU-55933 的敏感性，说明 RAP80 抑制剂和 ATM 抑制剂的潜在组合，有助于提高 ESCC 患者的疗效。

结论：RAP80 在食管鳞状细胞癌中起到促进作用，其水平可作为患者预后的独立生物标志物。我们的结果支持了 RAP80 抑制剂与 ATM 抑制剂或 USP13 抑制剂联用以提高食管鳞癌疗效的可能。

关键字： RAP80

623. PD-1/PD-L1 相关的免疫检查点抑制剂在原发中枢神经系统淋巴瘤中的作用

石澳荣*、贾永峰、刘霞

内蒙古医科大学

随着人们对淋巴瘤发病机制和治疗的不断深入，2017 年 WHO 造血和淋巴组织分类更新以后，原发中枢神经系统淋巴瘤（PCNSL）被定义为一个新的独特的亚型。它是一种无系统性浸润，仅局限于中枢神经系统和眼部的结外非霍奇金淋巴瘤。PCNSL 发病率低（占所有淋巴瘤的 1%，占结外淋巴瘤的 4%-6%，占所有脑肿瘤的 4%），但具有高度恶性其预后极差，未经治疗患者的总生存期为 1.5-3 个月，因此寻找潜在的治疗靶点，为患者提供个体化治疗显得十分重要。90%以上的 PCNSL 属于弥漫性大 B 细胞淋巴瘤（DLBCL）（CD20+），因此目前临床治疗的重要手段就是针对 B 细胞表面抗原 CD20 的单克隆抗体利妥昔单抗合并传统用药甲氨蝶呤。但对于最佳治疗方案仍无统一共识，随着 PCNSL 发病机制的不断深

入，找到免疫检查点抑制剂治疗很有必要。活化 T 细胞表面表达的程序性细胞死亡蛋白 1(PD-1)/程序性死亡配体 1(PD-L1)是导致肿瘤免疫逃逸的重要免疫检查点分子，因此阻断 PD-1/PD-L1 可以重新激活细胞毒性 T 细胞对肿瘤的杀伤作用，是一种重要的肿瘤免疫治疗方式。目前 PD-1/PD-L1 抑制剂在多种实体恶性肿瘤的治疗中发挥重大作用，但在 PCNSL 中，其应用还较少。PD-1 和 PD-L1 高表达可能与较差生存率相关，且在 PCNSL 中 PD-1 和 PD-L1 过表达，这为我们找到更简单更有效的免疫检查点抑制剂治疗 PCNSL 提供了新证据。但目前存在临床样本少，具体作用机制并没有被系统阐明等问题，PD-1/PD-L1 免疫检查点抑制剂的治疗效果和预后需要进一步的研究。

关键字：原发中枢神经系统淋巴瘤；PD-1/PD-L1；免疫治疗

624. 血清精氨酸酶 1 作为新型生物学标志物用于肺癌的诊断

高恒兴*、张坤、陈明伟*

西安交通大学第一附属医院

背景和目的：肺癌是发病率和死亡率最高的恶性肿瘤，对人类健康造成严重损害，而目前大多数肺癌（LC）患者就诊时被诊断为晚期，因此预后较差。血清肿瘤标志物（TMs），如癌胚抗原（CEA）、细胞角蛋白-19 片段（CYFRA21-1）、鳞状细胞癌原（SCC）和神经元特异性烯醇化酶（NSE），因其易于应用而常规用于 LC 的诊断和预后评估。而随着年龄的增长或某些良性疾病，TMs 值可能会上升到高于参考水平，而某些癌症患者的 TMs 值仍保持正常。因此，目前还没有理想的肺癌诊断预测的血清学标志物。肿瘤免疫抑制微环境对于肿瘤发生发展起着重要作用，而巨噬细胞的 M2 型极化和对肿瘤微环境（TME）的浸润是肿瘤进展的关键决定因素。血清精氨酸酶 1（Arg1）是 M2 巨噬细胞极化的重要标志，而 Arg1 作为血清学标志物用于肺癌的诊断目前仍未见报道。由于单个 TM 值只能提供有限的参考，本研究拟选择四种常用的 TMs，CEA、CYFRA21-1、SCC 和 NSE，评价 Arg1 单独以及与上述指标联合用于肺癌诊断的效能和价值，以期能更准确地识别低剂量计算机断层扫描（LDCT）筛查的候选对象，为 LC 患者制定更科学的诊断、治疗和随访计划提供重要依据。

方法：收集来自呼吸科住院的肺癌（LC）和良性肺部疾病（BLD）患者的 CEA、CYFRA21-1、SCC 和 NSE 检测数据。利用酶联免疫吸附试验（ELISA）检测 LC 和 BLD 患者以及体检中心健康人群（HC）的 Arg1 表达水平。基于研究变量的不同统计学特性，采用独立样本 Student-t

检验、Mann-Whitney U 检验或方差分析来衡量组间差异。采用 Spearman 相关分析评估 Arg1 与其他 TMs 的关联性。通过计算受试者工作特征（ROC）曲线下面积（AUC）估计 Arg1 单独以及与其他指标联合用于 LC 诊断的效能，确定 LC 筛查的最佳临界值。

结果：血清 Arg1 水平在 LC 组显著高于 BLD 和 HC 组（$p<0.05$），而 HC 和 BLD 组之间无显著性差异（$p>0.05$）（图 1）。Arg1 将 LC 与 HC 和 BLD 区分开来的 AUC 为 0.853 (0.756-0.950)，该指标诊断 LC 的最佳截止值为 1.698 （图 2）。CEA 和 CYFRA21-1 在 LC 与 BLD 组之间的差异均具有统计学意义（$p<0.05$）。Arg1 与 CYFRA21-1 之间存在一定的相关性（r=0.335，$p=0.015$）。在鉴别肺部良恶性病变时，Arg1 与 CEA 和 CYFRA21-1 联合[AUC：0.888 (0.796-0.980)] 用于鉴别 LC 的检测效能均优于 CEA [AUC：0.804 (0.661-0.947)，$p=0.264$]和 CYFRA21-1 [AUC：0.774 (0.632-0.915)，$p=0.038$] 单独检测以及两者联合检测的效能 [AUC：0.879 (0.775-0.982)，$p=0.760$]（图 3）。

结论：血清 Arg1 可有效预测 LC 的诊断。在鉴别肺部良恶性病变时，与单独或联合的相同 TMs 相比，Arg1 与 CEA 和 CYFRA21-1 联合的诊断预测模型可以更准确地识别 LC 筛查的高危人群。

关键字：肺癌，CEA，CYFRA21-1，SCC，NSE 和 Arg1，诊断

625. HIPK2 或通过调节 STAT6 促进三阴乳腺癌的发生发展

李一*、黄婷、吴池华、刘锦平

四川省医学科学院·四川省人民医院

研究目的：乳腺癌是女性最常见的恶性肿瘤，分为管腔型、HER2 过表达型及三阴型，其中三阴性乳腺癌目仍缺乏有效的治疗靶标，与其他类型的乳腺癌相比，具有复发转移率高、预后差的特点，因此寻找三阴乳腺癌的治疗靶点成为国内外研究的热点。同源结构域相互作用蛋白激酶 2（HIPK2）是一种肿瘤抑制基因，在多种肿瘤的发生发展中发挥着重要作用，但在乳腺癌中的研究尚少。本研究拟探讨 HIPK2 对三阴乳腺癌细胞系增殖和迁移的能力的影响及其作用机制，为三阴乳腺癌的治疗提供潜在靶点。

材料与方法：本研究采用三阴乳腺癌细胞系 MDA-MB-231 进行体外、体内实验及机制探讨，最后进行临床相关性的验证。体外、体内实验采用构建沉默 HIPK2(shRNA)的慢病毒感染 231 细胞系，感染成功后应用流式细胞术检测 231 细胞的凋亡能力的变化，Transwell 检测 231

细胞的迁移能力的变化，并将感染后的细胞注射到 BALB/c 裸鼠皮下，构建模型，通过活体荧光成像显示成瘤差异；通过蛋白芯片检测沉默 HIPK2 后相关通路蛋白的表达情况，并用 Western Blot 验证其表达差异；通过组织芯片验证 HIPK2 表达与临床病理资料的相关性。

结果：1. qPCR 检测显示 HIPK2 在 231 细胞中表达显著升高（*P*<0.001）（图 1）。2. 流式检测结果显示 shHIPK2 组细胞凋亡水平显著下降（*P*<0.001）；Transwell 检测结果显示 shHIPK2 组细胞迁移水平显著降低（*P*<0.001）（图 2）。3. 活体荧光成像显示 shHIPK2 组裸鼠体内移植瘤的荧光强度明显较低（*P*<0.01）（图 3）。4. 沉默 HIPK2 后检测人磷酸化激酶芯片中相关蛋白磷酸化水平，其中 $p<0.05$ 时，蛋白 Hsp27、p53 和 STAT6 的表达水平显著下调。WB 检测 231 中 HSP27、p-HSP27、P53、p-P53、STAT6 和 p-STAT6 的表达，结果显示沉默 HIPK2 后 p-STAT6 蛋白的表达水平有所降低（图 4）。5. 组织芯片分析结果显示 HIPK2 的表达与年龄、病理分级、肿瘤大小和临床分期等病理资料中呈显著正相关，生存分析显示 HIPK2 的表达与乳腺癌的总生存期显著相关，即 HIPK2 表达越高，患者的生存期越短（图 5）。

结论: HIPK2 或可通过 STAT6 信号通路促进三阴乳腺癌细胞的增殖和迁移能力，可能与乳腺癌的发生发展及预后相关。

关键字: HIPK2，三阴乳腺癌，STAT6

626. 影响晚期上皮性卵巢癌患者满意肿瘤减灭术的相关因素分析

祖逸峥*

福建医科大学妇儿临床医学院

目的: 通过对 154 例晚期上皮性卵巢癌患者的临床资料进行回顾性分析，探讨影响晚期上皮性卵巢癌患者初次肿瘤细胞减灭术满意程度的相关因素。

方法: 回顾性分析 2016 年 1 月至 2021 年 12 月于我院行初次肿瘤细胞减灭术晚期上皮性卵巢癌患者的临床病理资料。收集患者一般情况（发病年龄、民族、绝经状态、妊娠次数、分娩次数）、术前血清学指标（肿瘤标记物如 CA125、HE4 及术前外周血 WBC、NLR、MLR、PLR、PAR、ALB、PLT、D-D）、术中探查肿瘤病灶情况（肿瘤单双侧情况、肿瘤大小、腹水量、大网膜状态、有无上腹部转移）、术后病理情况（FIGO 分期、病理学类型、组织学分化），

通过手术记录评估肿瘤细胞减灭手术满意程度，分析各相关因素与手术满意程度的关系。应用 SPSS 25.0 软件对数据进行单因素及多因素相关分析，并通过 MedCalc 20.0 绘制 ROC 曲线，分别计算比较上腹部转移、大网膜状态、FIGO 分期、组织学分化、CA125 单一指标及联合预测的效能。

结果: 1.满意减瘤情况：纳入研究的 154 例晚期上皮性卵巢癌患者中满意组 106 例，满意率 68.8%，不满意组 48 例，不满意率 31.2%。2.影响晚期上皮性卵巢癌患者初次肿瘤细胞减灭术的满意程度的单因素分析：结果显示 CA125、HE4、NLR、MLR、PLR、PAR、PLT、D-D、肿瘤单双侧、肿瘤大小、大网膜状态、上腹部转移、FIGO 分期、病理学类型、组织学分化对 AEOC 患者行 PDS 满意程度有影响（*P* 均＜0.05）。3.影响 AEOC 患者 PDS 的满意程度的多因素分析：结果显示上腹部转移、大网膜状态、FIGO 分期、组织学分化、CA125 均是影响 AEOC 患者满意肿瘤细胞减灭术的独立危险因素（*P* 均＜0.05）。4.各影响因素在预测不满意肿瘤细胞减灭术中的价值：上腹部转移、大网膜状态、FIGO 分期、组织学分级、CA125 的 ROC 曲线下面积（AUC）分别为 0.663（95%CI:0.583-0.739）、0.688（95%CI:0.609-0.760）、0.564（95%CI:0.482-0.644）、0.621（95%CI:0.539-0.698）、0.764（95%CI:0.689-0.829）；上腹部转移的敏感性、特异性、准确性分别为 56.25%、76.42%、32.67%，大网膜状态的敏感性、特异性、准确性分别为 79.17%、58.49%、37.66%，FIGO 分期的敏感性、特异性、准确性分别为 16.67%、96.23%、12.89%，组织学分化的敏感性、特异性、准确性分别为 95.83%、28.30%、24.14%，CA125 的敏感性、特异性、准确性分别为 77.08%、68.87%、45.95%。5.多因素联合预测不满意肿瘤细胞减灭术的价值：AUC 为 0.862（95%CI:0.797-0.912），其敏感性、特异性、准确性、阳性预测值、阴性预测值分别为 83.33%、81.13%、64.47%、66.67%、91.49%。

结论： 1.CA125、HE4、NLR、MLR、PLR、PAR、PLT、D-D、肿瘤单双侧、肿瘤大小、大网膜状态、上腹部转移、FIGO 分期、病理学类型、组织学分化是影响晚期上皮性卵巢癌患者满意肿瘤细胞减灭术的相关因素；而上腹部转移、大网膜状态、FIGO 分期、组织学分化、CA125 是影响 AEOC 患者满意肿瘤细胞减灭术的独立危险因素；2.单因素预测不满意肿瘤细胞减灭术中，以组织学分化程度预测的敏感性高但特异性低；FIGO 分期预测的特异性高但敏感性低；3.上腹部转移联合大网膜状态、FIGO 分期、组织学分化及 CA125 明显提高预测不满意肿瘤细胞减灭术的百分比。

关键字： 晚期上皮性卵巢癌，肿瘤细胞减灭术，满意程度，相关因素分析

627. 焦亡—肿瘤研究的新前沿

谯坤*

贵州医科大学

细胞焦亡（Pyroptosis）是一种伴随着炎症反应的细胞程序性死亡形式，主要由 gasdermin D (GSDMD) 的炎性半胱天冬酶（caspase）裂解和 gasdermin E (GSDME) 的凋亡性半胱天冬酶(caspase)裂解诱导。其过程伴随着炎症小体的激活、促炎细胞因子白细胞介素 1β（IL-1β）和白细胞介素 18（IL-18）的成熟和分泌。细胞焦亡参与多种疾病的发生发展。近年来，随着 gasdermin 家族的进一步研究，对细胞焦亡的研究和认识逐渐深入，尤其在肿瘤中的作用和意义受到广泛关注。目前大量研究证据表明，细胞焦亡会影响肿瘤的发生发展。本综述旨在复习和总结肿瘤中细胞焦亡发生的分子机制和功能。

关键字： 细胞焦亡，caspase，gasdermin 家族，炎症小体，肿瘤免疫

628. 序列相似家族 135 成员 A 的表达与结直肠癌的预后和免疫微环境关系

赵龙、杨长江、叶颖江、申占龙*

北京大学人民医院

目的：探讨序列相似家族 135 成员 A(FAM135)在结直肠癌中的表达及其与结直肠癌免疫微环境的关系。

方法：从癌症基因组图谱数据库(TCGA)下载结直肠癌及癌旁正常组织的基因表达及临床数据，分析 CLCN3 其在结直肠癌样本中的表达水平及与患者临床病理指标及预后的关系，采用配对样本 t 检验分析其表达差异检验分析其与相关临床病理指标的关系，Kaplan-Meier 法分析其与预后的关系。通过基因本体(GO)生物进程分析、京都基因与基因组百科全书(KEGG)信号通路分析探讨 CLCN3 参与结直肠癌发生发展的可能机制，通过单样本基因集富集分析(ssGSEA)及 Spearman 相关性分析探索 CLCN3 表达与结直肠癌不同亚型免疫细胞浸润的相关性。

结果：与正常组织比较,结直肠癌中 CLCN3 低表达(4.131±0.609 比 4.401±0.409，t= -3.105, *P*= 0.002)。CLCN3 的表达水平与肿瘤淋巴结侵犯($\chi 2$=9.07, *P*=0.011)呈明显相关。CLCN3 低表

达与患者不良预后有关($\chi2$=6.41, *P*=0.011)。多因素分析结果表明 CLCN3 表达[风险比(HR)=0.654 ,95%可信区间(CI):0.441~0.970,*P*=0.035]为影响结直肠癌预后的独立因素。功能富集分析表明这些基因共涉及 42 个生物学过程，15 种细胞成分和 7 个分子功能,这些基因主要参与味觉传导、系统性红斑狼疮、病毒致癌、mRNA 剪接等通路。肿瘤微环境中免疫细胞相关性分析结果表明 CLCN3 表达与 DC 细胞(r=-0.279, *P*<0.001)、细胞毒细胞(r=-0.212，*P*<0.001)、中性粒细胞(r=-0.206，*P*<0.001)、巨噬细胞(r=-0.099，*P*=0.002)等多种免疫细胞浸润相关。

结论：CLCN3 在结直肠癌中显著低表达，且与结直肠癌预后相关，可能作为结直肠癌的潜在预后标志物及治疗靶点。

关键字：结直肠癌；电压门控氯离子通道 3；免疫微环境；癌症基因组图谱

629. CDS1 通过脂滴重塑促进抑制肾透明细胞癌恶性生物学行为

郑倩*、赵冉、王怡方、潘能慧、周晓莹

广西医科大学

背景：肾透明细胞癌（Kidney renal clear cell carcinoma，KIRC）是肾细胞癌最常见的病理类型。尽管手术、靶向和免疫治疗极大地改善了 KIRC 的疗效，但是晚期 KIRC 患者的预后仍较差。因此，探寻新的生物标志物及治疗靶点，对于肾透明细胞癌的诊断及治疗具有重要的意义。KIRC 最显著的病理特征是细胞内含有大量的脂肪成分，胞苷二磷酸二酰基甘油合成酶 1（CDP-diacylglycerol synthase 1，CDS1）负责将磷脂酸转化为胞苷二磷酸二酰甘油（CDP-DAG），抑制细胞内脂滴的合成。因此，我们以 CDS1 为切入点，探究其在 KIRC 中的表达改变及其生物学调控作用。

方法：分别利用 TCGA 和 GEO 数据库比较 CDS1 在 KIRC 和正常组织中表达，通过实时荧光定量 PCR、免疫组化对转录和表达水平进行验证。构建过表达 CDS1 的 KIRC 细胞株，利用 CCK8、划痕和侵袭实验，检测其对 KIRC 的恶性生物学行为的影响。利用中性树脂 BODIPY 染色检测胞内游离脂肪酸的含量，通过 ELISA 技术检测胞内的甘油三酯含量。通过流式细胞术检测过表达 CDS1 的细胞株，探究其对 KIRC 细胞周期和凋亡的影响。同时，采用 RNA 测序技术探究 CDS1 可能参与和调控的分子机制。

结果：相比正常肾组织，CDS1 mRNA 和蛋白表达水平在 KIRC 组织中下调。CDS1 表达越低，则 KIRC 患者的预后越差，提示 CDS1 是患者预后的有效分子标志物。通过绘制 ROC 曲线，我们发现基于 CDS1 mRNA 和蛋白表达水平均可有效区分 KIRC 和正常肾组织，AUC 分别等于 0.940 和 0.960（p<0.05）。为进一步探索 CDS1 在 KIRC 中的生物学调控作用，我们构建过表达 CDS1 的瞬转肾癌细胞株，发现过表达 CDS1 抑制肿瘤的增殖能力，阻滞细胞周期于 G2/M 期，诱导细胞发生凋亡，减弱细胞迁移及侵袭能力。相比对照组，过表达 CDS1 的 KIRC 细胞株中脂滴堆积增加，甘油三酯含量增多。运用 RNA 测序技术，通过聚类分析发现，过表达 CDS1 上调 KIRC 的差异基因主要参与 TNF-α和 NF-κB 信号通路。

结论：我们的结果表明，CDS1 可能是 KIRC 新的肿瘤抑制基因，而且是有效的 KIRC 诊断和预后标志物，以及潜在的治疗靶点，为临床诊疗提供新思路。

关键字：肾透明细胞癌、CDS1、脂滴、恶性生物学行为

630. 肢端黑色素瘤基因变异和肿瘤微环境特征及其预后价值探索

邹征云*[1]、黄蓉[1]、任宇[1]、郑科琳[3]、王佳钰[3]、秦岚群[4]、张桂颖[3]、赵梦珂[2]

1. 南京大学医学院附属鼓楼医院

2. 南京医科大学鼓楼临床医学院

3. 南京中医药大学鼓楼临床医学院

4. 南京医科大学附属常州第二人民医院

研究目的：肢端黑色素瘤是中国黑色素瘤中最常见的亚型，预后极差，对免疫检查点抑制剂（ICIs）应答不佳。肿瘤组织内免疫浸润水平是影响 ICIs 疗效的一个重要因素。然而，目前关于肢端黑色素瘤肿瘤微环境的研究较少。本研究的目的是探究肢端黑色素瘤基因变异和肿瘤微环境特征及其预后价值。

方法：收集 90 例肢端黑色素瘤患者的临床病理信息，包括年龄、性别、分期、组织学亚型、原发部位、有无溃疡、是否治疗等因素；通过二代测序（NGS）检测 425 个癌症相关基因包括体细胞突变、拷贝数变异在内的改变；利用多重荧光免疫组化染色（mIHC）技术对肿瘤微环境中的 CD8、CD68、HLA-DR、CD56、PanCK / S100 进行标记，并使用 Pannoramic/HALO 组织定量病理扫描分析软件进行分析计数。

结果：通过对患者的临床病理信息进行回顾性分析，发现高龄、分期晚、肢端雀斑样或结节型、未接受治疗这四种因素与肢端黑色素瘤患者预后不良显著相关（分别为：p=0.03，p<0.01，p<0.01，p=0.01）。NGS 检测提示肢端黑色素瘤的基因拷贝数变异较为频繁，常见 CCND1、CDK4、MDM2、FGF19 等拷贝数变异。通过预后分析发现存在 CDK4 扩增或 PTPN11 突变的肢端黑色素瘤患者生存时间显著更短（p<0.01，p<0.01）。分析 mIHC 检测结果发现肢端黑色素瘤肿瘤微环境中的免疫细胞浸润水平普遍偏低，肿瘤实质区的 CD8+T 细胞和 M1 巨噬细胞浸润显著低于间质区（p<0.01，p=0.05），且间质区 M1 巨噬细胞高浸润与更长的生存显著相关（p<0.01）。最后，通过将基因畸变和免疫浸润进行关联分析发现间质区 M1 巨噬细胞浸润与 CDK4 扩增呈显著负相关的趋势（p=0.06）。

结论：这是首个同时探索肢端黑色素瘤患者的基因畸变和肿瘤微环境特征的大样本研究。我们的研究表明，肢端黑色素瘤患者肿瘤微环境的免疫浸润水平普遍偏低，这可能是其 ICIs 治疗应答不佳的原因之一。CDK4 扩增和间质区 M1 巨噬细胞低浸润均与更差的生存相关，而 CDK4 扩增与间质区 M1 巨噬细胞浸润呈显著负相关的趋势，这或许是 CDK4 扩增肢端黑色素瘤患者预后不良的重要原因。

关键字：肢端黑色素瘤；肿瘤微环境；免疫浸润；CDK4 扩增；M1 巨噬细胞

631. PRMT1-MLXIP 蛋白复合体通过β-Catenin 信号通路促进胃癌细胞增殖和迁移的机制研究

王锋*、周旭军、陈施彤

重庆西南大学

研究目的：探究精氨酸甲基转移酶 1（PRMT1）在胃癌患者中表达及对患者预后的影响，明确 PRMT1 对胃癌细胞增殖和迁移能力的影响，并阐明 PRMT1 在胃癌中的作用机制，为胃癌的靶向治疗提供理论依据。

材料和方法：利用在线数据库比较 PRMT1 在正常组织和胃癌组织中的表达差异，并分析其对患者预后的影响，同时通过组织芯片及胃癌细胞系验证数据库结果。利用 shRNA 技术，构建 PRMT1 沉默的胃癌细胞系，并通过 MTT、Soft Agar、小鼠皮下移植瘤及尾静脉注射实验，检测 PRMT1 沉默对胃癌细胞增殖和迁移侵袭能力的影响。通过免疫沉淀实验结合质谱

分析，鉴定 PRMT1 结合蛋白，并通过邻位连接实验进行验证。同时分析 PRMT1 与结合蛋白间的作用关系，解析其在胃癌细胞中的作用机制。

结果：通过在线数据库及胃癌患者芯片分析我们发现，PRMT1 在胃癌中高表达，并会导致患者预后变差。敲低 PRMT1 后，胃癌细胞的增殖能力、迁移和侵袭能力、皮下成瘤能力以及体内转移能力均显著减弱，据此我们推测 PRMT1 在胃癌中发挥着促癌作用。通过结合蛋白的解析，我们发现 PRMT1 能够促进 MLXIP 蛋白对β-Catenin 的转录激活作用，从而发挥其促进增殖和迁移的作用。同时我们还发现 KTN1 蛋白能够通过与 PRMT1 蛋白结合，抑制 TRIM48 蛋白对 PRMT1 的泛素化降解作用，从而稳定 PRMT1 的蛋白表达。

结论：在胃癌细胞中，PRMT1-MLXIP 蛋白复合体通过转录激活β-Catenin 信号通路，从而提高胃癌细胞的增殖和迁移能力，其可以作为胃癌治疗的候选靶点之一。而 KTN1 蛋白能够通过稳定 PRMT1 的蛋白表达，从而稳定该蛋白复合体的活动（图 1）。图 1.PRMT1 在胃癌细胞中作用机制图

关键字：胃癌，增殖和迁移，PRMT1

632. 一种新型宫颈癌前病变分子标志物及其应用

崔倩文*、杨武林

中国科学院合肥物质科学研究院

研究目的：临床诊断宫颈病变依赖于 P16INK4a (P16)标记物，但其对低级别鳞状宫颈上皮内瘤变(cervical intraepithelial neoplasia, CIN)的敏感性非常有限。本研究的目的是证明 Pre-CN 对宫颈病变早期诊断是一个可靠的生物标志物。

材料与方法：我们从 GEO，TCGA 数据库的数据集中提取不同病理阶段宫颈组织筛选差异表达基因，并将其与人类蛋白免疫组化数据库相印证，筛选可靠的宫颈病变的候选标志物。进而收集临床样本通过免疫组化(IHC)和免疫细胞化学(ICC)检测候选标志物的表达情况。

结果：免疫组化结果显示，Pre-CN 染色效果与 P16 都对正常宫颈上皮不染色。但 Pre-CN 标记宫颈早期病变的阳性率明显高于 P16，对 CIN1 和 CIN2 的阳性标记率都达到 95%以上。另外，基于对宫颈鳞状上皮细胞增生病例的回顾性分析显示，通过 Pre-CN 染色对增生病例进行随访监测可以预测疾病的预后，即若 Pre-CN 转阴则病情减退，而 Pre-CN 持续阳性或

者由阴转阳则预示病情进展。ICC 检测结果与免疫组化结果一致，Pre-CN 染色可以有效标记各种类型的病理细胞，并依此对疾病进行病例分级。

结论：总结来说，Pre-CN 可以有效标记所有病理阶段的宫颈病变细胞，在 CIN 早期组织的标记上比传统的 P16 标记更有效。因此，Pre-CN 有可能取代 p16 标志物用于宫颈癌前病变早期筛查。

关键字：宫颈病变；早筛；诊断标志物；宫颈鳞状上皮内瘤变；免疫组化

633. Let-7c-5p 靶向调控 CTHRC1 抑制食管鳞状细胞癌进展的研究

郑雅心*[1]、张键[3]、黄春梅[1]、方霖[1]、康敏[2]

1. 眉山市人民医院（眉山市传染病医院）

2. 西南医科大学附属医院

3. 宜宾市第二人民医院

目的：miRNAs 作为潜在的肿瘤生物标记物，具有很好的临床应用前景。let-7c-5p 在食管鳞状细胞癌（ESCC）中的功能和潜在机制尚不清楚。本研究旨在通过检测 let-7c-5p 在 ESCC 组织和细胞系中的表达水平，研究 let-7c-5p 对 ESCC 细胞生物学功能的影响，进一步探讨 let-7c-5p 对 CTHRC1 的靶向调控作用及其对下游 AKT/ERK 信号传导通路的影响，最终查明 let-7c-5p 在 ESCC 发生发展过程中的作用和分子调控机制。

方法：本研究采用 PCR 检测 let-7c-5p、CTHRC1 在食管鳞癌组织中的 mRNA 表达水平，通过细胞转染试验过表达及抑制 let-7c-5p 表达后，检测 ESCC 中 CTHRC1 mRNA 及蛋白的表达情况以及对细胞生物学功能的影响；采用双荧光素酶报告基因试验来验证 let-7c-5p 和 CTHRC1 的靶向调控关系。Western Blot 检测 CTHRC1 蛋白表达水平以及下游信号传导通路 p-AKT、p-ERK 磷酸化水平变化。

结果：PCR 证实 let-7c-5p 在 ESCC 组织和细胞系中表达明显下调，而 CTHRC1 在 ESCC 中明显高表达，且 let-7c-5p 表达水平与 CTHRC1 呈负相关。let-7c-5p 与晚期 TNM 分期和淋巴结转移有相关性。双萤光素酶报告基因试验证实了 CTHRC1 是 let-7c-5p 的直接靶基因。CCK-8 试验证实 let-7c-5p 过表达能显著抑制食管鳞癌细胞的增殖能力；流式细胞学分析检测细胞凋亡结果显示过表达 let-7c-5p 可导致早期和晚期凋亡细胞百分比升高；伤口愈合测

定试验和 Transwell 迁移试验结果表明上调 let-7c-5p 能够明显抑制食管鳞癌细胞的迁移能力。Western Blot 结果显示过表达 let-7c-5p 可明显抑制 CTHRC1 的蛋白表达水平，进而抑制下游 p-AKT 和 p-ERK 磷酸化水平。

结论：（1）let-7c-5p 在人食管鳞癌组织中低表达，其低表达与晚期 TNM 分期和淋巴结转移相关；CTHRC1 在食管鳞癌组织中高表达，let-7c-5p 和 CTHRC1 表达呈负相关关系。（2）上调 let-7c-5p 可明显抑制食管鳞癌细胞株 TE1、KYSE150 的增殖和迁移活性，诱导细胞凋亡。（3）let-7c-5p 通过直接靶向调控 CTHRC1 表达，进而调节下游 AKT/ERK 信号传导通路，从而影响食管鳞状细胞癌的进展。

关键字：食管鳞状细胞癌；let-7c-5p；CTHRC1；p-AKT；p-ERK

634. 乳腺癌合并直肠癌 1 例并文献复习

于少雨、简亿*、朱梅、包宇航、杨美、郭敏、谢仟、胡晓倩

遵义医科大学附属医院

目的：乳腺癌合并直肠癌属于多原发性恶性肿瘤，临床少见，通过本文，探讨其临床表现、诊断及治疗，提高临床医师对该类疾病的认识。

方法：回顾性分析遵义医科大学附属医院收治的 1 例乳腺癌合并直肠癌临床特点并进行文献复习。

结果：44 岁女患，因“排便习惯改变及血便 20 天”于 2019 年 3 月 29 日入我院。20 天前无明显诱因出现血便，伴里急后重，伴小腹隐痛，于当地外院行肠镜提示直肠癌？直肠息肉？为进一步就诊，遂就诊于我院。查体：胸膝位肛门约 7cm 触及一肿块，环绕肠腔一周，包块凸向肠腔，质硬，表面不规则，压痛明显，不活动，手指可触及范围不能触及肿块上极。既往史：9 月前因触及右侧乳腺肿块于我院行右乳空心针穿刺活检病理示右乳非特殊型浸润性导管癌，免疫组化示浸润性癌，E-cadherin（+），P120（膜+），ER（+），PR（+），Her-2(2+),Ki67(60%),诊断为右乳腺浸润性导管癌（cT4N2MO III 期）行右侧乳腺癌改良根治术，术后予以 TEC 放疗及化疗。入院后完善相关检查后行“腹腔镜直肠癌根治术”，送检（直肠）腺癌，II 级，肿瘤浸润性肠壁肌层。明确诊断为直肠癌，后我院规律放化疗，1 年后失访。

结论：当触及乳腺肿块时尽早完善检查取病理活检明确，大便习惯性改变等症状且患者有肿瘤病史这类患者应高度警惕是否为多原发性恶性肿瘤或肿瘤转移，尽快行肠镜检查取病理明确，必要时完善 PET-CT 评估全身情况，早发现、早诊断及早治疗，以改善患者预后。多原发性恶性肿瘤临床表现无特异性，诊断主要为病理学，治疗需个体化，预后差。

关键字：乳腺癌；直肠癌；多原发性恶性肿瘤；诊断

635. 人工智能在乳腺癌 HER2 IHC 0 和 1+准确判读中的作用

吴偲*、岳萌、刘月平

河北医科大学第四医院/河北省肿瘤医院

背景：新型 HER2 靶向抗体药物结合物的出现为 HER2 低表达乳腺癌患者带来了新的治疗机会。由于 HER2 的异质性和观察者的主观评分差异导致的 HER2 ^{0} 和 HER2 $^{1+}$判读一致性很差，因此精准区分 HER2 $^{1+}$和 HER2 ^{0} 是非常必要的。在本研究中，我们旨在通过人工智能（AI）算法提高 HER2 ^{0} 和 $^{1+}$的判读的准确性和一致性。并且通过 AI 算法，评估其对异质性肿瘤 HER2 IHC 评分中的作用。

方法：AI 辅助判读是由人工智能算法和显微镜增强现实模块组成的。我们组织了一项多中心的两轮环状研究，收集 246 例非特殊浸润性导管癌病例，并从 3 家医院招募 15 名病理学家进行判读（初级、中级和高级病理学家各 5 名）。在第一轮环状研究（RS1）中，病理医师在没有 AI 辅助的情况下通过普通显微镜判读了 246 张 HER2 IHC 切片。经过 2 周的遗忘期后，在第二轮环状研究（RS2）中，病理医师在 AI 算法辅助下重新判读了该 246 例切片。

结果：在 AI 算法辅助下显著提高了判读的准确性（准确率为 0.93 *vs.* 0.80）以及 HER2 ^{0} 判读的精确度和 HER2 $^{1+}$的召回率。并且 AI 算法提高了总体判读的一致性（ICC=0.542 提升到 0.812），尤其对 HER2 $^{1+}$病例的一致性有明显提高。在异质性病例中，AI 算法辅助判读后准确率显著提高（准确率为 0.69 提升到 0.89），可与同质性病例判读准确性媲美（准确率为 0.95）。与中、高级病理医师相比，初级病理医师的准确性和一致性提升最多。

结论：我们的研究首次表明，AI 算法辅助判读可以显著提高 HER2 ^{0} 和 $^{1+}$判读的准确性和一致性，以及其在提升异质性病例判读的准确性上也有很好的性能。

关键字：乳腺癌；HER2 低表达；人工智能

636. 使用全幻灯片图像自动评估提高 Ki67 评分的一致性及预后分析

蔡丽静*、刘月平

河北医科大学第四医院

背景：2020 年 12 月，IKWG 发布了 Ki67 共识更新，从而提高 KI67 评估的一致性。在本研究中，我们开发了一种使用全幻灯片图像自动评估（WSI-AA，图 1）的方法来提高 KI67 评分的一致性和准确性，并分析 WSI-AA 评分的预后意义以及与其他临床病理特征的相关性。

方法：在前期研究中，我们开发了一种人工智能（AI）显微镜，即传统显微镜配备了 Ki67 评分人工智能算法。分析 2021 版 Ki67 共识评分软件算法（CSSA）应用程序与深度学习算法（DLA）的一致性，然后选择 150 例 Ki67 切片进行 DLA 验证，其中 50 例用于一致性分析，其余 100 例用于预后预测。选择 5 名病理医生对 50 例浸润性乳腺癌 Ki67 切片进行三轮研究，在第一轮研究（RS1）中，病理医生在常规显微镜下进行视觉评估（VA）；第二轮（RS2），计数评估（CA）；第三轮（RS3），辅助 AI 显微镜（AAM）（图 2）。然后根据 2021 版共识评估要求开发了 WSI-AA，并进行预后分析。

结果：CSSA 和 DLA 的 ICC 为 0.982（95%IC：0.954，0.993），与预期结果一致，并且不同病理医生 VA 的 ICC 为 0.960（95% IC：0.926、0.982)，CA 的 ICC 为 0.956（95% IC：0.919, 0.981）。其次，RS1 结果显示，VA 的 ICC 为 0.790（95% IC：0.693，0.865）；RS2，CA 的 ICC 为 0.914（95% IC：0.869，0.947）；RS3，AAM 的 ICC 为 0.950（ 95% IC: 0.922, 0.970)。最后，我们根据中位数原则将 WSI-AA 评分切点定义为 10%、18%和 38%，将 KI67 分为低、中、高表达，Kaplan Meier 生存曲线表明，Ki67 表达类别(低、中、高)分别与较差的无疾病生存期（disease free survival，DFS）显着相关(P=0.017)（图 3）；Ki67 表达类别与其他临床病理特征的相关性表明，Ki67 表达类别与较高的组织学分级、淋巴血管侵犯（Lymphovascular invasion，LVI）和神经侵犯（nerve invasion，NI)有统计学意义。

结论：结合 2021 版 Ki67 共识评分要求，AI-显微镜和 WSI-AA 可以帮助病理医生获得更高的 Ki67 评估一致性和准确性。此外，WSI-AA 评分与 DFS 具有显着相关性。

关键字：乳腺癌，AI-显微镜，WSI-AA,一致性分析

637. 基于 WSI 图像的人工智能模型提高三阴性乳腺癌 PD-L1 CPS 的精准判读

李金泽*、王心然、刘月平

河北医科大学第四医院/河北省肿瘤医院

目的：三阴性乳腺癌（Triple-negative breast cancer，TNBC）因具有较高的侵袭性，且预后不良而越来越受到关注。随着免疫疗法在 TNBC 中的应用，评估 PD-L1（DAKO 22C3）联合阳性评分（Combined positive score，CPS）的一致性和准确性越来越重要，但是病理医师在对其判读时存在很大的变异性，因此需要建立一种客观有效、简便易重复且准确的评分方法，为临床精准筛选 TNBC 免疫治疗患者奠定基础。

方法：本研究建立了一个能够对全切片图像（Whole slide images，WSIs）进行机器深度学习的人工智能（Artificial intelligence，AI）模型，采用区域分割和细胞检测算法对 PD-L1 CPS 进行判读。同时为了使 AI 模型达最佳性能，本研究独创了 H&E 联合 PD-L1（DAKO 22C3）序贯交替退色染色的方法对模型进行训练。本研究共进行了三轮环状判读研究（Ring study，RS），由 12 名不同级别的病理医师通过视觉评估和 AI 辅助判读对 TNBC 患者以连续性评分进行 PD-L1 CPS 的评估，最后比较判读结果的差异性、一致性和准确性。应用 SPSS 26.0 及 GraphPad Prism 8.0.1 进行统计学分析。Shapiro-Wilk（S-W）方法进行正态性检验，采用 Friedman M 及 Bonferroni 校正检验进行差异性分析，一致性分析采用组内相关系数（Intraclass correlation coefficient，ICC）进行研究。

结果：1. 在视觉评估中，所有病理医师 PD-L1 判读结果均不服从正态分布（P<0.05），不同级别病理医师对 PD-L1（DAKO 22C3）CPS 判读结果之间存在明显差异（P<0.05），而经过 AI 辅助判读，所有病理医师判读结果之间无明显差异（P= 0.473），判读结果的一致性得到提升。2. 一致性分析 1）在 RS1 和 RS2 视觉评估中，所有病理医师判读结果的一致性较弱，最低的一致性 ICC 值为 0.581（95%CI：0.479-0.690），在 AI 模型的辅助下，ICC 值提高至 0.883（95%CI：0.836-0.922），提高了判读结果的一致性和可重复性，其中中级病理医师提升的最明显。2）视觉评估中所有病理医师判读结果的内部一致性较弱，前后判读的可重复性较弱，其中初级医师组判读 PD-L1 的可重复性最差，ICC 值为 0.664（95%CI：0.564-0.762）。通过 AI 辅助评估后，高级病理医师判读结果内部一致性最高。3. 在 RS3 中，

所有病理医师判读结果的准确性提升近 30%，其中中级病理医师表现最优。同时初级病理医师对 AI 结果的接受程度较高，并且 80%以上的 AI 结果被普遍接受。

结论：在基于 WSI 图像的 AI 辅助诊断模型的帮助下，不同级别的病理医师对 TNBC 患者 PD-L1 CPS 评分之间达到了良好的一致性和准确性，判读水平有大幅提升，人工智能模型为病理学家在临床实践中进行 PD-L1 评分提供了一种提高一致性和准确性的良好方法，并对中级和初级医师更有帮助。

关键字：三阴性乳腺癌，PD-L1，人工智能，联合阳性评分，一致性

638. TAE 序贯奥沙利铂+雷替曲塞联合安罗替尼二线治疗中晚期原发性肝癌的临床研究

韩朝稳*、梁秀群、沈永奇、李凯旋、康中强、何沙

柳州市柳铁中心医院

目的：观察 TAE 序贯奥沙利铂+雷替曲塞联合安罗替尼治疗中晚期原发性肝癌（PLC）的疗效及毒性反应。

方法：2019 年 1 月～2020 年 06 月来自 4 个肿瘤中心的一线治疗后复发、进展的中晚期 PLC 患者 81 例，根据患者及家属的意愿，分为治疗组（采用 TAE 序贯安罗替尼联合奥沙利铂+雷替曲塞治疗进行治疗，40 例）和对照组（采用对症支持治疗的方法进行治疗，41 例）。

结果：观察组 40 例患者中，完全缓解（CR）1 例（2.5%），部分缓解（PR） 13 例（32.5%），稳定（SD）19 例(47.5%)，进展（PD）7 例（17.5%），客观缓解率（ORR）为 35.0%，疾病控制率（DCR）为 82.5%，中位总生存期（mOS）为 18.2 个月，中位无疾病进展期（mPFS）为 8.6 个月，1 年存活率（SR）为 52.5%。I-IV度副反应主要表现为消化道反应（40%）、骨髓抑制（67.5%）、肝毒性（27.5%）、周围神经毒性（25.0%）、高血压（22.5%）、声音嘶哑（35.0%）、皮肤反应（52.5%）和发热（20%），III-IV度毒副反应分别为消化道反应（2.5%）、骨髓抑制（27.5%）、发热（2.5%），经积极处理均可缓解。对症支持治疗组 41 例中，CR 0 例、PR 0 例，SD 11 例（26.8%），PD 30 例（73.2%），ORR 为 0，DCR 为 26.8%，mOS 为 4.6 个月, mPFS 为 1.8 个月，1 年 SR 为 0。两组相比 ORR、DCR、mPFS、mOS 和 1 年存活率，P 值均小于 0.05。

结论：TAE 序贯安罗替尼联合奥沙利铂+雷替曲塞治疗中晚期原发性肝癌安全有效，患者有临床获益，副反应可耐受，患者依从性良好。

关键字：原发性肝癌；奥沙利铂；雷替曲塞；TAE；安罗替尼

639. 微小膜壳绦虫感染对 ICR 小鼠小肠干细胞相关基因 mRNA 表达的影响

杨汉蕾*

上海市胸科医院

目的：探讨微小膜壳绦虫（*H.nana*）感染对美国癌症研究所（ICR）小鼠小肠中干细胞相关基因信使核糖核酸（mRNA）表达的影响。

材料和方法：取野生小鼠小肠内获取的 *H.nana* 虫体于显微镜下观察其形态，同时利用保守引物，采用聚合酶链式反应（PCR）技术扩增细胞色素 C 氧化酶亚基 I 基因（*COX*1）部分序列（*PCOX*1），并与 GeneBank 中记录的 *H.nana* 的 *COX*1 参考株核苷酸序列进行同源性比对分析；60 只 ICR 雌鼠随机均分为实验组（灌胃 *H.nana* 虫卵 500 个）和对照组（灌胃等量生理盐水），灌胃处理后 1~10 天分别取 2 组小鼠距离回盲部 6~8cm 处小肠肠段，观察 2 组小鼠小肠组织内虫体检获情况，采用实时荧光定量 PCR（qRT-PCR）技术检测 2 组小鼠小肠组织内 G 蛋白偶联受体 5 基因（*Lgr*5）、多梳复合蛋白基因（*Bmi*1）、武藏 RNA 结合蛋白基因（*Msi*1）及淋巴细胞抗原 6 复合物基因（*Ly6a*）的 mRNA 相对表达量。

结果：野生小鼠体内获取的虫体符合 *H.nana* 的形态学特征，*PCOX*1 基因与 GeneBank 中记录的 *H.nana* 的 *COX*1 参考株核苷酸序列同源性为 99%；qRT-PCR 结果显示 *H.nana* 发育的似囊尾蚴阶段 *Lgr*5 和 *Bmi*1 表达上调（$p<0.05$）、*Ly6a* 表达下调（$p<0.05$），成虫阶段 *Lgr*5 和 *Bmi*1 表达下调（$p<0.05$）、*Ly6a* 上调（$p<0.05$），*Msi*1 在虫体发育的似囊尾蚴阶段和成虫阶段表达均下调（$p<0.05$）。

结论：*H.nana* 感染可明显影响 ICR 小鼠 *Lgr*5、*Bmi*1、*Msi*1 及 *Ly6a* 基因的 mRNA 水平，基因表达差异主要分 2 个阶段，分别对应 *H.nana* 虫体发育的似囊尾蚴阶段和成虫阶段。

关键字：微小膜壳绦虫；小鼠；小肠；干细胞标志物；信使核糖核酸；实时荧光定量聚合酶链式反应

640. DUOX1 基因在鼻咽癌中转录失活的研究

张海山*

广西医科大学

目的：探索 DUOX1 基因在鼻咽癌（NPC）中 mRNA 转录和蛋白表达情况，分析其在 NPC 中转录失活可能的分子机制，评价 DUOX1 基因作为 NPC 诊断标志物的价值。

方法：利用 GEO 数据库进行 Meta 分析，比较 DUOX1 基因在 NPC 和正常鼻咽上皮（NNE）中 mRNA 转录水平的差异；通过 HPA 网站预测 DUOX1 基因在 NPC 中的蛋白表达情况；分别使用实时荧光定量 PCR 和免疫组织化学染色法对生信分析结果进行验证。EMBOSS 网站预测 DUOX1 基因 DNA 启动子区 CpG 岛含量；亚硫酸氢盐测序比较 NPC 组织和 NNE 组织 DNA 启动子区 CpG 位点的甲基化率；甲基转移酶抑制剂 5-aza-dC 处理 NPC 细胞株后检测 DUOX1 基因 mRNA 转录恢复情况。

结果：NPC 中 DUOX1 基因 mRNA 转录和蛋白表达水平均下调（$P<0.05$）；NPC 组织 DNA 启动子区甲基化程度高于 NNE 组织；5-aza-dC 处理过的 NPC 细胞株 DUOX1 基因 mRNA 转录水平得以恢复（$P<0.05$）。

结论：DUOX1 基因由于 DNA 启动子区甲基化在 NPC 中 mRNA 转录和蛋白表达失活，可作为 NPC 潜在的诊断标志物和治疗靶点。

关键字: DUOX1；鼻咽癌；DNA 甲基化；诊断标志物

641. 新型快速高通量融合检测技术的开发与验证

孙瑞[1,2]、王志中[1,2]、刘红霞[1,2]、马杰*[1,2]

1. 郑州大学附属肿瘤医院，河南省肿瘤医院分子病理科

2. 河南省分子病理学重点实验室

研究目的: 基因融合是肿瘤中一类重要的变异类型，它在辅助诊断、靶向治疗等方面有很重要的应用价值。在 RNA 水平检测融合具有更高的检出率，可以避免在 DNA 水平检测造成的假阴性结果。目前多种分子检测技术应用在基因融合的检测上，但大多数是在 DNA 水平进行检测的，主要的影响因素是 RNA 的不稳定性。另外，目前的一些在 RNA 水平上检测融合的技术往往还存在一定的问题，比如检测通量低或者检测周期过长。鉴于目前的临床应

用问题，我们设计了一种新型高通量融合检测技术，涉及的癌种主要为应用较为明确的肺癌以及软组织肿瘤，并对该项技术进行了性能验证。

材料与方法：该技术是在一种新型融合检测平台 NanoString 上进行设计的。中文又称荧光条形码技术，是可以在 RNA 水平上检测融合的一种检测方法。我们首先基于不同数据库筛选肺癌和软组织肿瘤相关融合断点以及用作质控和标准化的管家基因，然后采用 element 方法对融合断点以及管家基因进行探针设计。收集已进行过 NGS 检测（利用 NMPA 获批试剂盒）的 39 例肺癌样本（33 例融合阳性、6 例融合阴性）和已进行过 FISH 检测的 30 例软组织肿瘤样本（19 例融合阳性、11 例融合阴性）。自主搭建分析流程进行数据分析，并将分析结果与历史检测结果进行比对，同时通过 ROC 曲线计算阳性阈值。

结果：最终设计形成涵盖肺癌相关的 40 个融合断点（20 个融合亚型）以及软组织肿瘤相关的 166 个融合断点（53 个融合亚型）的 panel。其中在 3 个基因（ALK、ROS1、RET）的好发断点处上下游分别设计 4 段探针，利用基因表达的不平衡来检测未知融合类型。对比标准检测方法该项检测技术的灵敏度可以达到 97.1%，特异性可以达到 100%。不同融合的阳性阈值有一定差异，其中因为 ROS1 不平衡的检测受到本底高表达的影响，导致检测结果: 更加依赖于融合探针。该项检测已在临床中进行了应用。截至目前已检测 213 例，其中肺癌患者检测的阳性率达到 4.7%。在常规 FFPE 样本中检测的合格率达到 98.9%。

结论：目前临床应用中检测融合的方法有很多，但各有弊端。临床中急需一种既快速又高通量的检测方法。该项技术不需要逆转录和扩增，周期仅为两天，大大缩短临床检测周期。探针的设计最大可以扩充至几百个，最大限度满足临床需求。该技术对比金标准方法有非常高的准确性，说明其检测结果的可靠性。另外，该项技术对样本的兼容性较高，可以避免由于样本不足或完整度低带来的无法检测的后果。总之，这是一项可靠的快速高通量融合检测技术。

关键字：基因融合，高通量检测技术，RNA 水平

642. hnRNPM 细胞核亚定位调控可变剪接及肿瘤转移

郭佳维、李科、明月、潘怡潼、刘文荣、沈舒、徐富澔、刘宇、程健、王瑾、王成弟、戴伦治、李为民、彭勇*

Sichuan University

研究目的：可变剪接异常调控与肿瘤发生发展相关，剪接因子 hnRNPM 的异常激活促进上皮-间充质转化（EMT）和肿瘤转移，但 hnRNPM 本身尚无有效干预手段，且其上游调控机制仍不清楚。我们前期研究发现 hnRNPM 的细胞核亚定位改变与包括乳腺癌和肠癌在内的临床肿瘤转移密切相关，提示其亚定位改变可能作为 hnRNPM 失调的关键环节参与肿瘤转移。为此，本研究将揭示 hnRNPM 细胞核亚定位的精细调控机制，并初步探讨其相关的诊疗前景。

材料方法：通过可变剪接分析筛选参与肿瘤转移过程的关键剪接因子 hnRNPM；通过免疫组化精细分析大样本肿瘤组织中 hnRNPM 的细胞核亚定位情况；通过 RNA 免疫共沉淀偶联建库测序筛选出 EMT 过程中，与 hnRNPM 结合显著削弱的环状 RNA 分子 MASCOT；在多种细胞、动物模型上验证 MASCOT 在 EMT 及肿瘤转移中的生物学功能；利用生信预测结合 RNA pull-down/RNA EMSA 实验解析 MASCOT 与 hnRNPM 互作的关键序列，并构建 MASCOT 突变体干预其与 hnRNPM 的分子互作；利用共聚焦实验检测不同 MASCOT 突变体对 hnRNPM 定位及其下游可变剪接事件的调控作用；通过体内回补 MASCOT 探究其对在体肿瘤转移的治疗作用；通过 RNA 原位杂交结合免疫荧光实验在转移肿瘤样本中验证 MASCOT-hnRNPM 的临床相关性。

结果：1.发现 hnRNPM 的核斑定位与肿瘤转移呈显著正相关；2.发现 hnRNPM 作为关键剪接因子促进 EMT 相关的可变剪接重编程；3.MASCOT 与 hnRNPM 的结合在 EMT 过程中明显减弱；4.MASCOT 显著抑制肿瘤转移；5.鉴定出 MASCOT 序列内两段富含 GU 的序列负责其与 hnRNPM 的直接结合；6.MASCOT 作为支架分子结合 hnRNPM 与核仁骨架蛋白 NCL；7.核基质中，MASCOT 通过竞争性结合 hnRNPM C-端结构域阻止 hnRNPM 被 U2 剪接体招募；8.核仁中，MASCOT 通过锚定 hnRNPM 于核仁蛋白 NCL，在时空上阻止 hnRNPM 参与核斑中剪接体组装；9.体内重建 MASCOT 表达显著抑制肿瘤的在体转移过程；10.在肿瘤样本中，MASCOT 高表达与 hnRNPM 核斑定位呈现显著负相；11.MASCOT 高表达与肺癌淋巴结转移倾向和不良预后呈现负相关。

结论：MASCOT 作为内源性抑制分子调控 hnRNPM 在细胞核内的精细亚定位，阻止 hnRNPM 激活下游的可变剪接事件，从而抑制 EMT 及肿瘤转移过程。这表明 MASCOT 可作为潜在靶点用于开发监测临床肿瘤转移的关键标志物和 RNA 药物。

关键字：肿瘤转移；可变剪接；hnRNPM；环状 RNA

643. 灌洗液样本可作为基因检测的有效来源

张成娟[1]、吴新新[2,3]、吴敏清[1]、常玉喜[2,3]、魏冰[2,3]、马杰*[2,3]

1. 郑州大学附属肿瘤医院，河南省肿瘤医院生物样本中心

2. 郑州大学附属肿瘤医院，河南省肿瘤医院分子病理科

3. 河南省分子病理学重点实验室

研究目的：基因融合是肿瘤中一类重要的变异类型，它在辅助诊断、靶向治疗等方面有很重要的应用价值。在 RNA 水平检测融合具有更高的检出率，可以避免在 DNA 水平检测造成的假阴性结果。目前多种分子检测技术应用在基因融合的检测上，但大多数是在 DNA 水平进行检测的，主要的影响因素是 RNA 的不稳定性。另外，目前的一些在 RNA 水平上检测融合的技术往往还存在一定的问题，比如检测通量低或者检测周期过长。鉴于目前的临床应用问题，我们设计了一种新型高通量融合检测技术，涉及的癌种主要为应用较为明确的肺癌以及软组织肿瘤，并对该项技术进行了性能验证。

材料与方法：该技术是在一种新型融合检测平台 NanoString 上进行设计的。中文又称荧光条形码技术，是可以在 RNA 水平上检测融合的一种检测方法。我们首先基于不同数据库筛选肺癌和软组织肿瘤相关融合断点以及用作质控和标准化的管家基因，然后采用 element 方法对融合断点以及管家基因进行探针设计。收集已进行过 NGS 检测（利用 NMPA 获批试剂盒）的 39 例肺癌样本（33 例融合阳性、6 例融合阴性）和已进行过 FISH 检测的 30 例软组织肿瘤样本（19 例融合阳性、11 例融合阴性）。自主搭建分析流程进行数据分析，并将分析结果与历史检测结果进行比对，同时通过 ROC 曲线计算阳性阈值。

结果：最终设计形成涵盖肺癌相关的 40 个融合断点（20 个融合亚型）以及软组织肿瘤相关的 166 个融合断点（53 个融合亚型）的 panel。其中在 3 个基因（ALK、ROS1、RET）的好发断点处上下游分别设计 4 段探针，利用基因表达的不平衡来检测未知融合类型。对比标准检测方法该项检测技术的灵敏度可以达到 97.1%，特异性可以达到 100%。不同融合的阳性

阈值有一定差异，其中因为 ROS1 不平衡的检测受到本底高表达的影响，导致检测结果更加依赖于融合探针。该项检测已在临床中进行了应用。截至目前已检测 213 例，其中肺癌患者检测的阳性率达到 4.7%。在常规 FFPE 样本中检测的合格率达到 98.9%。

结论：目前临床应用中检测融合的方法有很多，但各有弊端。临床中急需一种既快速又高通量的检测方法。该项技术不需要逆转录和扩增，周期仅为两天，大大缩短临床检测周期。探针的设计最大可以扩充至几百个，最大限度满足临床需求。该技术对比金标准方法有非常高的准确性，说明其检测结果的可靠性。另外，该项技术对样本的兼容性较高，可以避免由于样本不足或完整度低带来的无法检测的后果。总之，这是一项可靠的快速高通量融合检测技术。

关键字：基因融合，高通量检测技术，RNA 水平

644. miR-19a-3p/CDS1/脂滴/NF-κB 信号通路轴对鼻咽癌炎症反应的影响

周晓莹*、王怡方

广西医科大学

背景：脂肪代谢紊乱是肿瘤细胞代谢重编程的标志之一。作为细胞脂肪代谢的重要细胞器，脂滴（lipid droplets, LDs）已被认为是细胞新陈代谢的主要调节者，参与包括信号转导、膜运输、脂质和蛋白质代谢等生物过程的调节。我们在前期研究中发现鼻咽癌细胞存在 LDs 储存现象，抑制 LDs 分解可以显著增强细胞的迁移能力，而 LDs 合成的调控机制在鼻咽癌中尚未见报道。研究表明，胞苷二磷酸二酰基甘油合成酶 1（CDP-diacylglycerol synthase 1，CDS1）是调控 LDs 合成的关键分子，推测 CDS1 的失活可能是鼻咽癌 LDs 储存的一项重要机制。

方法：分别通过 RT-qPCR 和 IHC 方法检测 CDS1 基因在鼻咽癌细胞和组织中的转录和蛋白表达水平。利用 CCK-8 实验、裸鼠成瘤实验、划痕和侵袭实验评价 CDS1 对鼻咽癌细胞增殖和转移能力的影响。通过共聚焦显微镜、流式细胞术和甘油三酯测试剂盒等评价细胞内 LDs 储存含量。利用 RNA 测序分析过表达 CDS1 对鼻咽癌细胞转录谱的调控，并以 RT-qPCR、Western blot 和 ELISA 分别验证测序结果。

结果：我们发现 CDS1 在鼻咽癌细胞和组织中表达显著下调。进一步探究发现，过表达 CDS1 的鼻咽癌细胞中 LDs 堆积显著减少，证实 CDS1 参与调控细胞的脂滴合成代谢。此外，CDS1 显著抑制鼻咽癌细胞的体外增殖能力、转移能力以及体内成瘤能力。利用油酸 OA 处理过表达 CDS1 的鼻咽癌细胞以达到外源性补充细胞脂滴的目的，发现 OA 处理可以逆转 CDS1 对鼻咽癌细胞增殖和侵袭的抑制作用，这提示 CDS1 发挥抑制鼻咽癌增殖和转移的能力可能依赖于细胞内 LDs 储存减少。进一步探索其分子机制，RNA 测序数据提示 LDs 堆积减少激活 TNF-α/NF-κB 信号通路，及其下游炎症因子 IL-6、IL-8、CXCL2 和 IL-1α的转录。我们证实过表达 CDS1 诱导鼻咽癌细胞发生 NF-κB（p65）核转运，激活上述炎症因子的转录表达，增加 IL-6 和 IL-8 的胞外分泌。这些数据说明，CDS1 可能通过 LDs 调控了鼻咽癌的炎症反应。最后，通过生物信息学预测软件发现 miR-19a-3p 与 CDS1 的 3'UTR 具有潜在结合位点。双萤光素酶实验结果提示，miR-19a-3p 与 CDS1 形成良好结合，抑制 CDS1 的转录表达。miR-19a-3p mimic 能够显著抑制 CDS1 的表达水平，并且提高鼻咽癌细胞的 LDs 含量。

结论：miR-19a-3p 靶向下调鼻咽癌中 CDS1 的表达。CDS1 通过抑制鼻咽癌细胞 LDs 储存，从而激活 NF-κB 信号通路以及下游炎症因子的转录表达，发挥肿瘤抑制基因的作用。

关键字：鼻咽癌；CDS1；脂滴储存；NF-κB 信号通路；miR-19a-3p

645. 自主神经在口腔黏膜癌变及防治中的作用

陈倩 [1,2]、江涵 [1,3]、神应强*[1]

1. 四川大学华西口腔医院

2. 浙江大学医学院附属口腔医院

3. 苏州科技城医院

口腔鳞癌患者的 5 年生存率为 50～60%左右，多年未有提高，严重威胁患者的健康和生命。明确口腔黏膜癌变机制，对阻断或逆转口腔黏膜癌变具有重要意义。研究表明肿瘤微环境中的神经组分在肿瘤发生发展中发挥了重要作用，但自主神经在口腔黏膜癌变中的作用及防治意义尚需探明。我们通过分析口腔白斑病及口腔鳞癌患者组织的病损微环境，同时利用 4NQO 诱导的小鼠口腔黏膜癌变模型及异种移植瘤模型，结合体外实验发现：自主神经是口腔黏膜癌前病损口腔白斑病及口腔鳞癌微环境中的重要组分；β和 m 受体基因在多种口腔鳞癌细胞系中高表达且 chrm3 的高表达与不良预后相关；交感神经化学阻断剂或β受体抑制剂

奈必洛尔可抑制小鼠口腔黏膜癌变；奈必洛尔可通过诱导蛋白质亚硝基化激活内质网应激及诱导线粒体功能异常来抑制口腔鳞癌细胞的增殖；m 受体激动剂卡巴胆碱可激活 YAP 信号通路促进口腔鳞癌细胞的增殖和侵袭。基于上述发现，我们得出结论：自主神经通过分泌神经递质促进了口腔黏膜癌变，阻断自主神经或相应神经递质受体能够阻断口腔黏膜癌变进程。我们的研究提出了口腔黏膜癌变的新机制，同时为阻断口腔黏膜癌变提供了新的靶点。

关键字：口腔黏膜癌变；自主神经；神经递质；奈必洛尔；卡巴胆碱；β受体；m 受体

646. 羰基化合物：一类新型肺癌诊断标志物

张沫[1]、赖治臻[1]、张仁俊[1]、刘帅[1]、田洪涛[1]、李丹[1]、周江[2]、李智立*[1]

1. 中国医学科学院基础医学研究所

2. 北京大学化学与分子工程学院

脂肪醛和脂肪酮类羰基化合物在人类生理和病理学中起着重要作用，与多种疾病密切相关。目前对羰基化合物的定量分析仍面临诸多挑战。本研究利用捕获能力超过 1200 μmol/g 的酰肼修饰磁微粒实现羰基化合物化学选择性捕获分离。利用质谱技术实现高通量和高覆盖的快速定量分析，共在人类血清中定性定量了 1500 多种羰基代谢物。进而研究了 113 例血清样本，其中包括 40 例健康人群、36 例肺部良性患者和 37 例肺癌患者。研究结果表明，六种羰基代谢标志物的组合能够区分健康与肺部疾病患者，受试者曲线下面积(AUC)优于 0.9。五种羰基代谢标志物的组合能够区分肺良性疾病和肺癌，AUC 优于 0.9。

关键字：羰基化合物，肺癌，肿瘤标志物，质谱

647. HIGD1A 的表观遗传失活促进肾透明细胞癌转移的研究

赵军*

广西医科大学

背景：肾透明细胞癌（Kidney renal clear cell carcinoma, KIRC）具有死亡率高、预后差、无并发症转移和缺乏有效治疗靶点等特点。HIG1 缺氧诱导结构域家族成员 1A（HIG1 hypoxia inducible domain family member 1A，HIGD1A）参与线粒体功能的维持，并在多种癌症发展

中起着重要的作用。然而，HIGD1A 在 KIRC 中的作用仍不清楚。因此，本研究了探讨了 HIGD1A 在 KIRC 中的转录失活机制及其抑癌机理。

方法：利用 GEO 数据库比较 KIRC 及正常对照组织中 HIGD1A mRNA 表达水平差异。基于 TCGA 数据库中收录数据研究了 KIRC 中 HIGD1A 的 mRNA 表达与患者临床病理指标的相关程度和生存时间的关联,并分析 HIGD1A mRNA 表达水平作为 KIRC 的诊断效能。RT-qPCR 检测 HIGD1A 在 KIRC 组织及细胞系中转录水平，免疫组化染色和 Western Blot 印迹检测 KIRC 组织、非肿瘤组织和 KIRC 细胞系中的蛋白表达。UALCAN 网站用于比较 KIRC 和正常组织中 HIGD1A 启动子区的甲基化水平，并对 KIRC 细胞进行 5-aza-dC 去甲基化处理。构建过表达 HIGD1A 的细胞株，利用 CCK8、侵袭、划痕验证 HIGD1A 对 KIRC 细胞恶性生物学行为的影响。GSEA 富集分析 HIGD1A 在 KIRC 中可能的调控通路。利用 TCGA 数据库进行 HIGD1A 与主要通路分子标志物之间的相关性分析，并用 RT-qPCR 对结果进行验证。

结果：HIGD1A 在 KIRC 中表达水平显著下调，且其低表达与 KIRC 的肿瘤分期及远处和病理分期呈负相关。生存分析显示 HIGD1A 低表达与 KIRC 患者不良预后有关，提示 HIGD1A 是 KIRC 潜在的预后分子生物标志物。分别基于 TCGA 数据库、RT-qPCR 结果和免疫组化评分绘制 ROC 曲线，发现曲线下面积(AUC）分别为 0.928、0.956 和 0.904(P <0.001）。KIRC 中 HIGD1A 启动子区的高甲基化水平与其表达呈负相关，且经 5-aza-dC 处理后，KIRC 细胞系中的 HIGD1A mRNA 表达恢复（p<0.05）。过表达 HIGD1A 以后发现能抑制肾透明细胞癌细胞的侵袭与迁移能力，对增殖无明显影响。此外，GSEA 富集发现 KIRC 中 HIGD1A 主要可能参与缺氧与 EMT 通路调节。过表达 HIGD1A 后 RT-qPCR 结果显示 HIGD1A mRNA 表达与 EMT 通路中上皮标志物 CDH1 和 EpCAM 表达正相关，与间充质标志物 VIM 和 SPARC 表达负相关。

结论：我们的实验结果说明 HIGD1A 由于启动子区高甲基化导致在 KIRC 中表达下调，并且通过 EMT 通路调控 KIRC 的转移，是 KIRC 有效地诊断和预后分子标志物，可能是 KIRC 潜在的治疗靶点，能够为临床治疗提供新的参考依据。

关键字：肾透明细胞癌；HIGD1A；DNA 甲基化；EMT；分子标志物

648. 泛癌的蛋白糖基化修饰标志物研究

赖治臻[1]、王志刚[1]、张继匀[1]、袁钟浩[1]、李丹[1]、徐雅莉[3]、张丹[1]、李娜[1]、周江[2]、李智立*[1]

1. 中国医学科学院基础医学研究所

2. 北京大学化学与分子工程学院

3. 中国医学科学院北京协和医院

癌症已成为威胁人类健康的重要死因，2020 年已有 1930 万新癌症病例和近 1000 万患者因癌症死亡。触珠蛋白在免疫和炎症反应方面起着重要作用，其糖基化修饰的变化与多种癌症有关。本研究共纳入了 9488 例，其中癌症 6025 例(包含 13 种癌症类型（食道癌、胃癌、肝癌、胰腺癌、结肠癌，直肠癌、肺癌、甲状腺癌、乳腺癌、子宫癌、卵巢癌、宫颈癌和前列腺癌）和 3463 例良性疾病患者，采用本研究团队研发的疾病特异蛋白质分离技术平台，获得疾病特异的触珠蛋白β链。应用聚苯胺纳米磁珠特异性地富集分离触珠蛋白β链完整 N-糖肽，采用 MALDI-MS 技术获得触珠蛋白β链 N184，N207/211 和 N241 位点上共 99 种完整 N-糖肽。利用机器学习分析方法，发现触珠蛋白β链完整 N-糖肽具有良好的区分癌症和良性疾病患者，其诊断精度为 0.721,灵敏度为 64.2%，特异度为 65.9%。

关键字：泛癌研究，触珠蛋白，N-糖基化，质谱，机器学习

649. PSMB1 在 II/III 期结直肠癌复发转移中的作用及其 机制研究

蒋雪飞、刘依婷、冯杏芝、高倩玲、杨兰兰、龙家慧、杨孜欢*

中山大学附属第六医院

背景：结直肠癌（Colorectal cancer，CRC）已成为我国第二高发的恶性肿瘤。其中局部进展期（II/III 期）的 CRC 患者接受标准治疗后有约 30%会发生复发转移，由于缺乏准确预测复发转移的生物标志物，临床干预措施仍十分有限，发生复发转移的 CRC 患者 5 年生存率仅约 13%。因此，寻找预测 II/III 期 CRC 患者复发转移的标志物，明确其调控机制，开发新的治疗靶点和疗法，是亟待解决的临床问题。

方法：对接受标准治疗的 II/III 期 CRC 患者的肿瘤组织进行蛋白组学质谱分析，分为 5 年无复发转移和 3 年内复发转移组，比较两组差异表达蛋白及结合文献确定目的基因 PSMB1。CRC 组织芯片分析病人预后情况；全基因组表达谱分析 PSMB1 调控的信号通路。表型和动物实验探究 PSMB1 在体内外对 CRC 细胞恶性能力的影响。蛋白质谱鉴定过表达 PSMB1 后显著富集的 RAB 蛋白家族，筛选出高表达与预后不良相关的 RAB34 蛋白。免疫共沉淀（CO-IP）和免疫印迹（WB）实验探究 PSMB1 和 RAB34 是否存在相互作用，以及 PSMB1 是否通过调控 RAB34 蛋白的表达来影响 ERK 通路的激活。

结果：PSMB1 在术后复发转移组中低表达，与 CRC 发生复发转移以及较差的预后相关；细胞实验证实，敲低 PSMB1 促进 CRC 细胞的恶性表型，过表达反之。动物实验表明，敲低 PSMB1 促进 CRC 细胞在体内的生长。PSMB1 通过与 RAB34 相互作用，促进 RAB34 被蛋白酶体识别和降解，从而抑制 ERK 信号通路的激活，进而影响 CRC 的复发转移过程。

结论：本研究揭示了 PSMB1 低表达与 II/III 期 CRC 术后复发转移显著相关；PSMB1 通过促进 RAB34 被蛋白酶体识别和降解，抑制 ERK 通路激活，从而抑制 CRC 的复发转移。PSMB1 可能作为 II/III 期 CRC 复发转移的潜在治疗靶点。

关键字：蛋白酶体；PSMB1；结直肠癌；复发转移

650. 跨人群研究肺癌筛查中特征的肠道微生物标志物及评估其诊断效能

韩文婕[1]、王娜[1]、韩梦真[1]、孙涛[2]、徐君南*[2]

1. 中国医科大学附属肿瘤医院

2. 辽宁省肿瘤医院

研究目的：肺癌在全球范围内的发病率和死亡率均在逐年上升，是对人群健康和生命威胁最大的恶性肿瘤之一。但肺癌的病因尚不明确，大部分患者在疾病晚期才获得初步确诊，导致患者的预后效果极差。所以癌症的早期筛查对于疾病的控制和改善预后均有重要意义，而精准的生物标志物是实现这一目标的关键之处。近年来许多研究揭示了肠道微生物组在疾病中的作用，然而对于肺癌之前的研究大都集中于肺部微生物，这种侵入性检查仅针对肺部有结节的患者展开研究，无法得知一般人群是否有早期癌变可能，所以我们想通过荟萃分析挖掘肺癌人群的标志性肠道差异微生物来开发一种便捷的、非侵入性的诊疗手段。

研究方法：我们采用 16s rRNA 基因扩增子测序分析来自 6 个地区的人群共 597 个粪便样本（肺癌组=323，健康对照组=274）。对这些患者肠道微生物组进行生物信息学分析，主要包括物种多样性分析，物种差异分析，微生物群的关联性和相关性分析和 CCA 分析等。然后我们利用物种注释结果构造机器学习模型，并评估模型的适用性及特异性，然后我们对模型进行内部交叉验证和外部验证评估其准确性和稳健性。最后我们根据 KEGG 和 COG 对差异菌群进行功能注释，寻找菌群可能参与的关键代谢通路。

研究结果：在不同的多样性指数中，肺癌组总是略低于健康对照组，其中以 Chao1 指数和 Shanno 指数最明显。PCOA 分析也显示两组的组成存在显著性差异（p=0.001）。结合 LeFse 检测结果，物种差异主要来源于变形菌门、普雷沃氏菌属、肠球菌属。然后，我们利用物种注释结果开发了诊断模型（AUC=0.80），并评估了其适用性和特异性，结果表明高 BMI 人群有更好的适用性，且哮喘和肺结核人群不会干扰肺癌的诊断。最后我们还对模型进行了内部交叉验证（AUC 值范围为 0.58-0.94）和外部验证（AUC=0.77），LODO 分析中的 AUC 值也升高（0.62-0.71），均表明此模型有良好的预测效能。此外我们还对肺癌人群的差异菌群进行功能预测,发现肺癌组的菌群所参与二级胆汁酸生物合成途径表达增强，亮氨酸，缬氨酸，异亮氨酸生物合成途径明显弱化。

结论：肺癌患者与健康人群的肠道菌群有显著性差异。通过构造模型筛选出 43 个核心标记生物可以很好地用于区分癌症和健康人群。这项工作证明了肺癌肠道特异性标志物在多人群中的有效性，可以为将来的非侵入性早期筛查研究或开发靶向治疗生物标志物提供线索。

关键字：肺癌，肠道菌群，机器学习，16s rRNA 测序，微生物标志物

651. 基于蛋白质糖基化修饰的肝癌诊断研究

张继匀[1]、赖治臻[1]、丁锐[3]、袁钟浩[1]、周巾煜[2]、李丹[2]、秦绪珍[3]、周江[4]、李智立*[2]

1. 中国医学科学院基础医学研究所/北京协和医学院基础学院

2. 中国医学科学院基础医学研究所

3. 中国医学科学院北京协和医院

4. 北京大学化学与分子工程学院

肝癌是最致命的恶性肿瘤之一，其发病率在全球范围内呈上升趋势。由于早期肝癌的临床症状不明显，其常在晚期被诊断且预后较差。大部分血清糖蛋白由肝脏合成，其糖基化修饰的

异常改变可以反映肝脏病理生理状态的变化。本研究旨在探索蛋白质糖基化修饰在肝癌早期诊断中的应用潜力。利用聚苯胺磁珠对 92 例良性肝病患者和 180 例肝癌患者（包含 123 例原发性肝癌患者和 57 例转移性肝癌患者）的血清中的完整糖肽进行分离，并采用质谱技术对糖肽进行定性和定量分析。共检测到 34 种完整糖肽，经统计分析发现糖肽可以很好地区分良性肝病患者和肝癌患者以及原发性肝癌患者和转移性肝癌患者，其诊断精度分别优于为 0.80 和 0.90。结果表明，蛋白质糖基化修饰可作为肝癌诊断的潜在标志物。

关键字：蛋白质糖基化修饰；肝癌；标志物

652. 循环肿瘤细胞异倍体检测在鼻咽癌患者治疗和 预后中的临床意义

汪玉兰[1,2]、程进[2]、黄倩*[2]

1. 上海市胸科医院

2. 上海市第一人民医院

探讨：鼻咽癌(NPC) 患者外周血循环肿瘤细胞(CTC) 变化与治疗效果和预后的关系。

方法：回顾性分析在本院接受同步放化疗的 35 例 NPC 者，采用两两配对样本的非参数检验法分析患者治疗前后的 CTC 数目差异。根据细胞形态大小将 CTC 分为大细胞 CTC 和小细胞 CTC，根据 8 号染色体数目分为三倍体、四倍体和多倍体（五倍体及以上）三类，比较患者治疗前后大小细胞差异与患者疗效的关系。以无进展生存期为预后评价指标，采用 Kaplan-Meier 法分析患者治疗前后 CTC 差值与预后的关系。

结果：NPC 患者治疗前后 CTC 变化与年龄、性别、TNM 分期、WHO 分型、外周血 EB 病毒抗体和转移情况无关(P>0. 05) 。在部分缓解患者中，同步放化疗后 CTC 水平有所下降，特别是三倍体和四倍体的小细胞 CTC 下降明显(P<0. 05) 。治疗前后三倍体 CTC 差值与预后相关且差异有统计学意义(P<0. 05) 。

结论：NPC 患者外周血 CTC 亚型水平与患者疗效和预后相关，动态监测患者外周血 CTC 水平对于 NPC 治疗指导和预后预测具有一定的临床意义。

关键字：鼻咽癌；循环肿瘤细胞；异倍体细胞；疗效评估

653. 原发性肺弥漫大 B 细胞淋巴瘤 1 例并文献复习

简亿、于少雨*、朱梅、包宇航、杨美、余枝娟、胡晓倩、路庚辛

遵义医科大学附属医院

目的：探讨原发性肺弥漫大 B 细胞淋巴瘤临床表现、诊断、鉴别诊断及治疗，提高临床医生对该病的认识。

方法：回顾性分析我院原发性肺弥漫大 B 细胞淋巴瘤 1 例临床特征并文献复习。

结果：65 岁男患 因“咳嗽、咳痰 20 天 ”于 2021 年 8 月 9 日就诊于我院。既往有高血压 3 年。入院行胸部 CT 提示左下肺中央型肺癌并阻塞性肺炎，纵膈及左肺门多发淋巴肿大，PET-CT 左肺门至左肺下叶高代谢结节，考虑左下肺中央型肺癌。初步诊断：左侧原发性支气管肺癌？并阻塞性肺炎。为进一步明确诊断行支气管镜检查隆突、左右主支气管和左下叶外侧基底段支气管改变，考虑恶性肿瘤，送检（隆突）支气管黏膜活检组织，纤维组织增生伴淋巴样异型细胞浸润，免疫组化：弥漫性大 B 细胞淋巴瘤，非生发中心来源， CK（-），P40（-），CD56（-），Syn（-），TTF1（-），LCA（+），CD20（+）CD3（-）CD5（-）Bcl-2（+）CD（-）Bcl-6（+）CD138（-）CD30（-）cyclinD1（-），SOX-11（-），P53（-），Ki-67（80%，+）。排除化疗禁忌后予以行 R-CHOP 方案化疗(利妥昔单抗 600mg d1、注射用环磷酰胺 1.2g d2、盐酸多柔比星脂质体注射液 40mg d2、注射用硫酸长春地辛 4mg d2、地塞米松磷酸钠注射液 10mg d1-d5)、化疗，同时予以制酸护胃、止吐、碱化尿液等治疗后症状好转出院，后继续予以上述化疗方案 6 个周期， 2022 年 3 月 25 日返院化疗时无呼吸道症状，复查胸部 CT 提示双肺少量纤维化，现规律随访中。

结论：原发于肺部的淋巴瘤较为少见，临床表现及影像学缺乏特异性，临床上容易漏诊及误诊，需要与肺癌、肺结核及肺部真菌病等鉴别，确诊主要依靠活组织检查获得病理学依据，治疗上根据临床表现、组织病理学类型、生物学特性等综合评估后可选择放疗、化疗、手术或综合治疗方案。

关键字：原发性肺淋巴瘤；诊断；治疗

654. 急性淋巴细胞白血病化疗中诱发肺结核活动 1 例

朱梅、包宇航、袁亚婷、黄敏、李小鹏、于少雨、杨美、简亿*

遵义医科大学附属医院

目的：结核病治疗诱发白血病临床少见，白血病使用免疫抑制剂及激素治疗时警惕结核活动，本文通过急性淋巴细胞白血病（ALL）化疗中诱发肺结核活动，总结该类疾病的临床特征，提高对该类疾病的认识。

方法：分析我院 ALL 化疗中诱发肺结核活动 1 例的临床特点。

结果：37 岁男患，因“胸痛 2 月，乏力、纳差伴头晕 1 月”于 2021 年 12 月 8 日就诊于我院。2 月前因胸痛于外院考虑“胸膜炎”予以 HRZE（异烟肼、利福平、吡嗪酰胺、乙胺丁醇）抗结核好转后出院，1 月后出现乏力、纳差伴头晕、头痛，停用抗结核药物，遂就诊于我院。既往史：10 年前诊断“肺结核”，以 HRZE 治疗 1 年后遵医嘱停药。（12 月 8 日）血常规：白细胞总数 2.43x10^9/L，血红蛋白 61.0g/L 血小板总数 29 x10^9/L。痰结核感染多次均阴性，（12 月 8 日）胸部 CT 双肺多发纤维化、钙化灶，为陈旧性肺结核，停用抗结核药物加用升白细胞药治疗 1 周后复查血常规：白细胞 1.0x10^9/L，原幼细胞 0.20，血红蛋白 61.0g/L，血小板 29 x 10^9/L。骨髓象：淋巴细胞异常增生，原幼稚淋巴细胞比例占 82%，考虑 ALL。骨髓流式：异常细胞群 BLast，占有核细胞 73.83%，普通-B-ALL，诊断为 ALL。患者一般情况差，第一个周期 VP 方案（长春新碱、强的松）化疗 1 周后换为 VDLP 方案（长春新碱、柔红霉素、培门冬酶、强的松）。第二周期时完善结核分枝杆菌核酸阳性，（2022 年 3 月 22 日）胸部 CT 双肺见多发结节状、斑点状及条索状高密度影。骨髓象原幼淋巴细胞占 43.9%。外周血见幼粒、幼红、泪滴红。予 VICLP 方案（长春新碱、伊达比星、环磷酰胺、培门冬酶）化疗同时 HRZE 方案抗结核。第三个周期 VDCLP 方案化疗(长春新碱、伊达比星、环磷酰胺、培门冬酶) ，复查骨髓象原幼淋巴细胞比例占 1.5%。第四个周期 MTX+PEG 方案化疗（甲氨蝶呤、多柔比星），第五个周期甲氨蝶呤+培门冬酶方案化疗。5 个周期结束后复查骨髓象及流式细胞学未见白血病细胞，达到完全缓解。随访至今症状好转。

结论：结核病治疗时易致白细胞减少，通常考虑药物副作用，忽视是否为白血病，停用抗结核药加用升白细胞药后白细胞计数仍低，临床医生需考虑是否为血液系统肿瘤，尽快完善结核相关病原学、骨髓象、骨髓活检等明确。肺结核使用免疫抑制剂及激素应评估预防性抗结核治疗，警惕结核病活动。

关键字：白血病；结核；化疗；完全缓解

655. 原位突变检测新策略及其在肿瘤精准治疗中的应用研究

汪慧聪、牛霞、郑直*

北京协和医学院

确定致癌突变已被证明是选择靶向肿瘤疗法的关键，在治疗前和治疗期间持续监测突变状态是非常必要的。现有的基于核酸提取的突变检测方法只能提供整个细胞群的平均信息，缺乏单个细胞的有意义的信息，包括肿瘤细胞的异质性以及具有特定突变的肿瘤细胞在整个细胞群中的比例，并且大量的野生背景容易造成漏检或者错失更多的基因信息。因此，为了准确评估肿瘤状态并指导患者治疗，以可接受的成本识别多种与药物相关的致癌基因突变及其丰度已成为迫切的临床需求，尚待在单细胞水平上实现。本研究拟开发一种基于原位检测的突变检测新策略，在 RNA 水平靶向突变位点进行原位 RCA 扩增，将突变信息转化为放大的荧光信号或化学信号，仅使用一组荧光探针或化学发光底物即可进行快速信号获取，能特异的识别较难检测的点突变。将该技术运用到循环肿瘤细胞(CTC)中，与差相富集结合免疫染色-荧光原位杂交技术(SE-iFISH)相结合，可同时对 CTC 进行综合表征、染色体核型分析与分子分型，多角度全方面地对 CTC 进行解析，以获得更加准确系统的信息。 本研究建立的原位检测突变的方法在人源 A549 细胞与鼠源 NIH-3T3 细胞的共培养体系中，用仅单碱基区别的 padlock 探针分别检测出不同荧光的人源和鼠源 ACTB mRNA 信号，表明该方法具备单碱基区分能力。在 293T 细胞中分别构建肾上腺皮质瘤的肿瘤驱动基因-KCNJ5 的野生型稳转株与 KCNJ5 G/C 突变型稳转株。用针对突变型的探针检测突变型稳转株中有信号，而在野生型稳转株中无信号。这说明我们已经成功研发了可用于检测外源基因突变的原位检测方法。基于该方法，用针对 EGFR T790M 突变的探针检测 T790M 突变型 H1975 细胞有信号而检测 T790M 野生型 A549 细胞无信号，这表明方法亦可特异性地检测内源突变 RNA。此外，在肿瘤组织样本、肺癌细胞混合外周血的 CTC 模拟样本中也证实了该突变检测方法的可行性。 因此，本研究初步建立了一种原位检测突变的新策略，避免了因核酸提取造成的大量野生背景的干扰，具有单碱基区分能力，能在原位特异的识别较难检测的点突变，可为组织切片中的突变检测提供突变在整个切片中的细胞比例信息与丰度信息。此外，对捕获的特定

CTC 进行突变及染色体异倍体同时检测，可多角度全方面地解析疾病信息，以在更早阶段动态监测肿瘤进展，为指导治疗提供更加可靠的基因信息。

关键字：驱动基因突变；原位检测；肿瘤精准治疗；循环肿瘤细胞

656. 氨基酸类代谢物：一类新型肺癌诊断标志物

田洪涛[1]、仇宇明[1]、赖治臻[1]、张沫[1]、刘帅[1]、张仁俊[1]、李丹[1]、周江[2]、李智立*[1]

1. 中国医学科学院基础医学研究所

2. 北京大学化学与分子工程学院

目前，肺癌是死亡率最高的癌症之一。肿瘤发生发展伴随着代谢重编程和代谢物表达水平变化。氨基类化合物是体内重要基础代谢物，是合成蛋白质主要原料。本研究采用一种新型氨基类亚代谢组定性定量方法，对 37 例肺部良性疾病患者、37 例肺癌患者以及 29 例健康对照血清中的氨基类代谢物进行定量和定性分析。研究结果表明，7 种氨基酸代谢物在对照组与肺癌、肺部良性疾病与肺癌和对照组与肺部良性疾病之间均存在显著差异。其中两种氨基酸的组合，在对照组与肺部性疾病之间的区分能力 AUC 优于 0.90；在肺部良性疾病与肺癌之间的区分能力 AUC 优于 0.95。

关键字：肺癌，氨基类代谢物，质谱分析，肿瘤标志物

657. 肿瘤干细胞来源外泌体分离鉴定及表达特征分析

产柳佳、王文敬*、王阳

首都医科大学附属北京佑安医院

目的: 3D 培养肿瘤干细胞微球，通过超速离心法分离提取肿瘤细胞外泌体，并鉴定表面蛋白表达（CD90、CD63、CD133、EpCAM、PD-L1）的表达。

方法：采用无血清低黏附 3D 培养体系培养 95D 肺癌细胞以及 HepG2 肝癌细胞微球，通过超速离心提取外泌体，透射电镜及激光纳米粒度仪测定其形态及尺寸特征，通过流式细胞术检测在 2D 培养和 3D 培养条件下提取的外泌体表面 CD90、CD63、CD133、EpCAM、PD-L1 的表达水平。

结果：透射电镜表征显示提取的外泌体具有典型的双层膜囊泡特征，尺寸在 50-170nm 之间。成像流式细胞仪检测显示外泌体 CD63 表达显著。3D 培养来源外泌体与 2D 培养来源外泌体相比其表面具有更高的干细胞标志蛋白（CD90、CD133、EpCAM）表达，且免检点蛋白 PD-L1 显著升高。

结论：成功地构建了 3D 肿瘤干细胞培养体系，并分离提取其来源外泌体，鉴定外泌体表面表达特征。结果提示肿瘤干细胞来源外泌体可能参与肿瘤耐药和免疫逃逸，是具有进一步研究价值的重要标志物。

关键字：外泌体；肿瘤干细胞；免疫检查点蛋白

658. 合并骨髓转移及弥散性血管内凝血的胃癌病人的临床病理特征及治疗

杜格、曹泰源、翟晓慧、练磊、杨祖立、肖健*

中山大学附属第六医院

研究目的：骨髓（BM）浸润是胃癌（GC）骨转移的一种特殊亚型，常并发弥散性血管内凝血（DIC）和其他血液系统疾病，构成严重临床综合征，最佳支持治疗效果欠佳。目前，只有关于这种特殊疾病的病例报告。该汇总分析旨在描述其详细的临床病理学特征和治疗结果。

方法：对 2000-2022 年在我院收治的病例进行系统审查。纳入标准为：胃食管交界处或胃部腺癌，骨髓浸润和 DIC 同时出现的病人。审查了详细的临床和病理数据。将治疗前胃癌、浸润和 DIC 同时出现的定义为同时性；将先出现胃癌，接受化疗或手术治疗后，同时发生骨髓浸润和 DIC 的定义为异时性类型。根据起病时是否接受化学药物治疗，将病人分为化疗组和最佳支持治疗组。利用 SPSS 进行描述性统计、卡方检验、Fisher 精确检验和生存分析。

结果：共纳入 58 例病人。 41（70.7%）是同时性转移病人，17 例（29.3%）为异时性转移。女性患者（32，55.2%）稍多于男性患者。中位年龄较正常 GC 相对年轻为 51 岁（28-76 岁）。ECOG PS 3-4 出现在 41 例 (70.7%) 病例中。 52 (89.6%) 为低分化腺癌。 Her-2 过度表达仅见于 4 例 (6.9%) 病例，且无 d-MMR。58 例患者中 51 例患者完善了 CKMB 检查，显示出显著的 CKMB 升高，这在以前的报告中没有提到。 LDH 和 ALP 水平异常分别见于 91.2%和 64.3%的病例。22 例（37.9%）病人血小板严重下降至低于 20×10^9/L。共有 32 名患

者接受了化疗治疗，26 名患者接受了最佳支持治疗，其中位 OS 分别为 151 天（6-598 天）和 14 天（2-61 天）（*P*<0.01)。 23 名 (71.8%) 化疗组患者在接受化疗后 DIC 得到改善。BSC 组没有病人达到 DIC 的改善，12 名患者重复发生 DIC，均伴随 CKMB 增高，且化疗后得到 DIC 改善。化疗药物中，5-氟尿嘧啶和多西他赛是应用最多的药物。

结论：CKMB 可能是合并骨髓转移及 DIC 类型的胃癌的一个独特标志物。积极的化疗可使合并骨髓转移及 DIC 的胃癌患者得到 DIC 的改善且显著提高其生存周期。

关键字：胃癌，骨髓转移，DIC，生存周期，化疗

659. 一种基于尿液 DNA 低深度全基因组甲基化测序的尿路上皮癌早期诊断和复发监测的新方法研究

史悦、王平、慈维敏*

中科院北京基因组所

研究目的：目前尿路上皮癌的临床诊断和复发监测主要通过侵入性的膀胱或输尿管镜结合病理活检。同时现有的无创诊断方法如尿脱落细胞学灵敏度偏低。虽然 FISH 灵敏度较高，但这些方法对低级别或小肿瘤的敏感性均较低，无法满足临床需求。因此，亟须找到一种新型、无创、低成本、准确度高的诊断及监测方法指导临床。我们前期建立了针对尿液 DNA 拷贝数及甲基化变异的不同模型用于诊断包括尿路上皮癌在内的泌尿系统肿瘤,相关成果已发表在 European Urology 和 Clinical Chemistry 上。我们拟在扩大规模的尿路上皮癌队列中进行 DNA 拷贝数联合甲基化变异模型的优化和验证,提升模型对低级别及小肿瘤的敏感性，及复发监测能效。最终开发出针低/高级别、早/晚期尿路上皮癌的高敏感性和特异性的尿液无创诊断技术。

材料与方法：我们共收集了 373 例患者尿液,包含尿路上皮癌病例共 199 例,非癌对照 174 例。基于 DNA 拷贝数和甲基化变异特征构建出了一个新的分类诊断整合模型 UCseek,并将其与目前临床常用的膀胱镜及 FISH 进行诊断效能的比较分析。另外我们还收集了 42 例膀胱癌复发患者尿液，对 UCseek 的复发监测能效进行了评估。

研究结果：我们发现新模型 UCseek 在独立验证集中具有高敏感性(92.7%)、高特异性(90.7%)和高准确性(91.7%)。同时该模型在低级别和 Ta/T1 肿瘤患者中的准确率分别为 91.8%和

94.3%。值得注意的是，UCseek 在超低测序深度(0.3X-0.5X)时仍可保持了良好性能。与膀胱镜检查相比，它在复发监测队列中也显示了强大诊断能效(90.91% *vs.* 59.09%)。

结论：我们基于尿液 DNA 的多组学整合分析成功优化了一种命名为 UCseek 的检测方法，适用于低/高级别、早/晚期尿路上皮癌的无创诊断和监测。在超低测序深度下，该模型仍可维持较好能效，可极大地降低检测成本。该方法的应用可减少不必要的膀胱镜或输尿管镜检和盲目的二次手术负担,为尿路上皮癌精准诊断和复发监测提供高效新方法。

关键字：尿路上皮癌； 尿液无创诊断； DNA 拷贝数；DNA 甲基化；二代测序

660. 基于全转录组测序的中国肝癌新亚群发现与临床转化研究

徐俊杰*[1]、姜是[2]、滕学奕[3]、张程晨[1]、梁霄[1]、蔡秀军[1]

1. 浙江大学医学院附属邵逸夫医院

2. 宁波市第一医院

3. 中国科学院生物物理所

目的：基于中国肝癌病人的转录组测序数据，发现肝癌新亚群，明确特异性标记物，以期为肝癌精准诊断和个体化治疗提供新思路。

方法：收集 296 例来自浙江大学附属邵逸夫医院的肝癌患者的癌组织和癌旁组织样本进行高通量转录组测序，并对所得数据进行基因差异表达分析、功能富集分析、免疫浸润、代谢通路的谱系分析、共表达网络分析等。分析 HCC_1 亚群的特异性差异表达基因，并在接受索拉非尼治疗的肝癌患者组织芯片中进行验证，明确 HCC_1 亚群标记基因与疗效标记基因。

结果：我们找到了一个和胆管细胞癌非常相似的肝细胞肝癌新亚群 HCC_1，转录组测序数据分析显示，HCC_1 和 ICC 在预后、免疫浸润、代谢通路、缺氧状态等方面存在高度相似性。在接受索拉非尼治疗的肝癌患者组织芯片中进行验证，明确了 HCC_1 的亚群标记基因 CEACEM5/6 与疗效标记基因 FGFR1。

结论: HCC_1 是一类和胆管细胞癌非常相似的肝细胞肝癌新亚群，与胆管细胞癌具有相似的表达谱，CEACEM5/6 可作为 HCC_1 的标记基因与其他 HCC 样本区别开来，FGFR1 可预测肝癌患者对索拉非尼的应答效果。

关键字：原发性肝癌；HCC_1；CEACEM5/6；FGFR1

661. 基于相对表达秩序关系的差异基因识别算法 RankCompV3

严婧、曾秋红、王先龙*

福建医科大学医学技术与工程学院生物信息学系，福州 350122

研究目的：样本内基因对的相对表达秩次关系（REO）在相同表型样本中保持稳定，在不同表型中差异显著，可用于生物标志构建和差异基因（DEG）分析。基于 REO，前期发展了 RankComp 和 RankCompV2 两个版本的算法，应用于两种组别中的差异基因识别，但算法中未考虑到两组样本中 REO 的配对实验关系，造成假阳性过高的问题。RankCompV3 算法中对此进行改进，并将算法拓展到单细胞转录组差异基因识别研究中。

材料与方法：算法以累积二项式分布识别在同一个组别中基因对构成的显著稳定对；对于任一基因，构建组别与 REO 方向的列联表；使用 P. McCullagh 检验列联表中 REO 数量分布与组别关联的显著性，判断该基因是否显著失调；初始使用管家基因作为非差异基因，后续迭代使用上一步的非差异基因构建列联表直至差异基因数目稳定。算法分别使用源自小鼠胚胎干细胞的单细胞数据集 GSE54695 作为阴性测试集，以 scDD R 包模拟的多模态单细胞数据和真实单细胞转录组数据集 GSE29087 等作为阳性测试集，与常见差异基因识别算法 MAST、DEsingle、Wilcoxon、Bimod、LR、limma 和 DEseq2 进行性能比较。

结果：在阴性对照样本（GSE54695）中本方法识别到较少的差异基因，十次随机实验检测到的差异基因平均数目为 172.2，假阳性极低。在模拟的多模态单细胞数据中，本算法假阳率低至 0.001，精度和准确率分别高为 0.981 和 0.945，性能优于或近似其他算法。其中，非差异基因 EE 和 EP 平均真阴率为 0.9994；差异基因 DD、DP、DB 和 DM 真阳率最高达 0.93。真实数据集 GSE29087 中，本算法的 AUC 值为 0.669，与其他 7 种算法（0.670、0.629、0.674、0.700、0.688、0.571 和 0.611）具有相似的性能。

结论：本研究基于 REO 开发的 RankCompV3 算法，在模拟数据和真实数据中都展现了较好的性能，能够检测到真实的生物学变异信号，不仅可以应用于常规高通量表达谱分析中，也可应用于单细胞转录组研究。

关键字：REOs 差异基因识别方法 高通量测序数据 单细胞数据

662. 基于肠道大肠杆菌及其代谢物靶基因构建胰腺癌特异性预后相关 mRNA-miRNA-lncRNA 三元调控网络

曹舒清*[1]、郭晨洁[2]、陈梦[2]、张钰婧[3]、贾天琪[4]、张潇月[2]

1. *山西医科大学法医学院*
2. *山西医科大学临床医学院*
3. *山西医科大学公共卫生学院*
4. *山西医科大学药学院*

目的：肠道菌群会通过各种途径影响恶性肿瘤发生发展，以往研究表明胰腺癌（pancreatic adenocarcinoma，PAAD）患者相比正常人其肠道大肠杆菌丰度发生明显变化，但大肠杆菌及其代谢产物如何影响 PAAD 患者预后尚不清楚。本文旨在通过生物信息学方法，从分子层面讨论肠道大肠杆菌及其代谢产物作用靶基因对患者的预后干预作用，为 PAAD 临床早期诊断及靶向治疗提供参考。

方法：通过 gutMGene 数据库获得肠道大肠杆菌及其代谢产物的靶基因，结合 TGCA 和 GTEx 数据库筛选在 PAAD 组织中差异表达的靶基因（DEGs），导入 DAVID 数据库进行生物富集分析。从 TCGA 数据库下载 176 例 PAAD 患者的转录组数据和临床信息，基于 DEGs 采用 Cox 回归和 Lasso 回归分析建立患者预后分析评估模型，获得预后相关靶基因（PRGs）。通过 miRDB 和 miRWalk 数据库筛选各个 PRGs 上游 microRNA，选取交集后以频次高于 PRGs 数目中位数的 miRNA 为主要 miRNA，将其导入 miRCancer 数据库分析获取与 PAAD 预后相关的核心 miRNA，再利用 TCGA、GSE106817 和 GSE112264 数据集验证其在癌症组织及外周血中的表达水平。然后通过 starbase V3.0 数据库获取核心 miRNA 的上游调控 lncRNA，利用 GEPIA 平台筛选并验证其在 PAAD 组织中的表达情况及与患者预后相关性。

结果：获得 34 个人肠道大肠杆菌及其代谢产物相关靶基因，其中 29 个在 PAAD 组织中差异表达，富集分析结果显示，DEGs 主要通过免疫炎症反应影响疾病进程。分析获得 8 个 PRGs，模型风险评分＝（0.11×Exp TJP2）＋（0.45×Exp TLR3）＋（0.13×Exp PIK3CA）＋（-0.03×Exp PIK3CD）＋（-0.47×Exp AKT1）＋（0.03×Exp CX3CL1）＋（0.33×Exp DUSP10）＋（-0.29×Exp SLC19A3）。整体队列中的 1 年、3 年和 5 年 ROC 曲线下面积分别为 0.70、0.79 和 0.92。免疫浸润分析发现，PRGs 与 CD8＋T 细胞、中性粒细胞、巨噬细胞等免疫细胞浸润程度相关。通过筛选合并每个 PRGs 结果，共获得 3746 条 PRGs 上游 miRNA，取出现频次＞4 的

miRNA 进行分析验证，得到 hsa-miR-380-3p 为 5 个 PRGs（TLR3、PIK3CA、PIK3CD、DUSP10 和 SLC19A3）对应的预后相关核心 miRNA，其在癌症组织和外周血中均显著上调表达，与较好的预后有关（$P<0.05$）。最后基于 starbase V3.0 和 GEPIA 数据库筛选获得一条 lncRNA，BLACAT1 在 PAAD 组织中上调表达，并且与更差的预后相关（$P<0.05$），完全符合 lncRNA 与 miRNA 负相关的 ceRNA 假说。

结论：TLR3/PIK3CA/PIK3CD/DUSP10/SLC19A3/hsa-miR-380-3p/BLACAT1 核心 RNA 调控网络可能是大肠杆菌及其代谢产物干预 PAAD 预后的潜在 ceRNA 网络，其中所有 RNA 均对 PAAD 预后具有显著预测价值。

关键字：大肠杆菌；胰腺癌；预后分析；ceRNA 网络；生物信息学分析

663. 基于空间转录组学研究造釉型颅咽管瘤的异质性

涂志伟[1]、王先龙*[1]、赵传[2]、林志雄[2]、林金城[1]、张恩[1]

1. 福建医科大学生物信息学系

2. 首都医科大学附属三博脑科医院

研究目的：釉型颅咽管瘤（ACP）是一种好发于蝶鞍或鞍上区域的脑肿瘤。ACP 存在显著的个体间差异，免疫浸润程度不同，实性和囊性成分变化大，对免疫调节治疗的响应也不同。本研究拟通过空间转录组学结合单细胞转录组学等解析 ACP 肿瘤免疫微环境，阐述异质性产生的机制。

材料和方法：采用 10x-Genomics 单细胞转录组测序技术对 12 例 ACP 新鲜冷冻标本进行单细胞转录组测序，使用 10x Genomics Visium 空间转录组测序技术对 3 例 ACP 石蜡包埋样本进行空间转录组测序。使用 cellranger、spaceranger、seurat、stlearn 软件包对单细胞转录、空间分辨转录谱，并结合苏木精伊红染色病理图片进行整合分析。

结果：研究发现成纤维细胞生长因子（FGF）、Wnt 靶基因（NOTUM）、WNT 信号通路负调控因子（AXIN2）等在 ACP 漩涡状细胞簇和栅栏样上皮细胞中显著高表达；在不同 ACP 样本中，这些基因的表达水平在 WNT 激活型样本中表达最高。一个样本中 CTNNB1 及其负调控因子 AXIN2 等 WNT 通路相关基因表达显著高于另外 2 个免疫浸润型样本，WNT 通路显著激活。同时，在 WNT 激活型样本中对 PD-1 和 PD-L1 的表达水平也显著高于另外两个样本。

结论：研究揭示了 ACP 不同分子亚型在空间结构上表达模式的异质性，为 ACP 的靶向治疗方案的设计提供思路。

关键字：造釉型颅咽管瘤，空间转录组，Wnt/β-catenin 信号通路

664. 造釉型颅咽管瘤中 Wnt/β-catenin 通路激活与免疫浸润互斥关系研究

张恩、林金城、陈雯、林金玉、徐默萍、徐达鹏、涂志伟、王先龙*

福建医科大学医学技术与工程学院生物信息学系，福州 350122

研究目的：造釉型颅咽管瘤（ACP）是常见于鞍区的原发性上皮瘤，具有高侵袭性、易复发、预后差等特点。课题组前期研究发现在同样 CTNNB1 突变的驱动下，不同肿瘤发展成为三种分子亚型。本研究旨在阐明分子亚型产生机制，特别是 Wnt/β-catenin 通路激活与免疫浸润互斥的分子机制。

材料与方法：自测和从公开数据库收集 ACP 多组学数据，包括 36 例转录谱、16 例蛋白质表达谱和 51 例 DNA 甲基化谱。使用共识聚类方法确定分子亚型，通过去卷积方法估计细胞组分，使用通路富集方法评估样本中激活的信号通路，揭示 ACP 不同亚型间特点。结合 DNA 甲基化启动子区域β值与 RNA 转录水平相关性分析以及 RNA 和蛋白质表达水平相关性分析，评价异常甲基化在分子分型形成中的角色。

结果：造釉型颅咽管瘤异质性高，依据表达谱和 DNA 甲基化谱可分成三种分子亚型，分别命名为 ImA、ImB 和 WNT 型。其中 ImA 和 ImB 两型表现为免疫浸润程度较高，免疫相关因子激活程度高；WNT 型则表现为 Wnt/β-catenin 通路异常激活，但免疫浸润程度低，呈现 Wnt/β-catenin 通路激活与免疫浸润互斥的关系。星形胶质细胞标志基因在 ImA 型中显著高表达，巨噬细胞标志基因在 ImB 型中富集程度较高。通过 DNA 甲基化、RNA 转录和蛋白表达水平进行关联分析，发现 36 个显著相关基因，其中免疫相关的 IL16、与癌症发生发展相关的 SMAD3、SSH3 等基因的异常甲基化可能在分子亚型形成中发挥重要作用。

结论：造釉型颅咽管瘤存在较大的异质性，存在三种分子特征迥异的亚型，呈现 Wnt/β-catenin 通路激活与免疫浸润互斥的现象。SMAD3 等基因异常 DNA 甲基化可能是导致不同亚型产生的原因。

关键字：造釉型颅咽管瘤 Wnt/β-catenin 通路 免疫浸润 多组学分析

665. 新型含氮双氢青蒿素二聚体对人白血病细胞株 NB4-R1 细胞凋亡的影响

崔雯[1,2]、薛征[1]、赵玲玲[2]、李英[3]、糜坚青*[2]

1. 上海市中医医院

2. 上海交通大学医学院附属瑞金医院

3. 中国科学院上海药物研究

目的：急性早幼粒细胞白血病（APL）是急性髓细胞白血病（AML）的特殊亚型，它的特点是 t（15；17）（q22；21）染色体易位形成的 PML-RARα融合基因。靶向治疗药物全反式维甲酸（all trans retinoic acid, ATRA）以及三氧化二砷的联合使用，极大地提高了 APL 的预后。但是，仍有小部分患者会产生 ATRA 耐药，尤其是那些多次复发或在分子学水平未缓解的病例。因此，寻找新的治疗药物改善 ATRA 耐药具有非常重要的意义。从传统中药中寻找开发新型抗肿瘤药物已成为研究热点。研究发现，中药黄花蒿有效成分青蒿素及其衍生物具有抗炎、抗肿瘤活性，且对人体正常细胞毒副作用小，具有广阔的应用前景。本研究分别以 ATRA 敏感株 NB4 以及 ATRA 耐药株 NB4-R1 为模型，探讨新型水溶性含氮双氢青蒿素二聚体（SM 1044）对其凋亡的影响及其可能的分子机制。

材料与方法：流式细胞术检测 SM 1044 对细胞凋亡的影响和线粒体跨膜电位的影响；Western blot 检测凋亡相关蛋白（caspase-3，-8，-9 以及 PARP）表达的变化；流式细胞术检测 SM 1044 对细胞活性氧（ROS）水平的影响；Western blot 检测 SM 1044 对 MAPK（ERK、JNK）信号通路以及 PML-RARα融合蛋白的影响。

结果：SM 1044 能够显著诱导 NB4、NB4-R1 细胞发生细胞凋亡，总凋亡率随着浓度的升高而增加。与 NB4 细胞相比，SM 1044 诱导 NB4-R1 细胞凋亡更明显。SM 1044 可诱导 NB4-R1 细胞线粒体跨膜电位丢失，丢失的细胞百分比随着浓度的升高而增加。SM 1044 处理 NB4-R1 细胞后，凋亡相关蛋白 caspase-3、caspase-8、caspase-9 以及 PARP 的剪切片段表达均明显增加。SM 1044 可诱导 NB4-R1 细胞产生活性氧。SM 1044 能够激活 MAPK（ERK、JNK）信号通路的磷酸化，同时下调 PML-RARα融合蛋白的表达。

结论：与 ATRA 敏感株 NB4 相比，SM 1044 具有更显著诱导 ATRA 耐药株 NB4-R1 细胞凋亡的作用。SM 1044 处理后，凋亡相关蛋白被激活，同时线粒体跨膜电位丢失明显，SM 1044 可通过凋亡内在和外在途径诱导 NB4-R1 细胞凋亡。其诱导凋亡可能与 ROS/ERK 以及

ROS/JNK 信号通路有关。此外，与大多数其他恶性肿瘤不同，PML/RARα可能是大部分 APL 发生发展的唯一驱动因素，SM 1044 还可通过下调 PML/RARα蛋白诱导细胞凋亡。因此，SM 1044 有望成为治疗 APL 尤其是 ATRA 耐药 APL 的潜在药物。

关键字：青蒿素衍生物；急性早幼粒细胞白血病；NB4-R1 细胞；细胞凋亡

666. 外周血 PD-1、CTLA-4、T-reg、pDC 与鼻咽癌临床特征及疗效相关性研究

徐歆宇、金风*

贵州医科大学附属肿瘤医院

目的：探讨初治鼻咽癌患者治疗前外周血 PD-1/CTL(%)、CTLA-4/CTL(%)、T-reg(%)、pDC 与鼻咽癌临床特征及即刻疗效的关系。

方法：收集 2019 年 3 月—2021 年 3 月在贵州医科大学附属肿瘤医院住院治疗的 112 例初治鼻咽癌患者治疗前淋巴细胞亚群及树突细胞亚群流式细胞术检测结果。采用 R 语言分析 PD-1/CTL(%)、CTLA-4/CTL(%)、T-reg(%)、 pDC 与鼻咽癌临床特征及即刻疗效的相关性，然后筛选出具有统计学意义数据进行进一步分析，二分类临床特征的组间比较用独立样本 t 检验，多分类临床特征及即刻疗效与上述指标构建线性回归模型拟合线性关系，使用平滑曲线拟合来解决非线性问题。

结果：NPC 患者年龄＜50 岁组 PD-1/CTL(%)为（31.66±13.23）%，NPC 患者年龄≥50 岁组 PD-1/CTL(%)为（38.21±10.62）%，两组 PD-1/CTL(%)总体均数存在着统计学差异（差值－6.55%，95%CI －11.03% -－2.07%，t＝－2.899，p＝0.005）； PD-1/CTL(%)在不同性别、慢性病史、吸烟史、饮酒史、T 分期、N 分期、M 分期、TNM 分期、EBV-DNA 拷贝数（＜500，≥500）中比较，差异无统计学意义（均 p＞0.05）。CTLA-4/CT(%)与 T 分期存在线性关系，且负相关（p＜0.05）；CTLA-4/CT(%)与 N 分期存在线性关系，且负相关（p＜0.05）；CTLA-4/CT(%)与 TNM 分期存在线性关系，且负相关（p＜0.05）；CTLA-4/CT(%)与即刻疗效存在线性关系，CTLA-4/CT(%)越高，疗效越好；CTLA-4/CTL(%)在不同性别、年龄（＜50 岁，≥50 岁）、慢性病史、吸烟史、饮酒史、M 分期、EBV-DNA 拷贝数（＜500，≥500）中比较，差异无统计学意义（均 p＞0.05）。T-reg(%)与 N 分期存在线性关系，且正相关（p＜0.05）； T-reg(%)与 M 分期存在“S”型曲线关系，当 T-reg(%)＜20%时，M 分期

无限接近于 0，当 T-reg(%)为 20%-50%时，T-reg(%)与 M 分期呈正相关（p＜0.05），当 T-reg(%)＞50%时，M 分期无限接近于 1；T-reg(%)在不同性别、年龄（＜50 岁，≥50 岁）、慢性病史、吸烟史、饮酒史、T 分期、TNM 分期、EBV-DNA 拷贝数（＜500，≥500）中比较，差异无统计学意义（均 p＞0.05）。pDC 与 N 分期存在线性关系，且负相关（p＜0.05）；pDC 与 TNM 分期存在线性关系，且负相关（p＜0.05），pDC 在不同性别、年龄（＜50 岁，≥50 岁）、慢性病史、吸烟史、饮酒史、T 分期、M 分期、EBV-DNA 拷贝数（＜500，≥500）中比较，差异无统计学意义（均 p＞0.05）。

结论：外周血 CTLA-4/CT(%)、T-reg(%)及 pDC 与鼻咽癌分期相关，CTLA-4/CT(%)与即刻疗效相关，有望成为预测鼻咽癌患者预后及疗效的生物标志物。

关键字：鼻咽癌；临床特征；即刻疗效；PD-1；CTLA-4；T-reg；pDC

667. 个体化免疫炎症相关蛋白复合物监测肺癌患者疾病进展

李丹、张慧娟、赖治臻、周巾煜、张继匀、李智立*

中国医学科学院基础医学研究所

目的：免疫炎症相关蛋白质与肿瘤转移复发密切相关。本研究以体液免疫相关蛋白为监测对象，验证个体化的血液免疫炎症相关复合物与肺癌疾病进展的关系。

方法：采用凝胶电泳方法对 119 例肺癌患者随访期间不同时间点血液（1331 个样本）中的免疫炎症相关蛋白复合物进行定量分析。构建免疫炎症相关蛋白复合物量变与随访时间的曲线。

结果：肺癌患者随访期间血液中免疫炎症相关蛋白复合物水平的变化率与临床病理特征和无进展生存期等指标有显著相关性，且具有个体化特征。113 例临床影像学确诊发生疾病进展的患者中，有 108 例患者在疾病进展之前免疫炎症相关蛋白质复合物水平发生显著变化，与临床影像学诊断相比，中位数提前 61.9 周。

结论：免疫炎症相关蛋白复合物具有早期预警肺癌患者疾病进展的潜力。

关键字：免疫炎症相关蛋白复合物，肺癌，疾病进展

668. 基于 TCGA 数据库分析 AKR1B1 在胃癌中的表达及临床意义

王乃雪[1]、郑振东*[2]、杜成[2]、王美玲[2]

1. 锦州医科大学中国人民解放军北部战区总医院研究生培养基地

2. 中国人民解放军北部战区总医院

目的：利用在线数据库和生物信息学方法分析 AKR1B1 基因在胃癌中的差异表达对其预后的意义，寻找胃癌新的生物标志物。

方法：使用 TCGA 公共数据库获取胃癌患者的基本临床信息、AKR1B1 的表达情况，通过使用 R 语言分析患者癌组织与癌旁组织的表达差异，以及 AKR1B1 的表达与临床信息相关性;利用 Kaplan-Meier Plotter 分析不同 AKR1B1 表达水平的胃癌患者生存曲线，同时利用 ROC 曲线行进一步的验证； Cox 比例风险回归模型对可能影响胃癌患者预后的因素进行单因素及多因素分析,并着重分析 AKR1B1 能否成为影响胃癌患者预后的独立因素;使用 TIMER 数据库分析 AKR1B1 在胃癌中与各种免疫细胞浸润的相关性;GEPIA 数据库分析 AKR1B1 的表达与免疫标志物的相关性。

结果：癌组织 AKR1B1 分子表达水平高于癌旁组织，差异有统计学意义（$p<0.05$）。AKR1B1 高表达患者的总生存（OS）明显低于低表达的患者($p<0.001$, HR= 1.83 (1.31−2.55)),通过 ROC 曲线进行验证得到曲线下面积为 0.625。通过 COX 模型进行分析，在单因素及多因素分析中 AKR1B1（$P<0.001$；$P<0.001$）可作为胃癌患者预后的独立影响因素。AKR1B1 的表达与胃癌中的多种免疫细胞浸润呈正相关，例如 CD4+T 细胞（P<0.001）、$CD8^+$T 细胞（$P<0.001$）、巨噬细胞（$P<0.001$）、中性粒细胞（$P<0.001$）、树突细胞（$P<0.001$）。在胃癌中，通过数据库分析发现 AKR1B1 的表达与 PD-L1（$P<0.001$）、PD-1($P<0.001$)、CTLA-4($P<0.001$)的表达呈正相关。

结论：AKR1B1 可作为胃癌患者的不良预后标志物，其高表达的患者生存预后差。AKR1B1 的表达与大部分免疫细胞呈正相关，同时也与免疫检查点抑制剂的表达呈正相关，AKR1B1 可为胃癌患者生存及免疫治疗的疗效提供一定预测价值。

关键字：AKR1B1、胃癌、预后标志物

669. ARA55 基因在 CNE2 鼻咽癌细胞中的功能研究

崔兆磊、陈燕*

福建省肿瘤医院

目的：研究 ARA55 过表达对 CNE2 鼻咽癌细胞生物学特性的影响，明确 ARA55 在 TGFβ1 介导的 CNE2 细胞上皮间质转化及侵袭、迁移中的作用。

方法：构建 pCMV-ARA55-EGFP 真核表达载体，经 ZLip2000 转染至 CNE2 鼻咽癌细胞，荧光显微镜和免疫印迹检测 ARA55-EGFP 融合蛋白的表达；通过 CCK-8 比色、划痕修复实验、Transwell 小室、Annexin V-PE/7-AAD 双荧光染色、DNA 梯状电泳等实验，探讨 ARA55 过表达对 CNE2 鼻咽癌细胞生物学特性的影响。一定浓度的 TGFβ1 诱导 CNE2 细胞株中 ARA55 的表达，免疫印迹检测 ARA55 蛋白及 EMT 相关标志物 N-cadherin、Claudin-1 等的表达变化；采用 ARA55 的 siRNA 质粒，经 X-treme GENE siRNA 转染至 CNE2 细胞株；通过 CCK-8 比色、划痕修复、Transwell 侵袭迁移等实验，研究 TGFβ1 介导的 ARA55 表达上调及沉默以 ARA55 表达对 CNE2 鼻咽癌细胞 EMT 及侵袭迁移的影响。

结果：DNA 测序及双酶切分析显示 pCMV-ARA55-EGFP 重组载体构建成功。pCMV-ARA55-EGFP 组细胞生长增殖、侵袭迁移能力明显低于 pCMV-C-EGFP 空载体组和/或空白对照组（$P<0.05$ 或 0.01）；Annexin V-PE/7-AAD 双荧光染色及 DNA 梯状电泳结果可见，pCMV-ARA55-EGFP 组细胞产生凋亡，且凋亡率明显高于 pCMV-C-EGFP 空载体组（$P<0.05$）；免疫印迹显示 pCMV-ARA55-EGFP 组细胞 Bcl-2 表达下调，Cytochrome C 表达上调，同时伴有 Caspase-9 和 Caspase-3 的激活。TGFβ1 诱导后，免疫印迹显示 ARA55 在 CNE2 细胞中的表达上调；ARA55 诱导组细胞发生间质样改变，N-cadherin 的表达上升，Claudin-1 表达下降，同时细胞的生长增殖及侵袭迁移能力明显高于对照组（$P<0.05$ 或 0.01）；诱导表达的 ARA55 通过 siRNA 下调后，siRNA-ARA55 组细胞生长增殖及侵袭迁移能力下降（$P<0.05$ 或 0.01）。

结论：成功构建 pCMV-ARA55-EGFP 重组载体； ARA55 过表达可抑制 CNE2 鼻咽癌细胞生长增殖，诱导凋亡；3. ARA55 参与了 TGFβ1 介导的 CNE2 细胞 EMT 及侵袭迁移过程。

关键字：鼻咽癌；ARA55；TGFβ1；上皮间质转化；CNE2

670. 中性粒细胞与淋巴细胞、血小板与淋巴细胞和单核细胞与淋巴细胞比值作为实体瘤免疫治疗的预后因素

纪宏娟[1,2]、杜成*[1]

1. 中国人民解放军北部战区总医院

2. 锦州医科大学

目的：中性粒细胞-淋巴细胞比值（NLR）、血小板-淋巴细胞比值（PLR）和单核细胞-淋巴细胞比值（MLR）被用作实体瘤免疫治疗的预后指标，本研究的目的是评估炎症标志物对接受免疫检查点抑制剂（ICIs）治疗的实体瘤患者预后的预测价值。

方法：纳入 2019 年 4 月-2021 年 10 月在北部战区总医院肿瘤科就诊的 184 例接受 ICIs 治疗的实体瘤患者的外周血常规参数和其他临床资料。生成了 NLR、PLR 和 MLR 的受试者工作特征（ROC）曲线，最佳截止值确定为约登指数（灵敏度+特异性-1）的最大点。根据 ROC 曲线分析结果，将患者分别分为两组。利用 Kaplan-Meier 生存分析及 Cox 模型分析 NLR、PLR、MLR 的预后预测价值。

结果：中位年龄 63 岁，女性 55 例，男性 129 例。外周血 NLR、PLR、MLR 曲线下面积（AUC）分别为 0.607（*P*=0.012）、0.664（*P*<0.0001）、0.668（*P*<0.0001），最佳截止值分别为 2.6549、226.002、0.3578。生存分析显示，NLR>2.654（*P*=0.006）、PLR>226.002（*P*<0.0001）和 MLR>0.3578（*P*<0.0001）与较差的 OS 相关。在单变量分析中，高 PLR 是整体生存的独立预后因素（HR：1.004，95%CI：1.001-1.007，*P*=0.006）。

结论：因此，我们的研究表明，NLR、PLR、MLR 可以作为预测实体瘤免疫治疗的预后因素。

关键字：中性粒细胞与淋巴细胞；血小板与淋巴细胞；单核细胞与淋巴细胞；免疫治疗；

671. 肝星状细胞活化过程中超氧阴离子介导肝癌细胞免疫逃逸机制的荧光成像研究

毛元涛、武传琛、张芳慧、王昕、李平*、唐波

山东师范大学

肝癌免疫逃逸是造成肝癌死亡的重要原因，其相关机制不清楚，使肝癌的免疫治疗面临巨大挑战。活化的肝星状细胞（aHSCs）在肝脏免疫过程中扮演关键角色，其活化过程产生的超氧阴离子（$O_2^{\bullet-}$）在肝癌免疫逃逸过程中发挥重要作用。为了探究活化的 aHSCs 如何通过 $O_2^{\bullet-}$的水平变化调控肝癌免疫逃逸的详细分子机制，我们设计合成了双光子荧光探针 TPH，开发了一种实时、原位检测 HSCs 活化过程中 $O_2^{\bullet-}$水平变化的研究策略。TPH 利用咖啡酸残基的酚醌互变和多肽的靶向实现了对 HSCs 内 $O_2^{\bullet-}$的特异性检测。借助双光子荧光成像技术，我们在体内和体外实验中观察到 HSCs 活化过程中 $O_2^{\bullet-}$水平升高的现象。在具有不同 HSCs 活化程度的肝癌小鼠模型中，升高的 $O_2^{\bullet-}$水平削弱了肝癌细胞周围 $CD8^+$ T 细胞浸润，增强了肝癌免疫逃逸的程度。进一步研究发现，HSCs 活化过程产生的 $O_2^{\bullet-}$损伤了 CDK4 蛋白的功能区域，诱导 PD-L1 水平升高，从而促进肝癌细胞免疫逃逸。我们的工作为 HSCs 活化过程中 $O_2^{\bullet-}$介导肝癌细胞免疫逃逸提供了证据，有望为肝癌免疫治疗提供潜在的靶点。

关键字：肝星状细胞，超氧阴离子，荧光成像，肝癌免疫逃逸

672. 基于 TCGA 数据库分析 CA9 在肾透明细胞癌中的表达及临床意义

丁瀚、韩起鹏*

中国人民解放军北部战区总医院

目的：利用在线数据库和生物信息学方法分析 CA9 基因在肾透明细胞癌中的差异表达对其预后的意义，寻找肾透明细胞癌新的生物标志物。

方法：使用 GEPIA 数据库分析肾透明细胞癌的差异基因，并分析基因表达情况。利用 TIMER 数据库对 GEPIA 数据库中基因表达情况进行验证，在 TIMER 数据库中分析 CA9 在肾透明细胞癌中与各种免疫细胞浸润的相关性。使用 TCGA 公共数据库获取肾透明细胞癌患者的

基本临床信息、CA9 的表达情况，通过使用 R 语言分析患者癌组织与癌旁组织的表达差异，CA9 的表达与临床信息相关性, Kaplan-Meier Plotter 分析基因表达与患者的生存曲线。

结果：使用 GEPIA 数据库分析出 CA9 在肾透明细胞癌中高表达，其表达高于其他肿瘤。肿瘤患者癌组织 CA9 表达均高于癌旁组织，差异具有统计学意义（*P*<0.001）。CA9 高表达患者的总生存时间（OS）高于大表达患者的总生存（*P*=0.02, HR=0.70(0.52-0.95)），从 THE HUMAN PROTEIN ATLAS 数据库中得出 CA9 为肾癌的不良预后标志物，并有免疫组化结果进行验证，癌组织中 CA9 的表达高于癌旁组织。CA9 的表达与多种免疫细胞息息相关，例如巨噬细胞（*p*<0.05）、肥大细胞（*p*<0.05）、细胞毒性 T 细胞（*p*<0.05）、CD8+T 细胞（*p*<0.05）等。

结论: CA9 可作为肾透明细胞癌患者的不良预后标志物，其高表达的患者生存预后差。CA9 的表达与大部分免疫细胞息息相关，AKR1B1 可为肾透明细胞癌患者的生存预后及免疫治疗的疗效提供一定预测价值。

关键字: CA9，肾透明细胞癌，预后标志物，免疫治疗

673. 环状 RNA 作为肺癌诊断标志的 meta 分析

李孟鹏、魏传飞、徐丽、刘延明、韩发彬*

聊城市人民医院

目的: 采用 meta 分析的方法评价环状 RNA 作为肺癌诊断标记物的价值。

方法: 全面检索 PubMed、Embase 和 Web of science 数据库，检索截止日期至 2022 年 8 月 1 日，检索关于环状 RNA 与肺癌诊断的相关研究，采用 Review Manager 5.3 软件对数据进行 Meta 分析。

结果: 共纳入 22 篇文章共 30 条 circRNAs。Meta 分析结果显示，在诊断价值方面，circRNAs 可区分肺癌患者和正常个体，其曲线下汇集面积(AUC)较高，为 0.86 (95%CI: 0.83-0.89)

结论：环状 RNA 可能作为肺癌的新型诊断标记物。

674. 用于诊断卵巢癌的肿瘤标志物（CA125、HE4）和算法(ROMA)

李晓*、薛丰民

郑州安图生物工程股份有限公司

目的：卵巢癌（OC）在女性癌症发病率中排第 7 位，在中国女性癌症发病率排第 9 位，但病死率却居首位，是全世界女性妇科肿瘤的首要死因。因卵巢癌病变位于盆腔深部,早期症状不典型，且无法进行筛查和术前活检进行组织学诊断。几种肿瘤标记物、影像学检查和组合算法已用于区分良性和恶性上皮性卵巢癌，本文将汇总近几年发表的文献，用于诊断卵巢癌的肿瘤标志物（CA125、HE4）和算法(ROMA)联合检测对提高卵巢癌检测的敏感性和特异性做出参考。

方法：汇总国内外近几年发表的用于诊断卵巢癌的标志物及算法的文献，为临床医生提供可用于指导诊断或治疗的可靠结果。

结果：糖类抗原 CA125 是目前使用最广泛的卵巢癌标志物，1981 年，Bast 等人使用针对 OVCA433 卵巢细胞系的抗体（OC125）首次定义了 CA 125，该标志物在卵巢癌早期的敏感性较低，在其他生理或病理条件下，如月经、妊娠、子宫内膜异位症和腹膜炎性疾病，CA125 会高表达。人类附睾蛋白 4（HE4）是一种新的卵巢癌肿瘤标志物，不受月经影响，但是跟年龄增长存在一定关系，一般根据更年期状态，建议参考值值为 70 和 140 pmol/l，有研究报告了 HE4 的特异性为 86%，AUC 高于单独的 CA125，分别为 0.893 和 0.865。另外一项研究表明 CA125 和 HE4 关联的特异性更好（80%）。当结合两种标记物时，ROC AUC 很高，从 0.96 到 0.91 不等。2009 年，Moore 提出了一种新算法：卵巢恶性肿瘤风险算法（ROMA），他根据绝经状态（定义为 6 个月内无月经或绝经的临床症状）关联 HE4 和 CA125 水平，有研究表明 ROMA 算法的特异性低于 HE4 水平（84%对 94%），但与 CA125 水平（84%对 78%）的相关性更好。另外一项研究 ROMA 算法的 AUC 优于 HE4 或 CA125（分别为 0.93、0.82 和 0.88），另外一项研究表明 ROMA 指数的敏感性和特异性为 88.5%和 72.3%。绝经后妇女的结果更好：ROMA 指数敏感性达到 95.5%，特异性为 60.7%。对于绝经前患者，使用 ROMA 结果的敏感性有所下降。

结论：用于诊断卵巢癌的肿瘤标志物（CA125、HE4）单独使用会受一些月经、卵巢癌良性病、年龄等因素的影响，影响医师判断，而联合检测 CA125 和 HE4，配合算法（ROMA）会提高对卵巢癌检测的灵敏度和特异性，能够在癌症早期发现，提高患者生存期。

关键字：卵巢癌，CA125，HE4，ROMA

675. 血清鳞状细胞癌抗原检测的假性升高结果分析及处理对策

姚汶励*、张来星

安图生物股份有限公司

目的：SCCA 是最早用于诊断鳞状上皮细胞癌的肿瘤标志物，具有较好的特异性，可作为宫颈癌、肺癌、结直肠癌、食管癌等辅助诊断、监测病情变化和推测疾病预后的依据。而 SCCA 的假性升高，不但会造成临床大夫诊断结果异常，也会给病人带来精神上的压力，引起不必要的医疗纠纷。然而在工作中，仪器、方法学灵敏度、工作人员操作、标本状态等都会对检验结果造成一定影响。如何发现、最大程度降低假性升高是值得我们思考和分析的问题。本文将从磁微粒化学发光检测过程逐一对异常原因进行分析汇总，消除大家因检测结果异常带来的担忧。

方法：汇总有关引起人血清 SCCA 结果异常的文献，同时收集安图生物工程股份有限公司所生产的鳞状细胞癌抗原定量检测试剂盒(磁微粒化学发光法)在临床使用过程中出现的部分异常结果样本，采用化学发光法雅培 I2000、罗氏 Cobas e602 试剂盒分别进行测定，通过查找排除影响 SCCA 检测准确性的因素，最终提高实验室检测 SCCA 的准确性。

结果：SCCA 出现结果偏高的影响因素通常分为 3 种：分析前因素、分析中因素、分析后因素。分析前主要在标本的采集与保存，SCCA 也常见于唾液、汗液、呼吸道分泌物，因此在 SCCA 检测过程中易被人体体表的物质所污染，导致假阳性结果，如果操作过程中样本和试剂受到污染，会造成结果异常升高；分析中主要在：仪器状态、测定方法和试剂、交叉污染、嗜异性抗体、质量控制等，比如仪器长期使用未保养维护，吸液针异常，影响光检测，可导致结果的假阳性；实验过程中消耗品不足也可能导致结果升高；样本中存在某些干扰物质，如血红蛋白、胆红素、甘油三酯，嗜异性抗体如 RF、HAMA 等相关物质均可能引起标本呈

现假阳性。分析后主要在参考值范围、与临床相关沟通等，不同地区、人群，参考值范围存在差异，实验室应建立自己的参考区间。

结论：实验前应佩戴好手套和口罩，严格按照标准操作规程（SOP）进行操作，避免人为因素或技术误差，同时应对仪器做好保养维护工作，仔细核对试剂信息正确，定标正常，储存条件正常，确保每天室内质控测定结果在控；实验过程中应随时查看，确认消耗品无缺少；若确认样本存在干扰，可进行稀释、聚乙二醇 6000 处理等确定干扰类型。总之，本研究为提高 SCCA 检测准确性进行了相关分析，可通过控制分析前、分析中、分析后影响因素，有效提高 SCCA 检测准确性，并为临床应用提供良好的指导。

关键字: SCCA；假阳性；定量检测

676. 原发性食管恶性黑色素瘤伴全身多处转移 1 例

黎徐*、韩书雯、何玲

遵义医科大学附属医院

目的：黑色素瘤可发生于身体各部位，最常见于皮肤。而原发性消化道黑色素瘤（PGIM）较罕见，多为转移性，临床缺乏特异性表现，总结发生在食管的恶性黑色素瘤临床特点、病理特征、内镜下表现及治疗方案，以提高临床医生对原发性食管恶性黑色素瘤的诊疗水平。

方法：回顾性分析遵义医科大学附属医院收治的原发性食管恶性黑色素瘤伴全身多处转移 1 例，并进行文献复习。

结果：患者女，60 岁，2 年前因“嗳气半年，右侧头痛 3 月，加重 15 天”入院。胃镜下病理活检：(食管、十二指肠乳头开口)恶性黑色素瘤，食管多发原发病灶，十二指肠多处累及。免疫组化：HMB45(+)、Melan-A(-)、S100(+)、CK(-)、CK7(-)、CK 5/6(-)、P40(-)、P63(-)，SMA(-)、Ki67(约 30+)。头颅 MRI+MRA：颅骨多发肿瘤性病变。PET-CT：右侧顶骨骨质破坏并代谢增高。右侧髋臼代谢增高结节。左侧鼻咽部、双侧颈部淋巴结、直肠上段代谢均增高。综合上述检查明确诊断为原发性食管恶性黑色素瘤伴全身多处转移。治疗上予以达拉非尼 150mg Q12h 、曲美替尼 2mg Qd、定期输注怕铂骊珠单抗、地舒单抗，针对头部转移予以放射治疗。靶向治疗后 2 月后复查 PET-CT：原右侧顶骨代谢不高；右侧髋臼代谢不高，结节较前缩小，上述考虑治疗后肿瘤活性受抑。对比上述新增脾脏代谢增高结节、左侧盆腔肠系膜、L4 左侧椎弓代谢增高。考虑转移病变。该患者目前仍在随访中。

结论：恶性黑色素瘤侵袭性强、预后差，发现时常为晚期。文献报道发生在食管时可仅表现为吞咽困难，缺乏特异性临床表现，内镜下以结节隆起型为主，极易漏诊误诊。诊断主要依赖于病理及免疫组化。目前早发现、早诊断仍是治疗该病的关键所在。

关键字：食管；恶性黑色素瘤；

677. 十二指肠神经内分泌肿瘤肝转移 1 例

黎徐*、车文怡、李华美

遵义医科大学附属医院

目的：十二指肠神经内分泌肿瘤（NENs）约占所有胃肠道 NENs 的 2%-3%，占十二指肠肿瘤的 3%，较为罕见。分析十二指肠 NENs 的临床特点及内镜下特征，以期提高临床医生对该病的诊疗水平。

方法： 回顾性分析遵义医科大学附属医院收治的十二指肠神经内分泌肿瘤肝转移 1 例并进行文献复习。

结果：患者女，37 岁，因“反复腹胀 4 年，加重伴腹痛 1 月”就诊于外院胃镜提示慢性胃炎，对症治疗后未见好转。故于 2022 年 03 月 04 日就诊我院。腹部 CT：十二指肠水平段-升段不规则增厚，考虑肿瘤。肝脏多发转移瘤多中心肝癌,最大者 100×95mm。胃肠镜:十二指肠肿瘤；慢性非萎缩性胃炎；胃体息肉。十二指肠黏膜活检：十二指肠神经内分泌瘤（G2），中级别。免疫组化：Ki-67 热点区 11%（+）、CK（++）、CD56（+）、Syn(+)、SSTR-2（3+）、CDX-2（++）、Villin(+++)、Cgn(-)、Insulin(-)、p53(-)。肝穿刺病理活检：部分细胞见大小一致的小圆细胞，结合组织形态考虑神经内分泌瘤。上述病灶符合 NENs 肝转移。明确诊断后予以注射用醋酸奥曲肽微球 30mg 1 次/月 控制肿瘤。并分别于 03 月 25 日、05 月 20 日行“经导管肝动脉栓塞术+肝动脉造影术”。治疗 5 月后复查腹部 CT 见肝脏转移瘤明显缩小（58×51mm）、减少。目前仍在随访中。

结论：十二指肠 NENs 生长缓慢，临床表现不典型，不易早期发现及诊断。相关文献报道其内镜下表现多为半球形、息肉形或盘状黏膜隆起，表面可有充血、糜烂或溃疡。该患者内镜下仅表现为慢性胃炎，极易漏诊和误诊，临床医生应高度警惕该病，应注意与息肉、间质瘤、平滑肌瘤等良性疾病相鉴别。目前该病主要以手术治疗为主，可辅以生物治疗及靶向治疗。

关键字：十二指肠；神经内分泌瘤；肝转移

678. 原发性卵巢小细胞型神经内分泌癌 1 例

黎徐*、李华美、何玲、杨珊

遵义医科大学附属医院

目的：总结原发性卵巢小细胞型神经内分泌癌（SCNEC）的临床特点及病理特征，以提高临床医生对该病的诊疗水平。

方法：回顾性分析遵义医科大学附属医院收治的原发性卵巢小细胞型神经内分泌癌 1 例并进行文献复习。

结果：患者女，69 岁，因“尿频 2 月，下腹痛 1 月”于 2022 年 01 月 13 日就诊我院。查体：宫颈充血，子宫稍大，有压痛。腹部 CT 提示双侧附件区占位性病变。PET-CT：1.双侧附件区肿块，代谢异常增高，考虑恶性肿瘤病变；2.胰腺多发代谢增高结节；3.左侧锁骨上区、腹膜后、肠系膜区、盆腔淋巴结代谢增高，考虑转移性病变，可疑卵巢恶性肿瘤；病检：（双侧卵巢、双侧输卵管)均见小细胞型神经内分泌癌累及；送检（宫体、宫颈）示小细胞型神经内分泌癌，癌组织侵及宫壁全层，伴片状坏死。神经、脉管均侵犯；送检（部分肠壁、膀胱病灶）均见累及。结合患者检查诊断为：卵巢 SCNEC T4N1M1 IV 期（伴双侧输卵管、子宫、膀胱、盆腔、腹膜后、胰腺等多处转移）。入院 1 周后行腹腔镜检查+开腹探查术+全子宫双侧附件切除术+膀胱表面病灶切除术+膀胱修补术+部分乙状结肠直肠切除术+乙状结肠造瘘术+盆腔淋巴结切除术+腹主动脉旁淋巴结切除术+骶前病损切除术+盆腔粘连松解术。术后规律予以 EP 方案（依托泊苷 10mg d1-5 +顺铂 30mg d1-5 ）规律化疗，目前仍在随访中。

结论：小细胞神经内分泌癌(SCNEC)在女性生殖系统中极为罕见，占所有妇科恶性肿瘤＜1%，其中以宫颈最为常见。卵巢 SCNEC 侵袭性强，主要依赖病理及免疫组化明确诊断。神经内分泌癌首选手术治疗，但由于早期就极易发生远处转移，且卵巢 SCNEC 患者平均发病年龄较大，患者预后较差。因此，临床上应警惕该病，早发现、早诊断、早治疗有助于患者预后。

关键字：卵巢；神经内分泌癌；

679. 基于单细胞转录组的 MSI-H/dMMR 结直肠癌患者免疫治疗疗效影响因素的综合分析

杨博文、车晓芳*

中国医科大学附属第一医院

免疫检查点抑制剂（ICI，如 PD-1/PD-L1 抑制剂）的应用使部分结直肠癌（CRC）患者获得长期生存获益。尽管 FDA 已经批准免疫治疗在 MSI-H/dMMR 结直肠癌患者中的应用，但现有证据表明，仍然有大约 50% 的 MSI-H/dMMR 的结直肠癌患者对免疫治疗耐药。因此，我们对结直肠癌患者的公开数据进行综合分析，数据纳入了 28 名 MSI-H 患者和 34 名 MSS 患者的单细胞转录组数据，从而确定结直肠癌患者对 ICI 敏感性的免疫相关决定因素以及 MSI-H/dMMR 结直肠癌患者可能的免疫治疗耐药机制。聚类分析表明，MSI-H/dMMR 结直肠癌患者中 T 细胞和 NK 细胞的比例较高。在上皮细胞和免疫细胞中都观察到 MSI-H/dMMR 和 MSS/pMMR 肿瘤之间转录组的显著差异。两组的恶性上皮细胞的差异表达基因（DEG）分析显示与抗原呈递过程相关的基因（如 HLA-DRA、HLA-DRB1、CD74、B2M 和 HLA-DPA1）在 MSI-H 患者亚群中显著上调。从而我们建立了基于 MSI-H/dMMR CRCs 恶性上皮细胞中的 19 个 DEGs 的免疫治疗疗效预测模型，并且在公开的 RNA-seq 数据集中显示出准确的 ICI 疗效预测能力（AUC= 0.91）。针对免疫细胞的亚群分析提示在 MSI-H/dMMR CRCs 中，CD8（+）T 细胞、CD4（+） T 细胞、γδT 细胞和 NK 细胞这几个亚群的浸润程度更高。值得注意的是，CD8（+）T 细胞的细胞簇 3 (C3)、C2 和 C1，这些亚群的特点在于其增殖相关特征基因（Ki-67、STMN1、TUBB）、激活相关特征基因（TNFRSF4、TNFRSF18、TNFRSF25）和免疫抑制检查点特征基因（LAG3、TIGIT、PDCD1 和 HAVCR2)在 MSI-H/dMMR CRCs 中的表达显著升高，提示激活的肿瘤免疫微环境能够提高 dMMR 患者对 ICB 的应答。此外，细胞通讯分析表明，PVR-TIGIT 通路是 MSS/pMMR 患者 CD8（+）T 细胞与恶性肿瘤细胞之间的主要相互作用通路。有趣的是，在部分 MSI-H/dMMR CRC 中也发现了 PVR 的高表达。因此，激活的 PVR-TIGIT 通路可能对应着大多数 MSS/pMMR 结直肠癌患者的免疫耗竭状态，这也是部分 MSI-H/dMMR CRCs 可能的耐药机制之一。总之，我们的研究描述了结直肠癌患者中不同细胞亚群的分子特征，并且确定了不同细胞亚群在 MSI-H/dMMR 和 MSS/pMMR 结直肠癌的单细胞转录组及 bulk 转

录组测序水平上的细胞互作网络。同时，我们构建了一个 ICI 疗效预测模型，为结直肠癌患者应用免疫治疗的临床决策提供证据。

关键字：肠癌；单细胞分析；MSI；免疫治疗

680. HSP90α、EBVCA-IgA、EBV DNA 在鼻咽癌诊断及预后相关性研究

崔兆磊、陈燕*

福建省肿瘤医院

目的：探讨热休克蛋白 90α（HSP90α）、EB 病毒衣壳抗原 IgA 抗体（EBVCA-IgA）、EBV DNA 对鼻咽癌(NPC)诊断及预后的价值。

方法：选取福建医科大学附属肿瘤医院 113 例鼻咽癌患者和 40 例健康体检者，采用 ELISA 法检测 HSP90α和 EBVCA-IgA、采用实时定量 PCR 法检测 EBV DNA，分析 HSP90α、EBVCA-IgA、EBV DNA 水平并进行统计分析和临床评价。

结果：NPC 组 HSP90α、EBVCA-IgA、EBV DNA 水平均显著高于健康对照组(t/Z=15.317,11.459,24.261, $P<0.05$)，在 NPC 不同分期的患者中，III 和 IV 期患者的 HSP90α、EBVCA-IgA、EBV DNA 的表达水平均高于 I 和 II 期，IV 期 HSP90α、EBVCA-IgA、EBV DNA 表达水平均明显高于 III 期，差异有统计学意义(Z=5.347,4.768,6.418, $p<0.05$)。采用 ROC 曲线分析 HSP90α、EBVCA-IgA、EBV DNA 水平对 NPC 的预测价值,曲线下面积分别为 0.884 (95% CI 0.832～0.935)、0.841(95% CI0.781～0.901)、0.934(95% CI 0.897～0.970),最佳截断值分别为 121.70 ng/ml, 1.84 S/CO, 2.7×103 copies/ml，联合检测 ROC 曲线下面积最大为 0.954，灵敏度为 92.5%，特异性为 86.0%。预后不良组患者 HSP90α、EBVCA-IgA、EBV DNA 水平均显著高于预后良好组($p<0.05$), Pearson 相关分析显示，NPC 患者 HSP90α与 EBVCA-IgA、EBV DNA，呈正相关(r=0.768，0.873，$p<0.05$)，随访 3 年患者总体生存率,经绘制生存曲线，低 HSP90α、EBV DNA 组患者 3 年总体生存率高于高 HSP90α、EBV DNA 组,差异有统计学意义($\chi2$=9.715,12.805, $P<0.001$)。

结论：HSP90α、EBV DNA 对 NPC 具有较高的诊断价值和预后预测价值，EBV DNA 诊断价值优于 HSP90α、EBVCA-IgA，联合检测诊断价值最高，HSP90α可作为临床治疗监测指标之一，具有较好临床应用价值。

关键字：鼻咽癌；热休克蛋白 90α；EB 病毒衣壳抗原 IgA 抗体；EBV DNA；诊断；预后

681. 基于芯片数据对肝内胆管癌 circRNA 差异表达谱及预后标志物的生物信息学分析

张钰婧*[1]、曹舒清[2]、贾天琪[3]、陈梦[4]、郭晨洁[4]

1. 山西医科大学公共卫生学院

2. 山西医科大学法医学院

3. 山西医科大学药学院

4. 山西医科大学临床医学院

目的：肝内胆管癌是一种常见的原发性肝癌，发病率仅次于肝细胞癌，其发病机制尚不明确且预后极差。circRNA 为一种闭环非编码 RNA，具有重要的基因调控功能，本研究旨在通过生物信息学方法分析肝内胆管癌差异表达的 circRNA，筛选其预后标志物。

方法：通过 GEO 数据库获得肝内胆管癌相关 circRNA 数据集 GSE181523 及 miRNA 数据集 GSE53870，运用 GEO2R 工具筛选差异表达 circRNA。分别选取差异显著的上调及下调 circRNA 各 5 个，利用 circBank 数据库预测与其相结合的 miRNA，并与 miRNA 数据集取交集获得可能与肝内胆管癌进展相关的 miRNA。选取差异显著的 miRNA 使用 TargetScan，miRDB 及 miRWalk 数据库预测靶基因，通过 DAVID 数据库对靶基因进行 GO 注释和 KEGG 富集分析。通过 STRING 构建蛋白互作网络(PPI)，用 Cytoscape 构建 circRNA-miRNA-核心基因调控网络，筛选核心靶基因。在 GEPIA 数据库中验证核心靶基因在肝内胆管癌的表达水平及对患者预后的影响。

结果：共筛选出 374 个差异表达 circRNA，上调 246 个，下调 128 个。通过位点预测网站与数据集取交集后得到 20 个与 circRNA 结合的 miRNA。三个数据库预测得到靶基因 791 个。GO 富集分析结果显示，靶基因主要参与蛋白质磷酸化、RNA 聚合酶 II 启动子对转录的正调控。KEGG 富集分析结果显示，靶基因主要富集在蛋白多糖与癌症、FOXO 信号通路。GEPIA2 分析发现 UBE2W 在肝内胆管癌中呈低表达，与较差预后相关（$p<0.05$）。根据生存分析结果获得与患者预后相关的三条调控网络 hsa_circ_0025332-has_miR_27a_3p-UBE2W，hsa_circ_0025332-has_miR_27b_3p-UBE2W，hsa_circ_0091419-has_miR_145_5p-UBE2W）。

结论：本研究通过生物信息学方法分析鉴定了肝内胆管癌差异 circRNA 及预后标志物，为肝内胆管癌的诊断提供新的生物标志物及潜在药物治疗靶点。

关键字：肝内胆管癌；生物信息学分析；circRNA；预后标志物

682. 白细胞介素 6 在结直肠癌患者中的表达及与肿瘤疗效关系

崔兆磊、陈燕*

福建省肿瘤医院

目的：探讨人白细胞介素 6（Interleukin-6，IL-6）在结直肠癌患者中的表达及意义。

方法：收集 132 例首诊结直肠癌患者（CRC）、34 例肠道良性疾病患者(CBD)及 84 例表观健康体检者(HC)血清,采用电化学发光双抗体夹心免疫分析法（ECLIA）检测血清中白细胞介素 6（IL-6）及癌胚抗原（CEA）含量，分析 IL-6 水平与结直肠癌患者临床病理特征的相关性；应用受试者工作特性曲线（ROC）和二元 Logistic 法回归分析 IL-6 和 CEA 两指标对结直肠癌的诊断价值；对随访资料完整的 120 例结直肠癌患者动态观察治疗前后血清 IL-6 和 CEA 水平，分析两指标与肿瘤疗效的关系。

结果：结直肠癌患者血清 IL-6 水平显著高于肠道良性疾病组(P<0.01)和健康对照组(P<0.01)，结直肠癌患者血清 CEA 水平显著高于肠道良性疾病组(p<0.05)和健康对照组(P<0.01),差异均有统计学意义。CRC 患者血清 IL-6 水平与肿瘤直径、分化程度、组织类型、淋巴结转移、远处转移、TNM 分期均显著相关(p<0.05)，而与年龄、性别及肿瘤发生部位无明显相关。IL-6 诊断结直肠癌的灵敏度（72.7%）和准确性（78.6%）均高于 CEA(分别为 68.2%和 77.9%，特异性（85.2%）低于 CEA（88.9%），两指标联合检测能够提高灵敏度（97.2%）和准确性（85.6%）。结直肠癌肿瘤控制组(CR+PR+SD)治疗后两指标均较治疗前有显著下降(p<0.05)，差异有统计学意义，而肿瘤进展组(PD)治疗后两指标均未显著下降(P>0.05)。

结论：IL-6 和 CEA 两指标联合检测有助于结直肠癌的诊断和疗效观察。

关键字：结直肠癌、白细胞介素 6、癌胚抗原

683. 鼻咽癌患者血浆外泌体 miR-BART 水平与临床转移之间的关系

崔兆磊、陈燕*

福建省肿瘤医院

目的：检测鼻咽癌患者血浆外泌体中 miR-BART 的含量，分析和鼻咽癌 miR-BART 的表达和患者临床病理参数之间的相关性，探讨它在 NPC 侵袭转移过程中的作用。

方法：收集 24 对鼻咽癌患者的配对血浆（治疗前和发生转移时总共 48 份血浆）和 12 名健康人的血浆，通过 exoRNeasy 血清/血浆 Maxi 试剂盒对鼻咽癌患者血浆中外泌体和外泌体中总 RNA 的提取。再通过 TaqMan MicroRNA 逆转录试剂盒进行多重 RT-PCR 完成 60 份标本的 miR-BART3、miR-BART7 和 miR-BART13 的检测。用 SPASS13.0 进行数据分析，探讨鼻咽癌患者血浆外泌体中 miR-BART 的表达水平与鼻咽癌临床病理参数(年龄、远处转移和临床分期)之间和复发转移的关系。

结果：血浆外泌体中的 miR-BART3 和 miR-BART7 对鼻咽癌有诊断意义，诊断的准确率为 0.794 和 0.817（95%置信区间分别为：0.641-0.946 和 0.671-0.964）；血浆外泌体中的 miR-BART13 在 NPC 组合健康对照组间不存在相关性。不同性别血浆外泌体中的 miR-BART3、miR-BART7、miR-BART13 表达量无差别；血浆外泌体中的 BART7、BART13 表达水平与年龄不存在相关性，但年龄大于 50 岁患者血浆外泌体中的 BART3 呈现高表达；BART7 与 T 分期、N 分期、临床分期均无相关性；而 BART13 与 T 分期、N 分期及临床分期都存在相关性，但由于其表达量很低，因此无意义；BART3 则与 N 分期存在较强相关性，但是随着 N 分期越晚，miR-BART3 表达量增加。

结论：miR-BART3 和 miR-BART7 对鼻咽癌有诊断意义，诊断的准确率分别为 0.794 和 0.817；转移前后的 miR-BART3 表达量有较大差别，但二者在统计学上的差异并不十分显著；miR-BART3 在 50 岁以上的鼻咽癌患者中高表达，且二者存在相关性；miR-BART3 则与 N 分期存在较强相关性，随着 N 分期越晚，miR-BART3 表达量增加。

关键字：鼻咽癌；血浆外泌体；miR-BART；转移

684. 藤黄酸下调蛋白 C 受体对 MDA-MB-231 细胞增殖的抑制作用

李溯、杨蕊、陈道桢*

南京医科大学附属无锡妇幼保健院

目的：探究藤黄酸影响蛋白 C 受体 PROCR 对三阴性乳腺癌细胞 MDA-MB-231 增殖凋亡的影响及其机制。

方法：以 MDA-MB-231 细胞为研究对象，采用 CCK8 法评估藤黄酸对 MDA-MB-231 细胞的增殖影响，并计算其 IC50 值。使用倒置显微镜观察不同浓度藤黄酸对 231 细胞形态影响。利用网络药理学和 KEGG 信号通路分析筛选藤黄酸可能的作用靶点及其相关信号通路，并进行作用机制研究。利用 Western blot 实验分析藤黄酸对 PROCR、Akt 和 p-Akt 蛋白表达水平影响，qPCR 实验验证不同浓度藤黄酸对 PROCR 基因水平情况。采用 TUNEL 法评估藤黄酸对 231 细胞凋亡的影响。

结果：经不同浓度藤黄酸作用 231 细胞 24 小时后，发现藤黄酸对 231 细胞具有显著的增殖抑制作用，呈现浓度依赖性，其 IC50 为 1.78 μM。经倒置显微镜观察显示，相较对照组梭形 231 细胞，实验组 231 细胞逐渐皱缩变圆，胞质凝缩，并与其周围细胞分离，细胞贴壁性下降；通过网络药理学筛选证实，PROCR 是藤黄酸的作用靶点之一，经 KEGG 信号通路分析，PI3K-Akt 信号在藤黄酸药物作用中发挥重要作用。通过 Western blot 实验证实，藤黄酸可以下调 PROCR、p-Akt 蛋白表达，但不影响 Akt 蛋白的表达；qPCR 实验也从基因层面证实藤黄酸可以降低 PROCR 基因表达水平，差异具有统计学意义（$p<0.05$）。经 TUNEL 法检测证实，随藤黄酸浓度增加，231 细胞凋亡率明显增加。

结论：藤黄酸下调 PROCR 影响 MDA-MB-231 细胞的增殖并诱导其凋亡，其可能作用机制和 PI3K-Akt 通路密切相关。

关键字：藤黄酸；乳腺癌；增殖；凋亡；作用机制

685. 肿瘤外泌体检测新策略研究

梁君婷[1]、朱晓娴[1]、陈慧芝[1]、周清[1,2]、周郁斌*[1]

1. 广东医科大学

2. 广州中医药大学

研究目的: 外泌体（exosomes）是一种由细胞分泌的、具有脂质结构的细胞外微囊泡，包含蛋白质、脂质、核酸等生物分子，存在于各种体液中。外泌体可携带供体细胞中的一些物质，被认为是细胞间通讯和物质交换的重要载体，可通过直接或间接的形式调控细胞的功能和生物学行为。研究表明，外泌体参与肿瘤疾病的发展进程，可作为肿瘤的无创液体活检中重要的标志物，其分析检测方法的建立具有重要意义。本研究旨在开发一种动力学型荧光生物传感器，对肿瘤外泌体进行便捷、快速地分析检测。

材料与方法: 本研究通过“一步法”制备动力学型生物传感器；另一方面，通过经典超高速冷冻离心法提取肿瘤外泌体。通过生物传感器与肿瘤外泌体的特异性结合，在一定波长的光激发下，收集其荧光变化信号，进而计算其表观荧光动力学参数，从而实现外泌体的检测并进行定性定量分析。

结果: 表征数据显示动力学型生物传感器和肿瘤外泌体已成功制备。该传感器性能考查结果表明，其对肿瘤外泌体具有较好的响应，表观荧光衰减动力学参数变化较为明显，有一定检测外泌体的能力。进一步研究表明，该传感器在肿瘤外泌体的检测中具有较好的线性关系及检测限。

结论: 本研究构建了一种用于肿瘤外泌体检测的基于荧光动力学的生物传感器。该生物传感器对外泌体表现出较好的检测效果，有望成为一种用于肿瘤疾病早期诊断和进程监测的液体活检新方法。

关键字: 荧光衰减；生物传感器；肿瘤外泌体；肿瘤标志物

686. 乳酸脱氢酶 C4 在肺腺癌中的表达及意义

崔兆磊、陈燕*

福建省肿瘤医院

目的: 探讨 LDH-C4（lactate dehydrogenase C4）在肺腺癌中的表达及其与患者预后的关系。

方法：基于高通量肺腺癌组织芯片 HLugA180Su05，通过免疫组化技术检测 92 例肺腺癌患者癌组织及对应癌旁组织中 LDH-C4 蛋白的表达水平，分析 LDH-C4 蛋白在肺腺癌中的表达量及其与临床病理特征和预后的关系。

结果： LDH-C4 在癌组织中阳性表达率为 96.7%（89/92），明显高于癌旁组织 22.6%（19/84）（P<0.001），癌组织中 LDH-C4 阳性表达与患者年龄、性别、肿瘤大小、淋巴结转移、临床分期、表皮生长因子受体基因（EGFR）突变无关（均 P>0.05）。LDH-C4 高表达组患者中位生存时间（OS）为（35 个月），显著低于低表达组（62 个月）（p<0.05）；LDH-C4 高表达组患者 5 年生存率为（24.0%）显著低于低表达组（53.3%），进一步 COX 多因素回归分析显示 LDH-C4 高表达是肺腺癌患者总 OS 的独立因素，LDH-C4 高表达是低表达患者死亡风险的 3.619 倍。

结论: LDH-C4 在肺腺癌中的表达水平升高，LDH-C4 高表达肺腺癌患者的预后负相关，可成为肺腺癌患者潜在的治疗靶点。

关键字: 肺腺癌；LDH-C4；预后

687. 乳酸脱氢酶 C4 在肝癌中的表达及其生物学功能研究

崔兆磊、陈燕*

福建省肿瘤医院

目的: 通过分析乳酸脱氢酶 C4(LDH-C4)在(HCC)中的表达及其与 HCC 患者的临床病理特征及其预后的关系,明确 LDH-C4 过表达对 HCC 细胞 Bel-7402 的细胞生物学行为能力的影响，并探讨相关分子机制。

方法：基于高通量肝癌组织芯片，采用免疫组化染色技术检测 HCC 癌组织中 LDH-C4 蛋白的表达水平，分析 LDH-C4 表达情况与肝癌患者临床病理特征的关系。荧光显微镜观察 GV492-LDHC 病毒感染后的 Bel-7402HCC 细胞中 EGFP 表达情况，筛选 LDH-C4 表达呈阳性的细胞系。通过 RT-qPCR 鉴定 LDH-C4 mRNA 过表达的效果。通过 CCK-8 实验、划痕修复实验及 Transwell 小室等实验分别检测 LDH-C4 对 HCC 细胞 Bel-7402 在体外的增殖、迁移及侵袭能力的影响。基于建立的 LDH-C4 稳定过表达的 Bel-7402 细胞系基础上，对各组细胞中乳酸、丙酮酸等细胞能量代谢产物含量进行检测，同时检测各组肿瘤细胞中葡萄糖消

耗水平，探究 LDH-C4 过表达对 Bel-7402HCC 细胞能量代谢的影响；通过 Western blot 实验检测 AKT/mTOR 信号通路中相关蛋白表达水平受 LDH-C4 过表达的影响。

结果: HCC 中的 LDH-C4 呈现高表达状态，主要表达于 HCC 细胞的细胞质中，且 LDH-C4 的表达水平与 HCC 患者的 T 分期、临床分期及瘤体大小明显相关（p<0.05）；生存分析结果提示：LDH-C4 高表达患者的预后较低表达者更差（p<0.05）。CCK-8 实验、划痕修复实验及 Transwell 小室实验检测结果提示：LDH-C4 过表达可提升 Bel-7402HCC 细胞在体外的迁移侵袭能力，但对生长增殖无明显影响。3.能量代谢实验结果显示：Bel-7402 细胞中 LDH-C4 过表达可提高乳酸产生含量，降低丙酮酸含量，提高细胞对葡萄糖的利用；Western blot 结果提示：过表达 LDH-C4 可上调 AKT/mTOR 信号通路中 AKT 蛋白及 mTOR 蛋白的表达。

结论: HCC 组织中 LDH-C4 呈现较高表达状态，与 HCC 患者的肿瘤大小、T 分期以及临床分期呈现明显正相关；LDH-C4 可作为 HCC 患者预后监测的一项重要参考指标。Bel-7402HCC 细胞中 LDH-C4 过表达可促进该细胞在体外的迁移和侵袭能力,促进 Bel-7402HCC 细胞的能量代谢水平，可能与 AKT/mTOR 信号通路的激活有关。

关键字: 乳酸脱氢酶 C4, HCC, 增殖, 迁移, 侵袭, 机制

688. 治疗前异常凝血酶原血清水平与原发性肝癌预后相关性研究

崔兆磊、陈燕*

福建省肿瘤医院

目的：探讨治疗前异常凝血酶原（PIVKA-II）血清水平在原发性肝癌预后中的临床应用价

方法：收集 2013 年 12 月至 2014 年 3 月福建省肿瘤医院连续收治的 100 例未经治疗的肝细胞癌患者入院时血清样本，用化学发光免疫技术检测 PIVKA-II血清水平。收集患者临床资料，同时对患者每隔三个月至半年进行随访，对随访结果结合临床资料，运用 X-tile 软件确立 PIVKA-II对总生存期的最佳截断值，并用 SPSS16.0 软件包进行生存分析。

结果：截至 2017 年 3 月，100 例患者中位生存时间为 4.1 个月，3 年生存率为 20%。X-tile 软件确立 PIVKA-II对总生存期的最佳截断值为 55859mAU/ml，PIVKA-II>55859 mAU/ml 的患者 17 例（占总人数的 17%），中位生存期为 2.0 个月，与 PIVKA-II≤55859 mAU/ml 组相

比（中位生存期为 5.6 个月），差异有统计学意义（*P*=0.000）。PIVKA-II的表达与总胆红素、腹水、肿瘤直径和门脉癌栓呈正相关。单因素分析显示治疗前 PIVKA-II表达、发现肿瘤途径、肝功能生化指标、腹水、CH 分级、侵犯肝被膜、肿瘤大小、肿瘤数量、临床分期、门脉癌栓、下腔静脉癌栓、远处转移以及治疗方式是患者总体生存率的影响因素。多因素分析显示治疗前 PIVKA-II高表达（OR=5.405；95%CI： 0.219-0.879， *P*=0.020），下腔静脉癌栓和远处转移是患者预后较差的独立预测因素

结论：治疗前血清 PIVKA-II 水平可作为肝癌预后标志物，治疗前 PIVKA-II 高表达提示不良预后。

关键字：原发性肝癌；预后；异常凝血酶原；生存率

689. 肿瘤睾丸相关抗原 LDH-C4 在鼻咽癌中的表达及其功能研究

崔兆磊、陈燕*

福建省肿瘤医院

目的：研究乳酸脱氢酶 C4（LDH-C4）蛋白在鼻咽癌组织中的表达情况以及在临床诊疗过程中的价值。明确 LDHC 基因过表达在 CNE2 鼻咽癌细胞的生物学作用，并初步探讨相关分子机制。

方法：通过免疫组化染色方法检测高通量鼻咽癌组织芯片中 LDH-C4 蛋白的表达量，根据染色的结果进行评分，分析鼻咽癌患者的临床和病理分期、转移、复发及预后等临床病理特征和 LDH-C4 蛋白表达的高低的相关性。通过慢病毒载体将外源性 LDHC 基因导入 CNE2 鼻咽癌细胞，并采用稀释法结合绿荧光表达情况筛选出单克隆化且 LDH-C4 表达阳性的细胞系。通过 CCK-8 比色、平板克隆形成、划痕修复实验、Transwell 小室等实验，研究 LDH-C4 表达上调后，CNE2 鼻咽癌细胞在体外增殖能力、迁移和侵袭能力的改变；通过 Western blot 检测 AKT/mTOR 信号转导通路相关蛋白的表达改变。

结果：129 例高通量鼻咽癌组织标本结果显示：LDH-C4 主要表达于鼻咽癌细胞的细胞质中，阳性率为 88.4%（114/129）；Spearman 相关性分析结果表明，鼻咽癌的临床分期、颈部淋巴结转移均与 LDH-C4 的表达水平呈正相关（$P<0.05$）；Kaplan-Meier 生存分析表明，LDH-C4 低水平患者预后明显优于高水平患者（$P<0.05$）。CCK-8 比色实验、克隆形成、划痕实验、

基质胶 Transwell 小室等一系列实验，证明 LDH-C4 过表达可增强 CNE2 鼻咽癌细胞的生长增殖、克隆形成以及侵袭和迁移能力；Western blot 结果证实，LDH-C4 在 CNE2 细胞中过表达可上调 AKT、mTOR 等蛋白的表达。

结论：LDH-C4 蛋白在鼻咽癌组织中的表达量明显增高，并与患者的临床分期、颈部淋巴结转移呈现正相关关系；LDH-C4 可作为鼻咽癌预后监测的一项重要指标，其高表达提示患者临床预后不良。上调 LDH-C4 可明显增强 CNE2 细胞体外增殖、侵袭及迁移能力，可能通过激活 AKT/mTOR 信号通路起作用。

关键字：鼻咽癌，LDH-C4，CNE2，侵袭转移，机制

690. 综合多组学数据探析 TXNIP 在胰腺癌中的表达及临床意义

陈梦*[1]、曹舒清 [2]、张钰婧 [3]、郭晨洁 [1]、胡培婷 [1]、李晓鑫 [4]

1. 山西医科大学临床医学院

2. 山西医科大学法医学院

3. 山西医科大学公共卫生学院

4. 山西医科大学医学影像学院

目的：胰腺癌(pancreatic adenocarcinoma，PAAD)是消化系统的高度恶性肿瘤，总体五年生存率仅 6%，具有发病隐蔽、预后差和死亡率高等特点。硫氧还蛋白相互作用蛋白(TXNIP)是一种与氧化还原稳态密切相关的代谢蛋白，已被指出与多种恶性肿瘤发生发展密切相关。但 TXNIP 在 PAAD 中的作用尚不明确。本文旨在利用生物信息学方法，探究 TXNIP 在 PAAD 中的表达水平及其与临床分期、预后和免疫浸润的关系，以期为 PAAD 的早期诊断和临床治疗提供参考。

方法：利用 GEPIA 数据库研究 TXNIP 在泛癌中的表达水平，结合 TCGA 和 GTEx 数据库分析 TXNIP 在 PAAD 组织中的表达情况及预后相关性。再通过 CPTAC 数据库分析 TXNIP 蛋白在 PAAD 组织中的表达，并利用 HPA 数据库辅以免疫组化验证。从 GEO 数据库获取 PAAD 相关数据集 GSE62452 和 GSE28735，利用独立样本 T 检验验证 TXNIP mRNA 在 PAAD 组织中的表达情况，并绘制受试者工作（ROC）曲线。然后利用 UALCAN 数据库分析 TXNIP 表达与性别、年龄、肿瘤分期、分级等临床特征的关系。再通过 cBioportal 平台分析 TXNIP

在 PAAD 患者中的变异情况，结合 MethSurv 数据库探究 TXNIP 甲基化水平对 PAAD 患者的预后影响，并使用 TIMER2.0 分析 PAAD 组织 TXNIP 表达与免疫细胞浸润的相关性。通过 miRDB 和 miRWalk 数据库挖掘出调控 TXNIP 异常表达的上游 miRNA，导入 miEAA 数据库进行生物富集分析，最后利用 CancerMIRNome 数据库筛选核心 miRNA。

结果：泛癌分析显示，TXNIP 在 PAAD、多形性胶质母细胞瘤和脑低级别胶质瘤中显著上调表达，并且与 PAAD 患者较差预后相关（p<0.05）。CPTAC 数据库和免疫组化结果均表明，相较正常组织 TXNIP 蛋白在癌组织中高水平表达。GEO 数据集验证结果与 TCGA 相同，并且 TXNIP 可以较好地区分 PAAD 患者（AUC＝0.726）。另外，TXNIP 表达水平还与肿瘤分期分级有关，且在 40-80 岁高年龄组表达差异显著，但与性别、饮酒习惯、糖尿病程度、慢性胰腺炎、淋巴结转移等无关。癌症基因组学分析结果显示，来自 UTSW 和 TCGA 数据库的 294 例 PAAD 组织样本中有 18 例 TXNIP 发生变异，总变异率为 6.12%，其中 94%为基因扩增。TXNIP 的高甲基化使 PAAD 患者有着更差的预后（P<0.01）。免疫浸润分析结果显示，TXNIP 与 $CD8^+$T 细胞、$CD4^+$T 细胞、B 细胞、中性粒细胞、巨噬细胞、树突状细胞浸润均呈正相关，预示其可能与 PAAD 肿瘤微环境关系密切。通过筛选共获得 20 条 TXNIP 的上游调控 miRNA，其主要富集于肿瘤细胞反应、聚糖降解和 Cul2-RING 泛素连接酶复合物等生物功能。其中 hsa-miR-524-5p 在 PAAD 中显著下调表达，且其也可以较好的区分 PAAD 患者（AUC＝0.730）。

结论：TXNIP 在 PAAD 中上调表达，且可能通过影响肿瘤微环境干预患者预后，以 hsa-miR-524-5p 为核心的上游调控 miRNA 同样与肿瘤细胞关系紧密，是潜在的生物标志物。

关键字：胰腺癌，硫氧还蛋白相互作用蛋白，表达预后，免疫浸润，生物标志物

691. 急性淋巴细胞白血病化疗所致肺部罕见致病菌感染一例并文献复习

杨美、余枝娟、朱梅、包宇航、简亿*

遵义医科大学附属医院

目的：探讨急性淋巴细胞白血病（ALL)患者使用免疫抑制剂后致肺部罕见致病菌感染的临床特征，以提高临床医师对该类疾病的认识。

方法：回顾性分析我院收治的 1 例确诊为 ALL 化疗所致肺部罕见致病菌感染患者的临床特点、辅助检查及诊疗并进行文献复习。

结果：患者女，51 岁，因“乏力 6 月余”入院。入院后完善骨髓病理提示骨髓增生活跃（约>90%），幼稚阶段细胞增生，各阶段粒、红及淋巴细胞散在分布，纤维组织增生。骨髓活检组织象检查考虑急性淋巴细胞白血病伴纤维组织增生可能性大。白血病免疫分型检测及流式细胞学检测提示普通-B-ALL；基因检测报告提示 FLT3 基因、ETV6 基因阳性。91 种白血病基因检测提示 EP300-ZNF384 阳性。诊断为急性淋巴细胞白血病，予 DVCLP（柔红霉素 60mg+环磷酰胺 1.1g+培门冬梅 3750u+地塞米松 10mg）方案治疗，化疗 1 次后出现咳嗽、咳痰、发热等不适，完善痰液涂片提示 G+球菌阳性，血细菌培养（需氧）提示沃氏葡萄球菌感染，痰培养提示肺炎克雷伯杆菌感染，予万古霉素 1g 1 次/12 小时、左氧氟沙星 0.5g 1 次/日抗感染治疗后患者无发热，咳嗽、咳痰明显好转。

结论：急性白血病是一种常见恶性血液性疾病，其中 ALL 是最常见的类型， ALL 患者伴不同程度的免疫功能低下，而化疗加重了此种状态，易致机会性感染，在临床工作中遇到恶性肿瘤化疗患者出现发热、咳嗽、咳痰等感染症状时，需考虑化疗后机体免疫力低下所致病原菌感染，需及时完善痰培养，血培养、胸部 CT 等检验检查，必要时完善 NGS 检查、支气管镜检查明确感染病原菌。治疗上可根据菌培养结果选择敏感抗生素，预后需根据合并基础疾病综合评估。

关键字：急性淋巴细胞白血病；免疫抑制；机会性感染

692. POLE/POLD1 突变对结直肠癌影响的生物信息学分析

赵龙、杨长江、叶颖江、申占龙*

北京大学人民医院

目的：利用生物信息学方法对结直肠癌（CRC）中的 DNA 聚合酶ε（POLE）和 DNA 聚合酶δ1（POLD1）的突变情况进行分析，并探索其对 CRC 的预后以及免疫治疗的影响

方法：基于 TCGA 数据库的数据集，利用 cBioPortal 工具对所有癌症中的 POLE/POLD1 的改变及其预后进行分析，利用 MSIsensor、MINTIS 两种评分系统对 POLE/POLD1 野生型和突变型的 CRC 患者微卫星不稳定性（MSI）进行评价，最后利用 TIMER 数据库分析 CRC 的免疫细胞浸润以及免疫检查点表达与 POLE/POLD1 突变之间相关性。

结果：在 CRC 中 POLE/POLD1 基因的改变频率为 6%，且均为错义突变为主，在泛癌中 POLD1 的突变后患者无进展生存期(P<0.001)、无病生存期(P<0.001)及疾病特异性生存期(P=0.0178)均显著延长，CRC 中 POLE/POLD1 的突变与微卫星不稳定性、免疫检查点的表达以及 CD8+ T 细胞等免疫细胞的浸润相关。

结论: POLE/POLD1 基因的改变在 CRC 中较为常见，在泛癌中 POLD1 的突变与患者预后相关。POLE/POLD1 基因突变后可能造成微卫星不稳定性增高、免疫检查点的表达上调和免疫细胞浸润程度增加，可能成为免疫治疗的新靶点。

关键字: POLE 突变、POLD1 突变；结直肠癌；生物信息学；免疫

693. PRELP 通过激活整合素β3-FAK-AKT 通路促进淋巴结转移并可作为结直肠癌的预后生物标志物

张富强、包博文、曲秀娟、邢承忠、车晓芳*

中国医科大学附属第一医院

背景：结直肠癌(CRC)是一种常见的胃肠道恶性肿瘤，其发病率和死亡率位居全球各类肿瘤第三位。淋巴结转移是结直肠癌远处转移的主要途径，也是导致患者不良预后的关键因素。因此，筛选 CRC 淋巴结转移的生物标志物，并探索其分子机制，对于精准预测 CRC 患者预后、寻找新的治疗策略具有重要的意义。

研究方法：利用 R 语言筛选出与淋巴结转移阳性和不良预后相关的基因， GO 富集分析结合 GSE17536 数据集验证得到新的淋巴结转移标志物。运用免疫组化检测肠癌组织中 PRELP 蛋白的表达。利用 logistic 单因素及多因素分析研究与 PRELP 有关的参数。transwell 实验检测细胞迁移及侵袭能力、人淋巴内皮细胞(hLECs)成管及迁移实验和小鼠腘窝淋巴结转移模型来评估淋巴管新生能力。免疫共沉淀（co-IP）和 western blot 实验检测 PRELP 的互作蛋白及对下游通路的影响

结果：1. PRELP 在淋巴结转移的 CRC 患者组织中显著上调，并与 CRC 的淋巴结转移呈正相关，是肠癌的独立预后危险因素。2. PRELP 显著促进肠癌细胞的迁移及侵袭，增强淋巴管内皮细胞的管形成和迁移能力。3. 裸鼠淋巴结转移模型显示，过表达 PRELP 显著促进了 CRC 发生淋巴结转移。4. PRELP 分泌至肠癌细胞培养上清中，且在肠癌细胞及 hLECs 中均可与整合素β3 结合，激活 FAK-AKT 通路。

结论：PRELP 可通过激活整合素β3-FAK-AKT 通路促进肠癌细胞转移及淋巴管新生，导致肠癌不良预后。本研究鉴定出 CRC 淋巴结转移相关预后标志物 PRELP，为 CRC 患者提供了新的潜在治疗靶点。

关键字：肠癌，淋巴结转移，生物标志物，PRELP

694. 丝氨酸棕榈酰转移酶长链碱性亚基 1 通过调控有丝分裂灾难促进胃癌细胞增殖的机制研究

车晓芳、郑雪莹、刘云鹏*

中国医科大学附属第一医院

目的：通过代谢组学筛选胃癌中活跃的代谢通路，并探讨该途径关键酶的代谢相关“经典”作用及非代谢依赖途径的“非经典”作用在胃癌中的作用及机制。

方法：1、基于 UPLC-MS/MS 平台进行胃癌患者的癌和癌旁组织代谢组学分析；2、在线数据分析 SPT 酶亚基在胃癌组织及癌旁组织中的表达；3、qRT-PCR 和 Western Blot 实验验证胃癌细胞系中 SPTLC1 和 SPTLC2 的表达及转染效率；4、MTS 法和集落形成实验检测细胞增殖能力变化；5、裸鼠皮下成瘤模型进行体内验证，免疫组化检测相关指标的表达；6、利用 GSEA 预测胃癌中 SPTLC1 高表达的相关通路； 7、流式细胞术检测细胞周期；8、免疫共沉淀结合质谱分析筛选 SPTLC1 互作蛋白并验证；9、免疫荧光实验检测细胞内 SPTLC1 与纺锤体、KIF4A、PRC1 的共定位情况。

结果：1、人胃癌组织中鞘脂代谢产物升高、鞘脂代谢关键酶丝氨酸棕榈酰转移酶长链碱性亚基 1(SPTLC1)高表达。2、沉默 SPTLC1 后胃癌细胞增殖减弱、鞘脂代谢产物减少，但外源性补充鞘脂代谢产物仅部分回复沉默 SPTLC1 导致的增殖抑制。3、GSEA 分析显示 SPTLC1 高表达富集到 G2M 检查点等有丝分裂相关通路，敲减 SPTLC1 后胃癌细胞周期阻滞到 G2/M 期并发生有丝分裂灾难；4、SPTLC1 与纺锤体共定位、且敲减 SPTLC1 后 KIF4A 与 PRC1 结合减少发生有丝分裂灾难。5、敲减 SPTLC1 提高胃癌细胞对紫杉醇的敏感性。

结论：1、胃癌中 SPTLC1 高表达通过增强鞘脂合成代谢的代谢依赖途径轻度促进胃癌细胞增殖；2、沉默 SPTLC1 通过抑制 KIF4A 与 PRC1 结合诱导有丝分裂灾难而抑制胃癌细胞有丝分裂；3、SPTLC1 高表达降低胃癌细胞对紫杉醇的敏感性。

关键字：胃癌，丝氨酸棕榈酰转移酶长链碱性亚基 1，有丝分裂灾难

695. 基于肿瘤进化轨迹的染色质不稳定亚型胃癌免疫治疗获益人群特征鉴定

杨宇竞、车晓芳、刘云鹏*

中国医科大学附属第一医院

目的：染色质不稳定（CIN）亚型胃癌对免疫治疗应答普遍较差，但有极少数患者仍可从免疫治疗中获益。因此，本研究旨在识别可能对免疫治疗获益的 CIN 亚型胃癌的生物学特征。

材料方法：基于半监督机器学习法构建 TCGA 胃癌分子分型分类器后，以 TCGA 队列为参考，对包含 13 个队列的 GEO-meta 队列中 1075 例胃癌样本进行了 CIN 分子亚型的预测及再划分，并基于 singleR 算法对 GSE183904 中的 13 名 CIN 亚型胃癌患者的上皮细胞进行分子亚型的预测。使用流形学习算法，基于亚型特征基因的表达水平构建 CIN 亚型胃癌的肿瘤进化模型。使用 TIDE 算法和 submap 算法预测 CIN 亚型胃癌样本的免疫检查点抑制剂（ICB）应答水平。使用 cibersort 算法、细胞通讯分析和加权基因共表达网络分析评价 CIN 亚型胃癌样本的免疫浸润水平。基于核回归识别影响 CIN 亚型胃癌向不同免疫浸润方向进化的关键突变。

结果：我们发现 CIN 亚型胃癌具有异质性，其中一小部分 CIN 胃癌的肿瘤微环境特征与 MSI 肿瘤类似，可能对 ICB 治疗有应答。这部分患者的肿瘤微环境有更丰富的激活且未耗竭 CD8+T 细胞和 CD4+T 细胞浸润，CD8+T 细胞与恶性上皮细胞的 MHC-I 通讯更紧密，表现为炎性通路激活的非抑制性免疫微环境，并伴随更高水平的肿瘤突变负荷。我们进一步筛选出 ARID1A 和 LRRK2 基因突变，可能作为反映 CIN 亚型胃癌免疫激活和预测 ICB 治疗获益的生物标志物。

结论：少数 CIN 亚型胃癌患者在肿瘤进化过程中能够获得对 ICB 获益的生物学特征，表现为炎性微环境及以 ARID1A 和 LRRK2 为关键突变的特征。

关键字：胃癌，染色质不稳定，免疫检查点抑制剂，肿瘤微环境，基因突变

696. 细胞表面糖蛋白 Trop-2 病毒样颗粒中整合免疫佐剂 CD40 配体后增强病毒样颗粒抵抗肺癌免疫原性的研究

王希*、刘昕阳

空军军医大学唐都医院

细胞表面糖蛋白 Trop-2 在包括肺癌在内的各种癌症中过度表达，已被作为有效的免疫治疗靶点。CD40 配体 (cd40L) 是肿瘤坏死因子超家族成员，是一种很有应用价值的免疫佐剂。基于人类免疫缺陷病毒 (HIV) gag 蛋白的病毒样颗粒 (VLP) 具有较高免疫原性，并且可以将外来抗原掺入其包膜上用于肿瘤疫苗的研发。在本研究中，应用杆状病毒 Bac-to-Bac 表达系统构建了基于 Trop-2、cd40L 和 gag 的重组杆状病毒，杆状病毒以不同组合感染 TN5 昆虫细胞后形成了 Trop-2 VLP 或 Trop-2-CD40L VLP。使用透射电镜和 WB 方法对 VLP 进行鉴定。Trop-2 VLP 或 Trop-2-CD40L VLP 分别免疫 c57BL/6 小鼠，免疫后小鼠表现出较强的体液和细胞免疫反应，而与免疫 Trop-2 VLP 的小鼠相比，免疫 Trop-2-CD40L VLP 的小鼠表现出更强的免疫反应。另外，与 Trop-2 VLP 免疫相比，Trop-2-CD40L VLP 免疫能更显著地提高 Lewis 肺癌细胞荷瘤小鼠的存活率并更有效地减缓了肿瘤生长。总之，本研究提供了一种基于 Trop-2 肿瘤抗原和 CD40L 免疫佐剂相结合的新型病毒样颗粒疫苗设计，也许可作为肺癌免疫治疗中的替代疗法进行选择。

关键字：Trop-2, CD40 配体, 肺癌, 病毒样颗粒

697. 病理纤维化中 CCL19/21+肥大细胞对 CCR7+成纤维细胞/成纤维细胞募集的调控

张香梅、单保恩、刘运江*

河北医科大学第四医院

背景：慢性组织纤维化是结缔组织疾病和恶性肿瘤的常见病理特征。然而，组织定植免疫细胞在成纤维细胞迁移中的作用机制的细节尚不清楚。

材料方法：本研究选取结缔组织病组织标本和实体瘤标本，观察肥大细胞与间质纤维化的关系及肥大细胞的表达特征，为肥大细胞诱导成纤维细胞迁移的机制提供依据。

结果：我们的数据表明，在疾病组织纤维化中，肥大细胞的激活可能会增加组织中趋化因子的表达，尤其是 CCL19，从而诱导大量 ccr7 阳性的成纤维细胞/纤维细胞迁移到特定的组织。**结论：**我们的实验证据表明，在疾病组织纤维化中，肥大细胞的激活可能会增加组织中趋化因子的表达，尤其是 CCL19，从而诱导大量 ccr7 阳性的成纤维细胞/成纤维细胞迁移到特定的组织。这为组织纤维化的发生奠定了基础。

关键字：CCR7; CCL19; fibrosis; fibrocyte

698. 基于唾液基因组学的胰腺癌相关生物标志物筛选及免疫细胞浸润分析

曹舒清*[1]、陈梦[2]、胡培婷[2]、贾天琪[3]

1. 山西医科大学法医学院

2. 山西医科大学临床医学院

3. 山西医科大学药学院

目的：唾液生物标志物已被证明与人体免疫、代谢等生理活动密切相关，无创、准确度高和成本低等优点推动了其在肿瘤早筛及辅助诊断领域的发展。但有关胰腺癌（pancreatic adenocarcinoma，PAAD）的唾液相关标志物研究目前仍然较少，故本研究从唾液基因组学出发分析筛选相关标志物，从而为 PAAD 早期筛查提供参考。

方法：从 GEO 数据集 GSE14245 获取 PAAD 患者与正常人唾液差异表达基因（DEGs），利用 DAVID 数据库对 DEGs 进行生物富集分析。通过 ImmuCellAI 算法分析 PAAD 患者与正常人唾液基因的免疫细胞相关性。利用 STRING 数据库进行蛋白互作分析，并使用 Cytoscape 软件的 MCODE 和 CytoHubba 插件筛选 Hub 基因，通过 TCGA、GTEx 数据和 GSE28753、GSE16515 数据集验证 Hub 基因在 PAAD 组织中的表达水平，并结合 GEPIA、Kaplan-Meier Plotter 在线平台和 TIMER2.0 数据库分析其生存预后和免疫细胞浸润相关性。利用包含 69 名 PAAD 和 61 名正常胰腺组织的数据集 GSE62452 绘制 Hub 基因受试者工作（ROC）曲线并计算曲线下面积（AUC）。最后通过 COMPARTMENTS 数据库对 Hub 基因进行亚细胞定位。

结果：共获得 293 个差异表达基因，其中上调基因 198 个，下调基因 95 个。生物富集分析显示，DEGs 主要与细胞迁移、ECM-受体相互作用、整合素介导的信号通路和 T 细胞受体

信号通路等生物机制有关。免疫算法分析显示，与正常人唾液基因相比，PAAD 患者唾液基因与 nTreg 细胞呈负相关（$P<0.05$）。经过算法筛选，共获得 5 个 Hub 基因（SPP1、COL1A1、ITGB3、ITGA2B 和 ENG），经表达验证显示，SPP1、COL1A1、ITGB3 和 ENG 在 PAAD 组织中显著上调表达，ITGA2B 则显著下调表达。生存分析显示，SPP1、COL1A1、ITGB3 和 ITGA2B 的差异表达与患者更差的预后相关（$P<0.05$），但 ENG 差异表达却反映更好的预后，是 PAAD 的保护因素。免疫浸润显示，Hub 基因均与 PAAD 组织中 $CD8^+$T 细胞和中性粒细胞浸润呈显著正相关（$P<0.05$）。ROC 曲线结果显示，Hub 基因的 AUC 面积分别为 0.624、0.751、0.692、0.670 和 0.564，联合 5 条 Hub 进行 ROC 分析，其同样可以较好区分 PAAD 患者（AUC＝0.810，$P<0.001$）。亚细胞定位结果显示，Hub 基因主要定位于整合素αvβ3 复合物，与肿瘤细胞迁移侵袭有关。

结论：唾液基因可作为生物标志物区分 PAAD 患者，并且可能通过整合素复合物、T 细胞浸润等生物机制参与 PAAD 疾病进展。

关键字：唾液；基因组；胰腺癌；生存分析；免疫浸润；生物标志物

699. 基于高效液相色谱-质谱联用(HPLC-MS)技术的血浆代谢组学在早期胃癌诊断中的应用研究

王峰[1]、庞瑞芳[2]、尹玉新[2]、戎龙*[1]

1. 北京大学第一医院

2. 北京大学医学部

目的：我国是胃癌高发国家，但早期胃癌（局限于黏膜层或黏膜下层的腺癌）的诊治率不足10%，远低于日韩及欧美等国家，多数患者就诊时已处于进展期，预后较差。胃癌的早期发现和治疗可显著改善患者预后，然而，目前临床上仍缺乏理想的可用于早期胃癌诊断和筛查的血浆标志物。本研究旨在通过基于高效液相色谱-质谱联用(HPLC-MS)技术的非靶向代谢组学分析方法，研究早期胃癌患者和健康志愿者血浆代谢谱的差异，寻找潜在的早期胃癌血浆标志物，并初步探讨其涉及的相关代谢通路，为早期胃癌的筛查和发病机制研究提供理论依据。

方法：收集 15 例早期胃癌患者和 15 例健康志愿者的血浆样本，应用高效液相色谱-质谱联用(HPLC-MS)技术检测代谢物的表达。应用主成分分析(PCA)和正交偏最小二乘判别分析

（OPLS-DA）模型，分析并筛选差异代谢物。应用通路富集分析，寻找与早期胃癌相关的代谢通路。应用基于支持向量机(SVM)算法的受试者工作特征曲线(ROC)，探索早期胃癌患者潜在的血浆生物学标志物，评价其诊断效能。

结果：与健康志愿者相比，早期胃癌患者血浆中共有 19 种代谢物的表达水平发生了显著改变，且精氨酸生物合成、丙氨酸、天冬氨酸和谷氨酸代谢、乙醛酸和二羧酸代谢通路发生明显重编程，提示早期胃癌患者体内形成了新的代谢调控网络。在基于血浆代谢组学筛选发现的小分子代谢产物中，15 种代谢物构建的早期胃癌诊断模型具有较好的诊断效能，ROC 分析中 AUC 为 0.971。

结论：本研究发现了多种代谢物，以及代谢通路与早期胃癌密切相关，这些在早期胃癌患者血浆中差异表达的小分子代谢产物，有望成为潜在的早期胃癌生物标志物，对早期胃癌的诊断与筛查具有重要的临床应用价值。代谢通路的显著改变可能与早期胃癌的发病机制密切相关。

关键字：胃癌，早期筛查，代谢组学，生物标志物，高效液相色谱-质谱联用技术

700. alstonine 通过 AMPK 活化和 PGC-1α/TFAM 上调抑制小鼠体外骨肉瘤细胞增殖和体内肿瘤生长

严沁*

成都市第五人民医院

目的：研究 alstonine 作为体外抗骨肉瘤药物并评估其潜在机制。

方法：准备正常的人成骨细胞和两种骨肉瘤细胞系（MG63 和 U-2OS）进行培养、增殖、菌落形成、蛋白印迹分析、实时定量聚合酶链反应（qPCR）、细胞凋亡分析；50 只雄性 BALB/c 裸鼠（6 周龄；25-35g）被随机分为 5 组：正常组、alstonine（alstonine+生理盐水）、模型（肿瘤）、3 组 alstonine 治疗（在 5、10 和 20 mg/kg 剂量）组和正常（假）组。将 U-2OS 细胞植入模型小鼠和两组小鼠皮下区域，诱导肿瘤发展。

结果：应用 alstonine 治疗可导致 MG63 和 U-2OS 细胞活力显著降低（$p<0.05$）。与对照组细胞相比，alstonine 处理后的 MG63 和 U-2OS 细胞集落形成显著减少，凋亡细胞明显增加（$p<0.05$）。在 1.25~20μM 浓度范围内，alstonine 治疗不影响成骨细胞的活力。与未处理的细胞相比，用 alstonine 处理 MG63 和 U-2OS 细胞，导致 AMPKα（Thr172）磷酸化水平显

著升高，mtDNA 拷贝计数升高，PGC-1α和 TFAM 蛋白的表达显著增加。与对照组相比，alstonine 处理的小鼠肿瘤组织中 PGC-1α和 TFAM 蛋白的表达显著升高（$p<0.05$）。

结论：alstonine 通过 AMPK 依赖途径抑制骨肉瘤细胞生长，激活细胞凋亡。alstonine 能有效抑制小鼠肿瘤生长，可考虑用于治疗骨肉瘤。

关键字：alstonine，AMPK 活化，PGC-1α/TFAM，骨肉瘤

701. 56℃灭活 30min 对糖类抗原 CA242、CA19-9 和 CA50 检测结果的影响

史琦、韩冉冉、渠文涛、史小芹

郑州安图生物工程股份有限公司

目的：为保障临床实验室操作人员的生物安全，通常会对一些含有潜在传染源的血清样本进行灭活处理，即将样本在 56℃灭活处理 30min。但灭活后样本的检测结果是否受影响，一直是检验工作者关注的重点。本文研究了血清样本灭活前后糖类抗原 CA242、CA19-9 和 CA50 检测结果的变化，以指导临床实验室对检测糖类抗原 CA242、CA19-9 和 CA50 的样本采取正确的处理方法。

方法：取 10 例进行糖类抗原 CA242、CA19-9 和 CA50 检测的血清样本，等分成 2 份，一组作为对照，在 2-8℃保存，另一组样本在 56℃条件下灭活 30min。取出两组样本，待恢复至室温后，使用 AutoLumo A2000 检测系统和配套试剂盒，平行考核两组样本的 CA242、CA19-9 和 CA50 检测结果，并对灭活前后的结果进行比对分析，观察灭活对检测结果是否有影响。

结果：与对照组相比，样本灭活后，糖类抗原 CA242、CA19-9 和 CA50 的检测结果偏差不超过 5%，无统计学意义（$P>0.05$）

结论：血清样本在 56℃灭活 30min 处理后，糖类抗原 CA242、CA19-9 和 CA50 的检测结果均无明显变化，说明三种待测物在 56℃条件下较稳定。因此，临床实验室在进行糖类抗原 CA242、CA19-9 和 CA50 三项检测时，血清样本可以进行灭活处理。

702. S100 β蛋白在脑梗死和脑出血患者中的诊断价值研究

张绿萍、渠文涛

郑州安图生物工程股份有限公司

目的：探讨 S100 钙结合蛋白β（S100 β蛋白）在脑梗死和脑出血患者血清中的表达水平及诊断价值。

方法：分别收集 16 例脑梗死患者的血清样本，作为实验组 A；19 例脑出血患者的血清样本，作为实验组 B；30 例健康体检者血清样本作为对照组。使用 S100 蛋白检测试剂盒（磁微粒化学发光法）在 AutoLumo A2000 plus 上对上述三组血清样本进行检测，比较三组血清中 S100β蛋白的表达水平，分析其临床意义。

结果：脑梗死组血清中 S100 β蛋白表达水平为 0.716±0.112 ng/mL；脑出血组血清中 S100 β蛋白表达水平为 0.413±0.182 ng/mL；对照组血清中 S100β蛋白表达水平为 0.056±0.024 ng/mL；脑梗死组和脑出血组的 S100β蛋白表达水平显著高于对照组，差异具有统计学意义（$P<0.05$），脑梗死组和脑出血组 S100β蛋白表达水平差异无统计学意义（$P>0.05$），但脑梗死患者 S100β血清水平检测值高于脑出血患者。S100β蛋白在脑梗死组和脑出血组的敏感性分别为：68.75%和 63.16%。

结论：S100 β蛋白在脑梗死和脑出血患者血清中的表达水平显著高于健康体检者，说明 S100 β蛋白对脑梗死和脑出血具有一定的诊断价值，提示血清 S100 β蛋白可作为脑梗死和脑出血的潜在标志物。

703. 联合放射组学评分和液体活检的恶性肺结节诊断预测多维度模型

许露、朱晓莉

东南大学附属中大医院

目的:本研究旨在建立一个理想、稳定、准确的恶性肺结节诊断多维度数学模型。

方法:本研究前瞻性纳入 2020 年 1 月至 2021 年 12 月共计 156 例通过 CT 检查确诊为肺结节的患者，他们接受了循环染色体异常细胞（Genetically Abnormal Cells，CAC）检测。我们收集了与肺结节性质密切相关的临床特征，如年龄、吸烟史和结节类型。通过开源软件对

CT 图像中的感兴趣区域（Region of Interest，ROI）进行分割。进一步对 ROI 进行放射组学特征提取，通过 LASSO 逻辑回归构建放射组学模型，得到放射组学评分。通过逻辑回归分析构建了结合临床特征、影像组学评分和液体活检的综合模型，构建 ROC 曲线评估模型的诊断性能。

结果:本研究筛选了五个放射组学特征用于模型构建，放射组学模型的 AUC 在训练集中可以达到 0.844（95%CI：0.766-0.915）。进一步联合影像组学评分、临床特征和 CAC，构建多维多维度综合模型，模型的 AUC 在训练集中达到 0.943（95% CI：0.900-0.986）。

结论:多维度综合模型是恶性肺结节无创诊断的有效工具，对现有的多种诊断方法的验证和联合应用是诊断恶性肺结节的研究趋势。

704. TPP1 介导的 DDR 及其下游信号通路在食管癌中的分子机制研究

文继林[1,2]、徐磊[2]、钟晓武[1,2]、郭晓兰[1,2]、方莉[1,2]

1. 川北医学院附属医院检验科

2. 川北医学院

目的: 探讨敲低 TPP1 对 DNA 损伤反应以及食管癌细胞增殖、衰老的影响及作用机制。

方法: 借助 UALCAN 和 Human Protein Atlas 数据库分析 TPP1 在食管癌组织和癌旁组织中的转录水平以及蛋白表达水平；构建 TPP1 基因的敲低质粒并转染食管癌细胞系；细胞计数盒-8（CCK-8）实验和β-半乳糖苷酶实验分别检测各组细胞的增殖能力和衰老变化；彗星实验评估各组细胞的 DNA 损伤严重程度；Western Blot 检测敲低 TPP1 后下游相关蛋白的表达水平；裸鼠成瘤实验在体内验证敲低 TPP1 对食管癌细胞增殖的影响；免疫组织化学实验检测下游相关蛋白在裸鼠体内癌组织中的表达水平。

结果：分析 UALCAN 和 Human Protein Atlas 数据库得知在食管癌组织中 TPP1 转录水平和蛋白表达量均高于癌旁组织（$P<0.005$）；在 48h 时间点，CCK-8 实验和β-半乳糖苷酶实验结果提示实验组细胞增殖速率显著低于对照组细胞，且衰老率明显高于对照组细胞（$P<0.05$）；彗星实验证实敲低 TPP1 后会加重食管癌细胞 DNA 受损，实验组细胞的彗星尾长、尾 DNA 比例、尾距较对照组均显著增加（$P<0.005$）；抑制食管癌细胞 TPP1 表达后，Western Blot 结果显示蛋白 p-ATM、p-P53、53BP1、γ-H2AX、P21 表达均上调；在食管癌裸鼠移植

瘤模型中，实验组裸鼠的肿瘤体积显著小于对照组（$P<0.005$）；免疫组织化学染色结果证实在裸鼠体内敲低 TPP1 后可上调蛋白 p-ATM、p-P53、53BP1、γ-H2AX 的表达，同时下调肿瘤标志蛋白 Ki-67 的表达。

结论：体外实验与体内实验均证实在食管癌细胞中敲低 TPP1 可激活 ATM-P53 信号通路，诱发 ATM 依赖 DNA 损伤反应和 P53 依赖生长阻滞，同时促进食管癌细胞衰老，发挥积极的抗肿瘤作用。

705. 基于生物信息学分析 Shelterin 在食管癌中表达及免疫浸润的临床意义

杨密渊[1,2]、钟晓武[1,2]、高川力[1,2]、袁梓纯[1,2]、王琴[1,2]、徐磊[1]、马强[1,2]、郭晓兰[1,2]

1. 川北医学院

2. 川北医学院附属医院检验科

目的：探讨 shelterin 在食管癌发生中可能的作用机制。

方法：首先利用 UALCAN 分析 shelterin 在食管癌组织中表达情况，再利用 Kaplan-Meier plotter 分析 shelterin 与食管癌患者生存预后关系。其次，利用多种生物信息学分析工具分析 shelterin 在食管癌发病过程中的潜在作用。

结果：Shelterin 中的 ACD、TERF1、TERF2、TERF2IP、POT1 在食管癌组织中高表达；TERF1 与食管腺癌患者的总生存率及无复发生存率相关，TERF2IP 与食管鳞癌患者的总生存率相关，TERF2 与食管鳞癌患者的无复发生存率相关；ACD、TERF1、TINF2 在食管癌中的启动子甲基化水平增加；Shelterin 的表达与遗传变异和免疫细胞浸润水平相关。功能富集分析发现 shelterin 及其相关基因主要富集到 DNA 损伤、细胞衰老等生物过程，主要富集在细胞周期、同源重组、端粒和端粒酶等通路。

结论：TERF1、TERF2 及 TERF2IP 在食管癌组织中高表达，且与生存预后相关；Shelterin 参与食管癌多种生物学过程，提示它们可能与食管癌的发生与发展密切相关。

706. KDM4B 对胶质母细胞瘤细胞增殖影响的初步研究

王忠泽、李泽昆、孙伟、赵二虎、崔红娟

西南大学

目的：根据 2020 年世界卫生组织最新统计数据显示，中国脑部和中枢神经系统肿瘤的新发病例和死亡人数均占据全球第一的位置，因此找到有效且合适的治疗手段迫在眉睫。组蛋白去甲基化酶 KDM4B 是一种组蛋白赖氨酸去甲基化酶，在细胞核内通过去除组蛋白尾部赖氨酸残基上的甲基基团，来调控靶基因的转录活性。在癌症中，KDM4B 的过表达主要去甲基化癌基因区域的 H3K9me3，从而开放染色质，促进癌基因转录。目前，KDM4B 在胶质母细胞瘤中的表达以及具体调控机制的研究尚未报道，我们的研究将深入探索这一新的领域，为胶质母细胞瘤的靶向治疗提供新的思路。

方法：使用 Western blot 实验和 TCGA 数据库分析 KDM4B 在胶质母细胞瘤和正常组织中的表达水平；构建 KDM4B 干涉载体（shKDM4B#1 和 shKDM4B#2），并用 qRT-PCR 和 Western blot 实验进行干涉验证。利用 MTT 实验、BrdU 免疫荧光实验、平板克隆形成实验以及 Soft Agar 实验分别探究 KDM4B 对于胶质母细胞瘤生长和增殖的影响，而后通过小鼠皮下成瘤检测 KDM4B 对体内成瘤能力的影响。最后，通过 Western blot 和 Co-IP 实验等分析 KDM4B 的调控机制。

结果：TCGA 数据库分析 KDM4B 在胶质母细胞瘤中高表达且对患者有较差的预后；Western Blot 实验结果表明 KDM4B 在 GBM 细胞系 U87-MG 和 LN229 中高表达；MTT、BrdU 及平板克隆实验表明敲低 GRTP1 后 U87-MG 和 LN229 细胞的生长及增殖受到明显的抑制，流式细胞术实验检测发现 GBM 细胞被阻滞在 G2/M 期；Soft Agar 实验表明在敲低 KDM4B 后 U87-MG 和 LN229 的体外成瘤能力得到明显抑制；小鼠皮下成瘤实验也发现敲低 KDM4B 后小鼠的体内成瘤能力也下降；Western blot 和 Co-IP 实验等分析发现敲低 KDM4B 可导致原癌基因 c-MYC 及其下游蛋白表达下调。

结论：KDM4B 在胶质母细胞瘤中高表达，且与病人的不良预后有关，说明 KDM4B 在胶质母细胞瘤中具有促癌功能。敲低 KDM4B 后明显抑制胶质母细胞瘤细胞的增殖和生长能力，且与 c-MYC 相关，后续研究将会围绕 KDM4B 与 c-MYC 相关的表观调控机制进行探究。本研究有望为胶质母细胞瘤靶向药物的研发提供了新的思路。

707. 基于转运 RNA 及其来源片段表达谱分析探讨乳腺癌细胞耐药机制

莫冬萍、严枫

江苏省肿瘤医院

目的:阿霉素(Adriamycin, ADR)是治疗乳腺癌的一线化疗药物，作用于 DNA 复制和转录过程，抑制肿瘤细胞增殖，导致凋亡。然而，ADR 破坏细胞膜结构及功能，产生细胞毒性及耐药性，使得化疗效果不佳，乳腺癌细胞产生耐药性是造成化疗失败和复发的首要原因。转运 RNA 及其来源片段(tRNA-Derived small RNAs, tDRs)源于 tRNA 前体及成熟体的特异性切割，参与多种肿瘤进展，但其在乳腺癌治疗耐药性的机制尚不清楚。

方法:高通量测序检测 MCF-7/ADR 细胞的 tDRs 表达谱，筛选出调控乳腺癌阿霉素耐药的 tDRs。基因本体（Gene Ontology，GO）和京都基因与基因组百科全书（Kyoto Encyclopedia of Genes and Genomes, KEGG）对差异 tDRs 进行生物学通路分析。Annexin V-FITC/PI 双染法检测细胞凋亡，实时定量聚合酶链反应检测转染后细胞凋亡能力和凋亡相关基因表达水平。Graph Pad Prism 8 处理实验数据，两两比较采用成组 t 检验。

结果:MCF-7/ADR 细胞中 73 条 tDRs 存在差异(差异倍数>2，p<0.05)。GO 和 KEGG 通路分析显示上调的 tDRs 和下调的 tDRs 分别参与多种不同的生物过程，涉及的主要功能与通路和肿瘤相关，尤其是上调的 tDRs(tRF-58-75-Ala-AGC-1, tRF-58-75-Ala-AGC-5, tRF-58-75-Pro-AGG-1-M7 和 tRF-59-76-Tyr-GTA-4)与细胞凋亡关系密切。细胞凋亡结果提示，tRF-58-75-Ala-AGC-1 抑制后，MCF-7/ADR 细胞凋亡能力显著高于阴性对照组，凋亡率分别是：(83.34±1.95)%和(71.12±5.01)%, (t=3.937, p<0.05)。抑制 tRF-58-75-Ala-AGC-1 表达，MCF-7/ADR 中 bcl-2 的 mRNA 表达水平（0.58±0.23）显著低于阴性对照组(1.00±0.05，t=3.025, p<0.05)；半胱氨酰天冬氨酸特异性蛋白酶(Caspase) -3，7，9 表达水平分别为 1.29±0.11,1.50±0.16,1.22±0.07 显著高于对照组 1.00±0.05(t 分别为 4.226,5.296,4.174，P 均小于 0.05)。

结论:MCF-7/ADR 细胞的 tDRs 表达存在差异，差异表达的基因可以为寻找新的化疗敏感靶点或生物标志物提供新思路和线索。

708. 皮下瘤切除与否尿液蛋白质组的变化

高友鹤、衡姊琦

北京师范大学

目的:本研究试图探索临床外科医生最关心的问题——实体肿瘤手术切除效果能否在尿蛋白质组得到反映。

方法:研究采用小鼠 MC38 细胞皮下瘤切除模型，将小鼠分为健康对照组，皮下瘤完全切除实验组和皮下瘤完全不切除实验组。对三组小鼠进行假手术或皮下瘤切除手术，皮下瘤完全切除组进行手术切除后饲养至 90 天未见复发，认为手术切除成功。收集手术后第 7 天、第 30 天的尿液，利用液相色谱联用质谱（LC-MS/MS），对尿液蛋白质组进行鉴定，分析差异蛋白和相关生物学通路。

结果:本章研究的结果有：（1）皮下瘤完全切除组和完全不切除组切除手术后 7 天，尿液蛋白质组可以筛选出能够区分两组的 20 个差异蛋白，富集到的生物学过程包括昼夜节律、Notch 信号通路、白细胞间粘附、异嗜性细胞通过质膜粘附细胞分子等。（2）皮下瘤完全切除组和完全不切除组切除手术后 30 天，尿液蛋白质组可以筛选出能够区分两组的 33 个差异蛋白，生物学过程包括细胞粘附、补体激活和替代途径、免疫系统的过程、血管生成等。（3）皮下瘤完全切除组和健康对照组切除手术后 30 天两组差异不明显。

结论:尿液蛋白质组的变化可以清晰反映肿瘤手术切除与否。

709. 新型血栓标志物对恶性肿瘤患者围手术期并发 VTE 的预警效能

张金彪[1]、曹蕾[1]、马飞[1]、代荣琴[2]

1. 河北省沧州中西医结合医院

2. 沧州医学高等专科学校

目的: 恶性肿瘤患者围手术期易并发静脉血栓栓塞症（VTE）,探讨新型血栓标志物对其的预警效能。

方法: 回顾性分析自 2020 年 7 月 1 日至 2021 年 2 月 1 日我院收治恶性肿瘤手术患者 150 例，为观察组，围手术期内并发 VTE 者 30 例，为血栓组；未并发 VTE 者 120 例，为无栓组。

另选同期健康体检者 60 例，为对照组。各组均检测凝血酶-抗凝血酶复合物（TAT）、纤溶酶-α2 纤溶酶抑制物复合物（PIC）、血栓调节蛋白（TM）、组织型纤溶酶原激活剂-纤溶酶原激活剂抑制剂-1 复合物（tPAI·C），对照组检测一次，观察组术前 1d 和术后 1d 各检测一次。采用 SPSS23.0 作统计学处理，评价血栓标志物预警效能。

结果: ①肺癌（$\chi2=12.532$，$P=0.014<0.05$）、老龄（$\chi2=6.685$，$P=0.036<0.05$）、肥胖（$\chi2=40.533$，$P=0.000<0.05$）、转移（$\chi2=5.383$，$P=0.031<0.05$）、晚期（$\chi2=5.827$，$P=0.023<0.05$）是恶性肿瘤患者术后并发 VTE 的高危因素；②观察组的 TAT、PIC、TM 均高于对照组，差异有统计学意义（$P<0.05$），术前 1d，血栓组的 TAT 和 TM 高于无栓组，差异有统计学意义（$P<0.05$），TM 预警效能最好（截断值 10.70，AUC=0.786，灵敏度 73.30%，特异度 81.70%，$P=0.000$），TAT 和 TM 联合可提升预警效能（AUC=0.796，灵敏度 80.00%，特异度 77.50%，$P=0.000$）；术后 1d，血栓组的 TAT、PIC、TM、tPAI·C 均高于无栓组，差异具有统计学意义（$P<0.05$），TAT 预警效能最好（截断值 16.50，AUC=0.887，灵敏度 82.36%，特异度 71.65%，$P=0.000$），四项联合可提升预警效能（AUC=0.913，灵敏度 90.00%，特异度 88.60%，$P=0.000$）；③PIC 作为纤溶激活标志物，与 TAT 均呈现良好的正相关（术前：$r=0.665$，$P=0.000<0.05$；术后：$r=0.638$，$P=0.000<0.05$）。

结论: 新型血栓标志物在恶性肿瘤患者围手术期预测 VTE 中具有重要的预警价值；TM 相对 TAT 能更早提示 VTE 风险，截断值为 10.70TU/ml；可选用 PIC 把控 VTE 发生前的纤溶状态，评估出血风险。

710. 血浆热休克蛋白 90α对胰腺癌诊断的临床意义

陈佳祺

吉林省肿瘤医院

目的:胰腺患者中热休克蛋白 90α（HSP 90α）表达情况及与传统肿瘤标志物（CA199、CA125）的相互关系。

方法:收集 120 例胰腺癌患者血浆中 HSP90α、CA199、CA125 数值，56 例胰腺良性疾病者 HSP90α数值。分析胰腺癌患者 HSP90α水平及与临床病理因素之间的关系,并与传统肿瘤标志物进行 spearman 相关性分析。

结果:胰腺癌患者血浆 HSP90α水平及阳性率均明显高于胰腺良性疾病组（83.28 *vs.* 50.72 ng/ml 和 48.7%vs.12.6%）,差异均有统计学意义（均 *P*<0.001）。（III+IV）期、存在淋巴结转移胰腺癌患者的 HSP 90α水平分别高于（I+II）期（*P*=0.013）、无淋巴结转移者（*P*=0.045）。胰腺癌患者的 HSP 90α水平与年龄、性别、肿瘤发生部位及肿瘤大小无关，差异均无统计学意义（均 *P*>0.05）。HSP 90α在胰腺癌诊断中的 ROC 曲线下面积为 0.751（95%CI:0.647～0.815），其敏感度和特异度分别为 54.1%和 86.0%。胰腺癌患者 HSP 90α水平与肿瘤标志物 CA199、CA125 之间没有明显的相关性（*P*>0.05）。HSP 90α与 CA199、CA125 项联合诊断胰腺癌的敏感度为 94.6%，明显高于单个肿瘤标志物（*p*<0.05），较 CA199+CA125 两项联合略增高，但差异无统计学意义（*P*>0.05）。

结论:胰腺癌患者 HSP 90α的表达明显高于良性疾病患者,与传统肿瘤标志物联合使用时可提高诊断胰腺癌的敏感度，对胰腺癌的辅助诊断有指导作用。

711. 肿瘤相关巨噬细胞代谢基因预测卵巢癌预后价值的研究

李泽、田菁、任丽

天津医科大学肿瘤医院

目的:近年来，肿瘤相关巨噬细胞(TAMs)与实体肿瘤的研究成为研究热点，本研究旨在探讨 TAMs 与卵巢癌（ovarian cancer，OV）中相关代谢基因的密切关系，为治疗 OV 提供新的方法。

方法:本研究选取癌症基因组图谱（TCGA）中生存信息完整（生存时间≥1 个月）的 OV 患者作为研究对象，通过加权基因共表达网络分析（Weighted Gene Correlation Network Analysis, WGCNA）找到与 OV 肿瘤相关巨噬细胞相关代谢基因模块，筛选出与预后相关的巨噬细胞代谢基因，构建预后风险预测模型并对模型的预测效能进行评估。运用 Lasso 回归算法对模块内肿瘤相关巨噬细胞相关代谢基因构建预后模型，并绘制时间依赖性 ROC 曲线并计算曲线下面积(AUC)，根据模型计算风险评分，根据计算出的风险评分中位值将 OV 分为高风险组和低风险组，利用 Kaplan-Meier 生存分析评估模型预测 OV 预后的能力。

结果:通过对 TCGA 数据库中的 593 例卵巢癌患者样本进行 WGCNA 分析，共获得 9 个基因模块，其中 diumpurple3 模块与巨噬细胞的相关性较高，将模块中的基因进行下一步分析得

到与预后显著相关的基因，并将这些基因纳入 LASSO-COX 回归模型里，最后确定下来 2 个基因（CHSY1、PLA2G2D）来构建我们的卵巢癌风险预测模型。

结论:我们通过对 TCGA 数据库中的数据进行相关分析，构建了一个具有预测卵巢癌预后能力的模型，该模型不仅可以帮助预测卵巢癌患者预后，还可能有助于临床治疗决策。

712. FoxQ1 在结直肠癌同期放化疗抵抗中的作用机制研究

刘艳艳、蒋永新、刘珊、安倩、范雪梅

云南省肿瘤医院（昆明医科大学第三附属医院）

目的：验证 FoxQ1 在结直肠癌同期放化疗抵抗细胞中的表达水平并在体外探索其对结直肠癌同期放化疗抵抗的作用机制。

方法：1.qRT-PCR 和 Western Blot 实验检测结直肠癌细胞 HCT116 及结直肠癌放化疗抵抗(chemoradiotherapy resistance, CRR) 细胞 HCT116CRR 中 FoxQ1 的 mRNA 和蛋白表达差异；并采用细胞转染技术对 HCT116CRR 细胞中的 FoxQ1 基因进行敲减，设置对照组、实验组；qRT-PCR 和 Western Blot 实验验证 FoxQ1 基因沉默效果。2. 采用 CCK-8、克隆形成、划痕、Transwell 实验检测 FoxQ1 对 HCT116CRR 细胞增殖、迁移及侵袭能力的影响；JC-1 和流式细胞术检测 FoxQ1 敲减后 HCT116CRR 细胞凋亡及细胞周期的变化。3. Western Blot 实验检测 FoxQ1 敲减后 HCT116CRR 细胞凋亡和细胞周期相关蛋白的变化；应用 STRING 数据库检索可能与 FoxQ1 发生相互作用的蛋白，并采用 Western Blot 验证 FoxQ1 对其蛋白表达的影响。

结果:1. qRT-PCR 和 Western Blot 实验检测 HCT116 及 HCT116CRR 细胞中 FoxQ1 的表达情况，结果显示，FoxQ1 在结直肠癌 HCTT116CRR 细胞中的 mRNA 水平及蛋白表达量均显著高于 HCT116 野生型细胞（P<0.001）。qRT-PCR 和 Western Blot 实验结果显示，构建的 FoxQ1 shRNA 显著降低 HCT116CRR 细胞中 FoxQ1 的 mRNA 水平（P<0.01）及蛋白表达量（P<0.001）。2. CCK-8 实验结果显示， shFoxQ1 组的细胞增殖能力低于 shNC 组（P<0.001）。克隆形成实验结果显示， shFoxQ1 组的细胞克隆形成能力显著低于 shNC 组（P<0.01）。划痕实验和 Transwell 实验结果显示，shFoxQ1 组的细胞迁移能力、侵袭能力相比于 shNC 组均显著减弱（P 均<0.01）。流式细胞术结果显示， shFoxQ1 组的细胞凋亡率显著高于 shNC 组（P<0.01）； shNC 组细胞周期分布为：G0/G1 期（43.42±1.27）%，G2/M 期（22.76±0.94）%，

shFoxQ1 组细胞周期分布为：G0/G1 期（57.19±1.15）%，G2/M 期（16.99±1.84）%， shFoxQ1 组 G0/G1 期细胞比例相较于 shNC 组明显增加（*P*<0.01），而 G2/M 期细胞比例降低（*P*<0.05）。JC-1 实验结果显示，相较于 shNC 组，shFoxQ1 组的细胞早期凋亡明显增加。Western Blot 实验结果显示在 HCT116CRR 细胞中，相较于 shNC 组，shFoxQ1 组 Bcl-2 蛋白、Caspase3 及 PARP 总蛋白的相对表达量均降低（*P* 均<0.01），而 Bax 蛋白、cleaved-Caspase3 及 cleaved-PARP 磷酸化蛋白的相对表达量均增高（*P* 均<0.01）；与 shNC 组相比，shFoxQ1 组 C-myc 和 cyclinD1 蛋白的相对表达量均降低（*P* 均<0.001）。3.应用 STRING 数据库分析可能与 FoxQ1 产生相互作用的蛋白，结果显示 FoxQ1 基因与 AKT 蛋白关系密切。Western Blot 实验结果显示，在 HCT116CRR 细胞中，与 shNC 组相比，shFoxQ1 组 p-AKT 磷酸化蛋白的相对表达量降低（*P*<0.001），而 AKT 总蛋白的相对表达量增加（*P*<0.01）。

结论：FoxQ1 基因可能通过激活 AKT 信号通路促进结直肠癌同期放化疗抵抗细胞的增殖、迁移和侵袭能力，抑制细胞凋亡。

713. 肺癌组织来源外泌体的蛋白质组学研究

纪东瑞、张庆华

上海华盈生物医药科技有限公司

目的:外泌体蛋白已经被广泛用于疾病诊断和预后标志物的研究，尤其是在肿瘤研究领域。但是外泌体在肺癌诊断及相关研究中却比较少。因此本研究的目的首先是分析肺癌组织来源外泌体的蛋白组特征，鉴别和肺癌相关的外泌体特异性的蛋白。然后鉴定用于肺癌诊断的潜在外泌体蛋白标志物。

方法:手术获得的肺癌病人配对的癌组织和癌旁组织被用来提取外泌体。我们通过液相串联质谱（LC-MS/MS）技术开展组织外泌体的蛋白组学分析。之后通过各种生信分析筛选癌组织和癌旁组织的差异性外泌体蛋白，进行了功能富集。最后通过特征选择，鉴别了潜在的标志物。

结果:蛋白组学鉴别了高可信的组织外泌体蛋白数量总共 2000 多个。主成分分析(Principal Component Analysis)表明了外泌体蛋白组可以完全区分癌组织和癌旁组织。加权基因共表达网络分析(WGCNA)发现了 6 个与样本类型癌组织显著相关的模块，其中最显著相关模块中的蛋白主要参与糖蛋白代谢、细胞外基质结构、颗粒细胞激活和内吞等生物学过程，蛋白互

作网络分析发现了这些蛋白形成了几个关键的互作网络，例如 Laminin interactions、Cellular amide metabolic process、Basigin interactions、Collagen biosynthesis and modifying enzymes、Glycosphingolipid metabolism 等。差异分析鉴别了 500 多个在癌组织和癌旁组织中显著差异的外泌体蛋白，联合肺癌组织蛋白组数据库和 TCGA 数据库发现了共有差异蛋白有 100 多个，这些蛋白可以作为候选标志物。通过集成算法进行特征选择，结果鉴别了高区分效能的外泌体蛋白。最后我们也发现了与肺癌分期相关的组织外泌体蛋白组特征。

结论:组织外泌体蛋白组可以反映肺癌组织特征性的信号。糖基化代谢、胞外基质结构相关的外泌体蛋白与癌组织显著相关。组织外泌体蛋白组可以区分癌组织和癌旁组织，可以作为潜在标志物的来源。

714. 阴沟肠杆菌促进肺上皮间充质转化促进肺癌增殖转移

林鑫、孙轶华

哈尔滨医科大学附属肿瘤医院

目的:探究肺癌组织中阴沟肠杆菌富集情况及其对肺癌增殖转移的影响

方法:通过 qRT-PCR 检测肺癌患者组织及血清中阴沟肠杆菌的富集情况。将阴沟肠杆菌与 HBE 及 A549 细胞共培养（MOI=100:1）后，CCK-8 检测细胞增殖情况，qRT-PCR 和 Western blot 分别检测上皮间质化（EMT）相关标志物的 mRNA 及蛋白表达水平，划痕试验评估细胞迁移能力。

结果:肺癌患者的组织及血清中均检测出阴沟肠杆菌的 DNA 的稳定富集，其中肿瘤组织的表达量明显高于癌旁组织，肺癌患者血清中的 E.cl 含量明显高于正常人，且存在远处转移的患者含量更高，而其他菌属（如大肠埃希菌，链球菌，具核梭杆菌，肠球菌等）表达情况并不一致。按照 MOI=100：1 的比例分别将阴沟肠杆菌和大肠杆菌与 HBE 及 A549 共培养后，HBE-$_{E.cl}$ 及 A549-$_{E.cl}$ 细胞增殖明显增加，E-Cadherin mRNA 及蛋白表达量减少，N-Cadherin、Vimentin 表达增加，划痕试验表明 E.cl 与 HBE 及 A549 共培养后，细胞迁移能力增强。而相同条件下，与大肠杆菌共培养的细胞并无明显变化。

结论:阴沟肠杆菌在肺癌患者体内稳定富集，并且可能通过增强肺癌细胞上皮间质化的能力，促进肺癌增殖转移，其中的具体机制有待后续继续探究。

715. 长链非编码 RNA LINC AC008063.3 在头颈鳞癌中的生物学功能及临床意义

买尔哈巴·米吉提[1,2]、郑希望[1,2]、田然[1,2]、郭庆博[1,2]、董阳洋[1,2]、吴勇延[3]、高伟[3]

1. 山西医科大学第一医院耳鼻咽喉头颈肿瘤实验室

2. 山西医科大学第一医院耳鼻咽喉头颈外科

3. 深圳大学总医院耳鼻咽喉头颈外科

目的:明确长链非编码 RNA LINC AC008063.3 表达水平与头颈鳞癌患者临床病理参数的关系，阐明 LINC AC008063.3 在头颈鳞癌细胞中的生物学功能，为头颈鳞癌诊疗及预后评估提供潜在分子标志物。

方法:分析 TCGA（The cancer genome atlas）数据库头颈鳞癌转录组数据中 LINC AC008063.3 的表达情况；利用实时荧光定量 PCR（real-time quantitative PCR，qPCR）检测人胚肺二倍体细胞 2BS，人永生化角质形成细胞 HACAT，头颈鳞癌细胞系 CAL-27, Detroit562, AMC-HN-8, FD-LSC-1, FaDu 和 WSU-HN30 中 LINC AC008063.3 的表达水平，RNAi（RNA interference）敲降头颈鳞癌细胞系中 LINC AC008063.3 的表达水平，利用 RT-qPCR 分别检测 LINC AC008063.3 在细胞核和胞质中的表达丰度；利用 CCK-8、平板克隆形成、流式细胞术、Transwell 迁移和侵袭，Seahorse 能量代谢等实验检测 LINC AC008063.3 敲降后肿瘤系的恶性表型变化。

结果:头颈鳞癌组织中 LINC AC008063.3 表达水平显著高于正常对照组织（头颈鳞癌组织：正常组织= 0.12：0.02，P<0.001）；生存分析显示 LINC AC008063.3 高表达组中患者总生存率显著低于低表达组患者总生存率，两组的中位生存时间分别为 33.10 个月和 61.27 个月（P<0.001）；临床相关性分析发现 LINC AC008063.3 表达水平与头颈鳞癌患者的年龄呈正相关（P<0.001），且与病理分期呈正相关（T3+T4＞T1+T2, P=0.03）；LINC AC008063.3 主要在细胞质内富集表达（细胞质：细胞核= 86.8 : 13.2，P=0.01）；敲降 LINC AC008063.3 可抑制头颈鳞癌细胞系增殖、克隆、迁移和侵袭能力，同时肿瘤细胞系糖酵解能力受到明显遏制（P＜0.05）。

结论:LINC AC008063.3 高表达与头颈鳞癌恶性进展相关，具有促进头颈鳞癌细胞增殖、克隆，迁移、侵袭等重要生物学功能，特别是肿瘤细胞系糖酵解能力受到抑制，有望作为头颈鳞癌诊疗标志物以及拮抗糖酵解的新型分子靶点。

716. 长链非编码 RNA MNX1-AS1 在头颈鳞癌中的生物学功能及临床意义

田然[1,2]、郑希望[1,3]、买尔哈巴·米吉提[1,3]、郭庆博[1,3]、董阳洋[1,3]、吴勇延[4]、高伟[4]

1. *山西医科大学第一医院耳鼻咽喉头颈肿瘤山西省重点实验室*
2. *山西医科大学基础医学院*
3. *山西医科大学第一医院耳鼻咽喉头颈外科*
4. *深圳大学总医院耳鼻咽喉头颈外科*

目的:探讨长链非编码 RNA MNX1-AS1（Long non-coding RNA MNX1-AS1，LncRNA MNX1-AS1）的表达水平与头颈鳞癌患者临床病理参数的关系，阐明 LncRNA MNX1-AS1 在头颈鳞癌细胞中的生物学功能，为头颈鳞癌诊疗及预后评估提供潜在分子标志物。

方法:分析 TCGA（The cancer genome atlas）数据库头颈鳞癌转录组数据中 LncRNA MNX1-AS1 的表达情况；利用实时荧光定量 PCR（real-time quantitative PCR，qPCR）检测人胚肺二倍体细胞 2BS 和人类永生化表皮细胞 HaCaT，头颈鳞癌细胞系 FD-LSC-1、CAL-27 和 Detroit562 中 LncRNA MNX1-AS1 的表达水平；使用 RNAi（RNAinterference）技术敲降头颈鳞癌细胞中 LncRNA MNX1-AS1 的表达，利用 CCK-8、平板克隆、流式细胞术、Transwell 迁移和侵袭等实验检测 LncRNA MNX1-AS1 被敲降后肿瘤细胞系恶性表型的变化。

结果:头颈鳞癌组织中 LncRNA MNX1-AS1 表达水平高于正常对照组织（头颈鳞癌组织；正常对照组织=0.41；0.09），差异具有统计学意义（$p<0.05$）；其表达水平与头颈鳞癌患者病理学分级呈正相关（$p<0.05$）。生存分析发现，LncRNA MNX1-AS1 高表达组的患者总生存率显著低于低表达组患者总生存率（$p<0.05$），其中中位生存时间分别为 42.97 月、61.27 月。临床相关性分析发现，有吸烟史患者组中其表达水平高于无吸烟史患者组（$p<0.05$）；临床中晚期患者组中其表达水平高于早中期患者组（$p<0.05$）。敲降 LncRNA MNX1-AS1 可抑制头颈鳞癌细胞增殖、克隆形成、迁移和侵袭能力（$p<0.05$）。

结论: LncRNA MNX1-AS1 高表达与头颈鳞癌恶性进展相关，具有促进头颈鳞癌细胞增殖、迁移、侵袭的重要生物学功能，是头颈鳞癌潜在的重要分子标志物。

717. 关于长链非编码 RNA HOXB-AS4 在头颈鳞癌中的调控作用及临床意义研究

汪洋[1]、郑希望[1]、王锦航[1]、张慧敏[1]、秦春红[1]、雷鹏祥[1]、高伟[2]、吴勇延[2]

1. 山西医科大学耳鼻咽喉实验室

2. 深圳大学总医院耳鼻咽喉头颈外科

目的:头颈鳞癌（Head and Neck Squamous Cell Carcinoma, HNSCC）作为全身肿瘤中排名第六位的恶性肿瘤，存在高增殖、局部侵袭和区域淋巴结转移等恶性生物学特征，其预后较差。研究发现，长链非编码 RNA（long non-coding RNA，lncRNA）在肿瘤进展过程中发挥重要作用。本研究旨在通过临床样本分析和细胞功能实验，以探究长链非编码 RNA HOXB-AS4 在头颈鳞癌细胞系中的生物学功能，讨论其与头颈鳞癌分期分型及预后的关系。

方法:首先利用 TCGA（The cancer genome atlas）数据库分析 HOXB-AS4 在头颈鳞癌和癌旁组织中的表达情况及与临床病理参数的联系，并探究其与头颈鳞癌患者预后不良的相关性；利用实时荧光定量 PCR（real-time quantitative PCR，qRT-PCR）检测人肾上皮细胞 293T、人胚肺二倍体细胞 2BS、人永生化角质形成细胞 HaCaT、头颈鳞癌细胞 AMC-HN-8、CAL-27、Detroit562、FaDu、FD-LSC-1 和 WSU-HN30 中 HOXB-AS4 的表达水平，并研究 HOXB-AS4 在头颈鳞癌细胞的胞核和胞质中分布情况；利用 RNA 干扰技术在头颈鳞癌细胞系中敲降 HOXB-AS4，通过 CCK-8、克隆形成、Transwell 迁移和侵袭等实验研究 HOXB-AS4 对头颈鳞癌细胞表型变化的影响。

结果:TCGA 头颈鳞癌转录组测序数据显示，HOXB-AS4 在头颈鳞癌组织的表达量显著高于正常组织；Kaplan-Meier 生存分析结果显示 HOXB-AS4 表达水平与头颈鳞癌患者预后呈负相关；临床相关性分析提示 HOXB-AS4 在高龄患者中高表达，能够促进肿瘤病理进展，并与肿瘤的侵袭和区域淋巴结转移呈正相关。qRT-PCR 结果显示，头颈鳞癌细胞中 HOXB-AS4 表达水平高于正常对照细胞，HOXB-AS4 主要分布于头颈鳞癌细胞胞质。细胞功能研究发现：敲降 HOXB-AS4 抑制头颈鳞癌细胞增殖、克隆形成、迁移及侵袭能力。

结论:长链非编码 RNA HOXB-AS4 在头颈鳞癌中表达显著上调，其在头颈鳞癌中扮演着促癌基因的角色，通过促进肿瘤细胞的增殖、迁移和侵袭能力，加快了肿瘤进展，与患者预后不良高度相关，提示 HOXB-AS4 可能作为头颈鳞癌诊断及预后评估的潜在标志物，同时也为头颈鳞癌的诊断以及治疗提供新的思路。

718. 长链非编码 RNA LINC02893 对头颈鳞癌细胞增殖及侵袭的影响

张慧敏[1]、郑希望[1]、秦春红[1]、汪洋[1]、王锦航[1]、雷鹏祥[1]、高伟[2]、吴勇延[2]

1. 山西医科大学第一医院

2. 深圳大学总医院

目的:头颈鳞癌（Head and Neck Squamous Cell Carcinoma, HNSCC）是头颈部常见的恶性肿瘤。虽然近年来针对头颈鳞癌的治疗手段有明显提高，但其复发率和死亡率仍呈上升趋势，预后水平较差。恶性增殖、侵袭及转移是导致头颈肿瘤预后不良的重要因素。长链非编码 RNA（long non-coding RNA，lncRNA）在肿瘤发生和发展过程中具有重要调控作用。本研究通过临床样本分析、细胞功能研究及裸鼠移植瘤实验，明确 lncRNA LINC02893 在头颈鳞癌细胞中的生物学功能及临床意义。

方法:利用 TCGA 数据库头颈鳞癌转录组测序数据分析 LINC02893 在头颈鳞癌中的表达水平及其与头颈鳞癌患者预后结局的相关性。利用实时荧光定量 PCR（qRT-PCR）技术检测头颈鳞癌组织及配对癌旁正常黏膜组织 LINC02893 表达水平。qRT-PCR 和荧光原位杂交技术（FISH）研究 LINC02893 在头颈鳞癌细胞中的表达水平及分布情况。CCK8、克隆形成、Transwell 迁移和侵袭等分析明确 LINC02893 对头颈鳞癌细胞表型的影响。构建裸鼠移植瘤模型，评估 LINC02893 对头颈鳞癌细胞体内成瘤能力的调控作用。

结果: TCGA 头颈鳞癌转录组测序数据显示，头颈鳞癌组织 LINC02893 表达水平显著上调，qRT-PCR 结果进一步证实头颈鳞癌组织 LINC02893 表达水平显著高于癌旁正常黏膜组织。统计学分析结果表明，LINC02893 高表达与头颈鳞癌患者预后不良相关。头颈鳞癌细胞 CAL-27、FaDu、Detroit562 和 FD-LSC-1 中 LINC02893 表达水平高于对照组正常细胞。荧光原位杂交结果显示，LINC02893 主要分布于头颈鳞癌细胞胞质。细胞功能研究发现：敲降 LINC02893 抑制头颈鳞癌细胞增殖、克隆形成、迁移及侵袭能力；相反，过表达 LINC02893 则促进头颈鳞癌细胞增殖、侵袭和迁移能力。裸鼠移植瘤实验结果表明，敲降 LINC02893 导致头颈鳞癌细胞体内成瘤能力降低。

结论:头颈鳞癌中 LINC02893 表达显著上调，且 LINC02893 高表达与 HNSCC 恶性不良预后相关。LINC02893 在头颈鳞癌中发挥癌基因功能，促进头颈鳞癌细胞增殖、迁移、侵袭和

体内成瘤能力。本研究结果将为头颈鳞癌的诊断和预后评估提供新的潜在标志物，同时为头颈鳞癌治疗提供新的思路和潜在分子靶点。

719. 人膀胱癌体外药物敏感性预测与临床应用

赵阳

中国科学院大学附属肿瘤医院（浙江省肿瘤医院）

目的:探讨人膀胱癌体外药敏试验在膀胱癌术后选药预防复发中的作用。

方法:药物选用 MMC、ADM、HPT、BCG、榄香稀乳。采用 MTT 法分别计算 5 种药物对人膀胱癌细胞的抑制率。并选择抑制率最高的药物应用于临床。

结果:所选 5 种药物对膀胱癌均有敏感性。但榄香稀乳始终显示出对癌细胞的抑制率最高，并获得临床证实。另外，在所选药物中抑制率与药物浓度呈正相关。

结论:人膀胱癌药物敏感性研究为膀胱癌术后灌注化疗的选药提供了一种更有针对性的方法。

720. 膀胱部分切除术在局限性肌层浸润性膀胱癌治疗中的作用

赵阳

中国科学院大学附属肿瘤医院（浙江省肿瘤医院）

目的:探讨膀胱部分切除术(PC)在局限性肌层浸润性膀胱癌(MIBC)治疗中的价值。

方法:回顾性分析 1999 年 9 月至 2005 年 4 月收治的 71 例局限性 MIBC 患者的临床资料，男 59 例，女 12 例。年龄 27-83 岁，平均 66 岁。肿瘤≤3 cm 34 例，肿瘤>3 cm 37 例。有脉管瘤栓 10 例。单发肿瘤 42 例，多发肿瘤 29 例。71 例均为 T2 – T3 期。肿瘤有蒂 18 例，广基 29 例。病理诊断为腺癌 6 例，肉瘤样癌 3 例，小细胞癌 1 例。低分级 11 例，高分级 50 例。47 例行 PC, 24 例行膀胱全切术(TC)。采用 Kaplan-Meier 法比较两种术式对患者 5 年总生存率(OS)和无病生存率(DFS)的影响。单因素与多因素分析临床病理特征与生存率的相关性。

结果:PC 组 OS 与 DFS 分别为 57%(27 例)与 53%(25 例),TC 组 OS 与 DFS 分别为 50%(12 例)与 4fi% (11 例)，两组比较差异无统计学意义(P>0.05)。单因素分析结果显示影响 MIBC 预后的因素为肿瘤是否有蒂及肿瘤浸润深度(包括是否有脉管瘤栓)，而患者年龄、性别、肿瘤

数量、大小及组织学类型与预后无相关性。多因素分析显示，肿瘤浸润深度是影响 MIBC 预后的独立危险因素，相对危险度=1.64(p<0.05)。

结论:PC 不会降低有选择的局限性 MIPC 患者的肿瘤控制率

721. 乳腺小粘蛋白在乳腺癌中的研究进展

刘良

西海岸新区人民医院

目的:国际癌症研究机构 2020 年 GLOBOCAN 统计估计显示，2020 年，全球估计有 1930 万新病例(不包括 NMSC，不包括基底细胞癌)和 1000 万癌症死亡。其中女性乳腺癌发病率高达 11.7%，超过肺癌的 11.4%成为发病率最高的恶性肿瘤，在女性恶性肿瘤的发病率和死亡率分别为 24.5%和 15.5%，严重威胁女性的健康和生命，大部分患者早期缺乏明显症状及有效的筛查方法导致其发现较晚，预后不佳。据报道，20%-30%的乳腺癌患者在诊断和原发肿瘤治疗后可能发生转移， 其中 90%的病人死亡为转移所致。没有转移的乳腺癌患者的 5 年总存活率高于 80%；然而，远处转移可以导致这一比率急剧下降至仅约 25%。转移性疾病是目前亟待解决的医学问题，因为转移性疾病通常对传统疗法具有抵抗力，只有姑息治疗方案可供选择。因此如早期诊断乳腺癌，有效发现乳腺癌微转移，及对治疗后的乳腺癌进行预后评估，需要开发有效的检测和治疗方法。远处转移是乳腺癌患者的主要死亡原因。为了尽早发现和防止肿瘤的扩散，迫切需要寻找新的肿瘤标志物用于诊断和预测肿瘤转移，并开发出肿瘤治疗新靶点，为此大量研究在不断探索中。

方法:本文将从 SBEM 对乳腺癌微转移在淋巴结、血液及骨髓中的检测价值、预后判断和治疗预测意义。

结果:SBEM 是一种仅在乳腺和唾液腺中特异性表达的分泌型蛋白，作为乳腺癌生物标志物具有很好的潜力。

结论:乳腺小粘蛋白（SBEM）它是一种仅在乳腺和唾液腺中特异性表达的分泌型蛋白，作为乳腺癌生物标志物具有很好的潜力。

722. 信迪利单抗联合安罗替尼一线治疗表皮生长因子受体（EGFR）阴性的晚期或转移性非小细胞肺癌（NSCLC）的疗效和安全性的研究

刘良

西海岸新区人民医院

目的:本研究是一项前瞻性、单臂、单中心 II 期研究，针对 EGFR 阴性的局部晚期或转移性 NSCLC 受试者，旨在评估信迪利单抗联合安罗替尼案一线治疗的疗效及安全性。

方法:本研究中研究药物定义为信迪利单抗、安罗替尼。研究药物的首次给药（第 1 周期，第 1 天）开始，在完成给药前评估之后，在每个周期的第 1 天开始研究给药。出于管理方面的原因，根据研究者的判断，可在每周期计划的第 1 天之前或者之后 3 天内给药。具体用药方法:信地利单抗剂量为每次 200mg，每 3 周给药 1 次，3 周（21 天）为一个疗程，直至疾病进展或出现不可耐受的不良反应。盐酸安罗替尼的推荐剂量为每次 12mg，每日 1 次，早餐前口服。连续服药 2 周，停药 1 周，即 3 周（21 天）为一个疗程，直至疾病进展或出现不可耐受的不良反应，用药期间如出现漏服。确认距下次用药时间短于 12 小时，则不再补服。

结果:本项目将免疫治疗及抗血管生成治疗肿瘤结合起来，用于一线 EGFR 阴性的 NSCLC 的治疗，具有较高的临床应用价值和创新性。两种不同作用机制的药物，可能在治疗中起到协同增强的效果，具有较高的科学性和先进性。为 EGFR 阴性的 NSCLC 一线治疗方案的选择、药物的应用、疗效预测及个体化治疗提供一定的理论依据。

结论:信地利单抗联合安罗替尼为 EGFR 阴性的 NSCLC 一线治疗方案的选择、药物的应用、疗效预测及个体化治疗提供一定的理论依据，安全可靠。

723. circ_MYLK 靶向 miR-324-3p 调控乳腺癌细胞增殖、迁移及侵袭的分子机制

刘良

西海岸新区人民医院

目的:本文探究 circ_MYLK 对乳腺癌细胞增殖、迁移及侵袭的影响；揭示 circ_MYLK 与 miR-324-3p 之间的靶向作用及作用机制；

方法:本研究探讨了 circ_MYLK、miR-324-3p 在乳腺癌组织及癌旁组织中的表达差异；采用分子克隆技术构建质粒，将研究基因利用共转染技术转染 T-47D 细胞，采用多种分子生物学方法，检测 circ_MYLK 对乳腺癌细胞增殖、迁移及侵袭的影响，探查通过干扰 circ_MYLK 靶向调控 miR-324-3p 表达的可能分子机制。

结果:与癌旁组织比较，乳腺癌组织中 circ_MYLK 的表达量升高（$P<0.05$），miR-324-3p 的表达量降低（$P<0.05$）；miR-324-3p 过表达可抑制 wt-circ_MYLK 的荧光素酶活性（$P<0.05$），而对 mut-circ_MYLK 的荧光素酶活性无明显影响；与 si-NC 组比较，si-circ_MYLK 组细胞增殖抑制率和 E-cadherin 蛋白水平升高（$P<0.05$），细胞克隆形成数、迁移及侵袭细胞数减少（$P<0.05$），N-cadherin 蛋白水平降低（$P<0.05$）；与 si-circ_MYLK+anti-miR-NC 组比较，si-circ_MYLK+anti-miR-324-3p 组细胞增殖抑制率和 E-cadherin 蛋白水平降低（$P<0.05$），细胞克隆形成数、迁移及侵袭细胞数增多（$P<0.05$），N-cadherin 蛋白水平升高（$P<0.05$）。

结论:干扰 circ_MYLK 表达可通过促进 miR-324-3p 表达而减弱乳腺癌细胞增殖、克隆形成、迁移及侵袭能力。

724. 胃癌功能性多基因风险评分的构建及跨人群的风险预测

谷元亮、颜财旺、汪天培、胡北平、朱猛、靳光付

南京医科大学

目的:胃癌是亚洲人群高发的恶性肿瘤之一，即使在发病率较低的欧洲人群中也有较高的死亡率。精准的构建多基因风险评分（PRS）有助于胃癌的早期预防。来源于中国人群胃癌全基因组关联荟萃分析研究（GWAS-meta，10254 胃癌病例，10914 正常对照）的 112 个标签单核苷酸多态性位点（SNP）构建的 PRS（PRS-112），作为一个有效的遗传风险预测工具已在中国人群大规模前瞻性队列中得到了验证。但由于遗传结构的差异，PRS-112 可能不适于跨人群应用。有研究认为大多数常见功能遗传变异在不同的人群中是共享的，识别功能遗传变异并以此构建 PRS 可以提高跨人群疾病风险预测的准确性。因此定位胃癌相关的功能遗传变异，可能有助于构建适用于欧洲人群的胃癌 PRS。

方法:本研究使用多个编码区变异功能预测工具及公共数据库下载的胃组织或细胞系的组蛋白修饰信号、转录因子结合位点、染色质互作信号、表达数量性状位点（eQTL）等信息，对 112 个标签 SNP 附近的高连锁不平衡 SNP 进行批量的功能注释，进而鉴定出可能影响蛋白编码或转录调控的功能 SNP，并使用 LDpred2 微效多基因模型（LDpred2-inf）构建功能性 PRS（fPRS）。最后在英国生物样本数据库（UKB）的欧洲人群中检验 PRS-112 和 fPRS 的胃癌风险预测效果。

结果:本研究共鉴定出 125 个功能性 SNP，其中包括 7 个预测为影响蛋白质编码的致病性 SNP 和 118 个可能影响转录调控的非编码 SNP，并以此构建了 fPRS。在 4,582,045 人年的随访中，UKB 队列的欧洲白人中共有 623 例新发胃癌，PRS-112 与胃癌风险之间没有显著关联（HR= 1.00, 95% CI= 0.93-1.09, *P= 0.846*），而 fPRS 与胃癌风险显著相关（HR= 1.11, 95% CI= 1.03-1.20, *P= 0.008*）。以 fPRS 将人群五等分，与低 fPRS（最低 1/5）人群相比，高 fPRS（最高 1/5）人群的胃癌发病风险更高（HR= 1.43, 95% CI= 1.12-1.84, *P*= 0.005）。同时，fPRS 较高的个体发生胃癌的 5 年绝对风险高于同龄人。另外，fPRS 在 UKB 全人群中的胃癌风险预测效果依然稳定（HR= 1.10, 95% CI= 1.02-1.19, *P*= 0.008）。

结论:本研究通过功能注释的方法鉴定了 125 个潜在功能遗传变异，并构建了适用于欧洲人群的胃癌 fPRS，在跨人群预测胃癌遗传风险方面明显优于 PRS-112。

725. 肺癌患者支气管肺泡灌洗液微生物组特征与非癌症病变的比较

孔昕

中国科学技术大学附属第一医院（安徽省立医院）

目的:比较非小细胞肺癌和非肿瘤性疾病患者的肺部微生物组的差异，对非小细胞肺癌和非癌症病变的肺部病变的微生物组进行表征，探索非小细胞肺癌患者独特的肺部菌群结构。

方法:前瞻性收集 2021 年 10 月至 12 月行支气管镜检查的患者的支气管肺泡灌洗液，纳入 14 例患者，其中 10 例诊断为非小细胞肺癌，4 例诊断为肺部感染。采用 16S rRNA 测序法对细菌种类进行测序，对获得数据进行生物信息学分析其 alpha、beta 多样性、物种组成以评估其中微生物菌群结构。

结果:受试者平均年龄 64 岁，两个组别中的微生物结构组成不同，在非小细胞肺癌患者中优势菌门组成主要是变形菌门（47%）、厚壁菌门（29%）、拟杆菌门（11%）、放线菌门（7%）和梭杆菌门（4%），而在非癌症病变的患者组中优势菌门组成主要是厚壁菌门（37%）、变形菌门（29%）、放线菌门（16%）、拟杆菌门（14%）和梭杆菌门（2%）。非小细胞肺癌组中的变形菌门的相对丰度显著增加（Wilcoxon 检验，p= 0.035）。两组样本共有 13 个优势种属，其中包括γ变形菌、卟啉单胞菌、链球菌、奈瑟氏菌、韦永氏球菌、普雷沃菌、棒状杆菌、消化链球菌、伯克氏菌、梭状芽孢杆菌等。进行 LEFse 分析进一步评估这 13 个种属在两组间的差异，发现属于变形菌门的γ变形菌在肺癌患者的肺泡灌洗液中显著升高（Wilcoxon 检验，p= 0.033）。

结论:结果表明，非小细胞肺癌患者与非癌症病变患者的肺部微生物群落结构存在差异，癌症的发生可能会改变肺部菌群结构，进而改变肿瘤微环境。微生物及其相关代谢物可能作为诊断性生物标志物用于治疗探索。

726. H3F3B 为免疫组化内参的新方法及其在肿瘤精准诊疗中的应用

金光植

上海交通大学医学院附属同仁医院

目的:采用免疫组织化学（IHC）的肿瘤标志物定性及定量对于肿瘤诊断、预测预后以及治疗评估具有重要指导意义。特别是以 Her2 及 PD-L1 表达水平为指导曲妥珠单抗及纳武利尤单抗、帕博利珠单抗疗效的重要依据。但是 Her2 及 PD-L1 表达水平受 IHC 实验过程中的样本制备、一抗及二抗反应、显色反应等许多参数的影响。此外，Her2 及 PD-L1 表达水平通常由病理医生根据染色强度和阳性表达的细胞率以及正确的细胞内定位情况给出评分。而，由病理医生打分的结果存在着差异，甚至差异超过 25%。Nat Biomed Eng (2019）也称报道免疫组织化学的精确定量是行业界的重大难题，是亟待解决的问题。因此，为了提高基于 IHC 方法的 Her2 及 PD-L1 表达水平的精准评分方法的开发迫在眉睫。

方法:们关注到组蛋白 H3F3B 通常作为核内参应用于免疫印迹（WB）。首先我们采用 HPA 数据库下载的 H3F3B 的免疫组化图像初步评估了其作为免疫组化内参的可行性。继而，我们采用肝癌组织评估了 H3F3B 在肿瘤组织的纵向和横向及切片内部的表达水平（以 H-Score 代表其表达水平）。我们对乳腺癌组织的 Her2 和肝癌组织中的 PD-L1 表达水平进行定量并采用连续切片的 H3F3B 表达水平进行了校正（即 Her2 的 H-Score/H3F3B 的 H-Score 或 PD-L1 的 H-Score/H3F3B 的 H-Score），并将 Her2 评分分类与乳腺癌患者转移复发风险进行了关联分析。另外，我们还采用同一张切片上的双染方法进行了 Her2/H3F3B 比值并与上述连续切片得出的比值进行一致性分析。

结果:通过 HPA 数据库 H3F3B 的免疫组化图像初步分析，我们发现 H3F3B 在 20 种人类癌组织中稳定且均匀地表达于细胞核，易于计数且与膜表达的 Her2 和 PD-L1 空间上易于区分。另外，H3F3B 在肝癌组织的纵向和横向及切片内部的表达水平高度一致，显示出作为免疫组化内参的高度可行性。采用连续切片的 H3F3B 表达水平校正的 Her2 表达水平与双染方法的 Her2/H3F3B 比值高度一致，且 2 种方法得出的 Her2/H3F3B 比值的均可有效分类出具有高转移复发风险的乳腺癌患者。

结论:以 H3F3B 为内参的 IHC 方法，可为 Her2 和 PD-L1 精准评分提供有效的工具，且 H3F3B 可作为实间质控和实内质控制的工具。

727. 预见性分阶段干预对预防肺癌 PICC 置置管患者血流感染的作用

谢娟秀

福建中医药大学附属人民医院

目的: 分析预见性分阶段干预对预防肺癌经外周静脉穿刺中心静脉置管（PICC 置管）患者血流感染的作用

方法: 选择我院 2019 年 4 月-2021 年 5 月收治的 68 例肺癌 PICC 置管患者作为研究对象，根据其入院治疗时间分组，将 2019 年 4 月-2020 年 4 月入院治疗患者纳入参照组（34 例），实施常规护理干预；将 2020 年 5 月-2021 年 5 月入院治疗患者纳入研究组（34 例），实施预见性分阶段干预。观察和比较两组患者护理前后自我效能感量表（GSES）评分、生活质量核心量表(EORTC QLQ－C30)评分和护理后患者血流感染发生率、护理满意率

结果: 干预后，两组 GSES 评分显著高于干预前，研究组 GSES 评分高于参照组，差异均有统计学意义（$p<0.05$）。干预后，两组 EORTC QLQ－C30 评分显著高于干预前，研究组 EORTC QLQ－C30 评分高于参照组，差异均有统计学意义（$p<0.05$）。研究组血流感染发生率低于参照组，差异有统计学意义（$p<0.05$）；研究组护理满意率高于参照组，差异有统计学意义（$p<0.05$）

结论: 实施预见性分阶段干预可显著提高患者自我效能，降低肺癌 PICC 置管血流感染发生率，并提升患者对护理的满意率。

728. 术前血清胱抑素 C 对 HBV 相关性肝细胞癌患者预后的影响

叶冬、余红平

广西医科大学附属肿瘤医院

目的:探讨术前血清胱抑素 C 水平（Cys-C）对行肝癌切除术后的乙型肝炎病毒（HBV）相关性肝细胞癌（HCC）患者预后的影响。

方法:收集 2014 年 1 月至 2019 年 6 月于广西医科大学附属肿瘤医院因首次发现肝癌就诊，且行肝癌切除术的 940 例 HBV 相关性 HCC 患者的临床病理和随访资料。基于 log-rank 检验方法确定术前 HBV 相关性 HCC 患者血清 Cys-C 水平的最佳临界值，将所有患者分为高血清 Cys-C 水平组和低血清 Cys-C 水平组。运用 Kaplan-Meier 法进行生存分析，单因素和多因素 Cox 回归模型分析影响患者术后总生存率的关系。

结果:HBV 相关性 HCC 患者术前血清 Cys-C 水平的最佳临界值为 0.71mg/L。高血清 Cys-C 水平组患者中的男性、年龄≥50 岁和无吸烟史者的比例高于低血清 Cys-C 水平组患者（P<0.001）。生存分析结果显示，术前血清 Cys-C 水平高的患者总生存期（overall survival, OS）较低血清 Cys-C 水平患者显著缩短（P= 0.02）。经多因素 cox 回归分析对 BCLC 分期、Child 分级和 AFP 因素进行校正后，结果发现血清 Cys-C 水平仍是 HBV 相关 HCC 患者术后 OS 的独立危险因素，与低血清 Cys-C 水平组患者相比，高血清 Cys-C 水平组患者行肝癌切除术后的死亡风险增加 1.82 倍（HR= 1.82，95%CI=1.14-2.91，P=0.012）。

结论:术前血清 Cys-C 水平是 HBV 相关性 HCC 患者行肝癌切除术后预后的独立危险因素。

729. 昆明小鼠 lewis 肺癌细胞种植后对心率变异的影响

刘雪莹、李炜健、凌永健、辜晓康、何雷、陈伟强

南方医科大学

目的:研究 Lewis 肺癌小鼠心率变异性（HRV）指标的变化规律，探索肺癌诊断的心率变异指标，为治疗肺癌提供新的研究方向。

方法:将 70 只雄性昆明小鼠随机分为健康组（正常小鼠）20 只和实验组（Lewis 肺癌建模组）50 只，实验组在建模之后根据是否成功分为未成瘤组和成瘤组。在建模后分别记录各组小鼠的 HRV 指标数值和统计分析。

结果:建模后成瘤组有 36 只小鼠，未成瘤组为 14 只，包括健康组在内各组小鼠均存活。由单因素 ANOVA 检验和 Kruskal-Wallis 检验得到差异具有统计学意义（P＜0.05）的指标有 sdnn，rmssd，lf，hf，且在三组的两两比较中，sdnn 的差异均具有统计学意义（P＜0.05）。根据成瘤可能性的大小对三个组进行由小到大排列（即健康组，未成瘤中，成瘤组）并进行斯皮尔曼相关分析得：sdnn、rmssd、lf、hf 与肿瘤都具有一定的负相关关系（p<0.05）。将成瘤组作为参照类别，由多项 Logistic 回归分析的 sdnn 在三个组别均产生显著性影响（P＜0.05），

rmssd 在健康组和成瘤组、未成瘤组和成瘤组产生显著影响（$P<0.05$）。在决策树模型中，sdnn 的特征重要性在差异具有统计学意义的 4 个指标中都是最高的，rmssd 次之。在三组中进行 ROC 曲线分析，sdnn 和 rmssd 对于成瘤均有很高的诊断价值，得到 sdnn 截止水平为 37.49ms，敏感性为 97.2%，特异性为 91.2%，曲线下面积（AUC）为 0.971，rmssd 的截止水平为 53.58ms，敏感性为 100%，特异性为 70.6%，AUC 为 0.936。

结论:低水平的 sdnn 和 rmssd 可能是 Lewis 肺癌移植的独立危险因素，HRV 中 sdnn、rmssd、hf 等下降能够反映自主神经紊乱，后者会影响肿瘤的进展。

730. 早期髓系来源抑制细胞通过下调 ARID1A 表达促进 luminal A 型乳腺癌上皮间充质转化过程

陈桂冬、李星晨、纪辰燕、刘芃芃、于津浦

天津医科大学肿瘤医院

目的:早期髓系来源抑制细胞（eMDSCs）是一种新的 MDSCs 亚群，与经典 MDSCs 相比具有更强的免疫抑制能力。在前期研究中，我们发现 eMDSCs 高浸润与乳腺癌的不良预后相关，但具体机制尚不清楚。

方法：我们构建了 21 个特征性基因来评估乳腺癌组织内 eMDSCs 的浸润状况，同时通过体外细胞实验探索 eMDSCs 对细胞行为的影响。此外，我们通过蛋白质组学的方法探索乳腺癌细胞中 eMDSCs 的目标蛋白，并在乳腺癌细胞中进行验证。

结果：21 个特征性基因能够很好地预测乳腺癌组织样本中 eMDSCs 的浸润情况，这一结果在我们收集到的乳腺癌样本中得到了验证，并且发现 eMDSCs 高浸润会影响乳腺癌患者的预后，特别是在 luminal A 型乳腺癌中。我们还在体外细胞实验中发现 eMDSCs 通过促进上皮-间质转化（EMT），加速细胞迁移和侵袭过程。eMDSCs 在 luminal A 型乳腺癌中明显下调了 ARID1A 的表达，这一蛋白与 EMT 密切相关，是乳腺癌患者的一个重要预后因素。此外，与 eMDSCs 共培养或敲除 ARID1A 后，luminal A 型乳腺癌细胞中 EMT 相关基因发生明显变化，而 ARID1A 的过表达明显逆转了这一过程。

结论：总之，eMDSCs 通过抑制 ARID1A 的表达促进 luminal A 型乳腺癌的 EMT 过程，为开发常规疗法后复发的 luminal A 型乳腺癌的新型治疗方案提供新的启示。

731. LINE-1 通过调控代谢重编程促进肺鳞癌发生发展

张蕊[1]、孙泽国[2]、刘芃芃[1]、于津浦[1]、张为家[2]

1. 天津医科大学肿瘤医院

2. 美国纽约西奈山伊坎医学院

目的：长散布元素-1（LINE-1，L1）是肿瘤遗传风险。L1 通过形成 L1 嵌合转录本（LCTs），在肿瘤发生发展中发挥重要作用。

方法：我们开发了逆转录转座子基因融合估算程序，识别和量化来自 TCGA 肺癌队列（n=1146）和单细胞 RNA 测序数据集中的 LCT，并在天津肿瘤医院独立队列（n=134）中进一步验证这些 LCT。然后我们研究了肿瘤特异性 LCT（L1-FGGY）在肺鳞癌细胞系和小鼠中细胞增殖和肿瘤进展中的功能作用。

结果：LCT 与特定的代谢过程和线粒体功能相关，并与基因组不稳定性、低甲基化、肿瘤分期和肿瘤免疫微环境相关。基于 L1-FGGY 的功能分析表明，L1-FGGY 引起花生四烯酸代谢重编程，促进肿瘤生长，联合使用抗 HIV 药物 NVR 和代谢抑制剂 ML355 可有效抑制肿瘤生长。最后，我们确定了一组转录组特征，以将预后不良风险较高的肺鳞癌患者分层，这些患者可能受益于单独使用 NVR 或与抗代谢药物联合使用的治疗。

结论：本研究首次阐明了 L1 在肺癌代谢重编程中的作用，为 L1 预测预后提供了理论依据，并为提出肺癌治疗新策略提供了潜在的可能。

732. 新辅助内分泌治疗联合放疗治疗寡转移性前列腺癌的前瞻性临床试验

肖雨田[1]、常易凡[1]、赵宪芝[1]、闫石[1]、王野[2]、张火俊[1]、任善成[2]

1. 海军军医大学第一附属医院（上海长海医院）

2. 海军军医大学第二附属医院（上海长征医院）

目的:寡转移性前列腺癌的最佳治疗方法仍未有定论。越来越多的临床试验证明了前列腺癌根治术以及肿瘤原位或转移灶定向放疗对寡转移前列腺癌患者的安全性和可行性。本临床试验的目的是证明转移灶定向新辅助放疗和新辅助雄激素剥夺疗法以及机器人辅助根治性前列腺切除术治疗寡转移性前列腺癌的安全性和可行性。

方法:本临床试验是一项前瞻性、开放标签、剂量递增的 I/II 期临床试验进行。受试者将接受 1 个月的新辅助内分泌治疗，然后进行转移灶定向放疗和腹部或盆腔放疗。放疗结束 4-8 周后，行机器人前列腺癌根治术。术后辅助内分泌治疗持续 2 年。该研究的主要终点是通过不良事件通用术语标准 (CTCAE) 5.0 评估治疗方法的安全性，以及通过 Clavien-Dindo 分类系统评估的围手术期并发症发病率。次要终点包括手术切缘阳性率、无生化复发生存期（bPFS）、放射学无进展生存期（rPFS）、术后尿控和生活质量指标。

结果:本研究已获得上海长海医院伦理委员会 (CHEC2019-110) 的批准，并在中国临床试验中心网站进行前瞻性注册(CHiCTR1900025743)。所有临床数据将由研究人员收集。该研究的结果预期投稿至同行评审的学术期刊，并在相关的医学会议上发表。所有受试者须书面签署知情同意书。

结论:近年来，前列腺癌根治术适应症逐步扩大，一些中心已对寡转移性前列腺癌患者开展前列腺癌根治术，但其价值尚无定论，有较高的并发症风险且生存获益有限。新辅助放疗已被证明对结直肠癌、乳腺癌和其他多种类型的恶性肿瘤安全有效，在降低转移性肿瘤细胞活性、临床降期和降低潜在术中风险方面显示出潜在优势。现有研究已经表明，对于高危局限性前列腺癌以及局部晚期前列腺癌，新辅助放疗具有良好的耐受性。因此，在这项研究中，我们希望通过 3+3 剂量递增的设计，进一步确定受试者对新辅助疗法的泌尿生殖、胃肠道和全身毒性的耐受性；此外，通过前列腺癌根治术，可以获得手术病理，以进一步确定治疗反应和后续治疗计划

733. 新型甾体化合物 by002 抑制食管癌细胞增殖及迁移机制研究

王赛琪[1,2,3,4]、聂彩云[1,2,3,4]、吕慧芳[1,2,3,4]、陈贝贝[2,3,4]、王建正[1,2,3,4]、徐伟锋[1,2,3,4]、赫云端[1,2,3,4]、赵静[1,2,3,4]、陈小兵[1,2,3,4]

1. *河南省肿瘤医院*
2. *郑州大学附属肿瘤医院*
3. *河南省消化道肿瘤精准治疗工程技术研究中心*
4. *郑州市消化道肿瘤精准治疗重点实验室*

目的：探索自主合成的甾体小分子化合物 by002 对食管癌细胞 EC109 的增殖及迁移的抑制作用及其潜在的分子机制。

方法:利用 MTT 法测定不同浓度 by002 处理后食管癌细胞的存活率并计算 IC_{50} 值；结晶紫染色法检测低剂量 by002 处理 24h 后 EC109 细胞的克隆形成能力；流式细胞术检测 by00 处理 24h 后 EC109 细胞的凋亡率；利用 Transwell 检测低剂量 by002 处理后 EC109 细胞的迁移能力；Western blot 检测 by002 处理 EC109 细胞后 active caspase-3、PARP1、p-Akt（Ser473）、E-cadherin 等蛋白的表达水平；建立人食管癌裸鼠荷瘤模型，连续给予小鼠 by002 治疗 21 天，观察 by002 对食管癌体内增殖抑制效果结果：化合物 by002 能够显著抑制 EC109 细胞体外增殖并呈浓度和时间依赖性。72 小时 IC_{50} 为 9μM；by002 处理 24h 之后，EC109 细胞所形成克隆的数量和大小均明显下降（$P<0.05$）并呈剂量依赖性；by002 处理 EC109 细胞 24h 之后诱导细胞发生凋亡，呈剂量和时间依赖性，同时 EC109 细胞的迁移率受到明显抑制；Western blot 结果显示，随着 by002 浓度的增加，EC109 细胞中 active caspase-3、PARP1 和 E-cadherin 表达量逐渐上升，而 p-Akt（Ser473）表达量逐渐下降同时 total-Akt 表达量未发生明显改变；体内实验结果显示，by002（100mg/kg/d）显著抑制食管癌细胞在体内的增殖抑制。

结论：新型甾体小分子化合物 by002 可能通过抑制 Akt 信号通路诱导细胞凋亡，从而抑制食管癌 EC109 细胞体内外增殖；此外，by002 可能通过上调上皮细胞标志物 E-cadherin 抑制 EC109 细胞体外迁移。

734. 构建免疫相关的预后模型以预测乙肝病毒感染肝癌患者的预后诊断和免疫治疗

付晨、刘超月、付佳

中国医科大学

目的：越来越多的证据表明，免疫相关基因在肝细胞癌(HCC)发生发展过程中起着至关重要的作用。然而，利用免疫相关基因进行评估乙肝病毒（HBV）感染肝癌患者的预后尚不明确。本研究的目的在于探讨具有预后价值的免疫相关基因在 HBV 感染的 HCC 中的作用。

方法：在癌症基因组图谱(TCGA)中整合 114 例 HBV 感染的 HCC 和 50 例正常组织的基因表达数据。分析差异表达免疫相关基因和单变量 Cox 回归分析以确定与总生存相关的免疫相关差异基因。免疫预后模型为使用 Lasso 和多元 Cox 回归分析构建。并进行多变量 Cox 回归分析用于确定 HBV 感染的 HCC 的独立预后因素。并对免疫相关性分析标记和免疫细胞浸润也进行了研究。

结果：共检测到 113 个免疫相关差异表达基因。免疫相关差异基因通过单因素 Cox 回归分析确定与 HCC 患者总生存率显著相关。应用多变量 Cox 回归分析构建基于免疫的预后模型，包括 7 个免疫相关基因，进一步分析表明，该免疫相关预后模型可能是一种和临床因素相关的独立预后指标。风险评分模型和免疫细胞浸润提示：该 7 个基因预后模型具有独立的预后价值，进一步能反映肿瘤免疫微环境。

结论：我们的研究筛选了潜在的预后免疫相关基因，并建立了一种新的基于免疫的 HBV 感染的 HCC 预后模型，不仅提供了新的潜在的预后生物标志物，同时也加深了我们对肿瘤免疫微环境状态的认识，为带有 HBV 的 HCC 奠定了免疫治疗的理论基础。

735. 敲低 Skp2 下调胃癌中 CD47 表达以促进巨噬细胞的抗肿瘤免疫作用

赵丽丹[1]、高可[1]、王研[1]、陈小兵[2]、石晓静[1]

1. 郑州大学医学科学院

2. 河南省肿瘤医院

目的:胃癌是全球最常见的确诊恶性肿瘤，在我国，2/3 胃癌在确诊时已处于进展期，预后较差，已成为癌症相关死亡的第三大常见原因。S 期激酶相关蛋白 2（S-Phase Kinase Associated Protein 2，Skp2）是 F-box 家族的成员，在食管癌、胃癌、乳腺癌、前列腺癌、肺癌等多种肿瘤中高表达，参与肿瘤细胞增殖、侵袭和转移等过程。此外，Skp2 在免疫微环境中发挥重要调控作用，然而 skp2 调控免疫微环境的机制尚不明晰。本研究旨在探索 Skp2 调控 CD47 表达，参与免疫微环境。

方法:通过 GEPIA、Ualcan、TIMER 等生物信息学工具探索 skp2 与 CD47 表达相关性；分别通过免疫组织化学、qRT-PCR 及 Western blot 进一步从肿瘤组织和细胞水平探索 skp2 与 CD47 表达相关性；运用体外共培养技术，使用流式细胞术和免疫荧光等实验方法进行了体外巨噬细胞吞噬能力测定；在免疫缺陷小鼠身上建立了异种移植模型进行了体内验证。

结果:在胃癌肿瘤组织和细胞中，skp2 与肿瘤浸润性巨噬细胞呈负相关；在胃癌细胞中，敲低 skp2 能够降低 CD47 蛋白的表达，同时下调增加了巨噬细胞对胃癌细胞的吞噬作用；动物实验结果也表明了敲低 skp2 具有诱导巨噬细胞吞噬作用的能力从而抑制肿瘤生长和转移。

结论:skp2 是胃癌巨噬细胞吞噬作用的重要调节因子，在肿瘤固有免疫调控中发挥了重要作用，从而为胃癌的预后和抗肿瘤免疫疗法的应用探索新的研究思路。

736. 肿瘤相关成纤维细胞通过 CXCL14/ANGPTL4/ERK 促进肺腺癌铂类耐药

李梦青、卢德华、杨晓东、高静

北京大学深圳医院

目的:肺癌是常见的恶性肿瘤，晚期肺癌化疗耐药仍是治疗的最大挑战之一。部分患者化疗后仍难免于肿瘤局部复发及远端转移。肿瘤相关成纤维细胞(Cancer-associated-fibroblas, CAF)是微环境中的主要成分之一，近年来越来越多研究发现其在肿瘤耐药中发挥重要作用，深入研究 CAFs 分泌蛋白在肺癌在耐药中的具体作用及机制，将有利于寻找肺癌治疗新的药物作用靶点，促进患者预后的改善。本研究在前期发现 CXCL14 在 CAFs 中高表达，以及体外证实 CXCL14 促进肿瘤细胞的耐药和转移的基础上进一步探索 CXCL14 介导下游信号转导的方式，以及促进化疗耐药的具体机制，同时初步探索干预上述信号通路逆转耐药的可能性，为临床非小细胞肺癌耐药及进展提供新治疗手段的理论依据。

方法:我们利用组织块培养方式获得原代肿瘤相关成纤维细胞。体外通过 CAFs 产生条件性培养基处理或真核重组蛋白进行功能实验。利用 CCK-8、迁移和侵袭实验、克隆形成能力、活-死细胞染色等在体外探索 CXCL14 对肺腺癌的功能。利用裸鼠皮下成瘤、腹腔化疗药注射我们确认 CXCL14 在体内实验中的促进耐药功能。利用表达谱测序探索 CXCL14 对肺癌细胞系基因的调控机制。

结果:研究首先在获取的原代 CAFs 中发现 CXCL14 基因的高表达，进一步通过生信数据和临床样本的组化芯片确认了其在间质的高表达情况。体外试验中，我们确认了 CXCL14 可以促进肺腺癌的铂类耐药，降低了铂类在体外诱导细胞凋亡的作用，并在体内实验中进一步验证该结果。通过 RNA-seq 我们发现 CXCL14 显著上调了 ANGPTL4 等基因，并在下游激活了 ERK 的磷酸化，从而促进耐药。敲低 ANGPTL4 或使用 ERK 抑制剂均可以逆转 CXCL14 的处理作用。

结论:CXCL14 在肺癌的间质中高表达，肿瘤相关成纤维细胞分泌的 CXCL14 可以促进肺腺的化疗耐药。该分子发挥作用很可能是通过激活了 ANGPTL4/ERK，而通过干预 ANGPTL4 或 ERK 可有效逆转 CXCL14 的作用。

737. 肿瘤标志物在免疫治疗过程中的作用

谢晓冬

中国人民解放军北部战区总医院

目的:免疫检查点抑制剂越来越多地出现在各种实体瘤的治疗策略中。免疫治疗时代来临。针对多种实体瘤，免疫治疗的长期生存获益均给人们带来惊喜，给肿瘤患者带来新的希望。然而，临床上对免疫检查抑制剂敏感的患者仅占少数；还会出现各种各样严重的不良反应，甚至有患者接受免疫治疗后出现肿瘤超进展。因此，免疫治疗过程中，有效的标志物必不可少。尤其是预测肿瘤免疫治疗疗效的标志物、预测免疫治疗相关不良反应和预测免疫治疗超进展的标志物。

方法:对肿瘤免疫治疗过程中出现假阳性进展、超进展、严重不良反应的案例进行检索和分析。并分别针对预测肿瘤免疫治疗疗效的标志物、预测免疫治疗超进展的标志物、预测免疫治疗相关不良反应的标志物进行综述。

结果:肿瘤标志物在肿瘤免疫治疗的过程中，对疗效、预后和不良反应有一定程度上的提示作用。不同肿瘤标志物在免疫治疗过程中发挥着不同的作用。通过一系列的综述，加深对在免疫治疗过程中起重要作用的标志物的了解和掌握。

结论:随着大量的免疫检查点抑制剂在中国上市，新的适应症不断获批，层出不穷的免疫治疗药物已正式登上中国肿瘤治疗的舞台。选择好有效的预测因子尤为重要。如何让肿瘤免疫治疗高效低毒，如何更加准确地预测肿瘤免疫治疗的疗效、预后及不良反应，是我们要共同面对的难题。

738. 肺癌患者循环肿瘤 DNA 的靶向治疗相关基因变异谱

白玲、宋佳佳、翟建昭、李晋、陆小军、陈飘飘、周易、周娟

四川大学华西医院

目的：循环肿瘤 DNA（ctDNA）测序是检测肺癌靶向基因变异的方法。这项研究调查了中国西南地区肺癌患者的 ctDNA 突变谱，以便为临床决策提供有价值的信息。

方法：这项回顾性研究纳入了 2017 年至 2019 年间到我院就诊的肺癌病人共 672 例，对其外周血血浆 ctDNA 下一代测序（NGS）结果及临床特征进行了回顾性分析。每名患者进行 ctDNA NGS 检测时均抽取 20ml 外周血，对与肺癌靶向治疗相关的 23 个基因进行靶向测序。

结果：672 例患者中约 73%在血浆 ctDNA 中检出至少有一个基因变异，并且有 306 例患者检出了靶向药物治疗相关的敏感或耐药位点。变异频率最高的基因是 EGFR（42.41%），其次是 ROS1（8.04%），HER2（7.59%），ALK（6.99%），FGFR1（5.51%），RET（5.51%），PIK3CA（4.46%），TSC1（4.46%），KRAS（3.87%），SMO（3.72%）等。EGFR 突变与女性，非吸烟者和腺癌有关，而 KRAS 突变倾向于在男性和吸烟者中发生。二者显著性互斥。吸烟史患者的 BRAF，KRAS，DDR2 和 MEK1 阳性率较高。HER2 和 RET 变异在腺癌中常见，未在鳞状细胞癌中检出。EGFR 19DEL，L858R，T790M 是最常见的 EGFR 突变类型，A1013T/A1013V，G719A/G719S，T273P 和 C264fs 等次之，同时也观察到了一些罕见的突变，包括 I1050T，K806R，S768I 和 L861Q。所有 C797S 突变均与 T790M 同时发生，其中 1 例患者同时存在 2 种 C797S 顺式突变。所有六个 T751A/T751I/T751P 突变均伴有 19DEL。与未靶向治疗的患者相比，有靶向治疗史的患者发生 EGFR 突变的频率更高，但 KRAS、PTEN、KIT、FGFR2 的突变率较低。此外，具有肾上腺、骨、脑、肝、多发转移的肺癌患者阳性检出率分别为 100%、82.40%、53.85%、80.00%、82.72%，其中脑转移的阳性率最低。

结论：这项研究表明近一半的患者在进行 ctDNA NGS 检测后可以获得靶向药物用药的实际指导，真正受益于 ctDNA 基因检测。血浆 ctDNA 的突变谱和阳性率与临床特征密切相关。不推荐将血浆用于患有脑转移的肺癌患者进行基因检测，因为其阳性率较低。当组织活检不可行时，液体活检将是肺癌靶向治疗选择的有效方法。然而，肿瘤 DNA 释放能力、ctDNA 含量和片段化挑战了其在血浆中的检测，尤其是结构变异和拷贝数变异。总之，液体活检领域仍需继续改进提升以更好地辅助临床治疗。

739. CDX-2 在胃癌中的研究现状

廖亦然、王炯

重庆大学附属肿瘤医院

目的：胃癌是常见的恶性肿瘤之一，它是一种由慢性胃炎经多步骤、多过程逐渐进展至癌变的疾病，众多基因及分子参与该演变过程。CDX-2 是同源框基因家族的一员，CDX-2 作为一种胃肠道特异性转录因子，能够特异性结合多种胃肠道基因启动子，调控这些基因在胃肠道的特异性表达及表达强度；同时还具有促进肠胎发育、胃肠道炎症及肿瘤发生等多种功能。CDX-2 作为抑癌基因与胃癌的发生发展相关，在诱导耐药、指导治疗、判断预后中起着重要作用。

方法：CDX-2 促进胃黏膜肠上皮化生，CDX-2 与肠上皮化生（intestinal metaplasia，IM）及胃癌时发现，CDX-2 表达阳性率不仅在不同 IM 亚型中有所差异（I 型表达最高，II 型表达居中，III 型表达最低），而且在萎缩性胃炎伴 IM、癌旁 IM 组织、肠型胃癌和弥漫型胃癌中表达阳性率亦各不相同，IM 越倾向恶性，CDX-2 阳性表达率越低，一定程度上反映出 CDX-2 的缺失可能是 IM 恶性进展的因素。CDX-2 阳性表达随着胃癌晚期逐渐减少，CDX-2 可上调细胞周期依赖性激酶抑制剂 p21/WAF1/CIP1 转录抑癌肿瘤细胞增殖，CDX-2 阳性表达可促进 IL-6、TNF-α 和 TNF-β 的表达而发挥抑癌基因作用，同时 CDX-2 的抑癌基因作用受 miRNA 的调节，miRNA-9 是可与 CDX-2 mRNA 3’UTR 互补序列相结合的 miRNA，它通过靶向负反馈调节 CDX-2 基因，进而促进肿瘤细胞增殖、迁移、侵袭。

结果：CDX-2 在逆转多药耐药(multidrug resistance，MDR)中起关键作用，人类 MDR 基因主要有 MDR1 和 MDR2 两个成员。在耐多药肿瘤细胞中，MDR1 被认为是过表达和扩增的基因，RNAi（RNA interference）介导的 CDX-2 可抑制内源性 MDR1 表达，进而可阻断 MDR1 参与的细胞耐药。CDX-2 阳性表达具有调控药物外排泵送、细胞周期和凋亡的作用，有助于逆转 MDR 的同源框转录 CDX-2 siRNA 可显著下调胃癌 7901/DDP 细胞中 CDX-2 mRNA 和 CDX-2 蛋白表达，导致细胞周期阻滞在 G0/G1 期，诱导细胞凋亡，还可显著降低 SGC7901/DDP 细胞对顺铂、5-氟尿嘧啶和阿霉素的敏感性及对阿霉素泵送能力。

结论：CDX-2 在胃癌药物治疗及基因治疗方面具有巨大潜力和临床应用价值，在指导治疗与预后方面可被用作靶向药物的靶标，也可被用作肿瘤预后和病情监控的标志物。随着 CDX-2 的深入研究，它在胃癌发生、发展中的作用机制将逐渐明确，或许能为新化疗药

物的筛选、基因靶向治疗及肿瘤个体化方案的选择提供了新的思路，未来通过对该基因表达调控的干预或许能为肿瘤治疗开辟新的途径。

740. 识别 IFN-γ促进癌症进展和癌症免疫逃避的负向作用

文小玲、王娜、李徐华、郭雨、符书恒、熊非凡、王珍珍、王宏久

海南医学院

目的:IFN-γ在癌症中发挥双重作用，外源性 IFN-γ的分子机制已明确，并已用于癌症治疗，但对内源性 IFN-γ负向作用的知识仍在癌症研究中。本研究旨在探讨内源性 IFN-γ在癌症中的作用。

方法:从 UCSC Xena、CellTalkDB 中获得 RNA-seq 数据、临床数据和配体受体网络数据。评估 IFN-γ相关基因表达与预后和临床分期的相关性，采用单变量和多变量 Cox 回归分析来确定生存结果的独立预测因子。使用 pearson 相关性分析识别与内源性 IFN-γ相关的配体受体，构建了病人特异配体受体网络。并且，STRING 数据库用于构建 IFN-γ相关蛋白质相互作用网络。利用肿瘤转录组反褶积的细胞特征分析，探索 IFN-γ与肿瘤微环境的关联。此外，SOAR 数据库用于分析 IFN-γ相关基因的空间变异性。

结果:我们根据表达谱及其与患者生存的关系对 IFN-γ相关基因（IFNL2，IFNL3）进行了全面分析。IFN-γ相关基因的表达与患者生存、临床分期、肿瘤突变、甲基化、拷贝数变异有关。内源性 IFN-γ的表达与癌症患者的不良预后显著相关，并且 IFN-γ相关基因（包括 IFNL2 和 IFNL3）可以作为生存结果的独立预测因子。在功能上，升高内源性 IFN-γ的表达可以驱动分子炎症机制，影响细胞-细胞粘附，参与调节免疫功能，影响肿瘤微环境，从而促进癌症的发生发展。同时，IFN-γ主要是由 Janus 酪氨酸激酶（Jak1 和 Jak2）与 IFNGR1 和 IFNGR2 受体结合，转录因子、信号转导和转录激活因子 (STAT1、STAT2、STAT3、STAT5) 的磷酸化启动，从而影响下游信号 JAK/STAT 通路对癌症的进展产生影响。此外，内源性 IFN-γ与自然杀伤 T 细胞如(NKT)细胞、CD8+细胞毒性 T 细胞和 M1 巨噬细胞中呈正相关，而 T 细胞与耗尽的 CD4+T 细胞呈负相关。而 IFN-γ被发现在多种细胞类型中表达，包括炎症、细胞周期和缺氧等。并且表达 IFN-γ的患者具有较高的免疫浸润，但由于 T 细胞紊乱和高炎症环境而发生癌症。此外，我们通过 SOAR 数据库的空间转录组分析了 IFNL2 和 IFNL3 的空间变异性，发现内源性 IFN-主要来源于 CD4+T 细胞。

结论:总之，我们通过多组学分析系统地认识到了 IFN-γ对癌症发展的影响，并为 IFN-γ在其临床治疗中的进一步应用提供了指导。

741. 肺鳞癌患者中铁死亡相关 lncRNA 预测模型的建立与分析

金山琇[1,2]、杜成[2]

1. 大连医科大学

2. 中国人民解放军北部战区总医院

目的:铁死亡是一种以铁离子和氧化应激为特点的细胞死亡，在肿瘤细胞死亡上发挥重要作用。lncRNA 可以通过改变表观遗传来改变肿瘤生长。本文将用与铁死亡相关的 lncRNA 构建预后预测模型来对肺鳞癌生存进行预测及探讨。

方法:从 FerrDb 网站下载铁死亡相关基因，并通过“R 4.2.1”进行分析。相关系数设定为 0.4 进行相关 lncRNA 的筛选。通过 TCGA 公用数据库对肺鳞癌患者信息进行下载，并将患者随机分为训练集与测试集。通过 lasso-cox 回归在训练集进行模型的构建并按中位值分为高低风险组，并在测试集进行验证。我们还利用 ROC 曲线对所构建的模型进行进一步验证，并且绘制了相关的线列图用于临床预测患者预后。根据基因与 lncRNA 的相关性绘制关系图，并进行基因富集分析（GSEA）以及对不同分组免疫检查点相关基因的表达进行探讨。

结果:在训练集通过 lasso-cox 回归最终确定了 6 个铁死亡相关的 lncRNA (AP006545.2、AC092143.3、LUCAT1、LINC02178、AP001189.3、C10orf55）。在测试集中，低风险评分患者有更好的 OS（*P=0.027*）和 PFS（*P*<0.001）。ROC 曲线预测 1 年、2 年、3 年的曲线下面积分别为 0.616、0.696、0.697。在高风险组中临床常用的免疫检查点 CTLA-4、PD1、PDL-1 的基因的表达显著高于低风险组（*P*<0.001）。通过基因富集分析可以看出高风险组患者 JAK-STAT 等信号传导通路更为活跃（*P=0.022*）。两组间免疫细胞浸润亚型及其相应功能存在显著差异。

结论:我们从铁死亡相关 lncRNAs 的角度研究了 LUSC 发展的潜在机制，并确定了 4 个 lncRNAs 作为预测 LUSC 患者预后的生物标志物。

742. 上调 T 抗原合成酶的表达抑制骨肉瘤 LM8 细胞增殖及机制

唐磊[1,2]、符策岗[1,3]、贾思宇[1]、王勃菲[1]、陈海丹[1,2]、蔡惠丽[4]

1. 三峡大学第一临床医学院宜昌市中心人民医院脊柱外科湖北宜昌 443003

2. 宁夏医科大学研究生院宁夏银川 750004

3. 上海市第六人民医院海口骨科与糖尿病医院，海南 海口 570000

4. 三峡大学第一临床医学院宜昌市中心人民医院血液内科湖北宜昌 443003

目的:探讨上调 T 合成酶表达对骨肉瘤 LM8 细胞凋亡的影响及其可能的作用机制。

方法:本研究将 T 合成酶特异性短发夹 RNA（shRNA）或 T 合成酶特异性真核表达载体（pcDNA3.1（+））转染小鼠骨肉瘤 LM8 细胞，观察不同 T 合成酶表达水平的 LM8 细胞在体内和体外的增殖影响及细胞毒性 T 淋巴细胞（CTL）对不同 T 合成酶表达水平的 LM8 细胞的致死率。

结果:T 合成酶的上调促进了骨肉瘤细胞的体外和体内增殖，但在体内 3 周后抑制了骨肉瘤细胞的增殖。体外具有高 T 合酶表达的骨肉瘤细胞促进增殖并抑制 $CD8^+$T 细胞的凋亡。此外，T 合酶上调促进细胞毒性 T 淋巴细胞（CTL）的肿瘤致死率增加。

结论:高 T 合成酶表达通过提高机体的抗肿瘤免疫力对肿瘤生长具有抑制作用。因此，利用这一特性制备具有高免疫原性的肿瘤细胞疫苗，为骨肉瘤的临床免疫治疗提供了新思路。

743. 一种新型 Hf-Ti 结合氟硼二吡咯染料（BODIPY）的纳米光敏剂用于肿瘤光动力治疗联合放疗

陈苗苗

河南省医药科学研究院

目的:为了解决临床上实体瘤中肿瘤细胞的放疗抵制性，将放疗增敏材料 Hf、Ti 与生物低毒光敏剂 BODIPY 结合，制备出一种能同时满足肿瘤光动力治疗和放疗增敏的 Hf-Ti-BODIPY，实现肿瘤的双模态协同治疗。

方法:首先设计并合成了具有 2D 纳米结构的光敏剂 Hf-Ti-BODIPY，通过扫描电子显微镜和透射电子显微镜对其形貌进行表征；验证该材料在蓝色可见光（450nm）下的 ROS 产生的能力；并通过细胞实验研究了其被肿瘤细胞摄取的能力，对正常组织细胞的低毒性，以及对肿瘤细胞光动力治疗和放疗增敏的能力；最后通过动物实验验证其生物相容性和对实体瘤的治疗能力。

结果:通过体外实验验证了该材料具有优越的光稳定性和 ROS 量子产率；共定位结果显示，Hf-Ti-BODIPY 主要定位于线粒体，在无光照的情况下对细胞低毒，在光照下具有良好的肿瘤细胞光杀伤能力。此外，该材料具有良好的生物相容性，血液分析和 H&E 结果显示该材料对正常组织器官无明显损伤，与对照组相比，Hf-Ti-BODIPY 对实体瘤的治疗效果显著。

结论:我们成功合成了一种 2D 纳米光敏剂 Hf-Ti-BODIPY，该材料能够应用于实体瘤治疗，增加肿瘤细胞的放疗敏感性。综上所述，我们希望该光敏剂的开发有助于肿瘤纳米药物的发展，促进肿瘤光动力治疗和放疗协同治疗的进程。

744. 结直肠癌非侵入精准检测方法的技术演替

陈书德、周忠坤、陈朋

兰州大学

目的：结直肠癌是临床常见恶性肿瘤，精准的早期筛查可有效降低结直肠癌死亡率。本文就结直肠癌非侵入精准检测方法及其临床应用的技术演替进行总结与梳理，通过归纳分析为同僚们提供研究思路。

方法：1.粪便隐血试验（FOBT）粪便中的血红素是含铁血红蛋白的主要成分，具有过氧化物酶活性，当它与试剂中的过氧化氢混合，愈创木脂将变为蓝色，即为粪隐血试验阳性。2.粪便分子检测 85%结直肠癌是由染色体不稳定引起的，其突变在腺瘤性结肠息肉 APC 基因，p53 肿瘤抑制基因和 K- ras 致癌基因中逐渐累积。另外 15%来自 DNA 错配修复所涉及的基因丢失。3.粪便微生物标志物筛查肠道菌群及其产物与结直肠癌密切相关，如 ROS 造成的 DNA 损伤、基因毒性的形成、T 细胞增殖增加和促癌通路的激活等。因此，可以检测结直肠癌特异性菌来进行早期筛查。4.血液肿瘤标志物检测血液中的分子（如 DNA、RNA、蛋白质）甚至细胞都可以作为标志物来检测疾病。血液肿瘤标志物用于结直肠癌筛查有广泛的研究，种类与数量较多。

结果：1.粪便隐血试验（FOBT）有效降低 CRC 患者死亡率，具有更高的敏感性和更好的成本效益，优于 gFOBT，定量化与自动化检测；对暂无出血的肿瘤可出现漏诊，炎症、痔疮、消化道出血等亦能出现假阳性结果。2.粪便分子检测使用粪便 DNA 作为分析物的优点是，随着研究进展，可以扩展或改进标记物组。结合隐血检测，可以弥补后者不能检测非出血息肉或腺瘤的缺陷。3.粪便微生物标志物筛查不依赖于已知核酸序列，可直接对未知病原微生物进行检测，突破了以往微生物检验的局限性这无疑将成为研究肠道微生物的有力工具，粪便微生物标识物筛查方法也将有更广阔的应用前景。4.血液肿瘤标志物检测一种微创、简便的体液检测方法，具有易操作、可实时监测癌症异质性变化、避免侵入性检查、利于实现个体化治疗等优点；显示治疗前和治疗期间的 CTC 数量是转移性结直肠癌患者的独立预测因子。此外，CTC 还提供预后信息。

结论：CRC 精准检测从 gFOBT，到 FIT 和 CologuardTM，非侵入性检测的敏感性、专一性逐步提升。微生物与疾病关系的揭秘，为我们开发更加精准的检验与诊断方法带来希望，而且血液标志物的联合检测也有广阔前景。除了理论研究进展的同时，从 Sanger 测序法到 Ion torrent 平台，创新实验技术的出现为我们提供了强有力的帮助。此外，我们也注意到从基础研究到临床应用是一个漫长的过程，伴随着技术、创新发现、临床验证、效率、费用等诸多挑战，譬如：新的免疫方法，更完善的基因检测技术，新的血液标志物的发现，新的粪便 CRC 相关微生物揭示，以及将得到实验室确认的方法在临床大样本验证、追踪、反馈等，这仍旧是限制我们改进非侵入性检测的障碍。而利用 NGS 技术对粪便 CRC 病变微生物进行筛选，结合粪便变异 DNA，开发多种标志物联合的检测方法会成为未来 CRC 精准检测的重要研究方向。

745. 基于脂肪酸代谢相关基因构建头颈部鳞癌的预后模型

肖雪、梁金凤

广西医科大学第一附属医院

目的:头颈部癌症是发生在舌、口腔、鼻咽、口咽、下咽和喉部的恶性肿瘤。大约 90%是头颈部鳞状细胞癌(head and neck squamous cell carcinoma , HNSC)。尽管综合治疗手段的提高，头颈部鳞癌患者的预后仍较差。脂肪酸代谢异常是恶性肿瘤的标志之一，肿瘤细胞通过上调

脂肪酸的摄取、储存和合成，促进自身的快速增殖。本研究旨在分析头颈部鳞癌的脂肪酸代谢相关的差异表达基因谱，并基于分子亚型建立脂肪酸代谢相关的头颈部鳞癌预后模型。

方法:通过基因表达综合数据库（GEO）和癌症基因组图谱数据库（TCGA）获取公共基因表达数据和临床注释，其中 TCGA_HNSC 作为测试集，GSE65858 作为验证集。脂肪酸相关基因来自 MsigDB 数据库中的脂肪酸相关因子。利用 R 语言“limma”包分析差异表达基因，通过“ConsensusClusterPlus” 软件包进行分子分型，通过 Kaplan-Meier 法描绘生存曲线，采用 Cox 回归模型进行单因素和多因素分析，通过 LASSO Cox 回归分析构建预后模型，通过基因表达水平及其对应的回归系数计算患者风险评分。

结果:基于 TCGA_HNSC 数据库的 495 例癌组织和 44 例癌旁组织，我们筛选出 436 个差异表达基因，其中包括 13 个脂肪酸紊乱相关的差异表达基因（如 ADH7、 ADH1B、 CYP4B1 和 APOD 等）。基于这 13 个差异表达基因，我们通过一致性聚类分析，对 TCGA-HNSC 队列样本进行亚型分类，获得 C1、C2 和 C3 三个亚型。Kaplan-Meier 分析结果提示，三个亚型之间的患者具有生存差异，C3 亚型患者的生存状态优于 C1 和 C2 亚型。临床病理学特征分析发现，C3 亚型的高分化肿瘤患者占比更高（高分化癌：C1 32.39%，C2 30.36%，C3 37.25%）。我们随后对三种分子亚型进行差异表达分析，发现 107 个差异表达基因，其中 26 个基因与头颈部鳞癌患者的总生存率显著相关（$P<0.05$）。采用最小绝对收缩和 Lasso 回归分析，我们发现 9 个候选基因构建的模型最佳，通过风险评分中位数将 TCGA-HNSC 队列样本分为高风险组和低风险组，对比发现高风险组的死亡病例比例更高，整体生存期更低。在验证集中，风险评分同样表现了良好的总体生存期预测能力。最后单变量和多变量 Cox 分析结果显示，风险评分可以作为头颈鳞癌患者总生存率的独立预测因子。

结论:头颈部鳞癌中存在脂肪酸代谢相关的差异表达基因。我们在分子分型基础上基于脂肪酸代谢相关基因构建的疾病模型可用于判断头颈部鳞癌患者的预后，筛选出的相关基因可用作头颈部鳞癌预后评估的分子标志物，为头颈部鳞癌的基础和临床研究提供前期数据。

746. 基于 TCGA 数据库分析 AKR1B1 在胃癌中的表达及临床意义

王乃雪[2]、郑振东[1]、杜成[1]、王美玲[1]

1. 中国人民解放军北部战区总医院

2. 锦州医科大学北部战区总医院研究生培养基地

目的：利用在线数据库和生物信息学方法分析 AKR1B1 基因在胃癌中的差异表达对其预后的意义，寻找胃癌新的生物标志物

方法：使用 TCGA 公共数据库获取胃癌患者的基本临床信息、AKR1B1 的表达情况，通过使用 R 语言分析患者癌组织与癌旁组织的表达差异，以及 AKR1B1 的表达与临床信息相关性;利用 Kaplan-Meier Plotter 分析不同 AKR1B1 表达水平的胃癌患者生存曲线，同时利用 ROC 曲线行进一步的验证； Cox 比例风险回归模型对可能影响胃癌患者预后的因素进行单因素及多因素分析,并着重分析 AKR1B1 能否成为影响胃癌患者预后的独立因素;使用 TIMER 数据库分析 AKR1B1 在胃癌中与各种免疫细胞浸润的相关性;GEPIA 数据库分析 AKR1B1 的表达与免疫标志物的相关性。

结果：癌组织 AKR1B1 分子表达水平高于癌旁组织，差异有统计学意义（$p<0.05$）。AKR1B1 高表达患者的总生存（OS）明显低于低表达的患者($p<0.001$, HR= 1.83 (1.31−2.55)),通过 ROC 曲线进行验证得到曲线下面积为 0.625。通过 COX 模型进行分析，在单因素及多因素分析中 AKR1B1（$P<0.001$；$P<0.001$）可作为胃癌患者预后的独立影响因素。AKR1B1 的表达与胃癌中的多种免疫细胞浸润呈正相关，例如 CD4+T 细胞（$P<0.001$）、CD8+T 细胞（$P<0.001$）、巨噬细胞（$P<0.001$）、中性粒细胞（$P<0.001$）、树突细胞（$P<0.001$）。在胃癌中，通过数据库分析发现 AKR1B1 的表达与 PD-L1（$P<0.001$）、PD-1($P<0.001$)、CTLA-4($P<0.001$)的表达呈正相关。

结论：AKR1B1 可作为胃癌患者的不良预后标志物，其高表达的患者生存预后差。AKR1B1 的表达与大部分免疫细胞呈正相关，同时也与免疫检查点抑制剂的表达呈正相关，AKR1B1 可为胃癌患者生存及免疫治疗的疗效提供一定预测价值。

747. 乳腺癌术后化疗患者抑郁发生的危险因素与其免疫状态的相关性

徐璐

永康市第一人民医院

目的:探讨乳腺癌术后化疗患者抑郁发生的危险因素，并分析其与免疫状态的相关性。

方法:收集永康市第一人民医院、永康市妇幼保健院、永康市中医院 2016 年 1 月至 2019 年 12 月收治的 140 例乳腺癌术后化疗患者的一般资料，依照汉密尔顿抑郁量表 24 项版（HAMD-24）分为抑郁组（62 例）与无抑郁组（78 例），比较两组患者一般资料，包括年龄、婚姻状况、文化程度、家庭月收入、付费方式、病理类型、临床分期、手术方式、化疗次数、WBC、Hb、血清白蛋白、血清肌酐、血清尿素氮；多因素 logistic 回归分析患者抑郁发生的危险因素，并通过 Spearman 秩相关分析 HAMD-24 各因子与 T 淋巴细胞亚群的相关性。

结果:抑郁组患者在婚姻状况、家庭月收入水平、临床分期、化疗次数、Hb、血清白蛋白水平方面与无抑郁组比较差异均有统计学意义（均 $P<0.05$）。logistic 回归分析结果显示乳腺癌术后化疗患者抑郁发生的独立危险因素主要为家庭月收入、临床分期、化疗次数、Hb、血清白蛋白水平（均 $P<0.05$）。HAMD-24 总分与 $CD3^+$、$CD4^+$、$CD4^+/CD8^+$、NK 细胞均呈负相关（均 $P<0.05$），与 $CD8^+$ 呈正 相关（$P<0.05$）；而在各因子分析中，睡眠障碍、焦虑/躯体化与 $CD3^+$、$CD4^+$ 均呈负相关（均 $P<0.05$），与 $CD8^+$呈正相关（$P<0.05$）。

结论:乳腺癌术后化疗患者抑郁的发生与婚姻状况、家庭月收入水平、临床分期、化疗次数、Hb、血清白蛋白水平密切相关，且与 CD3+、CD4+、CD4+/CD8+、NK 细胞呈负相关，与 CD8+ 呈正相关。临床应对上述因素及早干预，并给予抗抑郁治疗，改善患 者的免疫状态。

748. 新辅助治疗后激素受体阳性乳腺癌患者残留疾病肿瘤浸润淋巴细胞的预后意义

韩丹丹、岳萌、刘月平

河北医科大学第四医院

目的:研究报道治疗前肿瘤浸润淋巴细胞（Tumor-infiltrating lymphoeytes，TILs）高度浸润的乳腺癌与新辅助治疗（Neoadjuvant therapy，NAT）后较高的病理完全缓解（Pathologic complete response，pCR）率显著相关。但是新辅助治疗后 TILs 在激素受体阳性乳腺癌患者中的预后效果尚不清楚。因此，我们分析了激素受体阳性乳腺癌患者新辅助治疗后 TILs 对 pCR 和生存的预后价值，以预测 NAT 后患者的生存。

方法:回顾性研究 2010 年 1 月至 2016 年 6 月期间河北医科大学第四医院经术前空芯针穿刺活检病理确诊为激素受体阳性浸润性乳腺癌且行新辅助治疗后进行手术切除的原发性乳腺癌患者的临床病理资料，筛选符合入组条件的患者共 560 例，所有患者均进行了 6-8 个周期新辅助治疗和内分泌治疗。肿瘤浸润淋巴细胞分为低度浸润（＜10%）、中度浸润（10-40%）和高度浸润（＞40%）。主要研究终点是总生存期（Overall survival，OS）和无病生存期（Disease-free survival，DFS）。本研究的中位随访时间为 86±10 月（60-118 月）。Kaplan-Meier 及 Cox 回归进行单、多因素生存分析，Spearman 等级相关性分析间质 TILs 与临床病理特征的关联。应用 SPSS 26.0 进行统计分析，p<0.05 具有统计学意义。

结果:本研究共纳入 Luminal A 型乳腺癌 236 例，Luminal B HER2 阴性型乳腺癌 324 例。新辅助治疗前间质 TILs 水平与 NAT 后 pCR（P=0.005）呈正相关，即较高的 TILs 水平与 NAT 后较高的 pCR 率显著相关。新辅助治疗后较高的间质 TILs 与组织学分级(P<0.001)和 RCB 分级(P<0.001)呈负相关。间质 TILs 水平的升高与 DFS（P=0.004）和 OS（P＜0.001）的改善显著相关，并且在多变量分析中仍然是 DFS（P=0.005）和 OS（P=0.004）显著的预测因子。

结论:激素受体阳性乳腺癌患者 NAT 后较高的间质 TILs 水平与较长的 DFS 和 OS 显著相关，是预测预后的重要标志物。

749. 乳腺恶性叶状肿瘤临床病理特征及分子特征分析

岳萌、刘月平

河北医科大学第四医院

目的:乳腺叶状肿瘤（Phyllodes tumour, PT）是纤维上皮性病变中的一种罕见双相性肿瘤，有明显的管内生长模式。其中，恶性 PT 罕见，预后差，因此探索其临床病理特征及分子学基础，对于诊断、预后和治疗具有重要的意义。

方法:系统性回顾性搜集河北医科大学第四医院 2008.5-2021.5 月确诊的乳腺恶性叶状肿瘤病例共 39 例，采用 2019 版 WHO 诊断标准重新评估病例 HE 切片及免疫组化指标，搜集患者临床病理资料，对其中 2015.5-2021.5 的 18 例石蜡包埋标本（包括 5 例复发病例）进行 NGS 检测，分析临床病理特征及分子学改变。

结果:在 39 例病例中，均为女性患者，中位年龄 43 岁（18-67 岁），肿物大小 2cm×2cm×1.5cm-28cm×18cm×11cm，左乳 19 例，右乳 20 例。复发 7 例，远处转移 3 例，转移部位为肺部 2 例，腋下淋巴瘤 1 例。18 例 NGS 检测结果显示：10 例（55.6%）TP53，8 例（44.4%）MLL2，8 例（44.4%）MED12，6 例（33.3%）EGFR，6 例（33.3%）CDKN2A，6 例（33.3%）CDKN2B 基因发生改变。在 5 例复发性恶性叶状肿瘤中，原发病灶与复发病灶基因改变不大，其中 3 例复发前后均检测出 TP53 基因改变，2 例均检测出 TERT，CDKN2A，CDKN2B，LTK，MTAP，MUTYH，MTAP，PTCH1，TEK 的基因改变。

结论:恶性叶状肿瘤复发、转移率较高，基因检测有助于其病理诊断及复发预测。

750. 乳腺癌新辅助治疗后 HER2 状态的演变及临床意义

商久妍、刘月平

河北医科大学第四医院

目的:HER2 抗体偶联药物的出现为乳腺癌患者，尤其为 HER2 低表达患者提供新的治疗决策。为探讨 HER2 低表达乳腺癌的生物学特征，研究乳腺癌初发肿瘤和新辅助治疗后残余肿瘤中 HER2-Low 类别，来体现 HER2 表达从初发乳腺癌到新辅助治疗后残余肿瘤的演变，并比较 HER2 低表达和阴性乳腺癌的临床病理特征。

方法:根据 2018 版 ASCO/CAP 指南对 HER2 进行评估。HER2 阳性细胞染色的截断值为＞10%。HER2 阴性病例分为 HER2 低表达（IHC=1+/2+且 ISH 无扩增）和 HER2-0（IHC-0），并收集全部病例的临床病理特征。

结果:本研究纳入 775 例乳腺浸润性癌新辅助治疗非 pCR 患者。HER2-Low 病例在初发肿瘤中所占比例为 59.61%，在残余肿瘤中所占比例为 55.36%。在 HER2 阴性病例中，HR 阳性肿瘤与三阴性肿瘤相比，HER2 低表达的发生率更高（初发肿瘤中 80.27% VS 60.00%，残余肿瘤中 72.68% VS 50.77%）。HER2 表达不一致率为 21.42%（图 1），主要表现为 HER2-Low 病例转换为 HER2-0（10.19%）和 HER2-0 转换为 HER2-Low（6.45%）。在初发肿瘤 HER2 阴性病例中，HR 阳性病例的 HER2 不一致率低于三阴性病例（23.34% VS 36.92%）（图 2）。这一差异主要是病例由 HER2-Low 切换到 HER2-0 导致。与 HER2 0 病例相比，HER2 低表达病例中 RCB 分级、MP 分级及转移淋巴结个数差异有统计学意义。HER2 低表达病例的病理缓解率较低，转移淋巴结个数更多。

结论:HER2 低表达在疾病演变过程中高度不稳定，具有一定的生物学特征。新辅助治疗后乳腺癌 HER2 的重新检测可能为一定比例的患者带来新的治疗机会。

751. 肺细支气管腺瘤 3 例报道并文献复习

邓会岩、董政洋、刘月平

河北医科大学第四医院

目的:探讨肺细支气管腺瘤的临床病理特征。

方法:报道 3 例肺细支气管腺瘤，分析其临床病理特征、免疫表型、分子遗传学特征及鉴别诊断，并进行文献复习。

结果:患者基本信息：病例 1，52 岁男性，体检发现右肺下叶占位 2 个月，CT 显示双肺散在实性结节，较大者直径约 1cm。肉眼观：楔形切除肺组织，大小 8.0cm×3.5cm×2.0cm，距脏层胸膜约 0.2cm 见一灰褐色病灶，大小 0.7cm×0.7cm×0.5cm，界限尚清，切面灰白质韧。病例 2，73 岁男性，因咳嗽咳痰 1 个月入院。术前常规 CT 检查示：左肺下叶空洞性病变，界限清楚，内部可见血流信号。患者行左下肺楔形切除术。肉眼观：楔形切除肺组织，大小 8.0cm×3.5cm×2.0cm，距脏层胸膜约 0.2cm 见一灰褐色病灶，大小 0.7cm×0.7cm×0.5cm，界限尚清，切面灰白质韧。病例 3，65 岁女性，常规体检。CT 检查显示：左肺下叶多发结节，

不除外恶性病变。行左肺下叶切除，肉眼观：楔形切除肺组织，大小 10cm×5cm×2.5cm，距脏层胸膜约 0.1cm 见一灰褐色病灶，直径 0.8cm，界限尚清，切面灰褐质韧。3 例组织学形态均显示低倍镜下肿瘤与周围肺组织界限尚清，呈腺管状及少量乳头状结构，未见胸膜侵犯。肿瘤间质富于黏液，瘤细胞散在分布于黏液湖中；高倍镜下肿瘤由两种细胞构成，腔面细胞为含有纤毛的柱状细胞和黏液细胞，其下层细胞为单层或多层的基底样细胞，圆形、卵圆形，细胞大小较一致，未见核分裂象。免疫表型均为：上皮细胞 TTF1 阳性，基底细胞 P63、P40、CK5/6 阳性，KI67 增殖指数低（<1%）。其中病例 3 分子检测显示 BRAF 基因突变。

结论:肺细支气管腺瘤是一种易被诊断为恶性的良性肿瘤，其典型特征是由基底细胞层和腔面细胞层构成的双层细胞结构，免疫组化基底细胞 P40、P63、CK5/6、TTF1 表达多呈阳性，分子遗传学可有 BRAF 的突变，鉴别诊断主要包括. 浸润性黏液腺癌、腺泡型腺癌、含有微乳头成分的腺癌和细支气管周围化生等。

752. 研究 APC 与 BRCA1 共表达对于胃癌及结直肠癌或有胚系遗传价值

李诗、贾迎、刘月平

河北医科大学第四医院

目的:胃癌（GC）及结直肠癌（CRC）是最常见的消化系统恶性肿瘤，发病率和死亡率呈逐年上升，随着分子病理的发展，越来越多的证据证明其是由系列基因改变组成的分子疾病，且具有较高的遗传易感性。既往关注较多的为错配修复基因（MLH1，MSH2，MSH6 和 PMS2）、KRAS、BRAF 等等，结肠腺瘤性息肉病(APC)基因发生胚系突变也是结直肠癌易感因素，而 BRCA1/2 是与乳腺癌和卵巢癌的遗传易感风险密切相关的基因，目前与胃癌和结直肠癌遗传风险尚不明确。

方法:收集 2019 年 1 月至 2021 年 7 月河北医科大学第四医院胃癌和结直肠癌手术后且进行 NGS 检测患者，共有 152 人，其中发现同时存在 APC 与 BRCA1 共突变患者 3 人，收集患者的临床与病理资料进行回顾性研究。

结果:经过 NGS 检测，3 名患者均伴有高度微卫星不稳定性（2 例 MSH2 突变，1 例 MSH6 突变）且突变丰度高，为可疑胚系突变，同时伴有至少 3 种潜在临床意义的突变类型。3 名患者均有 APC 和 BRCA1 的突变，其中 2 例为 APC、BRCA1 及 TP53 同时突变，1 名为 APC、

BRCA1、EGFR、PIK3CA、PTCH1 突变，但突变丰度均不足证明为胚系。对患者家族史进行评估，发现此 3 人均有 1-2 名家属有肿瘤病史。

结论:结直肠恶性肿瘤中的 APC 与 BRCA1 共突变患者，其恶性肿瘤患病率高，常伴有恶性肿瘤家族史，APC 与 BRCA1 共表达对于胃癌及结直肠癌遗传价值。

753. 基因组驱动转录组一致性表达的整合分析揭示了一种新的混杂型乳腺癌亚型及其生物标志物

李徐华、王宏久、王娜、文小玲、郭雨、符书恒、熊非凡、王珍珍

海南医学院

目的:基于本文提出的基因组驱动转录组一致性表达的新的多组学整合方法来识别乳腺癌亚型。对确定的亚型进行深入分析，以揭示其独特的致病机制，并确定其生物标志物，以便在临床中对患者进行精确的诊断和个性化的治疗。

方法:使用 TCGA-BRCA 项目的突变数据、拷贝数变异数据和表达数据，构建了一个由二分变量组成的一致性矩阵，然后利用这个矩阵，对乳腺癌患者进行亚型的识别。

结果:基于构建的一致性矩阵对乳腺癌患者进行亚型的识别，确定了一个生存预后极差的混杂型乳腺癌分子亚型，且该混杂型亚型所包含的三阴性乳腺癌患者较少。对该混杂型亚型患者的深入研究发现，该亚型患者的临床表型混乱，其多种生物学功能发生了改变，患者的组织学构成复杂，具有较低的免疫浸润水平和较高的 T 细胞紊乱和肿瘤干性评分。基于 GDSC 数据库对其靶向治疗基因开展分析发现，该亚型患者可能更适合联合靶向治疗。与细胞循环、DNA 损伤和 DNA 修复等功能状态相关的基因在该亚型患者中显著高表达，导致其相关生物学功能发生了改变，细胞状态的正常调节被破坏。此外，由 NCAM1-FGFR1 配体受体对主导的细胞间通讯在该亚型患者中发生了改变，且这种改变已在多种癌症中得到证实。根据基因的一致性表达特征，确定了 31 个生物标志物，通过它们构建了混杂型亚型患者的预后风险模型和亚型分类器。从这 31 个生物标志物中选择了 18 个重要性最高的基因，仅在基因表达水平上为混合亚型患者构建了一个新的预后风险模型和亚型分类器，并在四个 GEO 数据集中验证了这 4 个预后风险模型和亚型分类器的泛化能力。最后，基于 SOAR 数据库，分析从两个水平确定的风险预后基因在不同细胞类型中的空间变化性，发现它们主要在恶性肿瘤细胞中有明显的空间表达变化模式，表明它们可能是恶性肿瘤细胞发展的关键因素。

结论:基于基因组驱动转录组一致性表达的新型多组学整合方法，确定了一种生存预后极差的混杂型乳腺癌亚型及其生物标志物。通过多角度的深入分析，揭示了该亚型独特的致病机制，为乳腺癌的分子分型研究和临床精准诊断、个性化治疗提供了参考。

754. 提升 fPSA 校准品稳定性的相关研究

卫影影、郑迪文

安图生物工程股份有限公司

目的：游离前列腺特异性抗原（fPSA）是前列腺癌相关的血清学肿瘤标志物，研究发现将 fPSA 抗原添加到商品化人血清中配制的校准品，在 2-8℃保存 7 天内，和首日相比，浓度值下降 30%左右；在-20℃保存，考核其冻融稳定性，反复冻融 1 次，浓度值下降约 30%。需要提升其稳定性。

方法：将商品化人血清平均分成 4 份，一份作为对照（A 组），不进行任何处理，另外 3 份分别置于 56℃水浴锅中灭活 30 分钟（B 组），1 小时（C 组），2 小时（D 组），恢复室温后，分别向 4 组基质中添加 fPSA 高值抗原（精浆提取物），置于 2-8℃和-20℃保存，使用安图 Auto Lumo A2000 Plus 磁微粒化学发光法（CMIA）进行考核，7 天内观察其不同保存条件下的浓度值变化。

结果：2-8℃保存条件稳定性：与第 1 天相比，A 组第 7 天的浓度值降幅约 30%，B 组第 7 天的浓度值降幅约 20%，C 组第 7 天的浓度值降幅约 15%；D 组第 7 天的浓度值降幅约 8%；-20℃冻融稳定性：A 组冻融 7 次后浓度值降幅约 30%，B,C 组降幅约 15%，D 组降幅在 5%内。

结论：商品化人血清作为校准品基质液，进行灭活后，可以使血清中丝氨酸蛋白酶变性失活，该处理有助于改善 fPSA 血清基质校准品的稳定性，灭活时间越长，稳定性越好。

755. 糖尿病患者 CA72-4 水平升高的原因分析

丁瑞红、郑迪文

郑州安图生物工程股份有限公司

目的:糖尿病是以高血糖为特征的代谢性疾病。中国第八次全国性糖尿病流行病学调查报告显示，18 岁及以上人群糖尿病患病率达到 11.2%，患病人数已跃居世界第一。糖尿病引起的高胰岛素血症、高血糖和慢性炎症会增加患者的患癌风险。研究表明 2 型糖尿病患者恶性肿瘤的发病率是正常人群的两倍以上，其中消化道肿瘤最为常见，因此肿瘤标志物被广泛用于糖尿病患者的癌症筛查和诊断。本文将汇总近几年发表的文献，为糖尿病患者的癌症筛查和诊断工作提供参考。

方法:汇总国内外近几年发表的糖尿病患者 CA72-4 升高的文献，为患者的癌症筛查和诊断工作提供参考。

结果:CA72-4 是一种由乳腺癌肝转移患者细胞膜提取的 B72.3 抗体特异性识别的粘蛋白样的高分子量糖蛋白，分子量为 220-400KD，其分泌或者膜脱落到血液中被检测到。对胃癌具有高特异性，其敏感性可达 28-80%，CA72-4 是目前诊断胃癌的最佳肿瘤标志物之一。正常人群的 95%置信区间为 12.1U/ml。然而，临床上观察到无恶性肿瘤的糖尿病患者 CA72-4 阳性率高于正常人群，并且在使用胰岛素治疗后，其血糖控制良好、胰岛功能得到改善或者恢复后，CA72-4 可以在短时间内恢复正常。有研究证实 CA72-4 水平与高血糖症之间有显著相关性，可能是由于高血糖引起的炎性造成的 CA72-4 水平可逆的升高。因此从正常人群中获得的肿瘤标志物 CA72-4 的临界值可能不适用于糖尿病患者，其 CA72-4 水平升高，应考虑除肿瘤外的良性或恶性疾病。

结论:临床上发现糖尿病患者 CA72-4 阳性时，应在控制代谢异常症状后，再次检测和跟踪肿瘤标志物，而不是通过影像学检查甚至侵入性活检，如胃镜检查以排除肿瘤。总的来说，在糖尿病患者中，CA72-4 水平应该被仔细地解释，以减少糖尿病患者不必要检查，减轻患者的经济负担和精神负担。

756. 跨人群研究早期肺癌筛查中特征的肠道微生物标志物

徐君南、韩文婕、孙涛

辽宁省肿瘤医院

目的:微生物群的生态失调与人体疾病密切相关。肺癌是最具侵袭性和最普遍的恶性肿瘤之一。肺微生物组与肺癌之间的关系已得到广泛研究，但是由于其侵袭性和易被口腔微生物污染的原因，使其不能广泛应用于肺癌早筛。

方法:为了开发更便捷的，非侵入性的筛查方法，在这里，我们整合了来自 5 个地区的人群共 549 个粪便样本的 16sRNA 基因序列数据，以识别在肺癌组和健康对照组之间始终存在差异的细菌分类群。

结果:目前的研究结果表明，肺癌组的肠道微生物物种多样性（α多样性）总是略小于健康对照组，且两组之间的组成（β多样性）有着显著的不同。在肺癌患者的分类群中，丰度显著较高的为拟杆菌属和瘤胃球菌属。而对照组中相对丰度较高的为粪杆菌属。在调整了潜在的混杂因素后,我们建立随机森林模型区分肺癌与对照（AUC=0.921）。根据最终模型预测，在属水平上筛选到 99 个生物标记物。此外，我们还进行了跨队列交叉验证，获得的 AUC 值范围为 0.51 至 0.98。

结论:这项工作证明了肺癌特异性标志物在多人群中的有效性，这将有助于 LC 的早期诊断和治疗。

757. 非小细胞肺癌免疫治疗生物标志物的研究进展

刘兆喆

中国人民解放军北部战区总医院

目的:免疫治疗的出现为非小细胞肺癌（non-small cell lung cancer, NSCLC）的治疗带来了重大的变革，然而，基于癌症类型的异质性，并非所有患者都能从免疫治疗中获益，因此寻找可靠的生物标志物用于指导临床免疫治疗成为关键。

方法:从外周血中的循环肿瘤细胞（circulating tumor cells，CTCs）、血浆肿瘤突变负荷(blood tumormutation burden，bTMB)、循环肿瘤 DNA(circulating tumor DNA，ctDNA）、中性粒细胞与淋巴细胞比率(neutrophil to lymphocyteratio，NLR)以及外泌体几方面展开分析。

结果:外周血液生物标志物因其安全性高、可重复检测等优点用于免疫治疗的临床探索，近些年来得到迅速发展，其在 NSCLC 中的应用尤为亮眼。多项临床研究表明，外周血生物标志物在早期诊断、辅助临床分期、精准治疗和预后评价等方面有很大潜力，但还需要用大量的基础实验和临床试验进行验证。

结论:探索这些生物标志物单独或联合应用的差异，进行阈值标准化，规范指导临床决策。

758. 胃癌腹膜转移药物治疗的回顾性分析与探索

侯宏霖[1,2]、吕慧芳[2]、聂彩云[2]、王茂勋[2]、张国耀[1]、张磊[1]、陈小兵[2]

1. 漯河市中心医院

2. 郑州大学附属肿瘤医院

目的：胃癌腹膜转移的主要特征是发病率高、预后极差、诊断率低。当前临床对胃癌腹膜转移的诊断主要依靠血清标志物检测、影像学诊断、诊断性腹腔、镜检查以及 CY 检查。这四种手段都存在或多或少的缺点。而在治疗方面，目前国内尚无专门的腹膜转移治疗指南。本研究拟从胃癌腹膜转移的治疗着手，通过分析郑州大学附属肿瘤医院收治的晚期胃癌腹膜转移病人的临床资料及随访信息，分析从一线治疗到二线、三线治疗的过程中最佳的治疗策略。

方法：1. 收集 2013 年 1 月～2017 年 1 月期间郑州大学附属肿瘤医院收治的经影像学及腹腔游离细胞学检测确诊的晚期胃癌腹膜转移病例共 253 例，并通过电话进行随访。2. 采用 SPSS23.0 统计软件包进行统计分析。①对基线信息进行统计描述，连续变量采用均数±标准差（Mean±SD）或中位数（Median）进行描述；分类变量采用率或构成比（%）进行统计描述。②对研究中各组间基线资料进行对比，定性资料采用卡方检验，定量资料采用 t 检验。③使用 Kaplan-Meier 法绘制生存曲线。④使用 Log-Rank 检验比较不同治疗方案的总生存时间或者无进展生存时间之间的差异。以上分析的 P 值均基于双侧检验，统计学显著性水准 a 为 0.05。

结果：1.对于一线胃癌腹膜转移患者，无/少量腹水组，S-1 联合 DDP 方案与 S-1 联合 OXA 方案 PFS 无统计学差异，两种方案 PFS 均优于 5-FU 静滴联合 DDP/OXA 组；中量腹水组，S-1 联合紫杉醇静脉滴注联合腹腔灌注紫杉醇局部化疗，可以明显提升 PFS；大量腹水组使用单药 S-1 治疗的患者 OS 优于最佳支持治疗组。以上结果均 $P<0.05$，差异有统计学意义。2.对于二线胃癌腹膜转移患者，紫杉类药物（紫杉醇/多西他赛）化疗组和伊立替康化疗组

PFS 无统计学差别，在化疗的基础上提线联合甲磺酸阿帕替尼（艾坦）也未能明显延长 PFS，*P* 均＞0.05。3.三线治疗单药阿帕替尼组中位 PFS 相较化疗（紫杉类药物/伊立替康）联合阿帕替尼组，无统计学差异，*P*＞0.05。4.对于二线治疗起即开始长期使用阿帕替尼联合化疗的患者，其 OS 优于三线开始使用阿帕替尼的患者，*P*＜0.05，差异有统计学意义。5.对于 HER-2 阳性的胃癌腹膜转移患者，因病例数较少，无法进行详细的分层研究，但观察到一线使用化疗联合曲妥珠单抗疾病进展后，继续长期使用赫赛汀的患者 OS 长于停用患者，*P*＜0.05，差异有统计学意义。

结论：1.对于晚期胃癌腹膜转移的病人，一线治疗应考虑首选 5-FU 类药物联合铂类的全身化疗，其中 S-1 的疗效可能优于 5-FU 静脉滴注。2.对于合并中量腹水的病人，在全身化疗的基础上联合腹腔灌注紫杉醇化疗，可能能够延长 PFS、提高疗效，使患者受益。3.在二线治疗时提线长期使用阿帕替尼并联合全身化疗，可能使患者总生存期受益。4.对于 HER-2 阳性的胃癌腹膜转移患者，一线曲妥珠单抗治疗失败后继续使用该药物可能仍然能使患者受益。

759. 肾癌坏死性凋亡相关 lncRNA 预后模型的建立与验证

宁静源、范小晴、孙克然、马翠卿

河北医科大学

目的：应用坏死性凋亡相关长链非编码 RNA（long noncoding RNA，lncRNA）构建肾癌患者的预后预测模型并加以验证。

方法：该研究使用美国癌症肿瘤基因组图谱(TCGA)数据库下载了临床和 RNA 测序的数据。通过单因素及多因素 COX 回归分析筛选出影响患者预后的坏死性凋亡相关 lncRNAs. 之后建立预后预测模型和在线版动态列线图。将 TCGA 的数据随机分为高危组和低危组，采用 Kaplan-Meier 方法分析病人总生存时间对预后预测模型进行验证。再将所有患者随机分为训练集和验证集并验证预后模型的有效性。

结果：使用筛选出的 6 个坏死性凋亡相关 lncRNAs(LINC02027、LINC00944、AC093278.2、AL162586.1、 LINC00605、LUCAT1) 构建肾癌预后预测模型，显示高危组患者的总体生存期（OS）都显著低于低危组（*p*<0.05）。在线版动态列线图具有良好的准确性和操作性。高危组和低危组的受试者工作特征曲线(receiver operating characteristic curve，ROC)发现风险

评分的曲线下面积（the area under the curve，AUC）值为 0.803，1、3、5 的 AUC 分别为 0.782、0.756、0.785。训练集和验证集的 ROC 曲线的 AUC 值在 1、3、5 年分别可以达到 0.81、0.728、0.763 和 0.762、0.784、0.812。

结论： 基于坏死性凋亡相关 lncRNAs 的肾癌预后预测模型可以有效预测患者预后，在线版动态列线图的开发为临床提供了更加方便地使用和指导作用。

760. GALAD 和 BALAD-2 模型在原发性肝细胞癌诊断及短期疗效评价中的临床意义研究

崔兆磊

福建省肿瘤医院

目的： 探讨 GALAD 模型在原发性肝细胞癌患者诊断价值以及 BALAD-2 模型在肝细胞癌短期疗效评估中的价值。

方法： 收集某院 2017 年 8 月—2018 年 2 月 87 例首诊肝癌（HCC）患者、53 例肝脏良性疾病（BLD）患者、49 例表观健康体检者(HC)血清，采用微流控免疫荧光电泳技术检测血清中 AFP、AFP-L3 和 DCP 水平，建立基于性别、年龄和血清中 AFP、AFP-L3 和 DCP 水平的 GALAD 模型，分析 GALAD 模型对于肝癌患者的诊断价值；采用溴甲酚紫法检测血清中白蛋白及重氮法检测血清中胆红素水平，建立基于 ALB、BIL、AFP、AFP-L3 和 DCP 的 BALAD-2 模型，对随访资料完整的 41 例原发性肝癌患者动态观察治疗前后 BALAD-2 模型变化，分析 BALAD-2 模型与肝癌患者短期疗效的关系。

结果: GALAD 模型评分与患者的性别和年龄显著相关，差异有统计学意义,多数肝癌患者伴有乙肝病毒感染，肝硬化是肝癌的高危因素；肝癌患者血清 AFP、AFP-L3、DCP 水平以及 GALAD 模型评分均显著高于肝脏良性疾病组(p<0.05)和表观健康对照组(p<0.05)，差异均有统计学意义；GALAD 的特异性（94.3%）和准确性（60.8%）均高于 AFP（分别为 85.1%和 55.7%）、AFP-L3(分别为 71.3%和 55.0%）、DCP（分别为 85.1%和 59.1%）,特异性(95.1%)低于 AFP-L3(97.1%)和 DCP(97.1%)，高于 AFP(90.2%),研究表明，GALAD 模型诊断肝癌优于单一指标；肿瘤控制组治疗后 AFP、AFP-L3、DCP 水平以及 BALAD-2 较治疗前均显著下降（p<0.05）差异有统计学意义；肿瘤进展组 AFP、AFP-L3、DCP 和 BALAD-2 均未显著下降（P>0.05）。

结论: GALAD 模型可提高原发性肝癌的早期诊断率，BALAD-2 模型有助于肝细胞癌患者短期疗效评估。

761. 肠内酯和曲贝替定通过上调 THBS1 协同抑制上皮性卵巢癌

林彩姬、刘慧迪

哈尔滨医科大学

目的:研究 ENL 和 Trabe 对 EOC 的联合抑制作用以及 THBS1 可能参与 ENL 和 Trabe 的抗癌活性。

方法:用慢病毒载体用过表达的 THBS1 转染的上皮性卵巢癌细胞系 ES-2。用血管形成试验来评估 THBS1 过表达后的抗血管生成活性，并建立药物干预和异种移植裸鼠癌症模型来评估药物之间的协同抑制和 THBS1 参与的体内效应。收集小鼠粪便样本进行 16S rDNA 测序和微生物群分析。

结果:我们检测到肠内酯和曲贝替定对癌细胞增殖和迁移的强抑制活性，并观察到肠内酯和曲贝替定在抑制上皮性卵巢癌的协同作用。肠内酯和 曲贝替定单独或联合给药可以抑制 HMEC-1 细胞的管形成能力，并且这种抑制作用随着 THBS1 过表达而变得更强。肠内酯和曲贝替定联合组 TIMP3 和 CD36 的表达均上调，而 MMP9、VEGF 和 CD47 的表达均降低。 随着 THBS1 的过表达，结果变得更加明显。 在动物实验中，肠内酯和曲贝替定的联合使用显示出优于任一单一药物的抑制作用，并且显著抑制了肿瘤生长，并且 THBS1 的过表达进一步增强了药物联合组的抗癌活性。

结论:肠内酯和曲贝替定协同抑制上皮性卵巢癌和 THBS1 可以显著促进肠内酯和曲贝替定的协同抗癌作用。

762. LPCAT1 在恶性肿瘤中的研究进展

郭艳玲

内蒙古医科大学附属医院

目的:代谢重组是恶性肿瘤细胞的基本特征之一,异常的脂质代谢通过干扰细胞的活动，并通过影响细胞增殖、分化来促进恶性肿瘤的形成及发展。溶血磷脂酰胆碱酰基转移酶 1 (lysophosphatidylcholine acyltransferase 1, LPCAT1) 参与了磷脂酰胆碱的生物合成与磷脂重塑，是磷脂代谢过程中在中重要的磷脂重构酶。LPCAT1 可以通过调节恶性肿瘤细胞中磷脂的饱和状态改变细胞膜结构和细胞内信号活性，在肿瘤细胞的发生、发展及侵袭中有着重要作用。最近的研究表明 LPCAT1 在非小细胞肺癌、乳腺癌、肝癌、结直肠癌等常见恶性肿瘤中过表达，并与恶性肿瘤的进展及预后密切相关，随着对 LPCAT1 的逐步研究及了解，我们认为 LPCAT1 可能成为恶性肿瘤的生物学标志及潜在的治疗靶点。

方法:恶性肿瘤是全球第二大死亡原因，严重威胁人类的生命健康。根据国际癌症研究机构最新数据统计显示，2018 年新增恶性肿瘤病例近 1810 万，且因恶性肿瘤而死亡的人数已达到 960 万。所以，恶性肿瘤已成为影响公共卫生保健的首要问题。近年来随着对恶性肿瘤了解的不断深入，我们发现异常的脂质代谢可以促进细胞增殖，导致恶性肿瘤的发生及发展。在最近的研究发现，细胞内溶血磷脂酰胆碱酰基转移酶-1 (lysophosphatidylcholine acyltransferase 1, LPCAT1)的表达水平可以影响细胞内的磷脂代谢，通过影响细胞内磷脂合成及重塑，与恶性肿瘤的侵袭、转移密切相关。本文将 LPCAT1 的生物特性、功能以及其在常见恶性肿瘤中的研究进展综述如下。

结果:恶性肿瘤细胞的快速增殖需要充足的能量供应以及由磷脂构成的独立细胞结构单元。LPCAT1 是磷脂代谢途径中的关键酶，通过调节细胞膜中磷脂的组成促进细胞的质膜重构，增加了细胞膜的流动性，影响细胞的增殖能力及细胞内的信号转导。多项研究表明，LPCAT1 在肺癌、乳腺癌、肝癌、结直肠癌等恶性肿瘤细胞及组织中高度表达，并伴有细胞内饱和磷脂酰胆碱水平的升高，影响恶性肿瘤的进展及预后。但是，目前关于恶性肿瘤细胞内 LPCAT1 如何影响并控制恶性肿瘤细胞行为并控制信号通路的活性仍不清楚，其具体的机制还有待进一步研究。综上所述，LPCAT1 有可能是恶性肿瘤早期诊断的潜在生物学标志物和治疗靶标，深入了解并研究 LPCAT1 对恶性肿瘤建立新的治疗方法具有重要意义。

结论:LPCAT1 在多种恶性肿瘤细胞内过表达，通过催化溶血磷脂酰胆碱转化为饱和磷脂酰胆碱，为肿瘤细胞的增殖提供更多生物来源。研究显示 LPCAT1 的上调可促进肿瘤细胞的增殖、侵袭和转移, LPCAT1 的下调通过诱导细胞周期阻滞于 G0/G1 期来抑制肿瘤细胞的生长，不仅影响恶性肿瘤的发生及进展，还与肿瘤患者的预后密切相关。

763. lncRNA RUN12 在胃癌中的表达及相关的机制研究

黄志艺[1,2]、邹长棪[2]、林贤东[2]

1. 福州大学化学学院

2. 福建省肿瘤医院

目的:探讨 lncRNA RUN12 基因表达与胃癌的进展的关系及相关的机制研究。

方法:收集胃腺癌患者 81 例,分析 RNU12 表达与胃癌病理特征的关系。利用慢病毒载体构建过表达和敲低 RNU12 的胃癌 AGS 细胞系，并通过 RT-qPCR、MTT 法、划痕实验和 transwell 侵袭实验，检测 RNU12 在胃癌细胞中的生物学功能。通过 lncRNASNP2 等数据库预测 RNU12 可能结合的 miRNA 及下游作用的靶基因，并利用 RIP、双萤光素酶实验进行验证。通过回复实验评估下游靶基因 BLID 与 RNU12 的关系。建立斑马鱼胃癌异种移植模型，探索 RNU12 与胃癌进展的关系。

结果:RUN12 在胃癌组织中低表达，而且其表达与病理特征密切相关。体外实验表明，RNU12 过表达抑制胃癌细胞的侵袭性。RNU12 和 BLID 的 3'UTR 都有 hsa-miR-575 结合位点，并且 Hsa-miR-575 是 RNU12 抑制剂和 BLID 抑制剂。BLID 在 RNU12 介导的胃癌细胞体外恶性行为起重要作用。斑马鱼胃癌移植模型研究表明，RNU12 过表达抑制胃癌细胞的增值和转移。RIP、双萤光素酶实验及回复实验显示，RUN12 通过 miR-575/BLID 信号轴调控胃癌的进展。同时，RNU12 可以抑制多种促瘤因子的作用，如 CCND1、PCNA、Cyclib D1、N-钙粘蛋白波形蛋白和 BCL-2。

结论:RNU12 在胃癌中异常表达，且与临床病理特征密切相关。RUN12 通过 miR-575/BLID 信号轴调控胃癌的进展。RUN12 可能是胃癌潜在肿瘤分子标志物。

764. 外周血 CTCs 联合血清肿瘤标志物检测在非小细胞肺癌患者中的临床意义

冯雨、崔东、张会民、刘渊源、李瑞杰、栾加强、徐明星、钱如林

河南省胸科医院

目的:探讨外周血 CTCs 联合血清肿瘤标志物检测在 NSCLC 中的临床意义。

方法:选取 102 例 NSCLC 患者资料（2020 年 1 月到 2022 年 1 月），将其设为研究组，另选取 87 例同时间进行健康体检者，作为对照组。比较研究组与对照组、不同临床分期患者外周血 CTCs、血清肿瘤标志物的表达情况，分析影响预后的因素、诊断价值。

结果:CTCs 阳性表达、CEA、NSE、CYFRA21-1 水平：研究组、III-IV期均高于对照组、I-II 期（$P<0.05$）；年龄、临床分期、CTCs、CEA、NSE、CYFRA21-1 为影响预后的因素（$P<0.05$）；外周血 CTCs 联合血清肿瘤标志物检测灵敏度、特异度、AUC 最高。

结论:外周血 CTCs 联合血清肿瘤标志物检测可有效诊断 NSCLC，可为临床病情诊断及预后评估提供参考。

765. 靶向敲降 LncRNA SLC25A25-AS1 对肺癌细胞生物学行为的影响及其机制

郭红艳、李林、孙晓杰、霍焰

齐齐哈尔医学院医学技术学院

目的: 观察长链非编码 RNA SLC25A25-AS1 靶向敲降对肺癌细胞增殖和凋亡的影响，探讨其作用机制。

方法: qPCR 检测 SLC25A25-AS1 在肺癌患者及健康对照者血清中的表达水平；靶向敲降肺癌 H1299 细胞中的 SLC25A25-AS1；MTT 实验和克隆形成实验观察细胞的生长增殖；流式细胞术检测细胞周期和细胞凋亡；qPCR 检测细胞增殖与凋亡相关基因表达；免疫印迹法检测 PI3K/Akt 信号通路关键分子及肿瘤增殖相关因子的表达。

结果: SLC25A25-AS1 在肺癌血清中的表达量显著高于健康对照组（$p<0.05$）。敲降 SLC25A25-AS1 可抑制 H1299 细胞增殖（$P<0.01$）和克隆形成（$p<0.05$），促进细胞凋亡并

影响细胞周期进程（*P*<0.01）。敲降 SLC25A25-AS1 使细胞增殖、凋亡相关基因 cyclin D1、mmp2、CDK1、vimentin 的表达降低，CCNG2 表达增加。免疫印迹结果显示，SLC25A25-AS1 敲降可使肿瘤相关蛋白 E-cadherin 的表达上调，而 Cyclin D1、vimentin、PI3K/Akt 信号通路关键分子 pAKT 及其下游靶蛋白 Bcl-2 的表达下调。

结论: LncRNA SLC25A25-AS1 可能通过 PI3K/Akt 信号通路调控 H1299 细胞增殖和凋亡。

766. ProGRP 和 NSE 联检在 SCLC 诊断中的应用价值研究

刘婷婷、渠文涛、史小芹

郑州安图生物工程股份有限公司

目的:与神经元特异性烯醇化酶（NSE）不同，胃泌素释放肽前体（ProGRP）作为一种新型的肺癌肿瘤标志物，不易受溶血的影响，特异性更优。本文探讨 ProGRP 和 NSE 联合检测在小细胞肺癌（SCLC）诊断中的应用价值

方法:选取健康人 80 例，良性肺病患者 72 例，非小细胞肺癌患者 51 例，小细胞肺癌患者 89 例。采用 AutoLumoA2000PLUS 对四组人群进行血清 ProGRP 和 NSE 的检测，分别统计四组人群 ProGRP 和 NSE 的阳性率。

结果:健康对照组，ProGRP 的阳性率为 2.5%（2/80），NSE 的阳性率为 3.75%（3/80）；良性肺病组，ProGRP 的阳性率为 6.94%（5/72），NSE 的阳性率为 9.72%（7/72）；非小细胞肺癌组，ProGRP 的阳性率为 31.37%（16/51），NSE 的阳性率为 29.41%（15/51）；小细胞肺癌组，ProGRP 的阳性率为 73.03%（65/89），NSE 的阳性率为 59.55%（53/89）；小细胞肺癌组 ProGRP 和 NSE 的阳性率显著高于其他组，差异有统计学意义(*P* <0.05)。ProGRP 和 NSE 联合检测（任意一项为阳性均算为阳性）可以进一步提高 SCLC 的阳性检测率，达到 80.89%（72/89）。

结论: ProGRP 和 NSE 联合检测有助于提高对小细胞肺癌的阳性检

767. 异常凝血酶原（PIVKA-II）、甲胎蛋白（AFP）联合检测原发性肝癌的价值

冉盼盼

郑州安图生物工程股份有限公司

目的:研究 PIVKA-II和 AFP 联合检测原发性肝癌（HCC）的临床价值。

方法:选择 2018 年 5 月至 2022 年 7 月河南省肿瘤医院收治的 HCC 患者 369 例为原发性肝癌组，良性肝病患者 106 例为良性肝病组，同期选择正常进行体检的健康者 351 名为健康对照组。分别检测三组的 PIVKA-II、AFP 水平，并对比各血清标志物单一及联合检测诊断 HCC 的阳性率。

结果:HCC 组患者的 PIVKA-II、AFP 检测值均高于良性肝病组，良性肝病组患者的上述指标检测值均高于健康对照组（$P<0.05$）；HCC 组患者的 PIVKA-II、AFP 检测阳性率明显高于良性肝病组，良性肝病组患者的各指标阳性率高于健康对照组（$P<0.05$）；HCC 组 PIVKA-II＋AFP 联合检测阳性率高于良性肝病组，良性肝病组高于健康对照组（$P<0.05$）；PIVKA-II＋AFP 联合诊断 HCC 的敏感度、特异性均高于单一指标检测（$P<0.05$）。

结论:PIVKA-II和 AFP 联合检测可提高 HCC 的检出率，有利于肝癌的早期诊断，有助于肝癌的早期筛查和治疗。

768. 甲胎蛋白和甲胎蛋白异质体联检对原发性肝癌诊断的临床价值

冉盼盼

郑州安图生物工程股份有限公司

目的:研究血清甲胎蛋白（AFP）和甲胎蛋白异质体（AFP-L3）联合检测对原发性肝癌（HCC）的诊断价值。

方法:选取患者共 259 例，原发性肝癌(HCC) 101 例，良性肝病(BLD) 158 例(其中肝炎 62 例，肝硬化 86 例，肝良性肿瘤 10 例) ，采用亲和吸附离心管分离 AFP-L3，磁微粒化学发光法检测 AFP 和 AFP-L3 含量，计算甲胎蛋白异质体比率（AFP-L3%）。

结果:HCC 组患者的 AFP、AFP-L3、AFP-L3%检测值均高于良性肝病组（$P<0.05$）；HCC 组患者的 AFP、AFP-L3%检测阳性率明显高于良性肝病组（$P<0.05$，特别是 AFP-L3 在肿瘤早期有较强的敏感性；HCC 组 AFP＋AFP-L3 联合检测阳性率高于良性肝病组（$P<0.05$）；AFP＋AFP-L3 联合诊断 HCC 的敏感度、特异性均高于单一指标检测（$P<0.05$）。

结论:AFP 和 AFP-L3 联合检测可提高 HCC 的检出率，有利于肝癌的早期诊断，有助于肝癌的早期筛查和治疗。

769. 去氢松香酸对肝癌细胞 HepG2 非靶标脂质组学及蛋白组学的影响

韩君

北京康仁堂药业有限公司

目的:前期本研究筛选影响去氢松香酸治疗肝癌与细胞焦亡相关的基因及生存列线图的建立。大鼠经口服和静脉注射去氢松香酸的绝对生物利用度为 16.5%。但是，缺少去氢松香酸对肝癌细胞 HepG2 的多组学研究，本研究通过脂质组学及蛋白组学研究，揭示去氢松香酸对肝癌细胞 HepG2 影响的分子机制。

方法:首先，通过去氢松香酸对肝癌细胞 HepG2 进行脂质组学分析，从脂质分子水平阐明去氢松香酸对肝癌细胞 HepG2 的影响；其次，通过去氢松香酸对肝癌细胞 HepG2 进行蛋白组学分析，筛选出差异蛋白并进行分析，比较差异蛋白的 Pathway 富集分析阐明其分子机制；最后通过显著富集铁死亡通路中的 17 个蛋白和差异显著脂质分子作联合分析研究去氢松香酸对肝癌细胞 HepG2 的影响。

结果:脂质组学共筛选鉴定 15 个显著差异代谢物表达上调，15 个显著差异代谢物表达下调。差异表达脂质主要与甘油磷脂代谢相关；蛋白组学研究共筛选出 260 种蛋白表达上调，961 种蛋白表达下调，富集显著性 Top5 的 Pathway 为铁死亡、氧化磷酸化和内质网中蛋白质加工等。结合蛋白组和脂质分析研究去氢松香酸对肝癌细胞 HepG2 影响，ACSL3 参与心磷脂代谢，沉默 ACSL3 后细胞裂解液和细胞上清中心磷脂的水平都显著增加。

结论:脂质组学及蛋白组学研究结果比较发现 ACSL3 是酰基辅酶 A 合成酶长链家族(ACSLs)中表达最多且功能复杂的一员其参与心磷脂代谢。

770. 98 例原发性颌骨内鳞状细胞癌预后影响因素的回顾性分析

杨金刚[1,2]、夏荣辉[1]、朱云[1]、吴思成[1]、董亚兵[1]、杨功鑫[1]、史俊隆[1]、崔迎慧[1]、朱凌[1]、周晌辉[1]

1. 上海交通大学医学院附属第九人民医院

2. 上海交通大学医学院附属同仁医院

目的:总结原发性颌骨内鳞状细胞癌（PIOSCC）的临床及病理特征，对其预后影响因素进行探讨。

方法:收集 2013 -2017 年上海交通大学医学院附属第九人民医院收治的原发性颌骨内鳞状细胞癌患者的临床、影像、组织病理及术后随访资料，采用描述性统计学方法分析影响预后的因素。采用 SPSS 23.0 软件包将基线资料进行单因素及多因素生存分析。

结果:共纳入 98 例患者，平均年龄为 56.6 岁，男 71 例，女 27 例，上颌骨 33 例，下颌骨 65 例。术后随访的 95 例患者中，24 例出现复发，10 例出现远处转移，复发和远处转移多发生于术后 2 年内。患者的 2 年和 5 年的总生存率分别为 74.7%，61.8%。单因素分析显示，肿瘤部位、肿瘤大小、切缘阳性、颈淋巴结转移对总生存率有显著影响，面部麻木、切缘阳性，肿瘤部位、颈淋巴结转移分别对复发和远处转移有显著影响；多因素分析显示，仅切缘阳性和颈淋巴结转移对总生存率的影响有统计学差异。

结论:术后前 2 年是 PIOSCC 患者复发、远处转移及死亡的高发期，切缘阳性及颈淋巴结转移是原发性颌骨内鳞状细胞癌的不良预后因素。

771. 晚期上皮性卵巢癌患者术前炎症指标联合 CA125、HE4 对肿瘤细胞减灭术满意度的预测价值

祖逸峥[1]、哈春芳[2]

1. 福建医科大学妇儿临床医学院

2. 宁夏医科大学总医院

目的：探讨晚期上皮性卵巢癌（AEOC）患者术前炎症指标联合糖类抗原 125（CA125）、人附睾蛋白 4（HE4）对初次肿瘤细胞减灭术满意程度的预测价值。

方法：回顾性分析自 2016 年 1 月至 2021 年 12 月于宁夏医科大学总医院经过初次肿瘤细胞减灭术的 AEOC 患者 144 例，其中满意组 101 例，不满意组 43 例。应用 MedCalc 20.0 软件绘制 ROC 曲线评估比较患者术前 NLR、MLR、PLR、CA125、HE4 单一预测及 PLR、CA125、HE4 两两联合预测不满意肿瘤细胞减灭术（SODS）的临床价值。

结果：1.不满意组术前 NLR、MLR、PLR、CA125、HE4 水平均高于满意组，差异有统计学意义（*P* 均＜0.05）；2.术前血清学指标单一预测 SODS 中，CA125 的 AUC 最大为 0.849（95%CI:0.780-0.903），其敏感性、特异性、准确性、阳性预测值、阴性预测值、阳性似然比、阴性似然比分别为 83.72%、73.27%、56.99%、57.14%、91.36%、3.13、0.22；3.术前血清学指标两两联合预测 SODS 中，术前 PLR＞262.11 联合 CA125＞748.4U/mol 的特异性最高为 94.06%。

结论：术前 PLR＞262.11 联合 CA125＞748.4U/mol 预测 AEOC 患者 SODS 的特异性高，在临床实践中可能成为预测 SODS 的有效手段。

772. 影响晚期上皮性卵巢癌患者满意肿瘤减灭术的相关因素分析

祖逸峥[1]、哈春芳[2]

1. 福建医科大学妇儿临床医学院

2. 宁夏医科大学总医院

目的：探讨影响晚期上皮性卵巢癌患者初次肿瘤细胞减灭术满意程度的相关因素。

方法：回顾性分析 2016 年 1 月至 2021 年 12 月于我院行初次肿瘤细胞减灭术晚期上皮性卵巢癌患者的临床病理资料。收集患者一般情况、术前血清学指标、术中探查肿瘤病灶情况、术后病理情况，分析各相关因素与手术满意程度的关系。应用 SPSS 25.0 软件对数据进行单因素及多因素相关分析，并通过 MedCalc 20.0 绘制 ROC 曲线，分别计算比较上腹部转移、大网膜状态、FIGO 分期、组织学分化、CA125 单一指标及联合预测的效能。

结果：1.满意减瘤情况：纳入研究的 154 例晚期上皮性卵巢癌患者中满意组 106 例，满意率 68.8%，不满意组 48 例，不满意率 31.2%。2.影响晚期上皮性卵巢癌患者初次肿瘤细胞减灭术的满意程度的单因素分析：结果显示 CA125、HE4、NLR、MLR、PLR、PAR、PLT、D-D、肿瘤单双侧、肿瘤大小、大网膜状态、上腹部转移、FIGO 分期、病理学类型、组织学分化对 AEOC 患者行 PDS 满意程度有影响（P 均＜0.05）。3.影响晚期上皮性卵巢癌患者初次肿瘤细胞减灭术的满意程度的多因素分析：结果显示上腹部转移、大网膜状态、FIGO 分期、组织学分化、CA125 均是影响 AEOC 患者满意肿瘤细胞减灭术的独立危险因素（P 均＜0.05）。4.各影响因素在预测不满意肿瘤细胞减灭术中的价值：上腹部转移、大网膜状态、FIGO 分期、组织学分级、CA125 的 ROC 曲线下面积（AUC）分别为 0.663（95%CI:0.583-0.739）、0.688（95%CI:0.609-0.760）、0.564（95%CI:0.482-0.644）、0.621（95%CI:0.539-0.698）、0.764（95%CI:0.689-0.829）；5.多因素联合预测不满意肿瘤细胞减灭术的价值：AUC 为 0.862（95%CI:0.797-0.912），其敏感性、特异性、准确性、阳性预测值、阴性预测值分别为 83.33%、81.13%、64.47%、66.67%、91.49%。

结论：1.CA125、HE4、NLR、MLR、PLR、PAR、PLT、D-D、肿瘤单双侧、肿瘤大小、大网膜状态、上腹部转移、FIGO 分期、病理学类型、组织学分化是影响晚期上皮性卵巢癌患者满意肿瘤细胞减灭术的相关因素；而上腹部转移、大网膜状态、FIGO 分期、组织学分化、CA125 是影响晚期上皮性卵巢癌患者满意肿瘤细胞减灭术的独立危险因素；2.上腹部转移联合大网膜状态、FIGO 分期、组织学分化及 CA125 明显提高预测不满意肿瘤细胞减灭术的百分比。

773. 达芬奇机器人手术在妇科恶性肿瘤应用中的临床效果分析

祖逸峥[1]、哈春芳[2]

1. 福建医科大学妇儿临床医学院

2. 宁夏医科大学总医院

目的：探讨妇科恶性肿瘤患者行达芬奇机器人辅助腹腔镜手术治疗的可行性及安全性，为临床实践中手术方式的确定提供依据。

方法：回顾性分析 2021 年 4 月至 2022 年 5 月就诊宁夏医科大学总医院妇科行手术治疗的 107 例妇科恶性肿瘤患者，按照手术方式不同分为机器人手术组（52 例）和传统腹腔镜手术组（55 例）。采用 SPSS23.0 软件对所有患者临床资料数据进行对比统计分析，以 $p<0.05$ 为差异有统计学意义。

结果：宫颈癌患者中，相比于传统腹腔镜手术组，机器人手术组的淋巴结清扫数目多（t=4.46）、术中出血量少（t=-2.878）、胃肠道功能恢复时间短（t=-4.716），但住院费用高（t=16.536）、手术时间长（t=2.037）（*P* 均＜0.05），而术后住院时间（t=-1.489）及引流管留置时间（t=-1.128），两组患者比较差异无统计学意义（*P* 均＞0.05）。子宫内膜癌患者中，相比传统腹腔镜手术组，机器人手术组的淋巴结清扫数目多（t=2.957）、术中出血量少（t=-2.603）、胃肠道功能恢复时间短（t=-2.889），但住院费用高（t=13.48）、手术时间长（t=2.378）（*P* 均＜0.05），而术后住院时间（t=0.076）及引流管留置时间（t=-1.310），两组患者比较差异无统计学意义（*P* 均＞0.05）。

结论：达芬奇机器人辅助腹腔镜手术在治疗妇科恶性肿瘤患者中具有淋巴结清扫数目多、术中出血量少、胃肠道功能恢复时间短的优势，是一种安全可行的手术方式。

774. 基于血管生成相关基因的结肠癌分子分型和免疫浸润分析

陈飞旭、张宁、杨飞翔、李昊、杜忆南

安徽医科大学

目的:结肠癌是常见的消化系统恶性肿瘤，其发病率和死亡率均位于全球所有癌症的第 5 位，对世界构成严重的健康威胁和经济负担。血管生成是指新血管从预先存在的血管网络发展而来的过程，相关研究表明，血管生成与结肠癌的进展和转移有关，从而显著影响患者疾病的进程。本研究旨在通过生物信息学方法，基于血管生成相关基因对结肠癌患者进行分子分型和免疫浸润分析，以期对结肠癌的精准治疗提供一定的参考。

方法:首先，我们从 TCGA 数据库获得结肠癌患者肿瘤样本和癌旁正常组织的 RNA-seq 数据，然后鉴定出在肿瘤样本和正常组织中差异表达的基因，再与血管生成相关的基因集取交集。接着，利用差异表达的血管生成相关基因构建蛋白质相互作用网络（PPI），并对它们的 GO 功能和 KEGG 途径进行富集分析。另外，利用血管生成相关基因通过一致性聚类对结肠癌患者进行亚型分组。在得到结果后，对不同亚组的临床特征和免疫相关性等进一步分析。

结果:我们共得到了 2692 个差异基因，与 36 个血管生成相关基因取交集后共得到了 13 个基因。基于这 13 个基因构建蛋白质相互作用网络，GO 分析和 KEGG 富集分析发现差异表达的血管生成相关基因主要富集在骨骼系统发育、组织形态发生和 PID 整合素 1 通路等。一致性分析得到样本分布均匀的两组亚型，临床病理特征分析显示两个亚组之间的 N 分期具有显著性差异。使用 EPIC 算法计算 2 组样本间的免疫浸润评分，发现有多种类型的免疫细胞在两组间的浸润评分存在显著性差异。免疫检查点相关基因表达分析显示，8 个免疫检查点相关基因在两亚组之间的表达均存在显著性差异。使用 TIDE 算法预测两亚组潜在的免疫治疗反应，第一组的 TIDE 评分高于第二组，且差异具有显著性，提示该亚组进行免疫检查点阻断治疗疗效差。

结论:本研究基于血管生成相关基因对结肠癌患者进行分子分型，并且不同亚型之间的免疫浸润和免疫治疗反应等存在显著性差异。该分型可以为结肠癌患者的人群分类提供新的参考，有助于结肠癌患者实现更精准的免疫治疗。

775. 硒化亚铜纳米通过化学动力疗法诱导胃癌铁死亡的研究

肖瑶、林铭珍、梁敏

广州医科大学附属第五医院

目的:探讨硒化亚铜（Cu2Se）纳米的制备、物化表征及其胃癌抗肿瘤效应的作用。

方法:采用透射电镜，水合粒径分析，Zeta 电位分析及紫外吸收光谱分析方法分析 Cu2Se 纳米的形貌、粒径大小及类芬顿性能，同时采用激光共聚焦、细胞毒性（CCK-8）、Transwell 实验评估该纳米的体外抗肿瘤作用效应毒性，最后构建单侧皮下荷瘤模型探究 Cu2Se 纳米的体内抗肿瘤作用。

结果:制备的 Cu2Se 纳米为 100nm 左右的类圆形中空结构，可催化过氧化氢生成单线氧。激光共聚焦实验表明 Cu2Se 可以促进胃癌细胞活性氧生成，诱导铁死亡发生；CCK-8 实验表明：Cu2Se 纳米对胃癌细胞具有浓度依赖性抑制增殖作用；Transwell 实验表明：Cu2Se 纳米能抑制胃癌细胞的侵袭迁移能力；裸鼠单侧皮下荷瘤模型表明 Cu2Se 纳米能安全高效抑制肿瘤增殖。

结论: Cu2Se 纳米具有良好的类芬顿效能，可诱导胃癌铁死亡发生，具备良好的体内外抑制抗肿瘤效应，是胃癌治疗的一种潜在新方法。

776. 长链非编码 RNA lncRNA MEG8 通过靶向 miR-181a-5p 调控脑胶质瘤细胞的增殖与转移潜能

林铭珍、肖瑶、梁敏

广州医科大学附属第五医院

目的：长链非编码 RNA（long non-coding RNA, lncRNA）在脑胶质瘤中发生和发展中起着重要作用，目前 lncRNA MEG8 在脑胶质瘤进展中的作用仍不清楚，因此本研究旨在阐明 lncRNA MEG8 在脑胶质瘤发生中的潜在作用和调控机制。

方法：公共数据库分析 lncRNA MEG8 在脑胶质瘤的表达量及与肿瘤预后关系，荧光定量 PCR 验证 lncRNA MEG8 和 miR-181a-5p 在本中心脑胶质瘤生物样本库中的表达水平。质粒

和微小 RNA（microRNA, miRNA）模拟物分别被转染进入脑胶质瘤细胞上调 lncRNA MEG8 和 miR-181a-5p 表达，通过 CCK-8 增殖、Transwell 实验、双萤光素酶报告检测 lncRNA MEG8 和 miR-181a-5p 对脑胶质瘤细胞增殖及转移能力的影响及潜在的调控机制。

结果：与邻近正常组织相比，lncRNA MEG8 在脑胶质瘤组织中呈低表达，其表达水平与患者的无瘤生存期密切相关。上调 lncRNA MEG8 的表达可显著抑制脑胶质瘤细胞的增殖能力、降低转移能力；miR-181a-5p 在脑胶质瘤组织中呈高表达，其表达水平与 lncRNA MEG8 呈负相关关系，且 miR-181a-5p 可逆转 lncRNA MEG8 的抑癌功能。

结论：LncRNA MEG8 通过下调 miR-181a-5p 的表达水平从而抑制脑胶质瘤细胞增殖及转移能力，是脑胶质瘤的潜在治疗靶点。

777. 数字 PCR 检测 CK19 的方法建立及其在 CTC 定量分析中的应用

马春辉[1,2]、胡海旭[2]、张丽娟[2]、刘毅[1,2]、刘天懿[2]

1. 安徽医科大学基础医学院

2. 解放军总医院第五医学中心

目的:循环肿瘤细胞（circulating tumor cells, CTC）介导的远处转移是肿瘤患者死亡的主要原因，其检测对患者的个体化诊疗具有重要的指导价值。通过 RT-qPCR 法检测上皮特异基因 CK19 是 CTC 检测的重要手段之一，具有敏感性高、结果客观、可多指标分析等优势，但不也存在不容易定量，可重复性差等不足。本研究拟建立针对 CK19 基因的数字 PCR 方法，利用该方法的超高敏感性和绝对定量优势对 CTC 进行定量分析。

方法:针对 CK19 基因的 mRNA 序列进行引物探针设计，采用人乳腺癌细胞系 MCF7 和健康人外周血有核细胞对引物探针进行筛选优化并获得最佳组合，之后进行如下测试：①以健康人的 RNA 为模板，进行空白检测限（Limit of blank，LOB）的分析。②将 MCF7 细胞系和健康人白细胞的模板按照不同浓度预混后进行检测限（Limit of detection，LOD）分析。③在 10^6 个健康人白细胞的背景下，分别混入不同数量的 MCF7 细胞进行 LOD 分析。④根据 LOB 和 LOD 检测结果建立判读阈值，并将健康人与临床患者的检测结果进行对比。

结果:经测试，采用特异逆转录引物的“一步法”检测效果优于采用通用逆转录引物的“两步法”。针对“一步法”的检测策略，在内参基因拷贝数为 2000、5000、10000、18000 时的 LOB

分别为 4.67、7.66、14.99、19.53。MCF7 细胞系与健康人白细胞模板预混后进行的 LOD 检测最低检测限可以达到 0.1%，R^2=0.9995。在 MCF7 细胞与健康人白细胞预混的试验中，最低可以检测到一个细胞，混入的肿瘤细胞小于 100 个时线性较好，R^2=0.9981。经统计学分析，健康人的检测结果与早期患者（*P*=0.093）之间不存在统计学差异，与治疗前的晚期患者（*P*<0.001）以及治疗中的晚期患者（*P*=0.026）之间均存在统计学差异。

结论:我们成功建立了一个检测 CK19 基因的数字 PCR 方法，该方法具有敏感、特异和定量准确等优势，未来经过进一步验证之后有望用于肿瘤患者的确诊及分期、微小残留疾病检测、预后评估及疗效评价，具有良好的应用前景。

778. 术前新辅助放疗增加口腔鳞状细胞癌预后不良的风险

许腾、宋晓萌、吴煜农

南京医科大学附属口腔医院

目的:整合医学的理念提倡恶性肿瘤的治疗需要多学科的资源的有序整合。近年来，术前新辅助放疗（Neoadjuvant radiotherapy）的理念在肝细胞癌、胰腺癌等恶性肿瘤的治疗中已开展了相应的临床随机对照实验，并取得了肯定的效果，而在口腔鳞癌中研究较少。本研究目的在于回顾性分析术前新辅助放疗在口腔鳞癌治疗中的效果，为未来的治疗方案设计提供依据。

方法:通过提取 SEER（Surveillance, Epidemiology, and End Results）中口腔鳞癌患者的临床信息，根据放疗时机分组后进行 KM 生存分析及单因素及多因素 Cox 回归分析，明确术前新辅助放疗对患者预后的影响。

结果:研究纳入 19970 名口腔癌患者，术后放疗组（n=19201）患者的总体生存期明显长于术前放疗组（n=769）（90.19±0.98 vs. 80.51±4.44，*p*<0.01），多因素 Cox 回归结果提示术前放疗为患者预后的独立风险因素（HR，1.161；95% CI，1.044-1.292；*p*=0.006）。倾向性评分匹配（PSM）后，术后放疗患者的总体生存期仍明显长于术前放疗患者（89.58±4.63 *vs.* 80.51±4.44，*p*=0.006），多因素 Cox 回归结果仍提示其为患者预后的独立风险因素（HR，1.294；95% CI，1.101-1.520；*p*=0.002）。

结论:术前新辅助放疗可能增加口腔鳞癌患者预后不良的风险，目前尚无证据支持其在口腔鳞癌诊疗中的应用价值。

779. TDP43 通过与 SEC31A 相互作用形成复合物影响头颈鳞癌细胞的增殖及凋亡

董孟杰

南京医科大学

目的:反式反应 DNA 结合蛋白 43(TDP43)，由 TARDBP 基因所编码，一种核酸结合蛋白，主要位于细胞核，可进行核质运输。参与 RNA 剪接、转录，调控包括肿瘤细胞在内的增殖及迁移等过程。然而，其在头颈鳞状细胞癌(HNSCC) 中的作用仍不清楚。

方法:采用免疫组织化学染色（IHC）综合分析 253 份样本中 TDP43 的表达特征。通过细胞表型实验探究 TDP43 对细胞增殖、迁移的影响，流式细胞术分析 TDP43 对细胞凋亡的作用；转录组测序检测基因组的基因功能及成分；蛋白质印迹、免疫荧光 (IF) 和免疫共沉淀 (co-IP) 实验进行进一步机制研究。

结果:我们发现 TDP43 在 HNSCC 组织中异常高表达且主要表达在细胞核中，其表达量为与肿瘤大小和临床分级有关。过表达 TDP43 促进了 HNSCC 细胞系增殖、迁移能力和裸鼠成瘤的能力，同时降低了肿瘤细胞对顺铂的敏感性。蛋白质印迹分析显示敲除 TDP43 抑制了 HNSCC 细胞的细胞周期蛋白表达。机制上，TDP43 通过与 SEC31A 相互作用并形成复合物激活 PI3K-AKT-mTOR 信号通路促进肿瘤发展。

结论:这些结果表明，TDP43 可能成为 HNSCC 的一个新的治疗靶点以提高其对顺铂的敏感性，从而为 HNSCC 患者的治疗提供一个新思路。

780. LIPI 评分对 PD-1 抑制剂治疗的晚期胰腺癌患者预后的预测价值

陈诗韵*、谭招丽、戴广海

中国人民解放军总医院第一医学中心

Background: There are currently no established biomarkers that can predict whether advanced pancreatic carcinoma (PC) patients would benefit from immune checkpoint inhibitors (ICIs). The lung Immune prognostic Index (LIPI) is a categorical biomarker based on derived

neutrophil-to-lymphocyte ratio (dNLR) and lactate dehydrogenase (LDH). Our study investigated the relationship between pretreatment LIPI and prognosis of patients receiving PD-1 inhibitors therapy.

Methods: Patients with advanced PC treated with PD-1 inhibitors at a single center from September 2015 to September 2020 were included. Based on baseline dNLR and LDH levels, patients were categorized according to pretreatment LIPI with an upper limit of normal (ULN) value of 250 U/L for lactate dehydrogenase and a classification point of 3 for dNLR. Overall survival (OS) and progression-free survival (PFS) served as this studys primary and secondary endpoints. Cox regression models were used to identify independent prognostic factors for survival benefit.

Results: There were 98 patients in our study. 61 (62.2%) patients had good LIPI (dNLR<3 and normal LDH) and 37 (37.8%) had intermediate/poor LIPI (dNLR ≥ 3 or/and LDH ≥ ULN). The overall patients with PC who received immunotherapy had median OS of 12.1 months, and patients with good LIPI score had significantly longer OS compared with those with intermediate/poor LIPI score (44.2 vs. 6.4 months; P<0.010), median PFS was 3.7 and 2.5 months (P=0.010). The number of metastatic sites >2 and the line of immunotherapy were associated with PFS, and the line of immunotherapy and the LIPI score were independent prognostic factors for OS, according to multivariate analysis.

Conclusion: Pretreatment LIPI can be used as a prognostic biomarker in patients with advanced PC treated with PD-1 inhibitors.

Key words： pancreatic cancer, immune checkpoint inhibitors, lung Immune prognostic Index, overall survival, progression-free survival

781. Survival and prognosis of metastatic breast cancer in young women: SEER 2010-2015

Hongna Sun*、Junnan Xu、Tao Sun

Department of Medical Oncology, Cancer Hospital of China Medical University, Liaoning Cancer Hospital & Institution, Shenyang, China

Objective: Female breast cancer is the most frequent malignant tumor with an estimated 2.3 million new cases, followed by lung cancer, and the fifth-biggest cause of cancer-related fatalities globally. While breast cancer is the leading cause of cancer death in women. Although breast cancer in young women (BCYW) is not as common as in older individuals, the incidence of BCYW is increasing. Due to the particular considerations regarding pregnancy, fertility preservation, early menopause, body image, lactation, and quality of life, BCYW deserves unique management. We sought to estimate the survival and prognosis of such patients.

Methods: We extracted primary breast cancer patients data between 2010 and 2015 from the Surveillance Epidemiology and End Results (SEER) database. We included patients under 70 years and divided them into two groups by age (＜40 *vs.* 40-69 years). Through Kaplan-Meier curves and Log-rank test, we analyzed and compared the overall survival (OS) and breast cancer-specific survival (BCSS) of metastatic breast cancer in young women and older patients among tumor subtypes. Furthermore, we divided metastatic BCYW into training and validation sets to create a nomogram for predicting patients risk and prognostic variables. The univariate and multivariate Cox proportional hazards model was used to determine essential independent prognostic factors for metastatic BCYW. A nomogram was developed to predict 1-, 3-, and 5-year OS based on the independent factors. The receiver operating characteristic (ROC) curve, concordance index (C-index), and calibration curves were employed to test the nomogram models prediction capacity as well as clinical applicability value.

Results: Kaplan-Meier curves suggest that patients under 40 years have longer OS and BCSS than older patients. Whereas these survival benefits are limited in HR+ or/and HER2+ patients, triple-negative breast cancer (TNBC) in young women has similar unfavorable outcomes to older patients. Cox regression analysis demonstrated that race, marital status, tumor subtypes, surgery,

liver metastasis, brain metastasis, and lung metastases were independent risk and prognostic factors for OS of BCYW patients. We used these independent variables to construct the nomogram. The training groups C-index for OS prediction was 0.721 (95% CI: 0.697–0.745), while the validation groups was 0.703 (95% CI: 0.664–0.742). The 1-, 3-, and 5-year AUCs in the training group were 0.802, 0.846, and 0.861, respectively, whereas the validation groups were 0.639, 0.703, and 0.692. The calibration curves for the probability of survival at 1-, 3-, and 5-year OS showed high agreement in the training group and satisfactory concordance in the validation group between the prediction by actual observation and nomogram.

Conclusion: We defined the clinicopathologic characteristics, comprehensively analyzed and compared the OS and BCSS of breast cancer between two age groups among tumor subtypes. Patients under 40 years have longer OS and BCSS than older patients, while these survival benefits are limited in HR+ or/and HER2+ patients, except for TNBC, which needs further investigation. In addition, we developed an efficient predictive nomogram to predict 1-, 3- and 5-year OS of metastatic BCYW. These nomograms can aid oncologists in distinguishing, assessing and evaluating the risk and prognosis of metastatic BCYW, which can help oncologists select next treatment strategies for BCYW.

Key words: Breast cancer in young women, Overall survival, Breast cancer-specific survival, Nomogram, Prognostic factors, SEER.

782. A Nomogram for Predicting Survival in Breast Infiltrating Duct Carcinoma Patients With Brain Metastasis: A Population-Based Study

Hongna Sun*、Junnan Xu、Tao Sun

Department of Medical Oncology, Cancer Hospital of China Medical University, Liaoning Cancer Hospital & Institution, Shenyang, China

Objective: Female breast cancer is the most frequent malignant tumor and the fifth-biggest cause of cancer-related fatalities globally. Breast cancer can spread to bone, liver, lung, and brain, and metastasizing to the brain has the worst outcomes. Brain metastases attack nearly 25% of

advanced breast cancer patients, significantly lowering their quality of life and overall survival (OS). The most frequent histological subtype of breast cancer is infiltrating duct carcinoma (IDC). However, several researches have focused on brain metastasis diagnostic and prognostic nomograms in newly diagnosed breast infiltrating duct carcinoma (BIDC) patients. The goal of the research was to create a nomogram utilizing the SEER (Surveillance Epidemiology and End Results) database, determining the independent factors that affect the prognosis of patients with brain metastases to make an optimal therapy plan for them.

Methods: We used the SEER database to determine 936 patients with brain metastases of breast infiltrating duct carcinoma (BIDC) and separated these patients into training (n=655) and validation (n=281) cohorts at random. The Cox proportional hazards model, both univariate and multivariate, was used to identify essential independent prognostic variables for brain metastasis of BIDC, and a nomogram was developed to forecast 1-, 2-, and 3-year overall survival (OS). In addition, we applied Kaplan-Meier curves to analyze survival and used the Log-rank test to compare the differences among the survivals. The receiver operating characteristic curve (ROC) and concordance index (C-index), and calibration curves were employed to test the nomogram models prediction capacity and clinical applicability value. All tests were two-tailed, and *P* values <0.05 were statistically significant. All statistical analyses were using R software (version 4.1.3; http://www.R-project.org).

Results: The major primary site was the upper outer (22.3%). The opportunity of tumors occurring in the left and right mammary was similar. Most tumors were grade II (32.4%) or grade III (48.9%), although tumor grade was unknown in 15.3% of patients. Hormone receptor-positive (HR+)/human epidermal growth factor receptor 2-negative (HER2−) breast cancer was the commonest subtype (40.5%), followed by HR-/HER2-(19.3%) and HR+/HER2+ (18.5%). In addition to brain metastasis, 618 patients (66.0%) had bone metastasis, 298 (31.8%) had liver metastasis and 428 (45.7%) had lung metastasis. Seven significant independent predictive indicators of OS (age, race, grade, tumor subtypes, surgery, chemotherapy, and liver metastasis) were discovered through univariate and multivariate Cox proportional hazard models, and we used these six independent variables to construct the nomogram. Then, we used the ROC and C-index, and calibration curves to test the nomogram models prediction capacity and clinical applicability value. The training groups C-index for OS prediction was 0.704 (95% CI: 0.677–0.731), whereas

the validation cohorts C-index was 0.678 (95% CI: 0.639–0.717), indicating that the model exhibited acceptable accuracy of prediction. The ROC curve demonstrated high predictive ability as well as clinical utility. The 1-, 2-, and 3-year AUC in the training group were 0.789, 0.786, and 0.778, respectively, and 0.745, 0.760, 0.740 in the validation group. Between the prediction by actual observation and nomogram, the calibration plot for the probability of survival at 1-, 2-, and 3-year OS demonstrated well accordance in the training group and satisfying concordance in the validation group.

Conclusions: We firstly developed an efficient predictive nomogram to predict 1-, 2- and 3-year OS in BIDC patients with brain metastases. These nomograms can aid oncologists in distinguishing, assessing and evaluating the risk and prognosis of BIDC with brain metastasis, which can help oncologists select next treatment strategies for BIDC brain metastasis patients.

Key words: infiltrating duct carcinoma, breast cancer, brain metastases, nomogram, prognostic factors, SEER.

783. Brief analysis on the role of RNA-binding proteins in the prognosis of endometrial cancer based on TCGA

Jing He[1]、Jiayi Zhou[2]、Yueming Zhang[1]、Wei Li[2]、Wenjie Hou[1]

1. Dushu Lake Hospital Affiliated to Soochow University

2. 苏州大学附属第一医院

Objective： To find out the prognostic role of RBPs in endometrial cancer.

Methods: Unit COX regression analysis, LASSO, multivariate COX regression analysis, Kaplan–Meier survival analysis.

Results： We obtained endometrial cancer RNA sequencing data and clinical data from TCGA, screened 284 differentially expressed genes that were differentially expressed between cancer tissues and normal tissues, performed functional enrichment analysis on them, and then screened from the differentially expressed genes identified prognostic-related genes (CD3EAP, EPHB6, CIRBP, LTK, ADARB2, RBPMS), developed a prognostic model to examine differences in OS

among patients in high- and low-risk cohorts, and constructed a nomogram to predict patient survival rate.

Conclusion： We use public databases to study that RBPs have certain value in the occurrence and development of endometrial cancer, and can be used as a prognostic marker for endometrial cancer.

784. Exploration of tumor-infiltrating immune cells on the prognosis of endometrial cancer

Jiayi Zhou[2]、Jing He[1]、Yueming Zhang[1]、Qiao Gu[3]、Wenjie Hou[1]

1. Dushu Lake Hospital Affiliated to Soochow University

2. 苏州大学附属第一医院

3. 常州市第一人民医院

Objective： To explore the landscape of tumor infiltrating immune cells in endometrial cancer and the correlation between TIICs and EC prognosis.

Methods: CIBERSORTx used an algorithm, based on the specifically gene expression to estimate the content and abundance of immune cells. Ranked data used Spearman coefficient to measure the relationship between immune cells and clinical characteristics. Univariate COX hazard analysis was performed to explore the relation between immune cells and clinical outcomes. Lasso regression was used to screen variables. Multivariate regression was performed for stepwise regression variable screening. Univariate and multivariate Independent prognosis analysis was performed to validate the reliability of the multivariate risk model. Furthermore, we used a nomographic chart to grade each patients and assess their prognosis.

Results: 11 types TIICs were remarkably increased in cancer tissues(p<0.05). Univariable regression revealed that 5 types TIICs were significantly related with EC prognosis. TTMMD model was constructed via lasso regression and multivariable cox regression. Log-rank was used to perform survival analysis, and the result was presented by Kaplan-Meier curve(p=5.13e-03). Roc curve was simultaneously fulfilled to validate the model's accuracy and predictability(AUC=0.676). The Kaplan-Meier curve of Training set was statistically

significant(p=3.807e-02). ROC curve replied the feasible of the model(AUC=0.678). The risk model was an independent factor for predicting EC prognosis(p<0.001).

Conclusion: 11 types TIICs were significantly associated with the prognosis of endometrial cancers. The immune cells based risk model was reliable for prognosis assessment.

785. The circular RNA, circRARS, promotes aerobic glycolysis of non-small cell lung cancer by binding with LDHA

Haoran Li[1]、*Qi Huang*[2]、*Haifa Guo*[3]、*Xiao Li*[1]、*Mantang Qiu*[1]

1. Peking University People's Hospital

2. The First Affiliated Hospital of Zhengzhou University

3. Beijing Chest Hospital, Capital Medical University

Objective: Accumulating evidence has highlighted critical roles of circular RNAs (circRNAs) in non-small-cell lung cancer (NSCLC). This study aims to unveil the roles of circRARS (hsa_circ_0001551) in NSCLC.

Methods: Quantitative real-time PCR was used to determine the expression of circRARS in NSCLC tissues and cells. Kaplan-Meier analysis was used to determine the prognostic value of circRARS expression. CCK8, transwell and wound healing assays was to assess the ability of proliferation, invasion and migration in NSCLC cells. RNA pull-down, cells fraction, glucose consumption, lactate production and lactate dehydrogenase activity were conducted to explore the potential mechanisms.

Results: circRARS is up-regulated in NSCLC tissues, and positively correlated with higher Tumor stages. NSCLC patients with high expression of circRARS have poor overall survival. Functional assays demonstrated that circRARS accelerates the proliferation, invasion and migration of NSCLC cells in vitro. Then, cell fraction suggests circRARS is mainly accumulated in cytoplasm and RNA pull-down assay shows LDHA could bind with circRARS. Furthermore, circRARS is positively regulate LDHA activity and its expression in transcription level. Moreover, down-regulated circRARS decreases glucose consumption and lactate production and

compromises aerobic glycolysis in NSCLC cells. Finally, rescue assays show circRARS could promote NSCLC cell proliferation via regulating LDHA activity.

Conclusion: This study shows that circRARS can promote glycolysis and tumor progression in NSCLC by regulating LDHA.

786. Identification of a 5-microRNA prognostic signature of patients with chromophobe renal cell carcinoma

Ziwei Liu[1,2]、Huiying Liang[1,2]

1. China Medical University

2. 广东省人民医院（广东省医学科学院）

Objective: This study aims to establish a prognostic-related model of miRNAs to assess patient prognosis. Simultaneously, developing a miRNA-mRNA regulatory network and contact the downstream target genes to screen further the hub target genes related to survival, to provide ideas for finding new targeted treatment strategies.

Methods: The miRNA datasets of CRCC and clinical information were extracted and screened from the TCGA database. Univariate and multivariate Cox regression analyses, as well as the Lasso regression analysis were utilized to screen out the miRNAs which were related to the prognosis of patients, and the risk prognosis model was constructed. Moreover, the target mRNA of DE-miRNA was analyzed by functional enrichment. Using String and Cytoscape tools, we constructed protein-protein interaction (PPI) and miRNA-mRNA regulatory networks, screened hub genes, and survival analysis was carried out.

Results: We identified 162 differentially expressed miRNAs, including 94 up-regulated miRNAs and 68 down-regulated miRNAs. Multivariate Cox regression analysis revealed five microRNAs (hsa-mir-517b、hsa-mir-580、hsa-mir-30e、hsa-mir-191、hsa-mir-598) which could be used to construct a risk model for predicting the prognosis of patients. Functional enrichment analysis revealed that these miRNAs' target genes are involved in biological processes and pathways that are closely related to cancer. In addition, We performed survival analysis on the top 10 hub genes,

and the results revealed that PTEN and NRAS were significantly correlated with overall survival (OS) of CRCC (p<0.05).

Conclusion： We identified a robust 5-miRNAs signature that can be utilized in assisting the prognosis of chromophobe renal cell carcinoma as biomarkers. And binding analysis with downstream target genes is helpful to understand the molecular regulation mechanism in the occurrence and development of CRCC. However, further experimental studies are required to validate our results.

787. Age-associated HAT1 expression instigates tumor heterogeneity and morphology in esophageal squamous cell carcinoma through the E2F transcription factor

Yuefeng Wu[1,2,3]、Bin Jiang[1]、Qi Wang[1]、Chuanqiang Wu[1]、Ming Wu[1]、Hai Song[1,2]

1. Department of Thoracic Surgery, Second Affiliated Hospital, School of Medicine, Zhejiang University, Hangzhou 310009, China.

2. Zhejiang University

3. Zhejiang University – University of Edingburgh Institute (ZJU-UoE), School of medicine, Zhejiang University, Haining 310000, China.

Objective: Esophageal squamous cell carcinoma (ESCC) and esophageal adenocarcinoma (ESAC) are two main subtypes of esophageal cancer. Esophageal squamous-cell carcinoma accounts for almost 90% of all esophageal cancer cases globally. The poor survival rate for people with esophageal cancer urgently calls for the clarification of the esophageal carcinoma development mechanism. Moreover, effective translation of the mechanistic findings into clinical applications is also rewarding.The diagnosis of cancer is typically based on histopathological examination of tumor tissue slides stained by hematoxylin and eosin (H&E) staining, and supplemented by immunohistochemistry (IHC) test. However, the histological based diagnosis and precision treatment need extensive experience. Recent development in convolutional neuron network (CNN) shines a light on the biomedical image analysis. The deep learning approaches have been applied to pathological region segmentation and disease classification on a variety of medical images,

such as X-ray, MRI, CT, and tissue slides. Translating tumor histopathological information into molecular alterations of tumor is urgent needed.

Methods: Here, we obtained three sets of H&E staining of tissue slides from The Cancer Genome Atlas (TCGA-ESC), the second affiliated hospital, School of medicine, Zhejiang University (SAHZJU-ESC), and a commercial tumor micro-array (TMA-ESC). The corresponding gene expression level was examined by accompanied RNA-sequencing data (TCGA-ESC) or immunohistochemistry (SAHZJU-ESC, TMA-ESC). The coloring scale differs greatly among different H&E slides. Therefore, all the H&E slides were subject to color normalization and sliced into smaller patches with precise patient identification and clinical information label.The cancerous regions were labeled by the experienced pathologists with a double-blind cross-check. A segmentation tool modified from U-net was used to segment the cancerous tissue and distinguish the ESCC from ESAC. The segmentation tool built here has 7 times downing-sampling and 7 times up-sampling. The model was trained for 100 epochs and verified the accuracy with a visual inspection.Thereafter, the Least absolute shrinkage and selection operator (LASSO) regression method is used to identify hub genes correlated with aging in both esophageal cancer and normal esophageal tissues. The RNA-seq data from TCGA was used to experiment. The expression of Histone acetyltransferase 1 (HAT1) was identified to be age-correlated. Expression array profiles from patients with ESCC (GSE45670, GSE20347) were also scaled and processed to verify that HAT1 is significantly up-regulated in ESCC. The Genotype-Tissue Expression (GTEx) data was used to verify that HAT1 expression is age-related in normal tissue as well. Most importantly, the HAT1 was stained with IHC on different age mice with the same genetic background (1 day, 10 days, 20 days, 6 months, 18 months, C57BL6). The HAT1 expression is gradually downregulated.Then, the patients with ESCC in the TCGA cohort were classified into the HAT1 high group and HAT1 low group based on average HAT1 expression. The Densenet-121 was used to distinguish the cell morphological difference in the HAT1 high versus low expression group. 70% of the patches were used for training, 30% of patches were used for validation. After 150 epochs, the best accuracy reaches 91.15%. The clarified patches were joined back to the full-face picture. The model was testified on SAHZJU-ESC and TMA-ESC datasets. The prediction results were confirmed with the HAT1 IHC staining results.

Results: It highlights the detail recognition and classification ability of a deep learning neuron network. However, how the computer vision is formed, and the classification criteria remain invisible, which makes it unreliable to be used in the clinic, and researchers cannot get beneficial insights from the convolutional neuron network. It appeared to be a 'black box. Therefore, interpreting the convolutional neuron network is essential. Here, the Grad-cam was used to quantitatively identify the weight of each identity and visualized by heatmap. The visual inspection made us hypothesize the HAT1 high-expression group has a smaller cell or nuclear size, whereas the cell shape is bigger in HAT1 low-expression group.To confirm the hypothesis, the single-hairpin RNA was stably transfected into the esophageal squamous carcinoma cell line (KYSE30). The HAT1 knockdown (KD) was confirmed by immunoblotting. After two passages, the cell images from the control group and KD group were captured and analyzed with ImageJ. The flow cytometry also confirmed the lagging of the cell cycle in the G2-M phase.Finally, the transcriptomics from the above experiment was obtained and another set of public ChIP sequencing (ChIP-Seq) data with HAT1 knockdown was analyzed with motif enrichment. The E2F was identified to be regulated by HAT1. Meanwhile, the gene ontology enrichment analysis identified mitochondria assembly process and regulation of sister chromatid separation process were involved. The gene set enrichment analysis identified E2F targets pathway as well.

Conclusion: Overall, our work systematically revealed the role of HAT1 in esophageal squamous carcinoma by regulating the E2F. Meanwhile, the trained segmentation and classification model may assist the clinical practice. Most importantly, the work design presents a novel genetic study approach. Although the CNN still cannot be fully explained yet and the well-annotated clinical image is also lacking, the advancement of technology and careful regulation of the clinical information make the artificial intelligence-based oncology translational study possible.

788. Heterogeneous distribution pattern of $CD3^+$ tumor-infiltrated lymphocytes (TILs) and high combined positive score (CPS) favored the prognosis of resected early stage small-cell lung cancer

Ying Jin [1,2,3]、Liang Zhu[1,2]、Guoping Cheng[1,2]、Meijuan Wu[1,2]、Ming Chen[4]

1. Zhejiang Cancer Hospital

2. 中国科学院肿瘤与基础医学研究所（筹）

3. 浙江省放射肿瘤学重点实验室

4. 中山大学肿瘤防治中心（中山大学附属肿瘤医院、中山大学肿瘤研究所）

Objective: This study aimed to illustrate the heterogeneity of immune features on prognosis in small cell lung cancer.

Methods: Immunohistochemistry (IHC) staining of CD3, CD4, CD8 and PD-L1 were performed in 55 FFPE samples derived from radical resection of SCLCs. Quantitative assessment of CD3+ tumor-infiltrated lymphocytes (TILs) was carried out to indicate the heterogeneity in the tumor and the stroma compartments. Hotspots of TILs were also evaluated to explore the potential relationship between TIL density and its immune function. PD-L1 expression was assessed in tumor and surrounding immune cells and the values of tumor positive score (TPS) and combined positive score (CPS) were compared. The clinical value of these factors was further identified according to their correlation with disease-free survival (DFS).

Results: More CD3+ TILs were infiltrated in the tumor stroma than that within the tumor cells (15.02±2.25% *vs.* 1.58±0.35%) and the $CD3^+$ s-TILs were positively correlated with DFS. The population of CD4+ subset of the TILs was found a favorable factor compared to the CD8+ subset. Hotspot of CD3+ TILs were observable in the SCLC and patients with more Hotspot areas have better outcome. CPS were more reliable than TPS to evaluate PD-L1 expression in SCLC and it was found positively correlated with tumor size and DFS.

Conclusion: The immune microenvironment of SCLC was heterogeneous. Hotspot, CD4 counts and CPS value of PD-L1 expression may valuable in determine the immune character and predicting the outcome of SCLC patients.

789. A Nomogram for Predicting Survival in Breast Infiltrating Duct Carcinoma Patients With Brain Metastasis: A Population-Based Study

Hongna Sun、Jun nan Xu、Tao Sun

Department of Medical Oncology, Cancer Hospital of China Medical University, Liaoning Cancer Hospital & Institution, Shenyang, China

Objective: Female breast cancer is the most frequent malignant tumor and the fifth-biggest cause of cancer-related fatalities globally. Breast cancer can spread to bone, liver, lung, and brain, and metastasizing to the brain has the worst outcomes. Brain metastases attack nearly 25% of advanced breast cancer patients, significantly lowering their quality of life and overall survival (OS). The most frequent histological subtype of breast cancer is infiltrating duct carcinoma (IDC). However, several researches have focused on brain metastasis diagnostic and prognostic nomograms in newly diagnosed breast infiltrating duct carcinoma (BIDC) patients. The goal of the research was to create a nomogram utilizing the SEER (Surveillance Epidemiology and End Results) database, determining the independent factors that affect the prognosis of patients with brain metastases to make an optimal therapy plan for them.

Methods: We used the SEER database to determine 936 patients with brain metastases of breast infiltrating duct carcinoma (BIDC) and separated these patients into training (n=655) and validation (n=281) cohorts at random. The Cox proportional hazards model, both univariate and multivariate, was used to identify essential independent prognostic variables for brain metastasis of BIDC, and a nomogram was developed to forecast 1-, 2-, and 3-year overall survival (OS). In addition, we applied Kaplan-Meier curves to analyze survival and used the Log-rank test to compare the differences among the survivals. The receiver operating characteristic curve (ROC) and concordance index (C-index), and calibration curves were employed to test the nomogram

models prediction capacity and clinical applicability value. All tests were two-tailed, and P values <0.05 were statistically significant. All statistical analyses were using R software (version 4.1.3; http://www.R-project.org).

Results: Most of the patients were white (73.7%). The major primary site was the upper outer (22.3%). The opportunity of tumors occurring in the left and right mammary was similar. Most tumors were grade II (32.4%) or grade III (49.0%), although tumor grade was unknown in 15.2% of patients. Hormone receptor-positive (HR+)/human epidermal growth factor receptor 2-negative (HER2−) breast cancer was the commonest subtype (40.5%), followed by HR-/HER2-(19.4%) and HR+/HER2+ (18.5%). In addition to brain metastasis, 618 patients (66.0%) had bone metastasis, 298 (31.8%) had liver metastasis and 427 (45.6%) had lung metastasis. Six significant independent predictive indicators of OS (age, grade, tumor subtypes, surgery, chemotherapy, and liver metastasis) were discovered through univariate and multivariate Cox proportional hazard models, and we used these six independent variables to construct the nomogram. Then, we used the ROC and C-index, and calibration curves to test the nomogram models prediction capacity and clinical applicability value. The validation cohorts concordance index (C-index) was 0.735 (95% CI: 0.706–0.764), while the training cohorts was 0.706 (95% CI: 0.682–0.730). The ROC confirmed high predictive ability as well as clinical utility. The 1-, 2-, and 3-year areas under the curve (AUC) were 0.822, 0.822, and 0.798 in the training group, respectively, and 0.777, 0.777, and 0.791 in the validation group. The 1-, 2-, and 3-year OS calibration curves were consistent between actual survival and nomogram predicted survival.

Conclusion: We firstly developed an efficient predictive nomogram to predict 1-, 2- and 3-year OS in BIDC patients with brain metastases. These nomograms can aid oncologists in distinguishing, assessing and evaluating the risk and prognosis of BIDC with brain metastasis, which can help oncologists select the optimal individual treatment strategies for BIDC brain metastasis patients.

790. Pan-cancer Analysis of LINC02535 and Its Oncogenic Role in Lung Adenocarcinoma

Shuang Dai、Feng Luo

Lung Cancer Center, West China Hospital, Sichuan University

Objective: Cancer has become the major public health problem worldwide for its leading cause of mortality. It is of great clinical significance to investigate the molecular mechanisms of carcinogenesis and to screen new therapeutic targets. LINC02535 has gained much attention for its oncogenic merits across several cancers, but the systematic pan-cancer analysis of LINC02535 has not yet been carried out. We aimed to illustrate its biological patterns in pan-cancer and biological function of LINC02535, particularly in lung adenocarcinoma (LUAD) that is the number one cancer killer.

Methods: Herein, we explored the expression, prognostic value, immunological function and hallmark pathways of LINC02535 across 33 cancers using the Cancer Genome Atlas (TCGA) and Genotype-Tissue Expression (GTEx) databases. Moreover, the expression and biological features of LINC02535 in LUAD were confirmed by qRT-PCR, in vitro and in vivo experiments including EdU cell proliferation assay, clone formation assay, construction of xenograft model, flow cytometry, scratch wound healing and Transwell migration assays.

Results: LINC02535 was aberrantly expressed in 13 of 30 human cancers and serves as a favorable or unfavorable biomarker in distinct cancers. Gene set enrichment analysis (GSEA) across all cancers indicated that proliferative or metastatic pathways/phenotypes were remarkably activated in most cancers. In LUAD, GSEA analysis revealed that LINC02535 may be involved in epithelial-mesenchymal transition (EMT), apoptosis, E2F targets, and KRAS-up signaling pathways. Interestingly, LINC02535 was positively correlated with the EMT- and immunosuppression-related gene NT5E (CD73) whether in LUAD or in other most cancers, based on the TCGA, GTEx and Cancer Cell Line Encyclopedia (CCLE) datasets (Spearman $R>0.5$, $p<0.001$). It was further confirmed by qRT-PCR that LINC02535 was upregulated in several lung cancer cells or tissues as opposed to Human bronchial epithelial cells or paratumor tissues. Furthermore, knockdown of LINC02535 inhibited proliferation, colony formation of lung cancer

cells and xenografted tumor growth. Downregulation of LINC02535 also suppressed migration ability of LUAD cells. Flow cytometry experiments indicated that silencing of LINC02535 induced apoptosis and led to G1/S cell cycle arrest.

Conclusion: Our study provided a comprehensive landscape of LINC02535 in pan-cancer, and highlighted the probability that LINC02535 regulated EMT involved in pan-cancer progression, particularly for LUAD progression, providing new insights into novel molecular therapeutic targets for LUAD.

791. Novel blood-based FUT7 DNA methylation is associated with lung cancer： especially for lung squamous cell carcinoma

Yifei Fang[1]、Yunhui Qu[2]、Longtao Ji[3,4,5]、Hao S[6]、Jiaqi Li[4,5]、Yutong Zhao[3,5]、Feifei Liang[3,4,5]、Zhi Wang[3,4,5]、Jiao Su[1]、Liping Dai[3,4,5]、Songyun Ouyang[1]

1. The First Affiliated Hospital of Zhengzhou University

2. Department of Clinical Laboratory, the First Affiliated Hospital of Zhengzhou University & Key Clinical Laboratory of Henan Province

3. Henan Institute of Medical and Pharmaceutical Sciences, Zhengzhou University

4. BGI College, Zhengzhou University

5. Henan Key Medical Laboratory of Tumor Molecular Biomarkers, Zhengzhou University

6. Department of Radiotherapy, the First Affiliated Hospital of Zhengzhou University

Objective: Lung cancer (LC) is the leading cause of death from cancer, with 1.8 million deaths worldwide in 2020. The mortality rate of LC in China is among the highest globally, and it remains on the rise. Therefore, initial diagnosis and proper treatment are efficient way to improve the survival of LC patients. Low-dose computed tomography (LDCT) screening has been proven to reduce LC mortality by 20% in high-risk populations, but the high false positives rate and overdiagnosis should also be concerned. DNA methylation performs a vital epigenetic mechanism that involves the regulation of X chromosome inactivation, genomic imprinting, tissue-specific gene expression and a variety of disorders. Changes of DNA methylation in peripheral blood may

be related to malignant tumors. It is necessary to explore blood-based biomarkers of methylation to detect LC. FUT7 belongs to the α1,3/4-fucosyltransferase family and catalyzes the synthesis of α1,3-fucose. Evidence is mounting that the expression of FUT7 is increased in liver cancer, lung cancer, breast cancer and other solid tumors. However, there is rare report about the association between blood-based FUT7 methylation and lung cancers. The purpose of our study is to explore the relationship of lung cancer with FUT7 methylation in peripheral blood and the detection value of FUT7 methylation in LC patients.

Methods: Mass spectrometry assays were performed to measure DNA methylation levels of seven CpG sites within FUT7 gene in the peripheral blood of 428 patients with LC, 233 patients with benign pulmonary nodule (BPN) and 862 normal controls (NC). The odds ratios (ORs) of all CpG sites were evaluated for their risk to LC using per SD change and tertiles analyses by logistic regression. The predictive ability of the seven FUT7 CpG sites and risk factors were evaluated by receiver operating characteristic curve (ROC).

Results: The methylation levels of seven CpG sites of FUT7 in LC were significantly lower than that in NC (P <0.05). The per SD decrement of methylation level in CpG_1-7 were significantly associated with 65%, 38%, 59%, 46%, 23%, 20% and 68% higher risk for LC versus NC respectively, and the adjusted ORs (95% CI) were 2.92 (2.17-3.96), 1.76 (1.29-2.38), 2.83 (2.09-3.82), 3.00 (2.17-4.16), 1.81 (1.35-2.43), 1.48 (1.11-1.97) and 3.04 (2.23-4.16) for the lowest tertiles of methylation level in CpG_1-7 compared with the top tertiles respectively. To explore the value of FUT7 methylation in the detection of LC, the combination analyses of seven CpG sites were performed. ROC analysis showed AUC of 0.659 (95%CI: 0.626-0.693) and 0.658 (CI: 0.614-0.701) in distinguishing LC from NC and LC versus BPN. Under the condition that BPN was a control group, each SD decrement of methylation level in CpG_4 and CpG_5 were significantly associated with 24% and 31% higher risk for LUAD. Compared with the top tertiles, the adjusted OR (95% CI) were 1.62 (1.03, 2.55) and 1.74 (1.08, 2.81) for the lowest tertiles of methylation level in CpG_4 and CpG_5. Meanwhile, the per SD decrement of methylation level in CpG_1, 2, 3, 4 and 7 were significantly associated with a 57%, 72%, 75%, 115% and 115% higher risk for LUSC respectively. Compared with the top tertiles, the adjusted ORs (95% CI) were 2.66 (1.16, 6.09), 2.97 (1.21, 7.29), 2.90 (1.31, 6.43), 5.19 (2.26, 11.92) and 4.52 (1.93, 10.57) for the lowest tertiles of methylation level in CpG_1, 2, 3, 4 and 7 respectively. ROC curves

demonstrated the AUC was 0.617 (CI: 0.577-0.657), 0.792 (CI: 0.736-0.848), 0.669 (CI: 0.622-0.716) and 0.729 (CI: 0.665-0.792) for seven FUT7 CpG sites in the discrimination of LUAD versus NC, LUSC versus NC, LUAD versus BPN and LUSC from BPN.

Conclusion: Our study revealed an association between FUT7 hypomethylation and LC, especially for LUSC, which provides novel support for the blood-based methylation signatures as potential marker for the evaluation of lung cancer risk.

792. Perspectives for immunotherapy of EBV-associated GLELC: A relatively "hot" tumor microenvironment

雷艳娜、刘明

West China Hospital, Sichuan University

Objective: Epstein–Barr virus (EBV)-associated gastric lymphoepithelioma-like carcinoma (EBVaGLELC) represents a small number of gastric cancer (GC), and research on tumor microenvironment(TME) and treatment strategy are still lacking.

Methods: A retrospective analysis was conducted between 2019 to 2022 in West China Hospital to reveal the immunological characteristics of EBV-positive GLELC. The difference of immune cell subset and tumor vascular structure between gastric denocarcinoma (GAC) and EBVaGLELC will be pointed out.

Results:13 patients with GELEC and 8 patients with GAC were retrospectively studied. After excluding the impact of tumor biological behavior, stage and other baseline characteristics on our research, the heterogeneity of immune cell profile was then confirmed through multiplexed immunofluorescence staining (mIF) which revealed a higher proportion of CD3+ T cells, CD8+ T cells, and Treg cells in the EBV-associated GLELC group. The tumor vascular structure was investigated using CD31 and α-smooth muscle actin (α-SMA) IF double staining. Results suggest that angiogenesis in EBV-positive GLELC may be less intense than in GAC, a feature that might decrease their susceptibility to antiangiogenic therapy. Such a distinct TME may provide therapeutic advantages and patients with this rare subtype of GC could be a good candidate for immunotherapy. Furthermore, we provide clinical treatment cases to confirm this hypothesis. We

reported a 52-year-old male with advanced EBV-positive GLELC who showed favourable response to the immunotherapy plus platinum-based chemotherapy. A repeat evaluation of this patient showed sustained partial response (PR), and the progression-free survival (PFS) was more than 21 months until now.

Conclusion: Compared with GAC, EBVaGLELC revealed higher T cell infiltration and less intense of angiogenesis. A relatively "hot" TME that may provide the rationality to treat with immunotherapy in EBV-related GLELC.

793. Survival Benefit of Radiation Therapy for Pancreatic Ductal Adenocarcinoma with Liver Metastases: A Propensity Score-Matched Study

Liyou Lian[1]、Shuwen Cheng[5]、Rujie Zheng[3]、Hongxia Yao[1]、Tianhui Chen[2]、Jinfei Chen[4]

1. the First Affiliated Hospital of Wenzhou Medical University

2. Department of Cancer Prevention, Cancer Hospital of the University of Chinese Academy of Sciences (Zhejiang Cancer Hospital), Hangzhou 310000, China

3. Department of Radiology, the First Affiliated Hospital of Wenzhou Medical University, Wenzhou 325000, China

4. Department of Oncology, the First Affiliated Hospital of Wenzhou Medical University, Wenzhou 325000, China

5. Nanjing University Medical School, Nanjing 210046, China

Objective: Pancreatic ductal adenocarcinoma (PDAC) remains refractory to existing treatments including the nucleosideanaloge gemcitabine. Approximately 10–20% of PDAC patients come with resectable PDAC stages, while the remaining patients display locally advanced, non–resectable stages, or distant metastases. Because of the high recurrence incidence following surgery, adjuvant therapy is strongly recommended, and both postoperative and preoperative adjuvant therapy have been utilized. It is a research priority due to its resistance to most treatments and its propensity to metastasize, prompting us to investigate the mechanism of tumor heterogeneity and hunt for viable treatment. Radiation therapy is one of the locoregional treatment modalities used to treat cancer, but not the primary treatment for PDAC with liver metastases. However, reports in some studies of selected patients suggested that radiation prolonged survival.

However, which patient groups can benefit from radiation therapy is a point of contention. Thus, we aimed to gather evidence for the benefits of radiation therapy by analyzing a national cohort and identifying prognostic factors that aid the selection of candidates for radiation therapy.

Methods: Data for patients with PDAC and liver metastasis were extracted from the population-based Surveillance, Epidemiology, and End Results (SEER) database from 1st January 2010 to 31st December 2015. We selected the pancreas as the primary disease site and used ICD-O-3 codes (C25.0–C25.3, C25.7–C25.9). Only patients diagnosed with ICD-O-3 histology/behavior codes of 8140/3 (adenocarcinoma) or 8500/3 (infiltrating duct adenocarcinoma) were included. The effect of radiation therapy on the original PDAC with liver metastases was assessed by separating patients into (a) those who received radiation therapy for cancer (Radiation Group) and (b) those who did not (No-Radiation Group). The bias between radiation and non-radiation groups was minimized with Propensity Score Matching (PSM). Overall survival was estimated using the Kaplan–Meier method. The difference in median survival between surgical groups was examined using the log-rank test. Univariate logistic regression was used to quantify the candidate predictors. Variables with $p<0.1$ were included in the multivariate logistic regression analysis for correction and construction of the final analysis.

Results: A total of 12945 patients with microscopically confirmed PDAC and liver metastases were extracted from the database, including 473 patients who underwent radiation therapy that were 1:1 propensity score-matched with patients who did not receive radiation therapy. The median overall survival for patients receiving radiation therapy (2-12 months) was significantly greater (log-rank test $P<0.0001$) than patients in the No- Radiation group (1-8 months). After performing univariate and multivariate regression analysis of potential risk factors, we also found that compared with the elderly, the young patients with radiation therapy could prolong the survival period ($P<0.0001$). Besides, patients with the treatment of combination of radiation and surgery or chemotherapy or T stage could significantly prolong the survival time. After performing a multivariate logistic regression analysis, we found whether receiving radiation therapy, chemotherapy therapy, surgery therapy or not and T stage and the age were associated with overall survival in PDAC patients with liver metastases (log-rank test $P<0.05$ each).

Conclusion: In conclusion, our findings show that the prognosis of PDAC with liver metastases improves after radiation therapy. Further studies are still needed to investigate the role of adjuvant radiation therapy in PDAC with liver metastases.

794. NTF4 exerts dual roles via ANXA1 pathway in breast cancer progression

Ran Sun[1,2]、Jin He[1]、Yijia Gong[1]、Yijiao Ning[1]、Chaoqun Deng[1]、Kexin Sun[1]、Mingjun Zhang[2]、Zhaobo Cheng[3]、Qin Xiang[1]、Xin Le[1]、Yongzhong Wu[3]、Tingxiu Xiang[1,3]

1. 重庆医科大学附属第一医院

2. the First Affiliated Hospital of Chongqing Medical University

3. 重庆大学附属肿瘤医院

Objective: The molecular underpinnings behind malignant progression of breast cancer from a localized lesion to an invasion and ultimately metastatic disease are incompletely understood. Here we report that neurotrophin 4 (NTF4) plays a dual role in mammary tumorigenesis and metastasis.

Methods: NTF4 functions were analyzed by various cell biology assays in vitro. Subcutaneous tumor model and metastatic lung colonization model were used to explore NTF4 effects in vivo. WB, IF, Co-IP, and iTRAQ were further applied to determine the detailed mechanism.

Results: NTF4 was downregulated in primary breast tumors, but upregulated in normal breast tissues and metastatic lymph nodes. NTF4 inhibited cell proliferation and colony formation and promoted cell apoptosis and cell cycle arrest in vitro. Meanwhile, NTF4 inhibited xenograft tumorigenicity in vivo. Surprisingly, NTF4 promoted epithelial-mesenchymal transition (EMT), cell motility, and invasiveness in vitro and metastatic lung colonization in vivo. Clinical data showed that expression levels of NTF4 were associated with poor clinical outcomes, supporting the notion that metastasis, rather than primary cancer, is the major determinant of the mortality of breast cancer patients. Mechanistic investigations further revealed that NTF4 elicits its pro-metastasis effects by targeting PRKDC and ANXA1. NTF4 could both activate PRKDC/AKT and ANXA1/NF-κB pathway to increase SNAIL stability, thereby strongly decreasing generation

of E-cadherin. Meanwhile, NTF4 can promote lysosomal degradation of E-cadherin. Using PRKDC and AKT inhibitor, and knockdown ANXA1 can reverse NTF4-mediated promotion of EMT, cell migration, and invasion, respectively. Interestingly, NTF4 exert its anti-proliferation effects by increasing the phosphoserine and sumoylation level of ANXA1 and the interaction between ANXA1 and importin β, which was important for ANXA1 to import into and retain in the nucleus. Then ANXA1 nuclear translocation induced expression of the pro-apoptotic Bid gene, and activated the caspase-3 apoptosis cascade, which was almost completely reversed by knocking down ANXA1.

Conclusion: Collectively, these findings uncover an unexpected dual role for NTF4 in mammary tumorigenesis and metastatic progression and represent a predictive and therapeutic target for breast cancer.

795. Plasma autoantibodies IgG and IgM to PD1/PDL1 as potential biomarkers and risk factors of lung cancer

Jiaqi Li、Man Liu、Xue Zhang、Longtao Ji、Ting Yang、Yutong Zhao、Zhi Wang、Feifei Liang、Liping Dai

Zhengzhou University

Objective: Antibodies targeting programmed cell death-1(PD1) and its ligand (PDL1) have transformed current cancer therapy. Nowadays, all anti-PD1/PDL1 antibodies approved by the FDA (Food and Drug Administration) of China (CFDA) are all of the IgG form. Autoantibodies (AAbs) directed against one or more of self-antigens and produced following immune reaction, which have been proved to be detectable in patients with different types of cancer. It has been reported that the preexisted anti-PD1/PDL1 IgG and their subclasses were distribution in a wide range of cancer types, and might serve as new predictive potential biomarkers for anti-PD1 therapy and guide immunosuppressive therapy. Although anti-PD1 IgG and anti-PDL1 IgG have been reported in some autoimmune diseases and cancer, there are no relevant studies on the detection of the differences in expressions between cancer patients and normal controls in a larger

sample size cohort. Moreover, little is known about the expressions of anti-PD1/PDL1 IgG and IgM in different clinical characteristics of LC.

Methods: The expression level of anti-PD1/PDL1 IgG and IgM were detected in plasma of 325 LC and 324 NC by indirect enzyme-linked immune sorbent assay (ELISA). Western blotting and indirect immunofluorescence (IIF) were used to verify the ELISA results. The association analysis was used to evaluate the risk factors of lung cancer.

Results: The expression level of anti-PD1/PDL1 IgG in all LC patients was significantly higher than NC ($P<0.001$ and $p<0.05$, respectively). The expression level of anti-PD1 IgG in both lung adenocarcinoma (ADC) and squamous cell carcinoma (SCC), subtypes of NSCLC, was significantly higher than NC ($P<0.001$), while the expression level of anti-PDL1 IgG in SCC was higher than NC ($p<0.05$). The positive rate of anti-PD1/PDL1 IgG in LC were significantly higher than NC in different clinical characteristics, such as clinical stage, nodules diameter, lymph node metastasis and distant metastasis ($P<0.001$). Moreover, expression of PD1/PDL1 in tissue showed no relationship with anti-PD1/PDL1 autoantibodies expression in plasma ($P>0.05$). Anti-PD1/PDL1 IgG were the risk factors related to LC (OR(95%CI):22.433(5.426-92.745) and 5.051(1.316-19.386)). The anti-PD1/PDL1 IgM were also the risk factors related to lung cancer after adjusting age and gender. The anti-PD1/PDL1 IgM were the risk factors for LC in ≤60 years population (OR(95%CI):6.122(1.365-27.455) and 7.664(1.715-34.251)) and anti-PD1 IgM was also the risk factor for LC in male (OR(95%CI):6.948(1.076-44.868)).

Conclusion: In this study, the expression levels of anti-PD1/PDL1 IgG and IgM autoantibodies were detected in plasma of LC and NC and plasma anti-PD1/PDL1 IgG and IgM might serve as potential biomarkers and risk factors for LC.

796. KLF15 suppresses tumor growth and metastasis in Triple-Negative Breast Cancer by downregulating CCL2 and CCL7

Xin Le[1]、Quist Kanyomse[1]、Jun Tang[1]、Fengsheng Dai[1]、Youchaou Mobet[2]、Chang Chen[2]、Zhaobo Cheng[1]、Chaoqun Deng[1]、Yijiao Ning[1]、Renjie Yu[1]、Xiaohua Zeng [3]、Tingxiu Xiang[3]

1. The First Affiliated Hospital of Chongqing Medical University

2. 重庆医科大学

3. 重庆大学附属肿瘤医院

Objective: TNBC is usually characterized by poor prognosis and high recurrence rate. Hence, clinical challenges of breast cancer patients treatment remain and it is vital to identify new biomarkers for comprehensive therapy.Kruppel like factor 15 (KLF15), a transcriptional factor belonging to the Kruppel-like factor (KLF) family of genes, has recently been reported as a tumor suppressor gene in breast cancer. However, the specific mechanisms by which KLF15 inhibits BrCa have not been elucidated. Here we investigated the role and mechanism of KLF15 in triple-negative breast cancer (TNBC),hoping to broaden related therapeutic strategies.

Methods: KLF15 expression and methylation were detected by qRT-PCR, RT-PCR and methylation-specific PCR in BrCa cell lines and tissues. The effects of KLF15 in TNBC cells were examined via CCK8, colony formation, flow cytometric assays, and Transwell assays. Xenografts and immunohistochemistry analyses were conducted to determine the effects of KLF15 on tumorigenesis in vivo. The specific mechanisms of KLF15 were further investigated using RNA sequencing, qRT-PCR, Western blot, luciferase assay, ChIP, and bioinformatics analysis.

Results: showed that KLF15 is significantly downregulated in breast cancer cell lines and tissues, which promoter methylation of KLF15 partially contributes to. Exogenous expression of KLF15 induced apoptosis and G2/M phase cell cycle arrest, suppressed cell proliferation , metastasis and in vivo tumorigenesis of TNBC cells. Mechanism studies revealed that KLF15 targeted and downregulated C-C motif chemokine ligand 2 (CCL2) and CCL7. Moreover, transcriptome and metabolome analysis revealed that KLF15 is involved in key anti-tumor regulatory and metabolic pathways in TNBC.

Conclusion: In general, our study identified KLF15 as a tumor suppressor in TNBC, and illustrated that KLF15 suppresses TNBC proliferation and metastasis by targeting and downregulating CCL2 and CCL7. This study also discovered key antitumor regulatory pathways of KLF15, presenting an opportunity for detailed studies concentrating on the alternative directions of the antitumor activity of KLF15 in TNBC.

797. Establishment of Differential Model for NSCLC and Benign Pulmonary Nodules Based on Serum miRNAs

Man Liu[1,3]、Jiaqi Li[1]、Longtao Ji[1]、Fenghui Liu[2]、Songyun Ouyang[2]、Yutong Zhao[1]、Zhi Wang[1]、Feifei Liang[1]、Liping Dai[1]

1. Department of Pathology and Pathophysiology, College of Basic Medicine, Zhengzhou University

2. Department of Respiratory and Sleep Medicine, the First Affiliated Hospital in Zhengzhou University, Zhengzhou 450052, Henan, China

3. Laboratory of Molecular Biology, Henan Luoyang Orthopedic Hospital (Henan Provincial Orthopedic Hospital), Zhengzhou 450000, Henan, China

Objective: Lung cancer is the leading cause of cancer-related death in China. With the widely application of low-dose spiral CT (LDCT), although the lung cancer-related death has declined, more pulmonary nodules have been detected. Differential diagnosis of benign and malignant pulmonary nodules has become an urgent clinic problem. Non-small cell lung cancer (NSCLC) accounts for 80% of LC. Effectively distinguishing NSCLC from benign pulmonary nodules (BPNs) is crucial to guide the management and treatment of pulmonary nodules, promote the rational distribution of medical resources and reduce lung cancer-related death.A diagnostic model of NSCLC and BPNs that combined the tumor biomarker and CT could reduce the high false positive rate (FPR) of the CT testing. MiRNA, a potential biomarker to assist clinical diagnosis, can exist in the serum stablely and is less affected by repeated freeze-thaw and PH changes.The study aimed to screen novel serum differentially expressed miRNAs (DEMs) which highly expressed in NSCLC, and owned favourable diagnostic performance for NSCLC and BPNs. Further, we established a diagnostic model based on serum DEMs, CT characteristics and clinical

information for discrimination of BPNs and NSCLC, which would provide new strategies for early diagnosis of NSCLC.

Methods: The sera of 496 participants (NSCLC, n=261; BPNs, n=225; healthy, n=10) were collected. Serum DEMs between NSCLC and healthy or NSCLC and BPNs were acquired via miRNA microarray screening. The expression of DEMs in NSCLC and BPNs was detected by qRT-PCR. The samples (NSCLC, n=163; BPNs, n=160) with complete information were selected for establishment and evaluation of the diagnostic model for distinguishing NSCLC from BPNs. 22 variables were analyzed by univariate analysis to screen out the variables with significant difference between NSCLC and BPNs. Differential models for identifying NSCLC from BPNs were constructed by three logistic methods (forward, backward, enter). The receiver operating characteristic (ROC) curve was used to evaluate the diagnostic ability of the DEMs and the differential models for differentiating NSCLC and BPNs Additionally, we compared the diagnostic ability of logistic model, the published Mayo model and Peking University model for NSCLC and BPNs. Delong test and nomogram drawing were proceeded via R software.

Results: After confirmation and verification, the expression level of miR-4678-3p, miR-4488 and miR-595 was significantly higher in the sera of NSCLC than BPNs. The Delong test showed that the logistic (forward) model containing age, miR-4687-3p, CYFRA21-1, nodule number, vascular notch sign, pleural indentation, and calcification owned strongest diagnostic stability (P=0.407). The AUC (95%CI), sensitivity, and specificity of the model in the training group and test group were 0.849 (0.802-0.897), 67.9%, 87.2% and 0.802 (0.702-0.902), 54.9%, 85.2%, respectively. In the CEA(-), CYFRA21-1(-), solitary, and solid subgroups, the diagnostic AUC was 0.784-0.849. Furthermore, it owned a good diagnostic performance for diagnosing early stage NSCLC and BPNs, the AUC(95%CI) was 0.800(0.725-0.874). Compared with Mayo model (AUC=0.511) and Peking University model (AUC=0.500), the logistic model in the study obtained the better diagnostic performance in the test group.

Conclusion: Based on the serum miRNA, we established the differential logistic model for identifying NSCLC and BPNs, which performed a favourable diagnostic ability for NSCLC and BPNs.

798. Construction of lncRNA TYMSOS/hsa-miR-101-3p /CEP55 and TYMSOS/hsa-miR-195-5p/CHEK1 axis in non-small cell lung cancer

Longtao Ji[1,2,3]、Jiaqi Li[2,3]、Feifei Liang[1,2,3]、Zhi Wang[1,2,3]、Yutong Zhao[2,3]、Fengqi Chen[2,3]、Yutong Li[1,2,3]、Liping Dai[1,2,3]

1. Henan Institute of Medical and Pharmaceutical Sciences，Zhengzhou University, Zhengzhou 450052, Henan, China

2. Henan Institute of Medical and Pharmaceutical Sciences & Henan Key Medical Laboratory of Tumor Molecular Biomarkers, Zhengzhou University, Zhengzhou, China

3. Henan Key Laboratory of Tumor Epidemiology & State Key Laboratory of Esophageal Cancer Prevention, Zhengzhou University, Zhengzhou, China

Objective: Lung cancer is one of the commonly diagnosed cancers and the leading cause of cancer death worldwide, and non-small cell lung cancer (NSCLC) is the most common type of lung cancer. Long non-coding RNAs (lncRNAs) as novel master regulators of initiation and progression can response to therapy in a wide variety of malignant tumors. Some lncRNAs may act as microRNA (miRNA) sponge to affect miRNA activities by regulating messenger RNA (mRNA) expression. This study aimed to explore the regulatory mechanisms in NSCLC by constructing lncRNA-miRNA-mRNA regulatory networks.

Methods: Whole transcriptome sequence was performed in five NSCLC tissues and the corresponding paired adjacent normal tissues. The expression of the selected lncRNAs were detected by GEPIA. Whereafter, the targeted miRNAs binding sites of DELs were predicted by the DIANA-LncBase Predicted V.2 (LncBase). Furthermore, targeted genes of integrated miRNAs were detected by miRDB, TargetScan and miRWalk databases. Then, in order to build an integral ceRNA regulatory network, we further performed analysis on the overlap of targeted miRNAs and mRNAs predicted on the website with differentially expressed miRNAs (DEMIs) and differentially expressed mRNAs (DEMs) in TCGA. Moreover, Gene Ontology (GO) and Kyoto Encyclopedia of Genes and Genomes (KEGG) pathway associated with the target genes were proceeded. Furthermore, lncRNA-miRNA and miRNA-mRNA interactions were predicted via

StarBase and lncRNA-miRNA-mRNA regulatory network was constructed by Cytoscape. In addition, the protein–protein interaction (PPI) network construction and survival analysis were performed by STRING and Kaplan-Meier plotter website.

Results: Totally 559 DELs (|log2FC|>1, p<0.05) were identified via whole transcriptome sequence，containing 235 up-regulated and 324 down-regulated DELs in NSCLC. Three candidate lncRNAs (LINC01426, TYMSOS, VPS9D1-AS1) were finally selected since there were few relative studies. Through bioinformatics prediction, the lncRNA-miRNA-mRNA network were further constructed centered TYMSOS, LINC01426 and VPS9D1-AS1 with 14 miRNAs and 218 mRNAs, respectively. Further analysis showed that the network contains 130 nodes and 402 edges. GO analysis showed that in biological process group terms, positive regulation of cell cycle, nuclear division, extracellular matrix organization were the top three enriched terms. In the molecular function group of GO analysis, DNA−binding transcription activator activity and RNA polymerase II−specific, DNA−binding transcription activator activity, cell adhesion molecule binding were the top terms. The terms associated with cellular component group may be linked with chromosomal region, condensed chromosome, midbody. KEGG analysis revealed that mRNAs were also significantly in microRNAs in cancer, cell cycle, cellular senescence, PI3K−Akt signaling pathway and human T−cell leukemia virus 1 infection. According to node degree, the ten most significant hub-genes were identified by PPI network.

Conclusion: Overall, TYMSOS/hsa-miR-101-3p/CEP55 and TYMSOS/hsa-miR-195-5p/CHEK1 ceRNA regulatory network constructed via bioinformatics prediction may play a vital role in the occurrence and development of NSCLC, and may serve as new therapeutic targets in the future.

799. BAP29 suppresses metastasis in triple negative breast cancer by inhibiting NOTCH pathway

hefen sun、wei jin

fudan university shanghai cancer center

Objective: Breast cancer is the most frequently diagnosed cancer and the leading cause of cancer-related death among women worldwide. Triple negative breast cancer (TNBC) constitutes

the most aggressive molecular subtype among breast cancer and the molecular mechanism of metastasis for TNBC unfortunately remain poor. Screening metastatic-related genes in TNBC and clarifying the mechanism will be helpful to find potential targets for intervention therapy. In our previous study, via iTRAQ assay using primary and metastatic breast cancer cell models, we identified BAP29 may regulate breast cancer metastasis. This study aims to identify the role and mechanism of BAP29 in TNBC.

Methods: A quantitative proteomic (iTRAQ) screen was performed to identify metastasis-related genes in triple-negative breast cancer. Multiple in vitro and in vivo functional analyses were used to study the effects of BAP29 on breast cancer metastasis. Next, transcriptomic sequencing (RNA-seq) and bioinformatics analysis was applied to screen the potential downstream pathways of BAP29. Moreover, immunoprecipitation assay was used to confirm the interaction of BAP29 with target proteins.

Results: We found that depletion of BAP29 promoted the metastasis in TNBC cell line and overexpression BAP29 inhibited cell metastasis in vivo and in vitro. RNA-Seq combining bioinformatic analysis indicated that BAP29 may regulate NOTCH Pathway. We next found that knockdown BAP29 upregulated the expression of NOTCH1 and NOTCH2 while overexpression BAP29 exhibited the reverse results. Further, knockdown BAP29 can significantly enhance the location of NOTCH1 and NOTCH2 in the Golgi. Then we found that BAP29 competed with SEC23A, a subunit of the COPII complex, to interact with Sec31A, another COPII subunit, thus disrupting the ER to Golgi transport of NOTCH1 and NOTCH2.

Conclusion： BAP29 suppressed TNBC metastasis by inhibiting NOTCH pathway. The potential mechanism was that BAP29 competed with SEC23A to interact with Sec31A and then disrupted the COPII dependent transport of NOTCH1 and NOTCH2. Our results might provide new candidate target for clinical treatment of breast cancer.

800. Differential Model Based on Novel Plasma Protein Markers for Lung Adenocarcinoma and Benign Pulmonary Nodules

Yutong Zhao、Xue Zhang、Jiaqi Li、Longtao Ji、Zhi Wang、Feifei Liang、Liping Dai

Henan Institute of Medical and Pharmaceutical Sciences

Objective: The purpose of this research mainly included the following aspects. Firstly, we aimed to discover and identify novel plasma protein biomarkers that can be used for the differential diagnosis of LUAD and BPN by label-free quantitative proteomics technology and enzyme-linked immunosorbent assay (ELISA). Secondly, we would like to construct a differential diagnosis model of LUAD and BPN by combining potential novel plasma proteins with CT indicators and clinical traditional tumor markers, which may be a promising alternative of the clinical management strategies of patients with pulmonary nodules.

Methods: 1. Screening of differentially expressed plasma proteins by label-free quantitative proteomics technology The plasma samples of ten LUAD patients and ten BPN patients were analyzed by label-free quantitative plasma proteomics technology. The differentially expressed proteins (DEPs) were screened with the criteria of FC > 1.2 or<1/1.2 and P<0.05. 2. Validation of DEPs by double-antibody sandwich ELISA method First, the plasma levels of DEPs were detected in validation cohort one by ELISA, which including 39 LUAD patients and 39 BPN patients. Candidate proteins with differential diagnosis ability (AUC > 0.5 and P<0.05) between LUAD and BPN were selected. Then, the abundances of candidate proteins were quantified in an independent validation cohort with 107 LUAD patients, 107 BPN patients, 58 lung squamous cell carcinoma (LUSC) patients, 48 small cell lung carcinoma (SCLC) and 44 normal controls (NCs) by ELISA.3. Construction of differential diagnosis model by combining candidate proteins with CT indicators and clinical traditional tumor markers Univariate analysis and receiver operating characteristic (ROC) curve analysis were adopted to screen promising indicators from twelve CT indicators and three traditional tumor biomarkers, which could be used to identify patients with LUAD and BPN. Logistic regression analysis (Enter method) was used to construct a differential diagnosis model for LUAD and BPN by combining candidate proteins with meaningful CT indicators and

traditional tumor markers. The diagnostic performance of this model in LUAD patients with different clinical characteristics was evaluated by ROC analysis.4. Statistical analysis The results of cell experiments were quantified by Image J and Image Pro plus 6.0 software. SPSS 26.0, GraphPad Prism 8.0 and R 4.0 software were used to analyze experimental data and visualize the results. The nonparametric test (Mann-Whitney U test) was used to analyze the differences of each indicator or model between different groups. The area under the ROC curve (AUC), sensitivity and specificity of each index or model in the differential diagnosis of LUAD and BPN were obtained using the ROC curve (The cutoff value was defined as the concentration of the indicator or the model-predicted probability at the maximum Youden index). All statistical analyses considered that the difference was statistically significant when $P<0.05$.

Results: 1. Through label-free quantitative plasma proteomic analysis, twelve protein markers with significant expression differences between LUAD and BPN were screened, including eight up-regulated proteins (ENPP2, FCGR3B, HGFAC,CLEC3B, SERPINA7, ICAM, LYZ, LUM) and four down-regulated proteins (PON1,PRDX2, CA2, APOC3). ENPP2 possessed the highest up-regulated fold (FC= 1.49)and APOC3 possessed the highest down-regulated fold (FC= 0.36).2. The expression levels of nine DEPs, which were validated by methodology among the twelve DEPs, were detected in the plasma samples of the validation cohort one by double-antibody sandwich ELISA. Three proteins (PRDX2, PON1, APOC3) possessed the ability to differentiate between LUAD and BPN, and the results were consistent with the plasma proteomics results. The diagnostic ability of the three candidate proteins was re-validated an independent validation cohort. The results showed that the AUCs (95%CI) of the three candidate proteins (PRDX2, PON1, APOC3) in the differential diagnosis of LUAD and BPN were 0.603 (0.527-0.678), 0.772 (0.710-0.835) and 0.706 (0.638-0.775), respectively. In addition, the expression level of APOC3 in LUAD was significantly lower than NCs ($P<0.05$). 3. Through univariate analysis and ROC analysis, three promising CT indicators(Spiculation, Vascular Notch Sign, Lobulation) and three traditional markers (CEA,CA125, CYFRA21-1) were screened out from twelve CT indicators and three traditional markers. Using logistic regression analysis, three candidate proteins, three CT indicators and three traditional markers were combined to construct a differential diagnosis model.The model was effective in distinguishing LUAD from BPN, with AUC (95%CI) of 0.904 (0.859-0.949), sensitivity of 81.44% and specificity of 90.14%.

Conclusion: 1. The plasma levels of three candidate proteins (PRDX2, PON1 and APOC3) in LUAD were lower than BPN, and they could be used as novel plasma protein markers for the differential diagnosis of LUAD and BPN.2. The differential diagnosis model, including PRDX2, PON1, APOC3, spiculation of nodules, vascular notch sign of nodules, lobulation of nodules, CEA,CA125 and CYFRA21-1, possessed remarkable diagnostic performance in differentiating LUAD and BPN.

801. Potentially functional variants of MAP3K14 in the NF-κB signaling pathway genes predict survival of HBV-related hepatocellular carcinoma patients

黄琼广

Guangxi Medical University

Objective: The NF-κB signal pathway plays an important role in associating inflammation with tumor development and progression. However, few studies have reported that roles of genetic variants of the NF-κB signal pathway genes in survival of patients with HBV-related hepatocellular carcinoma (HBV-HCC), especially with regards to potentially functional SNPs.

Methods: Multivariate Cox proportional hazards regression was used to evaluate associations between 2,060 single nucleotide polymorphisms (SNPs) in 20 NF-κB signal pathway genes and survival of 866 HBV-HCC patients, which were randomly split (1:1) into discovery and validation datasets. Expression quantitative trait loci (eQTL) analysis was conducted to identify associations between survival-associated SNPs and the corresponding mRNA expression. Kaplan-Meier curves and Online databases were used to assess the relationship between the genotypes and survival. Receiver operating characteristic (ROC) curves were used to assess the prediction accuracy of models integrating both clinical and genetic variables on HCC survival.

Results: A total of 6 SNPs in MAP3K14 remained significantly associated with OS of HBV-HCC patients (p<0.05, BFDP<0.8). Further expression quantitative trail loci (eQTL) analysis demonstrated that significant correlations between the rs2074292 (G>A) A allele was associated

with higher mRNA expression levels of MAP3K14 (*P*=0.044) in normal liver tissue, which was associated with worse survival of HBV-HCC patients. In the additive model, after adjusting for age, sex, smoking status, drinking status, AFP level, cirrhosis, embolus and BCLC stage, the combined dataset showed that HBV-HCC patients carrying the rs2074292 AA and GA genotypes (HR=1.71, 95%CI= 1.29-2.27, *P*=0.000) (HR=1.40, 95%CI=1.10-1.77, *P*=0.005) have worse OS than GG genotype, respectively. The addition of risk genotypes to the prediction models increased the AUC significantly from 71.15% to 73.11% (*P*=0.012) and from 72.55% to 74.21% (*P*=0.010) for one-year and three-year OS, respectively.

Conclusion: Our study indicates that MAP3K14 rs2074292 A allele may be a potential predictor of HBV-HCC survival, likely regulating MAP3K14 mRNA expression.

802. Bioinformatics analysis and validation of the development and prognosis role of lnc-RAB11B-AS1 in hepatocellular carcinoma

Xiangzhi Hu[1]、Dedong Wang[1,2]、Jinbin Chen[3]、Boheng Liang[2,4]、Pengzhe Qin[2,4]、Di Wu[2,4]

1.Department of Public Health and Preventive Medicine, School of Medicine, Jinan University

2.Guangzhou Center for Disease Control and Prevention, Guangzhou, PR China.

3.Guangzhou key laboratory for clinical rapid diagnosis and early warning of infectious diseases, KingMed School of Laboratory Medicine, Guangzhou Medical University, Guangzhou, Guangdong, China.

4.Institute of Public Health, Guangzhou Medical University & Guangzhou Center for Disease Control and Prevention, Guangzhou, PR China.

Objective: Lnc-RAB11B-AS1 was reported to be dysregulated in several types of cancers, and found could function as both an oncogene and tumor suppressor gene. The purpose of this study was to evaluate the potential role lnc-RAB11B-AS1 played in hepatocellular carcinoma (HCC).

Methods: Based on data-mining from The Cancer Genome Atlas (TCGA) and Gene Expression Omnibus (GEO), we investigated and evaluated the differential expression pattern and clinical significance of lnc-RAB11B-AS1 in HCC. Clinical correlation analysis of HCC was conducted using the chi-square test. Also, the Kaplan-Meier method and Cox regression models were utilized

to compare relationships between lnc-RAB11B-AS1 expression, survival, and multiple clinical characteristics. To make our results more credible at the histological level, immunohistochemical staining was applied to verify the expression of RAB11B protein in 90 HCC tissue chips and adjacent noncancerous tissues. Then we performed Gene Ontology (GO) functional annotation and Kyoto Encyclopedia of Genes and Genomes (KEGG) pathway enrichment analysis of RAB11B-related genes using Metascape. In addition, we use TIMER to explore the connection between RAB11B expression and immune infiltration level in HCC.

Results: Data showed downregulation of lnc-RAB11B-AS1 in HCC ($p<0.05$) and accompanied with the sync down expression of the proved target mRNA RAB11B and its protein, the low expressed lnc-RAB11B-AS1 would lead to both shortened overall survival (OS) and disease-free survival (DFS) of the HCC patients ($p<0.05$), the PD1/PD-L1 was correlated with the low expression of RAB11B protein. Multivariable Cox regression analysis indicated that advanced clinical stage (HR=2.628; $P<0.001$), lower expression of lnc-RAB11B-AS1 (HR=0.799; $P=0.025$), and RAB11B (HR=0.898; $P=0.041$) indicated a substantially higher risk of mortality. Moreover, GO functional annotation and KEGG pathway enrichment analysis showed a correlation with immune cells change and Non-alcoholic fatty liver disease (NAFLD). There were obvious positive relationships between six kinds of immune cells and RAB11B expression, including B cells, $CD8^+$ T cells, $CD4^+$ T cells, macrophages, neutrophils, and dendritic cells (all $p<0.05$).

Conclusion: Our findings revealed that lnc-RAB11B-AS1 was down-regulated in HCC and closely associated with the clinical stage of the HCC patients, suggesting that lnc-RAB11B-AS1 could be a possible predictor for HCC, which provides a new therapeutic target for the treatment of HCC.

803. Plasma D-dimer and IL-6 associated with treatment response and progress free survival in advanced non-small cell lung cancer patients treated with anti-PD-1 therapy

Chong Chen

Tianjin Medical University Cancer Institute and Hospital

Objective: The treatment response of immune checkpoint inhibitors (ICIs) remains unexpected and there is significant individual variability in the efficacy of different patients with advanced non-small cell lung cancer. This study aims to find peripheral blood biomarkers predicting the efficacy and PFS (progression-free survival) of anti-programmed death-1 (anti-PD-1) treatment in patients with advanced non-small cell lung cancer (NSCLC), which can be used to guide the adjustment of anti-PD-1 treatment regimens to bring greater clinical benefit to NSCLC patients.

Methods: A systematic review of 103 patients with advanced or recurrent NSCLC who received anti-PD-1 therapy (pembrolizumab or carrelixumab) inpatiently at Tianjin Medical University Cancer Hospital between January 2018 and April 2021. The cut-off values for carcinoembryonic antigen (CEA), cytokeratin19 fragment 21-1 (CYFR21-1), squamous cell carcinoma (SCC), tissue polypeptide-specific antigens (TPSA), D-dimer and serum inflammatory markers were determined by receiver operating characteristic curve analysis. Tumor response was assessed by computed tomography according to the Response Evaluation Criteria in Solid Tumors, version 1.1.

Results: Peripheral blood biomarkers IL-6 and D-dimer can predict the clinical value of treatment effect at 6-8 weeks of anti-PD-1 treatment, with AUC areas corresponding to 0.765 and 0.804. Analyses of survival showed that IL-6 ≥ 8.03 pg/mL and DD≥ 917.2 ng/mL were independent predictors of progression-free survival (PFS). A PFS prediction model for anti-PD-1 treatment of NSCLC using the new cut-off values: using "IL-6 ≥ 8.03 pg/mL" or "DD ≥ 917.20 ng/mL" as a score of “1”. The results showed that the higher the score of combined IL-6 and D-dimer, the shorter the PFS time.

Conclusion: High expression of IL-6 in patients with advanced NSCLC predicts poor efficacy and short duration of PFS with anti-PD-1 therapy; Increasing the cut-off value of D-dimer to 917.20ng/mL predicts the occurrence of disease progression in anti-PD-1 treated NSCLC patients, while high expression of D-dimer predicts short duration of PFS. Combined application of inflammatory index (IL-6) and fibrinolytic index (D-dimer) scores to predict the efficacy of anti-PD-1-treated NSCLC patients and to establish a predictive model for PFS in anti-PD-1-treated NSCLC.

804. MiRNA-625-3p promotes cell proliferation and metastasis of lung adenocarcinoma by targeting KLF9

Zhi Wang[1,2,3]、Longtao Ji[1,2,3]、Feifei Liang[1,2,3]、Jiaqi Li[2,3]、Yutong Zhao[2,3]、Yutong Li[1,2,3]、Fengqi Chen[2,3]、Liping Dai[1,2,3]

1. BGI College，Zhengzhou University, Zhengzhou, China

2. Henan Institute of Medical and Pharmaceutical Sciences & Henan Key Medical Laboratory of Tumor Molecular Biomarkers, Zhengzhou University, Zhengzhou, China

3. Henan Key Laboratory of Tumor Epidemiology, State Key Laboratory of Esophageal Cancer Prevention, Zhengzhou University, Zhengzhou, China

Objective: MicroRNAs (miRNAs) are a class of small, single-stranded endogenous non-coding RNA that generally contains 18~22 nucleotides. MiRNAs are emerging as potential blood-based biomarkers and involved in carcinogenesis for various cancers, including lung adenocarcinoma (LUAD). Unfortunately, most LUAD patients are diagnosed at advanced stage because there are no clinical symptoms in the early stage. Despite recent advances in treating LUAD which include chemotherapy, surgical resection and radiation therapy, the 5-year survival rate of LUAD is still less than 15%. Therefore, early diagnosis and treatment are crucial for improving the 5-year survival rate of LUAD. However, the regulatory roles of miR-625-3p had not been elucidated in LUAD. In this study, we aimed to investigate the role and mechanism of miR-625-3p in LUAD cells.

Methods: Human miRNA microarray 2.0 from Agilent Technologies including 2549 miRNAs were applied to screen candidate miRNAs in 14 serum samples. Total RNA was extracted from cells or serum using RNAiso Plus (TaKaRa, Japan) according to the manufacturer's protocol. Quantitative real-time PCR (qRT-PCR) was used to validate the expression of miRNA in 60 serum samples from LUAD and normal individuals. Loss-of-function and gain-of-function analysis of miR-625-3p were performed to assess its role in LUAD. Cell counting kit-8 assay (CCK-8) and transwell assays were used to explore cell proliferation, migration and invasion. Bioinformatics prediction was applied in the search for the target genes of miR-625-3p. qRT-PCR, western blot and dual luciferase assay were used to validate the target gene of miR-625-3p. A xenograft tumor model was established to evaluate cell proliferation in vivo.

Results: MiR-625-3p was the most increased miRNA expressed in LUAD serum samples compared with healthy ones according to microarray analysis, which was verified in independent serum samples, as well as in tissues based on TCGA database. ROC curve analysis showed that the area under the curve (AUC) of serum miR-625-3p in patients with LUAD was 0.789 (95%CI 0.664-0.915). Survival analysis suggested that high level of miR-625-3p was significantly correlated with a poor prognosis. Functionally, CCK-8 assay showed that overexpression of miR-625-3p increased the proliferation of LUAD cells, while inhibition of miR-625-3p repressed the proliferation of LUAD cells. Transwell assays showed that overexpression of miR-625-3p can promote the cell migration and invasion in LUAD cells, while inhibition of miR-625-3p repressed the migration and invasion in LUAD cells. Mechanistically, Dual luciferase reporter gene assay suggested that KLF9 is a direct target gene of miR-625-3p and miR-625-3p might promote LUAD proliferation, migration and invasion by targeting KLF9 in vitro. Tumor xenograft in nude mice showed that overexpression of miR-625-3p significant enhanced tumor growth in vivo. In addition, KLF9 reverses the effect of miR-625-3p on the proliferation, migration and invasion of LUAD cells. western blot showed that significant upregulation of Vimentin in miR-625-3p-overexpression tumor tissue, which were abolished by KLF9 overexpression. IHC staining revealed higher CD31 and Ki-67 levels in miR-625-3p-overexpressing tumors, whereas tumors from the KLF9-overexpressing group showed decreased CD31 and Ki-67 levels.

Conclusion: Our study identified that miR-625-3p plays an oncogenic role in LUAD, which promoted proliferation and migration through targeting KLF9. MiR-625-3p might be a potential novel diagnostic biomarker and target for LUAD therapy.

805. Potential Unreliability of ALK variant allele frequency in the efficacy prediction of targeted therapy in NSCLC

Weihua Li、Wei Rao、Jianming Ying

Departments of Pathology, National Cancer Center/National Clinical Research Center for Cancer/Cancer Hospital, Chinese Academy of Medical Sciences and Peking Union Medical College

Objective: Variable variant allele frequencies (VAFs) of ALK fusions are identified using hybrid capture-based next-generation sequencing (NGS) in non-small cell lung cancer (NSCLC). We investigate whether ALK VAF can assess intratumoral heterogeneity (ITH) and predict targeted therapy efficacy.

Methods: NGS, fluorescence in situ hybridization (FISH) and immunohistochemistry (IHC) were performed to identify ALK fusions.

Results: Through the application of NGS, FISH and IHC, ALK positive was detected in 7.4% (337/4548), 7.7% (368/4670) and 6.5% (794/12176) of NSCLCs, respectively. Based on adjusted VAF (adjVAF, VAF normalization for tumor purity), ALK subclonality was respectively estimated through 4 different threshold values (adjVAF=50%, 40%, 30% or 20%). Nonetheless, no statistical association was observed between median progression-free survival (PFS) and ALK subclonality, and poor correlation of adjVAF with PFS was found among the 85 patients who received first-line crizotinib or the 38 patients who received second-line alectinib. Moreover, ALK VAF had no correlation with FISH break-apart ratio and IHC-positively stained cell ratio in the same sample. When validated by another NGS platform, there were considerable discrepancies of VAFs between the two oncopanels. Unlike NGS, ALK subclonality was identified in only 2.3% (18/778) of NSCLCs by IHC. However, several concurrent actionable alterations involving EGFR, ROS1, KRAS, and FGFR2 were identified in these ALK IHC heterogeneous-expressed cases.

Conclusion: ALK VAF determined by hybrid capture-based NGS is probably unreliable for ITH assessment and targeted therapy efficacy prediction in NSCLC. ITH of ALK fusion may be a rare event that could be partly uncovered by IHC.

806. Reviewing the pathophysiological relationship between gut microbiota and depression to explore the optimal therapeutic pathway

徐君南、韩文婕、孙涛

辽宁省肿瘤医院

Objective: The gut microbes (GM) plays an important role in regulating the central nervous system (CNS) and disease progression. Thus it is also known as the “second brain” of humans. The relevance of abnormalities in the microbial-gut-brain axis (MGBA) to the development of depression has been demonstrated in many experiments, but the specific mechanisms and optimal therapies should be further studied.

Methods: we first describe the main roles of GM in the organism and the GM characteristics of depressed groups. Then some potential pathways around the MGBA focusing on how GM regulate brain depression level and how depressive state modulates GM structure are presented. Finally, new therapeutic ideas to intervene in the GM were introduced from the perspectives of Chinese materia medica (CMM), diet, and exogenous strains. At the same time, the application of combination therapy strategy can also greatly help to amplify the effect of antidepressant. These studies provide further insight into the role and potential pathways of GM in emotion-related disease, which holds important potential clinical outcomes for persons with MDD or related psychiatric disorders.

Results: Potential pathways for gut microbes to make connections with the brain in depression. Gut microbes transmits signals to the brain in two main forms. One is that metabolites stimulate neurons to transmit information to the brain, and the other is that metabolites cross the intestinal mucosal barrier and the blood-brain barrier successively through the blood circulation for information transmission. Metabolites use these two forms as vehicles to regulate depression

levels in four perspectives: alteration of depression on-m arkers in the brain, regulation of intracerebral inflammation, stimulation of neuroendocrine pathway and alteration of epigenetic modifications in the brain.

Conclusion: To explore new methods to prevent and treat depression and maximize the clinical value of intestinal flora, the flora analysis methods should be upgraded, and multi-omics studies should be performed. The improvement of depression symptoms should be scientifically evaluated. The application of accurate assessment criteria and an improved analysis system can help to promote depression prevention and treatment

807. Integrated proteomic analysis of human plasma and tumor tissue for liver cancer biomarker discovery

Zuoliang Dong[1]、Li Ren[2]

1. Tianjin Medical University General Hospital

2. 天津医科大学附属肿瘤医院

Objective: Biomarkers can be used as specific diagnostic tools, prognostic predictors, and potential therapeutic targets. Liver cancer is one of the most common causes of cancer-related deaths worldwide. Biomarkers for liver cancer such as α-Fetoprotein (AFP) show low sensitivity, and thus more sensitive biomarker is urgently needed. Here, we integrated plasma and tissue proteomics for liver cancer biomarker discovery, and investigated the proteins associated with liver cancer processes to better understand associated pathways during tumorigenesis in plasma.

Methods: We identified 3,177 proteins in the healthy and liver cancer compared cohort within 420 proteins significant changed, 38 markers were identified that can distinguish the liver cancer patients from health people, in which 8 proteins with the same change in liver cancer tissue were verified with paired tumor and adjacent liver tissue proteome.

Results: Two prognostic biomarkers were identified to be potential therapeutic targets of liver cancer. APEX, with available drugs approved by FDA, that is related to DNA repair and redox regulation of transcriptional factors. PON1 is synthesized in liver and secreted into the circulation

where it binds to high density lipoprotein (HDL) particles and hydrolyzes xenobiotics, and there are several potential agonist drugs available.

Conclusion: Finally, we summarize the proteins and pathways involved in liver cancer into three groups containing: proliferation, apoptosis and immune responses, which cloud not only represent the liver cancer tumorigenesis process but also the pan-cancer hallmarks in plasma.

808. A positive feedback loop between ID3 and PPARγ via DNA damage repair regulates the efficacy of radiotherapy for rectal cancer

Chuanzhong Huang、Ling Wang、Wankai Fu、Junxin Wu、Yunbin Ye

Fujian Cancer Hospital

Objective: To study the effect of inhibitor of differentiation 3 (ID3) on radiotherapy in patients with rectal cancer and to explore its primary mechanism.

Methods: Cell proliferation and clonogenic assays were used to study the relationship between ID3 and radiosensitivity. Co-immunoprecipitation and immunofluorescence were performed to analyze the possible mechanism of ID3 in the radiosensitivity of colorectal cancer. At the same time, a xenograft tumor model of HCT116 cells in nude mice was established to study the effect of irradiation on the tumorigenesis of ID3 knockdown colorectal cancer cells in vivo. Immunohistochemistry was performed to analyze the relationship between ID3 expression and the efficacy of radiotherapy in 46 patients with rectal cancer.

Results: Proliferation and clonogenic assays revealed that the radiosensitivity of colorectal cancer cells decreased with ID3 depletion through p53–independent pathway. With the decrease in ID3 expression, MDC1 was downregulated. Furthermore, the expression of ID3, MDC1, and γH2AX increased and formed foci after irradiation. ID3 interacted with PPARγ and form a positive feedback loop to enhance the effect of ID3 on the radiosensitivity of colorectal cancer. Irradiation tests in nude mice also confirmed that HCT116 cells with ID3 knockdown were more affected by irradiation. Immunohistochemical study showed that rectal cancer patients with low expression of ID3 had better radiotherapy efficacy.

Conclusion: ID3 and PPARγ influence the radiosensitivity of colorectal cancer cells by interacting with MDC1 to form a positive feedback loop that promotes DNA damage repair. Patients with low expression of ID3 who received neoadjuvant chemoradiotherapy can obtain a better curative effect.

809. Piezo1 protein affects the proliferation, cycle and apoptosis of esophageal squamous cell carcinoma through the p53 signaling pathway

Lulu Wang[1]、Guanglei Chang[1]、Zhaobin Xu[1]、Miaomiao Yang[2]、Liguo Zhang[1]

1. BGI College, Zhengzhou University

2. School of Basic Medical Sciences

Objective: Esophageal cancer ranks seventh in terms of incidence (604,000 new cases) and sixth in mortality overall (544,000 deaths), the latter signifying that esophageal cancer is responsible for one in every 18 cancer deaths in 2020. EC contains two types according to histological type: Adenocarcinoma (EAC) and Squamous cell carcinoma (ESCC). More than 80% of esophageal cancers are ESCC. ESCC is a malignant epithelial carcinoma of the esophageal epithelium. It has a poor prognosis, with an overall 5-year survival rate less than 20%. The formation of ESCC is a multi-step process, which involves a series of genetic and epigenetic changes. Therefore, it is urgent to seek new therapeutic targets for ESCC.Piezo1 is a mechanosensitive ion channel protein in mammals. This protein is a large transmembrane protein because it contains more than 2500 amino acids and 24-32 transmembrane helices. ESCC belongs to epithelial cell carcinoma, and the esophagus is a site that receives more mechanical stimulation. Therefore, research on the role of Piezo1 in ESCC can provide the basis for its clinical application.P53 signaling pathway is a classic apoptotic pathway. As a transcription factor, P53 can be induced by a variety of factors, leading to cell cycle arrest and apoptosis. Many studies have shown that p53-mediated cell cycle and apoptosis play an important role in preventing tumor progression. Piezo1 has been reported to cause apoptosis in breast cancer, prostate cancer and other cancer cells, but how Piezo1 affects THE apoptosis of ESCC cells is rarely reported. In addition, the relationship between Piezo1

protein causing apoptosis and the P53 signaling pathway has not been found yet and needs further exploration.

Methods: Immunohistochemistry and TCGA database data were used to validate the expression of Piezo1 in ESCC tissues. qRT-PCR (Real-time Fluorescent Quantitative Polymerase Chain Reaction) was used to detect the expression of Piezo1 protein in EC109, EC9706, TE-1, KYSE30 and KYSE510, and selected for subsequent experiments. Lentiviral transfection was used to construct ESCC lines with stable knockdown of Piezo1 protein. qRT-PCR and Western Blot were used to detect the mRNA and protein levels of Piezo1 in the selected ESCC lines. Flou-4-Ca2+ fluorescent probe was used to investigate the effect of knockdown Piezo1 protein on Ca2+ flux before and after adding Yoda1.CCK-8, scratch and transwell assay were used to detect the proliferation, migration and invasion ability of knockdown Piezo1 protein in ESCC. Flow cytometry was used to detect the effect of knockdown Piezo1 on the cell cycle of ESCC. TUNEL assay was used to detect the effect of knockdown Piezo1 on apoptosis of ESCC cells. Western Blot was used to detect the expression of knockdown Piezo1 on EMT pathway factors E-cadherin and N-cadherin. The protein expression of p53 pathway related factors p53, Bax and apoptosis factors Caspase3 and Cleaved-Caspase3 were detected by Western Blot. qRT-PCR was used to detect the p53, Bax mRNA expression in ESCC. Immunoprecipitation assay detected the interation between Piezo1 and p53 in ESCC. The cell lines of the ESCC knockdown group and the control group were inoculated subcutaneously into BALB/C nude mice to establish the mouse transplanted tumor model, the tumor weight and volume were observed and recorded. Western Blot was used to detect the expressions of p53, Bax, Caspase3, Cleaved-Caspase3, E-cadherin and N-cadherin protein of tumor tissue.

Results: The expression of Piezo1 protein was significantly higher in ESCC tissues than in paracancerous tissues via immunohistochemistry (P=0.004). The data of Piezo1 expression in 81 ESCC tissue samples and 11 normal esophageal tissue samples were collected from the TCGA database. The results showed that Piezo1 was highly expressed in ESCC compared with normal esophageal tissue (P<0.001). The mRNA expression of Piezo1 in EC109, EC9706, TE-1, KYSE30 and KYSE510 cells were verified by qRT-PCR, and it was found that the expression of Piezo1 in EC109 (p<0.05) and EC9706 (p<0.05) cells were higher than in other ESCC cells. Therefore, these two cell lines were selected for knockdown Piezo1. Knockdown Piezo1

(sh-Piezo1) and control (sh-NC) lentivirus were constructed and transfected into EC109 and EC9706 cells. qPCR and Western Blot results showed that the mRNA and protein levels of Piezo1 were significantly reduced (EC109, $p<0.05$; EC9706, $P<0.001$). Before and after addition of Yoda1, an agonist of Piezo1, the Ca2+flow in ESCC cells was decreased compared with the control group (EC109, $P<0.001$; EC9706, $p<0.05$). The results showed that the cell line of knockdown Piezo1 was successfully constructed.Compared with the control group, the migration (EC109, $P<0.001$; EC9706, $P<0.01$) and invasion (EC109, $P<0.01$; EC9706, $P<0.01$) ability of ESCC were significantly reduced after knockdown of Piezo1. In EC109 and EC9706 cells, compared with the control group, knockdown of Piezo1 increased the expression of the epithelial factors E-cadherin and decreased the expression of the mesenchymal factors N-cadherin.Compared with the control group, knockdown down Piezo1 could inhibited cell proligeration, blocked the number of G0/G1 phase cells to S phase and promoted cell apoptosis (EC109, $P<0.001$; EC9706, $P<0.001$); Knockdown of Piezo1 significantly increased the mRNA and protein expression of p53 (EC109, $P<0.01$; EC9706, $P<0.01$) and its downstream factor Bax (EC109, $P<0.01$; EC9706, $P<0.01$), The protein expression levels of apoptotic factors Caspase3 and Cleaved Caspase3 were also significantly increased. Immunoprecipitation results showed that Piezo1 interacted with p53 in ESCC. In vivo experiments showed that knockdown Piezo1 inhibited tumor growth compared with the control group($P<0.01$). The tumor tissues in mice were extracted, Western Blot results showed that compared with the control group, the expression of p53, Bax, Caspase3, Cleaved-Caspase3, and E-cadherin in the knockdown Piezo1 group were up-regulated, while the expression of N-cadherin was down-regulated.

Conclusion: Piezo1 protein was highly expressed in ESCC. Knockdown of Piezo1 inhibits the proliferation, migration and invasion of ESCC cells, promotes apoptosis, blocks the cell cycle and thus inhibits the development of ESCC. Piezo1 regulates the p53 pathway by interacting with p53, thereby affecting the apoptosis of ESCC cells.

810. Mir-421 and Mir-550a-1 are Potential Prognostic Markers in Esophageal Adenocarcinoma

Guanglei Chang[1,2,3]、Lulu Wang[1,2,3]、Miaomiao Yang[4]、Zhaobin Xu[1,2,3]、Liguo Zhang[1,2,3]

1. Zhengzhou University

2. Henan Institute of Medical and Pharmaceutical Sciences, Zhengzhou University, No. 40 Daxue Road, Zhengzhou 450052, China

3. Laboratory of Tumor Molecular Biomarkers, Zhengzhou University, Zhengzhou 450000, China

4. School of Basic Medical Sciences, Zhengzhou University, No. 100 Science Avenue, Zhengzhou, 450001, China

Objective: The miRNAs highly associated with prognosis of EAC and their target genes are identified by performing bioinformatics methods and the effects of prognostic miRNAs on EAC cell proliferation, migration and invasion are preliminarily explored, which provides a new reference for studies of molecular mechanism of EAC tumorigenesis and lays the theoretical and experiment foundation for development, prognosis and molecular target therapy of EAC.

Methods: To screen differentially expressed miRNAs highly correlated with EAC, EAC miRNA-seq data and corresponding clinical data were downloaded from TCGA database. Further, differentially expressed analysis and Weighted Gene Correlation Network Analysis (WGCNA) were performed to mining miRNA-seq data using "edgeR" and "WGCNA" function packages, respectively. Differentially expressed miRNAs were analyzed by univariate Cox and Lasso regression, and the EAC prognostic model was constructed based on multivariate Cox regression algorithm. Receiver operating characteristic (ROC) curve, concordance index and calibration curve were used to evaluate the prognostic model. Patients with EAC were randomly divided into internal validation sets 1 and 2 using the “Caret” function package to verify the predictive power of the prognostic model and separate survival analysis and ROC analysis for prognostic miRNAs were performed to identify the hub miRNAs of EAC prognosis. The expression level of prognostic hub miRNAs in EAC tissues, normal esophageal tissues and cells was verified by cell lines and integrated Xena database. EAC mRNA-seq data were derived from TCGA database. WGCNA and differential analysis were performed on EAC mRNA-seq data to screen differentially expressed mRNAs highly correlated with EAC. Target genes of prognostic

hub miRNAs were predicted using miRDB, miRWalk, miRTarBase and TargetScan databases, and the intersection of the predicted target genes and the differential mRNAs highly correlated with EAC was obtained. Functional enrichment analysis and survival analysis were performed on the overlapped target genes, and Xena database was used to verify the expression level of target genes in EAC and normal esophageal tissues, so as to identify the key target genes. The effects of prognostic hub miRNAs on OE33 cell proliferation, invasion and migration were detected by CCK-8 and Transwell

Results: 88 EAC tissue samples and 9 normal esophageal tissue samples were downloaded from TCGA. By differentially expressed analysis and WGCNA, 28 differential miRNAs highly associated with EAC were screened, among which 17 were up-regulated and 11 were down-regulated. ROC, concordance index and calibration curve showed that the prognostic model composed of mir-550a-1 and mir-421 had good predictive ability for EAC patients; ROC also showed that mir-550a-1 or mir-421 had a good predictive ability for prognosis of EAC patients, and the survival curve displayed that the up-regulation of mir-550a-1 and mir-421 was significantly associated with poor prognosis of EAC. Compared with normal esophageal tissues, verification of expression level found that the expressions of mir-550a-1 and mir-421 were significantly up-regulated in EAC tissues. Due to the mature bodies of mir-421 is miR-421; there are two mature body of mir-550a-1: mir-550a-3p and mir-550a-5p, the expressions of three mature bodies (miR-421, mir-550a-3p and mir-550a-5p) in EAC cell lines were verified, and they were found that the expressions of all three mature bodies (miR-421, miR-550a- 3p and miR-550a-5p) were up-regulated in EAC cells compared with normal esophageal epithelial cells. Among them, miR-421 and miR-550a-3p were most significantly expressed in EAC cells. By predicting and screening the target genes of prognostic miRNAs, a total of 9 target genes were identified, among which PPM1L and SLC18A2 was target genes of miR-421; ASAP3, LMF1, PRKACB and PDCD4 was target genes of miR-550a-3p; LMF1, BCL2L2, PTPN21 and RPS6KA5 were target genes of miR-550a-5p. Inhibition of miR-421 and miR-550a-3p expression in OE33 showed that the proliferation, migration and invasion abilities of OE33 cells were significantly suppressed compared with control.

Conclusion: The mir-421 and mir-550a-1 are potential molecular markers of EAC prognosis and their mature bodies (miR-421, miR-550a-3p and miR-550a-5p) could regulate (PPM1L and SLC18A2), (ASAP3, LMF1, PRKACB and PDCD4) and (BCL2L2, PTPN21 and RPS6KA5) affecting the tumorgensis and development of EAC, respectively. The expression of miR-421 and miR-550a-3p down-regulated significantly inhibited the proliferation, migration and invasion abilities of EAC cells

811. Peripheral Blood Markers Predictive of Outcome in Upper Gastrointestinal Cancers Patients Treated with Immune Checkpoint Inhibitors

Peiwei Wang、Jia Feng、Xue Cui、Yao Jin、Zexi Xu、Xinyi Chen、Jiayan Wei、Jinsong Wang、Yiming Weng、Min Peng

Renmin Hospital of Wuhan University

Objective: In view of the fact that peripheral blood parameters have been reported as predictors of immunotherapy to various cancers, this study aimed to determine the predictors of response to immune checkpoint inhibitors (ICIs) therapy in patients with upper gastrointestinal cancers from peripheral blood parameters.

Methods: The respective data of 93 patients with upper gastrointestinal tumor who received ICIs combination therapy were included in this study. The peripheral blood indexes of interest were neutrophil/lymphocyte ratio (NLR), platelet/lymphocyte ratio (PLR), lactate dehydrogenase (LDH), and fibrinogen/albumin ratio (FAR). Survival probabilities of progression-free survival (PFS) was estimated using Kaplan–Meier curves and log-rank tests and the multivariate Cox proportional hazards model. Receiver-operating characteristic curve was used to determine a cutoff value for parameters and area under the curve.

Results： The median PFS of all upper gastrointestinal cancers patients was 7.33 months. Baseline LDH0 ＜ 194.5,NLR0 ＜ 4.39,PLR0 ＜ 218.7 and FAR0 ＜ 0.13 were associated with longer PFS(13.4 *VS.* 4.9 months; p<0.001,10.8 *VS.* 4.2 months; p ＜0.001,10.8 *VS.* 6.7 months; p ＜ 0.05,8.4 *VS.* 5.0 months; p ＜0.05,respectively).The 6 weeks after treatment value, LDH1 ＜

264.5,PLR1＜117.2 were associated with longer PFS(7.5 *VS.* 2.7 months; p<0.05, 12.0 *VS.* 6.2 months; p ＜0.05, respectively). The first disease progression value,LDH2＜216.5 was associated with longer PFS(9.5 *VS.* 4.2 months; p<0.05). The NLR1 / NLR0<1.75 was associated with significant prolongation of PFS (7.5 *VS.* 4.9 months, P ＜0.05).

Conclusion: Our research illustrated that baseline LDH0,NLR0,PLR0,FAR0 and LDH1,LDH2,PLR1 at post-treatment are independent predictors for PFS in upper gastrointestinal tumor patients treated with ICIs.

812. ENKUR expression induced by chemically synthesized cinobufotalin suppresses malignant activities of hepatocellular carcinoma by modulating β-catenin/c-Jun/MYH9/USP7/c-Myc axis

Rentao Hou、Weiyi Fang

Cancer Center, Integrated Hospital of Traditional Chinese Medicine, Southern Medical University

Objective: ENKUR plays a crucial role in lung and colorectal cancers. Chemically synthesized cinobufotalin(CB) showed its significant anti-cancer effect in nasopharyngeal carcinoma. However, the roles of ENKUR and CB along with their correlation are still unknown in hepatocellular carcinoma (HCC).

Methods: In this study, ENKUR expression in HCC tissue and cells were detected. The relationship between ENKUR expression and clinical pathology was also assessed. In vivo and in vitro experiments were conducted to explore the effects and molecular basis of ENKUR and CB in HCC.

Results: ENKUR expression was correlated with HCC progression and patient prognosis. Furthermore, ENKUR could inhibit tumor proliferation, metastasis, and sorafenib resistance in HCC. Mechanistic studies showed that ENKUR or its Enkurin domain could bind to MYH9 and decrease its expression by binding to β-catenin and inhibiting its nuclear transfer, thus decreasing c-Jun level. Low expression of MYH9 suppressed recruitment of deubiquitination enzyme USP7,

promoting degradation of the c-Myc. Therefore, cell cycle and EMT signals were suppressed. CB as a safe and effective anti-cancer compound up-regulates the expression of ENKUR via inhibiting PI3K/AKT/c-Jun-mediated transcription suppression.

Conclusion: These findings show that ENKUR induced by CB antagonizes β-catenin/c-Jun/MYH9/USP7 pathway, thus increasing c-Myc ubiquitin degradation and finally suppressing cell cycle and EMT signals.

813. Experimental study of interference with calcitonin assay

Yixian Liu、Xiaofang Zhang、Zouliang Dong

Tianjin Medical University General Hospital

Background: Calcitonin is a sensitive serum marker for medullary thyroid carcinoma. CT levels favor the diagnosis, treatment, and prognostic assessment of MTC, but elevated basal CT levels can also be caused by other conditions, such as C cell-related diseases, hypercalcemia, chronic renal failure, bacterial diseases, certain medications, and foods. It is usually detected by immunoassay, and the method is susceptible to interference by substances that can be used to crosslink antibodies, such as heterophilic antibodies. The issue of whether elevated CT levels are consistent with clinical diagnosis must be determined. If they are not, then the cause should be clarified to exclude false positives, thereby avoiding misdiagnosis. Herein, we report a case with elevated CT results because of heterophilic antibodies encountered in clinical work. We discuss how elevated CT levels can be treated.

Methods: A patient came to our clinic with a physical examination ultrasound showing a slightly enlarged thyroid gland with small nodules. Relevant test results showed that thyroid hormone and thyroid antibody were normal. Results of ancillary tests, namely, liver and kidney function, calcium, phosphorus, magnesium, carcinoembryonic antigen, and rheumatoid factor, were all normal. But the patient was found to have elevated calcitonin level, which was inconsistent with the clinical presentation and other findings. Samples for CT tests treated with heparin anticoagulation and procoagulation tubes were analyzed via same platform. We also analyzed the

results via different platform validation.The patient's plasma was multiplex dilution, polyethylene glycol precipitation, heterophilic blocking test, and then then re-tested with same platform. Finally, DNA was extracted from peripheral blood and sequenced for the full exon-coding region of the RET gene.

Result: The results of the retest on the same platform were consistent with the original results and remained high, but the calcitonin levels tested on the other platforms were normal. The results were nonlinear after multiplier dilution, demonstrating the presence of other interfering factors. Calcitonin levels slightly decreased after polyethylene glycol treatment. The results were remarkably lower and normalized after three HBT treatment. Finally, sequencing of exons 5, 8, 10, 11, and 13–16 of the RET gene, including 98% of multiple endocrine neoplasia type 2 (MEN2) a, 95% of MEN2 b, and 95% of common MTC mutations revealed no pathological mutations.

Conclusion: Laboratory tests are an important adjunct to the diagnosis of clinical diseases. Usually, the results should be consistent with clinical presentation. Extra attention should be paid when the two do not match and problems with laboratory operations should be ruled out. By studying this case, when elevated calcitonin is inconsistent with clinical presentations and other findings, laboratory staff should communicate with clinicians, analyze the reasons for the inconsistent results, and use different means to verify whether the results are actually inaccurate. Moreover, close communication and cooperation with clinicians should be established to determine the cause, remove interference, and avoid misdiagnosis to enhance the effectiveness of diagnosis and better serve our patients. The aim is to provide realistic and reliable data for doctors and patients and to avoid unnecessary testing and overtreatment.

814. Systematic analysis of cuproptosis-related long non-coding RNA predicting prognosis in patients with lung squamous cell carcinoma

Shanxiu Jin[1,2]、Cheng Du[2]

1. 大连医科大学

2. General Hospital of Nothern Theater Command

Objective: Cuproptosis is a newly proposed copper dependent cell death mode. It is similar to ferroptosis found before, but there are different places. The main mechanism is that CU2+ directly combines with the ester acylation components in the tricarboxylic acid cycle.So, we will discuss whether cuproptosis related lncrna can be used to predict the prognosis of patients with lung squamous cell carcinoma（LSCA）.

Methods : A total of 19 genes related to cuproptosis（NFE2L2、NLRP3、SLC31A1、FDX1…) were identified through recently published articles. A total of 16 lncRNAs related to cuproptosis were identified by screening with the correlation coefficient of 0.4. The information of 504 lung squamous cell carcinoma patients were downloaded from TCGA public database and analyzed in R language (R version 4.2.1).We randomly divided them into train set and test set. The prognosis model was constructed by lasso-Cox regression in the train set and verified in the test set. We evaluated the prognostic power of this model receiver operating characteristic (ROC) curve and c-index curve, and drew a Nomogram for predict clinical prognosis of patients. In addition,the biological functions of the characterized lncRNAs were analyzed by Gene Ontology (GO) and Kyoto Encyclopedia of Genes and Genomes (KEGG).Finally, The gene mutation analysis obtained information on genetic alterations from the cBioPortal database.

Results: we finally identified four lncRNAs （AC079414.3、AC019080.1、AL449423.1、AC002467.1） for model construction, and divided them into high-risk and low-risk groups according to the median value. In the test set, Kaplan-Meier analysis revealed the high-risk group had poor OS ($p=0.002$) and PFS ($p<0.001$). The areas under the ROC curve in one year, three years and five years are 0.603, 0.630 and 0.603 respectively. In the model we constructed, there was no significant difference in tumor mutation burden between high-risk and low-risk

groups.Patients with high and low tumor mutation burden who had low risk scores also had better prognosis (p<0.001). The main mutations were TTN and TP53 gene mutations. Finally, the immune function was analyzed, and it was found that the immune function of high-risk group was more active.

Conclusion: We investigated the potential mechanisms of LUSC development from the perspective of cuproptosis-related lncRNAs,and identified 4 lncRNAs as biomarkers to predict the prognosis of LUSC patients.

815. ZNF503 combined with GATA3 is a prognostic factor in triple-negative breast cancer

Siyu Liu、Jingjing Liu

Henan Institute of Medical and Pharmaceutical Sciences

Objective: In this study, we explored whether ZNF503 and GATA3 could serve as prognostic markers independently or in combination.

Methods: We first analyzed the expression levels of GATA3 and ZNF503 in total breast cancer patients and their subtypes through the TCGA database, and predicted whether they could be used as prognostic biomarkers. Then and verify in TMA. We explored whether GATA3 and ZNF503 could serve as prognostic markers independently or in combination. Survival analysis and ROC analysis were performed on breast cancer patient data in the TCGA database and TMA to investigate their prognostic roles for future diagnostic and therapeutic strategies.Finally, the roles of these two genes in cell proliferation, migration and invasion were verified.

Results: We performed a survival analysis of 898 breast cancer patients from TCGA and 129 breast cancer patients from TMA. In TCGA database, the mRNA expression of GATA3 and ZNF503 could not predict TNBC prognosis alone, while the ratio index, ZNF503/GATA3 could be a novel prognostic biomarker in TNBC. In TNBC TMA database, we detected the protein expression of ZNF503 and GATA3 and found that the combination of two genes, ZNF503-GATA3, has a great improvement in predictive ability of clinical outcome.

Conclusion: In general, the predictive power of GATA3/ZNF503 in TNBC patients from TCGA was better than that of ZNF503 and GATA3 expression alone. In tissue microarrays, GATA3-ZNF503 index predicted TNBC survival. In conclusion, the combination of ZNF503 and GATA3 could be a useful prognostic factor in triple-negative breast cancer.

816. Antitumor effects of dictyophora polysaccharide against lung cancer by inhibiting recruitment of MDSCs

xiaohong wang

Zhejiang cancer hospital

Objective: Antitumor effects of dictyophora polysaccharide against lung cancer by inhibiting recruitment of MDSCs

Methods: Antitumor effects of dictyophora polysaccharide against lung cancer by inhibiting recruitment of MDSCsDP15 inhibits the tumour growth in mice. DP15 significantly deceased the proportion of CD11b+ Gr1+ MDSCs in splenocytes via p53/Bcl-2 related apoptosis pathway. The antitumor activity of DOC was enhanced when combined with DP15. The Infrared Radiation (IR) spectrum of DP15 showed the characteristic absorption peak of stretching vibration of the polysaccharide glycoside hydroxyl at 2600-3200 cm−1 and the peak of C-H stretching vibration appeared at 2800 cm−1. The peak at the 1600 cm−1 was attributed to the presence of water probably. The absorption peak around 1000 cm−1 indicated that it was a pyran-type polysaccharide, and the peak of absorption at 800 cm−1 was due to the existence of β-pyranose.LLC bearing mice treated with DP15 showed significantly extended survival compared with PBS-treated controls (Figure 2a, $p<0.05$). Tumour volume analysis also indicated that the volume of mice in DP15 group were obviously smaller than the controls (Figure 2b, $p<0.01$). according to these results, we found that DP15 has antitumor activities in lung cancer.Splenocytes isolated from the LLC bearing mice were cultured in the incubator and treated with DP15. The adherent cells adopted a branching type after incubation with DP15, while control cells keep in rounded shape.In vivo study， The mice were injected subcutaneously with 5 × 106 LLC in 100 μL 0.9% normal saline per flank, and randomly divided into different groups.

Preparation of spleen cell suspensions， After the end of observation, all mice were anaesthetized by carbon dioxide inhalation and sacrificed. The spleens were aseptically removed and transferred to the Ultra-clean bench. Flow cytometry for cell characterization,low cytometry for cell characterization.Western blot:The protein expression level of IL-2 was examined by Western blot. Briefly, Total protein of MDSCs was extracted using radioimmunoprecipitation assay (RIPA) and was determined the concentration by the bicinchoninic acid (BCA) kit. A total of 30 μg protein was separated with 10% of sodium dodecyl sulfate–polyacrylamide electrophoresis (SDS-PAGE) and transferred onto a polyvinylidene fluoride (PVDF) membrane, and then blocked with 3% bovine serum albumin at room temperature for 90 min. The membrane was subsequently incubated overnight at 4 °C with the IL-2 and β-actin antibodies (Abcam, Cambridge, UK). Then, the membrane was digitally photographed using the Bio-Rad image analysis system (Bio-Rad Laboratories, Hercules, CA, USA) after second antibodies incubation.

Results: The Infrared Radiation (IR) spectrum of DP15 showed the characteristic absorption peak of stretching vibration of the polysaccharide glycoside hydroxyl at 2600-3200 cm−1 and the peak of C-H stretching vibration appeared at 2800 cm−1. The peak at the 1600 cm−1 was attributed to the presence of water probably. The absorption peak around 1000 cm−1 indicated that it was a pyran-type polysaccharide, and the peak of absorption at 800 cm−1 was due to the existence of β-pyranose.

Conclusion: In conclusion, this study analysed the combined effect of chemotherapy and DP15, not only provided the strong antitumor activities of chemical drugs, but also helped ameliorated the tumour microenvironment. The combined use of DOC and DP15 strongly reduced the tumour growth and reduced MDSCs in tumour microenvironment, which also give the hint of clinical application of DP15 in lung cancer.

817. SLC7A5 promotes chemotherapy resistance of cervical cancer by mediating glutamine metabolism through ASNS

Lei Tang、Jian-Zhong He、ye Liu、Fa-Min Zeng

The Fifth Affiliated Hospital, Sun Yat-sen University, Zhuhai, Guangdong Province, China

Objective： Chemotherapy insensitivity are considered as the main cause of recurrence and metastasis of cervical cancer. SLC7A5 gene encodes an amino acid transporter and plays an important role in chemotherapy resistance. However, its underlying mechanism in cervical cancer chemotherapy resistance has not been investigated.

Methods： We performed immunohistochemistry and Kaplan-Meier survival analysis to explore the correlation SLC7A5 expression and sensitivity to chemotherapy in 101 cervical cancer samples and 60 normal adjacent tissue samples. In vitro experiments，cell proliferation, migration and invasion assay were used to study the effect of SLC7A5 expression on the function of cervical cancer cell lines. Dose response curve analysis was performed to further evaluate SLC7A5 cisplatin sensitivity of cervical cancer cell lines. RNA-sequencing, metabonomics analysis and western bolt was used to investigate the mechanism of SLC7A5-mediated cisplatin chemosensitivity.

Results： SLC7A5 was abnormally up-expressed in cervical cancer cells, and played a crucial role in the development of cervical cancer and cisplatin resistance. Knockdown of SLC7A5 was down-regulated the asparagine synthase (ASNS) expression and reduced the glutamine metabolism. Survival analysis revealed that the high expression of SLC7A5/ASNS decreased the survival rate and sensitivity to cisplatin chemotherapy of patients with cervical cancer. Above data suggests that SLC7A5 mediates ASNS to regulate the glutamine metabolism, and leads to cisplatin resistance in cervical cancer.

Conclusion： SLC7A5 regulates ASNS mediated glutamine metabolism to resist cervical cancer chemotherapy. Targeting SLC7A5 and ASNS will provide new strategies for clinical application of chemotherapy in cervical cancer.

818. A Nomogram for Predicting Survival in patients with Unresectable Hepatocellular Carcinoma treated with intensity modulated radiotherapy

Meiying Long[1]、Jianxu Li[2]、Moqin Qiu[3]、Meiying He[2]、Jialin Qiu[4]、Yingchun Li[4]、Hongping Yu[4]

1. Guangxi Medical University

2. Department of Radiotherapy, Guangxi Medical University Cancer Hospital, Nanning, Guangxi, China.

3. Department of Respiratory Oncology, Guangxi Medical University Cancer Hospital, Nanning, Guangxi, China.

4. Department of Experimental Research, Guangxi Medical University Cancer Hospital, Nanning, Guangxi, China.

Objective: Intensity modulated radiotherapy (IMRT) is an emerging treatment modality for hepatocellular carcinoma (HCC) with promising outcome. However, few survival prediction models have focused on the prognosis of patients with unresectable HCC undergoing IMRT. In this study, we aimed to identify predictors of survival in patients with unresectable HCC and to develop an easily clinically applicable prognostic nomogram to predict the overall survival(OS) in unresectable HCC treated with IMRT.

Methods: The patients in this study were collected from Guangxi Medical University Cancer Hospital. A total of 340 patients with unresectable HCC who received IMRT for liver tumors between March 2012 and December 2021 were included in the analysis. To develop prognostic nomograms and evaluate model predictive performance using a split-sample approach, 340 HCC patients were randomly divided into a training set (n=237) and a internal validation set (n=103) in a 7:3 ratio. Compare the balance of baseline patient characteristics in the two set. Cox proportional hazards models were used to identify prognostic variables, and significant variables (p<0.05) in univariate Cox analysis were included in multivariate Cox analyses. All variables that were statistically significant in the multivariate Cox analysis were used to construct a prognosis model and then to derive a predictive nomogram.The reliability and discriminatory of the predictive nomogram could be demonstrated in the validation set. The total area under the receiver operating characteristic(ROC) curve (AUC) was calculated to estimate the prediction performance of the

nomogram. Importance sampling (1,000 bootstraps) was used for the validation of nomogram and calibration curve construction.

Results: The median overall survival was 12.1 months (Interquartile range, 8.57-24.71) for all patients. The OS rates were 63.66%, 25.11%, and 13.78% at 1, 3, and 5 years, respectively. Multivariate analysis identified tumor numbers >3 (HR=1.69, 95%CI=1.21-2.37), AFP ≧ 400ng/ml (HR=1.52, 95%CI=1.10-2.10), PLT <100×10^9/L(HR=1.7495%CI=1.11-2.73) and ALP>150U/L (HR=1.65, 95%CI=1.15-2.37) were independent risk factors of OS, while prior surgery (HR=0.63, 95%CI=0.43-0.93) was an independent protective factor. The nomogram was developed by the prognosis model that was built using the five significant variables of the multivariate Cox analysis. The ROC plots showed that the nomogram exhibited a favorable predictive value in the training set, with the AUC at 1-year, 2-year, and 3-year models were 0.726, 0.739, and 0.753, respectively. Further, the clinical nomogram also demonstrated good discriminative ability in the validation set with AUC rates of 0.715, 0.756, and 0.780 for 1 year, 2 year, and 3 year, respectively. The Calibration curve srevealed satisfactory predictive accuracy for this predictive nomogram, which showed a considerable consistency between nomogram and actual observation at 1, 2, or 3 years in both training and validation set. The good prognostic discrimination of the predictive nomogram was reflected in the ability to stratify patients into two subgroups with distinct prognosis.

Conclusion: In this study, we developed a nomogram to predict survival in unresectable HCC patients treated with IMRT. The nomogram facilitates individualized prognosis prediction of unresectable HCC patients treated with IMRT and provides recommendations for pre-treatment decision-making by physicians and/or patients. Larger, multi-institutional patient cohorts are required to validate the models reliability and validity.

819. Cancer SLC6A6-Mediated Taurine Uptake Impairs CD8+ T Cell Antitumor Immunity via Regulating Immune Checkpoints

Tianyu Cao、Qi Wang、Wenyao Zhang、Yuanyuan Lu、Daiming Fan、Yongzhan Nie、xiaodi Zhao

Xijing Hospital, Fourth Military Medical University

Objective: One of the important features of tumor progression is changes in substance metabolism, known as metabolic remodeling or metabolic reprogramming. Tumor cells acquire apoptosis resistance, invasive growth and immune escape through metabolic remodeling, which is an important cause of tumor drug resistance and metastasis. One of the important mechanisms of metabolic remodeling is the change of substance absorption and efflux in tumor cells. Transporters are transmembrane proteins that transport endogenous and exogenous substances on cell membranes and can be divided into efflux and intake types according to function. Efflux transporters are represented by ATP-binding box transporters (e.g., P-GP), which expel substrates (e.g., anticancer drugs) by hydrolyzing ATP. This mechanism of tumor drug resistance has been widely studied and recognized. Ingestion transporters are represented by the Solute carrier (SLC) superfamily, which consists of more than 400 proteins in 65 subfamilies. They cannot hydrolyze ATP to produce energy, and promote the ingestion or bidirectional transport of substances in accordance with concentration or potential gradient. Solute vector mediated metabolism is not only involved in the physiological process that determines the fate of cells, but also has been found to be an important hub of cell components in the tumor immune microenvironment in recent years. According to a recent Nature study, the competitive uptake of methionine by tumor cells through SLC43A2 leads to the modification of T cell histone H3K79me2, which leads to the decrease of T cell immune function. SLC6A8 can be used by macrophages to take up the arginine metabolite creatine and regulate interferon and interleukin responses, resulting in macrophage polarization reprogramming. The gastrointestinal tract is the main site of material absorption, and a large number of solute vectors are expressed in the apical and basal-lateral membranes of mucosal epithelial cells. However, the function and mechanism of solute vectors in the progression of gastrointestinal cancer is still limited. It is an important scientific question to clarify

the change of solute carrier during the progression of gastrointestinal cancer and the mechanism of regulating substance metabolism in order to help tumor cells survive and grow under drug pressure.

Methods: Flow cytometry was used to detect cytokine secretion and immune checkpoint expression of T cells. Tumorigenesis assay in vivo was used to analyze the immune-promoting ability of taurine. Polychromatic histochemical staining was used to analyze the expression of immune cell markers. Single-cell sequencing was used to analyze the proportion of infiltrates of various immune cells. Westren blot and PCR were used to detect SLC6A6 and immune checkpoint expression.

Results: Transcriptome sequencing analysis showed that the expression profiles of solute vectors of SGC7901VCR and SGC7901ADR were significantly different from those of their parents, and the expression of solute vector SLC6A6 was most significantly up-regulated. Through the analysis of cancer public database, we found that the expression of SLC6A6 in gastric cancer and colorectal cancer was significantly higher than that in normal adjacent mucosa, and the expression level of SLC6A6 was highly negatively correlated with the survival of patients with gastrointestinal cancer. We further detected the expression of SLC6A6 in the clinical sample cohort of chemotherapy resistance and metastasis of GASTRIC cancer, and found that the expression of SLC6A6 in the chemotherapy resistance tissues of gastric cancer was significantly higher than that before chemotherapy. The expression of SLC6A6 in gastric cancer metastasis tissues was significantly higher than that in primary tissues. These results suggest that SLC6A6 may play an important role in promoting drug resistance and metastasis of gastrointestinal cancer. We established gastric cancer cell models with SLC6A6 function acquisition and function loss. Through in vitro cell experiments and in vivo animal experiments, it was found that upregulation of SLC6A6 expression or administration of taurine significantly enhanced drug resistance and metastasis ability of tumor cells. Down-regulation of SLC6A6 expression or down-regulation of SLC6A6 followed by taurine weakened drug resistance and metastasis ability of tumor cells. These results suggest that taurine transport by SLC6A6 promotes drug resistance and metastasis in tumor cells, leading to tumor progression, suggesting that taurine plays an important role in promoting drug resistance and metastasis of gastrointestinal cancer cells. We inoculated mouse gastric cancer cells and melanoma cells respectively in nude mice and

immunohealthy mice, and found that taurine had opposite effects on tumor progression in mice with different immune backgrounds: taurine promoted tumor progression in immunodeficient mice, but inhibited tumor progression in immunohealthy mice. We performed single-cell sequencing and immunofluorescence analysis on the tumors of immunohealthy mice and found that taurine significantly increased the number of infiltrated CD8+T cells in the tumors of mice. These results indicate that the antitumor effect of taurine depends on whether there are immune factors in the body, suggesting that the antitumor effect of taurine is attributed to the immune factors of the body, rather than the direct inhibitory effect on tumor cells. Plasma taurine levels in gastric cancer patients were significantly lower than those in healthy subjects, suggesting that patients with gastrointestinal cancer were in a state of taurine deficiency. Taurine was detected in different tissue cells of tumor-bearing mice, and it was found that the taurine content of tumor-infiltrating CD8+ T cells in mice was significantly lower than that in tumor cells, and also significantly lower than that in spleen CD8+ T cells. Further analysis of single cell sequencing results showed that the expression of SLC6A6 in murine tumor cells was significantly higher than that in tumor-infiltrating CD8+ T cells. By analyzing gastric cancer cells and clinical samples, we found that the expression of SLC6A6 in gastric cancer cells was significantly higher than that in CD8+ T cells. SLC6A6 expression was negatively correlated with the amount of infiltrated CD8+ T cells in clinical tumor samples. This suggests that taurine is deficient in the tumor microenvironment of gastrointestinal cancer, and tumor cells may compete with CD8+ T cells by overexpression of SLC6A6. Further RNA sequencing analysis of T cells showed that taurine could down-regulate T cell exhaustion score induced by TCM and reduce the expression of immune checkpoint molecules (PD-1, LAG3, TIM3, CTLA4, and TIGIT).

Conclusion: Taurine plays an important role in promoting the malignant behavior of gastrointestinal cancer cells and maintaining the anti-tumor function of T cells. By upregulating SLC6A6, gastrointestinal cancer cells compete with T cells for taurine in the microenvironment, on the one hand promoting their own drug resistance and metastasis, and on the other hand inducing T cell exhaustion to escape immune killing, ultimately leading to tumor progression

820. Identification of gut microbial markers for diagnosis across populations in early lung cancer

Junnan Xu、mengzhen Han、Tao Sun

Liaoning Cancer Hospital Institute

Objective: To investigate the dynamic changes of vaginal flora during cervical carcinogenesis and the value of cervical cancer-related vaginal and gut microbial markers as an adjunctive diagnostic tool.

Methods: We studied 416 public data samples of 16s rRNA from female vagina and 116 public data samples of 16s rRNA from female gut. The vaginal group was divided into Normal (n=180), cervical intraepithelial neoplasia (CINs) group (n=152) and Cervical_cancer group (n=84) according to severity. The gut group was divided into Normal (n=51), Cervical_cancer group (n=65). Reads were processed using vsearch, alpha diversity was determined by Chao1, Shannon and Simpson indices, beta diversity was assessed by principal-coordinate analysis (PCoA) based on weighted Unifrac distances and permutational multivariate analysis of variance (PERMANOVA) analysis based on bray-curtis distances. Microbial communities differences between groups were analyzed using Linear discriminant analysis (LDA) effect size (LEfSe), aiming to find biomarkers. Finally, a random forest model was constructed based on the results of ASVs and diversity analysis, combined with clinical data, and the model was evaluated to select the optimal prediction model.

Results: The structure of vaginal and gut microbial composition was significantly altered in patients with cervical cancer compared to the non-cancerous population. The increase in vaginal microbial diversity and abundance was positively correlated with disease severity and was accompanied by a decrease in commensal flora such as Lactobacillus spp. and an increase in the abundance of pathogenic bacteria such as Gardnerella spp. The diversity and abundance of gut microbes in patients with cervical cancer decreased, and the microbiological composition also changed significantly, including the enrichment of Bacteroides spp. and Prevotella spp. and the decrease of abundance of Faecalibacterium spp. and Roseburia spp. Overall, cervical carcinogenesis leads to microbial changes in both ecological niches that are significantly different

from the non-cancerous population. To determine the optimal microbiota profile for noninvasive diagnostic purposes, we achieved high accuracy in the diagnosis of cervical cancer in a predictive model based on biomarkers obtained from differential genera in both ecological sites (vaginal model AUC= 91.58%; gut model AUC= 99.95%).

Conclusion: Significant differences in vaginal and gut microbes were identified in patients with cervical cancer compared to the non-cancerous population, and there are also dynamic changes in microbes in the vagina that occur with changes in disease severity, and the flora was involved in the development of cervical cancer. The prediction models constructed based on the two ecologically distinct species all had good diagnostic value for cervical cancer.

821. Dynamic changes of vaginal flora during cervical carcinogenesis and clinical potential of vaginal and gut microbes as diagnostic tools for cervical cancer

Junnan Xu、mengzhen Han、Tao Sun

Liaoning Cancer Hospital Institute

Objective: To investigate the dynamic changes of vaginal flora during cervical carcinogenesis and the value of cervical cancer-related vaginal and gut microbial markers as an adjunctive diagnostic tool.

Methods: We studied 416 public data samples of 16s rRNA from female vagina and 116 public data samples of 16s rRNA from female gut. The vaginal group was divided into Normal (n=180), cervical intraepithelial neoplasia (CINs) group (n=152) and Cervical_cancer group (n=84) according to severity. The gut group was divided into Normal (n=51), Cervical_cancer group (n=65). Reads were processed using vsearch, alpha diversity was determined by Chao1, Shannon and Simpson indices, beta diversity was assessed by principal-coordinate analysis (PCoA) based on weighted Unifrac distances and permutational multivariate analysis of variance (PERMANOVA) analysis based on bray-curtis distances. Microbial communities differences between groups were analyzed using Linear discriminant analysis (LDA) effect size (LEfSe), aiming to find biomarkers. Finally, a random forest model was constructed based on the results of

ASVs and diversity analysis, combined with clinical data, and the model was evaluated to select the optimal prediction model.

Results: The structure of vaginal and gut microbial composition was significantly altered in patients with cervical cancer compared to the non-cancerous population. The increase in vaginal microbial diversity and abundance was positively correlated with disease severity and was accompanied by a decrease in commensal flora such as Lactobacillus spp. and an increase in the abundance of pathogenic bacteria such as Gardnerella spp. The diversity and abundance of gut microbes in patients with cervical cancer decreased, and the microbiological composition also changed significantly, including the enrichment of Bacteroides spp. and Prevotella spp. and the decrease of abundance of Faecalibacterium spp. and Roseburia spp. Overall, cervical carcinogenesis leads to microbial changes in both ecological niches that are significantly different from the non-cancerous population. To determine the optimal microbiota profile for noninvasive diagnostic purposes, we achieved high accuracy in the diagnosis of cervical cancer in a predictive model based on biomarkers obtained from differential genera in both ecological sites (vaginal model AUC= 91.58%; gut model AUC= 99.95%).

Conclusion: Significant differences in vaginal and gut microbes were identified in patients with cervical cancer compared to the non-cancerous population, and there are also dynamic changes in microbes in the vagina that occur with changes in disease severity, and the flora was involved in the development of cervical cancer. The prediction models constructed based on the two ecologically distinct species all had good diagnostic value for cervical cancer.

822. The peripheral blood CD4+ T cells/platelets can be used as indicator for prognosis of patients with metastatic/recurrent breast cancer

Xiaorui Li[1]、Yiwen Ma[1]、Shisheng Wang[2]、Tao Sun[1]

1. liaoning cancer hospital

2. 大连理工大学

Objective： To accurately predict the prognosis of breast cancer patients, the relationship between T cell subsets ($CD4^+$T cells, $CD8^+$T cells) , platelet counts and the median progressive free survival (mPFS), median overall survival (mOS) in patients with metastatic/recurrent breast cancer was investigated.

Methods： The first-line chemotherapy of 312 patients with metastatic and recurrent breast cancer was registered in this study. Meanwhile, the number of peripheral blood T cells, $CD4^+$T cells, $CD8^+$T cells, and the number of platelets were measured by flow cytometry. And the patients were followed up for 5 years to explore the relationship between T cells and their subgroups and the prognosis of metastatic breast cancer.

Results： The results suggested that the mPFS and mOS in patients with metastatic and recurrent breast cancer were correlated with the number of $CD4^+$ T cells/platelets, T cells and $CD4^+$ T cells in the peripheral blood ($p<0.05$); the mPFS and mOS was not related to the changes in $CD8^+$T ($P>0.05$).

Conclusion： In conclusion, the peripheral blood $CD4^+$ T cells/platelets, the number of T cells and the number of $CD4^+$ T in patients with metastatic and recurrent breast cancer can be used as indicators for judging the prognosis of patients and provide a basis for clinical diagnosis and treatment.

823. The Oleanolic Acid Derivative ZQL-3d Exerts Anticancer Effects via miR-221-3p/ASPP2 and Modulates Trastuzumab Resistance in Breast Cancer

Xiaorui Li[1]、Yiwen Ma[1]、Tao Sun[1]、Shisheng Wang[2]

1. liaoning cancer hospital

2. 大连理工大学

Objective： With the application of targeted drugs, survival and prognosis of HER2-positive breast cancer patients have improved significantly, but single-target small-molecule kinase inhibitors have developed resistance during clinical application due to mutations in residues at the target protein binding site. Therefore, the development of novel multi-target inhibitors that can overcome tumor resistance is an urgent problem in the current antitumor drug research. In recent years, oleanolic acid (OA) and its derivatives have attracted much attention because of their anti-tumor, anti-inflammatory, antiviral, anti-infective, immunomodulatory and other biological activities. In this study, we investigated the role of a novel OA derivative ZQL-3d in breast cancer and its relationship with trastuzumab resistance and its molecular mechanism.

Methods： The anticancer effect of ZQL-3d was detected by CCK8, cell cloning assay, flow cytometry, transwell, and scratch assay, and the expression levels of cell function-related pathway indicators were detected by qPCR and Western blotting and other molecular biology techniques. The micro RNA indicator miR-221-3p and downstream target ASPP2 related to drug resistance in HER2-positive breast cancer were predicted and screened by bioinformatics, and the correlation was verified by dual luciferase reporter gene assay. To investigate the overcoming effect of ZQL-3d on trastuzumab resistance in JIMT-1 and the changes of related pathway indicators when transfected with overexpression and silencing of miR-221-3p and ASPP2, respectively.

Results： ZQL-3d was able to exert anticancer effects in breast cancer cells of different molecular fractions, especially in JIMT-1, where ZQL-3d combined with trastuzumab showed significantly superior antitumor effects than trastuzumab alone. The miR-221-3p level was down-regulated after incubation of ZQL-3d in JIMT-1. JIMT-1 resistance to trastuzumab was alleviated after constructing a silent miR-221-3p model, and knockdown of ASPP2 restored resistance. In the

overexpression miR-221-3p model， SK-BR-3 appeared resistant to trastuzumab.Meanwhile, overexpression of ASPP2 could overcame the resistance.

Conclusion： The novel OA derivative (ZQL-3d) affects the apoptotic process through miR-221-3p regulation of ASPP2 to exert oncogenic effects and modulates the resistance to trastuzumab in HER2-positive breast cancer.

824. Necroptosis-related lncRNAs and Hepatocellular Carcinoma Undoubtedly Secret

Keran Sun[1]、Xiaobing Chen[1]、Jingyuan Ning[2]、Lin Wei[2]

1. Affiliated Tumor Hospital of Zhengzhou University

2. 河北医科大学

Background: The current study demonstrates that necroptosis is an important mechanism of carcinogenesis. However, the predictive value of necroptosis-associated long non-coding RNAs (LncRNAs) in hepatocellular carcinoma has not been investigated and demonstrated. The purpose of this study is to apply necroptosis-related lncRNAs to construct a predictive signature to predict the prognosis of hepatocellular carcinoma patients.

Methods: The clinical and RNA-seq data were downloaded using The Cancer Genome Atlas (TCGA) database, and necroptosis-related Genes were screened out. Univariate and multivariate COX analysis was used to screen out suitable necroptosis-related lncRNAs, and then predictive signature was constructed. The TCGA data were randomly divided into high- and low-risk groups, and the Kaplan-Meier method was used to analyze the overall survival (OS) of the two groups to verify the predictive signature. Gene set enrichment analysis (GSEA) was used to explore functional differences between high- and low-risk groups. Finally, a prognostic correlation model for predicting DFS in hepatocellular carcinoma was constructed and validated.

Results: We had screened out 9 necroptosis-related lncRNAs (BACE1-AS, LINC01188, LUCAT1, PI3KCD-AS2, Z83851.1, AC009283.1, AC012360.2, AC015908.3, AC103760.1), which were used to construct a predictive signature, and draw the ROC curve by the high- and low-risk group. It was found that the AUC value of risk score was 0.874, and the AUC values of 1-,3-,and

5-years were 0.8, 0.759, 0.787. The TCGA data were randomly divided into two cohorts. In two cohorts, The OS of the high-risk groups were significantly lower than that of the low-risk groups, and the AUC of the ROC curves of the two cohorts were 0.851, 0.804, 0.802 and 0.735, 0.716, 0.76 at 1-, 3-, and 5-years. The GSEA study found that the high-risk groups had cell cycle passway, complement and coagulation cascades passway, drug metabolism cytochrome p450 passway, metabolism of xenobiotics by cytochrome p450 passway, oocyte meiosis passway, peroxisome passway, fatty acid beta oxidation, azurophil granule, aromatase activity and purine metabolism passway significant enrichment. After quantifying immune cell subsets and related functions, it was found that the infiltration of active dendritic cells (aDCs), macrophages, mast cells, natural killer cells (NK), T regulatory cells (Tregs) were significantly different, and the expressions of immune checkpoints CD86, LAIR1, CTLA4, VTCN1, TNFRSF18, CD80, CD276, HHLA2, TNFSF4, TNFRSF8, TNFRSF4, TNFRSF9, LGALS9, HAVCR2 and TNFSF15 were also significantly different.

Conclusion: This predictive signature can accurately predict the prognosis of hepatocellular carcinoma patients and provide guidance for the clinical treatment of hepatocellular carcinoma patients.

825. Prognostic models for stomach adenocarcinoma patients based on hypoxia related long non code RNAs

Lina Wen[1]、Zongqiang Han[2]

1. 北京世纪坛医院

2. Beijing Xiaotangshan Hospital

Objective: Hypoxia plays an important role in the progression of gastric cancer, but its related biomarkers are not very clear. The objective of this study is to discover novel long non code RNA (lncRNA) biomarkers related to hypoxia and construct prognostic models of stomach adenocarcinoma (STAD) respectively.

Methods: Transcriptome datasets of STAD in The Cancer Genome Atlas (TCGA) database were downloaded. Hypxia genes were obtained from the hallmark xenobiotic metabolism set of

Molecular Signatures Database (MSigDB) database, and the differential lncRNA were acquired and analyzed for functional enrichment analysis by R software and . The lncRNA prognostic model was constructed by Cox regression analysis, and evaluated by Kaplan-Meier survival curve, risk curve, independent prognostic analysis, and receiver operating characteristic (ROC) curves. The clinical correlation analyses were performed and the nomograms of two prognostic models were conducted to predict outcome of STAD. Functional annotation of prognostic lncRNAs were explored by gene set enrichment analysis (GSEA).

Results: 31 differential lncRNAs were distinguished by STAD datasets in TCGA, but only 15 lncRNAs were identified as prognostic biomarkers by optimization, based on which the prognostic modes were constructed. The lncRNA model had high reliability for predicting prognosis of STAD. Clinical correlation analysis indicated that lncRNA was in the correlation with clinicopathological characteristics. The prognostic lncRNAs were mainly enriched in neuroactive ligand-receptor interaction pathway.

Conclusion: Hypxia related lncRNA prognostic model has a good evaluation effect on the prognosis of STAD patients.

826. Association of Genetic Variants of the Glycogen Metabolism Pathway with Risk of HBV-Related Hepatocellular Carcinoma

Yang Zuo[1]、Yingchun Liu[1]、Guanqiao Jin[1]、Xueyan Wei[2]、Shicheng Zhan[2]、Junjie Wei[2]、Hongping Yu[1]

1. The Guangxi Medical University Cancer Hospital

2. 广西医科大学公共卫生学院

Objective: Glycogen, a vital storage form of glucose and energy supply in cells, has been proved to be present in various cancer cells. Previous studies showed that glycogen could be consumed to sustain cancer cell growth and metastases regularly but accumulated as a deposit source of energy to survive under adverse conditions. This indicates that the level of glycogen metabolism might affect the occurrence of tumors. Glycogen metabolism plays an important role in the proliferation

and migration of hepatocellular carcinoma (HCC ） cells. Both genetic factors and microenvironmental factors could regulate the level of glycogen metabolism. In the present study, we investigated the association between variants of glycogen metabolism-related genes and the risk of HBV-related HCC.

Methods: Totally 2,482 HBV-related HCC cases and 2,707 cancer-free controls with positive HBV in 3 datasets (Guangxi 1 dataset, 1,036 cases/1,215controls, Guangxi 2 dataset, 966 cases /1,008 control, and Jiangsu dataset, 480cases/ 484control) were included in this case-control study. DNAs extracted from the whole blood of the included patients were collected for whole genome amplification and sequencing and analyzed for the occurrence of single nucleotide polymorphisms (SNPs). Candidate genes were selected in the glycogen metabolism pathway with the keyword "glycogen" from Gene Set Enrichment Analysis (GSEA) database. SNPs were selected if (a) Genotype call rate>95%; (b) minor allele frequency (MAF) ≥5%; (c) Hardy–Weinberg equilibrium (HWE) $\geq 1\times10^{-5}$. An additive logistic regression model adjusted by age, sex, and principal component analysis (PCA) was performed to assess the effects of SNPs on HCC risk. SNPs were discovered from Guangxi data 1 and Guangxi data 2, and a meta-analysis was further conducted to merge the genetic effect of the SNPs discovered on HCC risk by combining the Guangxi 1 and Guangxi 2 datasets. A random-effects model was used if the Cochrans Q test $P \leq 0.1$ or $I^2 > 50\%$; otherwise, a fixed-effects model was used. Then, we use the Jiangsu dataset as external validation. The odds ratio (OR), 95% confidence interval (CI), and P-value of 3 datasets were respectively calculated. Linkage disequilibrium (LD) analysis was performed to evaluate the independence of the SNPs with an r^2 threshold of 0.8.

Results: Forty-six genes from 4 glycogen metabolism-related datasets were selected as candidate genes. After adjusting by age, sex, and PCA, we identified 508 and 205 SNPs from Guangxi 1 and Guangxi 2 datasets, respectively. The meta-analysis combined the Guangxi 1 and Guangxi 2 datasets showed that 5 SNPs (rs7079157 T>C, rs10998747 A>G, rs12359036 A>G, rs7917338 A>G, and rs4543208 G>A) in 2 genes (*HK1* and *PPP2R2C*) were significantly associated with HCC risk. After an external validation by the Jiangsu dataset was performed, 4 SNPs (rs7079157, rs10998747, rs12359036, and rs7917338) in the *HK1* gene were identified, and all of the variant alleles in 4 SNPs were associated with decreased risk of HCC (rs7079157 T>C, $OR_{Guangxi\ 1}$= 0.74, 95% CI $_{Guangxi\ 1}$= 0.60~0.91, $P_{Guangxi\ 1} = 4\times10^{-3}$, $OR_{Guangxi\ 2}$= 0.79, 95% CI $_{Guangxi\ 2}$=

0.62~1.00, $P_{\text{Guangxi 2}} = 4.9\times10^{-2}$, $OR_{\text{Jiangsu}} = 0.74$, 95% $CI_{\text{Jiangsu}} = 0.57\sim0.97$, $P_{\text{Jiangsu}} = 3.1\times10^{-2}$; rs10998747 A>G, $OR_{\text{Guangxi 1}} = 0.74$, 95% $CI_{\text{Guangxi 1}} = 0.60\sim0.91$, $P_{\text{Guangxi 1}} = 4\times10^{-3}$, $OR_{\text{Guangxi 2}} = 0.79$, 95% $CI_{\text{Guangxi 2}} = 0.62\sim1.00$, $P_{\text{Guangxi 2}} = 4.9\times10^{-2}$, $OR_{\text{Jiangsu}} = 0.75$, 95% $CI_{\text{Jiangsu}} = 0.57\sim0.97$, $P_{\text{Jiangsu}} = 3.5\times10^{-2}$; rs12359036 A>G, $OR_{\text{Guangxi 1}} = 0.75$, 95% $CI_{\text{Guangxi 1}} = 0.61\sim0.92$, $P_{\text{Guangxi 1}} = 6\times10^{-3}$, $OR_{\text{Guangxi 2}} = 0.79$, 95% $CI_{\text{Guangxi 2}} = 0.62\sim1.00$, $P_{\text{Guangxi 2}} = 4.9\times10^{-2}$, $OR_{\text{Jiangsu}} = 0.75$, 95% $CI_{\text{Jiangsu}} = 0.57\sim0.97$, $P_{\text{Jiangsu}} = 3.5\times10^{-2}$;rs7917338 A>G, $OR_{\text{Guangxi 1}} = 0.75$, 95% $CI_{\text{Guangxi 1}} = 0.61\sim0.92$, $P_{\text{Guangxi 1}} = 7\times10^{-3}$, $OR_{\text{Guangxi 2}} = 0.78$, 95% $CI_{\text{Guangxi 2}} = 0.62\sim0.99$, $P_{\text{Guangxi 2}} = 4.4\times10^{-2}$, $OR_{\text{Jiangsu}} = 0.75$, 95% $CI_{\text{Jiangsu}} = 0.57\sim0.97$, $P_{\text{Jiangsu}} = 3.5\times10^{-2}$). The LD analysis showed that the 4 SNPs were highly linkage（r^2 0.94~0.98）.

Conclusion: SNPs (rs7079157, rs10998747, rs12359036, and rs7917338) identified in the *HK1* gene potentially might be a biomarker in risk prediction models for HCC and will decrease the risk.

827. Performance of A PLK1-Based Immune Risk Model for Prognosis and Response Prediction of Breast Cancer

Zhaolei Cui

Fujian Cancer Hospital

Objective: Polo-like kinase 1 (PLK1) belongs to a family of serine/threonine-protein kinases and acts as a powerful oncogene in tumor occurrence and development. We aimed to assess potential correlations between PLK1 expression and immune infiltration in BRCA and construct a PLK1-based immune risk model applicable for prognosis and response prediction.

Methods: We collected gene expression data of PLK1 in BRCA patients from TCGA. Associations of PLK1 expression with immune cell infiltration and immunomodulators were critically analyzed. A prognostic risk model based on seven genes for PLK1-related immunomodulators was established, and a nomogram was depicted for survival prediction.

Results: PLK1 expression was significantly associated with BRCA prognosis, clinical stage progression, and tumor classification. The PLK1 gene was significantly enriched in T cell and B cell receptors, and molecules of the chemokine signaling pathway. Specifically, PLK1 expression

was positively correlated with the degree of activated CD8+T cell, regulatory T cell (Tregs), and negatively correlated with M2 macrophage infiltration. The seven-gene-based risk model could serve as an independent prognostic factor of BRCA. The risk model was markedly correlated with PD-1/PD-L1 (both $P<0.001$) immune checkpoints expression and tumor mutation burden (TMB). Patients at high and low risk of BRCA identified by the risk model revealed different responses to anti-PD-1 and/or anti-CTLA4 therapy, as well as common chemotherapy drugs like cisplatin, paclitaxel, and gemcitabine.

Conclusion This PLK1-based immune risk model can effectively predict the prognosis and tumor progression of BRCA, identify gene mutations, and assess patient benefits from immunotherapy and chemotherapy regimens.

828. Diagnostic performance and efficacy evaluation of NSE and CA125 in sarcomas

Limei Min、Yuchen Ge、Hanxi Zhang、Wu Sun、Siyi Tan、Luxin Xue、Qin Wang、Zhijun Jia、Jie Shen、Baorui Liu、Xiaolu Wang、Rutian Li

The Comprehensive Cancer Center of Drum Tower Hospital, Medical School of Nanjing University & Clinical Cancer Institute of Nanjing University.

Objective: Soft tissue sarcomas(STSs) and bone sarcomas(BSs) are described as diseases with many classifications, complex conditions, and usually delayed diagnosis. There lacks a simple and sensitive methods for disease monitoring of sarcomas clinically. This study examined whether NSE and CA125 are available markers for the diagnosis and efficacy evaluation of sarcomas.

Methods: 110 patients with sarcomas were enrolled, and 60 healthy people were selected as controls. We collected serum NSE and CA125 levels at diagnosis, recurrence, during-treatment and post-treatment to analyze their values of diagnosis and therapeutic assessment.

Results: Elevated serum NSE at diagnosis suggested the possibility of STSs (AUC=0.513), while elevated serum CA125 was correlated with STSs(AUC=0.589) and BSs(AUC=0.602). The sensitivity and specificity of NSE for STSs were 46.25% and 63.33%, respectively. The sensitivity of CA125 for STSs and BSs were both 95.0%, though its specificity of both of them

were low(20.00% and 11.11%). During treatment of advanced sarcomas, the change of NSE was significantly correlated with the effectiveness of treatment(*P*=0.007 for SD, *P*=0.006 for PD). However, CA125 was not specific for the treatment evaluation of sarcomas(*P*=0.070 for SD, *P*=0.071 for PD).

Conclusion: NSE and CA125 can be used as potential markers to assist in diagnosing sarcomas. NSE is a promising marker for diseases monitoring of sarcomas.

829. 人类组蛋白修饰数据库 2.0

王洪利

哈尔滨工业大学

Objective: we developed HHMD version2.0 to provide more comprehensive information and reveal the regulatory functions and disease treatment targets of HMs.

Methods: We use Mysql to manage all analysis results and sample information. The web interface is implemented using a website based on the Struts2 web framework .

Results: HHMD version2.0 integrated 333 ChIP-seq datasets of 52 types of HMs in tissue/cell lines.We manually collected 1375 relationship information of 17 types of HM-regulated genes in 30 human disease states from the literature. HHMD version2.0 provides two self-developed online tools, HM-Gene-Net and HM_Disease_Diff. All HM data were visualized on the genome scale and integrated with Hi-C and ATAC-seq data. In addition, HMs enriched transcription factors or drug targets were also recorded.

Conclusion: The HHMD version2.0 is the most comprehensive database containing information on human histone modifications to date, and it provides multidimensional data support for functional studies of histone modifications. It will also play an active role in studying the role of histone modifications in disease pathogenesis, drug therapy, and developmental regulation in tissue and cell lines.

830. Prognostic of gastric cancer based on DNA methylation-driven EMT genes

Te Ma

Harbin Institute of Technology

Objective: Gastric cancer (GC) is one of the most common cancers, with one million new cases and approximately 769,000 deaths in 2020 (equating to one in every 13 deaths globally). Epithelial-mesenchymal transition, as a cell-biological program, plays an important role in gastric carcinogenesis. And the EMT status of cells is closely related to DNA methylation.We screened out methylation-driven EMT genes based on data from TCGA, GEO and dbEMT. Then, according to univariable and multivariable Cox regression analysis, the prognosis-related genes were screened, and finally a risk model for evaluating the prognosis of gastric cancer patients was constructed. Because of the molecular similarities between colorectal and gastric cancers, the model also extends well to colorectal cancer and rectal cancer

Methods: The genes affecting the prognosis of gastric cancer were derived from two gene sets, the DNA differentially methylated gene set and the EMT-related gene set from the dbEMT database. Consensus clustering was performed on the methylation data of the two gene sets separately to divide the subgroups. The QDMR tool was then used to filter specific genes for each subgroup. The integration of specific genes from two sources are the DNA methylation-driven EMT genes. This gene set was then used to perform analysis related to gastric cancer prognosis, including the establishment of prognostic models and validation of additional data.

Results: Consistent clustering of cancer samples from gastric cancer DNA methylation data resulted in 4 gastric cancer subgroups. Similarly, four subgroups were obtained using the methylation data of the EMT gene. The specific genes of each subgroup were extracted by QDMR, and the subgroup 3 of the two was found to be the same subgroup.A univariate cox proportional hazards regression model was used to screen 43 DNAmethylation-driven EMT genes and some clinical information. Factors that were significantly associated with patient prognosis were used to construct a multivariate cox proportional hazards regression model. High and low risk groups were divided according to the final score of the model. Significant differences in prognosis can be

found between high and low risk groups.Due to the molecular similarities among gastrointestinal cancers, this gastric cancer prognostic model is also instructive in the prognosis of patients with colon and rectal cancers.

Conclusion: A prognostic model of gastric cancer was established through DNA methylation-driven EMT genes. The model can divide gastric cancer patients into high and low risk groups, which has a good guiding significance for prognosis. In addition, this model also has good extended applications in colon cancer and rectal cancer.

831. Multi-Omics Integration Collective Variational Autoencoder for cancer-drug Sensitivity Prediction

Cong Wang、yan zhang

Harbin Institute of Technology

Objective: In this work, we proposed a new method MOICVAE (Multi-Omics Integration Collective Variational Autoencoder) based on deep learning to improve the drug sensitivity prediction on GDSC and CCLE datasets. As for the omics data of genomics and transcriptomics, we presented an encoder-decoder method to learn a low dimensional encoding for each cell-line. Through cell-line auxiliary information, the adopted collective variational autoencoder have an excellent performance to classify drug's sensitivities.

Methods: we introduced a workflow called MOICVAE, a novel approach that used multi-omics data to predict cancer drug sensitivity based on autoencoder. Firstly, we collected two kinds of omics data including genomics and transcriptomics from GDSC and CCLE database. After data interpolation and filtration, we acquired three feature matrices including gene expression, CNV, SNP separately. Then, we calculated the corresponding omics similarity matrices and the dimension for each matrix was . MOICVAE took three similarity matrices as input. Through a well-designed multimodal autoencoder architecture, we could get a fusion low dimension vector to represent each cell line. The second part of MOICVAE was a collective variational autoencoder. It included two deep neural networks that used to predict the drug sensitivity for a given cell-line, which was represented by its multi-omics profile. Although drug sensitivity and cell-line data were

different sources of information, they contained rich information associating with drug. Hence, we took sensitivity from each drug and cell-line fusion information as the input for VAE. To ensure samples from both sources of information had the same dimensionality (number of drugs). We could feed sensitivities and cell-line information into the same inference network and generation network. Like pretraining strategy, training a VAE through side information could improve neural networks robustness. Our experiments indicated that the proposed model MOICVAE achieved state-of-the-art performance for drug-cell line sensitivity prediction.

Results: In this study, we presented a novel method of Multi-Omics Integration Collective Variational Autoencoder (MOICVAE) for drug cell-line sensitivities' prediction which was able to acquire latent low-dimensional vector by fusing different omics data. Through compared to SNF, the multi-model autoencoder got an excellent outcome on silhouette score nearly 0.2 improved on both GDSC and CCLE datasets.For the second step, we trained a VAE through feeding it with omics information just as a pre-training operation, which had a key significance for developing a strong neural network. By 10-fold cross validation, MOICVAE had compared a lot of classification indicator with many other methods on GDSC and CCLE datasets. We achieved the highest auc of 0.771 on GDSC and highest precision of 0.694 on CCLE.

Conclusion: MOICVAE had advantage to fuse multi-omics features and achieved state-of-the-art performance for drug sensitivity classification. However, sufficient training data is beneficial to the superior performance of the deep learning model. If more data on the CCLE database, our model could achieve superior performance comparable to those on GDSC.In conclusion, our study indicates that our models MOICVAE have a huge potential in drug response prediction and multi-omics fusion would be a potential biomarker for cellline-drug response.

832. Acquired EGFR exon 19 deletion as a resistance mechanism to BRAF/MRK inhibition in BRAF V600E-mutant NSCLC

fang wu、yuxuan liu、yue zeng、yurong peng、yue pan、yizheng li

The Second Xiangya Hospital of Central South University

Objective： BRAF mutation, commonly BRAFV600E, occurs in approximately 2% of non-small cell lung cancer (NSCLC) patients. FDA has approved dabrafenib plus trametinib as the standard therapy for BRAFV600E-mutant NSCLC. The objective response rate is 64% with a median progression-free survival of about 10 months. Despite great anti-tumor activities of BRAF/MRK inhibitors, the resistance mechanism is not fully understood. Here, we reported a NSCLC patient whose acquired resistance to BRAF/MRK inhibition was caused by EGFR exon 19 deletion. We expect that this will help elucidate the mechanisms of EGFR inhibitor resistance and lead to better treatment of patients.

Methods: We followed up a 57 year old smoking male who was diagnosed as lung adenocarcinoma with metastases to mediastinal and supraclavicular lymph nodes in March 2018 (cT1bN3M0, stage IIIB).

Results： Next-generation sequencing (NGS) (Nanjing Geneseeq Technology Inc, Jiangsu, China) revealed an EGFR exon 19 deletion and BRAFV600E mutation in plasma at first. Finally, the patient died of diffuse intravascular coagulation (DIC). Acquired EGFR T790M mutation was also detected in plasma by NGS. In addition, the EGFR exon 19 deletion and the BRAFV600E mutation could still be observed.

Conclusion： The mechanisms of resistance in BRAFV600E-positive NSCLC treated with the combination of BRAF and MRK inhibitors mainly included alterations in the mitogen-activated protein kinase (MAPK) pathway (e.g., KRASG12V, KRASQ61R, NRASQ61K，NRASQ61R, and MEK1K57N) and phosphoinositide-3-kinase (PI3K) pathway (PI3KH1047R). Moreover, autocrine activation of the fibroblast growth factor receptor (FGFR) pathway caused by FGF1 upregulation was also an in vitro mechanism of adaptive resistance. So far, no EGFR mutation has been reported in NSCLC with acquired resistance to the combined BRAF and MRK inhibition. To

our knowledge, we reported for the first time EGFR exon 19 deletion as an acquired resistance mechanism to BRAF/MRK inhibition in NSCLC. Exon 19 deletion in the EGFR kinase domain leaded to overexpression of EGFR and triggered activation of the downstream signaling pathways including RAS/MAPK and PI3K, which promoted tumor proliferation in a BRAFV600E-positive patient resistant to BRAF/MEK inhibition.Our case showed triple BRAF/MRK/EGFR inhibition is an efficacious therapeutic strategy for patients with acquired EGFR exon 19 deletion after progression on BRAF/MRK inhibition. Moreover, the patient acquired a secondary T790M mutation after the triple-combination therapy. Although the third-generation EGFR TKI osimertinib may have a robust efficacy as third-line therapy, it was not timely administered due to rapid deterioration to death. A double-blind, phase 3 trial showed that osimertinib facilitated a longer PFS and had a similar safety profile when compared to the current standard first-line treatment in EGFR-mutant NSCLC. Therefore, if the patient had received osimertinib treatment rather than the first-generation EGFR TKI icotinib, he might have achieved better survival benefits. Notably, although the primary lung lesion was well controlled, metastases inevitably developed elsewhere, eventually making the patient dying of DIC. Therefore, more attention should be paid to the metastasis and targeted treatment should be carried out as soon as possible. In addition, ambulatory monitoring of gene mutation status during treatment could more effectively explore the mechanism of resistance and provide more targeted therapy opportunities for patients that develop drug resistance. For patients with advanced lung cancer, especially those who can not do tissue biopsy due to poor physical condition, liquid biopsy plays an important role in diagnosis.

833. Overexpression of ErbB3 promotes metastasis of ErbB2-positive breast cancer and its underlying molecular mechanisms

Ruxue Jia、Zhuolin Li、Yating Wu、Huimin Niu、Xiaofeng Lai、Meng Zhao、Shenghang Zhang、Shuiliang Wang

Affiliated Dongfang Hospital (the 900th Hospital) of School of Medicine, Xiamen University

Objective： ErbB2-positive breast cancer is a type of breast cancer with higher malignancy. However, our understanding of the molecular mechanism of breast cancer metastasis is still very limited. Here, we mainly investigate the role of ErbB3 overexpression in the metastasis of ErbB2-positive breast cancer and other malignant biological phenotypes.

Methods： ErbB3 overexpressing ErbB2-positive breast cancer cell lines were constructed by lentivirus transduction. MTS and cell cloning assay were used to detect the effect of ErbB3 overexpression on the proliferation of ErbB2-positive breast cancer. The effect of ErbB3 overexpression on metastasis and invasive growth of ErbB2-positive breast cancer was detected by transwell and transwell invasion assay. Western blot analyses were performed to determine the expression and activation of proteins. qRT-PCR was carried out to analyze the mRNAs and miRNAs expression levels. Clinical samples of ErbB2-positive breast cancer were analyzed by immunohistochemical assay.

Results： ErbB3 overexpression not only significantly promoted the growth and proliferation of ErbB2 positive breast cancer, but also significantly enhanced its invasion and migration. The preliminary mechanism investigation showed that ErbB3 overexpression could not only significantly induce the up-regulation of transcription factors such as ZEB1 in ErbB2-positive breast cancer cells to promote the EMT phenotype, but also significantly promote the up-regulation of MMP2 and MMP9 expressions with activation of downstream Akt and MAPK signalling pathways at the same time. In addition, RT-qPCR analysis also confirmed that ErbB3 overexpression down-regulated the expression of miR-203 and miR-542-3p, both of which may target ZEB1 and other EMT-regulating transcription factors. Analysis of clinical samples

preliminarily suggested that ErbB3 overexpression may be associated with clinical metastasis in patients with ErbB2-positive breast cancer.

Conclusion： Our data strongly suggest that ErbB3 overexpression can significantly enhance ErbB2 positive breast cancer metastasis and other related malignant biological phenotypes through activation of downstream signalings of ErbB2/ErbB3

834. Mesenchymal stem cell promotes metastasis of bladder cancer with co-expression of ErbB2 and ErbB3 mainly via paracrine of NRG-1

Zhuolin Li、Ruxue Jia、Yating Wu、Huimin Niu、Xiaofeng Lai、Jin Chen、Meng Zhao、Shenghang Zhang、Shuiliang Wang

Affiliated Dongfang Hospital (the 900th Hospital) of School of Medicine, Xiamen University

Objective： Tumor progression towards metastasis is often depicted as a multistage process. Each stage of metastasis is closely related to the genetic and epigenetic changes of tumor cells and the regulation of many factors in the microenvironment. In recent years, studies have shown that mesenchymal stem cells (MSC), as an important cell component of tumor microenvironment, are closely related to tumor metastasis. Our study focused on the role of MSC in the metastasis of bladder cancer with co-expression of ErbB2 and ErbB3 as well as its underlying mechanism.

Methods： ErbB3 overexpression ErbB2-positive bladder cancer cell line was constructed by lentiviral transfection. Transwell migration and invasion assay was used to detect the effect of MSC on the metastasis and invasive growth of ErbB2-positive bladder cancer and its ErbB3 overexpression subline. Western blot assay was used to detect the expression and activation of related proteins after co-culture with MSC. In the animal experiment, the xenograft tumor model of bladder cancer was established by injecting the above two cell lines through the tail vein of nude mice, and the ability of MSC to promote formation of metastatic tumor of ErbB2-positive bladder cancer in vivo was explored by injecting mesenchymal stem cells.

Results： At the cellular level, MSC could promote the metastasis of ErbB2-positive bladder cancer cells and ErbB3 overexpression ErbB2-positive bladder cancer cells, and the promotion

effect was more significant in ErbB3 overexpression cell lines. Mesenchymal stem cells were evidenced to secrete a large amount of NRG-1, a ligand of ErbB3. In addition, Western blot analysis showed that the expression of MMP2 and MMP9 was up-regulated after co-culture with MSC. The results of animal experiment were consistent with that of cell experiment, that is, MSC could promote the formation of metastatic tumor in ErbB2-positive bladder cancer cells in vivo, and this effect was more significant in the model of ErbB3 overexpression.

Conclusion： Our data suggest that MSC can promote the metastasis of bladder cancer with co-expression of ErbB2 and ErbB3, and this effect may be achieved by activating ErbB2/ErbB3 and its downstream signaling pathway via paracrine of NRG-1.

835. Long noncoding RNA lnc-POP1-1 upregulated by VN1R5 promotes cisplatin resistance in head and neck squamous cell carcinoma through interaction with MCM5

Yingying Jiang [1]、Wantao Chen[2]、Jianjun Zhang[2]

1. School of Stomatology, Weifang Medical University

2. 上海交通大学医学院附属第九人民医院

Objective: Cisplatin resistance is a major therapeutic challenge in advanced head and neck squamous cell carcinoma (HNSCC). Here, we aimed to investigate the key signaling pathway for cisplatin resistance in HNSCC cells.

Methods: The abnormally expressed proteins associated with cisplatin resistance were analyzed by Isobaric tags for relative and absolute quantitation (iTRAQ). The downstream genes regulated by Vomeronasal type-1 receptor 5 (VN1R5) were detected with RNA microarray. Luciferase reporter and chromatin immunoprecipitation (ChIP) assays were used to identify the functional transcription factors for lnc-POP1-1 gene promoter. RNA pull-down assays, LC-MS/MS mass spectrometry analysis and RNA immunoprecipitation assays (RIPs) were

performed to identify the RNA binding proteins (RBPs) for lnc-POP1-1. Comet assay and AP Site Counting assay were used to identify the condition of DNA damage.

Results:VN1R5 was identified as a cisplatin resistance-related protein and was highly expressed in cisplatin-resistant HNSCC cells and tissues. The long noncoding RNA (lncRNA) lnc-POP1-1 was confirmed to be a downstream target induced by VN1R5. VN1R5 transcriptionally regulated lnc-POP1-1 expression by activating the specificity protein 1 (Sp1) transcription factor via the cyclic AMP (cAMP)/protein kinase A (PKA) pathway. VN1R5 promoted cisplatin resistance in HNSCC cells in a lnc-POP1-1-dependent manner. Mechanistically, lnc-POP1-1 bound to the Minichromosome Maintenance Deficient 5 (MCM5) protein directly and decelerated MCM5 degradation by inhibiting ubiquitination of the MCM5 protein, which facilitated the repair of DNA damage caused by cisplatin.

Conclusion: In summary, we identified the cisplatin resistance-related protein VN1R5 and its downstream target lnc-POP1-1. Upon upregulation by VN1R5, lnc-POP1-1 promotes DNA repair in HNSCC cells through interaction with MCM5 and deceleration of its degradation.

从发现到临床研究的完整解决方案

——整个组织切片上基于单细胞的空间表型分析

Akoya Biosciences作为全球领先的空间生物公司，提供全面的单细胞成像解决方案，允许研究人员在空间环境背景下对细胞进行表型分析，并可视化它们如何组织和相互作用，以影响疾病进展和对治疗的反应。Akoya所提供的完整连续的空间表型解决方案，通过关键平台：PhenoCycler™，PhenoImager Fusion™及PhenoImage HT™ 服务于跨越发现、转化和临床研究的多样化需求。

探索发现 | **转化医学** | **临床研究**

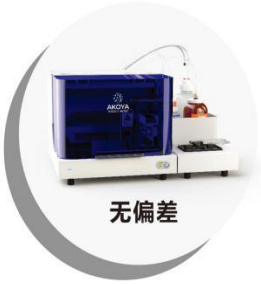

PhenoCycler-Fusion 解决方案
规模化的空间发现
快速全片成像检测 100+ 种生物标志物

PhenoImager 解决方案
规模化的空间特征验证
每周超过 300 张 6 种生物标志物快速全片成像

 # 每个反应运行的标志物数

 # 每天运行的样本数

了解更多，可访问 AKOYABIO.COM
或发邮件至 APACMARKETING@AKOYABIO.COM

仅用于研究，不用于诊断

illumina®

Who we are

Illumina is a leading developer, manufacturer, and marketer of life science tools and integrated systems dedicated to making genomics useful for all. Innovating at the intersection of technology, biology, and health, we are reimagining what's possible for human health and the health of our planet, including how diseases—from cancer to COVID-19—are discovered, detected, diagnosed, and treated. We provide sequencing innovations that are enabling researchers and clinicians to usher in the future of personalized medicine.

Fast facts

Founded in
1998

Number of employees
>9100

Annual revenue (2021)[1]
$4.5B USD

Cumulative sequencing installed base
>20,000

Headquarters
San Diego, California, USA

Countries served
>140

President and CEO
Francis deSouza

Sequencing systems

Next-generation sequencing (NGS) is revolutionizing research, enabling experiments that weren't possible before. Illumina offers a range of innovative NGS platforms that deliver exceptional data quality and accuracy, at a massive scale.

NovaSeq™ X/X Plus | NovaSeq 6000/6000Dx | NextSeq™ 550Dx* | NextSeq 1000/2000

Production-scale systems

MiSeq™ and MiSeqDx* | MiniSeq™ | iSeq™ 100

Benchtop systems

For Research Use Only. Not for use in diagnostic procedures.
*For In Vitro Diagnostic Use. Not available in all regions and countries.

Applications

- Oncology
- Genetic disease
- Infectious disease
- Multiomics
- Drug discovery
- Microbial genomics
- Reproductive health
- Molecular and cell biology
- Agriculture
- Conservation and sustainability

Customers

- Clinics
- Hospitals
- Research labs
- Health care systems
- Academic institutions
- Government agencies
- Pharmaceutical companies

超越单个循环肿瘤细胞（CTC）的循环肿瘤细胞及其血液微环境（CME）全活检

活性肿瘤相关循环稀有细胞（簇）检测（LTCRC）

大多数循环肿瘤细胞（CTC）自然凋亡、休眠及缺氧或在血液中受到血液剪切力损伤、药物及免疫攻击，失去肿瘤细胞生物活性，只有极其稀有的（<0.01%）单个CTC具有治疗抗性和较高的转移潜能，引起远处转移；循环肿瘤细胞与肿瘤相关非肿瘤细胞聚集成簇共同构建有利于生存和转移的血液微环境（CME），促进生存、转移。

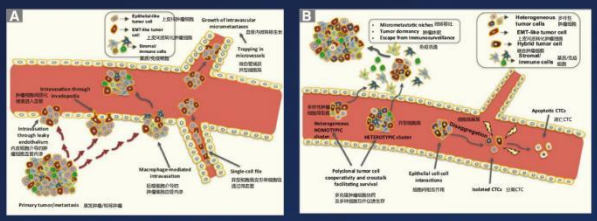

安泰康生物首次创造性提出CTC血液微环境（CME）概念，开发2.5D柔性高密度微孔阵列膜微流场超滤系统（微流控+阵列膜），非依赖、同步、自然、高保真捕获活性循环肿瘤相关稀有细胞，特别是完整细胞簇，支持细胞（簇）计数、分型、表型检测、体外培养、单细胞测序、类器官和动物模型构建，全面、系统、精准揭示肿瘤发生、耐药、转移、免疫逃逸等。

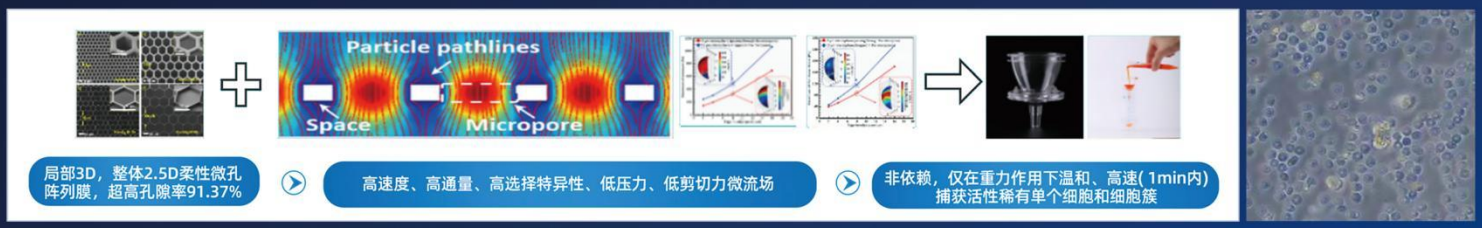

- ★ 不依赖任何化学试剂及抗体，不依赖任何外在驱动动力和设备，仅在重力作用下分离；
- ★ 1分钟高速、高通量、高回收率分离，较高中位值、低检测下限并保持良好的线性和平行性；
- ★ 活细胞无损伤、低损失、高效率捕获，细胞形态、抗原表达、遗传信息、细胞数量高保真度捕获；
- ★ 血液、体液中的肿瘤相关单细胞、细胞簇同步捕获，并保持细胞簇天然微生态环境。

扫码关注

IF+FISH进行单个LCTC和LCEC数量、染色体倍体及肿瘤相关同型细胞簇（CTC-CTC）和异型细胞簇（CTC-WBC）（CTC-CEC）数量、团簇组成和大小可视化同步检测分析。多维度多指标分析，实现肿瘤复发转移、治疗抗性、生存风险量化动态评估及辅助诊断、补存分期，精准分层和患者管理。

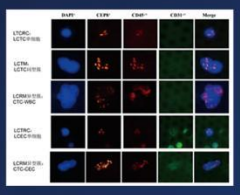

检测项目	LTCRC单细胞							LTCRC细胞簇					
	LCTC单细胞数量(个)				LCEC单细胞数量(个)			LTCRC细胞簇（LCTM）数量（个）			最大细胞簇所含细胞数量(个)或长短径(um)		
	LCTC单细胞	倍体类型			LCEC单细胞	倍体类型							
		三倍体	四倍体	高倍体		三倍体	四倍体	高倍体	LCTM（CTC-CTC）	LCTM（CTC-WBC）	LCTM（CTC-CEC）	LCTM（CTC-CTC）	LCTM（CTC-WBC）	LCTM（CTC-CEC）
	7	2	4	1	11	3	5	3	3	1	3	2	3	5

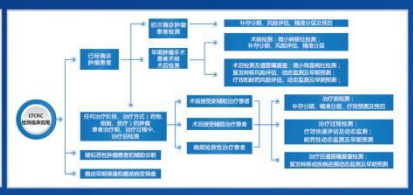

活性肿瘤相关循环稀有细胞（簇）靶分子表达评估（IF）

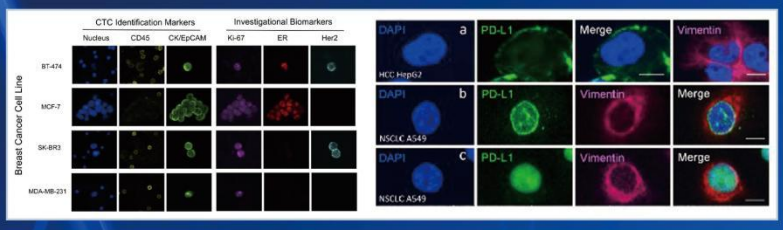

IF/FISH/NGS同步检测活性肿瘤相关循环稀有细胞及细胞簇

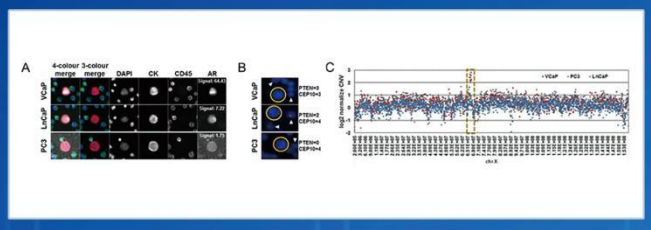

活性肿瘤相关循环稀有细胞（簇）如巨噬细胞、成纤维细胞、中性粒细胞及细胞簇全活检（IF）

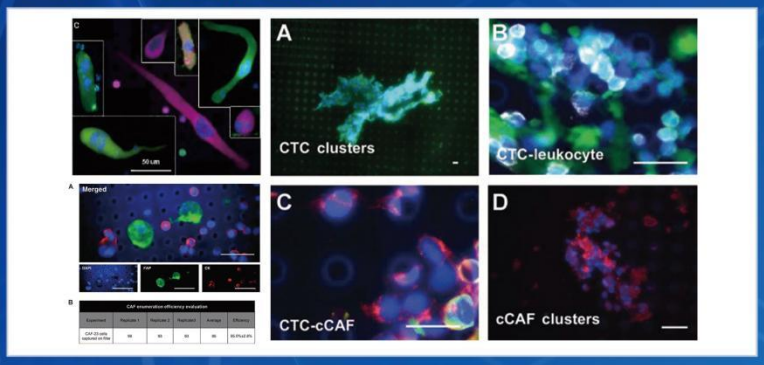

LTCRC体外培养药敏检测

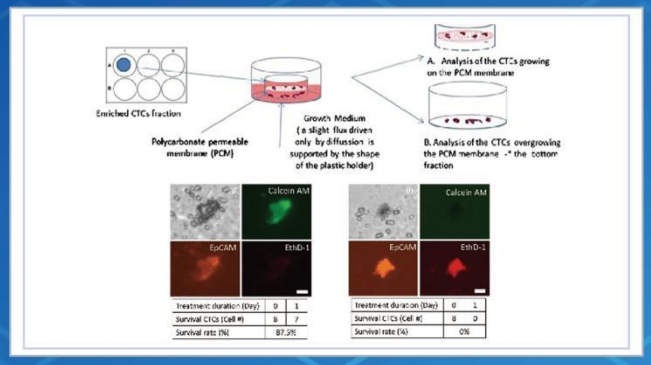

地址：北京市昌平区中关村科技园华通路11号207 咨询电话：13522810102 展位号：B051号 网址：www.anticancerchina.com.

Labway 兰卫医学

股票简称:兰卫医学
股票代码:301060

多组学平台助力肿瘤精准诊疗

服务内容

- 临床样本基础检验
- 临床样本病理服务
- 临床样本多组学分析
- 生物信息学分析
- 科研服务平台
- 模式动物服务平台

肿瘤真实世界研究　多组学大数据分析　肿瘤Biomarker预后研究

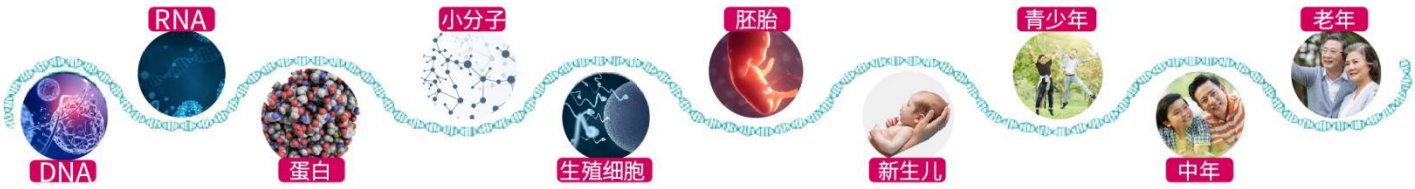

肿瘤多组学分析

基因组测序	转录组测序	表观组测序	三维基因组
WGS/WES	mRNA/miRNA/ IncRNA	WGBS/ChIP	群体Hi-C
突变位点注释 CNV/SV分析 高频基因筛查 驱动/高频突变	变异表达分析 可变剪切分析 富集分析 功能注释	甲基化图谱 组蛋白结合位点 DMR区域分析 甲基化变异分析	染色体互作 染色体顺反式 相互作用

多组学联合分析

www.labway.cn

兰卫医学上海总部地址：上海市长宁区临新路268弄1号楼

客户热线：400-021-9090

新产业生物

- 拥有“免疫磁性微球”专利（ZL2014102326566）并将其作为化学发光系统关键分离材料的公司
- 拥有“人工合成的小分子有机化合物-ABEI”专利（ZL2006100604488）并用其代替传统的酶作为发光标记物的公司
- 获得美国FDA准入的化学发光厂家
- HBV、HCV、HIV拿齐CE list A 认证的化学发光厂家

全面的化学发光项目
已获得注册证156项

Thyroid 甲状腺

TSH	促甲状腺素
TT4	总甲状腺素
TT3	总三碘甲状腺原氨酸
FT4	游离甲状腺素
FT3	游离三碘甲状腺原氨酸
rT$_3$	血清反三碘甲状腺原氨酸
TG	甲状腺球蛋白
Anti-Tg	抗甲状腺球蛋白抗体
TRAb	促甲状腺激素受体抗体
Anti-TM	抗甲状腺微粒体抗体
Anti-TPO	抗甲状腺过氧化物酶抗体
T-Uptake	甲状腺素结合力

Gonad 性腺

T-β-HCG	总β人绒毛膜促性腺激素
FSH	促卵泡生成素
LH	促黄体生成素
PRL	泌乳素
E$_2$	雌二醇
PROG	孕酮
TEST	睾酮
F-T	游离睾酮
FE$_3$	游离雌三醇
AMH	抗缪勒氏管激素
SHBG	性激素结合球蛋白
Androstenedione	雄烯二酮
DHEA-S	硫酸去氢表雄酮
17α-OHP	17α-羟孕酮
• PlGF	胎盘生长因子
• sFlt-1	可溶性fms样酪氨酸激酶-1

Glyco Metabolism 糖代谢

Pro-INS	胰岛素原
INS	胰岛素
C-P	C肽
GAD65	谷氨酸脱羧酶抗体
ICA	抗胰岛细胞抗体
Anti-IA2	抗酪氨酸磷酸酶抗体IgG
IAA	抗胰岛素抗体

Hepatic Fibrosis 肝纤维化

HA	血清透明质酸
PⅢP N-P	三型前胶原N端肽
C Ⅳ	Ⅳ型胶原
LN	层粘连蛋白
CG	甘胆酸
• GP73	高尔基体蛋白73

Drug Monitoring 药物监测

CSA	环孢霉素A
FK506	他克莫司
Digoxin	地高辛

Renal 肾功能

β$_2$-MG	β$_2$微球蛋白
H-ALB	人尿微量白蛋白

Tumor Markers 肿瘤标志物

AFP	甲胎蛋白
CEA	癌胚抗原
CA50	糖类抗原50
CA242	糖类抗原242
CA15-3	糖类抗原15-3
CA19-9	细胞角蛋白19片段
CA72-4	糖类抗原72-4
CA125	糖类抗原125
HE4	人附睾蛋白4
NSE	神经元特异性烯醇化酶
CYFRA21-1	细胞角蛋白19片段
SCCA	鳞状上皮细胞癌抗原
tPSA	总前列腺特异性抗原
fPSA	游离前列腺特异性抗原
PAP	前列腺酸性磷酸酶
ProGRP	胃泌素释放肽前体
PIVKA-□	异常凝血酶原
HER-2	人表皮生长因子受体2
• TPA	组织多肽抗原

Gastric 胃功能

Gastrin-17	胃泌素-17
PG Ⅰ	胃蛋白酶原Ⅰ
PG Ⅱ	胃蛋白酶原 Ⅱ
H.pylori IgG	幽门螺杆菌IgG抗体

Nerve and Brain Injury 神经及脑损伤

NSE	神经元特异性烯醇化酶
S100	S100 蛋白

Inflammation Monitoring 炎症监测

PCT	降钙素原
CRP	C反应蛋白
IL-6	白介素6
SAA	血清淀粉样蛋白A
• TNF-α	α肿瘤坏死因子
• PCT（STAT）	降钙素原（急诊）
• CRP（STAT）	C反应蛋白（急诊）

Bone Metabolism 骨代谢

25-OH VD	25-羟基维生素D
PTH	血清甲状旁腺素
CT	血清降钙素
BGP	骨钙素
P1NP	总Ⅰ型胶原氨基端延长肽
β-CTx	β-胶原特殊序列

Immunoglobulin 免疫球蛋白

IgM	人免疫球蛋白M
IgA	人免疫球蛋白A
IgE	人免疫球蛋白E
IgG	人免疫球蛋白G

Cardiac Markers 心血管及心肌标志物

hs-cTnI	超敏肌钙蛋白I
cTnI	肌钙蛋白I
CK-MB	肌酸激酶同工酶
Myoglobin	肌红蛋白
Lp-PLA2	脂蛋白相关磷脂酶A2
H-FABP	心脏型脂肪酸结合蛋白
NT-proBNP	氨基末端B型利钠肽前体
BNP	B型利钠肽
D-dimer	D-二聚体
MPO	髓过氧化物酶
HCY	同型半胱氨酸
• hs-cTnI（STAT）	超敏肌钙蛋白I（急诊）
• NT-proBNP（STAT）	氨基末端B型利钠肽前体（急诊）
• Myoglobin（STAT）	肌红蛋白（急诊）
• D-dimer（STAT）	D-二聚体（急诊）

Thrombus 血栓

D-dimer	D-二聚体
TAT	凝血酶-抗凝血酶Ⅲ复合物
PIC	纤溶酶-α2纤溶酶抑制剂复合物
tPAIC	组织型纤溶酶原激活剂-抑制剂1复合物
TM	血栓调节蛋白

Hypertension 高血压

Direct Renin	肾素
A Ⅰ	血管紧张素 Ⅰ
A Ⅱ	血管紧张素 Ⅱ
ALD	醛固酮
Cortisol	皮质醇
ACTH	促肾上腺皮质激素

Anemia 贫血

Ferritin	铁蛋白
VB$_{12}$	维生素B$_{12}$
FA	叶酸
EPO	促红细胞生成素

Autoimmune 自免抗体

Anti-CCP	抗环瓜氨酸肽抗体
ANA	抗核抗体
ENA	抗可提取性核抗原(6项)总抗体
Anti-dsDNA IgG	抗双链DNA抗体IgG
Anti-Histones IgG	抗组蛋白抗体IgG
Anti-Rib-P IgG	抗核糖体核蛋白抗体IgG
Anti-Sm/RNPIgG	抗Sm/RNP抗体IgG
Anti-Sm IgG	抗Sm抗体IgG
Anti-SS-A/Ro IgG	抗SS-A/Ro抗体IgG
Anti-SS-B IgG	抗SS-B抗体IgG
Anti-Jo-1 IgG	抗Jo-1抗体IgG
Anti-Scl-70 IgG	抗Scl-70抗体IgG
Anti-Centromeres IgG	抗着丝点抗体IgG
AMA-M2 IgG	抗线粒体M2抗体IgG
Anti-MPO	抗髓过氧化物酶抗体 IgG
• aCL IgG	抗心磷脂抗体IgG
• aCL IgM	抗心磷脂抗体IgM
• β2-GP1 IgG	抗β2糖蛋白1 IgG抗体
• β2-GP1 IgM	抗β2糖蛋白1 IgM抗体

Infectious Disease 传染病

HBsAg	乙型肝炎病毒表面抗原
Anti-HBs	乙型肝炎病毒表面抗体
HBeAg	乙型肝炎病毒e抗原
Anti-HBe	乙型肝炎病毒e抗体
Anti-HBc	乙型肝炎病毒核心抗体
Anti-HBc IgM	乙型肝炎病毒核心抗体IgM
HCVIgG	丙型肝炎病毒IgG抗体
HIV Ab/Ag Combi	人类免疫缺陷病毒抗原和抗体
Syphilis	梅毒螺旋体抗体

Respiratory Infection 呼吸道感染

2019-nCoV IgM	新型冠状病毒2019-nCoV IgM抗体
2019-nCoV IgG	新型冠状病毒2019-nCoV IgG抗体
• MP IgG	肺炎支原体IgG抗体
• MP IgM	肺炎支原体IgM抗体
• CP IgG	肺炎衣原体IgG抗体
• CP IgM	肺炎衣原体IgM抗体
• IAV IgM	甲型流行性感冒病毒IgM抗体
• IBV IgM	乙型流行性感冒病毒IgM抗体
• RSV IgM	呼吸道合胞病毒IgM抗体

TORCH 优生优育

Toxo IgG	弓形虫IgG抗体
Toxo IgM	弓形虫IgM抗体
Rubella IgG	风疹病毒IgG抗体
Rubella IgM	风疹病毒IgM抗体
CMV IgG	巨细胞病毒IgG抗体
CMV IgM	巨细胞病毒IgM抗体
HSV-1/2 IgG	Ⅰ、Ⅱ型单纯疱疹病毒IgG抗体
HSV-2 IgG	Ⅱ型单纯疱疹病毒IgG抗体
HSV-1/2 IgM	Ⅰ、Ⅱ型单纯疱疹病毒IgM抗体
HSV-1 IgG	Ⅰ型单纯疱疹病毒IgG抗体
• HSV-1 IgM	Ⅰ型单纯疱疹病毒IgM抗体
• HSV-2 IgM	Ⅱ型单纯疱疹病毒IgM抗体

Prenatal Screening 产前筛查

AFP	甲胎蛋白
Free-β-HCG	游离绒毛膜促性腺激素β亚单位
PAPP-A	妊娠相关血浆蛋白A
FE$_3$	游离雌三醇

EBV EB病毒

EBV EA IgG	EB病毒早期抗原IgG抗体
EBV EA IgA	EB病毒早期抗原IgA抗体
EBV VCA IgG	EB病毒衣壳抗原IgG抗体
EBV VCA IgM	EB病毒衣壳抗原IgM抗体
EBV VCA IgA	EB病毒衣壳抗原IgA抗体
EBV NA IgG	EB病毒核抗原IgG抗体
• EBV NA IgA	EB病毒核抗原IgA抗体

Growth 生长发育

GH	生长激素
IGF-I	胰岛素样生长因子 Ⅰ
IGFBP-3	胰岛素样生长因子结合蛋白3

• 紧张进产品即将上市

深圳市新产业生物医学工程股份有限公司

地址：深圳市坪山区坑梓街道金沙社区锦绣东路23号新产业生物大厦

邮箱：marketsnibe@snibe.cn

新产业生物公众号

全自动化学发光免疫分析系统 X系列

Snibe Diagnostic 新产业生物

MAGLUMI® X8
超高速 600T/H

MAGLUMI® X6
高速:450T/H

MAGLUMI® X3
中速:200T/H

智慧实验室整体解决方案

新产业-赛默飞 SATLARS®-TCA
全实验室智能化流水线

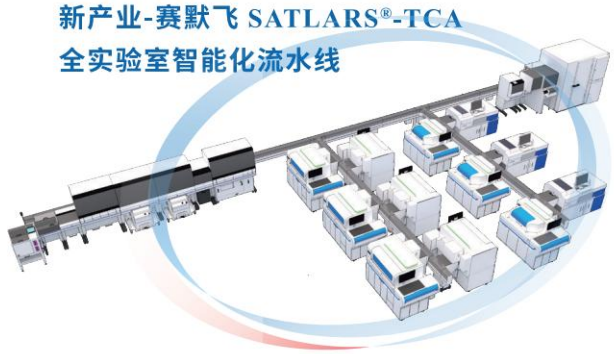

新产业-日立 TS
全实验室智能化流水线

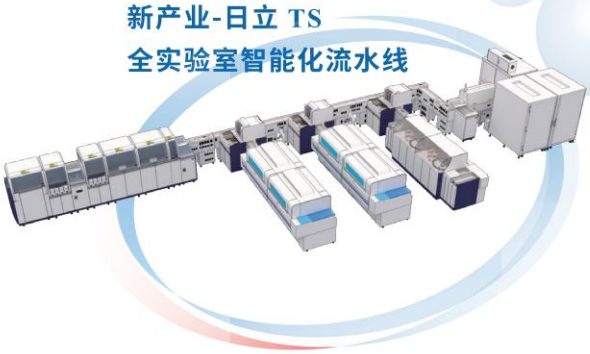

超高速生化免疫流水线SIB

超高速生化免疫流水线HX8

高速生化免疫流水线CX8

Genecast 臻和

朗微博® | MinerVa®
MRD DETECTION PLATFORM
—专业的MRD检测产品，值得信赖

专设平台 创新算法

针对ctDNA检测挑战，多维设计MRD专属检测平台——MinerVa®

MinerVa®
MRD DETECTION PLATFORM

"Miner-Va"
—Variant Miner，变异挖矿机

特异度挑战
- ◇ 克隆性造血影响
- ◇ 检测技术噪音
- ◇ 多变异信号的整合

灵敏度挑战
- ◇ ctDNA释放受多因素影响
- ◇ ctDNA丰度低

深度
- ◇ 30000X超高深度
- ◇ 差异化权重panel设计，肿瘤热点区域超高深度测序

洁净度
专利算法：
- ◇ 分子标签降噪
- ◇ 臻和大样本中国人群基线数据库
- ◇ 多变异联合置信概率分析

广度
- ◇ 769基因固定的大Panel
- ◇ 同时追踪热点功能突变和克隆性搭车变异
- ◇ 持续大Panel追踪

利用创新的多变异联合置信概率分析算法进行MRD阳性值判断，并获得国家专利保护

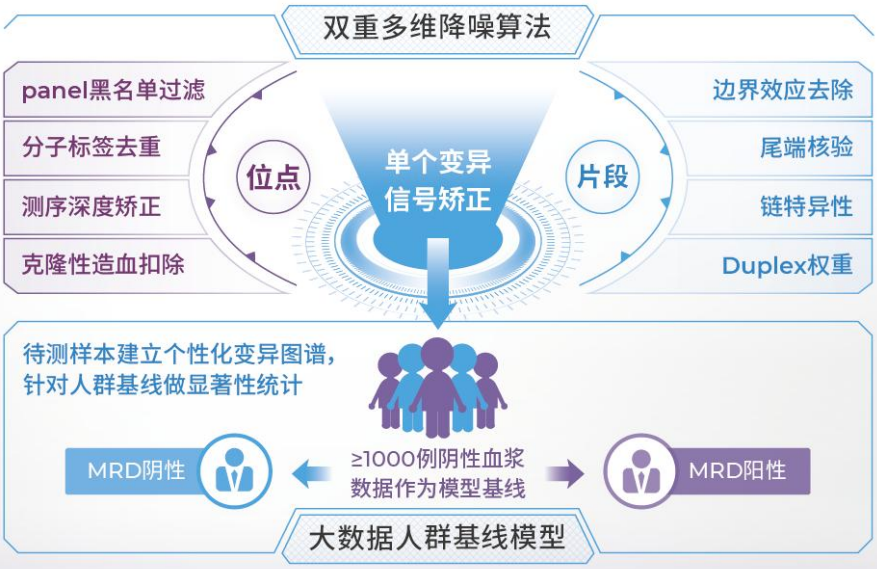

发明专利证书

无锡臻和生物科技有限公司
臻和精准医学检验实验室无锡有限公司

百奥智汇

单细胞测序
数据分析领军者

百奥智汇专注于为用户提供灵活、高效的一站式单细胞及空间多组学解决方案。实验方面，公司已经处理过100多种组织类型，包括肠、血管等多种疑难样本，并在北京、上海、广州、旧金山等多地布局实验室，方便就近送样；分析方面，公司自主开发等十余种算法，分析的细胞数超过2000万。截至目前，百奥智汇共支持客户在*Cell*、*Science*、*Gut* 等期刊发表16篇项目文章，总IF超过540，单篇平均IF达33.8。

产品介绍

实验检测方案

单细胞转录组
- 3' scRNA-seq
- Flex
- CITE-seq
- 5' scRNA-seq+TCR/BCR
- Hash-tag
- scATAC-seq+scRNA-seq
- Smart-seq3xpress

空间转录组
- 10x Visium CytAssist (FFPE)
- 10x Visium (FF)
- 原位RNA检测

蛋白检测
- Bulk蛋白质检测
- 空间蛋白质组学
- 原位蛋白质检测

DNA检测
- scDNA-seq
- 全基因组测序WGS
- 全外显子测序WES

单细胞悬液制备服务

流式分选服务

生信分析方案

标准分析
- 帮助研究者快速从单细胞测序数据中获得细胞异质性信息，得到功能性细胞亚群

高级分析
- 满足研究者对特定生物学和临床问题的需求，进行深入的针对性分析

定制化分析
- 由专门的生信分析工程师利用前沿的数据分析算法为研究者提供分析服务，并针对课题提出科学建议

软件产品

OmniAnalyzer® Pro

单细胞多组学数据分析定制机

大数据平台

OmniBrowser™

OmniDatasets
- Integration Services
- Curation Services
- Customized Services

资质认证

10x Genomics 亚洲唯一的全球数据分析合作伙伴

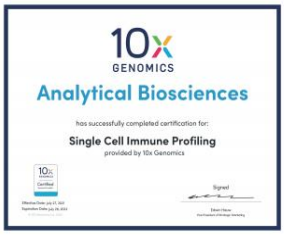

国内率先获得单细胞免疫组库CSP认证

国家高新技术企业认证

ISO27001信息安全管理体系认证

010-62566819
bd_china@abiosciences.com
www.abiosciences.com.cn

欢迎莅临 **百奥智汇展台B090** 交流学习

BIOBASE博科

集团简介

博科控股集团有限公司（简称博科集团）是经国家工商总局核准成立的高新技术产业公司，拥有国际品牌BIOBASE\MF\OLABO，下辖博科生物、博科建筑、鑫贝西智造、来宝网、美华国际等系列制造及运营实体，总部位于山东济南，博科集团以生命健康产业为核心，主营全场景医疗器械、生命安全防护产品及工程、实验室整体解决方案等，为全球用户提供一站式整体解决方案以及相关产品。

博科战略合作阐述

新基建业务（推荐居间合作）

净化工程

医用净化工程
- 净化工程装修
- 净化工程配套设备
- 净化工程维保
- 净化工程装修

净化工程材料及设备
- 各类净化空调
- 各类净化材料

装饰装修

各类一般工程装饰及
特殊需求的装饰工程

基建

EPC、交钥匙、DB
设计咨询
施工总承包
任意阶段任务承接

移动空间

方舱系列
打包箱系列
特种车系列

新消费业务(线下线上门店直营、加盟以及药店供应链合作)

健康美丽产品

医美系列	臻选产品系列
佰欧美系列	臻选酒品、茶系列
曼夕系列	甄选健康食品系列
其他系列	其他甄选礼品系列

家用医疗产品

康养系列(轮椅、病床、自动洗澡机、移位机、手杖等）
家庭检测系列(抗原、血氧、电子体温计等)
家庭治疗系到(家用制氧机、家用呼吸机、各类治疗仪)
家用防护系列(家用消毒机系到及其它消毒产品、口等防护产品)

新营销(直销、代理、配套、居间、经销)

医疗产品

IVD检测产品	基础医疗产品
生化及试剂系列	冷链系列
化学发光及试剂系列、酶免系列	防护系列
POCT及试剂系列	样本前处理系列
分子诊断系列	培养箱系列
IVD试剂、质控及耗材	其他基础医疗产品

病理科系列产品药房系列产品新生儿科系列产品
其他科室系列产品（毒供应中心、病房、静配中心等）

基础科学仪器

环保产品系列
各类实验室产品系列

第三方检测服务 产品及工程维保服务

庄物安全柜等
防护产品检测及维保
环境监测

JIYAN 济研生物

企业公众号　商务洽谈微信号

产品优势

- 长期培养，构建的类器官可持续增殖，冻存复苏传代
- 普遍适用，适用于多种病理分型组织的类器官构建
- 使用便捷，“即用型”试剂盒涵盖必备试剂和耗材
- 高成功率，类器官构建的成功率达90%以上
- 高性价比，全流程条件优化，节省摸索成本

类器官构建试剂盒/类器官培养基

货号	产品名称
OCK-001	肠癌类器官构建试剂盒
OCK-003	胃癌类器官构建试剂盒
OCK-005	卵巢癌类器官构建试剂盒
OCK-007	宫颈癌类器官构建试剂盒
OCK-009	肺癌类器官构建试剂盒
OCK-011	肝胆管癌类器官构建试剂盒
OCK-002	肠类器官构建试剂盒
OCK-004	胃类器官构建试剂盒
OCM-001	肠癌类器官完全培养基
OCM-003	胃癌类器官完全培养基
OCM-005	卵巢癌类器官完全培养基
OCM-007	宫颈癌类器官完全培养基
OCM-009	肺癌类器官完全培养基
OCM-011	肝胆管癌类器官完全培养基
OCM-002	肠类器官完全培养基
OCM-004	胃类器官完全培养基

“一站式” 类器官构建试剂盒（以肠癌为例）

货号	试剂名称	规格
B001-10	Tissue Storage Solution 组织保存液	10mL×1
B002-50	Tissue Wash Buffer 组织清洗液	50mL×1
B003-1	Tissue Fix Solution 组织固定液	1mL×1
D001-10	Dissociation Solution Ⅰ 酶解液Ⅰ	10mL×1
B004-100	Organoid Wash Buffer 类器官清洗液	100mL×1
B005-1	Red Blood Cell Lysis Buffer 红细胞裂解液	1mL×1
B006-5	Coating Buffer 润洗液	5mL×1
B007-01	Trypan Blue 台盼蓝	100μL×1
M001-04	Matrix 基质胶	400μL×2
OCM001-25	Colorectal Cancer Organoids Culture Medium 肠癌类器官完全培养基	25mL×2
S001-02	Supplement Ⅰ 添加物Ⅰ	200μL×1
B008-5	Organoid Recovery Solution 类器官回收液	5mL×1
D002-1	Dissociation Solution Ⅱ 酶解液Ⅱ	1mL×1
D003-1	Dissociation Solution Ⅲ 酶解液Ⅲ	1mL×1
B009-5	Organoid Cryopreservation Solution 类器官冻存液	5mL×1
试剂盒中另附相关必备耗材		

本页仅展示部分产品，更多产品请联系我们

邮箱： info@jiyanbio.com　**网址：** www.jiyanbio.com

电话： 13913789040　**地址：** 苏州市太仓生物医药产业园研发楼1023室

meikang 美康生物

股票代码：300439

MS-P5000系列

新一代全自动生化免疫分析流水线

占地面积最小的全自动样品处理系统，**前处理模块**占地面积≈1㎡

配套生化试剂140+

配套免疫试剂70+

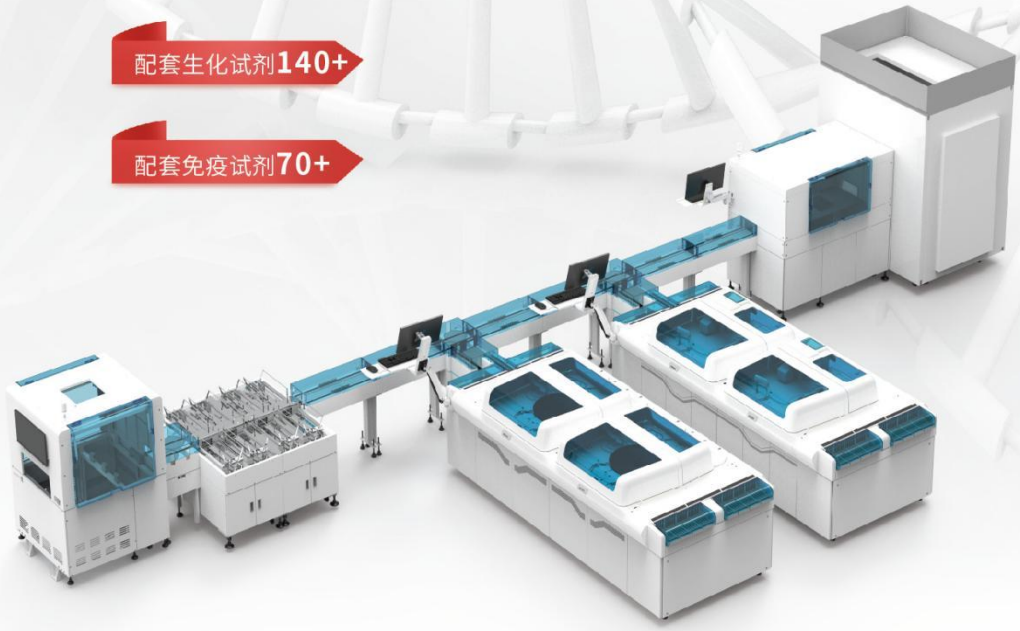

通过轨道+转盘/原机试管架提篮/试管架在线缓存平台/分析仪对接平台等方式，MS-P5000系列涵盖了血液样本前处理、运输、后处理全部环节，将整个样本周转流程打通，实现了样本自动分拣、自动离心、自动开盖、 自动判读不合格样本、自动滤除气溶胶污染、自动装载、自动回收加盖、自动冰箱存储、自动复检、自动抛弃过期样本等功能，从而提高实验室工作效率、避免差错与风险，提升整个实验室运行质量。

● 生化试剂推荐

脂联素（ADPN）
II型糖尿病早期风险筛查新指标

脂蛋白相关磷脂酶A2（质量法）（Lp-pLA2）
《中国临床血脂检测指南》推荐Lp-pLA2采用浓度测定

β2微球蛋白（β2-MG）
线性范围上限提高至50mg/L，满足各类透析患者检测需求

谷胱甘肽还原酶（GR）
急性肝炎早期敏感标志物，且可以用于药物性肝损检测

中性粒细胞明胶酶相关脂质运载蛋白（NGAL）
急性肾损伤早期敏感标志物

特异性生长因子（TSGF）
高灵敏度广谱肿瘤标记物

● 免疫试剂推荐

壳多糖酶3样蛋白1（CHI3L1）
肝纤维化早期敏感指标

胃蛋白酶原+胃泌素17（PG Ⅰ+PG Ⅱ+PG R+G-17）
胃癌早期筛查标志物

抗缪勒管激素（AMH）
全方位评估女性卵巢储备功能

促甲状腺素（TSH）
第三代技术，一流的检测灵敏度

降钙素原+白介素6（PCT+IL-6）
炎症检测双剑客

心肌标志物（Hs-cTnI、CK-MB、MYO、NT-proBNP）
新冠康复建议检测项目

美康生物科技股份有限公司
地址：宁波市鄞州区金达南路1228号
客户服务热线：400-8574-710
网址：www.nbmksw.com

青莲百奥 QLBio　BioLadder　蛋白质诊疗标志物发现创新平台

专注低丰度检测蛋白质标志物发现创新平台

血浆蛋白组学作为寻找生物标志物的专业技术，具有更高的临床转化价值，与临床化学参数具有很强的相关性。血清血浆均可用于蛋白组学研究，血浆中最丰富的蛋白质有白蛋白(约60%)、球蛋白(35%)、纤维蛋白原(4%)、脂蛋白(1%)和铁结合/转移蛋白(1%)。血液中有22种高丰度蛋白约占血浆蛋白的99%，其余1%的血液蛋白由数千个低丰度的循环蛋白以及由活细胞、凋亡细胞和坏死细胞释放的潜在生物标志物蛋白组成。由于高丰度蛋白的信号干扰，成分复杂的血液在筛选生物标志物时更具挑战，低丰度的蛋白检测往往需要跨越10-12个浓度数量级的检测挑战。同时，质谱技术在血浆蛋白开放式研究中是强有力的发现技术。

血浆蛋白质组蕴含巨量生理信息

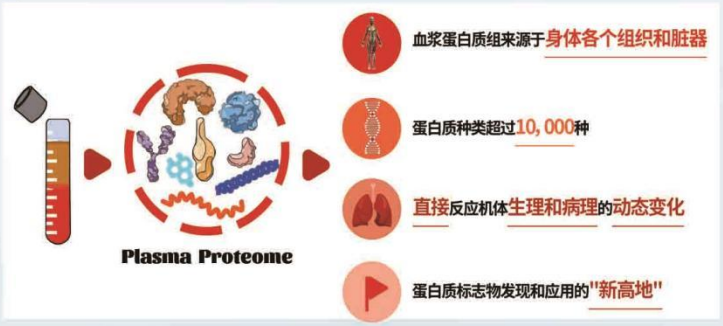

血浆蛋白质组的独特性

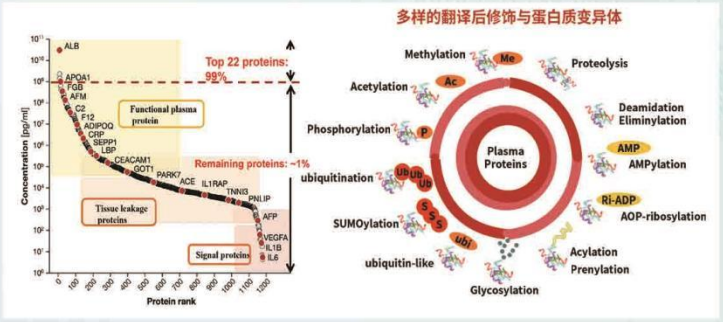

应用场景

纳米磁珠技术--不依赖于抗体

新一代蛋白质组学完整解决方案

青莲百奥自主研发的多功能独创性纳米磁珠富集试剂盒，不断突破蛋白检测的灵敏度、特异性瓶颈，搭配自主研发的蛋白质组学全流程前处理智能机器人及全自动大数据分析系统，全力打造“新一代蛋白质组学智能平台”。

独创性纳米磁珠富集试剂盒

1.覆盖体液类，外泌体类等7大样品类别

2.μl级样本起始量，损耗极低

3.高灵敏度，高深度捕获低丰度蛋白

试剂盒

蛋白质组学机器人

1.内置多种蛋白质组学前处理功能，一键启动

2.拥有磁吸附、精准温控、微量移液工作站多个模块

3.实现临床质谱蛋白质样本处理的全自动化和标准化操作

机器人

蛋白质组学生物信息分析一体机

1.自主研发简单易用的个性化云平台

2.自主创建高效、灵活的自动化流程

3.整合大规模多层次数据库，建立强大的信息学平台

生信分析

想了解更多详情可以扫描右下方二维码关键词回复&前往展会B189展台

北京青莲百奥生物科技有限公司

地址：北京市海淀区永捷南路2号院1号楼中关村科学城5层　网址：www.qinglianbio.com　电话：010-53395839

格诺 GENO

叶酸受体阳性循环肿瘤细胞检测（FR+CTC）

- 肿瘤Ⅰ期灵敏度可达**82.7%**，利于肿瘤早期发现；
- **一管血**实时监测肿瘤活性状态，助力患者精准管理

国械注准 20163400061

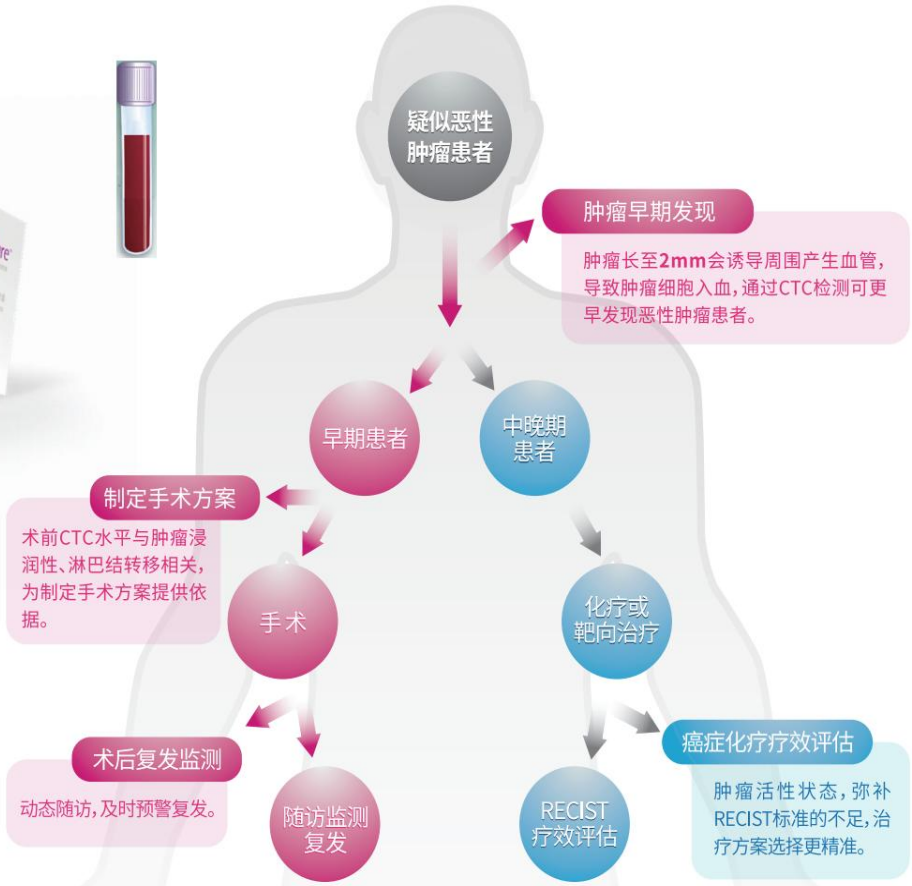

格诺生物于2010年11月在上海张江药谷成立，始终致力于液体活检完整解决方案的开发和推广，包括一系列基于CTC、ctDNA、代谢物等的全癌种诊断产品，涉及多种液体活检试剂的研发、生产、销售、临床检测服务、肿瘤云数据等业务。格诺生物自主研发生产的“叶酸受体阳性循环肿瘤细胞检测试剂盒”于2016年获得NMPA认证并正式上市，是国内首个通过NMPA批准的III类CTC检测试剂。格诺生物积极与全球顶级科研和临床机构达成协作推动技术在临床中的应用。其中与同济大学等单位合作的项目“肺癌精准诊疗关键研究与推广应用”荣获2019年度“国家科技进步二等奖”。

关注格诺，了解更多

公众号　　视频号

格诺生物（中国）科技有限公司

电话：+86（21）6106 6776
网址：www.genosaber.com
地址：上海市浦东新区周浦镇紫萍路908弄26号楼

汇芯生物
HUIXIN LIFETECH

泌芯安™
——基于尿液外泌体的前列腺癌基因检测试剂盒

基于外泌体的检测产品 独立于PSA和其他检测指标
提供独特的、可实现的癌症筛查路径 帮助您决定是否需要活检

无创采样 | 创新技术 | 质量保证 | 结果稳定

EXODUS
全自动外泌体提取系统

高速泌集 | 纯产兼得 | 以少见大 | 完泌归赵 | 智能便捷

适用于多种生物样本

植物囊泡 | 泪液 | 脑脊液 | 房水 | 细菌上清 | 唾液

血液 | 尿液 | 挤出囊泡 | 细胞上清 | 关节液 | 组织液

0755-61017077 | 深圳汇芯生物医疗科技有限公司

chIVD®
Chemclin Diagnostics Corporation
科美诊断

创新高通量诊断技术助推医疗机构健康管理

基于创新光激化学发光技术，可控型发光

单机检测通量高，及时发出报告

LiCA® 800
全自动化学发光免疫分析系统

HOOK-FREE专利技术

优异的加样精度

智能化试剂管理

一体化机身，便捷操作

免洗免分离，运行稳定，性价比高

科美诊断
地址：北京市海淀区永丰基地丰贤中路7号
北科院(100094)
电话：+86 10 58717511
传真：+86 10 58717500
服务热线：800 990 5090/400 880 5090

产品名称：全自动化学发光免疫分析仪
产品型号：LiCA® 800
注册证号：浙械注准20182400322
生产企业：嘉兴凯实生物科技有限公司
禁忌内容或注意事项详见说明书
广告批准文号：浙械广审（文）第230704-04871号
专利号：ZL201611034252.1（专利种类：中国发明专利）

创新服务人类健康

cobas t 711 coagulation analyzer 全自动凝血分析仪

W.A.R.M.开启凝血检测新视界

* 以活化部分凝血活酶时间检测试剂盒(凝固法)为例，一个试剂盒内包含3个试剂瓶，仪器内可放56盒。
** 以抗凝血酶检测试剂盒(发色底物法)为例。

全自动凝血分析仪 coagulation analyzer	国械注进 20202220253
活化部分凝血活酶时间检测试剂盒（凝固法）	国械注进 20202400331
抗凝血酶检测试剂盒（发色底物法）	国械注进 20202400239

生产企业：罗氏诊断公司 Roche Diagnostics GmbH
专业资料，仅供医疗卫生专业人士参考
禁忌内容和注意事项详见说明书　沪械广审（文）第 250428-03852 号

罗氏诊断产品(上海)有限公司

上海
中国(上海)自由贸易试验区希雅路330号
7号厂房第二层I部位
电话：021-3397 1000
传真：021-3397 1888
邮编：200131

北京
北京市东城区东长安街1号东方经贸城
西二办公楼二层201-208及三层301-312
电话：010-8515 4100
传真：010-8515 4188
邮编：100738

广州
广州市环市东路403号
广州国际电子大厦25楼
电话：020-8713 2600
传真：020-8713 2700
邮编：510095

服务热线： 800 820 8864　400 820 8864

MC-CN-01122　有效期至：2025年04月28日

cobas®

Roche

罗氏诊断

6类检测产品助力健康管理

专注专业 先知先行

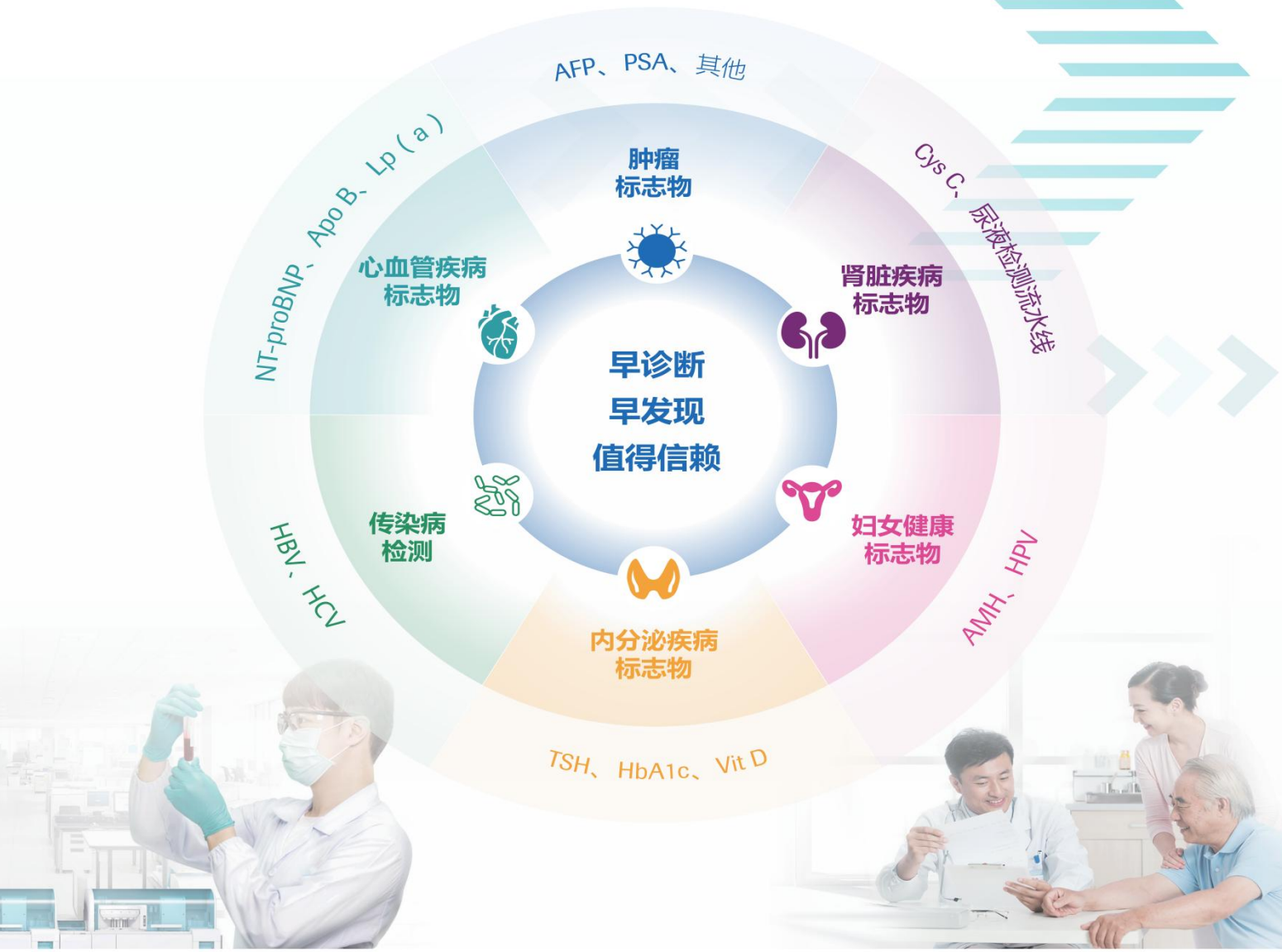

专业资料，仅供医疗卫生专业人士参考

罗氏诊断产品(上海)有限公司

上海

中国(上海)自由贸易试验区希雅路330号
7号厂房第二层I部位
电话: 021-3397 1000
传真: 021-3397 1888
邮编: 200131

北京

北京市东城区东长安街1号东方经贸城
西二办公楼2层至3层
电话: 010-8515 4100
传真: 010-8515 4188
邮编: 100738

广州

广州市环市东路403号
广州国际电子大厦25楼
电话: 020-8713 2600
传真: 020-8713 2700
邮编: 510095

服务热线： 800 820 8864 400 820 8864

mindray 迈瑞

CAL 7000

您需要的**功能**，全面集成

三位一体 全能单机

BC-7500 CRP & BC-7500 CS
荧光五分类/CRP/SAA 检测一步到位
高效集成

支持全样本： 静脉血&末梢血

全自动进样、混匀、检测、复测
一放、一取、实现全面自动化

MC-80 全自动细胞形态学分析仪

集合多项首发科技，快速智能化阅片
并实现如镜下一致的清晰图像
开辟自动化镜检新纪元

SC-120 全自动推片染色机

标准、高效、免维护
支持25ul微量血推片染色
是您值得信赖的推片染色专家

JOINSTAR

中 翰 生 物

Jet-iStar Max

全自动免疫荧光分析仪

为/优/化/检/验/流/程/而/生

1项 全球独家项目

6大 疾病检测板块

22 项 多指标平台

3-18分钟 快速检测

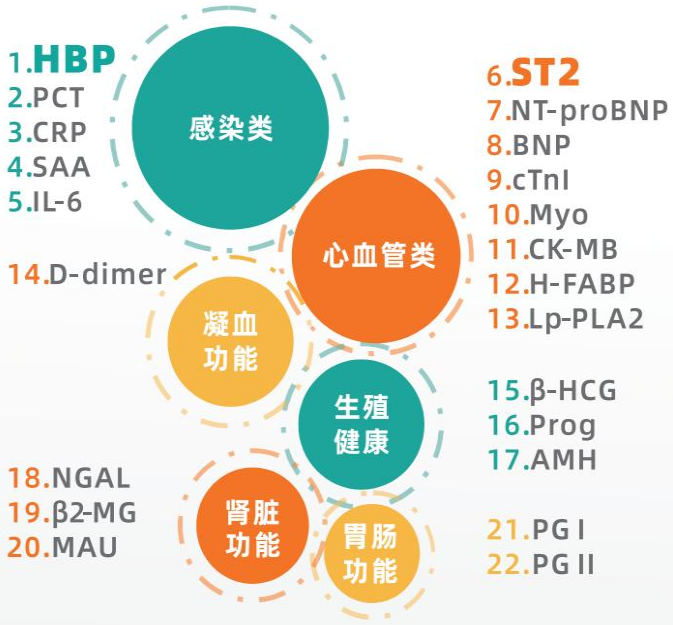

展位地址：上海跨国采购会展中心B028展位

联系电话：施 总 15026859598

ADICON艾迪康

成为每个人身边的医学检验专家

艾迪康医学检验中心成立于2004年1月16日，是全国连锁经营的独立医学实验室，已在全国设立了30余家医学实验室。企业采用欧美独立实验室的先进管理体系，引进国际高端质量标准，与全球医学检验同行广泛开展合作交流。目前，艾迪康拥有研发中心、药物临床、检验服务三大服务平台，其中检验服务平台下设临床实验室、病理实验室、生殖遗传实验室、基因实验室、质谱实验室，拥有200余项专利，提供4000余项检测项目，与全国1.9万家医疗机构建立了合作。

From Eye to Insight

Leica
MICROSYSTEMS

Cell DIVE

超多标组织成像整体解决方案

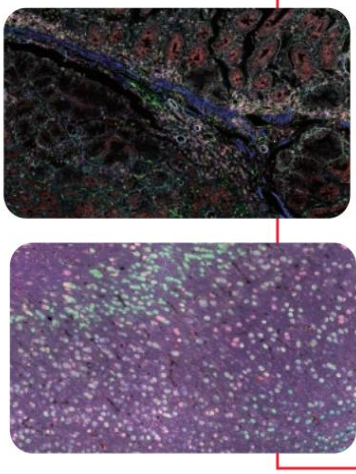

胰腺癌组织 11 个 Biomarker 成像：
CD3, CD4, CD20, CD45, HLA1, SMA1, Vimentin, Cytokeratin, NaK, Collagen, CD31

小鼠大脑 12 个 Biomarker 成像：
Beta-Tubulin, CNPase, FUS, HUD, IBA1, LC3A, MAP2, GFAP, Vimentin, SMA, NEUN, SORLA

THUNDER

高分辨率快速组织成像系统

成年大鼠大脑切片全景成像：
绿色，NeuN neuron；红色，astrocyte；蓝色，nucleus

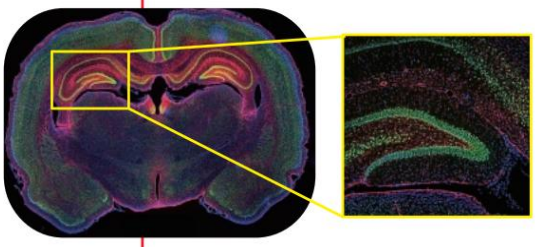

Leica LMD6/7

激光显微切割系统
——您的精准显微手术刀

从组织样本、活细胞样本中，采用激光切割、收集特定细胞，从而进行下游基因组、转录组、蛋白组、或代谢组水平的分析及验证。

- 重力收集，无污染
- 可收集到多孔板，连接自动化
- 精细灵活的激光移动
- 自动识别目标细胞

联系我们

徕卡显微系统（上海）贸易有限公司
地址：上海市长宁区福泉北路518号2座5楼，200335　　电话：400-650-6632
Web: www.leica-microsystems.com.cn

2022 中国肿瘤标志物学术大会
暨CACA整合肿瘤学峰会
暨第十六届肿瘤标志物青年科学家论坛
暨中国肿瘤标志物产业创新大会

2023年4月7日-9日

大会支持企业

Abbott 雅培
SIEMENS Healthineers
Snibe Diagnostic 新产业生物
mindray 迈瑞 生命科技如此亲近
华润智检
illumina 因美纳
创芯(国际) Accurate International
桐树基因 TONGSHU GENE
华大基因 BGI
Hotgen 热景生物
APPLIED PROTEIN TECHNOLOGY 中科新生命
景杰生物 PTM BIO
燃石医学 Burning Rock Dx
Roche
Tellgen 透景
Cyttel
abcam
DUNWILL
GENEWIZ A Brooks Life Sciences Company
格诺 GENO
迪安诊断 DIAN DIAGNOSTICS
基迪奥生物 GENE DENOVO
10x GENOMICS
BIOTREE 百趣 | 提升生命质量
百奥智汇
Runda MEDICAL
oebiotech 欧易生物
Elite Bio
LUMINGBIO 鹿明生物
Autobio 安图生物
Agilent
AKOYA BIOSCIENCES
Create Lab Instruments
新羿生物 TARGETINGONE
康华生物 | HIGHTOP 汉唐
ALLSHENG
中科纳泰 nanopep
YZY MED 友芝友医疗科技
瑞普基因科技 Repugene Technology
Singleron 新格元生物科技
晶准医学 CELLOMICS
CEGER 赛基生物
PinGene 品级基因
Genecast 臻和
ZEISS Seeing beyond
鼎晶生物 TOPGEN
诺辉健康 NEW HORIZON HEALTH 香港交易所上市公司(6606.HK)
阅尔基因 NUPRBE
佰诺全景 PANOVUE
Gene Create 金开瑞

2022 中国肿瘤标志物学术大会
暨CACA整合肿瘤学峰会
暨第十六届肿瘤标志物青年科学家论坛
暨中国肿瘤标志物产业创新大会

2023年4月7日-9日

大会支持企业

JOINSTAR 中翰生物
北京艾沐必康医疗科技有限公司 IMB (CHINA) MEDICAL TECHNOLOGIES CO., LTD.
isoplexis
Olink
西湖欧米 WESTLAKE OMICS
烈冰生物 NovelBio
EP BIOTEK 表观生物
拜谱生物 SHANGHAI BIOPROFILE
biomedicines an Open Access Journal by MDPI
cancers an Open Access Journal by MDPI
先声诊断 Simcere 用精准医疗帮助每个人
APExBIO Achieve Perfection, Explore the Unknown
奕谱生物 EPIPROBE
KHB 科华生物
华得森生物
SPH 上海医药 SHANGHAI PHARMA
普罗亭 PLT TECH
BIO-RAD
AXB® 艾克发
青莲百奥 QL Bio
日和貿易有限公司 NICHIWA TRADING CO.,LTD.
Leica MICROSYSTEMS
Promega
Sciendox 信道生物
FreeThinking 弗瑞思 做病理找弗瑞思
海尔施 HEALTH BioMed
EV BIOMED 亿微
BECKMAN COULTER
pilot Gene Technologies
GENE 吉凯基因
secretech 泌码科技
METWARE 迈维代谢
上海艾研生物科技有限公司 SHANGHAI OUTDO BIOTECH CO.,LTD.
TISSUEGNOSTICS PRECISION THAT INSPIRES
ThunderBio Life Sciences 达普生物
NORMAN Biological Technology
ABclonal Technology
YEASEN
YUBIO 裕策生物
HAMAMATSU PHOTON IS OUR BUSINESS
伯豪生物 SHBIO
腾辰 TANTICA
DANLI
chivd® Chemclin Diagnostics Corporation 科美诊断
砾云医疗
昂凯生命 ONCOCARE LIFETECH
maccura 迈克生物
生工® Sangon Biotech
Insilico Medicine
Shang Zhi Bao Medical

2022

2023年4月7日-9日

中国肿瘤标志物学术大会
暨CACA整合肿瘤学峰会
暨第十六届肿瘤标志物青年科学家论坛
暨中国肿瘤标志物产业创新大会

大会支持企业

沃吉基因 GENE Biotech
NEWON
Geekgene 极客基因
MCE MedChemExpress
Gene+ 吉因加
燊川实业 shenchuan Industry
zaiLab 再鼎医药
light of life 莱拓福
上海睿康生物 Shanghai Reigncom Biotech
SPH 上海医药 SHANGHAI PHARMA
天普策業 TECHPOOL
GenVista 星云基因
圣湘生物 Sansure Biotech
心禹医疗
麦特绘谱 Metabo-Profile
Novogene 诺禾致源
CYTEK TRANSCEND THE CONVENTIONAL
bio-techne
EVbio 益微生物
eppendorf
ThermoFisher SCIENTIFIC
ADICON 艾迪康
迈基诺 MyGenostics Toward the promise of Genomics
RunLab
国药集团 SINOPHARM
sysmex Lighting the way with diagnostics
AmoyDx 艾德生物
BD
astellas 安斯泰来中国
每一次检测都关乎生命 Ortho Clinical Diagnostics 奥森多医疗
华安生物 HUABIO
Labway 兰卫医学
indica labs HALO QUANTITATIVE PATHOLOGY
BIOBASE博科
Oxford NANOPORE Technologies
百迈客生物科技 BIOMARKER TECHNOLOGIES
FOCUSGEN 纳奥生物
MENARINI silicon biosystems
丹力医疗
Byron 柏荣诊断
VMT 上海卫宸医疗科技有限公司 Vecan Medical Tech Limited
达承 Dacheng
HANOL 汉诺生物
应脉医疗 Enlight Medical
迪英加科技
云舟生物
汇芯生物 HUIXIN LIFETECH
Aginome
seer
诺米代谢 PANOMIX

2022 中国肿瘤标志物学术大会
暨CACA整合肿瘤学峰会
暨第十六届肿瘤标志物青年科学家论坛
暨中国肿瘤标志物产业创新大会

2023年4月7日-9日

大会支持企业

博尔诚®
为真生物医药 MicroDiag Biomedicine
武汉国家级人类遗传资源库 WUHAN BIOBANK
BIOTREE百趣
BayOmics 贝普奥
DANAHER Life Sciences · 丹纳赫生命科学
JIYAN 济研生物
亿航生物 CARRIER BIOMED
proteintech™
AntCancer 安科康生物技术（北京）有限公司
CTI 华测艾研 PRECISION FOR LIFE
RayBiotech Empowering your proteomics
睿昂基因 Righton Gene
ANNGEEN Technologies 安智因
达科为 DAKEWE
sptlabtech
圆心科技 — 就医 用药 保险 —
环特生物 Hunter Biotech
JIYAN 济研生物
SANMED BIOTECH
proteintech™
Nanodigmbio 纳昂达
慧算基因 SMARTQUERIERGENE